British Journal of Pharmacology

July 1994

Volume 112 Number 3 pages 717–998

Br. J. Pharmacol. (1994), **112**, 717–719

SPECIAL REPORT

Presence of NK_3-sensitive neurones in different proportions in the medial habenula of guinea-pig, rat and gerbil

[1]P. Boden & G.N. Woodruff

Parke-Davis Neuroscience Research Centre, Addenbrookes Hospital Site, Hills Road, Cambridge CB2 2QB

Electrophysiological recordings were made from neurones of the medial habenula (Mhb) in brain slices obtained from guinea-pig, rat and gerbil brain. The selective NK_3 agonist, senktide, was used to determine the relative number of NK_3-sensitive-neurones in the Mhb of each species. The proportion of neurones responding to NK_1 ($Sar^9Met(O_2)^{11}SP$) and NK_2 ($\beta Ala^8NKA(4-10)$) agonists was also assessed. All (65/65) of the guinea-pig Mhb neurones tested were excited by the NK_3 agonist, but NK_1 and NK_2 agonists were without effect. NK_3 responses in the guinea-pig were not altered by the presence of a selective NK_1 antagonist, CP-99,994. NK_1, NK_2 and NK_3 agonists were without effect on Mhb neurones from gerbil brain slices. In agreement with findings from previous studies, a population of rat Mhb neurones responded to NK_1 or NK_3 agonists alone or were excited by both. These data show that there is a difference in both the number of NK-sensitive neurones and the type of NK response found in the medial habenula of the three species. The high sensitivity to an NK_3 agonist, combined with the apparent lack of NK_1 and NK_2 responses in the guinea-pig Mhb makes this preparation ideal for studies of central NK_3-mediated events.

Keywords: NK_3 receptor; medial habenula

Introduction Three types of neurokinin (NK) receptor have been identified in mammalian brain (see review by Guard & Watson, 1991), and functional data exist to support the presence of both NK_1 and NK_3 receptors in differing relative densities throughout various brain regions. In the rat, *in vitro* electrophysiological recordings have demonstrated the presence of NK responses in a sub-population of *substantia nigra* neurones which are excited only by NK_3 agonists (Keegan *et al.*, 1992), whilst in the medial habenula nucleus (Mhb), neurones are found which respond to either, or both, NK_1 and NK_3 agonists (Norris *et al.*, 1993).

The use of selective antagonists for NK_1 receptors has shown that a species difference exists between NK_1 antagonist binding sites in the rat and guinea-pig brain, with the latter being more representative of the human NK_1 receptor (Gitter *et al.*, 1991). There is now evidence to support the same conclusion for central NK_3 receptors (Petitet *et al.*, 1991). To date, although experiments on the expressed human NK_3 receptor sugggest an intra-species difference (Buell *et al.*, 1992), confirmation of an inter-species difference between NK_3 receptors awaits the development of selective NK_3 antagonists.

Given the possibility that NK_3 receptors in the guinea-pig brain might mirror more accurately those found in the human brain than the rat brain, the purpose of this study was to investigate the nature and type of NK response found in the Mhb of three species. We chose to use guinea-pig, where information on the nature of NK receptor types in the brain is restricted to the *locus coeruleus* which possesses sub-populations of neurones responding to both NK_1 and NK_3 agonists (Seabrook *et al.*, 1992; McLean, 1993) rat and gerbil. No data are available on functional NK responses in the gerbil brain.

Methods *Brain slice preparation* Coronal slices (350 μm) were prepared from brains of guinea-pig (Dunkin-Hartley, 300–500 g), gerbil (Mongolian, 40–60 g) or rat (Wistar, 150–300 g) brain using a Vibratome (Oxford Instruments). One such slice, cut at the level of the Mhb (bregma – 3.8 to – 4.2 mm) was placed in a perfusion chamber and perfused with artificial cerebrospinal fluid (ACSF) flowing at 4 ml min^{-1}. All experiments were performed at 37°C. Extracellular recordings were made from individual spontaneously firing neurones in the Mhb. Agonists were applied for 1 min. Slices were pretreated with antagonists for 30 min before addition of agonists in the continued presence of the antagonist. Details of the subsequent data analysis have been reported elsewhere (Boden *et al.*, 1991).

Drugs All NK agonists were obtained from Peninsula Labs. and applied at known concentrations directly dissolved in the ACSF from a 1 mM stock solution in dimethyl sulphoxide (DMSO). The agonists used were; senktide (succinyl-[Asp^6MePhe^8]substance P(6–11)); $Sar^9SP(Sar^9Met(O_2)^{11}$substance P); neurokinin B(NKB); β-$Ala^8NKA(4-10)$; SpOMe (substance P methyl ester). The highly selective NK_1 antagonist, CP-99,994 ((+)-2S,3S)-3-(2-methoxybenzylamino)-2-phenylpiperidine) (McLean *et al.*, 1993) (100 nM), used in some guinea-pig Mhb experiments, was synthesized in the Medicinal Chemistry Labs., Parke-Davis.

Results Table 1 shows the results for a series of neurokinin agonists on the firing rate of spontaneously firing guinea-pig Mhb neurones. All (65/65) guinea-pig Mhb neurones were excited in a concentration-dependent fashion by senktide (Figure 1) but none of those tested were affected by the presence of agonists for the NK_1(0/21) or NK_2(0/8) receptor. Further to this the response to senktide was not altered in the presence of CP-99,994 (100 nM) to eliminate any possible interference from NK_1 receptors. A mean EC_{50} value of 24.5 nM (range 5.0 to 42.0 nM, $n = 9$) was obtained for senktide at NK_3 sites in the guinea-pig Mhb. We compared the relative potencies of senktide and NKB on the same neurones (3 neurones from 3 slices). The mean EC_{50} values revealed like-potencies for the two agonists (Table 1A). A proportion (approximately 50%) of rat Mhb neurones was excited either by the NK_1 agonist or NK_3 agonist alone (Table 1B). EC_{50} values of 45.4 nM (range 24.0 to 60.0 nM, $n = 5$) and 76.0 nM (range 16.0 to 220.0 nM, $n = 5$) were obtained for senktide and $Sar^9Met(O_2)^{11}SP$ respectively in the rat Mhb. Three of 21 neurones in the rat Mhb were excited by both NK_1 and NK_3 agonists.

In contrast to the high incidence of NK_3-receptive neurones in the guinea-pig Mhb, studies of the same region in the gerbil failed to produce any indication of the presence of NK-sensitive neurones in the Mhb. The spontaneous firing

[1] Author for correspondence.

Table 1 Summary of data for NK agonist action on medial habenula neurones of guinea-pig, rat and gerbil

A *Guinea-pig*

No of slices	*No of neurones*	*No of neurones responding to tachykinin agonists* Sar^{9}Met(O$_2$)^{11}SP	NKB	β-Ala^{8}NKA(4–10)	Senktide
31	65	0/21	5/5	0/8	65/65

EC_{50} for senktide = 24.5 nM (5.0–42.0, $n = 9$)
EC_{50} for senktide cf. NKB ($n = 3$) = 27.0 nM (4.4–66.0) cf. 39.1 nM (2.7–87.0)

B *Rat*

No of slices	*No of neurones*	*No of neurones responding to tachykinin agonists* Sar^{9}Met(O$_2$)^{11}SP	β-Ala^{8}NKA(4–10)	Senktide
18	21	11/21	0/21	9/21

EC_{50} for senktide = 45.4 nM (24–60, $n = 5$)
EC_{50} for Sar^{9}Met(O$_2$)^{11}SP = 76.0 nM (16–220, $n = 5$)

C *Gerbil*

No of slices	*No of neurones*	*No of neurones responding to tachykinin agonists* Sar^{9}Met(O$_2$)^{11}SP	SpoMe	β-Ala^{8}NKA(4–10)	Senktide
4	13	0/13	0/13	0/13	0/13

EC_{50} values are given at the end of each data set as the mean of n values followed by the range.

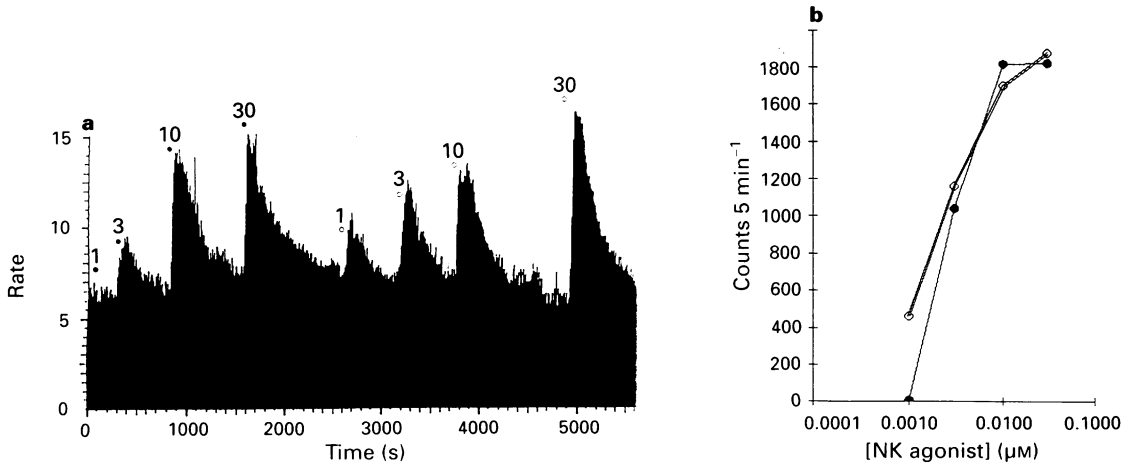

Figure 1 Concentration-dependent excitations of a spontaneously firing guinea-pig medial habenula neurone by the two neurokinin (NK) agonists, senktide and NKB: (a) shows a ratemeter histogram of the experiment with the firing rate (Hz) plotted against time of the experiment (seconds). NK agonists were applied for 1 min at the nanomolar concentrations shown ((●) senktide; (○) NKB). (b) Shows the resulting concentration-response curves. The two compounds were approximately equipotent with EC_{50} values of 4.4 nM (senktide, ●) and 2.7 nM (NKB, ○).

of 13 neurones (4 slices) was unaffected by NK_1, NK_2 or NK_3 agonists, suggesting, few if any, NK-sensitive neurones are present in the gerbil Mhb (Table 1C).

Discussion This study reveals that differences exist in the proportion and type of NK response on neurones within the same brain region in different species. While we were able to confirm that the rat Mhb has both NK_1 and NK_3-receptive neurones, we have also demonstrated for the first time the apparent lack of any functional NK responses in the gerbil Mhb. This is of interest given the recent finding that i.c.v. injection of NK_1 and NK_3 agonists caused hind-limb thumping in the same species (Graham *et al.*, 1993). We also report here for the first time the overwhelming predominance of neurones which are excited by an NK_3 agonist in the guinea-pig Mhb.

The data presented show that the guinea-pig Mhb is an excellent preparation for functional NK_3 receptor studies. The absence of a selective NK_3 antagonist meant that the only test for the presence of NK_3 sites lay in the use of an NK_3-selective agonist combined with an NK_1 antagonist. Under these conditions every guinea-pig Mhb neurone was excited in a concentration-dependent manner by senktide, indicative of a high density of NK_3-sensitive neurones in the guinea-pig Mhb.

The finding that senktide and NKB were approximately equipotent was also important, since this echoes the rank affinities in radioligand binding studies of the two agonists at the cloned human brain NK_3 receptor (Buell *et al.*, 1993). In other rodent brain slice preparations where comparisons of the potencies of NK agonists have been made NKB was considerably less potent than senktide (Seabrook *et al.*, 1992; Norris *et al.*, 1993).

References

BODEN, P.R., WOODRUFF, G.N. & PINNOCK, R.D. (1991). Pharmacology of a cholecystokinin receptor on 5-hydroxytryptamine neurones in the dorsal raphe of the rat brain. *Br. J. Pharmacol.*, **102,** 635–638.

BUELL, G., SCHULZ, M.F., ARKINSTALL, S.J., MAURY, K., MISSOTTEN, M., ADAMI, N., TALABOT, F. & KAWASHIMA, E. (1992). Molecular characterisation, expression and localisation of human NK_3 receptor. *FEBS Lett.*, **299,** 90–95.

GITTER, B.D., WATERS, D.C., BRUNS, R.F., MASON, N.R., NIXON, J.A. & HOWBERT, J.J. (1991). Species differences in affinities of non-peptide antagonists for substance P receptors. *Eur. J. Pharmacol.*, **197,** 237–238.

GRAHAM, E.A., TURPIN, M.P. & STUBBS, C.M. (1993). Characterisation of the tachykinin-induced hindlimb thumping response in gerbils. *Neuropeptides*, **228,** 100P.

GUARD, S. & WATSON, S.P. (1991). Tachykinin receptor types: classification and membrane signalling membranes. *Neurochem. Int.*, **18,** 149–165.

KEEGAN, K.D., WOODRUFF, G.N. & PINNOCK, R.D. (1992). The selective NK_3 receptor agonist senktide excites a subpopulation of dopamine-sensitive neurones in the rat substantia nigra pars compacta *in vitro*. *Br. J. Pharmacol.*, **105,** 3–5.

McLEAN, S., GANONG, A., SEYMOUR, P.A., SNIDER, R.M., DESAI, M.C., ROSEN, T., BRYCE, D.K., LONGO, K.P., REYNOLDS, L.S., ROBINSON, G., SCHMIDT, A.W., SIOK, C. & HEYM, J. (1993). Pharmacology of CP-99,994; a nonpeptide antagonist of the tachykinin neurokinin-1 receptor. *J. Pharmacol. Exp. Ther.*, **267,** 472–476.

NORRIS, S.K., BODEN, P.R. & WOODRUFF, G.N. (1993). Agonists selective for tachykinin NK_1 and NK_3 receptors excite subpopulations of neurons in the rat medial habenula nucleus *in vitro*. *Eur. J. Pharmacol.*, **234,** 223–228.

PETITET, F., BEAUJOUAN, J.-C., SAFFROY, M., TORRENS, Y. & GLOWINSKI, J. (1993). The nonpeptide NK_2 antagonist SR 48968 is also a NK_3 antagonist in the guinea-pig but not in the rat. *Biochem. Biophys. Res. Commun.*, **191,** 180–187.

SEABROOK, G.R., MAIN, M.J. & HILL, R.G. (1992). Pharmacology of neurokinin receptors on neurones within brain slices of the guinea-pig *locus coeruleus*. *Br. J. Pharmacol.*, **107,** 228P.

(Received March 1, 1994
Accepted March 21, 1994)

Br. J. Pharmacol. (1994), **112**, 720–722

SPECIAL REPORT

Expression of inducible nitric oxide synthase by neurones following exposure to endotoxin and cytokine

[1]Dahlia Minc-Golomb, *Ilan Tsarfaty & Joan P. Schwartz

Clinical Neuroscience Branch, National Institute of Neurological Disorders and Stroke, National Institutes of Health and *ABL-National Cancer Institute, National Institutes of Health, Bethesda, Maryland, U.S.A.

In the CNS, nitric oxide (NO) has been implicated as both a mediator of neurotoxicity and a neuromodulator. The inducible NO synthase (iNOS), thought to mediate toxic effects of NO, has been attributed to glial cells in the CNS. We now report that cerebellar granule cell neurones can be stimulated by lipopolysaccharide and interferon-γ to express iNOS *in vitro*, as demonstrated by reverse transcription-polymerase chain reaction and fluorescent *in situ* hybridisation. The expression of both constitutive NO synthase (cNOS) and iNOS by neurones suggests that NO has diverse functions in the brain, and supports the possibility that iNOS plays a role in neuronal damage and inflammation following activation of brain microglia and production of cytokines.

Keywords: Cerebellar granule cells; macrophage; cerebellum; interferon-γ; lipopolysaccharide

Introduction Two forms of nitric oxide synthase (NOS) have been described: a constitutive form (cNOS), expressed tonically, and an inducible form (iNOS), only present following exposure to agents such as cytokines and endotoxins. NO formed by cNOS functions in intercellular interactions, whereas NO produced by iNOS is mainly a cytotoxic agent (Moncada *et al.*, 1991). In the CNS, NO functions as a neuromodulator, but also mediates N-methyl-D-aspartate (NMDA) excitotoxicity on cortical neurones in culture (Dawson *et al.*, 1991). Induction of iNOS has not been demonstrated in neurones, but attributed to glial cells (Murphy *et al.*, 1993). Because of the potential role of iNOS in neurotoxicity, we have examined whether iNOS could be induced in neurones by cytokines, which increase in the brain following various insults (Morganti-Kossmann *et al.*, 1992).

Methods Cerebellar granule cells (CGC) were prepared from 8-day old rat pups (Novelli *et al.*, 1988) and used after 10–12 days *in vitro*. Previous characterization of these cultures has shown that greater than 95% of the cells are CGC. The absence of microglia and astrocytes in cultures (< 1/100 cells) was verified by staining with antibodies to ED-1 and glial fibrillary acidic protein respectively. A macrophage cell line, P388D1 (Koren *et al.*, 1975), was used as a positive control for the induction of the iNOS gene. Lipopolysaccharide (LPS, 10 μg ml^{-1} *E. coli* serotype 0128:B12, Sigma) and mouse interferon-γ (IFN-γ, 100 u ml^{-1}, Genzyme) were used to induce iNOS.

RNA was prepared using RNAzol (Tel-Test). RNA-specific (Shuldiner *et al.*, 1991) or standard reverse transcription – polymerase chain reaction (RS- or RT – PCR) were used to amplify iNOS mRNA, or the mRNA of the unchanging gene cyclophilin, which served as a quantity control, respectively. The primer for the reverse transcription of iNOS mRNA (GenEMBL No. M84373) corresponded to the antisense sequence of nucleotides 3554-3573, with the addition of the T30 tag (Shuldiner *et al.*, 1991). PCR primers for the amplification of iNOS cDNA corresponded to nucleotides 3440-3461 (upstream) and the T30 tag (downstream, Shuldiner *et al.*, 1991). RT-PCR primers for the gene encoding cyclophilin (GenEMBL No. M19533) corresponded to nucleotides 53–71 (upstream) and 679–696 (downstream). Each PCR cycle consisted of: 1'-94°C, 1'-59°C, 1'-72°C (30 cycles). Aliquots of the amplification products were electrophoresed, visualised by ethidium bromide staining, and transferred onto a nylon membrane. The blot was hybridised with ^{32}P-labelled iNOS cDNA from activated macrophages, washed under conditions of high stringency (0.1 × SSC, 0.1% SDS at 60°C), and exposed to X-ray film. Negative controls that underwent the same procedures without reverse transcriptase, or without RNA, did not yield PCR products.

CGC grown on glass slides, with or without application of LPS-IFN-γ for 4 h prior to fixation, were used for fluorescent *in situ* hybridisation (FISH). The slides were hybridised with 350 ng ml^{-1} of each of two biotinylated complementary or identical oligonucleotide probes to the iNOS mRNA (nucleotides 3440–3461 and 3554–3573), in a solution of 50% formamide, 4 × SSC, 1 × Denhardt's solution, 25 μg ml^{-1} tRNA, 50 μg ml^{-1} salmon sperm DNA, overnight at 37°C. Following hybridisation, the slides were washed 4 times in 2 × SSC and 50% formamide at 40°C for 15 min, twice for 1 h in 1 × SSC at 22°C. Following rinsing in ethanol, the slides were incubated with Streptavidin fluorescein (Amersham), washed, mounted, and examined by confocal laser scanning microscopy (CLSM), as described (Tsarfaty *et al.*, 1992).

Results Treatment of CGC with LPS-IFN-γ resulted in induction of transcription of the iNOS gene, as evidenced by RS-PCR. The iNOS PCR product in stimulated macrophages and CGC was the expected size (164 bases including the T30 tag) and hybridised with a macrophage iNOS cDNA, but not with a brain cNOS cDNA. iNOS mRNA was detectable 2–6 h following application of LPS-IFN-γ, in CGC as well as in macrophages, but not in untreated cultures (Figure 1a). Sequence of the PCR product from stimulated CGC revealed greater than 90% homology to the mouse macrophage sequence and 100% homology at the amino acid level. All samples gave rise to comparable amounts of PCR product for the nonchanging cyclophilin mRNA (Figure 1b).

FISH followed by CLSM demonstrated that iNOS was expressed by CGC, rather than by possible contaminating cells in the culture. This method showed iNOS mRNA in 80–90% of CGC treated with LPS-IFN-γ for 4 h (Figure 2a) but not in untreated cells (Figure 2g). Hybridisation of CGC with sense oligoprobes yielded no signal under identical microscope parameters (Figure 2e). Overlay analyses of the fluorescent hybridisation in treated CGC with the Nomarski optic morphology, which shows the typical appearance of cultured CGC (Figure 2a, b), demonstrated that iNOS mRNA is localised in the CGC cell bodies (Figure 2c). NOS

[1] Author for correspondence.

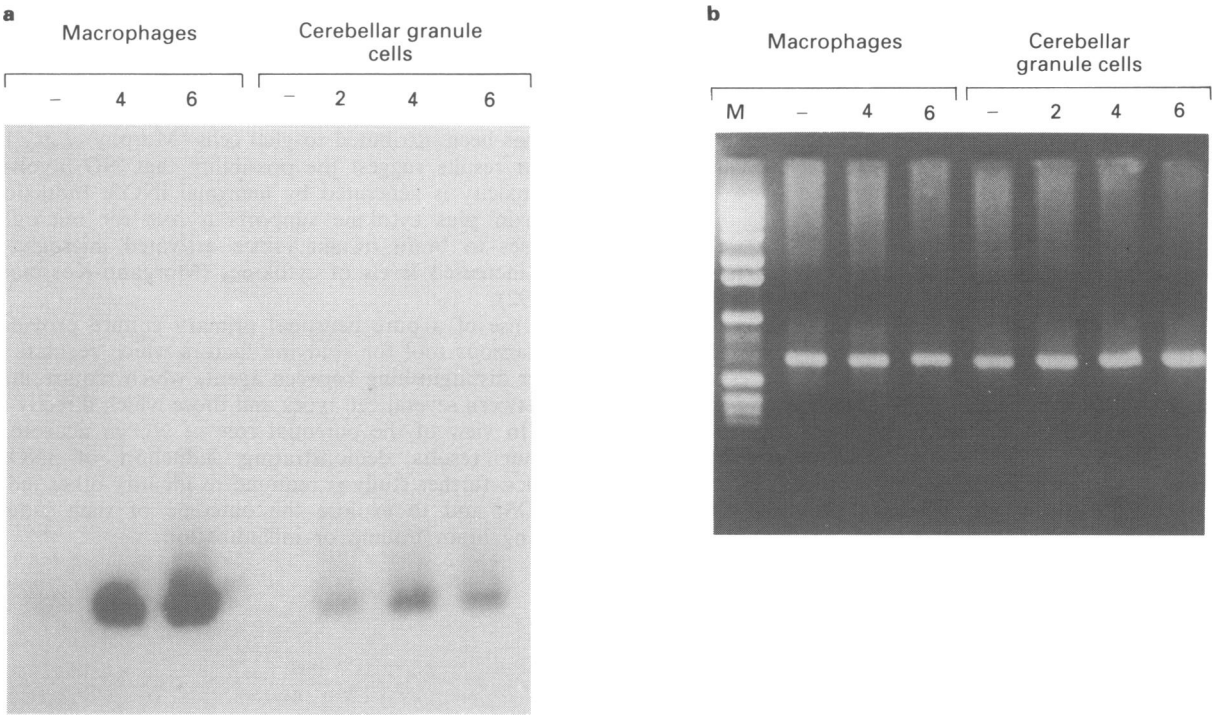

Figure 1 Inducible NO synthase (iNOS) mRNA in macrophages and in cerebellar granule cells (CGC). (a) Southern blot of RS-PCR product (164 bases) of the iNOS gene, after exposure of macrophages or CGC to LPS-IFN-γ for 0–6 h. (b) Ethidium bromide-stained gel of RT-PCR products for cyclophilin mRNA using the same RNA samples as in (a). The left lane is 1 Kb DNA ladder (GIBCO). The cyclophilin product is the expected size 644 bases. The numbers above the lanes show the hours of exposure to LPS-IFN-γ. For abbreviations, see text.

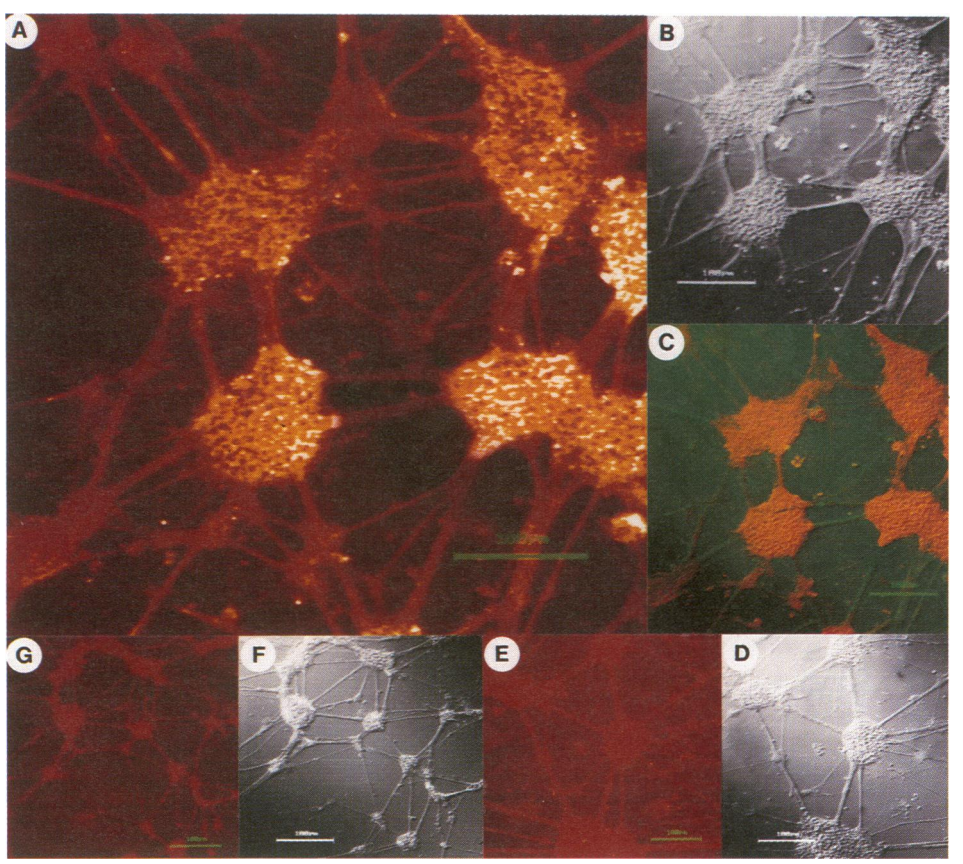

Figure 2 Fluorescent *in situ* hybridisation (FISH) analysis of inducible NO synthase (iNOS) mRNA in cerebellar granule cells (CGC) treated with lipopolysaccharide-interferon-γ (LPS-IFN-γ). FISH for the iNOS gene transcript was carried out as described in Methods. (a) Fluorescent *in situ* signal in the cell bodies. (b) Nomarski image of the same region as in (a). (c) Overlay analysis between iNOS mRNA fluorescence (a) and morphology (b) (yellow indicates overlap). (d, e) A treated sister culture hybridised with the sense probes and (f, g) an untreated sister culture hybridised with the antisense probes. Nomarski images (d, f); fluorescent images (e, g). Scale bars are 100 μm.

enzymatic activity was measured by assessing conversion of L-[^{3}H]-arginine to L-[^{3}H]-citrulline. Exposure of CGC to LPS-IFN-γ increased the rate of conversion from 0.21 ± 0.02 pmol min^{-1} mg^{-1} protein in untreated cells to 0.41 ± 0.04 pmol min^{-1} mg^{-1} protein in stimulated cells, indicating that the iNOS message is translated to an active enzyme in these cultured neurones. Either LPS or IFN-γ alone increased the activity to a lesser extent (data not shown).

Discussion Our results demonstrate that CGC express iNOS following exposure to LPS-IFN-γ in culture. In contrast to neurones, macrophages contain only iNOS which requires gene transcription, and the NO produced by this enzyme function as a cytotoxic agent. The level of expression of iNOS mRNA in macrophages is higher than that in neurones (Figure 1), perhaps because cytotoxicity is a major function of macrophages. Since CGC are the richest in cNOS in the CNS, these neurones can express two different forms of NOS, supporting the view that NO has a variety of different functions in nerve cells. In addition to its function as a neuronal messenger, NO has been implicated in neurotoxicity (Dawson *et al.*, 1991). iNOS mRNA was induced in whole brain extracts in experimentally-induced models of neurological disorders (Koprowski *et al.*, 1993). NOS inhibitors attenuated NMDA excitotoxicity and reduced ischaemic damage (Nowicki *et al.*, 1991). iNOS activity in the CNS has been attributed to glial cells (Murphy *et al.*, 1993), but our results suggest the possibility that NO involved in neurotoxicity is generated by neuronal iNOS. Induction by endotoxin plus cytokine supports a role for microglia in responses to brain trauma, since activated microglia produced increased levels of cytokines (Morganti-Kossmann *et al.*, 1992).

The use of a pure neuronal primary culture provides an advantageous tool for studying factors which regulate NOS and for distinguishing between agents which require interaction between several cell types and those which directly affect NOS. In view of the potential role of NO in neurotoxicity and our results demonstrating induction of iNOS in neurones, further study is required to identify other inducers of iNOS, and to explore the outcome of such induction following brain trauma or inflammation.

References

DAWSON, V.L., DAWSON, T.M., LONDON, E.D., BREDT, D.S. & SNYDER, S.H. (1991). Nitric oxide mediates glutamate neurotoxicity in primary cultures. *Proc. Natl. Acad. Sci. U.S.A.*, **88,** 6368–6371.

KOPROWSKI, H., ZHENG, Y.M., HEBER-KATZ, E., FRASER, N., RORKE, L., FU, Z.F., HANLON, C. & DIETZSCHOLD, B. (1993). In vivo expression of inducible nitric oxide synthase in experimentally induced neurologic diseases. *Proc. Natl. Acad. Sci. U.S.A.*, **90,** 3024–3027.

KOREN, H.S., HANDWERGER, B.S. & WUNDERLICH, J.R. (1975). Identification of macrophage-like characteristics in cultured murine tumor line. *J. Immunol.*, **114,** 894–897.

MONCADA, S., PALMER, R.M.J. & HIGGS, E.A. (1991). Nitric oxide: physiology, pathology, and pharmacology. *Pharmacol. Rev.*, **43,** 109–142.

MORGANTI-KOSSMANN, M.C., KOSSMANN, T. & WAHL, S.M. (1992). Cytokines and neuropathology. *Trends Pharmacol. Sci.*, **13,** 286–291.

MURPHY, S., SIMMONS, M.L., AGULLO, L., GARCIA, A., FEINSTEIN, D.L., GALEA, E., REIS, D.J., MINC-GOLOMB, D. & SCHWARTZ, J.P. (1993). Synthesis of nitric oxide in CNS glial cells. *Trends Neurosci.*, **16,** 323–328.

NOVELLI, A., REILLY, J.A., LYSKO, P.G. & HENNEBERRY, R.C. (1988). Glutamate becomes neurotoxic via the N-methyl-D-aspartate receptor when intraceullar energy levels are reduced. *Brain Res.*, **451,** 205–212.

NOWICKI, J.P., DUVAL, D., POIGNET, H. & SCATTON, B. (1991). Nitric oxide mediates neuronal death after focal cerebral ischemia in the mouse. *Eur. J. Pharmacol.*, **204,** 339–340.

SHULDINER, A.R., TANNER, K., MOORE, C.A. & ROTH, J. (1991). RNA template-specific PCR: an improved method that dramatically reduces false positives in RT-PCR. *BioTechniques*, **11,** 760–763.

TSARFATY, I., RESAU, J.H., RULONG, S., KEYDAR, I., FALETTO, D.L. & VANDE WOUDE, G.F. (1992). The met proto-oncogene receptor and lumen formation. *Science*, **257,** 1258–1261.

(Received January 11, 1994
Accepted April 7, 1994)

Br. J. Pharmacol. (1994), **112**, 723–727

Pro-inflammatory activities in elapid snake venoms

Denise V. Tambourgi, Maria Cristina dos Santos, *Maria de Fátima D. Furtado, *Maria Cristina W. de Freitas, *Wilmar Dias da Silva & [1]Thereza L. Kipnis

Departamento de Imunologia, Instituto de Ciências Biomédicas, Universidade de São Paulo, Av. Prof. Lineu Prestes, 2415, São Paulo, CEP 05508-900, Brazil and *Laboratório de Herpetologia and Laboratório de Imunoquímica, Instituto Butantan, São Paulo, S.P, Brazil

1 Snake venoms from the genera *Micrurus* (*M. ibiboboca* and *M. spixii*) and *Naja* (*N. naja*, *N. melanoleuca* and *N. nigricollis*) were analysed, using biological and immunochemical methods, to detect pro-inflammatory activities, cobra venom factor (COF), proteolytic enzymes, thrombin-like substances, haemorrhagic and oedema-producing substances.

2 The venoms of the five snake species activate the complement system (C) in normal human serum (NHS) in a dose-related fashion, at concentrations ranging from 5 μg to 200 μg ml^{-1} serum. Electrophoretic conversion of C3 was observed with all venoms in NHS containing normal concentrations of Ca^{2+} and Mg^{2+}, but only by venoms from *N. naja* and *N. melanoleuca* when Ca^{2+} was chelated by adding Mg^{2+}-EGTA.

3 Purified human C3 was electrophoretically converted, in the absence of other C components, by the venoms from *N. naja*, *N. nigricollis* and *M. ibiboboca*. However, only the venoms from *N. naja* and *N. melanoleuca* contained a 144 kDa protein revealed in Western blot with sera against COF or human C3.

4 All venoms, at minimum concentrations of 30 ng ml^{-1}, were capable of lysing sheep red blood cells, also in a dose-related fashion, when incubated with these cells in presence of egg yolk as a source of lecithin. Although the venoms from *M. spixii* and *N. nigricollis* showed detectable thrombin-like activity, these and the other venoms were free of proteolytic activity when fibrin, gelatin and casein, were used as substrates.

5 When tested on mice skin, all five venoms were capable of inducing an increase in vascular permeability and oedema, but were devoid of haemorrhagic producing substances (haemorrhagins).

6 These data provide evidence indicating that Elapidae venoms contain various pro-inflammatory factors which may be important in the spreading of neurotoxins throughout the tissues of the prey or human victim.

Keywords: Pro-inflammatory activities; snake venoms; complement activation; cobra venom factor; haemolytic activity; haemorrhagic; oedema and vascular increasing activities

Introduction

Venomous snakes belong to five families: elapidae, crotalidae, viperidae, hydrophidae and colubridae, and their venoms contain a vast number of substances with different biochemical and pharmacological activities. The venoms from some members of the Elapidae contain a 144 kDa glycoprotein, designated cobra venom factor (COF) (Müller-Eberhard & Fjellström, 1971). This protein displays some structural similarities and antigenic cross-reactivity with human C3 (Alper & Balavitch, 1976). There is evidence that COF is a physiological breakdown product of cobra C3 (Eggertsen *et al.*, 1983). COF generates active C3 convertase, COFBb by interacting with the C alternative components, factors B and D in the presence of Mg^{2+} (Götze & Müller-Eberhard, 1971; Götze, 1975). COFBb cleaves C3 into C3a and C3b (Shin *et al.*, 1969); C3a is released into the fluid phase while C3b binds to the bimolecular complex COFBb generating the trimolecular complex COFBbC3b, which now as a C5 convertase is able to cleave C5, the next component of the C cascade, into C5a and C5b (Smith *et al.*, 1982). Although the peptides C3a and C5a are mediators of the early events of the inflammatory process (Dias da Silva & Lepow, 1967; Dias da Silva *et al.*, 1967; Lepow *et al.*, 1967), C3b can be recognized by C receptors displayed on the phagocyte cell surface (Ross & Medof, 1985) and C5b serves as the starting for the C5b-C9 cytolytic complex organization (Pickering *et al.*, 1969).

Crotalidae venoms are abundant in proteases, some of which possess kinin-releasing activity (Rocha da Silva *et al.*, 1950; Geiger & Kortmann, 1977), others are capable of attacking fibrinogen catalyzing the release of fibrin peptides A and B from the terminal dissulphide knots of fibrinogen α and β chains (thrombin-like enzymes), or of splitting off fragments from the COOH terminals of α, β and γ chains of fibrinogen (fibrinogenolytic enzymes). Some may also act as fibrinolysins (plasminogen activating enzymes) (Stocker & Barlow, 1976; Stocker *et al.*, 1982), and others, present in venoms of viperidae, act on the vessel walls inducing haemorrhage (Mandelbaum & Assakura, 1988). Therefore, snake venoms are rich sources of enzyme-generating factors or enzymes capable of mediating, directly or indirectly, the early events of the inflammatory process. Inflammation at the site of the snake bite, together with the spreading action exerted by the hyaluronidase (Zeller, 1948), could facilitate the distribution of other toxic venom components, throughout the tissues of the prey.

The aims of the present work were to verify if the venoms of *Naja* and *Micrurus* contain substances endowed with pro-inflammatory activities as proteases, COF-like proteins, thrombin-like, haemolytic, C activators, haemorrhage inductors and mediators of vascular permeability.

Methods

Snake venoms

Venoms of *M. ibiboboca*, *M. spixii*, *N. naja*, *N. melanoleuca*, and *N. nigricollis* were provided by the Instituto Butantan,

[1] Author for correspondence.

São Paulo, SP, Brazil, and the Bombain Institute, India. The venoms were extracted from 5–10 adult snakes using standard procedures, the samples from each species pooled, vacuum dried and stored at 4°C. Stock solutions were prepared in pH 7.2, 0.15 M phosphate buffered-saline (PBS) at 1.0 mg ml^{-1}. Cobra venom factor (COF) from *N. naja* venom was purchased from Diamedix FL, U.S.A.

Sera and anti-sera

Normal human serum (NHS) was obtained from healthy donors; rabbit anti-COF was kindly provided by Dr Ramalho-Pinto, Instituto de Ciências Biológicas, UFMG, Belo Horizonte, MG, Brazil; goat anti-human C3, (Atlantic Antibodies, Scarborough, ME, U.S.A.); peroxidase goat anti-rabbit IgG (Sigma Chemical Co., St. Louis, MO, U.S.A.) and rabbit anti-goat IgG (Kirkegaard and Perry Lab. Inc., Gaithersburg, MA, U.S.A.).

Activation of C

Samples of 200 µl of normal human serum (NHS) were treated with 1.0, 5.0, 15.0 and 40.0 µg of snake venoms previously dissolved in PBS, or with PBS alone (control samples), for 1 h at 37°C and stored at − 20°C until assay.

Haemolytic C-assay

Volumes of NHS pretreated as described above, diluted 1:30 in pH 7.4 triethanolamine-saline buffer containing 0.1% gelatin, 15 mM $CaCl_2$ and 5 mM $MgCl_2$ (TBS^{2+}). Volumes of NHS ranged from 50 µl to 450 µl in 50 µl increments, and the volumes were adjusted to a final volume of 450 µl with TBS^{2+}. Two control tubes each containing 450 µl TBS^{2+} (cell blank) or distilled water (100% lysis) were always included. Three hundred microliters of EA, [sheep erythrocytes (E) optimally sensitized with rabbit antibodies (A) against E] at 5×10^8 ml^{-1} in TBS^{2+} were added to each tube. The mixtures were incubated for 1 h at 37°C; the reaction was then stopped by the addition of 2.0 ml cold saline to all tubes, except in the 100% lysis control to which 2.0 ml water was added. Tubes were centrifuged at 1300 r.p.m. for 10 min and the haemoglobin released into the supernatants determined spectrophotometrically at 412 µm, and the number of haemolytic sites (Z) calculated. The number of haemolytically active sites of each C component can be represented by $Z = -\ln (1-Y)$, the negative natural logarithm of the number of erythrocytes not lysed. For 63% haemolysis, $Z = 1$, which corresponds to one haemolytically active site per erythrocyte.

SDS-polyacrylamide gel electrophoresis (SDS–PAGE), Western blot (WB), double immunodiffusion (DID) and immunoelectrophoresis (IE)

SDS–PAGE and WB Whole snake venoms are analysed in 10% polyacrylamide slab gel using a Protean II (Bio-Rad Laboratories, Richmond, CA, U.S.A.). All samples (25 µl) were used at concentrations of 1 mg ml^{-1}. Some gels were silver stained by conventional methods to analyse the electrophoretic patterns of the snake venoms, while others were used for transblotting the electrophoretically separated protein bands onto nitrocellulose (Trans-Blot Transfer Medium, Bio-Rad Laboratories, Richmond, St. Louis, MO, U.S.A.). After transblotting, the nitrocellulose membranes were blocked with 5% skimmed milk in Tris-buffered saline (TBS), incubated for 1 h at room temperature with rabbit anti-COF (diluted 1:2000) or with goat anti-human C3 (diluted 1:100). After thorough washing with TBS, the membranes were incubated with the peroxidase conjugated anti-rabbit IgG or anti-goat IgG, diluted 1:3000, and the affinity staining for horseradish peroxidase was developed with 3,3′-diaminobenzidine (Sigma Chemical Co., St. Louis, MO, U.S.A.).

NHS or purified human C3 pretreated or untreated with snake venoms were analysed by IE according to described method (Grabar & Burtin, 1964), the C3, and its cleavage products were revealed with goat IgG anti-C3. DID analyses were performed as described by Crowle (1961).

Analysis of proteolytic activity

The proteolytic activity of the snake venoms was tested either using gelatin incorporated in SDS–PAGE gel (zymogram method) or casein in solution (caseinolytic method), according to described methods (Heussen & Dowdle, 1980; Lomonte & Gutiérrez, 1983). Thrombin-like and fibrinolytic activities were tested by the method of Baughman (1970).

Determination of indirect haemolytic activity

Increasing amounts of venoms starting from 30.0 ng and increasing to 300.0 ng (30.0 ng increments), in a volume of 100 µl were added to a row of test tubes. To 100 µl of egg yolk solution (300 µl of 10% egg yolk solution in saline plus 250 µl of 0.001 M $CaCl_2$), and 200 µl of sheep red blood cells (E) at 1.5×10^8 in saline were added to each tube. Three control tubes each containing 200 µl saline and 200 µl E (cell blank, egg yolk-control, and 100% lysis) were always included. After incubation for 1 h at 37°C, the reaction was stopped by adding 2.0 ml of cold saline to all tubes, except for the 100% lysis tube to which was added 2.0 ml water. The tubes were centrifuged for 10 min and the haemoglobin released in the supernatants determined spectrophotometrically at 412 nm, and the number of Z calculated.

Haemorrhagic (HPS), oedema and increasing vascular permeability (IVP) producing substances

The presence of HPS in the snake venoms was evaluated as described by Kondo *et al.* (1960). EPS and IVP producing substances in the venoms were determined according to the procedures of Yamakawa *et al.* (1976) with some modifications. Briefly, hind paw oedema was produced by a subplantar injection of 50 µl venom solution (100 µg ml^{-1}) or an equal volume of PBS into the right and left hind-paw of outbred mice, respectively. After different periods of time, the animals were killed according to ethical procedures and both feet were cut at the proximal joint and weighted in analytical balance. Oedema was expressed as the percentage increase in weight of the envenomed foot relative to the weight of the saline-injected foot.

Ten minutes before the animals were killed, mice were injected intravenously with a 80 µl solution of Evans blue dye 2.5% (w/v) in PBS. The feet used for determination of oedema were cut in small pieces incubated with formamide and the quantity of extracted material was determined from an Evan's blue dye standard curve (Garcia Leme & Wilhelm, 1975). Capillary permeability increasing activity was expressed as the increase (µl ml^{-1}) in the dye-complexed albumin of the envenomed foot relative to the dye complexed albumin of the saline-injected foot.

Results

C-activation

Figure 1 shows that all five snake venoms used in this work, were able to activate C, in a dose-related fashion, and under conditions in which the classical and alternative pathways of C activation were allowed to function. At a concentration of 250 µg ml^{-1} the C consumption induced by all venoms was near 100% (Figure 1). This C activation was followed by a conversion of the C3 electrophoretic mobility by the venoms of *N. naja* and *N. melanoleuca* (total conversion), *N. nigricollis*, *M. ibiboboca* and *M. spixii* (partial conversion) (Figure 2). When, however, Mg^{2+}-EGTA was added into the incuba-

tion mixtures at final concentrations of 1 mM $MgCl_2$ plus 10 mM EGTA, only the venom of *N. naja* and *N. melanoleuca* retained the ability to convert C3 (data not shown). Purified human C3 was electrophoretically converted, in the absence of other C components, by the venoms from *N. naja*, *N. nigricollis* and *M. ibiboboca* (Figure 3).

Presence of COF-like and C3-like proteins in the snake venoms

A COF-like or C3-like 144 kDa protein was clearly detected in the venoms of *N. melanoleuca* and *N. naja* but not in the venoms of the other species, in immunoblots using anti-COF or anti-human C3 (Figure 4). These proteins showed complete immunological identity with purified COF in double immunodiffusion analysis (data not shown).

Proteolytic, thrombin-like and fibrinolytic activities

Proteolytic activities assayed either using gelatin dispersed in SDS-polyacrilamide gels or casein and fibrinogen in solution, were not detected in any of the five venoms studied. When, however, the venoms were tested for their capacity to induce bovine fibrinogen coagulation, the venoms of *M. spixii* and *N. nigricollis* presented a small but clear thrombin-like activity (Table 1).

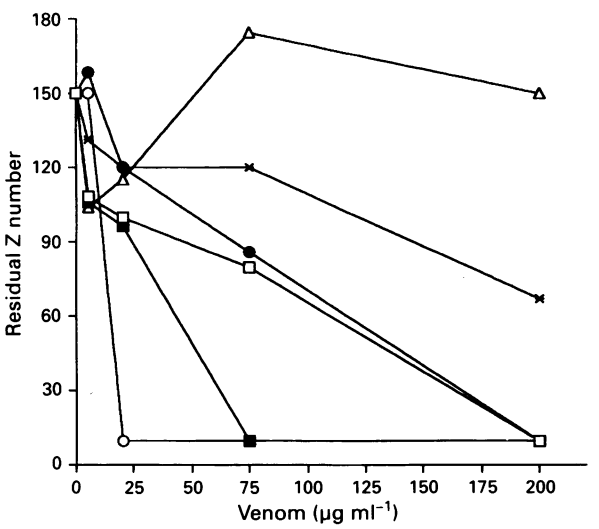

Figure 1 Consumption of complement in normal human serum by different amounts of elapid venoms using *C. d. terrificus* (△), *N. naja* (●), *N. nigricollis* (×), *N. melanoleuca* (●), *M. ibiboboca* (■) and *M. spixii* (□).

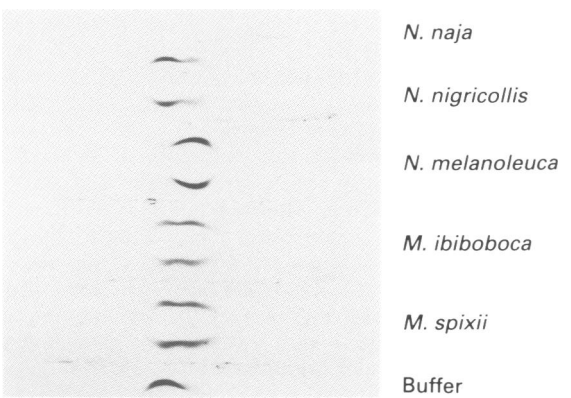

Figure 2 C3 conversion by elapid venoms. Immunoelectrophoresis analysis of normal human serum treated with the following venoms: *N. naja* (a), *N. nigricollis* (b), *N. melanoleuca* (c), *M. ibiboboca* (d) and *M. spixii* (e) on C3 in serum.

Haemorrhagic, oedema-inducing and increasing vascular permeability activities

The elapid venoms were able to increase the vascular permeability and oedema (Figure 5a,b). These venoms were devoid of haemorrhagic inducing activity (data not shown).

Haemolytic activity

All five venoms were able to induce lysis of sheep red blood cells, in a dose-related fashion, when incubated with these cells in the presence of egg yolk as a source of lecithin (Figure 6).

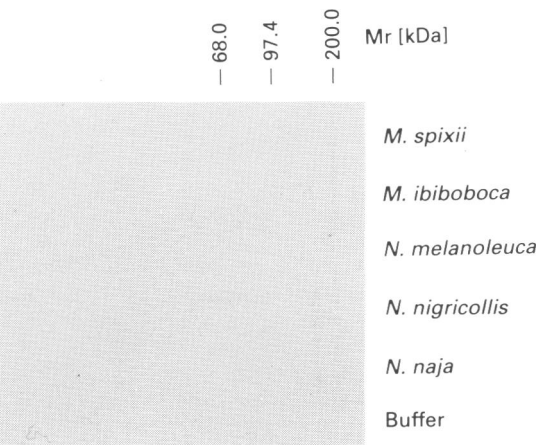

Figure 3 Proteolytic action of the elapid venoms on purified C3 Western blot analysis of purified human C3 samples treated with the venoms from *M. spixii* (a), *M. ibiboboca* (b), *N. melanoleuca* (c), *N. nigricollis* (d), *N. naja* (e) or with buffer (f) and developed with anti-human C3 antibodies.

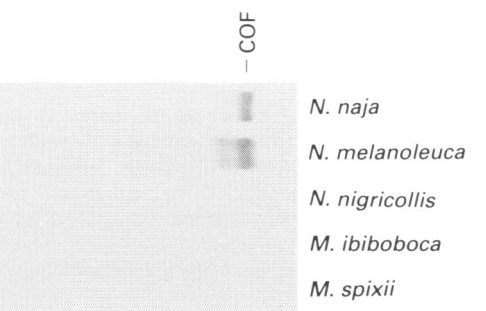

Figure 4 Identification of COF-like proteins in elapid venoms. Western blot analysis of venoms from *N. naja* (a), *N. melanoleuca* (b), *N. nigricollis* (c), *M. ibiboboca* (d), *M. spixii* (e) developed with anti-COF.

Table 1 Thrombin-like activity of *micrurus* and *naja* venoms

Venoms	*Thrombin-like activity* 500 μg ml^{-1}	1000 μg ml^{-1}
M. ibiboboca	–	–
M. spixii	60 min*	25 min*
N. naja	–	–
N. nigricollis	200 min*	75 min*
N. melanoleuca	–	–

– No clot
*Fibrinogen coagulation time
Samples of purified bovine fibrinogen in buffer containing Ca^{2+} were mixed with equal volume of venom solutions containing 5 μg and allowed to clot at room temperature. Clotting time was recorded.

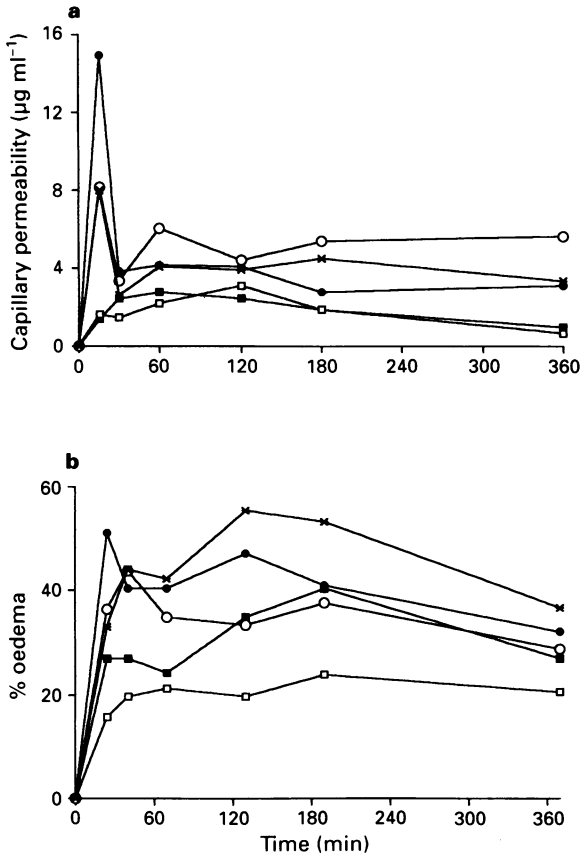

Figure 5 Time-course of the increasing vascular permeability (a) and oedema forming activity (b) by injection of 5 μg of elapidic venom into hind paw of mice. *N. naja* (●), *N. nigricollis* (×), *N. melanoleuca* (○), *M. ibiboboca* (□) and *M. spixii* (■).

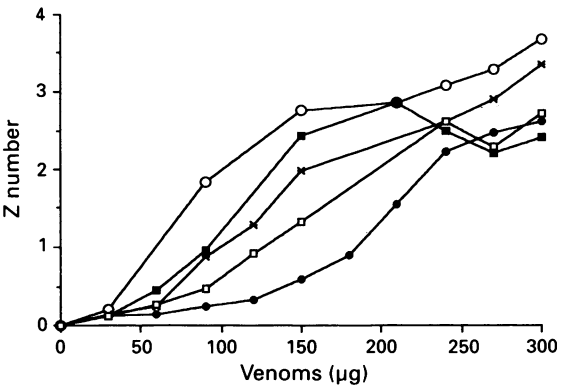

Figure 6 Haemolytic activity present in elapid venoms. Increasing amounts of venoms (30.0–300.0 ng), were added to a series of tubes containing egg yolk and sheep red blood cells. Haemolysis was spectrophotometrically determined and the number of Z calculated. *N. naja* (●), *N. nigricollis* (×), *N. melanoleuca* (○), *M. ibiboboca* (□) and *M. spixii* (■).

Discussion

The toxins present in snake venoms, used by snakes for effective immobilization of prey and for protection against predators, must rapidly reach the target organs. Therefore, mechanisms facilitating the distribution of the toxins throughout the tissues of the bitten animal must be activated. Hyaluronidase, which is present in almost all venoms, was the first of such mechanisms to be described (Zeller, 1948)., Another mechanism which could fulfil this spreading function is local acute inflammation at the site of bite or injection of the venoms. Some potentially pro-inflammatory factors such as proteolytic enzymes and activators of clotting, C and kallicrein-kinin systems have been detected in Crotalidae and Viperidae venoms. The action of these factors on the corresponding host substrates may release endogenous mediators of inflammation (Rocha e Silva *et al.*, 1950; Müller-Eberhard & Fjellström, 1971; Stocker & Barlow, 1976; Geiger & Kortmann, 1977; Stocker *et al.*, 1982).

The elapid venoms analysed contain components able to activate the C system. Consumption of haemolytic activity and conversion of C3 into products with electrophoretic mobility distinct from the native C3 molecule were observed in samples of human serum treated with these venoms. Some, such as *N. naja* and *N. melanoleuca* venoms which contain COF activate C by forming a COF-B complex, a C3-like convertase (Götze, 1975). *N. naja*, *N. nigricollis* and *M. ibiboboca* venoms cleave human purified C3 in the absence of other C factors. This effect could be attributed to some proteolytic enzymes present in these venoms. *M. spixii* venom, which is free of COF and is unable to cleave C3 directly, may enter into the C cascade through a Ca^{2+}-dependent mechanism. The C-activators certainly contribute to the local lesions induced by venoms, through the release into the injured tissues of the anaphylatoxins C3a and C5a. These two peptides are known to be mediators of the early events of the acute inflammation by increasing local vascular permeability, contracting smooth muscle, releasing histamine from mast cells, and by attracting leukocytes (Dias da Silva & Lepow, 1967; Dias da Silva *et al.*, 1967; Lepow *et al.*, 1967).

The thrombin-like enzymes detected in some venoms such as *M. spixii* and *N. nigricollis* by converting *in vitro* fibrinogen into a fibrin clot, may alter the local microcirculation through precipitous formation of thrombin. Formation of small thrombi could disturb the circulation (Stocker *et al.*, 1982).

The haemolytic inducing-activity present in all elapid venoms tested in this work can be attributed to their phospholipase A_2 contents since haemolysis only occurs when venom, sheep erythrocytes, and a lecithin as source of lysolecithin were mixed simultaneously. In animal or human tissues where snake venoms had previously been injected, phospholipase A_2 can degrade the cell membrane phospholipids into arachidonic acid. This compound can be metabolized by the enzyme cyclo-oxygenase to prostaglandins and by the enzyme lipoxygenase to hydroxy-eicosatetraenoic acids (HETEs) and derivatives of 5-hydroperoxy-eicosatetraenoic acid termed leukotrienes (Lewis & Austen, 1988). According to the type of isomerase enzymes present in the affected tissues, distinct cyclo-oxygenase products will result including prostaglandins, thromboxane, or prostacyclins. Some are vasoconstrictors (thromboxanes), others are vasodilators (prostacyclins), while others can increase vascular permeability (prostaglandins E_2).

The proteolytic enzymes present in these venoms could be responsible for the bradykinin formation and for breakdown of some clotting or C components.

The synergistic effect of the mediators of inflammation released by the action of proteolytic enzymes and activators of C, clotting and kallikrein-kinin systems or resulting from degradation of cell membrane phospholipids, by phospholipase A_2, may facilitate a rapid passage of the neurotoxins from the tissues to the blood. The observed oedema surrounding the sites of injection of the venoms, reinforces the suggestion that the *in vitro* formation of mediators, may also occur *in vivo* under conditions allowing their action.

This work was supported by Conselho Nacional de Pesquisa e Desenvolvimento Cientifico, CNPq and Fundação Butantan.

References

ALPER, C.A. & BALAVITCH, D. (1976). Cobra venom factor: evidence for its being altered cobra C3 (the third component of complement). *Science*, **191**, 1275–1276.

BAUGHMAN, D.J. (1970). Thrombin assay. In *Methods in Enzymology-Proteolytic Enzymes*. ed. Perlman, G.E. & Lorand, L. New York: Academic Press.

CROWLE, A.J. (1961). *Immunodiffusion*. New York: Academic Press.

DIAS DA SILVA, W., EISELE, J. & LEPOW, I.H. (1967). Complement as a mediator of inflammation. III. Purification of the activity with anaphylatoxin properties generated by interaction of the first four components of components of complement and its identification as cleavage product of C'3. *J. Exp. Med.*, **126**, 1027–1038.

DIAS DA SILVA, W. & LEPOW, I.H. (1967). Complement as a mediator of inflammation. II. Biological properties of anaphylatoxin prepared with purified components of human complement. *J. Exp. Med.*, **125**, 921–926.

EGGERTSEN, G., LUNDWALL, A., HELLMAN, U. & SJÖQUIST, J. (1983). Antigenic relationships between human and cobra complement factors C3 and cobra venom factor (CVF) from the Indian cobra (*Naja naja*). *J. Immunol.*, **131**, 1920–1923.

GARCIA LEME, J. & WILHELM, D.L. (1975). The effects of adrenalectomy and corticosterone on vascular permeability in the skin of the rat. *Br. J. Exp. Path.*, **56**, 402–407.

GEIGER, R. & KORTMANN, H. (1977). Esterolytic and proteolytic activities of snake venoms and their inhibition by proteinase inhibitors. *Toxicon*, **15**, 257–259.

GÖTZE, O. (1975). Proteases of properdin system. In *Proteases and Biological Control*. ed. Reich, E., Rifkin, D.B. & Shaw, E. Cold Spring Harbor Lab.

GÖTZE, O. & MÜLLER-EBERHARD, H.J. (1971). The C3-activator system: an alternate pathway of complement activation. In *Immune Complexes Diseases* (Proceedings) *J. Exp. Med.*, **134**, 90.

GRABAR, P. & BURTIN, P. (1964). *Immuno-electrophoretic Analysis*. Paris, Amsterdam: Elsevier Publishing Company.

HEUSSEN, C. & DOWDLE, E.B (1980). Electrophoretic analysis of plasminogen activators in polyacrylamide gels containing sodium dodecyl sulfate and copolymerized substrates. *Anal. Biochem.*, **102**, 196–202.

KONDO, H., KONDO, S., IKESAWA, H., MURATA, R. & OHSAKA, A. (1960). Studies on the quantitative method for determination of haemorrhagic activity of Habu snake venom. *Jpn. J. Med. Sci. Biol.*, **13**, 43–51.

LEPOW, I.H., DIAS DA SILVA, W. & EISELE, J. (1967). Nature and biological properties of human anaphylatoxin. In *International Symposium on the Biochemistry of Allergic Reactions*. Punta Alta, Italy, 5–7 July.

LEWIS, R.A. & AUSTEN, K.F. (1988). Leukotrienes. In *Inflammation: Basic Principles and Clinical Correlates*. ed. Gallin, J.T., Goldstein, I.M. & Snyderman, R. New York: Raven Press.

LOMONTE, B. & GUTIÉRREZ, J.M. (1983). La actividad proteolítica de los venenos de serpientes de Costa Rica sobre la caseina. *Rev. Biol. Trop.*, **31**, 37–40.

MANDELBAUM, F.R. & ASSAKURA, M.T. (1988). Antigenic relationship of haemorragic factors and proteases isolated from the venoms of three species of *Bothrops* snakes. *Toxicon*, **26**, 379–385.

MÜLLER-EBERHARD, H.J. & FJELLSTRÖM, K.E. (1971). Isolation of the anti-complementary protein from cobra venom and its mode of action on C3. *J. Immunol.*, **107**, 1666–1672.

PICKERING, R.J., WOLFSON, M.R., GOOD, R.A. & GEWURZ, H. (1969). Passive hemolysis by serum and cobra venom factor: a new mechanism inducing membrane damage by complement. *Proc. Natl. Acad. Sci. U.S.A.*, **62**, 521–527.

ROCHA E SILVA, M., BERALDO, W.T. & ROSENFELD, G. (1950). Bradykinin, a hypotensive and smooth muscle stimulating factor released from plasma globulin by snake venoms and trypsin. *Am. J. Physiol.*, **156**, 261–273.

ROSS, G.D. & MEDOF, M. (1985). Membrane complement receptors specific for bound fragments of C3. *Adv. Immunol.*, **37**, 217–267.

SHIN, H.S., GEWURZ, H. & SNYDERMAN, R. (1969). Reaction of a cobra venom factor with guinea pig complement and generation of an activity chemotactic for polimorphonuclear leukocytes. *Proc. Soc. Exp. Biol. Med.*, **131**, 203–207.

SMITH, C.A., VOGEL, C.W. & MÜLLER-EBERHARD, H.J. (1982). Ultrastructure of cobra venom factor dependent C3/C5 convertase and its zymogen, factor B of human complement. *J. Biol. Chem.*, **257**, 879–882.

STOCKER, K. & BARLOW, G.H. (1976). The coagulant enzyme from *Bothrops atrox* venom (batroxobin). *Methods Enzymol.*, **45**, 214–223.

STOCKER, K., FISHER, H. & MEIER, J. (1982). Thrombin-like snake venom proteinases. *Toxicon*, **20**, 265–273.

YAMAKAWA, M., NOZAKI, M. & HOKAMA, Z. (1976). Fractionation of sakishima habu (*Trimeresurus elegans*) venom and lethal hemorrhagic, and edema forming activities of the fractions. In *Animal Plant and Microbial Toxins*. ed. Ohsaka, A., Hayashi, K. & Saway, Y. New York: Plenum Press.

ZELLER, E.A. (1948). Enzymes of snake venoms and their biological significance. *Adv. Enzymol.*, **8**, 459–495.

(Received January 4, 1994
Revised March 14, 1994
Accepted March 17, 1994)

Br. J. Pharmacol. (1994), **112**, 728–734

Pharmacology of high-threshold calcium currents in GH_4C_1 pituitary cells and their regulation by activation of human D_2 and D_4 dopamine receptors

[1]G.R. Seabrook, M. Knowles, N. Brown, J. Myers, H. Sinclair, S. Patel, S.B. Freedman & G. McAllister

Merck Sharp & Dohme Research Laboratories, Neuroscience Research Centre, Terlings Park, Eastwick Road, Harlow, Essex CM20 2QR

1 The objective of this study was to characterize the pharmacology of calcium currents in GH_4C_1 pituitary cells and determine whether activation of heterologously expressed human dopamine receptors can regulate their function. Human D_2(short), D_3 and $D_{4.2}$ receptor cDNA's were separately transfected into GH_4C_1 cells and whole cell calcium currents were recorded by use of nystatin-perforated patch clamp techniques.

2 High-threshold calcium currents were antagonized in a biphasic manner by the dihydropyridine, nisoldipine. The half-maximally effective concentration for each site was 0.2 nM ($pIC_{50} = 9.78 \pm 0.21$, $n = 4$) and 339 nM ($pIC_{50} = 6.47 \pm 0.12$, $n = 4$). The component of current inhibited by 10 nM nisoldipine was also blocked by ω-conotoxin GVIA ($30 \pm 9\%$ at 30 nM, $n = 6$) or by ω-agatoxin IVA ($34 \pm 7\%$ at 100 nM, $n = 4$).

3 Activation of either D_2 or D_4 receptors by dopamine (10 μM) or quinpirole (0.1 to 10 μM) reduced the peak calcium current by ca. 20% in the majority of cells studied. No inhibition was observed in control or D_3 transfected GH_4C_1 cell lines.

4 The mobilisation of intracellular calcium by thyrotropin releasing hormone in hD_4-GH_4C_1 cells was also studied using Fura-2 AM microspectrofluorimetry. Thyrotropin releasing hormone caused a concentration-dependent increase in calcium mobilisation with an EC_{50} of 7 nM. D_4 receptor activation had no effect upon either basal or hormone-induced $[Ca^{2+}]_i$ transients.

5 These results demonstrate that GH_4C_1 pituitary cells have at least two types of dihydropyridine-sensitive high-threshold calcium currents and that like D_2 receptors, human D_4 receptors can also regulate calcium channel function.

Keywords: Dopamine; D4 dopamine receptor; dihydropyridine; calcium channel current; pituitary; GH_4C_1 cells

Introduction

Dopamine receptors of the D_2, D_3 and D_4 structural classes are highly homologous (Schwartz *et al.*, 1992; Sibley & Monsma, 1992), and consequently the mechanism by which these receptors couple to cellular effector systems may be similar. Cloned rat D_2 receptors couple to G-proteins which are negatively linked to adenylate cyclase, activate potassium conductances, and reduce intracellular calcium mobilisation (Albert *et al.*, 1990; Vallar *et al.*, 1990; Kanterman *et al.*, 1991; Castellano *et al.*, 1993). Such effects are also observed when endogenous D_2-like dopamine receptors in rat brain tissue are activated, and similarly human D_2 receptors expressed in Chinese hamster ovary (CHO) cells are also negatively linked to adenylate cyclase (Freedman *et al.*, 1994). In contrast, no clear evidence of functional coupling of hD_3 has been described in CHO cells; this may be because the appropriate type of G-protein(s) to which these receptors normally couple are absent (Sokoloff *et al.*, 1990; McAllister *et al.*, 1993; Freedman *et al.*, 1994). Consistent with this view, we have recently demonstrated that human D_3 receptors can couple to the inhibition of adenylate cyclase, and inhibition of calcium currents when expressed in appropriate cell lines (McAllister *et al.*, unpublished observations; Seabrook *et al.*, 1994a). Attempts to express hD_4 receptors (Van Tol *et al.*, 1991) in CHO cells by stable transfection, a prerequisite to definitive functional studies, have proved difficult. Whether hD_4 receptors can modulate neuronal excitability by coupling to effector mechanisms linked to ion channels has yet to be established.

To investigate the mechanism by which human D_2, D_3 and D_4 receptors may couple to ion channels, the rat pituitary GH_4C_1 cell line was chosen for electrophysiological studies of stably transfected receptors. GH_4C_1 cells do not normally express dopamine receptors and when transfected with rat D_2 receptors endogenous potassium currents can be activated by dopamine (Einhorn *et al.*, 1991). Furthermore this clonal cell line has both transient low-threshold calcium currents, and dihydropyridine-sensitive high-threshold calcium currents and inactivation of which is modulated by adenosine 3′:5′-cyclic monophosphate (cyclic AMP) (Cohen & McCarthy, 1987; Kalman *et al.*, 1988). High-threshold calcium currents in GH_4C_1 cells are also depressed by G-protein α-subunits liberated upon activation of somatostatin receptors (Luthin *et al.*, 1992; Kleuss *et al.*, 1993). In this study we describe the selective ability of hD_2 and hD_4, but not hD_3 receptors, to couple to the depression of calcium currents in transfected GH_4C_1 cell lines.

Methods

Cell culture

GH_4C_1 pituitary cells were obtained from Dr P. Guest (Cambridge University) and grown in tissue culture in a medium that contained Dulbecco's Modified Eagle's Medium (GIBCO), 10% foetal calf serum and 2 mM L-glutamine (Geneticin). Cells were plated on poly-L-lysine coated coverslips.

Transfection procedures

Human D_2 and D_3 receptor cDNA was separately subcloned into the mammalian expression vector pcDNAneo(Invitro-

[1] Author for correspondence.

gen) as described previously (McAllister *et al.*, 1993). D_4 receptor cDNA in the pRSVneo expression vector (Invitrogen) was obtained from Dr O. Civelli (Oregon). Stably transfected cell lines were obtained by transfecting the appropriate cDNA into GH_4C_1 cells by calcium phosphate precipitation. Transfected cells were selected for their resistance to the antibiotic G418 and assayed for their ability to bind [^{125}I]-iodosulpiride or [^{3}H]-spiperone. Expression of the appropriate dopamine receptor subtype mRNA in each cell line was confirmed by PCR analysis (e.g. McAllister *et al.*, 1993) and/or ribonuclease protection assay.

Radioligand binding

Cells were harvested in PBS and then lysed by polytroning (in 10 mM Tris-HCl, pH 7.4 containing 5 mM $MgSO_4$) for 10 s on ice. Membranes were centrifuged at 50,000 *g* for 15 min at 4°C and the resulting pellet resuspended at 20 mg ml^{-1} wet weight in assay buffer that contained (in mM): NaCl 118, HEPES 20, KCl 4.7, $MgSO_4$ 1.2, $NaHCO_3$ 5, KH_2PO_4 1.2, $CaCl_2$ 2.5, pargyline 10 μM and 0.1% ascorbic acid. Incubations, 30 min at 30°C, were carried out in the presence of 0.05–1 nM [^{125}I]-iodosulpiride or [^{3}H]-spiperone, and were initiated by the addition of 100–200 μg protein to final assay volumes of 0.1 ml for [^{125}I]-iodosulpiride and 1 ml for [^{3}H]-spiperone binding. The incubation was terminated by rapid filtration over GF/B filters presoaked in 0.3% PEI and washed with 10 ml ice cold 0.9% NaCl saline for [^{125}I]-iodosulpiride binding and 50 mM Tris (pH 7.4) for [^{3}H]-spiperone binding. Specific binding was defined by 1 μM haloperidol and radioactivity measured in a LKB 127 Clinigamma γ-counter, or liquid scintillation spectrophotometry.

Whole cell and nystatin perforated patch clamp recording

Whole cell patch clamp recordings were made using borosilicate glass microelectrodes (Clark Electromedical Instruments) that were filled with a solution which contained (in mM): CsCl 140, tetraethylammonium.Cl 25, EGTA 3, HEPES 40 and $MgCl_2$ 3, adjusted to pH 7.3 with CsOH. Cells were perfused at a rate of 1 to 2 ml min^{-1} with an extracellular solution that contained (in mM): NaCl 155, glucose 10, HEPES 10, KCl 5, $CaCl_2$ 5 and tetrodotoxin (0.5 μM), pH 7.4, at 22°C. Drugs were applied via the superfusion system. Nystatin perforated patch clamp recordings were made as previously described (Seabrook *et al.*, 1994b) using a pipette solution that contained (in mM): CsH_3O_3SCs 100, CsCl 25, $MgCl_2$ 3, HEPES 40, adjusted to pH 7.3 with CsOH. Cells were voltage-clamped and calcium currents were elicited by 100 ms depolarizing pulses from −80 to 0 or −20 mV at 0.033 Hz. Calcium currents were amplified using an Axopatch 200 patch clamp amplifier (Axon Instruments), and captured on line via a CED1401 interface (Cambridge Electronic Design) which was connected to a Compaq 386 microcomputer. Leak currents were subtracted with the amplifier, and by the CED voltage-clamp analysis software. Data are expressed as the mean ± standard error of the mean (s.e. mean). The inhibition of calcium currents by agonists was quantified as the mean depression in those cells which responded with >5% change in current amplitude. These data are cited along with the proportion of cells that responded to drug application in each sample.

Measurement of intracellular Ca^{2+}

Methods for determination of intracellular calcium were the same as previously described (Seabrook & Fong, 1993). Briefly, GH_4C_1 cells were loaded, prior to experimentation, with the membrane permeant fluorescent indicator Fura-2 AM (2 μM; 30 min) in a solution containing (in mM): NaCl 150, KCl 3, HEPES 10, glucose 10, sucrose 20, $CaCl_2$ 2 and $MgCl_2$ 3 at pH 7.4. The dye fluorescence at 540 nM was measured during alternate excitations at 340 and 380 nm wavelength light (0.1–1 Hz) using an MCID imaging system (Imaging Research Inc., Canada). Calcium levels were estimated from the R_{max} and R_{min} values which were determined after permeabilization of cells with ionomycin (10 μM), and following perfusion with solution containing 0 mM Ca^{2+} + 1 mM EGTA, and then 10 mM [Ca^{2+}] + 0 mM EGTA. Drugs were applied by superfusion for a period of 5 s, followed by a 40 min wash to minimize tachyphylaxis.

Drugs

Drugs were obtained from the following companies: synthetic ω-Aga IVA was purchased from the Peptide Institute (Osaka, Japan). ω-Conotoxin GVIA, ethylene glycol *bis*(β-aminoethyl ether)-*N,N,N',N'*-tetraacetic acid (EGTA), and 4-(2-hydroxyethyl)-1-piperazineethanesulphonic acid (HEPES) were purchased from Sigma. Dopamine and quinpirole were purchased from Research Biochemicals Inc., and nisoldipine was obtained from Miles Pharmaceuticals.

Results

Characterization of cell lines

Cells that had been transfected with either the hD_2, hD_3 or hD_4 receptor cDNA and that exhibited resistance to the antibiotic G418 were examined for their ability to bind [^{125}I]-iodosulpiride (Table 1). Saturable [^{125}I]-iodosulpiride binding was observed in approximately half of the G418 resistant clones that had been transfected with hD_2 (11/22 clones), or hD_3 receptor cDNA (15/35 clones). In contrast only one cell line transfected with hD_4 receptor cDNA (1/23 clones) exhibited significant [^{3}H]-spiperone binding. Transfection procedures under some circumstances have been reported to induce the expression of endogenous dopamine receptors in pituitary cell lines (e.g. Allard *et al.*, 1993). However, in this study no expression of endogenous D_2 receptor mRNA was detected using PCR analysis or ribonuclease protection in

Table 1 Comparison of the ligand binding properties of cell lines which had been transfected with human dopamine receptors

	D_2(short)		D_3		$D_{4.2}$
	CHO	GH_4C_1	CHO	GH_4C_1	GH_4C_1
Number of clones with binding	–	11/22	–	15/35	1/23
Clone studied	–	N4	–	18	21-NN
K_d iodosulpiride (nM)	0.2	0.4	0.4	0.3	0.1*
B_{max} (fmol mg^{-1} protein)	700	235	290	89	115
% inhibition of [^{3}H]-N-0437 binding by GTP-γ-S	70–80%	40–80%	0	0–10%	20–40%

Values for experiments on CHO cells are from Freedman *et al.* (1994). *[^{3}H]-spiperone was used as the ligand for determining the expression of hD_4 receptors because [^{125}I]-iodosulpiride binds with low affinity to these receptors.

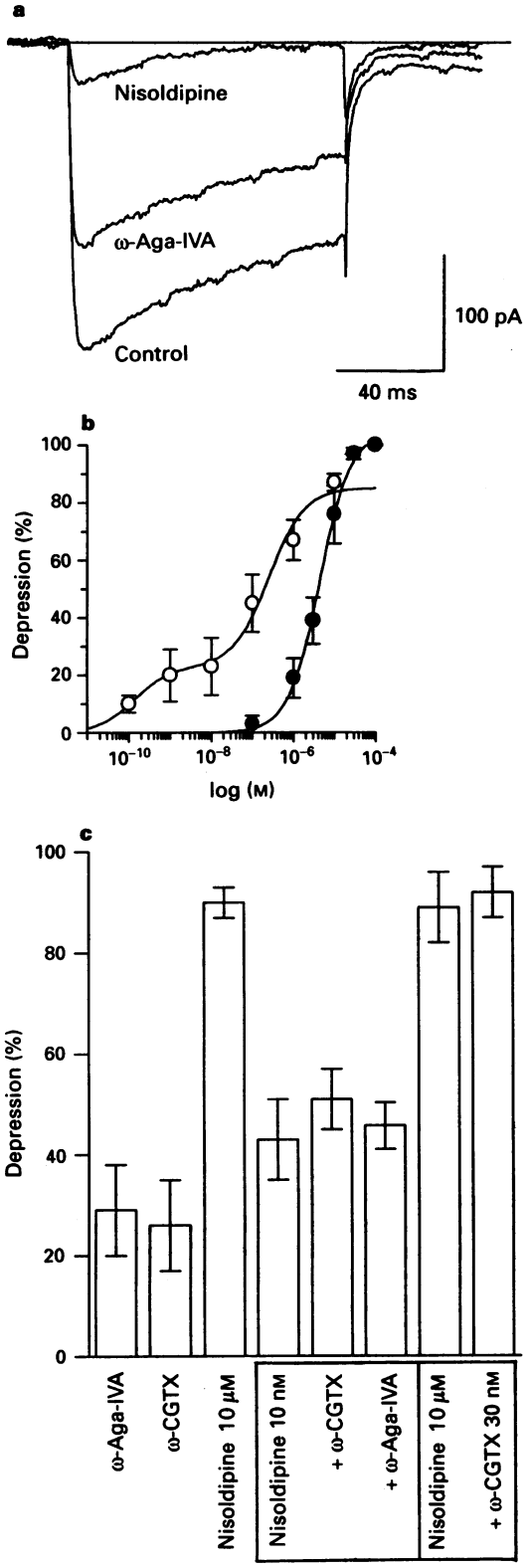

Figure 1 Block of high-threshold calcium currents in GH_4C_1 cells by calcium channel antagonists. (a) Depression of whole cell calcium currents by nisoldipine. Traces are the inward current that occurred in response to a 100 ms depolarization from −80 to 0 mV, in control, after ω-Aga IVA (100 nM), and after 5 min application of nisoldipine (10 μM). (b) Concentration-effect curves for the inhibition of the peak calcium current by nisoldipine (○) and cadmium ions (●). The depression by nisoldipine was biphasic (see text and Figure 2; $n = 5$) the estimated K_d for each site was 0.2 and 339 nM. The IC_{50} for cadmium was 4 μM ($n = 4$). (c) The nisoldipine-sensitive calcium current was partly, and reversibly inhibited by bath application of either ω-CGTX-GVIA (30 nM) or ω-Aga-IVA (100 nM). Inhibition of the high affinity component of the calcium current by 10 nM nisoldipine precluded the block by either ω-CGTX-GVIA or ω-Aga-IVA ($n = 4$ to 8 cells).

either the parent or transfected cell lines. The sensitivity of [^{3}H]-N-0437 (1 nM) binding to modulation by GTP-γ-S (10 μM) was used as an indicator for functional coupling in the transfected cell lines. Significant inhibition of [^{3}H]-N-0437 binding by GTP-γ-S was detected only in the hD_2 (40–80%) and hD_4 cell lines (20–40%), but not in the hD_3 line (0–10%).

Identification of two types of high-threshold calcium current

Both low-threshold (steps from −100 to −30 mV) and high-threshold (steps from −80 to >0 mV) calcium currents were observed in this study. Under these recording conditions the high-threshold calcium current was confirmed to be dihydropyridine-sensitive (Figure 1). However, the inhibition of the high-threshold calcium current by nisoldipine was biphasic over the concentration-range of 0.1 nM to 10 μM. The negative logarithm of the half-maximally effective concentration for each site, determined separately for each cell, was 9.78 ± 0.21 (= 0.2 nM; 27 ± 9%; $n = 4$) and 6.47 ± 0.12 (= 339 nM; 66 ± 8%; $n = 4$). The biphasic effect of nisoldipine was evident on both the peak and non-inactivating components of the high-threshold calcium current. The non-inactivating component of the high-threshold calcium current, measured at 95 ms into the voltage-step, was still only partly inhibited by 10 nM nisoldipine (37 ± 8%; $n = 7$; Figure 2). Consequently contamination by transient low-threshold calcium currents, which inactivate with a time constant of 39 ± 5 ms ($n = 5$), cannot account for the biphasic inhibition of high-threshold calcium currents by nisoldipine.

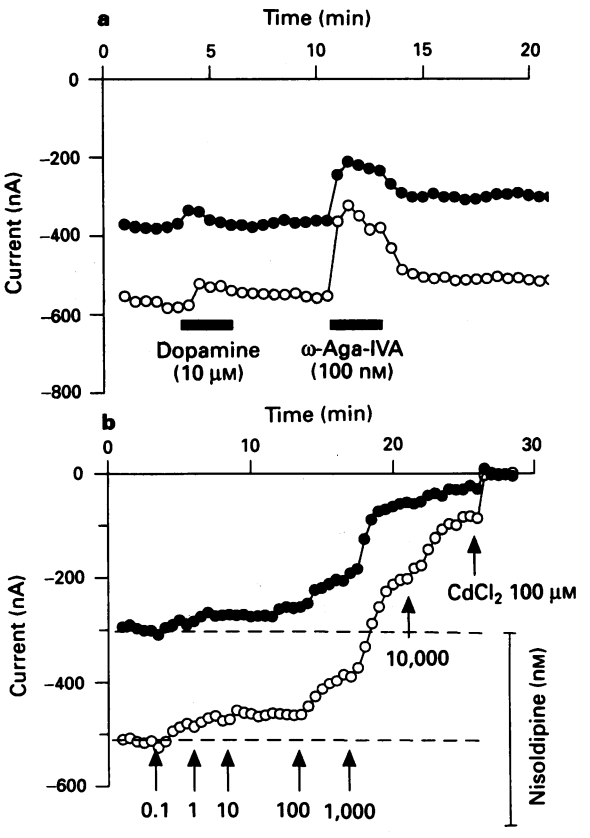

Figure 2 Comparison of the time course of the depression of the peak (○) and 'non-inactivating' high-threshold calcium current (●) in an individual hD_4-GH_4C_1 cell by (a) dopamine (10 μM) and ω-Aga-IVA (100 nM), and in (b) by increasing concentrations of nisoldipine and cadmium ions. Drugs were applied to the superfusion solution for either the duration of the horizontal bar as in (a) or were applied continuously at the time points indicated by the arrows in (b).

Nanomolar concentrations of both ω-agatoxin-IVA (34 ± 7% at 100 nM; $n = 4$) and ω-conotoxin GVIA (30 ± 9% at 30 nM; $n = 6$) reversibly blocked a proportion of the nisoldipine-sensitive calcium current in GH_4C_1 pituitary cells. Furthermore, pretreatment with 10 nM nisoldipine blocked the component of the calcium current that was sensitive to these peptides (Figure 1). Consequently, GH_4C_1 cells have at least two types of dihydropyridine-sensitive calcium currents, one of which is potently blocked by nisoldipine ($IC_{50} < 1$ nM), ω-Aga-IVA and ω-CGTX, and a second type that is less sensitive to nisoldipine (IC_{50} ca. 300 nM) but not blocked by nanomolar concentrations of these peptide neurotoxins.

Depression of calcium currents by activation of D_2 and D_4 but not D_3 receptors

In untransfected GH_4C_1 cells dopamine (10 μM) did not affect whole cell calcium currents ($n = 10$ cells). This observation was consistent with the lack of endogenous dopamine receptors and was confirmed by both PCR and binding ex-

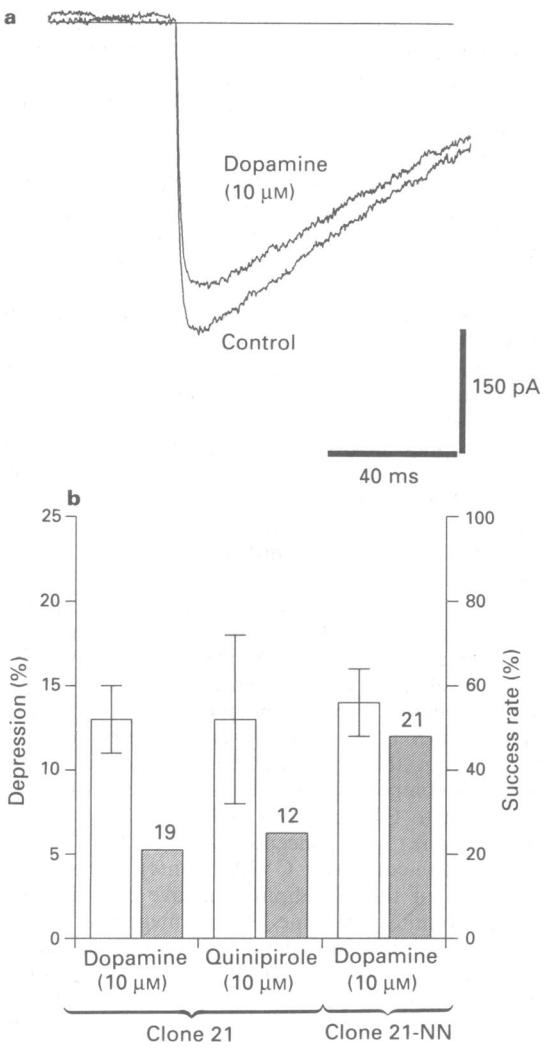

Figure 3 Depression of high-threshold calcium currents by activation of hD_4 receptors. (a) Inhibition of calcium currents by dopamine in an individual cell. Superimposed traces are the calcium currents elicited during a single 100 ms depolarizing pulse from − 80 to 0 mV before and after application of 10 μM dopamine demonstrating that in some cells the inhibition of the peak current was more pronounced. (b) Comparison between the depression of calcium currents caused by either dopamine or quinpirole in hD_4-GH_4C_1 clone 21, and in the single cell clone 21-NN (open columns). The increase in number of cells responding to dopamine in the single cell clone was not accompanied by an increase in the maximal depression. Filled columns represent the proportion of cells which responded with a > 5% depression with each agonist. Numbers represent the sample size.

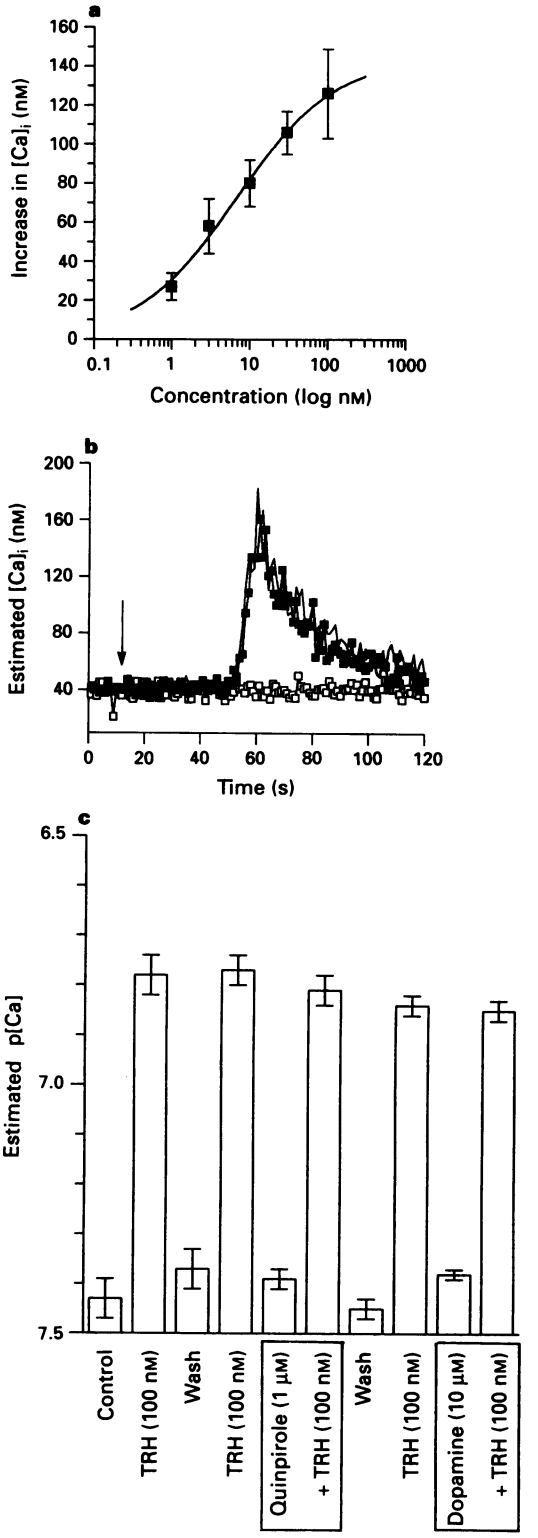

Figure 4 Mobilization of intracellular calcium in hD_4-GH_4C_1 cells by thyrotropin releasing hormone (TRH) measured using Fura-2 microspectrofluorimetry. (a) Concentration-effect curve for TRH. The half-maximally effective concentration of TRH was 7 ± 3 nM. (b) Time course of the TRH-induced calcium mobilization in an individual cell (solid line), and superimposed calcium levels measured during subsequent (30 min later) perfusion with quinpirole (1 μM; □), and then quinpirole + TRH (■). (c) Histogram showing the ability of repeated applications of TRH to release $[Ca^{2+}]_i$. Data are expressed as the geometric mean of the negative logarithm of the estimated intracellular calcium concentration (pEC_{50}). Despite the depression of whole cell calcium currents caused by activation of hD_4 receptors (Figure 3) neither quinpirole nor dopamine reduced the TRH-induced mobilization of intracellular calcium levels in hD_4-GH_4C_1 cells (clone 21-NN). $n = 4$ cells in this experiment.

periments. In both the D_2 and D_4 transfected cell lines, high-threshold calcium currents were depressed by 23 ± 7% (9/21 cells) and 13 ± 2% (4/19 cells) respectively upon application of dopamine (10 μM). In the hD_4-GH_4C_1 cell line a similar degree of inhibition of the whole cell calcium current was seen with the dopamine receptor agonist, quinpirole (13 ± 5% at 10 μM in 3/12 cells; Figure 3). Despite the availability of a functional second messenger system that could couple to calcium currents in the hD_3-GH_4C_1 cell line, as was indicated by the ability of somatostatin-14 to depress calcium currents in these cells (33 ± 18% at 1 μM in 4/5 cells), no inhibition of calcium currents by hD_3 receptor activation was observed ($n = 14$). The maximal depression of the high-threshold calcium current by somatostatin-14 in the hD_3 transfected cell line was comparable to that seen in hD_4-GH_4C_1 cells (27 ± 10% at 200 nM; $n = 3/4$ cells).

To examine whether the variation in coupling between cells or the fractional inhibition of the current was due to a low receptor density, cells were pretreated with Na-butyrate (3 mM) for 20–48 h. This treatment has previously been shown to upregulate transfected receptors in other cell types, including $5\text{-}HT_{1E}$ receptors expressed in HEK-293 cells (McAllister et al., 1992). However, in GH_4C_1 cells Na^+ butyrate treatment alone caused a mean 80% decrease in the density of calcium currents and thus was unsuitable for these experiments. After 48 h exposure to Na^+-butyrate, the mean calcium conductance per cell capacitance decreased from 277 ± 46 pS/pF to 59 ± 13 pS/pF ($n = 8$). We therefore used an alternative approach to improve experimental success rates using single cell cloning of the hD_4-GH_4C_1 cell line. A hD_4-GH_4C_1 single cell clone (21-NN) was obtained with enhanced [^{125}I]-iodosulpiride binding in which 48% of cells (10/21 cells) responded to agonist application. However, despite the increase in proportion of cells responding to agonist application the maximal inhibition was still limited to 10–20% of the peak current similar to that in the parent clone (Figure 3). Depression of calcium currents by hD_4 receptor activation was blocked by w-Aga-IVa (100 nM; $n = 6$).

D_4 receptors do not regulate TRH-induced calcium mobilisation

To determine whether the depression of calcium currents in GH_4C_1 cells was associated with a reduction in the driving force for Ca^{2+}, for example by that which may be caused following the mobilisation of $[Ca^{2+}]_i$, the ability of D4 receptor activation to regulate thyrotropin releasing hormone (TRH) induced increases in $[Ca^{2+}]_i$ was examined using Fura-2-AM microspectrofluorimetry. TRH caused a monophasic and concentration-dependent increase in $[Ca^{2+}]_i$ from an estimated mean of 48 nM to 195 nM ($EC_{50} = 7$ nM; Figure 4). Activation of hD_4 receptor by pretreatment of cells with quinpirole neither reduced basal calcium levels, nor significantly reduced the mobilisation-induced by TRH (100 nM, $n = 11$ cells from three separate experiments).

Discussion

Endogenous dopamine receptors in freshly dissociated pituitary cells modulate calcium currents as well as outward potassium currents (Stack & Suprenant, 1991; Keja et al., 1992; Lledo et al., 1992; Nussinovitch & Kleinhaus, 1992). Similarly in pituitary-derived cell lines which lack dopamine receptors, transfection with rat D_2 (short) or D_2 (long) receptors restores the ability of dopamine to activate potassium channels (Einhorn et al., 1990) and inhibit adenylate cyclase (Albert et al., 1990). We have previously reported that human D_3 receptors when transfected into GH_4C_1 cells do not couple to the activation of voltage-dependent potassium currents (Seabrook et al., 1992), but that when expressed in differentiated NG108-15 cells can couple to the depression of calcium currents (Seabrook et al., 1994a). To investigate further the mechanism by which dopamine receptors may couple to ion channels, the ability of heterologously expressed hD_2(short), hD_3 and hD_4 receptors to regulate endogenous calcium currents in GH_4C_1 cells was examined.

Activation of either hD_2 or hD_4 receptors caused approximately 20% depression of the high-threshold calcium currents in transfected GH_4C_1 cells. The maximal inhibition of calcium currents by these dopamine receptor subtypes was consistent with that caused by activation of endogenous dopamine receptors in dissociated rat pituitary cells (Stack & Suprenant, 1991; Keja et al., 1992). The inhibition achieved by the somatostatin-induced activation of $\alpha_{o2}\beta_1\gamma_3$ G-protein subunits in GH_3 cells is similarly limited to ca. 25% (Kleuss et al., 1993), comparable to that seen with somatostatin-14 in the hD_3- and hD_4-GH_4C_1 transfected cells. These data suggest that the inhibition caused by dopamine receptor activation was limited by either the signal transduction system or to a subpopulation of the high-threshold calcium current. Indeed in the present study evidence for two types of dihydropyridine-sensitive calcium currents was found.

Rat pituitary cells have at least two types of calcium current with either a low- or a high-threshold potential for activation, these currents can be distinguished by both physiological and pharmacological criteria (Armstrong & Matteson, 1985; Cohen & McCarthy, 1987). Consistent with this, both low-threshold (−100 to −30 mV) and high-threshold (−80 to >0 mV) currents were observed in this study. Furthermore, the high-threshold calcium currents were antagonized by nisoldipine in a biphasic manner. Low-threshold calcium currents in clonal pituitary cells are also weakly antagonized by dihydropyridines like nimodipine (Cohen & McCarthy, 1987); however, it was unlikely that the biphasic effect of nisoldipine was due to contamination by a low threshold current because the effect was evident on both the peak and non-inactivating components of the high-threshold calcium current.

Several peptide neurotoxins have proved valuable in that they can selectively block subtypes of calcium channels. These include ω-conotoxin GVIA which preferentially blocks neuronal 'N' type calcium currents (McCleskey et al., 1987) and the more recently identified ω-Aga-IVA. This toxin blocks a type of calcium channel that underlies most of the whole cell calcium current found in cerebellar purkinje cells (hence 'P' type) and is thought to be involved in the regulation of transmitter release (Mintz et al., 1992). Biphasic effects of nisoldipine on the high-threshold calcium currents in GH_4C_1 cells may reflect the presence of more than one calcium channel type; thus it was of interest to determine whether or not these peptides could selectively antagonize one or both components of the nisoldipine-sensitive current.

In contrast to GH_3 pituitary cells (Dr C. Cohen, personal communication), low concentrations of both ω-Aga-IVA (100 nM) and ω-conotoxin GVIA (30 nM) reversibly blocked a proportion of the nisoldipine-sensitive calcium current in this GH_4C_1 pituitary cell line. Pretreatment with 10 nM nisoldipine blocked the component of the calcium current that was sensitive to these peptides (Figure 1). Consequently, GH_4C_1 cells may have at least two types of dihydropyridine-sensitive calcium currents, one of which is potently blocked by nisoldipine ($IC_{50} < 1$ nM), ω-Aga-IVA and ω-CGTX, and a second type that is less sensitive to nisoldipine (IC_{50} ca. 300 nM) but not blocked by nanomolar concentrations of these peptide neurotoxins. The partial and reversible block of dihydropyridine-sensitive calcium currents by ω-CGTX GVIA is consistent with that seen in rat and chick sensory neurones (McCleskey et al., 1987; Kasai et al., 1987). Although ω-Aga-IVA has not previously been shown to depress dihydropyridine-sensitive calcium currents, purified ω-Aga-IVA toxin has also been reported to have non-selective effects on ω-CGTX sensitive currents in rat cerebellar neurones (Sutton et al., 1993) and T-type calcium currents in neuroblastoma cells (Seabrook et al., 1994b).

A number of structural subtypes of calcium channel α-subunits, which have different sensitivities to calcium channel antagonists, have been identified (Snutch & Reiner, 1992). Indeed there is a much greater diversity of structural forms of calcium channels relative to the number of calcium current types which have been identified using pharmacological criteria, partly because of the limited number of ligands that have the necessary selectivity for these channel subtypes. Despite the overlapping effects of toxins like ω-Aga-IVA, when used in conjunction with other calcium channel antagonists they will remain important tools in advancing our understanding of calcium channel function.

Thyrotropin-releasing hormone mobilizes intracellular calcium in pituitary cells and can regulate Ca^{2+}-activated K channel activity in both GH_3 and GH_4C_1 cells (Dubinsky & Oxford, 1985; Barros *et al.*, 1991). Rat D_2 receptors have been reported to suppress the intracellular calcium mobilisation caused by activation of receptors to thyrotropin releasing hormone in GH_4C_1 cells (Valar *et al.*, 1990). We have recently reported that hD_3 receptors, in contrast to rat D_2 receptors, do not modulate this signal transduction pathway although in this cell line hD_3 receptors did not couple efficiently to either arachidonic acid release, adenylate cyclase, or voltage-dependent potassium currents (Seabrook *et al.*, 1992). Although human D_4 receptors can regulate calcium currents when expressed in GH_4C_1 cells, no effects of quinpirole or dopamine were seen on either basal $[Ca^{2+}]_i$ levels or TRH-induced calcium mobilisation in this cell line. Consequently, the mechanism by which hD_4 receptors to calcium currents in GH_4C_1 cells is distinct from that of TRH-induced calcium mobilization.

Unlike hD_2 and hD_4 receptors, in hD_3 transfected GH_4C_1 cells no effect of receptor activation was seen upon endogenous high-threshold calcium currents. Lack of coupling of hD_3 receptors in GH_4C_1 cells was not due to 'wash-out' of a cytosolic second messenger system, such as that which can be observed with some muscarinic receptors (Hille, 1992), because these results were unaffected by using either whole cell or nystatin perforated patch clamp recording. It is also unlikely that the lack of coupling of hD_3 receptors simply reflects the low levels of receptor expression achieved with the hD_3 receptor cDNA (Table 1) because similar levels of expression were obtained in NG108-15 cells in which hD_3 receptors were functional (Seabrook *et al.*, 1994a). Furthermore other hD_2-GH_4C_1 clones which exhibited lower levels of binding can still couple to adenylate cyclase (unpublished observations).

GH_4C_1 cells have several types of G-protein alpha subunits which are thought to be involved in the regulation of ion channels. These include $G_{i\alpha1,2\&3}$, as well as $G_{o\alpha}$ subunits (Luthin *et al.*, 1992). Similarly differentiated NG108-15 cells, in which hD_2 (short) and hD_3 receptors can couple to calcium currents (Seabrook *et al.*, 1994a,b), also have $G_{i\alpha2\&3}$ and $G_{o\alpha}$, but minimal $G_{i\alpha1}$ (Milligan, 1989; Mullaney & Milligan, 1990). Thus there is no obvious deficiency of an alpha subunit commonly linked to calcium current regulation, that can account for the lack of coupling of hD_3 receptors in these cells.

Only limited information is available on the specificity of D_2-like dopamine receptor subtypes for different G-proteins and hence their transduction pathways. However, antibodies generated against the C-terminus of G-protein α subunits have proved useful in studies of their role in the regulation of calcium channel function. In dissociated pituitary cells antibodies raised against $G_{o\alpha}$ but not $G_{i\alpha1,2\text{ or }3}$ block the coupling of dopamine receptors to calcium currents, whereas only antibodies raised against $G_{i\alpha3}$ and not $G_{o\alpha}$ or $G_{i\alpha1,2}$ mediate D_2 receptor coupling to the activation of K^+ channels (Lledo *et al.*, 1992). The restricted ability of dopamine receptors to couple G-protein subtypes may explain not only differences in the effector mechanisms to which they couple, but also their cellular specificities. Indeed Tang and colleagues have recently shown that coupling of rat dopamine receptor subtypes is different between the D_2 and D_4 subtypes an effect correlated with the distribution of different G protein α-subunits. In this study the rat D_2 receptor inhibited adenylate cyclase activity in cell lines with high levels of $G_{i\alpha2}$ subunits including mouse fibroblasts CCL1.3 and the mesencephalic cell line NM9D, whereas the rat D4 receptor only coupled efficiently in MN9D cell line (Tang *et al.*, 1994).

Recent studies have also implicated the β and γ subunits of G-protein heterotrimers as important determinants of receptor function (Hille, 1992). Using antisense oligonucleotide 'knock-out' experiments, muscarinic and somatostatin receptors in GH_3 pituitary cells have been shown to couple selectively to the inhibition of dihydropyridine-sensitive calcium channels via αo1/β3/γ4, and αo2/β1/γ3, subunit combinations respectively (Kleuss *et al.*, 1993). It remains to be determined whether the restricted distribution of such β and/or γ subunits, or indeed subtypes of $G_{o\alpha}$ (Mullaney & Milligan, 1990), can account for the restricted functional coupling of the human D_3 receptor. Nevertheless, it is apparent from the present study that hD_3 receptors do not utilise G-protein(s) by which hD_2 and hD_4 receptors may couple to dihydropyridine-sensitive calcium currents in GH_4C_1 cells.

In conclusion, this study demonstrates that this GH_4C_1 pituitary cell line has at least two types of high-threshold calcium current that are differentially sensitive to nisoldipine, ω-Aga-IVA, and ω-CGTX GVIA. A subpopulation of these dihydropyridine-sensitive calcium currents was depressed following activation of transfected human D_2 and D_4 receptors, but not by D_3 dopamine receptors. Furthermore, the mechanism by which hD_4 receptors couple to these calcium currents was distinct from that of TRH-induced calcium mobilization. It is considered that the lack of coupling of hD_3 receptors, unlike that of the hD_2 and hD_4 receptors, may reflect fundamental differences in the ability of these dopamine receptor types to activate endogenous G-proteins in GH_4C_1 pituitary cells.

We are grateful to Dr J.A. Kemp for his constructive comments on this manuscript, as well as to Drs P. Sokoloff and O. Civelli for supplying the hD_3 and hD_4 receptor cDNA respectively.

References

ALBERT, P.R., NEVE, K.A., BUNZOW, J.R. & CIVELLI, O. (1990). Coupling of a cloned rat dopamine D_2 receptor to inhibition of adenylyl cyclase and prolactin secretion. *J. Biol. Chem.*, **265**, 2098–2104.

ALLARD, S., LAPOINTE, S. & FALARDEAU, P. (1993). Specific induction of a functional endogenous D_2 short dopamine receptor in GH_4C_1 cells. *Biochem. Biophys. Res. Commun.*, **193**, 801–807.

ARMSTRONG, C.M. & MATTESON, D.R. (1985). Two distinct populations of calcium channels in a clonal line of pituitary cells. *Science*, **227**, 65–67.

BARROS, F., DELGADO, L.M., MACIA, C. & DE LA PENA, P. (1991). Effects of hypothalamic peptides on electrical activity and membrane currents of patch perforated clamped GH_3 anterior pituitary cells. *FEBS Lett.*, **279**, 33–37.

CASTELLANO, M.A., LIU, L.-X., MONSMA, F.J., SIBLEY, D.S. & KAPATOS, G. (1993). Transfected D2 short dopamine receptors inhibit voltage-dependent potassium current in neuroblastoma × glioma hybrid (NG108-15) cells. *Mol. Pharmacol.*, **44**, 649–656.

COHEN, C.J. & MCCARTHY, R.T. (1987). Nimodipine block of calcium channels in rat anterior pituitary cells. *J. Physiol.*, **387**, 195–225.

DUBINSKY, J.M. & OXFORD, G.S. (1985). Dual modulation of K channels by thyrotropin-releasing hormone in clonal pituitary cells. *Proc. Natl. Acad. Sci. U.S.A.*, **82**, 4282–4286.

EINHORN, L.C., FALARDEAU, P., CARON, M., CIVELLI, O. & OXFORD, G.S. (1990). Both isoforms of the D_2 receptor couple to a G-protein-activated K channel when expressed in GH_4 cells. *Soc. Neurosci. Abstr.*, **16**, 382.

EINHORN, L.C., GREGERSON, K.A. & OXFORD, G.S. (1991). D_2 dopamine receptor activation of potassium channels in identified rat lactotrophs: whole cell and single channel recording. *J. Neurosci.*, **11**, 3727–3737.

FREEDMAN, S.B., PATEL, S., MARWOOD, R., EMMS, F., SEABROOK, G.R., KNOWLES, M.R. & MCALLISTER, G. (1994). Expression and pharmacological characterisation of the human D_3 receptor. *J. Pharmacol. Exp. Ther.*, **268**, 417–426.

HILLE, B. (1992). G-protein coupled mechanisms and nervous signalling. *Neuron*, **9**, 187–195.

KALMAN, D., O'LAGUE, P.H., ERXLEBEN, C. & ARMSTRONG, D.L. (1988). Calcium-dependent inactivation of the dihydropyridine-sensitive calcium channels in GH_3 cells. *J. Gen. Physiol.*, **92**, 531–548.

KANTERMAN, R.Y., MAHAN, L.C., BRILEY, E.M., MONSMA, F.J., SIBLEY, D.R., AXELROD, J. & FELDER, C.C. (1991). Transfected D_2 dopamine receptors mediate the potentiation of arachidonic acid release in Chinese hamster ovary cells. *Mol. Pharmacol.*, **39**, 364–369.

KASAI, H., AOSAKI, T. & FUKUDA, J. (1987). Presynaptic Ca-antagonist ω-conotoxin irreversibly blocks N-type Ca-channels in chick sensory neurons. *Neurosci. Res.*, **4**, 228–235.

KEJA, J.A., STOOF, J.C. & KITS, K.S. (1992). Dopamine D_2 receptor stimulation differentially affects voltage-activated calcium channels in rat pituitary melanotropic cells. *J. Physiol.*, **450**, 409–435.

KLEUSS, C., SCHERUBL, H., HESCHELER, J., SCHULTZ, G. & WITTIG, B. (1993). Selectivity in signal transduction determined by γ subunits of heterotrimeric G proteins. *Science*, **259**, 832–834.

LLEDO, P.M., HOMBURGER, V., BOCKAERT, J. & VINCENT, J.-D. (1992). Differential G protein-mediated coupling of D_2 dopamine receptors to K^+ and Ca^{2+} currents in rat anterior pituitary cells. *Neuron*, **8**, 455–463.

LUTHIN, D.R., EPPLER, C.M. & LINDEN, J. (1992). Somatostatin couples preferentially to Gi-type GTP-binding proteins in a pituitary cell line. *Proc. Fed. Exp. Biol.*, A1561.

MCALLISTER, G., CHARLESWORTH, A., SNODIN, C., BEER, M.S., NOBLE, A.J., MIDDLEMISS, D.N., IVERSEN, L.L. & WHITING, P. (1992). Molecular cloning of a serotonin receptor from human brain (5HT1E): a fifth 5HT1-like subtype. *Proc. Natl. Acad. Sci.*, **89**, 5517–5521.

MCALLISTER, G., KNOWLES, M.R., PATEL, S., MARWOOD, R., EMMS, F., SEABROOK, G.R., GRAZIANO, M., BORKOWSKI, D., HEY, P.J. & FREEDMAN, S.B. (1993). Characterisation of a chimeric hD_3/hD_2 dopamine receptor expressed in CHO cells. *FEBS Letts.*, **324**, 81–86.

MCCLESKEY, E.W., FOX, A.P., FELDMAN, D.H., CRUZ, L.J., OLIVERA, B.M., TSIEN, R.W. & YOSHIKAMI, D. (1987). ω-Conotoxin: direct and persistent blockade of specific types of calcium channels in neurons but not muscle. *Proc. Natl. Acad. Sci. U.S.A.*, **84**, 4327–4331.

MILLIGAN, G. (1989). Tissue distribution and subcellular location of guanine nucleotide binding proteins:- implications for cellular signalling. *Cell. Signal.*, **1**, 411–419.

MINTZ, I.M., ADAMS, M.E. & BEAN, B.P. (1992). P-type calcium channels in rat central and peripheral neurons. *Neuron*, **9**, 85–95.

MULLANEY, I. & MILLIGAN, G. (1990). Identification of two distinct isoforms of the guanine nucleotide binding protein Go in neuroblastoma × glioma hybrid cells: independent regulation during cyclic AMP-induced differentiation. *J. Neurochem.*, **55**, 1890–1898.

NUSSINOVITCH, I. & KLEINHAUS, A.L. (1992). Dopamine inhibits voltage-activated calcium channel currents in rat pars intermedia pituitary cells. *Brain Res.*, **574**, 49–55.

SCHWARTZ, J.-C., GIROS, B., MARTRES, M.-P. & SOKOLOFF, P. (1992). The dopamine receptor family: molecular biology and pharmacology. *Seminars Neurosci.*, **4**, 99–108.

SEABROOK, G.R. & FONG, T.M. (1993). Thapsigargin blocks the mobilisation of intracellular calcium caused by the activation of human NK1(long) receptors expressed in chinese hamster ovary cells. *Neurosci. Lett.*, **152**, 9–12.

SEABROOK, G.R., PATEL, S., MARWOOD, R., EMMS, F., KNOWLES, M.R., FREEDMAN, S.B. & MCALLISTER, G. (1992). Stable expression of human D_3 dopamine receptors in GH_4C_1 pituitary cells. *FEBS Lett.*, **312**, 123–126.

SEABROOK, G.R., PATEL, S., MARWOOD, R., EMMS, F., KNOWLES, M.R., FREEDMAN, S.B. & MCALLISTER, G. (1994a). Human D_3 dopamine receptors couple to the depression of calcium currents in a neuroblastoma-x-glioma cell line. *Br. J. Pharmacol.*, **111**, 391–393.

SEABROOK, G.R., KNOWLES, M., MYERS, J., SINCLAIR, H., PATEL, S., FREEDMAN, S.B. & MCALLISTER, G. (1994b). Depression of high-threshold calcium currents by activation of human D_2(short) dopamine receptors expressed in differentiated NG108-15 cells. *Br. J. Pharmacol.*, **111**, 1061–1066.

SIBLEY, D.R. & MONSMA, F.J. (1992). Molecular biology of dopamine receptors. *Trends Pharmacol. Sci.*, **13**, 61–69.

SNUTCH, T.P. & REINER, P.B. (1992). Ca^{2+} channels: diversity of form and function. *Current Opinions Neurobiol.*, **2**, 247–253.

SOKOLOFF, P., GIROS, B., MARTRES, M.-P., BOUTHENET, M.-L. & SCHWARTZ, J.-C. (1990). Molecular cloning and characterisation of a novel dopamine receptor (D_3) as a target for neuroleptics. *Nature*, **347**, 146–151.

STACK, J. & SUPRENANT, A. (1991). Dopamine actions on calcium currents, potassium currents and hormone release in rat melanotrophs. *J. Physiol.*, **439**, 37–58.

SUTTON, K.G., PEARSON, H., SCOTT, R.H. & DOLPHIN, A.C. (1993). Inhibition of Ca^{2+} channel currents in cultured rat cerebellar granule neurones by the Funnel Web spider toxin ω-Agatoxin IVA. *J. Physiol.*, **467**, 271P.

TANG, L., TODD, R.D., HELLER, A. & O'MALEY, K.L. (1994). Pharmacological and functional characterisation of D2, D3 and D4 dopamine receptors in fibroblast and dopaminergic cell lines. *J. Pharmacol. Exp. Ther.*, **268**, 495–502.

VALLAR, L., MUCA, C., MAGNI, M., ALBERT, P., BUNZOW, J., MELDOLESI, J. & CIVELLI, O. (1990). Differential coupling of dopaminergic D_2 receptors expressed in different cell types. *J. Biol. Chem.*, **265**, 10320–10326.

VAN TOL, H,. BUNZOW, J.R., GUAN, H.-C., SUNAHARA, R.K., SEEMAN, P., NIZNIK, H.B. & CIVELLI, O. (1991). Cloning of the gene for a human dopamine D_4 receptor with high affinity for the antipsychotic clozapine. *Nature*, **350**, 610–614.

(Received February 21, 1994
Accepted March 25, 1994)

Br. J. Pharmacol. (1994), **112**, 735–740

Characterization of EP-receptor subtypes involved in allodynia and hyperalgesia induced by intrathecal administration of prostaglandin E_2 to mice

*†Toshiaki Minami, *†Isao Nishihara, *Rumiko Uda, [1]†‡Seiji Ito, *Masayoshi Hyodo & †Osamu Hayaishi

*Department of Anesthesiology, Osaka Medical College, Takatsuki 569; †Department of Cell Biology, Osaka Bioscience Institute, Suita 565 and ‡Department of Medical Chemistry, Kansai Medical University, Moriguchi 570, Japan

1 Intrathecal (i.t.) administration of prostaglandin E_2 (PGE_2) to conscious mice induced allodynia, a state of discomfort and pain evoked by innocuous tactile stimuli, and hyperalgesia as assessed by the hot plate test. We characterized prostaglandin E receptor subtypes (EP_{1-3}) involved in these sensory disorders by use of 7 synthetic prostanoid analogues.

2 Sulprostone ($EP_1 < EP_3$) induced allodynia over a wide range of dosages from 50 pg to 5 $\mu g\,kg^{-1}$. The maximal allodynic effect was observed at 5 min after i.t. injection, and the response gradually decreased over the experimental period of 50 min. This sulprostone-induced allodynia showed a time course similar to that induced by PGE_2.

3 17-Phenyl-ω-trinor PGE_2 ($EP_1 > EP_3$) and 16,16-dimethyl PGE_2 ($EP_1 = EP_2 = EP_3$) were as potent as PGE_2 in inducing allodynia, and more potent than sulprostone. Butaprost (EP_2), 11-deoxy PGE_1 ($EP_2 = EP_3$), MB 28767 (EP_3), and cicaprost (prostaglandin I_2 (IP-) receptor) induced allodynia, but with much lower scores. 13,14-Dihydro-15-keto PGE_2, a metabolite of PGE_2, did not induce allodynia.

4 16,16-Dimethyl PGE_2 as well as PGE_2 induced hyperalgesia over a wide range of dosages (16,16-dimethyl PGE_2: 5 pg–0.5 $\mu g\,kg^{-1}$ PGE_2: 50 pg–0.5 $\mu g\,kg^{-1}$) with two apparent peaks at 0.5 $ng\,kg^{-1}$ and 0.5 $\mu g\,kg^{-1}$. Sulprostone ($EP_1 < EP_3$) and 17-phenyl-ω-trinor PGE_2 ($EP_1 > EP_3$) showed a bell-shaped hyperalgesia at lower doses of 5 pg–5 $ng\,kg^{-1}$ and 50 pg–50 $ng\,kg^{-1}$, respectively. MB 28767 (EP_3) showed a monophasic hyperalgesic action over a wide range of dosages at 50 pg–5 $\mu g\,kg^{-1}$. Butaprost (EP_2) induced hyperalgesia at doses higher than 50 $ng\,kg^{-1}$.

5 These results demonstrate that PGE_2 may exert allodynia through the EP_1-receptor and hyperalgesia through EP_2- and EP_3-receptors in the mouse spinal cord.

Keywords: EP agonist; IP agonist; allodynia; hyperalgesia; spinal cord

Introduction

Prostaglandins are ubiquitously distributed in virtually all mammalian tissues and organs, and it has been well documented that they are involved in various aspects of inflammation including pain (Coleman *et al.*, 1989). Accumulating evidence indicates that prostaglandins are critical for the augmented processing of pain information at the spinal level. Intrathecal (i.t.) injection of acetylsalicylic acid, indomethacin, and other nonsteroidal anti-inflammatory drugs has been shown to produce analgesia (Yaksh, 1982; Malmberg & Yaksh, 1992a,b). We and others (Taiwo & Levine, 1986; 1988; Uda *et al.*, 1990) previously reported that i.t. injection of PGD_2 and PGE_2 induced hyperalgesic effects.

Quite recently, we demonstrated that i.t. administration of PGE_2 into mice also induces allodynia, a state of discomfort and pain evoked by innocuous tactile stimuli; the mice showed squeaking, biting, and scratching movements in response to low-threshold stimuli (Minami *et al.*, 1994a,b). Hyperalgesia is defined as an increased response to a stimulus that is normally painful, whereas the closely related term allodynia is defined as pain due to a stimulus that does not normally provoke pain (Merskey, 1986). Although hyperalgesia and allodynia are often associated consequences of damage to peripheral nerves or the central nervous system, it has recently been suggested that different receptor systems in the spinal cord may be involved in these two sensory disorders (Yaksh & Aimone, 1989).

PGE_2 produces a broad range of biological actions in diverse tissues through its binding to specific receptors on plasma membranes (Samuelsson *et al.*, 1978; Moncada *et al.*, 1985). The diversity of PGE_2 actions is due to PGE-receptor subtypes coupled to different signal transduction pathways. PGE receptors are pharmacologically divided into at least three subtypes, EP_1, EP_2 and EP_3, and they are considered to be coupled to Ca^{2+} mobilization and stimulation and inhibition of adenylate cyclase, respectively (Coleman *et al.*, 1987; 1989). It has been suggested that the EP_1-receptor is involved in contraction of gastrointestinal and tracheal smooth muscles (Coleman & Kennedy, 1985), and stimulation of neurotransmitter release (Ehrenpreis *et al.*, 1973). Important functions of PGE_2 mediated via EP_2-receptors include the negative regulation of the immune system (Monick *et al.*, 1987) and inflammation (Coleman *et al.*, 1989). It has also been suggested that the EP_2-receptor may be involved in relaxation in trachea (Gardiner, 1986) and ileum circular muscle (Lawrence *et al.*, 1992), and vasodilatation of various blood vessels (Coleman *et al.*, 1989). On the other hand, the EP_3-receptor is assumed to be involved in inhibition of gastric acid secretion (Chen *et al.*, 1988), modulation of neurotransmitter release in central and peripheral neurones (Hedqvist & von Euler, 1972), and inhibition of sodium and water reabsorption in kidney tubules (Sonnenburg & Smith, 1988; Nakao *et al.*, 1989). However, the EP-receptor subtypes in the spinal cord have not yet been characterized. Although there are few prostanoid analogues which show absolute selectivity for the individual EP_1-, EP_2- and EP_3-subtypes, many are now known as potent agonists for EP-receptors.

In the present study, we examined the effect of i.t. admini-

[1] Author for correspondence at Suita address.

stration of various agonists selective for EP-receptor subtypes on nociception and non-nociception in the spinal cord of conscious mice.

Methods

Intrathecal administration

Male ddY-mice weighing 22 ± 2 g were used in this study. The animals were housed under conditions of a 12-h light-dark cycle and a constant temperature of 22 ± 2°C and 60 ± 10% humidity. A 27-gauge stainless-steel needle (0.35 mm, o.d.) attached to a microsyringe was inserted between the L_5 and L_6 vertebrae by a slight modification of the method of Hylden & Wilcox (1980). Drugs in vehicle were injected slowly into the subarachnoid space of conscious mice at 22 ± 2°C. The volume of the i.t. injection was 5 μl. It was previously confirmed by use of Commassie brilliant blue and ^{3}H-labelled prostaglandins that the injected solution does not extend to the cervical segments (Uda *et al.*, 1990).

Studies on allodynia

Studies on allodynia were carried out essentially according to the method of Yaksh & Harty (1988). The mice were divided into various groups ($n = 6-8$/group). Control mice were given physiological saline (5 μl). Drug-treated groups were injected with 5 μl of vehicle containing various doses of test agents. After the i.t. injection, each mouse was placed in an individual 13 × 8.5 × 13 cm Plexiglas enclosure with wood chips on the floor and observed. Allodynia was assessed once every 5 min over a 50-min period by light stroking of the flank of the mice with a paintbrush. The allodynia response was ranked as follows: 0, no response; 1, mild squeaking with attempts to move away from the stroking probe; 2, vigorous squeaking evoked by the stroking probe, biting at the probe, and strong efforts to escape.

Hot plate test

Mice were placed on a hot plate maintained at 55°C, and the elapsed time until the mice showed the first avoidance responses (licking the feet, jumping, or rapidly stamping the paws) was recorded as described by Woolfe & MacDonald (1944). The response time of the mice to the hot plate was measured at 30 min after i.t. injection.

The animals were used for only one measurement in each experiment. This study was conducted in accordance with the guidelines of the Ethics Committee of the International Association for the Study of Pain (Zimmermann, 1983).

Drugs

13,14-Dihydro-15-keto PGE_2, 16,16-dimethyl PGE_2, and 17-phenyl-ω-trinor PGE_2 were purchased from Cayman Chemical (Ann Arbor, MI, U.S.A.). The following prostaglandin analogues were generous gifts: PGE_2 and 11-deoxy PGE_1 from Ono Central Research Institute (Osaka, Japan); butaprost from Dr P.J. Gardiner of Bayer, U.K.; sulprostone and cicaprost from Dr K.-H. Thierauch, Schering AG, Berlin; MB 28767 (15S-hydroxy-9-oxo-16-phenoxy-ω-tetranorprost-13E-enoic acid) from Rhône-Poulenc Rorer, U.K. Table 1 summarizes the selectivity profiles of the EP- and IP-receptor agonists employed here as reported by Lawrence *et al.* (1992).

Stock solutions of the prostanoids were stored in ethanol solution at − 20°C. For injection, an aliquot of the desired stock agonist solution was put into a borosilicate tube and the ethanol was removed by evaporation to dryness under nitrogen gas. Sterile saline was then added to dissolve the agonist. Each agonist was dissolved in sterile saline on the day of the experiment and kept on ice until used. All drugs, including saline, were coded to assure blind testing.

Statistics

The statistical analyses were carried out by analysis of variance (ANOVA). Statistical significance ($P < 0.05$) was further examined with Duncan's test for multiple comparison.

Results

Effect of i.t. EP agonists on allodynia

Recently we reported that PGE_2 induced allodynia and hyperalgesia over a wide range of dosages from 0.5 pg to 50 μg kg^{-1} (Minami *et al.*, 1994a). In order to specify the EP-receptor(s) involved in the PGE_2-induced allodynia, we examined the effect of various EP agonists and cicaprost, an IP agonist, on allodynia in conscious mice. The i.t. administration of sulprostone (0.5 μg kg^{-1}), an EP_1 and EP_3 agonist, resulted in prominent agitation responses such as vocalization, biting, and escape from the probe, to tactile stimuli applied to the flank. Brushing of the face or tactile stimulation of the forepaws did not give any response, indicating that allodynia appeared limited to the caudal dermatomes of the body. The i.t. administration of saline had no effect on allodynia. As shown in Figure 1, the sulprostone (0.5 μg kg^{-1})-induced allodynia showed its maximum expression at 5 min after i.t. injection and gradually decreased during the 50-min experimental period in a manner similar to that induced by PGE_2. When the score obtained for the overall 50 min was cumulated and expressed as a percentage of the maximum possible score, the score of sulprostone was comparable to that of PGE_2 at 0.5 μg kg^{-1} (Figure 2). Allodynic scores of butaprost, an EP_2 agonist, MB 28767, an EP_3 agonist, and cicaprost were much lower than that of PGE_2 at 0.5 μg kg^{-1}.

Figure 3 shows the dose-dependencies of allodynia evoked

Table 1 Specificity of prostaglandin E and prostaglandin I analogues at EP- and IP-receptors

Prostanoid	*EP_1*	*EP_2*	*EP_3*	*IP*
PGE analogue				
PGE_2	+++	+++	+++	
16,16-Dimethyl PGE_2	++++	++(+)	++++	
Sulprostone	++	0	++++	
17-Phenyl-ω-trinor PGE_2	+++	+	++	
Butaprost	(+)	++	0	
11-Deoxy PGE_1	+	++(+)	++	
MB 28767	(+)	(+)	+++	
PGI analogue				
Cicaprost	(+)	(+)	0	++++

Rankings of EP- and IP-receptors are from Lawrence *et al.* (1992). One + corresponds to a potency difference of approximately one order of magnitude.

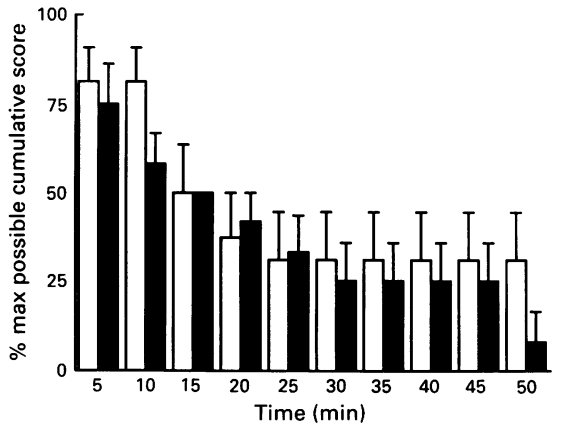

Figure 1 Time courses of allodynia induced by i.t. prostaglandin E_2 (PGE_2) and sulprostone. Mice were injected i.t. with 0.5 $\mu g\,kg^{-1}$ of PGE_2 (open columns) or sulprostone (solid columns). Assessment of allodynia was made as described under Methods. Each column (mean ± s.e.mean) represents the percentage of the maximum possible cumulative score of 6 mice evaluated every 5 min.

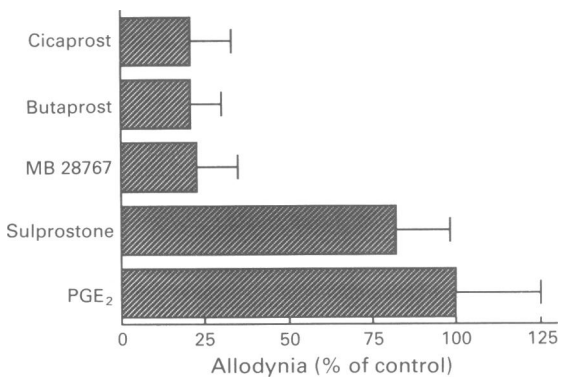

Figure 2 Effect of prostaglandin E_2 (PGE_2) and prostanoid agonists on allodynia in conscious mice. PGE_2 or prostanoid agonist (0.5 $\mu g\,kg^{-1}$) was injected into the subarachnoid space. Assessment of allodynia was made as described under Methods. When the score obtained for the overall 50-min experimental period was cumulated and expressed as a percentage of the maximum possible score, the allodynic score of PGE_2 was 43.8% and taken as 100%. Values shown are the mean ± s.e.mean of responses in 6 mice.

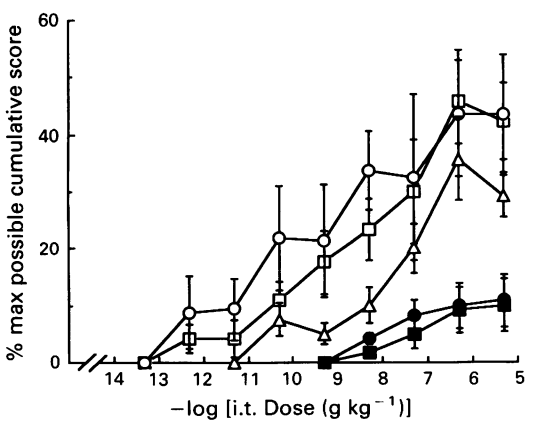

Figure 3 Dose-dependent effects of i.t. injection of prostaglandin E_2 (PGE_2) and various EP agonists on allodynia in conscious mice. Mice were injected with various doses of PGE_2 (○), 17-phenyl-ω-trinor PGE_2 (□), sulprostone (△), MB 28767 (●), or butaprost (■) into the subarachnoid space. Assessment of allodynia was made as described under Methods. Values shown are the mean ± s.e.mean of responses in 6 mice.

by EP agonists. The allodynia induced by sulprostone was observed at a dose as low as 50 $pg\,kg^{-1}$ and the maximal effect (35.8% of the maximum possible score) was observed at 5 $\mu g\,kg^{-1}$, with a half-maximal stimulation occurring at about 50 $\mu g\,kg^{-1}$. This agonist-induced allodynia showed similar time courses over a wide range of doses of 50 pg–5 $\mu g\,kg^{-1}$ (data not shown). Sulprostone-induced mice did not display clonic seizure and convulsion even at a dose as high as 5 $\mu g\,kg^{-1}$. 17-Phenyl-ω-trinor PGE_2 ($EP_1 > EP_3$) showed its maximum effect (45.8% of the maximum possible score) at 0.5 $\mu g\,kg^{-1}$, with a half-maximal stimulation occurring at about 5 $ng\,kg^{-1}$. Dose-dependency of 16,16-dimethyl PGE_2, a potent EP_1, EP_2 and EP_3 agonist, for allodynia showed a bell-shaped curve, and the maximum effect was observed at 50 $ng\,kg^{-1}$ (data not shown). Butaprost (Figure 3), MB 28767 (Figure 3), and 11-deoxy PGE_1 (data not shown) showed shallow log concentration-response curves with 10% of the maximum possible score at 5 $\mu g\,kg^{-1}$. 13,14-Dihydro-15-keto PGE_2, a metabolite of PGE_2, did not induce allodynia. Taken together, these results demonstrate that the EP_1-receptor may be involved in the PGE_2-induced allodynia in the spinal cord.

Effect of i.t.-administered EP agonists on hyperalgesia assessed by the hot plate test

As reported previously (Uda *et al.*, 1990), PGE_2-induced hyperalgesia was observed between 3 and 30 min after i.t. injection of PGE_2. In the present study, the response time of mice to the hot plate (55°C) was measured at 30 min after i.t. injection of various doses of EP agonists or vehicle so that the effect of EP agonist-induced allodynia would be minimized. There was no significant difference in the latency

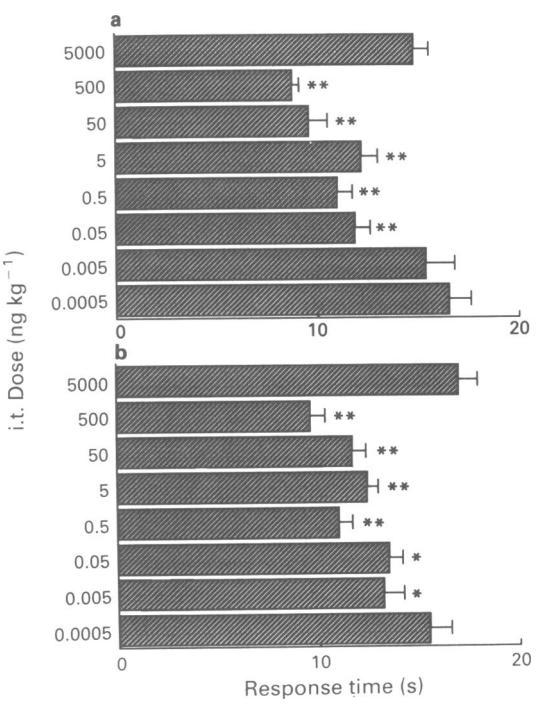

Figure 4 Dose-dependent effects of i.t. injection of prostaglandin E_2 (PGE_2) and 16,16-dimethyl PGE_2 on hyperalgesia assessed by the hot plate test. Mice were injected with various doses of PGE_2 (a) or 16,16-dimethyl PGE_2 (b) into the subarachnoid space. The time until the mice showed the first avoidance response to the hot plate test (55°C) was measured at 30 min after i.t. injection. Each column represents the mean ± s.e.mean of responses in ten mice. Statistical analyses were carried out by Duncan's test. $0.01 \leqslant {}^{*}P < 0.05$; $^{**}P < 0.01$, as compared with the saline-injected control group (16.2 ± 0.5 s).

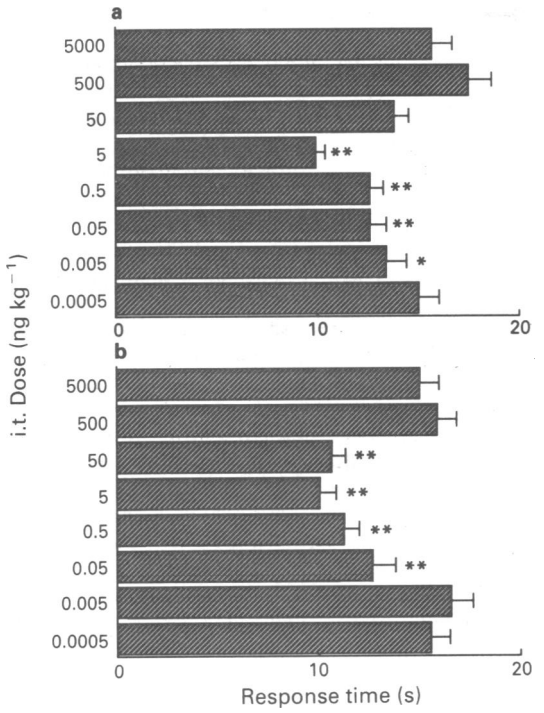

Figure 5 Dose-dependent effects of i.t. injection of sulprostone and 17-phenyl-ω-trinor PGE_2 on hyperalgesia assessed by the hot plate test. Mice were injected with various doses of sulprostone (a) or 17-phenyl-ω-trinor PGE_2 (b) into the subarachnoid space. Details as in the legend for Figure 4, $0.01 \leqslant {}^{*}P < 0.05$; ${}^{**}P < 0.01$, as compared with the saline-injected control group (16.2 ± 0.5 s).

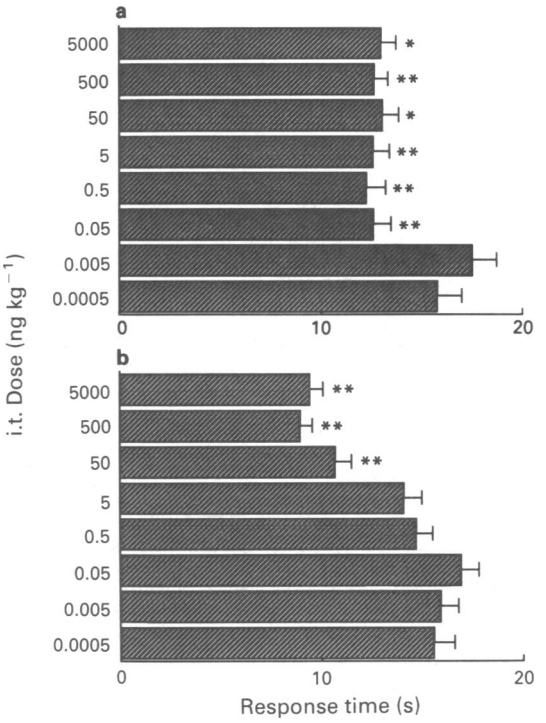

Figure 6 Dose-dependent effects of i.t. injection of MB 28767 and butaprost on hyperalgesia assessed by the hot plate test. Mice were injected with various doses of MB 28767 (a) or butaprost (b) into the subarachnoid space. Details as in the legend for Figure 4. $0.01 \leqslant {}^{*}P < 0.05$; ${}^{**}P < 0.01$, as compared with the saline-injected control group (16.2 ± 0.5 s).

period between the saline control (16.2 ± 0.5 s, mean ± s.e. mean) and the untreated control (15.4 ± 0.4 s).

As reported previously (Minami *et al.*, 1994a), PGE_2 (EP_1, EP_2, EP_3) produced its hyperalgesic action over a wide range of dosages from 50 pg to 0.5 μg kg^{-1}. Similarly, 16,16-dimethyl PGE_2 (EP_1, EP_2, EP_3) produced its hyperalgesic action at doses of 5 pg–0.5 μg kg^{-1} (Figure 4); this action showed two peaks, one at 0.5 ng kg^{-1} (11.0 ± 0.7 vs. 16.2 ± 0.5 s for the control) and one at 0.5 μg kg^{-1} (9.6 ± 0.7 s), and returned to the control level at 5 μg kg^{-1}, the highest concentration employed. On the other hand, sulprostone ($EP_1 < EP_3$) and 17-phenyl-ω-trinor PGE_2 ($EP_1 > EP_3$) produced bell-shaped dose dependency for hyperalgesic action at doses of 5 pg–5 ng kg^{-1} and 50 ng kg^{-1}, respectively (Figure 5). Neither sulprostone nor 17-phenyl-ω-trinor PGE_2 produced a significant change at higher doses examined. Unlike its effects on allodynia, MB 28767 (EP_3) produced its hyperalgesic action over a wide range of dosages from 50 pg to 5 μg kg^{-1}, and butaprost (EP_2) produced its hyperalgesic action at higher doses of 50 ng–5 μg kg^{-1} (Figure 6). 13,14-Dihydro-15-keto PGE_2 produced a weak hyperalgesic action at doses of 0.5 ng and 5 ng kg^{-1} (data not shown). Cicaprost (IP) produced no significant change. These results demonstrate that EP_2- and EP_3-receptors may be involved in the PGE_2-induced hyperalgesia in the spinal cord.

Discussion

We recently reported that the i.t. administration of PGE_2 to conscious mice induced allodynia and hyperalgesia (Uda *et al.*, 1990; Minami *et al.*, 1994a,b). The dose-dependency of PGE_2 for allodynia was apparently correlated with that for hyperalgesia. While the PGE_2-induced allodynia was dose-dependently relieved by the strychnine-sensitive glycine receptor agonist, taurine, the NMDA receptor antagonist ketamine, and a high dose of the α_2-adrenoceptor agonist, clonidine, the PGE_2-induced hyperalgesia assessed by the hot plate test was not suppressed by taurine or clonidine. To test the hypothesis that the mechanism of PGE_2-induced allodynia might be different from that of PGE_2-induced hyperalgesia (Minami *et al.*, 1994a), we used 7 synthetic prostaglandin analogues having different specificities for EP-receptor subtypes as summarized in Table 1.

The present study provides evidence that allodynia and hyperalgesia induced by PGE_2 are mediated by different EP-receptor subtypes. It is clear that the EP_1-receptor is involved in the PGE_2-induced allodynia for the following reasons: first, 17-phenyl-ω-trinor PGE_2 ($EP_1 > EP_3$) was more potent than sulprostone ($EP_1 < EP_3$) (Figure 3). Second, butaprost (EP_2), 11-deoxy PGE_1 ($EP_2 = EP_3 > EP_1$) and MB 28767 (EP_3) induced allodynia, but with much lower scores. On the other hand, the PGE_2-induced hyperalgesia was complicated, demonstrating that the hyperalgesia observed here may reflect the action of PGE_2 or EP agonists at multiple sites inherent in *in vivo* experiments. Both PGE_2 and 16,16-dimethyl PGE_2 induced a biphasic hyperalgesia over a wide range of dosages (PGE_2: 50 pg–0.5 μg kg^{-1}, 16,16-dimethyl PGE_2: 5 pg–0.5 μg kg^{-1}) with two apparent peaks at 0.5 ng and 0.5 μg kg^{-1} (Figure 4). Sulprostone ($EP_1 < EP_3$) and 17-phenyl-ω-trinor PGE_2 ($EP_1 > EP_3$) showed a bell-shaped dose-response for hyperalgesia at lower doses of 5 pg–5 ng kg^{-1} and 50 pg–50 ng kg^{-1}, respectively (Figure 5). MB 28767 (EP_3) showed a monophasic hyperalgesic action over a wide range of dosages of 50 pg–5 μg kg^{-1}. Butaprost (EP_2) induced hyperalgesia at doses higher than 50 ng kg^{-1} (Figure 6). These results suggest that PGE_2 may exert hyperalgesia through EP_2- and EP_3-receptors. Collectively, with the data obtained with butaprost, sulprostone, and MB 28767, the PGE_2-induced hyperalgesia is likely to be mediated by the EP_3-receptor at lower doses of PGE_2 and by the EP_2-receptor at higher doses. However, differences in receptor density or efficiency of receptor-effector coupling in the central nervous system could dramatically alter relative agonist potencies.

Therefore we cannot neglect the possibility that butaprost may exert hyperalgesia through the EP_3-receptor.

Prostaglandins have been studied as potential nociceptive transmitters, but as observed in the present experiments, these studies are complicated by the existence of multiple receptor subtypes and hampered by the absence of selective antagonists. Recently EP_1-, EP_2- and EP_3-receptors have been successfully cloned from mouse cDNA libraries (Sugimoto *et al.*, 1992; Honda *et al.*, 1993; Watabe *et al.*, 1993). There are some discrepancies in specificities of EP agonists and antagonists for EP-receptors between membranes from cDNA-transfected cells and tissues reported previously. For example, EP-receptors in isolated tissues that are susceptible to blockade by SC19220 and AH6809 have been designated as EP_1-receptors (Coleman *et al.*, 1985). However, because AH6809 showed only weak inhibition of the binding of [^{3}H]-PGE_2 to membranes prepared from EP_1-receptor cDNA-transfected CHO cells, it was suggested that there may be other forms of EP_1-receptor sensitive to AH6809 or that the action of AH6809 is species-specific and does not work on the mouse receptor (Watabe *et al.*, 1993). In this context, our previous observation that PGE_2-induced hyperalgesia was blocked by AH6809 (Uda *et al.*, 1990) is not inconsistent with the present results indicating that hyperalgesia induced by PGE_2 was mediated by EP_3- and/or EP_2-receptors (Figures 5 and 6). It was also reported that the lack of binding activity of butaprost toward the EP_2-receptor cloned from mouse mastocytoma P-815 cells suggests another form of EP_2-receptor subtype (Honda *et al.*, 1993). Furthermore, there are two isoforms of EP_3-receptor with different properties at the levels of signalling and desensitization in mice (Negishi *et al.*, 1993). It has also been shown that four isoforms exist of bovine EP_3-receptor that couple to different G proteins to activate different second messenger systems (Namba *et al.*, 1993). In addition to these findings, precise localization of EP-receptor subtypes in the spinal cord by *in situ* hybridization will be of help in understanding the diversity of cellular responses to PGE_2.

In summary, we have demonstrated here, on the basis of rankings of specificities of EP agonists for EP-receptor subtypes, that EP_1- and EP_3-receptors, and possibly EP_2-receptor, may exist in mouse spinal cord and be involved in pain transmission at the level of spinal cord. Spinal EP-receptor systems may exert pain transmission on high and low threshold afferents with mutual interactions of L-glutamate and other neuroactive substances (Taiwo & Levine, 1986; Uda *et al.*, 1990; Malmberg & Yaksh, 1992a,b; Minami *et al.*, 1994a,b). This is relevant because there is renewed interest and investigation into the mechanisms of hyperalgesia and associated allodynia (Willis, 1992). Because PGE_2 clearly plays important but complex roles in both acute and chronic pain via different pain processing pathways, the continued pharmacological approach along with the development of specific EP-receptor agonists and antagonists may provide us with an opportunity to learn more about the physiological and pathological roles of PGE_2 in pain.

This work was supported in part by Grants-in-Aid for Scientific Research on Priority Areas and for Scientific Research (C) (04670170) from the Ministry of Education, Science, and Culture of Japan, and by grants from the Ono Medical Research Foundation, Yamanouchi Foundation for Research on Metabolic Disorders and the Naito Foundation.

References

CHEN, M.C.Y., AMIRIAN, D.A., TOOMEY, M., SANDERS, M.J. & SOLL, A.H. (1988). Prostanoid inhibition of canine parietal cells: mediation by the inhibitory guanosine triphosphate-binding protein of adenylate cyclase. *Gastroenterology*, **94**, 1121–1129.

COLEMAN, R.A. & KENNEDY, I. (1985). Characterization of the prostanoid receptors mediating contraction of guinea-pig isolated trachea. *Prostaglandins*, **29**, 363–375.

COLEMAN, R.A., KENNEDY, I., HUMPHREY, P.P.A., BUNCE, K. & LUMLEY, P. (1989). Prostanoids and their receptors. In *Comprehensive Medical Chemistry. The Rational Design, Mechanistic Study and Therapeutic Application of Chemical Compounds*, Vol. 3. ed. Hansch, C., Sammes, P.G., Taylor, J.B. & Emmett, J.C. pp. 643–714. Oxford: Pergamon Press.

COLEMAN, R.A., KENNEDY, I. & SHELDRICK, R.L.G. (1987). Evidence for the existence of three subtypes of PGE_2 (EP) sensitive receptors in smooth muscle. *Br. J. Pharmacol.*, **91**, 323P.

EHRENPREIS, S., GREENBERG, J. & BELMAN, S. (1973). Prostaglandins reverse inhibition of electrically-induced contractions of guinea pig ileum by morphine, indomethacin and acetylsalicylic acid. *Nature New Biol.*, **245**, 280–282.

GARDINER, P.J. (1986). Characterization of prostanoid relaxant/inhibitory receptor (ψ) using a highly selective agonist, TR4979. *Br. J. Pharmacol.*, **87**, 45–56.

HEDQVIST, P. & VON EULER, U.S. (1972). Prostaglandin-induced neurotransmission failure in the field-stimulated, isolated vas deferens. *Neuropharmacology*, **11**, 177–187.

HONDA, A., SUGIMOTO, Y., NAMBA, T., WATABE, A., IRIE, A., NEGISHI, M., NARUMIYA, S. & ICHIKAWA, A. (1993). Cloning and expression of a cDNA for mouse prostaglandin E receptor EP_2 subtype. *J. Biol. Chem.*, **268**, 7759–7762.

HYLDEN, J.L.K. & WILCOX, G.L. (1980). Intrathecal morphine in mice: a new technique. *Eur. J. Pharmacol.*, **67**, 313–316.

LAWRENCE, R.A., JONES, R.L. & WILSON, N.H. (1992). Characterization of receptors involved in the direct and indirect actions of prostaglandins E and I on the guinea-pig ileum. *Br. J. Pharmacol.*, **105**, 271–278.

MALMBERG, A.B. & YAKSH, T.L. (1992a). Hyperalgesia mediated by spinal glutamate or substance P receptor blocked by spinal cyclooxygenase inhibition. *Science*, **257**, 1276–1279.

MALMBERG, A.B. & YAKSH, T.L. (1992b). Antinociceptive actions of spinal nonsteroidal anti-inflammatory agents on the formalin test in the rat. *J. Pharmacol. Exp. Ther.*, **263**, 136–146.

MERSKEY, H. (1986). Pain terms: a current list with definitions and notes on usage. *Pain*, Suppl. 3, S216–221.

MINAMI, T., UDA, R., HORIGUCHI, S., ITO, S., HYODO, M. & HAYAISHI, O. (1994a). Allodynia evoked by intrathecal administration of prostaglandin E_2 to conscious mice. *Pain* (in press).

MINAMI, T., NISHIHARA, I., UDA, R., ITO, S., HYODO, M. & HAYAISHI, O. (1994b). Involvement of glutamate receptors in allodynia induced by prostaglandins E_2 and $F_{2\alpha}$ injected into conscious mice. *Pain*, (in press).

MONCADA, S., FLOWER, R.J. & VANE, J.R. (1985). Prostaglandin, prostacyclin, thromboxane A_2 and leukotrienes. In *The Pharmacological Basis of Therapeutics*, 7th edn. ed. Gilman, A.G., Goodman, L.S., Rall, T.W. & Murad, F. pp. 660–673. New York: Macmillan Publishing Co.

MONICK, M., GLAZIER, J. & HUNNIGHAKE, G.W. (1987). Human alveolar macrophages suppress interleukin-1 (IL-1) activity via the secretion of prostaglandin E_2. *Am. Rev. Respir. Dis.*, **135**, 72–77.

NAKAO, A., ALLEN, M.L., SONNENBURG, W.K. & SMITH, W.L. (1989). Regulation of cAMP metabolism by PGE_2 in cortical and medullary thick ascending limb of Henle's loop. *Am. J. Physiol.*, **256**, C652–C657.

NAMBA, T., SUGIMOTO, Y., NEGISHI, M., IRIE, A., USHIKUBI, F., KAKIZUKA, A., ITO, S., ICHIKAWA, A. & NARUMIYA, S. (1993). Alternative splicing of C-terminal tail of prostaglandin E receptor subtype EP3 determines G-protein specificity. *Nature*, **365**, 166–170.

NEGISHI, M., SUGIMOTO, Y., IRIE, A., NARUMIYA, S. & ICHIKAWA, A. (1993). Two isoforms of prostaglandin E receptor EP_3 subtype. *J. Biol. Chem.*, **268**, 9517–9521.

SAMUELSSON, B., GOLDYNE, M., GRANSTRÖM, E., HAMBERG, M., HAMMARSTRÖM, S. & MALMSTEN, C. (1978). Prostaglandins and thromboxanes. *Annu. Rev. Biochem.*, **47**, 997–1029.

SONNENBURG, W.K. & SMITH, W.L. (1988). Regulation of cyclic AMP metabolism in rabbit cortical collecting tubule cells by prostaglandins. *J. Biol. Chem.*, **263**, 6155–6160.

SUGIMOTO, Y., NAMBA, T., HONDA, A., HAYASHI, Y., NEGISHI, M., ICHIKAWA, A. & NARUMIYA, S. (1992). Cloning and expression of a cDNA for mouse prostaglandin E receptor EP_3 subtype. *J. Biol. Chem.*, **267**, 6463–6466.

TAIWO, Y.O. & LEVINE, J.D. (1986). Indomethacin blocks central nociceptive effects of $PGF_{2\alpha}$. *Brain Res.*, **373**, 81–84.

TAIWO, Y.O. & LEVINE, J.D. (1988). Prostaglandins inhibit endogenous pain control mechanism by blocking transmission at spinal noradrenergic synapses. *J. Neurosci.*, **8**, 1346–1349.

UDA, R., HORIGUCHI, S., ITO, S., HYODO, M. & HAYAISHI, O. (1990). Nociceptive effects induced by intrathecal administration of prostaglandin D_2, E_2 or $F_{2\alpha}$ to conscious mice. *Brain Res.*, **510**, 26–32.

WATABE, A., SUGIMOTO, Y., HONDA, A., IRIE, A., NAMBA, T., NEGISHI, M., ITO, S., NARUMIYA, S. & ICHIKAWA, A. (1993). Cloning and expression of cDNA for a mouse prostaglandin E receptor EP_1 subtype. *J. Biol. Chem.*, **268**, 20715–20718.

WILLIS, W.D. Jr. (1992). In *Hyperalgesia and Allodynia*, New York: Raven Press.

WOOLFE, G. & MACDONALD, A.D. (1944). The evaluation of the analgesic action of pethidine hydrochloride (Demerol). *J. Pharmacol. Exp. Ther.*, **80**, 300–307.

YAKSH, T.L. (1982). Central and peripheral mechanisms for the antialgesic action of acetylsalicylic acid. In *Acetylsalicyclic Acid: New Uses for an Old Drug*, ed. Barett, H.J.M., Hirsh, J. & Mustard, J.F. pp. 137–151. New York: Raven Press.

YAKSH, T.L. & AIMONE, L. (1989). The central pharmacology of pain transmission. In *Textbook of Pain*. ed. Wall, P.D. & Melzack, R. pp. 283–320. Edinburgh: Churchill Livingstone.

YAKSH, T.L. & HARTY, G.J. (1988). Pharmacology of the allodynia in rats evoked by high dose intrathecal morphine. *J. Pharmacol. Exp. Ther.*, **244**, 501–507.

ZIMMERMANN, M. (1983). Ethical guidelines for investigations of experimental pain in conscious animals. *Pain*, **16**, 109–110.

(Received February 7, 1994
Revised March 2, 1994
Accepted March 8, 1994)

Br. J. Pharmacol. (1994), **112**, 741–744

Effects of antidepressants on the inward current mediated by 5-HT_3 receptors in rat nodose ganglion neurones

Ping Fan

Laboratory of Molecular and Cellular Neurobiology, National Institute on Alcohol Abuse and Alcoholism, 12501 Washington Ave., Rockville, MD 20852, U.S.A.

1 Effects of three different categories of antidepressants, imipramine (tricyclic), fluoxetine (selective 5-hydroxytryptamine (5-HT) uptake inhibitor), phenelzine and iproniazid (monoamine oxidase (MAO) inhibitor) on the inward current mediated by 5-HT_3 receptors were investigated in rat nodose ganglion neurones. The whole-cell patch-clamp technique was used for recording the 5-HT current.

2 All the antidepressants tested inhibited the peak 5-HT current. The inhibition gradually reached a steady level and the recovery was incomplete when antidepressants were removed. IC_{50} values for imipramine, fluoxetine and phenelzine were 0.54 μM, 1.3 μM and 4.2 μM respectively. The correspondent Hill coefficients were 0.9, 0.87 and 0.92.

3 The antidepressants examined increased the rate of 5-HT current desensitization. IC_{50} values for imipramine, fluoxetine and phenelzine on the decrease in desensitization time constant were 0.11 μM, 0.18 μM and 2.4 μM respectively. The correspondent Hill coefficients were 0.9, 1.14 and 1.06.

4 Intracellular applications of the protein kinase inhibitor, H-7 (100 μM), GDP-β-S (2 mM) and the calcium chelator BAPTA (20 mM) did not affect the 5-HT current and the actions of antidepressants on 5-HT current.

5 These results suggest that the 5-HT_3 receptor is an acting site for the therapeutic use of antidepressants. The present observation is also helpful in explaining the analgesic effect of antidepressants seen in pain clinics.

Keywords: 5-HT_3 receptor; desensitization; patch clamp; nodose ganglion neurone; imipramine; fluoxetine; phenelzine

Introduction

The 5-HT_3 receptor mediates fast synaptic transmission in the central nervous system (Sugita *et al.*, 1992). There is evidence that 5-HT_3 receptors and possibly the 5-HT_3 receptor-mediated synaptic transmission are involved in some psychiatric disorders such as depression (Fozard, 1992; Greenshaw, 1993). Behavioural studies have shown that 5-HT_3 receptor antagonists have a similar effect of that of antidepressants in an animal model of depression (Martin *et al.*, 1992). Receptor binding studies demonstrated a nanomolar binding of antidepressants to quipazine-labelled 5-HT_3 receptor sites in rat cortical membranes (Schmidt & Peroutka, 1989), but this observation was not confirmed by a study using the ICS205930-labelled 5-HT_3 receptor binding sites in neuroblastoma N1E-115 cells and zacopride-labelled binding sites in rat entorhinal cortex (Hoyer *et al.*, 1989). On the other hand, antidepressants are well known to block the 5-hydroxytryptamine (5-HT) reuptake pump and affect 5-hydroxytryptamine neurotransmission. Tricyclic antidepressants block the uptake of both noradrenaline and 5-HT and the antidepressant of the second-generation, fluoxetine, is a highly specific 5-HT uptake inhibitor (Fuller *et al.*, 1991; Hollister, 1992). At concentrations that inhibit the process of amine reuptake, antidepressants have no significant effect on neurotransmitter receptors investigated so far (Richelson & Nelson, 1984; Wander *et al.*, 1986). Antidepressants are also known to produce analgesia in pain clinics and to be especially useful for treating a variety of chronic pain (Hollister, 1992), while 5-HT_3 receptors have been shown to mediate various forms of pain such as the pain perception in peripheral, migraine, angina and irritable bowel syndrome (Fozard & Kalkman, 1992; Greenshaw, 1993). In the present study, the effects of three categories of widely used antidepressants on the inward current mediated by 5-HT_3 receptors in rat nodose ganglion neurones were investigated. They were: imipramine (tricyclic), fluoxetine (the selective 5-HT reuptake inhibitor), phenelzine and iproniazid (monoamine oxidase (MAO) inhibitor).

Methods

Preparation of nodose ganglion neurones

Single neurones were isolated from rat nodose ganglion. The procedure used has been described previously (Ikeda *et al.*, 1986) although some minor changes were made. Briefly, male, adult Sprague-Dawley rats (150–300 g) were killed by decapitation; nodose ganglia were rapidly dissected and placed in cold Dulbecco's modified Eagle's medium (DMEM). Nodose ganglia were then minced with iridectomy scissors and placed in DMEM containing 1.25 mg ml^{-1} collagenase (Sigma type IA), 0.8 mg ml^{-1} trypsin (Sigma type III) and 0.125 mg ml^{-1} deoxyribonuclease (Sigma type IV). The minced tissue was then digested in a waterbath shaker at 35°C for 30 to 45 min, after which soybean trypsin inhibitor (Sigma type IIs, 1 mg ml^{-1}) was added. Neurones were then plated in petri dishes.

Whole cell patch-clamp recording

Neurones were viewed with an inverted microscope and superfused with extracellular solution at 1 ml min^{-1}. The extracellular solution contained (in mM): NaCl 150, KCl 5, $CaCl_2$ 2.5, $MgCl_2$ 1, HEPES 10, D-glucose 10; the pH was adjusted to 7.4 with NaOH, and sucrose was added to adjust the osmolality to 340 mmol kg^{-1}. Experiments were performed at room temperature. The whole cell version of the patch-clamp technique was used by means of an Axopatch-1D amplifier (Axon Instruments). Patch electrodes (2–5 Mohm) were pulled from borosilicate glass (World Precision Instrument Co.) and filled with an internal solution containing (in mM): KCl 140, $MgCl_2$ 2, $CaCl_2$ 1, HEPES 10, EGTA 11, ATP (magnesium salt) 2; the pH was adjusted to 7.4 with KOH and osmolality to 310 mmol kg^{-1} with sucrose. Neurotransmitters and other drugs were dissolved in external solution and applied through a fast perfusion system consisting of a series of fused silica tubes (200–300 μm) glued together and held by a micromanipulator (Narishige). These tubes

were connected to several different reservoirs containing either control or test solutions. The neurone under study was placed within 50 μm of the opening of these tubes and the solution was allowed to perfuse the cell. By rapidly moving the perfusion system laterally, a different solution was applied to the cell. Ion substitution experiment shows that solution exchange is completed within 60 ms (Fan *et al.*, unpublished observations).

Values in the text and figures are means ± s.e.mean. Data were statistically compared by variance analysis or paired *t* test. Concentration-response curves were fitted with the logistic equation (De Lean *et al.*, 1978). Current decay was fitted by the use of Clampfit (Axon Instruments, Inc.). Fits were considered to be good if *r* values were >0.97.

5-HT hydrochloride, iproniazid and H-7 (1-(5 isoquinolinesulphonyl)-2-methyl-piperazine) were purchased from Research Biochemicals Inc. Imipramine, phenelzine and BAPTA (1,2-bis(2-aminophenoxy)ethane-N,N,N′,N′-tetraacetic acid) were from Sigma. GDP-β-S (guanosine-5′-O-(2-thiodiphosphate)) was from Boehringer Mannheim. Fluoxetine hydrochloride was a generous gift from Eli Lilly and Company.

Results

In acutely isolated rat nodose ganglion neurones, 5-HT produced an inward current mediated by 5-HT_3 receptors (Lovinger & White, 1991; Fan *et al.*, 1992). Usually, a stable 5-HT current can be observed 30 to 40 min after establishing whole cell recording conditions. The antidepressants tested (imipramine, fluoxetine, phenelzine and iproniazid) had similar effects on the 5-HT current. The effects of imipramine, fluoxetine and phenelzine were investigated in detail. A current was induced by 3 μM 5-HT which is close to the EC_{50} value of 2.6 μM in rat nodose neurones (Fan and Weight, unpublished data).

Effect of antidepressants on the peak 5-HT current

Data in Figure 1 show that a 3–4 min application of antidepressants inhibited the peak 5-HT current. After the introduction of antidepressants, the 5-HT current was gradually inhibited and the inhibition reached a steady level thereafter (Figure 4a). The recovery of the 5-HT current from the effects of antidepressants was incomplete (Figures 1 and 4a). Concentration-response curves of antidepressants are shown in Figure 2. IC_{50} values for imipramine, fluoxetine and phenelzine were 0.54 μM, 1.3 μM and 4.2 μM. The correspondent Hill coefficients were 0.9, 0.87 and 0.92.

Effect of antidepressants on the desensitization of the 5-HT current

Desensitization of the 5-HT current in the present study was best fitted by a single exponential function (fitting not shown). Antidepressants increased the rate of 5-HT current desensitization by reducing the desensitization time constant (Figures 1 and 3). Figure 3b shows superimposed currents induced by 3 μM 5-HT in control and in the presence of 1 μM fluoxetine. Concentration-response curves of the antidepressant effect on desensitization time constant are shown in Figure 3a. IC_{50} values for imipramine, fluoxetine and phenelzine were 0.11 μM, 0.18 μM and 2.4 μM respectively. The corresponding Hill coefficients were 0.9, 1.14 and 1.06. Similar to their effects on peak current, the reduction of 5-HT current desensitization time constant by antidepressants gradually reached a steady state level and the recovery was incomplete (Figure 4b).

Intracellular messengers in the actions of antidepressants on 5-HT current

There is evidence that intracellular messengers may influence the 5-HT_3 receptor desensitization (Yakel & Jackson, 1988; Yakel *et al.*, 1991). The slow effect of antidepressants on the 5-HT current and the incomplete recovery appear to be the characteristics of the second messenger-mediated actions. Therefore, effects of antidepressants on 5-HT current were investigated in the presence of the protein kinase inhibitor H-7, GDP-β-S, and calcium chelator, BAPTA. Intracellular applications of H-7 (100 μM), GDP-β-S (2 mM) and BAPTA (20 mM with 0 mM intracellular Ca^{2+}) for 10 to 15 min had no effect on the 5-HT current and the actions of antidepressants on 5-HT current (paired *t* test, $P>0.1-0.2$, Figure 5).

Discussion

Results in the present experiments demonstrate that the widely used antidepressants inhibit the peak 5-HT current

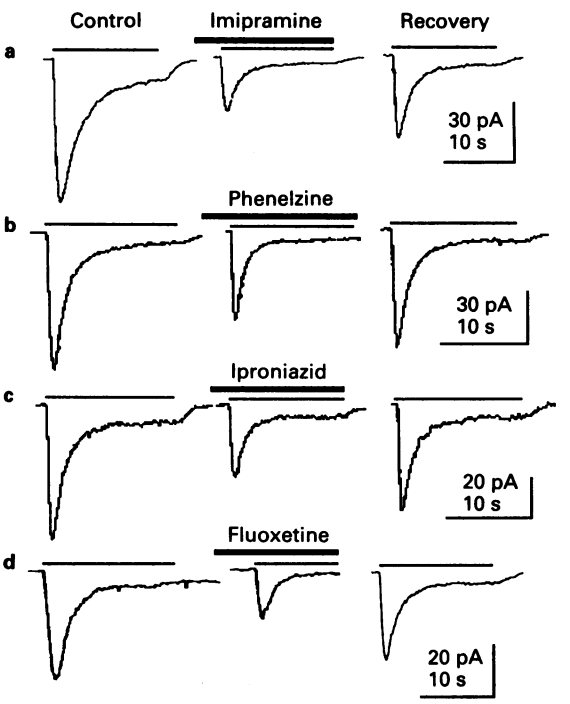

Figure 1 Effects of antidepressants on 5-hydroxytryptamine (5-HT) current. Currents were induced by 3 μM 5-HT which is indicated by thin bars. Recordings in (a), (b), (c) and (d) were from four different cells. Antidepressants (indicated by thick bars) were applied for 3–4 min and then applied together with 5-HT.

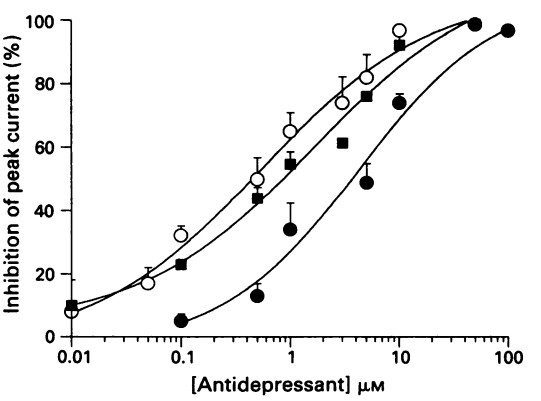

Figure 2 Concentration-response curves of antidepressants on the inhibition of peak current induced by 3 μM 5-hydroxytryptamine (5-HT). Each point represents the average data from 4–9 cells. Data were collected after 5 min application of the tested antidepressant. Standard errors are shown: (○) imipramine; (●) phenelzine; (■) fluoxetine.

and increase the rate of current desensitization. Their effects on 5-HT current were slow, concentration-dependent and the recovery was incomplete. Desensitization of the 5-HT current is obviously more sensitive to antidepressants than the peak current. IC_{50} values of imipramine, fluoxetine and phenelzine on current desensitization are 0.11 μM, 0.18 μM and 2.4 μM while those on peak current are 0.54 μM, 1.6 μM and 4.2 μM. It is possible that the increased desensitization contributes to the inhibition of peak current by antidepressants. Since the effects of antidepressants on 5-HT current were not affected by H-7, GDP-β-S and calcium chelator BAPTA, it is unlikely that G-protein, protein kinases and calcium-dependent processes are involved in the action of these antidepressants.

The daily dosage of imipramine for the treatment of depression is 75–200 mg and those for fluoxetine and phenelzine are 20–80 mg and 45–75 mg respectively (Hollister, 1992). It has been reported that after a single dose of 40 mg fluoxetine, the patient's peak plasma fluoxetine concentration was from 0.042 μM to 0.16 μM and a steady-state plasma concentration of 0.26 to 0.88 μM of fluoxetine was found in patients after thirty-day administration of 40 mg per day (Goodnick, 1991). It has also been reported that the effective plasma concentration of imipramine is between 100 ng ml^{-1} to 300 ng ml^{-1} (0.36 μM to 1.07 μM, Hollister, 1992). Therefore, the effective concentrations of imipramine and fluoxetine observed in the present study are within their therapeutic concentrations. The effective plasma concentration of phenelzine is not well documented. Usually, desirable inhibition of monoamine oxidase can be achieved with a daily dosage of 1 mg kg^{-1} (Hollister, 1992) or 7.3 μM if it is completely absorbed, which is close to the IC_{50} values of phenelzine on 5-HT current (2.4 μM and 4.2 μM). These data suggest that the 5-HT$_3$ receptor is an acting site for the therapeutic use of antidepressants.

Fluoxetine has been shown to increase the synaptic poten-

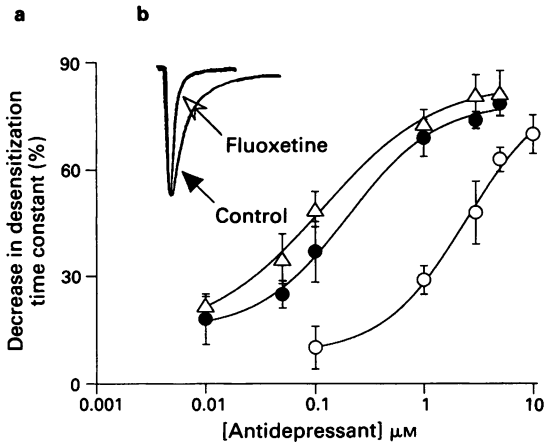

Figure 3 Effect of antidepressants on 5-hydroxytryptamine (5-HT) current desensitization. All currents were induced by 3 μM 5-HT. (a) Concentration-response curves of antidepressants on the reduction of desensitization time constant. Decreases in desensitization time constant were plotted against concentrations of antidepressants (in μM). Each point represents the average data from 3–9 cells. Data were collected after 5 min application of tested antidepressant. Standard errors are shown. (△) Imipramine; (○) phenelzine; (●) fluoxetine. (b) Sample recordings obtained in control (time constant: 1698 ms) and the presence of 5 μM fluoxetine (amplitude normalized to that of control, time constant: 355 ms).

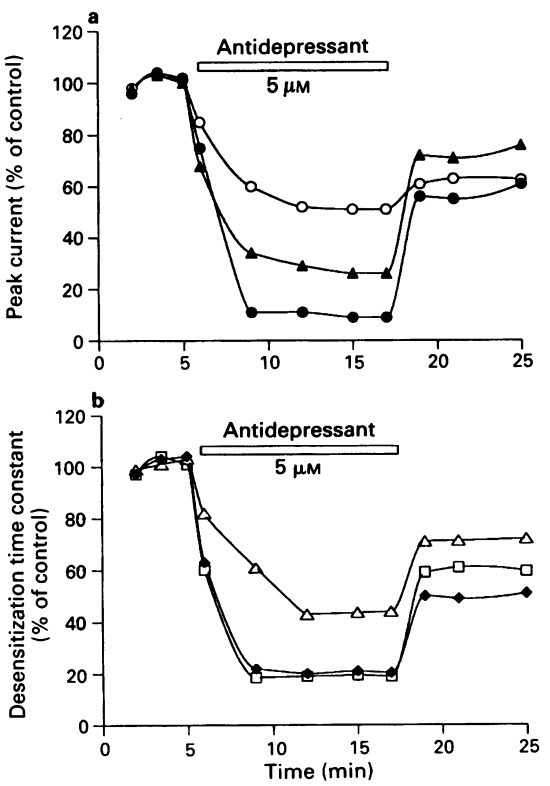

Figure 4 Time course of the effects of antidepressants on 5-hydroxytryptamine (5-HT) current. Currents were induced by 3 μM 5-HT. Three samples were collected before the administration of antidepressants and the average was taken as 100%. Compared to control, the difference for all the points after the application of 5 μM antidepressants (indicated by a bar) is highly significant ($P<0.05$–0.001), $n = 7$; 5, 9 for phenelzine, imipramine and fluoxetine respectively. (a) Effect on peak current: (●) imipramine; (○) phenelzine; (▲) fluoxetine. (b) Effect on current desensitization: (□) imipramine; (△) phenelzine; (◆) fluoxetine.

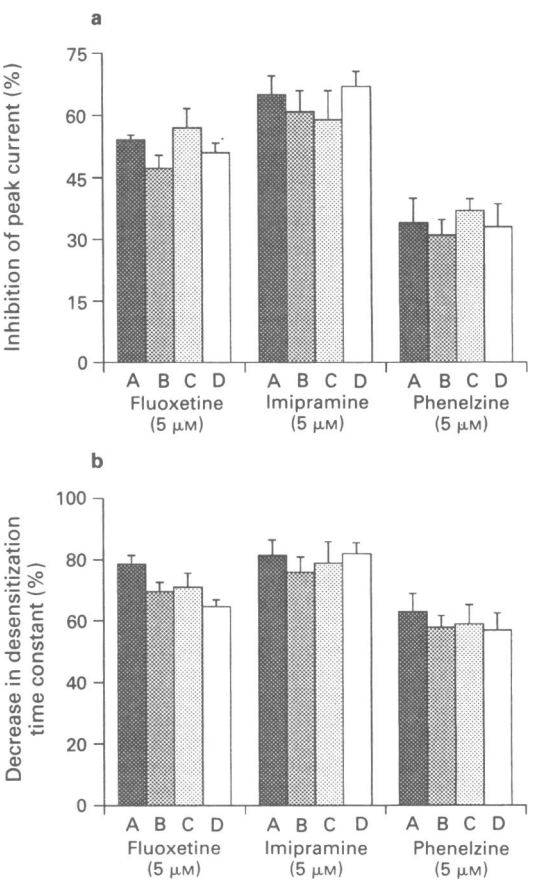

Figure 5 Effects of antidepressants on 5-hydroxytryptamine (5-HT) current under different conditions. Currents were induced by 3 μM 5-HT. Effects of 1 μM antidepressants were examined with and without intracellular H-7, GDP-β-S and BAPTA. Each category of experiment contains the average data from 4–7 cells. Standard errors are shown: (A) control; (B) H-7; (C) BAPTA; (D) GDP-β-S.

tials mediated by 5-HT_3 receptors in brain slices (Sugita *et al.*, 1992), while the present study demonstrates a 5-HT_3 receptor antagonist property of fluoxetine in isolated nodose ganglion neurones. There may be several reasons for the different effects of fluoxetine. First, it is likely that fluoxetine inhibited 5-HT uptake in brain slices and therefore increased the concentration of 5-HT in the synaptic cleft, resulting in increased synaptic potentials. In the present experiments, isolated nodose neurones were rapidly superfused and flooded with 5-HT when the agonist was applied. Thus, inhibition of 5-HT uptake by fluoxetine in this study should not have altered the concentration of 5-HT bathing the neurones. Second, stimulation of presynaptic terminals may activate both excitatory and inhibitory synaptic transmissions. Fluoxetine may inhibit the 5-HT_3 receptor-mediated excitation on inhibitory interneurones, block some of the inhibitory transmissions and therefore increase the excitatory synaptic potential. Third, 5-HT_3 receptors may have different pharmacological properties in different species and different tissues (Tyers, 1990; Newberry *et al.*, 1991; Peters *et al.*, 1992). The 5-HT_3 receptor in the central nervous system may be less sensitive or insensitive to fluoxetine. If this is the case, the antidepressant effect of fluoxetine is not mediated by its action on the peripheral 5-HT_3 receptors.

Antidepressants have been used in patients to produce pain relief (Hollister, 1992) and 5-HT_3 receptors have been reported to mediate the peripheral pain perception and the flare response induced by local application of 5-HT in man (Richardson *et al.*, 1985; Orwin & Fozard, 1986). 5-HT_3 receptor antagonists blocked these painful responses and reduced acute and chronic inflammatory pain (Eschalier *et al.*, 1989; Giordano & Rogers, 1989; Giordano & Dyche, 1989). 5-HT_3 receptor antagonists may also be effective in migraine, angina and irritable bowel syndrome (for review, see Fozard & Kalkman, 1992; Greenshaw, 1993). These observations suggest that the inhibition of 5-HT_3 receptors by antidepressants may help to explain the analgesic effect of antidepressants.

References

DE LEAN, A., MUNSON, P.J. & RODBARD, D. (1978). Simultaneous analysis of families of sigmoidal curves. *Am. J. Physiol.*, **235**, E97–E102.

ESCHALIER, A., KAYSER, V. & GUILBAUD, G. (1989). Influence of a specific 5-HT3 antagonist on carrageenan-induced hyperalgesia in rats. *Pain*, **36**, 249–255.

FAN, P., VISENTIN, S. & WEIGHT, F.F. (1992). 5-HT_3 channel activation by serotonin is antagonized by cocaine in neurons from rat nodose ganglion. *Soc. Neurosci. Abstr.*, **18**, 800.

FOZARD, J.R. (1992). Pharmacological relevance of 5-HT_3 receptors. In *Serotonin Receptor Subtypes: Pharmacological Significance and Clinical Implications*. ed. Langer, S.Z., Brunello, N., Racagni, G. & Mendlewicz, J. *Int. Acad. Biomed. Drug Res.*, Vol. 1, pp. 44–55. Basel: Karger.

FOZARD, J.R. & KALKMAN, H.O. (1992). 5-HT in nervous system disease and migraine. *Curr. Opin. Neurol.*, **5**, 496–502.

FULLER, R.W., WONG, D.T. & ROBERTSON, D.W. (1991). Fluoxetine, a selective inhibitor of serotonin uptake. *Med. Res. Rev.*, **11**, 17–34.

GIORDANO, J. & DYCHE, J. (1989). Differential analgesic actions of serotonin 5-HT3 receptor antagonists in the mouse. *Neuropharmacol.*, **28**, 423–427.

GIORDANO, J. & ROGERS, L.V. (1989). Peripherally administered serotonin 5-HT3 receptor antagonists reduce inflammatory pain in rats. *Eur. J. Pharmacol.*, **170**, 83–86.

GOODNICK, P.J. (1991). Pharmacokinetics of second generation antidepressants: fluoxetine. *Psychopharmacol. Bull.*, **27**, 503–512.

GREENSHAW, A.J. (1993). Behavioural pharmacology of 5-HT_3 receptor antagonists: a critical update on therapeutic potential. *Trends Pharmacol. Sci.*, **14**, 265–270.

HOLLISTER, L.E. (1992). Antidepressant agents. In *Basic and Clinical Pharmacology*. ed. Katzung, B. pp. 410–419. Norwalk: Appleton & Lange.

HOYER, D., GOZLAN, H., BOLANOS, F., SCHECHTER, L.E. & HAMON, M. (1989). Interaction of psychotropic drugs with central 5-HT_3 recognition sites: fact or artifact? *Eur. J. Pharmacol.*, **171**, 137–139.

IKEDA, S.R., SCHOFIELD, G.G. & WEIGHT, F.F. (1986). Na^+ and Ca^{2+} currents of acutely isolated adult rat nodose ganglion cells. *J. Neurophysiol.*, **55**, 527–539.

LOVINGER, D.M. & WHITE, G. (1991). Ethanol potentiation of 5-hydroxytryptamine$_3$ receptors-mediated ion current in neuroblastoma cells and isolated adult mammalian neurons. *Mol. Pharmacol.*, **40**, 263–270.

MARTIN, P., GOZLAN, H. & PUECH, A.J. (1992). 5-HT_3 receptor antagonists reverse helpless behaviour in rats. *Eur. J. Pharmacol.*, **212**, 73–78.

NEWBERRY, N.R., CHESHIRE, S.H. & GILBERT, M.J. (1991). Evidence that the 5-HT_3 receptors of rat, mouse and guinea-pig superior cervical ganglion may be different. *Br. J. Pharmacol.*, **102**, 615–620.

ORWIN, J.M. & FOZARD, J.R. (1986). Blockade of the flare response to intradermal 5-hydroxytryptamine in man by MDL 72222, a selective antagonist at neuronal 5-hydroxytryptamine receptors. *Eur. J. Clin. Pharmacol.*, **30**, 209–212.

PETERS, J.A., MALONE, H.M. & LAMBERT, J.J. (1992). Recent advances in the electrophysiological characterization of 5-HT_3 receptors. *Trends Pharmacol. Sci.*, **13**, 391–397.

RICHARDSON, B.P., ENGEL, G., DONATSCH, P. & STADLER, P.A. (1985). Identification of serotonin receptor subtypes and their specific blockade by a new class of drugs. *Nature*, **316**, 126–131.

RICHELSON, E. & NELSON, A. (1984). Antagonism by antidepressants of neurotransmitter receptors of normal human brain in vivo. *J. Pharmacol. Exp. Ther.*, **230**, 94–102.

SCHMIDT, A.W. & PEROUTKA, S.J. (1989). Antidepressant interactions with 5-hydroxytryptamine3 receptor binding sites. *Eur. J. Pharmacol.*, **163**, 397–398.

SUGITA, S., SHEN, K.Z. & NORTH, R.A. (1992). 5-Hydroxytryptamine is a fast excitatory transmitter at 5-HT_3 receptors in rat amygdala. *Neuron*, **8**, 199–203.

TYERS, M.B. (1990). 5-HT_3 receptors. *Ann. N.Y. Acad. Sci.*, **600**, 194–205.

WANDER, T., NELSON, A. & OKASAKI, H. (1986). Antagonism by antidepressants of serotonin S_1 and S_2 receptors of normal human brain in vivo. *Eur. J. Pharmacol.*, **132**, 115–121.

YAKEL, J.L. & JACKSON, M.B. (1988). 5-HT_3 receptors mediated rapid responses in cultured hippocampus and a cloned cell line. *Neuron*, **1**, 615–621.

YAKEL, J.L., SHAO, X.M. & JACKSON, M.B. (1991). Activation and desensitization of the 5-HT_3 receptor in a rat glioma + mouse neuroblastoma hybrid cell. *J. Physiol.*, **436**, 293–308.

(Received January 17, 1994
Revised March 8, 1994
Accepted March 9, 1994)

Br. J. Pharmacol. (1994), **112**, 745–748

Mepacrine-induced inhibition of the inward current mediated by 5-HT_3 receptors in rat nodose ganglion neurones

Ping Fan

Laboratory of Molecular and Cellular Neurobiology, National Institute on Alcohol Abuse and Alcoholism, 12501 Washington Ave., Rockville, MD 20852, U.S.A.

1 With the whole-cell patch clamp technique, the effect of the antimalarial drug, mepacrine (quinacrine) on the inward current mediated by 5-HT_3 receptors (5-hydroxytryptamine (5-HT)-induced current) was investigated in isolated nodose ganglion neurones of the rat.

2 5-HT and the selective 5-HT_3 receptor agonists, 2-methyl-5-HT and *m*-chlorophenylbiguanide elicited an inward current which reversed at around 0 mV and quickly desensitized to a steady state level.

3 Mepacrine dose-dependently inhibited the peak current induced by 5-HT with an IC_{50} of 2.1 μM and an apparent Hill coefficient of 0.99.

4 Mepacrine increased the decay rate of the 5-HT-induced current.

5 The effect of mepacrine on the 5-HT-induced current was reversible and not dependent on membrane potential. The reversal potential of the 5-HT-induced current was not affected.

6 Intracellular mepacrine had no significant effect on the 5-HT-induced current and did not block the extracellular action of mepacrine.

7 Concentration-response curves in the presence and absence of mepacrine suggest a non-competitive inhibition of 5-HT-induced current by mepacrine.

Keywords: Nodose ganglion; mepacrine; quinacrine; 5-HT_3 receptor; patch-clamp

Introduction

Mepacrine (quinacrine) is an antimalarial drug (Webster, 1990). It has been widely used as an inhibitor for phospholipase A_2 which is a major enzyme in the release of free arachidonic acid (Vernon & Bell, 1992; Glaser *et al.*, 1993). Treatment with mepacrine has become one of the pharmacological tools to evaluate the role of arachidonic acid in cellular functions (Blackwell *et al.*, 1977; Billah *et al.*, 1981; Snyder *et al.*, 1992). However, mepacrine also has other effects on cellular physiology. It binds to DNA (Darzynkiewicz *et al.*, 1984), increases the pH of lysosomes (DiCerbo *et al.*, 1984), competes with the binding of acetylcholine to muscarinic and nicotinic receptors (O'Donnell & Howlett, 1991; Grunhagen & Changeux, 1976; Cox *et al.*, 1985) and may have local anaesthetic-like actions (Grunhagen & Changeux, 1976). Several studies have shown that mepacrine interacts with voltage-gated ion channels such as the fast transient outward K^+ channels in rat melanotrophs (Kehl, 1991) and the high-threshold Ca^{2+} channel in rat hippocampal cells (Mironov & Lux, 1992). Mepacrine has also been reported to inhibit Na^+/H^+ exchange (Karmazyn *et al.*, 1990), Na^+/Ca^{2+} exchange (Shepherd *et al.*, 1991) and to protect animals from myocardial ischaemia (Chariello *et al.*, 1987; Sargent *et al.*, 1992). In the present study, mepacrine was found to inhibit the inward current mediated by 5-HT_3 receptors in rat nodose ganglion neurones and to increase the rate of current decay. Results presented here also indicate that inhibition of phospholipase A_2 may not be involved in the effect of mepacrine on the 5-HT_3 receptor-mediated inward current.

Methods

Preparation of nodose ganglion neurones

Single neurones were isolated from rat nodose ganglion. The procedure used has been described previously (Ikeda *et al.*, 1986) although some minor changes were made. Briefly, male, adult Sprague-Dawley rats (150–300 g) were killed by decapitation; nodose ganglia were rapidly dissected and placed in cold Dulbecco's modified Eagle's medium (DMEM). Nodose ganglia were then minced wih iridectomy scissors and digested in DMEM containing 1.25 mg ml^{-1} collagenase (type IA), 0.8 mg ml^{-1} trypsin (type III) and 0.125 mg ml^{-1} deoxyribonuclease (type IV) at 35°C for 30 to 45 min, after which soybean trypsin inhibitor (Sigma type IIs, 1 mg ml^{-1}) was added. Neurones were then plated in petri dishes.

Whole cell patch-clamp recording

Neurones were viewed with an inverted microscope and superfused with extracellular solution at 1 ml min^{-1}. The extracellular solution contained (in mM): NaCl 150, KCl 5, $CaCl_2$ 2.5, $MgCl_2$ 1, HEPES 10, D-glucose 10; the pH was adjusted to 7.4 with NaOH, and sucrose was added to adjust the osmolality to 340 mmol kg^{-1}. Experiments were performed at room temperature. The whole cell version of the patch-clamp technique was used by means of an Axopatch-1D amplifier (Axon Instruments). Patch electrodes (2–5 Mohm) were pulled from borosilicate glass (World Precision Instrument Co.) and filled with an internal solution containing (in mM): KCl 140, $MgCl_2$ 2, $CaCl_2$ 1, HEPES 10, ATP (magnesium salt) 2; the pH was adjusted to 7.4 with KOH and osmolality to 310 mmol kg^{-1} with sucrose. Neurotransmitters and other drugs were dissolved in external solution and applied through a fast perfusion system consisting of a series of fused silica tubes (200–300 μm) glued together and held by a micromanipulator (Narishige). These tubes were connected to several different reservoirs containing either control or test solutions. The neurone under study was placed within 50 μm of the opening of these tubes and the solution was allowed to perfuse the cell. By rapidly moving the perfusion system laterally, a different solution was applied to the cell.

Values in the text and figures are means ± s.e.mean. Data were statistically compared by variance analysis of paired *t* test. Concentration-response curves were fitted with the logis-

tic equation (De Lean *et al.*, 1978). Current decay was fitted by the use of Clampfit (Axon Instruments, Inc.). Fits were considered to be good if r values were >0.97.

5-Hydroxytryptamine (5-HT) hydrochloride, 2-methyl-5-HT and *m*-chlorophenylbiguanide were purchased from Research Biochemicals Inc. Quinacrine dihydrochloride was from Sigma.

Results

Previous studies have demonstrated that in rat nodose ganglion neurones, 5-HT produced an inward current mediated by 5-HT_3 receptors (Lovinger & White, 1991; Lovinger, 1991; Fan *et al.*, 1992). This current was induced in the present study at a holding potential of -50 mV. The selective 5-HT_3 agonists, 2-methyl-5-HT and *m*-chlorophenylbiguanide induced a current with similar kinetics (Figure 1a). Mepacrine reduced the peak current induced by 5-HT in a concentration-dependent manner (Figure 1b,c). The effect of mepacrine reached a steady level after 3–4 min of application. The concentration-response curve revealed an IC_{50} of 2.1 μM and an apparent Hill coefficient of 0.99 (Figure 1c). The effect of mepacrine was reversible (Figure 1b).

The 5-HT-induced current reverses at around 0 mV. Mepacrine did not change the reversal potential of 5-HT-induced current and its effect on 5-HT-induced current was not dependent on membrane potential ($n = 5$). The current-

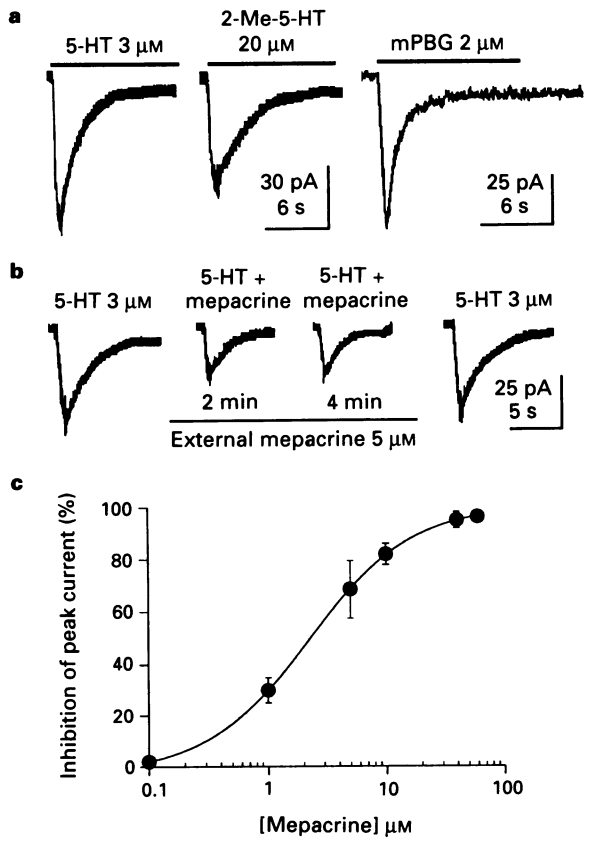

Figure 1 Effect of mepacrine on the inward current mediated by 5-HT_3 receptors. (a) Inward currents induced by 5-hydroxytryptamine (5-HT), 2-methyl-5-HT (2-Me-5-HT) and *m*-chlorophenylbiguanide (mPBG). Currents induced by 5-HT and 2-Me-5-HT were from the same cell. (b) Mepacrine inhibited the current induced by 3 μM 5-HT. (c) Concentration-response curve for mepacrine. Each point represents the average data from 4–9 cells. Mepacrine was applied for 3–4 min and then applied together with 5-HT. Standard errors are shown.

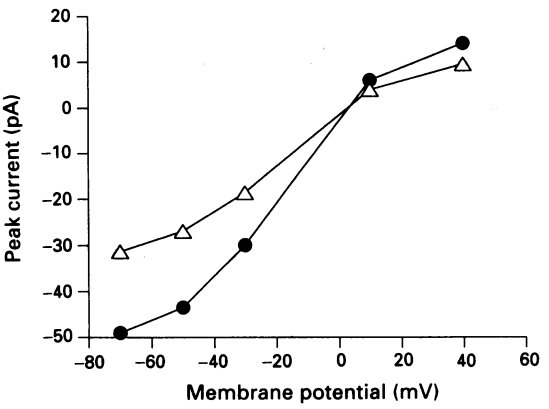

Figure 2 The current-voltage relationship for the 5-hydroxytryptamine (5-HT)-induced current. The curve was obtained by measuring the 5-HT-induced current at different membrane potentials (from -75 to $+40$ mV). Mepacrine did not affect the current reversal potential, which was $+1$ mV in this cell, and antagonized the 5-HT-induced current with no voltage-dependency. A similar effect was observed in another four cells. (●) Control; (△) 5 μM mepacrine.

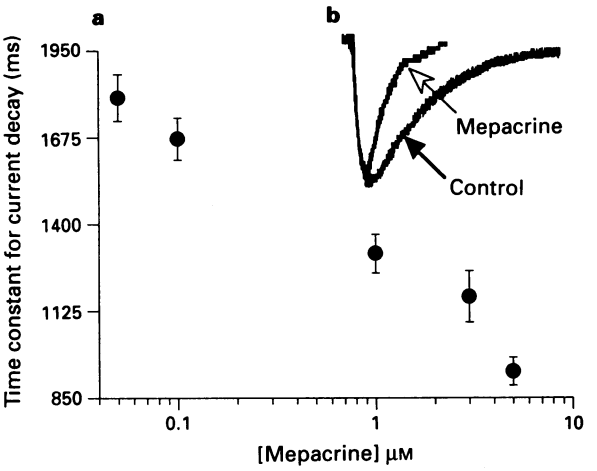

Figure 3 Mepacrine increased the rate of the 5-hydroxytryptamine (5-HT)-induced current decay. (a) The time constant for the 5-HT-induced current decay was plotted against mepacrine concentrations. Each point represents the average data from 3–6 cells. Mepacrine was applied for 3–4 min and then applied together with 3 μM 5-HT. (b) An example of the mepacrine effect on current decay. Amplitude of the 5-HT-induced current after 3 min application of mepacrine (5 μM) was normalized to that of control.

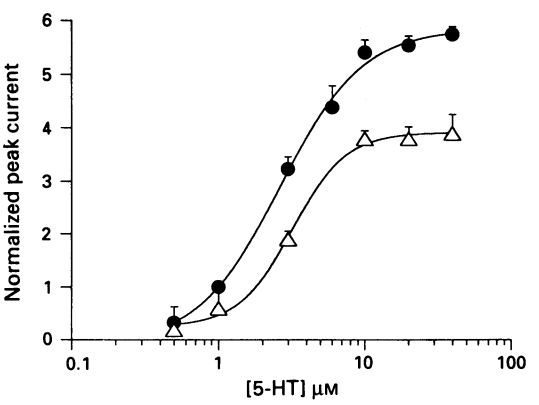

Figure 4 Concentration-response curves for 5-hydroxytryptamine (5-HT) in control (●) and in the presence of 5 μM mepacrine (△). Mepacrine (5 μM) was applied for 3–4 min and then applied together with 5-HT. Current amplitude was normalized relative to that induced by 1 μM 5-HT. Each point contains data from four to five cells. Standard errors are shown when they are bigger than the size of the symbols.

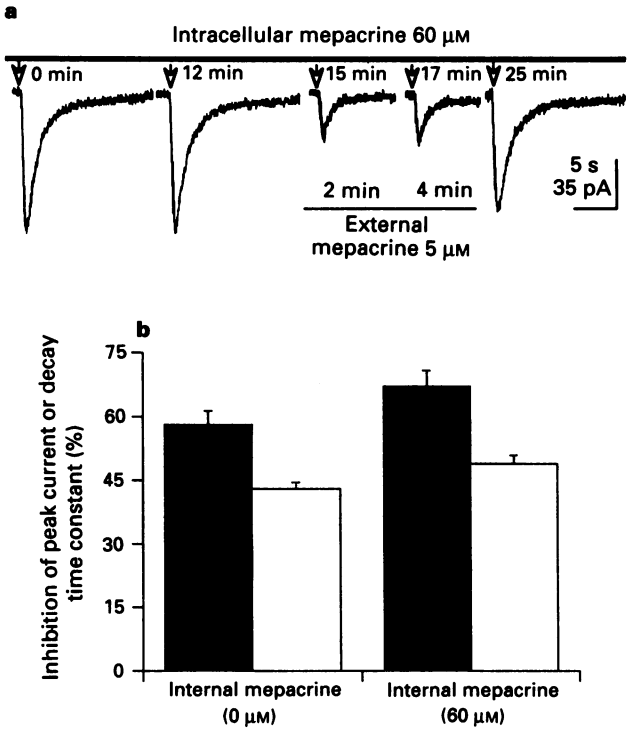

Figure 5 Effect of extracellular mepacrine on the 5-hydroxytryptamine (5-HT)-induced current in the presence of intracellular mepacrine (60 μM, a, $n = 5$). Intracellular mepacrine is indicated by a thick bar and time after cell rupture is shown above each tracing. Four minute application of 5 μM extracellular mepacrine is indicated by a thin bar. Arrows: 15 s application of 3 μM 5-HT. (b) Averaged data for the effect of mepacrine on the 5-HT-induced current under different conditions: solid column: peak current: open column: decay time constant.

voltage relation curves in the absence and presence of mepacrine are shown in Figure 2.

During prolonged application of agonist, the 5-HT-induced current decayed to a steady state level in a few seconds (Figure 1a,b). Decay of the 5-HT-induced current was best fitted by a single exponential function (fitting not shown). In the presence of mepacrine, the rate of the 5-HT-induced current decay was increased and the current decay was still best fitted by a single exponential function. Data in Figure 3a show the time constant for the 5-HT-induced current decay at different mepacrine concentrations.

Figure 4 shows the concentration-response curves with or without 5 μM mepacrine. Mepacrine was applied for 3–4 min and then applied together with 5-HT. All the responses were normalized to the peak response induced by 1 μM 5-HT. Mepacrine depressed the maximal response without an apparent shift of EC_{50} values. The EC_{50} was 2.6 μM in control conditions and was 3.1 μM in the presence of mepacrine. This observation suggests a non-competitive inhibition of the 5-HT-induced current by mepacrine.

To investigate the involvement of intracellular messengers, mepacrine was also applied intracellularly through recording electrodes. The current immediately after the cell was ruptured was taken as control. Intracellular mepacrine (60 μM, $n = 7$) had no significant effect on the 5-HT-induced current at 20 to 30 min after the cell was ruptured and did not block the effect of extracellular mepacrine (Figure 5). Mepacrine (5 μM) reduced the peak current and time constant of current decay by 58 ± 5.6% and 43 ± 2.6% respectively in the absence of intracellular mepacrine. With 60 μM intracellular mepacrine, the inhibitions of peak current and time constant by 5 μM extracellular mepacrine were 67 ± 5.5% and 49 ± 2.8% respectively (Figure 5b).

Discussion

The present study demonstrates that micromolar concentrations of mepacrine non-competitively inhibit the inward current mediated by 5-HT$_3$ receptors with an IC_{50} of 2.1 μM. At this concentration-range, mepacrine inhibited acetylcholine bindings to muscarinic (O'Donnell & Howlett, 1991) and nicotinic receptors (Grunhagen & Changeux, 1976; Cox *et al.*, 1985), decreased voltage-gated Ca^{2+} currents (Mironov & Lux, 1992; Sargent *et al.*, 1992) and a fast transient outward K^+ current (Kehl, 1991), depressed Na^+/Ca^{2+} and Na^+/H^+ exchange (Shepherd *et al.*, 1991; Karmazyn *et al.*, 1990) and had a cardioprotective effect against ischaemia (Chiariello *et al.*, 1987; Sargent *et al.*, 1992). All these mepacrine effects were independent of phospholipase A_2 activity, although the effective mepacrine concentration for the inhibition of phospholipase A_2 is also in this range (Billah *et al.*, 1981). The present observation that intracellular mepacrine exhibits no significant effect on the 5-HT-induced current does not support the involvement of phospholipase A_2 in the effect of mepacrine. Therefore, the results with mepacrine treatment should be interpreted with care.

The effect of mepacrine on the 5-HT-induced current was not voltage-dependent and mepacrine did not change the reversal potential of the 5-HT-induced current (Figure 2). These results indicate that the ionic permeability of the 5-HT$_3$ receptor-ion channel was not affected by mepacrine. Lack of effect by internal mepacrine (Figure 5) reveals that the mepacrine binding site is most likely to be on the external face of the membrane, while the non-competitive dose-response curve suggests that this site is different from the agonist binding site. From these observations, the effect of mepacrine on 5-HT$_3$ receptors appears to be different from its effect on acetylcholine receptors. O'Donnell & Howlett (1991) reported that mepacrine acted at the agonist binding site on acetylcholine muscarinic receptors and shifted the dose-response curve in a parallel fashion. Similarly, mepacrine also acted at the acetylcholine binding site on nicotinic receptors (Grunhagen & Changeux, 1976; Cox *et al.*, 1985), although mepacrine may affect other sites of acetylcholine binding such as acetylcholine uptake protein (Anderson *et al.*, 1983).

Mepacrine increased the rate of the 5-HT-induced current decay. This effect is also concentration-dependent. It seems that mepacrine is similar to some non-competitive antagonists of ligand-gated ion channels, which usually act at sites other than the agonist binding sites and increase receptor desensitization. A well known example is the effect of local anaesthetics on nicotinic receptors (Neher & Steinbach, 1978). A local anaesthetic-like effect of mepacrine on nicotinic receptors has been reported (Grunhagen & Changeux, 1976). However, our previous results demonstrate that local anesthetics such as cocaine, procaine and tetracaine exhibit a competitive blockade on the activation of 5-HT$_3$ receptors (Fan *et al.*, 1992; Fan & Weight, 1993). Therefore, for the 5-HT$_3$ receptors, the effect of mepacrine is obviously different from that caused by local anaesthetics.

Recently, Kooyman *et al.* (1993) demonstrated that tetraethylammonium ion, a potassium channel blocker like mepacrine, blocks the 5-HT$_3$ receptor-mediated ion current in neuroblastoma N1E-115 cells. However, the effect of tetraethylammonium ions is different from that of mepacrine. It acts at the 5-HT recognition site and prevents desensitization while mepacrine increases the receptor desensitization.

In conclusion, the inhibition of the 5-HT-induced current by mepacrine was through an action on the extracellular face of the membrane, was non-competitive, voltage-independent and was probably not connected with phospholipase A_2 activity.

The author is grateful to Dr J.C. Szerb for reading the manuscript.

References

ANDERSON, D.C., KING, S.C. & PARSONS, S.M. (1983). Pharmacological characterization of acetylcholine transport system in purified Torpedo electric organ synaptic vesicles. *Mol. Pharmacol.*, **24**, 48–54.

BILLAH, M.M., LAPETINA, E.G. & CUATRECASAS, P. (1981). Phospholipase A_2 activity specific for phosphatidic acid. *J. Biol. Chem.*, **256**, 5399–5403.

BLACKWELL, G.J., DUNCOMBE, W.G., FLOWER, R.J., PARSONS, M.F. & VANE, J.R. (1977). The distribution and metabolism of arachidonic acid in rabbit platelets during aggregation and its modification by drugs. *Br. J. Pharmacol.*, **59**, 353–366.

CHIARIELLO, M., AMBROSIO, G., CAPPELLI-BIGAZZI, M., NEVOLA, E., PERONE-FILARDI, P., MARONE, G. & CONDORELLI, M. (1987). Inhibition of ischemia-induced phospholipase activation by quinacrine protects jeopardized myocardium in rats with coronary artery occlusion. *J. Pharmacol. Exp. Ther.*, **241**, 560–568.

COX, R.N., KALDANY, R.R.J., DIPOALA, M. & KARLIN, A. (1985). Time-resolved photolabelling by quinacrine azide of a non-competitive inhibitor site of the nicotinic acetylcholine receptor in a transient, agonist-induced state. *J. Biol. Chem.*, **260**, 7186–7193.

DARZYNKIEWICZ, Z., TRAGANOS, F., KAPUSCINSKI, J., STAIANO-COICO, L. & MELAMED, M.R. (1984). Accessibility of DNA in situ to various fluorchromes. *Cytometry*, **5**, 355–363.

DE LEAN, A., MUNSON, P.J. & RODBARD, D. (1978). Simultaneous analysis of families of sigmoidal curves. *Am. J. Physiol.*, **235**, E97–E102.

DiCERBO, A., NANDI, P.K. & EDELHOCH, H. (1984). Interaction of basic compounds with coated vesicles. *Biochemistry*, **23**, 6036–6040.

FAN, P., VISENTIN, S. & WEIGHT, F.F. (1992). 5-HT_3 channel activation by serotonin is antagonized by cocaine in neurons from rat nodose ganglion. *Soc. Neurosci. Abstr.*, **18**, 800.

FAN, P. & WEIGHT, F.F. (1993). Effect of procaine on the function of 5-HT_3 receptor ion-channels. *Soc. Neurosci. Abstr.*, **19**, 282.

GLASER, K.B., MOBILIO, D., CHANG, J.Y. & SENKO, N. (1993). Phospholipase A_2 enzymes: regulation and inhibition. *Trends Pharmacol. Sci.*, **14**, 92–98.

GRUNHAGEN, H.H. & CHANGEUX, J.P. (1976). Studies on the electrogenic action of acetylcholine with Torpedo marmorata electric organ. *J. Mol. Biol.*, **106**, 497–516.

IKEDA, S.R., SCHOFIELD, G.G. & WEIGHT, F.F. (1986). Na^+ and Ca^{2+} currents of acutely isolated adult rat nodose ganglion cells. *J. Neurophysiol.*, **55**, 527–539.

KARMAZYN, M., WATSON, J.E. & MOFFAT, M.P. (1990). Mechanisms of cardiac depression induced by phorbol myristate acetate in working rat hearts. *Br. J. Pharmacol.*, **100**, 826–830.

KEHL, S.J. (1991). Quinidine-induced inhibition of the fast transient outward K^+ current in rat melanotrophs. *Br. J. Pharmacol.*, **103**, 1807–1813.

KOOYMAN, A.R., ZWART, R. & VIJVERBERG, H.P. (1993). Tetraethylammonium ions block 5-HT3 receptor-mediated ion current at the agonist recognition site and prevent desensitization in cultured mouse neuroblastoma cells. *Eur. J. Pharmacol.*, **246**, 247–254.

LOVINGER, D.M. (1991). Ethanol potentiation of 5-hydroxytryptamine$_3$ receptors-mediated ion current in NCB 20 neuroblastoma cells. *Neurosci. Lett.*, **122**, 57–60.

LOVINGER, D.M. & WHITE, G. (1991). Ethanol potentiation of 5-hydroxytryptamine$_3$ receptors-mediated ion current in neuroblastoma cells and isolated adult mammalian neurons. *Mol. Pharmacol.*, **40**, 263–270.

MIRONOV, S.L. & LUX, H.D. (1992). The selective action of quinacrine on high threshold calcium channels in rat hippocampal cells. *Br. J. Pharmacol.*, **106**, 751–755.

NEHER, E. & STEINBACH, J.H. (1978). Local anesthetics transiently block currents through single acetylcholine receptor channels. *J. Physiol.*, **277**, 153–176.

O'DONNELL, K.A. & HOWLETT, A.C. (1991). Muscarinic receptor binding is inhibited by quinacrine. *Neurosci. Lett.*, **127**, 46–48.

SARGENT, C.A., VESTERQVIST, O., MCCULLOUGH, J.R., OGLETREE, M.L. & GROVER, G.J. (1992). Effect of the phospholipase A_2 inhibitors quinacrine and 7,7-dimethyleicosadienoic acid in isolated globally ischemic rat hearts. *J. Pharmacol. Exp. Ther.*, **262**, 1161–1167.

SHEPHERD, N., KAVALER, F. & SPIELMAN, W. (1991). Cadmium block of isometric contractions of isolated bullfrog atrial cells. *Am. J. Physiol.*, **260**, C249–C258.

SNYDER, D.W., SOMMERS, C.D., BOBBITT, J.L. & MIHELICH, E.D. (1992). Evidence that phospholipase A_2 inhibitors can selectively block PLA_2-mediated contraction of guinea pig lung pleural strips. *J. Pharmacol. Exp. Ther.*, **262**, 1147–1153.

VERNON, L.P. & BELL, J.D. (1992). Membrane structure toxins and phospholipase A_2 activity. *Pharmacol. Ther.*, **54**, 269–295.

WEBSTER, L.T. (1990). Drugs used in the chemotherapy of protozoal infection. In *The Pharmacological Basis of Therapeutics*. ed. Gilman, A.G., Rall, T.W., Nies, A.S. & Taylor, P. pp. 978–1018. New York: Pergamon Press.

(Received January 21, 1994
Revised March 8, 1994
Accepted March 9, 1994).

Br. J. Pharmacol. (1994), **112**, 749–756

Predominance of endothelin$_A$ (ET_A) receptors in ovine airway smooth muscle and their mediation of ET-1-induced contraction

[1]Roy G. Goldie, Peta S. Grayson, Patrick G. Knott, Glenn J. Self & Peter J. Henry

Department of Pharmacology, University of Western Australia, Nedlands, 6009, Australia

1 Autoradiographic studies were conducted to investigate the receptor subtypes for endothelin-1 (ET-1) that were present in the ovine respiratory tract. In addition, the receptor subtypes mediating contraction of airway smooth muscle and the possible involvement of extracellular Ca^{2+} and inositol phosphate generation in intracellular signal transduction were assessed.

2 Specific [^{125}I]-ET-1 binding in ovine trachea increased in a time- and concentration-dependent manner. Autoradiographic studies demonstrated that significant binding was associated with airway smooth muscle, although higher densities of specific binding were associated with submucosal glands and with cells immediately below the epithelial basement membrane (lamina propria). The ET_A receptor-selective antagonist, BQ 123 (1 μM), virtually abolished specific binding to airway smooth muscle. Quantitative analyses of autoradiographic data describing the time-dependence of specific [^{125}I]-ET-1 binding in ovine airway smooth muscle in the presence and absence of BQ 123 or sarafotoxin S6c, revealed a homogeneous population of ET_A receptors. BQ 123 (1 μM) also abolished specific binding to structures associated with submucosal glands, whereas the ET_B receptor selective agonist, sarafotoxin S6c (100 nM) had little effect on this binding, indicating the predominance of ET_A receptors at these sites. In contrast, ET_B receptors predominated in the lamina propria, since sarafotoxin S6c abolished specific binding in this tissue.

3 High levels of specific [^{125}I]-ET-1 binding were also detected in the alveoli and in the walls of blood vessels and small airways in ovine peripheral lung. Specific binding associated with alveoli was reduced to similar extents by BQ 123 (1 μM; 54%) and sarafotoxin S6c (100 nM; 40%), suggesting the co-existence of both ET_A and ET_B receptors in approximately equal proportions in this tissue. In contrast, specific binding to blood vessels and to peripheral bronchial smooth muscle was abolished in the presence of BQ 123 (1 μM), but was unaffected by sarafotoxin S6c, indicating the presence of only ET_A receptors at these sites.

4 ET-1 caused concentration-dependent contractions of ovine tracheal smooth muscle which were inhibited in the presence of BQ 123 (1 μM). ET-1 also caused concentration-dependent contraction of ovine lung parenchyma strips. In contrast, the ET_B receptor-selective agonists, sarafotoxin S6c and BQ 3020, were virtually inactive as spasmogens in both tracheal smooth muscle and lung strip preparations. Thus contraction was mediated by ET_A receptors in ovine tracheal smooth muscle and this is consistent with binding and autoradiographic data demonstrating a homogeneous population of these binding sites in this tissue. Contraction of parenchymal lung strip preparations to ET-1 was mediated via non-ET_B receptors, presumably ET_A receptors, with contributions to this response perhaps coming from airway and vascular smooth muscle and from alveolar wall contractile cells.

5 ET-1-induced contraction of tracheal smooth muscle was not significantly altered in the presence of indomethacin (5 μM), indicating that cyclo-oxygenase metabolites of arachidonic acid were not involved in this response. Contraction induced by ET-1 was virtually abolished in Ca^{2+}-free medium containing 0.1 mM EGTA, indicating that this response was dependent upon the influx of extracellular Ca^{2+}. Contraction was inhibited by about 50% in the presence of nicardipine (1 μM), indicating that a significant component of this response was mediated via the activation of L-type Ca^{2+} channels.

6 ET-1 caused poorly defined increases in the accumulation of intracellular inositol phosphates in ovine tracheal smooth muscle. The maximal response to ET-1 was less than 20% of that to the cholinoceptor agonist, carbachol. Furthermore, sarafotoxin S6c was inactive. These data, when taken together with the results of autoradiographic and contraction studies, indicate that ovine airway smooth muscle contraction in response to ET-1 is mediated via ET_A receptors which are linked to the influx of extracellular Ca^{2+}, partly through voltage-dependent channels. ET_B receptors also exist in the lamina propria of ovine trachea and in peripheral alveoli, perhaps residing in vascular endothelial cells.

Keywords: Ovine tracheal smooth muscle; contraction; endothelin; ET_A receptors; autoradiography

Introduction

It is now established that both ET_A and ET_B receptors can mediate endothelin-1 (ET-1)-induced contraction of airway smooth muscle (Hay, 1992; Henry, 1993). ET-1-induced contraction of guinea-pig tracheal smooth muscle (Tschirhart *et al.*, 1991; Hay, 1992) is mediated predominantly via ET_B receptors, which are selectively stimulated by sarafotoxin S6c and BQ 3020 (Williams *et al.*, 1991; Ihara *et al.*, 1992b). ET-1-induced stimulation of these receptors appears to be linked to the activation of the inositol phosphate cascade (Hay, 1990), and thus presumably to the mobilization of intracellular Ca^{2+} stores. In contrast, it has been suggested that in sheep airways, the ET_A receptor subtype predom-

[1] Author for correspondence.

inates (Araham et al., 1993). This is consistent with data showing that the ET_A receptor-selective antagonist, BQ 123 (Ihara et al., 1992a) markedly attenuated ET-1-induced bronchoconstriction in allergic sheep and of contraction of tracheal smooth muscle isolated from such animals (Noguchi et al., 1992). In contrast, in rat trachea, powerful contraction was mediated via both ET_A receptors linked to inositol phosphate generation and ET_B receptors which facilitated the influx of extracellular Ca^{2+} (Henry, 1993). In the present study, we assessed the autoradiographic distribution and density of both ET_A and ET_B receptors in ovine tracheal smooth muscle and evaluated their role in ET-1-induced contraction and in the generation of intracellular inositol phosphates.

Methods

Tissue preparation

Sheep tracheal and lung parenchymal tissue was obtained at a local abattoir from freshly slaughtered lambs 4–9 months of age. Tissue was transferred to the laboratory in ice-cold Krebs bicarbonate solution, the composition of which was (mM): NaCl 117, KCl 5.36, $NaHCO_3$ 25.0, KH_2PO_4 1.03, $MgSO_4.7H_2O$ 0.57, $CaCl_2.H_2O$ 2.5 and glucose 11.1. Surrounding fat and other adherring tissue was removed from the trachea and a longitudinal cut was made through the cartilage down the length of the airway opposite the smooth muscle band. Tissue containing the smooth muscle was removed with the epithelium and some cartilage still attached. These preparations were then submerged in Macrodex and frozen by immersion in isopentane, quenched with liquid nitrogen. In addition, tracheal smooth muscle dissected free of all epithelium, submucosal tissue and cartilage, was obtained from six sheep and a piece (approx. 10 mm × 10 mm) from each animal stacked in layers in Macrodex and frozen as described above. Transverse sections (10 μm) of all preparations were cut at − 20°C and thaw-mounted onto gelatin/chrome alum-coated glass slides. Parenchymal tissue was inflated by bronchial instillation with OCT embedding medium diluted 1:4 with 0.9% w/v NaCl solution before snap freezing, sectioning and thaw-mounting on glass slides as described above.

Autoradiographic studies

[^{125}I]-ET-1 autoradiographic studies in sheep tracheal and lung parenchymal tissue were conducted essentially as previously described for other species (Henry et al., 1990). Slide-mounted tissue sections (10 μm) were incubated for 2 × 10 min at 22°C in Tris-HCl buffer (50 mM Tris, 100 mM NaCl; pH 7.4) containing 0.25% (w/v) bovine serum albumin and the protease inhibitor phenylmethylsulphonyl fluoride (10 μM). For some autoradiographic experiments, tissue sections were incubated with 0.5 nM [^{125}I]-ET-1 for 60 min in the presence and absence of the ET_A receptor-selective antagonist, BQ 123 (1 μM) or the ET_B receptor-selective agonist, sarafotoxin S6c (100 nM). Non-specific binding was determined in the combined presence of 1 μM BQ 123 and 100 nM sarafotoxin S6c. Autoradiographic grain densities over alveolar wall tissue were determined with an automated grain detection and counting system (Henry et al., 1990). Four separate fields (three over tissue and one over a non-tissue area) were viewed from each parenchymal section and triplicate slides were analysed. Thus, a total of 192 fields were analysed [(four fields per section) × (four tissue sections per slide) × (three slides per treatment) × (four treatments)]. Autoradiographic densities were expressed as grains 1000 μm^{-2}.

Time course of [^{125}I]-ET-1 binding in tracheal smooth muscle In these experiments, ovine tracheal smooth muscle sections were incubated with 0.35 nM [^{125}I]-ET-1 for 10–180 min in the presence and absence of 1 μM BQ 123, or 100 nM sarafotoxin S6c or in the combined presence of 1 μM BQ 123 and 100 nM sarafotoxin S6c (to assess non-specific binding). Autoradiographic grain densities were measured as described above. A total of 1152 fields were analysed [(four fields per section) × (six tissue sections per slide) × (two slides per treatment) × (four treatments) for each of six time points].

Functional studies

Trachea Sheep trachea was cut transversely at intervals of approximately 3 mm to provide a series of ring segments. The epithelium and attached submucosa was dissected away from the smooth muscle band. The exterior connective tissue and other deep submucosal elements were also dissected from the preparation to leave the intact airway smooth muscle stretched across the cartilage ring as a thin band. This muscle was trimmed to leave a fine filament. Two ligatures approximately 5 mm apart were tied around this muscle filament to provide points of attachment to anchorage sites in the organ bath system. Tracheal preparations were suspended under a resting tension of 500 mg and placed in organ baths containing 2 ml of Krebs bicarbonate solution of 37°C, bubbled continuously with 5% CO_2 in O_2. Changes in isometric tension were recorded via FT03 force-displacement transducers (Grass Instruments).

Tracheal segments were allowed to equilibrate for 45 min before exposure to the cumulative addition of 0.3 μM and 10 μM carbachol. Upon reaching a contraction plateau the preparations were washed in drug-free Krebs bicarbonate solution for 15 min. Concentration-effect curves were constructed to ET-1 in the presence and absence of the ET_A receptor antagonist, BQ 123 (1 μM), or the cyclo-oxygenase inhibitor, indomethacin (5 μM). In these experiments, preparations were exposed for 20 min to one of these agents or its solvent (paired control preparation) and then to cumulative additions (0.5 log-concentration increments) of ET-1 (1 nM to 300 nM). In some experiments, tracheal responsiveness to sarafotoxin S6c or BQ 3020 was also evaluated (1 nM to 300 nM). In a separate series of experiments, the influence of the L-type Ca^{2+} channel antagonist nicardipine (1 μM) or reducing the extracellular Ca^{2+} concentration nominally to zero was assessed on tracheal smooth muscle contraction to potassium (K^+), carbachol and ET-1. In the latter experiments, Krebs bicarbonate solution was replaced three times at intervals of 15 min, with Ca^{2+}-free Krebs bicarbonate solution containing EGTA (0.1 mM). In all experiments, only one agonist cumulative concentration-effect curve was constructed in each preparation. ET-1, BQ 3020-, sarafotoxin S6c-, carbachol- and K^+-induced contractions were plotted as a percentage of the initial contraction induced by 10 μM carbachol (C_{max}). Agonist potencies were assessed as pD_2 values where $pD_2 = -\log EC_{50}$ and EC_{50} = the concentration of agonist producing 50% of the maximal response (E_{max}).

Lung parenchyma strips The marginal edge of the primary lung lobe was cut away as a strip to expose the underlying parenchymal tissue. A strip of parenchyma approximately 2 mm × 2 mm × 6 mm, free of pleural lining tissue, was then dissected from the exposed edge. Such preparations were suspended in organ baths as described for tracheal preparations and their responsiveness to cumulative concentrations of carbachol, ET-1, sarafotoxin S6c or BQ 3020 tested. Contractions were assessed as % of the response to 400 μM carbachol (C_{max}). Agonist potencies were assessed as the concentration producing 50% of the contraction to 400 μM carbachol (95% confidence limits).

[^{3}H]-inositol phosphate accumulation

Inositol phosphates accumulation in response to ET-1, sarafotoxin S6c and carbachol were determined as previously described (Henry et al., 1992). Lengths (approximately 5 cm)

of sheep tracheal smooth muscle were dissected free of all surrounding tissue including epithelium and submucosa and cut along the fibre axis at intervals of 1 mm. Tissue pieces from each of three animals were pooled to provide separate tissue samples. Tissue samples were weighed, preincubated for 30 min in 5 ml of Krebs bicarbonate solution at 37°C and then incubated with [^{3}H]-*myo*-inositol (5 μCi) in 1 ml of carbogen-aerated Krebs bicarbonate solution for 3 h at 37°C with gentle shaking. Tissues were washed twice with 5 ml Krebs bicarbonate solution for 15 min to remove excess [^{3}H]-*myo*-inositol and a third time for a further 15 min. After washing, the tissues were incubated for a further 15 min in 1 ml Krebs bicarbonate solution containing 5 mM LiCl to inhibit the breakdown of inositol monophosphate to inositol and thus enhance the accumulation of inositol phosphates. The tissues were stimulated for 15 min by the addition of 20 μl ET-1 (10 nM to 3 μM) or sarafotoxin S6c (1 nM to 2.5 μM) and the stimulation terminated by the addition of 1.5 ml chloroform:methanol (1:2, v/v) with vigorous shaking. After standing for 15 min, chloroform (0.5 ml) and distilled water (0.5 ml) were added sequentially. The entire upper methanol/water phase was applied to an anion exchange chromatography column (1 ml of Dowex AG1-X8 in formate form). Inositol was eluted with 10 ml of water and glycerophosphoinositol with 15 ml of a buffer containing 5 mM sodium tetraborate and 60 mM sodium formate. [^{3}H]-inositol phosphates were eluted with a buffer containing 0.1 mM formic acid and 0.75 M ammonium formate. Three 1 ml aliquots of the final fraction were mixed with 10 ml of scintillant (5.8 g l^{-1} 2,5-diphenyloxazol (PPO) in Triton X100:toluene, 1:2) and radioactivity counted in a Tricarb liquid scintillation counter (Packard, Model 1500). Total [^{3}H]-inositol phosphate accumulation was expressed as d.p.m. mg^{-1} wet wt. tracheal smooth muscle.

Drugs

Drugs used were: [^{125}I]-ET-1 (2000 Ci mmol^{-1}), ET-1, sarafotoxin S6c, BQ 3020 ([Ala^{11,15}]Ac-ET-1(6–21)]; Auspep, Melbourne, Australia), carbamylcholine chloride, indomethacin,

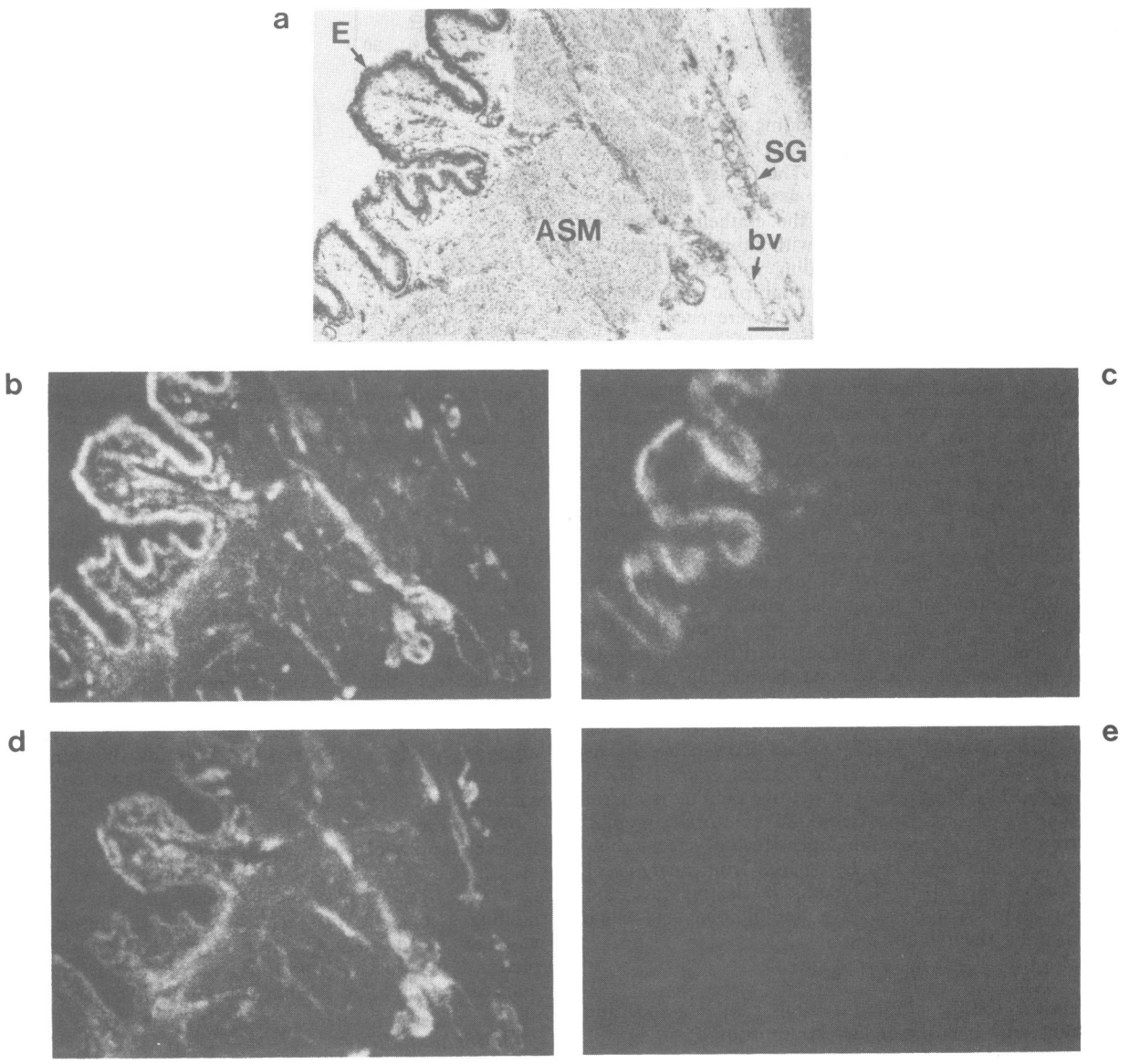

Figure 1 (a) Bright-field photomicrograph of a 10 μm transverse frozen section of ovine trachea. ASM = airway smooth muscle, E = epithelium, SG = submucosal gland, bv = blood vessel. (b–e) Dark-field photomicrographs showing the distribution of autoradiographic grains derived from [^{125}I]-endothelin-1 ([^{125}I]-ET-1). (b) Total [^{125}I]-ET-1 binding in the section shown in the light-field photomicrograph. (c–e) Serial sections showing [^{125}I]-ET-1 binding (c) in the presence of the ET_A receptor-selective antagonist, BQ-123 (1 μM); (d) the ET_B receptor-selective agonist sarafotoxin S6c (100 nM); and (e) in the combined presence of 1 μM BQ 123 and 100 nM sarafotoxin S6c (i.e. nonspecific binding). Bar = 200 μm.

nicardipine hydrochloride (Sigma Chemical Company, St Louis, U.S.A.), potassium chloride (Fluka), phenylmethylsulphonyl fluoride (Calbiochem, La Jolla, U.S.A.), BQ 123 (cyclo[D-Trp-D-Asp-L-Pro-D-Val-L-Leu]; gift from Dr D.W.P. Hay of SmithKline Beecham Pharmaceuticals, U.S.A.). Stock solutions (50 μM) of ET-1 and sarafotoxin S6c were prepared in 0.1 M acetic acid and dilutions made in 0.9% NaCl solution (saline). Stock solutions (50 μM) of BQ 3020 were prepared in 0.1 M ammonium chloride. BQ-123 and indomethacin were prepared in 100 mM Na_2CO_3 and diluted in saline as required. All other drugs were dissolved in saline. Drugs were kept on ice and protected from light.

Statistical analyses

Differences between treatment means were assessed by analysis of variance followed by a modified *t*-statistic (Wallenstein *et al.*, 1980) or by Student's unpaired *t* test as appropriate. *P* values less than 0.05 were considered to be statistically significant.

Results

Autoradiography

Trachea The distribution of total binding sites for [^{125}I]-ET-1 (0.5 nM; 60 min) in a transverse frozen section (10 μm) of sheep trachea is shown in Figure 1b. The highest densities of specific autoradiographic grains were associated with cells in the submucosa, immediately below the epithelial basement membrane and with cells associated with submucosal glands. However, high levels of specific binding were also observed over airway smooth muscle. Autoradiographic grains representing non-specific binding (Figure 1e) were evenly distributed over the tissue with no evidence of localization to particular tissue structures. The ET_A receptor antagonist BQ 123 (1 μM), reduced the density of specific autoradiographic grains over airway smooth muscle and submucosal glands to levels similar to non-specific binding (Figure 1c), indicating that only ET_A-receptors existed in these tissues, but did not appear to reduce significantly binding to cells immediately beneath the epithelial basement membrane. In sharp contrast, the ET_B-selective agonist sarafotoxin S6c (100 nM, Figure 1d), abolished specific binding to these cells, but appeared to have little affect on specific binding to airway smooth muscle or submucosal glands.

To assess more accurately the relative proportions of specific ET_A and ET_B binding sites in sheep tracheal smooth muscle, it was necessary to determine the binding maximum (B_{max}) for all specific binding in sheep tracheal smooth muscle, as well as the binding maxima for these separate binding site populations. Since [^{125}I]-ET-1 binds irreversibly to its specific sites (Marsault *et al.*, 1991; Waggoner *et al.*, 1992), it was not appropriate to apply a competitive binding isotherm to derive binding maxima from quantitative autoradiographic data describing the concentration-dependence of specific binding. However, these data can be derived from analyses of the time courses of [^{125}I]-ET-1 binding in the presence and absence of receptor subtype-selective binding inhibitors which are described by the relationship

$$Bt = B_{max}\ (1-e^{-tk_1L}),$$

where *Bt* is the specific binding at time *t*, k_1 is association rate constant and L is the ligand concentration.

Results show that specific [^{125}I]-ET-1 (0.35 nM) binding increased in a time-dependent manner to a plateau (Figure 2a). However, this specific binding could not be described as consisting of two components. Specific binding was abolished in the presence of BQ 123 (1 μM), but was unaffected by sarafotoxin S6c (100 nM), consistent with the presence of only ET_A sites in airway smooth muscle (Figure 1b).

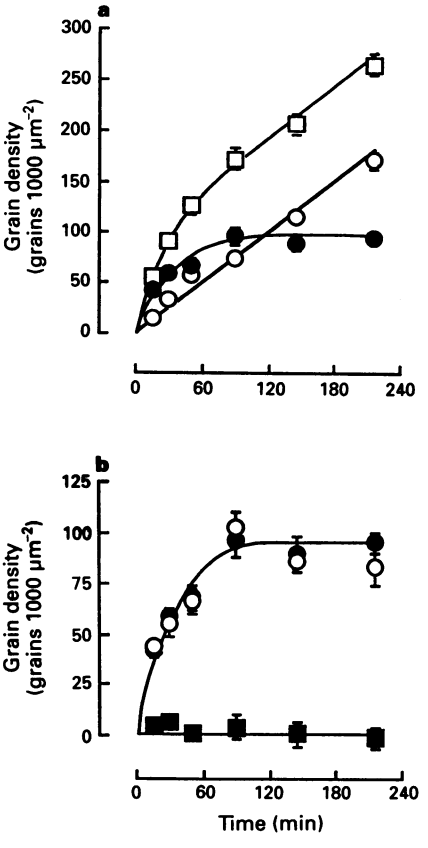

Figure 2 (a) Time-dependence of [^{125}I]-endothelin-1 ([^{125}I]-ET-1, 0.35 nM) binding in 10 μm transverse frozen sections of slide-mounted ovine tracheal smooth muscle. Total (□), specific (●) and non-specific binding (○) is shown. Non-specific binding was assessed in the combined presence of 1 μM BQ 123 and 100 nM sarafotoxin S6c. (b) Specific [^{125}I]-ET-1 binding (●) assessed in the presence of 1 μM BQ 123 (■) (i.e. binding to ET_B sites) or 100 nM sarafotoxin S6c (○) (i.e. binding to ET_A sites). Data are presented as mean ± s.e.mean of six mean estimates.

Peripheral lung Figure 3b shows the distribution of autoradiographic grains derived from total [^{125}I]-ET-1 (0.5 nM, 60 min) binding in a frozen section (10 μm) of ovine peripheral lung tissue. The highest levels of binding were associated with alveolar septae and vascular smooth muscle, with lower levels over bronchial airway smooth muscle. It can be seen that specific grain density (230 ± 16 grains 1000 μm^{-2}) was markedly reduced over alveolar wall tissue, but not abolished in the presence of the ET_A-selective antagonist, BQ 123 (1 μM; 107 ± 8 grains 1000 μm^{-2}; 53.5% inhibition) alone (Figure 3c), or the ET_B-selective agonist, sarafotoxin S6c (100 nM; 139 ± 8 grains 1000 μm^{-2}; 39.6% inhibition) alone (Figure 3d). However, binding was reduced to levels approaching background in the combined presence of 1 μM BQ 123 and 100 nM sarafotoxin S6c (non-specific = 8 ± 7 grains 1000 μm^{-2}; Figure 3e). In contrast, the binding associated with bronchial smooth muscle and with vascular smooth muscle, was virtually abolished in the presence of BQ 123 (1 μM) only (Figure 3c), but was not markedly altered by 100 nM sarafotoxin S6c (Figure 3d).

Functional studies

Trachea Carbachol and ET-1 caused concentration-dependent contraction of ovine tracheal smooth muscle preparations. ET-1 (pD_2 = 8.36 ± 0.06, *n* = 14) was approximately 35 times more potent than carbachol (pD_2 = 6.81 ± 0.07, *n* = 12; $P < 0.001$), but the maximal contractile response (E_{max}) was only 71 ± 6% of that to carbachol (pooled value from data

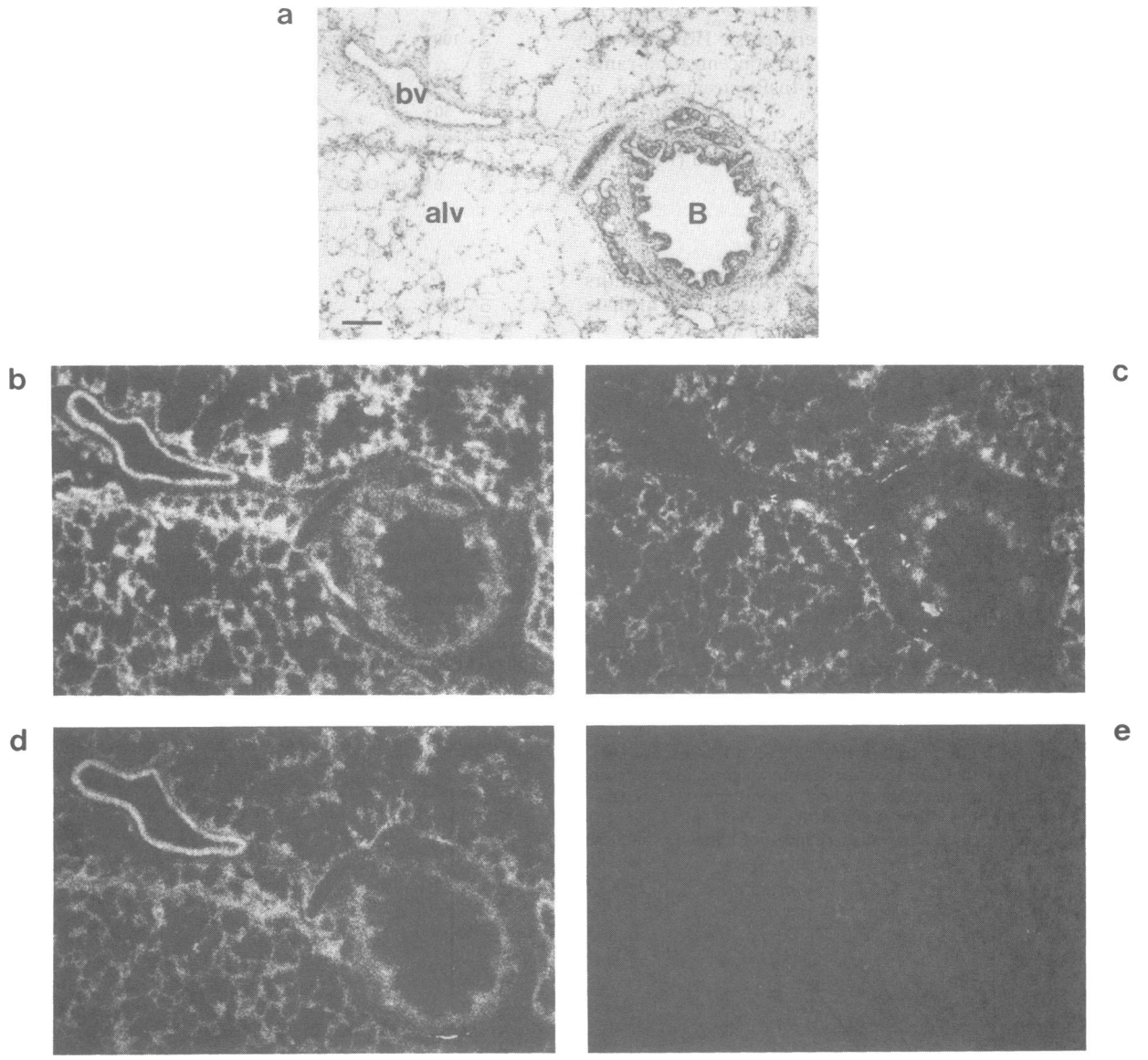

Figure 3 (a) Bright-field photomicrograph of a 10 μm transverse frozen section of ovine peripheral lung. B = bronchus, alv- = alveolus, bv = blood vessel. (b–e) Dark-field photomicrographs showing the distribution of autoradiographic grains derived from [^{125}I]-endothelin-1 ([^{125}I]-ET-1, 0.5 nM, 60 min). (b) Total [^{125}I]-ET-1 binding in the section shown in the light-field photomicrograph. (c–e) Serial sections showing [^{125}I]-ET-1 binding in the presence of (c) the ET_A receptor-selective antagonist BQ 123 (1 μM); (d) the ET_B receptor-selective agonist sarafotoxin S6c (100 nM); and (e) in the combined presence of 1 μM BQ 123 and 100 nM sarafotoxin S6c (i.e. non-specific binding). Bar = 200 μm.

in Figures 4,5 and 6). In contrast, neither of the ET_B receptor-selective agonists, sarafotoxin S6c (Figure 4) or BQ 3020 (data not shown) were active as contractile agonists to any significant extent. The ET_A receptor-selective antagonist, BQ 123 (1 μM) shifted the concentration-effect curve to ET-1 to the right by 5.4 fold (apparent $pK_B = 6.7$), but did not alter tracheal responsiveness to carbachol (Figure 5). Contractions to K^+ and ET-1 were virtually abolished in Ca^{2+}-free medium (Figure 6a and b). Under similar conditions, carbachol potency was reduced by less than 2 fold ($P > 0.05$), although E_{max} was reduced by 50% ($P < 0.001$) (control $n = 7$, test $n = 6$; data not shown). Furthermore, the voltage-dependent Ca^{2+} channel antagonist, nicardipine (1 μM), markedly attenuated responses to K^+ and reduced E_{max} for ET-1 by approximately 45% from 76 ± 8% ($n = 8$) to 42 ± 7% ($n = 8$) of the E_{max} to carbachol ($P < 0.01$) (Figure 6c and d), whereas carbachol potency was only reduced by approximately 2 fold ($P < 0.05$) and E_{max} remained unaffected ($P > 0.1$) (control $n = 5$, test $n = 6$; data not shown). In contrast, indomethacin (5 μM) failed to alter significantly either the pD_2 or E_{max} for ET-1 or carbachol ($P > 0.1$) (control $n = 3$, test $n = 3$; data not shown).

Peripheral lung strips ET-1 and carbachol caused concentration-dependent increases in isometric tension in ovine lung strip preparations, whereas sarafotoxin S6c (Figure 7) and BQ 3020 (data not shown) were virtually inactive. Since maximal response was not obtained with either ET_1 or carbachol, relative agonist potency was assessed in terms of the concentrations of agonist causing 50% of the greatest response to carbachol (C_{max}; 95% confidence limits, CL). ET-1 was approximately 180 times more potent than carbachol (50% C_{max} carbachol = 26.1 (CL: 15.8–42.7) μM ($n = 4$); ET-1 = 148 (CL: 90–230) mM ($n = 4$).

[^{3}H]-inositol phosphate generation

Carbachol caused significant concentration-dependent increases in the accumulation of total [^{3}H]-inositol phosphates ([^{3}H]-InsPs) above basal levels in ovine tracheal smooth mus-

cle (Figure 8; pD_2 carbachol = 6.02 ± 0.18; E_{max} = 15.0 ± 2.1 fold increase above basal; n = 3 experiments). However, the response to ET-1 was variable across the concentration-range tested. The maximum level of [^{3}H]-InsPs accumulated in response to ET-1 was less than 20% of that to carbachol ($P<0.05$), while the ET_B receptor-selective agonist, sarafotoxin S6c was inactive at all concentrations tested (Figure 8).

Discussion

This study has clearly demonstrated that ET_A receptors predominate in ovine tracheal smooth muscle and mediate

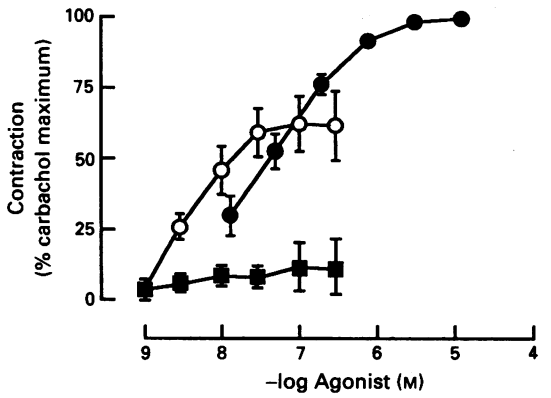

Figure 4 Cumulative concentration-effect curves to carbachol (●), endothelin-1 (○) and the ET_B receptor-selective agonist sarafotoxin S6c (■) for contraction in ovine tracheal smooth muscle preparations. Four preparations were derived from each of 3–12 (n) animals. Data are presented as mean ± s.e.mean of n mean estimates.

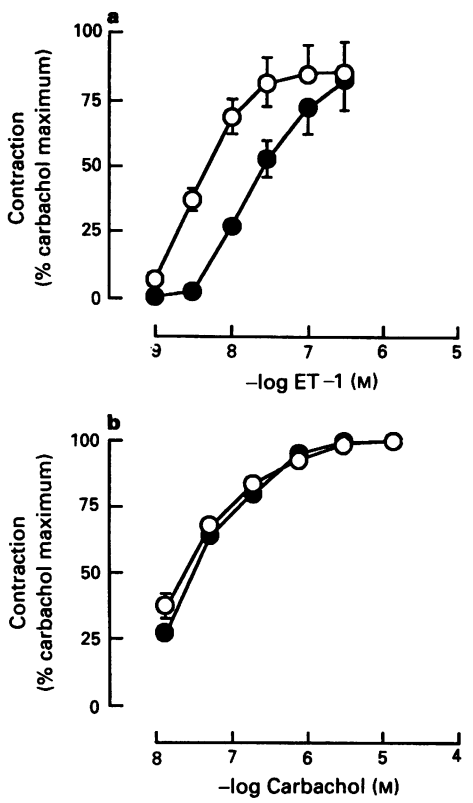

Figure 5 Cumulative concentration-effect curves to (a) endothelin-1 (ET-1) and (b) carbachol for contraction in ovine tracheal smooth muscle preparations in the absence (○) or presence (●) of the ET_A receptor-selective antagonist, BQ 123 (1 μM). Four preparations were derived from each of three animals. Data are presented as mean ± s.e.mean of three mean estimates.

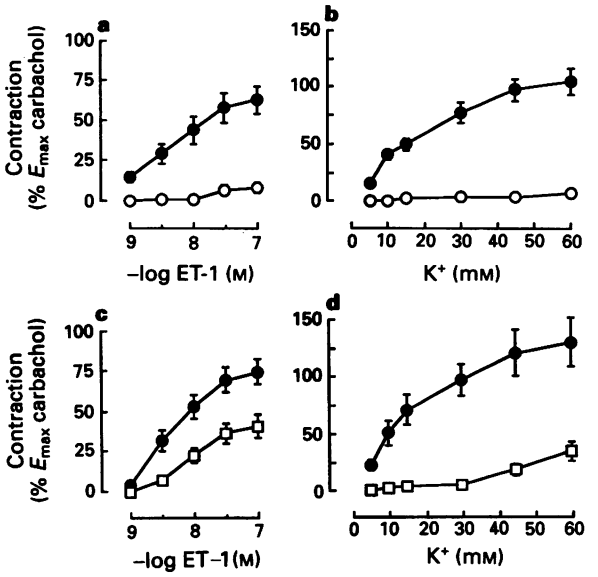

Figure 6 Cumulative concentration-effect curves to K^+ and endothelin-1 (ET-1) in ovine tracheal smooth muscle preparations in Krebs bicarbonate solution containing 2.5 mM Ca^{2+} (●). (a and b) Contraction measured in Ca^{2+}-free Krebs bicarbonate solution containing 0.1 mM EGTA (○) and (c and d) in the presence of nicardipine (1 μM) (□). For each treatment group, one preparation was derived from each of 5–8 animals. Data are presented as mean ± s.e.mean.

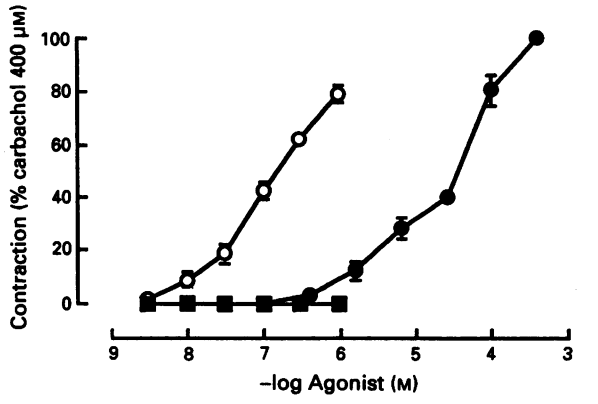

Figure 7 Cumulative-concentration-effect curves to carbachol (●), endothelin-1 (○) and sarafotoxin S6c (■) for contraction in ovine parenchymal lung strip preparations. Four preparations were derived from each of n = 4 animals. Data are presented as mean ± s.e.mean.

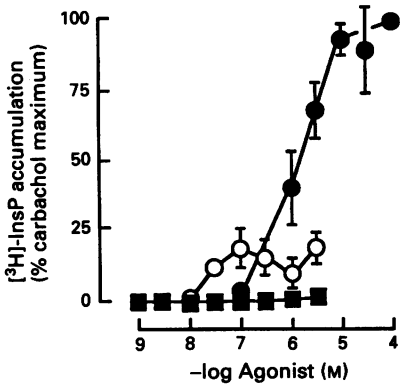

Figure 8 Cumulative concentration-effect curves to carbachol (●), endothelin-1 (○) and the ET_B receptor-selective agonist sarafotoxin S6c (■) for the accumulation of intracellular total inositol phosphates (InsPs) in ovine tracheal smooth muscle. Data are presented as mean ± s.e.mean of observations in tissue from three separate experiments.

contraction in response to ET-1. The primary evidence in support of this contention includes the fact that specific [^{125}I]-ET-1 binding in tracheal smooth muscle was abolished in the presence of the ET_A receptor-selective antagonist, BQ 123 (1 μM). Quantitative autoradiographic data produced in the presence and absence of ET_A and ET_B receptor-selective ligands, also showed that all of the specific binding to airway smooth muscle cells could be accounted for as binding to ET_A receptors. In addition, ET-1-induced contraction of this tissue was significantly inhibited in the presence of BQ 123. The apparent pK_B of 6.7 for BQ 123 against ET-1 is consistent with a value of 7.1 in guinea-pig aorta (Hay, 1992) and with its pA_2 value of 6.9 in rat thoracic aorta (Sumner *et al.*, 1992). Furthermore, the ET_B receptor-selective agonists, sarafotoxin S6c (Williams *et al.*, 1991) and BQ 3020 (Ihara *et al.*, 1992b) were virtually inactive as spasmogens in ovine tracheal smooth muscle preparations. This is consistent with evidence in sheep that ET-1-induced bronchial smooth muscle contraction was mediated via ET_A receptors (Noguchi *et al.*, 1992; Abraham *et al.*, 1993).

However, the present data contrast sharply with results obtained in airway smooth muscle from other species. For example, ET-1-induced contraction in guinea-pig bronchus was mediated predominantly via ET_B receptors (Hay, 1992), although evidence for multiple receptor subtypes in this tissue has been reported (Tschirhart *et al.*, 1991). Furthermore, ET_B receptors were also primarily responsible for mediating ET-1-induced contraction in human bronchus (Hay *et al.*, 1993). However, in rat trachea, both ET_A and ET_B receptors co-existed in approximately equal proportions and mediated responses which made approximately equivalent contributions to ET-1-induced increases in airway smooth muscle tone (Henry, 1993).

Species differences are also apparent with respect to the signal transduction mechanisms to which ET receptor subtypes are linked. In rat tracheal smooth muscle, ET-1-induced contraction mediated via ET_A receptors was linked to the phosphoinositide generating pathway, whereas ET_B receptors were linked to the influx of extracellular Ca^{2+} via non L-type Ca^{2+} channels (Henry, 1993). In contrast, in the present study, ET-1-induced contraction was completely dependent upon extracellular Ca^{2+} influx and this response was only partially associated with voltage-dependent L-type Ca^{2+} channels. Furthermore, the dependence on extracellular Ca^{2+} influx of ET-1-induced contraction mediated via ET_A receptors is consistent with the trivial increases in intracellular inositol phosphate accumulation observed in response to this peptide and to sarafotoxin S6c.

Autoradiographic data showed that a homogeneous population of ET_A receptors was also present at sites associated with submucosal glands and in clearly defined blood vessels and the density of these sites was greater than that seen over airway smooth muscle cells. In contrast, ET_B receptors were detected in the tracheal wall in association with submucosal cells residing at or near the epithelial basement membrane. The density of these sites was also greater than that for ET_A receptors in airway smooth muscle. While the cell type associated with these sites could not be accurately resolved, endothelial cells from the bronchial microcirculation are a likely location of these receptors, since it is established that vascular endothelial cells contain ET_B receptors (Masaki *et al.*, 1991; Hirata *et al.*, 1993).

ET_B receptors were also detected in ovine lung parenchyma, most noticeably in association with the alveolar wall, where sarafotoxin S6c-sensitive binding accounted for approximately 40% of the specific binding of [^{125}I]-ET-1. Almost all of the remaining specific binding was BQ 123-sensitive and was thus defined as ET_A receptor-associated. As observed in the trachea, the ET_B receptor-selective agonist sarafotoxin S6c abolished [^{125}I]-ET-1 binding to cells at or near the epithelial basement membrane in peripheral bronchi. In contrast, BQ 123 abolished bronchial smooth muscle binding, indicating that ET_A receptors predominated in ovine peripheral airway smooth muscle, as well as in tracheal airway smooth muscle.

ET-1-induced contraction of ovine peripheral lung strips was also apparently mediated via ET_A receptors, since the ET_B receptor-selective agonists sarafotoxin S6c and BQ 3020 were virtually inactive as spasmogens in this tissue. The precise locations of all of the ET_A receptors mediating contractile responses of ovine lung strips is not known. However, it seems likely that ET_A receptors in bronchial smooth muscle mediated a large proportion of the total response. Vascular smooth muscle contraction mediated via ET_A receptors may also have contributed to lung strip responses to ET-1, since this tissue component in lung strips has been reported previously to be active in response to spasmogens (Bertram *et al.*, 1983). It is also possible that some alveolar wall ET_A receptors existed in contractile cells such as interstitial myofibroblasts (Kapanci *et al.*, 1974) which may contribute to the increase in lung strip tone in response to ET-1. However, evidence from electron microscopic autoradiography suggests that specific [^{125}I]-ET-1 binding in the alveolar wall primarily involves vascular endothelial cells and fibroblasts (Furuya *et al.*, 1991; 1992). It seems likely that ovine alveolar ET_B receptors reside in capillary endothelial cells (Hirata *et al.*, 1993) and are thus unlikely to contribute to ET-1-induced lung strip contraction.

In conclusion, this study has demonstrated that although both ET_A and ET_B receptors exist in the ovine respiratory tract, it is the ET_A receptor subtype which mediates airway smooth muscle contraction. This contrasts sharply with human airway smooth muscle in which ET-1-induced contraction is mediated primarily via ET_B receptors.

This research was supported by grants from the National Health and Medical Research Council of Australia and the Child Health Research Foundation of Western Australia.

References

ABRAHAM, W.M., AHMED, A., CORTES, A., SPINELLA, M.J., MALIK, A.B. & ANDERSEN, T.T. (1993). A specific endothelin-1 antagonist blocks inhaled endothelin-1-induced bronchoconstriction in sheep. *J. Appl. Physiol.*, **74**, 2537–2542.

BERTRAM, J.F., GOLDIE, R.G., PAPADIMITRIOU, J.M. & PATERSON, J.W. (1983). Correlations between pharmacological responses and structure of human lung parenchyma strips. *Br. J. Pharmacol.*, **80**, 107–114.

FURUYA, S., NARUSE, S., NAKAYAMA, T., FURUYA, K. & NOKIHARA, K. (1991). Localization of [^{125}I]-endothelin-1 in rat tissues observed by electron microscopic autoradiography. *J. Cardiovasc. Pharmacol.*, **17** (Suppl 7), S452–S454.

FURUYA, S., NARUSE, S., NAKAYAMA, T., FURUYA, K. & NOKIHARA, K. (1992). Effect and distribution of intravenously injected ^{125}I-endothelin-1 in rat kidney and lung examined by electron microscopic radioautography. *Anat. Embryol.*, **185**, 87–96.

HAY, D.W.P. (1990). Mechanism of endothelin-induced contraction in guinea-pig trachea. *Br. J. Pharmacol.*, **100**, 383–392.

HAY, D.W.P. (1992). Pharmacological evidence for distinct endothelin receptors in guinea-pig bronchus and aorta. *Br. J. Pharmacol.*, **106**, 759–761.

HAY, D.W.P., LUTTMANN, M.A., HUBBARD, W.C. & UNDEM, B.J. (1993). Endothelin receptor subtypes in human and guinea-pig pulmonary tissues. *Br. J. Pharmacol.*, **110**, 1175–1183.

HENRY, P.J. (1993). Endothelin-1 (ET-1)-induced contraction in rat isolated trachea: involvement of ET_A and ET_B receptors and multiple signal transduction systems. *Br. J. Pharmacol.*, **110**, 435–441.

HENRY, P.J., RIGBY, P.J., SELF, G.J., PREUSS, J.M.H. & GOLDIE, R.G. (1990). Relationship between endothelin-1 binding site densities and constrictor activities in human and animal airway smooth muscle. *Br. J. Pharmacol.*, **100**, 786–792.

HENRY, P.J., RIGBY, P.J., SELF, G.J., PREUSS, J.M.H. & GOLDIE, R.G. (1992). Endothelin-1-induced [^{3}H]-inositol phosphate accumulation in rat trachea. *Br. J. Pharmacol.*, **105**, 135–141.

HIRATA, Y., EMORI, T., EGUCHI, S., KANNO, K., IMAI, T., OHTA, K. & MARUMO, F. (1993). Endothelin receptor subtype B mediates synthesis of nitric oxide by cultured bovine endothelial cells. *J. Clin. Invest.*, **91**, 1367–1373.

IHARA, M., NOGUCHI, K., SAEKI, T., FUKURODA, T., TSCHIDA, S., KIMURA, S., FUKAMI, T., NISHIKIBE, M. & YANO, M. (1992a). Biological profiles of highly potent novel endothelin antagonists selective for the ET_A receptor. *Life Sci.*, **50**, 247–255.

IHARA, M., SAEKI, T,. FUKURODA, T., KIMURA, S., OZAKI, S., PATEL, A.C. & YANO, M. (1992b). A novel radioligand [^{125}I]-BQ-3020 selective for endothelin (ET_B) receptors. *Life Sci.*, **51**, PL47–PL52.

KAPANCI, Y., ASSIMACOPOULOS, A., IRLE, C., ZWAHLEN, A. & GABBIANI, G. (1974). Contractile interstitial cells in pulmonary alveolar septa: a possible regulator of ventilation/perfusion ratio? *J. Cell Biol.*, **60**, 375–392.

MARSAULT, R., VIGNE, P., BREITTMAYER, J.P. & FRELIN, C. (1991). Kinetics of vasoconstrictor action of endothelins. *Am. J. Physiol.*, **261**, (Cell Physiol., 30), C986–C993.

MASAKI, T., KIMURA, S., YANAGISAWA, M. & GOTO, K. (1991). Molecular and cellular mechanism of endothelin regulation. Implications for vascular function. *Circulation*, **84**, 1457–1468.

NOGUCHI, K., ISHIKAWA, K., YANO, M., AHMED, A., CORTES, J., HALLMON, J. & ABRAHAM, W.M. (1992). An endothelin $(ET)_A$ receptor antagonist, BQ 123, blocks ET-1-induced bronchoconstriction and tracheal smooth muscle (TSM) contraction in allergic sheep. *Am. Rev. Respir. Dis.*, **145**, A858.

SUMNER, M.J., CANNON, T.R., MUNDIN, J.W., WHITE, D.G. & WATTS, I.S. (1992). Endothelin ET_A and ET_B receptors mediate vascular smooth muscle contraction. *Br. J. Pharmacol.*, **107**, 858–860.

TSCHIRHART, E.J., DRIJHOUT, J.W., PELTON, J.T., MILLER, R.C. & JONES, C.R. (1991). Endothelins: functional and autoradiographic studies in guinea-pig trachea. *J. Pharmacol. Exp. Ther.*, **258**, 381–387.

WAGGONER, W.G., GENOVA, S.L. & RASH, V.A. (1992). Kinetic analyses demonstrate that the equilibrium assumption does not apply to [^{125}I]-endothelin-1 binding data. *Life Sci.*, **51**, 1869–1876.

WALLENSTEIN, S., ZUCKER, C.L. & FLEISS, J.L. (1980). Some statistical methods useful in circulation research. *Circ. Res.*, **47**, 1–9.

WILLIAMS, D.L. Jr., JONES, K.L., PETTIBONE, D.J., LIS, E.V. & CLINESCHMIDT, B.V. (1991). Sarafotoxin S6c; an agonist which distinguishes between endothelin receptor subtypes. *Biochem. Biophys. Res. Commun.*, **175**, 556–561.

(Received December 21, 1993
Revised March 4, 1994
Accepted March 9, 1994)

Br. J. Pharmacol. (1994), **112**, 757–762

A quantitative comparison of functional and anti-ischaemic effects of the phosphodiesterase-inhibitors, amrinone, milrinone and levosimendan in rabbit isolated hearts

[1]A.F.E. Rump, D. Acar & W. Klaus

Institut für Pharmakologie, Universität Köln, Gleuelerstr. 24, 50931 Köln, Germany

1 The functional and anti-ischaemic effects of the phosphodiesterase (PDE)-inhibitors, amrinone, milrinone and levosimendan, a new agent combining PDE-inhibitory with calcium-sensitizing properties, were investigated in rabbit isolated hearts (Langendorff, constant pressure: 70 cmH_2O, Tyrode solution, Ca^{2+} 1.8 mmol l^{-1}, 37°C). Anti-ischaemic effects were studied in electrically-driven hearts (200 beats min^{-1}). Acute regional ischaemia was induced by ligature of a branch of the circumflex coronary artery and quantified from epicardial NADH-fluorescence photography.

2 Cumulative concentration-response curves in spontaneously beating hearts in the presence of isoprenaline (10^{-10} M), showed a higher inotropic and coronary vasodilator potency for levosimendan (EC_{50}: 7×10^{-7} M) compared to milrinone (EC_{50}: 7.7×10^{-6} M) or amrinone (EC_{50}: 2×10^{-5} M). Although the maximal coronary dilator activity was similar for the three agents, the maximal inotropic and chronotropic effects were lower for levosimendan than for amrinone or milrinone ($P<0.05$).

3 In regionally ischaemic hearts, milrinone (10^{-5} M) or levosimendan (5×10^{-6} M) similarly enhanced the left ventricular pressure (+15–20%) ($P<0.05$) and the global coronary flow (+40–50%) ($P<0.05$). The epicardial NADH-fluorescence area was significantly diminished by milrinone or levosimendan (−20–30%) ($P<0.05$) and there was no significant difference between the anti-ischaemic effects of either agent ($P>0.05$).

4 It is concluded that amrinone and milrinone possess similar functional profiles in rabbit isolated hearts and a higher inotropic and chronotropic efficacy than levosimendan. At functionally equieffective concentrations, milrinone and levosimendan show similar anti-ischaemic effects, related to an improvement of myocardial perfusion. The calcium-sensitizing properties seem not to be relevant for cardioprotection by levosimendan at the concentration used.

Keywords: NADH-fluorescence; myocardial ischaemia; cardioprotection; inotropes; phosphodiesterase-inhibitors; calcium-sensitizers; amrinone; milrinone; levosimendan

Introduction

Phosphodiesterase (PDE)-inhibitors represent a class of agents combining inotropic and vasodilator properties (Leyen *et al.*, 1989). Several of these agents have been shown to possess anti-ischaemic properties that could be demonstrated in experimental (Jentzer *et al.*, 1981; Rump *et al.*, 1993a,e) and clinical situations (Benotti *et al.*, 1980). These anti-ischaemic effects have often been explained by peripheral dilatation and a reduction in myocardial oxygen-consumption. Moreover, it has been suggested that an improvement of myocardial perfusion might also contribute to the beneficial effects observed in isolated heart preparations (Rump *et al.*, 1993a,e). Thus, the relation of inotropic effects to vasodilator effects seems to be of prime importance for the anti-ischaemic properties of PDE-inhibitors. It was, however, demonstrated that PDE-inhibitors may differ in their influence on intracellular calcium recirculation (Morner, 1990; Holmberg *et al.*, 1991). Moreover, several agents combining PDE-inhibitory and calcium-sensitizing properties have been described (Kitzen & Winbury, 1989; Herzig & Quast, 1992). The sensitization of the myofilaments to calcium may not only represent a new inotropic principle; theoretically, a calcium-sensitizing effect might be accompanied by an oxygen-sparing effect (Van Zwieten, 1991). Therefore, PDE-inhibitors with calcium-sensitizing properties might possibly be expected to be particularly effective as anti-ischaemic inotropes.

Simendan is a novel compound combining PDE-inhibitory and calcium-sensitizing properties (Edes *et al.*, 1992; Haikala *et al.*, 1992a,b; Ovaska *et al.*, 1992; Raasmuja *et al.*, 1992). It was demonstrated that simendan augmented the tension developed by guinea-pig papillary muscles and chemically skinned fibres to the same extent in micromolar concentrations (100% tension increase at 3×10^{-6} M) (Haikala *et al.*, 1992a). In comparison, milrinone had no effect on the skinned fibres up to 10^{-4} M (Haikala *et al.*, 1992a). These findings indicate that at a micromolar concentration the positive inotropic action of simendan is actually caused by an increased calcium-sensitivity of contractile proteins and not by an increased calcium influx (Haikala *et al.*, 1992a). The precise mechanisms involved at the molecular level are still unclear, but it was shown that simendan binds to troponin (Ovaska *et al.*, 1992) and does not enhance myosin ATPase activity (Haikala *et al.*, 1992b). Although a potential drawback in the use of myofilament sensitizers is the possibility that they may impair diastolic function (Katz, 1986; Ventura *et al.*, 1992), it was shown that simendan does not delay relaxation (Haikala *et al.*, 1992b). Moreover, an inhibitory action on the voltage-sensitive Ca^{2+} current may explain the antiarrhythmic effects observed (Raasmaja *et al.*, 1992). Thus, several mechanisms of action may confer cardioprotective properties to simendan.

In the present study, we have investigated the functional and anti-ischaemic effects of levosimendan, the active enantiomer of simendan, in comparison to the 'pure' bipyridine-type PDE-inhibitors, amrinone and milrinone, in a rabbit isolated heart preparation.

Methods

Hearts from male rabbits (White New Zealand) (1.6–2.0 kg body weight) were prepared as published previously (Rump

[1] Author for correspondence.

et al., 1993d) and perfused according to Langendorff (Langendorff, 1895) at a constant pressure of 70 cmH_2O with Tyrode solution equilibrated with 95% O_2 and 5% CO_2 at 37°C. The Tyrode solution had the following millimolar composition: Na^+ 161, K^+ 5.36, Ca^{2+} 1.8, Mg^{2+} 1.05, Cl^- 148, HCO_3^- 23.8, $H_2PO_4^-$ 0.42, glucose 10. Left ventricular pressure was measured continuously with a pressure transducer (Trantec Modell 800, Bentley) attached to a fluid-filled rubber balloon which was inserted via the left atrium into the left ventricle. The volume was adapted to give an end-diastolic pressure of 0 mmHg. Left ventricular pressure was measured as actively developed left ventricular pressure, i.e. systolic minus end-diastolic left ventricular pressure. Global coronary flow was measured with graded glass cylinders. The hearts were electrically-driven (Stimulator-S, Hugo-Sachs Elektronik) as described in the experimental protocol.

For quantification of the ischaemic myoepicardium, photographs using endogenous NADH-fluorescence were taken and submitted to image processing (Rump et al., 1993d). The excitation light was provided by a Xe-flash (100 J in 120 μs, model Strobe 1001 S.O. 1, Drello), the light filtered through an excitation filter (UG1, 0.5 mm, Schott) and directed towards the heart by a 4 point quartz light guide (diameter 10 mm, Volpi). A selected pulse of the electrical stimulator was used to trigger the flash lights without delay so that the pictures were always taken during the same phase of the cardiac contraction cycle (late ventricular diastole). NADH-fluorescence was recorded in a dark room on high sensitivity film (Polaroid type 667, 36 DIN) with a cut on emission filter (GG 435/3 mm, Schott) in front of a Rolleiflex SL66 camera (shutter open) fitted with an 80 mm retro lens and bellow attachment which allowed an image magnification of up to 1.5.

Epicardial NADH-fluorescence photographs were digitized into a matrix of 768 × 512 pixels and 255 grey levels, and image processing was performed on a Lion 486 PC (CCD-video-camera 1000 WOL, Mintron Enterprise Ltd; frame graver board, Data translation, Marlboro, U.S.A.; JAVA and Sigma Plot Software, Jandel Scientific, Corte Madera, U.S.A.). After coronary occlusion, enhanced NADH-fluorescence was shown by an increase in the number of pixels with higher grey values. The number of pixels with enhanced NADH-fluorescence after coronary occlusion was proportional to the size of the ischaemic area.

The absolute size of the ischaemic zone was determined as the quotient of the NADH-fluorescence area 30 min after coronary occlusion and left ventricle size, as determined on epicardial NADH-fluorescence photographs.

Influence of the heart-rate on the left ventricular pressure and the coronary flow

Electrically-driven hearts ($n = 8$) were allowed to stabilize for 45 min before accelerating the pacing-rate stepwise by 30 beats min^{-1}, every 10 min from 180 beats min^{-1} up to 300 beats min^{-1}.

Concentration-response relationships

To investigate the haemodynamic effects of amrinone, milrinone or levosimendan, cumulative concentration-response curves were obtained in rabbit isolated spontaneously beating hearts. Hearts were allowed to stabilize for 45 min after preparation. Isoprenaline 10^{-10} M was added to the perfusion buffer to provide a β-adrenergic drive before applying amrinone ($n = 7$), milrinone ($n = 6$) or levosimendan ($n = 6$) at increasing concentrations at intervals of 10 min. Control hearts were examined to correct the haemodynamic parameters for changes occurring over time. The inotropic and coronary dilator activities were corrected for the influence of the heart-rate.

Influence of milrinone or levosimendan on acute regional ischaemia

Hearts were allowed to stabilize for 45 min after preparation before occluding a postero-lateral branch of the circumflex artery for 120 min. Milrinone (10^{-5} M, $n = 5$) or levosimendan-treatment (5×10^{-6} M, $n = 6$) was started after an ischaemic period of 30 min and continued over the experimental time. Untreated control hearts were examined for comparison ($n = 5$).

Epicardial NADH-fluorescence photographs were taken at $t = 30$ min, before starting the treatment, as well as at $t = 40$, 60, 90 and 120 min. The NADH-fluorescence area after an ischaemic period of 30 min was taken as a reference and set 100%.

Materials

The following substances were used: Amrinone (Sigma, St Louis, U.S.A.), milrinone (Sanofi-Winthrop, München, Germany), levosimendan ((−)-OR-125) ((**R**)-(−)-[[4-(1,4,5,6-tetrahydro-4- methyl-6-oxo-3- pyridazinyl) phenyl]-hydrazono] propanedinitril) (gift from Orion Pharmaceutica, Espoo, Finland), isoprenaline (Sigma, St Louis, U.S.A.).

Data analysis and statistics

Data are given as mean ± s.e.mean of n experiments. The relationship between heart-rate, left ventricular pressure and coronary flow was examined by linear regression analysis (Backhaus et al., 1994). Data from cumulative concentration-response curves were submitted to logit analysis to determine EC_{50} values (Hafner et al., 1977). Statistical significance was evaluated at 95% confidence limits by one way or two way ANOVA and Scheffée test.

Results

Influence of the heart-rate on the left ventricular pressure and the coronary flow

Accelerating the pacing-rate from 180 min^{-1} up to 300 min^{-1} was accompanied by a reduction of the left ventricular pressure (Δ LVP% = $-0.178 \times \Delta$ HR(%) + 1.248, linear correlation coefficient $r = -0.46$) and by an increase of the coronary flow (Δ CF(%) = $0.093 \times \Delta$ HR(%) + 2.301, $r = 0.54$).

Concentration-response relationships

The functional parameters did not differ significantly between the groups at the end of the equilibration period ($P > 0.05$) (Table 1), and they were not significantly affected by isoprenaline 10^{-10} M ($P > 0.05$). Amrinone, milrinone and levosimendan concentration-dependently increased the heart-rate (Figure 1), the left ventricular pressure (Figure 2) and the coronary flow (Figure 3). Milrinone showed a higher inotropic and coronary vasodilator potency than amrinone (Table 2), but the relation of inotropy to coronary dilatation was similar for both agents. There was also no significant difference between the maximal inotropic and coronary vasodilator effects of amrinone and milrinone ($P > 0.05$). The chronotropic potency was not determined as the maximal increase of the heart-rate could not be ascertained (Figure 1). Levosimendan showed a higher inotropic and coronary vasodilator potency than milrinone (Table 2). Whereas the maximal coronary vasodilatation was similar for the three agents ($P > 0.05$) (Figure 3), the maximal inotropic effect was significantly lower for levosimendan compared to amrinone or milrinone ($P < 0.05$) (Figure 2). Similarly, the maximal increase in heart-rate by levosimendan was significantly lower than that induced by amrinone or milrinone at the highest concentration used ($P < 0.05$) (Figure 1).

Table 1 Actual values of the heart-rate (HR), the left ventricular pressure (LVP) and the coronary flow (CF) at the end of the equilibration period before adding isoprenaline

	HR (min^{-1})	*LVP* (mmHg)	*CF* ($ml\ min^{-1}$)
Amrinone	117 ± 12	62 ± 8	18 ± 3
Milrinone	134 ± 13	59 ± 3	18 ± 2
Levosimendan	136 ± 5	61 ± 6	21 ± 1

There was no significant difference between the three groups ($P > 0.05$).

Table 2 EC_{50} values ($mol\ l^{-1}$) for the chronotropic, inotropic and coronary vasodilator activity of amrinone, milrinone and levosimendan

	Chronotropy	*Inotropy*	*Coronary dilatation*
Amrinone	–	2×10^{-5}	9.1×10^{-6}
Milrinone	–	7.7×10^{-6}	3×10^{-6}
Levosimendan	2.3×10^{-7}	7×10^{-7}	4.9×10^{-7}

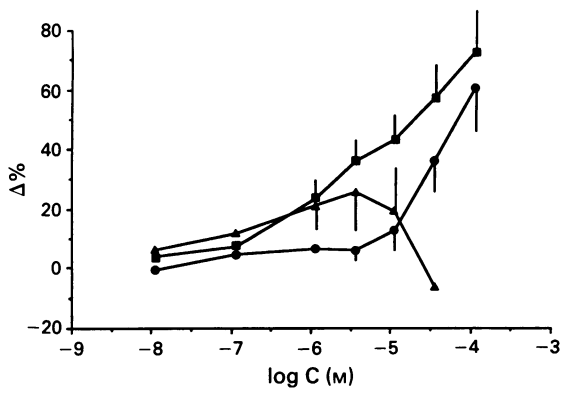

Figure 1 Cumulative concentration-response curves for the chronotropic effects of amrinone (●, $n = 7$), milrinone (■, $n = 6$) or levosimendan (▲, $n = 6$) in the presence of isoprenaline (10^{-10} M) in the perfusion buffer. Ordinate scale: increase in the heart-rate relative to the actual values before PDE-inhibitor application. Symbols represent the mean ± s.e.mean.

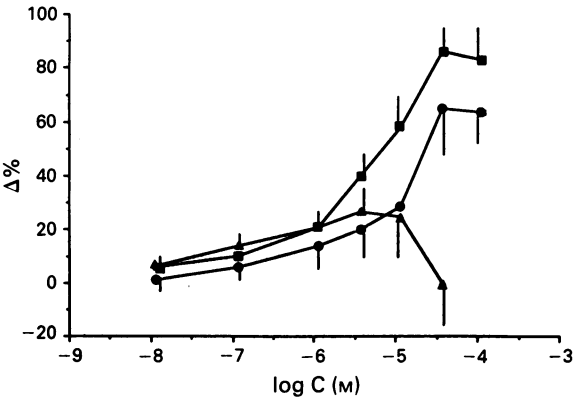

Figure 2 Cumulative concentration-response curves for the inotropic effects of amrinone (●, $n = 7$), milrinone (■, $n = 6$) or levosimendan (▲, $n = 6$) in the presence of isoprenaline (10^{-10} M) in the perfusion buffer. Ordinate scale: increase in the left ventricular pressure relative to the actual values before PDE-inhibitor application. Symbols represent the mean ± s.e.mean.

Effects of milrinone and levosimendan in regionally ischaemic hearts

There was no significant difference in pacing-rate, left ventricular pressure or coronary flow between treated hearts and controls at the end of the equilibration period when coronary occlusion was started ($P > 0.05$) (Table 3).

The coronary flow and concomitantly the left ventricular pressure were significantly decreased by coronary occlusion ($P < 0.05$) (Figures 4 and 5). The end-diastolic pressure was not significantly affected ($P > 0.05$) (data not shown). The left ventricular pressure and the pressure-rate-product were significantly increased to a similar extent by milrinone or levosimendan ($P < 0.05$) (Figure 5), whereas the end-diastolic pressure remained unaffected ($P > 0.05$) (data not shown). The coronary flow was enhanced by both agents ($P < 0.05$) (Figure 4) and the enhancement was similar for both agents over most of the time ($P > 0.05$) but was temporarily higher at $t = 40$ and 60 min in hearts treated with levosimendan ($P < 0.05$). Ventricular fibrillation did not occur in either group.

After coronary occlusion, myocardial ischaemia was visualized by a significant epicardial NADH-fluorescence enhancement distal to the occlusion site ($P < 0.05$). The size of the ischaemic zone (%) 30 min after coronary occlusion, prior to drug administration was not significantly different in the control (10 ± 3), milrinone-(11 ± 3) and levosimendan-(12 ± 3) treated hearts. In control hearts, myocardial ischaemia remained unchanged over the experimental time ($P > 0.05$) (Figure 6). Milrinone or levosimendan significantly reduced the epicardial NADH-fluorescence area ($P < 0.05$) (Figure 6). There was no significant difference between myocardial ischaemia reduction by milrinone or levosimendan ($P > 0.05$).

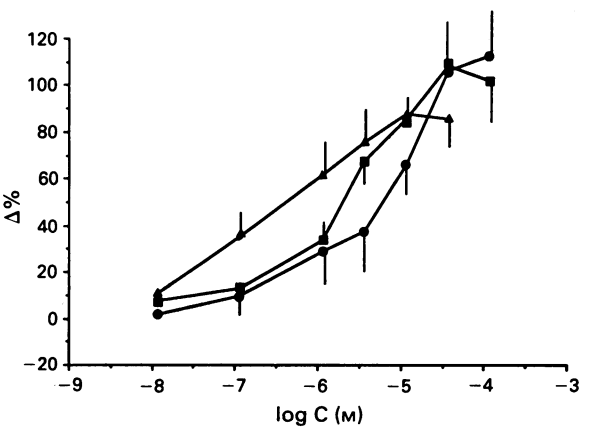

Figure 3 Cumulative concentration-response curves for the coronary vasodilator activity of amrinone (●, $n = 7$), milrinone (■, $n = 6$) or levosimendan (▲, $n = 6$) in the presence of isoprenaline (10^{-10} M) in the perfusion buffer. Ordinate scale: increase of the coronary flow relative to the actual values before PDE-inhibitor application. Symbols represent the mean ± s.e.mean.

Table 3 Actual values of the pacing-rate (HR), the left ventricular pressure (LVP) and the coronary flow (CF) at the end of the equilibration period, before coronary occlusion, and after an ischaemic period of 30 min, before starting the inotropic treatment

	HR (min^{-1})		*LVP* (mmHg)		*CF* ($ml\ min^{-1}$)	
Time (min)	0	30	0	30	0	30
Controls	202 ± 8		72 ± 4	61 ± 6	25 ± 3	18 ± 3
Milrinone	194 ± 5		65 ± 5	53 ± 5	24 ± 3	18 ± 3
Levosimendan	207 ± 10		68 ± 4	48 ± 6	24 ± 3	14 ± 2

There was no significant difference between the groups ($P > 0.05$).

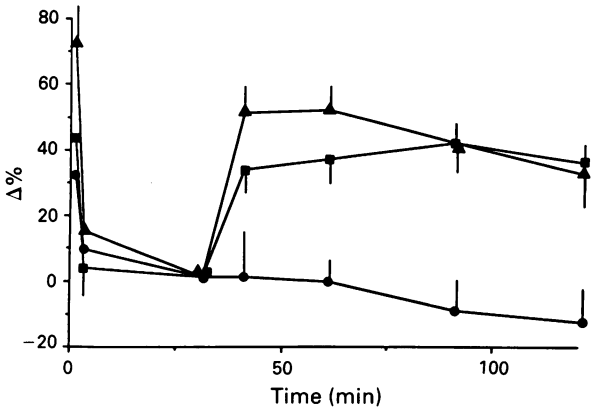

Figure 4 Time course of the relative changes of the coronary flow (CF) over the experimental time: (●) controls ($n = 5$); (■) milrinone 10^{-5} M ($n = 5$); (▲) levosimendan 5×10^{-6} M ($n = 6$). The actual values at $t = 30$ min, before starting the inotropic treatment, were taken as a reference (100%). Symbols represent the mean ± s.e.mean. CF enhancement was temporarily higher after levosimendan compared to milrinone-treatment at $t = 40$ and 60 min ($P < 0.05$).

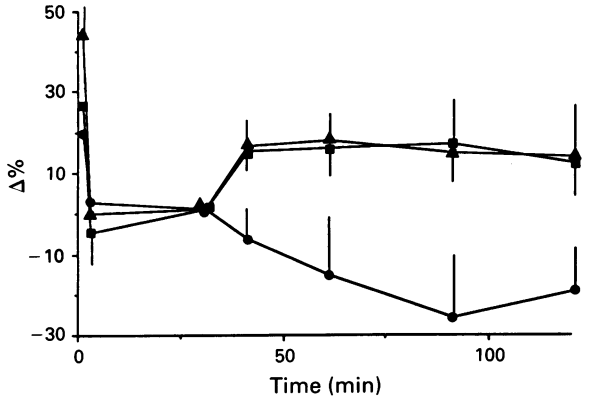

Figure 5 Time course of the relative changes of the left ventricular pressure (LVP) over the experimental time: (●) controls ($n = 5$); (■) milrinone 10^{-5} M ($n = 5$); (▲) levosimendan 5×10^{-6} M ($n = 6$). The actual values at $t = 30$ min, before starting the inotropic treatment, were taken as a reference (100%). Symbols represent the mean ± s.e. mean. There was no significant difference between LVP enhancement by milrinone and levosimendan ($P > 0.05$).

Discussion

The relation of inotropy to coronary vasodilatation was similar for the PDE-inhibitors, amrinone and milrinone. Although peripheral dilatation was not assessed in our experiments, these findings suggest that the haemodynamic profiles of both agents are very similar, and therefore similar anti-ischaemic potencies might also be expected. This is in accordance with previous findings showing that, at functionally equieffective concentrations, amrinone and milrinone

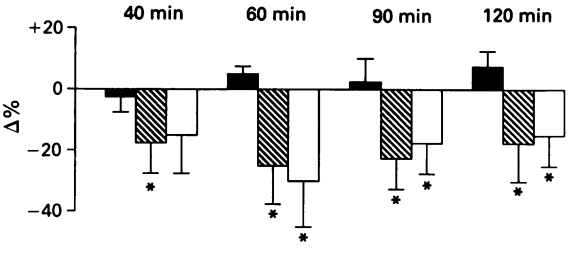

Figure 6 Epicardial NADH-fluorescence area over the experimental time. Filled columns: untreated control hearts ($n = 5$); hatched columns: milrinone-treated hearts ($n = 5$); open columns: levosimendan-treated hearts ($n = 6$). The fluorescence area 30 min after coronary occlusion was used as a reference (100%). Columns represent the mean ± s.e.mean, $*P < 0.05$.

diminished myocardial ischaemia and infarct size to a similar extent (Rump *et al.*, 1993a). Levosimendan showed a different functional profile with lower maximal effects on heart-rate and inotropy. The lower chronotropic and inotropic efficacy may be caused by an inhibitory action of levosimendan on the voltage-sensitive Ca^{2+} current (Raasmaja *et al.*, 1992), counteracting the chronotropic and inotropic effects of PDE-inhibition at higher concentrations. A decrease of the voltage-sensitive Ca^{2+} current in guinea-pig cardiomyocytes has been described for simendan at a concentration of 10^{-6} M, whereas twitch tension enhancement in guinea-pig papillary muscle shows an EC_{50} of 0.2×10^{-6} M (Raasmaja *et al.*, 1992). Calcium-channel blocking properties are also consistent with a marked coronary dilator activity, in spite of a lower maximal inotropic effect. Thus, a contribution of the calcium-antagonistic properties to cardioprotection, mediated by beneficial effects on the oxygen-demand/supply balance or by direct cytoprotection, must also be considered.

To assess the anti-ischaemic properties of milrinone and levosimendan, myocardial ischaemia was quantitated from epicardial NADH-fluorescence photography. This technique has been shown to be a very sensitive indicator of myocardial oxygenation (Barlow *et al.*, 1977). Moreover, tissue injury by toxic agents such as oxygen free radicals also induces an increase in NADH-fluorescence intensity (Rump *et al.*, 1993b,c). However, NAD redox state is measured only in the myoepicardium, which may not be characteristic of the myoendocardium. It was nevertheless demonstrated that a diminution of epicardial NADH-fluorescence during the experiment by pharmacological interventions is accompanied by infarct size reduction, as assessed by macrohistochemistry (Rump *et al.*, 1993a). Therefore, epicardial NADH-fluorescence seems to be a valid indicator of transmural ischaemic damage.

Myocardial oxygen-demand depends on heart-rate, wall tension and contractility (Baller *et al.*, 1979). The influence of the heart-rate can be negated in our model as hearts were paced at a constant rate. Furthermore, left ventricular pressure was measured isovolumetrically, excluding a reduction in wall-tension by ventricular geometry changes. The main determinants of myocardial oxygen consumption is therefore contractility and the only variable determinant of myocardial

oxygen-supply in our model is the global coronary flow. The anti-ischaemic effects of milrinone or levosimendan suggest an improvement of the oxygen-demand/supply balance. Several mechanisms must be considered: residual coronary flow to the ischaemic area is one of the most important determinants of the rate and extent of cell death within an ischaemic zone (Jennings & Reimer, 1983; Nienaber *et al.*, 1983; Hearse & Yellon, 1984). It was however demonstrated by NADH-surface fluorophotography (Harken *et al.*, 1981), anatomically (Flores *et al.*, 1984) and by microsphere techniques (Winkler *et al.*, 1984; Maxwell *et al.*, 1987) that collateral flow is essentially zero in rabbit hearts. Therefore, the likelihood of cardioprotection by drug-induced collateral flow enhancement seems remote. Concomitantly, direct cytoprotective effects may be largely excluded as the presence of the protective agent in the ischaemic tissue is required. As levosimendan was applied after the coronary occlusion was started, it may not have entered the ischaemic zone in substantial amounts. Calcium-channel blocking properties may re-inforce coronary vasodilatation, but a contribution to cardioprotection by inhibiting calcium-overload of cardiomyocytes in the ischaemic zone seems unlikely. It must rather be assumed that the beneficial effects of milrinone and levosimendan may be related to an increase of myocardial perfusion in the tissue surrounding the ischaemic zone, improving the oxygen-supply and metabolite elimination by diffusion exchanges. Moreover, as levosimendan and milrinone showed similar anti-ischaemic effects at equieffective concentrations, it seems that oxygen-sparing effects by sensitization of myofilaments to calcium do not contribute to the beneficial effects observed.

Although conclusions from *in vitro* experiments to a clinical setting must be drawn cautiously, our findings suggest that the bipyridine-type PDE-inhibitors amrinone and milrinone possess similar functional profiles, and therefore similar anti-ischaemic potencies might be expected. The anti-ischaemic properties of levosimendan are comparable to those of milrinone, at higher haemodynamically equieffective concentrations, associated with a marked coronary dilator activity. It remains to be seen whether oxygen-sparing effects, related to the calcium-sensitizing properties of levosimendan, confer to that compound particular cardioprotective properties at lower concentrations, when myocardial perfusion is less affected.

References

BACKHAUS, K., ERICHSON, B., PLINKE, W. & WEIBER, R. (1994). *Multivariate Analysenmethoden.* Berlin, Heidelberg, New York, London, Paris, Tokio, Hong Kong, Barcelona, Budapest: Springer Verlag.

BALLER, D., BRETSCHNEIDER, H.J. & HELLIGE, G. (1979). Validity of myocardial oxygen consumption parameters. *Clin. Cardiol.*, **2**, 317–327.

BARLOW, C.H., HARKEN, A.D. & CHANCE, B. (1977). Evaluation of cardiac ischemia by NADH fluorescence photography. *Ann. Surg.*, **186**, 737–740.

BENOTTI, J.R., GROSSMAN, W., BRAUNWALD, E. & CARABELLO, B.A. (1980). Effects of amrinone on myocardial energy metabolism and haemodynamics in patients with severe congestive heart failure due to coronary artery disease. *Circulation*, **62**, 24–34.

EDES, I., PAPP, G.J. & CSANADY, M. (1992). The effects of a new calcium sensitizer, simendan, on intracellular protein phosphorylation. *J. Mol. Cell. Cardiol.*, **24** (Suppl. V), 93.

FLORES, N.A., DAVIES, R.L., PENNY, W.J. & SHERIDAN, D.J. (1984). Coronary microangiography in the guinea pig, rabbit and ferret. *Int. J. Cardiol.*, **6**, 459–471.

HAFNER, D., HEINEN, E. & NOACK, E. (1977). Mathematical analysis of concentration-response relationships. *Arzneim.-Forsch./Drug Res.*, **27**, 1871–1873.

HAIKALA, H., LINDÉN, I.B. & POHTO, P. (1992a). Simendan, a novel calcium sensitizer, is as potent and efficient in the skinned fibre as in the electrically paced papillary muscle. *J. Mol. Cell. Cardiol.*, **24** (Suppl. I), 260.

HAIKALA, H., NISSINEN, E., ETEMADZADEH, E., LINDEN, I.B. & POHTO, P. (1992b). Levosimendan increases calcium sensitivity without enhancing myosin ATPase activity and impairing relaxation. *J. Mol. Cell. Cardiol.*, **24** (Suppl V), 97.

HARKEN, A.H., SIMSON, M.B., HASELGROVE, J., WETSTEIN, L., HARDEN, W.R. & BARLOW, C.H. (1981). Early ischemia after complete coronary ligation in the rabbit, dog, pig and monkey. *Am. J. Physiol.*, **241**, H202–H210.

HEARSE, D.J. & YELLON, D.M. (1984). Why are we still in doubt about infarct size limitation? The experimentalist's viewpoint. In *Therapeutic Approaches to Myocardial Infarct Size Limitation.* ed. Hearse, D.J. & Yellon, D.M. pp. 17–42. New York: Raven Press.

HERZIG, J.W. & QUAST, U. (1992). On the role of Ca^{++} binding proteins as possible targets for Ca^{++} sensitizing agents. *Z. Kardiol.*, **81** (Suppl. 4), 49–55.

HOLMBERG, S.R.M. & WILLIAMS, A.J. (1991). Phosphodiesterase inhibitors and the cardiac sarcoplasmic reticulum calcium release channel: differential effects of milrinone and enoximone. *Cardiovasc. Res.*, **25**, 537–545.

JENNINGS, R.B. & REIMAR, K.A. (1983). Factors involved in salvaging ischaemic myocardium: effect of reperfusion of arterial blood. *Circulation*, **68** (Suppl I), 125–136.

JENTZER, J.H., LEJEMTEL, T.H., SONNENBLICK, E.H. & KIRK, E.S. (1981). Beneficial effect of amrinone on myocardial oxygen consumption during acute left ventricular failure in dogs. *Am. J. Cardiol.*, **48**, 75–83.

KATZ, A.M. (1986). Potential deleterious effects of inotropic agents in the therapy of chronic heart failure. *Circulation*, **73** (Suppl. III), 184–190.

KITZEN, J.M. & WINBURY, M.M. (1989). Pimobendan. *Cardiovasc. Drug Res.*, **6**, 265–291.

LANGENDORFF, O. (1895). Untersuchungen am überlebenden Säugetier-herzen. *Arch. Ges. Physiol.*, **61**, 291–332.

LEYEN V DER, H., SCHMITZ, W., SCHOLZ, H. & SCHOLZ, J. (1989). New positive inotropic agents acting by phosphodiesterase inhibition or alpha1-adrenergic stimulation. *Pharmacol. Res.*, **21**, 329–337.

MAXWELL, M.P., HEARSE, D.J. & YELLON, D.M. (1987). Species variation in the corona collateral circulation during regional myocardial ischaemia: A critical determinant of the rate of evolution and extent of myocardial infarction. *Cardiovasc. Res.*, **21**, 737–746.

MORNER, S.E.J.N. (1990). Phosphodiesterase inhibitors increase calcium recirculation within the myocyte. In *Phosphodiesterase Inhibitors and the Heart.* pp. 6–7. Abingdon: The Medicine Group (UK) Ltd.

NIENABER, C., GOTTWICK, M., WINKLER, B. & SCHAPER, W. (1983). The relationship between perfusion deficit, infarct size and time after experimental coronary occlusion. *Basic Res. Cardiol.*, **78**, 210–226.

OVASKA, M., HAIKALA, H., LUNDSTROM, K., KORKOLAINEN, T., TASKINEN, J. & LINDÉN, I.B. (1992). Studies on calcium-dependent binding of simendan to troponin complex and troponin C. *J. Mol. Cell. Cardiol.*, **24** (Suppl. I), 260.

RAASMAJA, A., TALO, A., HAIKALA, H., NISSINEN, E., LINDÉN, I.B. & POHTO, P. (1992). In *Excitation-Contraction Coupling in Skeletal, Cardiac and Smooth Muscles.* ed. Frank, G.B., Bianchi, C.P. & Keuers, H.E.D. p. 423. New York, London: Plenum Press.

RUMP, A.F.E., BLAZINCIC, B. & KLAUS, W. (1993a). Effect of amrinone and milrinone on myocardial ischemia extent and infarct size in isolated rabbit hearts. *Drug Res.*, **43**, 1262–1266.

RUMP, A.F.E., RÖSEN, R. & KLAUS, W. (1993b). Cardioprotection by superoxide dismutase: A catecholamine-dependent process? *Anesth. Analg.*, **76**, 239–246.

RUMP, A.F.E., RÖSEN, R. & KLAUS, W. (1993c). Free radical scavenging properties of β-adrenoceptor blockers are not relevant for cardioprotection in isolated rabbit hearts. *Naunyn-Schmied. Arch. Pharmacol.*, **348**, 431–434.

RUMP, A.F.E., RÖSEN, R., KORTH, A. & KLAUS, W. (1993d). Deleterious effect of exogenous angiotensin-I on the extent of regional ischaemia and its inhibition by captopril. *Eur. Heart J.*, **14**, 106–112.

RUMP, A.F.E., RÖSEN, R., SIGMUND, B., FUCHS, J., DHEIN, S. & KLAUS, W. (1993e). Beneficial effect of amrinone on the size of acute regional ischemia in isolated rabbit hearts. *J. Cardiothor. Vasc. Anesth.*, **7**, 573–578.

VAN ZWIETEN, P.A. (1991). Background to the drug treatment of heart failure. In *The Role of Phosphodiesterase-Inhibitors in Heart Failure*. ed. Van Zwieten, P.A. pp. 1–12. London, New York: Royal Society of Medicine Services.

VENTURA, C., MILLER, R., WOLF, H.P., BEIER, N., JONAS, R., KLOCKOW, M., LUES, I., HANO, O., SPURGEON, H.A., LAKATTA, E.G. & CAPOGROSSI, M.C. (1992). Novel Diazinone Derivatives separate myofilament Ca^{2+} sensitization and phosphodiesterase III inhibitory effects in guinea pig myocardium. *Circ. Res.*, **70**, 1081–1090.

WINKLER, B., SASS, S., BINZ, K. & SCHAPER, W. (1984). Myocardial blood flow and myocardial infarction in rats, guinea pig and rabbits. *J. Mol. Cell. Cardiol.*, **16** (Supp 2), 48.

(Received July 1, 1993
Revised February 24, 1994
Accepted March 9, 1994)

Br. J. Pharmacol. (1994), **112**, 763–768

A pharmacological analysis of receptors mediating the excitatory response to 5-hydroxytryptamine in the guinea-pig isolated trachea

[1]Adele Lucchelli, Maria Grazia Santagostino-Barbone, Annalisa Barbieri & *Marcello Tonini

Institute of Pharmacology, School of Pharmacy, University of Pavia, Viale Taramelli 14, 27100 Pavia and *Department of Internal Medicine and Therapeutics, Division of Pharmacology and Toxicology, University of Pavia, Piazza Botta 10, 27100 Pavia, Italy

1 Experiments were carried out to characterize the receptors mediating the indirect excitatory response to 5-hydroxytryptamine (5-HT) in the guinea-pig isolated trachea.

2 5-HT caused concentration-dependent contractions of tracheal strips, and the resulting concentration-response curve was biphasic in nature. The first phase was obtained with agonist concentrations in the range of 0.01–3 nM and achieved a maximum which was 30% of the total 5-HT response, while the second phase was in the range 10 nM–1 μM.

3 Atropine (0.1 μM) and tetrodotoxin (TTX: 0.3 μM) significantly reduced both phases of the 5-HT curve. Morphine (10 μM), which can act to inhibit neuronal acetylcholine release, abolished the first phase and reduced the second phase. This suggests that the first phase is mainly neurogenic (cholinergic) in nature, while the second phase is in part neurogenic and in part due to direct activation of the effector cells.

4 The 5-HT_{2A} receptor antagonist, ketanserin (0.01, 0.1 μM) markedly depressed the first phase and shifted the second phase to the right in a parallel manner, with some depression of the 5-HT response maximum. The less selective (5-HT_1/5-HT_{2A}) antagonist, methiothepin (0.1 μM) mimicked the action of ketanserin, albeit with less potency. Concomitant administration of ketanserin and methiothepin (each at 0.1 μM) produced an antagonism similar to that caused by ketanserin (0.1 μM) alone.

5 The 5-HT_3 receptor antagonists, ondansetron (0.1 μM) and granisetron (0.01 μM) slightly but significantly inhibited the first phase of the 5-HT curve without altering the second phase. SDZ 205,557 (0.3 μM), a 5-HT_4 receptor antagonist, was ineffective.

6 Our results suggest that neural 5-HT_{2A} and, to a lesser extent, 5-HT_3 receptor subtypes mediate the first phase of the 5-HT curve in the guinea-pig trachea. The second phase is mediated by 5-HT_{2A} receptors, which are probably located at both the neural and muscular level. No evidence for the participation of 5-HT_1 receptors in the 5-HT response has been obtained.

Keywords: 5-HT; 5-HT-mediated contractions; 5-HT receptor antagonists; guinea-pig trachea

Introduction

Increasing evidence suggests that 5-hydroxytryptamine (5-HT) produces bronchoconstriction in a number of animal species, including man. In *in vivo* experiments in the dog, this response was partially antagonized by atropine (Islam *et al.*, 1974) and by procedures that reduce vagal nerve function (Hahn *et al.*, 1978), indicating an interaction of 5-HT with the extrinsic parasympathetic innervation. This mode of action has been substantiated by experiments in which 5-HT caused hyperresponsiveness of canine airways to vagal stimulation (Hahn *et al.*, 1978; Dixon *et al.*, 1980; Sheller *et al.*, 1982). Activation of cholinergic pathways by 5-HT has also been demonstrated in the airways of the guinea-pig (Macquin-Mavier *et al.*, 1991). Although in this species bilateral cervical vagotomy or nicotinic ganglionic blockade had little or no effect on 5-HT-induced bronchoconstriction, the latter was significantly reduced by atropine. This led to the hypothesis that excitatory 5-HT receptors might also be located in postganglionic parasympathetic nerves (Macquin-Mavier *et al.*, 1991).

In the guinea-pig isolated trachea, however, the excitatory response to 5-HT is sustained by two distinct mechanisms. These include a direct action on smooth muscle mediated by post-junctional 5-HT_2 receptors (Cohen *et al.*, 1985; Lemoine & Kaumann, 1986; Baumgartner *et al.*, 1990; Watts & Cohen, 1993), and an indirect action caused by activation of cholinergic nerves (McCaig, 1986; Baumgartner *et al.*, 1990), as observed in *in vivo* experiments. Although 5-HT receptors mediating the neurogenic component of the 5-HT response have not as yet been characterized in guinea-pig isolated preparations, results from *in vivo* experiments indicate that 5-HT_2 receptors may also contribute to the indirect response (Macquin-Mavier *et al.*, 1991).

Recently, in peripheral tissues like the mouse isolated trachea (Van Oosterhout *et al.*, 1991) and guinea-pig intestinal preparations (Craig & Clarke, 1990; Eglen *et al.*, 1990; Tonini *et al.*, 1992a), 5-HT was found to activate cholinergic nerves via multiple receptors including 5-HT_1-like, 5-HT_3 and 5-HT_4 subtypes. The present study was designed to characterize the receptors mediating the indirect excitatory response to 5-HT in the guinea-pig isolated trachea by use of selective antagonists of various 5-HT receptor subtypes. The new nomenclature for 5-HT receptors recently proposed (Humphrey *et al.*, 1993) will be used throughout the text.

Methods

Male guinea-pigs (400–500 g) were killed by CO_2 asphyxation. The entire trachea was removed, cleared of adhering connective tissue and cut into two segments similar in length. Each segment was opened through the cartilage and a zig-zag strip (4.5 cm long, 2 mm wide) was prepared according to the method of Emmerson & MacKay (1979). Strips were mount-

[1] Author for correspondence.

ed in a 10 ml organ bath containing Krebs-Henseleit solution (composition in mM: NaCl 118, KCl 5.6, $CaCl_2 \cdot 2H_2O$ 2.5, $MgSO_4 \cdot 7H_2O$ 1.19, NaH_2PO_4 1.3, $NaHCO_3$ 25, glucose 10), maintained at 37°C and gassed with a mixture of 95% O_2 and 5% CO_2 (pH 7.4).

Contractions were recorded by U. Basile 7006 isotonic transducers loaded at 0.5 g and connected to LNI recorders. All experiments were started after an equilibration period of 60 min, during which solutions were changed every 15 min.

Protocol

Cumulative concentration-response curves to 5-HT were constructed in paired tissues using half logarithmic dosing increments. Each 5-HT concentration was added to the bath as soon as the previous concentration had reached a plateau. After an initial concentration-response curve had been obtained (first curve), tissues were washed for 60 min, then a second curve was constructed either in the absence (second control curve) or presence of different pharmacological agents which were left in contact with the preparation for 20 min. These agents were: cocaine, a neuronal 5-HT uptake blocker (Verbeuren, 1989), morphine, an inhibitor of acetylcholine (ACh) release (Schaumann, 1957; Tonini *et al.*, 1992b), atropine, a non selective muscarinic receptor antagonist, tetrodotoxin (TTX), a neuronal Na^+-channel blocker, ketanserin, a $5\text{-}HT_{2A}$ receptor antagonist (Humphrey *et al.*, 1993), methiothepin, a $5\text{-}HT_1/5\text{-}HT_{2A}$ receptor antagonist (Humphrey *et al.*, 1993), granisetron and ondansetron, selective $5\text{-}HT_3$ receptor antagonists (Richardson *et al.*, 1985; Sanger & Nelson, 1989) and SDZ 205,557, a $5\text{-}HT_4$ receptor antagonist (Buchheit *et al.*, 1992). In each tissue, only one inhibitor/antagonist concentration was tested, with the exception of a few experiments in which ketanserin and methiothepin were administered concomitantly at equimolar concentrations.

In a separate set of experiments, the contractile response to 5-HT was investigated in tissues obtained from reserpine-pretreated guinea-pigs (5 mg kg^{-1}, i.p., once daily for 2 days) killed 24 h after the last drug injection. This dose schedule was previously found to produce effective central and peripheral noradrenaline depletion in the rat (Wakade, 1980) and to abolish the responses to tyramine in the guinea-pig intestine (Lucchelli *et al.*, 1990).

Data analysis

In control tissues, following the determination of the first concentration-response curve, removal of 5-HT by prolonged rinsing caused basal muscle tone to decrease to a level lower than that observed initially. Nevertheless, the second administration of 5-HT caused a maximum effect comparable to that obtained in the first curve. Data from the second curve were then normalized, i.e. corrected for the change in basal tone and expressed as a percentage of the maximum effect, as previously suggested by Lemoine & Kaumann (1986).

Control curves were analysed by fitting them to a logistic equation of the form; $\text{Effect} = E_{\text{maximum}}/1 + e^{(-2.303 \cdot \text{slope} \cdot (\log[A] - \log[A_{50}]))}$ where: E_{maximum} = maximum response; [A] = molar agonist concentration; $[A_{50}]$ = molar agonist concentration inducing 50% of the maximum response. All data were fitted either to a single logistic expression or to the sum of two logistics. Goodness of fit to a single or double logistic expression was evaluated by the *F*-test of the residual variances using a significance criterion of $P \leqslant 0.05$ (SAS Institute Inc., 1988).

In biphasic curves, maximum responses were determined graphically for each phase and indicated as max_1 and max_2, respectively. Potency values were expressed as $-\log EC_1$ and $-\log EC_2$ for the first and second phase, respectively, where EC indicates the molar concentration of 5-HT inducing 50% of the maximum effect.

In the experiments in which inhibitors/antagonists were tested, any drug-induced depression of the 5-HT curve was calculated as a percentage of the maximum effect of the first curve, with no correction for between-curve differences in control agonist curves.

All data in the text are mean ± s.e.mean. Differences between means were analysed by Student's paired two-tailed *t* test or by ANOVA followed by *a posteriori* Bonferroni's test when applicable. Values of $P \leqslant 0.05$ were taken as statistically significant.

Drugs

5-Hydroxytryptamine hydrochloride, reserpine, tetrodotoxin and atropine sulphate were obtained from Sigma; ketanserin tartrate and methiothepin mesylate from RBI; granisetron (BRL 43694: endo-N-(9-methyl-9-azabicyclo 3.3.1 non-3-yl)-1-methyl-1H-indazole-3-carboxamide hydrochloride) and ondansetron (GR 38032F: 1,2,3,9-tetrahydro-9-methyl-3-(2-methylimidazol-1) methyl carbazole-4-one hydrochloride hydrate) were donated by Smith Kline Beecham and Glaxo, respectively; SDZ 205,557: (2-methoxy-4-amino-5-chloro-benzoic acid 2-(diethyl-amino)-ethyl ester hydrochloride) was a gift from Sandoz; morphine hydrochloride and cocaine hydrochloride were from SALARS (Società Azionaria Laboratori Alcaloidi Rifornimenti Sanitari, Como, Italy).

With the exception of ketanserin and reserpine, all drugs were dissolved in distilled water and administered in volumes not exceeding 1% v/v of the bath volume. Stock solutions of ketanserin were prepared in 1:100 v/v ethanol/water, while those of reserpine in 20:100 v/v ethanol/water with the addition of 1.6% w/v ascorbic acid. Further dilutions were in water.

Results

Effects of 5-HT on tracheal strips

5-HT produced concentration-dependent contractions of the guinea-pig isolated trachea and the resulting concentration-response curve was biphasic in nature (Figure 1), since it was better fitted to a summation of two logistics than to a single logistic function ($F = 6.3$, $P < 0.05$).

The first phase was obtained with concentrations of 5-HT in the range 0.01–3 nM, while the second phase was in the range 10 nM–1 μM. The mean maximum response of the first phase (max_1) was 31.0 ± 2.5% of the total response while that of the second phase (max_2) was 98.0 ± 0.2%. The mean

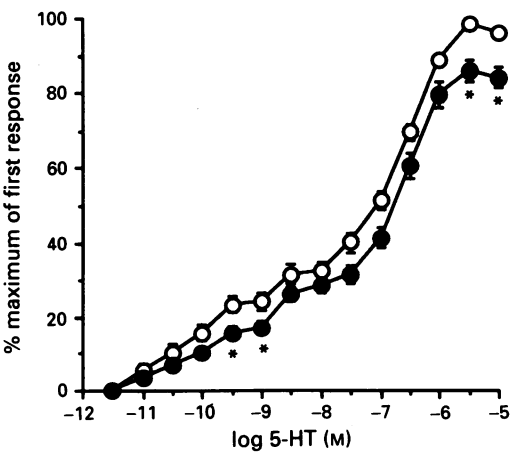

Figure 1 Concentration-response curves to 5-hydroxytryptamine (5-HT) obtained in the guinea-pig isolated trachea. (○) First curve; (●) second curve determined after a 60 min interval. Results are mean ± s.e.mean; $n = 30$. $^*P < 0.05$ versus respective values of the first curve.

potency values were 9.9 ± 0.07 for the first phase (− log EC_1) and 6.7 ± 0.03 for the second phase (− log EC_2).

In control experiments designed to determine any time-dependent changes in tissue sensitivity, a slight change in 5-HT responsiveness was observed after 60 min recovery from the first 5-HT curve (Figure 1). The second concentration-response curve to 5-HT was biphasic exhibiting the following values: max_1 23.0 ± 2.1% and max_2 82.0 ± 2.8%; − log EC_1 9.9 ± 0.05 and − log EC_2 6.7 ± 0.03. While max_1 and max_2 values of the second curve were significantly different ($P<0.05$) from the corresponding values of the first curve, potency values of the two phases in both curves were not different.

Reserpine pretreatment ($n = 4$) did not alter the sensitivity of the trachea to 5-HT. Potency (− log EC_1, 9.7 ± 0.09; − log EC_2, 6.8 ± 0.04) and maximum contractility (max_1, 33.0 ± 3.0%; max_2, 99.0 ± 1.0%) values obtained in tissues from reserpinized animals were not different from those obtained in tissues of untreated animals.

Effects of 5-HT receptor antagonists on 5-HT-induced contractions

None of the pharmacological agents, incubated with tracheal strips before 5-HT administration, changed the basal tone of the preparation. Cocaine (10 μM) did not affect the sensitivity of trachea to 5-HT (Figure 2). In the presence of atropine (0.1 μM), both phases of the 5-HT curve were greatly inhibited (Figure 3). Like atropine, TTX (0.3 μM) significantly reduced both phases of the concentration-response curve to 5-HT. In the presence of TTX, the first phase was scarcely dependent on agonist concentration, while the second phase was shifted to the right with max_2 reduced to 53.2 ± 10.1% (Figure 4). Morphine (10 μM) greatly affected 5-HT responses causing the curve to become monophasic, due to abolition of the first phase. Moreover, the second phase was shifted to the right and reduced in its maximum (Figure 5).

Ketanserin (0.01 μM) markedly reduced the first phase of the 5-HT curve and shifted the second phase to the right in a parallel manner with some depression of the maximum effect (max_2: 66.7 ± 13.3%). A higher concentration of ketanserin (0.1 μM) did not further inhibit the first phase, while it caused an additional shift of the second phase to the right and a further reduction of the maximum effect (max_2: 50.8 ± 11.2%) (Figure 6a). Methiothepin (0.1 μM) greatly inhibited the first phase and shifted to the right and depressed the second phase of the curve (Figure 6b). Preincubation of tracheal strips with both ketanserin (0.1 μM) and methiothepin (0.1 μM) led to a reduction of both 5-HT phases

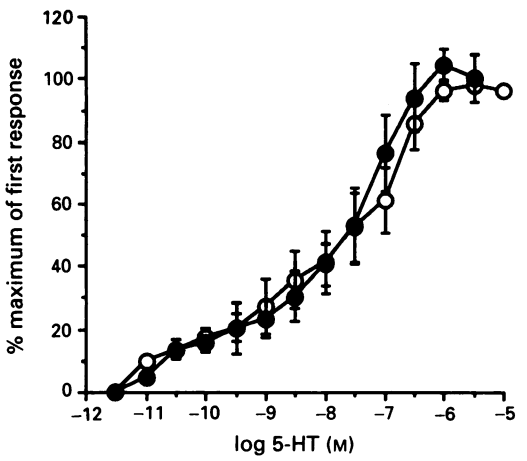

Figure 2 Concentration-response curves to 5-HT obtained in guinea-pig tracheal strips in the absence (○) or presence of 10 μM cocaine (●). Results are mean ± s.e.mean; $n = 4$.

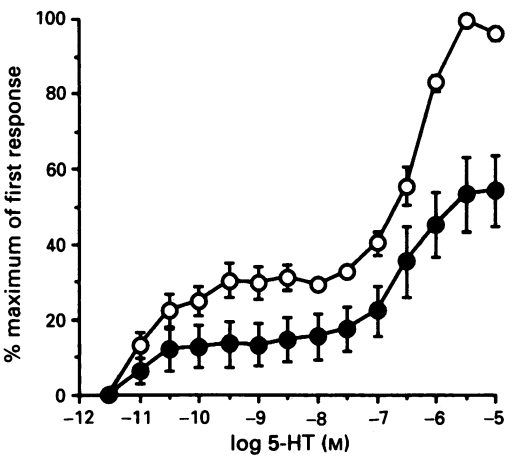

Figure 4 5-HT concentration-response curves obtained in guinea-pig tracheal strips in the absence (○) or presence of 0.3 μM tetrodotoxin (TTX) (●). Results are mean ± s.e.mean; $n = 4$. All values in the presence of TTX are significantly different ($P<0.05$) from their respective controls.

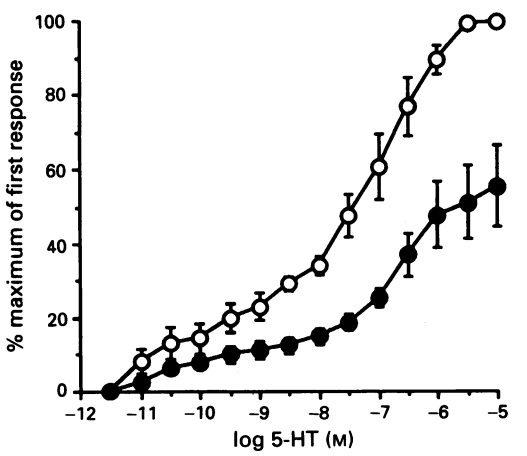

Figure 3 5-HT concentration-response curves obtained in guinea-pig tracheal strips in the absence (○) or presence of 0.1 μM atropine (●). Results are mean ± s.e.mean; $n = 4$. All values in the presence of atropine are significantly different ($P<0.05$) from their respective controls.

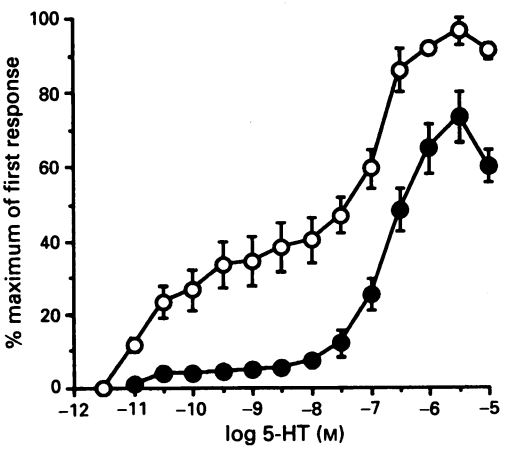

Figure 5 5-HT concentration-response curves obtained in guinea-pig tracheal strips in the absence (○) or presence of 10 μM morphine (●). Results are mean ± s.e.mean; $n = 4$. All values in the presence of morphine are significantly different ($P<0.05$) from their respective controls.

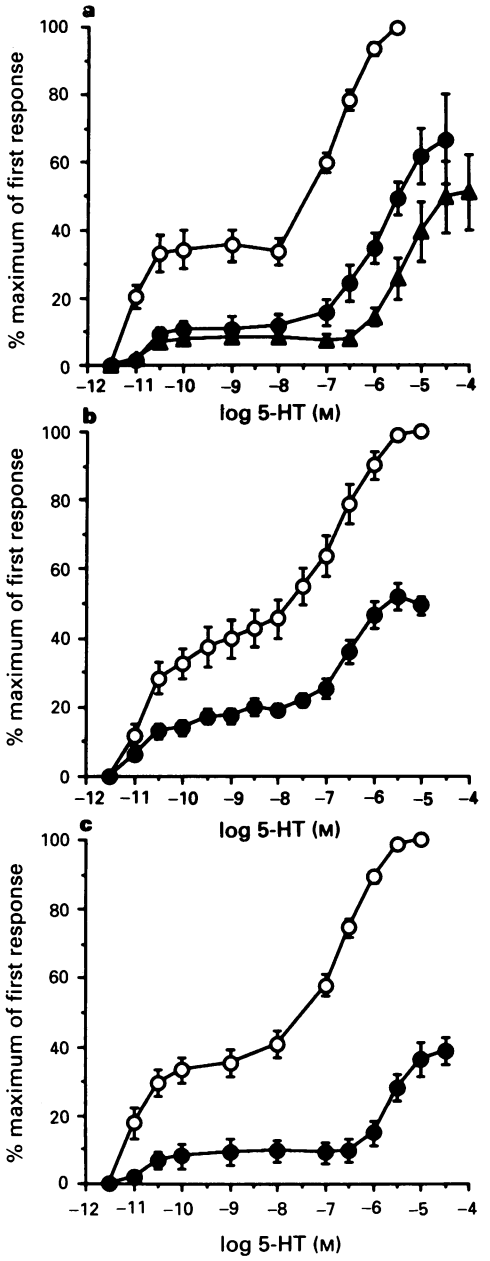

Figure 6 Effect of 0.01 (●) and 0.1 μM (▲) ketanserin (a), 0.1 μM (●) methiothepin (b), and a combination of ketanserin and methiothepin (each at 0.1 μM: ●) (c) on the concentration-response curves to 5-HT (control: ○). Results are mean ± s.e.mean; $n = 4-8$. Each point of 5-HT curve in the presence of antagonists is significantly different ($P<0.05$) from the corresponding control value (Student's paired two-tailed t test). The antagonism caused by 0.1 μM ketanserin (a) was not different from that caused by a combination of ketanserin and methiothepin (c) (ANOVA followed by Bonferroni's test).

similar to that obtained with ketanserin (0.1 μM) alone (Figure 6c). The comparison of the 5-HT curve in the presence of 0.1 μM ketanserin with those obtained in the presence of methiothepin (0.1 μM) or of a combination of both antagonists rèvealed that the antagonism exerted by ketanserin was significantly higher ($P<0.05$) than that exerted by methiothepin and was not different from that exerted by the concomitant administration of the two antagonists.

Granisetron (0.01 μM) slightly, but significantly, reduced the first phase of the 5-HT curve without affecting the second phase. Max_1 was reduced to 21.0 ± 2.4% (control: 32.5 ± 3.3%) (Figure 7a). Like granisetron, ondansetron (0.1 μM) reduced max_1 from 28.4 ± 4.8% to 19.1 ± 3.1% without alteration of the second phase (Figure 7b).

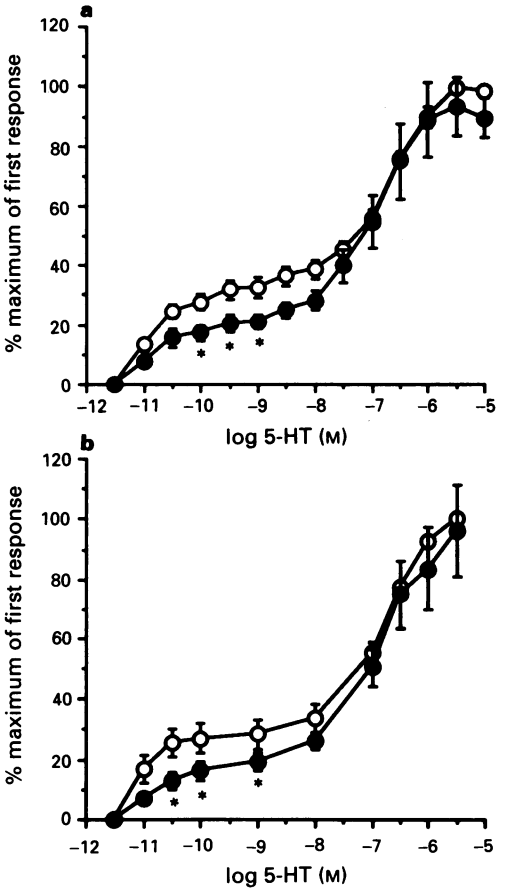

Figure 7 Effect of 0.01 μM (●) granisetron (a) and 0.1 μM (●) ondansetron (b) on the concentration-response curves to 5-HT obtained in guinea-pig tracheal strips (control: ○). Results are mean ± s.e.mean; $n = 4-8$. $^*P<0.05$.

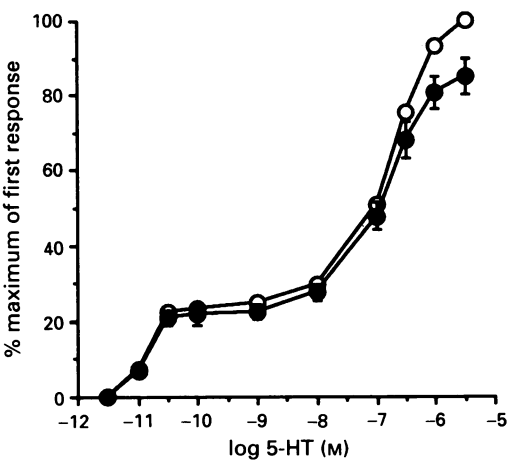

Figure 8 Effect of 0.3 μM SDZ 205,557 (●) on the concentration-response curve to 5-HT obtained in guinea-pig tracheal strips (control: ○). Results are mean ± s.e.mean; $n = 4$.

SDZ 205,557 (0.3 μM) was ineffective on both phases of the 5-HT curve (Figure 8).

Discussion

To our knowledge, this is the first work indicating that the concentration-response curve to 5-HT in contracting the guinea-pig isolated trachea is biphasic in nature.

The first phase, which accounts for approximately 30% of the maximal agonist response, is obtained with 5-HT concentrations up to 3 nM, while the second phase is generated at higher concentrations. In previous works with isolated trachea, concentration-response curves to the contractile effect of 5-HT were described as monophasic and the minimal effective agonist concentration was in the 1–10 nM range (Lemoine & Kaumann, 1986; Baumgartner *et al.*, 1990; Cortijo *et al.*, 1992; Watts & Cohen, 1992; 1993). Inclusion of indomethacin in the bathing solution or a lower tissue incubation temperature (32°C) could account for the failure to detect a 5-HT contractile response at sub-nanomolar concentrations.

The response of the tissue to repeated administrations of 5-HT was fairly reproducible. Slight time-related changes in sensitivity to 5-HT were detected in both phases of the curve. However, they were restricted only to a reduction of the maximum effect in each phase, without changes in the sensitivity to 5-HT. Similar results have been reported for the 'second phase' by Baumgartner *et al.* (1990) and by Watts & Cohen (1992).

It is well known that 5-HT can induce noradrenaline release in various tissues (Feniuk & Humphrey, 1989; Lucchelli *et al.*, 1984) via receptor-mediated mechanisms (e.g. 5-HT_3 receptors; Fozard & Mobarok Ali, 1978) and by a tyramine-like action on sympathetic neurones (Humphrey, 1978), which might influence the constrictor effect of 5-HT. The similarity of results obtained with 5-HT in tissues from control and reserpine-pretreated animals indicate that, in the guinea-pig trachea, 5-HT is devoid of noradrenaline releasing properties. Furthermore, the failure of cocaine, a blocker of neuronal 5-HT uptake (Verbeuren, 1989), to modify 5-HT-induced contractions, suggests that uptake mechanisms play a minor, if any, role in the trachea.

TTX and atropine inhibited both phases of the contractile response to 5-HT. This observation suggests that at least part of the effect of 5-HT is neurogenic in nature and mediated by ACh release from postganglionic cholinergic neurones. Inhibitory effects of atropine on the contractile response to 5-HT in the guinea-pig airways have been previously reported both *in vitro* (McCaig, 1986; Baumgartner *et al.*, 1990) and *in vivo* (Macquin-Mavier *et al.*, 1991). The cholinergic component of the 5-HT response is probably most prominent in the first phase, since the latter was abolished by a high concentration of morphine, which is known to inhibit ACh release from peripheral tissues (Schaumann, 1957; Tonini *et al.*, 1992b). The second phase of 5-HT curve was partially resistant to morphine (as it was to TTX and atropine), indicating that 5-HT may directly activate the effector cells, especially at high concentrations.

As far as the influence of 5-HT receptor antagonism is concerned, the effects of various antagonists on both phases of 5-HT response need to be considered. The ketanserin-induced inhibition of the first phase of the 5-HT curve and the rightward displacement of the second phase is entirely consistent with antagonism at 5-HT_{2A} receptors. These findings support the concept that 5-HT_{2A} receptors are involved not only in the direct contractile responses induced by high 5-HT concentrations, but also in the nerve-mediated cholinergic responses produced by sub-nanomolar concentrations of 5-HT. Our results are in agreement with those of Macquin-Mavier *et al.* (1991), who reported that the neural 5-HT receptors mediating the facilitation of parasympathetic contraction in the guinea-pig airways *in vivo* may be ascribed to the 5-HT_2 subtype. We are aware, however, that a sub-nanomolar potency for 5-HT, such as that suggested in our study, has never been reported for neural (central) 5-HT_2 receptors (Hoyer, 1989). To clarify this point, experiments evaluating ACh release induced by 5-HT receptor agonists (in the absence and in the presence of antagonists) are required. The rightward displacement of the second phase and the reduction in the maximum effect of 5-HT produced by ketanserin, confirms previous findings (Cohen *et al.*, 1985; Lemoine & Kaumann, 1986; Baumgartner *et al.*, 1990; Watts & Cohen, 1992) and corroborates the results of Watts & Cohen (1992), who found that the reduction of the maximum effect of 5-HT increased with increasing antagonist concentrations. The same pattern of antagonism was obtained with ritanserin, another competitive 5-HT_{2A} receptor antagonist (Watts & Cohen, 1992). In addition to 5-HT_{2A} receptor antagonist properties, ketanserin also displays antagonism at 5-HT_{2C}-receptors (Humphrey *et al.*, 1993), although with 100 fold lower affinity (Hoyer, 1989). The involvement of 5-HT_{2C} receptors in the contractile effect of 5-HT in the trachea has been ruled out by Watts & Cohen (1993).

Our findings with methiothepin tend to exclude the participation of 5-HT_1 receptors in the 5-HT-induced neurogenic response of guinea-pig airways, even though these receptors have been claimed to facilitate cholinergic transmission in the trachea of other animal species (i.e. the mouse) (Van Oosterhout *et al.*, 1991). In fact, based on our results, the antagonism exerted by methiothepin on both phases of the 5-HT curve can be explained in terms of blockade of 5-HT_{2A} receptors. Methiothepin, which is generally employed as a 5-HT_1 antagonist, has an affinity value for brain 5-HT_{2A} receptors which is almost 30 times greater than that for any other type of 5-HT_1 receptor (Hoyer, 1989). Therefore, at the concentration employed in this study (0.1 μM), which is in the range of the affinity of methiothepin for the 5-HT_1 receptors, the possibility exists that methiothepin also interacts with 5-HT_{2A} receptors. The observation that ketanserin (0.1 μM) or a combination of ketanserin and methiothepin (each at 0.1 μM) antagonized 5-HT responses to a similar extent, suggests the involvement of 5-HT_{2A} receptors only. In fact, for an interaction between antagonists at a single receptor type, addition of concentration-ratios is expected, whereas multiplication is expected when the antagonists act at different receptors.

The 5-HT_3 receptor antagonists, ondansetron and granisetron slightly, but significantly, reduced the first phase of 5-HT curve without affecting the second phase. These findings suggest that neuronal 5-HT_3 receptors may contribute to the 5-HT-induced cholinergic response in the first phase. The inefficacy of cocaine, a compound that has antagonistic properties at 5-HT_3 receptors (Fozard *et al.*, 1979) is difficult to explain, but might reflect 5-HT_3 receptors heterogeneity (Richardson & Engel, 1986). In this respect, the potent cocaine derivative antagonist, MDL 72222, was found to antagonize central but not peripheral 5-HT_3 receptors (Fozard, 1984; Richardson & Engel, 1986). Nevertheless, caution is required in interpreting our findings, since a slight reduction of the first 5-HT phase is also observed following repeated agonist curves, and because the affinity of 5-HT for 5-HT_3 receptors is in the micromolar range of concentrations (Eglen *et al.*, 1990). In our experiments, the failure of 5-HT_3 receptor blockade to affect the second phase of 5-HT curve is in agreement with the results of Kameda *et al.* (1988) and Baumgartner *et al.* (1990), who found that the $5\text{-HT}_3/5\text{-HT}_4$ blocker ICS 205,930 (tropisetron) had no effect on 5-HT-induced contractions. Indeed, a moderate inhibitory effect of high concentrations of tropisetron was reported by Watts & Cohen (1992). Recently, the participation of 5-HT_3 receptors in facilitating electrically-induced cholinergic transmission in the guinea-pig trachea has been reported by Rizzo *et al.* (1993). Finally, we investigated the possible contribution of 5-HT_4 receptors to the excitatory action of 5-HT. The 5-HT_4 receptor antagonist SDZ 205,557 (Buchheit *et al.*, 1992), at a concentration not interfering with 5-HT_3 receptors in guinea-pig peripheral tissues (Eglen *et al.*, 1993), was ineffective on the 5-HT curve, indicating that 5-HT_4 receptors are not involved in the contractile effect of 5-HT in the trachea.

In conclusion, 5-HT has been shown to induce a biphasic contractile response in the guinea-pig trachea. The first phase appears to be almost totally cholinergic in nature and is mediated by neural receptors displaying the characteristics of a 5-HT_{2A} receptor. The slight antagonism caused by

ondansetron and granisetron on this phase, might suggest a minor contribution of 5-HT_3 receptors. The second phase of the 5-HT response is mediated by direct and indirect mechanisms, involving both neural and smooth muscle 5-HT_{2A} receptors (Macquin-Mavier *et al.*, 1991; Watts & Cohen, 1993; and present results). However, an unequivocal receptor classification awaits the development of truly selective antagonists for the various members of the 5-HT_2 receptor subtypes.

This study was supported in part by a grant from the Italian Ministry for University and Scientific Research (MURST). The generous gifts of ondansetron (Glaxo), granisetron (Smith Kline Beecham) and SDZ 205,557 (Sandoz) are gratefully acknowledged.

References

BAUMGARTNER, R.A., WILLS-KARP, M., KAUFMAN, M.J., MUNAKATA, M. & HIRSHMAN, C. (1990). Serotonin induces constriction and relaxation of the guinea pig airway. *J. Pharmacol. Exp. Ther.*, **255**, 165–173.

BUCHHEIT, K.H., GAMSE, R. & PFANNKUCHE, H.J. (1992). SDZ 205-557, a selective, surmountable antagonist for 5-HT_4 receptors in the isolated guinea pig ileum. *Naunyn-Schmied. Arch. Pharmacol.*, **345**, 387–393.

COHEN, M.L., SCHENCK, K.W., COLBERT, W. & WITTENAUER, L. (1985). Role of 5-HT_2 receptors in serotonin-induced contractions of nonvascular smooth muscle. *J. Pharmacol. Exp. Ther.*, **232**, 770–774.

CORTIJO, J., GONZALEZ, M., ORTIZ, J.L. & MORCILLO, E. (1992). Effects of low temperature and pharmacological interventions on the responses of the isolated guinea-pig trachea. *Naunyn-Schmied. Arch. Pharmacol.*, **346**, 573–580.

CRAIG, D.A. & CLARKE, D.E. (1990). Pharmacological characterization of a neuronal receptor to 5-hydroxytryptamine in guinea pig ileum with properties similar to 5-hydroxytryptamine$_4$ receptor. *J. Pharmacol. Exp. Ther.*, **252**, 1378–1386.

DIXON, M., JACKSON, D.M. & RICHARDS, I.M. (1980). The effects of 5-hydroxytryptamine, histamine and acetylcholine on the reactivity of the lung of the anaesthetised dog. *J. Physiol.*, **307**, 85–96.

EGLEN, R.M., ALVAREZ, R., JOHNSON, L.G., LEUNG, E. & WONG, E.H.F. (1993). The action of SDZ 205,557 at 5-hydroxytryptamine (5-HT_3 and 5-HT_4) receptors. *Br. J. Pharmacol.*, **108**, 376–382.

EGLEN, R.M., SWANK, S.R., WALSH, L.K.M. & WHITING, R.L. (1990). Characterization of 5-HT_3 and 'atypical' 5-HT receptors mediating ileal contractions *in vitro*. *Br. J. Pharmacol.*, **101**, 513–520.

EMMERSON, J. & MACKAY, D. (1979). The zig-zag tracheal strip. *J. Pharm. Pharmacol.*, **31**, 798.

FENIUK, W. & HUMPHREY, P.P.A. (1989). Mechanisms of 5-hydroxytryptamine-induced vasoconstriction. In *The Peripheral Actions of 5-Hydroxytryptamine*. ed. Fozard, J.R. pp. 100–122. Oxford: Oxford Medical Publications.

FOZARD, J.R. (1984). MDL 72222: a potent and highly selective antagonist at neuronal 5-hydroxytryptamine receptors. *Naunyn-Schmied. Arch. Pharmacol.*, **326**, 36–44.

FOZARD, J.R., MOBAROK ALI, A.T.M. & NEWGROSH, G. (1979). Blockade of serotonin receptors on autonomic neurones by (−)-cocaine and some related compounds. *Eur. J. Pharmacol.*, **59**, 195–210.

Blockade of serotinin receptors on autonomic neurones by (−)-cocaine and some related compounds. *Eur. J. Pharmacol.*, **59**, 195–210.

HAHN, H.L., WILSON, A.G., GRAF, P.D., FISCHER, S.P. & NADEL, J.A. (1978). Interaction between serotonin and efferent vagus nerves in dog lungs. *J. Appl. Physiol.*, **44**, 144–149.

HOYER, D. (1989). 5-Hydroxytryptamine receptors and effector coupling mechanisms in peripheral tissues. In *The Peripheral Actions of 5-Hydroxytryptamine*. ed. Fozard, J.R. pp. 72–99. Oxford: Oxford Medical Publications.

HUMPHREY, P.P.A. (1978). The effects of α-adrenoceptor antagonists on contractile responses to 5-hydroxytryptamine in dog saphenous vein. *Br. J. Pharmacol.*, **63**, 671–675.

HUMPHREY, P.P.A., HARTIG, P. & HOYER, D. (1993). A proposed new nomenclature for 5-HT receptors. *Trends Pharmacol. Sci.*, **14**, 233–236.

ISLAM, M.D., MELVILLE, G.N. & ULMER, W.T. (1974). Role of atropine in antagonizing the effect of 5-hydroxytryptamine (5-HT) on bronchial and pulmonary vascular systems. *Respiration*, **31**, 47–50.

KAMEDA, H., MINAMI, M., YOSHIOKA, M. & SAITO, H. (1988). The effects of ICS 205-930, a novel 5-HT_3 antagonist, on the responses to 5-HT in the guinea pig ileum and trachea. *Biog. Amines*, **5**, 465–474.

LEMOINE, H. & KAUMANN, A.J. (1986). Allosteric properties of 5-HT_2 receptors in tracheal smooth muscle. *Naunyn-Schmied. Arch. Pharmacol.*, **333**, 91–97.

LUCCHELLI, A., BOSELLI, C. & GRANA, E. (1990). Dopamine-induced relaxation of the guinea-pig isolated jejunum is not mediated through dopamine receptors. *Pharmacol. Res.*, **22**, 433–444.

LUCCHELLI, A., SANTAGOSTINO-BARBONE, M.G., MODESTO, F. & GRANA, E. (1984). Direct and indirect actions of 5-hydroxytryptamine on the rat isolated vas deferens. *Arch. Int. Pharmacodyn. Ther.*, **269**, 236–251.

MACQUIN-MAVIER, I., JARREAU, P.H., ISTIN, N. & HARF, A. (1991). 5-Hydroxytryptamine-induced bronchoconstriction in the guinea-pig: effect of 5-HT_2 receptor activation on acetylcholine release. *Br. J. Pharmacol.*, **102**, 1003–1007.

MCCAIG, D. (1986). Autonomic responses of the isolated, innervated trachea of the guinea-pig: interaction with autonomic drugs, histamine and 5-hydroxytryptamine. *Br. J. Pharmacol.*, **88**, 239–248.

RICHARDSON, B.P. & ENGEL, G. (1986). The pharmacology and function of 5-HT_3 receptors. *Trends Neurosci.*, **7**, 424–428.

RICHARDSON, B.P., ENGEL, G., DONATSCH, P. & STADLER, P.A. (1985). Identification of serotonin M-receptor subtypes and their specific blockade by a new class of drugs. *Nature*, **316**, 126–131.

RIZZO, A.C., KREUTNER, W. & CHAPMAN, R.W. (1993). 5-HT_3 receptors augment neuronal cholinergic contractions in guinea-pig trachea. *Eur. J. Pharmacol.*, **234**, 109–112.

SANGER, G.J. & NELSON, D.R. (1989). Selective and functional 5-hydroxytryptamine$_3$ receptor antagonism by GR 43694 (granisetron). *Eur. J. Pharmacol.*, **159**, 113–124.

SAS INSTITUTE INC. (1988). *SAS/STAT User's Guide*, Release 6.03 Edition, Cary, North Carolina: SAS Institute Inc.

SCHAUMANN, W. (1957). Inhibition by morphine of release of acetylcholine from the intestine of guinea-pig. *Br. J. Pharmacol. Chemother.*, **12**, 115–118.

SHELLER, J.R., HOLTZMAN, M.J., SKOOGH, B.E. & NADEL, J.A. (1982). Interaction of serotonin with vagal- and ACh-induced bronchoconstriction in canine lungs. *J. Appl. Physiol.*, **52**, 964–966.

TONINI, M., CANDURA, S.M., ONORI, L., COCCINI, T., MANZO, L. & RIZZI, C.A. (1992a). 5-Hydroxytryptamine$_4$ receptor agonists facilitate cholinergic transmission in the circular muscle of guinea-pig ileum: antagonism by tropisetron and DAU 6285. *Life Sci.*, **50**, PL173–PL178.

TONINI, M., WATERMAN, S.A., CANDURA, S.M., COCCINI, T. & COSTA, M. (1992b). Site of action of morphine on the ascending excitatory reflex in the guinea-pig small intestine. *Neurosci. Lett.*, **144**, 195–198.

VAN OOSTERHOUT, A.J.M., HOFMAN, G., WOUTERSEN-VAN KIJNANTEN, F.M.A. & NIJKAMP, F.P. (1991). 5-HT_1 like receptors mediate potentiation of cholinergic nerve-mediated contraction of isolated mouse trachea. *Eur. J. Pharmacol.*, **209**, 237–244.

VERBEUREN, T.J. (1989). Synthesis, storage, release and metabolism of 5-hydroxytryptamine in peripheral tissues. In *The Peripheral Actions of 5-Hydroxytryptamine*. ed. Fozard, J.R. pp. 1–25. Oxford: Oxford Medical Publications.

WAKADE, A.R. (1980). A comparison of rates of depletion and recovery of noradrenaline stores of peripheral and central noradrenergic neurones after reserpine administration: importance of neuronal activity. *Br. J. Pharmacol.*, **68**, 93–98.

WATTS, S.W. & COHEN, M.L. (1992). Characterization of the contractile serotonergic receptor in guinea pig trachea with agonists and antagonists. *J. Pharmacol. Exp. Ther.*, **260**, 1101–1106.

WATTS, S.W. & COHEN, M.L. (1993). Further evidence that the guinea pig tracheal contractile serotonergic receptor is a 5-hydroxytryptamine$_2$ receptor: use of 5-methyltryptamine and dipropyl-5-carboxamidotryptamine. *J. Pharmacol. Exp. Ther.*, **264**, 271–275.

(Received November 8, 1993
Revised March 11, 1994
Accepted March 15, 1994)

Br. J. Pharmacol. (1994), **112**, 769–774

Peripheral and central adrenoceptor modulation of the behavioural effects of clozapine in the paw test

[1]Eric P.M. Prinssen, Bart A. Ellenbroek & Alexander R. Cools

Department of Psycho- and Neuropharmacology, University of Nijmegen, P.O. Box 9101, 6500 HB Nijmegen, The Netherlands

1 In rats, the atypical neuroleptic, clozapine, has been found to increase the hindlimb retraction time but not the forelimb retraction time, in the paw test. These parameters have predictive validity for the antipsychotic efficacy and extrapyramidal side-effects of drugs, respectively. The present study analysed to what extent drugs acting on adrenoceptors affect the behavioural effect of clozapine in the paw test.

2 The α_1-adrenoceptor agonist, ST 587 but not the peripherally working α_1-agonist, methoxamine, decreased the effect of clozapine on the hindlimb retraction time. The α_1-antagonist phenoxybenzamine increased this effect of clozapine, and blocked the effect of ST 587 on clozapine at low doses. Only the combination of phenoxybenzamine with clozapine produced an increase in forelimb retraction time.

3 The α_2-adrenoceptor agonist, clonidine, decreased the effect of clozapine on the hindlimb retraction time. This effect was neither antagonized by the α_2-antagonist rauwolscine nor by the α_1-antagonist phenoxybenzamine. Rauwolscine or the peripherally working α_2-antagonist L-659,066 did not influence the effect of clozapine on the hindlimb retraction time. The forelimb retraction time was not affected by any of the drug combinations.

4 In contrast to the β_2-adrenoceptor agonist, clenbuterol, which was ineffective, the peripherally acting β-agonist, (−)-isoprenaline, increased the effects of clozapine on the hindlimb retraction time. The β-antagonist, (−)-propranolol as well as the peripherally acting β-antagonist, nadolol decreased this effect of clozapine. Low doses of the peripherally acting β_1-antagonist, atenolol, as well as low doses of the β_2-antagonist, ICI-118,551, decreased the effect of clozapine. A low dose of nadolol blocked the effect of (−)-isoprenaline on clozapine. Only the combination of clenbuterol with clozapine produced an increase in forelimb retraction time.

5 It is concluded that blockade of central α_1-adrenoceptors plays an important role in the effect of clozapine on the hindlimb retraction time. Furthermore, the effect of clozapine on the hindlimb retraction time is strongly modulated by peripheral β_1- and/or β_2-adrenoceptors. Given the predictive validity of the paw test, the presented data suggest that the α_1-adrenoceptor antagonist properties of clozapine are important for its therapeutic effects, but not for its lack of extrapyramidal side-effects.

Keywords: Neuroleptics; peripheral adrenoceptors; central adrenoceptors; α_1-adrenoceptors; α_2-adrenoceptors; β_1-adrenoceptors; β_2-adrenoceptors; paw test

Introduction

Many studies point towards a role for the noradrenergic system in schizophrenia (Maas *et al.*, 1993; for review Van Kammen *et al.*, 1986). There are also many studies suggesting a role for α-adrenoceptors in the therapeutic effects of neuroleptics (Petersen, 1981; Marwaha & Aghajanian, 1982; Cohen & Lipinsky, 1986; Baldessarini *et al.*, 1992), although blockade of dopamine D_2 receptors is believed to be crucial (Creese *et al.*, 1976; Seeman *et al.*, 1976; Peroutka & Snyder, 1980; but see, Cohen & Lipinsky, 1986). However, clozapine is a much weaker antagonist of the dopamine D_2 receptor than most neuroleptics (Richelson & Nelson, 1984; Anderson, 1988; Farde & Nordström, 1992), while it is effective in patients who are unresponsive to other neuroleptics (Kane *et al.*, 1988). Moreover, clozapine is superior to most other neuroleptics with respect to lack of extrapyramidal side-effects (Angst *et al.*, 1971) and amelioration of negative symptoms (Honigfeld *et al.*, 1987). Together, this implies that clozapine must have a working mechanism that is different from that of other neuroleptics. One of the prominent features of clozapine is its potent α_1- as well as α_2-adrenoceptor antagonist properties (Hall *et al.*, 1986; Richelson & Nelson, 1984), which are even more pronounced since clozapine is administered in high doses (Wyatt, 1976). Therefore, the present study examined to what extent α_1- and α_2-adrenoceptors play a role in the effects of clozapine. Moreover, since α- and β-adrenoceptors can interact strongly (e.g. Stone *et al.*, 1987), the possible modulation of the effects of clozapine by β-adrenoceptors was also studied. The animal model used was the so-called paw test which models both the antipsychotic efficacy and the extrapyramidal side-effects of drugs (Ellenbroek *et al.*, 1987). With regard to a large number of criteria (such as false positives and false negatives, response to chronic treatment, interactions between neuroleptics and anticholinergics, etc.), this model has been shown to have predictive validity for both the antipsychotic efficacy and the extrapyramidal side-effects of drugs (Ellenbroek *et al.*, 1987; Ellenbroek & Cools, 1988; Ellenbroek, 1993).

Methods

The procedure followed was similar to that described by Prinssen *et al.* (1993). Male Wistar rats (weighing between 220 and 250 g) were housed individually 24 h before the experiment. Experiments were performed between 10 h 00 min and 16 h 00 min, and rats were used only once. On the day of the experiment, the rats received one or two intraperitoneal injections. In the case of single injections, each rat was injected at $t = 0$ min. In the case of two injections, the first injection (an adrenoceptor antagonist) was given at $t = -10$ min and the second (clozapine) at $t = 0$ min. When a (putative) adrenoceptor antagonist was combined with its agonist, the two drugs were administered as a cocktail at $t = -10$. The injection volume was always 1 ml kg^{-1}, except for phenoxybenzamine dissolved in propylene glycol

[1] Author for correspondence.

(0.5 ml kg^{-1}). All drugs were dissolved in distilled water, except for clozapine to which a drop of HCl was added (1 N), phenoxybenzamine which was dissolved in propylene glycol, and the combination of clonidine or ST 587 and phenoxybenzamine which was dissolved in 50% alcohol. Control injections consisted of distilled water, since combinations of propylene glycol or 50% alcohol with clozapine did not differ from the combination of distilled water with clozapine (data not shown).

Thirty minutes after the last injection the paw test was performed and repeated at 40 and 50 min. In the paw test a rat was placed on a Perspex platform which has four holes. The rat was placed on the platform by positioning first the hind- and then the forelimbs in the holes. Two variables were measured in this test, namely the time it takes the animal to retract its first hindlimb (hindlimb retraction time; HRT) and the time it takes the animal to retract its first forelimb (forelimb retraction time; FRT) with a minimum time of 1 s and a maximum time of 60 s. Since only robust effects are considered to be important, the window (1 to 60 s) was chosen so that both significant decreases and significant increases could be easily detected. The individual score was calculated for each animal as the mean of the three trials. The data are presented as the median value of these means per group ($n = 6-15$ rats) together with the corresponding 25 and 75 percentiles. Group differences were calculated with a two-tailed Mann-Whitney U-test.

The following drugs were used (for the sake of clarity, peripherally working drugs are defined as drugs that do not readily pass the blood-brain barrier): the atypical neuroleptic clozapine (Sandoz, The Netherlands), the α_1-agonist ST 587 (2-(2-chloro-5-trifluoromethyl-phenyl imino)imidazolidine; Boehringer Ingelheim, Germany), the peripherally working α_1-agonist, methoxamine HCl (Wellcome, U.S.A.), the α_1-antagonist, phenoxybenzamine HCl (SK&F, U.S.A.), the α_2-agonist, clonidine HCl (Boehringer Ingelheim, The Netherlands), the α_2-antagonist rauwolscine HCl (Carl Roth, Germany), the peripherally working α_2-antagonist L 659,066 ((2**R**-trans)-N-(2-(1,3,4,6,7,12b-hexahydro-2'-oxospiro(2H-benzo-furo(2,3-a)quinolizine-2,3-imidazolin)-3'-yl)ethyl)methane-sulphonamide monohydrochloride; Merck, U.S.A.), the β_2-agonist clenbuterol HCl (Sigma, The Netherlands), the peripherally working β-agonist, (−)-isoprenaline HCl (Sigma, U.S.A.), the β-antagonist, (−)-propranolol HCl (RBI, U.S.A.), the peripherally working β-antagonist, nadolol (Sigma, St. Louis, U.S.A.), the peripherally working β_1-antagonist (±)-atenolol (RBI, U.S.A.) and the β_2-antagonist, ICI-118,551 (erythro-DL-1-(7-methylindan-4-yloxyl)-3-(isopropylaminobutan-2-ol) hydrochloride; Zeneca, U.S.A.).

Results

Effects of drugs acting on adrenoceptors

The purpose of this study was to analyse the interaction of drugs acting on adrenoceptors with clozapine. To avoid the use of doses of drugs that were effective on their own, all drugs used in interaction with clozapine, were also tested alone in high doses. In case of strong behavioural effects of such a drug, a sub-threshold dose was used in the interaction study with clozapine. ST 587 (1 mg kg^{-1}), phenoxybenzamine (10 mg kg^{-1}), rauwolscine (5 mg kg^{-1}), L 659,066 (5 mg kg^{-1}), (−)-isoprenaline (5 mg kg^{-1}), (−)-propranolol (10 mg kg^{-1}), nadolol (10 mg kg^{-1}), atenolol (1 mg kg^{-1}) and ICI-118,551 (1 mg kg^{-1}) did not significantly influence HRT or FRT compared with controls (distilled water, median values: HRT 1.1 s; FRT: 1.0 s). Methoxamine (10 mg kg^{-1}) and clenbuterol (10 mg kg^{-1}) induced small, but significant increases in HRT (median value of HRT: 2.9 and 4.3 s, respectively). Since higher doses of clonidine induced strong effects on the HRT [(clonidine (0.3 mg kg^{-1}) induced a HRT of 22.0 s (median value)], the highest dose used in this study was limited to 0.1 mg kg^{-1}, a dose that was without significant effects.

Effects of clozapine alone

In line with earlier findings, clozapine (15–20 mg kg^{-1}) significantly increased the HRT ($P<0.01$; Figure 1), but not the FRT (data not shown) compared with controls (distilled water; see above).

Effects of α_1-selective drugs on clozapine

ST 587 (0.25–1 mg kg^{-1}) decreased the effect of clozapine (20 mg kg^{-1}) on the HRT (Figure 1): higher doses produced stronger effects. On the other hand, the peripherally acting α_1-agonist, methoxamine (10 mg kg^{-1}) combined with clozapine (20 mg kg^{-1}), did not influence the HRT (median value: 56.6 s) compared with clozapine alone (median value: 60.0 s; Figure 1). Phenoxybenzamine increased the effect of clozapine (15 mg kg^{-1}) on the HRT (Figure 1): the lowest dose which was significantly effective, already produced a maximal increase (60.0 s). The effect of ST 587 on clozapine could be antagonized by phenoxybenzamine (1 mg kg^{-1}; Figure 3), in a dose that itself did not affect clozapine (15 mg kg^{-1}; Figure 1).

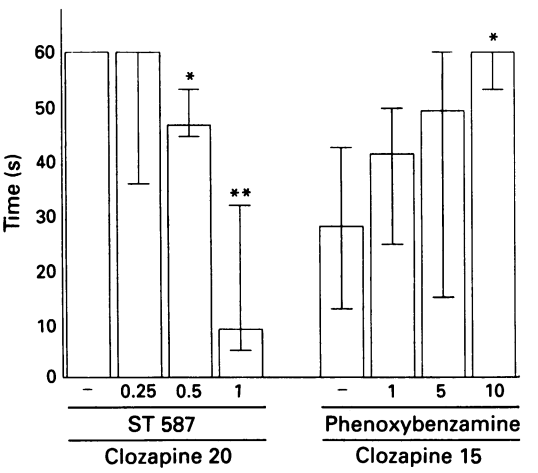

Figure 1 The effect of ST 587 and phenoxybenzamine on the hindlimb retraction time (HRT) induced by clozapine. The doses used (in mg kg^{-1}) are shown in the figure. Median values and percentiles (25 and 75%) of the HRT are shown. $*P<0.05$; $**P<0.01$.

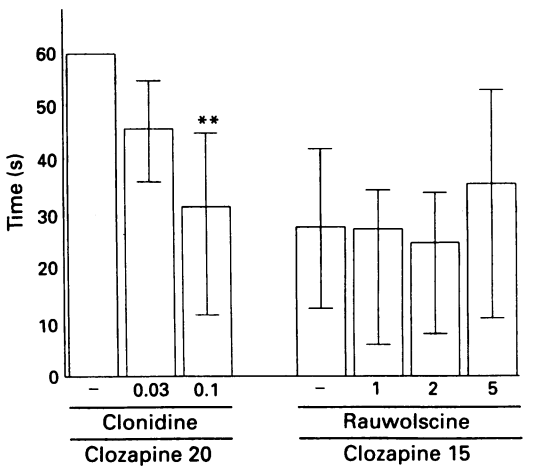

Figure 2 The effect of clonidine and rauwolscine on the hindlimb retraction time (HRT) induced by clozapine. The doses used (in mg kg^{-1}) are shown in the figure. Median values and percentiles (25 and 75%) of the HRT are shown. $**P<0.01$.

The FRT was not affected by any of the combinations, apart from the combination of phenoxybenzamine (10 mg kg^{-1}) and clozapine (15 mg kg^{-1}) that produced a small, but significant effect ($P<0.05$) on the FRT (median value: 6.2 s) compared with clozapine alone (median value: 1.0 s).

Effects of α_2-selective drugs on clozapine

Clonidine (0.03–0.1 mg kg^{-1}) significantly decreased the effect of clozapine (20 mg kg^{-1}) on the HRT (Figure 2): higher doses could not be tested since they produced strong effects when given alone (see above). Rauwolscine (1–5 mg kg^{-1}; Figure 2), as well as L-659,066 (5 mg kg^{-1}; HRT, median value: 35.8), did not influence the effect of clozapine (15 mg kg^{-1}) on the HRT. The inhibitory effect of clonidine (0.1 mg kg^{-1}) on clozapine (20 mg kg^{-1}) could not be antagonized by relatively high doses (see Discussion) of rauwolscine (1 mg kg^{-1}) or phenoxybenzamine (1 mg kg^{-1}; Figure 3).

The FRT was not affected by any of the drug combinations.

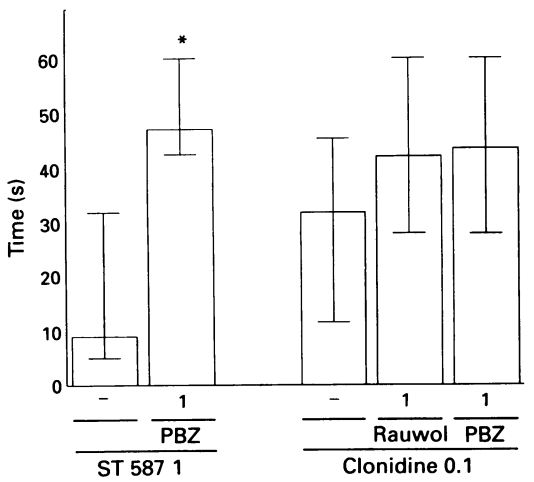

Figure 3 All groups received 20 mg kg^{-1} clozapine. The left part of the figure shows that the inhibition of clozapine by ST 587 is antagonized by phenoxybenzamine. The right part of the figure shows that the inhibition of clozapine by clonidine is neither antagonized by rauwolscine (Rauwol) nor by phenoxybenzamine (PBZ). The doses used (in mg kg^{-1}) are shown in the figure. Median values and percentiles (25 and 75%) of the hindlimb retraction time (HRT) are shown. $*P<0.05$.

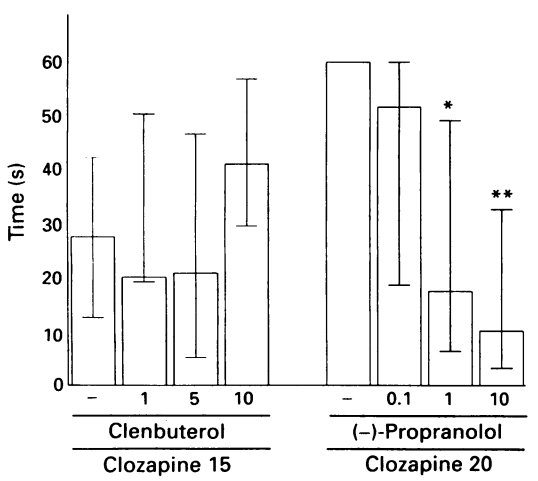

Figure 4 The effect of clenbuterol and (−)-propranolol on the hindlimb retraction time (HRT) induced by clozapine. The doses used (in mg kg^{-1}) are shown in the figure. Median values and percentiles (25 and 75%) of the HRT are shown. $*P<0.05$; $**P<0.01$.

Effects of β-selective drugs on clozapine

Clenbuterol (1–10 mg kg^{-1}) did not influence the effect of clozapine on the HRT (15 mg kg^{-1}; Figure 4). In contrast, the peripherally acting β-agonist, (−)-isoprenaline (1–5 mg kg^{-1}) increased the effects of clozapine (15 mg kg^{-1}) on the HRT (Figure 5): the lowest dose that was significantly effective, already produced maximal effects (60.0 s). (−)-Propranolol (0.1–10 mg kg^{-1}), nadolol (1–10 mg kg^{-1}), atenolol (0.1–1 mg kg^{-1}) and ICI-118,551 (0.1–1 mg kg^{-1}) decreased the effect of clozapine (20 mg kg^{-1}) on the HRT (Figures 4–6). The effect of (−)-isoprenaline (5 mg kg^{-1}) on clozapine (15 mg kg^{-1}) was blocked by a dose of nadolol (1 mg kg^{-1}) that itself had no effect (Figure 5).

The FRT was not affected, apart from the combination of clenbuterol (10 mg kg^{-1}) and clozapine (15 mg kg^{-1}), which produced a significant increase in the FRT (median value: 15.7 s) compared with clozapine alone (median value: 1.0 s).

Discussion

The role of α_1-adrenoceptors in the effects of clozapine

In line with earlier findings, clozapine (15–20 mg kg^{-1}) enhanced the hindlimb retraction time (HRT) in the paw test. The α_1-agonist, ST 587, decreased this effect of clozapine. The effect of ST 587 appeared to be α_1-adrenoceptor-specific: (1) ST 587 is highly selective for α_1- over α_2-adrenoceptor stimulation (De Jonge *et al.*, 1981); (2) the effect of ST 587 could be attenuated by a dose of the α_1-antagonist, phenoxybenzamine, that itself did not affect clozapine; (3) when combined with clozapine, higher doses of phenyoxybenzamine produced effects opposite to those of ST 587.

A high dose (cf. Liebau *et al.*, 1989) of the peripherally acting α_1-agonist, methoxamine, did not alter the effect of clozapine on the HRT. Even when a possible effect of methoxamine was obscured by the ceiling effect of clozapine, the contribution of peripheral α_1-adrenoceptors to the effects of ST 587 can be excluded since the effective dose of ST 587 (0.5 mg kg^{-1}) was 20 times smaller than the ineffective dose of methoxamine (10 mg kg^{-1}). Thus, the attenuation of the effects of clozapine by α_1-adrenoceptor stimulation did not seem to involve peripheral α_1-adrenoceptors. Therefore, it is concluded that central α_1-adrenoceptor stimulation decreased the effects of clozapine on the HRT in the paw test. These

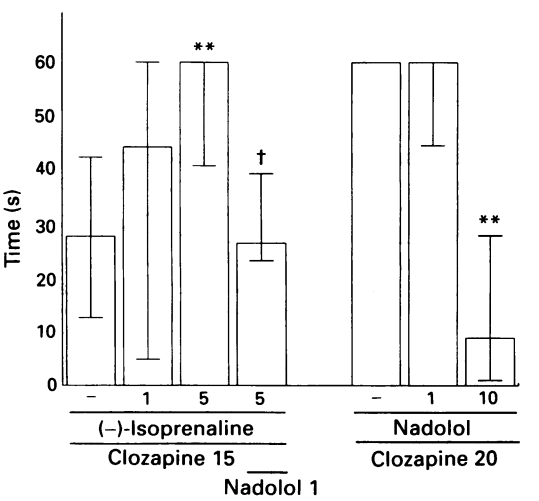

Figure 5 The effect of (−)-isoprenaline and/or nadolol on the hindlimb retraction time (HRT) induced by clozapine. The doses used (in mg kg^{-1}) are shown in the figure. Median values and percentiles (25 and 75%) of the HRT are shown. $**P<0.01$; $\dagger P<0.05$, compared with the combination of (−)-isoprenaline (5 mg kg^{-1}) and clozapine.

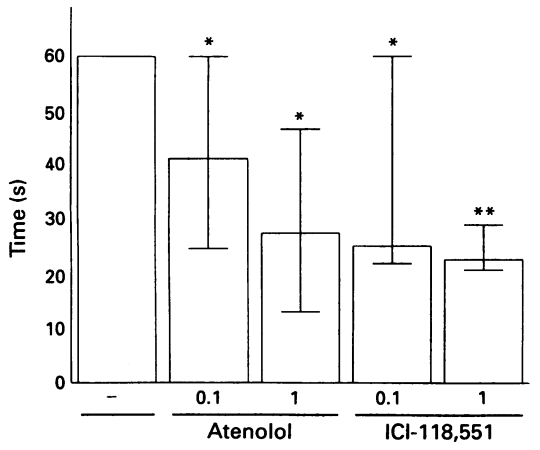

Figure 6 All groups received 20 mg kg^{-1} clozapine. The effect of atenolol and ICI-118,551 on the hindlimb retraction time (HRT) induced by clozapine is shown. The doses used (in mg kg^{-1}) are shown in the figure. Median values and percentiles (25 and 75%) of the HRT are shown. *$P<0.05$; **$P<0.01$.

data together with the fact that clozapine potently antagonizes α_1-adrenoceptors (Hall *et al.*, 1986; Mennon *et al.*, 1988) strongly suggest that blockade of central α_1-adrenoceptors contribute significantly to the HRT elicited by clozapine. Since the HRT is a parameter with predictive validity for the antipsychotic efficacy of drugs (Ellenbroek *et al.*, 1987; Ellenbroek & Cools, 1988; Ellenbroek, 1993), the present study implies that inhibition of central α_1-adrenoceptors is important for the antipsychotic effects of clozapine. On the other hand, a high dose of phenoxybenzamine alone (10 mg kg^{-1}) did not increase the HRT, suggesting that blockade of α_1-adrenoceptors alone is not enough to produce such an effect. Indeed, recent studies have shown that the 5-hydroxytryptamine 5-HT$_2$ receptor antagonist properties (Ellenbroek *et al.*, 1994) as well as the dopamine D$_1$ receptor antagonist properties, but not the dopamine D$_2$ receptor antagonist properties of clozapine (Ellenbroek *et al.*, 1991) also play a role in the effects of clozapine on the HRT. We are now studying to what extent combined antagonism of 5-HT$_2$ receptors, dopamine D$_1$ receptors and α_1-adrenoceptors may produce a clozapine-like profile in the paw test.

As previously reported (Ellenbroek *et al.*, 1987), unlike classical neuroleptics, clozapine did not induce an increase in the forelimb retraction time (FRT). When combined with clozapine, ST 587 did not induce an increase in FRT, indicating that the α_1-antagonist properties of clozapine do not play a role in its lack of FRT. Since the FRT is a parameter with predictive validity for extrapyramidal side-effects (Ellenbroek *et al.*, 1987; Ellenbroek & Cools, 1988), the present data indicate that the α_1-antagonist properties of clozapine do not play a role in its lack of extrapyramidal side-effects. Moreover, phenoxybenzamine in combination with clozapine, did induce an increase in FRT, suggesting that additional blockade of α_1-adrenoceptors together with clozapine, may increase, but not decrease, extrapyramidal side-effects (cf. Chiodo & Bunney, 1985).

The role of α_2-adrenoceptors in the effects of clozapine

As mentioned, clozapine enhanced the HRT in the paw test. The higher dose of clonidine (0.1 mg kg^{-1}) decreased this effect of clozapine. This effect of clonidine could not be blocked by a relatively high dose of rauwolscine (cf. Timmermans *et al.*, 1981), suggesting that α_2-adrenoceptor stimulation does not affect clozapine with respect to the HRT. This is underlined by the finding that both rauwolscine and L 659,066 did not modulate the effect of clozapine on the HRT. Since the HRT is a parameter with predictive validity for the antipsychotic efficacy of drugs (see above), the present study implies that inhibition of α_2-adrenoceptors does not contribute to the antipsychotic effects of clozapine.

Since clonidine also has α_1-adrenoceptor agonist properties (Liebau *et al.*, 1989), the role of these adrenoceptors was evaluated as well. However, a dose of phenoxybenzamine (1 mg kg^{-1}) that strongly attenuated the effect of ST 587, did not attenuate the effect of clonidine on clozapine. This suggests that the effects of clonidine on clozapine are not due to its α_1-adrenoceptor properties. However, until more is known about the pharmacology of the many different α_1- and α_2-adrenoceptor subtypes that have recently been identified (Johnson & Minneman, 1986; Morrow & Creese, 1986; Bylund *et al.*, 1988) a role for these receptor subtypes cannot be fully excluded. Moreover, the effect of clonidine may involve an interaction between α_1- and α_2-adrenoceptor (sub)types. Alternatively, other receptors for which clonidine has a high affinity may be involved, e.g. imidazoline receptors (Molderings *et al.*, 1993).

As mentioned clozapine did not induce an effect on the FRT; nor did the combination of clonidine with clozapine induce an increase in FRT, indicating that the α_2-antagonist properties of clozapine do not play a role in its lack of effect on FRT. Since the FRT is a parameter with predictive validity for extrapyramidal side-effects (see above), the present data indicate that the α_2-antagonist properties of clozapine do not play a role in its lack of extrapyramidal side-effects.

The role of β-adrenoceptors in the effects of clozapine

The peripherally acting β-agonist, (−)-isoprenaline, increased the effect of clozapine on the HRT, which could be attenuated by an ineffective dose of the peripherally acting β-antagonist, nadolol (1 mg kg^{-1}). Moreover, when given alone, higher doses of nadolol decreased the effects of clozapine. Together, these data imply that peripheral β-adrenoceptors modulate the effect of clozapine on the HRT. The decrease in the effect of clozapine on the HRT by β-adrenoceptor blockade seems to be mediated via β_1- as well as β_2-adrenoceptors, since atenolol and ICI-118,551 were both effective in doses that are receptor-specific (Bilsky *et al.*, 1983). The significant effect of a low dose of atenolol (0.1 mg kg^{-1}) furthermore underlines the involvement of peripheral receptors. The β_2-agonist, clenbuterol, had no effect on clozapine, in contrast with (−)-isoprenaline. This was especially surprising since selective β_2-adrenoceptor blockade did affect clozapine (see above). These data may indicate that stimulation of β_2-adrenoceptors, as opposed to non-selective β-adrenoceptor stimulation, is not sufficient to enhance the effect of clozapine on the HRT. However, one has to be careful since clenbuterol also seems to possess β_1-antagonist properties (Ordway *et al.*, 1987). Since a β_1-antagonist (atenolol) decreased the clozapine-induced HRT, the possibility cannot be excluded that the lack of effect of clenbuterol is due to its ability to interact with both β_1- and β_2-adrenoceptors in an opposite manner.

As mentioned, clozapine did not induce an increase on the FRT. Neither did the combination of any of the peripherally acting drugs with clozapine produce an effect on the FRT. Interestingly, clenbuterol, which readily passes the blood-brain barrier, did induce an increase in FRT, when combined with clozapine, suggesting that central β_2-adrenoceptors may be involved in this increase in FRT.

Since clozapine has a very low affinity for β-adrenoceptors (Hall *et al.*, 1986), it becomes difficult to ascribe the effects of peripheral β-adrenoceptor agents on the clozapine-induced increase of HRT to clozapine's ability to interact with β-adrenoceptors. While the precise mechanisms of action by which peripheral β-adrenoceptors might modulate the effects of clozapine are unknown, we can exclude the following ones. First, the effects of the β-ligands do not seem to be mediated by a change in the pharmacokinetics of clozapine.

Propranolol has been shown to increase, and not to decrease, the plasma concentration of neuroleptics (the classical neuroleptic, chlorpromazine and the atypical neuroleptic, thioridazine; clozapine was not studied), thereby increasing their therapeutic efficacy (Peet *et al.*, 1980; Silver *et al.*, 1986). Indeed, (−)-propranolol has been found to increase, but not to decrease, the effects of haloperidol on the HRT (unpublished observations). Second, the effect of the β-ligands could not be ascribed to a direct influence on the extrafusal fibres in the hindlimb muscles, thereby influencing the contractability of these muscles, despite the fact that these muscle fibres contain β_2-adrenoceptors (Buckenmeyer *et al.*, 1990): for, both β_1- and β_2-adrenoceptors were found to be involved in the effects studied. Moreover, (−)-propranolol increased the effects of haloperidol on the HRT (see above), while it decreased the effects of clozapine (Figure 4): such effects seem incompatible with a direct action on muscle fibres. Further research on the mechanisms of action by which peripheral β-adrenoceptors modulate the effects of clozapine is necessary.

Summary

The present study shows that central α_1-adrenoceptor stimulation decreases the effects of clozapine on the hindlimb retraction time (HRT), a parameter with predictive validity for the antipsychotic efficacy of drugs. As discussed, these data imply that blockade of central α_1-adrenoceptors by clozapine is important for the antipsychotic effects of clozapine. The present study also shows that blockade of β_1- and/or β_2-adrenoceptors decreased the effect of clozapine on the HRT, an effect that seemed to be mediated by peripheral receptors. The forelimb retraction time (FRT), a parameter with predictive validity for extrapyramidal side-effects, on which clozapine has no effect, was not increased when clozapine was combined with α_1-agonists. Therefore, these data imply that α_1-adrenoceptors do not play a role in the lack of extrapyramidal side-effects of clozapine.

The authors would like to thank Anne-Marie Boerboom for her contribution in the experiments. We thank Sandoz, The Netherlands (clozapine), Boehringer Ingelheim, Germany (ST 587), Merck, U.S.A. (L 659,066) and Zeneca, U.S.A. (ICI-118,551) for generously supplying the drugs. This study is supported by the Dutch Society for Scientific Research (NWO), no. 900-548-119.

References

ANDERSON, P.H. (1988). Comparison of the pharmacological characteristics of [^{3}H]raclopride and [^{3}H]SCH 23390 binding to dopamine receptors in vivo in mouse brain. *Eur. J. Pharmacol.*, **146**, 113–120.

ANGST, J., BENTE, D., BERNER, P., HEIMANN, H., HELMCHEN, H. & HIPPIUS, H. (1971). Das klinische wirkungsbild von clozapin (untersuchung mit dem AMP-system). *Pharmakopsychiatrie*, **4**, 200–211.

BALDESSARINI, R.J., HUSTON-LYONS, D., CAMPBELL, A., MARSH, E. & COHEN, B.M. (1992). Do central antiadrenergic actions contribute to the atypical properties of clozapine? *Br. J. Psychiat.*, **160**, 12–16.

BILSKY, A.J., HALLIDAY, S.E., FITZGERALD, J.D. & WALE, J.L. (1983). The pharmacology of a β_2-selective adrenoceptor antagonist (ICI 118,551). *J. Cardiovasc. Pharmacol.*, **5**, 430–437.

BUCKENMEYER, P.J., GOLDFARB, A.H., PARTILLA, J.S., PINEYRO, M.A. & DAX, E.M. (1990). Endurance training, not acute exercise, differentially alters β-receptors and cyclase in skeletal fiber types. *Am. J. Physiol.*, **258**, E72–E77.

BYLUND, D.B., RAY-PRENGER, C. & MURPHY, T.J. (1988). Alpha-2A and alpha-2B adrenergic subtypes: antagonist binding in tissues and cell lines containing only one subtype. *J. Pharmacol. Exp. Ther.*, **245**, 600–607.

CHIODO, L.A. & BUNNEY, B.S. (1985). Possible mechanisms by which repeated clozapine administration differentially affects the activity of two subpopulations of midbrain dopamine neurons. *J. Neurosci.*, **5**, 2539–2544.

COHEN, B.M. & LIPINSKY, J.F. (1986). In vivo potencies of antipsychotic drugs in blocking alpha 1 noradrenergic and dopamine D2 receptors: implications for drug mechanisms of action. *Life Sci.*, **39**, 2571–2580.

CREESE, I., BURT, D.R. & SNYDER, S.H. (1976). Dopamine receptor binding predicts clinical and pharmacological potencies of antischizophrenic drugs. *Science*, **192**, 481–483.

DE JONGE, A., VAN MEEL, J.C.A., TIMMERMANS, P.B.M.W.M. & VAN ZWIETEN, P.A. (1981). A lipophilic, selective α_1-adrenoceptor agonist: 2-(2-chloro-5-trifluoromethylphenylimino)imidazolidine (St 587). *Life Sci.*, **28**, 2009–2016.

ELLENBROEK, B.A. (1993). Treatment of schizophrenia: a clinical and preclinical evaluation of neuroleptic drugs. *Pharmacol. Ther.*, **57**, 1–78.

ELLENBROEK, B.A., ARTZ, M.T. & COOLS, A.R. (1991). The involvement of dopamine D_1 and D_2 receptors in the effects of the classical neuroleptic haloperidol and the atypical neuroleptic clozapine. *Eur. J. Pharmacol.*, **196**, 103–108.

ELLENBROEK, B.A. & COOLS, A.R. (1988). The paw test: an animal model for neuroleptic drugs which fulfils the criteria for pharmacological isomorphism. *Life Sci.*, **42**, 1205–1213.

ELLENBROEK, B.A., PEETERS, B.W., HONIG, W.M. & COOLS, A.R. (1987). The paw test: a behavioural paradigm for differentiating between classical and atypical neuroleptic drugs. *Psychopharmacology*, **93**, 343–348.

ELLENBROEK, B.A., PRINSSEN, E.P.M. & COOLS, A.R. (1994). The role of serotonin receptor subtypes in the behavioural effects of neuroleptic drugs. A paw test study in rats. *Eur. J. Neurosci.*, **6**, 1–8.

FARDE, L. & NORDSTRÖM, A.-L. (1992). PET analysis indicates atypical central dopamine receptor occupancy in clozapine-treated patients. *Br. J. Psychiat.*, **169**, 30–33.

HALL, H., SALLEMARK, M. & JERNING, E. (1986). Effects of remoxipride and some related new substituted salicylamides on rat brain receptors. *Acta Pharmacol. Toxicol.*, **58**, 61–70.

HONIGFELD, G., SINGER, J. & PATTON, J. (1987). Clozapine: antipsychotic activity in treatment resistant schizophrenics. *Adv. Ther.*, **1**, 77–97.

JOHNSON, R.D. & MINNEMAN, K.P. (1986). Differentiation of alpha-1-adrenergic receptors linked to phosphoinositol turnover and cyclic AMP accumulations in rat brain. *J. Pharmacol. Exp. Ther.*, **31**, 329–346.

KANE, J.M., HONIGFELD, G., SINGER, J. & MELTZER, H. (1988). Clozapine in treatment-resistant schizophrenics. *Psychopharmacol. Bull.*, **24**, 62–67.

LIEBAU, S., HOHLFELD, J. & FÖRSTERMANN, U. (1989). The inhibition of α_1-adrenoceptor-mediated contractions of rabbit pulmonary artery by Ca^{2+}-withdrawal, pertussin toxin and N-ethylmaleimide is dependent on agonist intrinsic efficacy. *Naunyn-Schmied. Arch. Pharmacol.*, **339**, 496–502.

MAAS, J.W., CONTRERAS, S.A., MILLER, A.L., BERMAN, N., BOWDEN, C.L., JAVORS, M.A., SELESHI, E. & WEINTRAUB, E. (1993). Studies of catecholamine metabolism in schizophrenia/psychosis-1. *Neuropsychopharmacol.*, **8**, 97–109.

MARWAHA, J. & AGHAJANIAN, G.K. (1982). Typical and atypical neuroleptics are potent antagonists at α_1-adrenoceptors of the dorsal geniculate nucleus. *Naunyn-Schmied. Arch. Pharmacol.*, **321**, 32–37.

MENNON, M.K., GORDON, L.I. & FITTEN, J. (1988). Interaction between clozapine and a lipophilic α_1-adrenergic agonist. *Life Sci.*, **43**, 1791–1804.

MOLDERINGS, G.J., MOURA, D., FINK, K., BÖNISCH, H. & GÖTHERT, M. (1993). Binding of [^{3}H]clonidine to I_1-imidazoline sites in bovine adrenal medullary membranes. *Naunyn-Schmied. Arch. Pharmacol.*, **348**, 70–76.

MORROW, A.L. & CREESE, I. (1986). Characterization of α_1-adrenergic receptor subtypes in rat brain: a reevaluation of [^{3}H]WB-4101 and [^{3}H]prazosin binding. *Mol. Pharmacol.*, **29**, 321–330.

ORDWAY, G.A., O'DONNEL, J.M. & FRAZER, A. (1987). Effects of clenbuterol on central beta-1 and beta-2 adrenergic receptors of the rat. *J. Pharmacol. Exp. Ther.*, **241,** 187–195.

PEET, M., MIDDLEMISS, D.N. & YATES, R.A. (1980). Pharmacokinetic interaction between propranolol and chlorpromazine in schizophrenic patients. *Lancet*, **ii,** 978.

PEROUTKA, S.J. & SNYDER, S.H. (1980). Relationship of neuroleptic drug effects at dopamine, serotonin, α-adrenergic, and histamine receptors to clinical potency. *Am. J. Psychiat.*, **137,** 1518–1522.

PETERSEN, E.N. (1981). Pre- and postsynaptic α-adrenoceptor antagonism by neuroleptics in vivo. *Eur. J. Pharmacol.*, **69,** 399–405.

PRINSSEN, E.P.M., ELLENBROEK, B.A., STAMATOVIC, B. & COOLS, A.R. (1993). The effects of haloperidol and raclopride in the paw test are influenced similarly by SCH 39166. *Eur. J. Pharmacol.*, **231,** 275–280.

RICHELSON, E. & NELSON, A. (1984). Antagonism by neuroleptics of neurotransmitter receptors of normal human brain in vitro. *Eur. J. Pharmacol.*, **103,** 197–204.

SEEMAN, P., LEE, T., CHOA-WONG, M. & WONG, K. (1976). Antipsychotic drugs doses and neuroleptic/dopamine receptors. *Nature*, **261,** 717–719.

SILVER, J.M., YODUFSKY, S.C., KOGAN, M. & KATZ, B.L. (1986). Elevation of thioridazine plasma levels by propranolol. *Am. J. Psychiat.*, **143,** 1290–1292.

STONE, E.A., MCEWEN, B.S., HERRERA, A.S. & CARR, K.D. (1987). Regulation of α and β components of noradrenergic cyclic AMP response in cortical slices. *Eur. J. Pharmacol.*, **141,** 347–356.

TIMMERMANS, P.B.M.W.M., SCHOOP, A.M.C., KWA, H.Y. & VAN ZWIETEN, P.A. (1981). Characterization of α-adrenoceptors participating in the central hypotensive and sedative effects of clonidine using yohimbine, rauwolscine and corynanthine. *Eur. J. Pharmacol.*, **70,** 7–15.

VAN KAMMEN, D.P., PETERS, J. & VAN KAMMEN, W.B. (1986). Cerebrospinal fluid studies of monoamine metabolism in schizophrenia. *Psychiatric Clinics North Am.*, **9,** 81–97.

WYATT, R.J. (1976). Biochemistry and schizophrenia (part 4) the neuroleptics – their mechanism of action: a review of biochemical literature. *Psychopharmacol. Bull.*, **12,** 5–50.

(Received December 23, 1993
Revised February 22, 1994
Accepted March 16, 1994)

Br. J. Pharmacol. (1994), **112**, 775–780

Characterization of the effects of 2-methylthio-ATP and 2-chloro-ATP on brain capillary endothelial cells: similarities to ADP and differences from ATP

Paul Vigne, Erick Feolde, *Jean Philippe Breittmayer & [1]Christian Frelin

Institut de Pharmacologie Moléculaire et Cellulaire du CNRS, 660 Route des Lucioles, Sophia Antipolis, 06560 Valbonne, France and *INSERM U343, Faculté de Médecine, Université de Nice-Sophia Antipolis 06034 Nice Cedex, France

1 Brain capillary endothelial cells responded to 2-methylthio-ATP (2MeSATP) by large increases in $[Ca^{2+}]_i$ (EC_{50} = 27 nM) that were partially dependent on the presence of extracellular Ca^{2+} and that were not associated with a measurable production of inositol phosphates.

2 2-chloro-ATP (2ClATP) raised $[Ca^{2+}]_i$ in a biphasic manner. At low concentrations, intracellular Ca^{2+} mobilization was not associated with a measurable production of inositol phosphates. At concentrations > 30 μM, 2ClATP activated phospholipase C.

3 The actions of 2ClATP, 2MeSATP and ADP on $[Ca^{2+}]_i$ were additive to those of ATP and UTP. Non-additive actions of 2MeSATP and of low concentrations of ADP or of 2ClATP were observed.

4 Cross desensitizations of the actions of ADP, 2MeSATP and 2ClATP were observed. None of them desensitized cells to the action of ATP.

5 It is concluded that 2MeSATP and low concentrations of 2ClATP and ADP induce intracellular Ca^{2+} mobilization by acting via an atypical P_{2y} purinoceptor that is not coupled to phospholipase C. At high concentrations, 2ClATP also activates phospholipase C and further increases $[Ca^{2+}]_i$ probably by acting on P_{2u} purinoceptors.

Keywords: Blood brain barrier; purinoceptor; 2-chloro-ATP; 2MeSATP; 2-methylthio-ATP

Introduction

Phosphorylated adenine nucleotides play an important role in modulating a variety of cellular functions in the cardiovascular system (Pirotton *et al.*, 1993; Gordon, 1986). Their action is mediated via at least five distinct P_2 purinoceptors (Burnstock & Kennedy, 1985; Gordon, 1986). P_{2x} receptors are receptor operated channels that are mainly found in vascular smooth muscle cells. P_{2y} receptors are phospholipase C-coupled receptors that are more specific for 2-methylthio-ATP (2MeSATP) than for adenosine 5′ triphosphate (ATP) and that are found in aortic endothelial cells. P_{2t} receptors are adenosine 5′ diphosphate (ADP)-specific receptors of platelets. P_{2z} receptors specifically recognize the tetrabasic form of ATP and are responsible for the permeabilizing effects of ATP in various transformed cell lines. Finally the recently identified P_{2u} receptors recognize ATP and uridine 5′ triphosphate (UTP) and couple to phospholipase C (O'Connor *et al.*, 1991). The structures of P_{2y} and P_{2u} receptors have recently been elucidated. Both receptors belong to the family of G protein coupled, seven transmembrane domain receptors (Lustig *et al.*, 1993; Webb *et al.*, 1993).

In a previous study we analyzed the responses of rat brain capillary endothelial cells (BCEC) to nucleotides and provided evidence for the presence of two types of receptors for nucleotides: (i) a P_{2u}-like receptor coupled to phospholipase C and (ii) an ADP-specific receptor the occupancy of which induced a mobilization of intracellular Ca^{2+} stores without activation of phospholipase C (Frelin *et al.*, 1993). In this paper we analyze the actions of 2MeSATP and 2-chloro-ATP (2ClATP) on BCEC. 2MeSATP is a well known agonist of P_{2y} receptors in aortic endothelial cells (Motte *et al.*, 1993; Wilkinson *et al.*, 1993). 2ClATP and 2MeSATP are antagonists of ADP responses mediated by P_{2t} receptors in platelets (Cusack & Hourani, 1982; Hall & Hourani, 1993). 2ClATP is also a potent P_{2y} agonist (Needham *et al.*, 1987).

[1] Author for correspondence.

Methods

BCEC were prepared as previously described (Vigne *et al.*, 1989). Cells were grown in Dulbecco's modified Eagle's medium (GIBCO) supplemented with 10% foetal calf serum (Dutscher, Strasbourg, France), 100 units ml^{-1} penicillin and 100 μg ml^{-1} streptomycin. For intracellular Ca^{2+} measurements, cells were loaded with 5 μM indo-1/AM for 2 h in complete culture medium at 37°C. After dissociation from the culture dishes, cells were centrifuged at low speed and suspended into an Earle's salt solution (composition, mM: NaCl 140, KCl 5, $CaCl_2$ 1.8, $MgSO_4$ 0.8, glucose 5, buffered at pH 7.4 with N-2-hydroxyethylpiperazine-N′-2-ethane sulphonic acid-NaOH 25). Flow cytometric analysis of the indo-1 fluorescence was performed as described previously (Frelin *et al.*, 1993) using a FacStar Plus (Becton-Dickinson). Indo-1 fluorescence ratio were measured in single cells and collected in real time at a rate of 500 cells s^{-1}. Means of 1000–3000 individual measurements were computed and collected at different times following the addition of agonists. The values of the fluorescence ratio given by the computer are arbitrary values. The technique, because it reduces the incidence of the cell to cell variability in the responses, is well suited for a pharmacological analysis of the action of Ca^{2+} mobilizing agents (Frelin *et al.*, 1993). To define dose-response curves for agonists, cells were treated with the desired concentration of agonists and analyzed. The indo-1 fluorescence ratio of 1000 cells, sampled during 1.5 s, 20 s after the addition of agonists were collected and the mean ratio computed. Each experiment was repeated at least three times. Low $[Ca^{2+}]$ (50 nM) solutions were prepared using 0.5 mM $CaCl_2$ and 1.2 mM ethyleneglycol *bis*-(β-aminoethyl ether)-*N*,*N*,*N*′,*N*′-tetraacetic acid. All experiments were performed at 20°C.

To measure the production of inositol phosphates, BCEC were grown to confluency in six well plates and labelled to equilibrium with 2 μCi ml^{-1} of *myo*-[2-^{3}H]-inositol in complete culture medium. After washing with Earle's salt solution, cells were incubated for 10 min at 37°C in a 110 mM NaCl, 40 mM LiCl modified Earle's salt solution. After 5 min

of exposure to agonists, the radioactivity incorporated into total inositol phosphates (InsP) was determined as previously described (Frelin *et al.*, 1993).

Proteins were determined according to Bradford (1976).

Means ± s.e.mean are shown. When no error bar is presented in the Figures, it was smaller than the size of the points. Dose-response curves were fitted to a four parameter logistic function using the SigmaPlot software.

Materials

2ClATP and 2MeSATP were purchased from Research Biochemicals Inc. Other nucleotides were from the Sigma Chemical Co. Indo-1/AM was from Calbiochem. Endothelin-1 was from Neosystems (Strasbourg, France). *myo*-[2-^{3}H] inositol (19 Ci mmol^{-1}) was from Amersham.

Results

Figure 1a shows that the addition of 1 μM 2MeSATP to BCEC increased $[Ca^{2+}]_i$ in a manner partially dependent on the presence of external Ca^{2+}. The dose-response curve for the action of 2MeSATP on $[Ca^{2+}]_i$ is presented in Figure 1b. It was monophasic with an EC_{50} value of 27 ± 4 nM. Figure 2a shows that like 2MeSATP, 2ClATP raised $[Ca^{2+}]_i$ in a manner partially dependent on the presence of external Ca^{2+}. The dose-response curve for 2ClATP action on $[Ca^{2+}]_i$ is shown in Figure 2b. It extended over at least five orders of magnitude and showed a marked shoulder at 3 to 10 μM.

We next measured the production of total inositol phosphates. Figure 3 shows that 2MeSATP had no effect on InsP production up to the highest concentration tested (1 mM).

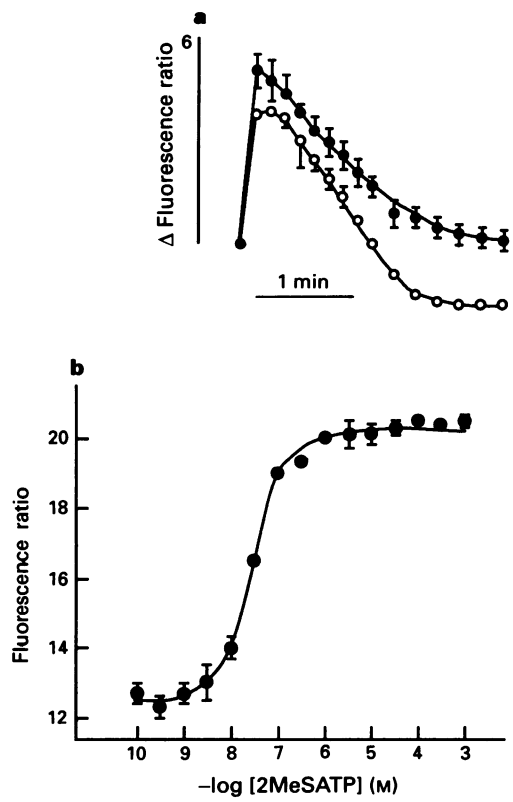

Figure 1 The action of 2-methylthio-ATP (2MeSATP) on $[Ca^{2+}]_i$: (a) Changes in indo-1 fluorescence ratio observed after the addition of 1 μM 2MeSATP. Experiments were performed in the presence of 1.8 mM Ca^{2+} (●) or of 50 nM Ca^{2+} (○). (b) Dose-response curve for the action of 2MeSATP on $[Ca^{2+}]_i$. Mean indo-1 fluorescence ratio was measured 20 s after the addition of the nucleotide to the cells. Means ± s.e. ($n = 3$) are shown.

Similarly, 2ClATP had no action up to concentrations of 10 μM. At higher concentrations, 2ClATP increased InsP production up to 1.8 fold. Under the same conditions ATP (30 μM) and endothelin-1 (100 nM) increased InsP production 2 and 2.6 fold (Figure 3). An obvious possibility for these results is that 2ClATP had two distinct actions on BCEC. At low concentrations it increased $[Ca^{2+}]_i$ in the absence of

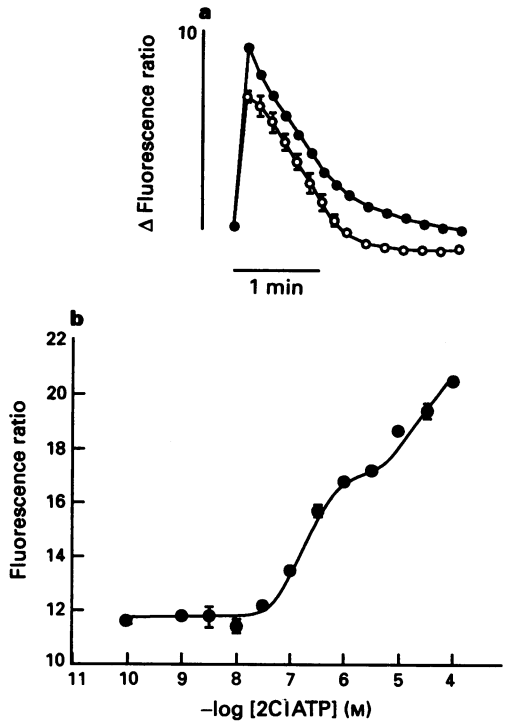

Figure 2 The action of 2-chloro-ATP (2ClATP) on $[Ca^{2+}]_i$: (a) Changes in indo-1 fluorescence ratio observed after the addition of 1 μM 2ClATP. Experiments were performed in the presence of 1.8 mM Ca^{2+} (●) or of 50 nM Ca^{2+} (○). (b) Dose-response curve for the action of 2ClATP on $[Ca^{2+}]_i$. Mean indo-1 fluorescence ratio were measured 20 s after the addition of the nucleotide to the cells. Means ± s.e. ($n = 3$) are shown.

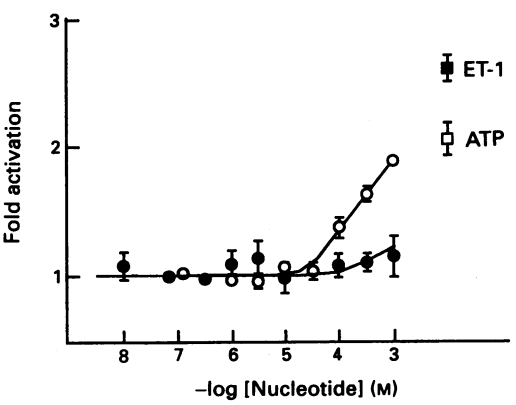

Figure 3 The action of 2-methylthio-ATP (2MeSATP) and 2-chloro-ATP (2ClATP) on inositol phosphates (InsP) production. Cells were exposed for 5 min to the indicated concentrations of 2MeSATP (●) and 2ClATP (○) and the production of total InsP was measured as described in Methods. The figure also shows for comparison the effects of 100 nM endothelin-1 (ET-1) and of 30 μM ATP in the same cells. Means ± s.e. ($n = 8$) are shown. It was checked that the clones used in these experiments responded to low concentrations of 2MeSATP and 2ClATP by large changes in $[Ca^{2+}]_i$.

measurable InsP production. At high concentrations (>30 μM) it further increased $[Ca^{2+}]_i$ by activating phospholipase C. Very similar results have been previously reported for ADP (Frelin *et al.*, 1993).

A useful way to assess receptor heterogeneity is to look for additive responses. Additive actions of maximally effective concentrations of agonists are expected if they bind to different receptor sites. Non additive actions are expected if they bind to the same receptor. They are also expected if they bind to different sites but maximally increase $[Ca^{2+}]_i$ by depleting intracellular Ca^{2+} stores. However, one difficulty with this approach is that ADP and 2ClATP which have a complex action of $[Ca^{2+}]_i$ (e.g. Figure 2) may recognize more than one type of receptor. For this reason, dose-response curves for each nucleotide were established in the presence of fixed concentrations of 2MeSATP, 2ClATP or ADP. In a first series of experiments, cells were treated at the same time with 1 μM 2MeSATP and different concentrations of ATP, UTP, ADP or 2ClATP. At a concentration of 1 μM, 2MeSATP induced maximum InsP-independent intracellular Ca^{2+} changes (Figure 1b). Figure 4 shows that ATP and UTP still increased $[Ca^{2+}]_i$ in the presence of 2MeSATP. EC_{50} values were 7.9 ± 1.4 μM and 4.3 ± 1.9 μM for ATP and UTP respectively. These values were close to the EC_{50} values measured in the absence of 2MeSATP (ATP: 10 μM, UTP: 15 μM; Frelin *et al.*, 1993). Thus the presence of 2MeSATP hardly altered the responses to ATP and UTP. Figure 4 further shows that in the presence of 1 μM 2MeSATP, ADP and 2ClATP increased $[Ca^{2+}]_i$ but only at concentrations >10 μM. EC_{50} values were 0.15 ± 0.02 mM and 0.19 ± 0.06 mM for ADP and 2ClATP respectively. A conspicious effect of 2MeSATP was to transform the biphasic action of 2ClATP (Figure 2b) into a monophasic action (Figure 4). It suppressed the actions of low concentrations of 2ClATP that are independent of the formation of InsP and left unaltered the action of large concentrations of 2ClATP that are associated with an activation of phospholipase C. 2MeSATP also transformed the biphasic action of ADP into a monophasic, InsP-associated action.

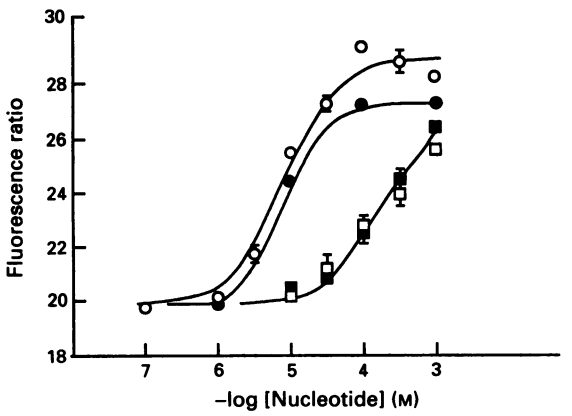

Figure 4 The action of nucleotides on $[Ca^{2+}]_i$ in the presence of 2-methylthio-ATP (2MeSATP). Cells were exposed at the same time to 1 μM 2MeSATP and different concentrations of ATP (○), UTP (●), ADP (■) and 2-chloro-ATP (2ClATP) (□). The mean indo-1 fluorescence ratio was measured 20 s later and plotted as a function of the concentration of nucleotide used. The mean indo-1 fluorescence ratio in the absence of agonists was 10. Means ± s.e. ($n = 3$) are shown. All experiments shown were performed on the same batch of cells and are directly comparable.

Figure 5 shows the results of similar experiments performed in the presence of 1 μM 2ClATP. At this concentration, 2ClATP increased $[Ca^{2+}]_i$ to a large extent (Figure 2b) but had no action on the formation of InsP (Figure 3). In the presence of 1 μM 2ClATP, ATP and UTP still increased $[Ca^{2+}]_i$. EC_{50} values were 21 ± 2 μM and 13 ± 3 μM for ATP and UTP respectively, close to the values previously observed in the absence of 2ClATP. Thus low concentrations of 2ClATP hardly modified the responses to ATP and UTP. Figure 5 further shows that 2ClATP almost completely suppressed the action of 2MeSATP. It also prevented low concentrations (<10 μM) of ADP from raising $[Ca^{2+}]_i$ and transformed its biphasic action into a monophasic action. The EC_{50} value for the action of ADP on $[Ca^{2+}]_i$ in the presence of 2ClATP was 0.24 ± 0.03 mM. At these concentrations, ADP induced a measurable production of InsP (Frelin *et al.*, 1993).

Figure 6 shows the results of similar experiments performed in the presence of 10 μM ADP. This concentration induced maximum InsP-independent Ca^{2+} mobilization (Frelin *et al.*, 1993). As previously reported (Frelin *et al.*, 1993), ADP did not prevent ATP from increasing $[Ca^{2+}]_i$, thus indicating additive actions. The EC_{50} value for the action of ATP in the presence of ADP was 11 ± 2 μM. Figure 6 further shows that ADP completely suppressed the actions of

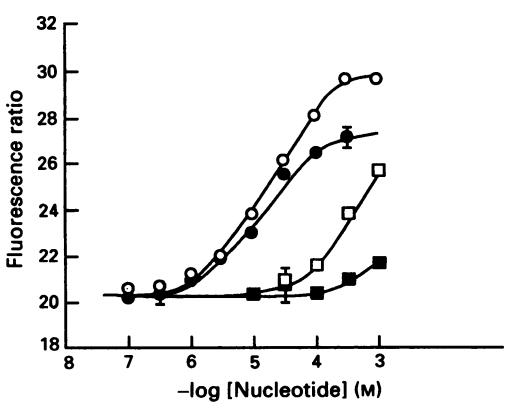

Figure 5 The action of nucleotides on $[Ca^{2+}]_i$ in the presence of 2-chloro-ATP (2ClATP). Cells were exposed at the same time to 1 μM 2ClATP and different concentrations of ATP (○), UTP (●), ADP (□) and 2-methylthio-ATP (2MeSATP) (■). The mean indo-1 fluorescence ratio was measured 20 s later and plotted as a function of the concentration of nucleotide used. The mean indo-1 fluorescence ratio in the absence of agonists was 10. Means ± s.e. ($n = 3$) are shown. All experiments shown were performed on the same batch of cells and are directly comparable.

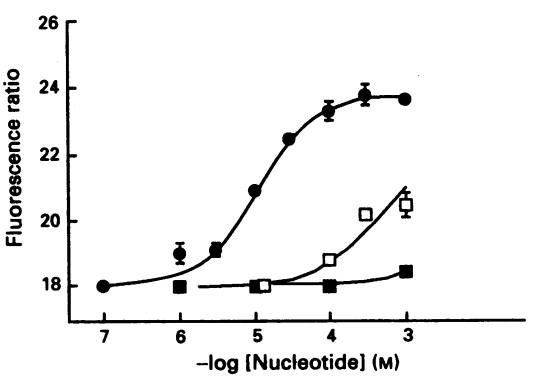

Figure 6 The action of nucleotides on $[Ca^{2+}]_i$ in the presence of ADP. Cells were exposed at the same time to 10 μM ADP and different concentrations of ATP (●), 2-methylthio-ATP (2MeSATP) (■) and 2-chloro-ATP (2ClATP) (□). The mean indo-1 fluorescence ratio was measured 20 s later and plotted as a function of the concentration of nucleotide used. The mean indo-1 fluorescence ratio in the absence of agonists was 10. Means ± s.e. ($n = 3$) are shown. All experiments shown were performed on the same batch of cells and are directly comparable.

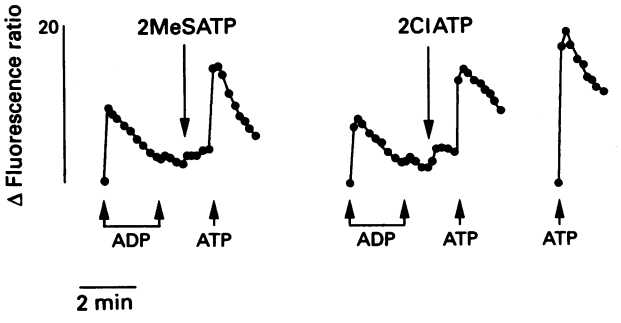

Figure 7 ADP desensitized cells to the actions of 2-methylthio-ATP (2MeSATP) and 2-chloro-ATP (2ClATP) but not to that of ATP. Cells were exposed twice to 3 μM ADP and then to 1 μM 2MeSATP, 1 μM 2ClATP and 0.3 mM ATP as indicated and changes in the indo-1 fluorescence ratio were monitored. The right panel shows for comparison, a Ca^{2+} transient obtained in the same batch of cells using 0.3 nM ATP. Each point was the mean of 1000 individual cell measurements.

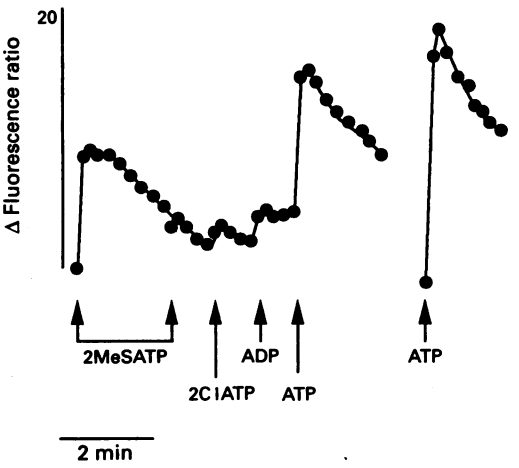

Figure 8 2-Methylthio-ATP (2MeSATP) desensitized cells to the actions of ADP and 2-chloro-ATP (2ClATP) but not to that of ATP. Cells were exposed twice to 1 μM 2MeATP and then to 1 μM 2ClATP, 3 μM ADP and 0.3 mM ATP as indicated and changes in the indo-1 fluorescence ratio were monitored. The right panel shows for comparison, a Ca^{2+} transient obtained in the same batch of cells using 0.3 mM ATP. Each point was the mean of 1000 individual cell measurements.

2MeSATP and of low concentrations of 2ClATP. ADP did not prevent large (>30 μM) concentrations of 2ClATP from raising $[Ca^{2+}]_i$. At these concentrations, 2ClATP induced a measurable production of InsP (Figure 3).

Taken together, the results presented in Figures 4 to 6 indicated that 2MeSATP, 2ClATP and ADP acted in very similar ways. They hardly modified the cellular responses to ATP and UTP. They prevented their high affinity, InsP independent responses but had no action on the low affinity responses, associated with a measurable production of InsP.

Another way to assess receptor heterogeneity is to perform desensitization experiments. We previously reported that ADP desensitized cells still responded to ATP (Frelin *et al.*, 1993). Figure 7 shows that a first treatment of BCEC with 3 μM ADP desensitized cells to further applications of ADP and also to the applications of 2MeSATP and 2ClATP. Yet desensitized cells still responded to 0.3 mM ATP by a large $[Ca^{2+}]_i$ transient. Figure 8 further shows that cells that had been treated with 1 μM 2MeSATP no longer responded to 1 μM 2ClATP or to 3 μM ADP, yet they retained large responses to 0.3 mM ATP. Finally, Figure 9 shows that 1 μM 2ClATP-treated cells were desensitized to the actions of

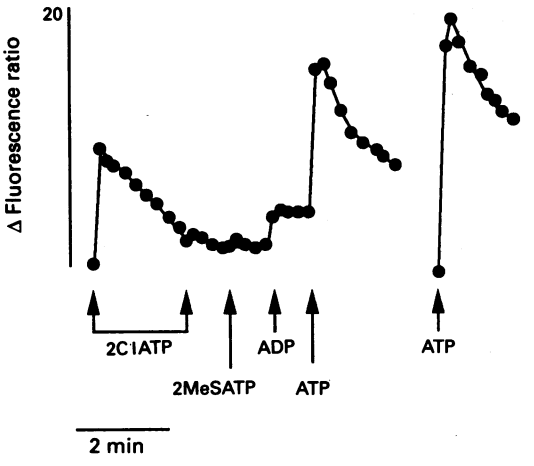

Figure 9 2-Chloro-ATP (2ClATP) desensitized cells to the actions of 2-methylthio-ATP (2MeSATP) and ADP but not to that of ATP. Cells were exposed twice to 1 μM 2ClATP and then to 1 μM 2MeATP, 3 μM ADP and 0.3 mM ATP as indicated and changes in the indo-1 fluorescence ratio were monitored. The right panel shows for comparison, a Ca^{2+} transient obtained in the same batch of cells using 0.3 mM ATP. Each point was the mean of 1000 individual cell measurements. Experiments shown in Figures 7–9 were performed on the same batch of cells and are therefore directly comparable. They are representative of three independent experiments.

2MeSATP and ADP but not to that of ATP. Thus cross desensitizations of the actions of ADP, 2MeSATP and 2ClATP were observed. None of these substances desensitized cells to the action of ATP.

Discussion

2MeSATP is a potent agonist of P_{2y} receptors in aortic endothelial cells (Motte *et al.*, 1993; Wilkinson *et al.*, 1993) and an antagonist of P_{2t} receptors of platelets (Hall & Hourani, 1993). Conversely, 2ClATP is an agonist of P_{2y} receptors (Needham *et al.*, 1987), a weak agonist of P_{2u} receptors (Lustig *et al.*, 1993) and an antagonist of P_{2t} receptors (Cusack & Hourani, 1982; Hall & Hourani, 1993). We previously described the presence in rat BCEC of two distinct receptor sites for nucleotides: (i) a P_{2u} purinoceptor for ATP and UTP and (ii) an ADP receptor that induced the mobilization of thapsigargin-sensitive intracellular Ca^{2+} stores in the absence of formation of inositol phosphates (Frelin *et al.*, 1993). This paper defines the actions of 2MeSATP and 2ClATP in BCEC and shows that the two nucleotides act in a manner similar to that of ADP and distinct from that of ATP.

Evidence that 2MeSATP and low concentrations of ADP have similar actions is as follows: (i) 2MeSATP (Figure 3) and low concentrations of ADP (Frelin *et al.*, 1993) induce intracellular Ca^{2+} mobilization in the absence of measurable InsP production. (ii) 2MeSATP hardly alters the cell responses to ATP and UTP but it prevents the action of low concentrations of ADP (Figure 4). Conversely ADP prevents the action of 2MeSATP but not that of ATP (Figure 6). (iii) 2MeSATP and ADP desensitize each other's action. 2MeSATP and ADP do not desensitize cells to the action of ATP (Figure 7–9).

Evidence that low concentrations of 2ClATP and ADP act similarly are as follows: (i) Low concentrations of 2ClATP (Figures 2 and 3) and ADP (Frelin *et al.*, 1993) induce intracellular Ca^{2+} mobilization in the absence of measurable InsP production. (ii) Low concentrations of 2ClATP do not prevent ATP or UTP from raising $[Ca^{2+}]_i$ with EC_{50} values

close to those observed in the absence of 2ClATP (Figure 5). Low concentrations of 2ClATP prevent the action of low concentrations of ADP (Figure 4). Conversely ADP prevents the action of low concentrations of 2ClATP but not that of ATP (Figure 6). (iii) 2ClATP and ADP desensitize each other's action. 2ClATP and ADP do not desensitize cells to the action of ATP (Figures 7–9).

The close similarities of the actions of 2MeSATP and of 2ClATP suggest that they may recognize the same receptor. The observations that 2MeSATP and low concentrations of 2ClATP have no additive actions (Figures 4 and 5) and desensitize each other's action (Figures 8 and 9) are fully consistent with this hypothesis.

Very similar properties have previously been reported in rat hepatocytes which respond to ATP, UTP, 2MeSATP and ADP by large increases in $[Ca^{2+}]_i$ and by increased glycogenolytic rates. First ATP and ADP induce different intracellular $[Ca^{2+}]_i$ oscillations (Dixon *et al.*, 1990). Second, while the actions of ATP and UTP are clearly associated to an activation of phospholipase C (Keppens *et al.*, 1992), those of ADβS and 2MeSATP are not (Keppens & DeWulf, 1991; Keppens *et al.*, 1993). Finally, it is worth noting that the EC_{50} value for the action of 2MeSATP on glycogen phosphorylase in hepatocytes (20 nM, Keppens & DeWulf, 1991) is close to the EC_{50} value for the action of 2MeSATP on $[Ca^{2+}]_i$ in BCEC (27 nM, Figure 1b). This could suggest that a similar receptor is expressed by rat BCEC and by rat hepatocytes. This receptor recognises low concentrations of 2MeSATP, 2ClATP and ADP and it induces intracellular Ca^{2+} mobilization in the absence of formation of inositol phosphates. Its pharmacological profile, defined from the InsP-independent actions of nucleotides on $[Ca^{2+}]_i$ is: 2MeSATP (EC_{50} = 27 nM, Figure 1b) > 2ClATP (EC_{50} ~0.3 μM, Figure 2b) > ADP (EC_{50} ~1 μM; Frelin *et al.*, 1993). This receptor although pharmacologically similar to P_{2y} receptors differs from known P_{2y} purinoceptors in that it is not coupled to phospholipase C. It differs from P_{2t} purinoceptors for 2ClATP and 2MeSATP act as agonists rather than as antagonists. It is unlikely a P_{2x} or P_{2z} purinoceptor for changes in $[Ca^{2+}]_i$ induced by 2MeSATP and 2ClATP are not suppressed when the external Ca^{2+} concentration is lowered (Figures 1 and 2) and mostly result from the mobilization of intracellular stores. This is also suggested by the observation that α, β methylene ATP, a potent agonist of P_{2x} receptors is inactive on BCEC (Frelin *et al.*, 1993). 2MeSATP is usually considered as a high affinity and specific agonist of P_{2y} receptors and is thought to act primarily by activating phospholipase C (Motte *et al.*, 1993; Wilkinson *et al.*, 1993; Webb *et al.*, 1993). It is worth noting that at low concentrations 2MeSATP may also act in a manner independent of the formation of inositol phosphates both in rat BCEC (this study) and in rat hepatocytes (Keppens & DeWulf, 1991).

At high concentrations, 2ClATP increases $[Ca^{2+}]_i$ in parallel to an activation of phospholipase C (Figures 2 and 3). The properties of the receptor involved can be defined from the experiments presented in Figures 5 to 7 in which the InsP-independent responses were masked by the use of low concentrations of ADP, 2MeSATP or 2ClATP. Under these conditions ATP (EC_{50} = 7–21 μM), UTP (EC_{50} = 4–13 μM), 2ClATP (EC_{50} = 0.19 mM) and ADP (EC_{50} = 0.15–0.24 mM) increase $[Ca^{2+}]_i$. Similar values have been found for their action on phospholipase C activity (ATP: 10 μM, UTP: 15 μM, 2ClATP: >0.1 mM, ADP: >0.1 mM) (Frelin *et al.*, 1993, Figure 2). Both profiles are typical of a P_{2u} receptor (Fine *et al.*, 1989; Pfeilschrifter, 1990; Brown *et al.*, 1991; O'Connor *et al.*, 1991; Lustig *et al.*, 1993; Raha *et al.*, 1993), suggesting that the InsP-dependent action of nucleotides was mediated by P_{2u} purinoceptors. Further evidence for the presence of a P_{2u} receptor on BCEC is provided by the observation that ATP and UTP have non-additive and cross-desensitizing actions (Frelin *et al.*, 1993). Finally, clear evidence that the P_{2u} receptor is distinct from the ADP receptor described above is that some of the cell clones used in this study responded to ATP and UTP but not to low concentrations of 2ClATP or of 2MeSATP (data not shown).

In conclusion, the results presented in this paper provide further support for the presence of at least two types of purinoceptors in rat BCEC: a P_{2u} purinoceptor and an atypical P_{2y} receptor that induces intracellular Ca^{2+} mobilization via a phospholipase C independent mechanism.

This work was supported by the Centre National de la Recherche Scientifique and the Association pour la Recherche sur le Cancer. We thank N. Boyer and V. Chéron for expert technical assistance.

References

BRADFORD, M.M. (1976). A rapid and sensitive method for the quantification of microgram quantities of protein utilizing the principle of protein-dye coupling. *Anal. Biochem.*, **72**, 248–254.

BROWN, H.A., LAZAROWSKI, E.R., BOUCHER, R.C. & HARDEN, T.K. (1991). Evidence that UTP and ATP regulate phospholipase C through a common extracellular 5'nucleotide receptor in human airway epithelial cells. *Mol. Pharmacol.*, **40**, 648–655.

BURNSTOCK, G. & KENNEDY, C. (1985). Is there a basis for distinguishing two types of P_2-purinoceptors. *Gen. Pharmacol.*, **16**, 433–440.

CUSACK, N.J. & HOURANI, S.M.O. (1982). Specific but non competitive inhibition by 2-alkylthio analogues of adenosine 5'-monophosphate and adenosine 5'-triphosphate of human platelet aggregation induced by adenosine 5'-diphosphate. *Br. J. Pharmacol.*, **75**, 397–400.

DIXON, C.J., WOODS, N.M., CUTHBERTSON, K.S.R. & COBBOLD, P.H. (1990). Evidence for two Ca^{2+} mobilizing purinoceptors on rat hepatocytes. *Biochem. J.*, **269**, 499–502.

FINE, J., COLE, P. & DAVIDSON, J.S. (1989). Extracellular nucleotides stimulate receptor-mediated calcium mobilization and inositol phosphate production in human fibroblasts. *Biochem. J.*, **263**, 371–376.

FRELIN, C., BREITTMAYER, J.P. & VIGNE, P. (1993). ADP induces inositol phosphate independent intracellular Ca^{2+} mobilization in brain capillary endothelial cells. *J. Biol. Chem.*, **268**, 8787–8792.

GORDON, J.L. (1986). Extracellular ATP: effects, sources and fate. *Biochem. J.*, **233**, 309–319.

HALL, D.A. & HOURANI, S.M.O. (1993). Effects of analogues of adenine nucleotides on increases in intracellular calcium mediated by P_{2t}-purinoceptors on human platelets. *Br. J. Pharmacol.*, **108**, 728–733.

KEPPENS, S. & DEWULF, H. (1991). Characterization of the biological effects of 2-methylthio-ATP on rat hepatocytes: clear cut differences with ATP. *Br. J. Pharmacol.*, **104**, 301–304.

KEPPENS, S., VANDEKERCKOVE, A. & DEWULF, H. (1992). Extracellular ATP and UTP exert similar effects on rat isolated hepatocytes. *Br. J. Pharmacol.*, **105**, 475–479.

KEPPENS, S., VANDEKERCKOVE, A. & DEWULF, H. (1993). Characterization of the effects of adenosine 5'-[β-thio]-diphosphate in rat liver. *Br. J. Pharmacol.*, **108**, 663–668.

LUSTIG, K.D., SHIAU, A.K., BRAKE, A.J. & JULIUS, D. (1993). Expression cloning of an ATP receptor from mouse neuroblastoma cells. *Proc. Natl. Acad. Sci. U.S.A.*, **90**, 5113–5117.

MOTTE, S., PIROTTON, S. & BOEYNAEMS, J.M. (1993). Heterogeneity of ATP receptors in aortic endothelial cells. Involvement of P_{2y} and P_{2u} receptors in inositol phosphate response. *Circ. Res.*, **72**, 504–510.

NEEDHAM, L., CUSACK, N.J., PEARSON, J.D. & GORDON, J.L. (1987). Characteristics of the P2 purinoceptor that mediates prostacyclin production by pig aortic endothelial cells. *Eur. J. Pharmacol.*, **134**, 199–209.

O'CONNOR, S.E., DAINTY, I.A. & LEFF, P. (1991). Further subclassification of ATP receptors based on agonist studies. *Trends Pharmacol. Sci.*, **12**, 137–141.

PFEILSCHRIFTER, J. (1990). Comparison of extracellular ATP and UTP signalling in rat renal mesangial cells. *Biochem. J.*, **272,** 469–472.

PIROTTON, S., MOTTE, S., CÔTE, S. & BOEYNAEMS, J.M. (1993). Control of endothelial function by nucleotides: multiple receptors and transducing mechanisms. *Cell Signalling*, **5,** 1–8.

RAHA, S., DESOUZA, L.R. & REED, J.K. (1993). Intracellular signalling by nucleotide receptors in PC12 pheochromocytoma cells. *J. Cell. Physiol.*, **154,** 623–630.

VIGNE, P., CHAMPIGNY, G., MARSAULT, R., BARBRY, P., FRELIN, C. & LAZDUNSKI, M. (1989). A new type of amiloride sensitive cationic channel in endothelial cells of brain microvessels. *J. Biol. Chem.*, **264,** 7663–7668.

WEBB, T.E., SIMON, J., KRISHEK, B.J., BATESON, A.N., SMART, T.G., KING, B.F., BURNSTOCK, G. & BARNARD, E.A. (1993). Cloning and functional expression of a brain G-protein coupled ATP receptor. *FEBS Lett.*, **324,** 219–225.

WILKINSON, G.F., PURKISS, J.R. & BOARDER, M.R. (1993). The regulation of aortic endothelial cells by purines and pyrimidines involves co-existing P_{2y}-purinoceptors and nucleotide receptors linked to phospholipase C. *Br. J. Pharmacol.*, **108,** 689–693.

(Received September 20, 1993
Revised February 10, 1994
Accepted March 16, 1994)

Br. J. Pharmacol. (1994), **112**, 781–788

The effect of cyclic AMP elevating agents on bradykinin- and carbachol-induced signal transduction in canine cultured tracheal smooth muscle cells

[1]Chuen Mao Yang, Hui-Chuan Hsia, *Shue-Fen Luo, Jen-Tsung Hsieh & Richard Ong

Department of Pharmacology and *Department of Internal Medicine, Chang Gung Medical College, Kwei-San, Tao-Yuan, Taiwan

1 The effects of cholera toxin (CTX), forskolin and dibutyryl cyclic AMP on bradykinin (BK)- and carbachol-induced accumulation of inositol phosphates (IPs) and Ca^{2+} mobilization were investigated in canine cultured tracheal smooth muscle cells (TSMCs). The BK-induced responses were mediated via a G protein which was not inhibited by CTX or pertussis toxin treatment.

2 BK-stimulated IPs accumulation and Ca^{2+} mobilization were potentiated by CTX (10 $\mu g\,ml^{-1}$) pretreatment which was time-dependent. Maximal increase of these responses occurred after 24 h treatment with CTX. The concentration-effect relationship of BK-induced responses were shifted to the left and BK was substantially more effective in CTX-treated cells than in the control cells. This enhancing effect of CTX did not occur with carbachol.

3 Short-term (<4 h) treatment with forskolin (10 μM) or dibutyryl cyclic AMP (1 mM) failed to accentuate BK-induced responses, but long-term (>4 h) treatment of TSMCs with these agents mimicked the enhancing effect of CTX, suggesting that CTX-induced enhancement of BK responsiveness might be due to a rise in cyclic AMP.

4 Prolonged treatment of TSMCs with these agents was accompanied by an increase in cell surface [^{3}H]-BK binding sites, which was inhibited by concurrent incubation with cycloheximide, an inhibitor of protein biosynthesis. Cycloheximide also abolished the potentiating actions of CTX, forskolin, and dibutyryl cyclic AMP on BK-induced IPs formation and Ca^{2+} mobilization.

5 The locus of this enhancement was further investigated by examining the effects of CTX, forskolin and dibutyryl cyclic AMP on AlF_4^--induced IPs accumulation in canine TSMCs. AlF_4^--induced IPs accumulation was not affected by CTX, forskolin, or dibutyryl cyclic AMP treatment, supporting the contention that this stimulatory effect is located at the BK receptor level.

6 These results demonstrate that the augmentation of BK-induced IPs accumulation and Ca^{2+} mobilization produced by CTX, forskolin and dibutyryl cyclic AMP involves a cyclic AMP-dependent mechanism which is induced by a sustained increase in the level of intracellular cyclic AMP. CTX and forskolin may promote an increase of the synthesis of BK receptors, and thereby enhance BK-induced responses.

Keywords: Inositol phosphates; Ca^{2+}; G protein; cyclic AMP; BK receptor

Introduction

Bradykinin (BK) is a classic mediator of inflammatory diseases of the airways and may be implicated in allergic asthma (Christiansen *et al.*, 1987). In the airways, BK causes bronchoconstriction, pulmonary and bronchial vasodilatation, mucus secretion and microvascular leakage (Barnes, 1992). One possible mechanism of BK-induced tracheal smooth muscle contraction has been attributed to an increase in phosphoinositide (PI) hydrolysis (Marsh & Hill, 1992; Yang *et al.*, 1994) and a rise in intracellular Ca^{2+} ($[Ca^{2+}]_i$) (Murray & Kotlikoff, 1991; Marsh & Hill, 1993). Many studies have suggested that G proteins are involved in the coupling of the BK receptor to phospholipase C (PLC) in various cells (Higashida *et al.*, 1986; Burch & Axelrod, 1987; Murayama & Ui, 1987), since BK-induced inositol phosphates (IPs) accumulation was found to be sensitive to guanine nucleotide analogues (Higashida *et al.*, 1986; Murayama & Ui, 1987). BK stimulates IPs accumulation by mechanisms involving both pertussis toxin-sensitive and insensitive G proteins (Higashida *et al.*, 1986; Lambert *et al.*, 1986; Liebmann *et al.*, 1990).

Several lines of evidence have demonstrated that cholera toxin (CTX) affects signal transduction in various cell types (Hepler & Gilman, 1992). Preincubation of cells with CTX causes inhibition of PI turnover, which is partly due to a reduction in number of hormonal receptors (Gardner *et al.*, 1989; Guillon *et al.*, 1989; Socorro *et al.*, 1990). It has also been shown that CTX potentiates the BK-stimulated PI turnover in human foreskin fibroblasts, the osteoblast-like cell line MC3T3-E1 and BALB/c/3T3 cells (Olashaw & Pledger, 1988; Etscheid & Villereal, 1989; Banno *et al.*, 1993). This potentiating action was inhibited by cycloheximide. This response may therefore involve an increase in protein synthesis following elevation of the concentration of cyclic AMP, probably through BK receptors (Etscheid *et al.*, 1991; Banno *et al.*, 1993). Moreover, elevation of cyclic AMP concentration caused by CTX promotes transcription of mRNA encoding a protein that stimulates the release of arachidonic acid metabolites (Peterson *et al.*, 1991).

We have previously shown that BK-induced IPs accumulation was potentiated by CTX treatment for 4 h in canine TSMCs (Yang *et al.*, 1994). In this study, experiments were undertaken to investigate the effects of CTX, forskolin and dibutyryl cyclic AMP on BK- and carbachol-induced IPs accumulation and Ca^{2+} mobilization, as well as the mechanism underlying the enhancement by these agents of BK responsiveness in canine TSMCs. Our results show that CTX, forskolin, and dibutyryl cyclic AMP greatly enhance the accumulation of IPs induced by BK, but not by carbachol in canine TSMCs. This enhancement is accompanied

[1] Author for correspondence.

by an increase in effectiveness of BK in inducing Ca^{2+} mobilization. Finally, we demonstrate that the increased responsiveness of the TSMCs results, at least in part, from an increase in the number of BK receptors.

Methods

Animals

Mongrel dogs, 10–20 kg, of either sex were purchased from a local supplier, and used throughout this study. Dogs were housed indoors in the animal facilities under automatically controlled temperature and light cycle conditions and fed standard laboratory chow and tap water *ad libitum*. Dogs were anaesthetized with pentobarbitone (30 mg kg^{-1}, intravenously) and ventilated mechanically via an orotracheal tube. The tracheae were surgically removed.

Isolation of tracheal smooth muscle cells

The TSMCs were isolated according to the methods previously reported (Yang, 1990; Yang *et al.*, 1991a,b). The trachea was cut longitudinally through the cartilage rings and the smooth muscle was dissected. The muscle was minced and transferred to the dissociation medium containing 0.1% collagenase IV, 0.025% DNase I, 0.025% elastase IV, and antibiotics in physiological solution. The physiological solution contained (mM): NaCl 137, KCl 5, $CaCl_2$ 1.1, $NaHCO_3$ 20, NaH_2PO_4 1, glucose 11 and HEPES 25 (pH 7.4). The tissue pieces were gently agitated at 37°C in a rotary shaker for 1 h. The released cells were collected and the residual was again digested with fresh enzyme solution for an additional 1 h at 37°C. The released cells were pooled and washed twice with Dulbecco's modified Eagle's medium (DMEM) and Ham's nutrient mixture F-12 (F-12) medium (1:1, vol/vol). The cells, suspended in DMEM/F-12 containing 10% foetal bovine serum (FBS), were plated onto a 60 mm culture dish and incubated at 37°C for 1 h to remove fibroblasts. The cells were counted and diluted with DMEM/F-12 to a final concentration of 2×10^5 cells ml^{-1}. The cell suspension was plated onto (0.5 ml/well) 24-well (1 ml/well) 12-well or (2 ml/well) 6-well culture plates containing glass coverslips coated with collagen for receptor binding assay, IPs accumulation and Ca^{2+} measurement, respectively. The medium was changed after 24 h and then every 3 days. After 5 days in culture, the cells were cultured in DMEM/F-12 containing 1% FBS for 24 h at 37°C. Then, the cells were grown in DMEM/F-12 containing 1% FBS supplemented with insulin-like growth factor I (IGF-I, 10 ng ml^{-1}) and insulin (1 μg ml^{-1}) for 12–14 days. These culture conditions were used to facilitate the expression of muscarinic receptors on cultured TSMCs (Yang *et al.*, 1991b).

In order to characterize the isolated and cultured TSMCs and to exclude contamination by epithelial cells and fibroblasts, the cells were identified by an indirect immunofluorescence method using a monoclonal antibody of light chain myosin (Gown *et al.*, 1985). Under the above culture conditions, over 95% of the cells were smooth muscle cells.

Accumulation of inositol phosphates

Effect of BK on the hydrolysis of PI was assayed by monitoring the accumulation of ^3H-labelled IPs as described by Berridge *et al.* (1983). Cultured TSMCs were incubated with 5 μCi ml^{-1} of *myo*-[2-^3H]-inositol at 37°C for 2 days. TSMCs were washed two times with PBS and incubated in Krebs-Henseleit buffer (KHS, pH 7.4) containing (in mM): NaCl 117, KCl 4.7, $MgSO_4$ 1.1, KH_2PO_4 1.2, $NaHCO_3$ 20, $CaCl_2$ 2.4, glucose 1, HEPES 20, and LiCl 10 at 37°C for 30 min. After BK was added at the concentration indicated, incubation was continued for another 60 min in the presence of 10 μM phosphoramidon. Reactions were terminated by addition of 5% perchloric acid followed by sonication and centrifugation at 3000 *g* for 15 min.

The perchloric acid soluble supernatants were extracted four times with ether, neutralized with potassium hydroxide, and applied to a column of AG1-X8, formate form, 100–200 mesh (Bio-Rad). The resin was washed successively with 5 ml of water and 5 ml of 60 mM ammonium formate: 5 mM sodium tetraborate to eliminate free *myo*-[^3H]-inositol and glycerophosphoinositol, respectively. Total IPs was eluted with 5 ml of 1 M ammonium formate: 0.1 M formic acid. The amount of [^3H]-IPs was determined in a radiospectrometer (Beckman LS5000TA, Fullerton, CA, U.S.A.).

Measurement of intracellular Ca^{2+} level

$[Ca^{2+}]_i$ was measured in confluent monolayers with the calcium-sensitive dye fura-2/AM as described by Grynkiewicz *et al.* (1985). Upon confluence, the cells were cultured in DMEM/F-12 with 1% FBS one day before measurements were taken. The monolayers were covered with 1 ml of DMEM/F-12 with 1% FBS containing 5 μM fura-2/AM and incubated at 37°C for 45 min. At the end of the loading period, the coverslips were washed twice with the physiological buffer solution (PBS) containing (mM): NaCl 125, KCl 5, $CaCl_2$ 1.8, $MgCl_2$ 2, NaH_2PO_4 0.5, $NaHCO_3$ 5, HEPES 10, and glucose 10, pH 7.4. The cells were incubated in PBS for another 30 min to complete dye deesterification. The coverslip was inserted into a quartz cuvette at an angle of approximately 45° to the excitation beam and placed in the thermostatted holder of a SLM 8000C spectrofluorometer. Continuous stirring was achieved with a magnetic stirrer.

Fluorescence of Ca^{2+}-bound and unbound fura-2 was measured by rapidly alternating the dual excitation wavelengths between 340 and 380 nm and electronically separating the resultant fluorescence signals at an emission wavelength of 510 nm. The autofluorescence of each monolayer was subtracted from the fluorescence data. The ratios (R) of the fluorescence at the two wavelengths were computed and used to calculate changes in $[Ca^{2+}]_i$. The ratios of maximum (R_{max}) and minimum (R_{min}) fluorescence of fura-2 were determined by the addition of ionomycin (10 μM) in the presence of PBS containing 5 mM Ca^{2+} and by adding 5 mM EGTA at pH 8 in Ca^{2+}-free PBS, respectively. Values obtained were 14.09, 0.96, and 22.07 for R_{max}, R_{min}, and β, respectively. The K_d of fura-2 for Ca^{2+} was assumed to be 224 nM (Grynkiewicz *et al.*, 1985).

[^3H]-BK binding assay

For detection of the effects of CTX, forskolin, and dibutyryl cyclic AMP on BK receptor density of TSMCs, [^3H]-BK was used as a ligand for binding studies. Binding assays were performed with confluent TSMCs in 24-well culture plates, with or without CTX, forskolin or dibutyryl cyclic AMP treatment in DMEM/F-12 containing 1% FBS for 24 h prior to the binding experiments, as described by Lambert *et al.* (1986). Culture medium was removed and 1 ml of binding buffer (composition, mM HEPES 20, pH 7.4, NaCl 17, KCl 5.4, KH_2PO_4 0.44, $CaCl_2$ 0.63, $MgSO_4$ 0.21, Na_2HPO_4 0.34, N-methylglucamine 110, 0.1% (w/v)BSA and bacitracin 2) was added to each well. Plates were equilibrated on ice for 10 min, after which the binding buffer was replaced with 0.25 ml of binding buffer containing the appropriate concentration of [^3H]-BK in the absence or presence of unlabelled BK (10 μM). After 4 h incubation at 4°C, binding buffer was removed and cells were washed three times with 2 ml of binding buffer at 4°C. Cells were suspended in 0.25 ml of 0.1 N NaOH and counted in a radiospectrometer. Counting data were corrected for the specific activity and quenching. The amount of specific binding was calculated as the total binding minus the binding in the presence of 10 μM unlabelled BK. Total receptor density (B_{max}) and dissociation

constant (K_d) were calculated by the Ligand programme, as described previously (Yang, 1991).

Analysis of data

The EC_{50} values were estimated by the Graph Pad Programme (Graph Pad, San Diego, CA, U.S.A.). The data were expressed as the mean ± s.e.mean of at least four experiments with statistical comparisons based on a Student's two-tailed t test at a $P < 0.05$ level of significance.

Chemicals

DMEM/F-12 medium and FBS were purchased from J. R. Scientific (Woodland, CA, U.S.A.). Insulin and IGF-1 were from Boehringer Mannheim (GmbH, Germany). Fura-2 was from Molecular Probes Inc (Eugene, OR, U.S.A.). [^{3}H]-bradykinin (67 Ci mmol^{-1}) was from Du Pont NEN (Boston, MA, U.S.A.). [^{3}H]-*myo*-inositol (18 Ci mmol^{-1}) was from Amersham (Buckinghamshire, England). Enzymes and other chemicals were from Sigma Co (St. Louis, MO, U.S.A.)

Results

Effect of BK on IPs accumulation

We have previously reported that the BK-induced IPs accumulation is enhanced by CTX treatment (10 μg ml^{-1}, 4 h; Yang *et al.*, 1994). To characterize the effect of CTX on BK-induced IPs accumulation, TSMCs were prelabelled with [^{3}H]-inositol for 48 h, with or without CTX (10 μg ml^{-1}) for 24 h, before addition of BK (1 μM). As shown in Table 1, the BK-induced IPs accumulation was significantly enhanced by approximately 4 fold in TSMCs incubated with CTX ($P < 0.001$, $n = 5$), but CTX alone did not stimulate IPs accumulation, indicating that CTX-induced enhancement of BK responsiveness might indirectly result from a rise in adenosine 3′:5′-cyclic monophosphate (cyclic AMP). To test this hypothesis, TSMCs were treated with either 10 μM forskolin, an agent that raises cyclic AMP levels via activation of adenylate cyclase, or 1 mM dibutyryl cyclic AMP for 24 h, and then exposed to 1 μM BK. Forskolin and dibutyryl cyclic AMP also markedly enhanced the BK-induced IPs accumulation ($P < 0.001$, $n = 5$, Table 1), but these agents alone did not induce IPs accumulation. To determine whether the cyclic AMP-dependent enhancement of the BK-induced responses is related to protein synthesis, cycloheximide, an inhibitor of protein synthesis, was used with either CTX, forskolin, or dibutyryl-cyclic AMP. Concurrent exposure of TSMCs with cycloheximide (1 μM) blocked the CTX-, forskolin-, and dibutyryl cyclic AMP-induced enhancement of the IPs accumulation response to BK (Table 1). Importantly, an exposure to these cyclic AMP elevating agents significantly decreases carbachol-induced IPs accumulation ($P < 0.05$, $n = 5$). These results suggest that cyclic AMP elevating agents might induce changes in some components unique to the BK pathway.

The CTX and forskolin enhanced BK-induced IPs accumulation was time-dependent (Figure 1). The enhancement of BK-induced IPs accumulation was not seen until 6 h of treatment, and enhancement apparently still occurred after 24 h treatment with these agents (Figure 1). These results suggest that a prolonged increase in cyclic AMP levels might be a prerequisite for the increased BK-responsiveness of TSMCs that had been treated with cyclic AMP elevating agents. Parallel experiments were carried out with carbachol. There was no enhancement of carbachol-induced IPs accumulation during treatment with CTX (Figure 1). The enhancement of IPs accumulation by pretreatment with CTX and forskolin was dependent upon the BK concentrations

Table 1 Effects of cholera toxin (CTX), forskolin, and dibutyryl cyclic AMP on bradykinin (BK)-induced accumulation of inositol phosphates (IPs)

	IPs accumulation (d.p.m./well × 10^{-4})	
Treatment	*Carbachol*	*Bradykinin*
Control		
Untreated	14.6 ± 0.3	5.6 ± 0.4
Cholera toxin	11.7 ± 0.6**	23.8 ± 0.6*
Forskolin	9.5 ± 0.2**	22.4 ± 0.8*
Dibutyryl cyclic AMP	10.4 ± 0.4**	19.5 ± 0.5*
Cycloheximide		
Untreated	13.3 ± 0.4	5.3 ± 0.4
Cholera toxin	11.8 ± 0.9	8.0 ± 0.8
Forskolin	11.7 ± 0.5	7.2 ± 0.6
Dibutyryl cyclic AMP	12.8 ± 0.8	7.3 ± 0.5

Tracheal smooth muscle cells were prelabelled with [^{3}H]-inositol for 48 h, and then treated with cholera toxin (10 μg ml^{-1}), forskolin (10 μM), or dibutyryl cyclic AMP (1 mM) in the absence (control) or presence of cycloheximide (1 μM) for 24 h, and then exposed to BK (1 μM) or carbachol (100 μM) for 60 min. The basal levels of [^{3}H]-IPs accumulation in the absence and presence of cycloheximide were 10400 ± 780 and 11310 ± 1820 d.p.m./well, respectively. The results are expressed as the mean ± s.e.mean of five separate experiments determined in triplicate. *$P < 0.001$; **$P < 0.05$, as compared with untreated cells stimulated by respective agonists.

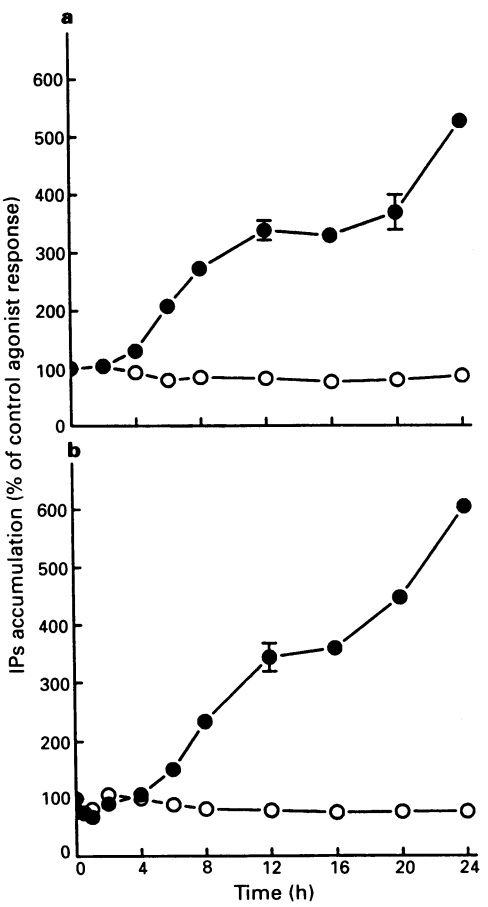

Figure 1 Time-dependence of cholera toxin (CTX) (a) and forksolin (b) treatment on bradykinin (BK)-induced inositol phosphates (IPs) accumulation. [^{3}H]-inositol prelabelled tracheal smooth muscle cells (TSMCs) were incubated with either CTX (10 μg ml^{-1}) or forskolin (10 μM) at 37°C for the indicated time, and then exposed to BK (1 μM, ●) or carbachol (100 μM, ○) for another 60 min. The accumulation of IPs was determined, as described under Methods. Results are expressed as the mean ± s.e.mean of five separate experiments determined in triplicate.

when measured 60 min after exposure to BK (Figure 2). These agents increased the maximal BK-induced IPs accumulation, but did not change the basal level (10400 ± 780 d.p.m./well) obtained when these agents were used alone. The concentration-effect relationship of BK-induced IPs accumulation was shifted to the left and BK was substantially more effective in TSMCs treated with CTX and forskolin than in the control (Figure 2). Moreover, pretreatment with pertussis toxin did not change IPs accumulation induced by BK and carbachol (data not shown).

Effect of BK on $[Ca^{2+}]_i$

Since cyclic AMP elevating agents increased the magnitude of BK-induced IPs accumulation, and it has been established that generation of inositol, 1,4,5-trisphosphate leads to a rise in $[Ca^{2+}]_i$ (Murray & Kotlikoff, 1991; Marsh & Hill, 1993), we therefore investigated the effects of CTX, forskolin and dibutyryl cyclic AMP on the BK-induced increase in $[Ca^{2+}]_i$. The data in Table 2 show that the BK-induced increase in $[Ca^{2+}]_i$ was significantly enhanced in TSMCs incubated with either CTX, forskolin or dibutyryl cyclic AMP for 24 h ($P < 0.001$, $n = 6$). Similarly, the enhancing effects of these agents on protein synthesis may be mediated through activation of a cyclic AMP-dependent protein kinase, since concurrent exposure of TSMCs to cycloheximide (1 μM), blocked the stimulatory effect of these agents on the calcium response to BK (Table 2). However, pretreatment of TSMCs with these agents for 24 h did not affect the mobilization of Ca^{2+} induced by carbachol. These results suggest that prolonged treatment with CTX and forskolin might be required to induce protein synthesis in canine TSMCs.

CTX and forskolin enhanced the BK-induced rise in $[Ca^{2+}]_i$ in a time-dependent manner (Figure 3). The augmentation of BK-induced rise in $[Ca^{2+}]_i$ was not observed until 12 h after treatment and increase in $[Ca^{2+}]_i$ induced by BK apparently still occurred after treatment with these agents for 24 h. The magnitude of the effect of BK on $[Ca^{2+}]_i$ was markedly greater in the TSMCs pretreated with CTX and forskolin for 24 h ($P < 0.001$, $n = 6$, Figure 3), whereas treatment with CTX and forskolin for 4 h led to a small decrease in the calcium response to BK or carbachol (Figure 3). However, treatment of TSMCs with forskolin for 24 h led to a small increase in the calcium response to carbachol. The data in Figure 4 show further details the relationship between BK concentrations and $[Ca^{2+}]_i$ changes in TSMCs pretreated with these agents. CTX and forskolin increased the maximal BK-induced rise in $[Ca^{2+}]_i$, but did not change the resting level of $[Ca^{2+}]_i$ (115 ± 18 nM, $n = 30$). The concentration-effect relationship of BK-induced increase in $[Ca^{2+}]_i$ was shifted to the left and BK was substantially more effective in TSMCs treated with CTX and forskolin than in the control (Figure 4). The greater sensitivity of the TSMCs pretreated with these agents is clearly evident in the presence of BK concentrations as low as 30 nM. Furthermore, pretreatment of the cells with pertussis toxin did not significantly change the increase in $[Ca^{2+}]_i$ induced by BK or carbachol (data not shown).

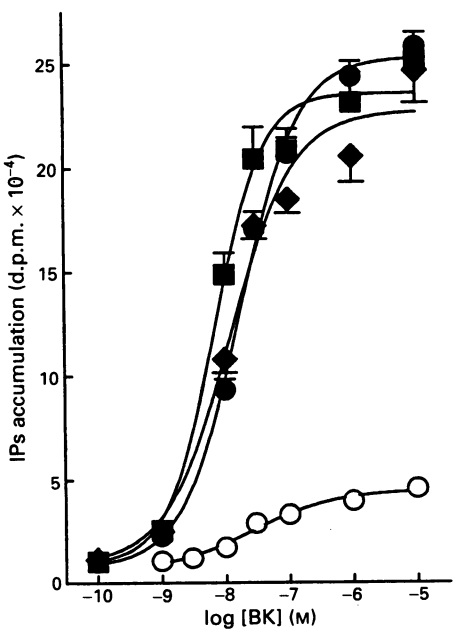

Figure 2 Effects of cholera toxin (CTX), forskolin, and dibutyryl cyclic AMP treatment on concentration-effect relationship of bradykinin (BK)-induced inositol phosphates (IPs) accumulation. [^{3}H]-inositol prelabelled TSMCs were incubated with either CTX (10 μg ml^{-1}), forskolin (10 μM) or dibutyryl cyclic AMP (1 μM) for 24 h and then exposed to various concentrations of BK for 60 min. Results are expressed as the mean ± s.e.mean of five separate experiments determined in triplicate. (○) Control; (●) CTX; (◆) forskolin; (■) dibutyryl cyclic AMP.

Effects of CTX, forskolin and dibutyryl cyclic AMP on [^{3}H]-BK binding

Cyclic AMP elevating agents have been shown to exert their effect by modulating the binding of a hormone to its receptors, (Gardner *et al.*, 1989; Guillon *et al.*, 1989; Socorro *et al.*, 1990; Etscheid *et al.*, 1991; Banno *et al.*, 1993). From our study, it is evident that pretreatment of TSMCs with CTX, forskolin, and dibutyryl cyclic AMP enhances BK-induced accumulation of IPs and the rise in $[Ca^{2+}]_i$. This might be due to changes in the affinity (dissociation constant, K_d) and/or to an increase in density of the BK receptor (B_{max}). To determine whether the potentiation by CTX, forskolin, and dibutyryl cyclic AMP on BK-stimulated responses in TSMCs occurs at the level of BK receptors, we further measured B_{max} and K_d in cells pretreated with CTX, forskolin or dibutyryl cyclic AMP for 24 h, using [^{3}H]-BK. As shown in Table 3, the B_{max} values were increased from 23.1 to 252.3, 189.3 and 228.2 fmol mg^{-1} protein in TSMCs pretreated with CTX, forskolin, and dibutyryl cyclic AMP, respectively. The K_d values were not significantly changed as compared with that of the control (Table 3).

Effects of cyclic AMP elevating agents on direct stimulation of G proteins

To determine whether treatment with CTX, forskolin, and dibutyryl cyclic AMP influences the coupling of G protein to

Table 2 Effects of cholera toxin (CTX), forskolin, and dibutyryl cyclic AMP on bradykinin (BK)-induced Ca^{2+} mobilization

	Increased $[Ca^{2+}]_i$ (nM)	
Treatment	*Carbachol*	*Bradykinin*
Control		
Untreated	185 ± 13	188 ± 14
Cholera toxin	202 ± 29	494 ± 22*
Forskolin	237 ± 27	462 ± 20*
Dibutyryl cyclic AMP	192 ± 12	479 ± 17*
Cycloheximide		
Untreated	172 ± 19	179 ± 10
Cholera toxin	191 ± 22	197 ± 18
Forskolin	197 ± 21	207 ± 18
Dibutyryl cyclic AMP	171 ± 17	204 ± 13

Tracheal smooth muscle cells were prelabelled with cholera toxin (10 μg ml^{-1}), forskolin (10 μM), or dibutyryl cyclic AMP (1 mM) in the absence (control) or presence of cycloheximide (1 μM) for 24 h, and then exposed to BK (1 μM) or carbachol (100 μM). The results are expressed as the mean ± s.e.mean of six separate measurements. *$P < 0.001$ as compared with untreated cells stimulated by BK.

phospholipase C (PLC), AlF_4^- (10 μM; 10 μM $AlCl_3$ + 10 mM NaF) was used to stimulate G proteins directly and then hydrolyze PI to generate IPs. Data in Figure 5 reveals that pretreatment of TSMCs with one of these three agents for 24 h enhanced BK-induced IPs accumulation, but there was no effect on the AlF_4^--induced response.

Discussion

It has been reported that BK-stimulated IPs accumulation can be inhibited or stimulated by CTX treatment, depending on the physiological assay and cell type studied (Etscheid & Villereal, 1989; Etscheid *et al.*, 1991; Banno *et al.*, 1993). The

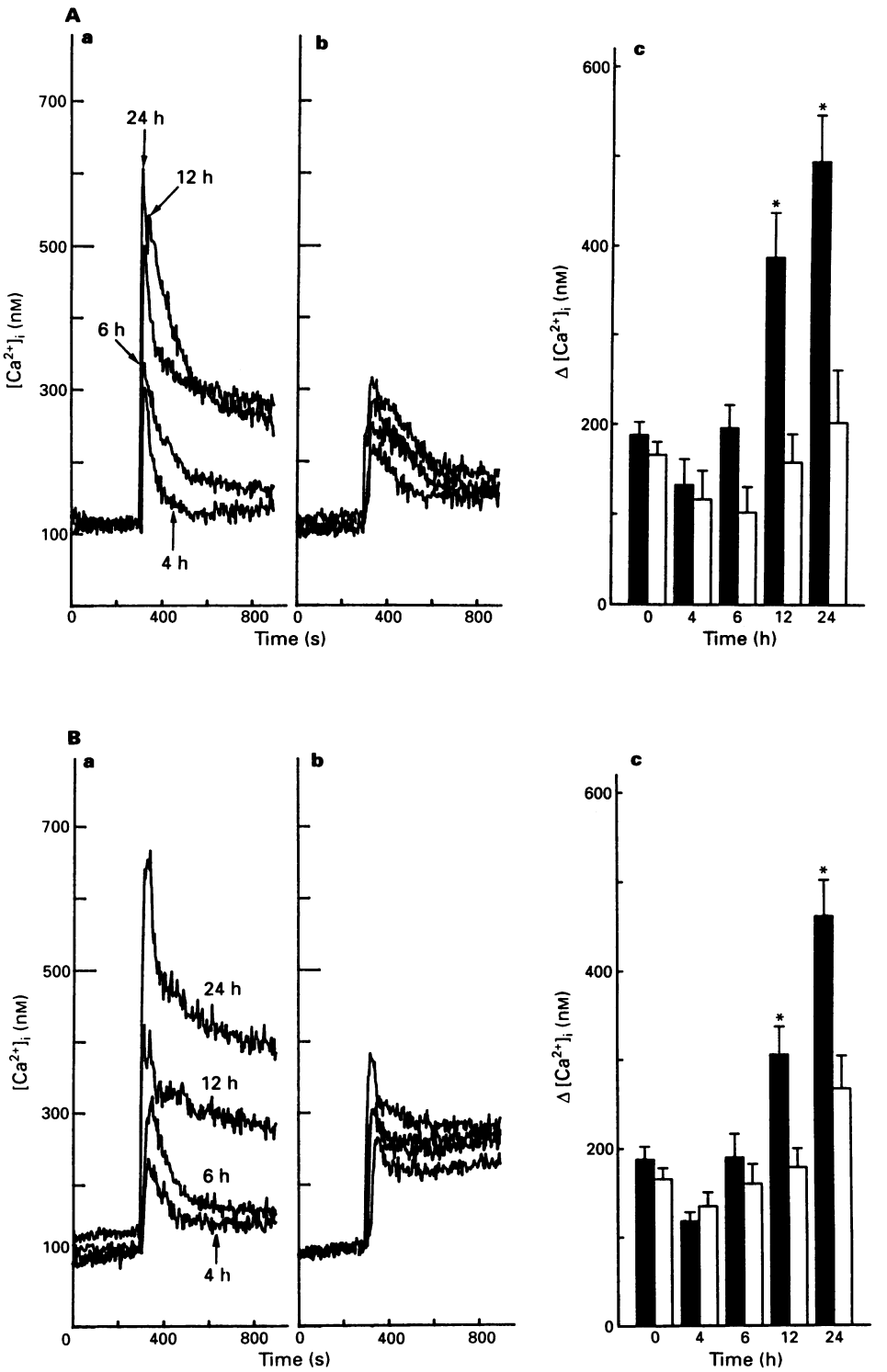

Figure 3 Time dependence of cholera toxin (CTX) (A) and forskolin (B) treatment on bradykinin (BK)-induced rise in $[Ca^{2+}]_i$. Tracheal smooth muscle cells (TSMCs) were incubated with either CTX (10 μg ml^{-1}) or forskolin (10 μM) at 37°C for the indicated time, and then exposed to BK (1 μM; a) or carbachol (100 μM; b). The cells on glass coverslips were loaded with 5 μM fura-2 and fluorescent measurement of $[Ca^{2+}]_i$ was carried out in a dual excitation wavelength (340 and 380 nm) spectrofluorometer. Agonist was added to the cells at 300 s. The resting $[Ca^{2+}]_i$ level was 105 ± 10 nM. The data expressed as the mean ± s.e.mean of six separate experiments are shown in (c). Open column, exposed to carbachol; solid column, exposed to BK. $^*P < 0.001$, as compared with control cells.

purpose of this study was to determine the mechanisms by which CTX, forskolin and dibutyryl cyclic AMP enhance the cellular responsiveness to BK stimulation. We demonstrate that BK is a more effective stimulator of IPs accumulation and Ca^{2+} mobilization in canine TSMCs that had been pretreated with CTX, forskolin, and dibutyryl cyclic AMP (Figures 2 and 4). The increased sensitivity of $[Ca^{2+}]_i$ to BK in cells treated with cyclic AMP elevating agents probably results directly from an enhanced accumulation of IPs. However, treatment of TSMCs with these cyclic AMP elevating agents did not enhance the carbachol-induced responses (Figures 1 and 3). The site of action of these agents might be unique to the BK pathway and associated with BK receptor synthesis, since cycloheximide reversed these effects. The selective increase in the responsiveness of TSMCs to BK upon treatment of cells with these cyclic AMP elevating agents appears to result largely from an increase in the number of BK receptors (Table 3). The increased expression of BK receptors probably contributes to the greater effectiveness of BK in inducing these responses.

The enhancing effect of CTX on the PI-PLC pathway may be due to the activation of the stimulatory G_s protein, which in turn activates adenylate cyclase, and which leads to an increased intracellular cyclic AMP level (Gilman, 1984). The

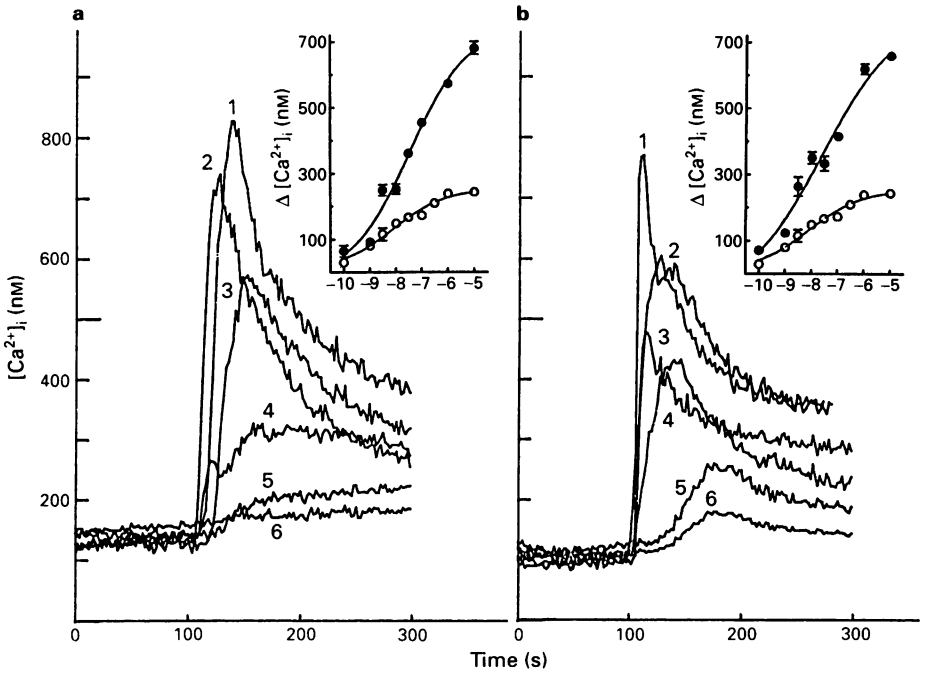

Figure 4 Effects of cholera toxin (CTX) (a) and forskolin (b) treatment on concentration curve of bradykinin (BK)-induced Ca^{2+} mobilization. Tracheal smooth muscle cells (TSMCs) were incubated with either CTX (10 μg ml^{-1}), or forskolin (10 μM) for 24 h and then exposed to various concentrations of BK; (1) 10 μM; (2) 1 μM; (3) 0.1 μM; (4) 10 nM; (5) 1 nM and (6) 0.1 nM. Inset: The concentration-response curves of BK for the increase in $[Ca^{2+}]_i$ by (○) control, (●) CTX (a) or (●) forskolin (b) treatment. Results are expressed as the mean ± s.e.mean of five separate experiments determined in triplicate.

Table 3 Effects of cholera toxin (CTX), forskolin and dibutyryl cyclic AMP treatment on [^{3}H]-bradykinin ([^{3}H]-BK) binding in canine tracheal smooth muscle cells (TSMCs)

Treatment	K_d (nM)	B_{max} (fmol mg^{-1} protein)
Control		
Untreated	2.3 ± 0.3	23.1 ± 0.3
Cholera toxin	2.4 ± 0.3	252.3 ± 35.8*
Forskolin	2.2 ± 0.3	189.3 ± 18.1*
Dibutyryl cyclic AMP	1.9 ± 0.3	228.2 ± 32.2*
Cycloheximide		
Untreated	2.6 ± 0.6	21.9 ± 3.9
Cholera toxin	2.3 ± 0.5	46.4 ± 6.0**
Forskolin	2.4 ± 0.7	42.4 ± 9.8**
Dibutyryl cyclic AMP	2.7 ± 0.6	42.6 ± 6.7**

Cultured TSMCs were incubated in the absence or presence of cycloheximide (1 μM) with either cholera toxin (10 μg ml^{-1}), forskolin (10 μM), or dibutyryl cyclic AMP (1 mM) for 24 h. Binding assays were performed in triplicate with concentrations of [^{3}H]-BK ranging from 0.2 to 10 nM and incubated at 4°C for 4 h. Data are expressed as the mean ± s.e.mean of three individual experiments. *$P < 0.001$; **$P < 0.05$ as compared with untreated cells.

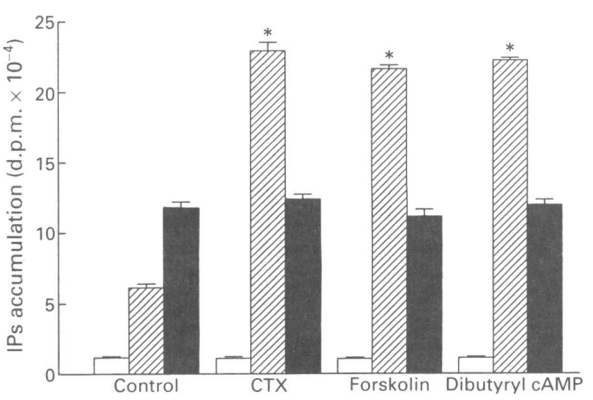

Figure 5 Effects of cholera toxin (CTX), forskolin, and dibutyryl cyclic AMP on direct stimulation of G protein coupling to PI hydrolysis in TSMCs. Cells prelabelled with [^{3}H]-inositol were incubated with either CTX (10 μg ml^{-1}), forskolin (10 μM), or dibutyryl cyclic AMP (1 mM) for 24 h and then exposed to BK (1 μM) or AlF_4^- (10 μM; 10 μM $AlCl_3$ and 10 mM NaF) for 60 min. The accumulation of IPs was determined as described under Methods. Data are expressed as the mean ± s.e.mean from three separate experiments determined in triplicate. *$P < 0.001$, as compared with untreated cells stimulated with BK. Open column, basal level; hatched column, BK; cross-hatched bar, AlF_4^-.

increase in the concentration of cyclic AMP caused by CTX and forskolin is responsible for the enhancement of BK-induced IPs accumulation (Etscheid *et al.*, 1991; Banno *et al.*, 1993). In contrast, several lines of evidence have shown that CTX and forskolin exert a negative feedback regulation on receptor-activated signal transduction through activation of the cyclic AMP-dependent protein kinase. It has been reported that cyclic AMP elevating agents inhibit agonist-induced IPs accumulation in Jurkat T lymphocytes (Imboden *et al.*, 1986), skeletal myoblasts (Gardner *et al.*, 1989), and glomerulosa cells (Guillon *et al.*, 1989). In those cells, treatment with the cyclic AMP elevating agents caused a decrease in the numbers of vasopressin and angiotensin II receptors (Gardner *et al.*, 1989; Guillon *et al.*, 1989). This inhibitory mechanism of CTX and forskolin is thought to result from desensitization or uncoupling of receptors by phosphorylation.

In the present work, the results obtained are consistent with previous studies showing that the accumulation of IPs induced by BK was enhanced by CTX treatment in human forskin fibroblasts (Etscheid & Villereal, 1989) and in the osteoblast-like cell line, MC3T3-E1 (Banno *et al.*, 1993). Short-term treatment with forskolin and dibutyryl cyclic AMP showed that a large increase in the intracellular cyclic AMP level is not sufficient to cause augmentation of IPs accumulation and Ca^{2+} mobilization induced by BK (Figures 1 and 3). However, long-term treatment (24 h) with these two agents mimicked the enhancement effect of CTX on BK-induced responses. These results suggest that the elevation of cyclic AMP concentration requires to be maintained for several hours before it can exert a potentiating effect. Therefore, the enhancing effect of CTX is caused by a rise in cyclic AMP, but it is unlikely that it is due to phosphorylation of the BK receptors. Indeed, the enhancing effects induced by cyclic AMP elevating agents were abolished by concurrent exposure to cycloheximide (Tables 1 and 2). It can be concluded that the enhancing effects of these agents on BK receptor-linked PI-PLC activation in canine TSMCs requires induction of certain protein(s) synthesis. Several lines of evidence have demonstrated that the effects of cyclic AMP elevating agents are blocked by cycloheximide (Etscheid *et al.*, 1991; Banno *et al.*, 1993). It has been shown that the action of CTX is involved in protein synthesis; elevation in cyclic AMP levels caused by CTX promoted transcription of mRNA encoding a protein that stimulates the release of arachidonic acid metabolites (Peterson *et al.*, 1991). Also, epidermal growth factor-stimulated IPs accumulation was potentiated by CTX pretreatment and inhibited by cycloheximide (Olashaw & Pledger, 1988). Therefore, the stimulatory effects of these agents might involve the induction of unidentified proteins synthesis via a cyclic AMP-dependent mechanism in canine TSMCs.

Furthermore, it has been reported that CTX increases the synthesis of cell surface BK receptors and thereby enhances IPs accumulation in response to BK in various cell types (Etscheid *et al.*, 1991; Banno *et al.*, 1993). In this study, we found that CTX, forskolin, and dibutyryl cyclic AMP increased total [^{3}H]-BK binding sites in canine TSMCs (Table 3). We speculate that these agents affect the receptor number at the gene level, associated with the sustained elevation of intracellular cyclic AMP, since TSMCs require to be exposed to CTX, forskolin, or dibutyryl cyclic AMP for several hours before any enhancing effect occurs. This hypothesis is supported by the evidence that treatment with cyclic AMP elevating agents did not affect AlF_4^--induced IPs accumulation in canine TSMCs (Figure 5). It is therefore conceivable that CTX, forskolin and dibutyryl cyclic AMP induce an increase in the number of BK receptors, which in turn potentiate BK-induced IPs accumulation and Ca^{2+} mobilization in canine TSMCs.

This work was supported by grants CMRP-340 from the Chang Gung Medical Research Foundation and NSC83-0412-B182-026 to C.M.Y., and CMRP-403 and NSC83-0420-B182-001-M03 to S.F.L. from the National Science Council, Taiwan. The authors are greatly indebted to Dr Anthony Herp at Chang Gund Medical College for his critical reading of the manuscript and suggestions. Appreciation is also expressed to Dr Delon Wu for his encouragement.

References

BANNO, U., SAKAI, T., KUMADA, T. & NOZAWA, Y. (1993). Potentiation by cholera toxin of bradykinin-induced inositol phosphates production in the osteoblast-like cell line MC3T3-E1. *Biochem. J.*, **292**, 401–408.

BARNES, P.J. (1992). Modulation of neurotransmission in airways. *Physiol. Rev.*, **72**, 699–729.

BERRIDGE, M.J., DAWSON, R.M.C., DOWNES, C.P., HESLOP, J.P. & IRVINE, R.F. (1983). Changes in the levels of inositol phosphates after agonist-dependent hydrolysis of membrane phosphoinositides. *Biochem. J.*, **212**, 473–482.

BURCH, R.M. & AXELROD, J. (1987). Dissociation of bradykinin-induced prostaglandin formation from phosphoinositol turnover in Swiss 3T3 fibroblasts: evidence for G-protein regulation of phospholipase A_2. *Proc. Natl. Acad. Sci. USA*, **84**, 6374–6378.

CHRISTIANSEN, S.C., PROOD, D. & COCHRANE, C.G. (1987). Detection of tissue kallikrein in the bronchoalveolar lavage fluid of asthmatic patient. *J. Clin. Invest.*, **79**, 188–197.

ETSCHEID, B.G. & VILLEREAL, M.L. (1989). Coupling of bradykinin receptors to phospholipase C in cultured fibroblasts is mediated by a G-protein. *J. Cell. Physiol.*, **140**, 264–271.

ETSCHEID, B.G., KO, P.H. & VILLEREAL, M. (1991). Regulation of bradykinin receptor level by cholera toxin, pertussis toxin and forskolin in cultured human fibroblasts. *Br. J. Pharmacol.*, **103**, 1347–1350.

GARDNER, S.D., MILLIGAN, G., RICE, J.E. & WAKELAM, M.J.O. (1989). The effect of cholera toxin on the inhibition of vasopressin-stimulated inositol phospholipid hydrolysis is a cyclic AMP-mediated event at the level of receptor binding. *Biochem. J.*, **259**, 679–684.

GILMAN, A.G. (1984). G-proteins and dual control of adenylate cyclase. *Cell*, **36**, 577–579.

GOWN, A.M., VOGEL, A.N., GORDON, D. & LU, P.L. (1985). A smooth muscle-specific monoclonal antibody recognizes smooth muscle actin isozymes. *J. Cell. Biol.*, **100**, 807–813.

GRYNKIEWICZ, G., POENIE, M. & TSIEN, R.Y. (1985). A new generation of Ca^{2+} indicators with improved fluorescence properties. *J. Biol. Chem.*, **260**, 3440–3450.

GUILLON, G., BALESTRE, M.N., LOMBARD, C., RASSENDREN, F. & KIRK, C.T. (1989). Influence of bacterial toxins and forskolin upon vasopressin-induced inositol phosphate accumulation in WRK 1 cells. *Biochem. J.*, **260**, 665–672.

HEPLER, J.R. & GILMAN, A. (1992). G proteins. *Trends Biochem. Sci.*, **17**, 383–388.

HIGASHIDA, H., STREATY, R.A., KLEE, W.A. & NIRENBERG, M. (1986). Bradykinin-activated transmembrane signals are coupled via No or Ni to production of inositol 1,4,5-trisphosphate, a second messenger in NG108-15 neuroblastoma-glioma hybrid cells. *Proc. Natl. Acad. Sci. USA*, **83**, 942–946.

IMBODEN, J.B., SHOBACK, D.M., PATTISON, G. & STOBO, J.D. (1986). Cholera toxin inhibits the T-cell antigen receptor-mediated increase in inositol triphosphate and cytoplasmic free calcium. *Proc. Natl. Acad. Sci. USA*, **83**, 5673–5677.

LAMBERT, T.L., KENT, R.S. & WHORTON, A.R. (1986). Bradykinin stimulation of inositol polyphosphate production in porcine aortic endothelial cells. *J. Biol. Chem.*, **261**, 15288–15293.

LIEBMANN, C., SCHNITTLER, M., STEWART, J.M. & REISSMANN, S. (1991). Antagonist binding reveals two heterogeneous B_2 bradykinin receptors in rat myometrial membranes. *Eur. J. Pharmacol.*, **199**, 363–365.

MARSH, K.A. & HILL, S.J. (1992). Bradykinin B_2 receptor-mediated phosphoinositide hydrolysis in bovine cultured tracheal smooth muscle cells. *Br. J. Pharmacol.*, **107**, 443–447.

MARSH, K.A. & HILL, S.J. (1993). Characteristics of the bradykinin-induced increases in intracellular calcium ion concentration of single cultured bovine tracheal smooth muscle cells. *Br. J. Pharmacol.*, **108**, 60P.

MURAYAMA, T. & UI, M. (1987). Phosphatidic acid may stimulate membrane receptors mediating adenylate cyclase inhibition and phospholipid breakdown in 3T3 fibroblasts. *J. Biol. Chem.*, **262**, 5522–5529.

MURRAY, R.K. & KOTLIKOFF, M.I. (1991). Receptor-activated calcium influx in human airway smooth muscle cells. *J. Physiol.*, **435**, 123–144.

OLASHAW, N.E. & PLEDGER, W.J. (1988). Epidermal growth factor stimulates formation of inositol phosphates in BALB/c/3T3 cells pretreated with cholera toxin and isobutylmethylxanthine. *J. Biol. Chem.*, **263**, 1111–1114.

PETERSON, J.W., REITMEYER, J.C., JACKSON, C.A. & ANSARI, G.A.S. (1991). Protein synthesis is required for cholera toxin-induced stimulation of arachidonic acid metabolism. *Biochim. Biophys. Acta*, **1092**, 79–84.

SOCORRO, L., ALEXANDER, R.W. & GRIENDLING, K.K. (1990). Cholera toxin modulation of angiotensin II-stimulated inositol phosphate production in cultured vascular smooth muscle cells. *Biochem. J.*, **265**, 799–807.

STERNWEIS, P.C. & SMRCKA, A.V. (1992). Regulation of phospholipase C by G proteins. *Trends Biochem. Sci.*, **17**, 502–506.

YANG, C.M. (1990). Muscarinic receptor expression in the primary culture of tracheal smooth muscle cells. *J. Receptor Res.*, **10**, 235–247.

YANG, C.M. (1991). Characterization of muscarinic receptors in dog tracheal smooth muscle cells. *J. Autonom. Pharmacol.*, **11**, 51–61.

YANG, C.M., CHOU, S.-P. & SUNG, T.-C. (1991a). Muscarinic receptor subtypes coupled to generation of different second messengers in isolated tracheal smooth muscle cells. *Br. J. Pharmacol.*, **104**, 613–618.

YANG, C.M., CHOI, S.-P. & SUNG, T.-C. (1991b). Regulation of functional muscarinic receptor expression in tracheal smooth muscle cells. *Am. J. Physiol.*, **261**, C1123–C1129.

YANG, C.M., HSIA, H.-C., CHOU, S.-P., ONG, R., HSIEH, J.-T. & LUO, S.-F. (1994). Bradykinin-stimulated phosphoinositide metabolism in cultured canine tracheal smooth muscle cells. *Br. J. Pharmacol.*, **111**, 21–28.

(Received December 9, 1993
Revised March 8, 1994
Accepted March 16, 1994)

Br. J. Pharmacol. (1994), **112**, 789–794

The effects of SB 204070, a highly potent and selective 5-HT_4 receptor antagonist, on guinea-pig distal colon

[1]K.A. Wardle, E.S. Ellis, G.S. Baxter, G.A. Kennett, L.M. Gaster & G.J. Sanger

SmithKline Beecham Pharmaceuticals, Coldharbour Road, The Pinnacles, Harlow, Essex CM19 5AD

1 The pharmacology of a novel 5-HT_4 receptor antagonist, SB 204070 has been evaluated in the guinea-pig isolated distal colon longitudinal muscle-myenteric plexus (LMMP).

2 SB 204070 is a highly potent antagonist of 5-HT-evoked cholinergically-mediated contractions in the guinea-pig distal colon. Low concentrations (10–100 pM) produced a shift to the right of the curve (apparent pA_2 10.8 ± 0.1) with no significant effect on the maximum response. With higher concentrations of SB 204070 (300 pM and above), the maximum response to 5-HT was reduced.

3 When tested against the partial 5-HT_4 receptor agonist, BIMU 1, SB 204070 was active at similar low concentrations (10 pM and above) but produced a reduction in maximum, with no prior shift to the right of the curve, at all concentrations tested (10–300 pM).

4 The antagonism seen with SB 204070 is unlikely to be due to a non-selective effect since high concentrations (10 nM and 1 μM) of the compound had no effect on cholinergically-mediated contractions evoked by the nicotinic receptor agonist, DMPP, in the same preparation. SB 204070 is unlikely to be an irreversible antagonist since the effects of the compound could be reversed upon washing of the tissue.

5 Radioligand binding studies show that SB 204070 has a greater that 5000 fold selectivity for the 5-HT_4 receptor over 5-HT_{1A}, 5-HT_{1D}, 5-HT_{1E}, 5-HT_{2A}, 5-HT_{2C}, 5-HT_3, $GABA_A$, BDZ, TBPS, A_1 adenosine receptors, α_1, α_2, β_1, β_2 adrenoceptors and D_1, D_2 and D_3 dopamine receptors.

6 SB 204070 is a highly potent, highly selective 5-HT_4 receptor antagonist and as such is an important new tool in evaluating the functional role of the 5-HT_4 receptor.

Keywords: 5-HT (5-hydroxytryptamine); 5-HT_4 receptors; SB 204070; guinea-pig distal colon

Introduction

A novel 5-hydroxytryptamine (5-HT) receptor, positively coupled with adenylate cyclase was identified in mouse embryo colliculi neurones byDumuis and co-workers as far back as 1988 (Dumuis *et al.*, 1988a,b). The receptor was tentatively named 5-HT_4 due to its inability to fit into the Bradley *et al.* (1986) classification. Since then, the 5-HT_4 receptor has been officially recognised (Humphrey *et al.*, 1993) and identified in a variety of tissues across many species (for review see Ford & Clarke, 1993).

Until recently, much of the characterization of the 5-HT_4 receptor has been based on the activity of agonists. Thus, the 5-HT_4 receptor is activated by indoleamine agonists (5-HT and 5-methoxytryptamine (5-MeOT)), by substituted benzamides (such as metoclopramide, renzapride, cisapride and zacopride) and by azabicycloalkyl benzimidazolones (such as BIMU 1 and BIMU 8). The antagonist profile of the 5-HT_4 receptor has been based largely on exclusion. Tropisetron was the first compound to be identified as having antagonist activity at the 5-HT_4 receptor (Dumuis *et al.*, 1988a). Tropisetron, however, possesses a 10 to 100 times higher affinity for the 5-HT_3 receptor than for the 5-HT_4 receptor (Clarke *et al.*, 1989). Furthermore, tropisetron has been shown to block both muscarinic receptors (Clarke *et al.*, 1989) and sodium channels (Scholtysik, 1987). An alternative antagonist, SDZ 205 557 has been shown to display around 50 fold selectivity for the 5-HT_4 receptor over the 5-HT_3 receptor in the guinea-pig isolated ileum (Buchheit *et al.*, 1992). However, since the 5-HT_3 receptors in guinea-pig yield lower antagonist affinity estimates than other species (Butler *et al.*, 1990), this selectivity appears to be an over-estimation (see Eglen *et al.*, 1992a).

More recently, compounds with much greater selectivity for the 5-HT_4 receptor have been reported. These include RS-23597-190 (Eglen *et al.*, 1992b) and GR 113808 (Grossman *et al.*, 1993). RS-23597-190 has been shown to antagonize 5-HT_4 receptor-mediated relaxations in the rat oesophagus, yielding a pA_2 estimate of 7.8 (Eglen *et al.*, 1992b) and has selectivity over 5-HT_3 and dopamine receptors of greater than 125 fold. GR 113808 has been shown to act as a competitive antagonist of 5-HT_4 receptor-mediated responses in both the guinea-pig proximal colon and rat oesophagus, with pA_2 values of 9.2 and 9.5 respectively, with selectivity over a range of receptors of approximately 3000 fold (Grossman *et al.*, 1993).

In the present study we describe details of another highly potent and selective 5-HT_4 receptor antagonist, the benzodioxan derivative, SB 204070. The pharmacology of this compound has been characterized in the guinea-pig distal colon (Wardle & Sanger, 1992; 1993). Preliminary results have previously been reported (Wardle *et al.*, 1993; Gaster *et al.*, 1993).

Methods

Preparation of guinea-pig distal colon tissue

Distal colon (discarding the terminal 7–8 cm) was removed from young male Dunkin Hartley guinea-pigs (200–300 g) and placed in Krebs solution of the following composition (mM): NaCl 121.5, $CaCl_2$ 2.5, KH_2PO_4 1.2, KCl 4.7, $MgSO_4$ 1.2, $NaHCO_3$ 25.0, glucose 5.6.

Sections of longitudinal muscle-myenteric plexus (LMMP, 2–3 cm in length) were dissected as previously described (Wardle & Sanger, 1993) and mounted under a 0.5 g load in 10 ml tissue baths. Tissues were bathed with Krebs solution at 37°C gassed with 5% CO_2 in O_2 and containing granisetron (1 μM) and methiothepin (100 nM) to inhibit responses mediated by 5-HT_3 and 5-HT_1-like and 5-HT_2 receptors

[1] Author for correspondence.

respectively. Responses were recorded isotonically and displayed on a Lectromed MT8P multitrace chart recorder.

Experimental protocol and concentration-effect curves

Tissues were left to stabilize and sensitized to 5-HT as previously described (Wardle & Sanger, 1993). Sensitization was viewed as being complete when three consistent responses were obtained to 5-HT (1 μM). Agonist concentration-effect curves were constructed non-cumulatively by adding increasing concentrations of agonist at 15 min intervals. The agonist was left in contact with the tissue until a maximum response was obtained (usually 30 s), then washed out. Two agonist concentration-effect curves were constructed in each tissue, the first in the absence, the second in the presence of SB 204070. In all experiments, the antagonist was left to equilibrate with the tissues for a minimum of 45 min. Responses were expressed as a percentage of the maximum 5-HT-evoked contraction in each tissue obtained in the control concentration-effect curve. Results were expressed as mean ± s.e.mean of a number (n) of observations.

All agonist concentration-effect curves were fitted to the following equation using Kaleidagraph (Synergy Software, PCS Inc. Reading, PA, U.S.A.) on an Apple Macintosh II Ci computer.

$$E = \alpha/1 + (EC_{50}/[A])^n$$

α, [A] and n represent the maximum response, agonist concentration and curve mid point slope factor respectively. The EC_{50} is the concentration of agonist that produces 50% of the maximal response. EC_{50} values from individual curves were converted to $\log_{10}$ values prior to calculation of the arithmetic mean.

Where the maximum response to the agonist was not significantly reduced, affinity estimates for the antagonist (SB 204070) were expressed as pA_2 values, calculated according to the method of Arunlakshana & Schild (1959). However, as higher concentrations of SB 204070 reduced the maximum response, it would appear that something other than simple competitive antagonism was taking place. For this reason, the term 'apparent pA_2' will be used throughout this paper.

Onset/recovery of effects of SB 204070

The rate of onset and time to wash out of the antagonistic effects of SB 204070 were investigated in the guinea-pig distal colon LMMP. Tissues were set up as previously described and exposed repeatedly to the approximate EC_{50} concentration of 5-HT (generally 1 nM) at 15 min intervals until consistent responses were obtained. Immediately after washout of 5-HT, SB 204070 was added to the bathing solution and left in contact with the tissues for 30 min, during which time tissues were exposed to the same concentration of 5-HT twice. The bathing solution was then replaced with drug-free Krebs and the tissues challenged with the same concentration of 5-HT every 15 min until responses returned to control level. The rate of recovery from the antagonistic effects of SB 204070 was calculated as the time taken for the response to 5-HT to recover to 50% of its control value ($t_1$off).

Radioligand binding studies

Radioligand binding studies were performed as described by Sanger & Nelson (1989), except that [^{3}H]-idazoxan (0.5 nM), [^{3}H]-SCH 23390 (0.1 nM), and [^{125}I]-iodosulpiride (0.1 nM) were used to label the α_2 adrenoceptor, dopamine D_1 and dopamine D_2 receptors respectively. Iodosulpiride (100 μM) was used to define non-specific binding in this latter assay. In addition the following assays were used: 5-HT_{1D} [^{3}H]-5-HT (4 nM) in guinea-pig cortex in the presence of 100 nM 8-OH-DPAT and 100 nM pizotifen (Waeber et al., 1989); 5-HT_{2C}, [^{3}H]-mesulergine (2 nM) in pig choroid plexus tissue in the presence of 30 nM spiperone (Pazos et al., 1985); 5-HT_3, [^{3}H]-granisetron in pooled rat hippocampus and entorhinal cortex, non-specific binding defined by 100 μM metoclopramide (Nelson & Thomas, 1990); 5-HT_{1E}, [^{3}H]-5-HT (10 nM) in CHO cells expressing human 5-HT_{1E} clones using the conditions of Hamblin & Metcalf (1991) and defining non-specific binding with 10 μM 5-HT; dopamine D_3, [^{125}I]-iodosulpiride (200 pM) in CHO cells expressing human D_3 clones, non-specific binding defined by 100 μM iodosulpiride (Bowen et al., 1993); β_1 adrenoceptor, [^{125}I]-iodocyanopindolol (0.024 nM) on cloned human β_1 receptors expressed in CHO cells, non-specific binding defined by 30 nM isoprenaline; β_2 adrenoceptor, [^{125}I]-iodocyanopindolol (12 pM) on cloned human β_2 receptors expressed in CHO cells, non-specific binding defined with 30 nM isoprenaline; $GABA_A$, [^{3}H]-muscimol (10 nM) in rat cortex, non-specific binding defined by 100 μM bicuculline (Peters et al., 1988); adenosine A_1; [^{3}H]-phenylisopropyladenosine in rat cortex, non-specific binding defined by 100 μM 2-chloroadenosine (Schwabe & Trost, 1980).

Statistics and data analysis for radioligand binding studies

The concentration of inhibitor required to inhibit 50% of specific binding (IC_{50}) was derived using the four parameter logistic function 'Allfit' (DeLean et al., 1978) and corrected to inhibitory affinity constant (K_i) according to Cheng & Prusoff (1973). For all binding studies, n values were greater than or equal to 2.

Drugs

The following drugs were used: 5-hydroxytryptamine creatinine sulphate (5-HT), 1,1-dimethyl-4-phenyl-piperazinium iodide (DMPP), isoprenaline hydrochloride and 2-chloroadenosine (+)-bicuculline (Sigma), 8-hydroxy-n,n-dipropylaminotetralin hydrogen bromide (8-OH-DPAT, RBI), spiperone (Janssen), methiothepin hydrochloride (Roche), granisetron, renzapride, iodosulpiride hydrochloride, metoclopramide, and pizotifen hydrogen maleate (SmithKline Beecham), SB 204070 ((1-butyl-4-piperidinyl)methyl 8-amino-7-chloro-1,4-benzodioxan-5-carboxylate hydrochloride, synthesized in house). BIMU 1 was a kind gift from Dr Carlo Rizzi, Boehringer Ingelheim, Italy.

All drugs were dissolved in 0.9% w/v saline and diluted with Krebs solution. Glass was used at all times in the making up and dilution of SB 204070 since the compound may adhere to certain types of plastic (see Discussion).

Radiochemical sources were as follows (specific activity Ci mmol^{-1}): [^{3}H]-5-HT (20), [^{3}H]-8-OH-DPAT (161), [^{125}I]-iodocyanopindolol (2200), [^{3}H]-granisetron (61), [^{3}H]-prazosin (80), [^{3}H]-ter-butyl-bicyclphosphorothionate (TPBS, 127) – New England Nuclear; [^{3}H]-mesulergine (80), [^{3}H]-idazoxan (43), [^{3}H]-SCH 23390 (73), [^{3}H]-muscimol (19), [^{3}H]-flunitrazepam (84), [^{3}H]-phenylisopropyladenosine (50), [^{125}I]-iodosulpride (2000) – Amersham International.

Results

Effects of SB 204070 in the guinea-pig distal colon LMMP

In the presence of methiothepin (100 nM) and granisetron (1 μM), 5-HT (10 pM–10 nM) evoked a monophasic concentration-dependent contraction with a pEC_{50} of 9.2 ± 0.1 (n = 38). This response has previously been shown to be antagonized by tropisetron (pA_2 6.4 ± 0.1, slope of Schild plot 1.3 ± 0.1) and SDZ 205 557 (pA_2 7.8 ± 0.1, slope of Schild plot 1.1 ± 0.1), suggesting that the response is 5-HT_4 receptor-mediated (Wardle & Sanger, 1993).

Low concentrations of SB 204070 (10, 30 and 100 pM, $n = 6$, Figure 1a) caused concentration-dependent, surmountable antagonism of the 5-HT curve, yielding apparent pA_2 values of 11.1 ± 0.2, 10.7 ± 0.2 and 10.7 ± 0.1 respectively. At higher concentrations (0.3, 1 and 3 nM), rightward displacements of the concentration-effect curve to 5-HT were associated with a reduction in the maximum response. SB 204070 did not display agonism at any concentration tested.

SB 204070 was also examined as an antagonist of the responses mediated by two other classes of 5-HT_4 receptor agonists, namely the substituted benzamide, renzapride and the benzimidazolone derivative, BIMU 1. Renzapride was a full agonist in the guinea-pig distal colon (intrinsic activity cf. 5-HT = 1.0 ± 0.02, $n = 4$) with a pEC_{50} of 7.2 ± 0.1. SB 204070 (10–300 pM, $n = 4$, Figure 1b) evoked a concentration-dependent reduction in the maximum response to renzapride, with no prior shift to the right of the curve. Similar results were obtained with the partial agonist, BIMU 1 (intrinsic activity cf. 5-HT = 0.6 ± 0.03, $pEC_{50} = 6.9 \pm 0.2$, $n = 4$, Figure 1c).

Onset and recovery of antagonistic effects of SB 204070

A 30 min incubation with SB 204070 (30 pM, 100 pM, 300 pM and 1 nM, $n = 6$) caused maximum antagonism of the contraction evoked by a pEC_{50} dose of 5-HT of $50 \pm 3\%$, $84 \pm 2\%$, $100 \pm 0\%$ and $100 \pm 0\%$ respectively (Figure 2).

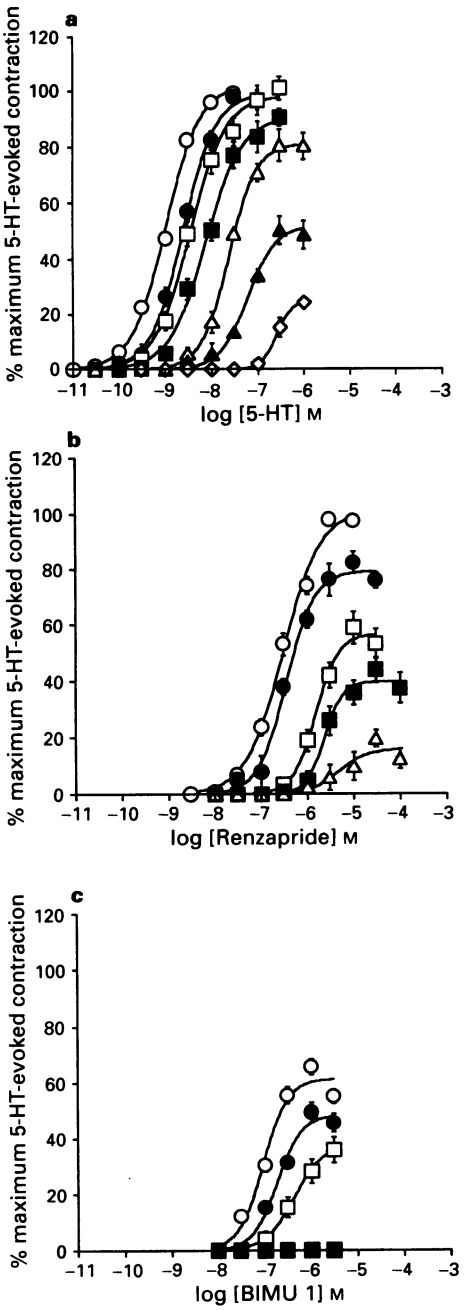

Figure 1 Concentration-response curves to 5-HT (a), renzapride (b) and BIMU 1 (c) in the absence (○) and presence of 10 pM (●), 30 pM (□), 100 pM (■), 300 pM (△), 1 nM (▲) and 3 nM (◇) SB 204070 in the guinea-pig distal colon longitudinal muscle-myenteric plexus preparation. Experiments were carried out in the presence of methiothepin (100 nM) and granisetron (1 μM). Each point represents the mean ± s.e.mean of 6, 4 and 4 observations respectively.

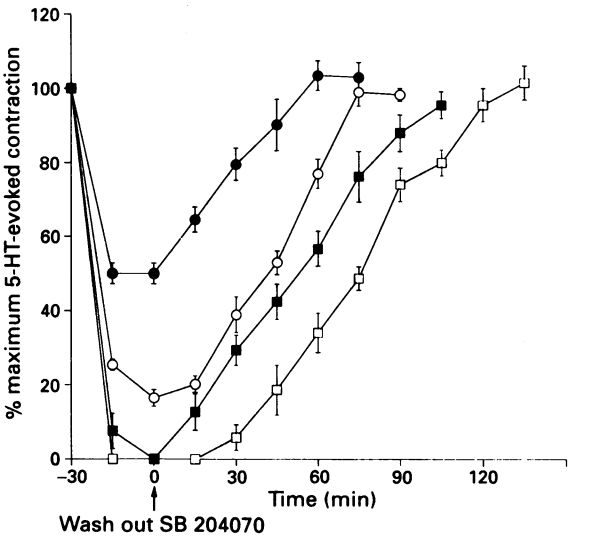

Figure 2 Onset and recovery of the antagonistic effects of SB 204070 in the guinea-pig distal colon longitudinal muscle-myenteric plexus preparation. A standard pEC_{50} concentration of 5-HT was added to tissues until stable responses were produced. At time $t = -30$ min, various concentrations of SB 204070 (30 pM (●), 100 pM (○), 300 pM (■) and 1 nM (□)) were added to the bath. Following a 30 min incubation with SB 204070 the antagonist was washed from the bath and 5-HT added at 15 min intervals until responses returned to control levels. Experiments were carried out in the presence of methiothepin (100 nM) and granisetron (1 μM). Each point represents the mean ± s.e.mean of 4 observations.

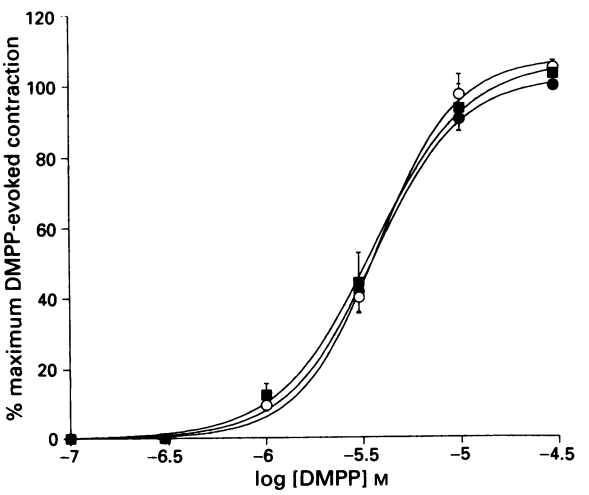

Figure 3 Concentration-response curves to 1,1-dimethyl-4-phenylpiperazinium (DMPP) in the absence (○) and presence of 10 nM (●) and 1 μM (■) SB 204070 in the guinea-pig distal colon longitudinal muscle-myenteric plexus preparation. Experiments were carried out in the presence of methiothepin (100 nM) and granisetron (1 μM). Each point represents the mean ± s.e.mean of 6 observations.

Table 1 *In vitro* binding profile of SB 204070

Receptor	*Affinity* (pK_I) (range)
5-HT_{1A}	<6.0
5-HT_{1D}	<5.0
5-HT_{1E}	<5.0
5-HT_{2A}	<6.0
5-HT_{2C}	(6.9–7.1)
5-HT_3	(6.4–6.8)
Dopamine D_1	<6.0
Dopamine D_2	<5.0
Dopamine D_3	<6.0
Adrenoceptor α_1	<6.0
Adrenoceptor α_2	<6.0
Adrenoceptor β_1	<6.0
Adrenoceptor β_2	<6.0
$GABA_A$	<4.0
BDZ	<5.0
TBPS	<5.0
A_1	<4.5

Longer incubations with SB 204070 revealed no further antagonism (results not shown). Upon washout, the responses to 5-HT recovered to control levels with $t_{\frac{1}{2}off}$ values of 36 ± 5 min, 47 ± 5 min and 70 ± 7 min for concentrations of SB 204070 of 100 pM, 300 pM and 1 nM respectively.

Selectivity studies

In the guinea-pig distal colon the nicotine receptor agonist DMPP (3–300 μM, $n = 4$) evoked concentration-dependent, cholinergically-mediated contractions. These responses were not affected by SB 204070 (10 nM and 1 μM) at concentrations significantly greater than those required to antagonize the cholinergically-mediated contractions evoked by 5-HT in the same preparations (Figure 3).

The effects of SB 204070 in a number of radioligand binding systems were studied *in vitro*. Results are summarized in Table 1. SB 204070 had little or no affinity for the 5-HT_{1A}, 5-HT_{1D}, 5-HT_{1E} or 5-HT_{2A} receptors. Weak affinity was observed for the 5-HT_{2C} (pK_I 6.9–7.1) and 5-HT_3 (pK_I 6.4 ± 6.8) sites. In the following binding systems: dopamine D_1, D_2 and D_3, α_1, α_2, β_1 and β_2 adrenoceptors, $GABA_A$, BDZ, TBPS and adenosine A_1, no inhibition of binding was observed for SB 204070 at concentrations up to and including 1 μM.

Discussion

The tools currently available for the study of the 5-HT_4 receptor, including tropisetron, SDZ 205 557 and DAU 6285 are limited by selectivity and bioavailability. For example, tropisetron has affinity for the 5-HT_4 receptor in the micromolar range (Dumuis *et al.*, 1988a; Kaumann *et al.*, 1990), but antagonizes 5-HT_3 receptor-mediated responses at nanomolar concentrations (Richardson *et al.*, 1985). Both SDZ 205 557 and DAU 6285 show a greater affinity for the 5-HT_4 receptor over the 5-HT_3 site, but with pA_2 estimates in the range of 7.4 for SDZ 205 557 (Buchheit *et al.*, 1992) and 7.0 for DAU 6285 (Turconi *et al.*, 1991; Baxter *et al.*, 1992), potency values are still relatively low. More recently, two highly potent and selective 5-HT_4 receptor antagonists, GR 113808 (Grossman *et al.*, 1993) and SB 204070 (Wardle *et al.*, 1993; Gaster *et al.*, 1993) have been identified. At the present time the bio-availability of the former compound, GR 113808 is unknown, and based on its structure, may be speculated to be low. In the present investigation we describe a more detailed study of the latter compound, SB 204070. This compound has previously been shown to have good bio-availability when dosed sub-cutaneously (Banner *et al.*, 1993) and as such represents a useful tool in the evaluation of 5-HT_4 receptor-mediated responses both *in vitro* and *in vivo*.

The activity of SB 204070 has been investigated against 5-HT_4 receptor-mediated contractions in the guinea-pig distal colon (Wardle & Sanger, 1992; 1993). SB 204070 alone had no effects on resting tone, suggesting that it is devoid of agonist effects at the 5-HT_4 receptor. When examined against 5-HT-evoked contractions, low concentrations of SB 204070 shifted the curve in an apparently competitive manner (mean apparent pA_2 value over this concentration-range: 10.8 ± 0.1). Higher concentrations produced a further shift to the right of the curve with a concomitant reduction in the maximum response.

There are many plausible mechanisms of non-surmountable antagonism including multiple receptor subtypes, allosteric receptor modulation, irreversible antagonism and pseudo-irreversible antagonism (see Bond *et al.*, 1989).

The possibility that SB 204070 mediates its effects through multiple receptors is unlikely. Thus, radioligand binding studies indicate a lack of affinity of SB 204070 for other 5-HT receptors and other classical neurotransmitter receptors. When compared to activity at the 5-HT_4 receptor in functional systems, binding studies indicate that SB 204070 has a greater than 5,000 fold selectivity for the 5-HT_4 receptor over 5-HT_{1A}, 5-HT_{1D}, 5-HT_{1E}, 5-HT_{2A}, 5-HT_{2C}, 5-HT_3, $GABA_A$, BDZ, TBPS, A_1 adenosine receptors, α_1, α_2, β_1, β_2 adrenoceptors and D_1, D_2 and D_3 dopamine receptors. These findings suggest that SB 204070 is highly selective for the 5-HT_4 receptor and that the non-surmountable effects are unlikely to be due to antagonism of a non-5-HT_4 site.

It has previously been shown that, in the guinea-pig distal colon, 5-HT_4 receptor-mediated contractions are evoked indirectly via acetylcholine release (Wardle & Sanger, 1993). Thus, the possibility that the apparent non-surmountable antagonism observed with SB 204070 was due to a non-selective effect was investigated against DMPP-evoked, cholinergically-mediated contraction in the same preparation. SB 204070, at concentrations of up to 10,000 fold greater than those required to block the 5-HT_4 receptor had no significant effect on DMPP-evoked contractions, suggesting that the reduction in maximum seen with SB 204070 is unlikely to be due to either a local anaesthetic or anticholinergic effect of the antagonist.

The possibility of an allosteric binding site or of pseudo-irreversible antagonism are difficult to evaluate in the present system. However, irreversible or pseudo-irreversible antagonism are preferred mechanism in explaining the non-surmountable activity of SB 204070 because they are intrinsically less complicated than allosteric modulation. Thus, this latter mechanism involves the postulation of a second binding site, in addition to the 5-HT_4 receptor, which in turn mediates a change in receptor state. While this possibility cannot be ruled out, the observed effects of SB 204070 can be better accounted for by a simpler explanation.

The apparent non-surmountable effects of SB 204070 in the guinea-pig distal colon may be explained if the compound behaved as an irreversible antagonist at the 5-HT_4 receptor. Such an effect, however, is unlikely since, upon repeated washing of the compound from the bathing solution, the responses to a pEC_{50} concentration of 5-HT were restored to control levels for all concentrations of SB 204070 tested. This observation strongly suggests that the effects of SB 204070 are reversible in this system. Further evaluation of the washout profile of SB 204070 against a complete concentration-effect curve to 5-HT was not possible to obtain. Thus, control experiments, in which three consecutive concentration-effect curves were constructed to 5-HT, indicated that the third curve was not super-imposable on the first two, an effect probably due to fatigue of the tissues (unpublished observation).

The most likely explanation for the reduction in the maximum response to 5-HT observed with higher concentrations

of SB 204070 is that, in this preparation, SB 204070 is a slowly reversible or 'persistent' antagonist and acts in a pseudo-irreversible manner (Rang, 1966). Thus, since the 5-HT_4 receptor-mediated response in the guinea-pig distal colon has previously been proposed to be a well coupled system (Wardle & Sanger, 1993), the initial shift to the right of the curve seen with the low concentrations of SB 204070 may be attributed to the occupation and removal of spare receptors in a manner similar to that expected for an irreversible antagonist (Kenakin, 1993). Furthermore, in this model, BIMU 1 acts as a partial agonist relative to 5-HT and, by definition, must occupy all of the available receptors to produce its maximum response (Kenakin, 1993). Thus, when tested against BIMU 1, SB 204070, at all concentrations, produced an immediate reduction in maximum, without any prior shift to the right of the curve.

Non-surmountable antagonism is a common phenomenon in 5-HT receptor systems (see Leff & Martin, 1988; Martin, 1990) and in particular with highly potent compounds. It is relevant to note that, in the guinea-pig proximal colon, the potent 5-HT_4 receptor antagonist GR 113808 (pA_2 9.2), has also been reported to cause a small suppression of the maximum response to 5-HT at concentrations approximately 100 fold higher than its pA_2 value (Grossman *et al.*, 1993). Such an effect is consistent with that seen in the present study. Furthermore, in the present study, tissues were exposed to the agonist for a period of 30 s, during which time the response to the agonist reached a plateau. Considering the possible slow offset of SB 204070 from the receptor, it is likely that re-equilibration between SB 204070 and 5-HT is incomplete in this short time period, an effect contributing to the observed reduction in maximum response. If the depression in the maximum response is simply due to a problem of drug-receptor kinetics, then it should be possible to protect against agonist curve depression by co-incubation with an excess of a simple competitive antagonist, such as SDZ 205,557. Such an investigation is currently under way.

Radio-ligand binding studies with an iodinated derivative of SB 204070 (SB 207710, Brown *et al.*, 1993) are currently ongoing in piglet hippocampus. Preliminary data suggest a binding affinity of 9.9 ± 0.1 (T. Young, personal communication). This value is clearly lower than that predicted by the present study. The reason for this difference is at present unclear. While it may reflect differences in the 5-HT_4 receptor in the two models, an alternative explanation is that of tissue accumulation of SB 204070 in the functional studies. Thus, the compound may become concentrated in the tissue elements close to the receptor phase, disturbing equilibrium. Such a suggestion is supported by the apparent high lipophilicity of SB 204070 (see below) and by the washout data presented in the present study.

While studying the antagonistic effect of SB 204070 it was noted that when the compound was diluted using plastic pipettes, variations were observed in the potency of SB 204070. This variation could be eliminated by carrying out all dilutions in glass test tubes and using glass pipettes (as was the case in the present results). The reason for this is unclear, but may reflect adsorption and release of SB 204070 from the plastic throughout the dilution procedure. Such a possibility is currently being investigated further.

The antagonistic effects of SB 204070 were investigated against each of the three chemical classes of 5-HT_4 receptor agonists (indoles; 5-HT, 4-amino-5-chloro-2-methoxy substituted benzamides; renzapride and azabicycloalkyl benzimidazolone derivatives; BIMU 1). Since the mechanism of antagonism of SB 204070 in this preparation cannot be described as simple competition, a comparison of pA_2 values against different agonists was not possible. What can be concluded from the present data, however, is that, when tested against each of the three types of 5-HT_4 receptor agonists, SB 204070 is consistently active at very low concentrations (10 pM and above). From this it may be suggested that the potency of SB 204070 in the guinea-pig distal colon is agonist-dependent.

In conclusion, SB 204070 has been evaluated for its ability to antagonize 5-HT_4 receptor mediated-contractions in the guinea-pig distal colon LMMP. This compound is shown to be a highly potent, highly selective 5-HT_4 receptor antagonist in this preparation. The nature of the antagonism is complex. While the binding of the compound *in vitro* is reversible, dissociation from the receptor appears to be slow, thus preventing the attainment of equilibrium between 5-HT and the receptor within the time course of the experiment. The simplest explanation for the observed results is that SB 204070 behaves as a pseudo-irreversible antagonist. It is worth pointing out that the non-surmountable nature of the antagonism observed with SB 204070 suggests a need for caution when using this ligand for comparison of 5-HT_4 receptors in different tissues or in the discrimination of putative 5-HT_4 receptor subtypes. Indeed, the behaviour of SB 204070 and its apparent affinity may be influenced by the receptor reserve of the particular preparation under investigation (see Baxter *et al.*, 1994). Notwithstanding this caveat, the high potency and selectivity of SB 204070 suggest that it will be a useful tool in the study of the physiology and pathophysiology of the $5HT_4$ receptor. We eagerly await results from other functional studies to see if the nature of this antagonism is a peculiarity to the model currently used and from whole animal studies to see how this observation manifests itself *in vivo*.

The authors wish to thank all members of the Neuroscience Research at SmithKline Beecham involved in the radio-ligand binding studies on SB 204070.

References

ARUNLAKSHANA, O. & SCHILD, H.O. (1959). Some quantitative uses of drug antagonism. *Br. J. Pharmacol. Chemother.*, **14**, 48–58.

BANNER, S.E., SMITH, M.I. & SANGER, G.J. (1993). 5-HT receptors and 5-hydroxytryptophan-evoked defecation in mice. *Br. J. Pharmacol.*, **110**, 17P.

BAXTER, G.S., BLACKBURN, T.P., SANGER, G.J. & WARDLE, K.A. (1992). Actions of DAU 6285 at putative 5-HT_4 receptors in guinea-pig colon and rat oesophagus. *Br. J. Pharmacol.*, **106**, 99P.

BAXTER, G.S., SANGER, G.J., GASTER, L.M. & WARDLE, K.A. (1994). Tissue and agonist dependent non-surmountable antagonism by the selective 5-HT_4 receptor antagonist SB 204070. *Br. J. Pharmacol.*, **112**, 105P.

BOND, R.A., ORNSTEIN, A.G. & CLARKE, D.E. (1989). Unsurmountable antagonism to 5-hydroxytryptamine in rat kidney results from pseudoirreversible inhibition rather than multiple receptors or allosteric modulation. *J. Pharmacol. Exp. Ther.*, **249**, 401–410.

BOWEN, W.P., COLDWELL, M.C., HICKS, F.R. & RILEY, G.J. (1993). Further characterisation of human D_2 and D_3 dopamine receptors: GppNHp shifts are explained by the presence of more than one binding site in each clone. *Br. J. Pharmacol.*, **108**, 277P.

BRADLEY, P.B., ENGEL, G., FENIUK, W., FOZARD, J.R., HUMPHREY, P.P.A., MIDDLEMISS, D.N., MYLECHRANE, E.J., RICHARDSON, B.P. & SAXENA, P.R. (1986). Proposals for the classification and nomenclature of functional receptors for 5-hydroxytryptamine. *Neuropharmacol.*, **25**, 563–576.

BROWN, A.M., YOUNG, T.J., PATCH, T.L., CHEUNG, C.W., KAUMANN, A.J. & KING, F.D. (1993). [^{125}I]-SB 207710, a potent, selective radioligand for 5-HT_4 receptors. *Br. J. Pharmacol.*, **110**, 10P.

BUCHHEIT, K.-H., GAMSE, R. & PFANNKUCHE, H.-J. (1992). SDZ 205-557, a selective, surmountable antagonist for 5-HT_4 receptors in the isolated guinea-pig ileum. *Naunyn-Schmied. Arch. Pharmacol.*, **345**, 387–393.

BUTLER, A., ELSWOOD, C.J., BURRIDGE, J., IRELAND, S.J., BUNCE, K.T., KILPATRICK, G.J. & TYRES, M.B. (1990). The pharmacological characterisation of 5-HT_3 receptors in three isolated preparations derived from guinea-pig tissues. *Br. J. Pharmacol.*, **101**, 591–598.

CHENG, Y. & PRUSOFF, W.H. (1973). Relationship between the inhibition constant (Ki) and the concentration of inhibitor which causes 50 percent inhibition (IC_{50}) of an enzymatic reaction. *Biochem. Pharmacol.*, **22**, 3099–3108.

CLARKE, D.E., CRAIG, D.A. & FOZARD, J.R. (1989). The 5-HT_4 receptor: naughty, but nice. *Trends Pharmacol. Sci.*, **10**, 385–386.

DELEAN, A., MUNSON, P.J. & RODBARD, D. (1978). Simultaneous analysis of families of sigmoidal curves: application to bioassay, radioligand assay and physiological dose-response curve. *Am. J. Physiol.*, **235**, E97–E102.

DUMUIS, A., BOUHELAL, R., SEBBEN, M. & BOCKAERT, J. (1988a). A 5-HT receptor in the central nervous system, positively coupled with adenylate cyclase, is antagonised by ICS 205 930. *Eur. J. Pharmacol.*, **146**, 187–188.

DUMUIS, A., BOUHELAL, R., SEBBEN, M., CORY, R. & BOCKAERT, J. (1988b). A non-classical 5-hydroxytryptamine receptor positively coupled with adenylate cyclase in the central nervous system. *Mol. Pharmacol.*, **34**, 880–887.

EGLEN, R.M., ALVAREZ, R., WONG, E.H.F., JOHNSON, L., PERKINS, L.A., RAMSEY, S., LOURY, D.N., TANG, H.-M., WALLACE, S. & WHITING, R.L. (1992a). Characterisation of the interaction of SDZ 205 557 at putative 5-HT_4 receptors. *Br. J. Pharmacol.*, **105**, 275P.

EGLEN, R.M., BONHAUS, D.W., CLARKE, R., HEGDE, S., LEUNG, E. & WHITING, R.L. (1992b). RS-23597-190: a potent and selective 5-HT_4 receptor antagonist. *Br. J. Pharmacol.*, **107**, 439P.

ELSWOOD, C.J., BUNCE, K.T. & HUMPHREY, P.P.A. (1991). Identification of putative 5-HT_4 receptors in guinea-pig ascending colon. *Eur. J. Pharmacol.*, **196**, 149–155.

FORD, P.D.W. & CLARKE, D.E. (1993). The 5-HT_4 receptor. *Med. Res. Rev.*, **13**, 633–662.

GASTER, L.M., JENNINGS, A.J., JOINER, G.F., KING, F.D., MULHOLLAND, K.R., RAHMAN, S.K., STARR, S., WYMAN, P.A., WARDLE, K.A., ELLIS, E.S. & SANGER, G.J. (1993). (1-Butyl-4-piperidinyl)methyl 8-amino-7-chloro-1,4-benzodioxan-5-carboxylate hydrochloride: a highly potent and selective 5-HT_4 receptor antagonist derived from metoclopramide. *J. Med. Chem.*, **36**, 4121–4123.

GROSSMAN, C.J., KILPATRICK, G.J. & BUNCE, K.T. (1993). Development of a radioligand binding assay for 5-HT_4 receptors in guinea-pig and rat brain. *Br. J. Pharmacol.*, **109**, 618–624.

HAMBLIN, M.W. & METCALF, M.A. (1991). Primary structure and functional characterisation of a human 5-HT_{1D}-type serotonin receptor. *Mol. Pharmacol.*, **40**, 143–148.

HUMPHREY, P.P.A., HARTIG, G. & HOYER, D. (1993). A proposed new nomenclature for 5-HT receptors. *Trends Pharmacol. Sci.*, **14**, 233–236.

KAUMANN, A.J., SANDERS, L., BROWN, A.M., MURRAY, K.J. & BROWN, M.J. (1990). A 5-hydroxytryptamine receptor in human atrium. *Br. J. Pharmacol.*, **100**, 879–885.

KENAKIN, T. (1993). In *Pharmacological Analysis of Drug-Receptor Interaction* Second edition. New York: Raven Press.

LEFF, P. & MARTIN, G.R. (1988). The classification of 5-hydroxytryptamine receptors. *Med. Res. Rev.*, **8**, 187–202.

MARTIN, G.R. (1990). Current problems and future requirements for 5-hydroxytryptamine receptor classification. *Neuropsychopharmacol.*, **3**, 321–333.

NELSON, D.L. & THOMAS, D.L. (1990). [^{3}H]-BRL 43694 (Granisetron), a specific ligand for 5-HT_3 binding sites in rat brain cortical membranes. *Biochem. Pharmacol.*, **38**, 1693–1695.

PAZOS, A., HOYER, D. & PALACIOS, J.M. (1985). The binding of serotonergic ligands to the porcine choroid plexus: characterisation of a new type of serotonin recognition site. *Eur. J. Pharmacol.*, **106**, 539–546.

PETERS, J.A., KIRKNESS, E.F., CALLACHAN, H., LAMBERT, J.J. & TURNER, A.J. (1988). Modulation of the $GABA_A$ receptor by depressant barbiturates and pregnone steroids. *Br. J. Pharmacol.*, **94**, 1257–1269.

RANG, H.P. (1966). The kinetics of action of acetylcholine antagonists in smooth muscle. *Proc. R. Soc. B*, **164**, 488–510.

RICHARDSON, B.P., ENGEL, G., DONATSCH, P. & STADLER, P.A. (1985). Identification of serotonin M-receptor subtypes and their specific blockade by a new class of drugs. *Nature*, **316**, 126–131.

SANGER, G.J. & NELSON, D.R. (1989). Selective and functional 5-hydroxytryptamine$_3$ receptor antagonism by BRL 43694 (granisetron). *Eur. J. Pharmacol.*, **159**, 113–124.

SCHOLTYSIK, G. (1987). Evidence for inhibition by ICS 205 930 and stimulation by BRL 34915 of K^+ conductance in cardiac muscle. *Naunyn-Schmied. Arch. Pharmacol.*, **335**, 692–696.

SCHWABE, U. & TROST, T. (1980). Characterisation of adenosine receptors in rat brain by (−) [^{3}H]-N^6-phenylisopropyladenosine. *Naunyn-Schmied. Arch. Pharmacol.*, **313**, 179–187.

TURCONI, M., SCHIANTARELLI, P., BORSINI, F., RIZZI, C.A., LADINSKY, H. & DONETTI, A. (1991). Azabicycloalkyl benzimidazalones: interaction with serotonergic 5-HT_3 and 5-HT_4 receptors and potential therapeutic implications. *Drugs Future*, **16**, 1011–1026.

WAEBER, C., SCHOEFFTER, P., PALACIOS, J.M. & HOYER, D. (1989). 5-HT_{1D} receptors in guinea-pig and pigeon brain. Radioligand binding and biochemical studies. *Naunyn-Schmied. Arch. Pharmacol.*, **340**, 479–485.

WARDLE, K.A., ELLIS, L.M., GASTER, L.M., KING, F.D. & SANGER, G.J. (1993). SB 204070 – a potent and selective 5-HT_4 receptor antagonist. *Br. J. Pharmacol.*, **110**, 15P.

WARDLE, K.A. & SANGER, G.J. (1992). Guinea-pig distal colon: a sensitive model of the putative 5-HT_4 receptor. *Br. J. Pharmacol.*, **105**, 279P.

WARDLE, K.A. & SANGER, G.J. (1993). The guinea-pig distal colon – a sensitive preparation for the investigation of 5-HT_4 receptor mediated contractions. *Br. J. Pharmacol.*, **110**, 1593–1599.

(Received December 9, 1993
Revised March 14, 1994
Accepted March 16, 1994)

Br. J. Pharmacol. (1994), **112**, 795–800

Moguisteine: a novel peripheral non-narcotic antitussive drug

[1]L. Gallico, A. Borghi, C. Dalla Rosa, R. Ceserani & S. Tognella

Boehringer Mannheim Italia, Research Center, Viale della Libertà, Km 0.750, I-20052 Monza, Italy

1 The antitussive effects of moguisteine have been compared with codeine in several experimental models of cough in guinea-pigs and dogs.

2 Moguisteine and codeine dose-dependently (respective ED_{50} values are given in parentheses) inhibited cough induced in guinea-pigs by 7.5% citric acid aerosol (25.2 and 29.2 mg kg^{-1}, p.o.), by 30 μM capsaicin aerosol (19.3 and 15.2 mg kg^{-1}, p.o.), by mechanical stimulation (22.9 and 26.4 mg kg^{-1}, p.o.) and by tracheal electrical stimulation (12.5 and 13.9 mg kg^{-1}, p.o.).

3 Moguisteine was effective against cough induced by tracheal electrical stimulation in dogs (ED_{50} 17.2 mg kg^{-1}, p.o.); codeine was not tested because of its emetic effect.

4 After repeated dosing (12–15 days), moguisteine did not induce tolerance in either guinea-pigs or dogs.

5 Moguisteine did not interact with opiate receptors, since it did not show affinity for [^{3}H]-naloxone binding sites and furthermore naloxone (5 mg kg^{-1}, s.c.) did not antagonize its antitussive effects.

6 Moguisteine had no antitussive effect after i.c.v. administration (20 μg), whilst codeine (2–10 μg) and dextromethorphan (2.5–20 μg) were highly effective.

7 Our findings demonstrate that moguisteine is a novel peripherally acting non-narcotic antitussive agent, the mode of action of which remains to be elucidated fully.

Keywords: Cough; antitussive agents; moguisteine; codeine; naloxone

Introduction

Cough is a physiological defence mechanism for the clearance of foreign materials and of excessive bronchial secretion in the airways, but it is also a common symptom of a variety of respiratory diseases (Irwin *et al.*, 1981). The cough reflex is triggered by the activation of rapidly adapting receptors (or 'irritant' receptors) within the larynx, trachea and the proximal bronchi, and of C-fibre endings found in the airway walls of bronchi (Karlsson *et al.*, 1988b). Afferent signals are transmitted through the sensory vagal fibres to the cough centre, which has been experimentally identified as being in the region of the solitary nucleus in the medulla within the brain (Kasè *et al.*, 1970). From the cough centre the impulses travel through the efferent pathways to the respiratory muscles (diaphragm, intercostal and abdominal muscles) and the airways (Irwin *et al.*, 1977).

Current cough therapy is based on the use of drugs that are classified according to their site of action, which may be central (applicable to both narcotic and non narcotic drugs), or peripheral. The centrally acting antitussives, such as codeine and dextromethorphan, which depress the cough centre, are considered the most clinically effective, although sedative and addictive effects can limit their use (Eddy *et al.*, 1969). However recent experimental studies have clearly shown that codeine acts also at the peripheral level, as its antitussive effect was reversed by opiate antagonists with scanty penetration of the blood-brain barrier (Adcock *et al.*, 1988; Karlsson *et al.*, 1988a). Further support for the concept of the peripheral component in the action of opiates was provided by the investigations performed with BW 443C, a novel agonist of opioid receptors that has poor penetration of the blood-brain barrier, which in turn inhibits cough in animals. The drug's effect was antagonized by peripherally acting opioid receptor antagonists (Adcock *et al.*, 1988). BW 443C was also shown to act on sensory nerve endings, since it reduced spontaneous and chemically induced activity in both irritant and C-fibre receptors (Adcock, 1991). The peripherally acting non opiate drugs, such as oxolamine, benzonatate and dropropizine are believed to reduce the afferent fibre nerve inputs or to inhibit the activation of airway sensory receptors: however, very few studies have attempted to clarify their mechanism of action (Irwin & Curley, 1990). Furthermore, the effectiveness in cough therapy of peripherally acting drugs has not been conclusively demonstrated, given the paucity of controlled clinical trials (Banner, 1986). Only local anaesthetics that interfere with the conduction of afferent nerve impulses have been shown to be peripherally active antitussive compounds, but their considerable side effects make their use unsuitable (Karlsson, 1983). Therefore the availability of a novel, non-narcotic peripheral and effective drug could represent a considerable improvement in the treatment of cough.

This paper describes the antitussive profile of moguisteine, (**R,S**)-2- (2-methoxyphenoxy) -methyl-3-ethoxycarbonyl-acetyl -1,3 thiazolidine (Figure 1), a non-narcotic compound, in comparison with that of codeine, as assessed in animal models. Part of this work has been published in abstract form (Gallico *et al.*, 1990).

Methods

Cough induced by citric acid aerosol in the guinea-pig

Male Dunkin Hartley guinea-pigs (Charles River, Calco, Italy) 350–400 g were maintained in conditioned quarters (temperature 21 ± 2°C, relative humidity 55 ± 10%, 12 h on–12 h off, light cycle) with food and water *ad libitum* for at least 1 week before use.

Guinea-pigs were put into a Perspex box (20 × 12 × 14 cm) and exposed to a 7.5% citric acid aerosol (Charlier *et al.*, 1961) delivered by an ultrasonic nebulizer (G.B. Elbisonic, Bielin Milan, Italy, particle size 0.5–6 μm, mean output 0.5 ml min^{-1}) for 5 min. During this period the animals were continuously watched by a trained observer and the number of coughs was counted manually and taken as the control basal value. Coughs can be recognized easily on the basis of sound associated with a rapid inspiration followed by a rapid expiration. Only the guinea-pigs responding within the range of 14–22 coughs were selected for further studies. Twenty

[1] Author for correspondence.

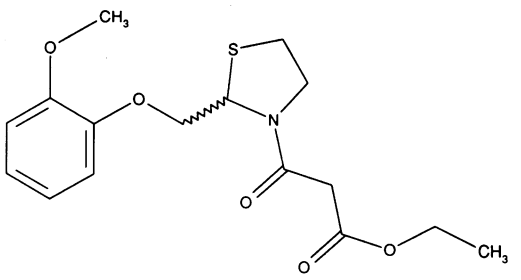

Figure 1 Chemical structure of moguisteine.

four hours later, after overnight fasting with water *ad libitum*, the guinea-pigs ($n = 8$ for each dose), were randomly pretreated by gavage with moguisteine (15, 30 and 60 mg kg^{-1}) and codeine (20, 40 and 80 mg kg^{-1}) 1 h before re-exposure to the citric acid aerosol. The experiments were performed with a blind design so that the observer was unaware of the treatment. Antitussive activity was evaluated in each guinea-pig as the reduction in the number of coughs in comparison with the previously established control basal value. In the repeated dosing study (15 days), antitussive activity for each guinea-pig was determined as described above, 1 h after the last administration of either moguisteine or codeine (the control basal values having been recorded before the beginning of the treatment).

Preliminary experiments demonstrated that cough, checked for two consecutive days per week, was consistently reproducible in the same animal for at least 3 weeks.

Cough induced by capsaicin aerosol in the guinea-pig

In this experimental model, the guinea-pigs could not be used as their own controls because of the tachyphylactic effect of capsaicin, which occurs after two repeated exposures; the experimental schedule was therefore modified. After overnight fasting with water *ad libitum*, the guinea-pigs were randomly assigned to the experimental groups ($n = 10$ for each dose) and orally pretreated with vehicle (controls), moguisteine (7.5, 15 and 30 mg kg^{-1}) or codeine (10, 20 and 40 mg kg^{-1}) 1 h before exposure for 5 min to a 30 μM capsaicin aerosol (Forsberg & Karlsson, 1986). The aerosol characteristics and the cough counting were as previously described; in control animals capsaicin induced 7–12 coughs. Antitussive activity was evaluated as the reduction in the number of coughs in comparison with the control group.

Cough induced by mechanical stimulation of the trachea in anaesthetized guinea-pigs

After overnight fasting with water *ad libitum*, the guinea-pigs were lightly anaesthetized with 25% w/v urethane (4 ml kg^{-1}, i.p.) which induces surgical levels of analgesia without depressant effects on respiratory function. Analgesia was monitored throughout the experiment as the disappearance of head shaking in response to an ear pinch (Green, 1982). The animals were maintained at a constant body temperature of 37°C by means of a heated plate. A thin steel wire was gently inserted into the trachea through a small incision near the cricoid cartilage. Coughs were evoked by pushing the steel wire to reach the bifurcation of the trachea 35 and 5 min before oral drug administration and 30, 60 and 120 min after treatment (Takagi *et al.*, 1960). One violent cough (the intensity was not recorded) occurred upon each stimulation. We only selected those guinea-pigs that responded to both mechanical stimulations before dosing; the animals were then randomly assigned to receive moguisteine (7.5, 15 and 30 mg kg^{-1}) and codeine (15, 30 and 60 mg kg^{-1}) ($n = 10$ for each dose). The pretreatment was considered to be effective when, after administration of the test compounds, an animal failed to respond to any one of the stimulations.

Cough induced by electrical stimulation of the trachea in conscious guinea-pigs

The guinea-pigs were anaesthetized (ketamine, 10 mg kg^{-1}, i.m. and xylazine 3 mg kg^{-1}, i.m.) and the neck region caudal to the cricoid cartilage was incised in the midline and the trachea was exposed. Care was taken to not disturb the recurrent vagus nerves along the dorsolateral side of the trachea. A silver-plated cuprum electrode (Awg 32-Habia) was wrapped around the trachea at about 1.5 cm above the bifurcation, fixed to the muscular tissue and brought through the skin incision (Cavanagh *et al.*, 1976). The indifferent electrode (a stainless steel clip) was fixed to the dorsal skin. The animals were then allowed to recover from the anaesthesia under aseptic conditions in warmed cages. After overnight fasting with water *ad libitum*, the guinea-pigs were assessed, 48 h after the surgical implant, for tussive threshold to electrical stimulation by the determination of the minimum voltage (range of 4–10 V) required to elicit cough with the following stimulus conditions: square wave pulses of 0.6 ms, 40 Hz, 10 s train duration (Stimulator S, Ugo Sachs Elektronik, Germany). The number of coughs (7–12) during the electrical stimulation was recorded for each guinea-pig and considered as a basal value. The guinea-pigs were then randomly assigned to different experimental groups and pretreated by gavage with the test compounds i.e. moguisteine (7.5, 15 and 30 mg kg^{-1}) and codeine (7.5, 15 and 30 mg kg^{-1}) ($n = 8$ for each dose).

In a further experiment, animals were treated by the intracerebroventricular route (i.c.v.) with moguisteine (10 and 20 μg), codeine (1, 2.5, 5 and 10 μg) and dextromethorphan (2.5, 5, 10 and 20 μg) respectively ($n = 7$ animals for each dose). The i.c.v. administration (50 μl volume) was performed through a small cannula inserted under light general anaesthesia (25% urethane, 4 ml kg^{-1}, i.p.) at the level of the bregma above the right cerebral lateral ventricle. At the end of the experiment, 50 μl of methylene blue was injected i.c.v. into each guinea-pig; homogeneous spreading of the dye within the ventricle demonstrated that the drug had been correctly administered.

Antitussive activity was evaluated as the reduction in the number of coughs in comparison with the control responses in the same guinea-pig at either 1 h after oral treatment or at 1, 3 and 5 min after i.c.v. treatment.

Cough induced by electrical stimulation of trachea in conscious dogs

Six Beagle dogs of either sex (Morini, S. Polo d'Enza, Italy) 10–15 kg, were maintained in conditioned quarters with food and water *ad libitum* for at least two weeks before use. The animals were anaesthetized with a mixture of xylazine (1 mg kg^{-1}, i.v.), ketamine (2 mg kg^{-1}, i.v.) and pancuronium bromide (2 mg i.v.); surgical anaesthesia was judged and controlled by loss of the pedal, corneal and photomotor reflexes (Green, 1982). The effect lasts about 60–90 min which is the time required for surgical operation. After orotracheal intubation the dogs were artificially ventilated by an automatic apparatus (Bird Mark 4 – Mark 8).

A short midline incision was made in the neck of the dogs, caudal to the cricoid cartilage. After the exposure and the isolation of the trachea, two electrodes, connected to insulated wires, were inserted (i.e. penetrated the mucosa) between two tracheal rings (at about 6 cm down the cricoid cartilage) and properly secured (Stefko & Benson, 1953). The wires were brought through the subcutaneous tissue and exteriorized on the back. The muscle relaxant effect of pancuronium was reversed with neostigmine (0.5 mg kg^{-1}, i.v.). The animals were allowed to recover from the anaesthesia in aseptic warmed boxes. One week after surgery, the unres-

trained animals were placed in a cage to which the animals had previously been accustomed. The tracheal mucosa was stimulated with a Grass S48 stimulator according to the following parameters: 10 stimulations of 1 s with square wave pulse of 1 ms, 50 Hz, 10–30 V, at intervals of 5 s each. The cough basal value response determined for each dog ranged from 10 to 12. The antitussive activity of moguisteine (10, 20 and 40 mg kg^{-1}, p.o.) and of codeine (10 and 20 mg kg^{-1}, p.o.), evaluated as reduction in coughs versus basal value in the same animal, was recorded 1 h after oral treatment. In the repeated dosing study (12 days), antitussive activity in each dog was determined as described above, 1 h after the last administration (the control basal values having been recorded before the beginning of the treatment).

[^{3}H]-naloxone binding assay

Male Sprague Dawley rats (Charles River, Calco, Italy) 175–225 g were used. The animals, maintained in conditioned quarters with food and water *ad libitum* for at least 1 week, were used.

The animals were killed by decapitation and the cortices rapidly removed and homogenized in 20 volumes of ice-cold 50 mM Tris-Cl buffer (pH 7.7) with a Polytron tissue disruptor. After centrifugation at 38,000 *g*, the pellet was resuspended in 100 volumes of buffer. Binding assays were carried out by incubation for 20 min of approximately 0.5 mg membrane protein with 1.6 nM [^{3}H]-naloxone at 25°C in the dark in a final incubation volume of 1 ml (Stengaard-Pedersen & Larsson, 1981). We incubated, for 30 min, moguisteine at up to a concentration of 0.05 mM, codeine from 5 μM to 0.05 mM, morphine and naloxone from 1 nM to 5 μM. At the end of the incubation period, samples were rapidly filtered through Whatman GF/B glass-fibre filters and washed three times with 4 ml of ice-cold 50 mM Tris-Cl buffer. The filters were then placed in scintillation vials; radioactivity was determined with a beta-counter (TRI-CARB, Packard). Specific [^{3}H]-naloxone binding was defined as the difference in binding in the presence and absence of morphine 6 μM.

Effect on pulmonary mechanics in spontaneously breathing anaesthetized guinea-pigs

Guinea-pigs, fasted overnight, were anaesthetized with urethane 1.2 g kg^{-1}, i.p. The animals were tracheotomized and connected through a tracheal cannula to a Fleisch pneumotachograph (type 0000, HSE) which was coupled to a differential pressure transducer (type DP45-14, Basile, Italy) for the measurement of respiratory airflow. Transpulmonary pressure was measured with a differential pressure transducer (mod. MPX-11DP, HSE); one end of the differential pressure transducer was connected to an intrapleural catheter and the other end was exposed to atmospheric pressure. Using a respiratory analyzer (Model 6, Buxco, U.S.A.) we applied the breath by breath principle of Amdur & Mead, (1958) to calculate values for respiratory rate (breath min^{-1}), tidal volume (ml), minute volume (ml min^{-1}), total lung resistance (cmH_2O ml^{-1} s^{-1}), and dynamic compliance (ml cmH_2O^{-1}). The values were recorded on a dynograph (Beckman R611) and registered on a printer. During the experiments, the animals were maintained at the constant body temperature of 37°C. Respiratory function was assessed under baseline conditions and 10, 20, 30, 60 and 90 min after either vehicle or moguisteine or codeine treatment (60 mg kg^{-1}, p.o.). Five animals per group were used.

Compounds

The following compounds were used: moguisteine [(**R**,**S**)-2-(2-methoxyphenoxy)-methyl-3-ethoxycarbonyl-acetyl-1,3 thiazolidine] (Boehringer Mannheim Italia) either suspended in 0.5% methylcellulose or dissolved in 0.4% dimethyl sulphoxide (DMSO); codeine phosphate and morphine HCl (Carlo Erba, Italy), dextromethorphan (Roche, Italy) and urethane (Fluka Chemie, Switzerland) dissolved in saline; citric acid (Carlo Erba, Italy) dissolved in distilled water; capsaicin (Fluka Chemie, Switzerland) dissolved in 10% ethanol, 10% Tween 80 and diluted with saline; ketamine (Ketalar, Parke Davis); xylazine (Rompum, Bayer); pancuronium bromide (Pavulon, Organon); naloxone (Narcan, Crinos); neostigmine methylsulphate (Prostigmin, Roche); [^{3}H]-naloxone (Dupont/NEN). The vehicles (1 ml kg^{-1}, p.o. or 50 μl, i.c.v.) used to dissolve and/or prepare suspensions of moguisteine and codeine were demonstrated in preliminary studies not to affect cough. The doses quoted for codeine refer to its phosphate salt.

Statistical analysis

Evaluation of the statistical significance of the results was performed with Student's test for both paired data and unpaired data (cough induced by capsaicin). ED_{50} values with 95% confidence limits were either determined according to Snedecor & Cochran (1967) (cough induced by citric acid, capsaicin, electrical stimulation) or by logit transformation (Ashton, 1972) (mechanical stimulation).

Results

Antitussive effect

Cough induced by citric acid aerosol in the guinea-pig Moguisteine dose-dependently inhibited the cough elicited by the 5 min 7.5% citric acid aerosol, with an ED_{50} (95% CL) of 25.2 (16.2–39.3) mg kg^{-1}, p.o. (Table 1). Codeine displayed a similar activity with an ED_{50} (95% CL) of 29.2 (18.6–45.6) mg kg^{-1}, p.o. (Table 1).

In further experiments, the effect of moguisteine (30 mg kg^{-1}) and codeine (40 mg kg^{-1}) over a repeated dosing period (15 days) were compared with those observed after a single treatment. Single and repeated moguisteine dosing caused similar levels of cough inhibition (64% and 70% respectively). The results for codeine under identical dosing conditions were almost the same (64% and 71% reductions respectively).

Cough induced by capsaicin aerosol in the guinea-pig Moguisteine dose-dependently inhibited capsaicin (30 μM) aerosol-induced cough with an ED_{50} (95% CL) of 19.3 (12.1–26.5) mg kg^{-1}, p.o. (Table 2). Similarly, codeine reduced cough with an ED_{50} (95% CL) of 15.2 (6.2–35.8) mg kg^{-1}, p.o. (Table 2).

Cough induced by mechanical stimulation of the trachea in anaesthetized guinea-pigs The inhibition values for mechanically induced cough by moguisteine were very similar to

Table 1 Inhibition by moguisteine and codeine of cough induced by citric acid (7.5%) aerosol in conscious guinea-pigs

Treatment	*Dose* (mg kg^{-1} p.o.)	*No. of coughs* (mean ± s.e.mean)	ED_{50} (95% CL)
Basal values	–	17.1 ± 0.8	
Moguisteine	15	10.7 ± 0.9*	25.2
	30	7.7 ± 0.9*	(16.2–39.3)
	60	4.8 ± 0.7*	
Basal values	–	17.3 ± 0.6	
Codeine	20	10.5 ± 0.9*	29.2
	40	7.6 ± 0.5*	(18.6–45.6)
	80	3.6 ± 0.9*	

*$P < 0.001$ compared to basal values; $n = 8$ per group.

those obtained with codeine (Table 3), with ED_{50} (95% CL) of 22.9 (12.3–33.6) and 26.4 (18.6–34.1) mg kg^{-1}, p.o., respectively.

Cough induced by electrical stimulation of the guinea-pig and dog trachea Moguisteine effectively reduced cough in guinea-pigs, with an ED_{50} (95% CL) of 12.5 (7.7–17.5) mg kg^{-1}, p.o. (Table 4); codeine, at the same doses, displayed a very similar effect, with an ED_{50} (95% CL) of 13.9 (11.2–17.2) mg kg^{-1}, p.o. (Table 4).

In the dog experiments, the oral administration of moguisteine produced a dose-related inhibition of cough, ED_{50} (95% CL) of 17 (8–37) mg kg^{-1}. After multiple dosing (12 days), moguisteine (20 mg kg^{-1} day^{-1}, p.o.) produced a reduction in cough (53%) that was not significantly different from that recorded after single treatment (50%). A comparative study with codeine was not feasible due to the emetic effect induced by codeine at 10 and 20 mg kg^{-1} p.o.; lower dosages were better tolerated but proved to be inactive.

Table 2 Inhibition by moguisteine and codeine of cough induced by capsaicin (30 μM) aerosol in conscious guinea-pigs

Treatment	Dose (mg kg^{-1} p.o.)	No. of coughs (mean ± s.e.mean)	ED_{50} (95% CL)
Control	–	8.7 ± 0.6	
Moguisteine	7.5	6.6 ± 0.7	19.3
	15	4.4 ± 0.8*	(12.1–26.5)
	30	2.2 ± 0.5*	
Control	–	9.1 ± 0.8	
Codeine	10	5.7 ± 0.4*	15.2
	20	4.4 ± 0.7*	(6.2–35.8)
	40	2.7 ± 0.5*	

*$P<0.01$ compared to control group, unpaired t test; $n = 10$ per group.

Table 3 Inhibition by moguisteine and codeine of cough induced by trachea mechanical stimulation in anaesthetized guinea-pigs

Treatment	Dose (mg kg^{-1} p.o.)	No. of animals without cough/treated	ED_{50} (95% CL)
Moguisteine	7.5	2/10	
	15	4/10	22.9
	30	6/10	(12.3–33.6)
	60	9/10	
Codeine	15	2/10	26.4
	30	5/10	(18.6–34.1)
	60	10/10	

$n = 10$ per dose.

Table 4 Inhibition by moguisteine and codeine of cough induced by trachea electrical stimulation in conscious guinea-pigs

Treatment	Dose (mg kg^{-1} p.o.)	No. of coughs (mean ± s.e.mean)	ED_{50} (95% CL)
Basal values	–	9.1 ± 0.5	
Moguisteine	7.5	5.6 ± 0.4*	12.5
	15	4.0 ± 0.3*	(7.7–17.5)
	30	0.4 ± 0.2*	
Basal values	–	9.3 ± 0.5	
Codeine	7.5	7.0 ± 0.4*	13.9
	15	4.6 ± 0.4*	(11.2–17.2)
	30	1.5 ± 0.3*	

*$P<0.05$ compared to basal values; $n = 8$ per group.

Mechanism of action

Effect of naloxone on the antitussive activity of moguisteine and codeine in the guinea-pig Naloxone, 5 mg kg^{-1}, s.c., injected 10 min before either citric acid aerosol or electrical stimulation (as previously described) did not significantly affect cough responses and did not antagonize the antitussive properties of moguisteine in either experimental model, whereas it did abolish the effectiveness of codeine (Figure 2a and b).

[^{3}H]-naloxone binding assay Moguisteine did not show any affinity for opiate receptors, since it was unable to displace [^{3}H]-naloxone from its binding sites; in contrast, codeine, morphine and naloxone were highly effective with IC_{50}s of 0.02 mM, 15 nM and 2 nM respectively.

Antitussive effect after intracerebroventricular (i.c.v.) administration in the guinea-pig When injected into the right cerebral lateral ventricle, moguisteine failed to inhibit significantly cough induced by electrical stimulation (Table 5) whereas codeine and dextromethorphan reduced the cough in a dose-related way (Table 5). The onset of the effect of codeine was very rapid (1 min after administration), and after 5 min the percentage reduction in cough was already significant at a

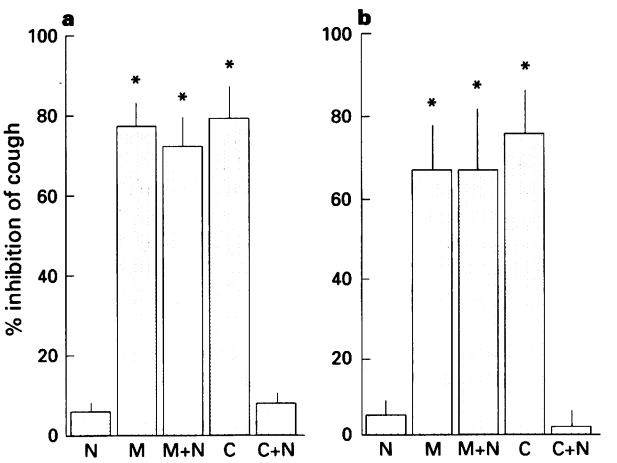

Figure 2 Effect of naloxone (N) on antitussive activity of moguisteine (M) and codeine (C) on cough induced by citric acid (a) or by electrical stimulation (b) of guinea-pig trachea. N: 5 mg kg^{-1} s.c. (a and b); M: 60 mg kg^{-1} p.o. (a) and 30 mg kg^{-1} p.o. (b): C: 80 mg kg^{-1} p.o. (a) and 30 mg kg^{-1} p.o. (b). M and C were given 1 h and N 10 min before the challenge. *$P<0.05$ vs control basal value.

Table 5 Intracerebroventricular (i.c.v.) antitussive effect of moguisteine, codeine and dextromethorphan on cough induced by electrical stimulation of the trachea in conscious guinea-pigs

Compound	Dose (μg)	% Reduction in cough (mean ± s.e.mean) at each time point (min) 1	3	5
Moguisteine	10	19 ± 6	3.5 ± 4	17 ± 10
	20	0	0	9 ± 7
Codeine	1	10 ± 5	25 ± 8	17 ± 9
	2.5	22 ± 6	40 ± 9	41 ± 5*
	5	39 ± 15	65 ± 10*	45 ± 7*
	10	63 ± 8*	75 ± 8*	70 ± 4*
Dextromethorphan	2.5	0	22 ± 8	27 ± 7
	5	15 ± 9	31 ± 9	48 ± 6*
	10	23 ± 11	51 ± 9*	57 ± 14*
	20	36 ± 10	61 ± 5*	74 ± 7*

*$P<0.05$ vs control basal value; $n = 7$ per dose.

Table 6 Effect of moguisteine (60 mg kg^{-1}, p.o.) on respiratory function in spontaneously breathing anaesthetized guinea-pigs

		Time after treatment (min)					
		0	10	20	30	60	90
Respiratory rate	Control	100 ± 13	92 ± 14	88 ± 6	88 ± 10	89 ± 13	85 ± 10
(breath min^{-1})	Moguisteine	92 ± 12	75 ± 22	76 ± 14	75 ± 16	80 ± 12	79 ± 11
Tidal volume (ml)	Control	2.2 ± 0.2	2.2 ± 0.2	2.3 ± 0.1	2.3 ± 0.2	2.3 ± 0.2	2.4 ± 0.2
	Moguisteine	2.3 ± 0.1	2.6 ± 0.2*	2.6 ± 0.2*	2.5 ± 0.3	2.5 ± 0.2	2.5 ± 0.2
Minute volume	Control	196 ± 55	183 ± 39	182 ± 50	184 ± 47	184 ± 47	180 ± 51
(ml min^{-1})	Moguisteine	210 ± 20	192 ± 38	193 ± 20	189 ± 22	201 ± 17	201 ± 18
Total lung resistance	Control	0.22 ± 0.01	0.22 ± 0.02	0.22 ± 0.01	0.21 ± 0.02	0.23 ± 0.01	0.24 ± 0.02
(cmH_2O ml^{-1} s^{-1})	Moguisteine	0.24 ± 0.02	0.23 ± 0.03	0.24 ± 0.02	0.24 ± 0.01	0.25 ± 0.02	0.25 ± 0.02
Dynamic compliance	Control	0.51 ± 0.12	0.59 ± 0.16	0.58 ± 0.14	0.58 ± 0.11	0.53 ± 0.10	0.56 ± 0.11
(ml cmH_2O^{-1})	Moguisteine	0.59 ± 0.12	0.62 ± 0.13	0.60 ± 0.10	0.63 ± 0.13	0.62 ± 0.11	0.60 ± 0.09

Means ± s.e.mean for five guinea-pigs.
*$P < 0.05$ vs control group.

Table 7 Effect of codeine (60 mg kg^{-1}, p.o.) on respiratory function in spontaneously breathing anaesthetized guinea-pigs

		Time after treatment (min)					
		0	10	20	30	60	90
Respiratory rate	Control	87 ± 8	78 ± 7	75 ± 8	71 ± 8	68 ± 8	67 ± 8
(breath min^{-1})	Codeine	93 ± 12	59 ± 13*	60 ± 15*	57 ± 16*	54 ± 11*	52 ± 11*
Tidal volume (ml)	Control	2.3 ± 0.2	2.4 ± 0.2	2.4 ± 0.2	2.5 ± 0.2	2.5 ± 0.2	2.5 ± 0.2
	Codeine	2.4 ± 0.2	2.7 ± 0.3*	2.7 ± 0.4*	2.7 ± 0.3	2.8 ± 0.3*	2.8 ± 0.3
Minute volume	Control	206 ± 11	191 ± 15	185 ± 18	180 ± 14	173 ± 17	172 ± 16
(ml min^{-1})	Codeine	225 ± 29	163 ± 24*	163 ± 26*	154 ± 31*	156 ± 23*	150 ± 27*
Total lung resistance	Control	0.28 ± 0.03	0.29 ± 0.03	0.30 ± 0.05	0.29 ± 0.03	0.27 ± 0.04	0.28 ± 0.06
(cmH_2O ml^{-1} s^{-1})	Codeine	0.29 ± 0.02	0.27 ± 0.05	0.26 ± 0.04	0.28 ± 0.02	0.26 ± 0.04	0.27 ± 0.02
Dynamic compliance	Control	0.65 ± 0.12	0.66 ± 0.14	0.67 ± 0.15	0.65 ± 0.16	0.68 ± 0.17	0.75 ± 0.17
(ml cmH_2O^{-1})	Codeine	0.60 ± 0.03	0.68 ± 0.08	0.71 ± 0.08	0.70 ± 0.05	0.69 ± 0.08	0.70 ± 0.12

Means ± s.e.mean for five guinea-pigs.
*$P < 0.05$ vs control group.

dose of 2.5 μg; the greatest effect was observed with 10 μg (75 ± 8% and 70 ± 4% reduction 3 and 5 min respectively after treatment). A significant antitussive effect of dextromethorphan occurred after 3 min at the maximum tested dose and was higher 5 min after treatment. The maximal activity was observed with 20 μg (74 ± 7% cough reduction); the lowest tested dose, 2.5 μg, was scarcely effective.

Effect on pulmonary mechanics in spontaneously breathing anaesthetized guinea-pigs Moguisteine (60 mg kg^{-1}, p.o.) did not affect respiratory rate, minute volume, total lung resistance and dynamic compliance; it produced only a transient (10–20 min after treatment), although significant, increase in tidal volume (Table 6). In contrast, codeine (60 mg kg^{-1}, p.o.) produced a significant depressant effect on ventilation, as shown by the significant reduction in minute volume which lasted for all the recording period. The most notable effect of codeine was on respiratory rate. A significant increase in the tidal volume values was recorded at 10, 20 and 60 min (Table 7).

Discussion

Moguisteine is an effective antitussive agent in a number of commonly used experimental cough models. It proved to be as active as codeine in cough induced in guinea-pigs both by chemical irritants, such as citric acid and capsaicin, and by mechanical or electrical stimulation of the trachea.

Its antitussive efficacy is also clearly demonstrated by its prevention of electrically induced cough in conscious dogs. Moguisteine did not induce tolerance either in guinea-pigs or in dogs after repeated (15 and 12 days respectively) dosing. In addition, it did not depress ventilation, whereas an opposite effect was observed after codeine administration.

Further studies proved the antitussive efficacy of moguisteine and its safety in controlled clinical trials in patients with persistent cough (Morrone *et al.*, 1993; Del Donno *et al.*, 1993).

To investigate the mechanism of action of moguisteine it was important to define whether the drug interacts with opiate receptors (Chan & Harris, 1984; Karlsson *et al.*, 1990). Naloxone, an opiate antagonist which does not affect the cough reflex *per se*, abolished the antitussive effect of codeine both in electrically stimulated and citric acid-induced cough in guinea-pigs, but not that of moguisteine. Moreover, binding studies on rat brain homogenates with [^{3}H]-naloxone as the ligand showed that moguisteine (at up to 0.05 mM) had no affinity for opiate binding sites. These *in vivo* and *in vitro* results exclude the hypothesis of interaction with the opiate receptors. As the evaluation of a drug's pharmacological effect after direct intracerebral administration is a reliable method to clarify whether a drug acts at the central level (Kasè, 1980), we checked the antitussive effect of moguisteine following i.c.v. dosing in guinea-pig. This approach had already been used to define the site of action of antitussive drugs and it has been shown conclusively by this approach that codeine has a clearcut central effect (Kasè, 1980). Our results show that moguisteine 10 and 20 μg i.c.v. in guinea-pigs proved to be completely inactive against electrically induced cough, whereas codeine (1–10 μg i.c.v. guinea-pig) and dextromethorphan (2.5–20 μg) were dose-dependently effective in the same experimental conditions. That moguisteine lacks central activity is further demonstrated by its poor penetration of the blood brain barrier (0.01% of the administered dose), which we observed in the tissue distribution studies in guinea-pigs with the labelled compound (unpublished observations). Altogether, these findings suggest that the site of action of moguisteine is at a peripheral level.

It is well known that local anaesthetics can be used to

suppress cough (Karlsson, 1983; Howard *et al.*, 1977) and they have recently been shown to inhibit reflex cough provoked in volunteers by capsaicin (Choudry *et al.*, 1990). A significant local anaesthetic effect, as well as a direct inhibition of the cough centre, is responsible for the effectiveness of vadocaine, which is chemically related to such anaesthetics as lignocaine and procainamide, and which has been shown to be effective, though weaker than codeine, in several experimental cough models (Mannisto *et al.*, 1988). However, the above mechanism cannot account for the antitussive properties of moguisteine, since this drug is devoid of a local anaesthetic effect (unpublished observations).

Further experiments to elucidate more fully the mode of action of moguisteine are currently in progress.

References

ADCOCK, J.J. (1991). Peripheral opioid receptors and the cough reflex. *Resp. Med.*, **85**, (suppl A), 43–46.

ADCOCK, J.J., SCHNEIDER, C. & SMITH, T.W. (1988). Effects of codeine, morphine and a novel opioid pentapeptide BW 443C on cough, nociception and ventilation in the unanaesthetised guinea-pig. *Br. J. Pharmacol.*, **93**, 93–100.

AMDUR, M.O. & MEAD, J. (1958). Mechanics of respiration in unaesthetized guinea pigs. *Am. J. Physiol.*, **19**, 364–368.

ASHTON, W.D. (1972). *The Logit Transformation.* ed. Stuart A. London: Charles Griffin & Co Ltd.

BANNER, S.A. (1986). Cough: physiology, evaluation, treatment. *Lung*, **164**, 79–92.

CAVANAGH, R.L., GYLYS, J.A. & BIERWAGEN, M.E. (1976). Antitussive properties of butorphanol. *Arch. Int. Pharmacodyn.*, **220**, 258–268.

CHAN, T.T. & HARRIS, L.S. (1984). Antitussive potencies of opiates and their inhibition of codeine binding. *NIDA Res. Monogr.*, **49**, 77–84.

CHARLIER, R., PROST, M., BINON, F. & DELTOUR, G. (1961). Etude pharmacologique d'un antitussif, le fumarate acide de phenethyl-1 (propyne-2-yl)-4 propionoxy-4 piperidine. *Arch. Int. Pharmacodyn.*, **84**, 306–327.

CHOUDRY, N.B., FULLER, R.W., ANDERSON, N. & KARLSSON, J.A. (1990). Separation of cough and reflex bronchoconstriction by inhaled local anaesthetics. *Eur. Respir. J.*, **3**, 579–583.

DEL DONNO, M., AVERSA, C., CORSICO, R., FORESI, A., GRASSI, B., MASTROPASQUA, B., SCODITTI, S. & OLIVIERI, D. (1993). Efficacy and safety of moguisteine in comparison with dextromethorphan in patients with persistent cough. *Eur. Respir. J.*, **6**, Suppl 17, 324s.

EDDY, N.B., FRIEBEL, H., HAHN, K.J. & HALLSACH, H. (1969). Codeine and its alternates for pain and cough relief. 3. The antitussive action of codeine. Mechanisms, methodology and evaluation. *Bull. WHO*, **40**, 425–454.

FORSBERG, K. & KARLSSON, J.A. (1986). Cough induced by stimulation of capsaicin-sensitive sensory neurons in conscious guinea pigs. *Acta Physiol. Scand.*, **128**, 319–320.

GALLICO, L., BORGHI, A., DALLA ROSA, C., OGGIONI, N., LUMACHI, B., TOFANETTI, O. & TOGNELLA,S. (1990). Moguisteine: a new drug effective in experimental cough and hyperreactivity. *Am. Rev. Respir. Dis.*, **141**, Suppl, A840.

GREEN, C.J. (1982). General and balanced anaesthesia. In *Animal Anaesthesia.* pp. 53–84. London: Laboratory Animals Ltd.

HOWARD, P., CAYTON, R.M., BRENNAN, S.R. & ANDERSON, P.B. (1977). Lignocaine aerosol and persistent cough. *Br. J. Dis. Chest*, **71**, 19–24.

IRWIN, S.R., CORRAO, W.M. & PRATTER, M.R. (1981). Chronic persistent cough in the adult: the spectrum and frequency causes and successful outcome of specific therapy. *Am. Rev. Respir. Dis.*, **123**, 413–417.

IRWIN, S.R. & CURLEY, F.J. (1990). The treatment of cough. A comprehensive review. *Chest*, **99**, 1477–1484.

IRWIN, S.R., ROSEN, M.J. & BRAMAN, S.S. (1977). Cough. A comprehensive review. *Arch. Intern. Med.*, **137**, 1186–1191.

KARLSSON, J.A. (1983). Airway anaesthesia and the cough reflex. *Bull. Eur. Physiopathol. Respir.*, **23** Suppl. 10, 29S–36S.

KARLSSON, J.A., LANNER, A.S., FORSBERG, K., FULLER, R.W. & PERSSON, G.G.A. (1988a). Inhibition of cough and bronchoconstriction in the guinea-pig by opiates: evidence for a peripheral action. *Br. J. Pharmacol.*, **93**, 233P.

KARLSSON, J.A., SANT'AMBROGIO, G. & WIDDICOMBE, J.G. (1988b). Afferent neural pathways in cough and reflex bronchoconstriction. *J. Appl. Physiol.*, **65**, 1007–1023.

KARLSSON, J.A., LANNER, A.S. & PERSSON, C.G.A. (1990). Airway opioid receptors mediate inhibition of cough and reflex bronchoconstriction in guinea pigs. *J. Pharmacol. Exp. Ther.*, **252**, 863–868.

KASE, Y. (1980). Antitussive agents and their sites of action. *Trends Pharmacol. Sci.*, **5**, 237–239.

KASE, Y., WAKITA, Y., KITO, G., MIYATA, T., YUIZONO, T. & KATAOKA, M. (1970). Centrally induced cough in the cat. *Life Sci.*, **9**, 49–59.

MANNISTO, P.T., KARTTUNEN, P., LAHOVAARA, S., NISSINEN, E., DAVIES, J.E., ALGATE, D.R. & BAINES, M.W. (1988). Antitussive action of the new anilide derivative vadocaine hydrochloride compared with codeine phosphate in four animal models. *Arzneim. Forsch.*, **38**, 598–604.

MORRONE, L., PIZZA, A., MARTINELLI, A., MERLO, G., MAIORANO, V. & CHIANESE, R. (1993). Pilot study on efficacy and safety of a new antitussive drug, moguisteine: a double blind placebo controlled trial. *Adv. Ther.*, **10**, 67–73.

SNEDECOR, G.W. & COCHRAN, W.G. (1967). *Statistical Methods.* Ames, Iowa: The Iowa State University Press.

STEFKO, P.L. & BENSON, W.M. (1953). A method for the evaluation of antitussive agents in the unanesthetized dog. *J. Pharmacol. Exp. Ther.*, **108**, 217–223.

STENGAARD-PEDERSEN, K. & LARSSON, L. (1981). Interaction of putative opioid peptides with opiate receptors. *Acta Pharmacol. Toxicol.*, **48**, 39–46.

TAKAGI, K., FUKUDA, H. & YANO, K. (1960). Studies on antitussives I. Bioassay of antitussives. *Yakugaku Zasshi*, **80**, 1497–1501.

(Received August 2, 1993
Revised March 17, 1994
Accepted March 21, 1994)

Br. J. Pharmacol. (1994), **112**, 801–808

A role for endogenous histamine in interleukin-8-induced neutrophil infiltration into mouse air-pouch: investigation of the modulatory action of systemic and local dexamethasone

[1]Mauro Perretti, Jeanette G. Harris & Roderick J. Flower

Department of Biochemical Pharmacology, The William Harvey Research Institute, The Medical College of Saint Bartholomew's Hospital, Charterhouse Square, London EC1M 6BQ

1 When injected into a 6-day-old mouse air-pouch, human recombinant interleukin-8 (IL-8; 0.03–3 μg) induced, in a dose-dependent fashion, an accumulation of neutrophils which could be reliably assessed 4 h after the injection. No protein extravasation was measured above the values obtained with the vehicle alone (carboxymethylcellulose, CMC, 0.5% w/v in phosphate-buffered solution, PBS).

2 The IL-8 effect (routinely evaluated at 1 μg dose) was inhibited neither by local administration of actinomycin D (1 μg) nor by systemic treatment with indomethacin (1 mg kg^{-1}, i.v.), BWA4C (5 mg kg^{-1}, p.o.), methysergide (6 mg kg^{-1}, i.p.) and RP67580 (2 mg kg^{-1}, i.p.).

3 Treatment of mice with the H_1 antagonist, mepyramine (1–10 mg kg^{-1}, i.p.) resulted in a dose-dependent inhibition of the cell accumulation elicited by the chemokine, with a maximal reduction of approximately 50–60%. The mepyramine effect was not due to a non specific reduction of neutrophil function, since treatment with this drug (6 mg kg^{-1}, i.p.) did not modify the cell infiltration measured in response to a challenge with interleukin-1β (20 ng) or with the vehicle CMC to any extent. Moreover, treatment of mice with mepyramine did not modify cell counts in a peripheral blood film with respect to controls. Two other H_1 antagonists, chemically unrelated to mepyramine, diphenhydramine (9 mg kg^{-1}, i.p.) and triprolidine (0.5 mg kg^{-1}, i.p.), inhibited IL-8-induced migration to a similar extent (≈50–60%), whereas the H_2 antagonist, ranitidine (5 mg kg^{-1}, i.p.) was without effect.

4 The concept that endogenous histamine could be involved in the IL-8 effect was strengthened in two ways: (i) addition of histamine (0.2–2 μg) to a small dose of IL-8 (0.3 μg) potentiated the cell elicitation induced by the chemokine without having any effect on its own; (ii) IL-8-induced neutrophil accumulation was greatly impaired in animals depleted of mast cell amines by sub-chronic (5 day) treatment with compound 48/80 according to an established protocol.

5 The glucocorticoid dexamethasone (Dex; 1–50 μg per mouse, i.v., corresponding approximately to 0.03–1.5 mg kg^{-1}, given i.v. 2 h prior to challenge with IL-8) potently inhibited neutrophil infiltration with an approximate ED_{50} of 5 μg per mouse (≈0.3 mg kg^{-1}, i.v.). Passive immunisation of mice with a polyclonal sheep serum raised against the steroid-inducible anti-inflammatory protein lipocortin 1 (LC1) abolished the inhibitory action of Dex whereas a control serum was without effect.

6 Local administration of Dex at a dose which was ineffective when given systemically (1 μg) also reduced neutrophil migration induced by IL-8, either alone or in combination with histamine. This local inhibition (≈50%), also seen with hydrocortisone (30 μg), was prevented by the concomitant administration of the steroid antagonist RU38486 (10 μg) indicating the involvement of glucocorticoid receptor in the response.

7 These findings characterize further the mechanisms underlying PMN recruitment induced by IL-8 *in vivo*, and point to a role for histamine. The anti-inflammatory action of the glucocorticoids, as in some other models, appears to be LC1-dependent when these drugs are given systemically and LC1-independent when the steroids are given locally.

Keywords: Inflammation; interleukin-8; histamine; dexamethasone; lipocortin 1

Introduction

Interleukin-8 (IL-8) is the prototype of a new class of chemotactic cytokines recently named chemokines (Miller & Krangel, 1992). Since its discovery (Yoshimura *et al.*, 1987) it has always been clear that the polymorphonuclear leucocyte (PMN) was the main target cell for this cytokine. Indeed, IL-8 induces the classical pattern of phenomena typical of PMN activation, i.e. enzyme release, superoxide and leukotriene generation, β_2-integrin activation and *in vitro* chemotaxis (Carveth *et al.*, 1989; Schroder, 1989; Baggiolini *et al.*, 1989). The administration of IL-8 into specific tissue sites *in vivo* causes a potent and selective PMN accumulation which is distinguishable from the migration induced by other pro-inflammatory cytokines, such as interleukin-1 (IL-1) and tumour necrosis factor (TNF) as it does not require continuing DNA-dependent RNA synthesis (Rampart & Williams, 1988; Colditz *et al.*, 1989; Foster *et al.*, 1989; Rampart *et al.*, 1989). In this respect, IL-8 is considered to be a direct chemoattractant as are C5a and leukotriene B_4. Moreover, it is very likely that the endogenous release of IL-8 is involved in the chemotactic action of IL-1 (Huber *et al.*, 1991) although this interrelationship has yet to be confirmed *in vivo*.

We have recently characterized a murine air-pouch model for the evaluation of PMN migration using IL-1 as a stimulus (Perretti & Flower, 1993). In this study it was possible to determine that IL-1 acted through a type I receptor-mediated mechanism and in a manner dependent upon *de novo* protein synthesis. Moreover, a role for endogenous PAF, but not for arachidonic acid metabolites, was proposed on the basis of the differential effects of selective drugs. IL-1-induced PMN migration was sensitive to the

[1] Author for correspondence.

anti-inflammatory glucocorticoid hormone, dexamethasone (Dex). The inhibition which followed systemic treatment with Dex was mediated by the steroid-inducible anti-inflammatory protein lipocortin 1 (LC1), whereas the inhibition observed after local treatment with Dex was LC1-independent (Perretti & Flower, 1993).

In the present study we have used the murine air-pouch model to investigate the immunopharmacological modulation of IL-8-induced PMN migration. We describe the kinetics of the PMN accumulation into the air-pouch caused by this cytokine and the effect of various anti-inflammatory drugs which were evaluated to investigate potential endogenous mediators of the action of IL-8.

Methods

Mouse air-pouch model

Male Swiss Albino mice (22–25 g; Tuck, Essex) were used for all the experiments. Air-pouches were formed by s.c. injection of 2.5 ml of air on day 0 and day 3 (Perretti & Flower, 1993). Six days after the initial injection of air, mice (28–32 g) received a local injection of human recombinant IL-8 (72aa monocyte-derived form, generous gift of Dr I. Lindley, Sandoz Forschunginstitut, Wien, Austria) in 0.5 ml of carboxymethylcellulose (CMC; BDH, Dorset) 0.5% (w/v) in sterile phosphate-buffered solution (PBS). Control mice received CMC alone. This protocol was chosen on the basis of preliminary experiments, confirming the findings observed with IL-1 (Perretti & Flower, 1993), that is a poor migration in the absence of CMC. Using PBS + BSA 0.01% (w/v) as vehicle only $0.07 \pm 0.03 \times 10^6$ PMN and $0.21 \pm 0.11 \times 10^6$ PMN per mouse were recovered in the absence and presence of 1 μg IL-8, respectively (mean ± s.e.mean, $n = 4$ in both cases, not significant).

At various times after IL-8 administration mice were killed by CO_2 exposure and the pouches washed thoroughly with 2 ml of PBS containing 1 mM ethylenediaminetetracetic acid (EDTA) and 50 u ml^{-1} heparin. Lavage fluids were centrifuged at 220 *g* for 10 min at 4°C and the pellet was resuspended in 2 ml of PBS-EDTA-heparin. Leucocytes were counted after staining (1:10) in Turk's solution (crystal violet 0.01% w/v in acetic acid 3%) in an improved Neubauer hemocytometer. The number of PMN recovered from each pouch was then calculated.

In further experiments the migration caused by local administration of 20 ng human recombinant IL-1β (generous gift of Dr L. Parente, IRIS, Siena, Italy) was assessed, this dose of the cytokine being chosen on the basis of a previous study (Perretti & Flower, 1993). Pouches were washed at the 4-h time point, and PMN infiltration measured as described above.

Protein concentration in cell-free lavage fluids was measured according to the methodology described by Bradford (1976).

Drug treatment

The effect of putative inhibitors and/or antagonists was assessed either by local administration or by systemic treatment.

The role of *de novo* RNA synthesis was ascertained by co-administration into the air-pouch of actinomycin D (1 μg) together with IL-8 (1 μg). The potential synergism between IL-8 and histamine was evaluated in co-administration experiments in which a mixture of the cytokine, at a dose of 0.3 μg, and histamine (0.2 to 4 μg) in 0.5 ml CMC was injected in the air-pouches at time 0. The leucocyte accumulation was measured 4 h later.

The potential role of inflammatory mediators was investigated by systemic administration of selective drugs. Indomethacin (Sigma, Poole, Dorset) was given i.v. into the tail vein. Mepyramine (maleate, May and Baker Ltd., Essex), diphenhydramine (hydrochloride, Research Biomedical International, Natick, MA, U.S.A.), triprolidine (hydrochloride, Research Biomedical International, Natick, MA, U.S.A.), methysergide (maleate, Sandoz, U.K.), RP-67580 (*3aR,7aR*)-7,7-diphenyl-2-[1-imino-2-(2-methoxyphenyl)-ethyl]perhydroisoindol-4-one; generous gift of Dr C. Garret, Rhone-Poulenc Rorer, Vitry-sur-Seine, France) and ranitidine (Sigma, Poole, Dorset) were administered i.p. whereas BWA4C (N-(3-phenoxycinnamyl)-acetohydroxamic acid; The Wellcome Research Laboratories, Beckenham, Kent) was given by oral gavage; in all cases drug treatment was performed 15–20 min before IL-8 challenge. PMN migration was always evaluated 4 h following cytokine administration.

The inhibitory action of the anti-inflammatory glucocorticoid, Dex (sodium phosphate salt, David Ball Laboratories, Warwick) was carefully investigated. Mice were treated with Dex (1–50 μg per mouse corresponding to 0.03–1.5 mg kg^{-1}) i.v. 2 h before the local administration of IL-8. The role of endogenous LC1 in this action of the steroid was evaluated by passive immunisation of the mice with a specific anti-LC1 (αLC1) sheep antiserum (50 μl s.c., 24 h before Dex) using the time and dose protocol found to prevent Dex inhibition of IL-1-induced migration (Perretti & Flower, 1993). Control animals received an identical volume of normal sheep serum (Sigma). To evaluate its effectiveness following local treatment, Dex (at the dose of 1 μg shown to be effective against IL-1-induced cell migration, see Perretti & Flower, 1993) was given directly into the pouch either with IL-8 (1 μg) or with the mixture of IL-8 plus histamine (0.3 μg and 2 μg, respectively) as described above. The glucocorticoid nature of the Dex effect observed following local treatment was confirmed in two ways: first, the action of another glucocorticoid, hydrocortisone (30 μg; sodium succinate salt, Upjohn Ltd, U.K.) was assessed; second, the effect of the specific compound with anti-glucocorticoid properties, RU38486 (10 μg; Roussel-Uclaf, Paris, France) upon Dex-induced inhibition was evaluated.

To deplete mast-cell amines an established protocol was followed (Di Rosa *et al.*, 1971). Mice received six doses of compound 48/80 (Sigma) at 0.6 mg kg^{-1} i.p. at 12 h intervals followed by three doses of the same agent at 1.2 mg kg^{-1} i.p., after which the experiment was started by local administration of CMC alone or in combination with 1 μg IL-8. Control mice received repeated doses of PBS (5 ml kg^{-1}, i.p.) prior to challenge with the cytokine. Migration was assessed 4 h later.

In some experiments blood samples were obtained by cardiac puncture from a number of mice 4.5 h after treatment with mepyramine, or 2 h after treatment i.v. with Dex and the total number of leucocytes measured with a Coulter Counter (Coulter Electronics, Luton, Bedfordshire). The percentage of PMN and mononuclear cells was then assessed by staining in Turk's and the total number of each cell type then calculated.

Data and statistics

Data, PMN (10^6) migrated per mouse, are reported either as total migration or as net migration by subtracting the effect of CMC alone: this is stated for each table and figure. Statistical differences between treatments were assessed by analysis of variance followed by the Bonferroni test. Values of probability less than 0.05 were taken as significant.

Results

Characterization of IL-8-induced PMN migration into the mouse air-pouch

The dose of 1 μg of human recombinant IL-8 caused a time-dependent PMN infiltration into the pouch, with a max-

imal rate of influx between 2 and 4 h (3.1×10^6 PMN per h). The cell accumulation reached maximum by the 8-h time point and was greatly reduced by 24 h (Figure 1a). At the 4-h time point, the cumulative data for CMC and CMC + IL-8 1 μg were as follows (mean ± s.e.mean): $1.56 \pm 0.18 \times 10^6$ PMN ($n = 47$) and $5.84 \pm 0.28 \times 10^6$ PMN per mouse ($n = 70$), respectively ($P < 0.01$). The IL-8 effect appeared to be specific for PMN because no mononuclear cell infiltration was observed at any time point. PMN infiltration was not accompanied by any increase in plasma protein extravasation above that caused by CMC alone (2.18 ± 0.14 and 1.88 ± 0.12 mg protein in CMC and CMC plus 1 μg IL-8 groups, respectively, $n = 5$). The 4-h time point was selected and used in all subsequent experiments.

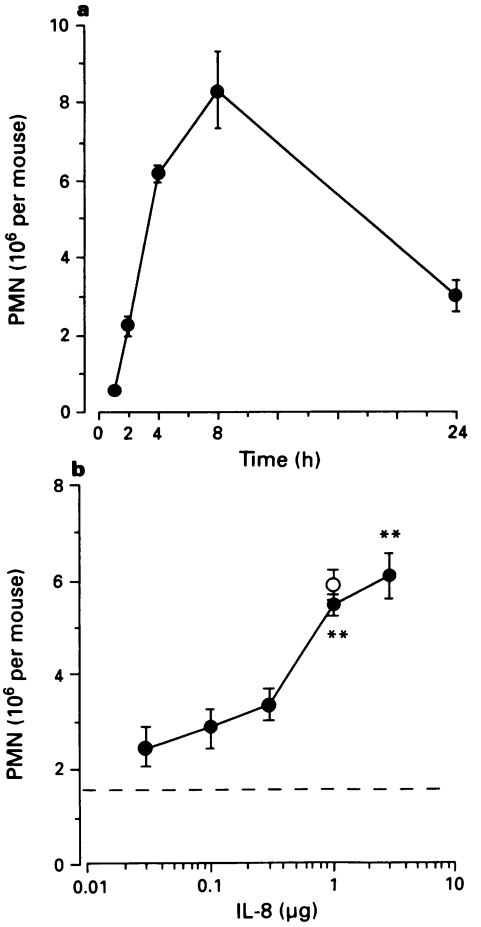

Figure 1 Characterization of interleukin-8 (IL-8)-induced PMN infiltration into the mouse air-pouch. (a) Time-course: 1 μg of IL-8 in 0.5 ml CMC was injected at time 0 directly in the air-pouch. At different times following treatment with the cytokine mice were sacrificed and PMN infiltration measured. Values are mean ± s.e. mean of 5–6 mice per time point. (b) Dose-response: different doses of IL-8 were injected in 0.5 ml CMC at time 0 and PMN migration evaluated 4 h later (●). Values are mean ± s.e.mean of 6–8 mice per group. In one case, actinomycin D 1 μg was injected concomitantly with IL-8 1 μg and migration evaluated 4 h later (○). The dotted line indicates the migration measured with CMC alone ($1.6 \pm 0.7 \times 10^6$ PMN, $n = 5$). $^{**}P < 0.01$ vs CMC.

The IL-8 effect was dose-dependent. Figure 1b shows that the dose of 0.3 μg per pouch caused a consistent effect, with an apparent peak observed at 3 μg. The dose of 1 μg, which caused a consistent infiltration and corresponded to ≈80% of maximal migration (Figure 1b), was selected and used in experiments to evaluate the potential role of inflammatory mediators. IL-8-induced PMN infiltration was not dependent upon DNA-dependent RNA synthesis: co-administration of actinomycin D (1 μg) was without effect on the response elicited by 1 μg IL-8 (Figure 1b).

Drug effect

The PMN accumulation which follows IL-8 administration into the pouch does not appear to depend upon arachidonic

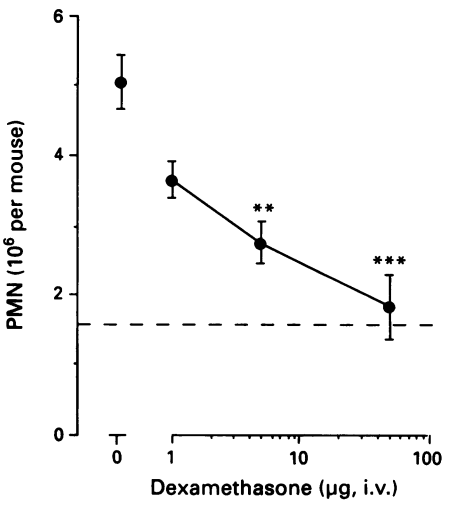

Figure 2 Systemic treatment with dexamethasone (Dex) inhibits interleukin-8 (IL-8)-induced PMN migration. Mice received an intravenous treatment with Dex 2 h prior to challenge with 1 μg of IL-8 (in 0.5 ml CMC directly into the pouch). PMN infiltration was measured 4 h later. Values are mean ± s.e.mean of 5–7 mice per dose. The dotted line indicates CMC-induced migration ($1.69 \pm 0.28 \times 10^6$ PMN, $n = 11$). $^{**}P < 0.01$ and $^{***}P < 0.001$ vs controls (dose 0 group).

Table 1 Drug effects on interleukin-8 (IL-8)-induced PMN migration

Treatment	*PMN* (10^6 per mouse)	*% inhibition*
CMC	1.90 ± 0.19 (4)	–
IL-8 1 μg	5.70 ± 0.64 (8)	0
+ Methysergide 6 mg kg^{-1}, i.p.	4.60 ± 0.83 (7)	19
CMC	1.90 ± 0.19 (4)	–
IL-8 1 μg	4.40 ± 1.18 (4)	0
+ Indomethacin 1 mg kg^{-1}, i.v.	3.40 ± 0.37 (4)	23
CMC	1.40 ± 0.72 (3)	–
IL-8 1 μg	4.75 ± 0.54 (4)	0
+ BWA4C 5 mg kg^{-1}, p.o.	3.50 ± 0.50 (6)	26
CMC	1.40 ± 0.50 (3)	–
IL-8 1 μg	5.65 ± 0.49 (4)	0
+ RP67580 2 mg kg^{-1}, i.p.	7.45 ± 1.50 (4)	– 31

Either vehicle or selective drugs were administered 10–20 min before local challenge with IL-8 (0.5 ml in carboxymethylcellulose (CMC) 0.5%). Control mice received CMC alone. In all cases migration was measured at the 4 h time-point. Results (mean ± s.e.mean, n) of each single experiment are reported. No treatment was statistically different from its respective IL-8 group.

acid metabolism, since both the cyclo-oxygenase inhibitor, indomethacin, and the 5'-lipoxygenase inhibitor, BWA4C, exerted no significant inhibition on this migration, when tested at doses which have been demonstrated to inhibit the appropriate enzyme (Table 1). The 5-hydroxytryptamine (5-HT) antagonist, methysergide, and the tachykinin antagonist to the NK_1 receptor, RP-67580, were also without effect (Table 1).

Systemic Dex was a powerful inhibitor of IL-8-induced migration with an ED_{50} of approximately 5 μg per mouse and a maximal inhibition of 91% if assessed as net migration (Figure 2). Passive immunisation of mice, according to a pre-determined protocol (Perretti & Flower, 1993), with a specific αLC1 sheep serum completely prevented the action of Dex (Figure 3). By contrast, a control sheep serum was without effect. In the absence of Dex treatment, the αLCl antiserum did not modify IL-8-induced migration (Figure 3). Dex 5 μg dose was also tested on the number of circulating PMN finding no effect with respect to control mice at the 2 h time point (mean ± s.e.mean): $0.69 \pm 0.20 \times 10^6$ PMN ml^{-1}, $n = 4$, and $0.80 \pm 0.17 \times 10^6$ PMN ml^{-1}, $n = 8$, in PBS- and Dex-treated mice, respectively.

Dex exerted a profound inhibition of IL-1-induced cell migration also after local injection into the pouch at time 0, an effect which is LC1-independent (Perretti & Flower, 1993). At the same dose used in the previous study (1 μg), local Dex significantly inhibited IL-8-induced PMN migration (Table 2). This inhibition was not due to a systemic absorption and action, inasmuch as 1 μg Dex was ineffective when given i.v. at time 0 (mean ± s.e.mean): $4.08 \pm 0.79 \times 10^6$ PMN ($n = 5$) and $3.48 \pm 0.43 \times 10^6$ PMN per mouse ($n = 5$), not significant, in PBS- and Dex-pretreated mice, respectively, in response to IL-8 1 μg at 4-h time point. Moreover, the effect of local Dex was mimicked by hydrocortisone, although a higher dose was necessary to inhibit PMN migration to a similar extent (Table 2). Dex-induced inhibition was prevented by co-injection of the antagonist RU38486, which alone had no action on the IL-8 response (Table 2).

The role of endogenous histamine on IL-8-induced PMN migration

A dose-dependent inhibition of IL-8-induced PMN migration was consistently observed with the selective H_1 antagonist, mepyramine (Figure 4) with a maximal inhibition of 50–60%. The action of mepyramine was not the result of a non-specific depression of PMN function because at a dose (6 mg kg^{-1}, i.p.) which greatly affected PMN infiltration caused by IL-8, this drug did not modify the cell influx measured in response to IL-1β (Table 3). Similarly, mepyramine treatment did not alter the 4 h-migration observed with CMC alone (mean ± s.e.mean): $1.56 \pm 0.48 \times 10^6$ PMN ($n = 5$) and $2.33 \pm 0.42 \times 10^6$ PMN per mouse ($n = 6$) in PBS- and mepyramine-treated mice, respectively. To exclude the possibility that mepyramine lowered peripheral PMN, the number of circulating mononuclear leucocytes and

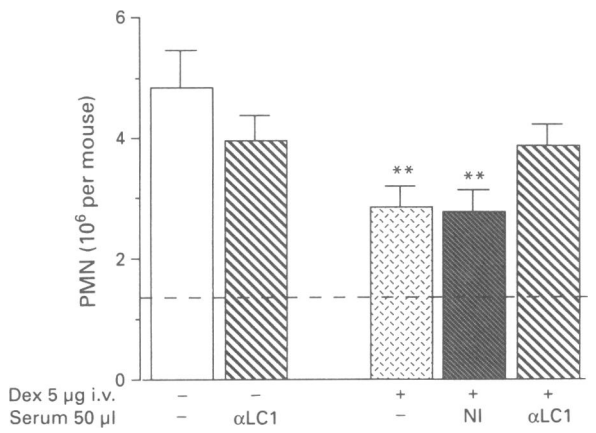

Figure 3 Anti-lipocortin 1 (αLC1) polyclonal serum prevents the inhibition exerted by systemic dexamethasone (Dex) upon interleukin-8 (IL-8)-induced PMN infiltration into the mouse air-pouch. Mice received either PBS (0.2 ml s.c.), non-immune (NI) or αLC1 sheep serum (50 μl s.c. in both cases) 24 h prior to the i.v. administration of Dex (5 μg per mouse). IL-8 (1 μg in 0.5 ml CMC) was injected 2 h after the steroid, and the PMN migration assessed at 4 h-time point. Values are mean ± s.e.mean for 9–12 mice per group. The dotted line indicates the migration measured with CMC alone ($1.36 \pm 0.13 \times 10^6$ PMN, $n = 6$). $^{**}P < 0.01$ vs PBS/PBS group.

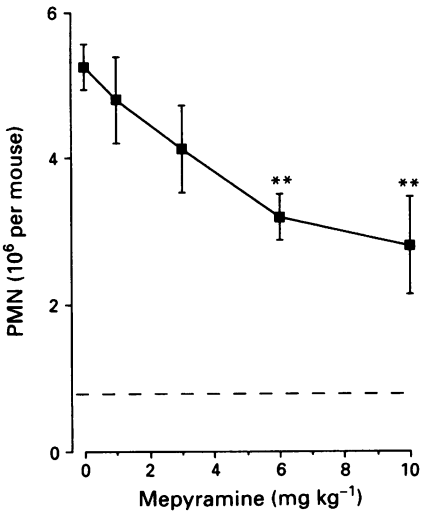

Figure 4 Mepyramine inhibits interleukin-8 (IL-8)-induced PMN influx into the mouse air-pouch. Mice received either PBS (10 ml kg^{-1}, i.p.) or mepyramine (i.p.) 10–20 min before local administration of IL-8 (1 μg in 0.5 ml CMC). PMN migration was measured 4 h later. Values are mean ± s.e.mean for 5–12 mice per dose. The dotted line indicates CMC-induced migration ($0.69 \pm 0.12 \times 10^6$ PMN, $n = 11$). $^{**}P < 0.01$ vs PBS-treated group (dose 0 group).

Table 2 Local effect of dexamethasone (Dex) and hydrocortisone on interleukin-8 (IL-8)-induced PMN migration into mouse air-pouch

Pretreatment	*PMN* (10^6 per mouse)	*% inhibition*
PBS	5.00 ± 0.42 (18)	0
Dex	3.00 ± 0.36** (20)	40
RU38486	4.67 ± 0.66 (6)	7
Dex + RU38486	4.12 ± 0.66 (6)	18
Hydrocortisone	2.43 ± 0.62** (6)	51

All treatments were done by co-administration with IL-8 (1 μg/0.5 ml carboxymethylcellulose (CMC)). Doses used: Dex 1 μg; RU38486 10 μg; hydrocortisone 30 μg. PMN influx was measured at 4 h-time point. Values are mean ± s.e.mean (n) and are reported as total migration since the effect of CMC ($1.17 \pm 0.38 \times 10^6$ PMN, $n = 7$) has not been subtracted. % inhibition was calculated vs IL-8-induced migration in control group (PBS-pretreated group).
$^{**}P < 0.01$ vs PBS-treated group.

PMN after i.p. treatment with either PBS (10 ml kg^{-1}) or mepyramine (6 mg kg^{-1}) was counted. The values found were: $4.29 \pm 0.6 \times 10^6$ ml^{-1} mononuclear cells and $0.74 \pm 0.06 \times 10^6$ ml^{-1} PMN in control animals ($n = 4$), and $4.33 \pm 0.36 \times 10^6$ ml^{-1} mononuclear leucocytes and $0.80 \pm 0.19 \times 10^6$ ml^{-1} PMN in mepyramine-treated mice ($n = 4$, not significant). The mepyramine effect was mimicked by two other H_1 antagonists, diphenhydramine and triprolidine, whereas the H_2 antagonist, ranitidine, was inactive (Figure 5).

Histamine co-injection with IL-8 into the air-pouch potentiated PMN infiltration. A significant and consistent migration was measured with IL-8 0.3 μg in the presence of 2 μg (10 nmol) histamine, a dose which did not potentiate the mild infiltration caused by CMC alone (Table 4). The histamine effect followed a bell-shaped curve, with an optimal dose of 2 μg (Figure 6). To further clarify the mechanism underlying the effectiveness of the local treatment with Dex, the effect of the steroid upon the IL-8/histamine mixture was evaluated. At a dose of 1 μg, Dex greatly affected (60% inhibition) the PMN accumulation measured under these conditions (Figure 7).

IL-8-induced PMN migration was impaired in mice depleted of mast cell amines by sub-chronic treatment with compound 48/80 (Figure 8). Cell accumulation in response to IL-8 was reduced by ≈50% in depleted animals, with no effect on the aspecific stimulus CMC (Figure 8).

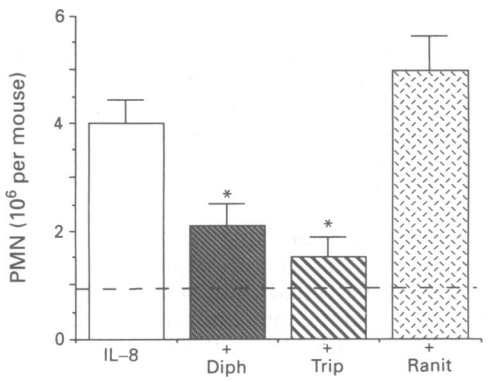

Figure 5 Effect of diphenhydramine (Diph), triprolidine (Trip) and ranitidine (Ranit) on interleukin-8 (IL-8)-induced PMN influx into the mouse air-pouch. Mice received either PBS (10 ml kg^{-1}, i.p.), Diph (9 mg kg^{-1}, i.p.), Trip (0.5 mg kg^{-1}, i.p.) or Ranit (5 mg kg^{-1}, i.p.) 10–20 min before local administration of IL-8 (1 μg in 0.5 ml CMC). PMN migration was measured 4 h later. Values are mean ± s.e.mean for six mice. The dotted line indicates CMC-induced migration ($0.89 \pm 0.15 \times 10^6$ PMN, $n = 6$). *$P < 0.05$ vs PBS-treated group.

Discussion

In this study we have observed a selective and consistent PMN infiltration following IL-8 administration into a 6-day-old subcutaneous air-pouch in the mouse. The kinetics of

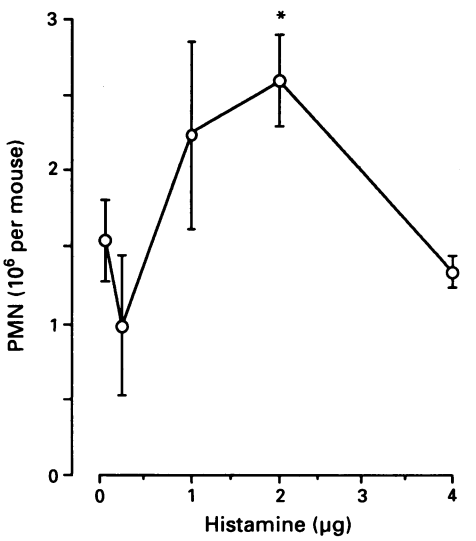

Figure 6 Dose-dependent histamine potentiation of interleukin-8 (IL-8)-induced PMN migration. Local treatment with IL-8 0.3 μg alone or with different doses of histamine was made at time 0, and PMN migration evaluated 4 h later. Values are mean ± s.e.mean for 15 mice (doses 0 and 2 μg) or for five mice (all other doses). The 4 h-migration induced by CMC alone has been subtracted and it was as in Table 4. *$P < 0.05$ vs IL-8 0.3 μg alone (histamine dose 0).

Table 3 Effect of mepyramine on cytokine-induced PMN migration into mouse air-pouch

Treatment (i.p.)	*IL-8* PMN	*IL-8* % inhibition	*IL-1β* PMN	*IL-1β* % inhibition
PBS	5.55 ± 0.36 (8)	0	5.33 ± 0.33 (6)	0
Mepyramine	2.32 ± 0.33 (12)**	58	6.52 ± 0.75 (6)	− 22

Mepyramine (6 mg kg^{-1}) or PBS (10 ml kg^{-1}) were injected i.p. 10 min before treatment with IL-8 (1 μg) or with IL-1β (20 ng) and PMN migration measured 4 h later. Values (10^6 per mouse) are mean ± s.e.mean (n) and express net migration having been corrected for the carboxymethylcellulose (CMC)-induced migration (0.86 ± 0.12, $n = 7$).
**$P < 0.01$ vs appropriate PBS-treated group.

Table 4 Histamine potentiates interleukin-8 (IL-8)-induced PMN migration into mouse air-pouch

Treatment	*PMN migration* (10^6 per mouse)	Net migration	*Protein* (mg per mouse)
CMC	1.74 ± 0.26 (13)	0	2.50 ± 0.27
Histamine 2 μg	1.54 ± 0.30 (5)	0	2.23 ± 0.52
IL-8 0.3 μg	3.28 ± 0.27 (15)**	1.54	2.77 ± 0.10
IL-8 0.3 μg + Histamine 2 μg	4.34 ± 0.30 (14)**‡	2.60	3.18 ± 0.39

Histamine and IL-8 were injected concomitantly in 0.5 ml carboxymethylcellulose (CMC) and PMN migration was evaluated 4 h later. Values are mean ± s.e.mean (n).
**$P < 0.01$ vs CMC alone.
‡$P < 0.05$ vs. IL-8 alone.

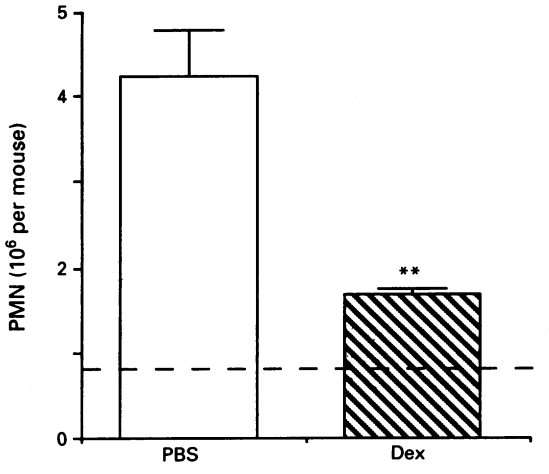

Figure 7 Effect of dexamethasone (Dex) on PMN migration induced by interleukin-8 (IL-8) in combination with histamine. Mice were given 0.5 ml of CMC containing histamine (2 μg) and IL-8 (0.3 μg), with or without 1 μg Dex, directly into the air-pouch. PMN influx was measured 4 h later. Values are mean ± s.e.mean for 6 mice per group. The dotted line indicates the migration observed with CMC alone ($0.8 \pm 0.3 \times 10^6$ PMN, $n = 6$). $^{**}P < 0.01$ vs PBS-treated group.

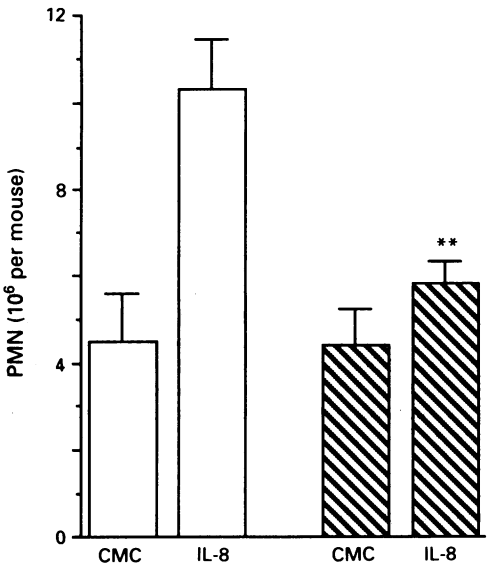

Figure 8 Effect of mast cell amine depletion on interleukin-8 (IL-8)-induced PMN migration. Mice received either PBS 5 ml kg^{-1}, i.p. (open columns) or compound 48/80 (hatched columns) as described in the Methods section for 5 days. IL-8 1 μg was then injected locally in 0.5 ml CMC, controls receiving CMC alone, and PMN migration measured 4 h later. Values are mean ± s.e.mean ($n = 4$ for CMC group and $n = 7$ for IL-8 group). $^{**}P < 0.01$ vs IL-8 group in PBS-treated mice.

the cell accumulation displayed the typical profile of an acute inflammatory process, with a maximal rate of influx between 2 and 4 h after injection of the cytokine. The IL-8 chemotactic response was not blocked by actinomycin D suggesting that continuing DNA-dependent RNA synthesis was not important for its action. Furthermore, the intense PMN accumulation was not paralleled by plasma protein extravasation. These characteristics, already observed after IL-8 intradermal injection in the rabbit skin (Colditz *et al.*, 1989; Foster *et al.*, 1989; Rampart *et al.*, 1989; Forrest *et al.*, 1992), confirmed that the murine air-pouch model was suitable for studying IL-8 chemotactic response and for assessing the effect of putative inhibitors.

Several conclusions can be drawn from the experiments performed with selective inhibitors of lipid mediator generation or action. Neither the cyclo-oxygenase inhibitor indomethacin (Higgs *et al.*, 1980) nor the selective 5'-lipoxygenase inhibitor BWA4C (Tateson *et al.*, 1988) had any effect upon the PMN migration into the pouch suggesting that eicosanoid formation is not a requisite for this response to occur. In contrast to IL-1-induced migration (Perretti *et al.*, 1993a), the IL-8 elicited response was insensitive to the selective NK_1 antagonist, RP-67580 (Garret *et al.*, 1991), which confirms the lack of effect of sensory neurone depletion obtained by pretreatment with capsaicin (J.G.H. and M.P., unpublished observation).

An interesting observation of this study is that the H_1 antagonist, mepyramine, inhibited IL-8-induced PMN migration into the air-pouch in a dose-dependent way. Its effect was not the consequence of a non-specific depression of cell function since this drug did not modify either CMC- or IL-1β-induced cell infiltration. The effect of two chemically distinct H_1 antagonists was also tested; we found that both diphenhydramine and triprolidine mimicked mepyramine, causing a similar reduction of cell accumulation in response to IL-8 (≈50–60%). The H_2 antagonist, ranitidine, was ineffective though tested at a dose reported to be active and specific (Del Soldato *et al.*, 1982). These data suggest a specific role for endogenous histamine and H_1 receptors in the response to IL-8. The specificity of its role is also highlighted by the ineffectiveness of methysergide treatment, which excludes the involvement of another endogenous amine, 5-HT.

It has been proposed that IL-8 may induce PMN infiltration *in vivo* through a haptotactic (i.e. migration induced by substrate bound chemoattractants) rather than a chemotactic (i.e. migration in response to soluble gradients of chemoattractants) action (Rot, 1993), and, that endothelial cells have specific binding sites for this cytokine (Rot, 1992; Tanaka *et al.*, 1993). According to this recently proposed model, the involvement of a co-factor(s) which facilitates leucocyte rolling on the endothelial wall (Rot, 1992), is a fundamental requisite for a subsequent firm adhesion via β_2-integrins (Lawrence & Springer, 1991; Von Andrian *et al.*, 1992). Previous studies have suggested that IL-8-induced PMN infiltration in the rat peritoneal cavity may require the presence of resident mast cells (Ribeiro *et al.*, 1991), and that a genetic strain of mice deficient of this cell type have an impaired response to IL-8 (reported in Rot, 1993). We have mimicked this situation by a subchronic treatment with compound 48/80, according to an accepted protocol (Di Rosa *et al.*, 1971), finding a marked reduction in the number of PMN migrated in response to IL-8 challenge. Migration due to CMC alone was not altered. The role of histamine was finally investigated in co-administration experiments. Exogenously added histamine, ineffective when given alone, dose-dependently potentiated PMN accumulation into the air-pouches in response to IL-8, with an optimal effect at the dose of 2 μg. Histamine potentiation of IL-8-induced migration was not accompanied by significant changes in protein extravasation. Histamine is well known to cause vascular leakage (Majno & Palade, 1961), however, the lack of effect on protein extravasation observed when administered into the pouch is unlikely to be due to the timing of the experiments, in that a single histamine injection causes significant plasma protein extravasation at the 4 h-time point (Collins *et al.*, 1993). Rather, the lack of effect is probably more related to the dose of histamine and/or the experimental model used. All these observations, together with the effect of the selective drug mepyramine and of compound 48/80 depletion experiments, suggest strongly that histamine, a mast cell product, is the co-factor required for manifestation of this important property of IL-8 *in vivo*. As stated above, PMN must roll on the endothelial wall before firmly adhering to these cells (Lawrence & Springer, 1991; Tanaka *et al.*, 1993), and the rolling process is brought about by selectins (Lasky, 1992),

one of which, P-selectin, is induced by histamine on endothelial cell membranes within minutes of the application (Lorant *et al.*, 1991; Lasky, 1992).

The anti-inflammatory glucocorticoid hormone, Dex, potently inhibited IL-8-induced PMN infiltration into the murine air-pouch, with an ED_{50} of approximately 5 μg per mouse ($\approx 150\ \mu g\ kg^{-1}$, i.v.). This inhibitory effect is likely to be brought about by endogenous LC1, since it was abrogated by passive immunisation of mice with a specific αLC1 polyclonal antibody. In this respect, this study confirms the observations obtained in IL-1-induced PMN migration (Perretti & Flower, 1993), and indicates that induction of LC1 can be a general mechanism by which systemic anti-inflammatory steroids can affect cytokine induced cell migration, and, more generally, the cellular response characteristic of the inflammatory process. Moreover, treatment with either the full length LC1 molecule, as well as with a N-terminal peptide of this protein, amino acids 2–26, resulted in a significant reduction of both IL-1- and IL-8-induced PMN accumulation (Cirino *et al.*, 1993; Perretti & Flower, 1993; Perretti *et al.*, 1993b), again strengthening the concept of LC1 as the mediator of the effect observed with systemic steroid treatment.

Local injection of Dex together with IL-8 resulted in a significant and consistent inhibitory effect of the action of this cytokine. The steroid had a similar action on IL-1-induced migration, with a mechanism which was LC1-independent (Perretti & Flower, 1993). The efficacy of Dex against IL-8 is, at a first glance, surprising because local administration of anti-inflammatory glucocorticoid hormones is well known to inhibit cell recruitment elicited by indirect agents, like IL-1, TNF and endotoxin, but not those induced by direct-acting agents, like C5a and formyl-Met-Leu-Phe (Ribeiro *et al.*, 1991; Perretti & Flower, 1993; Yarwood *et al.*, 1993). However, the Dex effect was specific and brought about by an interaction with the endogenous corticoid receptors, as evidenced by the antagonism exerted by RU38486 (Peers *et al.*, 1988). Moreover, another glucocorticoid, hydrocortisone, was similarly a potent inhibitor of cell infiltration. As discussed above, IL-8 should no longer be considered a classical direct-acting chemoattractant as we have reported here a role for endogenous histamine in its action. Dexamethasone inhibited the PMN influx induced by IL-8 plus histamine to a similar extent as the cell accumulation observed in response to IL-8 alone. It is likely that under these experimental conditions Dex and hydrocortisone are interfering with the action of histamine, rather than with its endogenous release. It is noteworthy that a recent study has shown Dex to be a potent inhibitor of histamine-induced PMN adherence to endothelial cells (Watanabe *et al.*, 1991). The exact molecular mechanism of the Dex effect, i.e. inhibition of histamine-induced P-selectin expression and/or of the biological effect of this adhesion molecule is at the moment a matter of speculation and requires further studies to be clarified.

In conclusion, this study identifies the mouse air-pouch model as a useful experimental system for the study of IL-8-induced PMN accumulation and suggests that this phenomenon may require endogenous histamine. The involvement of this biogenic amine may provide an explanation for the inhibitory action of locally injected Dex upon the cell response to the cytokine. As in other studies, the inhibition of PMN migration exerted by systemic Dex appears to be brought about by endogenous LC1.

This work was supported by the Ono Pharmaceutical Company (Osaka, Japan). R.J.F. is supported by an endowment from Lilly (Surrey, U.K.). The authors thank Dr J.D. Croxtall for the preparation and validation of the αLC1 sheep polyclonal serum. The technical support of Mr A. Mustafa is also acknowledged.

References

BAGGIOLINI, M., WALZ, A. & KUNKEL, S.L. (1989). Neutrophil-activating peptide-1/interleukin 8, a novel cytokine that activates neutrophils. *J. Clin. Invest.*, **84**, 1045–1049.

BRADFORD, M.M. (1976). A rapid and sensitive method for the quantitation of microgram quantities of protein utilizing the principle of protein-dye binding. *Anal. Biochem.*, **72**, 248–254.

CARVETH, H.J., BOHNSACK, J.F., MCINTYRE, T.M., BAGGIOLINI, M., PRESCOTT, S.M. & ZIMMERMANN, G.A. (1989). Neutrophil activating factor (NAF) induces polymorphonuclear leukocyte adherence to endothelial cells and to subendothelial matrix proteins. *Biochem. Biophys. Res. Commun.*, **162**, 387–393.

CIRINO, G., CICALA, C., SORRENTINO, L., CILIBERTO, G., ARPAIA, G., PERRETTI, M. & FLOWER, R.J. (1993). Anti-inflammatory actions of a N-terminal peptide from human lipocortin 1. *Br. J. Pharmacol.*, **108**, 573–574.

COLDITZ, I., ZWAHLEN, R., DEWALD, B. & BAGGIOLINI, M. (1989). *In vivo* inflammatory activity of neutrophil-activating factor, a novel chemotactic peptide derived from human monocytes. *Am. J. Pathol.*, **134**, 755–760.

COLLINS, P.D., WEG, V.B., FACCIOLI, L.H., WATSON, M.L., MOQBEL, R. & WILLIAMS, T.J. (1993). Eosinophil accumulation induced by human interleukin-8 in the guinea pig *in vivo*. *Immunology*, **79**, 312–318.

DEL SOLDATO, P., GHIORZI, A. & BUAROTTI, L. (1982). A rat model based on the histamine H_2-receptor-activation-induced gastric pathology. *Pharmacol. Res. Commun.*, **14**, 175–185.

DI ROSA, M., GIROUD, J.P. & WILLOUGHBY, D.A. (1971). Studies of the mediators of the acute inflammatory response induced in rats in different sites by carrageenan and turpentine. *J. Pathol.*, **104**, 15–29.

FORREST, M.J., EIERMANN, G.J., MEUER, R., WALAKOVITS, L.A. & MACINTYRE, D.E. (1992). The role of CD18 in IL-8 induced dermal and synovial inflammation. *Br. J. Pharmacol.*, **106**, 287–294.

FOSTER, S.J., AKED, D.M., SCHRODER, J.-M. & CHRISTOPHERS, E. (1989). Acute inflammatory effects of a monocyte-derived neutrophil-activating peptide in rabbit skin. *Immunology*, **67**, 181–183.

GARRET, C., CARRUETTE, A., FARDIN, V., MOUSSAOUI, S., PEYRONEL, J.-F., BLANCHARD, J.-C. & LADURON, P.M. (1991). Pharmacological properties of a potent and selective nonpeptide substance P antagonist. *Proc. Natl. Acad. Sci. U.S.A.*, **88**, 10208–10212.

HIGGS, G.A., EAKINS, K.E., MUGRIDGE, K.G., MONCADA, S. & VANE, J.R. (1980). The effect of non-steroid anti-inflammatory drugs on leukocyte migration in carrageenin-induced inflammation. *Eur. J. Pharmacol.*, **66**, 81–86.

HUBER, A.R, KUNKEL, S.L., TODD III, R.F. & WEISS, S.J. (1991). Regulation of transendothelial neutrophil migration by endogenous interleukin-8. *Science*, **254**, 99–102.

LASKY, L.A. (1992). Selectins: interpreters of cell-specific carbohydrate information during inflammation. *Science*, **258**, 964–969.

LAWRENCE, M.B. & SPRINGER, T.A. (1991). Leukocytes roll on a selectin at physiologic flow rates: distinction from and prerequisite for adhesion through integrins. *Cell*, **65**, 859–873.

LORANT, D.E., PATEL, K.D., MCINTYRE, T.M., MCEVER, R.P., PRESCOTT, S.M. & ZIMMERMAN, G.A. (1991). Coexpression of GMP-140 and PAF by endothelium stimulated by histamine and thrombin: a juxtacrine system for adhesion and activation of neutrophils. *J. Cell Biol.*, **115**, 223–234.

MAJNO, G. & PALADE, G.E. (1961). Studies on inflammation. I. Effect of histamine and serotonin on vascular permeability. An electron microscopy study. *J. Biophys. Biochem. Cytol.*, **11**, 571–606.

MILLER, M.D. & KRANGEL, M.S. (1992). Biology and biochemistry of the chemokines: a family of chemotactic and inflammatory cytokines. *Crit. Rev. Immunol.*, **12**, 17–46.

PEERS, S.H., MOON, D. & FLOWER, R.J. (1988). Reversal of the anti-inflammatory effects of dexamethasone by the glucocorticoid antagonist RU38486. *Biochem. Pharmacol.*, **37**, 556–557.

PERRETTI, M., AHLUWALIA, A., FLOWER, R.J. & MANZINI, S. (1993a). Endogenous tachykinins play a role in IL-1-induced neutrophil accumulation: involvement of NK-1 receptors. *Immunology*, **80**, 73–77.

PERRETTI, M., AHLUWALIA, A., HARRIS, J.G., GOULDING, N.J. & FLOWER, R.J. (1993b). Lipocortin-1 fragments inhibit neutrophil accumulation and neutrophil-dependent edema in the mouse: a qualitative comparison with an anti-CD11b monoclonal antibody. *J. Immunol.*, **151**, 4306–4314.

PERRETTI, M. & FLOWER, R.J. (1993). Modulation of IL-1-induced neutrophil migration by dexamethasone and lipocortin 1. *J. Immunol.*, **150**, 992–999.

RAMPART, M., VAN DAMME, J., ZONNEKEYN, L. & HERMAN, A.G. (1989). Granulocyte chemotactic protein/Interleukin-8 induces plasma leakage and neutrophil accumulation in rabbit skin. *Am. J. Pathol.*, **135**, 21–25.

RAMPART, M. & WILLIAMS, T.J. (1988). Evidence that neutrophil accumulation induced by interleukin-1 requires both local protein biosynthesis and neutrophil CD18 antigen expression *in vivo*. *Br. J. Pharmacol.*, **94**, 1143–1148.

RIBEIRO, R.A., FLORES, C.A., CUNHA, F.Q. & FERREIRA, S.H. (1991). IL-8 causes *in vivo* neutrophil migration by a cell-dependent mechanism. *Immunology*, **73**, 472–477.

ROT, A. (1992). Endothelial cell binding of NAP-1/IL-8: role in neutrophil emigration. *Immunol. Today*, **13**, 291–294.

ROT, A. (1993). Neutrophil attractant/activation protein-1 (interleukin-8) induces *in vitro* neutrophil migration by haptotactic mechanism. *Eur. J. Immunol.*, **23**, 303–306.

SCHRODER, J.-M. (1989). The monocyte-derived neutrophil activating peptide (NAP/Interleukin 8) stimulates human neutrophil arachidonate-5-lipoxygenase, but not the release of cellular arachidonate. *J. Exp. Med.*, **170**, 847–863.

TANAKA, Y., ADAMS, D.H. & SHAW, S. (1993). Proteoglycans on endothelial cell present adhesion-inducing cytokines to leukocytes. *Immunol. Today*, **14**, 111–115.

TATESON, J.E., RANDALL, R.W., REYNOLDS, C.H., JACKSON, W.P., BHATTACHERJEE, P., SALMON, J.A. & GARLAND, L.G. (1988). Selective inhibition of arachidonate-5-lipoxygenase by novel acetohydroxamic acids: biochemical assessment *in vitro* and *ex vivo*. *Br. J. Pharmacol.*, **94**, 528–539.

VON ANDRIAN, U.H., HANSELL, P., CHAMBERS, J.D., BERGER, E.M., FILHO, I.T., BUTCHER, E.C. & ARFORS, K.-E. (1992). L-selectin function is required for β_2-integrin-mediated neutrophil adhesion at physiological shear rates in vivo. *Am. J. Physiol.*, **263**, H1034–H1044.

WATANABE, M., YAGI, M., OMATA, M., HIRASAWA, N., MUE, S., TSURUFUJI, S. & OHUCHI, K. (1991). Stimulation of neutrophil adherence to vascular endothelial cells by histamine and thrombin and its inhibition by PAF antagonists and dexamethasone. *Br. J. Pharmacol.*, **102**, 239–245.

YARWOOD, H., NOURSHARGH, S., BRAIN, S. & WILLIAMS, T.J. (1993). Effect of dexamethasone on neutrophil accumulation and oedema formation in rabbit skin: an investigation of site of action. *Br. J. Pharmacol.*, **108**, 959–966.

YOSHIMURA, T., MATSUSHIMA, K., OPPENHEIM, J.J. & LEONARD, E.J. (1987). Neutrophil chemotactic factor produced by lipopolysaccharide (LPS)-stimulated human blood mononuclear leukocytes: partial characterization and separation from interleukin 1 (IL-1). *J. Immunol.*, **139**, 788–793.

(Received December 6, 1993
Revised March 11, 1994
Accepted March 21, 1994)

Br. J. Pharmacol. (1994), **112**, 809–816

Actions of two new antagonists showing selectivity for different sub-types of metabotropic glutamate receptor in the neonatal rat spinal cord

D.E. Jane, P.L.St.J. Jones, P.C-K. Pook, H-W. Tse & [1]J.C. Watkins

Department of Pharmacology, School of Medical Sciences, Bristol BS8 1TD

1 The presynaptic depressant action of L-2-amino-4-phosphonobutyrate (L-AP4) on the monosynaptic excitation of neonatal rat motoneurones has been differentiated from the similar effects produced by (1S,3R)-1-aminocyclopentane-1,3-dicarboxylate ((1S,3R)-ACPD), (1S,3S)-ACPD and (2S,3S,4S)-α-(carboxycyclopropyl)glycine (L-CCG-I), and from the postsynaptic motoneuronal depolarization produced by (1S,3R)-ACPD, by the actions of two new antagonists, α-methyl-L-AP4 (MAP4) and α-methyl-L-CCG-I (MCCG). Such selectivity was not seen with a previously reported antagonist, (+)-α-methyl-4-carboxyphenylglycine (MCPG).

2 MAP4 selectively and competitively antagonized the depression of monosynaptic excitation produced by L-AP4 (K_D 22 μM). At ten fold higher concentrations, MAP4 also antagonized synaptic depression produced by L-CCG-I but in an apparently non-competitive manner. MAP4 was virtually without effect on depression produced by (1S,3R)- or (1S,3S)-ACPD.

3 MCCG differentially antagonized the presynaptic depression produced by the range of agonists used. This antagonist had minimal effect on L-AP4-induced depression. The antagonism of the synaptic depression effected by (1S,3S)-ACPD and L-CCG-I was apparently competitive in each case but of varying effectiveness, with apparent K_D values for the interaction between MCCG and the receptors activated by the two depressants calculated as 103 and 259 μM, respectively. MCCG also antagonized the presynaptic depression produced by (1S,3R)-ACPD.

4 Neither MAP4 nor MCCG (200–500 μM) significantly affected motoneuronal depolarizations produced by (1S,3R)-ACPD. At the same concentrations the two antagonists produced only very weak and variable effects (slight antagonism or potentiation) on depolarizations produced by (S)-α-amino-3-hydroxy-5-methylisoxazole-4-propionic acid (AMPA) and N-methyl-D-aspartate (NMDA).

5 It is concluded that MAP4 is a potent and selective antagonist for those excitatory amino acid (EAA) receptors on neonatal rat primary afferent terminals that are preferentially activated by L-AP4, and that MCCG is a relatively selective antagonist for different presynaptic EAA receptors that are preferentially activated by (1S,3S)-ACPD and (perhaps less selectively) by L-CCG-I. These receptors probably comprise two sub-types of metabotropic glutamate receptors negatively linked to adenylyl cyclase activity.

Keywords: Excitatory amino acids; metabotropic glutamate receptors; antagonism; neonatal rat; spinal cord; α-methyl amino acids; L-AP4; (1S,3R)-ACPD; (1S,3S)-ACPD; L-CCG-I; MAP4; MCCG

Introduction

Investigation of the role of metabotropic glutamate receptors (mGluRs) in central nervous function requires the development of selective agonists and antagonists for the various sub-types of these receptors now known to exist (Tanabe *et al.*, 1992; 1993; Nakajima *et al.*, 1993; Okamoto *et al.*, 1994; for reviews, see Nakanishi, 1992; Schoepp & Conn, 1993). Such receptors appear to comprise two main families, those coupled to phosphoinositide (PI) hydrolysis (mGluR1 and 5) and those negatively coupled to adenylyl cyclase activity (mGluR2,3,4,6 and 7). Recently, members of a series of phenylglycine derivatives were shown to possess a range of neurochemical and electrophysiological properties compatible with differential activity at mGluR sub-types (Birse *et al.*, 1993; Eaton *et al.*, 1993b; Kemp *et al.*, 1994). Thus, certain phenolic glycines have agonist activity. For example, (S)-3-hydroxyphenylglycine (3HPG) stimulates PI hydrolysis in rat pup cerebrocortical slices (Birse *et al.*, 1993) and in mGluR1-expressing Chinese hamster ovary (CHO) cells (Hayashi *et al.*, 1994) while (RS)-3,5-dihydroxyphenylglycine (DHPG) has a similar (and more potent) action in mGluR1-expressing *Xenopus* oocytes (Ito *et al.*, 1992). In contrast, (S)-4-carboxyphenylglycine (4CPG) antagonizes (1S,3R)-1-amino-1,3-cyclopentane dicarboxylate (ACPD)-stimulated PI hydrolysis in rat pup cerebrocortical slices (Birse *et al.*, 1993) while both (S)-4CPG and (S)-4-carboxy-3-hydroxyphenylglycine (4C3-HPG) were found to be antagonists of L-glutamate-stimulated PI hydrolysis in CHO cells expressing mGluR1 (Hayashi *et al.*, 1994). In addition, (S)-4C3HPG and (S)-4CPG (less effectively) are agonists at mGluR2 receptors expressed in CHO cells, while a related substance, (+)-α-methyl-4-carboxyphenylglycine (MCPG), is an antagonist at both mGluR1 and mGluR2 receptor sub-types expressed in these cells (Hayashi *et al.*, 1994). MCPG is also an antagonist at guinea-pig cerebrocortical receptors activated by the agonist (S)-2-amino-4-phosphonobutyrate (L-AP4) and negatively linked to the cyclic AMP cascade (Kemp *et al.*, 1994). These L-AP4-activated receptors are currently unidentified but are not of the mGluR4 sub-type, which is one of three cloned metabotropic glutamate receptors that have been shown to be highly sensitive to this agonist (Nakanishi, 1992; Nakajima *et al.*, 1993; Okamoto *et al.*, 1994), since MCPG has no action at mGluR4 (Hayashi *et al.*, 1994).

In electrophysiological experiments (S)-4C3HPG, (S)-4CPG and (+)-MCPG antagonize a number of effects produced by the mGluR-selective agonist (1S,3R)-ACPD. Thus, each of these phenylglycine compounds blocks the (1S,3R)-ACPD-induced depolarization of neonatal rat motoneurones

[1] Author for correspondence.

in vitro (Birse *et al.*, 1993; Eaton *et al.*, 1993b; Jane *et al.*, 1993) and the excitation of rat thalamic neurones *in vivo* (Eaton *et al.*, 1993a). Also, in neurones of the nucleus tractus solitarius (NTS) in the rat brain stem *in vitro*, these same three phenylglycines antagonize the depression of excitatory postsynaptic currents (e.p.s.cs), the depression of inhibitory postsynaptic currents (i.p.s.cs), the depression of muscimol-induced currents and the potentiation of (**RS**)-α-amino-3-hydroxy-5-methylisoxazole-4-propionic acid (AMPA)-induced currents that is effected in each case by (1**S**,3**R**)-ACPD (Glaum *et al.*, 1993). These three phenylglycines selectively block nociceptive responses in rat thalamic neurones *in vivo*, relative to non-nociceptive sensory responses (Eaton *et al.*, 1993a; Salt *et al.*, 1993), and MCPG has been reported to block the induction of both NMDA-receptor dependent and NMDA receptor-independent long-term potentiation (LTP) in rat hippocampal slices (Bashir *et al.*, 1993).

While highly promising as lead compounds for the development of more specific antagonists, (S)-4C3HPG, (S)-4CPG and (+)-MCPG, which all show little or no activity at NMDA and non-NMDA ionotropic glutamate receptors (Birse *et al.*, 1993; Eaton *et al.*, 1993a,b; Jane *et al.*, 1993; Bashir *et al.*, 1993), present a spectrum of activity that may make it difficult in some cases to identify the precise mGluR sub-type(s) involved in particular synaptic phenomena. Thus (S)-4C3HPG and (S)-4CPG are agonists (Birse *et al.*, 1992; Pook *et al.*, 1993), and MCPG an antagonist (Pook *et al.*, 1993; Kemp *et al.*, 1994), at presynaptic receptors activated by (1S,3R)-ACPD to effect depression of monosynaptic excitation of neonatal rat motoneurones. Together with the neurochemical effects of these three phenylglycines at specific mGluR sub-types (Hayashi *et al.*, 1994) such results would point to mGluR2 being the presynaptic receptor on the terminals of neonatal rat primary afferent fibres. However, MCPG also antagonizes L-AP4-induced depression of monosynaptic excitation in neonatal rat motoneurones (Kemp *et al.*, 1994) but L-AP4 is not an agonist at mGluR2 receptors (Tanabe *et al.*, 1992) while none of the phenylglycines affect mGluR4 receptors (Hayashi *et al.*, 1994), which are potently activated by L-AP4 (Tanabe *et al.*, 1992; Nakanishi, 1992). The range of potencies observed for (+)-MCPG as an antagonist of the depression of monosynaptic excitation of neonatal rat motoneurones depending on the agonist used to produce the depression (Kemp *et al.*, 1994) suggested to us the possibility that more than a single mGluR sub-type was involved in such presynaptically-mediated effects. These and other considerations have led us to seek more sub-type-specific mGluR agonists and antagonists which would help us to identify receptor sub-types more definitively. To aid this search, we included the mGluR agonist (2S,3S,4S)-α-(car-

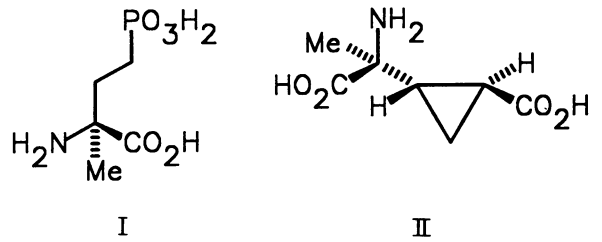

I II

Figure 1 Structures of MAP4 (I) and MCCG (II). For abbreviations, see text.

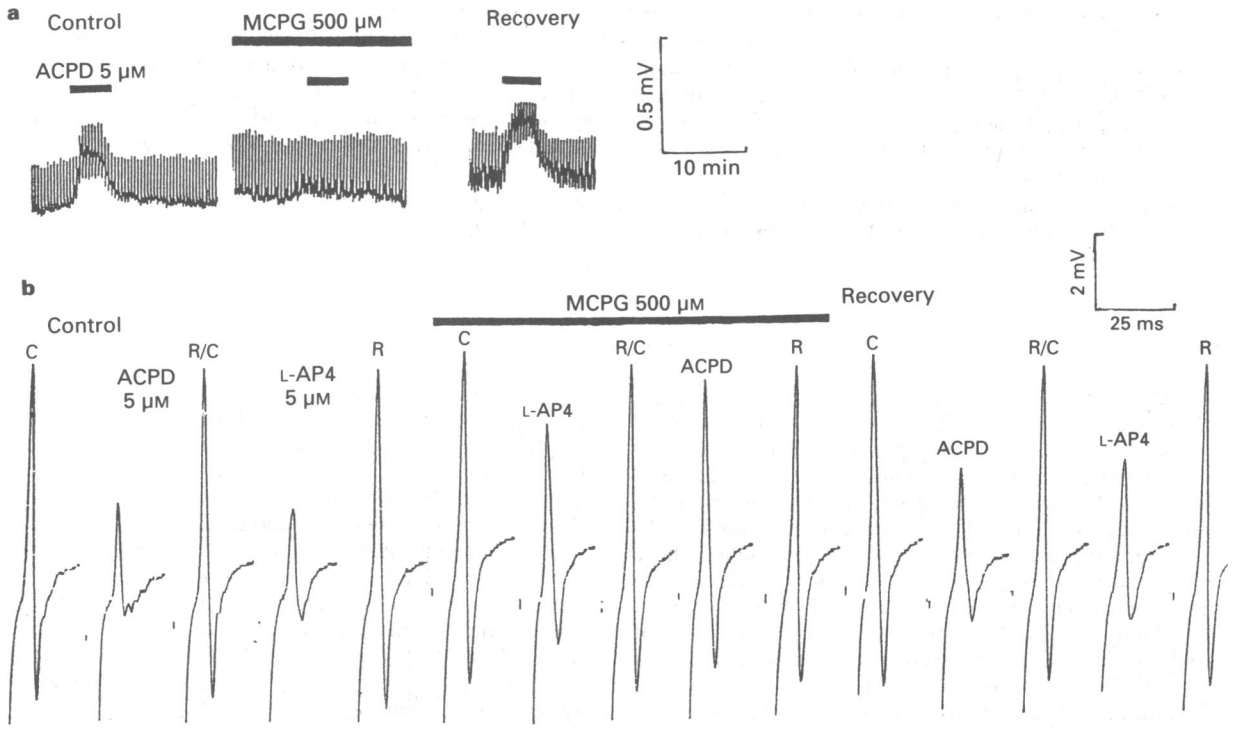

Figure 2 Non-selective antagonism of (1S,3R)-ACPD- and L-AP4-induced responses in neonatal rat motoneurones by (+)-α-methyl-4-carboxyphenylglycine (MCPG). (a) Shows chart recordings, in Mg^{2+}/D-AP5-containing medium, of slow components of the DR-VRP and depolarizing base line shift produced by 5 μM (1S,3R)-ACPD. L-AP4 (5 μM) produced no base-line shift (not shown; see Figure 2). Left, control response; centre, recorded during superfusion with medium containing 500 μM (+)-MCPG, showing abolition of the (1S,3R)-ACPD-induced depolarization; right, recovery, recorded 20 min after washout of antagonist. (b) In the same preparation as (a), both (1S,3R)-ACPD (5 μM) and L-AP4 (5 μM) produced a similar depression of the monosynaptic component of the DR-VRP. C denotes control responses recorded immediately prior to the addition of synaptic-depressant agonists; R denotes recovery responses, recorded 10 min after return to agonist-free medium; R/C, recovered response used as control for next agonist-induced depression. The centre panel of responses were recorded 30 min after the addition of (+)-MCPG (500 μM) to the superfusion medium; the depressant effects of both (1S,3R)-ACPD and L-AP4 were antagonized. The final sequence of responses, showing recovery from antagonism, was recorded 20 min after return to antagonist-free medium. For abbreviations, see text.

boxycyclopropyl)glycine (L-CCG-I) (Ishida *et al.*, 1993) among the substances we used to produce depression of monosynaptic excitation of neonatal rat motoneurones. Monosynaptic depression effected by L-CCG-I was less susceptible to antagonism by (+)-MCPG than that produced by L-AP4 (Kemp *et al.*, 1994) and may have involved a different receptor sub-type. We have also included (1S,3S)-ACPD which, like L-CCG-I and L-AP4, and unlike (1S,3R)-ACPD, causes presynaptic depression without causing postsynaptic depolarization (Pook *et al.*, 1992). We report here that two new mGluR antagonists, α-methyl-L-AP4 (MAP4) and α-methyl-L-CCG-I (MCCG) have selective actions at L-AP4-sensitive and (1S,3S)-ACPD/L-CCG-I-sensitive presynaptic receptors, respectively, on primary afferents to neonatal rat motoneurones. The structures of these compounds are shown in Figure 1.

Methods

MAP4 and MCCG were synthesized in our laboratory by methods that will be described in a subsequent publication. Hemisected isolated spinal cords from 1- to 5-day old rats were used (Evans *et al.*, 1982). Recordings were made from a ventral root of monosynaptic responses of motoneurones evoked by stimulation of the corresponding dorsal root (30 V, 2 pulses min^{-1}). The standard medium contained: (mM) NaCl 118, $NaHCO_3$ 25, KCl 3, $CaCl_2$ 2.5, D-glucose 12, gassed with 5% CO_2/95% O_2. In addition, for most experiments, 2 mM $MgSO_4$ and 50 μM D-2-amino-5-phosphonopentanoate (D-AP5) were included in the standard medium to eliminate slow synaptic responses mediated by N-methyl-D-aspartate (NMDA) receptors and to isolate the main component of the monosynaptic response which is mediated by

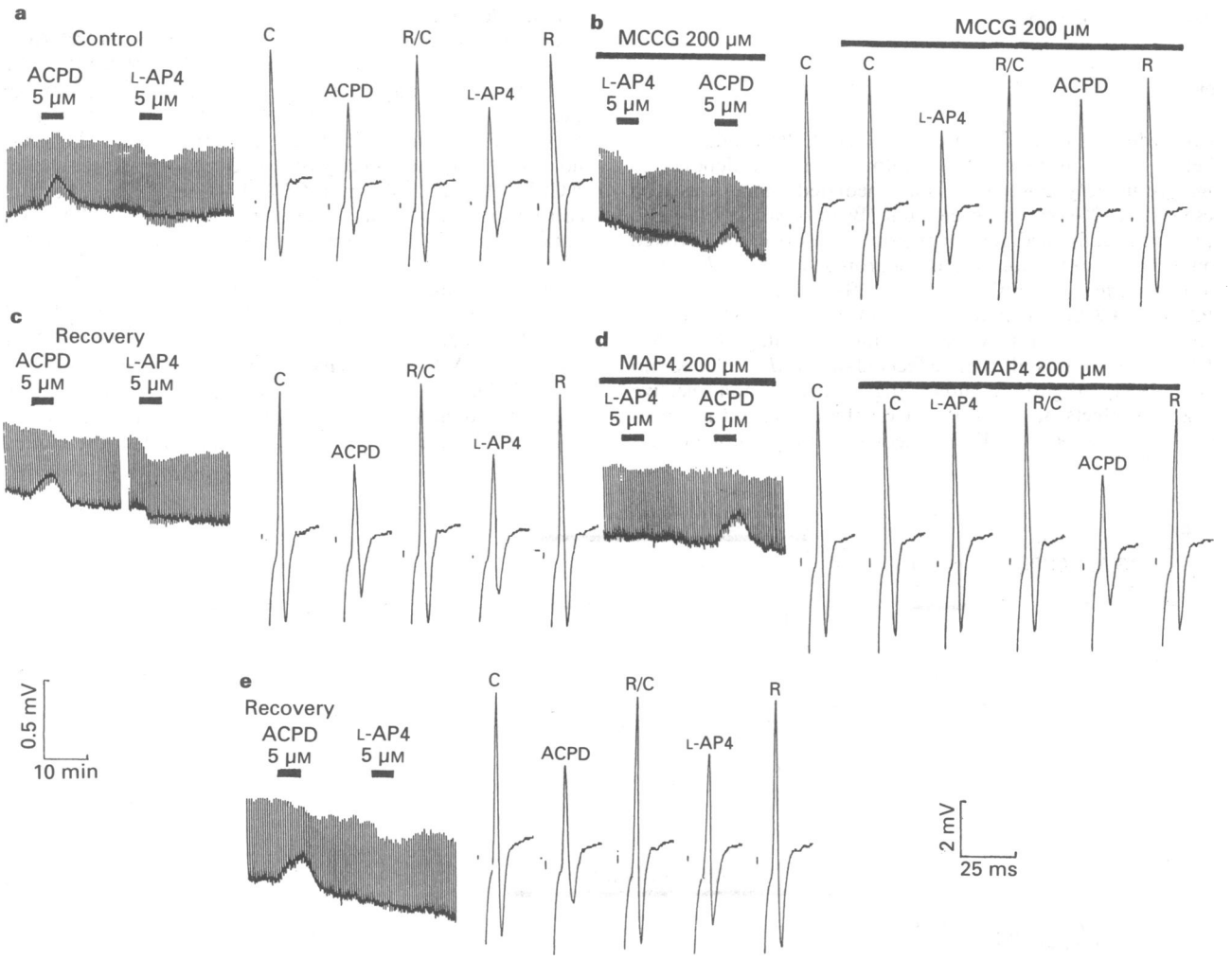

Figure 3 Selective antagonist effects of MCCG and MAP4 on (1S,3R)-ACPD and L-AP4-induced responses in neonatal rat motoneurones. All responses recorded in the same spinal cord preparation; Mg^{2+}/D-AP5-containing medium. (a–e) Each two-part section shows slow (left hand sequences, direct chart recordings) and fast (right hand sequences, oscilloscope traces) DR-VRPs. (a) Control responses showing the depolarizing base line shift produced by (1S,3R)-ACPD (5 μM), and small depressant effects of L-AP4 (5 μM) on the slow DR-VRP and the depressant effects of both (1S,3R)-ACPD and L-AP4 on the fast component of the DR-VRP. (b) Recorded 15 min after addition of 200 μM MCCG to the medium. This antagonist, which itself had no overt action on the slow or fast components of the synaptic response, selectively reduced the depression of the fast component of the DR-VRP produced by (1S,3R)-ACPD without altering the effects of L-AP4 on slow and fast components of the DR-VRP or the depolarizing effect of (1S,3R)-ACPD. (c) Responses recorded 35 min after return to normal (antagonist-free) medium. (d) Recorded 15 min after changing to medium containing 200 μM MAP4, which had no effect on the amplitude of the evoked synaptic responses. The depressant effects of L-AP4 on both the slow and fast components of the DR-VRP were antagonized by MAP4, without antagonism of either the deloparizing effect of (1S,3R)-ACPD or the depression of the fast component of the DR-VRP produced by (1S,3R)-ACPD. (e) Recorded 25 min after returning to normal medium, showing near-complete recovery of the L-AP4-induced depression. C, control; R/C, recovery responses for fast component of DR-VRP following removal of depressant agonists and representing control responses preceding the next addition of depressant; R, recovery at end of sequence of medium changes. Left hand calibration (0.5 mV, 10 min) applies to slow, chart recorded components of DR-VRP; right hand calibration (2 mV, 25 ms) refers to oscilloscope traces of fast components of DR-VRP. For abbreviations, see text.

receptors of the α-amino-3-hydroxy-5-methylisoxazole-4-propionic acid (AMPA) and/or kainate types (Long *et al.*, 1990). The rate of superfusion of the medium over the cord was 1 ml min^{-1}. After control responses to dorsal root stimulation were obtained, flow of standard medium was changed to agonist-containing medium (5 ml) at various concentrations, in order to cause depression of the monosynaptic response within the range of approximately 5–95% (usually 25–75%). Following the determination of control levels of depression by L-AP4, (1S,3S)-ACPD, (1S,3R)-ACPD or L-CCG-I the depression of the response was then measured in each case in a medium containing MAP4 or MCCG (both 200–500 μM). Some experiments were also conducted with standard medium (excluding $MgSO_4$ and D-AP5) that contained tetrodotoxin (TTX; 10^{-5} M for 2 min, then 10^{-7} M continuously) in order to investigate the effects of the antagonists on depolarization directly generated in motoneurones by (1S,3R)-ACPD, or by the inotropic receptor agonists NMDA and AMPA.

Results

As recorded from ventral roots (1S,3R)-ACPD produces two different effects in neonatal rat motoneurones – a depolarization, presumably postsynaptically mediated, since it is also present in TTX-containing medium (Birse *et al.*, 1993) – and a presynaptically-mediated depression of dorsal root-evoked monosynaptic excitation of motoneurones (Pook *et al.*, 1992). The latter effect is simulated by (1S,3S)-ACPD (Pook *et al.*, 1992), by L-CCG-I (Ishida *et al.*, 1993) and by L-AP4 (Evans *et al.*, 1982). A previously reported mGluR antagonist, (+)-MCPG, antagonizes all these effects (Jane *et al.*, 1993; Kemp *et al.*, 1994). Figure 2 shows the relatively non-selective antagonist effects of (+)-MCPG on the depolarization produced by (1S,3R)-ACPD in neonatal rat motoneurones (Figure 2a) and on the (1S,3R)-ACPD- and L-AP4-induced depression of monosynaptic excitation of these motoneurones (Figure 2b).

In contrast, MCCG and MAP4 both showed differential antagonism of these three responses, each antagonist producing a characteristic pattern of activity. Figure 3a and b shows that neither the postsynaptic motoneurone depolarization produced by (1S,3R)-ACPD, nor the presynaptic depression of monosynaptic excitation produced by L-AP4, was affected by 200 μM MCCG; however, this antagonist attenuated the presynaptic depression produced by (1S,3R)-ACPD. On the other hand, MAP4 (Figure 3c and d) greatly attenuated the presynaptic depression produced by L-AP4 without affecting the depolarization of presynaptic depression produced by (1S,3R)-ACPD. Neither MCCG nor MAP4 affected either the slow or fast components of the DR-VRP when added alone to the superfusion medium (Figure 3b and d). Rapid recovery was obtained after each antagonist was washed out (Figure 3c and e).

In addition to its effect as an antagonist of (1S,3R)-ACPD-induced depression of the monosynaptic DR-VRP, MCCG (200 μM) also antagonized the depression of monosynaptic excitation produced by (1S,3S)-ACPD (Figure 4a) and L-CCG-I (Figure 4b). In contrast, MAP4 (200 μM) had little or no effect on the depression produced by either (1S,3S)-ACPD (Figure 5a) or L-CCG-I (Figure 5b). At higher concentrations (1 mM), however, MAP4 did show some antagonism of the synaptic depression affected by L-CCG-I (Figure 5c).

Dose-response curves were constructed for the depression of monosynaptic excitation produced by L-AP4, L-CCG-I and (1S,3S)-ACPD in the presence and absence of MAP4 (300 μM) or MCCG (300 μM). MAP4 produced a consistently parallel shift to the right in the curve for L-AP4 (Figure 6a), a lesser and non-parallel shift to the right in the curve for L-CCG-I (Figure 6b) and no significant shift in the curve for

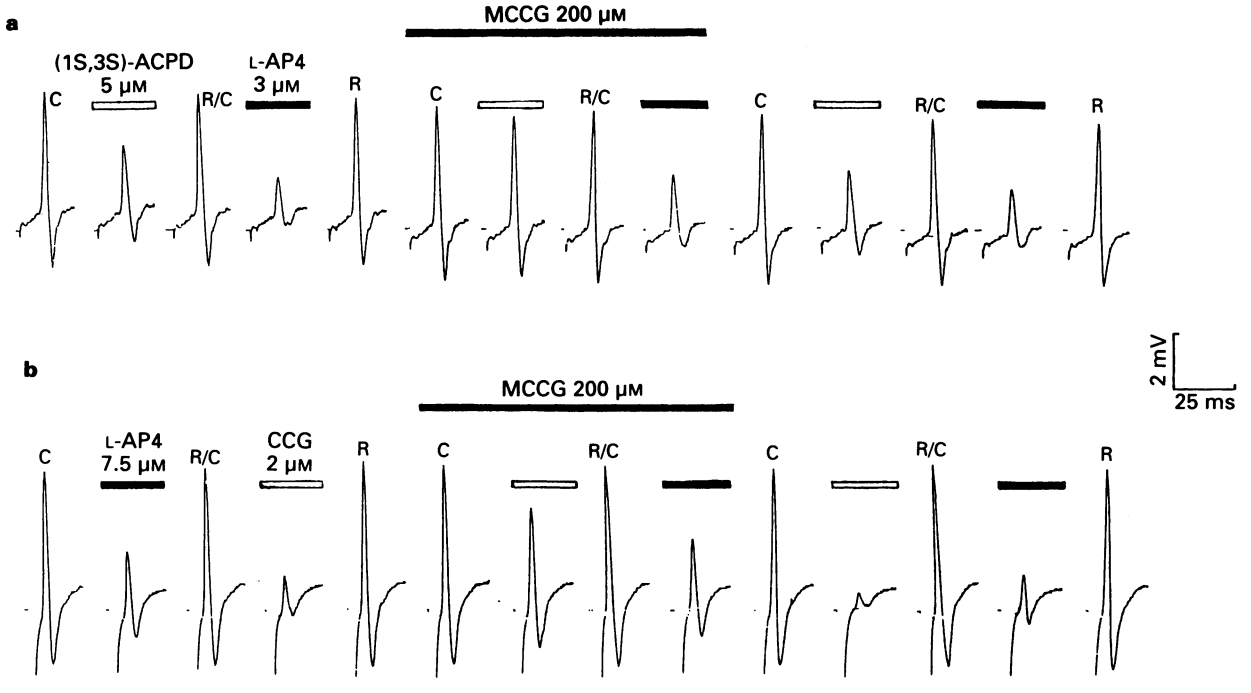

Figure 4 Selective antagonism by MCCG of (1S,3S)-ACPD and L-CCG-I-induced depression of monosynaptic DR-VRP in neonatal rat motoneurones. (a) Shows depression of synaptic response by (1S,3S)-ACPD (5 μM) and L-AP4 (3 μM). MCCG (200 μM) almost completely abolished the depression produced by (1S,3S)-ACPD and was less effective versus L-AP4. (b) Shows selective antagonism by MCCG (200 μM) of L-CCG-I (2 μM)-induced depression of the monosynaptic DR-VRP relative to L-AP4 (7.5 μM)-induced depression. (a) and (b) are from different preparations; Mg^{2+}/D-AP5-containing medium. The centre sequences of responses were recorded 20 min after beginning superfusion with antagonist-containing medium. The two sequences of responses showing recovery from the antagonists were recorded 30–35 min after return to antagonist-free medium. C, control responses recorded before each addition of depressant agonist. R/C, recovered response acting as control for subsequent agonist-induced depression. R, recovery, recorded at end of each sequence of medium changes. For abbreviations, see text.

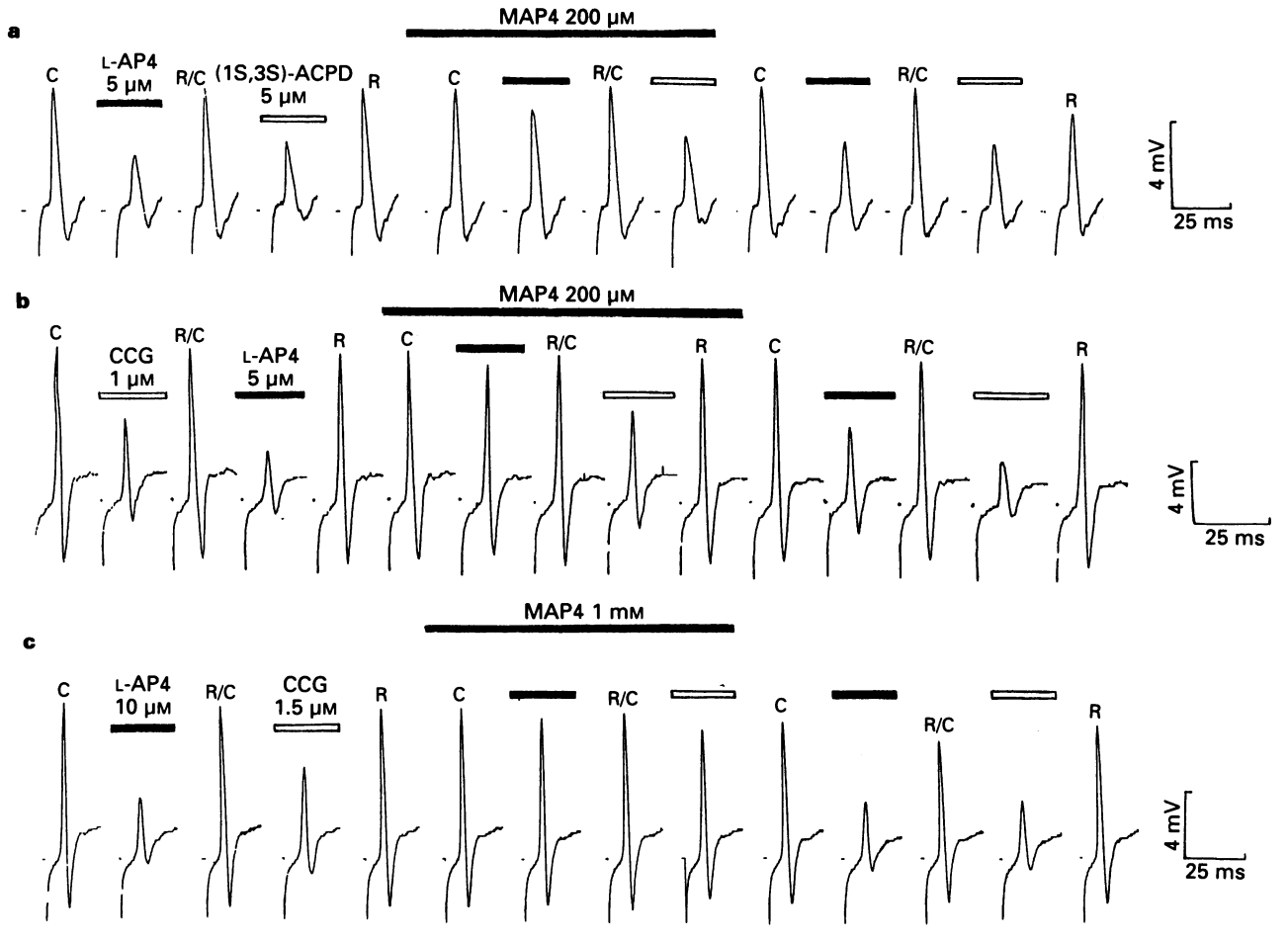

Figure 5 Three separate preparations showing selective antagonism by MAP4 of L-AP4-induced synaptic depression relative to (1S,3S)-ACPD- and L-CCG-I-induced depression. (a) MAP4 (200 μM) antagonized the depression produced by 5 μM L-AP4 with little or no effect on the depression produced by 5 μM (1S,3S)-ACPD. (b) MAP4 (200 μM) selectively antagonized the depression produced by 5 μM L-AP4 with little or no effect on the depression produced by 1 μM L-CCG-I. (c) MAP4 (1 mM), almost abolished the depression produced by 10 μM L-AP4 and also antagonized the lesser depression produced by 1.5 μM L-CCG-I. Other details as Figure 4. For abbreviations, see text.

(1S,3S)-ACPD (Figure 6c). MCCG produced a parallel rightward shift in the curve for L-CCG-I (Figure 6e), a similar parallel shift in the case of (1S,3S)-ACPD (Figure 6f) and either no effect or a slight potentiation (Figure 6d) in the case of L-AP4. A feature of such experiments was the tendency of the preparation to become more sensitive to the agonists after prolonged treatment with an antagonist. This is reflected in the recovery dose-response curves shown in Figure 6b,e and f.

Table 1 gives apparent K_D values calculated for the interactions between MAP4 or MCCG and the receptors activated by L-AP4, L-CCG-I and (1S,3S)-ACPD. The most potent action was the antagonism by MAP4 of L-AP4-induced synaptic depression; the apparently non-competitive action of MAP4 versus L-CCG-I was more than ten fold weaker. The apparent K_D values calculated for the antagonism by MCCG of the depressant responses produced by (1S,3S)-ACPD and L-CCG-I were relatively close to one another, but the difference between them did reach statistical significance.

It was important to establish the selectivity of MAP4 and MCCG as antagonists of presynaptic excitatory amino acid (EAA) receptors mediating synaptic depression, relative to postsynaptic metabotropic and ionotropic excitatory receptors causing depolarization. Table 2 indicates that, in a TTX-containing medium, and at a concentration (250 μM) which antagonized presynaptic depressant responses, neither of the two antagonists significantly affected similar magnitude depolarizations produced by (1S,3R)-ACPD (25 μM) or N-methyl-D-aspartate (NMDA, 7 μM). Each of the antagonists produced a small depression of the depolarizations induced by (S)-α-amino-3-hydroxy-5-methylisoxazole-4-propionic acid (AMPA, 1.2–1.5 μM). However, this was significant only in the case of MAP4 versus AMPA-induced depolarizations, and the failure to achieve complete recovery of the AMPA depolarizations after washout in these cases may have reflected a slight change in the responsiveness of the preparations during the course of these experiments. At higher concentrations, slight potentiation of depolarizations produced by AMPA (in the case of MCCG) or NMDA (in the case of MAP4) were sometimes observed (Figure 7).

Discussion

These results indicate that MAP4 and MCCG, which had relatively little effect on responses mediated by ionotropic EAA receptors (Table 2; Figure 7), discriminate effectively between three types of responses produced in neonatal rat motoneurones by specific metabotropic glutamate receptor agonists as recorded electrophysiologically: (a) the depolarization produced by (1S,3R)-ACPD; (b) the depression of monosynaptic excitation effected by L-CCG-I, (1S,3S)-ACPD and (1S,3R)-ACPD, and (c) the depression of monosynaptic excitation mediated by L-AP4. MAP4 was selective for L-AP4-induced depression, and MCCG preferentially antagonized (1S,3R)-ACPD-induced depression. At the same concentrations of MAP4 and MCCG used to show their selective presynaptic antagonist effects, neither of these two substances

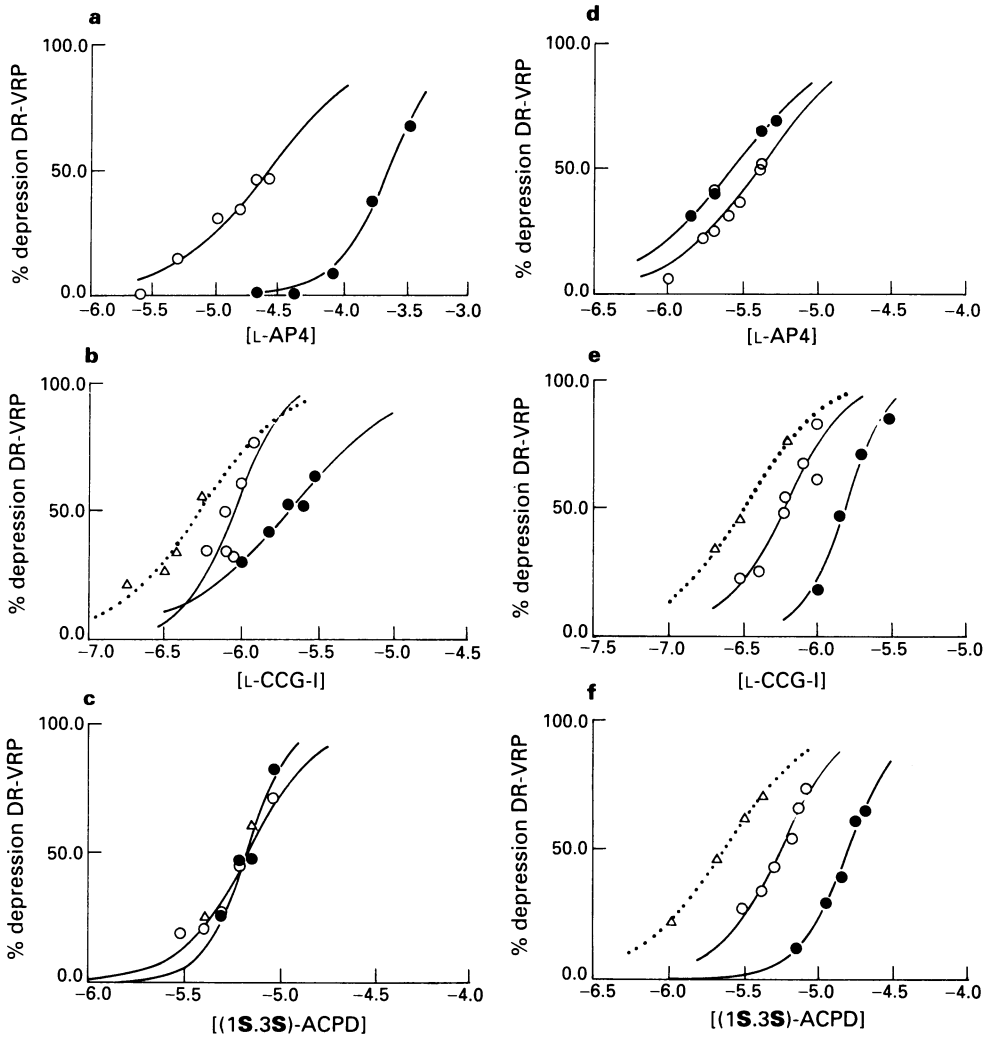

Figure 6 Dose-response curves for depression of monosynaptic DR-VRP by L-AP4, (1S,3S)-ACPD and L-CCG-I in presence and absence of MAP4 or MCCG. (a,d) Depression by L-AP4; (b,e) depression by L-CCG-I; (c,f) depression by (1S,3S)-ACPD. (a–c) Antagonist MAP4 (300 μM); (d–f) antagonist MCCG (300 μM). (○) Control responses; (●) responses recorded in presence of antagonist; (△) responses recorded after removal of antagonist. Parallel shifts to the right, showing competitive antagonism, observed for MAP4/L-AP4 (a), MCCG/L-CCG-I (e) and MCCG/(1S,3S)-ACPD (f); non-parallel shift to the right, showing non-competitive antagonism for MAP4/LCCG-I (b). A slight potentiation (shift to the left) seen for MCCG/L-AP4 (d). Note that after washout of the antagonists the preparation became more sensitive to the depressant agonists than before exposure to the antagonists. Ordinates: % depression of the monosynaptic response; abcissae, log concentration of depressant agonist. For abbreviations, see text.

antagonized the depolarizations produced in neonatal rat motoneurones by (1S,3R)-ACPD, which were previously shown to be blocked by (S)-4C3H-PG, (S)-4CPG and (+)-MCPG (Birse *et al.*, 1993; Eaton *et al.*, 1993b; Jane *et al.*, 1993; Kemp *et al.*, 1994). Such depolarizations are probably mediated postsynaptically by mGluR1 receptors since the three phenylglycine derivatives that antagonize these responses are also antagonists at mGluR1 receptors expressed in CHO cells (Hayashi *et al.*, 1994). However, the same three mGluR1 receptor antagonists also have actions at presynaptic EAA receptors, activation of which effects depression of monosynaptic excitation of neonatal rat motoneurones. (S)-4C3HPG is a moderately potent agonist and (S)-4CPG a relatively weak agonist at presynaptic EAA receptors (Pook *et al.*, 1993), while (+)-MCPG is an antagonist at these receptors, reducing depression of excitation mediated by (1S,3R)-ACPD, (1S,3S)-ACPD, L-AP4, (S)4C3HPG (and the positional isomer (S)-3C4HPG) and L-CCG-I (Kemp *et al.*, 1994 and Figure 1). Except in the case of L-AP4, such depression is likely to be mediated by mGluR2 receptors since the depressant effects of L-CCG-I, (1S,3R)-ACPD, (S)-4C3HPG, (S)-3C4HPG and (S)-4CPG on monosynaptic excitation and the antagonism of these effects by (+)-MCPG parallel their effects on mGluR2 expressed in CHO cells (Hayashi *et al.*, 1994). However, L-AP4 is not an agonist at mGluR2 receptors (Tanabe *et al.*, 1992; Nakanishi *et al.*,

Table 1 Apparent K_D values calculated for the interaction between MAP4 or MCCG and metabotropic glutamate receptors mediating the presynaptic depressant effects of L-AP4, (1S,3S)-ACPD and L-CCG-I

	Antagonist (App K_D, μM) versus		
Antagonist	L-AP4	(1S,3S)-ACPD	L-CCG-I
MAP4	22 ± 5(5)	n.e.(4)[1]	>200(6)[2]
MCCG	n.e.(3)[1]	103 ± 28(5)*	259 ± 34(5)*

Values are μM ± s.e.mean (no. of experiments).
[1]n.e. = no effect (no consistent antagonism at 300 μM).
[2]Non-parallel dose-response curves in presence and absence of antagonist.
*Difference statistically significant ($P<0.02$, Student's t test).
For abbreviations, see text.

Table 2 Effects of MCCG and MAP4 on neonatal rat motoneuronal depolarizations induced by (1S,3R)-ACPD, NMDA or AMPA

		% control depolarization	
Agonist	*Conc.* (μM)	*MCCG* (250 μM)	*MAP4* (250 μM)
(1S,3R)-ACPD	25	103 ± 6(6)[1,2]	95 ± 8(5)*[3]
NMDA	7	87 ± 6(4)[1]	100 ± 6(3)[3]
AMPA	1.2–1.5	79 ± 7(4)[2]	73 ± 2(3)*

All agonists tested in the same preparations; TTX-containing medium.
*Difference statistically significant ($P<0.05$); pairs 1,2,3 not significantly different (Mann-Whitney U-Test).

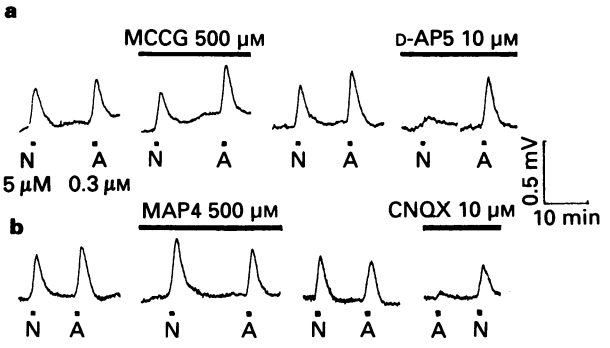

Figure 7 Effects of MCCG and MAP4 on depolarizing responses mediated by NMDA or AMPA receptors. (a) Shows lack of depressant effect of MCCG (500 μM) on either NMDA (5 μM, N)- or AMPA (0.3 μM, A)-induced depolarizations, and subsequent selective depression of NMDA-induced responses by 10 μM D-AP5. (b) Recorded in same spinal cord preparation following recovery from D-AP5-containing medium (approx 1 h), shows lack of effect of MAP4 (500 μM) on AMPA-induced responses and slight potentiation of NMDA-induced responses, with subsequent selective depression of AMPA-induced responses by CNQX (10 μM). Left to right: control responses, responses recorded 20 min after beginning MCCG- or MAP4-containing medium, responses recorded 20 min after washout or MCCG or MAP4, responses recorded 20 min after perfusion with D-AP5 or CNQX-containing medium. For abbreviations, see text.

1992). Therefore the presynaptic depressant effect of L-AP4 and its antagonism by (+)-MCPG must be mediated at receptors other than mGluR2. The present work shows that depression produced by L-AP4 is selectively blocked by MAP4 while the depressions produced by L-CCG-I, (1S,3R)-ACPD and (1S,3S)-ACPD are selectively blocked by MCCG. These results thus confirm the participation of at least two types of presynaptic receptor in the mediation of such depressant effects, and implicate mGluR2 as one of the mGluR sub-types involved.

The nature of the receptor type mediating the depression produced by L-AP4 is currently unknown, but is probably neither mGluR4 nor mGluR6, which, with mGluR7, comprise the range of L-AP4-sensitive mGluR receptors currently identified (Tanabe *et al.*, 1992; Nakajima *et al.*, 1993; Okamoto *et al.*, 1994). Sub-type mGluR4 is not sensitive to (+)-MCPG (Hayashi *et al.*, 1994), which is a less-specific L-AP4 antagonist than MAP4 (Kemp *et al.*, 1994 and Figure 1), and mGluR6 appears to be highly localized to retina (Nakajima *et al.*, 1993). This question of the identity of the L-AP4/MAP4-sensitive receptors remains to be answered.

Of the two sub-type-selective mGluR antagonists described in this work, MAP4 is the more potent. The K_D value found for the interaction of this antagonist with L-AP4-sensitive presynaptic receptors was 22 μM whereas that for MCCG versus (1S,3S)-ACPD- or L-CCG-I-sensitive receptors was in excess of 100 μM and dependent on the agonist. This agonist-dependency raises the question of the selectivity not only of the two antagonists but also of the agonists used. While MAP4 had little or no action at receptors sensitive to (1S,3S)-ACPD, this antagonist did show significant antagonist activity against L-CCG-I-induced depression of synaptic excitation. Such antagonism, however, was at least ten fold weaker than the antagonism shown at L-AP4-sensitive receptors and was probably non-competitive. MCCG had only minimal effect on L-AP4-induced synaptic depression and was more potent as an antagonist of (1S,3S)-ACPD-induced synaptic depression (apparent K_D 103 μM) than as an antagonist of L-CCG-I-induced synaptic depression (apparent K_D 259 μM). These results can be explained on the hypothesis that (1S,3S)-ACPD is a more specific agonist at non-L-AP4 presynaptic receptors on primary afferent terminals in neonatal rat spinal cord than is L-CCG-I, and that the depressant responses produced by L-CCG-I in this preparation were predominantly mediated by (1S,3S)-ACPD-sensitive receptors, but partly also by L-AP4-sensitive receptors. In this case since MAP4 had no action on (1S,3S)-ACPD-sensitive receptors, and MCCG had no action at L-AP4-sensitive receptors, the two antagonists are possibly both highly selective for the two different types of metabotropic receptor on presynaptic terminals at which they act. On this basis L-AP4 and (1S,3S)-ACPD would be regarded as the agonists of choice for the selective activation of these two receptors.

This work was supported by the Medical Research Council and US PHS Grant No. 26540.

References

BASHIR, Z.I., BORTOLOTTO, Z.A., DAVIES, C.H,. BERRETTA, N., IRVING, A.J., SEAL, A.J., HENLEY, J.M., JANE, D.E., WATKINS, J.C. & COLLINGRIDGE, G.L. (1993). Induction of LTP in the hippocampus needs synaptic activation of glutamate metabotropic receptors. *Nature*, **363**, 347–350.

BIRSE, E.F., EATON, S.A., JANE, D.E., JONES, P.L.St.J., PORTER, R.H.P., POOK, P.C.-K., SUNTER, D.C., UDVARHELYI, P.M., WHARTON, B., ROBERTS, P.J., SALT, T.E. & WATKINS, J.C. (1993). Phenylglycine derivatives as new pharmacological tools for investigating the role of metabotropic glutamate receptors in the central nervous system. *Neuroscience*, **52**, 481–488.

BIRSE, E.F., MEWETT, K.N., POOK, P.C.-K., TYRELL, K., UDVARHELYI, P.M., WHARTON, B. & WATKINS, J.C. (1992). Enantiomer specific depressant actions of 4-carboxy-3-hydroxyphenylglycine on synaptic excitation of motoneurones in newborn rat spinal cord. *J. Physiol.*, **452**, 185P.

EATON, S.A., BIRSE, E.F., WHARTON, B., SUNTER, D.C., UDVARHELYI, P.M., WATKINS, J.C. & SALT, T.E. (1993a). Mediation of thalamic sensory responses in vivo by ACPD-activated excitatory amino acid receptors. *Eur. J. Neurosci.*, **5**, 186–189.

EATON, S.A., JANE, D.E., JONES, P.L.St.J., PORTER, R.H.P., POOK, P.C.-K., SUNTER, D.C., UDVARHELYI, P.M., ROBERTS, P.J., SALT, T.E. & WATKINS, J.C. (1993b). Competitive antagonism at metabotropic glutamate receptors by (S)-4-carboxyphenylglycine (CPG) and (RS)-α-methyl-4-carboxyphenylglycine (MCPG). *Eur. J. Pharmacol., Mol. Pharmacol.*, **244**, 195–197.

EVANS, R.H., FRANCIS, A.A., JONES, A.W., SMITH, D.A.S. & WATKINS, J.C. (1982). The effects of a series of ω-phosphonic α-carboxylic amino acids on electrically evoked and amino acid induced responses in isolated spinal cord preparations. *Br. J. Pharmacol.*, **75**, 65–75.

GLAUM, S.R., SUNTER, D.C., UDVARHELYI, P.M, WATKINS, J.C. & MILLER, R.J. (1993). The actions of phenylglycine derived metabotropic glutamate receptor antagonists on multiple (1S,3R)-ACPD responses in the rat nucleus of the tractus solitarius. *Neuropharmacology*, **32**, 1419–1425.

HAYASHI, Y., SEKIYAMA, N., NAKANISHI, S., JANE, D.E., SUNTER, D.C., BIRSE, E.F., UDVARHELYI, P.M. & WATKINS, J.C. (1994). Analysis of agonist and antagonist activities of phenylglycine derivatives for different cloned metabotropic glutamate receptor sub-types. *J. Neuroscience*, (in press).

ISHIDA, M., SAITOH, T., SHIMAMOTO, K., OHFUNE, Y. & SHINOZAKI, H. (1993). A novel metabotropic glutamate receptor agonist; marked depression of monosynaptic excitation in the newborn rat isolated spinal cord. *Br. J. Pharmacol.*, **109**, 1169–1177.

ITO, I., KOHDA, A., TANABE, S., HIROSE, E., HAYASHI, M., MITSUNAGA, S. & SUGIYAMA, H. (1992). 3,5-Dihydroxyphenylglycine: a potent agonist of metabotropic glutamate receptors. *NeuroReport*, **3**, 1013–1016.

JANE, D.E., JONES, P.L.St.J., POOK, P.C.-K., SALT, T.E., SUNTER, D.C. & WATKINS, J.C. (1993). Stereospecific antagonism by (+)-α-methyl-4-carboxyphenylglycine of (1S,3R)-ACPD-induced effects in neonatal rat motoneurones and rat thalamic neurones. *Neuropharmacology*, **32**, 725–727.

KEMP, M., ROBERTS, P.J., POOK, P.C.-K., JANE, D.E., JONES, A.W., JONES, P.L.St.J., SUNTER, D.C., UDVARHELYI, P.M. & WATKINS, J.C. (1994). Antagonism of presynaptically mediated depressant responses and cyclic AMP-coupled metabotropic glutamate receptors. *Eur. J. Pharmacol., Mol. Pharmacol.*, **266**, 187–192.

LONG, S.K., SMITH, D.A.S., SIAREY, R.J. & EVANS, R.H. (1990). Effect of 6-cyano-2,3-dihydroxy-7-nitroquinoxaline (CNQX) on dorsal root-, NMDA-, kainate- and quisqualate-mediated depolarization of rat motoneurones *in vitro*. *Br. J. Pharmacol.*, **100**, 850–854.

NAKAJIMA, Y., IWAKABE, H., AKAWAZA, C., NAWA, H., SHIGEMOTO, R., MIZUNO, N. & NAKANISHI, S. (1993). Molecular characterization of a novel retinal metabotropic glutamate receptor mGluR6 with a high agonist selectivity for L-2-amino-4-phosphonobutyrate. *J. Biol. Chem.*, **268**, 11868–11873.

NAKANISHI, S. (1992). Molecular diversity of glutamate receptors and implications for brain function. *Science*, **258**, 597–603.

OKAMOTO, N., HORI, S., AKAZAWA, C,. HAYASHI, Y., SHIGEMOTO, R., MIZUNO, N. & NAKANISHI, S. (1994). Molecular characterization of a new metabotropic glutamate receptor mGluR7 coupled to inhibitory cyclic AMP signal transduction. *J. Biol. Chem.*, **269**, 1231–1236.

POOK, P.C.-K., BIRSE, E.F., JANE, D.E., JONES, A.W., JONES, P.L.St.J., MEWETT, K.N., SUNTER, D.C., UDVARHELYI, P.M., WHARTON, B. & WATKINS, J.C. (1993). Differential actions of the metabotropic glutamate receptor antagonists 4C-PG and αM4C-PG at L-AP4-like receptors in neonatal rat spinal cord. *Br. J. Pharmacol.*, **108**, 87P.

POOK, P.C.-K., SUNTER, D.E., UDVARHELYI, P.M. & WATKINS, J.C. (1992). Evidence for presynaptic depression of monosynaptic excitation in neonatal rat motoneurones by (1S,3S)- and (1S,3R)-ACPD. *Exp. Physiol.*, **77**, 529–532.

SALT, T.E., EATON, S.A., JANE, D.E. & WATKINS, J.C. (1993). Actions of the metabotropic glutamate receptor antagonist (RS)-α-methyl-4-carboxyphenylglycine on responses of thalamic neurones to ACPD. *Br. J. Pharmacol.*, **108**, 88P.

SCHOEPP, D.D. & CONN, P.J. (1993). Metabotropic glutamate receptors in brain function and pathology. *Trends Pharmacol. Sci.*, **14**, 13–20.

TANABE, Y., MASU, M., ISHII, T., SHIGEMOTO, R. & NAKANISHI, S. (1992). A family of metabotropic glutamate receptors. *Neuron*, **8**, 169–179.

TANABE, Y., NOMURA, A., MASU, M., SHIGEMOTO, R., MIZUNO, N. & NAKANISHI, S. (1993). Signal transduction, pharmacological properties, and expression patterns of two rat metabotropic glutamate receptors, mGluR3 and mGluR4. *J. Neurosci.*, **13**, 1372–1378.

(Received January 12, 1994
Revised March 16, 1994
Accepted March 22, 1994)

Br. J. Pharmacol. (1994), **112**, 817–822

Comparison of antinociception induced by supraspinally administered L-arginine and kyotorphin

Atsufumi Kawabata, Sachiko Manabe & [1]Hiroshi Takagi

Department of Pharmacology, Faculty of Pharmaceutical Sciences, Kinki University, 3-4-1 Kowakae, Higashi-Osaka 577, Japan

1 Intracerebroventricular (i.c.v.) or intracisternal (i.cist.) administration of kyotorphin (KTP), an endogenous Met-enkephalin releaser, at 5 μg per mouse, and L-arginine (L-Arg), a possible KTP precursor, at 30 μg per mouse, elicited antinociception in mice to a similar extent, as assessed by the tail-flick test.

2 Intracisternal preadministration of anti-KTP serum abolished the effects of i.cist. KTP and i.c.v. or i.cist. L-Arg, but not of i.c.v. KTP.

3 The antinociceptive effects of i.cist. KTP and of i.c.v. or i.cist. L-Arg disappeared in reserpinized mice, whereas the effect of i.c.v. KTP was unaffected by treatment of mice with reserpine.

4 Intrathecal (i.t.) phentolamine markedly reduced the antinocieption induced by i.cist. KTP and by i.c.v. or i.cist. L-Arg, but not by i.c.v. KTP.

5 Intrathecal methysergide attenuated the antinociceptive effects of i.cist. KTP, but not of i.c.v. KTP and i.c.v. or i.cist. L-Arg.

6 These results suggest that the antinociception produced by i.cist. KTP, but not by i.c.v. KTP, is mediated by the brainstem-spinal noradrenergic and 5-hydroxytryptaminergic systems, and that L-Arg given i.c.v. or i.cist. increases KTP formation in the lower brain, possibly the brainstem, resulting in antinociception mediated by the descending noradrenergic system. Therefore, the regional distribution of KTP receptors and KTP synthetase in the brain does not appear to be common.

Keywords: L-Arginine; kyotorphin; enkephalin; antinociception; antiserum; phentolamine; methysergide; brainstem-spinal noradrenergic system; brainstem-spinal 5-hydroxytryptaminergic system

Introduction

Kyotorphin (KTP), an endogenous antinociceptive dipeptide (L-tyrosyl-L-arginine), enhances the release of [Met^5]enkephalin (Met-Enk) in the brain and in the spinal cord (Takagi *et al.*, 1979a,b) and functions as a neurotransmitter or neuromodulator in nociceptive processing in the CNS (Takagi & Ueda, 1988). KTP, when administered intracerebroventricularly (i.c.v.) or intracisternally (i.cist.), produces naloxone-reversible antinociception in the mouse, and this effect is inhibited by the selective δ-opioid receptor antagonist, naltrindole and by the KTP receptor antagonist, L-leucyl-L-arginine (Leu-Arg) (Takagi *et al.*, 1979a; Kawabata *et al.*, 1992b).

KTP is formed by a specific enzyme, KTP synthetase, from L-tyrosine and L-arginine (L-Arg) in the presence of ATP and Mg^{2+} (Ueda *et al.*, 1987b), and is also formed by a Ca^{2+}-activated processing enzyme from a precursor protein in the brain (Yoshihara *et al.*, 1988; 1990). In the former pathway, exogenously applied L-Arg acts as an effective KTP precursor, since the K_m value for L-Arg of KTP synthetase is much higher than its concentration in the mammalian brain (Ueda *et al.*, 1987b). In fact, i.c.v. or s.c. administration of L-Arg exhibits potent antinociceptive activity that is blocked by naloxone, naltrindole or Leu-Arg in mice and rats (Kawabata *et al.*, 1992a,b; 1993). Clinical studies have also demonstrated naloxone-reversible analgesic effects of L-arginine in chronic pain patients (Takagi *et al.*, 1990; Harima *et al.*, 1991). On the other hand, L-Arg is also a source of nitric oxide (NO) that is now considered a novel type of neuronal messenger involved in various biological events (for review, see Garthwaite, 1991; Bredt & Snyder, 1992; Vincent & Hope, 1992). However, constitutive NO synthase in the brain is probably saturated by L-Arg under physiological conditions, since the K_m value for L-Arg of this enzyme is much lower than its brain levels (Bredt & Snyder, 1990; Knowles *et al.*, 1990), suggesting that exogenously applied L-Arg does not increase NO production (Garthwaite, 1991). In addition, NO synthase inhibitors, administered i.c.v., exhibit antinociceptive activity in the mouse, suggesting a nociceptive role of NO in the brain (Moore *et al.*, 1991; Babbedge *et al.*, 1993; Kawabata *et al.*, 1993). It is unlikely that brain NO is involved in the production of the antinociceptive effect of L-Arg. In this paper, we show that i.cist. preadministration of anti-KTP serum abolishes the antinociception elicited by i.c.v. or i.cist. L-Arg, further suggesting that L-Arg-induced antinociception is mediated by KTP formation in the brain.

The brainstem-spinal monoaminergic systems contribute to the antinociception exerted by systemic and supraspinal administration of opioids (Takagi, 1980; 1982; Bashaum & Fields, 1984; Besson & Chaouch, 1987; Kuraishi *et al.*, 1987; Wigder & Wilcox, 1987). The antinociceptive effects of i.cist. KTP are also inhibited by intrathecal (i.t.) injection of phentolamine, an α-adrenoceptor antagonist (Ueda *et al.*, 1987a), suggesting involvement of the brainstem-spinal descending noradrenergic system. To clarify the antinociceptive mechanisms of L-Arg, we also examined the contribution of the brainstem-spinal noradrenergic and 5-hydroxytryptaminergic systems to antinociception induced by i.c.v. or i.cist. L-arginine, compared with that induced by i.c.v. or i.cist. KTP.

Methods

Animals

Male ddy mice weighing 15–25 g (Japan SLC, Inc.) were given food and water *ad libitum* except on the experimental day.

[1] Author for correspondence.

Tail-flick test

To determine thermal nociception, mice were tested for responsiveness to radiant heat by use of a tail-flick analgesia meter (MK-330, Muromachi Kikai Co. Ltd., Japan). The tail of each mouse was placed in the path of a light beam connected via a photoelectric cell to a digital monitor and recorder. The latency to remove the tail was monitored and recorded automatically via the photoelectric cell. The stimulus intensity was adjusted to obtain base-line latencies of 2–2.5 s, and a cut-off latency of 8 s was used to avoid damage to the tail. The tail-flick latency of each mouse was measured 4–5 times at 20 min intervals and the basal latency was defined as the mean of the last 3 stable latencies. Fluctuation in base-line latencies for each mouse employed in the experiments was within 0.4 s. Results are expressed as the changes in latencies, which were obtained by subtracting the basal latency from the test latency.

Experimental protocol

Effects of anti-kyotorphin serum on antinociception induced by kyotorphin and by L-arginine After measurement of the baseline latencies, 10 μl of anti-kyotorphin serum without dilution or of control serum was administered i.cist. (Ueda *et al.*, 1979) to mice, and KTP at 5 μg per mouse or L-Arg at 30 μg per mouse in a volume of 5 μl was administered intracerebroventricularly (i.c.v.) (Haley & McCormick, 1957) or i.cist. 60 min later. The tail-flick latency was repeatedly assessed at 5, 10, 20, 40 and 60 min after KTP or L-Arg administration.

Antinociceptive effects of kyotorphin and L-arginine in reserpinizied mice Reserpine, a monoamine depletor, at 5 mg kg^{-1} was administered intraperitoneally (i.p.) to mice 24 h before i.c.v. or i.cist. administration of KTP (5 μg per mouse) or L-Arg (30 μg per mouse).

Effects of intrathecal administration of phentolamine and methysergide on the antinociceptive activity of kyotorphin or L-arginine Phentolamine, an α-adrenoceptor antagonist, at 1–10 μg per mouse, or methysergide, a 5-hydroxytryptamine (5-HT) receptor antagonist, at 1–5 μg per mouse, was administered intrathecally (i.t.) (Hylden & Wilcox, 1980) to mice 5 min before i.c.v. or i.cist. injections with KTP (5 μg per mouse) or L-Arg (30 μg per mouse).

Anti-kyotorphin serum

Anti-KTP serum was a gift from Dr Shiomi *et al.* (Fukuyama Univ., Japan). They produced this antiserum from the rabbit immunized with KTP conjugated with bovine serum albumin, according to the method of Ueda *et al.* (1987b). The binding activity and specificity of the antiserum were also tested by radioimmunoassay (Ueda *et al.*, 1987b) in our laboratory. The relative cross-reactivity (%) of the antiserum to endogenous and synthetic substances was as follows: KTP, 100; L-Tyr, <0.001; L- and D-Arg, <0.001; L-ornithine (L-Orn), <0.001; L-citrulline, <0.001; Met- and Leu-enkephalin, <0.001; L-Tyr-D-Arg, 0.15; L-Leu-L-Arg, 0.22; L-Tyr-L-N^G-nitroarginine methyl ester, 0.39; L-Tyr-L-Orn, 3.02. Control serum was prepared from a non-immunized rabbit.

Drugs

Drugs used were L-arginine hydrochloride (L-Arg) (Nacalai Tesque, Japan), kyotorphin acetate (KTP), reserpine (Sigma, U.S.A.), phentolamine mesylate (Regitin, Inj.; Ciba-Geigy), and methysergide hydrogen maleate (a gift from Dr Kuraishi). Reserpine was suspended in 0.2% Tween 80 solution, and all other drugs were dissolved in physiological saline.

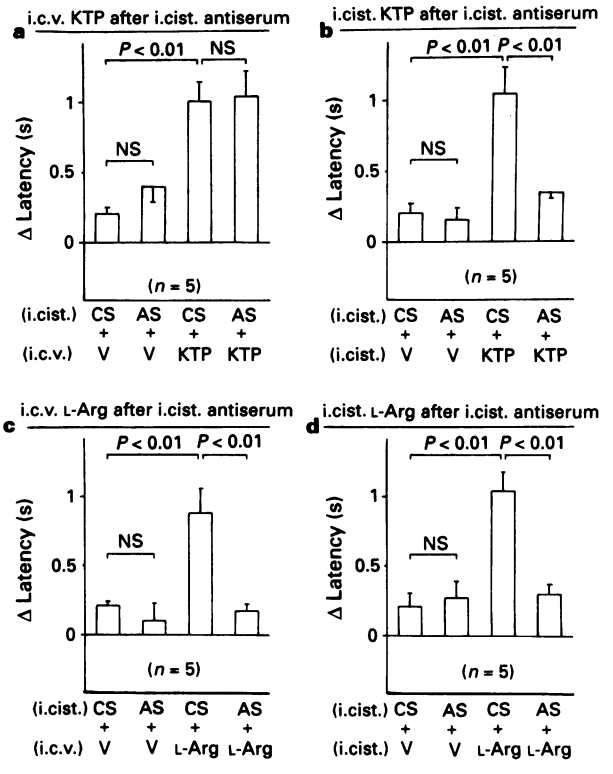

Figure 1 Effects of i.cist. preadministratin of anti-kyotorphin serum on the antinociception produced by i.c.v. or i.cist. kyotorphin (KTP) and by i.c.v. or i.cist. L-arginine (L-Arg) in the tail-flick test in mice. KTP at 5 μg per mouse and L-Arg at 30 μg per mouse were administered i.c.v. or i.cist. 1 h after i.cist. injection of 10 μl of anti-KTP serum (AS) without dilution or control serum (CS). Data indicate Δ latencies 10 min after KTP or L-Arg; values are mean with s.e.mean. V, vehicles; NS, not significant.

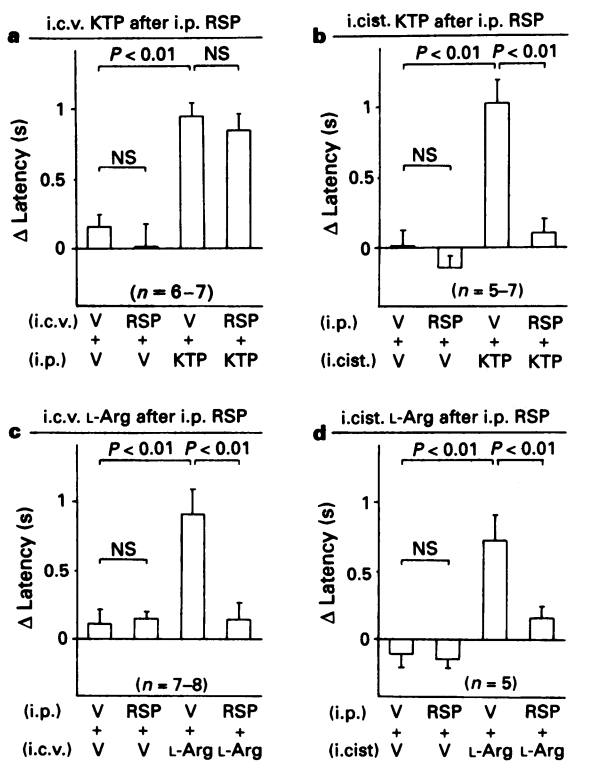

Figure 2 Antinociceptive activity of i.c.v. or i.cist. kyotorphin (KTP) and of i.c.v. or i.cist. L-arginine (L-Arg) in reserpinized mice as assessed by the tail-flick test. KTP at 5 μg per mouse and L-Arg at 30 μg per mouse were administered i.c.v. or i.cist. 24 h after i.p. injection of reserpine (RSP) at 5 mg kg^{-1}. Data indicate Δ latencies 10 min after KTP or L-Arg; values are mean with s.e.mean. V, vehicle; NS, not significant.

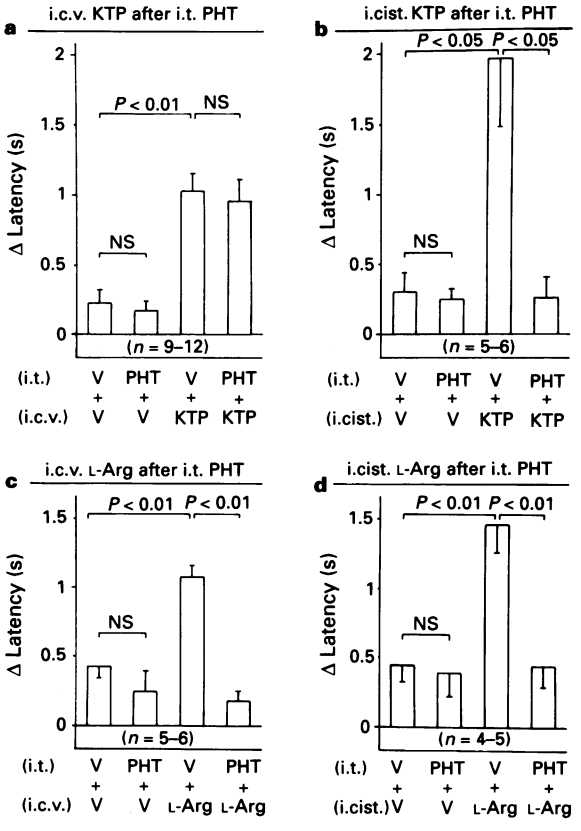

Figure 3 Effects of i.t. phentolamine on the antinociception elicited by i.c.v. or i.cist. kyotorphin (KTP) and by i.c.v. or i.cist. L-arginine (L-Arg) in the tail-flick test in mice. KTP at 5 μg per mouse and L-Arg at 30 μg per mouse were administered i.c.v. or i.cist. 5 min after i.t. injection of phentolamine (PHT) at 10 μg per mouse (a) or at 1 μg per mouse (b, c and d). Data indicate Δ latencies 10 min after KTP or L-Arg; values are mean with s.e.mean. V, vehicle; NS, not significant.

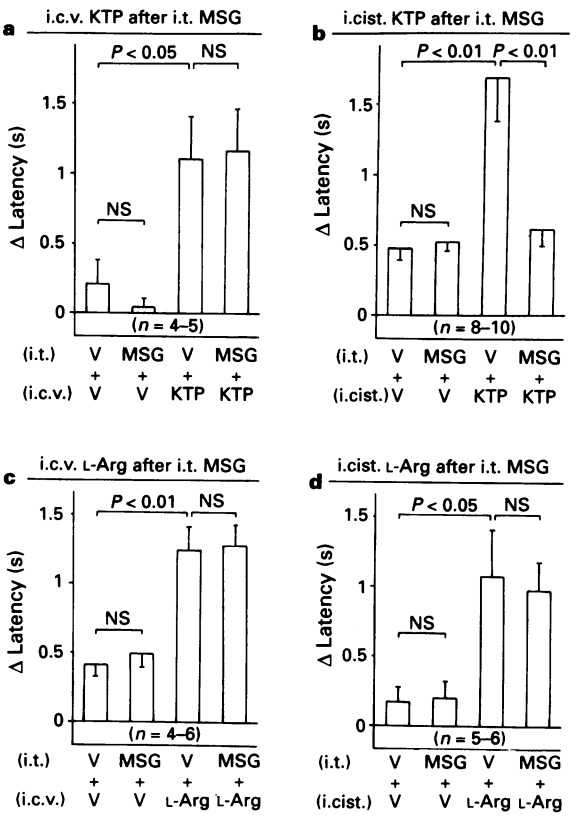

Figure 4 Effects of i.t. methysergide on the antinociception induced by i.c.v. or i.cist. kyotorphin (KTP) and by i.c.v. or i.cist. L-arginine (L-Arg) in the tail-flick test in mice. KTP at 5 μg per mouse and L-Arg at 30 μg per mouse were administered i.c.v. or i.cist. 5 min after i.t. injection of methysergide (MSG) at 5 μg per mouse (a, c and d) or at 1 μg per mouse (b). Data indicate Δ latencies 10 min after KTP or L-Arg; values are mean with s.e.mean. V, vehicle; NS, not significant.

Statistics

The results are expressed as means with s.e.mean. Statistical significance between groups was analyzed by Newman-Keuls' multiple comparison test and was set at $P<0.05$.

Results

Effects of i.cist. preadministration of anti-kyotorphin serum on the antinociception exerted by i.c.v. and by i.cist injections of kyotorphin or L-arginine

KTP, given i.c.v. or i.cist. at 5 μg per mouse, and L-Arg, given i.c.v. or i.cist. at 30 μg per mouse, significantly prolonged the tail-flick latency, to a similar extent, 10 min after administration (Figure 1), the effects disappearing at 40 min. Anti-KTP serum, administered i.cist. 1 h before KTP, abolished the antinociceptive effects of i.cist. KTP, although the antiserum itself did not affect the latency (Figure 1b). However, i.c.v. KTP-induced antinociception was resistant to i.cist pretreatment with the antiserum (Figure 1a). In contrast, the antinociception produced by either i.c.v. or i.cist. L-Arg was significantly inhibited by i.cist. preadministration of anti-KTP serum (Figure 1c,d).

Antinociceptive activity of kyotorphin and L-arginine (i.c.v. or i.cist.) in reserpinized mice

Preadministration (i.p.) of reserpine at 5 mg kg^{-1} markedly reduced the antinociceptive activity exerted by i.cist. KTP at 5 μg per mouse, without having a significant effect by itself (Figure 2b). However, the same dose of reserpine did not inhibit the antinociception induced by i.c.v. KTP at the same dose (Figure 2a). By contrast, the antinociceptive effects of either i.c.v. or i.cist. L-Arg at 30 μg per mouse were abolished by preadministered reserpine (5 mg kg^{-1}) (Figure 2c,d).

Effects of intrathecal phentolamine on the antinociception produced by i.c.v. or i.cist. administration of kyotorphin or L-arginine

Intrathecal preadministration of phentolamine at 1 μg per mouse, which had no significant effect when administered alone, considerably suppressed i.cist. KTP-induced antinociception (Figure 3b), in agreement with the report of Ueda *et al.* (1987a). However, i.c.v. KTP-induced antinociception was not significantly altered by i.t. phentolamine even at 10 μg per mouse (Figure 3a). On the other hand, the antinociception elicited by i.c.v. and i.cist. L-Arg at 30 μg per mouse was significantly attenuated by 1 μg per mouse of phentolamine (i.t.) (Figure 3c,d).

Effects of intrathecal methysergide on supraspinally applied kyotorphin- or L-arginine-induced antinociception

Methysergide, preadministered i.t. at 1 μg per mouse, markedly blocked the antinociceptive effect of i.cist. KTP at 5 μg per mouse, although it alone had no effect (Figure 4b). However, methysergide even at 5 μg per mouse failed to inhibit the antinociception induced by i.c.v. KTP at 5 μg per mouse and by i.c.v. or i.cist. L-Arg at 30 μg per mouse (Figure 4a,c,d).

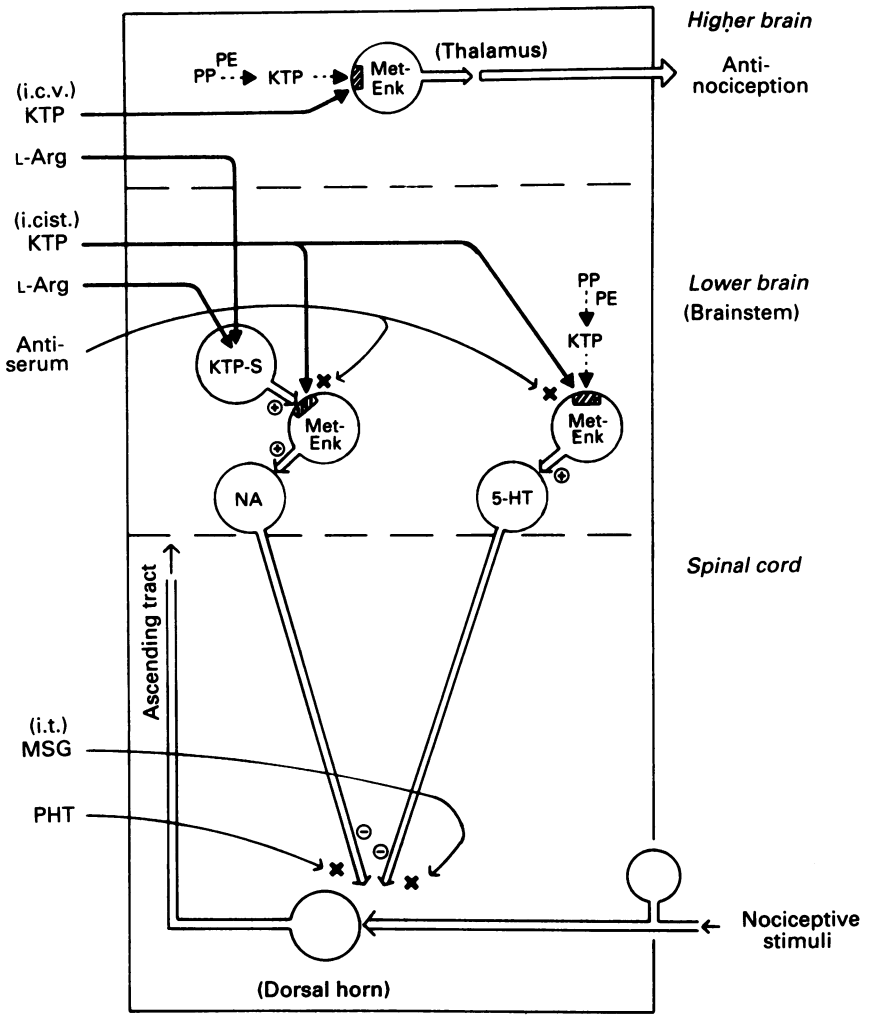

Figure 5 A working hypothesis concerning the antinociceptive mechanisms of kyotorphin (KTP) and L-arginine (L-Arg). PHT, phentolamine; MSG, methysergide; KTP-S, kyotorphin synthetase-containing neurone; Met-Enk, Met-enkephalin neurone; NA, noradrenergic neurone; 5-HT, 5-hydroxytryptaminergic neurone; PE, the processing enzyme of kyotorphin; PP, the precursor protein of kyotorphin. The hatched areas indicate kyotorphin receptors.

Discussion

The present findings suggest that i.cist. KTP produces antinociception via the brainstem-spinal noradrenergic and 5-hydroxytryptaminergic pathways, and that i.c.v. or i.cist. administration of L-Arg increases KTP formation in the lower brain, especially the brainstem, and subsequently activates the descending noradrenergic but not 5-hydroxytryptaminergic systems, resulting in antinociception. In addition, our results imply that the antinociceptive mechanism of i.c.v. KTP is independent of the brainstem-spinal monoaminergic systems, differing from that of i.cist. KTP.

Although dye distribution following i.c.v. and i.cist. injection using the techniques employed in the present study have been described previously by Haley & McCormick (1957) and Ueda *et al.* (1979), we have also examined distribution of dye after i.c.v. or i.cist. injections of 0.5% Evans blue in a volume of 5 or 10 μl in order to check the success of these injection techniques. The dye was always seen throughout the ventricular system 10 min after i.c.v. injection, suggesting that drugs, administered by this route, could be expected to exert effects in both the higher and lower brain. At 10 and 60 min after i.cist. injection, a high concentration of the dye was found in the area surrounding the cisterna magna and the ventral surface of the brainstem, while a very low concentration of the dye was found in the fourth, third and lateral ventricles. Therefore, drugs, administered by this route, would be expected to reach brainstem regions such as the nucleus reticularis paragigantocellularis (NRPG) and nucleus reticularis gigantocellularis (NRGC) that are highly sensitive to Met-Enk and KTP (Takagi, 1980; 1982; Satoh *et al.*, 1985). In our preliminary experiments, anti-KTP serum, when administered i.cist. 60 min, but not 30, 20 and 10 min, before i.cist. injection of L-Arg, abolished L-Arg (i.cist.)-induced antinociception. Thus, it appears to take about 60 min for the antibody to reach the effective site of L-Arg in the lower brain. Therefore, anti-KTP serum was administered i.cist. 60 min before i.c.v. or i.cist. injections of drugs in the present study.

We previously demonstrated that the antinociception induced by i.c.v. KTP is reversed by s.c. naltrindole, a δ-receptor antagonist, and by i.c.v. Leu-Arg, a KTP receptor antagonist (Kawabata *et al.*, 1992b). In this study, however, i.cist. preadministration of anti-KTP serum abolished the antinociceptive effects of i.cist. but not i.c.v. KTP, suggesting that KTP receptors existing in the higher brain predominantly contribute to the production of the effect of i.c.v. KTP. I.c.v. administration of KTP, at a dose of 5 μg per mouse, may not be adequate to increase its concentration in the lower brain to a level sufficient to activate KTP receptors, since KTP is easily degraded by aminopeptidase and kyotorphinase in the brain (Ueda *et al.*, 1985; Akasaki *et al.*, 1991; Orawski *et al.*, 1992). By contrast, the antinociceptive effects of either i.c.v. or i.cist. L-Arg were inhibited by i.cist. pread-

ministration of anti-KTP serum, thereby suggesting the involvement of KTP formation in the lower brain. In support of this finding, the activity of KTP synthetase in the lower brain regions such as the midbrain and medulla oblongata is much higher than that in the higher brain regions (Ueda *et al.*, 1987b). Taken together with the antagonism of L-Arg-induced antinociception by naloxone, naltrindole or Leu-Arg (Kawabata *et al.*, 1992a,b; 1993), we propose the antinociceptive mechanism of L-Arg is as follows: exogenously (i.c.v. and i.cist) applied L-Arg is effectively utilized for KTP synthesis by KTP synthetase in the lower brain, especially the brainstem, and subsequently KTP released in response to nociceptive stimuli enhances Met-Enk release via KTP receptors, resulting in antinociception through the activation of δ-opioid receptors. Furthermore, the above results imply a specific distribution of KTP receptors and KTP synthetase in the brain. In addition to KTP synthetase, KTP can also be formed by a Ca^{2+}-activated processing enzyme from a precursor protein (Yoshihara *et al.*, 1988; 1990). In the higher brain, therefore, this processing enzyme rather than KTP synthetase may be primarily responsible for KTP formation.

The findings that i.cist. KTP-induced antinociception disappeared in reserpinized mice and was abolished by i.t. phentolamine and by i.t. methysergide, suggest involvement of the brainstem-spinal noradrenergic and 5-hydroxytryptaminergic pathways in the induction of this effect. However, the antinociception produced by i.c.v. and by i.cist. L-Arg was inhibited by i.p. reserpine or i.t. phentolamine but not by i.t. methysergide, suggesting involvement of the brainstem-spinal noradrenergic but not 5-hydroxytryptaminergic pathways. The spinally projecting noradrenaline neurones originate primarily from pontine A1 or A7 cell groups. The NRPG and NRGC, which may be innervated by the periaqueductal gray matter (PAG) neurones, provide the major innervation of the descending noradrenergic system (Takagi, 1980; 1982; Kuraishi *et al.*, 1987; Clark & Proudfit, 1991; Yeomans *et al.*, 1992). In contrast, the spinally projecting 5-HT neurones originate in the nucleus raphe magnus (NRM) which are also innervated by PAG neurones (Takagi, 1982; Besson & Chaouch, 1987). Therefore, KTP synthetase-containing neurones appear to be localized mainly in the brainstem regions such as NRPG and NRGC that innervate the descending noradrenergic system. In the regions innervated by the descending 5-hydroxytryptaminergic neurones, KTP may be formed predominantly by the processing enzyme from a precursor protein but not by the synthetase.

We found that i.c.v. KTP-induced antinociception was resistant to i.p. reserpine, i.t. phentolamine or i.t. methysergide; this is compatible with the finding that i.cist. anti-KTP serum failed to antagonize the effect of i.c.v. KTP. These results suggest the presence of an antinociceptive mechanism independent of the brainstem-spinal monoaminergic systems. The antinociceptive effect of i.c.v. KTP is mediated by KTP receptors and by δ-opioid receptors, as indicated previously (Kawabata *et al.*, 1992b). It is unlikely that the opioid neurones, activated by i.c.v. KTP, directly innervate the spinal dorsal horn, contributing to antinociception, since i.t. administration of naloxone at 10 ng per mouse did not exhibit a significant inhibitory effect (data not shown). There is evidence for an ascending inhibitory system from the brainstem to the thalamus (Koyama & Yokota, 1993). KTP may activate this inhibitory system, thereby causing an inhibition of transmission of noxious input at the thalamus level.

Based upon the above evidence, we proposed a working hypothesis concerning the antinociceptive mechanisms of L-Arg and KTP in the CNS (Figure 5). A detailed analysis of the regional distribution of KTP receptors and KTP synthetase in the brain is necessary to confirm the proposed mechanism.

We are grateful to Dr H. Shiomi and Dr A. Nakamura (Fukuyama Univ., Japan) for the generous gift of anti-kyotorphin serum. This paper is the seventh on 'Pain modulation by neuroactive amino acids'.

References

AKASAKI, K., NAKAMURA, A., SHIOMI, H. & TSUJI, H. (1991). Identification and characterization of two distinct kyotorphin-hydrolyzing enzymes in rat brain. *Neuropeptides*, **20**, 103–107.

BABBEDGE, R.C., HART, S.L. & MOORE, P.K. (1993). Anti-nociceptive activity of nitric oxide synthase inhibitors in the mouse: dissociation between the effect of L-NAME and L-NMMA. *J. Pharm. Pharmacol.*, **45**, 77–79.

BASBAUM, A.I. & FIELDS, H.L. (1984). Endogenous pain control systems: brainstem spinal pathways and endorphin circuitry. *Annu. Rev. Neurosci.*, **7**, 309–338.

BESSON, J.M. & CHAOUCH, A. (1987). Descending serotonergic systems. In *Pain and Headache. Neurotransmitters and Pain Control*, vol. 9, ed. Akil, H. & Lewis, J.W. pp. 101–128. Basel: Karger.

BREDT, D.S. & SNYDER, S.H. (1990). Isolation of nitric oxide synthetase, a calmodulin-requiring enzyme. *Proc. Natl. Acad. Sci. U.S.A.*, **87**, 682–685.

BREDT, D.S. & SNYDER, S.H. (1992). Nitric oxide, a novel neuronal messenger. *Neuron*, **8**, 3–11.

CLARK, F.M. & PROUDFIT, H.K. (1991). The projection of noradrenergic neurons in the A7 catecholamine cell group to the spinal cord in the rat demonstrated by anterograde tracing combined with immunocytochemistry. *Brain Res.*, **547**, 279–288.

GARTHWAITE, J. (1991). Glutamate, nitric oxide and cell-cell signalling in the nervous system. *Trends Neurosci.*, **14**, 60–67.

HALEY, T.J. & MCCORMICK, W.G. (1957). Pharmacological effects produced by intracerebral injection of drugs in the conscious mouse. *Br. J. Pharmacol. Chemother.*, **12**, 12–15.

HARIMA, A., SHIMIZU, H. & TAKAGI, H. (1991). Analgesic effect of L-arginine in patients with persistent pain. *Eur. Neuropsychopharmacol.*, **1**, 529–533.

HYLDEN, J.K. & WILCOX, G.L. (1980). Intrathecal morphine in mice: a new technique. *Eur. J. Pharmacol.*, **67**, 313–316.

KAWABATA, A., FUKUZUMI, Y., FUKUSHIMA, Y. & TAKAGI, H. (1992a). Antinociceptive effect of L-arginine on carrageenin-induced hyperalgesia in rats: possible involvement of central opioidergic systems. *Eur. J. Pharmacol.*, **218**, 153–158.

KAWABATA, A., NISHIMURA, Y. & TAKAGI, H. (1992b). L-Leucyl-L-arginine, naltrindole and D-arginine block antinociception elicited by L-arginine in mice with carrageenin-induced hyperalgesia. *Br. J. Pharmacol.*, **107**, 1096–1101.

KAWABATA, A., UMEDA, N. & TAKAGI, H. (1993). L-Arginine exerts a dual role in nociceptive processing in the brain: involvement of the kyotorphin-Met-enkephalin pathway and NO-cyclic GMP pathway. *Br. J. Pharmacol.*, **109**, 73–79.

KNOWLES, R.G., PALACIOS, M., PALMERR, R.M .& MONCADA, S. (1990). Kinetic characteristics of nitric oxide synthase from rat brain. *Biochem. J.*, **269**, 207–210.

KOYAMA, N. & YOKOTA, T. (1993). Ascending inhibition of nociceptive neurons in the nucleus ventralis posterolateralis following conditioning stimulation of the nucleus raphe magnus. *Brain Res.*, **609**, 298–306.

KURAISHI, Y., SATOH, M. & TAKAGI, H. (1987). The descending noradrenergic system and analgesia. In *Pain and Headache. Neurotransmitters and Pain Control*, Vol. 9, ed. Akil, H. & Lewis, J.W., pp. 101–128. Basel: Karger.

MOORE, P.K., OLUYOMI, A.O., BABBEDGE, R.C., WALLACE, P. & HART, S.L. (1991). L-N^G-nitroarginine methyl ester exhibits antinociceptive activity in the mouse. *Br. J. Pharmacol.*, **102**, 198–202.

ORAWSKI, A.T. & SIMMONS, W.H. (1992). Dipeptidase activities in rat brain synaptosomes can be distinguished on the basis of inhibition by bestatin and amastatin: identification of a kyotorphin (Tyr-Arg)-degrading enzyme. *Neurochem. Res.*, **17**, 817–820.

SATOH, M., WADA, T., IWAMA, T. & TAKAGI, H. (1985). Sites of analgesic actions of kyotorphin and D-kyotorphin in the central nervous system of rats. *Neuropeptides*, **5**, 415–418.

TAKAGI, H. (1980). The nucleus reticularis paragigantocellularis as a site of analgesic action of morphine and enkephalin. *Trends Pharmacol. Sci.*, **1**, 182–184.

TAKAGI, H. (1982). Critical review of pain relieving procedures including acupuncture. In *Advances in Pharmacology and Therapeutics II*, Vol. 1 ed. Yoshida, H., Hagihara, Y. & Ebashi, S. pp. 79–92. New York: Pergamon Press.

TAKAGI, H., HARIMA, A. & SHIMIZU, H. (1990). A novel clinical treatment of persistent pain with L-arginine. *Eur. J. Pharmacol.*, **183**, 1443.

TAKAGI, H., SHIOMI, H., UEDA, H. & AMANO, H. (1979a). Morphine-like analgesia by a new dipeptide, L-tyrosyl-L-arginine (kyotorphin) and its analogue. *Eur. J. Pharmacol.*, **55**, 109–111.

TAKAGI, H., SHIOMI, H., UEDA, H. & AMANO, H. (1979b). A novel analgesic dipeptide from bovine brain is a possible Met-enkephalin releaser. *Nature*, **282**, 410–412.

TAKAGI, H. & UEDA, H. (1988). Kyotorphin as an endogenous pain modulator. In *The Biowarning System in the Brain*. ed. Takagi, H., Oomura, Y., Ito, M. & Otsuka, M. pp. 139–153, Tokyo: University of Tokyo Press.

UEDA, H., AMANO, H., SHIOMI, H. & TAKAGI, H. (1979). Comparison of the analgesic effects of various opioid peptides by a newly devised intracisternal injection technique in conscious mice. *Eur. J. Pharmacol.*, **56**, 265–268.

UEDA, H., GE, M., HAZATO, T., KATAYAMA, T. & TAKAGI, H. (1985). Degradation of kyotorphin by a purified membrane-bound-aminopeptidase from monkey brain: potentiation of kyotorphin-induced analgesia by a highly effective inhibitor, bestatin. *Life Sci.*, **36**, 1865–1871.

UEDA, H., GE, M., SATOH, M. & TAKAGI, H. (1987a). Non-opioid analgesia of the neuropeptide, neo-kyotorphin and possible mediation by inhibition of GABA release in the mouse brain. *Peptides*, **8**, 905–909.

UEDA, H., YOSHIHARA, Y., FUKUSHIMA, N., SHIMOI, H, NAKAMURA, A. & TAKAGI, H. (1987b). Kyotorphin (tyrosyl-arginine) synthetase in rat brain synaptosomes. *J. Biol. Chem.*, **262**, 8165–8173.

VINCENT, S.R. & HOPE, B.T. (1992). Neurons that say NO. *Trends Neurosci.*, **15**, 108–113.

WIGDER, S. & WILCOX, G.L. (1987). Central and systemic morphine-induced antinociception in mice: contribution of descending serotonergic and noradrenergic pathways. *J. Pharmacol. Exp. Ther.*, **242**, 90–95.

YEOMANS, D.C., CLARK, F.M., PAICE, J.A. & PROUDFIT, H.K. (1992). Antinociception induced by electrical stimulation of spinally projecting noradrenergic neurons in the A7 catecholamine cell group of the rat. *Pain*, **48**, 449–461.

YOSHIHARA, Y., UEDA, H,. FUJII, N., SHIDE, A., YAJIMA, H. & SATOH, M. (1990). Purification of a novel type of calcium-activated neutral protease from rat brain. *J. Biol. Chem.*, **265**, 5809–5815.

YOSHIHARA, Y., UEDA, H., IMAJOH, S., TAKAGI, H. & SATOH, M. (1988). Calcium-activated neutral proteases (CANP), a putative processing enzyme of the neuropeptide, kyotorphin, in the brain. *Biochem. Biophys. Res. Commun.*, **155**, 546–553.

(Received January 31, 1994
Revised March 17, 1994
Accepted March 22, 1994)

Br. J. Pharmacol. (1994), **112**, 823–830

Effects of bosentan (Ro 47-0203), an ET_A-, ET_B-receptor antagonist, on regional haemodynamic responses to endothelins in conscious rats

[1]S.M. Gardiner, P.A. Kemp, J.E. March & T. Bennett

Department of Physiology and Pharmacology, University of Nottingham Medical School, Queen's Medical Centre, Nottingham NG7 2UH

1 Regional haemodynamic responses to endothelin (ET)-1, -2 and -3 and big ET-1 (all at 500 pmol kg^{-1}) were assessed in the same conscious Long Evans rats ($n = 8$) in the absence or presence of the mixed ET_A-, ET_B-receptor antagonist, Ro 47-0203 (bosentan; 30 mg kg^{-1}).

2 Bosentan blocked the initial depressor, tachycardic and hindquarters hyperaemic vasodilator effects of ET-1, -2 and -3, and substantially curtailed the primary renal and secondary hindquarters vasoconstrictor responses. Bosentan did not inhibit the initial mesenteric vasoconstrictor action of ET-1, but reduced the duration of the later mesenteric vasoconstriction. In contrast, bosentan delayed the rate of onset, and reduced the duration, of the mesenteric vasoconstrictor actions of ET-2 and ET-3. The most likely explanation of this finding is that ET-1, but not ET-2 or ET-3, triggered a covert mesenteric vasodilator mechanism which was antagonized by bosentan.

3 Bosentan blocked all the effects of big ET-1, and, in a separate group of rats ($n = 7$), blocked all the haemodynamic effects of a lower dose of ET-1 (50 pmol kg^{-1}), with the exception of a slight mesenteric vasoconstriction.

4 The most straightforward explanation of the results is that the major haemodynamic effects of ET-1, -2 and -3, and all the effects of big ET-1, are mediated through ET_A- and/or ET_B-receptors that are effectively antagonized by bosentan.

Keywords: ET_A-receptors; ET_B-receptors; endothelins; big endothelin-1; bosentan

Introduction

Recent findings indicate that, while exogenous endothelin (ET)-1, and its analogues elicit initial depressor and vasodilator effects by activating ET_B-receptors, the subsequent pressor and vasoconstrictor actions of these peptides may involve both ET_A- and ET_B-receptors (Hiley *et al.*, 1989; Randall, 1991; Bigaud & Pelton, 1992; Clozel *et al.*, 1992; Gardiner *et al.*, 1992b; Moreland *et al.*, 1992; Cristol *et al.*, 1993; McMurdo *et al.*, 1993; Warner *et al.*, 1993).

These obervations raise the possibility that selective ET_A-receptor antagonists would be less useful than non-selective, ET_A-, ET_B-receptor antagonists in pathophysiological conditions in which impairment of regional blood flow was due to endogenous endothelin(s) (see Battistini *et al.*, 1993, for review). Recently, Clozel *et al.* (1993) demonstrated the ability of the non-selective ET_A-, ET_B-receptor antagonist, Ro 46-2005 (4-tert-butyl-*N*- [6-(2-hydroxy-ethoxy)-5-(3-methoxy-phenoxy)-4-pyrimidinyl]-benzenesulphonamide), to inhibit the decrease in renal blood flow following renal ischaemia, and also the cerebral vasospasm following subarachnoid haemorrhage in anaesthetized rats. In those models, Ro 46-2005 was without effect on systemic arterial blood pressure. However, Ro 46-2005 at a dose of 100 mg kg^{-1} caused a prolonged fall (30–40 mmHg) in mean arterial blood pressure in conscious, frusemide-treated, squirrel monkeys. Collectively, these results indicate that endogenous ETs may contribute to vasospasm in pathological conditions, and to the maintenance of mean arterial blood pressure in sodium depletion. However, at present, no data are available regarding the ability of non-selective ET_A-, ET_B-receptor antagonists to influence the regional haemodynamic actions of ETs.

Therefore, in the present work, we assessed regional haemodynamic responses to ET-1, ET-2 and ET-3, and big ET-1 in the absence and presence of the non-peptide, non-selective, ET_A-, and ET_B-receptor antagonist, bosentan (i.e., Ro 47-0203; 4-tert-butyl-*N*-[6-(2-hydroxy)-ethoxy)-5-(2-methoxy-phenoxy)-2, 2'-bipyrimidin-4yl] -benzenesulphonamide) (Clozel *et al.*, 1994).

Methods

Male Long Evans rats (350–450 g), bred in the Biomedical Services Unit, Queen's Medical Centre, Nottingham, were chronically instrumented with pulsed Doppler flow probes (renal, mesenteric and hindquarters) and intravascular catheters as described in detail previously (Gardiner *et al.*, 1991; 1992a). All surgery was carried out under sodium methohexitone anaesthesia (Brietal, Lilly; 40–60 mg kg^{-1}, i.p., supplemented as required). Experiments were not begun until at least 24 h after the last surgical intervention.

One group of animals ($n = 8$) was randomized to receive i.v. bolus doses of ET-1, ET-2, ET-3 and big ET-1 (all at 500 pmol kg^{-1}) on separate experimental days, before and 5 min after i.v. bolus injection of bosentan (30 mg kg^{-1}). The peptide injections on any experimental day were separated by at least 7 h; in pilot experiments we determined that repeated peptide injections at this interval evoked reproducible responses. The dose of the peptides was based on preliminary experiments showing that it evoked reproducible responses with respect to all components (see Results); the dose of bosentan was based on previous studies (Clozel *et al.*, 1994). Since bosentan did not abolish all the effects of the peptides (see Results), in a second group of animals ($n = 7$), responses to ET-1 at a 10 fold lower dose, i.e., 50 pmol kg^{-1}, were assessed before and 5 min after i.v. bolus injection of bosentan.

[1] Author for correspondence.

Data analysis

During an experimental run, continuous recordings were made of instantaneous heart rate, and mean and phasic arterial blood pressure and Doppler shift signals. Vascular conductance was calculated (mean Doppler shift divided by mean arterial blood pressure), and changes in all variables relative to baseline were used to assess responses to peptides. For ET-1, ET-2 and ET-3 at 500 pmol kg^{-1}, measurements were made at 0.25, 0.5, 0.75, 1, 2, 3, 4, 5, 10, 15, 20, 25, 30 and 60 min after injection. For big ET-1, measurements were made 1, 2, 3, 4, 5, 10, 15, 20, 25, 30 and 60 min after

Table 1 Resting cardiovascular variables in the two groups of conscious, Long Evans rats studied

	Group 1	*Group 2*
Heart rate (beats min^{-1})	324 ± 10	301 ± 4
Mean arterial blood pressure (mmHg)	96 ± 3	100 ± 1
Renal Doppler shift (kHz)	6.8 ± 0.8	5.6 ± 0.6
Mesenteric Doppler shift (kHz)	6.6 ± 0.5	6.2 ± 0.5
Hindquarters Doppler shift (kHz)	4.0 ± 0.2	3.5 ± 0.3
Renal vascular conductance ([kHz $mmHg^{-1}$]10^3)	72 ± 10	56 ± 6
Mesenteric vascular conductance ([kHz $mmHg^{-1}$]10^3)	70 ± 6	62 ± 4
Hindquarters vascular conductance ([kHz $mmHg^{-1}$]10^3)	42 ± 3	35 ± 3

Group 1 ($n = 8$) were those that received ET-1, ET-2, ET-3 and big ET-1 at 500 pmol kg^{-1}. Group 2 ($n = 7$) were given ET-1 at 50 pmol kg^{-1} only. Values are mean ± s.e.mean.

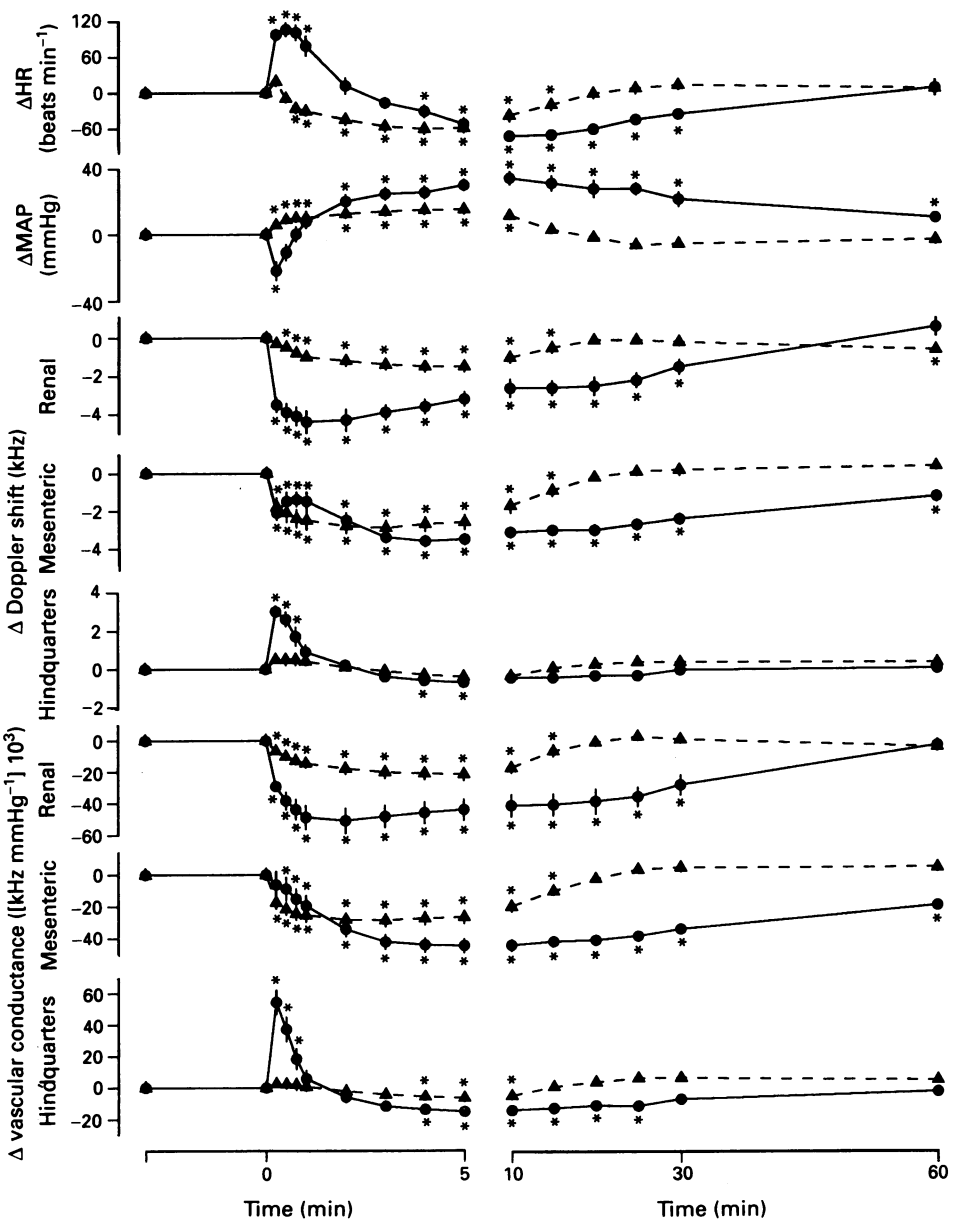

Figure 1 Cardiovascular responses to endothelin-1 (ET-1, 500 pmol kg^{-1}) in the absence (●) or presence (▲) of bosentan (30 mg kg^{-1}) in the same conscious, Long Evans rats ($n = 8$). Values are mean ± s.e.mean; $*P < 0.05$ versus baseline. Statistics for the differences between the responses in the absence and presence of bosentan are given in the text and Table 2.

injection. Responses to peptides were assessed by applying Friedman's test to the changes relative to the preinjection baseline; responses in the absence and presence of bosentan were compared by applying Wilcoxon's ranks sums test to integrated responses (areas under or over curves AUC_{0-60} min, AOC_{0-60} min, respectively). The same procedures were followed with the lower dose of ET-1 (50 pmol kg^{-1}), except that measurements were made only up to 10 min post-injection, since most variables were back to baseline levels by then. A P value <0.05 was taken as significant.

Peptides and drugs

ET-1, ET-2, ET-3 and big ET-1 were obtained from the Peptide Institute (Osaka, Japan), through their UK agents (Scientific Research Associates). Peptides were dissolved in saline containing 1% bovine serum albumin (Sigma, U.K.), and injected in a volume of 0.1 ml, flushed in with 0.1 ml saline. Bosentan (sodium salt) was synthesized at F. Hoffman – LaRoche Ltd., Basel Switzerland; it was dissolved in sterile water (60 mg ml^{-1}) and injected in a volume of 0.2 ml, flushed in with 0.1 ml saline.

Results

Resting cardiovascular variables in the two groups of rats studied are shown in Table 1.

Responses to ET-1 in the absence and presence of bosentan

High dose ET-1 ET-1 (500 pmol kg^{-1}) caused an initial fall in mean arterial blood pressure, and a tachycardia, accompanied by reductions in renal and mesenteric flows and conductances, but an increase in hindquarters flow and conductance (Figure 1, Table 2). Thereafter, there were pressor

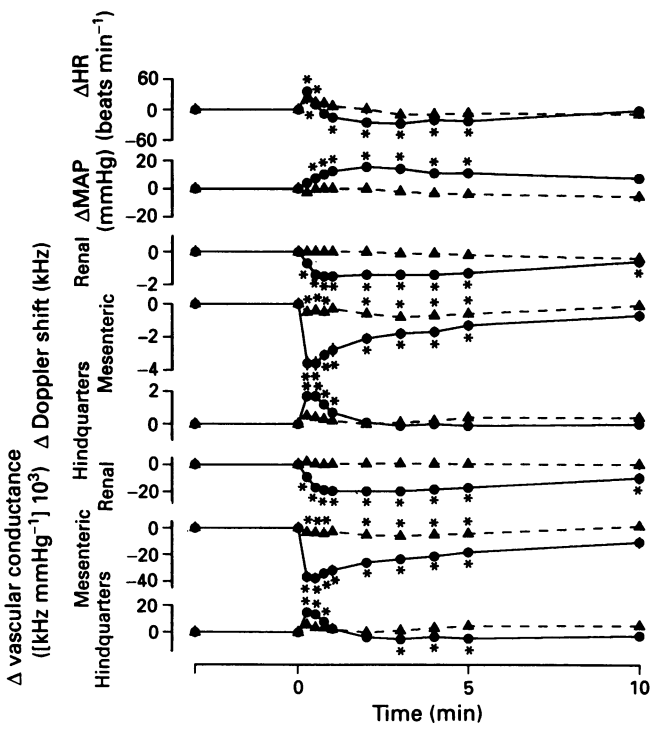

Figure 2 Cardiovascular responses to endothelin-1 (ET-1, 50 pmol kg^{-1}) in the absence (●) or presence (▲) of bosentan (30 mg kg^{-1}) in the same conscious, Long Evans rats ($n=7$). Values are mean ± s.e.mean; *$P<0.05$ versus baseline. Statistics for the differences between the responses in the absence and presence of bosentan are given in the text and Table 3.

Table 2 Integrated (AUC or AOC) cardiovascular responses to ET-1, ET-2, ET-3 or big ET-1 in the absence or presence of bosentan, respectively, in the same conscious, Long Evans rats ($n=8$)

	ET-1		*ET-2*		*ET-3*		*Big ET-1*	
	− *bosentan*	+ *bosentan*	− *bosentan*	+ *bosentan*	− *bosentan*	+ *bosentan*	− *bosentan*	+ *bosentan*
Heart rate (AUC, beats)	138 ± 23	7 ± 2†	30 ± 8*	14 ± 6	68 ± 17*	4 ± 4†	-	-
Heart rate (AOC, beats)	2529 ± 244	1117 ± 238†	1785 ± 227*	677 ± 188†	1387 ± 209*	833 ± 155†	3011 ± 549	473 ± 153†
Mean BP (AOC, mmHg min)	14 ± 4	0†	5 ± 2*	1 ± 1	6 ± 2	0†	-	-
Mean BP (AUC, mmHg min)	1212 ± 194	172 ± 32†	521 ± 113*	61 ± 23†	747 ± 90*	298 ± 41†	1121 ± 57	22 ± 19†
Renal conductance (AOC, [kHz mmHg^{-1}]10^3 min)	1742 ± 338	422 ± 85†	878 ± 136*	259 ± 101†	984 ± 88*	403 ± 114†	1068 ± 88*	330 ± 103†
Mesenteric conductance (AOC, [kHz mmHg^{-1}]10^3 min)	1962 ± 168	362 ± 65†	1161 ± 120*	308 ± 78†	1959 ± 251	498 ± 92†	1645 ± 215	388 ± 71†
Hindquarters conductance (AUC, [kHz mmHg^{-1}]10^3 min)	35 ± 8	7 ± 3†	15 ± 5*	8 ± 2	11 ± 2*	14 ± 3	-	-
Hindquarters conductance (AOC, [kHz mmHg^{-1}]10^3 min)	491 ± 109	75 ± 29†	375 ± 84*	32 ± 19†	475 ± 98	96 ± 78†	1158 ± 132*	40 ± 21†

Values are mean ± s.e.mean; †$P<0.05$ versus corresponding responses in the absence of bosentan; *$P<0.05$ versus corresponding responses to ET-1. The heart rate, mean arterial blood pressure and hindquarters vascular conductance changes evoked by ET-1, -2 and -3 were biphasic.

and bradycardic effects associated with reductions in renal, mesenteric and hindquarters flows and vascular conductances (Figure 1, Table 2).

When bosentan was injected, the majority of animals showed an alerting response and motor activity (such effects were not seen with vehicle injection). The motor activity was accompanied by a transient (less than 5 min) rise in heart rate and mean arterial blood pressure, but no reductions in regional blood flows. Hence, the pressor effect of bosentan was probably due to an activity-induced increase in cardiac output, and clearly was not an agonistic effect of the drug at ET-receptors, consisent with the findings of Clozel *et al.* (1994).

In the presence of bosentan, the initial depressor and tachycardic, and the hindquarters hyperaemic vasodilator effects of ET-1, were abolished (Figure 1, Table 2). Although the early (within 1 min) renal vasoconstrictor effect of ET-1 was attenuated (+ bosentan, Δ maximum vascular conductance = -15 ± 3 kHz mmHg$^{-1}10^3$;-bosentan, Δ maximum = -49 ± 8 kHz mmHg$^{-1}10^3$), the mesenteric vasoconstrictor response was not (Figure 1); however, the subsequent renal, mesenteric and hindquarters vasoconstrictor effects of ET-1, together with its pressor and bradycardic actions were all attenuated by bosentan (Figure 1, Table 2). Nevertheless, in the presence of bosentan, ET-1 still exerted significant cardiovascular effects (Figure 1).

Low dose ET-1 In the absence of bosentan, the 50 pmol kg^{-1} dose of ET-1 did not cause an initial depressor effect, and there was only a slight tachycardia (Figure 2). However, there were early increases in hindquarters flow and vascular conductance, in association with reductions in renal and mesenteric flows and vascular conductances (Figure 2, Table 3). Subsequently, there was a rise in mean arterial blood pressure and a bradycardia, together with a slight hindquarters vasoconstriction, but this was not accompanied by a reduction in flow (Figure 2, Table 3).

In the presence of bosentan, the pressor, bradycardic and renal and hindquarters haemodynamic effects of ET-1 were abolished. However, there were still significant, albeit slight, reductions in mesenteric flow and vascular conductance (Figure 2, Table 3).

Responses to ET-2 in the absence and presence of bosentan

Although the pattern of haemodynamic changes evoked by ET-2 (Figure 3) was similar to that of ET-1 (Figure 1), the initial depressor, tachycardic and hindquarters hyperaemic vasodilator effects of ET-2 were significantly less than those of ET-1 (Table 2; compare Figures 1 and 3), as was the initial renal vasoconstrictor effect (ET-2, Δ vascular conductance at 15 s = -9 ± 9 kHz mmHg$^{-1}10^3$; ET-1 = -29 ± 2 kHz mmHg$^{-1}10^3$). However, the initial mesenteric vasoconstrictor effect of ET-2 (Δ vascular conductance at 15 s = -45 ± 5 kHz mmHg$^{-1}10^3$) was significantly greater than that of ET-1 (-6 ± 9 kHz mmHg$^{-1}10^3$) (compare Figures 1 and 3). The subsequent pressor, bradycardic, and renal and mesenteric vasoconstrictor effects of ET-2 were less sustained than those of ET-1, and hence the integrated responses were smaller (Table 2).

In the presence of bosentan, the initial depressor effect of ET-2 was abolished, and there was no significant tachycardia, but since the responses in the absence of bosentan were small, there was no statistically significant effect of bosentan (Table 2). Likewise, the attentuation by bosentan of the initial hyperaemic hindquarters vasodilator response to ET-2 did not reach significance (Figure 3, Table 2). However, the early renal vasoconstriction was abolished, and the initial mesenteric vasoconstriction was attenuated (+ bosentan, Δ vascular conductance at 15 s = -14 ± 4 kHz mmHg$^{-1}10^3$) (Figure 3), and bosentan also reduced the durations of the renal and mesenteric vasoconstriction, and abolished the delayed hindquarters vasoconstriction (Figure 3, Table 2).

Responses to ET-3 in the absence and presence of bosentan

The profile of haemodynamic effect of ET-3 (Figure 4) was similar to that of ET-2 and ET-1, but compared to the latter, the initial tachycardia and hindquarters vasodilator actions of ET-3 were less (Table 2). Moreover, there was a significant difference between the early change in renal vascular conductance evoked by ET-3 (Δ vascular conductance at 15 s = 7 ± 4 kHz mmHg$^{-1}10^3$) and that seen with ET-1 (above), whereas the early mesenteric vasoconstrictor effect of ET-3 (Δ vascular conductance at 15 s = -41 ± 9 kHz mmHg^{-1} 10^3) was greater than that of ET-1 (above) (compare Figures 4 and 1). The durations of the pressor, bradycardic, renal vasoconstrictor effects, but not the mesenteric vasoconstrictor effect of ET-3, were less than those of ET-1 (Figure 4, Table 2).

Bosentan abolished the initial depressor and tachycardic effects of ET-3 (Figure 4, Table 2) and attenuated the early renal and mesenteric vasoconstrictions (renal, Δ vascular conductance at 1 min, + bosentan Δ = -10 ± 2 kHz mmHg^{-1} 10^3; − bosentan = -46 ± 5 kHz mmHg^{-1} 10^3; mesenteric, Δ vascular conductance at 15 s, + bosentan = -19 ± 3 kHz mmHg$^{-1}10^3$; − bosentan = -41 ± 9 kHz mmHg$^{-1}10^3$ (Figure 4, Table 2). Bosentan attenuated the subsequent pressor and bradycardic effects of ET-3, reduced the duration of the renal and mesenteric vasoconstrictor responses, and abolished the delayed hindquarters vasoconstrictor action of ET-3 (Figure 4, Table 2).

Response to big ET-1 in the absence and presence of bosentan

Big ET-1 evoked a slowly-developing pressor and bradycardic effect, accompanied by renal, mesenteric and hindquarters vasoconstrictions (Figure 5, Table 2). Big ET-1 thus differed from ET-1 in the absence of an initial depressor, tachycardic

Table 3 Integrated (AUC or AOC) cardiovascular responses to ET-1 (50 pmol kg^{-1}) in the absence or presence of bosentan in the same conscious, Long Evans rats ($n = 7$)

	ET-1	
	− bosentan	*+ bosentan*
Heart rate (AUC, beats)	14 ± 3	13 ± 5
Heart rate (AOC, beats)	191 ± 41	109 ± 45†
Mean BP (AUC, mmHg min)	110 ± 19	10 ± 5†
Renal conductance (AOC, [kHz mmHg^{-1}]10^3 min)	157 ± 32	16 ± 8†
Mesenteric conductance (AOC, [kHz mmHg^{-1}]10^3 min)	205 ± 34	41 ± 7†
Hindquarters conductance (AUC, [kHz mmHg^{-1}]10^3 min)	10 ± 2	4 ± 1
Hindquarters conductance (AOC, [kHz mmHg^{-1}]10^3 min)	38 ± 12	4 ± 2†

Values are mean ± s.e.mean; †$P < 0.05$ versus corresponding response in the absence of bosentan. The heart rate and hindquarters vascular conductance responses were biphasic.

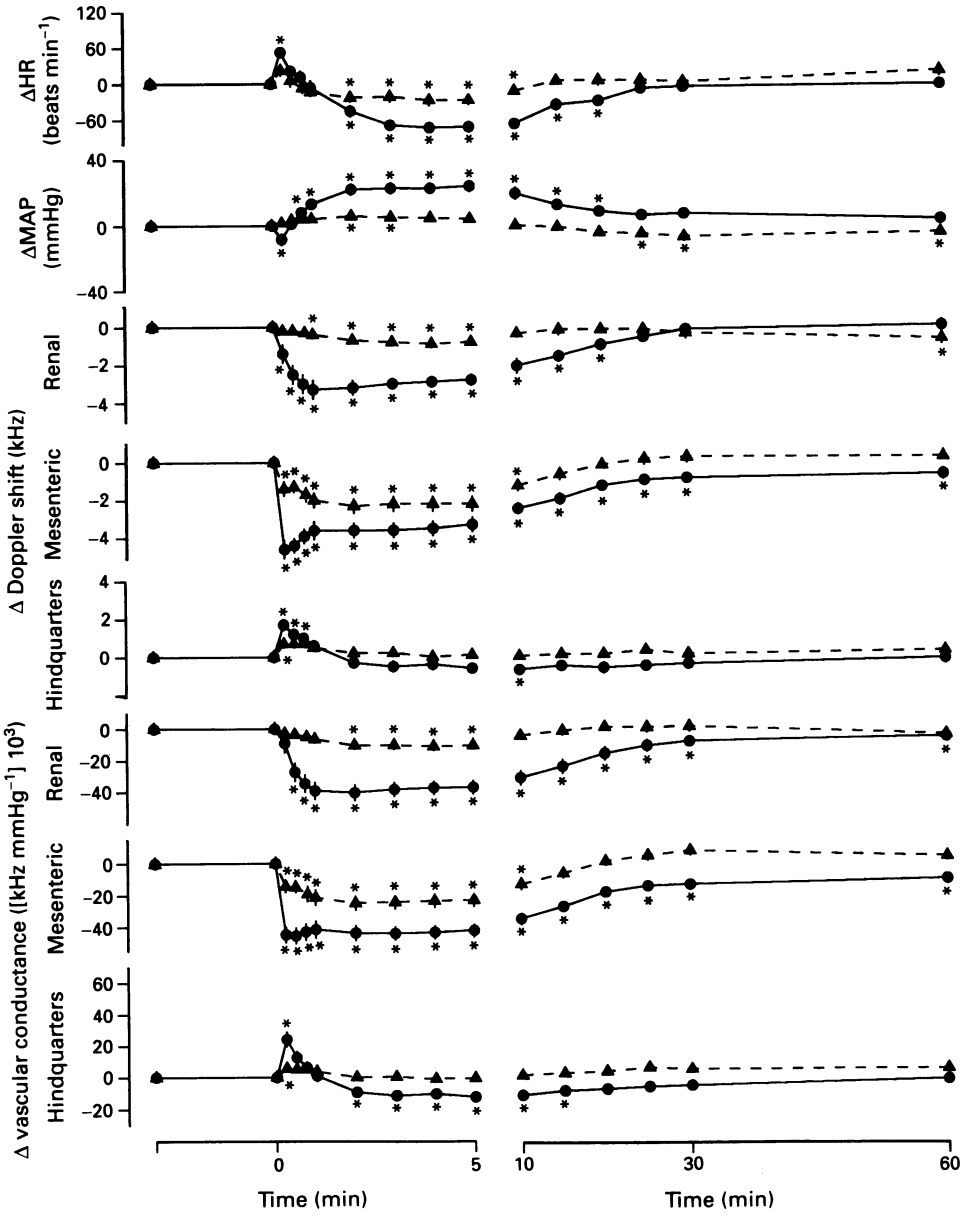

Figure 3 Cardiovascular responses to endothelin-2 (ET-2, 500 pmol kg^{-1}) in the absence (●) or presence (▲) of bosentan (30 mg kg^{-1}) in the same conscious, Long Evans rats ($n = 8$). Values are mean ± s.e.mean; *$P < 0.05$ versus baseline. Statistics for the differences between the responses in the absence and presence of bosentan are given in the text and Table 2.

and hindquarters vasodilator phase, although at a higher dose (10 nmol kg^{-1}), big ET-1 has such effects (Gardiner *et al.*, 1991). The integrated pressor and bradycardic, and mesenteric vasoconstrictor effects of big ET-1 were not different from those of ET-1, but the latter had greater renal vasoconstrictor and lesser hindquarters vasoconstrictor actions than did big ET-1 (Figure 5, Table 2).

Bosentan abolished the pressor, and renal, and hindquarters vasoconstrictor effects of big ET-1 (Figure 5, Table 2). In the presence of bosentan there were slight, delayed falls in mean arterial blood pressure and mesenteric flow and vascular conductance following administration of big ET-1 (Figure 5, Table 2).

Discussion

The major objectives of the present work were to assess the effectiveness of bosentan as an antagonist of the regional haemodynamic actions of ET-1, -2 and -3 and big ET-1 in conscious rats and, in so doing, to determine if there were residual responses to the peptides in the presence of bosentan, consistent with involvement of non-ET_A-, non-ET_B-receptors.

Effects of bosentan on responses to ET-1

At a dose of 500 pmol kg^{-1}, ET-1 elicited a marked initial hypotension, tachycardia and increases in hindquarters flow and vascular conductance; all these effects were blocked by bosentan. Furthermore, in the same experimental model, we have found that the ET_A-receptor antagonist, FR 139317, has no influence on these initial responses to ET-1 (Bennett *et al.*, 1993). Thus, these results, together, are consistent with an exclusive mediation of the hypotensive and hindquarters hyperaemic vasodilator effects of ET-1 by ET_B-receptors; it is likely that the tachycardia was a reflex response to the hypotension (Gardiner *et al.*, 1990a).

Although bosentan clearly attenuated the early renal vasoconstrictor effect of ET-1 at a dose of 500 pmol kg^{-1}, it tended to enhance the initial vasoconstrictor response in the mesenteric vascular bed. However, examination of the

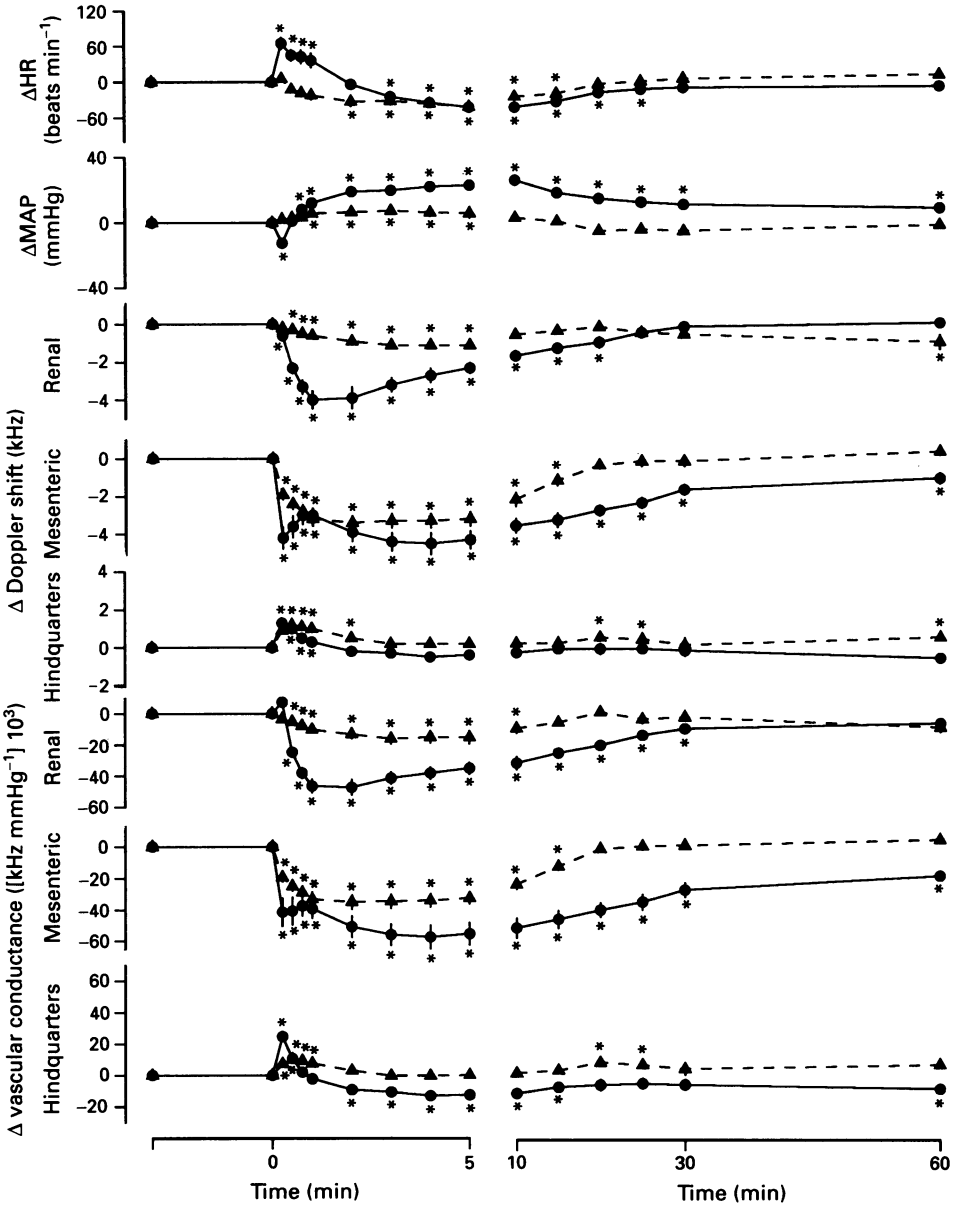

Figure 4 Cardiovascular responses to endothelin-3 (ET-3, 500 pmol kg^{-1}) in the absence (●) or presence (▲) of bosentan (30 mg kg^{-1}) in the same conscious, Long Evans rats ($n = 8$). Values are mean ± s.e.mean; *$P < 0.05$ versus baseline. Statistics for the differences between the responses in the absence and presence of bosentan are given in the text and Table 2.

changes in the arterial blood pressure and mesenteric blood flow showed that this was due to bosentan blocking a covert vasodilator component in this vascular bed that was acting to oppose the vasoconstrictor effect of ET-1. This interpretation is consistent with the finding that ET-1 at a dose of 50 pmol kg^{-1} had a rapid onset, mesenteric vasoconstrictor effect, that was clearly inhibited by bosentan. These observations indicate that, at a dose of 50 pmol kg^{-1}, ET-1 had a preferential mesenteric vasoconstrictor action, while at a dose of 500 pmol kg^{-1} addition mesenteric vasodilator mechanisms were activated by ET-1. It is feasible that the different pattern of haemodynamic changes in mesenteric and hindquarters vascular beds in response to ET-1, and the effect of bosentan thereupon, reflected different distributions of ET_A- and ET_B-receptors in the two vascular beds.

It is difficult to argue that bosentan more effectively blocked ET_B- than ET_A-receptors, if the latter predominate and, when activated, produce effects that oppose those due to ET_B-receptor stimulation. By the same token, it is not possible, straightforwardly, to quantitate the efffectiveness of bosentan in blocking the pressor and vasoconstrictor effects of ET-1, since, in the absence of bosentan, these actions were functionally antagonized by the depressor and vasodilator responses to ET-1 (Clozel *et al.*, 1994). Nonetheless, it was clear that bosentan markedly attenuated the pressor, and renal, mesenteric and hindquarters vasoconstrictor effects of ET-1 at a dose of 500 pmol kg^{-1}. Because, in the latter vascular bed, there was no reduction of flow in the presence of bosentan, it is possible that the vasoconstriction was an autoregulatory response to the rise in the perfusion pressure.

Although bosentan clearly shortened the duration of the pressor and vasoconstrictor effects, and diminished the maximum responses to ET-1 at a dose of 500 pmol kg^{-1}, significant responses remained. It is feasible that these were due to the involvement of receptors other than those of the ET_A- or ET_B-receptor subtype (see Huggins *et al.*, 1993, for review). However, since bosentan is a competitive antagonist (Clozel *et al.*, 1994) it is possible that the dose of bosentan was insufficient to inhibit fully the haemodynamic effects of this high dose of ET-1. Therefore, we assessed the effectiveness of bosentan against a lower dose of ET-1 (50 pmol kg^{-1}). Under these conditions, bosentan blocked all the

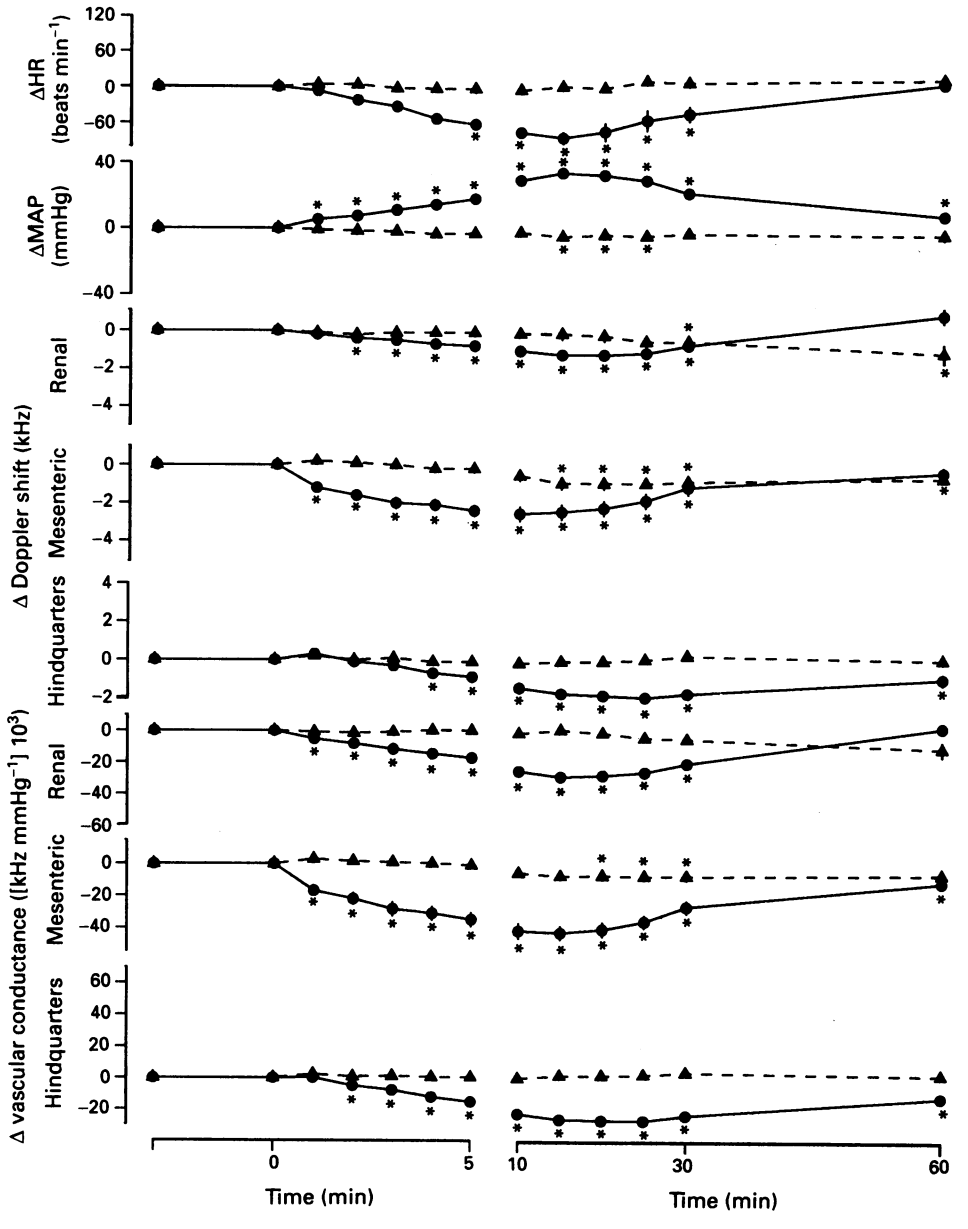

Figure 5 Cardiovascular responses to big endothelin-1 (big ET-1, 500 pmol kg^{-1}) in the absence (●) or presence (▲) of bosentan (30 mg kg^{-1}) in the same conscious, Long Evans rats ($n = 8$). Values are mean ± s.e.mean; $^*P < 0.05$ versus baseline. Statistics for the differences between the responses in the absence and presence of bosentan are given in the text and Table 2.

effects of ET-1, except for small reductions in mesenteric flow and vascular conductance. Thus, it seems likely that the majority of the effects of ET-1 were mediated through ET_A- and/or ET_B-receptors. However, we cannot dismiss an action of bosentan at other subtypes of ET receptors, in addition to ET_A- or ET_B-receptors. As mentioned above, it is feasible that, particularly at a dose of 500 pmol kg^{-1}, ET-1 activated other ET-receptor subtypes in addition to ET_A- and ET_B-receptors. Such a possibility is consistent with the finding that the maximum bradycardic effect of ET-1 was less inhibited by bosentan than was its maximum pressor effect (see Tables 2 and 3). Since the chronotropic actions of ET-1 are blocked by atropine and atenolol (Gardiner *et al.*, 1990a), it is feasible that any putative, non-ET_A-, non-ET_B-receptor-mediated influence of ET-1 on heart rate might be mediated through modulating cardiac autonomic control, possibly by an effect on baroreflex sensitivity.

Effects of bosentan on responses to ET-2 or ET-3

ET-2 and ET-3 had smaller initial depressor and hindquarters vasodilator effects than ET-1. Furthermore, they had more rapid onset vasoconstrictor actions in the mesenteric vascular bed than did ET-1, although this was not the case in the renal vascular bed. Thus, with the exception of the latter, we here, and previously (Gardiner *et al.*, 1990b, c,d), have not found *in vivo* functional evidence for more effective activation of vasodilator mechanisms, by ET- 3 or ET-2, than by ET-1.

In the majority of instances there was no evidence indicating that bosentan was less effective at inhibiting the actions of ET-2 or ET-3 than those of ET-1. Hence, our results are generally consistent with the proposal that the majority of the effects of ET-1, -2 and -3 are mediated through ET_A- and/or ET_B-receptors. The one apparent exception was the hindquarters hyperaemic vasodilator responses to ET-2 and ET-3 which, unlike those to ET-1, were not completely blocked by bosentan. However, these responses were so small their functional significance is doubtful.

Effects of bosentan on responses to big ET-1

All the effects of big ET-1 over the first 10 min after its administration were blocked by bosentan. Subsequently, even

in the presence of bosentan, there were slight reductions in mean arterial blood pressure and renal and mesenteric flows, and mesenteric vascular conductance. Considering the time course of these changes, it is likely they were due to the waning of the initial effects of bosentan (see Results), rather than to residual actions of big ET-1 in the presence of bosentan. Since bosentan so effectively blocked all the actions of big ET-1, it seems likely that the latter exerts its effects through ET_A- and/or ET_B-receptors. While this probably occurs after the local conversion of big ET-1 to ET-1 (Gardiner *et al.*, 1991), it has been suggested that unprocessed big ET-1 may also exert haemodynamic effects (Douglas & Hiley, 1991). If this is the case, then these actions appear to be mediated through ET_A- and/or ET_B-receptors, or possibly through another ET-receptor subtype that is antagonized by bosentan. Although it is theoretically possible that bosentan could have inhibited the haemodynamic effects of big ET-1 by preventing the generation of ET-1, Clozel *et al.* (1994) have reported that bosentan does not inhibit endothelin converting enzyme.

In conclusion, bosentan is an effective antagonist of the *in vivo* haemodynamic effects of ET-1, -2 and -3, and big ET-1 in conscious rats. Since previous studies have shown bosentan has no effect on responses to many substances, including catecholamines, prostanoids, angiotensin and vasopressin (Clozel *et al.*, 1994), this compound will be a powerful tool for discerning the putative role of endothelins in cardiovascular pathophysiology.

We are extremely grateful to Dr Martine Clozel (F. Hoffmann LaRoche Ltd.) for the gift of bosentan, and for useful discussions of the work herein.

References

BATTISTINI, B., D'ORLÉANS-JUSTE, P. & SIROIS, P. (1993). Endothelins: circulating plasma levels and presence in other biological fluids. *Lab. Invest.*, **68**, 600–628.

BENNETT, T., GARDINER, S.M., KEMP, P.A., DAVENPORT, A.P. & EDVINSSON, L. (1993). Influence of an ET_A-receptor antagonist on regional haemodynamic responses to endothelin-1 (ET-1) and [$Ala^{11,15}$]Ac-ET-1(6–21) in conscious rats. *Br. J. Pharmacol.*, **109**, suppl. 57P.

BIGAUD, M. & PELTON, J.T. (1992). Discrimination between ET_A- and ET_B-receptor-mediated effects of endothelin-1 and [$Ala^{1,3,11,15}$] endothelin-1 by BQ-123 in the anaesthetized rat. *Br. J. Pharmacol.*, **107**, 912–918.

CLOZEL, M., BREU, V., BURRI, K., CASSAL, J.M., FISHLI, W., GRAY, G.A., HIRTH, G., KALINA, B., LÖFFLER, B.M., MULLER, M., NEIDHART, W. & RAMUZ, H. (1993). Pathophysiological role of endothelin revealed by the first orally active endothelin receptor antagonist. *Nature*, **365**, 759–761.

CLOZEL, M., BREU, V., GRAY, G.A., KALINA, B., LÖFFLER, B.M., BURRI, K., CASSAL, J.M., HIRTH, G., MULLER, M., NEIDHART, W. & RAMUZ, H. (1994). Pharmacological characterization of bosentan, a new potent orally active non-peptide endothelin receptor antagonist. *J. Pharmacol. Exp. Ther.*, (in press).

CLOZEL, M., GRAY, G.A., BREU, V., LÖFFLER, B.-M. & OSTERWALDER, R. (1992). The endothelin ET_B-receptor mediates both vasodilatation and vasoconstriction *in vivo*. *Biochem. Biophys. Res. Commun.*, **186**, 867–873.

CRISTOL, J.-P., WARNER, T.D., THIEMERMANN, C. & VANE, J.R. (1993). Mediation via different receptors of the vasoconstrictor effects of endothelins and sarafotoxins in the systemic circulation and renal vasculature of the anaesthetized rat. *Br. J. Pharmacol.*, **108**, 776–779.

DOUGLAS, S.A. & HILEY, C.R. (1991). Responses to endothelin-1, human proendothelin [1-38] and porcine proendothelin [1–39] in the rat on intravenous administration and in the blood perfused mesentery. *Neurochem. Int.*, **18**, 445–454.

GARDINER, S.M., COMPTON, A.M. & BENNETT, T. (1990a). Effects of endothelin-1 on cardiac output in conscious rats in the absence and presence of cardiac autonomic blockade. *Eur. J. Pharmacol.*, **183**, 2232–2233.

GARDINER, S.M., COMPTON, A.M. & BENNETT, T. (1990b). Regional hemodynamic effect of endothelin-2 and sarafotoxin-S6b in conscious rats. *Am. J. Physiol.*, **258**, R912–R917.

GARDINER, S.M., COMPTON, A.M. & BENNETT, T. (1990c). Regional haemodynamic effects of endothelin-1 and endothelin-3 in conscious Long Evans and Brattleboro rats. *Br. J. Pharmacol.*, **99**, 107–112.

GARDINER, S.M., COMPTON, A.M. & BENNETT, T. (1990d). Effects of indomethacin on the regional haemodynamic responses to low doses of endothelins and sarafotoxin. *Br. J. Pharmacol.*, **100**, 158–162.

GARDINER, S.M., COMPTON, A.M., KEMP, P.A. & BENNETT, T. (1991). The effects of phosphoramidon on the regional haemodynamic responses to human proendothelin [1–38] in conscious rats. *Br. J. Pharmacol.*, **103**, 2009–2015.

GARDINER, S.M., KEMP, P.A. & BENNETT, T. (1992a). Inhibition by phosphoramidon of the regional haemodynamic effects of proendothelin-2 and -3 in conscious rats. *Br. J. Pharmacol.*, **107**, 584–590.

GARDINER, S.M., KEMP, P.A., BENNETT, T. & DAVENPORT, A.P. (1992b). Regional haemodynamic responses to [$Ala^{1,3,11,15}$]endothelin-1 in conscious rats. *Br. J. Pharmacol.*, **107**, 415P.

HILEY, C.R., DOUGLAS, S.A. & RANDALL, M.D. (1989). Pressor effects of endothelin-1 and some analogues in the perfused superior mesenteric arterial bed of the rat. *J. Cardiovasc. Pharmacol.*, **13** (suppl. 5), S197–S199.

HUGGINS, J.P., PELTON, J.T. & MILLER, R.C. (1993). The structure and specificity of endothelin receptors: their importance in physiology and medicine. *Pharmacol. Ther.*, **59**, 55–123.

MCMURDO, L., CORDER, R., THIEMERMANN, C. & VANE, J.R. (1993). Incomplete inhibition of the pressor effects of endothelin-1 and related peptides in the anaesthetized rat with BQ 123 provides evidence for more than one vasoconstrictor receptor. *Br. J. Pharmacol.*, **108**, 557–561.

MORELAND, S., MCMULLEN, D.M, DELANELY, C.L., LEE, V.G. & HUNT, J.T. (1992). Venous smooth muscle contains vasoconstrictor ET_B-like receptors. *Biochem. Biophys Res. Commun.*, **184**, 100–106.

RANDALL, M.D. (1991). Vascular activities of the endothelins. *Pharmacol. Ther.*, **50**, 73–93.

WARNER, T.D., ALLCOCK, G.H, CORDER, R. & VANE, J.R. (1993). Use of the endothelin antagonists BQ-123 and PD 142893 to reveal three endothelin receptors mediating smooth muscle contraction and the release of EDRF. *Br. J. Pharmacol.*, **110**, 777–782.

(Received December 17, 1993
Revised March 22, 1994
Accepted March 23, 1994)

Br. J. Pharmacol. (1994), **112**, 831–836

Contribution of both nitric oxide and a change in membrane potential to acetylcholine-induced relaxation in the rat small mesenteric artery

Gareth J. Waldron & [1]Christopher J. Garland

Department of Pharmacology, University of Bristol, University Walk, Bristol BS8 1TD

1 Acetylcholine stimulated repolarization and relaxation in isolated segments of rat small mesenteric artery ($D_{100} = 325 \pm 9\,\mu m$) in which the smooth muscle cells were depolarized and contracted by submaximal concentrations of noradrenaline (0.75–2.5 μM). There was no significant difference either in the time taken to initiate relaxation or hyperpolarization, or for these parameters to reach maximum in response to acetylcholine.

2 The nitric oxide synthase inhibitor, N^G-nitro L-arginine methyl ester (L-NAME, 100 μM) reduced the pD_2 for acetylcholine-induced relaxation from 7.5 to 7 and depressed the maximum relaxation from 89% to 68% in tissues stimulated with noradrenaline. The pD_2 for smooth muscle repolarization in these experiments was also reduced (7.4 to 6.6) but the maximum change in membrane potential in response to acetylcholine was unaltered. The increase in potential now clearly preceded relaxation by 3.7 s (to initiation) and 4.7 s (to maximum).

3 In the presence of noradrenaline and a raised potassium concentration (25 mM), the repolarization to acetylcholine was markedly attenuated. Simultaneous tension measurements also revealed a marked reduction in the maximal relaxation to acetylcholine, but the pD_2 was unchanged at 7.4.

4 The residual relaxation recorded in the absence of marked repolarization (in the presence of noradrenaline and 25 mM potassium) was abolished by the addition of 100 μM L-NAME.

5 Nitric oxide gas in solution (0.2–2.2 μM; NO_g) relaxed artery segments precontracted with noradrenaline. The magnitude of relaxation to NO_g was not altered in the presence of noradrenaline and 25 mM potassium.

6 These data provide additional evidence that acetylcholine-evoked endothelium-dependent increases in membrane potential provide a major mechanism for smooth muscle relaxation in the mesenteric artery. They also show that voltage-dependent and independent (initiated by NO) mechanisms can both contribute to relaxation, and suggest that NO may modulate the increase in membrane potential or the release of a hyperpolarizing factor.

Keywords: Vascular smooth muscle; endothelial cells; nitric oxide; EDHF; mesenteric artery

Introduction

Acetylcholine and related cholinomimetics stimulate endothelium-dependent smooth muscle relaxation which is associated with membrane hyperpolarization (Bolton *et al.*, 1984; Chen *et al.*, 1988; Feletou & Vanhoutte, 1988; Brayden, 1990; McPherson & Angus, 1991; Garland & McPherson, 1992; Rand & Garland, 1992). The smooth muscle hyperpolarization, like the relaxation, is apparently mediated by the release of a diffusible factor (Feletou & Vanhoutte, 1988; Chen *et al.*, 1991). Whether or not nitric oxide (NO), which is, or is very closely related to, endothelium-derived relaxant factor (EDRF), contributes to the membrane potential change in some arteries is not clear. In the rat aorta and pulmonary artery, the hyperpolarization to acetylcholine was not blocked by either oxyhaemoglobin or methylene blue, while relaxation was reduced. These data indicated the involvement of a distinct hyperpolarizing factor (EDHF) released at the same time as NO (Chen *et al.*, 1988; Taylor & Weston, 1988). This suggestion was supported by the failure of exogenous nitric oxide to induce smooth muscle hyperpolarization in concentrations which induced marked relaxation in a number of vascular preparations (Komori *et al.*, 1988; Huang *et al.*, 1988; Brayden, 1990; Rand & Garland, 1992; Plane & Garland, 1993), and the insensitivity of acetylcholine-induced hyperpolarization or repolarization to the action of nitric oxide synthase inhibitors in some arteries (Chen *et al.*, 1991; Nagao & Vanhoutte, 1991; Garland & McPherson, 1992).

In the rat small mesenteric artery, we recently presented evidence against a role for NO in the smooth muscle hyperpolarization and repolarization to acetylcholine (Garland & McPherson, 1992). Although exogenous NO caused glibenclamide-sensitive hyperpolarization in unstimulated smooth muscle cells, this effect was blocked by prior depolarization, while the membrane potential change to acetylcholine was not sensitive to glibenclamide and was increased in magnitude by prior depolarization. In addition, the hyperpolarization (in unstimulated arteries) and the repolarization and relaxation (in noradrenaline-stimulated arteries) to acetylcholine were not markedly altered by either the NO-synthase inhibitor, nitro-L-arginine, or by oxyhaemoglobin. While these results argue strongly against NO having a significant role in the membrane potential increases to acetylcholine, the possibility remains that NO does contribute to the smooth muscle relaxation. If NO and a hyperpolarizing factor are released simultaneously in response to acetylcholine, they may act in parallel to cause relaxation by different mechanisms, one independent of a change in membrane potential, the other dependent upon a change. Even if the production of NO were completely blocked, marked relaxation could still be caused by increases in membrane potential. To study the possibility that NO contributes to relaxation it is therefore necessary to block the increases in membrane potential. Endothelium-dependent hyperpolarization reflects an increase in smooth muscle potassium conductance and can be abolished by raising the external potassium

[1] Author for correspondence.

concentration (Taylor & Weston, 1988; Chen & Suzuki, 1989; Nagao & Vanhoutte, 1991).

In the present experiments, we have investigated the possibility that both NO and increases in smooth muscle membrane potential contribute to the endothelium-dependent relaxation that is induced by acetylcholine in the rat small mesenteric artery. Some of the results have been presented in preliminary form at the Cambridge meeting of the British Pharmacological Society (Waldron *et al.*, 1993).

Methods

Sprague-Dawley rats of either sex (approximately 300 g) were stunned and killed by cervical dislocation. The mesentery was removed and placed in physiological salt solution (PSS) at room temperature. A segment of a third order branch of the superior mesenteric artery was carefully removed and cut into cylindrical segments 1–2 mm in length. Segments were then mounted in a tissue chamber for recording simultaneous changes in smooth muscle membrane potential and tension, as previously described (Garland, 1987). Briefly, two tungsten wires (each of 25 μm diameter) were passed through the segment's lumen and each wire attached to a small plastic foot. One foot was coupled to an isometric force transducer (Harvard Biosciences, 52-9529) and the other to a microdrive (Prior, code 71). After 60 min equilibration, a passive diameter-tension curve was constructed, from which the effective transmural pressure was calculated. The segment was then set at a tension equivalent to that generated at 0.9 times the diameter of the vessel at 100 mmHg (D_{100}; Mulvany & Halpern, 1977). The segment was superfused (at 3–5 ml min^{-1}) with PSS which had been gassed with a mixture of 95% O_2/5% CO_2 and warmed to 37°C. Concentration-response curves were constructed from responses to cumulative concentrations of acetylcholine in segments precontracted to noradrenaline (0.25–2.5 μM). Nitric oxide synthase blocking drugs increase the size of contraction to a given concentration of spasmogen (Cocks & Angus, 1991). Thus, in experiments in which N^G-nitro L-arginine methyl ester (L-NAME) was present, the concentration of noradrenaline was decreased in an attempt to maintain impalements and obtain a similar level of tone compared to the experiments in which L-NAME was absent. Where this was not successful, control experiments were performed in which similar levels of tone were induced. All drugs were equilibrated with the superfusate before it entered the tissue chamber apart from nitric oxide gas – PSS containing the gas (usually 10–100 μl) was injected close to the artery segment from a gas-tight syringe.

Electrophysiology

Measurement of smooth muscle membrane potential was made with a glass microelectrode, advanced through the adventitial surface of the artery segment. The electrodes were filled with 2 M KCl and had resistances of 80–120 MΩ. Membrane electrical events were recorded through a high-input impedance d.c. preamplifier (Neurolog NL102G) and digitized, together with data from the isometric transducer, and stored on disc.

Solutions and drugs

Experiments were performed in physiological salt solution (PSS) of the following composition (mM): NaCl 119, $NaHCO_3$ 25, KCl 4.7, $MgSO_4$ 1.2, $CaCl_2$ 2.5, disodium EDTA 0.027 and glucose 11.

Drugs used were acetylcholine chloride (BDH); (−)-noradrenaline bitartrate (arterenol, Sigma); N^G-nitro L-arginine methyl ester (Sigma); nitric oxide gas (research grade, BDH).

Preparation of nitric oxide solution

One ml of 99% nitric oxide gas was injected, using a gas tight syringe, into a gas tight ampoule containing 100 ml of PSS which had been bubbled with research grade helium (BOC) for 45–60 min. Nitric oxide solution (NO_g) was then injected into the tissue chamber in volumes of 10–100 μl, with a gas tight syringe. Control injections of helium gassed PSS were always performed to assess the extent of potential injection artifacts.

Analysis of data

Where oscillations in tension or membrane potential occurred, the response to the agonist was taken to be the level of tension or membrane potential at half the amplitude of the oscillations. Relaxations are expressed as a percentage decrease in the initial tone to noradrenaline. Other data are expressed as mean ± s.e.mean. The significance between mean values was calculated by Student's *t* test, with rejection of the null hypothesis at the 5% level.

Results

Acetylcholine-induced changes in tension and membrane potential of mesenteric artery segments

The resting membrane potential of smooth muscle cells in the rat small mesenteric artery (D_{100} 325 ± 8.6 μm; $n = 23$) was −61.6 ± 2.1 mV ($n = 11$ cells). Noradrenaline (0.75–2.5 μM) depolarized the cells to −44.5 ± 2.0 mV ($n = 7$), with a subsequent increase in active tension to 1.41 ± 0.17 mN mm^{-1} ($n = 12$). In 78% of experiments, rhythmic oscillations in membrane potential and tension developed in the continued presence of noradrenaline (14.2 ± 0.5 cycles min^{-1}, $n = 11$). The application of acetylcholine (0.01–1 μM) stimulated concentration-dependent repolarization and relaxation (Figure 1). The pD_2 for relaxation was 7.5 ± 0.05 and the

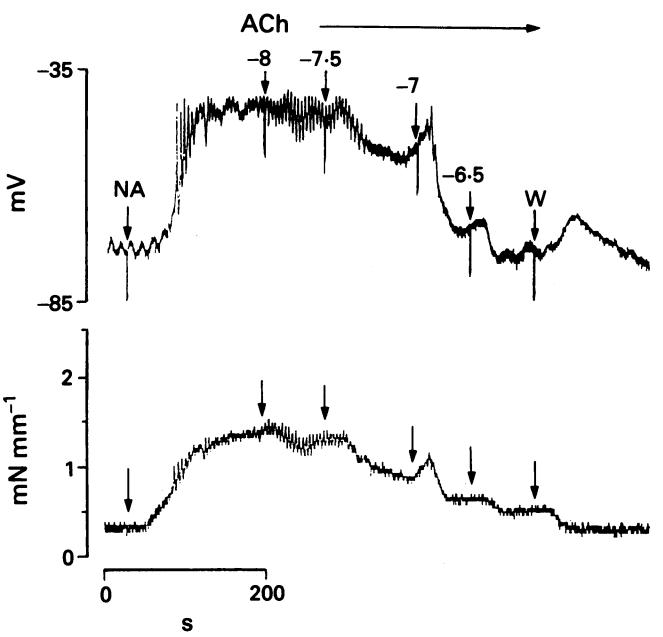

Figure 1 Representative experimental trace showing simultaneous recording of smooth muscle membrane potential (upper trace) and tension (lower trace). Noradrenaline (NA; 1 μM) depolarizes and contracts the cells and the subsequent addition of acetylcholine (ACh; 0.01–0.3 μM) stimulates concentration dependent repolarization and relaxation. Drugs were added to the superfusate chamber at the arrows. Washout is indicated by W.

maximum relaxation obtained was 92.1 ± 2.0% (all $n = 7$) with 1 μM (Figure 2a). Above 1 μM, acetylcholine stimulated an endothelium-independent smooth muscle contraction. The pD_2 for membrane repolarization was not significantly different at 7.4 ± 0.04 and the maximum increase in membrane potential was around 21 mV, changing the potential to − 66.9 ± 3.4 mV (all $n = 4$; Figure 2b). There was no difference in either the time taken to initiate relaxation or repolarization after the application of acetylcholine (relaxation preceded repolarization by 1.1 ± 1.8 s; $n = 21$), or the time taken to reach maximum (relaxation preceded repolarization by 1.6 ± 3.2 s; $n = 20$).

Acetylcholine-induced repolarization and relaxation in the presence of L-NAME

L-NAME (100 μM) was applied to the superfusate 30 min before noradrenaline and was present throughout the subsequent application of acetylcholine. In the presence of L-NAME, the concentration-response curve for relaxation was shifted to the right and the maximal relaxation reduced. The pD_2 changed from 7.5 ± 0.05 to 6.96 ± 0.12 ($P < 0.001$) and the maximal relaxation was reduced from 88.6 ± 5.1% to 67.6 ± 7.5% at 1 μM (all $n = 4$; Figure 2a). As in the absence of L-NAME, endothelium-independent contractions were obtained to higher concentrations of acetylcholine. With repolarization the pD_2 was also changed, from 7.4 ± 0.04 to 6.6 ± 0.13 ($P < 0.001$, $n = 4$; Figure 2b). L-NAME did not alter the amplitude of the maximal repolarization to acetylcholine, but it did alter the temporal relationship between increases in membrane potential and relaxation. Although in the absence of L-NAME there was no difference in the mean time taken to initiate repolarization and relaxation, or reach a maximal effect, in the presence of L-NAME the onset of repolarization always preceded the onset of relaxation by 3.7 ± 1.2 s and maximal repolarization was reached before maximal relaxation by 4.2 ± 1.8 s (both $n = 11$). In contrast to the experiments described above, in the presence of L-NAME rhythmic oscillations in membrane potential and tension were not observed indicating that NO may be involved in these oscillations, as suggested by Gustaffson *et al.* (1993).

Acetylcholine responses in the presence of raised extracellular potassium

Raising the concentration of potassium in the superfusate from 4.7 to 25 mM in the presence of prior smooth muscle depolarization and contraction to a submaximal concentration of noradrenaline, caused an additional increase in tension (0.52 mN mm^{-1}) and a depolarization of 13 mV (Table 1). Under these conditions, the subsequent addition of

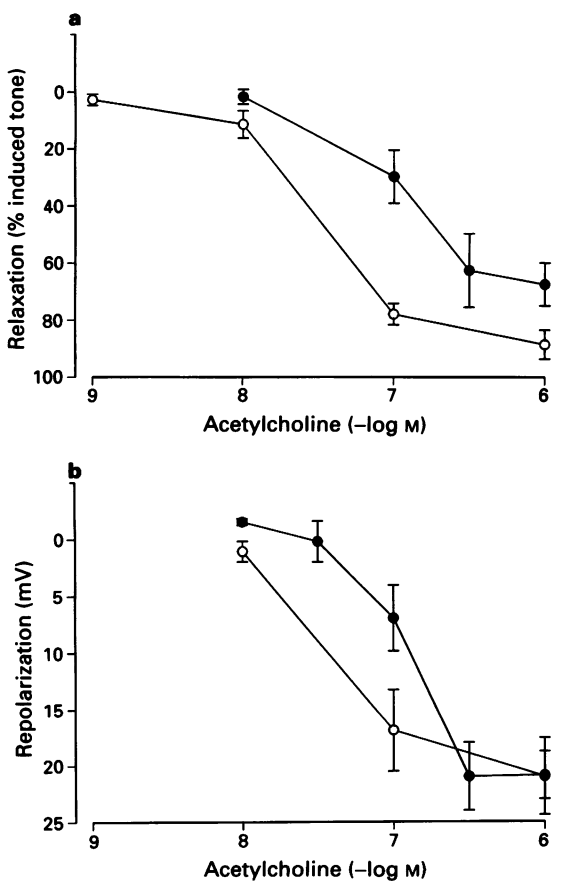

Figure 2 Mean concentration-effect curves constructed to acetylcholine in the absence (○) and presence (●) of the nitric oxide synthase inhibitor N^G-nitro-L-arginine methyl ester (L-NAME, 100 μM). (a) Relaxation of noradrenaline-induced contraction. (b) Reversal of noradrenaline-induced depolarization recorded simultaneously with the relaxations summarized in (a). Results are the mean ± s.e.means where they exceed symbol size ($n = 4$).

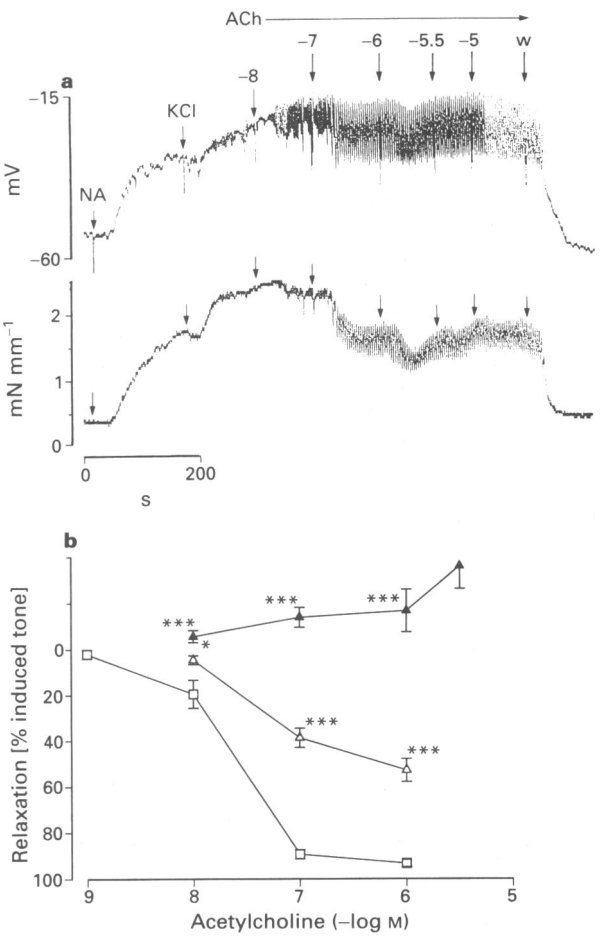

Figure 3 (a) Representative trace of a simultaneous record of membrane potential (upper trace) and tension (lower trace) showing the lack of any measurable repolarization and a marked reduction in the amount of relaxation to acetylcholine (ACh) in cells depolarized and contracted in the combined presence of 25 mM potassium and noradrenaline (NA). Drugs were added to the superfusate chamber at the arrows. Washout of all drugs is indicated by W. (b) Mean concentration-effect curves showing the effect of 25 mM potassium (△) and the combination of 25 mM potassium and 100 μM N^G-nitro-L-arginine methyl ester (L-NAME) (▲) on the relaxation to acetylcholine (□) in the presence of noradrenaline. Values are means ($n = 4$–11) with s.e.means. $P < 0.05$*; $P < 0.001$*** compared to control tissues.

Table 1 The effect of N^G-nitro-L-arginine methyl ester (L-NAME) and raised extracellular potassium on noradrenaline induced contraction and depolarization in rat small mesenteric artery

	Resting membrane potential (mV)	*Plus noradrenaline* *Membrane potential* (mV)	*Tension* ($mN\ mm^{-1}$)	*Concentration range noradrenaline* (μM)
Control	-61.6 ± 2.1 $n=11$	-44.5 ± 2.0 $n=7$	1.41 ± 0.17 $n=12$	0.75–2.5
L-NAME	-58.5 ± 2.2 $n=4$	-40.8 ± 2.2 $n=5$	1.81 ± 0.20 $n=8$	0.75–1
K^+ 25 mM	-57.2 ± 1.6 $n=4$	-31.6 ± 3.8 $n=4$**	1.93 ± 0.14 $n=5$	1–2.5
K^+ 25 mM and L-NAME	-59.2 ± 7.1 $n=3$	-33.8 ± 9.0 $n=3$	2.05 ± 0.14 $n=12$**	0.25–1

As nitric oxide synthase blocking drugs increase the magnitude of contraction the concentration of noradrenaline was varied (right-hand column) to as far as possible induce comparable levels of tone. Control experiments showed no functional antagonism between higher levels of tone (around 2 $mN\ mm^{-1}$) and relaxation to acetylcholine. Values are mean ± s.e.mean. Significant difference from control values $P<0.01$**.

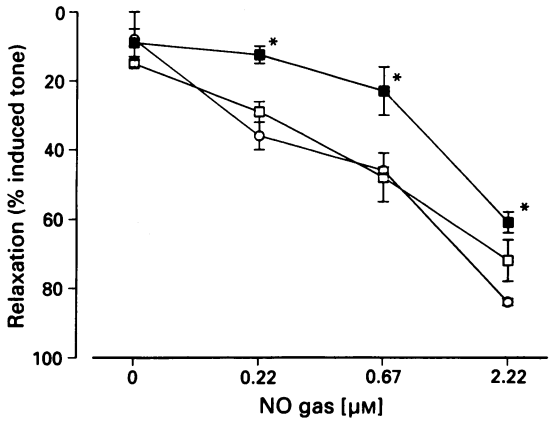

Figure 4 Mean concentration-effect curves showing the effect of raising external potassium from control levels of 4.7 mM (○) to 25 mM (□) or 30 mM (■), on the ability of nitric oxide gas (NO_g) injected directly into the organ bath to relax noradrenaline precontracted tissues. Values are means ($n=3$) ± s.e.mean. $P<0.05$* compared to 4.7 mM K^+ Krebs.

acetylcholine stimulated only a small increase in membrane potential (cf. 4 mV; Figure 3a). Rhythmic oscillations of the membrane potential and tension were still observed under these conditions (frequency 16.8 ± 0.6 cycles min^{-1}; $n=4$). The maximum smooth muscle relaxation to acetylcholine was markedly attenuated to $53.8 \pm 5.0\%$ and the pD_2 was not different from control values at 7.4 ± 0.07 ($n=5$). The residual relaxation to acetylcholine was abolished by incubating the artery segments with 100 μM L-NAME for 30 min prior to the addition of noradrenaline and increased potassium (Figure 3b). The contraction to noradrenaline and potassium in this series was close to 2 $mN\ mm^{-1}$ and the membrane potential was depolarized to −34 mV (Table 1). In experiments without L-NAME present, the potency and maximal relaxation to acetylcholine was not altered when applied against a similar level of noradrenaline-induced tone (2.04 ± 0.1 $mN\ mm^{-1}$; $n=3$). After washout and reincubation in a Krebs solution containing a normal potassium concentration, acetylcholine stimulated a transient response in the continuing presence of noradrenaline and L-NAME (six of eight experiments).

Effect of exogenous nitric oxide

Relaxation to nitric oxide (NO_g) injected directly into the tissue chamber, in artery segments contracted to noradrenaline, was not modified by the presence of 25 mM potassium. However, the magnitude of relaxation to NO_g was significantly reduced in the presence of noradrenaline and 30 mM potassium (Figure 4).

Discussion

The main conclusions from the work presented in this paper are that an increase in the smooth muscle membrane potential in response to acetylcholine provides a major drive to relaxation in the mesenteric artery, and also that nitric oxide is released in response to acetylcholine and contributes to relaxation by a mechanism independent of membrane potential change.

A close correlation between acetylcholine-induced increases in smooth muscle membrane potential and relaxation has been reported previously. Also, in unstimulated tissues, acetylcholine was shown to induce smooth muscle hyperpolarization. Both these responses to acetylcholine were endothelium-dependent (McPherson & Angus, 1991; Garland & McPherson, 1992). We have extended these observations in the present study, using simultaneous measurements of membrane potential and tension, to show that the concentration of acetylcholine required to change membrane potential and tension are not different. In addition, when the production of NO was blocked by the nitric oxide synthase inhibitor L-NAME, the onset of the change in membrane potential and the time to peak response always clearly preceded the accompanying changes in smooth muscle tension. In the absence of L-NAME there was no clear temporal relationship between these parameters.

Acetylcholine stimulates endothelium-dependent increases in smooth muscle potassium conductance, an effect which presumably underlies the increase in membrane potential observed in recent studies (Chen *et al.*, 1988; Chen & Suzuki, 1989). This idea is supported by the effect of raising the external concentration of potassium from 4.7 mM to 25 mM, which almost abolished the repolarization to acetylcholine and at the same time reduced the total relaxation by nearly 50%. This concentration of potassium did not reduce the relaxation to NO_g, so it would not be expected to modify the relaxant action of any NO released from the endothelium. Interestingly, higher concentrations of potassium did appear to reduce the relaxation to exogenous NO. An explanation for this effect is not apparent, as the levels of contraction were similar with both concentrations of potassium. This observation was not investigated further. Potassium (25 mM) would not be expected to reduce the production of NO by the endothelium as concentrations of 65 mM did not reduce endothelium-dependent relaxation to acetylcholine in the rabbit basilar artery which is predominantly due to the action of NO (Plane & Garland, 1993). So the fact that membrane

potential change in response to acetylcholine was closely correlated to smooth muscle relaxation, and that in the absence of a change in membrane potential of more than a couple of millivolts relaxation was reduced by around 50%, highlights the importance of voltage-sensitive mechanisms in the relaxant responses of the small mesenteric artery to this cholinomimetic.

Although an increase in the smooth muscle membrane potential appears to have a major role in causing relaxation to acetylcholine, several observations indicate that the increase does not reflect an action of NO *per se*. First, although exogenous NO_g or acidified sodium nitrite did stimulate smooth muscle hyperpolarization in the mesenteric artery, this action was blocked by prior depolarization to noradrenaline. In contrast, depolarization to noradrenaline increased rather than decreased the magnitude of the repolarization to acetylcholine and, in depolarized cells, NO stimulated marked smooth muscle relaxation in the absence of a change in membrane potential. Second, the hyperpolarization to NO was reversibly inhibited in the presence of the potassium channel blocker, glibenclamide. However, glibenclamide did not affect either the acetylcholine-induced hyperpolarization or the repolarization and relaxation in this artery. Third, neither repolarization nor relaxation to acetylcholine was blocked with either nitro-arginine or oxyhaemoglobin, although oxyhaemoglobin totally abolished the responses to exogenous NO (Garland & McPherson, 1992).

In light of the discrepancies between the membrane responses to exogenous NO and acetylcholine, the observations clearly indicate that changes in membrane potential to the latter do not reflect a direct action of NO on the smooth muscle cells in the mesenteric artery. Presumably, they are explained by the release of a separate diffusible factor, as demonstrated in the canine femoral and guinea-pig carotid arteries (Feletou & Vanhoutte, 1988; Chen *et al.*, 1991). Evidence for the action of a separate factor, EDHF, has been obtained in a large number of different vascular preparations (Chen *et al.*, 1988; Feletou & Vanhoutte, 1988; Taylor & Weston, 1988; Chen & Suzuki, 1989; Chen *et al.*, 1991; Garland & McPherson, 1992; Rand & Garland, 1992; Plane & Garland, 1992). Studies on the relative contribution which membrane potential changes make to relaxation are, however, limited. In the canine coronary artery, membrane potential changes to acetylcholine could be blocked with 60 mM potassium, an effect associated with a reduction in relaxation by around 60% (Nagao & Vanhoutte, 1991). As in the present study, the residual relaxation was abolished after inhibition of NO synthase. Based on the persistence of variable sized relaxations to acetylcholine in the presence of nitro-arginine in different arteries from the rat, it has been suggested that EDHF may make a greater contribution than EDRF to the relaxant response in small compared to large arteries (Nagao *et al.*, 1992). Studies with rabbit large cerebral arteries lend support to this suggestion, as the acetylcholine-induced relaxation in the basilar artery appears predominantly to reflect an action of NO (Rand & Garland, 1992; Plane & Garland, 1993).

While around half of the total relaxation to acetylcholine can be explained by a change in the smooth muscle membrane potential, the remainder appears to reflect a contribution from NO. Our original hypothesis that blocking hyperpolarization may reveal a contribution from NO was correct, as the residual relaxation in the absence of hyperpolarization was totally abolished by L-NAME. Our results are also in agreement with the observations of Gustafsson *et al.* (1993), who found that nitro-arginine and other manipulations to inhibit the action of NO blocked the rhythmic tension oscillations induced by noradrenaline in the mesenteric artery. However, we were also able to demonstrate an action of L-NAME against both relaxation and repolarization in smooth muscle cells in a normal potassium concentration. If the interpretation above is correct, and NO is not responsible for the change in membrane potential to acetylcholine, the shift in the curve for increases in membrane potential with L-NAME suggests that NO can modulate the response. A similar effect was observed with NO synthase inhibitors in the rabbit basilar artery (Rand & Garland, 1992). NO may modulate the release of an EDHF from the endothelium or act, either directly or indirectly via protein kinases, to modify changes in smooth muscle potassium conductance. Whatever the precise explanation, an effect of L-NAME was in contrast to our previous study, where nitro-arginine did not alter either smooth muscle repolarization or relaxation in similar size mesenteric arteries from Wistar-Kyoto rats (Garland & McPherson, 1992).

An explanation for the apparent discrepancy between the two studies is not obvious. The discrepancy is unlikely to reflect the use of L-NAME in the present study, rather than nitro-arginine, as similar sized relaxations to acetylcholine also persisted in the presence of nitro-arginine in larger diameter mesenteric arteries (Nagao *et al.*, 1992). In similar sized mesenteric arteries, nitro-arginine did not apparently reduce relaxation, but modified the response which became much more transient (Gustaffson *et al.*, 1993) suggestive of a response to EDHF (Chen & Suzuki, 1989). One possible explanation is that the variable effect of NO synthase inhibitors reflects the strain of rats used. Gustaffson *et al.* (1993) failed to find any effect with nitro-arginine in a number of their experiments with mesenteric arteries from Wistar rats, whilst it has been reported that nitro-arginine blocks acetylcholine-induced relaxation incompletely in mesenteric arteries from Sprague-Dawley rats (this study; Wu *et al.*, 1993). In the isolated perfused mesenteric bed from the colony of Sprague-Dawley rats used in the present study, we have found that the vasodilatation to acetylcholine is reduced by a similar extent, around 20–30%, with either nitro-arginine or its methyl ester (Parsons *et al.*, 1993). However, this reduction was observed in 80% of cases. In the remaining experiments, NO synthase inhibitors had no effect on the vasodilatation (Parsons *et al.*, unpublished data). The persistence of relaxation and changes in membrane potential to acetylcholine, in arteries from the inbred Wistar-Kyoto strain (Garland & McPherson, 1992) may be the functional expression of one aspect of this variability.

In summary, these data show that acetylcholine stimulates both voltage-dependent and independent mechanisms in the rat small mesenteric artery. The repolarization to acetylcholine, which is known to be endothelium-dependent, can account for approximately 50% of the relaxation to this agent. The remainder of the endothelium-dependent relaxation appears to be stimulated by NO, based on the sensitivity of the residual relaxation (in 25 mM potassium) to the NO synthase inhibitor L-NAME.

The support of the Wellcome Trust and Rhône-Poulenc Rorer (G.J.W.) is gratefully acknowledged.

References

BOLTON, T.B., LANG, R.J. & TAKEWAKI, T. (1984). Mechanisms of action of noradrenaline and carbachol on smooth muscle of guinea-pig anterior mesenteric artery. *J. Physiol.*, **351**, 549–572.

BRAYDEN, J.E. (1990). Membrane hyperpolarization is a mechanism of endothelium-dependent cerebral vasodilation. *Am. J. Physiol.*, **259**, H668–H673.

CHEN, G. & SUZUKI, H. (1989). Some electrical properties of the endothelium-dependent hyperpolarization recorded from rat arterial smooth muscle cells. *J. Physiol.*, **410**, 91–106.

CHEN, G., SUZUKI, H. & WESTON, A.H. (1988). Acetylcholine releases endothelium derived hyperpolarizing factor and EDRF from rat blood vessels. *Br. J. Pharmacol.*, **95**, 1165–1174.

CHEN, G., YAMAMOTO, Y., MIWA, K. & SUZUKI, H. (1991). Hyperpolarization of arterial smooth muscle induced by endothelial humoral substances. *Am. J. Physiol.*, **260**, H1888–H1892.

COCKS, T.M. & ANGUS, J.A. (1991). Evidence that contractions of isolated arteries by L-NMMA and NOLA are not due to inhibition of basal EDRF release. *J. Cardiovascular. Pharmacol.*, **17** (Suppl. 3), S159–S164.

FELETOU, M. & VANHOUTTE, P.M. (1988). Endothelium-dependent hyperpolarization of canine coronary artery smooth muscle. *Br. J. Pharmacol.*, **93**, 515–524.

GARLAND, C.J. (1987). The role of membrane depolarization in the contractile response of the rabbit basilar artery to 5-hydroxytryptamine. *J. Physiol.*, **392**, 333–348.

GARLAND, C.J. & MCPHERSON, G.A. (1992). Evidence that nitric oxide does not mediate the hyperpolarization and relaxation to acetylcholine in the rat small mesenteric artery. *Br. J. Pharmacol.*, **105**, 429–435.

GUSTAFSSON, H., MULVANY, M.J. & NILSSON, H. (1993). Rhythmic contractions of isolated arteries from the rat: influence of the endothelium. *Acta Physiol. Scand.*, **148**, 153–163.

HUANG, A.H., BUSSE, R. & BASSENGE, E. (1988). Endothelium-dependent hyperpolarization of smooth muscle cells in rabbit femoral arteries is not mediated by EDRF (nitric oxide). *Naunyn-Schmied. Arch. Pharmacol.*, **338**, 438–442.

KOMORI, K., LORENZ, R.R. & VANHOUTTE, P.M. (1988). Nitric oxide, ACh and electrical and mechanical properties of canine arterial smooth muscle. *Am. J. Physiol.*, **255**, H207–H212.

MCPHERSON, G.A. & ANGUS, J.A. (1991). Evidence that acetylcholine mediated hyperpolarization of the rat small mesenteric artery does not involve the K^+ channel opened by cromakalim. *Br. J. Pharmacol.*, **103**, 1184–1190.

MULVANY, M.J. & HALPERN, W. (1977). Contractile responses of small resistance arteries in spontaneously hypertensive and normotensive rats. *Circ. Res.*, **41**, 19–26.

NAGAO, T. & VANHOUTTE, P.M. (1991). Hyperpolarization contributes to endothelium-dependent relaxations to acetylcholine in femoral veins of rats. *Am. J. Physiol.*, **261**, H1034–H1037.

NAGAO, T., ILLIANO, S. & VANHOUTTE, P.M. (1992). Heterogeneous distribution of endothelium-dependent relaxations resistant to N^G-nitro-L-arginine in rats. *Am. J. Physiol.*, **263**, H1090–H1094.

PARSONS, S., GARLAND, C.J. & PLANE, F. (1993). The role of nitric oxide in acetylcholine-evoked dilatation of the rat isolated mesenteric bed. *Br. J. Pharmacol.*, **110**, 86P.

PLANE, F. & GARLAND, C.J. (1992). Electrophysiology of cerebral blood vessels. *Pharmacol. Ther.*, **56**, 341–358.

PLANE, F. & GARLAND, C.J. (1993). Differential effects of acetylcholine, nitric oxide and levcromakalim on smooth muscle membrane potential and tone in the rabbit basilar artery. *Br. J. Pharmacol.*, **110**, 651–656.

RAND, V.E. & GARLAND, C.J. (1992). Endothelium-dependent relaxation to acetylcholine in the rabbit basilar artery: importance of membrane hyperpolarization. *Br. J. Pharmacol.*, **106**, 143–150.

TAYLOR, S.G. & WESTON, A.H. (1988). Endothelium derived hyperpolarizing factor: an endogenous inhibitor released from the vascular endothelium. *Trends Pharmacol. Sci.*, **9**, 272–274.

WALDRON, G.J., MCPHERSON, G.A. & GARLAND, C.J. (1993). Acetylcholine-induced relaxation in the rat isolated mesenteric artery: relative importance of smooth muscle hyperpolarization. *Br. J. Pharmacol.*, **108**, 3P.

WU, C.-C., CHEN, S.-J. & YEN, M.-H. (1993). Different responses to acetylcholine in the presence of nitric oxide inhibitor in rat aortae and mesenteric arteries. *Clin. Exp. Pharmacol. Physiol.*, **20**, 405–412.

(Received February 1, 1994
Revised March 17, 1994
Accepted March 24, 1994)

Br. J. Pharmacol. (1994), **112**, 837–842

Lack of correlation of hypotensive effects with prevention of cardiac hypertrophy by perindopril after ligation of rat coronary artery

Kiyoshi Chiba, Sachiko Moriyama, Yutaka Ishigai, Akiko Fukuzawa, Kiyoshi Irie & [1]Toshiro Shibano

Exploratory Research Laboratories II, Tokyo R&D Center, Daiichi Pharmaceutical Co., Ltd., 1-16-13, Kita-Kasai, Edogawa-Ku, Tokyo 134, Japan

1 The present study was designed to test the hypothesis that beneficial effects of angiotensin converting enzyme (ACE)inhibitors are independent of a fall in blood pressure in rat experimental heart failure following coronary ligation.

2 The animals were assigned randomly to six groups; sham operation, controls subjected to coronary ligation (control), coronary ligation plus chronic treatment with ACE inhibitors at non- and hypotensive doses; perindopril (0.2 or 2 mg kg^{-1} day^{-1}) or enalapril (2 or 20 mg kg^{-1} day^{-1}) for three weeks starting one week after the ligation.

3 Systemic blood pressure was measured every week during the experiments. At the end of the treatments, cardiac function and heart weight (an index of myocardial hypertrophy) were determined. In the other animals, ACE activities in plasma and tissues including heart, kidney, lung and blood vessels were measured.

4 In the controls, cardiac ACE activity, weight of right ventricle and left ventricular end-diastolic pressure (LVEDP) were higher compared to those in the sham-operated animals four weeks after the coronary ligation. However, ACE activities were not changed in plasma, kidney, lung and aorta by ligation of the coronary artery.

5 The chronic treatment with perindopril at a dose of 0.2 mg kg^{-1} day^{-1} inhibited the increase in ACE activity in cardiac tissue and suppressed the right ventricular hypertrophy without affecting systemic haemodynamics. In contrast, enalapril at a dose of 20 mg kg^{-1} day^{-1}, but not 2 mg kg^{-1} day^{-1}, prevented the development of the right ventricular hypertrophy. Enalapril at 20 mg kg^{-1} day^{-1} also lowered systemic blood pressure.

6 There is no significant correlation between systemic blood pressure and right ventricular hypertrophy at the end of the treatment with perindopril ($r = 0.06$) or enalapril ($r = 0.1$).

7 These findings demonstrate that perindopril, an ACE inhibitor, prevents cardiac hypertrophy without affecting systemic blood pressure in the rat with heart failure after coronary ligation, and suggest that selective augmentation of ACE activity in cardiac tissue is involved in the progression of hypertrophy in this model.

Keywords: Angiotensin-converting enzyme; blood pressure; cardiac hypertrophy; coronary ligation; enalapril; perindopril

Introduction

Experimental myocardial infarction following ligation of the coronary artery results in compensatory hypertrophy in the non-infarcted myocardium. In the rat model of myocardial infarction, angiotensin converting enzyme (ACE) inhibitors, such as captopril and enalapril, prevent the progression of cardiac hypertrophy, though the exact mechanism of this prevention is unclear (Pfeffer *et al.*, 1985; 1988). The increase in pre- and afterload against the heart may favour the growth of myocytes. Indeed, ACE inhibitors are potent vasodilator agents and are likely to attenuate the pre- and afterload due to direct actions on haemodynamics. However, the reduction in blood pressure does not necessarily correlate with the prevention of cardiac hypertrophy since some classes of antihypertensive agents, such as calcium antagonists, do not significantly suppress the development of hypertrophy (Linz *et al.*, 1988; Kromer & Riegger, 1988). In the rat model of pressure overloaded cardiac hypertrophy by aortic stenosis, ACE inhibitors attenuate cardiac hypertrophy without affecting blood pressure (Linz *et al.*, 1989; Linz & Schölkens, 1992). Alternatively, earlier studies demonstrate that the renin-angiotensin system in the hearts may participate in the regulation of cardiac function and growth adaptation of the remaining viable myocytes (Campbel *et al.*, 1986; Hirsch *et al.*, 1991; Yamada *et al.*, 1991; Reiss *et al.*, 1993; Meggs *et al.*, 1993). Angiotensin II stimulates the growth of myocardium (Aceto *et al.*, 1990; Baker *et al.*, 1990) and also enhances the release of noradrenaline, which is another possible mediator of the cardiac hypertrophy via activation of α_1-adrenoceptors (Simpson, 1983). Furthermore, ACE inhibitors reduce the degradation of bradykinin in the heart (Baumgarten *et al.*, 1993; Noda *et al.*, 1993). This peptide may inhibit the cell growth due to release of nitric oxide by activation of kinin B_2 receptors (Farhy *et al.*, 1992; Linz & Schölkens, 1992). Taken in conjunction, these observations suggest that ACE inhibitors, independently of a fall in blood pressure, can prevent the progression of cardiac hypertrophy following coronary ligation. In the present study, the effects of chronic treatment with perindopril, a novel long-acting ACE inhibitor (Macfayden *et al.*, 1990), and enalapril at non-hypotensive doses were studied on cardiac hypertrophy after ligation of the coronary artery in rats.

[1] Author for correspondence.

Methods

Animals

Animals in the present study were treated according to the guidelines for animal experimentation prepared by the Japanese Association for Laboratory Animals Science. Sprague-Dawley male rats (Nihon SLC, Shizuoka, Japan), weighing 250–300 g, were assigned to sham-operation or myocardial infarction group after an observation period of three weeks.

Myocardial infarction was produced by ligation of the left coronary artery as described by Selye *et al.* (1960) with a modification. Briefly, the animals were anaesthetized by inhalation of 2% halothane, followed by 0.5% halothane during artificial respiration. A left thoracotomy was performed at the fourth intercostal space. The heart was gently exteriorized to ligate the left coronary artery 2 mm from its origin. Then, the heart was replaced in its normal position and the chest was compressed to remove air from the pleural cavity and stitched with a single suture. Successful occlusion of the artery was confirmed by appearance of Q waves in the electrocardiogram (Leads I, II and aVL), indicating the presence of myocardial ischaemia (Pfeffer *et al.*, 1987; Sweet *et al.*, 1987; 1988; Raya *et al.*, 1989). In the sham-operation group, the animals underwent left thoracotomy without ligation of the coronary artery.

One week after the surgery, the animals were anaesthetized with 2% halothane to record electrocardiograms. The animals with Q waves in leads I, II and aVL were randomly assigned to one of five groups: (a) control treatment, and chronic treatment with (b) perindopril (0.2 mg kg^{-1} day^{-1}), (c) perindopril (2 mg kg^{-1} day^{-1}), (d) enalapril (2 mg kg^{-1} day^{-1}), and (e) enalapril (20 mg kg^{-1} day^{-1}). The animals were allowed free access to tap water (sham-operation and control treatment groups) or drinking water including perindopril or enalapril for three weeks. The concentration of perindopril was adjusted to be equivalent to a daily dose of 0.2 and 2 mg kg^{-1} and enalapril, 2 and 20 mg kg^{-1} day^{-1}. The rats were weighed every week to readjust the concentrations of the compounds in the drinking water. The drug solutions were made freshly every two days. Systolic arterial pressure and heart rate were measured weekly during the treatment by means of a tail-cuff probe connected to a pressure monitor (BP-98, Softron, Japan). At the end of the treatments, cardiac function, cardiac weight and myocardial infarction size were measured. In the other animals, plasma and tissue ACE activities were determined.

Cardiac function

At the end of the treatment, cardiac function was measured under anaesthesia with thiopentone. A micro-tip catheter transducer (Model SPR-407, 2F, Miller Instruments Inc., Houston, U.S.A.) was introduced into the left ventricle through the right carotid artery for the measurement of systolic and end-diastolic pressure and maximum positive dP/dt.

Ventricular weight and myocardial infarction size

After the study of cardiac function, hearts were rapidly removed. The hearts were separated into right and left ventricle including septum, and the wet weight of the ventricles was measured. The hearts from coronary-ligated rats were fixed in 10% buffered formalin solution for determination of myocardial infarction size. The left ventricles were trimmed and sliced transversely, parallel to the atrioventricular groove, in five sections of 1.5–2.0 mm from apex to base. The sliced sections were dehydrated in methyl alcohol, cleared with xylene, and embedded in paraffin. Then, sections were cut, 5 μm in thickness and stained with Elastica-VanGieson trichrome. These serial sections were mounted on slides for photography. Infarct size was measured by planimetry and calculated as the mean percentage ratio of infarction to total left ventricular circumference (Fletcher *et al.*, 1981).

Measurement of ACE activity

Under anaesthesia with thiopentone, blood was collected from the carotid artery to obtain plasma. Tissues (heart, lung, kidney and aorta) were removed after exsanguination, and homogenized in 0.3% Triton X solution. After centrifugation of the homogenates at 29,200 *g* for 15 min, the supernatant was used for measurement of ACE activity which was determined by a modified fluorometric method according to Unger *et al.* (1982), using hippuryl-L-histidine-L-leucine as a substrate. Briefly, the tissue homogenate and plasma sample (50 μl) were incubated in 400 μl of PBS (pH 8.0): 300 mM NaCl for 2 min at 37°C. Then, 50 μl of 16.7 mM substrate solution was added to the reaction mixture and incubated at 37°C for 30 min for plasma, 180 min for cardiac tissue, 120 min for renal tissue, 10 min for pulmonary tissue and 60 min for thoracic aorta, respectively. The reaction solution (100 μl) was removed into 0.1 N NaOH solution and 25 μl of 2% *ortho*-phthaldialdehyde was added. Thirty

Table 1 Effects of oral treatment with perindopril or enalapril on systolic blood pressure and heart rate in rats with myocardial infarction

		n	Baseline	Treatment with ACE inhibitors: 1 week	2 weeks	3 weeks	4 weeks
Systolic blood pressure							
Sham		14	96.3 ± 2.8	101.7 ± 3.2*	109.2 ± 3.4*	107.4 ± 3.5*	103.8 ± 3.7*
Control		17	97.4 ± 2.9	81.9 ± 2.0	89.1 ± 2.0	90.9 ± 2.1	91.8 ± 2.2
Perindopril	0.2 mg kg^{-1} day^{-1}	17	97.6 ± 2.5	88.5 ± 2.2	92.0 ± 4.1	93.5 ± 3.6	93.6 ± 3.4
	2 mg kg^{-1} day^{-1}	17	98.8 ± 3.4	84.4 ± 2.7	74.6 ± 2.2*	72.6 ± 2.3*	75.2 ± 3.2*
Enalapril	2 mg kg^{-1} day^{-1}	17	97.3 ± 1.5	85.8 ± 2.0	88.5 ± 3.5	88.6 ± 2.6	89.3 ± 3.3
	20 mg kg^{-1} day^{-1}	17	102.3 ± 3.3	87.9 ± 3.4	80.8 ± 2.3*	82.4 ± 1.7*	78.8 ± 2.7*
Heart rate							
Sham		14	456.0 ± 12.0	410.4 ± 13.0*	417.1 ± 6.9	441.3 ± 13.4	431.3 ± 10.2
Control		17	441.3 ± 12.1	443.4 ± 10.2	416.1 ± 12.0	417.1 ± 12.8	433.1 ± 8.5
Perindopril	0.2 mg kg^{-1} day^{-1}	17	457.1 ± 10.5	456.0 ± 9.8	428.5 ± 10.8	436.3 ± 10.0	424.2 ± 8.4
	2 mg kg^{-1} day^{-1}	17	440.5 ± 8.1	426.1 ± 7.9	426.9 ± 7.2	439.3 ± 7.4	426.2 ± 7.5
Enalapril	2 mg kg^{-1} day^{-1}	17	443.9 ± 7.8	433.9 ± 7.0	429.3 ± 9.1	435.9 ± 7.3	438.8 ± 9.7
	20 mg kg^{-1} day^{-1}	17	420.3 ± 7.0	426.5 ± 9.1	442.7 ± 12.0	427.5 ± 7.2	441.3 ± 7.8

Values are mean ± s.e.mean. *n*, number of animals. *$P < 0.05$ vs. control treatment group.

minutes later, 1 ml of 0.8 N HCl was added and centrifuged at 900 *g* for 10 min. Then, fluorospectrometry of the sample was performed (excitation: 355 nm, emission: 460 nm) with a fluoroscanner (Titertek, Fluoroskan II, type 371, Flow Laboratories Japan Co. Ltd., Tokyo, Japan).

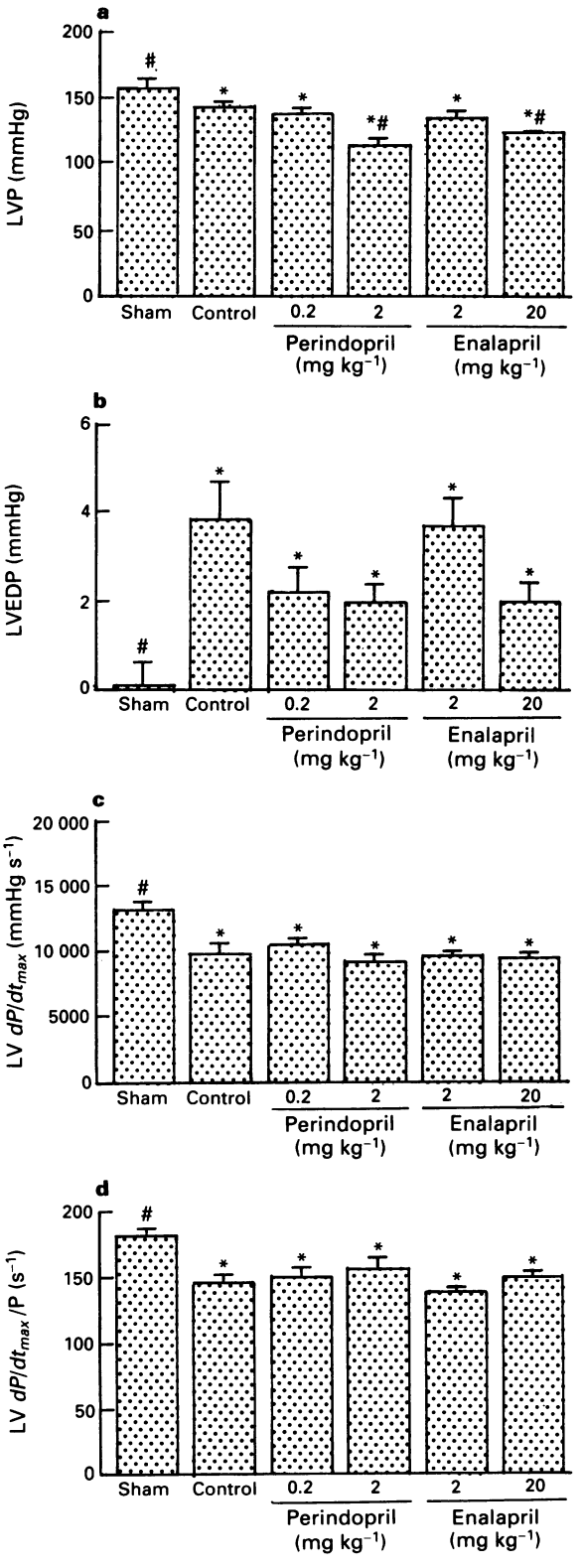

Figure 1 Cardiac function in sham-operated and coronary-ligated rats treated with perindopril (0.2 or 2 mg kg^{-1} day^{-1}), enalapril (2 or 20 mg kg^{-1} day^{-1}), or water (control). (a) LVP, left ventricular pressure; (b) LVEDP, left ventricular end-diastolic pressure; (c) LV dP/dt_{max}, the maximum rate of rise in LVP; (d) LV dP/dt_{max}/P, LV dP/dt_{max} divided by instantaneous LVP. *$P<0.05$ versus sham-operated rats; #$P<0.05$ versus control-treatment rats. Results are expressed as means ± s.e.mean of 18–23 animals.

Drugs

Perindopril tert-butylamin was obtained from Institut De Recherches Internationales Servier (Courbevoie Cedex, France). Enalapril malate was synthesized at Daiichi Pharmaceutical Co., Ltd. (Tokyo, Japan). Hippuryl-L-histidine-L-leucine and angiotensin I were obtained from Sigma Chemical Co. (St. Louis, MO, U.S.A.); *ortho*-phthaldialdehyde from Peptide Institute, Inc. (Osaka, Japan); halothane from Takeda Chemical Industries, Ltd. (Osaka, Japan).

Statistical analysis

Results are expressed as mean ± s.e.mean; *n* refers to the number of animals. Statistical comparison was performed by means of Kruskal-Wallis test, followed by Mann-Whitney test. A *P* value of less than 0.05 were considered to indicate statistically significant differences between groups.

Results

Changes in systemic blood pressure and heart rate after coronary ligation (Table 1)

There was no significant difference between the groups in systolic blood pressure and heart rate at the beginning of the experiments. In the coronary-ligated rats, systolic blood pressure decreased one week after the ligation from 98.7 ± 1.2 mmHg to 86.1 ± 1.2 mmHg (in total, $n = 85$). The oral administration of perindopril (2 mg kg^{-1} day^{-1}) and enalapril (20 mg kg^{-1} day^{-1}) reduced systolic blood pressure, which lasted until the end of the experiments. Neither perindopril nor enalapril affected heart rate.

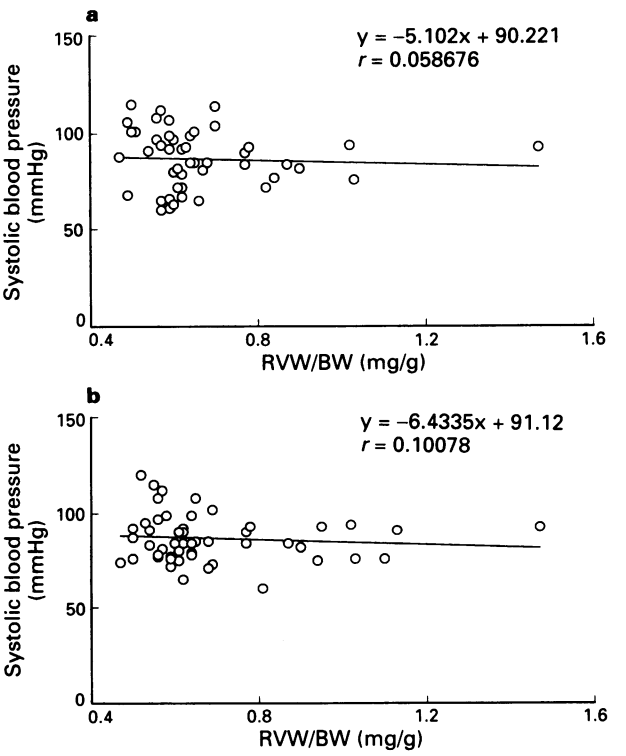

Figure 2 Correlation between cardiac hypertrophy and systemic blood pressure. (a) Controls and perindopril-treated group (0.2 and 2 mg kg^{-1} day^{-1}); (b) controls and enalapril-treated groups (2 and 20 mg kg^{-1} day^{-1}). RVW/BW, a ratio of right ventricular weight to body weight. *r* = correlation coefficient.

Table 2 Effects of oral treatment with perindopril or enalapril on cardiac hypertrophy and infarct size in rats with myocardial infarction

		Coronary ligation				
			Perindopril		*Enalapril*	
	Sham ($n = 14$)	*Control* ($n = 17$)	0.2 mg kg^{-1} day^{-1} ($n = 17$)	2 mg kg^{-1} day^{-1} ($n = 17$)	2 mg kg^{-1} day^{-1} ($n = 17$)	20 mg kg^{-1} day^{-1} ($n = 17$)
Weights						
BW (g)	434 ± 5‡	398 ± 6*	393 ± 6*	381 ± 7*	400 ± 6*	380 ± 7*‡
RVW (mg)	249 ± 7	301 ± 19	240 ± 9	229 ± 7	277 ± 20	228 ± 7*‡
LVW (mg)	846 ± 18	801 ± 16	786 ± 19*‡	678 ± 10*‡	757 ± 10*‡	707 ± 11*‡
WVW (mg)	1095 ± 24	1102 ± 19	1026 ± 25‡	906 ± 15*‡	1034 ± 24*‡	935 ± 14*‡
Cardiac hypertrophic indices						
RVW/BW (mg/g)	0.57 ± 0.01‡	0.76 ± 0.06*	0.61 ± 0.02‡	0.60 ± 0.02‡	0.69 ± 0.05	0.60 ± 0.02‡
LVW/BW (mg/g)	1.95 ± 0.03	2.02 ± 4.04	2.00 ± 0.04	1.78 ± 0.02	1.90 ± 0.02‡	1.87 ± 0.04‡
WVW/BW (mg/g)	2.52 ± 0.04‡	2.78 ± 0.07*	2.61 ± 0.05	2.38 ± 0.03*‡	2.59 ± 0.06‡	2.47 ± 0.04‡
Infarction size (%)		56 ± 3	49 ± 3	45 ± 3‡	44 ± 2‡	43 ± 3‡

Values are mean ± s.e.mean. BW, body weight; RVW, right ventricular weight; LVW, left ventricular weight; WVW, whole ventricular weight; infarction size, percent of the ventricle; n, number of animals. *$P < 0.05$ vs. sham; ‡$P < 0.05$ vs. control.

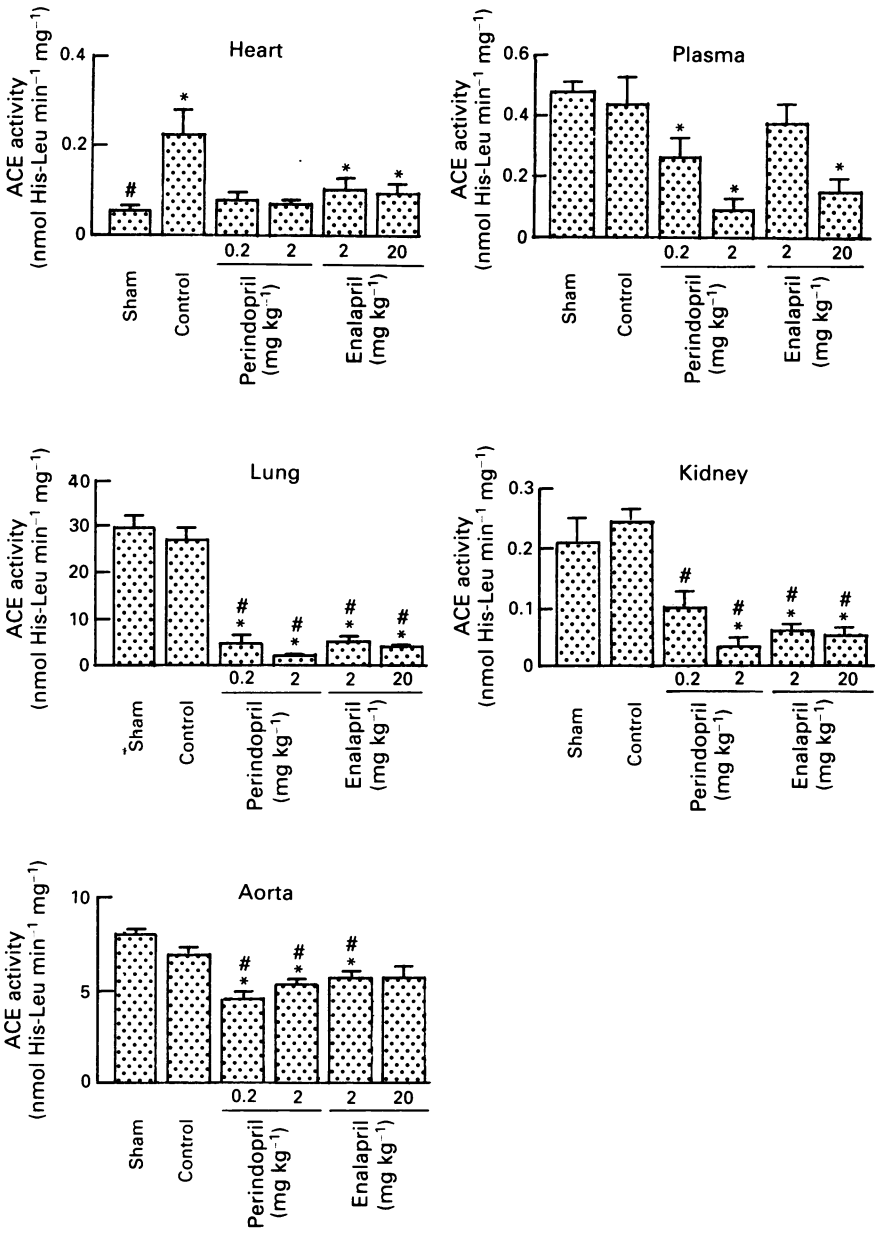

Figure 3 Angiotensin converting enzyme (ACE) activity in sham-operated and coronary-ligated rats treated with perindopril (0.2 or 2 mg kg^{-1} day^{-1}), enalapril (2 or 20 mg kg^{-1} day^{-1}), or water (control). *$P < 0.05$ versus sham-operated rats; #$P < 0.05$ versus control rats. Results are expressed as means ± s.e.mean of five animals.

Cardiac function at the end of treatment (Figure 1)

In the controls, left ventricular pressure (LVP), the maximum rate of rise of LVP (LV dP/dt_{max}) and LV dp/dt_{max} divided by instantaneous LVP (LV $dP/dt_{max}/P$; an index of cardiac contractility) were reduced, and left ventricular end-diastolic pressure (LVEDP) was increased compared to the sham-operated group. Perindopril (2 mg kg^{-1} day^{-1}) and enalapril (20 mg kg^{-1} day^{-1}) decreased LVP and LV dP/dt_{max}, respectively. There was no significant difference in LVEDP and LV $dp/dt_{max}/P$ between the controls, perindopril- and enalapril-treated groups.

Cardiac weight and myocardial infarction size (Table 2)

The ratio of right ventricular weight to body weight (RVW/BW) was higher in the controls than in the sham-operated group. This increase in RVW/BW was significantly attenuated in the animals treated with perindopril (0.2 mg kg^{-1} day^{-1} or 2 mg kg^{-1} day^{-1}) or enalapril (20 mg kg^{-1} day^{-1}), but not in the animals treated with 2 mg kg^{-1} day^{-1} enalapril. There was no significant correlation between RVW/BW and systemic blood pressure at the end of treatments with perindopril ($r = 0.06$) or enalapril ($r = 0.1$) (Figure 2). Although myocardial infarction size varied in a narrow range (43.0–56.2% of left ventricle) in all of the coronary-ligated rats, the size in animals treated with perindopril (2 mg kg^{-1} day^{-1}) and enalapril (2 and 20 mg kg^{-1} day^{-1}) was significantly smaller than in controls.

ACE activity (Figure 3)

Cardiac ACE activity was four fold higher in the control treatment group with coronary ligation (control) than in the sham-operated group. In contrast, there was no significant difference between control and sham-operated groups in ACE activities in plasma and kidney, lung and aorta. The increase in cardiac ACE activity was significantly inhibited by chronic treatment with perindopril (0.2 and 2 mg kg^{-1} day^{-1}), but not by treatment with enalapril (2 and 20 mg kg^{-1} day^{-1}). ACE activities in the kidney and lung were lowered in the groups treated with perindopril or enalapril at both doses, respectively. Aortic ACE activity was suppressed in the perindopril-treated (0.2 and 2 mg kg^{-1} day^{-1}) and 2 mg kg^{-1} day^{-1} enalapril-treated groups, but not in the 20 mg kg^{-1} day^{-1} enalapril-treated group.

Discussion

To clarify the beneficial effects of chronic treatment with ACE inhibitors on cardiac hypertrophy and dysfunction after coronary ligation, the present study focused on the changes in haemodynamics and tissue ACE activities. In the acute phase of myocardial infarction, the activation of renin in plasma can alter systemic haemodynamics, which may affect the chronic progression of cardiac hypertrophy and dysfunction (Dzau *et al.*, 1981). To avoid an interaction with the acute effects of ACE inhibitors on haemodynamics, the inhibitors were given to the rats from one week after ligation of coronary arteries, when the activities of circulating renin-angiotensin system return to baseline. The selection of two oral doses of each perindopril or enalapril was based on the effects of the compounds on systemic blood pressure in preliminary studies (data not shown); lower doses which did not alter blood pressure and higher doses which decreased systolic blood pressure by 10–15 mmHg.

At the end of the experiments, four weeks after coronary ligation, significant cardiac hypertrophies were induced in the right ventricles. The progression of right ventricular hypertrophy is an adaptive response to the increased pre- and afterload due to impaired function of left ventricle with myocardial infarction. The hypertrophy in the right ventricle was associated with the elevation of LVEDP and increase in cardiac ACE activity in the controls with coronary ligation compared to sham-operated animals. However, ACE activities were not enhanced in plasma, lung, kidney and aorta, indicating a selective activation of cardiac ACE in rats with myocardial infarction. The present results are consistent with previous findings (Hirsch *et al.*, 1991). Chronic treatment with perindopril at both doses of 0.2 and 2 mg kg^{-1} day^{-1} attenuated right ventricular hypertrophy and lowered ACE activities in heart, lung, aorta and kidney, but not in plasma. Perindopril at 0.2 mg kg^{-1} day^{-1} did not alter systemic blood pressure and heart rate during the experiments. The increase in LVEDP in controls may contribute to stimulate the progression of the cardiac hypertrophy. However, perindopril and enalapril did not significantly reduce LVEDP at the end of experiments. In contrast to perindopril, enalapril at non-hypotensive dose (2 mg kg^{-1} day^{-1}) did not inhibit right ventricular hypertrophy. A dose of 20 mg kg^{-1} day^{-1} of enalapril was required (which lowered blood pressure) to attenuate the hypertrophy in right ventricles. However, it is unlikely that enalapril inhibits cardiac hypertrophy due to its effects on haemodynamics since there is no correlation between systolic blood pressure and right ventricular hypertrophy at the end of treatment with enalapril. Hence, the present findings demonstrate that the beneficial effects of ACE inhibitors are independent of a significant fall in blood pressure on the cardiac hypertrophy. Thus, the direct influence on haemodynamics is separate from the anti-hypertrophic effects of ACE inhibitors in the rat heart failure model of coronary ligation. The present results are in agreement with previous studies showing that ramipril prevents left ventricular hypertrophy without blood pressure reduction in the aortic stenosis model in rats (Linz *et al.*, 1989; Linz & Schölkens, 1992). Alternatively, the present findings suggest that selective augmentation of ACE activities in cardiac tissues explains, at least in part, the progression of cardiac hypertrophy after coronary ligation. Stimulation of conversion of angiotensin I to angiotensin II may lead to cell growth of myocytes. The discrepancy between the two ACE inhibitors, perindopril and enalapril, in the selectivity of actions on cardiac hypertrophy and haemodynamics may be due to the different potency of ACE inhibition in hearts and vessels (Hirsch *et al.*, 1992). The attenuation by perindopril of the progression of cardiac hypertrophy and the increase in cardiac ACE activity is consistent with earlier observations (Pfeffer *et al.*, 1985; 1988; Hirsch *et al.*, 1991; Fornes *et al.*, 1992). Perindopril (2 mg kg^{-1} day^{-1}) and enalapril (2 and 20 mg kg^{-1} day^{-1}) lowered the weight of left ventricles including septum (LVW or LVW/BW). The inhibitors may suppress the cell growth in the non-infarcted region of the left ventricle; however, the interpretation of the present results requires caution since most of the infarcted myocardium had degenerated. The reduction of infarct size by perindopril and enalapril might attenuate the impaired cardiac function.

In addition, the results of the present study do not rule out other possibilities concerning the mechanism of action of ACE inhibitors. The enhanced concentration of bradykinin produced by ACE inhibitors in the hearts may participate in the regulation of cardiac hypertrophy since the anti-hypertrophy effect of ramipril is inhibited by Hoe 140, a kinin B_2 receptor antagonist (Linz & Schölkens, 1992). Furthermore, angiotensin II stimulates the release of noradrenaline from adrenergic nerve endings, which may accelerate cardiac hypertrophy due to the activation of α_1-adrenoceptors (Newling *et al.*, 1989).

In conclusion, the present study demonstrates a separation of hypotensive effects from anti-hypertrophic actions of ACE inhibitors after myocardial infarction in rats.

References

ACETO, J.F. & BAKER, K.M. (1990). [Sar1]angiotensin II receptor-mediated stimulation of protein synthesis in chick heart cells. *Am. J. Physiol.*, **259**, H806–H813.

BAKER, K.M., CHERMIN, M.I., WIXSON, S.K. & ACETO, J.F. (1990). Renin-angiotensin system involvement in pressure-overload cardiac hypertrophy in rats. *Am. J. Physiol.*, **259**, H324–H332.

BAUMGARTEN, C.R., LINZ, W., KUNKEL, G., SCHÖLKENS, B.A. & WIEMER, G. (1993). Ramiprilat increases bradykinin outflow from isolated hearts of rat. *Br. J. Pharmacol.*, **108**, 293–295.

CAMPBEL, D.J. & HABENER, J.F. (1986). The angiotensinogen gene is expressed and differentially regulated in multiple tissues of the rat. *J. Clin. Invest.*, **78**, 31–39.

DZAU, V.J., COLUCCI, W.S., HOLLENBERG, N.K. & WILLIAMS, G.H. (1981). Relation of the renin-angiotensin-aldosterone system to clinical state in congestive heart failure. *Circulation*, **63**, 645–651.

FARHY, R.D., HO, K.L., CARRETERO, O.A. & SCICLI, A.G. (1992). Kinins mediate the antiproliferative effect of ramipril in rat carotid artery. *Biochem. Biophys. Res. Commun.*, **182**, 283–288.

FLETCHER, P.J., PFEFFER, J.M., PFEFFER, M.A. & BRAUNWALD, E. (1981). Left ventricular diastolic-volume relations in rats with healed myocardial infarction. *Circ. Res.*, **49**, 618–626.

FORNES, P., RICHER, C., PUSSARD, E., HEUDES, D., DOMERGUE, V. & GIUDICELLI, J.F. (1992). Beneficial effects of trandolapril on experimentally induced congestive heart failure in rats. *Am. J. Cardiol.*, **70**, 43D–51D.

HIRSCH, A.T., TALSNESS, C.E., SCHUNKERT, H., PAUL, M. & DZAU, V.J. (1991). Tissue-specific activation of cardiac angiotensin converting enzyme in experimental heart failure. *Circ. Res.*, **69**, 475–482.

HIRSCH, A.T., TALSNESS, C.E., SMITH, A.D., SCHUNKERT, H., INGERLFINGER, J.R. & DZAU, V.J. (1992). Differential effects of captopril and enalapril on tissue renin-angiotensin systems in experimental heart failure. *Circulation*, **86**, 1566–1574.

KROMER, E.P. & RIEGGER, A.J. (1988). Effects of long-term angiotensin converting enzyme inhibition on myocardial hypertrophy in experimental aortic stenosis in the rat. *Am. J. Cardiol.*, **62**, 161–163.

LINZ, W. & SCHÖLKENS, B.A. (1992). A specific B_2-bradykinin-receptor antagonist Hoe 140 abolishes the antihypertrophic effect of ramipril. *Br. J. Pharmacol.*, **105**, 771–772.

LINZ, W., SCHÖLKENS, B.A., DONAUBAUER, H.AH. & GANTEN, D. (1988). Effects of ramipril, nifedipine and dihydralazine on cardiac hypertrophy in rats. *Clin. Exp. Hypertens*, **A10**, 711.

LINZ, W., SCHÖLKENS, B.A. & GATEN, D. (1989). Converting enyzme inhibition specifically prevents the development and induced the regression of cardiac hypertrophy in rats. *Clin. Exp. Hypertens*, **A11**, 1325–1350.

MACFAYDEN, R.J., LEES, K.R. & REID, J.L. (1990). Perindopril: a review of its pharmacokinetics and clinical pharmacology. *Drugs*, **39**, 49–63.

MEGGS, L.G., COUPET, J., HUANG, H., CHENG, W., LI, P., CAPASSO, J.M., HOMCY, C.J. & ANVERSA, P. (1993). Regulation of angiotensin II receptors on ventricular myocytes after myocardial infarction in rats. *Circ. Res.*, **72**, 1149–1162.

NEWLING, R.P., FLETCHER, P.J., CONTIS, M. & SHAW, J. (1989). Noradrenaline and cardiac hypertrophy in the rat: changes in morphology, blood pressure and ventricular performance. *J. Hypertens*, **7**, 561–567.

NODA, K., SASAGURI, M., IDEISHI, M., IKEDA, M. & ARAKAWA, K. (1993). Role of locally formed angiotensin II and bradykinin in the reduction of myocardial infarct size in dogs. *Cardiovasc. Res.*, **27**, 334–340.

PFEFFER, J.M., PFEFFER, M.A. & BRAUNWALD, E. (1987). Hemodynamic benefits and prolonged survival with long-term captopril therapy in rats with myocardial infarction and heart failure. *Circulation*, **75** (suppl. I), 1-149–1-155.

PFEFFER, M.A., PFEFFER, J.M., STEINBERG, C. & FINN, P. (1985). Survival after an experimental myocardial infarction: Beneficial effects of long-term therapy with captopril. *Circulation*, **72**, 406–412.

PFEFFER, M.A., LAMAS, G.A., VAUGHN, D.E., PARISI, A.F. & BRAUNWALD, E. (1988). Effect of captopril on progressive ventricular dilation after anterior myocardial infarction. *N. Engl. J. Med.*, **319**, 80–86.

RAYA, T.E., GAY, R.G., ARUIRRE, M. & GOLDMAN, S. (1989). Impertance of venodilation in prevention of left ventricular dilation after chronic large myocardial infarction in rats: a comparison of captopril and hydralazine. *Circ. Res.*, **64**, 330–337.

REISS, K., CAPASSO, J.M., HUANG, H.E., MEGGS, L.G., LI, P. & ANVERSA, P. (1993). ANG II receptors, c-mys, and c-jun in myocytes after myocardial infarction and ventricular failure. *Am. J. Physiol.*, **264**, H760–H769.

SELYE, H., BAJUSZ, E., GRASSO, S. & MENDELL, P. (1969). Simple techniques for the surgical occlusion of the coronary vessels in the rat. *Angiology*, **11**, 398–407.

SIMPSON, P. (1983). Norepinephrine-stimulated hypertrophy of cultured rat myocardial cells is an α1-adrenergic response. *J. Clin. Invest.*, **72**, 732–738.

SWEET, C.S., EMMERT, S.E., STABILITO, I.I. & RIBERIRO, L.G.T. (1987). Increased survival in rats with congestive heart failure treated with enalapril. *J. Cardiovasc. Pharmacol.*, **10**, 636–642.

SWEET, C.S., LUDDEN, C.T., STABILITO, I.I., EMMERT, S.E. & HEYSE, J.F. (1988). Beneficial effects of milrinone and enalapril on long-term survival of rats with healed myocardial infarction. *Eur. J. Pharmacol.*, **147**, 29–37.

UNGER, T., SCHÜL, B., RASCHER, W., LANG, R.E. & GANTEN, D. (1982). Selective activation of the converting enzyme inhibitor MK 421 and comparison of its active diacid form with captopril in different tissue of the rat. *Biochem. Pharmacol.*, **31**, 3063–3070.

YAMADA, H., FABRIS, B., ALLEN, A.M., JACKSON, B., JOHNSTON, C.I. & MENDELSOHN, A.O. (1991). Localization of angiotensin converting enzyme in rat heart. *Circ. Res.*, **68**, 141–149.

(Received October 8, 1993
Revised January 24, 1994
Accepted March 25, 1994)

Br. J. Pharmacol. (1994), **112**, 843–846

A comparison of intravenous NBQX and GYKI 53655 as AMPA antagonists in the rat spinal cord

[1]Boris A. Chizh, Michael J. Cumberbatch & [2]P. Max Headley

Department of Physiology, School of Medical Sciences, University of Bristol, University Walk, Bristol BS8 1TD

1 The effects of intravenous administration of two α-amino-3-hydroxy-5-methylisoxazole-4-propionic acid (AMPA) antagonists were studied on responses of single neurones to iontophoretically applied excitatory amino acids. The tests were performed on spinal neurones in α-chloralose anaesthetized, spinalized rats.

2 Both the quinoxaline, NBQX (2–16 mg kg^{-1}) and the 2,3-benzodiazepine, GYKI 53655 (2–8 mg kg^{-1}) dose-dependently decreased responses to AMPA.

3 Both compounds were short acting, with half-recovery times of 15 min for NBQX and 7 min for GYKI 53655.

4 The selectivity for responses to AMPA over those to N-methyl-D-aspartate (NMDA) was significantly poorer for systemic NBQX than for either systemic GYKI 53655 or iontophoretic NBQX, suggesting that systemic NBQX may be converted to a less selective metabolite.

5 GYKI 53655 is therefore likely to be a more valuable tool than NBQX for the study of AMPA receptor-mediated processes *in vivo*.

Keywords: Excitatory amino acids; AMPA; NBQX; GYKI 53655

Introduction

The pathogenesis of several neurological disorders, such as epilepsia and brain ischaemia, involves neurotoxicity mediated by excitatory amino acids (EAA; Rogawski, 1993). N-methyl-D-aspartate (NMDA) antagonists have been tested clinically in such disorders, but the serious side-effects of these compounds, and their limited effectiveness, have pushed interest towards drugs acting via non-NMDA receptors (Rogawski, 1993). Two classes of selective antagonists for AMPA (α-amino-3-hydroxy-5-methylisoxazole-4-propionic acid) have been developed recently. The first class comprises competitive quinoxalinedione antagonists (Honoré *et al.*, 1988) such as NBQX (2,3-dihydroxy-6-nitro-7-sulphamoyl-benzo(F) quinoxaline; Sheardown *et al.*, 1990). The second comprise a novel group of 2,3-benzodiazepines such as GYKI 53655 (1-(4'-aminophenyl)-3-methylcarbamoyl-4-methyl-3,4-dihydro-7,8-methylene-dioxy-5H-2,3-benzodiazepine HCl; Tarnawa *et al.*, 1993) that act via an allosteric site (Zorumski *et al.*, 1993). Some of these compounds have been found effective in models of epilepsia and brain ischaemia (Rogawski, 1993). However, the interpretation of these data is currently difficult because little is known about the selectivity of these antagonists for non-NMDA *vs* NMDA receptors after systemic administration *in vivo*, although the structurally similar benzodiazepine, GYKI 52466, appears to be selective (Engberg *et al.*, 1993). We have now compared the selectivity of NBQX and GYKI 53655, administered intravenously, between the response of spinal neurones to iontophoretically applied AMPA and NMDA.

Methods

Animal preparation

Experiments were performed on 27 male Wistar rats (260–350 g). Details of the experimental methods have been described elsewhere (Headley *et al.*, 1987). Briefly, rats were anaesthetized with halothane in O_2 and tracheal, carotid and jugular cannulae were inserted. The lumbo-thoracic spinal cord was exposed and cut at T9-T11 and the animal was prepared for extracellular recordings of single dorsal horn neurone action potentials. Anaesthesia after surgery was maintained with α-chloralose (50 mg kg^{-1}, i.v. initially, then 10 mg kg^{-1} as required). Arterial blood pressure was monitored continuously; systolic pressure remained above 100 mmHg. Core temperature was maintained close to 37°C. Extracellular recordings of single dorsal horn neurone action potentials were made with the central barrel of multibarrel glass micropipettes, filled with 3.5 M NaCl. Counts of evoked spike activity, in epochs related to the stimuli, were analysed on-line with a microcomputer. Cell discharge rates were monitored on a chart recorder. At the end of experiments, the rats were killed with an overdose of pentobarbitone.

Drugs

AMPA, NMDA and NBQX were administered microiontophoretically from the side barrels of the multibarrel pipettes, from solutions of the sodium salts of AMPA (Tocris Neuramin; 10 mM in 200 mM NaCl), NMDA (Tocris Neuramin; 100 mM in 100 mM NaCl) and NBQX (Merz + Co; 1 mM in 50 mM NaCl), all at pH 7.5–8. Another barrel contained 200 mM NaCl for current balancing. AMPA and NMDA were ejected in regular cycles. NBQX, and also GYKI 53655 (Lilly & Co), were administered intravenously.

Antagonist effects are expressed quantitatively as percentages of control EAA responses, where control was taken as the mean of the last 3 pre-drug counts; mean values ± s.e.mean are indicated. No corrections for spontaneous activity were made. Tests were accepted only if AMPA and NMDA responses recovered by at least 50% of the initial antagonist effect. Statistical analysis was performed with the Wilcoxon matched pairs test on original spike count data (except where indicated).

Results

In preliminary experiments, GYKI 53655 (4 mg kg^{-1}) was found to have a short-lasting depressant effect on neuronal

[1] Present address: Dept of Pharmacology, Moscow Sechenov Medical Academy, 2/6 B.Pirogovskaya St, Moscow 119881, Russia.
[2] Author for correspondence.

responses to iontophoretic AMPA, with a half-recovery time of approximately 7 min (Figure 1a). We assumed that this was due to drug elimination, so for the rest of the experiments, bolus injections of GYKI 53655 were supplemented with a constant infusion at a rate of half the bolus dose given over 7 min. When tested on dorsal horn neurone responses to AMPA and NMDA, GYKI 53655 (4 and 8 mg kg^{-1}) substantially depressed or completely abolished AMPA responses, while NMDA-evoked firing was less affected (Figure 1b). Pooled data from 14 such experiments show the dose-dependence of GYKI 53655 (2–8 mg kg^{-1}) in depressing responses to AMPA (Figure 2a). NBQX also dose-dependently decreased AMPA-evoked responses following either i.v. (2–16 mg kg^{-1}) or microiontophoretic administration (Figure 2b).

Both antagonists reduced responses to AMPA significantly more than those to NMDA ($P<0.002$ at all doses, based on a comparison of the percentage data). Nonetheless the results in Figure 2a and b indicate that, following i.v. administration, GYKI 53655 was more selective than NBQX. At the highest doses tested, GYKI 53655 and NBQX reduced AMPA responses to a comparable degree (23 ± 6% and 27 ± 6% control, respectively) whereas for NMDA the values were 77 ± 7% *vs* 59 ± 7% control respectively. Similar data that are more directly comparable were obtained by selecting those cells on which both antagonists were tested under directly comparable conditions (Figure 2c). On these cells the highest doses of each antagonist tested (NBQX 16 mg kg^{-1} and GYKI 53655 8 mg kg^{-1}) again reduced AMPA responses to a very similar degree, but NBQX reduced NMDA responses significantly more than did GYKI 53655 ($P<0.05$, based on percentage data).

When administered by iontophoresis as opposed to intravenously, NBQX was a highly selective antagonist at the top currents tested (5–10 nA), reducing AMPA responses to 14 ± 4% control ($P<0.001$ *vs* control) whilst NMDA responses remained at 85 ± 4% control (nonetheless significantly less than control, $P<0.01$).

Spontaneous firing rates were reduced by all antagonists, but significantly more by systemic GYKI 53655 and NBQX (respectively to 50 ± 13% and 36 ± 10% control at the highest doses tested on 10 cells having spontaneous activity) than by microiontophoretic NBQX (70 ± 7% control; 9 cells with spontaneous activity).

Discussion

Both the competitive AMPA antagonist NBQX, and a weaker analogue of the non-competitive antagonist, GYKI 53655, have been reported to be therapeutically effective in different animal models of epilepsy and global brain ischaemia (Rogawski, 1993). However, most of the data on the receptor profile of these compounds come from *in vitro* studies (e.g. Zeman & Lodge, 1992; Zorumski *et al.*, 1993). A variety of factors may change this profile of the drugs *in vivo*, particularly after systemic administration, making the interpretation of the mechanism of their effects difficult. Thus, GYKI 52466, which selectively blocked AMPA-activated currents in cultured hippocampal neurones (Donevan & Rogawski, 1993), has been reported to be a non-selective antagonist of both AMPA and NMDA-induced seizures when tested

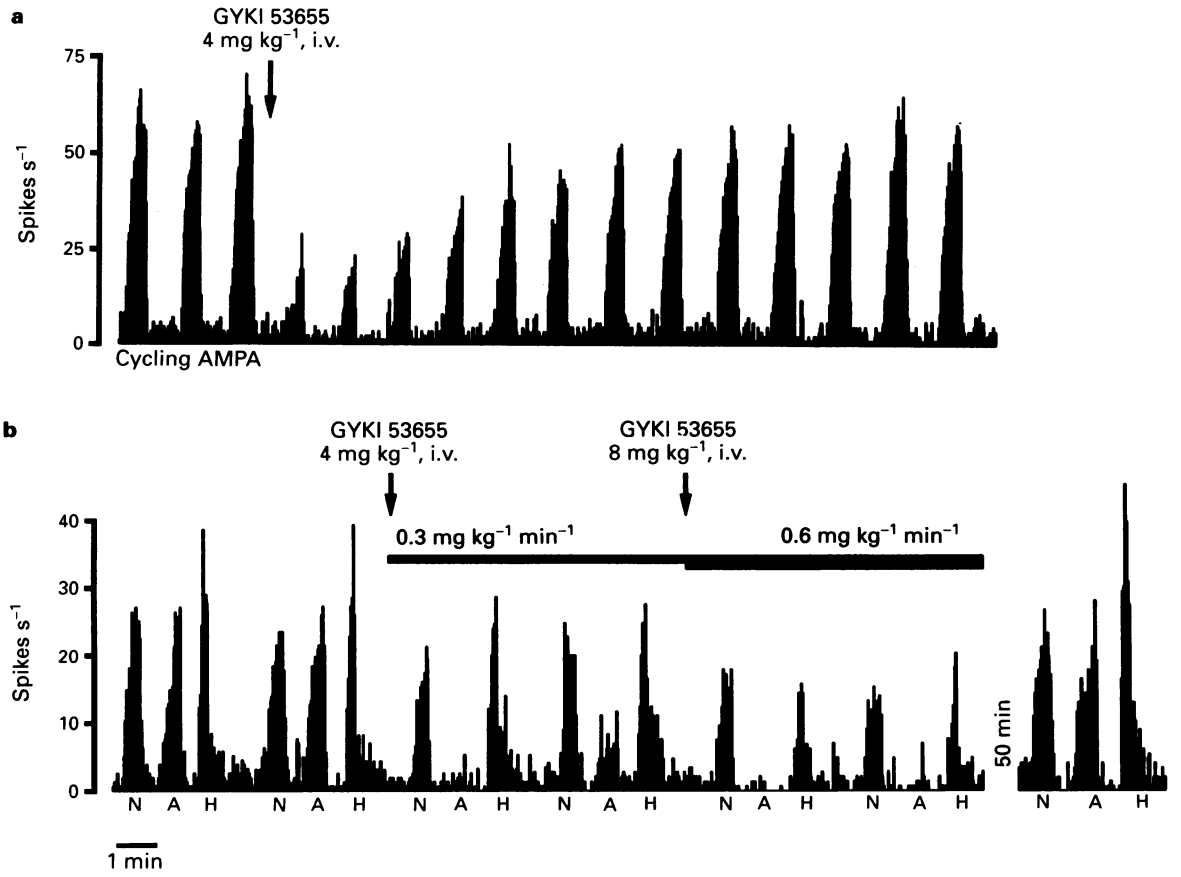

Figure 1 (a) Effects of a bolus intravenous injection of GYKI 53655 on neuronal responses to iontophoretic AMPA (8 nA). (b) Selectivity of GYKI 53655 between responses to iontophoretic NMDA (N, 25 nA) and AMPA (A, 7 nA), and to noxious heat stimulation applied to the plantar surface of the hindpaw (H, 49°C for 15 s); a bolus injection was supplemented by infusion of half the bolus dose over the half-recovery time estimated from experiments such as that in (a). Data from two spinal dorsal horn neurones in α-chloralose anaesthetized, spinalized rats.

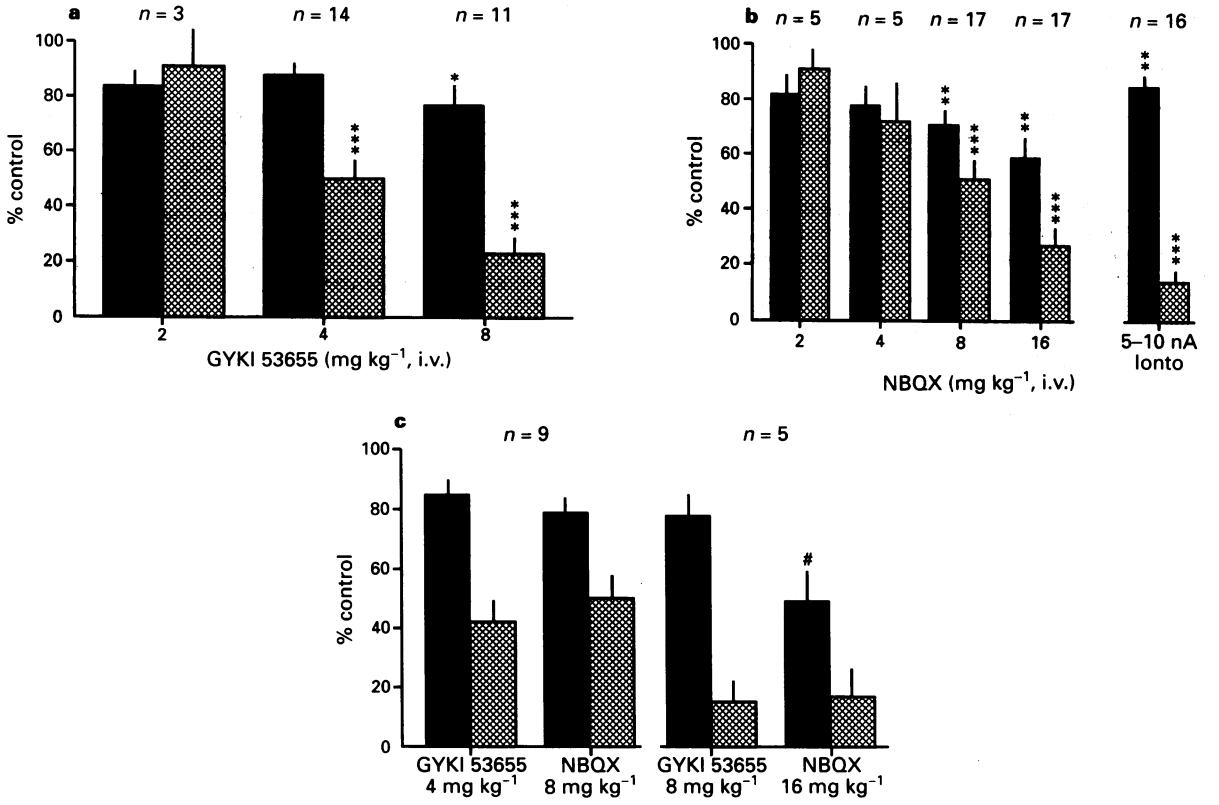

Figure 2 The effects of intravenous GYKI 53655 and NBQX (including tests with iontophoretically administered NBQX) on dorsal horn neurone responses to iontophoretic NMDA (solid columns) and AMPA (cross-hatched columns). (a) Pooled data for GYKI 53655; (b) pooled data for NBQX; (c) direct comparison of the selectivity of GYKI 53655 and NBQX when tested on the same cells at lower (left) and higher i.v. doses (right). Asterisks show significant difference from control: $*P<0.05$; $**P<0.01$; $***P<0.001$. #Significant difference between effects on NMDA responses of NBQX (16 mg kg^{-1}) and GYKI 53655 (8 mg kg^{-1}), $P<0.05$.

systemically (Bisaga *et al.*, 1993). When tested on a small number of spinal motoneurones by either iontophoretic or intravenous administration *in vivo*, this compound did, however, appear selective for AMPA-evoked responses (Engberg *et al.*, 1993). NBQX has also been shown to antagonize AMPA-induced responses in the spinal cord *in vitro* (Zeman & Lodge, 1992) and *in vivo* after localized iontophoretic administration (Lodge *et al.*, 1991) without marked effects on NMDA responses.

In this study GYKI 53655, a more potent derivative of GYKI 52466 (Tarnawa *et al.*, 1993) was more selective than NBQX in reducing responses to AMPA *vs* NMDA. Even GYKI 53655, however, did reduce NMDA responses to some extent. The reduction of background activity (which presumably results from antagonism of AMPA receptor-mediated spontaneous inputs onto the cells) reflects a decreased excitability that would in turn reduce responses to NMDA as well as those to AMPA; this effect is therefore likely to contribute to this minor degree of non-selectivity. Such a mechanism cannot, however, explain the difference in the degree of selectivity between systemic NBQX and either iontophoretic NBQX or systemic GYKI 53655 (see data in Figure 2), particularly when the two agents were compared on the same cells.

Since NBQX is evidently metabolized rapidly (the half-recovery time under these conditions was 15 min), it seems likely that a metabolic product may underlie the observed low selectivity of NBQX after systemic administration. GYKI 53655, whilst more selective, was even shorter-acting (half recovery time 7 min), which would limit the possible therapeutic use of this compound. Disubstituted reduced analogues of GYKI 52466 are longer lasting (Tarnawa *et al.*, 1993); development in this direction may yield more useful compounds.

In conclusion, the present work has demonstrated that both NBQX and GYKI 53655 can be effective AMPA antagonists following systemic administration. Care should, however, be taken in the interpretation of results obtained with systemic NBQX since its antagonist profile appears to be less selective than that observed either *in vitro* or following localized administration *in vivo*. This seems likely to be due to conversion of NBQX to a less selective metabolite. GYKI 53655 therefore seems to be a more valuable tool than NBQX for the investigation of AMPA receptor-mediated processes *in vivo*.

The authors are grateful to the Wellcome Trust and the Medical Research Council for financial support, and to Dr D. Lodge (Eli Lilly & Co., U.K.) and Dr Leimner (Merz + Co., Germany) for gifts of GYKI 53655 and NBQX, respectively.

References

BISAGA, A., KRZASCIK, P., JANKOWSKA, E., PALEJKO, W., KOSTOWSKI, W. & DANYSZ, W. (1993). Effect of glutamate receptor antagonists on *N*-methyl-D-aspartate- and α-amino-3-hydroxy-5-methyl-4-isoxazolepropionic acid-induced convulsant effects in mice and rats. *Eur. J. Pharmacol.*, **242**, 213–220.

DONEVAN, S.D. & ROGAWSKI, M.A. (1993). GYKI 52466, a 2,3-benzodiazepine, is a highly selective, non-competitive antagonist of AMPA/kainate receptor responses. *Neuron*, **10**, 51–59.

ENGBERG, I., TARNAWA, I., DURAND, J. & OUARDOUZ, M. (1993). An analysis of synaptic transmission to motoneurones in the cat spinal cord using a new selective receptor blocker. *Acta Physiol. Scand.*, **148**, 97–100.

HEADLEY, P.M., PARSONS, C.G. & WEST, D.C. (1987). The role of *N*-methylaspartate receptors in mediating responses of rat and cat spinal neurones to defined sensory stimuli. *J. Physiol.*, **385**, 169–188.

HONORÉ, T., DAVIES, S.N., DREJER, J., FLETCHER, E.J., JACOBSEN, P., LODGE, D. & NIELSEN, F.E. (1988). Quinoxalinediones: potent competitive non-NMDA glutamate receptor antagonists. *Science*, **241**, 701–703.

LODGE, D., JONES, M.G. & PALMER, A.J. (1991). Excitatory amino acids: new tools for old stories. *Can. J. Physiol. Pharmacol.*, **69**, 1123–1128.

ROGAWSKI, M.A. (1993). Therapeutic potential of excitatory amino acid antagonists: channel blockers and 2,3-benzodiazepines. *Trends Pharmacol. Sci.*, **14**, 325–331.

SHEARDOWN, M.J., NIELSEN, E.Ø., HANSEN, A.J., JACOBSEN, P. & HONORÉ, T. (1990). 2,3-dihydroxy-6-nitro-7-sulfamoyl-benzo(F) quinoxaline: a neuroprotectant for cerebral ischaemia. *Science*, **247**, 571–574.

TARNAWA, I., BERZSENYI, P., ANDRÁSI, F., BOTKA, P., HÁMORI, T., LING, I. & KÖRÖSI, J. (1993). Structure-activity relationships of 2,3-benzodiazepine compounds with glutamate antagonistic action. *Bioorganic Med. Chem. Lett.*, **3**, 99–104.

ZEMAN, S. & LODGE, D. (1992). Pharmacological characterization of non-NMDA subtypes of glutamate receptor in the neonatal rat hemisected spinal cord *in vitro*. *Br. J. Pharmacol.*, **106**, 367–372.

ZORUMSKI, C.F., YAMADA, K.A., PRICE, M.T. & OLNEY, J.W. (1993). A benzodiazepine recognition site associated with the non-NMDA glutamate receptor. *Neuron*, **10**, 61–67.

(Received March 16, 1994
Accepted March 25, 1994)

Br. J. Pharmacol. (1994), **112**, 847–854

Pharmacological characterization of the human histamine H_2 receptor stably expressed in Chinese hamster ovary cells

[1]Rob Leurs, Martine J. Smit, Wiro M.B.P. Menge & Hendrik Timmerman

Leiden/Amsterdam Center for Drug Research, Department of Pharmacochemistry, Vrije Universiteit, De Boelelaan 1083, 1081 HV Amsterdam, The Netherlands

1 The gene for the human histamine H_2 receptor was stably expressed in Chinese hamster ovary (CHO) cells and characterized by [^{125}I]-iodoaminopotentidine binding studies. In addition, the coupling of the expressed receptor protein to a variety of signal transduction pathways was investigated.

2 After cotransfection of CHO cells with pCMVhumH_2 and pUT626, a phleomycine-resistant clonal cell line (CHOhumH_2) was isolated that expressed 565 ± 35 fmol kg^{-1} protein binding sites with high affinity (0.21 ± 0.02 nM) for the H_2 antagonist, [^{125}I]-iodoaminopotentidine.

3 Displacement studies with a variety of H_2 antagonists indicated that the encoded protein was indistinguishable from the H_2 receptor identified in human brain membranes and guinea-pig right atrium. The K_i-values observed in the various preparations correlated very well ($r^2 = 0.996–0.920$).

4 Displacement studies with histamine showed that a limited fraction ($32 \pm 6\%$) of the binding sites showed a high affinity for histamine (2 ± 1.2 μM); the shallow displacement curves were reflected by a Hill-coefficient significantly different from unity ($n_H = 0.58 \pm 0.09$). The addition of 100 μM Gpp(NH)p resulted in a steepening of the displacement curve ($n_H = 0.79 \pm 0.02$) and a loss of high affinity sites for histamine.

5 Displacement studies with other agonists indicated that the recently developed specific H_2 agonists, amthamine and amselamine, showed an approximately 4–5 fold higher affinity for the human H_2 receptor than histamine.

6 Stimulation of CHOhumH_2 cells with histamine resulted in a rapid rise of the intracellular cyclic AMP levels. After 10 min an approximately 10 fold increase in cyclic AMP could be measured. The EC_{50} value for this response was 7 ± 1 nM for histamine. This response was effectively blocked by tiotidine and cimetidine, resulting in K_i values of 8 ± 1 nM and 0.56 ± 0.24 μM respectively.

7 Stimulation of CHOhumH_2 cells with histamine neither inhibited the A23187-induced release of [^{3}H]-arachidonic acid nor changed the intracellular IP_3 levels.

8 These results show that the cloned human gene encodes a histamine H_2 receptor that is indistinguishable from the H_2 receptor identified in human brain tissue. This receptor is functionally coupled to the adenylate cyclase in CHO cells, but does not influence the inositolphosphate turnover or arachidonic acid release.

Keywords: Human histamine H_2 receptor; Chinese hamster ovary cell (CHO); [^{125}I]-iodoaminopotentidine; cyclic AMP; arachidonic acid release; inositolphosphate production

Introduction

Following the original observations of Ash and Schild (1966) of possible histamine receptor heterogeneity, Black and colleagues (1972) initiated a successful search for histamine receptor ligands that could selectively block or mimic the actions of histamine on cardiac and stomach function. It was the development of burimamide and various analogues (Black *et al.*, 1972) that finally provided evidence for the existence of at least two different histamine receptor subtypes. With the availability of suitable pharmacological tools (for review see Leurs *et al.*, 1991) the role of the H_2 receptor in human (patho)physiology has been studied in detail. The receptor protein is present in e.g. various distinct human brain areas (Traiffort *et al.*, 1992a; Martinez-Mir *et al.*, 1993), human heart (Bristow *et al.*, 1982; Du *et al.*, 1993; Zerkowski *et al.*, 1993), human airway preparations (Barnes, 1992), human blood vessels (Keitoku *et al.*, 1990; Toda, 1990), human uterus (Martinez-Mir *et al.*, 1992) and human stomach (Bertaccini & Corruzi, 1992). As can be anticipated from this localization, the H_2 receptor subtype has been identified as an important target for (potential) pharmacotherapy. Besides a role of H_2 receptor antagonists in gastric acid secretion (Bertaccini & Corruzi, 1992) application of cardioselective H_2 receptor agonists in congestive heart failure has also been suggested (Felix *et al.*, 1991). Moreover, recently, a role for the H_2 receptor has been suggested in some neurological diseases (Kaminsky *et al.*, 1990; Deutsch *et al.*, 1993; Martinez-Mir *et al.*, 1993), indicating that CNS-active H_2 ligands might also have therapeutic potential. Due to these perspectives, the search for more potent and selective H_2 receptor agents still continues and has, for instance, recently resulted in the development of the new and highly specific H_2 receptor agonists, amthamine and amselamine (Eriks *et al.*, 1991; Timmerman, 1992; Van der Goot *et al.*, unpublished observations).

Despite the interesting therapeutic potential of the H_2 receptor, detailed studies of the human histamine H_2 receptor have been hampered by the lack of suitable model systems. Human tissue is not widely available for pharmacological studies and only a few human cell lines have been reported to contain histamine H_2 receptors (Arima *et al.*, 1991; Emani *et al.*, 1983; Gespach *et al.*, 1985). Yet, the reported pharmacology of the histamine receptor present on these cells is not always clear (Burde *et al.*, 1989; Mitsuhashi *et al.*, 1991; Reyl-Desmars *et al.*, 1991; Seifert *et al.*, 1992). Only in human monocytic U937 cells are pharmacologically clearly defined H_2 receptors present, but the density of receptor sites is too low for detailed receptor binding studies (Smit *et al.*, unpublished observations).

The recent introduction of molecular biology in the field of

[1] Author for correspondence.

G-protein coupled receptor research has greatly improved the knowledge of molecular aspects of these receptor proteins. Following the cloning of the gene encoding the hamster β_2-receptor by Dixon et al. (1986), a wide variety of genes encoding G-protein coupled receptors have been cloned by various techniques. Also in the field of histamine research the molecular biological approach has recently been successful. Using degenerated oligonucleotides based on conserved transmembrane regions of the receptor family and mRNA of canine parietal cells, Gantz et al. (1991b) succeeded in cloning the gene encoding a putative canine histamine H_2 receptor. Using the canine nucleotide sequence, soon thereafter a rat (Ruat et al., 1991) and human homologue (Gantz et al., 1991a) were cloned. The rat gene was expressed in Chinese hamster ovary cells and was shown to be a typical H_2 receptor (Traiffort et al., 1992b). No detailed information is available yet for the pharmacological profile of the proteins encoded by the canine and human gene.

A cellular system expressing the human histamine H_2 receptor protein would be very useful for the development of new histamine receptor ligands and would also allow detailed investigation of the regulation of the histamine H_2 receptor function. For the study of H_1 receptor regulation isolated cell systems have already proved to be extremely useful (see e.g. Smit et al., 1992). In view of the anticipated use of histamine H_2 receptor agonists in congestive heart failure (Felix et al., 1991) and the reported increase in β-receptor kinase expression in heart tissue of patients with congestive heart failure (Ungerer et al., 1993), a detailed study of the molecular mechanisms underlying the regulation of histamine H_2 receptor function is of great importance. Therefore, we decided to express stably the reported human gene in Chinese hamster ovary cells and to perform a molecular pharmacological characterization of the encoded protein. Besides receptor binding studies with a wide range of agents acting at histamine receptors we also investigated the signal transduction pathways that can be activated by the receptor protein in these cells.

Methods

Cell culture

Chinese hamster ovary cells (CHO cells) deficient in dihydrofolate reductase were maintained at 37°C in a humified atmosphere with 5% CO_2 in Dulbecco's Modified Eagle's Medium (DMEM), containing 10% (v/v) foetal calf serum and supplemented with 2 mM L-glutamine, hypoxanthine, thymidine, MEM amino acids, 50 iu ml^{-1} penicillin and 50 $\mu g\ ml^{-1}$ streptomycin. CHO cells were stably transfected with the eukaryotic expression vector pCMVhumH_2neo (Gantz et al., 1991a) and the plasmid pUT626, containing the *Sh ble* gene, conferring resistance to the antibiotic phleomycine (Cayla, France), using Lipofectine (Gibco BRL, The Netherlands). After 2 weeks of selection in the presence of 50 $\mu g\ ml^{-1}$ phleomycine, surviving CHO colonies were isolated by ring cloning and further expanded in culture medium supplemented with phleomycine.

CHO cells expressing the guinea-pig histamine H_1 receptor (CHOgpH_1, Leurs et al., 1994) were grown at 37°C in a humified atmosphere with 5% CO_2 in DMEM, containing 10% (v/v) dialysed foetal calf serum and supplemented with 2 mM L-glutamine, MEM amino acids, 50 iu ml^{-1} penicillin and 50 $\mu g\ ml^{-1}$ streptomycin.

Membrane preparation

CHOhumH_2 cells were trypsinized and recovered by a 10 min centrifugation at 500 *g*. Cells were homogenized in ice-cold 50 mM Na_2/K-phosphate buffer (pH = 7.4) with a Polytron homogenizer (5 s, maximal speed). The resulting homogenate was thereafter centrifuged for 30 min at 18,000 *g* at 4°C. The pellet was resuspended in 50 mM phosphate buffer and used for radioligand binding studies. Protein concentrations were determined according to Bradford (1976) with bovine serum albumin used as a standard.

Histamine H_2 receptor binding

The radiolabelled H_2 receptor antagonist [^{125}I]-iodoaminopotentidine ([^{125}I]-APT) was synthesized as described previously (Ruat et al., 1990), with some minor modifications. Briefly, the iodonation of aminopotentidine with $Na^{125}I$ was performed with H_2O_2 and acetic acid (2:1, v/v) instead of chloramine-T. In this way the [^{125}I]-APT was obtained carrier-free.

Triplicate assays were performed in polypropylene tubes in 50 mM phosphate buffer containing gelatine (0.1% final amount) to prevent adsorption of the radioligand. For competition experiments 0.2 nM [^{125}I]-APT was incubated with 5–10 μg of membrane proteins in the presence of increasing concentrations of the competitor in a total volume of 400 μl. In saturation studies increasing concentrations of [^{125}I]-APT were incubated with membrane protein in the absence or presence of 1 μM tiotidine. After 90 min at 30°C the incubations were stopped by rapid dilution with 3 ml ice-cold 20 mM Na_2/K phosphate buffer (pH = 7.4 at 4°C) supplemented with 0.1% bovine serum albumin. The bound radioactivity was subsequently separated by filtration with a Brandel cell harvester (Semat, UK) through Whatman GF/B glass fibre filters that had been treated with 0.3% polyethylenimine. Filters were washed twice with buffer and radioactivity retained on the filters was counted with a LKB-γ-counter at an efficiency of 63%. The binding data were evaluated by use of LIGAND, a non-linear, weighted, least-squares curve-fitting procedure (Munson & Rodbard, 1980). Fits for one or two binding sites were tested. Goodness of fit was considered with an F-test of residual sums of squares corrected for the differences in degrees of freedom. A more complex model was accepted if at the $P = 0.05$ level the F-value was greater than the critical value for the respective F statistic.

Cyclic AMP production

CHOhumH_2 cells were seeded in 24-well plates and cultured overnight in culture medium. Cells were washed twice with DMEM, supplemented with 50 mM HEPES (pH = 7.4 at 37°C) and preincubated for 30 min at 37°C. Thereafter the medium was aspirated, appropriate drugs in DMEM/HEPES were added and the cells were incubated for the indicated time at 37°. In most experiments the adenosine 3':5'-cyclic monophosphate (cyclic AMP) accumulation was measured in the presence of 300 μM of the phosphodiesterase inhibitor, isobutylmethylxanthine (IBMX). The reaction was stopped by the rapid aspiration of the culture medium and the addition of 200 μl of 0.1 N cold HCl. The cells were kept on ice and disrupted by sonication (5 s, 50 W, Labsonic 1510, Braun-Melsungen, Germany). The resulting homogenate was frozen at − 20°C or directly neutralized with 1 N NaOH and assayed for the presence of cyclic AMP.

Cyclic AMP assay

The amount of cyclic AMP in the CHO cells was determined according to Nordstedt & Fredholm (1990), although some minor modifications were introduced. Briefly, a protein kinase A containing fraction was isolated from bovine adrenal glands. Adrenal cortex was homogenized in 10 volumes 100 mM Tris/HCl, 250 mM NaCl, 10 mM EDTA, 0.25 M sucrose and 0.1% 2-mercaptoethanol (pH = 7.4 at 4°C, buffer A) using an Omni-Sorval mixer (30 s, maximal speed) and a Polytron homogenizer (10 s, maximal speed). The homogenate was centrifuged for 60 min at 30,000 *g* at 4°C. The supernatant, containing protein kinase A, was carefully recovered and frozen in 1 ml aliquots at − 80°C.

Before use the binding protein was diluted five fold in ice-cold buffer A without sucrose and 2-mercaptoethanol and kept on ice. Subsequently, 200 µl of the binding protein was mixed with 100 µl of the CHO homogenate or cyclic AMP standards and 30,000 d.p.m. [^{3}H]-cyclic AMP. After incubation for 150 min at 4°C the mixture was rapidly diluted with 3 ml ice-cold 50 mM Tris/HCl (pH = 7.4 at 4°C) and filtered through Whatman GF/B filters using a Brandel cell-harvester (Semat, UK). The radioactivity retained on the filters was measured by liquid scintillation counting.

[^{3}H]-arachidonic acid release

CHOhumH_2 cells were seeded in 24-well plates and cultured overnight in culture medium, containing 0.5 µCi ml^{-1} [^{3}H]-arachidonic acid ([^{3}H]-AA). To remove unincorporated [^{3}H]-AA, cells were washed twice with 1 ml DMEM supplemented with 0.2% bovine serum albumin (fatty acid-free). Thereafter the cells were incubated at 37°C for 30 min with the appropriate drugs in 1 ml of DMEM with 0.2% bovine serum albumin. In some experiments CHOhumH_2 cells were preincubated with histamine for 10 min before the release of [^{3}H]-AA was stimulated. The release of [^{3}H]-AA was determined by liquid scintillation counting of 0.5 ml sample of the incubation medium. Previously, it has been shown that over 90% of the released radioactivity corresponds to authentic [^{3}H]-AA (Traiffort *et al.*, 1992b).

Inositol phosphate production

CHOhumH_2 or CHOgpH_1 cells were seeded in 24-well plates and cultured overnight in culture medium. Cells were washed twice with DMEM, supplemented with 50 mM HEPES (pH = 7.4 at 37°C) and preincubated for 30 min at 37°C. Thereafter the medium was aspirated, 100 µM histamine in 100 µl DMEM/HEPES was added and the cells were incubated for the indicated time at 37°C. The reaction was stopped by the addition of 100 µl of 10% cold $HClO_4$. The cells were disrupted by sonication (5 s, 50 W, Labsonic 1510, Braun-Melsungen) and kept on ice for 10 min. The cell homogenate was centrifuged for 5 min in Eppendorf tubes at 11,000 *g*. The supernatant (190 µl) was transfered to another tube and 47.5 µl 10 mM EDTA (pH = 7.4) was added. The samples were neutralized with 300 µl of a freon:tri-octylamine mixture (1:1, v/v, freshly prepared). The samples were vortexed and centrifuged for 2 min at 11,000 *g*. The neutralized upper phase (150 µl) was mixed with 37.5 µl 1 M $NaHCO_3$ and assayed for the presence of inositol (1,4,5) trisphosphate (IP_3) using a IP_3-mass assay system (Amersham).

In some experiments cells were labelled overnight in culture medium supplemented with 1 µCi ml^{-1} [^{3}H]-inositol. Reactions were terminated with 1 ml cold $CHCl_3$/methanol and the [^{3}H]-inositol phosphates were isolated by anion exchange chromatography (Godfrey, 1992).

Chemicals

Histamine dihydrochloride, A23187, isobutylmethylxanthine, cyclic AMP, haloperidol and mepyramine were obtained from Sigma Chemical Company (U.S.A.). [^{3}H]-cyclic AMP (40 Ci mmol^{-1}), [^{3}H]-inositol (18.8 Ci mmol^{-1}) were obtained from Amersham, and [^{3}H]-arachidonic acid (232 Ci mmol^{-1}) was purchased from New England Nuclear. Dimaprit dihydrobromide, amthamine dihydrobromide, amselamine dihydrobromide, impromidine trihydrobromide, aminopotentidine and thioperamide were taken from laboratory stock. Gifts of burimamide, metiamide, cimetidine, icotidine, zolantidine (SmithKline Beecham), tiotidine (Imperial Chemical Industries), ranitidine (Glaxo), famotidine (Merck Sharp & Dohme) and mianserin (Organon) are gratefully acknowledged.

Results

Pharmacological characterization of the human H_2 receptor using [^{125}I]-APT

Cotransfection of CHO cells with the plasmid pCMVhumH_2 and pUT626 resulted after 10–12 days of selection in culture medium supplemented with 50 µg ml^{-1} phleomycine in the formation of several clonal cell lines, which expressed [^{125}I]-APT binding sites. Untransfected cells did not show any specific [^{125}I]-APT binding (data not shown). For subsequent experiments a cell line (CHOhumH_2) stably expressing [^{125}I]-APT binding sites was further analysed. Saturation experiments performed with CHOhumH_2 cell membranes indicated the expression of a single [^{125}I]-APT binding site (n_H = 1.0 ± 0.1) with a dissociation constant (K_d) of 0.21 ± 0.02 nM (n = 3, mean ± s.e.mean) and a maximal density of 565 ± 35 fmol mg^{-1} protein (n = 3) (Figure 1).

The specific binding of 0.2 nM [^{125}I]-APT represented more than 95% of the total binding and was monophasically (n_H not significantly different from unity) inhibited by a variety of H_2 receptor antagonists but was unaffected by the H_1- and H_3 antagonists, mepyramine and thioperamide (Figure 2a, Table 1). The K_i values of the H_2 antagonists correlated well with their biological activities at the H_2 receptor of the guinea-pig right atrium (Leurs *et al.*, 1991) (r^2 = 0.920, n = 10, Table 1) and the K_i-values determined for the H_2 receptor on *post-mortem* human brain membranes (Traiffort *et al.*, 1992a) (r^2 = 0.996, n = 6, Table 1). The antidepressant, mianserin and the neuroleptic, haloperidol also interacted with the cloned human H_2 receptor protein, although at only moderate concentrations (Table 1).

Various histamine H_2 agonists displaced the specific [^{125}I]-APT binding to CHOhumH_2 cell membranes too (Figure 2b, Table 2). Yet, histamine displacement curves were shallow (n_H = 0.58 ± 0.09, n = 5) and could be best analysed according to a two site model (Figure 2b). Simultaneous fitting of the five independent experiments resulted in an affinity of 2.0 ± 1.2 µM and 81 ± 15 µM for respectively the high- and low affinity binding site. The addition of 100 µM Gpp(NH)p resulted in a steepening and a rightward shift of the histamine displacement curve (Figure 2b), which was best analysed according to a single site model, leading to a K_i-value of 45 ± 4 µM (Table 2). The percentage high affinity sites for histamine was rather low (Figure 2b, Table 2) and not always obvious. Similar observations were made for the other H_2-receptor agonists. Under control conditions shallow displacements curves were obtained, which with the exception

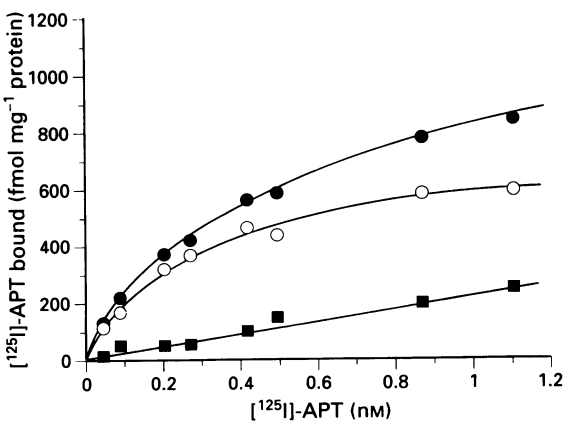

Figure 1 Concentration-dependent binding of [^{125}I]-iodoaminopotentidine ([^{125}I]-APT) to CHOhumH_2 cell membranes. Specific radioligand binding (○) was determined by subtracting the binding in the presence of 1 µM of tiotidine (■) from the total binding (●). Mean values of triplicate determinations of a typical experiment out of three are shown.

of the data for dimaprit, were best fitted according to a two sites model (Table 2). In the presence of Gpp(NH)p the specific agonists, amthamine (Eriks et al., 1991), amselamine (Van der Goot et al., unpublished observations), dimaprit and impromidine all displaced [^{125}I]-APT binding to CHO humH$_2$ membranes monophasically and showed a higher affinity for the human H$_2$ receptor than did histamine (Table 2).

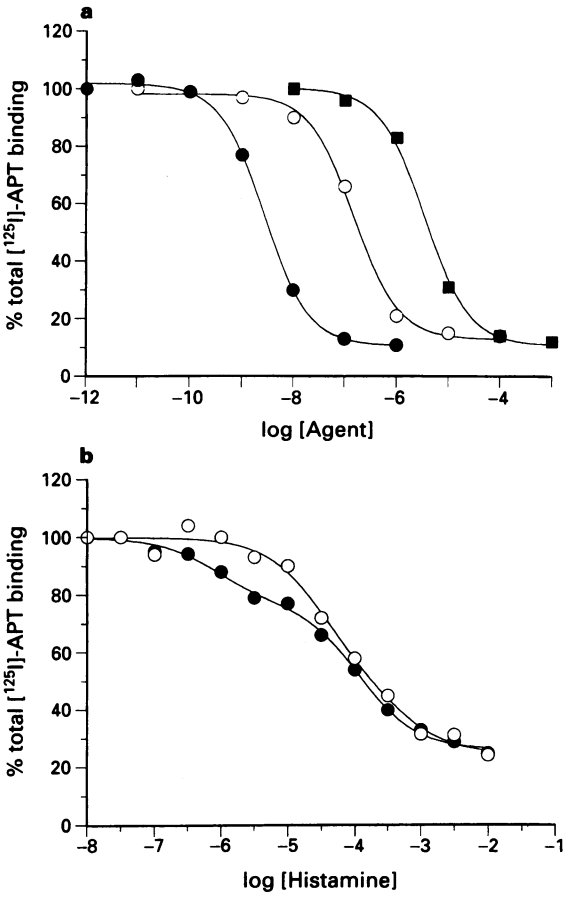

Figure 2 Pharmacological profile of the [^{125}I]-iodoaminopotentidine ([^{125}I]-ATP) binding site on CHOhumH$_2$ membranes. Displacement of [^{125}I]-APT binding by (a) APT (●), ranitidine (○), burimamide (■) or (b) histamine in the absence (●) or presence (○) of 100 μM Gpp(NH)p is shown. Data shown are the mean values of triplicate determinations from a typical experiment. Similar results were obtained in 2–4 other independent experiments.

Cyclic AMP production in CHOhumH$_2$ cells

In untransfected CHO cells, histamine (100 μM) did not affect the cellular cyclic AMP level (data not shown). Stimulation of the CHOhumH$_2$ cells in the absence of the cyclic AMP phosphodiesterase inhibitor, isobutylmethylxanthine (IBMX) with 1 μM histamine for 10 min resulted in a slight but significant increase of the basal cyclic AMP level of 6.6 ± 1.0 pmol/well to 10.7 ± 1.1 pmol/well ($P<0.05$, $n=3$). In the presence of increasing concentrations of IBMX, histamine stimulation resulted in a massive increase of the cellular cyclic AMP levels, which appeared to be maximal with 300–600 μM IBMX (data not shown). In subsequent experiments the cyclic AMP accumulation was measured in the presence of 300 μM IBMX.

Under these conditions addition of 1 μM histamine resulted in the rapid production of cellular cyclic AMP (inset Figure 3a); already 2 min after the application of histamine, increased levels of cyclic AMP were found. Maximal stimulation of the cellular cyclic AMP levels (approximately 10 fold) was observed after 10 min (inset Figure 3a). Stimulation of CHOhumH$_2$ cells with increasing concentrations of histamine for 10 min resulted in a concentration-dependent increase in cellular cyclic AMP levels. At relatively low concentrations, histamine stimulated the cyclic AMP production (Figure 3a); the EC$_{50}$-value of histamine for this response was 7 ± 1 nM ($n=5$). This histamine-induced (0.3 μM) cyclic AMP response was effectively inhibited by the H$_2$ receptor antagonists, tiotidine and cimetidine (Figure 3b), resulting in K_i values of 8 ± 1 nM and 0.56 ± 0.24 μM ($n=4$) respectively. These K_i-values correspond well with the K_i-values obtained from the [^{125}I]-APT displacement studies (Table 1). The histamine-induced cyclic AMP response was not affected by the H$_1$- and H$_3$ receptor antagonists mepyramine and thioperamide in concentrations up to 100 μM (Figure 3b).

Arachidonic acid release in CHOhumH$_2$ cells

In CHOhumH$_2$ cells prelabelled with [^{3}H]-AA application of the Ca^{2+} ionophore A23187 led to a massive increase of [^{3}H]-AA release (Figure 4). Whereas under basal conditions the [^{3}H]-AA release was 389 ± 17 d.p.m. ($n=4$), stimulation of CHOhumH$_2$ cells with 1 μM of the Ca^{2+} ionophore A23187 led to an elevation of the [^{3}H]-AA release to 3156 ± 88 d.p.m. ($n=4$). Histamine (1 μM and 100 μM) did not affect the basal [^{3}H]-AA release, whereas the A23187 (1 μM) induced [^{3}H]-AA release was slightly increased by 100 μM histamine (Figure 4). In some experiments CHOhum H$_2$ cells were preincubated with histamine in order to study its effect on the A23187-induced [^{3}H]-AA release. Also under

Table 1 K_i-values of various histamine receptor antagonists for competition with [^{125}I]-iodoaminopotentidine binding to CHOhumH$_2$ membranes

	CHOHumH$_2$		*Human brain*	*Guinea-pig atrium*
Compounds	K_i	n_H	K_i	K_B
APT	15 ± 5 nM	− 0.99 ± 0.06	−	−
Burimamide	3.9 ± 1.2 μM	− 1.10 ± 0.04	1.6 μM	7.8 μM
Cimetidine	0.66 ± 0.22 μM	− 0.89 ± 0.02	0.27 μM	0.79 μM
Famotidine	16 ± 3 nM	− 0.92 ± 0.07	−	16 nM
Metiamide	0.67 ± 0.16 μM	− 0.95 ± 0.03	−	0.92 μM
Ranitidine	85 ± 4 nM	− 0.96 ± 0.06	38 nM	63 nM
Tiotidine	17 ± 6 nM	− 0.88 ± 0.01	5 nM	15 nM
Zolantidine	40 ± 8 nM	− 1.05 ± 0.06	−	35 nM
Icotidine	15 ± 2 nM	− 1.01 ± 0.04	−	60 nM
Haloperidol	1.5 ± 0.3 μM	− 0.98 ± 0.03	0.65 μM	0.87 μM
Mianserine	0.56 ± 0.51 μM	− 1.08 ± 0.04	0.10 μM	0.11 μM
Mepyramine	> 10 μM			
Thioperamide	> 100 μM			

Reported values for [^{125}I]-iodoaminopotentidine binding to human brain membranes (Traiffort et al., 1991a) and antagonism of histamine-induced chronotropic responses of guinea-pig right atrium (Leurs et al., 1991) are shown for comparison. Data shown are mean ± s.e.mean of three to four independent experiments, each performed in triplicate.

Table 2 K_i-values of various histamine receptor agonists for competition with [^{125}I]-iodoaminopotentidine binding to CHOHumH_2 membranes in the absence or presence of 100 μM Gpp(NH)p

	− *Gpp(NH)p*			+ *Gpp(NH)p*		*Guinea-pig right atrium*
Compounds	$K_{i,high}$ (μM)	$K_{i,low}$(μM)	n_H	K_i (μM)	n_H	EC_{50} (μM)
Histamine	2.0 ± 1.2 (32 ± 6%)	81 ± 15 (68 ± 6%)	− 0.58 ± 0.09	45 ± 4	− 0.79 ± 0.02	0.72
Amthamine	0.15 ± 0.14 (23 ± 6%)	6.9 ± 0.8 (76 ± 6%)	− 0.68 ± 0.03	7.0 ± 1.7	− 0.88 ± 0.01	0.62
Amselamine	0.13 ± 0.09 (18 ± 3%)	9.6 ± 0.7 (82 ± 3%)	− 0.73 ± 0.02	10 ± 1	− 1.02 ± 0.11	0.39
Dimaprit	ND	25 ± 5 (100%)	− 0.79 ± 0.02	24 ± 5	− 0.96 ± 0.09	1.1
Impromidine	0.023 ± 0.028 (31 ± 15%)	0.38 ± 0.09 (69 ± 16%)	− 0.73 ± 0.04	0.47 ± 0.03	− 0.96 ± 0.04	0.016

Reported values for agonist-induced chronotropic responses of guinea-pig right atrium (Eriks *et al.*, 1991; Van Der Goot, unpublished) are shown for comparison. Values in parentheses indicate the relative densities of the respective sites. Data shown are mean ± s.e.mean of three to five independent experiments, each performed in triplicate.
ND = not detectable.

these conditions histamine had no inhibitory effect on the A23187 response (data not shown).

Inositol phosphate production in CHOhumH$_2$ cells

In CHOhumH$_2$ cells prelabelled overnight with [^{3}H]-inositol, application of 100 μM histamine in the presence of 20 mM LiCl for 10 min at 37°C did not result in an increase of the intracellular accumulation of [^{3}H]-inositol phosphates (107 ± 7% of the basal accumulation, $n = 3$). Yet, stimulation of the endogenous P_2-purinoceptor of CHOhumH$_2$ cells (Iredale & Hill, 1993; Traiffort *et al.*, 1992b) with 100 μM of ATP resulted in an increase of 580 ± 110% ($n = 3$) of the basal release of [^{3}H]-inositol phosphates. Since this approach might be too insensitive for small increases in the levels of IP_3 we analysed the effects of histamine in more detail. Using an IP_3 mass assay we measured the intracellular IP_3 levels in CHOhumH$_2$ and CHOgpH$_1$ cells after stimulation with 100 μM histamine. As can be seen in Figure 5, histamine had no effect on the basal levels of IP_3 in CHOhumH$_2$ cells. In CHOgpH$_1$ cells, 100 μM histamine rapidly elevated, as expected, the cellular IP_3 levels; within 10 s the IP_3 levels were more than doubled. This rise was transient and dropped to a lower level, which remained elevated up to 1 min of stimulation (Figure 5). In accordance with these findings we were unable to find any effect of histamine on the intracellular calcium levels in fura-2 loaded CHOhumH$_2$ cells, although in the same population of cells 100 μM of ATP resulted in a rapid rise of the basal level of 97 ± 12 nM to a peak value of 406 ± 55 nM ($n = 3$).

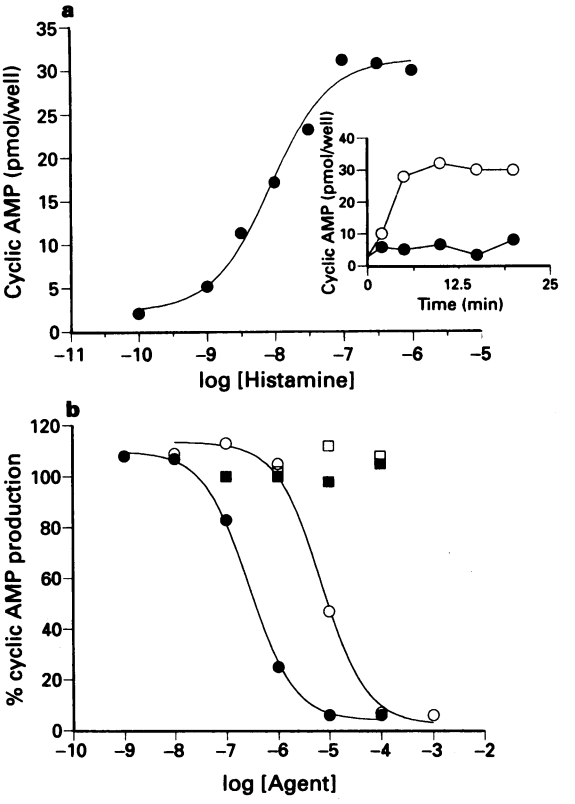

Figure 3 Histamine-induced cyclic-AMP accumulation in CHOhumH_2 cells. (a) CHOhumH$_2$ cells were stimulated with increasing concentrations of histamine for 10 min at 37°C in the presence of 300 μM isobutylmethylxanthine (IBMX). Data shown are the mean values of a typical experiment out of 6. In untransfected cells histamine did not alter the intracellular cyclic AMP concentration. Inset: CHOhumH_2 cells were stimulated with DMEM (●) or 1 μM of histamine (○) for various lengths of time at 37°C in the presence of 300 μM IBMX. Data shown are the mean values of a typical experiment out of 3. (b) Pharmacological characterization of the histamine-induced cyclic AMP response in CHOhumH$_2$ cells. Cells were incubated for 10 min at 37°C with 0.3 μM of histamine in the presence of increasing concentrations of tiotidine (●), cimetidine (○), mepyramine (■) and thioperamide (□) and 300 μM IBMX. A typical experiment out of 4 is shown.

Discussion

In this paper we present evidence that the receptor protein encoded by the putative human histamine H_2 receptor gene (Gantz *et al.*, 1991a) is indistinguishable from the pharmacologically characterized H_2 receptor of the guinea-pig atrium (Leurs *et al.*, 1991) or human brain tissue (Traiffort *et al.*, 1992a). In the initial paper on the cloning of the human gene (Gantz *et al.*, 1991a), some indications of the H_2 nature of the encoded receptor protein were presented; transfected cells bound the H_2 receptor antagonist, [^{3}H]-tiotidine, whereas histamine was found to induce a cimetidine-sensitive cyclic AMP accumulation (Gantz *et al.*, 1991a). In view of the reported pharmacological discrepancies of human H_2 receptor-like proteins in various cell systems (Burde *et al.*, 1989; Reyl-Desmars *et al.*, 1991; Seifert *et al.*, 1992) the observed actions of cimetidine and tiotidine do, however, not unambiguously define the encoded human receptor protein.

In human gastric HGT-1 tumour cells, Reyl-Desmars *et al.* (1991) reported the presence of an H_2 receptor with a rather low affinity for tiotidine. The pharmacological profile of the reported binding site was therefore quite different from the profile of standard H_2 receptor systems (Reyl-Desmars *et al.*, 1991) and still remains undefined. Nevertheless, functional H_2 receptors have been observed in the same cell line (Emani *et*

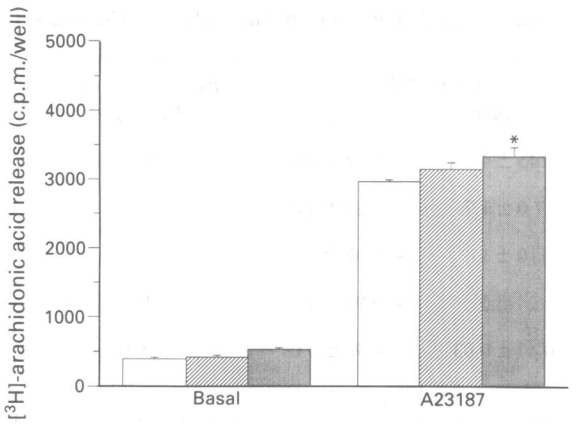

Figure 4 Effect of histamine on the basal and A23187-induced release of [^{3}H]-arachidonic acid ([^{3}H]-AA) from prelabelled CHOhum H_2 cells. Cells were incubated with DMEM (open column), 1 μM (hatched column) or 100 μM (stippled column) of histamine in the absence or presence of 1 μM A23187 for 30 min at 37°C, after which the released radioactivity was counted in the medium. A typical experiment out of 4 is shown. *Significant difference compared to stimulation with DMEM (ANOVA).

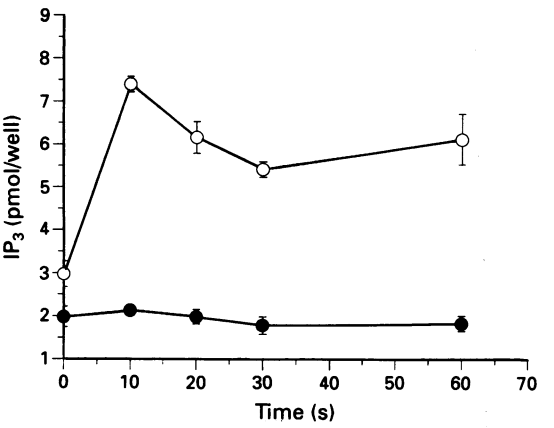

Figure 5 Effect of 100 μM histamine on the inositol (1,4,5) trisphosphate (IP_3) production in CHOhumH_2 (●) and CHOgpH_1 cells (○). Cells were incubated for the indicated times with histamine at 37°C, homogenized and the IP_3 levels were determined by radioreceptor assay. Data shown are the mean ± s.e.mean of a typical experiment out of 4.

al., 1983). Similar observations are made in human HL-60 promyelocytic leukemia cells. Also in these cells functional H_2 receptors have been described (Burde *et al.*, 1989; Mitsuhashi *et al.*, 1991; Seifert *et al.*, 1992). However, the pharmacological definition of the various functional responses is not always clear. A unique agonist/antagonist profile is reported for the inhibition of the oxidative burst (Burde *et al.*, 1989) and the increase of cytosolic calcium in HL-60 cells (Mitsuhashi *et al.*, 1991; Seifert *et al.*, 1992).

In view of these data and the lack of suitable systems for the study of the pharmacological properties of the human H_2 receptor and the regulation of its function, we stably expressed the cloned human gene (Gantz *et al.*, 1991a) in CHO cells. Our detailed pharmacological characterization of the encoded protein was performed with the highly specific H_2 receptor antagonist [^{125}H]-iodoaminepotentidine (Ruat *et al.*, 1990). This radiolabel has previously successfully been used for the labelling of the human H_2 receptor in brain tissue (Traiffort *et al.*, 1992a) and has many advantages over [^{3}H]-tiotidine. From our results with CHOhumH_2 cells, the H_2 nature of the encoded receptor protein is clear. Affinity constants calculated from displacement studies with 11 structurally different H_2 receptor antagonists perfectly match the pharmacological profile of the H_2 receptor from guinea-pig right atrium (Leurs *et al.*, 1991) and human brain (Traiffort *et al.*, 1992a); regression coefficients of 0.92–0.99 are obtained when the various K_i-values are correlated. It can therefore be concluded that the cloned gene (Gantz *et al.*, 1991a) encodes a classical human H_2 receptor.

In this study a complicated interaction of histamine with the [^{125}H]-iodoaminopotentidine binding site on CHOhumH_2 cell membranes is observed. Shallow displacement curves with Hill-coefficients of 0.58 were obtained, whereas the inclusion of the non-hydrolysable GTP analogue Gpp(NH)p resulted in a steepening of the curves. Approximately 30% of the [^{125}H]-iodoaminopotentidine binding sites showed high affinity for histamine (2 μM). The biphasic nature of the displacement curves of histamine indicate the coupling of the human H_2 receptor to G-proteins.

As far as we know, the coupling of the human H_2 receptor to a G-protein has not been reported before on the basis of radioligand binding studies. Yet, besides its deduced amino acid structure, adenylate cyclase studies with human heart tissue (Bristow *et al.*, 1982) and radioligand binding studies with the rat H_2 receptor expressed in CHO cells (Traiffort *et al.*, 1992b) also indicate the interaction of the H_2 receptor with G-proteins. There is a remarkable discrepancy between the results from the displacement studies with histamine using CHOhumH_2 cell membranes and *post-mortem* human brain membranes (Table 1). In human brain tissue, histamine was found to display a 10 fold higher affinity (4 μM) compared to guinea-pig brain tissue (Traiffort *et al.*, 1992a). The affinity of histamine for the high affinity site on CHOhumH_2 cell membranes is remarkably close to the reported affinity of histamine on human brain membranes (Traiffort *et al.*, 1992a). Unfortunately no data regarding GTP sensitivity was reported in the latter. Yet, the observed differences between guinea-pig and human brain tissue were suggested to be related to species differences or *post-mortem* or aging-induced changes in receptor characteristics (Traiffort *et al.*, 1992a). Based on the present findings we conclude that the previously reported high affinity of histamine in human brain membranes does not reflect a natural higher sensitivity of the human H_2 receptor to this neurotransmitter, but could be due to either conservation problems inherent in the use of *post-mortem* human samples or due to aging-related changes in receptor or G protein characteristics; it is possible that only high-affinity H_2 receptor sites have been measured in the *post-mortem* human brain membranes (Traiffort *et al.*, 1992a).

Following the characterization of the binding of the expressed protein we investigated the signal transduction pathways of the human H_2 receptor in CHO cells. Previously, it has been reported that H_2 receptors can elevate the cyclic AMP levels in a variety of human tissues (Platshon *et al.*, 1978; Bristow *et al.*, 1982; Emani *et al.*, 1983; Whitehead *et al.*, 1988; Arima *et al.*, 1991). We found that in stably expressed CHO cells stimulation of the human H_2 receptor also results in the rapid intracellular accumulation of cyclic AMP. Histamine is highly effective in this respect; the high potency in relation to its low affinity reflects a large receptor reserve for histamine and therefore a highly efficient coupling of the H_2 receptor to the adenylate cyclase system in the CHO cells. The histamine-induced cyclic AMP production in CHOhumH_2 cells was pharmacologically characterized as an H_2 receptor-mediated process; the response was not inhibited by the H_1- and H_3-receptor antagonists, mepyramine and thioperamide but could be inhibited potently by the H_2 antagonists, tiotidine and cimetidine. The resulting K_i-values obtained from the cyclic AMP inhibition experiments (8 nM and 0.56 μM) were quite similar to the K_i-values obtained from the radioligand binding studies (17 nM and 0.66 μM) for tiotidine and cimetidine respectively.

In some systems it has been suggested that histamine H_2 receptor stimulation is linked to other signal transduction mechanisms (Mitsuhashi *et al.*, 1989; Delvalle *et al.*, 1992; Seifert *et al.*, 1992; Traiffort *et al.*, 1992b). In HL-60 cells (Mitsuhashi *et al.*, 1989; Seifert *et al.*, 1992) and rat HEPA cells transfected with the canine H_2 receptor cDNA (Delvalle *et al.*, 1992) H_2 receptor stimulation has been reported to result in an increase of the intracellular Ca^{2+} concentration. In HEPA cells this response was clearly correlated with an increase of the IP_3 levels and appeared to be independent of cyclic AMP production (Delvalle *et al.*, 1992). Moreover, in CHO cells rat H_2 receptor stimulation inhibited A23187-induced arachidonic acid release via a cyclic AMP independent mechanism (Traiffort *et al.*, 1992b). These data indicate that H_2 receptors might interact with a variety of different G proteins in the membrane.

In CHOhumH_2 cells we were unable to observe a coupling to the phospholipase C and phospholipase A_2 pathway. In total agreement with our findings, a linkage of the rat H_2 receptor with the phospholipase C pathway could not be found either (Traiffort *et al.*, 1992b). These conflicting observations can be explained by assuming different G protein and/or phospholipase C isoenzyme distribution in CHO and HEPA cells. In contrast to the rat H_2 receptor (Traiffort *et al.*, 1992b) the human H_2 receptor was not able to reduce the A23187-induced arachidonic acid release from CHOhumH_2 cells. Instead, a slight stimulation was obtained, which can be explained by the reported modulation of arachidonic acid release from CHO cells by protein kinase A (Piomelli & Di Marzo, 1993). An explanation for the observed lack of inhibition could be found in the difference in receptor expression. For the rat H_2 receptor a CHO clone expressing 1.4 pmol mg^{-1} protein was used for the arachidonic acid release experiments (Traiffort *et al.*, 1992b), whereas in the present study, the human H_2 receptor was expressed at a more physiological level ($\pm$ 600 fmol mg^{-1} protein). It is also possible that the observed sequence differences between the rat (Ruat *et al.*, 1991) and human gene (Gantz *et al.*, 1991a,b) are responsible for the difference in signal transduction. It is known that intracellular receptor domains are involved in the interaction of G protein coupled receptors with different G proteins (Probst *et al.*, 1992). Although the rat and human H_2 receptor share a high degree of overall homology, differences are found especially in the intracellular parts of the receptor proteins (Gantz *et al.*, 1991a; Ruat *et al.*, 1991).

In conclusion, we have stably expressed the human H_2 receptor in CHO cells. The receptor protein is pharmacologically similar to the human H_2 receptor in brain tissue and is very efficiently coupled to the adenylate cyclase system. The availability of a cell system expressing the human H_2 receptor will play a key role in the development of new and selective ligands for this protein, an important target for today's human pharmacotherapy (Felix *et al.*, 1991; Bertaccini & Corruzi, 1992). Screening of large series of compounds for their affinities for the human H_2 receptor is possible now, and the regulation of the human H_2 receptor function can be studied in detail.

H_2 receptor agonists are investigated for future development and application in patients with congestive heart failure (Felix *et al.*, 1991). In this pathophysiological condition the cardiac adrenergic neurotransmission is greatly reduced. This is probably the result of an increase in the expression of the β-adrenoceptor kinase, which is responsible for the phosphorylation and desensitization of the β_2-adrenoceptor (Ungerer *et al.*, 1993). Recently, we observed a rapid desensitization of the human H_2 receptor-mediated cyclic AMP production in U-937 cells (Smit *et al.*, unpublished observations). Yet, the use of this cell line for detailed biochemical investigations is limited since the density of H_2 receptors is very low ($\pm$ 10 fmol mg^{-1} protein; M.J. Smit, unpublished observations). The use of the CHOhumH_2 cells will therefore also be of great importance for future mechanistic studies of the desensitization and regulation of H_2 receptor expression.

The authors wish to thank Dr I. Gantz for the gift of the human H_2 cDNA and Dr J. Eersels for the synthesis of [^{125}I]-APT. The research of R.L. has been made possible by a fellowship of the Royal Netherlands Academcy of Arts and Sciences.

References

ARIMA, N., YAMASHITA, Y., NAKATA, H., NAKAMURA, A., KONISHITA, Y. & CHIBA, T. (1991). Presence of histamine H_2 receptors on human gastric carcinoma cell line MKN-45 and their increase by retinoic acid treatment. *Biochem. Biophys. Res. Commun.*, **176**, 1027–1032.

ASH, A.S.F. & SCHILD, H.O. (1966). Receptors mediating some actions of histamine. *Br. J. Pharmacol. Chemother.*, **27**, 427–439.

BARNES, P.J. (1992). Histamine receptors in the respiratory tract. In *The Histamine Receptor*. ed Schwartz, J.C. & Haas, H. pp. 253–270. New York: Wiley-Liss.

BERTACCINI, G. & CORRUZI, G. (1992). Histamine receptors in the digestive systems. In *The Histamine Receptor*. ed. Schwartz, J.C. & Haas, H. pp. 193–230. New York: Wiley-Liss.

BLACK, J.W., DUNCAN, W.A.M,. DURANT, G.J., GANELLIN, C.R. & PARSONS, M.E. (1972). Definition and antagonism of histamine H_2 receptors. *Nature*, **236**, 385–390.

BRADFORD, M.M. (1976). A rapid and sensitive method for the quantitation of microgram quantities of protein utilizing the principle of protein-dye binding. *Anal. Biochem.*, **72**, 248–254.

BRISTOW, M.R., CUBICCIOTTI, R., GINSBURG, R., STINSON, E.B. & JOHNSON, C.L. (1982). Histamine-mediated adenylate cyclase stimulation in human myocardium. *Mol. Pharmacol.*, **21**, 671–679.

BURDE, R., SEIFERT, R., BUSCHAUER, A. & SCHULTZ, G. (1989). Histamine inhibits activation of human neutrophils and HL-60 leukemic cells via H-2-Receptors. *Arch. Pharmacol.*, **340**, 671–678.

DELVALLE, J., WANG, L., GANTZ, I. & YAMADA, T. (1992). Characterization of H_2 histamine receptor: linkage to both adenylate cyclase and $[Ca^{2+}]_i$ signalling systems. *Am. J. Physiol.*, **263**, G967–972.

DEUTSCH, S.T., ROSSE, R.B., KENDRICK, K.A., FAYMCCARTHY, M., COLLINS, J.P. & WYATT, R.J. (1993). Famotidine adjunctive pharmacotherapy for schizophrenia-preliminary data. *Clin. Neuropharmacol.*, **16**, 518–524.

DIXON, R.A.F., KOBILKA, B.K., STRADER, D.J., BENOVIC, J.L., DOHLMAN, H.G., FRIELLE, T., BOLANOWSKI, M.A., BENNETT, C.D., RANDS, E., DIEHL, R.E., MUMFORD, R.A., SLATER, E.E., SIGAL, I.S., CARON, M.G., LEFKOWITZ, R.J. & STRADER, C.D. (1986). Cloning of the gene and cDNA for mammalian β-adrenergic receptor and homology with rhodopsin. *Nature*, **321**, 75–79.

DU, X.Y., SCHOEMAKER, R.G., BAX, W.A., BOS, E. & SAXENA, P.R. (1993). Effects of histamine on porcine isolated myocardium: differentiation from effects on human tissue. *J. Cardiovasc. Res.*, **22**, 468–473.

EMANI, S., GESPACH, C., FORGUE-LAFITTE, M., BROER, Y. & ROSSELIN, G. (1983). Histamine and VIP interactions with receptor cyclic AMP systems in the human gastric cancer cell line HGT-1. *Life Sci.*, **33**, 415–423.

ERIKS, J.C., STERK, G.J., VAN DER AAR, E.M., VAN ACKER, S.A.B.E., VAN DER GOOT, H. & TIMMERMAN, H. (1991). 4- or 5-(2-aminoethyl)thiazoles and derivatives: new selective H_2-receptor agonists. In *New Perspectives in Histamine Research*. ed. Timmerman, H. & Van der Goot, H. pp. 301–314. Basel: Birkhauser Verlag.

FELIX, S.B., BUSCHAUER, A. & BAUMANN, G. (1991). Therapeutic value of H_2-receptor stimulation in congestive heart failure. Hemodynamic effects of BU-E-76, BU-E-75 and arpromidine (BU-E-50) in comparison to impromidine. In *New Perspectives in Histamine Research*. ed Timmerman, H. & Van der Goot, H. pp. 257–269. Basel: Birkhäuser Verlag.

GANTZ, I., MUNZERT, G., TASHIRO, T., SCHAFFER, M., WANG, L., DELVALLE, J. & YAMADA, T. (1991a). Molecular cloning of the human histamine H_2 receptor. *Biochem. Biophys. Res. Commun.*, **178,** 1386–1392.

GANTZ, I., SCHAFFER, M., DELVALLE, J., LOGDSON, G., CAMPBELL, V., UHLER, M. & YAMADA, T. (1991b). Molecular cloning of a gene encoding the histamine H_2 receptor. *Proc. Natl. Acad. Sci. U.S.A.*, **88,** 429–433.

GESPACH, C., COST, H. & ABITA, J. (1985). Histamine H_2 receptor activity during the differentiation of the human monocytic-like cell line U-937. *Febs Lett.*, **184,** 207–213.

GODFREY, P. (1992). Inositol lipids and and phosphates. In *Signal Transduction. A Practical Approach* ed. Milligan, G. pp. 105–121. Oxford: IRL Press.

IREDALE, P.A. & HILL, S.J. (1993). Increases in intracellular calcium via activation of an endogenous P_2-purinoceptor in cultured CHO-K1 cells. *Br. J. Pharmacol.*, **110,** 1305–1310.

KAMINSKY, R., MORIARTY, T.M., BODINE, J., WOLF. A.E. & DAVIDSON, M. (1990). Effect of famotidine on deficit symptoms of schizophrenia. *Lancet*, **335,** 1351–1352.

KEITOKU, M., MARUYAMA, Y. & TAKISHIMA, T. (1990). Different histamine actions in proximal and distal human coronary arteries in vitro. *Cardiovasc. Res.*, **24,** 614–622.

LEURS, R., VAN DER GOOT, H. & TIMMERMAN, H. (1991). Histaminergic agonist and antagonists: recent developments. In *Advances in Drug Research.* ed. Testa, B., Vol. 20, pp. 217–304. London: Academic Press.

LEURS, R., TRAIFFORT, E., ARRANG, J.M., TARDIVEL-LACOMBE, J., RUAT, M. & SCHWARTZ, J.C. (1994). Guinea-pig histamine H_1 receptor: II stable expression in Chinese Hamster Ovary cells reveals the interaction with three major signal transduction pathways. *J. Neurochem.*, **62,** 519–527.

MARTINEZ-MIR, M.I., ESTAN, L., MORALES-OLIVAS, F.J. & RUBIO, E. (1992). Effect of histamine and histamine analogues on human isolated myometrial strips. *Br. J. Pharmacol.*, **107,** 528–531.

MARTINEZ-MIR, M.I., POLLARD, H., MOREAU, J., TRAIFFORT, E., RUAT, M., SCHWARTZ, J.C. & PALACOIS, J.M. (1993). Loss of striatal histamine H_2 receptors in Huntington's Chorea but not in Parkinson's disease: comparison with animal models. *Synapse*, **15,** 209–220.

MITSUHASHI, M., MITSUHASHI, T., DAZIN, P.F. & PAYAN, D.G. (1991). Agonistic activities of histamine-albumin conjugates at the histamine H_2 receptors on human HL-60 promyelocytic leukemia cells. *Mol. Pharmacol.*, **40,** 271–275.

MITSUHASHI, M., MITSUHASHI, T. & PAYAN, D.G. (1989). Multiple signalling pathways of histamine H_2 receptors. *J. Biol. Chem.*, **264,** 18356–18362.

MUNSON, P.J. & RODBARD, D. (1980). LIGAND: a versatile computerized approach for characterization of ligand-binding systems. *Anal. Biochem.*, **107,** 220–239.

NORDSTEDT, C. & FREDHOLM, B.B. (1990). A modification of a protein-binding method for the rapid quantification of cAMP in cell-culture supernatant and body fluids. *Anal. Biochem.*, **189,** 231–234.

PIOMELLI, D. & DI MARZO, V. (1993). Dopamine D_2 receptor signalling via the arachidonic acid cascade: modulation by cAMP-dependent protein kinase A and prostaglandin E_2. *J. Lipid Mediators*, **6,** 433–443.

PLATHSON, L.F. & KALINER, M. (1978). The effect of the immunologic release of histamine upon human lung cyclic nucleotide levels and prostaglandin generation. *J. Clin. Invest.*, **62,** 1113–1121.

PROBST, W.C., SNYDER, L.A., SCHUSTER, D.T., BROSIUS, J. & SEALFON, S.C. (1992). Sequence alignment of the G-protein coupled receptor superfamily. *DNA Cell Biol.*, **11,** 1–20.

REYL-DESMARS, F., CHERIFI, Y., LE ROMANCER, M., PIGEON, C., LE ROUX, S. & LEWIN, M.J.M. (1991). Solubilisation, purification et caracterisation moleculaire du recepteur histaminique H_2 a partir des cellules tumorales gastrique humaines HGT-1. *C.R. Acad. Sci. Paris*, **312,** 221–224.

RUAT, M., TRAIFFORT, E., ARRANG, J., LEURS, R. & SCHWARTZ, J.C. (1991). Cloning and tissue expression of a rat histamine H_2-receptor gene. *Biochem. Biophys. Res. Commun.*, **179,** 1470–1478.

RUAT, M., TRAIFFORT, E., BOUTHENET, M.L., SCHWARTZ, J.-C., HIRSCHFELD, J., BUSCHAUER, A. & SCHUNACK, W. (1990). Reversible and irreversible labelling and autoradiographic localization of the cerebral histamine H_2 receptor using [^{125}I]iodonated probes. *Proc. Natl. Acad. Sci. U.S.A.*, **87,** 1658–1662.

SEIFERT, R., HOER, A., SCHWANNER, I. & BUSCHAUER, A. (1992). Histamine increases cytosolic calcium in HL-60 promyelocytes predominantly via H_2 receptors with a unique agonist/antagonist profile and induces functional differentiation. *Mol. Pharmacol.*, **42,** 235–241.

SMIT, M.J., BLOEMERS, S.M., LEURS, R., TERTOOLEN, L.G.J., BAST, A., DE LAAT, S.W. & TIMMERMAN, H. (1992). Short-term desensitization of the histamine H_1 receptor in human HeLa cells: involvement of protein kinase C dependent and independent pathways. *Br. J. Pharmacol.*, **107,** 448–455.

TIMMERMAN, H. (1992). Routes to histamine H_2 agonists. *Quant. Struct. Act. Relat.*, **11,** 219–223.

TODA, N. (1990). Mechanism underlying responses to histamine of isolated monkey and human cerebral arteries. *Am. J. Physiol.*, **258,** H311–317.

TRAIFFORT, E., POLLARD, H., MOREAU, J., RUAT, M., SCHWARTZ, J.C., MATRINEZ-MIR, M.I. & PALACOIS, J.M. (1992a). Pharmacological characterization and autoradiographic localization of histamine H_2 receptors in human brain identified with [^{125}I]iodoaminopotentidine. *J. Neurochem.*, **59,** 290–299.

TRAIFFORT, E., RUAT, M., ARRANG, J.M., LEURS, R., PIOMELLI, D. & SCHWARTZ, J.C. (1992b). Expression of a cloned rat histamine H_2 receptor mediating inhibition of arachidonate release and activation of cAMP accumulation. *Proc. Natl. Acad. U.S.A.*, **89,** 2649–2653.

UNGERER, M., BOHM, M., ELCE, J.S., ERDMANN, E. & LOHSE, M.J. (1993). Altered expression of beta-adrenergic receptor kinase and beta1-adrenergic receptors in the failing human heart. *Circulation*, **87,** 454–463.

WHITEHEAD, R.J., TAYLOR, D.J., EVANSON, J.M., HART, I.R. & WOOLLEY, D.E. (1988). Demonstration of histamine H_2 receptors on human melanoma cells. *Biochem. Biophys. Res. Commun.*, **151,** 518–523.

ZERKOWSKI, H., BROEDE, A., KUNDE, K., HILLEMAN, S., SCHÄFFER, E., VOGELSANG, M., MICHEL, M.C. & BRODDE, O. (1993). Comparison of the positive inotropic effect of serotonin, histamine, angiotensin II, endothelin and isoprenaline in the isolated human right atrium. *Arch. Pharmacol.*, **347,** 347–352.

(Received February 3, 1994
Revised March 24, 1994
Accepted March 25, 1994)

Br. J. Pharmacol. (1994), **112**, 855–860

Covariation of α_2-adrenoceptor density and function following irreversible antagonism with EEDQ

[1]Michael J. Durcan, Philip F. Morgan, Michelle L. Van Etten & Markku Linnoila

Laboratory of Clinical Studies, DICBR, National Institute on Alcohol Abuse and Alcoholism, 9000 Rockville Pike, Bethesda, MD 20892, U.S.A.

1 Administration of the irreversible antagonist, N-ethoxycarbonyl-2-ethoxy-1,2-dihydroquinoline, (EEDQ, 2 mg kg^{-1}, i.p.) to mice reduced binding of [^{3}H]-RX 821002 (2-methoxy-idazoxan) to α_2-adrenoceptors in whole mouse brain by 75% 24 h later. The receptor binding returned over time only being reduced by 25% by 16 days post administration; the time taken for binding to return to 50% of control levels was estimated to be 5.25 days.

2 EEDQ administration also resulted in the loss of the sedative effect of the α_2-adrenoceptor agonist, medetomidine, measured by the holeboard test of directed exploration and locomotor activity. Agonist-induced sedation returned to control values by 8 days post EEDQ administration.

3 EEDQ administration also resulted in the loss of the hypothermic response to medetomidine (0.1 mg kg^{-1}, i.p.). Medetomidine-induced hypothermia returned to control values by 12 days post EEDQ administration.

4 Pretreatment with the selective α_2-adrenoceptor antagonist, RX 821002 (0.1–3.0 mg kg^{-1}, i.p.) 45 min before EEDQ prevented the loss of α_2-adrenoceptors as well as the blockade of medetomide-induced sedation and hypothermia by EEDQ.

5 The results of these experiments indicate that there is significant receptor reserve for α_2-adrenoceptor-mediated behavioural and physiological responses.

Keywords: N-ethoxycarbonyl-2-ethoxy-1,2-dihydroquinoline (EEDQ); α_2-adrenoceptors; RX 821002; medetomidine; sedation; hypothermia; receptor binding in mice

Introduction

N-ethoxycarbonyl-2- ethoxy-1, 2-dihydroquinoline (EEDQ) (Belleau *et al.*, 1968; 1969) is a potent and irreversible antagonist of a number of neurotransmitter receptors (Meller *et al.*, 1988; Crocker & Cameron, 1989). Since EEDQ binds irreversibly to these receptors and they must be replaced for the return of function, it provides a useful tool for the investigation of receptor turnover as well as the relationship between receptor density and behavioural or physiological function. Additionally, by employing appropriate pharmacological treatments before EEDQ administration it is possible to explore the differential contributions of specific receptor subtypes. EEDQ has been extensively used for the investigation of the behavioural, neuropharmacological and electrophysiological effects of irreversible blockade of dopamine receptors (Hamblin & Creese, 1983; Meller *et al.*, 1985; Saller *et al.*, 1989; Cox & Waszcak, 1990). However, EEDQ has been reported to be more potent in irreversibly blocking α-adrenoceptors, in particular the α_2-adrenoceptor, than dopamine receptors (Adler *et al.*, 1985; Meller *et al.*, 1988; Pilc *et al.*, 1989). For example, the peripherally administered dose required to maximally block α_2-adrenoceptors is reported to be <2 mg kg^{-1} whereas doses of greater than 4 mg kg^{-1} are routinely used in investigation of dopamine receptors (Hamblin & Creese, 1983; Meller *et al.*, 1985; Saller *et al.*, 1989; Cox & Waszcak, 1990).

In the experiments described here the effect of EEDQ on radioligand binding to α_2-adrenoceptors was explored both over time following EEDQ treatment and in groups of animals in which the α_2-adrenoceptors were 'protected' by the prior administration of a selective α_2-adrenoceptor antagonist, RX 821002. In addition, the changes in responses to an α_2-adrenoceptor agonist *in vivo* following EEDQ treatment were also investigated both over time and in animals pretreated with RX 821002. The selective α_2-adrenoceptor agonist, medetomidine, was used to investigate α_2-mediated responses i.e., sedation and hypothermia. The dose used (0.1 mg kg^{-1}) was chosen on the basis of previous studies with this compound (Durcan *et al.*, 1989). The results are discussed in terms of the rate of α_2-adrenoceptor turnover and the relationship of receptor density to agonist-mediated function.

Methods

Animals

NIH Swiss male mice were housed in groups of ten on a 12:12 h light:dark cycle with food and water available *ad lib.* The mice weighed between 21 and 25 g (approximately 6–7 weeks of age) at the time of testing. All mice were naive to the testing apparatus.

[^{3}H]-RX 821002 binding

For binding studies mouse whole brains were rapidly removed and frozen at − 70°C. Individual brains were homogenized in 10 ml of buffer (50 mM Tris HCl; 0.5 mM $MgCl_2$, pH 7.4). The homogenates were centrifuged at 35,000 *g* for 20 min at 4°C, the supernatant discarded and resuspended in buffer. This procedure was repeated twice more.

For saturation binding tissue homogenates were incubated with 11 concentrations of [^{3}H]-RX 821002 (0.05–20 nM) for 30 min at room temperature. Non-specific binding was determined with 10 μM phentolamine. Bound and free radioligand were separated by rapid filtration through Whatman GF/B filters using a Brandel M-24 cell harvester. Filters were washed twice with 5 ml ice-cold assay buffer, placed in vials containing 10 ml scintillation fluid and the radioactivity

[1] Current address for correspondence: Div. of Pharmacology, Rm. 1237, Main Building, Wellcome Research Laboratories, 3030 Cornwallis Road, Durham, NC 27709 USA.

measured in a liquid scintillation counter. Protein levels were determined by the Coomassie blue method with gamma globulin standards using a Bio-Rad microplate reader and reagents (Bio-Rad, Melville, NY, U.S.A.). When a single concentration of radioligand was employed 1 nM [^{3}H]-RX 821002 was used under identical assay conditions.

Holeboard testing

The holeboard consisted of a Plexiglas box (40 × 40 × 30 cm) the floor of which had four equally spaced holes, each 3 cm in diameter. In two opposite walls, 2 cm above the floor, were four equally spaced infra-red photobeams to measure movement in the box. There were also photobeams beneath each hole to measure the number and duration of head-dips. The apparatus was interfaced with a PDP-11 computer running SKED-11 software (State Systems Inc., Kalamazoo, MI, U.S.A.).

The holeboard testing, which took place in a dimly lit room, involved placing a mouse in the centre of the floor and allowing it to explore for 8 min.

Temperature recording

Core body temperatures were measured with a rectal probe and a digital thermometer (Harvard Apparatus, South Natick, MA, U.S.A.). The probe was inserted 2.5 cm into the colon of each mouse.

Data analysis

The maximum number of binding sites (B_{max}) and the equilibrium dissociation constants (K_d) were calculated with Lundon-1 software (Lundon Software Inc., Chagrin Falls, OH, U.S.A.). Data were analysed by analysis of variance and *post hoc* Tukey tests to determine differences between individual means.

Effect of EEDQ on [^{3}H]-RX 821002 binding: time course and receptor protection studies

For the time course experiment, groups of animals ($n = 4$ each) were treated with EEDQ (2 mg kg^{-1}) or 5% DMSO vehicle 1, 2, 4, 8, 12 and 16 days before they were killed. Whole brain tissue was obtained and the magnitude of [^{3}H]-RX 821002 binding assessed using a single concentration of radioligand as described above.

For the receptor protection experiments groups of animals ($n = 4$ each) were pretreated with RX 821002 (0.1–3.0 mg kg^{-1}, i.p.) or distilled water vehicle 45 min before treatment with EEDQ (2 mg kg^{-1}, i.p.) or 5% DMSO vehicle. Twenty four hours later whole brain tissue was obtained and the magnitude of [^{3}H]-RX 821002 binding assessed using a single concentration of radioligand as described above. In addition in groups receiving pretreatments with vehicle or 3.0 mg kg^{-1} RX 821002, saturation binding curve analysis was also performed to obtain B_{max} and K_d estimates as described above.

Effect of EEDQ on medetomidine-induced sedation: time course and receptor protection studies

For the medetomidine-induced sedation experiments groups of animals ($n = 7–10$) were treated with EEDQ (2 mg kg^{-1}) or 5% DMSO vehicle 1, 2, 4, 8, 12 and 16 days before testing in the holeboard apparatus. On the day of testing the animals were injected with medetomidine (0.1 mg kg^{-1}, i.p.) or distilled water vehicle 30 min before testing in the holeboard apparatus as described above.

For the receptor protection experiments groups of animals ($n = 6–8$) were pretreated with RX 821002 (0.1–3.0 mg kg^{-1}, i.p.) or distilled water vehicle 45 min before treatment with EEDQ (2 mg kg^{-1}, i.p.) or 5% DMSO vehicle. Twenty four hours later they were tested in the holeboard apparatus. The animals were injected with medetomidine (0.1 mg kg^{-1}, i.p.) or distilled water vehicle 30 min before testing in the holeboard apparatus as described above.

Effect of EEDQ on medetomidine-induced hypothermia: time course and receptor protection studies

For the medetomidine-induced hypothermia experiments groups of animals ($n = 8–11$) were treated with EEDQ (2 mg kg^{-1}) or 5% DMSO vehicle 1, 2, 4, 8, 12 and 16 days prior to hypothermia testing. On the day of testing the core body temperature of each animal was measured immediately before it was injected with medetomidine (0.1 mg kg^{-1}, i.p.) or distilled water vehicle. Twenty minutes later the core body temperature of each animal was measured again.

For the receptor protection experiments groups of animals ($n = 6–8$) were pretreated with RX 821002 (0.1–3.0 mg kg^{-1}, i.p.) or distilled water vehicle 45 min before treatment with EEDQ (2 mg kg^{-1}, i.p.) or 5% DMSO vehicle. Twenty four hours later their core body temperatures were measured immediately before medetomidine (0.1 mg kg^{-1}, i.p.) administration. Twenty minutes later the core body temperature of each animal was measured again.

Drugs

N-ethoxycarbonyl-2-ethoxy-1,2-dihydroquinoline (EEDQ), 2-[2-(2-methoxy-1,4-benzodioxanyl)] imidazoline hydrochloride (RX 821002) and phentolamine were obtained from Research Biochemicals International, Natick, MA, U.S.A., and medetomidine was obtained from Farmos Ltd., Turku, Finland. [^{3}H]-RX 821002 was obtained from Amersham Life Science, Arlington Heights, IL, U.S.A. EEDQ was dissolved in 5% dimethylsulphoxide (DMSO) distilled water, RX 821002 and medetomidine were each dissolved in a distilled water vehicle. All injections were given i.p. at a volume of 10 ml kg^{-1}.

Results

Effect of EEDQ treatment on [^{3}H]-RX 821002 binding

Pretreatment with EEDQ (2 mg kg^{-1}) significantly reduced binding of [^{3}H]-RX 821002 in mouse whole brain homogenates obtained 24 h after administration (see Figure 1). The amount of binding in the EEDQ-treated animals was approximately 25% of that seen in the vehicle-treated animals 1 day following treatment; binding gradually returned towards control levels over time (see Figure 1b). By day 16 post EEDQ treatment the binding in the treated animals was not statistically significantly different from the control animals (Figure 1); however, it was still only approximately 75% of control levels (Figure 1b).

Pretreatment 45 min before EEDQ administration with RX 821002 dose-dependently protected against the loss of binding induced by EEDQ seen 24 h later (Figure 2). Animals pretreated with vehicle 45 min before EEDQ showed a reduction in [^{3}H]-RX 821002 binding consistent with that seen previously. Animals receiving 0.3, 1.0 and 3.0 RX 821002 prior to EEDQ all showed significantly greater binding than unpretreated controls (Figure 2). In the groups which were not treated with EEDQ, the administration of RX 821002 did not have any significant effect on receptor binding 24 h later. Analysis of saturation binding data revealed a significant ($P < 0.01$) reduction in the maximal binding (B_{max}) in the EEDQ only treated group as compared to controls (Table 1) whereas pretreatment with 3 mg kg^{-1} RX 821002 significantly ($P < 0.01$) attenuated the effect of EEDQ. No statistically significant change in affinity (K_d) was observed. Representative Scatchard plots for the four groups are shown in Figure 3.

Effect of EEDQ on medetomidine-induced sedation

Treatment with 0.1 mg kg^{-1} medetomidine produced a marked behavioural sedation in animals previously treated with the DMSO vehicle as shown by the reduction in locomotor activity and exploratory head-dipping in the holeboard ($P<0.01$). In animals treated with EEDQ the sedative effect of medetomidine was attenuated 1, 2 and 4 days after EEDQ treatment (Figure 4). A significant ($P<0.05$) attenuation of medetomidine-induced sedation was also observed on day 12 post EEDQ treatment but animals tested 8 and 16 days post EEDQ treatment did not differ from DMSO vehicle-treated controls. Whilst the attenuation seen on day 12 was significantly different from control ($P<0.05$ for head-dips, $P<0.01$ for locomotor activity), its magnitude was somewhat less than that seen earlier and not significantly different from values of EEDQ treated animals on days 8 and 16. Additionally, the medetomidine only treated control groups were somewhat more sedated on day 12 than on the other days. EEDQ treatment alone had no effect on either locomotor activity or exploratory head-dipping.

In the receptor protection experiment, the sedative effect of medetomidine was again reversed by administration of EEDQ 24 h earlier. However, in animals pretreated with RX 821002 45 min before EEDQ treatment, the sedation was less marked, an effect which was dose-dependent. For locomotor activity, groups given either 1 or 3 mg kg^{-1} RX 821002 treatment prior to EEDQ did not differ significantly from the 5% DMSO vehicle pretreated animals in

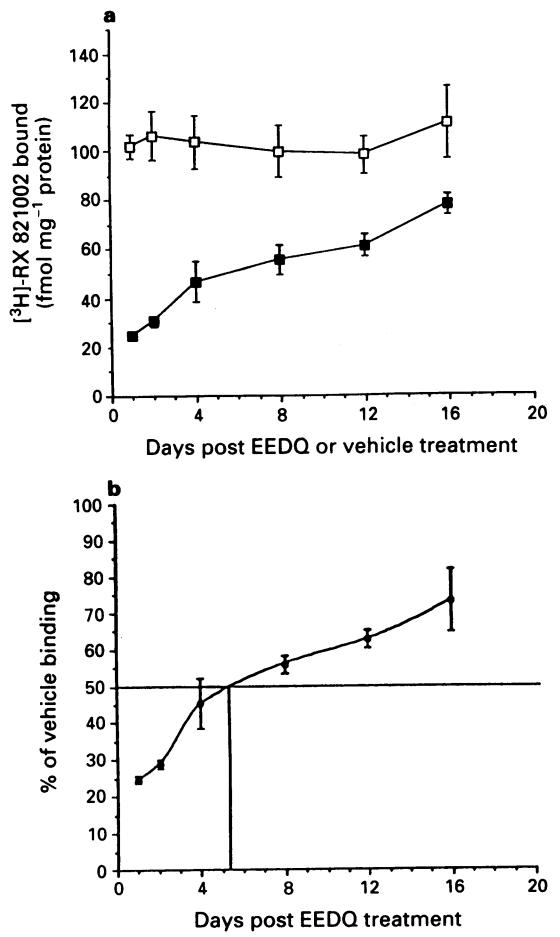

Figure 1 Time course of the effect of EEDQ on [^{3}H]-RX 821002 binding in mouse whole brain. (a) Animals were treated with either vehicle (□) or 2 mg kg^{-1} EEDQ (■) on day 0. (b) Stineman interpolation of the effect of EEDQ on [^{3}H]-RX 821002 binding expressed as a percentage of vehicle-treated values.

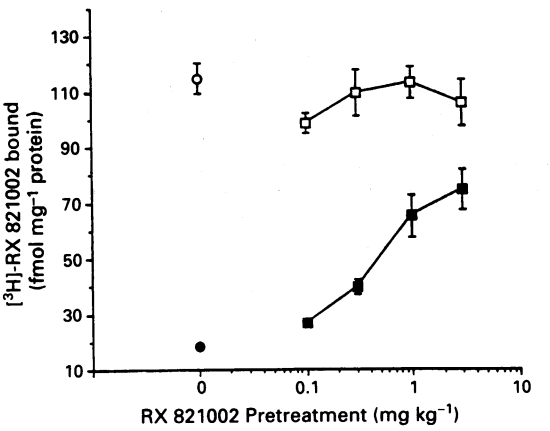

Figure 2 Effect of pretreatment with RX 821002 45 min prior to EEDQ on [^{3}H]-RX 821002 binding 24 h later: (□) animals treated with 0.1–3.0 mg kg^{-1} RX 821002 45 min before administration of 5% DMSO vehicle; (■) animals treated with 0.1–3.0 mg kg^{-1} RX 821002 45 min prior to administration of 2 mg kg^{-1} EEDQ; (○) vehicle + vehicle control; (●) vehicle + 2 mg kg^{-1} EEDQ control.

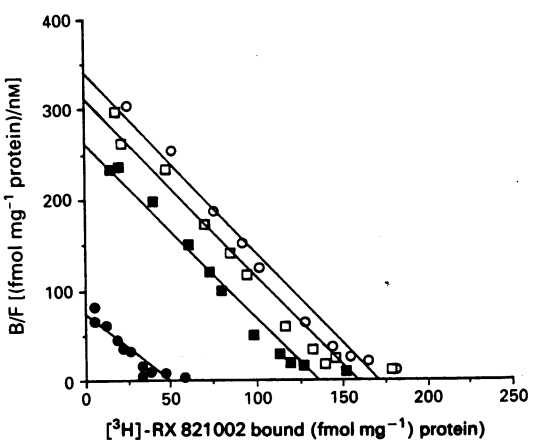

Figure 3 Representative Scatchard plots of [^{3}H]-RX 821002 binding data from animals killed 24 h after EEDQ administration with or without a pretreatment with RX 821002. (○) Vehicle + vehicle control; (●) vehicle + 2 mg kg^{-1} EEDQ control; (□) pretreatment with 3 mg kg^{-1} RX 821002 45 min prior to administration of 5% DMSO vehicle; (■) pretreatment with 3 mg kg^{-1} RX 821002 45 min prior to administration of 2 mg kg^{-1} EEDQ.

Table 1 Results of Scatchard analysis of [^{3}H]-RX 821002 binding isotherms from whole brain homogenates of animals treated 24 h previously with either EEDQ or its vehicle

Pretreatment	*Treatment*	B_{max} (fmol mg^{-1} protein)	K_d (nM)	n
Vehicle	Vehicle	165.13 ± 6.7	0.44 ± 0.02	4
Vehicle	EEDQ	60.55 ± 12.8***	1.13 ± 0.63	4
RX 821002 3 mg kg^{-1}	Vehicle	169.20 ± 7.1	0.43 ± 0.02	4
RX 821002 3 mg kg^{-1}	EEDQ	141.70 ± 19.2	0.49 ± 0.10	4

***$P<0.001$ vs. vehicle-treated controls.

their sedative response to medetomidine (Figure 5a). In the case of exploratory head-dipping, significant protection from the effect of EEDQ treatment was seen at doses of 0.3, 1.0 and 3.0 mg kg^{-1} RX 821002 (Figure 5b). Neither EEDQ nor RX 821002 treatment had any intrinsic effects on holeboard behaviours, however, animals pretreated with 3 mg kg^{-1} RX 821002 did show less sedation in response to medetomidine than animals pretreated with lower doses.

Effect of EEDQ on medetomidine-induced hypothermia

Medetomidine (0.1 mg kg^{-1}) produced a significant ($P<0.01$) drop in core body temperature (Figure 6). This hypothermic effect was significantly reversed by administration of EEDQ (2 mg kg^{-1}) 1, 2, 4 or 8 days prior to testing with medetomidine. The hypothermic effect of medetomidine returned by 16 days post EEDQ treatment. EEDQ did not have any intrinsic effect on core temperature at any time point during the experiment (Figure 6).

In the receptor protection experiment, pretreatment with RX 821002 again significantly reversed the effects of EEDQ on medetomidine-induced hypothermia (Figure 7). Groups receiving 1 and 3 mg kg^{-1} RX 821002 did not differ significantly from the 5% DMSO treated controls in the hypothermic response to medetomidine.

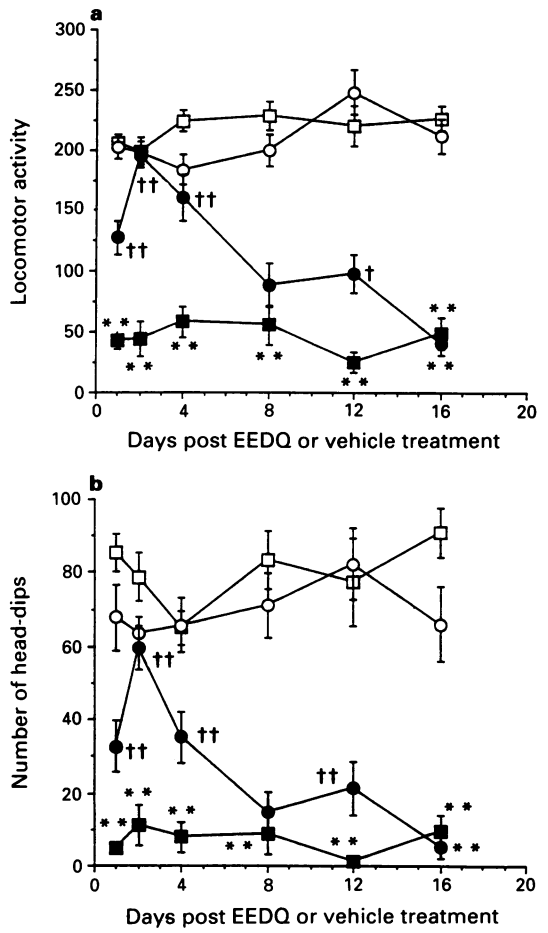

Figure 4 Time course of the effect of EEDQ on the sedative effects of medetomidine seen using the holeboard test. (a) Locomotor activity; (b) exploratory head-dipping. (□) 5% DMSO vehicle administered on day 0, vehicle administered on test day; (■) 5% DMSO vehicle administered on day 0, 0.1 mg kg^{-1} medetomidine administered on test day; (○) 2 mg kg^{-1} EEDQ administered on day 0, vehicle administered on test day; (●) 2 mg kg^{-1} EEDQ administered on day 0, 0.1 mg kg^{-1} medetomidine administered on test day. **$P<0.01$ vs vehicle/vehicle controls, ††$P<0.01$; †$P<0.05$, vs medetomidine only treated control.

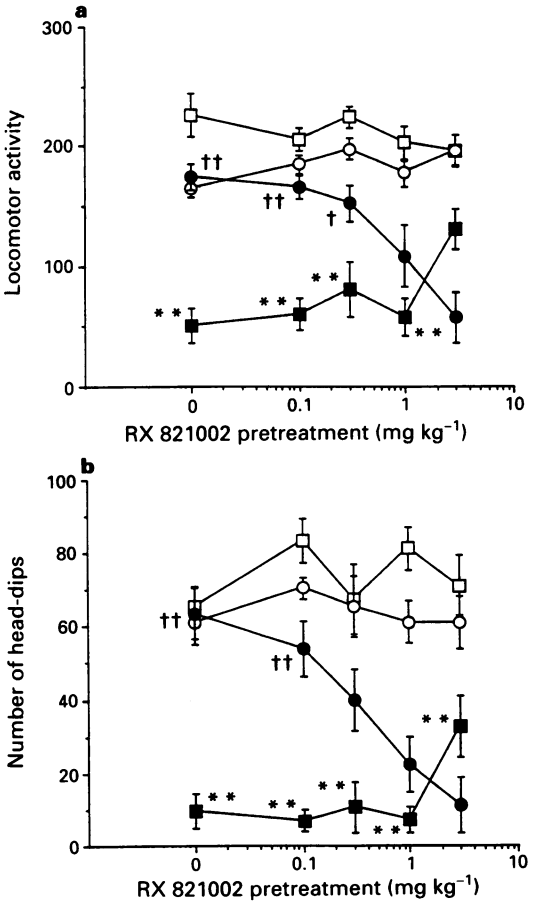

Figure 5 Effect of pretreatment with RX 821002 45 min before EEDQ on the sedative effects of medetomidine in the holeboard test 24 h later. (a) Locomotor activity; (b) exploratory head-dipping. (□) Animals treated with 0.0–3.0 mg kg^{-1} RX 8210002 45 min prior to administration of 5% DMSO vehicle and tested 24 h later with vehicle; (■) animals treated with 0.0–0.3 mg kg^{-1} RX 821002 45 min prior to administration of 5% DMSO vehicle and tested 24 h later with 0.1 mg kg^{-1} medetomidine; (○) animals treated with 0.0–3.0 mg kg^{-1} RX 821002 45 min prior to administration of 2 mg kg^{-1} EEDQ and tested 24 h later with vehicle; (●) animals treated with 0.0–3.0 mg kg^{-1} RX 821002 45 min prior to administration of 2 mg kg^{-1} EEDQ and tested 24 h later with 0.1 mg kg^{-1} medetomidine. **$P<0.01$ vs vehicle only control; ††$P<0.01$, †$P<0.05$, vs medetomidine only treated control.

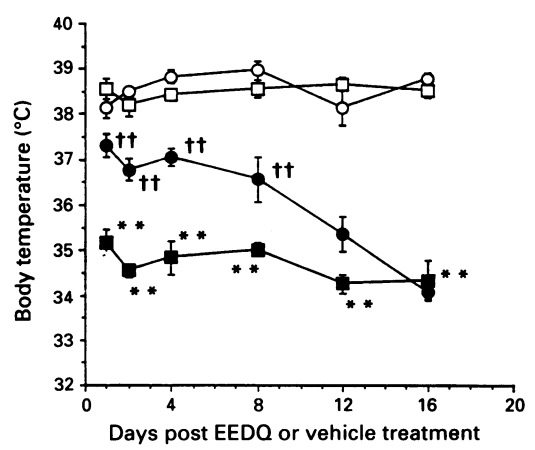

Figure 6 Time course of the effect of EEDQ on the hypothermic effect of medetomidine. (□) 5% DMSO vehicle administered on day 0, vehicle administered on test day; (■) 5% DMSO vehicle administered on day 0, 0.1 mg kg^{-1} medetomidine administered on test day; (○) 2 mg kg^{-1} EEDQ administered on day 0, vehicle administered on test day; (●) 2 mg kg^{-1} EEDQ administered on day 0, 0.1 mg kg^{-1} medetomidine administered on test day. **$P<0.01$ vs vehicle/vehicle control; ††$P<0.01$, vs medetomidine only treated control.

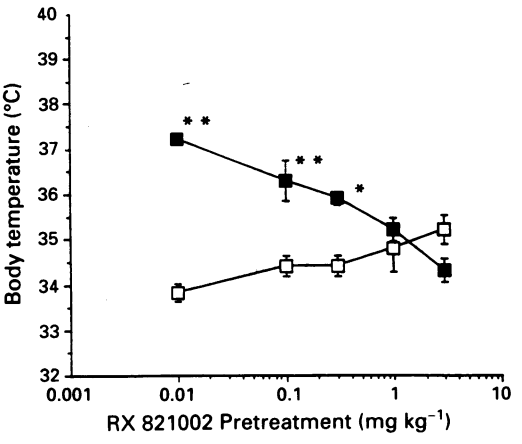

Figure 7 Effect of pretreatment with RX 821002 prior to EEDQ on hypothermic effect of medetomidine administered 24 h later; the RX 821002 pretreatment was administered 45 min before EEDQ administration and the animals were tested for medetomidine-induced hypothermia 24 h after the EEDQ. (□) Animals treated with 0.0–3.0 mg kg^{-1} RX 821002 45 min prior to administration of 5% DMSO vehicle and tested 24 h later with vehicle; (■) animals treated with 0.0–3.0 mg kg^{-1} RX 821002 45 min prior to administration of 2 mg kg^{-1} EEDQ and tested 24 h later with vehicle. $^{**}P<0.01$; $^{*}P<0.05$ vs vehicle only control.

Discussion

EEDQ (2 mg kg^{-1}) significantly reduced the number of α_2-adrenoceptor binding sites labelled by [^{3}H]-RX 821002 in mouse whole brain, 24 h after administration. The binding sites returned gradually over time, reaching 75% of control values by 16 days post EEDQ exposure. This finding is consistent with that reported with similar dosing regimes (Adler *et al.*, 1985; Pilc *et al.*, 1989; 1992). The effects of EEDQ on the α_2-adrenoceptor binding could be dose-dependently attenuated by administration of the selective α_2-adrenoceptor antagonist, RX 821002. Similar protective effects of the α_2-adrenoceptor agonist, clonidine and the less specific α_2-adrenoceptor antagonist, yohimbine have also been previously reported in rats (Pilc *et al.*, 1989; 1992). RX 821002 did not however produce any intrinsic change in α_2-adrenoceptor binding as has been previously reported for yohimbine (Pilc *et al.*, 1989). These results support the notion that EEDQ binds irreversibly to α_2-adrenoceptors which can be protected by the administration of selective ligands for those sites.

As a consequence of the irreversible binding of EEDQ to these sites, synthesis of new receptors is required for the return of functional receptors. In these experiments the time taken for the binding sites to return to 50% of control levels was estimated to be 5.25 days. Twenty-four hours after treatment with 2.0 mg kg^{-1} EEDQ the number of binding sites was reduced by 75–80% and previous studies have suggested this to be a maximal reduction, i.e. higher doses of EEDQ do not substantially increase this reduction (Adler *et al.*, 1985; Pilc *et al.*, 1992). This implies that either some binding sites return within 24 h or that there are some α_2-adrenoceptors that are unaffected by EEDQ treatment.

If there is an EEDQ-resistant sub-population of α_2-adrenoceptors, resistance may be due to neuroanatomical location or a particular subtype of receptor (or possibly both). For example, it has been reported that recovery rates for α_2-adrenoceptors (Bart & Garcia-Sevilla, 1992) and D_1 dopamine receptors (Giorgi *et al.*, 1991) following EEDQ treatment vary according to the brain region examined. A differential loss of an α_2-adrenoceptor subtype following EEDQ has also been suggested by Agenter *et al.* (1993). Investigating only presynaptic receptors, Agenter *et al.* (1993) found a much greater receptor inactivation than that reported for all α_2-adrenoceptors (Adler *et al.*, 1985; Pilc *et al.*, 1992; present study). If a resistant subtype of binding site does indeed exist, the present study suggests it is not the non-adrenoceptor imidazoline binding site (Michel & Insel, 1989; Lehmann *et al.*, 1989; Bousquet *et al.*, 1989), a site which binds a number of α_2-adrenoceptor ligands (most notably idazoxan). RX 821002, the methoxy derivative of idazoxan, (Stillings *et al.*, 1985) has little or no affinity for these sites (Langin *et al.*, 1990a,b; Hudson & Nutt, 1990; Miralles *et al.*, 1993a) and yet a similar proportion of binding sites labelled by this compound are lost following EEDQ treatment as seen with other ligands (Pilc *et al.*, 1989). However, recent evidence suggests that EEDQ may be able to inactivate at least partially I_2-imidazoline sites *in vivo*, probably through an indirect action since *in vitro* administration has little or no effect on these receptors (Miralles *et al.*, 1993b).

Although the binding returned towards control values relatively slowly, reaching 75% by day 16 post EEDQ, the α_2-adrenoceptor agonist effects returned much more quickly. The sedative effect of the α_2-adrenoceptor agonist, medetomidine, was significantly reduced 1, 2 and 4 days post EEDQ treatment but returned to control levels on days 8 and 16 post EEDQ. There was good agreement between the rate of return of the sedative effect of medetomidine with the rate of return of the hypothermia. As in the binding experiments, pretreatment with the selective α_2-adrenoceptor antagonist RX 821002 dose-dependently protected the animals against the effect of EEDQ on medetomidine-induced sedation. In animals not treated with EEDQ, 3 mg kg^{-1} RX 821002 showed some residual effect on the response to medetomidine administered 24 h later; a somewhat similar effect was also seen in the hypothermia protection experiment. The binding experiment did not suggest any change in receptor density resulting from this pretreatment. One possible explanation may be that sufficient RX 821002 remains in the animal to antagonize partially the effect of medetomidine 24 h later, although if this is the case one might have expected to see a similar effect in animals treated with EEDQ.

The hypothermic response to medetomidine returned to control levels by day 16 post EEDQ but the recovery of this effect was slower than that seen for sedation. A significantly reduced hypothermic response to medetomidine was seen for up to 8 days post EEDQ treatment. The loss of agonist hypothermic efficacy could also be protected against dose-dependently by pretreatment with the selective α_2-adrenoceptor antagonist, RX 821002.

Collectively the above results suggest that there is significant receptor reserve for the α_2-adrenoceptor agonist effects, at least as they pertain to behavioural sedation and hypothermia. The time course for the recovery of the sedative and hypothermic properties of medetomidine in mice is similar to that seen in rats for the return of the inhibition of noradrenaline release induced by the α_2-adrenoceptor agonist UK-14304 following EEDQ administration where the maximal response returns in 8 days (Adler *et al.*, 1987). For the measures used in these studies it would appear that they are largely mediated by α_2-adrenoceptors since it was possible to protect against the effects of EEDQ using a selective α_2-adrenoceptor antagonist. In studies using either this or higher concentrations of EEDQ to investigate other receptor systems, particularly if behavioural responses are under investigation, it is important to protect α-adrenoceptors or clearly establish the specificity of the effect for the receptor system under investigation in order to rule out the possibility of influences by α-adrenoceptors from the results.

References

ADLER, C.H., MELLER, E. & GOLDSTEIN, M. (1985). Recovery of α_2-adrenoceptor binding and function after irreversible inactivation by N-ethoxycarbonyl-2-ethoxy-1, 2-dihydroquinoline (EEDQ). *Eur. J. Pharmacol.*, **116**, 175–178.

ADLER, C.H., MELLER, E. & GOLDSTEIN, M. (1987). Receptor reserve at the α_2-adrenergic receptor in the rat cerebral cortex. *J. Pharmacol. Exp. Ther.*, **240**, 508–515.

AGENTER, E., DRODNY, H. & SINGER, E.A. (1993). Central α_2-autoreceptors: agonist dissociation constants and recovery after irreversible inactivation. *Br. J. Pharmacol.*, **108**, 370–375.

BARTEN, F. & GARCIA-SEVILLA, J.A. (1992). Long term treatment with desipramine increases the turnover of α_2-adrenoceptors in the rat brain. *Mol. Pharmacol.*, **42**, 846–855.

BELLEAU, B., DITULLIO, V. & GODIN, D. (1969). The mechanism of irreversible adrenergic blockade by N-carboxydihydroquinolines – model studies with typical serin hydrolases. *Biochem. Pharmacol.*, **18**, 1039–1044.

BELLEAU, B., MARTEL, R., LACASSE, G., HENARD, M., WEINBERG, N.L. & PETTON, Y.G. (1968). N-carboxylic esters of 1,2- and 1,4-dihydroquinolines. A new class of irreversible inactivators of the catecholamine α-receptors and potent central nervous system depressants. *J Am. Chem. Soc.*, **90**, 823–824.

BOUSQUET, P., FELDMAN, J., TIBIRICA, E., BRICCA, G., MOLINES, A., DONTENWILL, M. & BELCOURT, A. (1989). New concepts on the central regulation of blood pressure. Alpha$_2$-adrenoceptors and 'imidazoline receptors'. *Am. J. Med.*, **87**, 10S–13S.

COX, R.F. & WASZCAK, B.L. (1990). Irreversible receptor inactivation reveals differences in dopamine receptor reserve between A9 and A10 dopamine systems: an electrophysiological analysis. *Brain Res.*, **534**, 273–282.

CROCKER, A.D. & CAMERON, D.L. (1989). Receptor alkylating agents: novel tools for the study of receptor function in the central nervous system of the rat. *Clin. Exp. Pharmacol. Physiol.*, **16**, 545–548.

DURCAN, M.J., LISTER, R.G. & LINNOILA, M. (1989). Interactions of antagonists with medetomidine and with ethanol in a holeboard test. *Neuropharmacology*, **28**, 275–281.

GIORGI, O., PIBIRI, M.G. & BIGGIO, G. (1991). Differential turnover rates of D_1 dopamine receptors in the retina and disinct areas of rat brain. *J. Neurochem.*, **57**, 754–759.

HAMBLIN, M. & CREESE, I. (1983). Behavioural and radioligand binding evidence for irreversible dopamine receptor blockade by N-ethoxycarbonyl-2-ethoxy-1,2-dihydroquinoline. *Life Sci.*, **32**, 2247–2255.

HUDSON, A.L. & NUTT, D.J. (1991). *In vitro* autoradiography of [^{3}H]-RX 821002 in the rat CNS, a new ligand for identifying alpha$_2$-adrenoceptors. *Br. J. Pharmacol.*, **99**, 345P.

LANGIN, D., PARIS, H., DAUZATS, M. & LAFONTAN, M. (1990a). Discrimination between alpha$_2$-adrenoceptors and [^{3}H]idazoxan-labeled non-adrenergic sites in rabbit white fat cells. *Eur. J. Pharmacol.*, **188**, 261–272.

LANGIN, D., PARIS, H. & LAFONTAN, M. (1990b). Binding of [^{3}H]idazoxan and of its methoxy derivative [^{3}H]-RX 821002 in human fat cells: [^{3}H]Idazoxan but not [^{3}H]-RX 821002 labels additional non-alpha$_2$-adrenergic binding sites. *Mol. Pharmacol.*, **37**, 876–885.

LEHMANN, J., KOENIG-B., ERARD, E. & VITOU, P. (1989). The imidazoline-preferring receptor. *Life Sci.*, **45**, 1609–1615.

MELLER, E., BOHMAKER, K., GOLDSTEIN, M. & FRIEDHOFF, A.J. (1985). Inactivation of D1 and D2 dopamine receptors by N-ethoxycarbonyl-2-ethoxy-1, 2-dihydroquinoline *in vivo*: selective protection by neuroleptics. *J. Pharmacol. Exp. Ther.*, **233**, 656–662.

MELLER, E., GOLDSTEIN, M., FRIEDHOFF, A.J. & SCHWEITZER, J.W. (1988). N-ethoxycarbonyl-2-ethoxy-1, 2-dihydroquinoline (EEDQ): A new tool to probe CNS receptor function. *Adv. Exp. Med. Biol.*, **235**, 121–136.

MICHEL, M.C. & INSEL, P.A. (1989). Are there multiple imidazoline binding sites? *Trends Pharmacol. Sci.*, **10**, 342–344.

MIRALLES, A., OLMOS, G., SASTRE, M., BARTUREN, F., MARTIN, I. & GARCIA-SEVILLA, J.A. (1993a). Discrimination and pharmacological characterization of I_2-imidazoline sites with [^{3}H]-idazoxan and alpha-2 adrenoceptors with [^{3}H]RX 821002 (2-methoxy idazoxan) in the human and rat brains. *J. Pharmacol. Exp. Ther.*, **260**, 1000–1007.

MIRALLES, A., RIBAS, R., OLMOS, G. & GARCIA-SEVILLA, J.A. (1993b). Differential effects of the alkylating agent N-ethoxycarbonyl-2 ethoxy-1,2-dihydroquinoline on brain α_2-adrenoceptors and I_2-imidazoline sites in vitro and in vivo. *J. Neurochem.*, **61**, 1602–1610.

PILC, A., NOWAK, G. & ZAK, J. (1992). N-ethoxycarbonyl-2-ethoxy-1,2-dihydroquinoline, an irreversible receptor inactivator, as a tool for measurement of α_2-adrenoceptor occupany *in vivo*. *Eur. J. Pharmacol.*, **212**, 109–111.

PILC, A., VETULANI, J., NOMURA, S. & ENNA, S.J. (1989). An *in vivo* procedure for the selective inactivation of rat brain cerebral cortical alpha-adrenoceptors using N-ethoxycarbonyl-2-ethoxy-1,2-dihydroquinoline (EEDQ). *Brain Res.*, **493**, 8–13.

SALLER, C.F., KREAMER, L.D., ADAMOVAGE, L.A. & SALMA, A.I. (1989). Dopamine receptor occupancy *in vivo*: Measurement using N-ethoxycarbonyl-2-ethoxy-1,2-dihydroquinoline (EEDQ). *Life Sci.*, **45**, 917–929.

STILLINGS, M.R., CHAPELO, C.B., BUTLER, R.C., DAVIS, J.A., ENGLAND, C.D., MYERS, M., MYERS, P.L., TWEDDLE, N., WELBOURN, A.P., DOXEY, S.C. & SMITH, C.F.C. (1985). Alpha-adrenoceptor reagents. 3. Synthesis of some 2-substituted 1,4-benzodioxans as selective alpha-2-adrenoceptor antagonists. *J. Med. Chem.*, **28**, 1054–1062.

(Received January 5, 1994
Revised March 11, 1994
Accepted March 25, 1994)

Br. J. Pharmacol. (1994), **112**, 861–866

The effect of 5-HT_{1A} receptor agonists on locomotor activity in the guinea-pig

J.L. Evenden

Department of Behavioural Pharmacology, CNS Preclinical R & D, Astra Arcus, Södertälje, S-151 85 Sweden

1 The present study examined the effects of 8-hydroxy-2-(di-n-propylamino)tetralin (8-OH-DPAT), flesinoxan, ipsapirone and buspirone, all agonists at the 5-HT_{1A} receptor, on the locomotor activity of guinea-pigs. The effects of these drugs were contrasted with those of the non-selective 5-HT agonist, 5-methoxy-*N*,*N*-dimethyl tryptamine (5-MeO-DMT) and the dopamine D_2 antagonist, raclopride.

2 8-OH-DPAT, flesinoxan and 5-MeO-DMT markedly increased the locomotor activity of naive, unhabituated guinea-pigs in a dose-dependent manner. Buspirone also did so, although to a lesser extent and for a shorter time. The doses at which this effect was seen were higher than those normally employed in rats. Ipsapirone and raclopride had no significant effects on locomotor activity.

3 The locomotor activity increasing effect of 1.0 mg kg^{-1} 8-OH-DPAT was blocked by the selective 5-HT_{1A} antagonist (S)-UH-301 (3.0 and 10.0 mg kg^{-1}), but not by (−)-alprenolol (15.0 mg kg^{-1}). Ipsapirone (30.0 mg kg^{-1}) and raclopride (3.0 mg kg^{-1}) antagonized 8-OH-DPAT-induced locomotor activity but only to a small extent. The 5-HT reuptake inhibitor, zimelidine (10.0 mg kg^{-1}) had no effect.

4 The effect of the 5-HT_{1A} agonists in the guinea-pig contrasts with the effects of 8-OH-DPAT on the locomotor activity of unhabituated rats and mice tested in the same apparatus, but are similar to the effects of 8-OH-DPAT on habituated rats, which show a low baseline of activity.

5 These results support the suggestion that 5-HT_{1A} agonists may have an intrinsic activating effect which may be masked by other effects of the drug (e.g. hypothermia, 5-HT syndrome). The rank ordering of the 5-HT_{1A} agonists also suggests that the degree to which the drugs increase locomotor activity is related to their agonist efficacy at the postsynaptic 5-HT_{1A} receptor.

Keywords: 5-Hydroxytryptamine agonists; 8-OH-DPAT; locomotor activity in guinea-pig

Introduction

Agonists at the 5-hydroxytryptamine$_{1A}$ (5-HT_{1A}) receptor, exemplified by the selective agonist, 8-hydroxy-2-(di-n-propylamino)tetralin (8-OH-DPAT) elicit a characteristic set of behaviours in the naive rat, including aspects of the 5-HT syndrome, a long, flat, body posture and fore-paw treading (Tricklebank *et al.*, 1984), and hypothermia (Goodwin & Green, 1985). Partial agonists (such as the azapirones, buspirone, ipsapirone and gepirone) have a similar profile (Wilkinson & Dourish, 1991). 8-OH-DPAT also has clear effects on locomotor activity, which, however, are somewhat complex. If naive rats are tested soon after injection, overall activity is reduced but the proportion of forward locomotion is increased (Hillegaart *et al.*, 1989; Ericson *et al.*, 1991). However, if rats are continuously monitored for several hours, the initial reduction in activity passes over into an increase in activity (Evenden & Ängeby-Möller, 1990).

Evenden & Ängeby-Möller (1990) found very similar effects in mice to those in rats, on measures of both locomotor activity and rearing. In contrast, Buhot *et al.* (1989) noted that, in the same dose-range, 8-OH-DPAT did not alter exploratory activity in the hamster. Other effects of the drug also show marked species differences. For example, it has not proved easy to obtain signs of the 5-HT syndrome in mice in response to 8-OH-DPAT treatment that are seen in rats, except after intravenous administration of high doses (Yamada *et al.*, 1988). Bill *et al.* (1991) have also reported evidence for a species difference in the 8-OH-DPAT-induced hypothermic response. A species difference has also been noted in the effects of 5-HT_{1A} receptor agonists on responding punished by electric shocks in animal models of anxiety. In rats and monkeys the increase in punished behaviour after 5-HT_{1A} agonist treatment is inconsistent (Barrett & Witkin, 1990; Gleeson & Barrett, 1990), whereas in pigeons there is an increase comparable to that produced by benzodiazepines (Ahlers *et al.*, 1992).

Recently, interest has revived in the behavioural pharmacology of 5-HT in the guinea-pig, largely due to an apparent difference in the presynaptic receptor mediating 5-HT release (5-HT_{1B} in the rat vs 5-HT_{1D} in the guinea-pig and man; Hoyer & Middlemiss, 1989). However, differences in the effects of 8-OH-DPAT have also been reported. In contrast to its hypothermia-inducing effects in the rat, the drug increased body temperature in the guinea-pig, and differences were noted in the effect of the drug on cortical acetylcholine release and the electrocortigram (Siniscalchi *et al.*, 1990). Ryan (personal communication) has found that 8-OH-DPAT induces wet dog shakes in guinea-pigs but not in rats. As far as locomotor activity is concerned, a brief report by Skingle & Bradbury (1989) demonstrated that 8-OH-DPAT increased locomotor activity in the guinea-pig, in a dose-dependent manner from 0.1 to 1.0 mg kg^{-1} s.c., just such a treatment that suppresses activity in the rat. The partial agonist, gepirone, had a similar but weaker effect, and also partially blocked the effect of 8-OH-DPAT. These authors concluded that the overt behavioural effect of 8-OH-DPAT in the guinea-pig, including indices of the 5-HT syndome, were 'quite distinct from the syndrome reported in the rat.'

The present study was designed to provide a direct comparison between the effects of 5-HT_{1A} agonist on locomotor activity in the guinea-pig and rat, by using the same apparatus and experimental design employed by Evenden & Ängeby-Möller (1990). To explore the relationship between agonist efficacy and response, the effects of four 5-HT_{1A} receptor agonists were examined, 8-OH-DPAT, flesinoxan, ipsapirone and buspirone. Of these, 8-OH-DPAT and flexinoxan have highest efficacy (although see Millan *et al.*, 1991), whereas buspirone and ipsapirone are clearly partial agonists (Schoeffer & Hoyer, 1988; Boddeke *et al.*, 1992). These drugs were compared with the non-selective 5-HT

[1] Author for correspondence.

receptor agonist, 5-methoxy-*N*,*N*-dimethyl-tryptamine (5-MeO DMT), which is also a full agonist at the 5-HT_{1A} receptor (Dumuis *et al.*, 1988). The 5-HT_{1A} receptor agonists also vary in their selectivity vis-à-vis other neurotransmitter receptors. 8-OH-DPAT is relatively selective for the 5-HT_{1A} receptor, as is flesinoxan (Van Wijngaarden *et al.*, 1990; Schipper *et al.*, 1991). Buspirone has a well-documented affinity for the dopamine D_2 receptor, where it acts as an antagonist, and shares with ipsapirone the active metabolite 1-(2-pyrimidinyl)-piperazine which has α_2-adrenoceptor antagonist activity (Caccia *et al.*, 1986). The structurally unrelated 8-OH-DPAT and flesinoxan cannot generate this metabolite. Raclopride, a selective D_2 antagonist (Köhler *et al.*, 1985), was included both as a control for the D_2 antagonist activity of buspirone and as an active comparison.

To verify that the effect of 8-OH-DPAT is mediated by 5-HT_{1A} receptors, the 5-HT_{1A} receptor antagonists, (−)-alprenolol and (S)-UH-301 were used in combination with 8-OH-DPAT. Of the two, (S)-UH-301 is more selective (Björk *et al.*, 1991), whereas (−)-alprenolol has affinity for the 5-HT_{1B} site (Middlemiss *et al.*, 1985) as well as acting as a β-adrenoceptor antagonist. Comparisons were made with combinations of 8-OH-DPAT with ipsapirone, raclopride or the 5-HT reuptake inhibitor, zimelidine.

Methods

Animals

Male Dunkin Hartley guinea-pigs were used in the agonist experiments these were aged 3–6 months at the time of use, and weighed 500–1000 g. In the antagonist experiments these were 2–3 months old and weighed 350–500 g. The subjects were housed in groups of 3 or 4, under a 12:12 h cycle (lights on at 06 h 00 min), with free access to food and water. All experiments took place in the light phase of the cycle.

Apparatus

The apparatus consisted of four open field arenas, 70 × 70 cm, equipped with two rows of infra-red photo beams, each consisting of eight cells on the X- and eight on the Y-axis. These were situated 4.0 and 12.5 cm above the floor. The individual photocells were spaced 9.0 cm apart, with a gap of 2.5 cm between the end beams and the side walls of the test apparatus. The apparatus itself was constructed with side-walls and floor of clear plastic, and each was individually housed within an outer chamber, 100 cm square. These chambers were opaque, but open at the top, so that the subjects could hear, but not see, each other. During the experiment the apparatus was illuminated by the normal fluorescent room lighting. A locomotor count was defined as a movement which broke two different beams successively. The data were recorded by an IBM PC-compatible computer using software provided by Kungsbacka Mät- och Reglerteknik, Fjärås, Sweden. A more complete description of the characteristics of the apparatus may be found in Ericson *et al.* (1990).

Procedure

Guinea-pigs were generally tested in groups of three or four. In the agonist studies, each subject was weighed and then injected with one of the test drugs or vehicle according to a pseudo latin-square design. Immediately after injection, it was placed in one of the arenas: one animal to each arena. When all subjects had been treated, the session was started. Each session then continued for 4 h during which time the subjects were not disturbed. At the end of each session, the apparatus was cleaned prior to testing the next group. The antagonist experiment proceeded in a similar manner with two differences. The subjects were initially injected with one of the antagonist treatments or saline 30 min before receiving a second injection of either 1.0 mg kg^{-1} 8-OH-DPAT or saline. During the interval between injections the subjects remained in their home cage. After the second treatment they were placed in the locomotor apparatus for a period, in this case, of 2 h. Eight guinea-pigs received such treatment except for 3.0 mg kg^{-1} (S)-UH-301 + 8-OH-DPAT ($n = 9$) and zimelidine + 8-OH-DPAT ($n = 7$).

It may be noted that the experiments involving 8-OH-DPAT, buspirone and 5-MeODMT were carried out in late 1989, the experiments involving ipsapirone, flesinoxan and raclopride in mid 1992, and the antagonist experiment in late 1993, that is, over a period of four years. Each agonist was compared to its own vehicle control group. Since the antagonists were given in only single doses (two in the case of (S)-UH-301), these were all compared to a single set of vehicle- and 8-OH-DPAT-treated rats which were tested at the same time interspersed in the pseudo-latin square design.

Drugs

The drugs used were 8-hydroxy-2-(di-n-propylamino)tetralin hydrochloride (Research Biochemicals Inc.), flesinoxan hydrochloride (Duphar), buspirone hydrochloride (Sigma Chemical Co.), ipsapirone (Troponwerke), 5-methoxy-*N*,*N*-dimethyl tryptamine (Sigma Chemical Co.), raclopride tartrate (Astra Arcus), zimelidine (Astra Arcus), (−)-alprenolol hydrogentartrate monohydrate (Astra Hässle) and (S)-UH-301 hydrochloride (S-5-fluoro-8-hydroxy-2-(di-n-propylamino)tetralin hydrochloride, Dept of Organic Pharmaceutical Chemistry, University of Uppsala). All drugs were injected s.c. in the flank. Ipsapirone was injected in a volume of 2.0 ml kg^{-1}, the other drugs in a volume of 1.0 ml kg^{-1}. All drugs were dissolved in 0.9% saline, which served as a control.

Measurements and analysis

A locomotor count was recorded when the subject consecutively broke two different beams in the lower series. Locomotor counts were cumulated into 5 min bins. After square root transformation to normalize the distribution, data from these bins were subjected to two-factor analysis of variance Treatment Group by Ttime Bin (BMDP model 2V). Dunnett's *t* test was used *post hoc* to compare treatment groups with the saline control in each bin. A 5% level of significance was used for the analysis of variance, and a 2% level of significance for the Dunnett's test.

Results

Agonist experiments

The effects of the agonists on the locomotor activity of guinea-pigs may be seen in Figures 1 and 2. 5-MeO DMT increased locomotor activity in the first hour after treatment, but not thereafter ($F_{int}(141,1128) = 3.06$, $P < 0.0001$). Statistically significant increases in activity were obtained with 1.0 mg kg^{-1} in the first 10 min, with 3.0 mg kg^{-1} up to 35 min and with 10.0 mg kg^{-1} up to 55 min (Figure 1a). 8-OH-DPAT had a similar but longer lasting effect ($F_{int}(235,1974) = 4.74$, $P < 0.0001$). No significant increase in locomotor activity was seen with 0.01 and 0.1 mg kg^{-1}. A statistically significant increase in activity was seen with 1.0 mg kg^{-1} up to 70 min post injection, with 3.0 mg kg^{-1} up to 90 min post-injection and with 10.0 mg kg^{-1} up to 145 min post injection (Figure 1b). Flesinoxan also increased locomotor activity ($F_{int}(188,1645) = 3.07$, $P < 0.0001$). The minimum effective dose was 3.0 mg kg^{-1} which had significant effects up to 30 min post-injection. The dose of 10.0 mg kg^{-1} had effects up to 90 min post-injection (Figure 1c). In contrast, buspirone had only a weak effect

($F_{int}(141,1316) = 1.27$, $P < 0.05$). The lowest dose tested, a higher dose by the standards of rat studies, was 10.0 mg kg^{-1} which significantly increased locomotor activity in the first 5 min of testing. The two higher doses, 30.0 and 100.0 mg kg^{-1} significantly increased locomotor activity for a little longer, up to 20 min post-injection (Figure 2a). The weak effects of buspirone were complemented by the lack of effect of ipsapirone ($F_{int}(141,1316) = 0.86$, $P > 0.80$, Figure 2b). The dopamine D_2 receptor antagonist, raclopride, was also without effect ($F_{int}(188,1645) = 1.1$, $P > 0.10$, Figure 2c).

Antagonist experiments

The effects of the various drug treatments on 8-OH-DPAT-induced hyperactivity in the guinea-pig may be seen in Figure 3. Note that the curves for the saline- and 8-OH-DPAT-

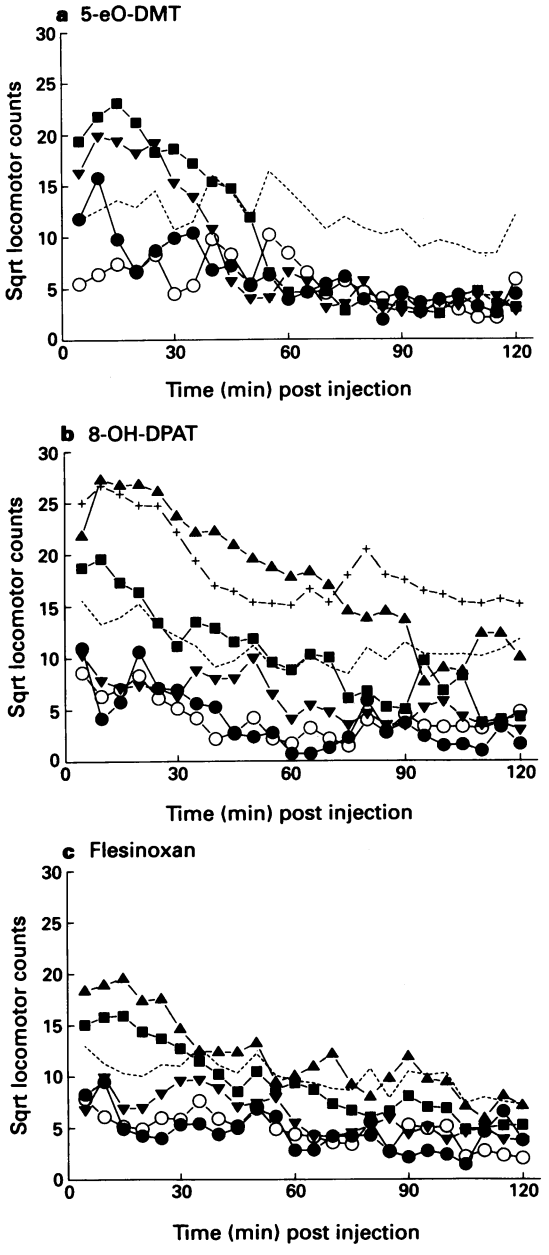

Figure 1 The effects of (a) 5-methoxy-*N*,*N*-dimethyltryptamine (5-MeO-DMT), (b), 8-hydroxy-2-(di-n-propylamino)tetralin (8-OH-DPAT) and (c), flesinoxan on horizontal activity in the guinea-pig. In all three panels the horizontal axis shows the time since the start of testing (substance administered at time 0), and the vertical axis the number of locomotor counts after square root (sq rt) transformation. Note that only the first 2 h of the 4 h test are shown in the figure. The doses used were (a) for 5-MeO-DMT: saline (○), 1.0 mg kg^{-1} (●), 3.0 mg kg^{-1} (◆) and 10.0 mg kg^{-1} (■); (b) for 8-OH-DPAT: saline (○), 0.01 mg kg^{-1} (●). 0.1 mg kg^{-1} (▼), 1.0 mg kg^{-1} (■), 3.0 mg kg^{-1} (▲) and 10.0 mg kg^{-1} (+); and (c) for flesinoxan: saline (○), 0.3 mg kg^{-1} (●), 1.0 mg kg^{-1} (▼), 3.0 mg kg^{-1} (■) and 10.0 mg kg^{-1} (▲). The dashed line shows the level of activity required to achieve a significant difference from the vehicle-treated group using Dunnett's t test ($P < 0.02$). Symbols appearing above this line illustrate a significant increase in activity compared to saline-treated guinea-pigs. All three drugs significantly increased locomotor activity.

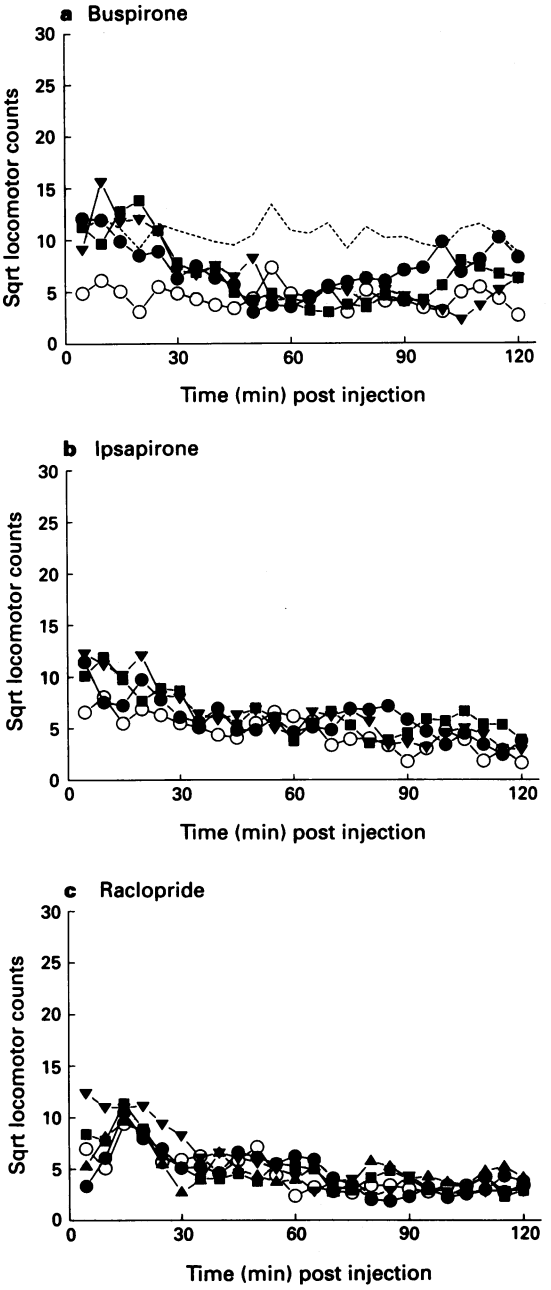

Figure 2 The effects of (a) buspirone, (b) ipsapirone and (c) raclopride on horizontal activity in the guinea-pig. In all three panels the horizontal axis shows the time since the start of testing (substance administered at time 0), and the vertical axis the number of locomotor counts after square root (sq rt) transformation. The doses used were (a) for buspirone; saline (○), 10.0 mg kg^{-1} (●), 30.0 mg kg^{-1} (▼) and 100.0 mg kg^{-1} (■); (b) for ipsapirone: saline (○), 3.0 mg kg^{-1} (●), 10.0 mg kg^{-1} (▼) and 30.0 mg kg^{-1} (■); and (c) for raclopride: saline (○), 0.1 mg kg^{-1} (●), 0.3 mg kg^{-1} (▼), 1.0 mg kg^{-1} (■) and 3.0 mg kg^{-1} (▲). The dashed line shows the level of activity required to achieve a significant difference from the vehicle-treated group using Dunnett's t test ($P < 0.02$). Symbols appearing above this line illustrate a significant increase in activity compared to saline-treated guinea-pigs. Buspirone slightly increased locomotor activity soon after injection. The other two drugs had no significant effect.

treated groups in the two panels represent the same data. Dunnett's t test was performed after a significant statistical interaction ($F_{int}(161,1288) = 4.95$, $P < 0.0001$), which confirms that there were differences amongst the treatment groups. Zimelidine (10.0 mg kg^{-1}) had little effect on 8-OH-DPAT-induced hyperactivity. A significant increase in activity was noted 50–55 min after 8-OH-DPAT treatment which may represent a slight prolonging of 8-OH-DPATs effect. Ipsapirone (30.0 mg kg^{-1}) and raclopride (3.0 mg kg^{-1}) had very similar effects to each other, in that both reduced the peak activity of the guinea-pigs. The effect of ipsapirone was statistically significant from 5–10 min and that of raclopride from 5–15 min after 8-OH-DPAT treatment. These statistically significant effects formed part of a clear trend (Figure 3a). In addition, there was also a slight increase in the activity of the raclopride + 8-OH-DPAT treated guinea-pigs compared to the guinea-pigs treated with 8-OH-DPAT alone from 55–60 min again suggesting a slight prolongation of the effect of 8-OH-DPAT.

Much clearer effects were obtained with the two 5-HT$_{1A}$ receptor antagonists. However, these were completely opposite in nature. (−)-Alprenolol clearly potentiated the effects of 8-OH-DPAT, in that the animals with the combined treatment were significantly more active than those treated with 8-OH-DPAT alone from 50–85 min (except 60–65). This difference can be seen in Figure 3b. (−)-Alprenolol had no effect on locomotor activity when given alone at a dose of 15.0 mg kg^{-1} ($F_{int}(47,470) = 0.86$, NS: data not shown). In contrast, (S)-UH-301 blocked the effects of 8-OH-DPAT. A dose of 3.0 mg kg^{-1} partially blocked the increase in activity, with significant effects from 0–35 min, whereas a dose of 10.0 mg kg^{-1} totally blocked the effects of 8-OH-DPAT from 0–55 min after which 8-OH-DPAT itself did not significantly increase activity compared to the saline-treated guinea-pigs (see Figure 3b).

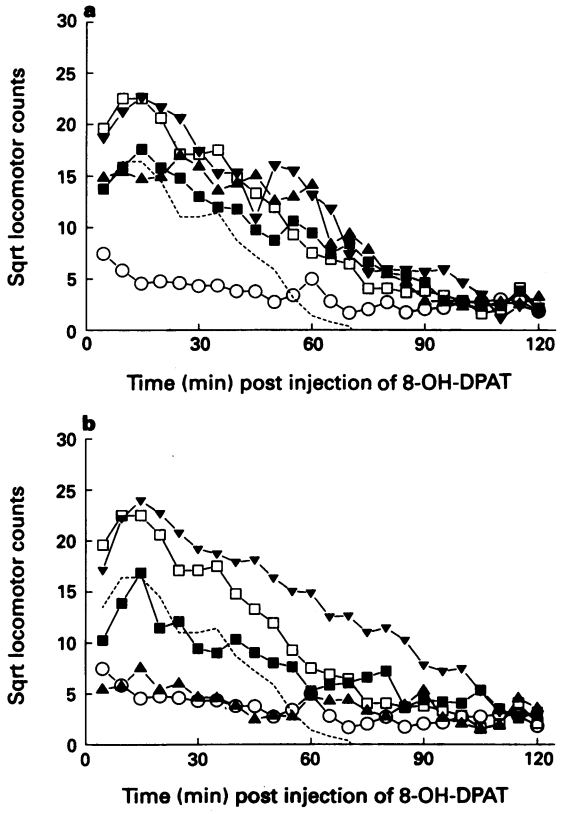

Figure 3 The effects of (a) zimelidine, ipsapirone, and raclopride, and (b) (−)-alprenolol and (S)-UH-301 on the 8-hydroxy-2-(di-n-propylamino)tetralin (8-OH-DPAT)-induced increase in horizontal activity in the guinea-pig. In all three panels the horizontal axis shows the time since the start of testing (8-OH-DPAT administered at time 0), and the vertical axis the number of locomotor counts after square root (sq rt) transformation. The treatments were as follows: (a) saline + saline (○); saline + 1.0 mg kg^{-1} 8-OH-DPAT (□); 10.0 mg kg^{-1} zimelidine + 1.0 mg kg^{-1} 8-OH-DPAT (▼); 30.0 mg kg^{-1} ipsapirone + 1.0 mg kg^{-1} 8-OH-DPAT (■) and 3.0 mg kg^{-1} raclopride + 1.0 mg kg^{-1} 8-OH-DPAT (▲); and (b) saline + saline (○); saline + 1.0 mg kg^{-1} 8-OH-DPAT (□); 15.0 mg kg^{-1} (−)-alprenolol + 1.0 mg kg^{-1} 8-OH-DPAT (▼); 3.0 mg kg^{-1} (S)-UH-301 + 1.0 mg kg^{-1} 8-OH-DPAT (■) and 10.0 mg kg^{-1} (S)-UH-301 + 1.0 mg kg^{-1} 8-OH-DPAT (▼). The dashed line shows the level of activity required to achieve a significant reduction in activity compared to the saline + 8-OH-DPAT-treated group using Dunnett's t test ($P < 0.02$). Symbols appearing below this line illustrate a significantly lower activity than this control group.

Discussion

In contrast to the effects in mice and rats, 8-OH-DPAT increased locomotor activity in a dose-dependent and straightforward manner. However, the doses required to obtain the greatest effect were around 10 times higher than the doses previously used in this procedure in rodents (Evenden & Ängeby-Möller, 1990). Flesinoxan had a similar effect. This drug also reduces locomotor activity in the rat when monitored in similar apparatus to that used here (Hillegaart *et al.*, 1989). Likewise, relatively high doses of flesinoxan were used in the present study to obtain a significant effect. The partial agonists at the 5-HT$_{1A}$ receptor, buspirone and ipsapirone, had, respectively, little and no effect on the locomotor activity of the guinea-pig. These drugs have also been reported to reduce locomotor activity in the rat (Mittman & Geyer, 1989). The weak effect of buspirone is unlikely to reflect the D_2 antagonist properties of the drug since ipsapirone does not have a significant affinity for the D_2 receptor. Furthermore, the D_2 antagonist, raclopride, did not itself affect guinea-pig locomotor activity, and only weakly blocked 8-OH-DPAT-induced hyperactivity. Although both buspirone and ipsapirone are rapidly metabolized giving a metabolite, 1-PP, which has antagonist activity at the α_2-adrenoceptor, this is also unlikely to be the reason for their lack of effect, since Skingle & Bradbury (1989) have reported that gepirone, which generates same active metabolite, does increase locomotor activity in the guinea-pig, but to a lesser extent than 8-OH-DPAT.

The 8-OH-DPAT-induced hyperactivity was clearly blocked by the selective 5-HT$_{1A}$ receptor antagonist, (S)-UH-301, but curiously, not by (−)-alprenolol, which has otherwise been reported to block 8-OH-DPAT-induced effects in other tests in rats (Middlemiss *et al.*, 1985; Rényi, 1991). The drug did not itself increase locomotor activity, and the dose used here has been found to block 8-OH-DPAT-induced wet dog shakes in the guinea-pig (Ryan & Pakh, unpublished). Kalkman & Soar (1990) found that β-adrenoceptor antagonists enhanced 8-OH-DPAT hyperlocomotion in rats, and it appears to be this aspect of the pharmacological profile of (−)-alprenolol which predominates in the present experiment. Ipsapirone, which is a partial agonist at the 5-HT$_{1A}$ receptor, did block the effects of 8-OH-DPAT to a certain extent. Previously, Skingle & Bradley (1989) noted that gepirone also partially blocked 8-OH-DPAT-induced hyperactivity in the guinea-pig, and Kalkman & Soar, (1990) found that buspirone blocked 8-OH-DPAT-induced hyperlocomotion in the rat. The effect of 8-OH-DPAT was not prevented by pretreatment with the 5-HT reuptake inhibitor, zimelidine, which suggests that the hyperactivity in the guinea-pig does not depend upon reduced extracellular levels of 5-HT.

Together, these results suggest that to increase locomotor activity in the guinea-pig, a 5-HT$_{1A}$ agonist must have high efficacy at the 5-HT$_{1A}$ receptor, since only drugs that are relatively full agonists had this effect (i.e. 8-OH-DPAT, flesinoxan and 5-MeO DMT). The prototypical selective 5-HT$_{1A}$ receptor antagonist, 8-OH-DPAT has been tested in

a range of species. As noted in the Introduction, in addition to the increase in locomotor activity reported here and by Skingle & Bradley (1989) in the guinea pig, the drug has been noted primarily to reduce locomotor activity in the rat and mouse. However, rats and mice do not necessarily appear to be sedated by the drug, since Tricklebank *et al.* (1984) in an observational study, found an increase in 'ambulation' in the rat after 8-OH-DPAT treatment. The drug appeared to have no effect on exploratory activity in the hamster (Buhot *et al.*, 1989). In the domestic pig, 8-OH-DPAT induced ataxia and general sedation (Löscher *et al.*, 1990), with sedation also being reported in the cynamolgus monkey (Mizuta *et al.*, 1990). However, these latter two were observational studies with no quantification of locomotor activity. Flesinoxan has also been reported to induce a feeling of relaxation and drowsiness in man (Annsseau *et al.*, 1992). From this list, the guinea-pig stands out as being the only species so far tested in which locomotor stimulation has clearly been observed.

The effects of 8-OH-DPAT may depend in part upon differences in the behaviour of the species. In the present study there were differences in the way in which guinea-pigs and rats behave in this apparatus. Guinea-pigs are very much less active when treated with saline than are rats. In the study of Evenden & Ängeby-Möller (1990), unhabituated rats made as many as 800 counts in the first 5 min of testing, falling to around 100–200 counts per 5 min up to about 80 min. In the present study, unhabituated guinea-pigs made only around 100 counts in the first 5 min and less than 50 counts per 5 min after around 30 min. In this respect the guinea-pigs more resembled habituated rats, which had been familiarized with the apparatus for 2 h before treatment. These rats were less active than unhabituated rats, and showed a hyperactivity in response to 1.0 mg kg^{-1} 8-OH-DPAT (Evenden & Ängeby-Möller, 1990). This suggests that obtaining an increase in locomotor-activity after 8-OH-DPAT treatment may depend in part on having a low baseline level of activity i.e. the effect may be baseline-dependent. This is confirmed by the findings of Björk *et al.* (1992) who tested rats either unhabituated or habituated in cages similar to the home cages. In this study (R)-8-OH-DPAT increased locomotor activity, and this increase was antagonized by (S)-UH-301.

These differences in locomotor activity form only part of the overall profile of differences between rats and guinea-pigs (see Introduction). There are also neuroanatomical differences between the two species (Sijbesma *et al.*, 1991). Furthermore, sub-chronic treatment of rats with 8-OH-DPAT induces a tolerance when hypothermia or induction of the 5-HT syndrome are monitored (Larsson *et al.*, 1990), but a progessively increasing hyperactivity has been seen in a two-way avoidance test (Evenden, 1992). Thus, in some respects, i.e. lack of obvious 5-HT syndrome, lack of hypothermic response and hyperactivity, the guinea-pig more closely resembles the '8-OH-DPAT-tolerant' than the '8-OH-DPAT-naive' rat.

In conclusion, these results lend support to suggestions that there are important species differences in the response to treatment with 5-HT$_{1A}$ receptor agonists. They indicate that it is necessary to take into account differences in the baseline behaviour between species but leave open the question of the biochemical mechanisms underlying this behaviour, and whether these may also be species specific.

The author acknowledges the technical assistance of K. Ängeby-Möller and the comments of C. Ryan and thanks Bayer Troponwerk, Duphar & Prof U. Hacksell for ipsapirone, flesinoxan and (S)-UH-301, respectively. These data have been presented in preliminary form to the European Behavioural Pharmacology Society, Cambridge, 1992 and the 23rd Annual Meeting of the Society for Neuroscience, 1993.

References

AHLERS, S.T., WEISSMAN, B.A. & BARRETT, L.E. (1992). Antagonism studies with BMY-7378 and NAN-190: effects on 8-hydroxy-2-(di-n-propylamino)tetralin-induced increases in punished responding of pigeons. *J. Pharmacol. Exp. Ther.*, **260**, 474–481.

ANNSSEAU, M., LEMBRECHTS, M., PITCHOT, W., GONZALEZ MORENO, A., LEGROS, J.J. & BRADFORD, L.D. (1992). Neuroendocrine responses to intravenous flesinoxan as an index of serotonergic neurotransmission. *Clin. Neuropharmacol.*, **15** (suppl 1B), 114.

BARRETT, J.E. & WITKIN, J.M. (1990). Buspirone in animal models of anxiety. In *Buspirone: Mechanisms and Clinical Aspects*. ed. Tunnicliff, G., Eison, A.S. & Taylor, D.P. pp. 37–79, New York: Academic Press.

BILL, D.J., KNIGHT, M., FORSTER, E.A. & FLETCHER, A. (1991). Direct evidence for an important species difference in the mechanism of 8-OH-DPAT-induced hypothermia. *Br. J. Pharmacol.*, **103**, 1857–1864.

BJÖRK, L., CORNFIELD, L.J., NELSON, D.L., HILLVER, S.-E., ANDÉN, N.-E., LEWANDER, T. & HACKSELL, U. (1991). Pharmacology of the novel 5-hydroxytryptamine IA receptor antagonist (S)-5-fluoro-8-hydroxy-2-(dipropylamino)tetralin: Inhibition of (R)-8-hydroxy-2-(di-n-propylamino)tetralin-induced effects. *J. Pharmacol. Exp. Ther.*, **258**, 58–65.

BJÖRK, L., FREDRIKSSON, A., HACKSELL, U. & LEWANDER, T. (1992). Effects of (R)-8-OH-DPAT and the enantiomers of UH-301 on motor activities in the rat: antagonism of (R)-8-OH-DPAT-induced effects. *Eur. J. Neuropsychopharmacol.*, **2**, 141–147.

BODDEKE, H.W.G.M., FARGIN, A., RAYMOND, J.R., SCHOEFFTER, P. & HOYER, D. (1992). Agonist/antagonist interactions with cloned human 5-HT$_{1A}$ receptors: variations in intrinsic activity studied in transfected HeLa cells. *Naunyn Schmied. Arch. Pharmacol.*, **345**, 257–263.

BUHOT, M.-C., RAGE, P. & SEGU, L. (1989). Changes in exploratory behaviour of hamsters following treatment with 8-hydroxy-2-(di-n-propylamino)tetralin. *Behav. Brain Res.*, **35**, 163–179.

CACCIA, S., CONTI, I., VIGANO, G. & GARATTINI, S. (1986). 1-(2-Pyrimidinyl)-piperazine as active metabolite of buspirone in man and rat. *Pharmacology*, **33**, 46–51.

DUMUIS, A., SEBBEN, M. & BOCKEAER, J. (1988). Pharmacology of 5-hydroxy-tryptamine-1A receptors which inhibit cAMP production in hippocampal and cortical neurones in primary culture. *Mol. Pharmacol.*, **33**, 176–186.

ERICSON, E., SAMUELSSON, J. & AHLENIUS, S. (1991). Photocell measurements of rat motor activity. *J. Pharmacol. Methods*, **34**, 111–122.

EVENDEN, J.L. (1992). Effects of 8-hydroxy-2-(di-n-propylamino)tetralin (8-OH-DPAT) after repeated administration on a conditioned avoidance response (CAR) in the rat. *Psychopharmacology*, **109**, 134–144.

EVENDEN, J.L. & ÄNGEBY-MÖLLER, K. (1990). Effects of 8-hydroxy-2-(di-n-propylamino)tetralin (8-OH-DPAT) on locomotor activity and rearing of mice and rats. *Psychopharmacology*, **102**, 485–491.

GLEESON, S. & BARRETT, J.E. (1990). 5-HT1A agonist effects on punished responding of squirrel monkeys. *Pharmacol. Biochem. Behav.*, **37**, 335–337.

GOODWIN, G.M. & GREEN, A.R. (1985). A behavioural and biochemical study in mice and rats of putative selective agonists and antagonists for 5-HT$_1$ and 5-HT$_2$ receptors. *Br. J. Pharmacol.*, **84**, 743–753.

HILLEGAART, V., WADENBURG, M.L. & AHELENIUS, S. (1989). Effects of 8-OH-DPAT on motor activity in the rat. *Pharmacol. Biochem. Behav.*, **32**, 797–800.

HOYER, D. & MIDDELMISS, D.N. (1989). Species difference in the pharmacology of terminal 5-HT autoreceptors in mammalian brain. *Trends Pharmacol. Sci.*, **10**, 130–132.

KALKMAN, H.O. & SOAR, J. (1990). Determination of the 5-HT receptor subtype involved in 8-OH-DPAT-induced hyperlocomotion: potential difficulties arising from inadequate pharmacological tools. *Eur. J. Pharmacol.*, **191**, 383–390.

KÖHLER, C., HALL, H., ÖGREN, S.O. & GAWELL, L. (1985). Specific in vitro and in vivo binding of ^{3}H-raclopride. A potent substituted benzamide drug with high affinity for dopamine D-2 receptors in the rat brain. *Biochem. Pharmacol.*, **34**, 2251–2259.

LARSSON, L.-G., RÉNYL, L., ROSS, S.B., SVENSSON, B. & ÄNGEBY-MÖLLER, K. (1990). Different effects on the responses of functional pre- and postsynaptic 5-HT_{1A} receptors by repeated treatment of rats with the 5-HT_{1A} receptor agonist 8-OH-DPAT. *Neuropharmacology*, **29**, 85–91.

LÖSCHER, W., WHITE, U., FREDOW, G., TRABER, J. & GLASER, T. (1990). The behavioural responses to 8-OH-DPAT, ipsapirone and the novel 5-HT_{1A} receptor agonist Bay Vq 7813 in the pig. *Naunyn-Schmied. Arch. Pharmacol.*, **342**, 271–277.

MIDDLEMISS, D.N., NEILL, J. & TRICKLEBANK, M.D. (1985). Subtypes of the 5-HT receptor involved in hypothermia and forepaw treading induced by 8-OH-DPAT. *Br. J. Pharmacol.*, **85**, 251P.

MILLAN, M.J., BERVOETS, K. & COLPEART, F.C. (1991). 5-Hydroxytryptamine (5-$HT)_{1A}$ receptors and the tail flick response. 1. 8-hydroxy-2-(di-n-propylamino)tetralin HBr-induced spontaneous tail-flicks in the rat as an in vivo model of 5-HT_{1A} receptor-mediated activity. *J. Pharmacol. Exp. Ther.*, **256**, 973–982.

MITTMAN, S.M. & GEYER, M.A. (1989). Effects of 5-HT-1A agonists on locomotor and investigatory behaviours in rats differ from those of hallucinogens. *Psychopharmacology*, **98**, 321–329.

MIZUTA, E., YAMAGUCHI, M. & KUNO, S. (1990). Behavioural effects of 8-hydroxy-2-(di-n-propylamino)tetralin (8-OH-DPAT) in monkeys. *Eur. J. Pharmacol.*, **178**, 125–127.

RÉNYL, L. (1991). The involvement of the 5-HT_1 and 5-HT_2 receptors and of catecholaminergic systems in different components of the 5-HT syndrome in the rat. *Pol. J. Pharmacol. Pharm.*, **43**, 405–419.

SCHIPPER, J., TULP, M.TH.M., BERKELMANS, B., MOS, J., VAN DER HEIJDEN, J.A.M. & OLIVIER, B. (1991). Preclinical pharmacology of flesinoxan: a potential anxiolytic and antidepressant drug. *Human Psychopharmacology*, **6**, S53–S61.

SCHOEFFTER, P. & HOYER, D. (1988). Centrally acting hypotensive agents with affinity for 5-HT1A binding sites inhibit forskolin-stimulated adenylate cyclase activity in calf hippocampus. *Br. J. Pharmacol.*, **95**, 975–985.

SIJBESMA, H., SCIPPER, J., CORNELISSEN, J.C.H.M. & DE KLOET, E.R. (1991). Species differences in the distribution of central 5-HT_1 binding sites: a comparative autoradiographic study between rat and guinea pig. *Brain Res.*, **555**, 295–304.

SINISCALCHI, A., BEANI, L. & BIANCHI, C. (1990). Different effects of 8-OH-DPAT, a 5-HT_{1A} receptor agonist on acetylcholine release, electrocortigram and body temperature in guinea pigs and rats. *Eur. J. Pharmacol.*, **175**, 219–223.

SKINGLE, M. & BRADBURY, A.J. (1989). Behavioural and biochemical effects of 8-OH-DPAT in the guinea pig. Poster presentation at *Serotonin from Cell Biology to Pharmacology and Therapeutics*, Florence, March 29–April 1, 1989.

TRICKLEBANK, M.D., FORLER, C. & FOZARD, J.R. (1984). The involvement of subtypes of the 5-HT_{1A} receptor and of catecholaminergic systems in the behavioural response to 8-hydroxy-2-(di-n-propylamino)tetralin in the rat. *Eur. J. Pharmacol.*, **106**, 271–282.

WILKINSON, L.O. & DOURISH, C.T. (1991). Serotonin and animal behaviour. In *Serotonin Receptor Subtypes: Basic and Clinical Aspects* ed. Peroutka, S.J. pp. 147–210. New York: Wiley-Liss Inc.

VAN WIJNGAARDEN, I., TULP, M.TH.M. & SOUDIJN, W. (1990). The concept of selectivity in 5-HT receptor research. *Eur. J. Pharmacol.*, **188**, 301–312.

YAMADA, J., SUGIMOTO, Y. & HORISAKA, K. (1988). The behavioural effects of 8-hydroxy-2-(di-n-propylamino)tetralin (8-OH-DPAT) in mice. *Eur. J. Pharmacol.*, **154**, 299–304.

(Received November 4, 1993
Revised February 10, 1994
Accepted March 28, 1994)

Br. J. Pharmacol. (1994), **112**, 867–872

Effects of cyclic GMP and analogues on neurogenic transmission in the rat tail artery

Sylvin Ouedraogo, Martin Tschöpl, Jean-Claude Stoclet & [1]Bernard Bucher

Laboratoire de Pharmacologie Cellulaire et Moléculaire, C.N.R.S., URA 600, Université Louis Pasteur Strasbourg, B.P. 24, 67401 Illkirch, France

1 The effects of membrane permeable analogues of guanosine 3':5'-cyclic monophosphate (cyclic GMP), and of the NO donor, 3-morpholinosydnonimine-N-ethylcarbamide (SIN-1) were investigated on [^{3}H]-noradrenaline release and neurogenic vasoconstriction in electrical field stimulated rat tail arteries.

2 Two 8-substituted analogues of cyclic GMP (8-bromoguanosine 3':5'-cyclic monophosphate; 8-bromo-cyclic GMP and 8-(4-chlorophenylthio)-guanosine 3':5'-cyclic monophosphate; 8-pCPT-cyclic GMP) concentration-dependently enhanced stimulation-induced [^{3}H]-noradrenaline release. These prejunctional effects were antagonized by the cyclic AMP-dependent protein kinase (PKA) inhibitor N-[2-((3-(4-bromophenyl)-2-propenyl)-amino)-ethyl]-5 isoquinolinesulphonamide dihydrochloride (H-89; 100 nM) but not by the cyclic GMP-dependent protein kinase (PKG) inhibitors, Rp-8-bromoguanosine 3':5'-cyclic monophosphorothioate (Rp-8-bromo-cyclic GMPS; 10 μM) or Rp-8-(4-chlorophenylthio)-guanosine 3':5'-cyclic monophosphorothioate (Rp-8-pCPT-cyclic GMPS; 10 μM).

3 β-Phenyl-1,N^2-ethenoguanosine 3':5'-cyclic monophosphate (PET-cyclic GMP) had no effect on stimulation-induced [^{3}H]-noradrenaline release but concentration-dependently decreased the stimulation-induced vasoconstriction.

4 The two 8-substituted cyclic GMP derivatives, PET-cyclic GMP and SIN-1, both decreased stimulation-induced vasoconstriction. In addition, SIN-1 relaxed rat tail arteries precontracted with phenylephrine (1 μM). The SIN-1 concentration-relaxation curve was shifted in parallel manner to the right by Rp-8-bromo-cyclic GMPS (10 μM) and Rp-8-pCPT-cyclic GMPS (10 μM) with no change in the maximum effect, showing that the relaxation was mediated by a cyclic GMP/PKG-dependent mechanism.

5 It is concluded that PKA activation is involved in the noradrenaline release enhancing effect of the two 8-substituted cyclic GMP analogues, whereas a cyclic GMP/PKG-operated pathway accounts for the inhibitory effects of the cyclic GMP and its analogues on vascular smooth muscle contraction.

Keywords: Neurogenic vasoconstriction; noradrenaline release; cyclic GMP; SIN-1; cyclic nucleotide-dependent protein kinases; rat tail artery

Introduction

Relaxation of vascular smooth muscle by nitrovasodilators, atrial natriuretic factor and endothelium-derived relaxing factor is mediated at least in part by guanosine 3':5'-cyclic monophosphate (cyclic GMP) (Schultz *et al.*, 1977; Gruetter *et al.*, 1979; Winquist *et al.*, 1981; Lincoln & Corbin, 1983; Ignarro, 1990). However, until recently, the role of this cyclic nucleotide in smooth muscle physiology has not been clearly defined. There is evidence indicating that protein kinase G (PKG) is involved in the cyclic GMP-induced smooth muscle relaxation (Lincoln & Corbin, 1983; Beebe & Corbin, 1986; Francis *et al.*, 1988) and in the reduction of intracellular Ca^{2+} concentration upon elevation of intracellular cyclic GMP in aortic smooth muscle cells (Cornwell & Lincoln, 1989).

Concerning the regulation of neurotransmitter release, two main trandsuction mechanisms triggered by receptor activation operate in sympathetic nerve endings. The activation of the adenylyl cyclase/cyclic AMP system and of the phospholipase C-inositol 1,4,5-trisphosphate/diacylglycerol system both result in an enhancement of stimulation-induced noradrenaline release (Starke *et al.*, 1989; Majewski *et al.*, 1990). The involvement of the guanylyl cyclase/cyclic GMP system is less clear. Previous studies on the effects of cell permeable cyclic GMP analogues on field stimulated-evoked release of noradrenaline have shown either no effect, e.g. in guinea-pig ileum and vas deferens (Stjärne *et al.*, 1979; Axelsson *et al.*, 1980; Alberts *et al.*, 1985), a small facilitatory effect, e.g. in cat spleen, mouse atria (Cubeddu *et al.*, 1975; Johnston *et al.*, 1987), or an inhibitory effect, e.g. in rat pineal (Pelayo *et al.*, 1978). We have recently demonstrated the lack of prejunctional effects of activators of both soluble and membrane associated guanylate cyclase, despite a large effect of 8-bromo-guanosine 3':5'-cyclic monophosphate (8-bromo-cyclic GMP), in the rat tail artery (Bucher *et al.*, 1992).

Therefore, it was the aim of the present study to examine further the effects of both cyclic GMP analogues and endogenously formed cyclic GMP on neurogenic vasoconstriction and modulation of noradrenaline release from the nerve terminals innervating the rat tail artery. These effects were studied in the presence and absence of selective inhibitors of cylic GMP- and cyclic AMP-dependent protein kinases.

Methods

Electrically-evoked [^{3}H]-noradrenaline release and vasoconstriction

The experiments were carried out as described previously (Illes *et al.*, 1987; Bucher *et al.*, 1992). Briefly, male Wistar rats (12 weeks old) were killed by cervical dislocation and exsanguinated. A segment of about 2–2.5 cm of the proximal part of the ventral tail artery was dissected out and kept in oxygenated (95% O_2/5% CO_2) medium of the following composition (mM): NaCl 118, KCl 4.8, $CaCl_2$ 2.5, KH_2PO_4 0.9, $NaHCO_3$ 25, glucose 11, ascorbic acid 0.3 and disodium

[1] Author for correspondence.

EDTA 0.03. The arteries were cannulated at one end and preincubated for 1 h in 1.5 ml of medium of the same composition as above containing in addition 2.2 μM (−)-[^{3}H]-noradrenaline (specific activity 4.4 Ci mmol^{-1}). They were then suspended vertically and perfused by means of a roller pump with medium containing in addition cocaine (10 μM) in order to block the re-uptake of released [^{3}H]-noradrenaline.

Each artery was subjected to 6 stimulation periods (24 pulses at 0.4 Hz; 0.3 ms; 200 mA; intervals between stimulation periods 16 min) as in previous experiments (Bucher *et al.*, 1992). The compounds were infused into the perfusion stream for 8 min before either S_1 or S_3 and this was maintained until the end of the experiment when the arteries were solubilized in 1 ml Soluene 100 (Packard Instrument, Paris, France).

The fractional rate of tritium outflow and stimulation-evoked tritium overflow were expressed as a percentage of the tissue tritium content at the start of the respective collection period. The effects of drugs added after S_2 were evaluated by calculating the ratio S_4/S_2 of the tritium overflow or vasoconstriction evoked during the respective stimulation periods.

Relaxation of phenylephrine-preconstricted arteries

Rat tail arteries were dissected as above and experiments carried out as described previously (Bucher *et al.*, 1992). Arteries were cannulated at both ends and suspended vertically in an organ bath containing 4 ml of medium maintained at 37°C and of the same composition as above but without ascorbic acid, disodium EDTA and cocaine. After 1 h equilibration, the contractile capacity was tested by exposing the arterial segment to phenylephrine (3 μM). The vessel was then repeatedly exposed to 1 μM phenylephrine for 10 min followed by washing for 20 min. The presence of functional endothelium was verified (Bucher *et al.*, 1992). Once three comparable and stable phenylephrine-elicited contractions were obtained, cumulative concentrations of the NO donor 3-morpholinosydnonimine-N-ethylcarbamide (SIN-1, 0.01–30 μM) were applied to arteries precontracted with 1 μM phenylephrine. After an interval of 2 h during which the medium was changed every 10 min, a second concentration-response curve to SIN-1 alone, or in the presence of either Rp-8-bromo-cyclic GMPS 10 μM or Rp-8-pCPT-cyclic GMPS 10 μM, was constructed. Tissues were incubated with Rp-bromo-cyclic-GMPS or Rp-8-pCPT-cyclic GMPS 30 min prior to the second SIN-1 concentration-response curve and left throughout in the solution. All experiments were carried out in the dark, due to the light sensitivity of some of the compounds (SIN-1 and Rp-8-pCPT-cyclic GMPS). The effects of cumulatively added SIN-1 concentrations were expressed as % reduction of precontractions induced by phenylephrine, and these values were calculated in each individual preparation.

Statistical analysis

Results are given as mean ± s.e.mean. *n* is the number of experiments. Unless stated otherwise, comparisons were made by the Mann-Whitney test if Kruskall-Wallis analysis indicated a significant difference between multiple groups. A probability level of 0.05 or less was considered significant. For multiple comparisons with the same control group, the limit of significance was divided by the number of comparisons according to Bonferroni (Wallenstein *et al.*, 1980).

Drugs

The following compounds were used: 8-bromo-guanosine 3′:5′-cyclic monophosphate (sodium salt; 8-bromo-cyclic GMP), (−)-noradrenaline hydrochloride, (−)-phenylephrine hydrochloride (Sigma, L'Isle d'Abeau Chesnes, France); β-phenyl-1,N^2-ethenoguanosine-3′:5′-cyclic monophosphate, (sodium salt; PET-cyclic GMP), 8-(4-chlorophenylthio)-guanosine 3′:5′-cyclic monophosphate (sodium salt; 8-pCPT-cyclic GMP), 8-bromo-guanosine 3′:5′-cyclic monophosphorothioate, Rp-isomer (sodium salt; Rp-8-Br-cyclic GMPS), 8-(4-chlorophenylthio)-guanosine 3′:5′-cyclic monophosphorothioate, Rp-isomer (sodium salt; Rp-8-pCPT-cyclic GMPS) (Biolog, Bremen, Germany); N-[2-((3-(4-bromophenyl)-2-propenyl)-amino)-ethyl]-5-isoquinolinesulphonamide dihydrochloride (H-89) (Calbiochem, Meudon, France); SIN-1 (3-morpholinosydnonimine-N-ethylcarbamide; kindly donated by Hoechst, France). Stock solutions of all other substances were prepared with Milli-Q water (Millipore) and diluted as required with the exception of SIN-1 which was initially dissolved in 5% glucose. (−)-[Ring-2,5,6-^{3}H]-noradrenaline, specific activity 43.7–56.9 Ci mmol^{-1} (New England Nuclear, Dreieich, Germany), was diluted with unlabelled (−)-noradrenaline hydrochloride in order to obtain a specific activity of 4.4 Ci mmol^{-1}.

Results

Electrically-evoked [^{3}H]-noradrenaline release and vasoconstriction

In control as well as in treated arteries, the tritium overflow and peak of vasoconstriction evoked by S_2 amounted respectively to 0.176 ± 0.006% of tissue tritium and 86.7 ± 4.6

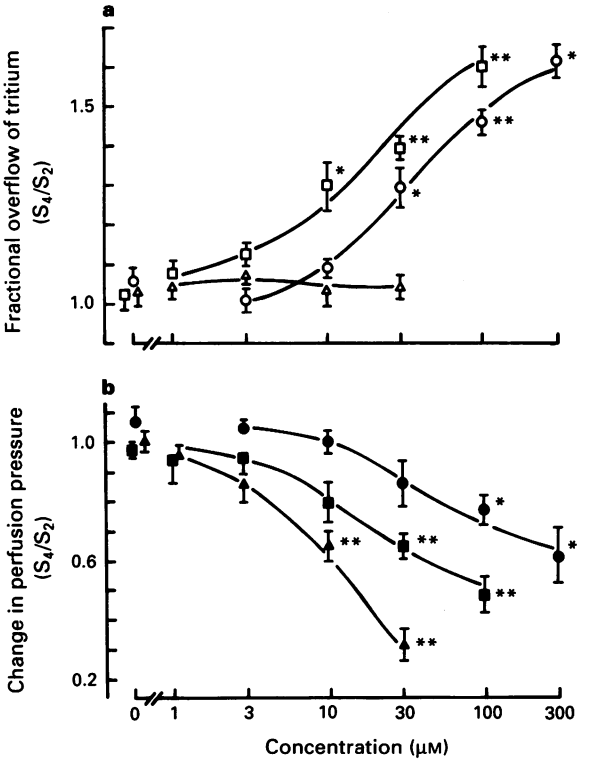

Figure 1 Effect of 8-Br-cGMP (circles), 8-pCPT-cGMP (squares) and PET-cGMP (triangles) on electrically-evoked overflow of tritium (open symbols, a) and change in perfusion pressure (solid symbols, b) in rat tail arteries with functional endothelium preincubated with [^{3}H]-noradrenaline. Four periods (S_1–S_4) of field stimulation were delivered at intervals of 16 min (24 pulses at 0.4 Hz, 200 mA, 0.3 ms duration). Each concentration of 8-Br-cGMP, 8-pCPT-cGMP and PET-cGMP or the solvent (control group) was added 8 min before S_3 and maintained in the medium for the duration of the experiment. The effect of the drug is presented as the ratio of tritium overflow or change in perfusion pressure evoked by S_4 over that evoked by S_2. Each point represents the mean ± s.e.mean from 5–6 arteries. Significant difference from control values: $^*P<0.05$; $^{**}P<0.01$. For abbreviations, see text.

mmHg ($n = 76$; all appropriate experiments pooled). Under control conditions, these values did not change significantly upon subsequent stimulations, resulting in S_4/S_2 ratios which were not different from unity. The fractional rate of basal tritium overflow declined with time ($b_n/b_2 < 1$) and infusion of solvent did not cause any change in basal perfusion pressure (not shown). 8-Bromo-cyclic GMP (3–300 μM) and 8-pCPT-cyclic GMP (1–100 μM) produced concentration-dependent increases in the electrically-induced tritium overflow whereas PET-cyclic GMP (1–30 μM) was without effect (Figure 1). In six experiments, SIN-1 (10 μM) had no significant effect on [^{3}H]-noradrenaline release.

In spite of the enhancement of stimulation-induced tritium overflow, 8-bromo-cyclic GMP and 8-pCPT-cyclic GMP produced a concentration-dependent decrease in the vasoconstrictor response (Figure 1). PET-cyclic GMP also concentration-dependently reduced the stimulation-elicited vasoconstriction, and it was more potent than 8-pCPT-cyclic GMP and 8-bromo-cyclic GMP in producing this effect. SIN-1 reduced vasoconstriction by about 50%, compared to the

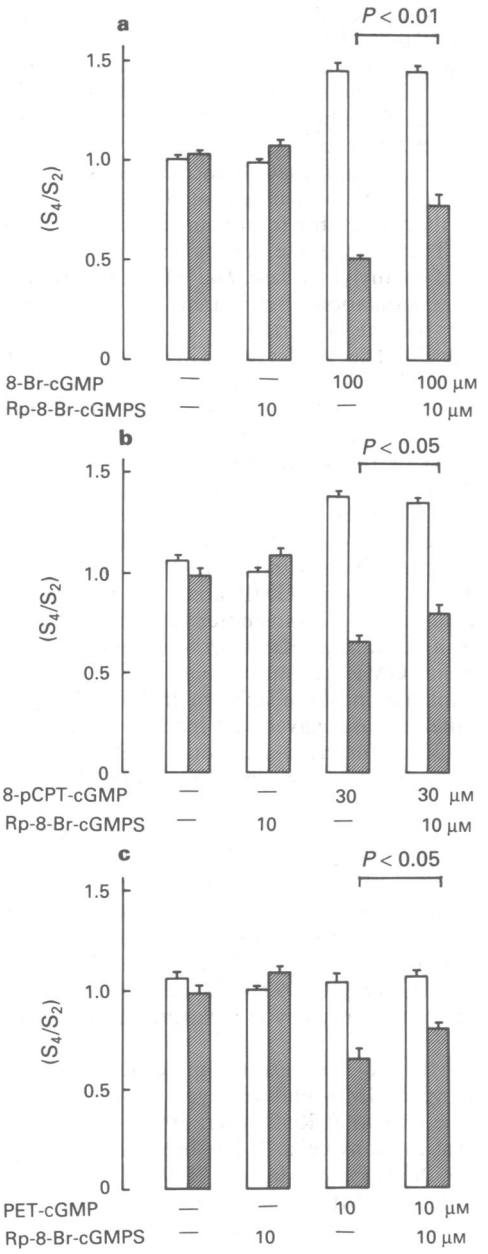

Figure 2 Interaction of Rp-8-Br-cGMPS with 8-Br-cGMP (a), 8-pCPT-cGMP (b) and PET-cGMP (c) on electrically-evoked tritium overflow (open columns) and change in perfusion pressure (hatched columns) in rat tail arteries preincubated with [^{3}H]-noradrenaline. Four periods (S_1–S_4) of field stimulation were delivered at intervals of 16 min (24 pulses at 0.4 Hz, 200 mA, 0.3 ms duration). The compounds or their solvents (control group) were added alone or in combination 8 min before S_3. They were maintained in the medium for the duration of the experiment. The effect of the drugs are presented as the ratio of tritium overflow or change in perfusion pressure evoked by S_4 over that evoked by S_2. Each column represents the mean ± s.e.mean from 4–8 arteries. The statistically significant differences between some values are indicated. For abbreviations, see text.

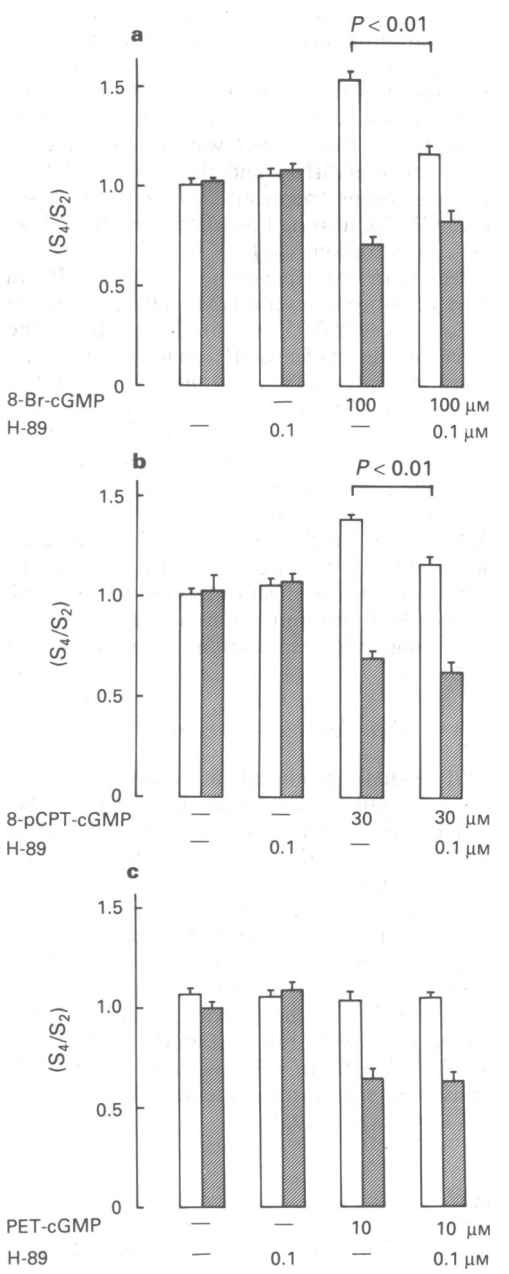

Figure 3 Interaction of H-89 with 8-Br-cGMP (a), 8-pCPT-cGMP (b) and PET-cGMP (c) on electrically-evoked tritium overflow (open columns) and change in perfusion pressure (hatched columns) in rat tail arteries preincubated with [^{3}H]-noradrenaline. Four periods (S_1–S_4) of field stimulation were delivered at intervals of 16 min (24 pulses at 0.4 Hz, 200 mA, 0.3 ms duration). The compounds or their solvents (control group) were added alone or in combination 8 min before S_3. They were maintained in the medium for the duration of the experiment. The effects of the drugs are presented as the ratio of tritium overflow or change in perfusion pressure evoked by S_4 over that evoked by S_2. Each column represents the mean ± s.e.mean from 6–8 arteries. The statistically significant differences between some values are indicated. For abbreviations, see text.

corresponding controls (S_4/S_2: 0.56 ± 0.04; $n = 6$ and 1.08 ± 0.09; $n = 6$; respectively; $P < 0.01$).

At the concentration tested (10 μM), the membrane permeant and metabolically stable competitive inhibitor of PKG, Rp-8-bromo-cyclic GMPS, did not itself modify the tritium overflow or the vasoconstrictor response induced by periarterial nerve stimulation (Figure 2). It significantly reduced the effects of 8-bromo-cyclic GMP (100 μM), 8-pCPT-cyclic GMP (30 μM) and PET-cyclic GMP (10 μM) on the stimulation-induced vasoconstriction, but did not modify their respective effects on the stimulation-evoked [^{3}H]-noradrenaline overflow (Figure 2). Rp-8-bromo-cyclic GMPS (10 μM) also attenuated the inhibitory effect of SIN-1 (10 μM) on the stimulation-induced vasoconstrictor response (S_4/S_2: 0.56 ± 0.04; $n = 6$ and S_4/S_2: 0.76 ± 0.04; $n = 4$; $P < 0.05$; in the absence and presence of the PKG inhibitor, respectively). The electrically-evoked overflow of tritium which was not modified by SIN-1 (see above) was also unaffected in the combined presence of SIN-1 and the PKG inhibitor ($n = 4$).

Another membrane permeant PKG antagonist, Rp-8-pCPT-cyclic GMPS, also had no effect by itself. However, at equimolar concentration (10 μM) it reduced to a slightly greater extent than did Rp-8-bromo-cyclic GMPS the inhibitory effect of 8-bromo-cyclic GMP (100 μM) on perfusion pressure (S_4/S_2: 0.84 ± 0.05; $n = 6$). By contrast, the facilitatory effect of the cyclic GMP analogue on the evoked tritium overflow (S_4/S_2: 1.48 ± 0.04; $n = 11$) was not modified in the presence of Rp-8-pCPT-cyclic GMPS (S_4/S_2: 1.55 ± 0.04; $n = 6$).

The PKA inhibitor H-89 (0.1 μM), like the PKG blockers had no effect by itself (Figure 3) but reduced by about 50% the effect of 8-bromo-cyclic GMP (100 μM) and 8-pCPT-cyclic GMP (30 μM) on the tritium overflow evoked by electrical field stimulation (Figure 3a, b). By contrast, H-89 did not modify the inhibitory effect of 8-bromo-cyclic GMP or of 8-pCPT-cyclic GMP on stimulation-induced vasoconstriction, nor did it change the responses obtained with PET-cyclic GMP (Figure 3c).

Relaxation of phenylephrine-precontracted arteries

SIN-1 (0.01–30 μM) produced a concentration-dependent relaxation of rat tail arteries precontracted with phenylephrine with a maximum relaxation to slightly above the pre-phenylephrine tension and an EC_{50} of 1.66 ± 0.51 μM ($n = 7$). A second concentration-response curve constructed 2 h after the first was not different from the former ($n = 7$). Rp-8-bromo-cyclic GMPS (10 μM) and Rp-8-pCPT-cyclic GMPS (10 μM) antagonized responses to SIN-1, resulting in a parallel rightward shift in the concentration-response curve with no depression of the maximum. Rp-8-bromo-cyclic GMPS shifted the concentration-response curve of SIN-1 by the factor 2.16 ± 0.22 ($n = 7$), whereas Rp-8-pCPT-cyclic GMPS caused a significantly greater shift by the factor 3.17 ± 0.28 ($n = 7$; $P < 0.05$).

Discussion

It has been previously shown that the presence of endothelium decreased the overflow of endogenous noradrenaline release from sympathetic nerves in rabbit carotid and canine pulmonary arteries (Cohen & Weisbrod, 1988; Tesfamarian *et al.*, 1989; Greenberg *et al.*, 1990a). Nitric oxide, which accounts for the biological activity of endothelium-derived relaxing factor (EDRF) (Palmer *et al.*, 1987) originally described by Furchgott & Zawadzki in 1980; stimulates soluble guanylyl cyclase in a variety of cells (Ignarro, 1990; Moncada *et al.*, 1991). Therefore, one of the postulated mechanisms of inhibition of noradrenaline release by EDRF was thought to be an increase of cyclic GMP (Greenberg *et al.*, 1990b). However, recent observations suggest that altering cyclic GMP levels has no major role in the prejunctional modulation of noradrenaline release in some arteries (Bucher *et al.*, 1992; Tesfamarian *et al.*, 1992), and the results of the present study are compatible with this.

The action of exogenously applied, cell membrane permeable, cyclic GMP analogues is thought to be primarily due to their ability to mimic the intracellular effects of the endogenously produced nucleotide. The present results in fact show that the two 8-substituted analogues of cyclic GMP were able to induce an increase in nerve-stimulated noradrenaline release. However, the derivative modified at the 1,N^2-position of the purine ring, PET-cyclic GMP, was without effect. Moreover, the two membrane permeant, metabolically stable, selective inhibitors of PKG, Rp-8-bromo cyclic GMPS and Rp-8pCPT cyclic GMPS, an 8-bromo and a 8-(4-chlorophenylthio) derivative of Rp-cyclic GMPS respectively (Butt *et al.*, 1990), had no effect on the enhancement of stimulated [^{3}H]-noradrenaline release by 8-bromo-cyclic GMP or 8-pCPT cyclic GMP. Neither poor membrane permeability nor inadequate concentrations of the PKG inhibitors could explain their lack of effects since, in the same conditions, they were able to attenuate cyclic GMP-mediated relaxation. Therefore, these results are not consistent with activation of guanylyl cyclase and of PKG being a major pathway for modulation of noradrenaline release from nerve terminals in the rat tail artery.

Other possible effects of cyclic GMP analogues on mechanisms affecting transmitter release were therefore investigated. The effects of the two 8-substituted analogues of cyclic GMP on stimulation-induced noradrenaline release were inhibited by the selective PKA inhibitor H-89 (Chijiwa *et al.*, 1990), suggesting an involvement of PKA. In the same experimental model H-89 significantly attenuates the enhancement of electrically-evoked release of [^{3}H]-noradrenaline by forskolin, isoprenaline and 8-bromo-cyclic AMP (Ouedraogo *et al.*, 1994). The cyclic GMP analogue PET-cyclic GMP, which had no effect on transmitter release is 10 to 20 times less potent in activating PKA than 8-bromo-cyclic GMP and 8-pCPT-cyclic GMP (Francis *et al.*, 1988). Therefore a plausible explanation of the lack of effect of PET-cyclic GMP on transmitter release may be its inability to activate PKA. There is evidence for cross-activation of PKA and PKG by adenyl and guanyl 3′:5′-cyclic nucleotides (for review see Schmidt *et al.*, 1993). Involvement of PKG in cyclic AMP mediated actions has been reported in rat aortic smooth muscle cells in culture (Lincoln *et al.*, 1990) and, more recently, in pig coronary arteries (Jiang *et al.*, 1992). Reciprosal cross-activation, i.e. cyclic GMP activation of PKA, could also occur. Several lines of evidence suggest such a cross-activation of PKA by cyclic GMP in T84 human intestinal cells (Forte *et al.*, 1992) and in PKG-deficient human platelets of chronic myelocytic leukaemia (Eigenthaler *et al.*, 1993).

Cyclic GMP may also exert significant functional effects through a cyclic GMP-inhibited type III cyclic AMP phosphodiesterase (Beavo & Reifsnyder, 1990), an enzyme known to be present in many cells. It has been suggested (Cubeddu *et al.*, 1975; Maurice & Haslam, 1990; Bowen & Haslam, 1991) that cyclic GMP or analogues therefore may achieve their effects by inhibiting this enzyme, resulting in elevated cyclic AMP levels and activation of cyclic AMP-mediated signal transduction. However, such effects are not likely to be involved in these experiments since 8-pCPT-cyclic GMP is not able to inhibit the cyclic GMP-inhibited phosphodiesterase (Butt *et al.*, 1992) but did enhance noradrenaline release. Whether the effects with the two 8-substituted analogues resulted from direct or indirect activation of PKA remains to be determined.

Exposure of the arteries to cyclic GMP analogues or to an NO donor, SIN-1, the active metabolite of molsidomine (Feelisch & Noack, 1987) which activates guanylyl cyclase (Böhme *et al.*, 1984), produced an inhibition of the neurogenic vasoconstriction. The PKG antagonists but not the PKA inhibitor attenuated this effect, providing further evi-

dence that activation of PKG mediates cyclic GMP-induced relaxation of smooth muscle cells (Cornwell & Lincoln, 1989; Lincoln *et al.*, 1990). At the postjunctional level, the efficiency of the three analogues tested in the present study fits well with that observed in pig coronary arteries (Sekhar *et al.*, 1992). It has previously been shown that bovine aorta contains two isozymic forms of PKG, designated type Iα and type Iβ (Lincoln *et al.*, 1988; Wolfe *et al.*, 1989). Type Iα and type Iβ have different cyclic nucleotide analogue selectivities for activation: analogues modified at the 1,N^2-position (PET-cyclic GMP) are equally active on the two isozymes whereas analogues modified at the 8-position (8-bromo- or 8-pCPT-cyclic GMP) are much more effective in activating the type Iα (Sekhar *et al.*, 1992). A good correlation between the potencies of cyclic GMP analogues for PKG Iα and relaxation has been reported, whereas the correlation was poor with PKG Iβ (Sekhar *et al.*, 1992). However, in the present study, PET-cyclic GMP was the most potent relaxing analogue. Therefore a role for the type Iβ isozyme in vascular relaxation in the rat tail artery cannot be excluded.

Altogether, the results obtained in the current study show that, in the rat tail artery, the postjunctional action of cyclic GMP and its analogues involves the activation of a PKG. On the other hand, they provide no evidence for the existence of a cyclic GMP-operated mechanism at the prejunctional level. The prejunctional effect of the two 8-substituted cyclic GMP analogues tested in this study involves the activation of a PKA.

We would like to thank Dr R.C. Miller for helpful comments on the manuscript.

References

ALBERTS, P., ÖGREN, V.R. & SELLSTRÖM, Å.I. (1985). Role of adenosine 3',5'-cyclic monophosphate in adrenoceptor-mediated control of ^{3}H-noradrenaline secretion in guinea-pig ileum myenteric nerve terminals. *Naunyn-Schmied. Arch. Pharmacol.*, **330**, 114–120.

AXELSSON, K.L., ANDERSSON, R.G.G. & WIKBERG, J.E.S. (1980). Effect of cGMP derivatives on contraction relaxation cycle, release of norepinephrine and protein kinase activity in guinea pig vas deferens. *Acta Pharmacol. Toxicol.*, **47**, 328–334.

BEAVO, J.A. & REIFSNYDER, D.H. (1990). Primary sequence of cyclic nucleotide phosphodiesterase isozymes and the design of selective inhibitors. *Trends Pharmacol. Sci.*, **11**, 150–155.

BEEBE, S.J. & CORBIN, J.D. (1986). Cyclic nucleotide dependent protein kinases. In *The Enzymes*, vol. XVII, ed. Boyer, P.D. & Krebs, E.G. pp. 43–111. New York: Academic Press.

BÖHME, E., GROSSMANN, G., HERZ, J., MÜLSCH, A., SPIES, C. & SCHULTZ, G. (1984). Regulation of cyclic GMP formation by soluble guanylate cyclase: stimulation by NO-containing compounds. In *Adv. Cyclic Nucleotide Protein Phosphorylation Res.*, Vol. 17, ed. Greengard, P., Paoletti, R. & Nicosia, S. pp. 259–266. New York: Raven Press.

BOWEN, R. & HASLAM, R.J. (1991). Effects of nitrovasodilators on platelet cyclic nucleotide levels in rabbit blood; role for cyclic AMP in synergistic inhibition of platelet function by SIN-1 and prostaglandin E_1. *J. Cardiovasc. Pharmacol.*, **17**, 424–433.

BUCHER, B., OUEDRAOGO, S., TSCHÖPL, M., PAYA, D. & STOCLET, J.-C. (1992). Role of the L-arginine-NO pathway and of cyclic GMP in electrical field-induced noradrenaline release and vasoconstriction in the rat tail artery. *Br. J. Pharmacol.*, **107**, 976–982.

BUTT, E., VAN BEMMELEN, M., FISCHER, L., WALTER, U. & JASTORFF, B. (1990). Inhibition of cGMP-dependent protein kinase by (Rp)-guanosine 3',5'-monophosphorothioates. *FEBS Lett.*, **263**, 47–50.

BUTT, E., NOLTE, C., SCHULZ, S., BELTMAN, J., BEAVO, J.A., JASTORFF, B. & WALTER, U. (1992). Analysis of the functional role of cGMP-dependent protein kinase in intact human platelets using a specific activator 8-parachlorophenylthio-cGMP. *Biochem. Pharmacol.*, **43**, 2591–2600.

CHIJIWA, T., MISHIMA, A., HAGIWARA, M., SANO, M., HAYASHI, K., INOUE, T., NAITO, K., TOSHIOKA, T. & HIDAKA, H. (1990). Inhibition of forskolin-induced neurite outgrowth and protein phosphorylation by a new synthesized selective inhibitor of cyclic AMP-dependent protein kinase, N-[2-(p-bromocinnamylamino) ethyl]-5-isoquinolinesulfonamide (H-89), of PC12D pheochromocytoma cells. *J. Biol. Chem.*, **265**, 5267–5272.

COHEN, R.A. & WEISBROD, R.M. (1988). Endothelium inhibits norepinephrine release from adrenergic nerves of rabbit carotid artery. *Am. J. Physiol.*, **254**, H871–H878.

CORNWELL, T.L. & LINCOLN, T.M. (1989). Regulation of intracellular Ca^{2+} levels in cultured vascular smooth muscle cells. *J. Biol. Chem.*, **264**, 1146–1155.

CUBEDDU, L., BARNES, X.E. & WEINER, N. (1975). Release of norepinephrine and dopamine-β-hydroxylase by nerve stimulation. IV. An evaluation of a role for cyclic adenosine monophosphate. *J. Pharmacol. Exp. Ther.*, **193**, 105–127.

EIGENTHALER, M., ULLRICH, H., GEIGER, J., HORSTRUP, K., HÖNIG-LIEDL, P., WIEBECKE, D. & WALTER, U. (1993). Defective nitrovasodilator-stimulated protein phosphorylation and calcium regulation in cGMP-dependent protein kinase-deficient human platelets of chronic myelocytic leukemia. *J. Biol. Chem.*, **268**, 13526–13531.

FEELISCH, M. & NOACK, E. (1987). Correlation between nitric oxide formation during degradation of organic nitrates and activation of guanylate cyclase. *Eur. J. Pharmacol.*, **139**, 19–30.

FORTE, L.R., THORNE, P.K., EBER, S.L., KRAUSSE, W.J., FREEMAN, R.H., FRANCIS, S.H. & CORBIN, J.D. (1992). Stimulation of intestinal Cl^- transport by heat-stable enterotoxin: activation of cAMP-dependent protein kinase by cGMP. *Am. J. Physiol.*, **263**, C607–C615.

FRANCIS, S.H., NOBLETT, B.D., TODD, B.W., WELLS, J.N. & CORBIN, J.D. (1988). Relaxation of vascular and tracheal smooth muscle by cyclic nucleotide analogs that preferentially activate purified cGMP-dependent protein kinase. *Mol. Pharmacol.*, **34**, 506–517.

FURCHGOTT, R.F. & ZAWADZKI, J.V. (1980). The obligatory role of endothelial cells in the relaxation of arterial smooth muscle by acetylcholine. *Nature*, **288**, 373–376.

GREENBERG, S.S., DIECKE, F.P.J., CANTOR, E., PEEVY, K. & TANAKA, T.P. (1990a). Inhibition of sympathetic neurotransmitter release by modulators of cyclic GMP in canine vascular smooth muscle. *Eur. J. Pharmacol.*, **187**, 409–423.

GREENBERG, S.S., DIECKE, F.P.J., PEEVY, K. & TANAKA, T.P. (1990b). Release of norepinephrine from adrenergic nerve endings of blood vessels is modulated by endothelium-derived relaxing factor. *Am. J. Hyperten.*, **3**, 211–218.

GRUETTER, C.A., BARRY, B., MCNAMARA, D., GRUETTER, D., KADOWITZ, P. & IGNARRO, L. (1979). Relaxation of bovine coronary artery and activation of coronary arterial guanylate cyclase by nitric oxide, nitroprusside, and carcinogenic nitrosoamine. *J. Cyclic Nucleotide Res.*, **5**, 211–224.

IGNARRO, L.J. (1990). Nitric oxide. A novel signal transduction mechanism for transcellular communication. *Hypertension*, **16**, 477–483.

ILLES, P., BETTERMANN, R., BROD, I. & BUCHER, B. (1987). β-Endorphin-sensitive opioid receptors in the rat tail artery. *Naunyn-Schmied. Arch. Pharmacol.*, **335**, 420–427.

JIANG, H., CILBRAN, J.L., FRANCIS, S.H. & CORBIN, J.D. (1992). Direct evidence for cross-activation of cGMP-dependent protein kinase by cAMP in pig coronary arteries. *J. Biol. Chem.*, **267**, 1015–1019.

JOHNSTON, H., MAJEWSKI, H. & MUSGRAVE, I.F. (1987). Involvement of cyclic nucleotides in prejunctional modulation of noradrenaline release in mouse atria. *Br. J. Pharmacol.*, **91**, 773–781.

LINCOLN, T.M. & CORBIN, J.D. (1983). Characterization and biological role of the cyclic GMP-dependent protein kinase. *Adv. Cyclic Nucleotide Res.*, **15**, 139–192.

LINCOLN, T.M., CORNWELL, T.L. & TAYLOR, A.E. (1990) cGMP-dependent protein kinase mediates the reduction of Ca^{2+} by cAMP in vascular smooth muscle cells. *Am. J. Physiol.*, **258**, C399–C407.

LINCOLN, T.M, THOMPSON, M. & CORNWELL, T.L. (1988). Purification and characterization of two forms of cyclic GMP-dependent protein kinase from bovine aorta. *J. Biol. Chem.*, **263**, 17632–17637.

MAJEWSKI, H., COSTA, M., FOUCART, S., MURPHY, T.V. & MUSGRAVE, I.F. (1990). Second messengers are involved in facilitatory but not inhibitory receptor actions at sympathetic nerve endings. *Ann. N.Y. Acad. Sci.*, **604**, 266–275.

MAURICE, D.H. & HASLAM, R.J. (1991). Molecular basis of the synergistic inhibition of platelet function by nitrovasodilators and activators of adenylate cyclase: inhibition of cyclic AMP breakdown by cyclic GMP. *Mol. Pharmacol.*, **37**, 671–681.

MONCADA, S., PALMER, R.M.J. & HIGGS, E.A. (1991). Nitric oxide: physiology, pathophysiology and pharmacology. *Pharmacol. Rev.*, **43**, 109–142.

OUEDRAOGO, S., STOCLET, J.C. & BUCHER, B. (1994). Effects of cyclic AMP and analogues on neurogenic transmission in the rat tail artery. *Br. J. Pharmacol.*, **111**, 625–631.

PALMER, R.M.J., FERRIGE, A.G. & MONCADA, S. (1987). Nitric oxide release accounts for the biological activity of endothelium-derived relaxing factor. *Nature*, **327**, 524–526.

PELAYO, F., DUBOCOVICH, M.L. & LANGER, S.Z. (1978). Possible role of cyclic nucleotides in regulation of noradrenaline release from rat pineal through presynaptic adrenoceptors. *Nature*, **274**, 76–78.

SCHMIDT, H.H.H.W., LOHMANN, S.M. & WALTER, U. (1993). The nitric oxide and cGMP signal transduction system; regulation and mechanism of action. *Biochim. Biophys. Acta*, **1178**, 153–175.

SCHULTZ, K.D., SCHULTZ, K. & SCHULTZ, G. (1977). Sodium nitroprusside and other smooth muscle relaxants increase cyclic GMP levels in rat ductus deferens. *Nature*, **265**, 750–751.

SEKHAR, K.R., HATCHETT, R.J., SHABB, J.B., WOLFE, L., FRANCIS, S.H., WELLS, J.N., JASTORFF, B., BUTT, E., CHAKINALA, M.M. & CORBIN, J.D. (1992). Relaxation of pig coronary arteries by new and potent cGMP analogs that selectively activate type Iα, compared with type Iβ, cGMP-dependent protein kinase. *Mol. Pharmacol.*, **42**, 103–108.

STARKE, K., GÖTHERT, M. & KILBINGER, H. (1989). Modulation of neurotransmitter release by presynaptic autoreceptors. *Physiol. Rev.*, **69**, 864–989.

STJÄRNE, L., BARTFAI, T. & ALBERTS, P. (1979). The influence of 8-Br-3′,5′-cyclic nucleotide analogs and of inhibitors of 3′,5′-cyclic nucleotide phosphodiesterase, on noradrenaline secretion and neuromuscular transmission in guinea-pig vas deferens. *Naunyn-Schmied. Arch. Pharmacol.*, **308**, 99–105.

TESFAMARIAM, B., WEISBROD, R.M. & COHEN, R.A. (1989). The endothelium inhibits activation by calcium of vascular neurotransmission. *Am. J. Physiol.*, **257**, H1871–H1877.

TESFAMARIAM, B., WEISBROD, R.M. & COHEN, R.A. (1992). Cyclic GMP modulators on vascular adrenergic neurotransmission. *J. Vasc. Res.*, **29**, 396–404.

WALLENSTEIN, S., ZUCKER, C.L. & FLEISS, J.L. (1980). Some statistical methods useful in circulation research. *Circ. Res.*, **47**, 1–9.

WINQUIST, R.J., FAISON, E.P., WALDMAN, S.A., SCHWARTZ, K., MURAD, F. & RAPOPORT, R.M. (1981). Atrial natriuretic factor elicits an endothelium-independent relaxation and activates particulate guanylate cyclase in vascular smooth muscle. *Proc. Natl. Acad. Sci. U.S.A.*, **81**, 7661–7664.

WOLFE, L., CORBIN, J.D. & FRANCIS, S.H. (1989). Characterization of a novel isozyme of cGMP-induced protein kinase from bovine aorta. *J. Biol. Chem.*, **264**, 7734–7741.

(Received November 15, 1993
Revised March 21, 1994
Accepted March 30, 1994)

Br. J. Pharmacol. (1994), **112**, 873–880

Comparison between the pharmacology of dopamine receptors mediating the inhibition of cell firing in rat brain slices through the substantia nigra pars compacta and ventral tegmental area

B. Bowery, L.A. Rothwell & [1]G.R. Seabrook

Merck Sharp & Dohme Research Laboratories, Neuroscience Research Centre, Terlings Park, Eastwick Road, Harlow, Essex CM20 2QR

1 Electrophysiological recordings were made from presumed dopaminergic neurones in the substantia nigra pars compacta and ventral tegmental area of rat brain slices. The ability of selective dopamine receptor agonists to hyperpolarize neurones and inhibit cell firing, as well as the ability of dopamine receptor antagonists to block responses to quinpirole were compared.

2 Six dopamine receptor agonists were examined for their ability to hyperpolarize neurones within the substantia nigra pars compacta. Of these, the most potent ligand tested was naxagolide with an EC_{50} value of 20 nM and estimated maximum of 10 mV. The rank order of agonist potency was naxagolide> quinpirole>apomorphine>dopamine.

3 Quinpirole was more potent at inhibiting cell firing in the substantia nigra pars compacta ($pIC_{50} = 7.65 \pm 0.06$, $n = 35$) than in the ventral tegmental area ($pIC_{50} = 7.24 \pm 0.06$, $n = 32$; $P < 0.01$, Student's t test). 7-Hydroxy-*N*,*N*-di-*n*-propyl-2-aminotetralin (7-OH-DPAT), a putative D_3 selective agonist, had a comparable potency to quinpirole in both the ventral tegmental area ($pIC_{50} = 7.39 \pm 0.26$, $n = 4$), and substantia nigra pars compacta ($pIC_{50} = 7.71 \pm 0.20$; $n = 4$).

4 The inhibition of cell firing by quinpirole was antagonized by haloperidol, S(-)-sulpiride, clozapine, and ritanserin. S(-)-sulpiride and haloperidol had the highest estimated affinities in the substantia nigra, with pA_2 values of 8.97 (slope = 0.85) and 8.20 (slope = 2.09) respectively. The pA_2 values for S(-)-sulpiride and haloperidol in the ventral tegmental area were 8.07 (slope = 0.87) and 8.11 (slope = 1.48) respectively. Clozapine had a lower functional affinity than S(-)-sulpiride and haloperidol in both the substantia nigra ($pA_2 = 6.47$, slope = 1.19) and ventral tegmental area ($pA_2 = 6.53$, slope 0.87). Ritanserin, a 5-HT_2 receptor antagonist that also binds to $D_{2\text{-like}}$ dopamine receptors, caused a slight but significant shift in the concentration-effect curve to quinpirole with an estimated pK_A of 6.97 ± 0.13 ($n = 4$) in the substantia nigra and pK_A of 7.12 ± 0.22 ($n = 4$) in the ventral tegmental area.

5 Comparison of these data with the binding affinity for cloned dopamine receptors demonstrates that the responses to quinpirole on dopaminergic neurones in both the A9 (substantia nigra) and A10 (ventral tegmental area) brain areas are consistent with the activation of predominantly D_2, and not D_3 or D_4 dopamine receptors. Furthermore, the similarity in functional affinity of antagonists for these receptors suggest that the mesolimbic selectivity of atypical neuroleptics, like clozapine, may be a consequence of their actions on other receptors or their effects elsewhere in the brain.

Keywords: Dopamine receptor; schizophrenia; naxagolide [(+)-PHNO]; quinpirole; clozapine; substantia nigra; ventral tegmental area; electrophysiology

Introduction

There are three principal dopaminergic projection pathways within the mammalian brain: the nigrostriatal system (A9), the mesolimbic system (A10), and the tubero-infundibular system (Fallon & Loughlin, 1985). Dopamine containing neurones of the nigrostriatal pathway project from the substantia nigra pars compacta (SNC) to the caudate nucleus-putamen complex (dorsal striatum). This pathway is involved in the integration of sensory stimuli and initiation of movement and in man the degeneration of neurones within the SNC results in the debilitating motor defects associated with Parkinson's disease. In contrast, the mesolimbic pathway is comprised of dopaminergic neurones which project principally from the ventral tegmental area (VTA) to regions which include the ventral striatum (nucleus accumbens) and prefrontal cortex. The mesolimbic system is implicated in emotional behaviour and the hyperactivity of the dopaminergic neurones in the VTA is thought to underlie some forms of psychosis (reviewed in Goldstein & Deutch, 1992; Reynolds, 1992). This hypothesis is supported by the fact that most efficacious antipsychotic agents act as dopamine receptor antagonists (reviewed in Seeman, 1992). However, many antipsychotic drugs have significant extrapyramidal side effects, which are thought to be due to the lack of selectivity of antagonists between the nigrostriatal and mesolimbic systems (e.g. White & Wang, 1983).

Recently, cloning studies have revealed the existence of several structural types of dopamine receptors that have a ligand binding profile similar to endogenous D_2 receptors (hereafter referred to as $D_{2\text{-like}}$). These structural subtypes include the D_2, D_3 and D_4 subtypes (Bunzow *et al.*, 1988; Sokoloff *et al.*, 1990; Van Tol *et al.*, 1991). Not only do neuroleptic drugs like clozapine and sulpiride differ in their affinity for these receptors, but D_3 and D_4 receptors appear to have a more restricted distribution within the brain. In particular D_3 receptors appear to be preferentially expressed within the mesolimbic system (Bouthenet *et al.*, 1991; Levesque *et al.*, 1992) and heterologous expression studies have shown that these receptors can couple to effector mechanisms similar to the D_2 receptor subtype (Seabrook *et al.*, 1994a,b; McAllister *et al.*, unpublished observations).

Several *in vivo* studies have shown that chronic administration of clozapine (White & Wang, 1983; Skarsfeldt, 1988) and novel putative antipsychotic agents such as sertindole

[1] Author for correspondence.

(Skarsfeldt & Perregaard, 1990), can selectively inhibit the activity of neurones within the VTA compared to the SNC. Indeed such activity may explain the atypical profile of clozapine in rodent behavioural assays, as well as its reduced propensity to induce extrapyramidal side-effects in man. Whether or not this selectivity reflects the asymmetrical distribution of dopamine receptor subtypes remains to be determined.

Conventionally, dopamine receptors have been characterized by functional criteria into $D_{1\text{-like}}$ receptors which activate adenylate cyclase, and $D_{2\text{-like}}$ receptors which can inhibit adenylate cyclase activity and exert inhibitory influences upon neuronal excitability (Kebabian & Calne, 1979). The action of dopaminergic ligands on catecholamine containing neurones of the rat midbrain have been extensively characterized both *in vitro* and *in vivo*. Dopamine, acting on $D_{2\text{-like}}$ receptors inhibits cell firing in both the substantia nigra pars compacta and ventral tegmental area by hyperpolarizing cells following the activation of G-proteins linked to the activation of potassium channels (Pinnock, 1983; Lacey *et al.*, 1987; Mercuri *et al.*, 1992; Momiyama *et al.*, 1993).

Although the receptors that regulate the release of dopamine in the dorsal and ventral striatum have been subject to extensive pharmacological comparisons, few direct and quantitative comparisons of the functional activity of dopamine receptor ligands on neurones within the VTA and SNC have been carried out *in vitro*. *In vivo* studies have compared the pharmacology of dopamine receptors that regulate the firing of A9 and A10 neurones (Bunney & Grace, 1979; White & Wang, 1983; Skarsfeldt, 1988; Skarsfeldt & Perregaard, 1990), however, the interpretation of these studies may be complicated by the actions of these drugs elsewhere in the brain. Indeed, clozapine appears to have little functional selectivity in its ability to block the dopamine-mediated inhibition of cell firing in A10 versus A9 neurones *in vitro* (Suppes & Pinnock, 1987). To investigate further the pharmacology of the dopamine receptors present on mid-brain neurones, this study compared the functional effects of a range of dopamine receptor ligands using a rat brain slice preparation and quantitative pharmacological analysis.

Methods

Experimental preparations and recording techniques

Intracellular and extracellular recordings were made from presumed dopamine-containing neurones in either the medial substantia nigra pars compacta, or ventral tegmental area within slices (300–350 μm thick) of rat brain. The techniques for preparation of, recording from, and application of substances to these neurones have previously been described (Pinnock, 1983; Lacey *et al.*, 1988). In brief, coronal slices of rat substantia nigra and ventral tegmental area (plate 25, Paxinos & Watson, 1944) were submerged in a tissue chamber (volume 0.4 ml) by a continuously superfused (at 1–2 ml min^{-1}) artificial cerebrospinal fluid (ACSF) kept at 36°C and gassed with 95% O_2 and 5% CO_2. The ACSF contained (in mM): NaCl 126, KCl 2.5, NaH_2PO_4 1.2, $MgCl_2$ 1.3, $CaCl_2$ 2.4, $NaHCO_3$ 26 and glucose 10. Electrophysiological recordings were made with glass microelectrodes filled either with 3 M KCl (30–70 MΩ) for intracellular recordings, or 3 M NaCl (5–10 MΩ) for extracellular recording. Care was taken to ensure that recordings were made from either the medial substantia nigra pars compacta, lateral and immediately adjacent to the medial terminal nucleus accessory optic tract (MT), or from within the ventral tegmental area, identified as medial to the MT and ventral to the medial lemniscus.

Analytical techniques

Drug effects were expressed as either the % inhibition of cell firing, or cell hyperpolarization in mV. To quantify the drug-induced hyperpolarization of spontaneously active cells, the membrane potential was initially hyperpolarized by a holding current of *ca.* 50 pA to approximately −60 mV. Concentration-effect data were fitted to a logistic equation, $A/(1+(B/X)^C)$ where A = maximum, B = EC_{50}, C = Hill slope, X = agonist concentration, by least squares analysis of variance (Grafit; Erithacus Software). Concentration-effect data for the hyperpolarization of substantia nigra neurones by agonists represent the data pooled from several cells as complete concentration-effect data were not always obtained on the same cell. For these data, values represent the mean ± s.e.mean of the fitting procedure. Agonist-induced inhibition of cell firing was determined using cumulative concentration-effect curves, allowing 7 min for the firing rate to stabilize in each concentration of the agonist. Agonist potency was quantified as the negative logarithm of the half-maximal inhibitory concentration (pIC_{50}), and pooled data are the geometric mean ± standard error. Antagonist affinities were estimated from pA_2 values determined from Schild analysis (Arunlakshana & Schild, 1959), or from estimated pK_A values at single antagonist concentrations where stated using the equation, K_A = [antagonist concentration]/(concentration-ratio − 1). Concentration-ratio shifts were determined from the concentration of agonist required to half-maximally inhibit cell firing in the absence and presence of each concentration of antagonist. For a more accurate estimate of the affinity of those antagonists whose Schild plots had slopes that did not significantly differ from unity, pK_B values were also calculated by fitting a line with a slope of one to the data (Kenakin, 1990).

Drugs

Drugs were applied in the superfusion medium in known concentrations, reaching the recording chamber after a delay of 20–30 s. The following drugs were used: quinpirole hydrochloride, R(+)-1-phenyl-2, 3, 4, 5-tetrahydro-(1H)-3-benzazepine-7, 8-diol hydrochloride [R(+)-SKF 38393], (+)-bromocryptine methanesulphonate, S(-)sulpiride (Research Biochemicals Inc.), apomorphine, dopamine hydrochloride (Sigma), haloperidol, ritanserin (Janssen Pharmaceuticals), and clozapine (Sandoz Pharmaceuticals). 7-Hydroxy-*N*-*N*-di-*n*-propyl-2-aminotetralin (7-OH-DPAT) was provided by Research Biochemicals Inc. as part of the Chemical Synthesis Program of the National Institute of Mental Health, contract 278-90-0007. Naxagolide [(+)-4-propyl-9-hydroxynaphthoxazine; (+)-PHNO] was synthesized at Merck Sharp & Dohme Research Laboratories. Where necessary drugs were dissolved in dimethylsuphoxide (DMSO), and diluted to a final bath concentration of <0.1% DMSO which alone had no effect on cell firing rate. Dopamine was applied after treatment of cells with cocaine (10 μM) to block catecholamine uptake (e.g. Lacey *et al.*, 1990).

Results

Substantia nigra pars compacta cell properties

Intracellular recordings were made from >40 neurones within the substantia nigra pars compacta of rat brain slices. The properties of these neurones were comparable to those of the principal, presumed dopamine-containing, cells of the substantia nigra pars compacta described previously (Lacey *et al.*, 1987; 1989). Most cells were spontaneously active, firing action potentials at rates of between 1 and 3 Hz. Spontaneously active cells were hyperpolarized by constant current injection (typically <-0.1 nA) through the recording electrode to membrane potentials negative to the firing threshold. The mean membrane potential at which drugs were tested was −55 ± 2 mV. The mean cell input resistance at this potential, using hyperpolarizing current of −0.1 to

−0.2 nA over the ohmic portion of the current-voltage relationship, was 167 ± 23 MΩ.

Effect of dopamine receptor agonists on membrane potential in the substantia nigra

Naxagolide, quinpirole, apomorphine, and dopamine hyperpolarized the membrane of substantia nigra pars compacta neurones in a concentration-dependent manner to a maximum of approximately 10 mV, accompanied by a fall in input resistance (Figure 1). The effects of all the agonists were maximal within 3 min of their application. As with the effect of $GABA_B$ receptor agonists on these neurones (Lacey *et al.*, 1988; Seabrook *et al.*, 1990), and particularly with the more potent agonists at high drug concentrations, responses occasionally failed to recover completely even following washout periods of >15 min. The pooled concentration-effect curves for each agonist were fitted to a logistic equation. The most potent agonist was naxagolide with an EC_{50} of 20 nM and estimated maximum of 9.7 mV. The rank order of agonist potency was naxagolide<quinpirole<apomorphine<dopamine (Table 1). The potency of (+)-bromocryptine was indeterminate because of its low efficacy. When applied at concentrations *ca.* 100 fold greater than its affinity for $D_{2\text{-like}}$ receptors, (+)-bromocryptine (10 μM) caused a hyperpolarization that was only a fraction (13%) of the maximum hyperpolarization caused by quinpirole. The D_1 agonist, SKF 38393 (1 μM), when applied alone neither hyperpolarized nor depolarized these neurones within the substantia nigra pars compacta.

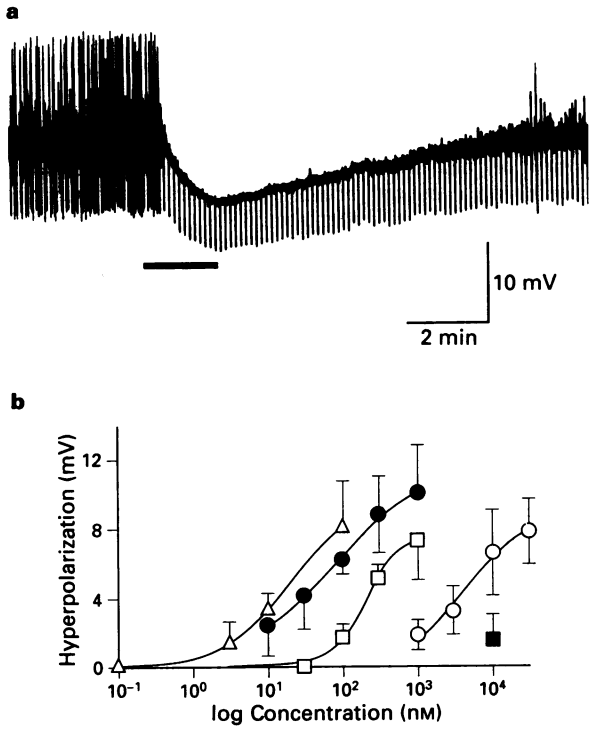

Figure 1 Hyperpolarization of neurones within substantia nigra pars compacta by dopamine receptor agonists. (a) Membrane potential recorded from an individual cell using an intracellular electrode. Quinpirole (300 nM), applied for the duration of the horizontal bar, caused a reversible hyperpolarization of the membrane potential which was accompanied by a block of spontaneous action potential firing. The amplitude of spontaneous action potentials in this figure are truncated by the chart recorder. Negative deflections on the trace represent the membrane transients in responses to the injection of a hyperpolarizing current through the recording electrode (0.1 nA for 100 ms duration). (b) Concentration-effect curves for the hyperpolarization of neurones within the substantia nigra by the dopamine receptor agonists naxagolide (△), quinpirole (●), apomorphine (□), dopamine (○), and (+)-bromocryptine (■). Each data point represents the mean ± s.e.mean of 4 to 6 cells. Solid lines are the fits of the logistic equation to the data (see Table 1).

Effects of dopamine receptor agonists and antagonists on cell firing in the substantia nigra

Quinpirole was chosen as the agonist to examine the pharmacology of the dopamine receptor on neurones within rat brain slices because of its high affinity for D_3/D_4 receptors compared to D_2 receptors, as well as its high functional potency and reversible effects upon neurones of the substantia nigra (Lacey *et al.*, 1987; Sheehan *et al.*, 1993). Extracellular single unit activity was used in preference to intracellular recording for antagonist studies because a hyperpolarization of only a few millivolts is necessary to inhibit cell firing. Thus the inhibition of cell firing would effectively have a higher receptor reserve. This is consistent with the 3 fold greater potency of quinpirole at inhibiting cell firing (22 nM) compared to hyperpolarizing cells within the substantia nigra pars compacta (77 nM; Tables 1 and 2).

In contrast to the effects of high concentrations of naxagolide on cell membrane potential, no tachyphylaxis of the inhibition of cell firing by quinpirole was seen during sustained agonist applications. This was partly because of the low agonist concentrations required to achieve the maximal response, typically at a concentration of 100 nM, but also because the effect of quinpirole was more readily reversible than that of other agonists. The concentration-effect curve for the inhibition of cell firing by quinpirole (nH = 1.96) (Figure 2) was steeper than that for cell hyperpolarizations (nH = 0.69; Table 1), probably because of the higher receptor reserve, and was therefore a more sensitive method of determining concentration-ratio shifts in the presence of antagonists.

The inhibition of cell firing caused by quinpirole in the substantia nigra pars compacta was antagonized in a surmountable manner by haloperidol, S(-)-sulpiride, and clozapine. No agonist-like effects of these compounds were observed. Antagonists were allowed to equilibrate for 40 min at each antagonist concentration before repeating agonist concentration-effect curves. Antagonist affinities were estimated from Schild plots using the concentration-ratio shifts produced by increasing concentrations of the antagonist. The Schild plot for haloperidol yielded a pA_2 value (the concentration of antagonist required to shift the agonist concentration-effect curve by two) of 8.20. However, the slope of the Schild plot for haloperidol was greater than unity (2.09; Table 2) which precluded the determination of pK_B values. The Schild plot for S(-)-sulpiride was 8.97 with a slope not significantly different from unity, consistent with competitive antagonism. Constraining the slope of the Schild plot to unity enabled the determination of the functional affinity of

Table 1 Comparison of the potency and ability of dopamine receptor agonists to hyperpolarize neurones within the substantia nigra pars compacta of rat brain

	EC_{50} (nM)	*Hyperpolarization maximum* (mV)	*Slope*	n
Naxagolide	20 ± 2	9.7 ± 0.4	0.97	6
Quinpirole	77 ± 25	11.8 ± 1.0	0.69	4
Apomorphine	205 ± 20	7.7 ± 0.4	1.84	8
Dopamine	4389 ± 2136	8.9 ± 1.6	1.07	4
(+)-Bromocryptine	indeterminate	1.5 mV at 10 μM	–	5
SKF 38393	>1000	no effect	–	4

Cell hyperpolarizations were recorded with intracellular electrodes and concentration-effect curves were fitted by least squares analysis of variance. The maximum hyperpolarization was estimated from the best fit to a single-site logistic equation.

Table 2 Inhibition of cell firing in the substantia nigra pars compacta by quinpirole and antagonism of responses by dopamine receptor antagonists

	pIC_{50}	n
Quinpirole	7.65 ± 0.06	35
7-OH-DPAT	7.71 ± 0.20	4

	pA_2	Slope	pK_B	Estimated pK_A	Estimated affinity (nM)	n
S(−)-sulpiride	8.97	0.85 ± 0.28	8.60 ± 0.15	–	3	8
Haloperidol	8.20	2.09 ± 0.43	–	–	<6	6
Clozapine	6.47	1.19 ± 0.19	6.63 ± 0.08	–	234	4
Ritanserin	–	–	–	6.97 ± 0.13	107	4

Values given ± s.e.mean.

Agonist responses were quantified as the negative logarithm of the half-maximal inhibitory concentration (pIC_{50}). Antagonist affinities were determined by Schild analysis, or in the case of ritanserin by estimating the affinity from the concentration-ratio shifts obtained at a concentration of 300 nM. For drugs which acted in a competitive manner and whose Schild plots did not significantly differ from unity, the negative logarithm of the antagonist dissociation constant was also calculated. These pK_B values were determined by constraining the slope of the Schild plot to one.

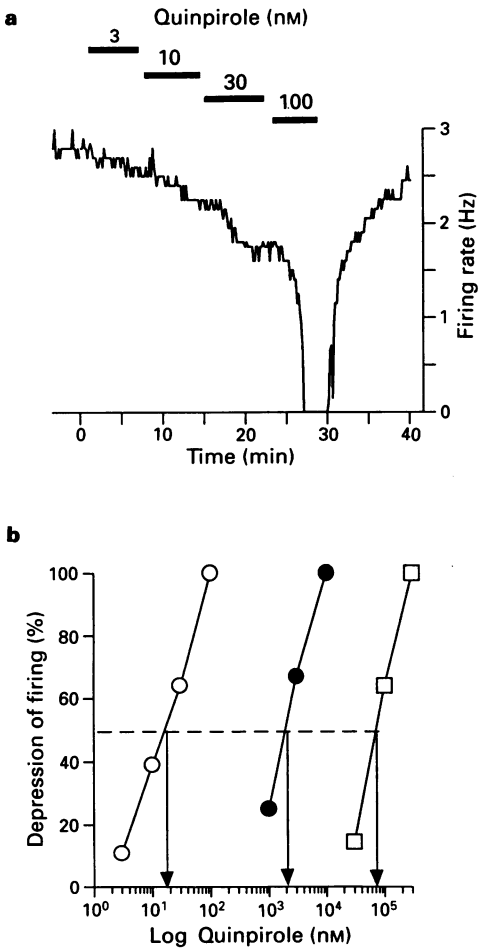

Figure 2 Inhibition of cell firing by quinpirole in rat substantia nigra pars compacta using extracellular recording and antagonism by S(−)-sulpiride. (a) Graph depicting the time course of the decrease in cell firing rate during the cumulative application of quinpirole in an individual cell. (b) Concentration-effect curve for the inhibition of cell firing caused by quinpirole (○), and the surmoutable antagonism caused by 100 nM (●) and 300 nM S(−)-sulpiride (□). The EC_{50} of quinpirole (arrows) was used to determine the concentration-ratio shift for each concentration of antagonist and this was then used to construct the Schild plots in Figure 3.

S(-)-sulpride (pK_B value; Kenakin, 1990) which was 8.60 ± 0.15, equivalent to 3 nM. Clozapine also antagonized the responses to quinpirole in a competitive manner. The Schild plot for clozapine yielded a pA_2 value 6.47 with a slope not significantly different from unity. The pK_B value for clozapine was 6.63 ± 0.08, equivalent to 234 nM (Table 2). The affinity of ritanserin was estimated from the shift in the concentration-effect curve to quinpirole produced by an antagonist concentration of 300 nM. This estimated pK_A value, which assumes competitive antagonism, was 6.97 ± 0.13, equivalent to 107 nM. Higher concentrations of ritanserin were not used because of non-specific effects on ion channels (e.g. Leysen *et al.*, 1993).

Effects of dopamine receptor agonists on neurones within the ventral tegmental area

Quinpirole and 7-OH-DPAT inhibited the firing of the majority of neurones within brain slices of the ventral tegmental area of rat brain. The potency of quinpirole, pIC_{50} = 7.24 ± 0.06 equivalent to 58 nM (n = 32), was slightly but significantly lower ($P < 0.01$, Student's t test) than that required to inhibit cell firing within the substantia nigra (pIC_{50} = 7.65 ± 0.06, n = 35; Tables 2 and 3). 7-OH-DPAT was equipotent to quinpirole in the VTA (pIC_{50} = 7.39 ± 0.26; n = 4) and the SNC (7.71 ± 0.20, n = 4).

The inhibition of cell firing caused by quinpirole in the ventral tegmental area was antagonized in a surmountable manner by S(-)-sulpiride, haloperidol, clozapine, and ritanserin (Figure 3; Table 3). The pA_2 value of haloperidol, determined from Schild analysis, was 8.11 with a slope significantly greater than unity (1.48). The Schild plot for S(-)-sulpiride yielded a pA_2 value of 8.24, with a slope not significantly different from unity (0.87). Constraining the slope to one gave a pK_B value for S(-)-sulpiride of 8.07 ± 0.05, equivalent to an affinity of 9 nM. Like sulpiride, clozapine also antagonized the responses to quinpirole in a competitive manner. The Schild plot for clozapine yielded a pA_2 value 6.53 (slope = 0.87; Table 3). The pK_B value for clozapine was 6.38 ± 0.08, equivalent to 417 nM. As for the experiments in the substantia nigra, the affinity of ritanserin was estimated from the shift in the concentration-effect curve to quinpirole produced by an antagonist concentration of 300 nM. The estimated pK_A value for ritanserin was 7.12 ± 0.22, equivalent to 76 nM.

Discussion

Using *in vitro* electrophysiological recording, this study compared the pharmacology of the dopamine receptors that mediate the inhibition of cell firing on dopaminergic-neurones within the substantia nigra pars compacta and ventral tegmental area of rat brain. The effects of several clinically effective neuroleptic drugs, including clozapine, on

Table 3 Inhibition of cell firing in the ventral tegmental area by quinpirole and antagonism of responses by dopamine receptor antagonists

	pIC_{50}	n
Quinpirole	7.24 ± 0.06	32
7-OH-DPAT	7.39 ± 0.26	4

	pA_2	Slope	pK_B	Estimated pK_A	Estimated affinity (nM)	n
S(−)-sulpiride	8.24	0.87 ± 0.09	8.07 ± 0.05	-	9	5
Haloperidol	8.11	1.48 ± 0.22	-	-	<8	8
Clozapine	6.53	0.87 ± 0.20	6.38 ± 0.08	-	417	5
Ritanserin	-	-	-	7.12 ± 0.22	76	4

Values given ± s.e.mean.
Data are presented as described in Table 2.

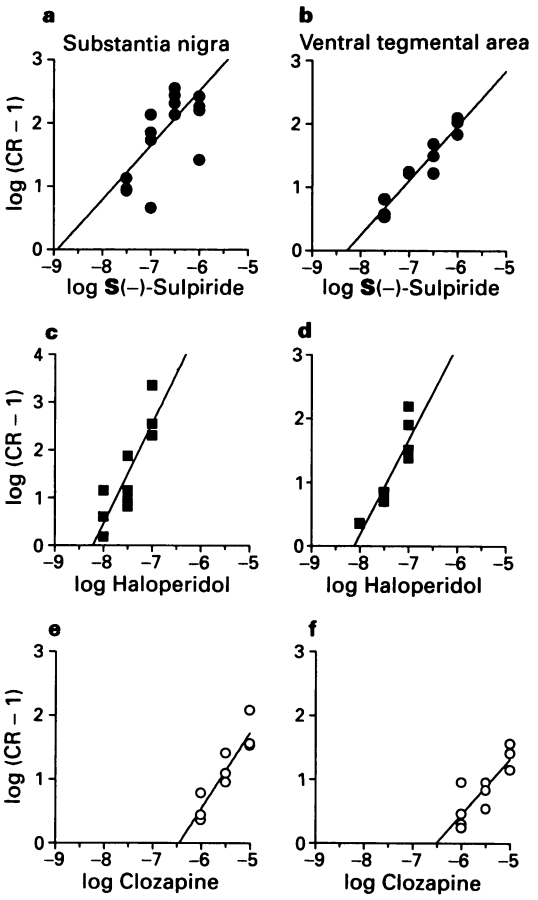

Figure 3 Comparison between the ability of S(−)sulpiride (●), haloperidol (■), and clozapine (○) to antagonize responses to quinpirole in the rat substantia nigra pars compacta (a, c and e) and ventral tegmental area (b, d and f). Lines fitted by linear regression were used to determine antagonist pA_2 values (Tables 2 and 3).

A9 and A10 dopamine neurones were contrasted with their affinity for cloned dopamine receptor subtypes.

Pharmacology of dopamine receptors on A9 and A10 neurones

In binding assays, naxagolide has approximately 50 fold binding selectivity for D_3 over D_2 and D_4 receptors (Table 4). Consistent with the high potency and ability of naxagolide to induce stereotyped behaviour in rodents (Martin *et al.*, 1984; 1985), this ligand was the most potent agonist tested in the

Table 4 Affinities of the ligands used in the present study for human D_2, D_3 and D_4 dopamine receptors

	D_2	D_3	D_4
Putative agonists			
(+)-Bromocryptine	1	2	190
Naxagolide	9	0.2	30
Apomorphine	30	16	0.5
7-OH-DPAT	60	1.6	270
Quinpirole	600	17	39
Dopamine	710	29	13
R(+)-SKF 38393	>1000	>1000	>1000
Putative antagonists			
Haloperidol	3	2	2
S(−)-sulpiride	6	8	250
Clozapine	38	88	13

Data from Freedman *et al.*, (1994, and unpublished observations). All data represent mean K_i values from >3 replicates, in nM concentrations.

SNC. Quinpirole also hyperpolarized neurones within the substantia nigra with a potency similar to that observed in previous studies (Lacey *et al.*, 1987). However, the ability of quinpirole to inhibit cell firing in the VTA was approximately 100 fold more potent than that reported by Momiyama *et al.* (1993). This can only partly be accounted for by the fact that the concentration of quinpirole required to inhibit cell firing is lower than that required to hyperpolarize maximally dopaminergic neurones. For example in the SNC this was 3 fold lower (Tables 1 and 2). However despite these differences, in the present study, quinpirole had a significant 3 fold lower potency in the ventral tegmental area compared to the substantia nigra. Agonist potency is dependent upon both the affinity of the ligand for the receptor as well as the number of receptors that need to be activated for a given functional response. In this respect, the lower potency of quinpirole in the ventral tegmental area may simply reflect a lower receptor reserve relative to the substantia nigra and not necessarily an action at a different receptor subtype. This hypothesis is supported by the *in vivo* studies of Cox & Waszczak (1990), who showed that the inhibition of cell firing caused by the dopamine receptor agonist R(-)-*N*-*n*-propylnorapomorphine (NPA) in A9 neurones was more sensitive to the actions of the irreversible receptor inactivator *N*-ethyoxycarbonyl-2-ethoxy-1,2-dihydroquinoline (EEDQ) than A10 neurones. In their study, Furchgott analysis revealed that the relative receptor reserves for responses to peripheral administration of NPA were 70% and 30%, in A9 and A10 neurones respectively.

In the present study, the overall rank order of agonist potency in the substantia nigra was naxagolide>quin-

pirole>apomorphine>dopamine. This was similar but not identical to that expected from the binding profile for D_2 receptors (naxagolide>apomorphine>quinpirole>dopamine). Despite minimizing transmitter uptake by blocking catecholamine transporters with cocaine (10 μM), the EC_{50} for dopamine was weaker than its binding affinity for D_2 receptors. Although an EC_{50} of 4 μM is consistent with previous functional studies it should be noted that cocaine may cause the extracellular accumulation of endogenous dopamine which would preclude the determination of meaningful potency values for this agonist (Lacey *et al.*, 1987; 1990).

In vivo studies using fast cyclic voltammetry (Stamford *et al.*, 1991) have shown that bromocryptine has little effect upon dopamine release within the striatum, supporting the hypothesis that this agonist acts preferentially on 'post-synaptic' D_2 receptors (Jenner *et al.*, 1979). In the present study (+)-bromocryptine (10 μM) produced a hyperpolarization that was 13% of the maximum produced by quinpirole. Although (+)-bromocryptine has approximately 100 fold selectivity for D_2 and D_3 receptors over D_4 receptors, it is likely that the fractional hyperpolarization obtained with this agonist was due to its low efficacy rather than an action on different receptor population since the concentration of agonist used was more than 100 fold greater than its binding affinity for D_2, D_3 or D_4 receptors.

The possibility that not all agonists have the same intrinsic efficacy, and because cells may express more than one type of dopamine receptor complicates receptor characterization using just agonist potency. Consequently, to test whether the dopamine receptors activated by quinpirole were different between the SNC and VTA, the functional affinity of several dopamine receptor antagonists were compared.

Antagonists like haloperidol bind with comparable affinity to the D_2, D_3 and D_4 dopamine receptor subtypes (Table 4) and consistent with this, its pA_2 for dopamine receptors was similar in both the VTA and SNC. The slope of the Schild plot for haloperidol was greater than unity in both the SNC and VTA (2.09 and 1.48 respectively; Tables 1, 2) indicating that despite an incubation period of 40 min, this antagonist may not have been at equilibrium with the receptors at the lower concentrations used. Consequently the pA_2 value for haloperidol may be an underestimate of antagonist affinity. Non-competitive antagonism of dopamine receptors by haloperidol in rat substantia nigra was also observed by Pinnock (1984).

S(−)-sulpiride has a significantly higher binding affinity for D_2 and D_3 receptors (6 to 18 nM respectively) compared to D_4 dopamine receptors (250 nM; Table 4). In both the SNC and VTA this antagonist had a functional affinity of *ca.* 10 nM and thus was more consistent with the effects of quinpirole being mediated by either D_2 or D_3 receptors. Furthermore, the estimated affinity of clozapine in both the SNC (234 nM) and VTA (417 nM) was more consistent with its lower binding affinity for D_2 and D_3 receptors than for D_4 receptors (Table 4).

The putative D_3 receptor agonist 7-OH-DPAT has approximately 40 fold greater affinity for D_3 over D_2 receptors and has been used in behavioural studies to attempt to define a functional role for the D_3 receptor (Daly & Waddington, 1993). In the present study, 7-OH-DPAT was equipotent to quinpirole in both the VTA and SNC, although like quinpirole the potency of 7-OH-DPAT was 2 fold weaker in the VTA, consistent with a lower receptor reserve in this area. However, as previously discussed, agonist potency is not necessarily a good criterion for distinguishing between receptor subtypes. Indeed despite the 10 fold binding selectivity of 7-OH-DPAT versus quinpirole for D_3 receptors (Table 4) the ability of 7-OH-DPAT to inhibit forskolin-stimulated adenylate cyclase activity in human embryonic kidney cells that have been transfected with human D_3 dopamine receptors was similar to the potency of quinpirole (McAllister *et al.*, unpublished observations). Furthermore in CHO cells transfected with rat D_3 receptors the functional selectivity of agonists varies according to whether one examines the inhibition of adenylate cyclase or cell mitogenesis (Chio *et al.*, 1994). Consequently confirmation that D_3 receptors are not involved in the function of midbrain dopamine neurones requires a selective antagonist of rat D_3 dopamine receptors, and these have yet to be described.

The $5\text{-}HT_2$ receptor antagonist, ritanserin (Leysen *et al.*, 1985; Humphrey *et al.*, 1993) also has high affinity for $D_{2\text{-like}}$ dopamine receptors in binding studies (Leysen *et al.*, 1993). *In vivo* studies have also shown that ritanserin dose-dependently increases the excitability of midbrain dopaminergic neurones, an effect that has been attributed to the antagonism of $5\text{-}HT_2$ receptors (Ugedo *et al.*, 1989). However, in the present study ritanserin when applied alone did not have any agonist-like activity and antagonized responses to quinpirole in both A9 and A10 neurones. The estimated functional affinity of ritanserin was 107 nM and 76 nM in the SNC and VTA respectively, assuming competitive antagonism. These affinities are compatible with ritanserin's ability to displace iodosulpiride binding to cloned rat D_2 and D_3 dopamine receptors (Leysen *et al.*, 1993). It is unlikely that the effect of quinpirole at nanomolar concentrations was mediated by an action on 5-HT receptors because quinpirole has little affinity for these receptors and furthermore its effects were blocked by S(-)-sulpiride which is selective for $D_{2\text{-like}}$ receptors over 5-HT receptors (Leysen *et al.*, 1993).

The functional affinities of the dopamine receptor antagonists used in the present study were more consistent with ligand binding profile of the D_2 receptor subtype than that of D_3 or D_4 receptors. Although the existence of a low density of functional D_3 or D_4 receptors in these brain areas cannot be excluded, these results indicate that they contribute little to the electrophysiological effects of exogenously applied quinpirole.

Implications for the mechanism of action of antipsychotic drugs

The effectiveness of clozapine as an atypical neuroleptic in the clinic (reviewed in Kane, 1992) has prompted numerous investigators to try and identify the properties of this compound that give it its antipsychotic profile. *In vivo* studies in rats have shown that chronic treatment with clozapine selectively reduces neuronal activity within the ventral tegmental area compared to the substantia nigra (White & Wang, 1983; Skarsfeldt, 1988), this preferential action on mesolimbic neurones is thought to underlie its atypical neuroleptic profile. The identification of novel D_3 and D_4 dopamine receptors that also bind clozapine with high affinity, as well as their localization in mesolimbic brain areas (Bouthenet *et al.*, 1991; Levesque *et al.*, 1992) has prompted speculation that actions on these receptors may account for the selective effects of clozapine on mesolimbic neurones. However, one argument that appears to militate against this hypothesis is that most neuroleptic drugs are functional antagonists of $D_{2\text{-like}}$ dopamine receptors. In that the selective antagonism of dopamine autoreceptors present on neurones in the VTA would be expected to increase and not decrease the firing rate of neurones in this area and may thus cause a concomitant increase in dopamine release. Although such a simplistic scenario excludes the involvement of feedback regulation of dopamine neurone activity (reviewed in Kalivas, 1993), it has been hypothesized that the resultant excitation may lead to a depolarization-induced block of cell firing, with drugs like clozapine exerting a preferential effect in the ventral tegmental area (reviewed in Bunney, 1992). Consistent with this hypothesis, acute treatment of rats *in vivo* with neuroleptics such as clozapine and haloperidol causes a transient increase in neuronal activity within the ventral tegmental area (Hand *et al.*, 1987; Skarsfeldt, 1988). However, the mechanism that underlies the eventual decrease in neuronal activity following chronic exposure to neuroleptics over a period of several weeks is less clear.

To test whether the mesolimbic selectivity of clozapine seen with *in vivo* studies was due to a direct and selective effect on A9 versus A10 dopaminergic neurones, the ability of this ligand to block the quinpirole-induced inhibition of cell firing was studied. Quinpirole was chosen as the agonist for this comparison because it has high affinity for the recently cloned D_3 and D_4 receptor subtypes and excellent selectivity over D_1-like receptors. As has previously been reported for the effects of dopamine on neurones within the substantia nigra pars compacta (Suppes & Pinnock, 1987; Bull *et al.*, 1993), clozapine also antagonized responses to quinpirole in the ventral tegmental area without any agonist-like effects. Furthermore, the affinity of clozapine for receptors that mediate the quinpirole-induced inhibition of firing in the SNC and VTA was indistinguishable. Consequently, the *in vivo* mesolimbic selectivity of clozapine in rat brain is not due to a differential action upon these dopamine receptors. This observation is supported by studies examining the effects of clozapine on dopamine release, using *in vitro* fast cyclic voltammetry within the striatum. Sheehan *et al.* (1993) have shown that clozapine has comparable affinity for dopamine autoreceptors on A9 and A10 fibres in the ventral and dorsal striatum respectively. Bull and colleagues have also shown that action potential firing by dopaminergic neurones in the SNC can also be inhibited by the dopamine receptor ligand dpADTN (N,N-dipropyl-2-aminotetralin), an effect which is antagonized albeit weakly, by haloperidol and (±)-sulpiride (Bull *et al.*, 1993). Furthermore, *in vitro* fast cyclic voltammetric studies also showed that dpADTN reduces dopamine release in the striatum (Sheehan *et al.*, 1993), but as with quinpirole, the estimated affinity of antagonists for these receptors did not exhibit any selectivity between the dorsal or ventral striatum. Although this ligand may be acting at a receptor population different from that of quinpirole, the absence of mesolimbic selectivity suggests that these receptors cannot account for atypical neuroleptic drug profiles and in accord with this the effects of dpADTN were insensitive to clozapine.

So how do clozapine and other related atypical antipsychotic drugs exert their mesolimbic selectivity? Clozapine also has high affinity for several other types of G-protein linked receptors, notably $5\text{-HT}_{2\text{-like}}$ receptors. Antagonism of these, or actions at other receptor types may be more important determinants for atypical antipsychotic activity than effects on $D_{2\text{-like}}$ dopamine receptors. Alternatively an effect of clozapine on dopamine receptors in other brain areas, in particular upon D_4 receptors that may be upregulated in schizophrenics (e.g. Seeman *et al.*, 1993), could contribute more significantly to its antipsychotic actions.

In conclusion, the pharmacology of the response to quinpirole in both A9 (substantia nigra) and A10 (ventral tegmental area) brain areas was consistent with the activation of predominantly D_2, and not D_3 or D_4 dopamine receptors. Furthermore, the comparable affinity of clozapine for receptors on A9 and A10 cell bodies suggest that the mesolimbic selectivity of this compound seen with *in vivo* studies of rat brain function is not due to a preferential affinity for $D_{2\text{-like}}$ receptors on dopamine neurones of the rat ventral tegmental area compared to that of the substantia nigra pars compacta.

We would like to thank Dr J.A. Kemp and Dr M. Tricklebank for their constructive comments on this manuscript.

References

ARUNLAKSHANA, O. & SCHILD, H.O. (1959). Some quantitative uses of drug antagonists. *Br. J. Pharmacol. Chemother.*, **14**, 48–58.

BOUTHENET, M.-L., SOUIL, E., MARTRES, M.-P., SOKOLOFF, P., GIROS, B. & SCHWARTZ, J.-C. (1991). Localisation of dopamine D_3 receptor mRNA in the rat brain using in situ hybridisation histochemistry: comparison with dopamine D_2 receptor mRNA. *Brain Res.*, **564**, 203–219.

BULL, D.R., HAYES, A.G. & SHEEHAN, M.J. (1993). A clozapine-insensitive response to dopamine agonists in rat substantia nigra. *Br. J. Pharmacol.*, **108**, 55P.

BUNNEY, B.S. (1992). Clozapine: a hypothesised mechanism for its unique clinical profile. *Br. J. Psychiatry*, **160** (suppl. 17), 17–21.

BUNNEY, B.S. & GRACE, A.A. (1978). Acute and chronic haloperidol treatment: comparison of effects on nigral dopaminergic cell activity. *Life Sci.*, **23**, 1715–1728.

BUNZOW, J.R., VAN TOL, H.H.M., GRANDY, D.K., ALBERT, P., SALON, J., CHRISTIE, M., MACHINDA, C.A., NEVE, K.A. & CIVELLI, O. (1988). Cloning and expression of a rat D_2 dopamine receptor cDNA. *Nature*, **336**, 783–787.

CHIO, C.L., LAJINESS, M.E. & HUFF, R.M. (1994). Activation of heterologously expressed D3 dopamine receptors: comparison with D2 dopamine receptors. *Mol. Pharmacol.*, **45**, 51–60.

COX, R.F. & WASZCZAK, B.L. (1990). Irreversible receptor inactivation reveals differences in dopamine receptor reserve between A9 and A10 dopamine systems: an electrophysiological analysis. *Brain Res.*, **534**, 273–282.

DALY, S.A. & WADDINGTON, J.L. (1993). Behavioural effects of the putative D_3 dopamine receptor agonist 7-OH-DPAT in relation to the other 'D2-like' agonists. *Neuropharmacology*, **32**, 509–510.

FALLON, J.H. & LOUGHLIN, S.E. (1985). Basal ganglia. In *The Rat Nervous System*, volume 1. ed. Paxinos, G. pp. 353–374. London: Academic Press.

FREEDMAN, S.B., PATEL, S., MARWOOD, R., EMMS, F., SEABROOK, G.R., KNOWLES, M.R. & MCALLISTER, G. (1994). Expression and pharmacological characterisation of the human D_3 dopamine receptor. *J. Pharmacol. Exp. Ther.*, **268**, 417–426.

GOLDSTEIN, M. & DEUTCH, A.Y. (1992). Dopaminergic mechanisms in the pathogenesis of schizophrenias. *FASEB J.*, **6**, 2413–2421.

HAND, T.H., HU, X.-T. & WANG, R.Y. (1987). Differential effects of acute clozapine and haloperidol on the activity of ventral tegmental (A10) and nigrostriatal (A9) dopamine neurones. *Brain Res.*, **415**, 257–269.

HUMPHREY, P.P.A., HARTIG, P. & HOYER, D. (1993). A proposed new nomenclature for 5-HT receptors. *Trends Pharmacol. Sci.*, **14**, 233–236.

JENNER, P., MARSDEN, C.A. & REAVILL, C. (1979). Evidence for metabolite involvement in bromocryptine-induced circling behaviour. *Br. J. Pharmacol.*, **24**, 744–747.

KALIVAS, P.W. (1993). Neurotransmitter regulation of dopamine neurons in the ventral tegmental area. *Brain Res. Rev.*, **18**, 75–113.

KANE, J.M. (1992). Clinical efficacy of clozapine in treatment-refractory schizophrenia: an overview. *Br. J. Psychiatry*, **160** (suppl. 17), 41–45.

KEBABIAN, J.W. & CALNE, D.B. (1979). Multiple receptors for dopamine. *Nature*, **277**, 93–96.

KENAKIN, T. (1990). Drugs and receptors: an overview of the current state of knowledge. *Drugs*, **40**, 666–687.

LACEY, M.G., MERCURI, N.B. & NORTH, R.A. (1987). Dopamine acts on D_2 receptors to increase potassium conductance in neurones of the rat substantia nigra zona compacta. *J. Physiol.*, **392**, 397–416.

LACEY, M.G., MERCURI, N.B. & NORTH, R.A. (1988). On the potassium conductance increase activated by $GABA_B$ and dopamine D_2 receptors in rat substantia nigra neurones. *J. Physiol.*, **401**, 437–453.

LACEY, M.G., MERCURI, N.B. & NORTH, R.A. (1989). Two cell types in rat substantia nigra zona compacta distinguished by membrane potential properties and the actions of dopamine and opioids. *J. Neurosci.*, **9**, 1233–1241.

LACEY, M.G., MERCURI, N.B. & NORTH, R.A. (1990). Actions of cocaine on rat dopaminergic neurones *in vitro*. *Br. J. Pharmacol.*, **99**, 731–735.

LEVESQUE, D., DIAZ, J., PILON, C., MARTRES, M.-P., GIROS, B., SOIUL, E., SCHOTT, D., MORGAT, J.-L., SCHWARTZ, J.-C. & SOKOLOFF, P. (1992). Identification, characterisation, and localisation of the dopamine D_3 receptor in rat brain using 7-[3H]hydroxy-N,N,di-n,propyl-2-aminotetralin. *Proc. Natl. Acad. Sci. U.S.A.*, **89**, 8155–8159.

LEYSEN, J.E., GOMMEREN, W., VAN GOMPEL, P., WYNANTS, J., JANSEEN, P.F.M. & LADURON, P.M. (1985). Receptor-binding properties in vitro and in vivo of ritanserin. *Mol. Pharmacol.*, **27**, 600–611.

LEYSEN, J.E., JANSSEN, P.M.F., SCHOTTE, A., LUYTEN, W.H.M.L. & MEGENS, A.A.H.P. (1993). Interaction of antipsychotic drugs with neurotransmitter receptor sites in vitro and in vivo in relation to pharmacological and clinical effects: role of $5HT_2$ receptors. *Psychopharmacology*, **112**, S40–S54.

MARTIN, G.E., WILLIAMS, M., PETTIBONE, D.J., YARBROUGH, G.G., CLINESCHMIDT, B.V. & JONES, J.H. (1984). Pharmacologic profile of a novel potent direct-acting dopamine agonist, (+)-4-propyl-9-hydroxynaphthoxazine [(+)-PHNO]. *J. Pharmacol. Exp. Ther.*, **230**, 569–576.

MARTIN, G.E., WILLIAMS, M., PETTIBONE, D.J., ZRADA, M.M., LOTTI, V.J. & JONES, J.H. (1985). Selectivity of (+)-4-propyl-9-hydroxynaphthoxazine [(+)-PHNO] for dopamine receptors in vitro and in vivo. *J. Pharmacol. Exp. Ther.*, **233**, 395–401.

MERCURI, N.B., CALABRESI, P. & BERNARDI, G. (1992). The electrophysiological actions of dopamine and dopaminergic drugs on neurons of the substantia nigra pars compacta and ventral tegmental area. *Life Sci.*, **51**, 711–718.

MOMIYAMA, T., TODO, N. & SASA, M. (1993). A mechanism underlying dopamine D_1 and D_2 receptor-mediated inhibition of dopaminergic neurones in the ventral tegmental area *in vitro*. *Br. J. Pharmacol.*, **109**, 933–940.

PAXINOS, G. & WATSON, C. (1944). *The Rat Brain in Stereotaxic Coordinates*. London: Academic Press.

PINNOCK, R.D. (1983). Sensitivity of compacta neurones in the rat substantia nigra slice to dopamine agonists. *Eur. J. Pharmacol.*, **96**, 269–276.

PINNOCK, R.D. (1984). The actions of antipsychotic drugs on dopamine receptors in the rat substantia nigra. *Br. J. Pharmacol.*, **81**, 631–635.

REYNOLDS, G.P. (1992). Developments in the drug treatment of schizophrenia. *Trends Pharmacol. Sci.*, **13**, 116–121.

SEABROOK, G.R., HOWSON, W. & LACEY, M.G. (1990). Electrophysiological characterisation of potent agonists and antagonists at pre- and post-synaptic $GABA_B$ receptors on neurones in rat brain slices. *Br. J. Pharmacol.*, **101**, 949–957.

SEABROOK, G.R., KEMP, J.A., FREEDMAN, S.B., PATEL, S., SINCLAIR, H.A. & MCALLISTER, G. (1994a). Functional expression of human D_3 dopamine receptors in differentiated neuroblastoma × glioma NG108-15 cells. *Br. J. Pharmacol.*, **111**, 391–393.

SEABROOK, G.R., MCALLISTER, G., KNOWLES, M.R., MYERS, J., SINCLAIR, H.A., PATEL, S., FREEDMAN, S.B. & KEMP, J.A. (1994b). Depression of high-threshold calcium currents by activation of human $D_{2(short)}$ dopamine receptors expressed in differentiated NG108-15 cells. *Br. J. Pharmacol.*, **111**, 1061–1066.

SEEMAN, P. (1992). Dopamine receptor sequences: therapeutic levels of neuroleptics occupy D_2 receptors, clozapine occupies D_4. *Neuropsychopharmacology*, **7**, 261–284.

SEEMAN, P., GUAN, H.-C. & VAN TOL, H.H.M. (1993). Dopamine D_4 receptors elevated in Schizophrenia. *Nature*, **365**, 441–445.

SHEEHAN, M.J., HAYES, A.G. & BULL, D.R. (1993). Evidence for a clozapine-insensitive response to the dopamine agonist, N,N,dipropylamino-5,6,dihydroxytetralin (dpADTN), on dopaminergic nerve terminals. *Br. J. Pharmacol.*, **108**, 56P.

SKARSFELDT, T. (1988). Differential effects after repeated treatment with haloperidol, clozapine, thioridazine and tefludazine on SNC and VTA dopamine neurones in rats. *Life Sci.*, **42**, 1037–1044.

SKARSFELDT, T. & PERREGAARD, J. (1990). Sertindole, a new neuroleptic with extreme selectivity on A10 versus A9 dopamine neurones in the rat. *Eur. J. Pharmacol.*, **182**, 613–614.

SOKOLOFF, P., GIROS, B., MARTRES, M.-P., BOUTHENET, M.-L. & SCHWARTZ, J.-C. (1990). Molecular cloning and characterisation of a novel dopamine receptor (D_3) as a target for neuroleptics. *Nature*, **347**, 146–151.

STAMFORD, J.A., KRUK, Z.L. & MILLAR, J. (1991). Differential effects of dopamine agonists upon stimulated limbic and striatal dopamine release: *in vivo* voltammetric data. *Br. J. Pharmacol.*, **102**, 45–50.

SUPPES, T. & PINNOCK, R.D. (1987). Sensitivity of neuronal dopamine responses in the substantia nigra and ventral tegmentum to clozapine, metoclopromine and SCH 23390. *Neuropharmacology*, **26**, 331–337.

UGEDO, L., GRENHOFF, J. & SVENSSON, T.H. (1989). Ritanserin, a $5\text{-}HT_2$ receptor antagonist activates midbrain dopamine neurons by blocking serotonergic inhibition. *Psychopharmacology*, **98**, 45–50.

VAN TOL, H.H.M., BUNZOW, J.R., GUAN, H.-C., SUNAHARA, R.K., SEEMAN, P., NIZNIK, H.B. & CIVELLI, O. (1991). Cloning of the gene for a human dopamine D_4 receptor with high affinity for the antipsychotic clozapine. *Nature*, **350**, 610–614.

WHITE, F.J. & WANG, R.Y. (1983). Differential effects of classical and atypical antipsychotic drugs on A9 and A10 dopamine neurones. *Science*, **221**, 1054–1056.

(Received November 19, 1993
Revised March 30, 1994
Accepted April 5, 1994)

Br. J. Pharmacol. (1994), **112**, 881–886

The influence of acetazolamide and amlodipine on the intracellular sodium content of rat proximal tubular cells

Patrick S.K. Wong, *Paul L. Barclay, *Michael J. Newman & [1]Edward J. Johns

Department of Physiology, The Medical School, Birmingham B15 2TT and *Pfizer Central Research, Sandwich, Kent CT13 9NJ

1 This investigation set out to use ^{23}Na n.m.r. spectroscopy to measure changes in intracellular levels of sodium in isolated suspensions of rat proximal tubules. The effects of temperature, an inhibitor of the sodium pump and known natriuretic drugs on intracellular sodium content of such tubular preparations were measured and compared with calcium channel antagonists where action at this level is unclear.

2 Rat kidneys were perfused with collagenase, roughly chopped, subjected to mechanical dispersion and washed to remove all traces of the enzyme. The proximal tubules were then purified and concentrated by Percoll density gradient centrifugation and then resuspended in buffer containing dysprosium tripolyphosphate shift reagent.

3 Distinct peaks corresponding to intracellular and extracellular sodium signals were observed when the tubules were placed into the n.m.r. spectrometer. As the temperature of the suspension rose to 37°C, there was an exponential decrease in sodium content, with a decay constant of $0.15 \pm 0.02\ min^{-1}$, which reached a stable level within 20 to 25 min. Addition of ouabain, 10^{-3} M, resulted in a significant ($P<0.01$) 30% increase in intracellular sodium content within 5 min which peaked at 70% 20 min later. Although acetazolamide (10^{-3} M) significantly ($P<0.01$) increased intracellular sodium content by 45%, amlodipine (10^{-4} M) had no effect.

4 These data show that changes in the activity of the Na^+/K^+/ATPase have a considerable influence on the intracellular levels of sodium in proximal tubule cells. Inhibition of carbonic anhydrase activity resulted in a rise in intracellular sodium content which is compatible with its action to reduce the turnover rate of the $Na^+/(HCO_3^-)_3$ symporter. The lack of effect of amlodipine was consistent with the suggestion that it does not have a direct action on the sodium handling processes at the level of the proximal tubule.

Keywords: ^{23}Na n.m.r. spectroscopy; proximal tubules; carbonic anhydrase inhibitor; calcium channel antagonist; sodium transport

Introduction

Currently it is accepted that at the proximal tubule of the kidney, sodium moves from the tubular fluid into the cells by a variety of sodium coupled transport systems (Silbernagl *et al.*, 1975; Krapf, 1989) and leaves at the basolateral surface, mainly facilitated by the sodium pump and $Na^+/(HCO_3^-)_3$ symporter, into the extracellular space, with water being passively reabsorbed with the sodium. Recent evidence suggests that along the proximal tubule there is a heterogeneity with respect to sodium handling, insofar as the S1 and S2 segments reabsorb the majority of the filtered $NaHCO_3$ whilst the late S2 and the S3 segments are in the main responsible for the reabsorption of NaCl (Berry, 1982). The characteristics of sodium transport across the tubular cells were elucidated by methods such as measurement of the transepithelial movement of radioactive ^{22}Na or measurement of potential differences or pH changes between the apical and basolateral sides of the epithelial cells (Baum, 1987; DuBose, 1990; Gesek & Schoolwerth, 1990). Very little is known of the dynamic response of sodium within the cell when challenged with physiological and pharmacological stimuli. The reason for this has been the difficulty with which intracellular sodium (Na_i) can be measured dynamically because of the lack of available methodologies. One method, ion selective microelectrodes, has been utilised to measure intracellular sodium in the face of physiological challenges (Kondo & Frömter, 1990). Another potentially important way in which intracellular sodium content can be measured is by ^{23}Na n.m.r. spectroscopy.

Dynamic measurement of changes in Na_i content in response to physiological challenges, for example temperature changes, and following drug administration has recently been reported in a variety of tissues and cells. ^{23}Na efflux and influx due to the effect of changing the Na^+ concentration of the incubation medium have been measured in dog and rabbit kidney tubules by Boulanger *et al.* (1987) and the effect of changing temperature on Na_i has been observed on the rabbit proximal tubules (Gullans *et al.*, 1985). ^{23}Na n.m.r. was also used by Kumar *et al.* (1986) to measure changes in sodium efflux in the rat proximal tubule when the tubular suspension temperature was raised from 4°C to 37°C and Gullans *et al.* (1985) induced sodium influx by using nystatin, a polyene antibiotic.

The transport of sodium across the proximal tubule is known to be inhibited by a number of drugs which give rise to natriuresis. One well described compound is acetazolamide (ACTZ), which is a mild diuretic and natriuretic agent, and its mechanism of action is inhibition of carbonic anhydrase. The consequence of its action is to reduce bicarbonate reabsorption thereby preventing sodium reabsorption and hence to increase sodium and water excretion (Preisig *et al.*, 1987). Calcium channel antagonists (CCA), especially the dihydropyridine variety, cause hyperpolarization of vascular smooth muscle resulting in vasodilatation. Interestingly, calcium channel antagonists have been reported to have natriuretic and diuretic properties (Struyker-Boudier *et al.*, 1990). There is a possibility that the calcium channel antagonists act directly on tubular transport processes to cause natriuresis, and Rodicio *et al.* (1990) reported that nifedipine increased sodium excretion in man without altering glomerular filtration rate (GFR) and renal plasma flow, suggesting a tubular action. Similarly, in *in vivo* experiments,

[1] Author for correspondence.

amlodipine has been demonstrated to have natriuretic properties in the absence of changes in renal blood flow or glomerular filtration (Johns, 1988). The dihydropyridine class, calcium channel antagonist, felodipine has also shown direct tubular actions in the kidney of anaesthetized normotensive dogs (DiBona, 1990). However, the site of action along the tubule has yet to be resolved.

The aim of this study was to use ^{23}Na n.m.r. spectroscopy to determine intracellular levels of sodium in suspensions of proximal tubules obtained from rat kidneys and to compare the effect of two natriuretic agents, acetazolamide and the calcium channel antagonist amlodipine on this Na_i content. In this way the action of a compound of known proximal tubular site of action, such as ACTZ, could be compared with that of a compound whose site of action is unknown but which could be acting at the proximal tubule.

Methods

General dissection

The methods used to isolate the proximal tubules were based on techniques described by Balaban *et al.* (1980), Vinay *et al.* (1981) and Gesek *et al.* (1987). Male Wistar rats, 350–400 g, were anaesthetized with Sagatal, 60 mg kg^{-1}, i.p., the kidneys were then exposed via a midline incision and the intestines were displaced to the left. The aorta and vena cava were then cannulated below the level of the kidneys and 500 u heparin was immediately injected intravenously to prevent blood coagulation. Loose ligatures were placed around the aorta and vena cava above the renal vessels and the mesenteric and coeliac arteries were tied off. Prior to the perfusion of the kidneys, the ligatures above the kidneys were tightened to form a closed system.

Both kidneys were then perfused with the physiological buffer solution (containing in mM: NaCl 115, $NaHCO_3$ 25, KCl 5, glucose 5, $MgSO_4$ 1, L-alanine 1, sodium lactate 4, mannitol 25, $CaCl_2$ 2, dextran 0.6%, NaH_2PO_4 2) which was saturated with 95% O_2/5% CO_2 and kept at 37°C, through the aortic cannula. Perfusion pressure was monitored with an on-line manometer and the perfusion rate adjusted to achieve a perfusion pressure of approximately 120 mmHg. When the venous effluent was seen to be clear of blood, the perfusate was changed to an enzyme solution (containing, in mM: NaCl 115, $NaHCO_3$ 25, KCl 5, glucose 5, $MgSO_4$ 1, L-alanine 1, sodium lactate 4, $CaCl_2$ 2, dextran 0.6%, NaH_2PO_4 2, collagenase 40 u ml^{-1}). The enzyme solution was collected from the venous cannula and reinfused into the kidneys until the perfusate had infiltrated into surrounding tissue and no perfusate could be collected at the venous end, which was typically achieved after approximately 10–15 min. The kidneys were immediately removed, placed into a beaker of ice-cold buffer (containing, in mM: NaCl 115, $NaHCO_3$ 25, KCl 5, glucose 5, $MgSO_4$ 1, L-alanine 1, sodium lactate 4, $CaCl_2$ 2, dextran 0.6%, NaH_2PO_4 2). The kidneys were then decapsulated, placed on a glass petri dish, which was kept on ice, and sliced into transverse sections approximately 2 mm thick. The medulla was dissected away and the cortical slices were minced with a razor blade and placed into 15 ml of the enzyme solution. This suspension was incubated at 37°C for 35 min under an atmosphere of 95% O_2/5% CO_2. At 7 min intervals during the incubation, the tubules were gently dispersed by pulling the suspension through a long Pasteur pipette. After 35 min the enzyme solution containing the suspension of dissociated tubules was centrifuged at 120 *g* at 4°C for 1 min (MSE Mistral 3000). The collagenase solution was decanted away and the tubules were placed into 10 ml of fresh ice-cold buffer solution. The new suspension was filtered through 3 layers of surgical gauze to remove any undissociated tissue and the centrifugation process was repeated 3 times.

The proximal tubules were then purified by differential centrifugation in Percoll. Fresh Percoll was made isotonic with a buffer solution (containing in mM: NaCl 1150, $NaHCO_3$ 250, KCl 50, $MgSO_4$ 0.5, mannitol 350, NaH_2PO_4 20) in a 9:1 ratio of undiluted Percoll to buffer. The isotonic Percoll was adjusted to pH 7.4 with HEPES. This isotonic Percoll was taken as 100% and subsequent dilutions were made from this isotonic stock. A 45% Percoll solution was prepared by diluting the 100% stock with a dilution solution (containing, in mM: NaCl 115, $NaHCO_3$ 25, KCl 5, $MgSO_4$ 0.05, mannitol 35, NaH_2PO_4 2). This was kept at 4°C and under an atmosphere of 95% O_2/5% CO_2 for at least 30 min before use.

The tubules were washed twice by low speed centrifugation (500 r.p.m. for 1 min) in 10 ml of the dilution solution and then placed into 30 ml of the 45% Percoll in a 50 ml centrifuge tube. Five millilitres of undiluted isotonic Percoll was then injected carefully into the bottom of the tube. This suspension was then centrifuged at 18,000 *g* at 4°C for 10 min (8 × 50 fixed head rotor on a MSE superspeed 50 or 17,540 *g* with a SS-34 rotor head on a Sorvall refrigerated centrifuge). The resulting four to five layers were then removed separately with a Pasteur pipette. The upper two thirds were discarded, whilst the bottom two layers, which contained the proximal tubules, were washed three times by low speed centrifugation (500 r.p.m. for 1 min) in 10 ml solutions of the ice-cold buffer solution to remove any remaining Percoll and then resuspended in the ice-cold buffer and kept on ice until use.

Physiological viability

The viability of the tubular suspensions was estimated by the trypan blue exclusion test and by ATP measurements of the tissues at the end of the preparation procedure. ATP concentrations were determined with an ATP analysis kit (Sigma UK, procedure No. 366-UV). At the same time samples were also taken for protein determination, which was performed with a Sigma kit (procedure No. P5656), utilising the principles of the Lowry procedure (Lowry *et al.*, 1951).

Nuclear magnetic resonance methods

The shift reagent, dysprosium tripolyphosphate, ($Dy(PPP_i)_2^{7-}$), was prepared, prior to use, by making up 100 mM $DyCl_3$ in a 50 mM HEPES-buffered solution containing 200 mM sodium tripolyphosphate. The working solution of the shift reagent was prepared by diluting the stock shift reagent with a low sodium buffer (containing, in mM: NaCl 85, $NaHCO_3$ 25, KCl 5, glucose 5, $MgSO_4$ 1, L-alanine 1, sodium lactate 4, $CaCl_2$ 2, dextran 0.6%, NaH_2PO_4 2) in a ratio of 1:25 with respect to the buffer. This gave a final concentration of 4 mM of $Dy(PPP_i)_2^{7-}$. The proximal tubules were then suspended in the buffer/shift reagent to give a protein concentration of approximately 40 mg protein ml^{-1}.

The n.m.r. spectra were collected using a Bruker 250 spectrometer operating at 66 MHz which accumulated 5000 scans for each spectrum using an acquisition time of 70 ms per scan; a total accumulation time of approximately 5.8 min. Application of 90° pulses every 70 ms ensured that the spectra were fully relaxed. In some experiments a Jeol JNM-GX270 was also used, operating at 71 MHz and 1024 scans were performed for each spectra with an acquisition time of 102 ms, plus a pulse delay of 150 ms, giving an accumulation time of approximately 4.5 min.

Between 1.5–2.0 ml of the suspension was placed in a 10 mm diameter n.m.r. tube. The shift reagent, containing 10% deuterium oxide to act as a frequency lock, and one drop of antifoam reagent B was added to the suspension prior to placing it in the n.m.r. probe. A single bubbling system was arranged to give very gentle agitation of the suspension during the experiment. The probe was kept at 37°C and acquisition was begun immediately after the tubule suspension was placed in the probe. The spectral peaks were

analysed by integration, using Bruker software, which gave an area under the curve for each peak.

It took approximately 10 min for the sample temperature to rise to 37°C after placing the n.m.r. tube, which had been kept at 0–4°C, in the probe. Agents with known effects on the sodium transport in the kidney were then infused into the suspension via an infusion line, 25–30 min after the suspension had been placed into the probe. The temperature of the probe was monitored by an internal thermometer.

Drug treatments

Ouabain (10^{-3} M), acetazolamide (10^{-3} M) or amlodipine (10^{-4} M) or vehicle alone (physiological buffer), was added to the suspension 25–30 min after the tubule suspension had been placed into the probe. The drugs were dissolved in the buffer solution and added to the suspension via the infusion line in a volume of 0.5 ml to give the final concentrations quoted above. After the test drug or vehicle only had been delivered to the suspension, further spectra were acquired over the subsequent 25–30 min to establish whether there was any effect on the intracellular sodium content. Changes were recorded as deviations from the steady state level (100%) just prior to the addition of the drug.

Calculations

Assuming that the intracellular sodium is 100% visible, the sodium content within the cells of the rat proximal tubules can be calculated by comparison of the intracellular sodium peak integral (area underneath the curve) with the integral of the extracellular peak, together with knowledge of the extracellular sodium concentration, which was determined by flame photometry, and the protein content of the sample, as described by Gullans *et al.* (1985). This ensures the derivation of the sodium content of the sample in a specific n.m.r. spectrum, with units of nmol mg^{-1} protein. Assuming that there is 0.75 mg protein mg^{-1} dry wt (Balaban *et al.*, 1980) the sodium content can be converted to units of nmol mg^{-1} dry wt.

Statistical analysis

The n.m.r. data were tested by one way analysis of variance followed by Bonferoni *post-hoc* analysis, comparing steady state intracellular sodium levels with changes due to the effect of the drug over time. All statistical computations were obtained with statistical software, Superanova (Abacus). Significant differences were taken when P was less than 5%.

Chemicals

Heparin was supplied as Multiparin (Fisons UK). Antifoam reagent B, ouabain, acetazolamide, collagenase (type IV, 1000 u ml^{-1}) and Percoll, supplied as 23% w/w colloidal solution were purchased from Sigma UK. Amlodipine was supplied by Pfizer UK.

Results

Proximal tubule morphology

Microscopic examination indicated that the fraction retained from the bottom two layers of the 45% Percoll purification step consisted of greater than 95% of proximal tubules. Examination by phase-contrast microscopy indicated that the proximal tubules were 250–400 μm in length and they had a characteristic brush border with open lumens.

Tubular viability

The majority of the tubules sampled excluded trypan blue for up to 15 min which indicated that the cells were still alive. More accurate measurements were provided by the ATP analysis of the tubule suspensions. The ATP levels for these experiments (Table 1) were between 6–12 nmol ATP mg^{-1} protein. No treatment group was significantly different from the proximal tubules incubated in buffer alone, which indicated that the tissues were still undergoing active respiration.

n.m.r. results

A typical ^{23}Na n.m.r. spectrum of a proximal tubule suspension is shown in Figure 1. The smaller peak (A_i) is the intracellular sodium signal and the larger peak (A_e), which has been shifted to the right, is the extracellular sodium signal. The horizontal scale is given in p.p.m. In all n.m.r. experiments, the shift difference between the intra- and extracellular peaks was between 7–10 p.p.m. which provided a good resolution between the two peaks.

Effect of temperature on sodium content in suspensions of proximal tubules

Figure 2 shows the effect on the intracellular sodium content due to warming suspensions of proximal tubules from 4°C to 37°C. On placing the suspension in the probe, which was at 37°C, sodium content fell significantly ($P < 0.001$) over the subsequent 15 min. The sodium efflux followed an exponential rate which gave a value of $k = 0.15 \pm 0.02$ min^{-1}. The rate constant, k, was calculated from the gradient of the graph by regression analysis. Steady state levels of intracellular sodium, at 37°C, were calculated to be 79.9 ± 5.1 nmol mg^{-1} protein which was equivalent to 60.0 ± 3.8 nmol mg^{-1} dry wt and 19.0 ± 1.2 mM ($n = 57$) and this level was chosen as the 100% level from which deviations due to drug application would be recorded.

Table 1 ATP levels in proximal tubule suspensions

Control	*Ouabain*	*ACTZ*	*Amlodipine*
11.1 ± 0.9	10.7 ± 1.9	13.1 ± 2.7	10.4 ± 1.5
$n = 22$	$n = 3$	$n = 3$	$n = 4$

All ATP concentrations given as nmol ATP mg^{-1} protein. No treatment group was significantly different from the proximal tubules incubated in buffer alone when tested using analysis of variance. ACTZ = acetazolamide.

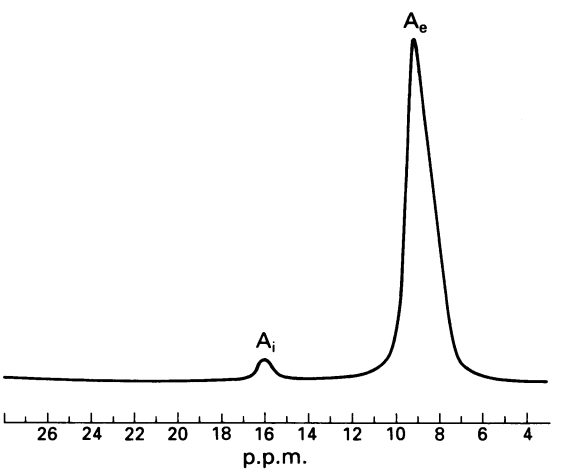

Figure 1 A typical ^{23}Na n.m.r. spectra of intra- and extracellular sodium intensities in a suspension of rat proximal tubules. A_i represents the intracellular sodium peak and A_e represents the extracellular sodium peak. The horizontal scale is given in p.p.m. In all n.m.r. experiments, the shift difference between the intra- and extracellular peaks was between 7–10 p.p.m. which provided a good resolution between the two peaks.

The effect of pharmacological agents on $[Na]_i$ using n.m.r.

In the 7 experiments performed for the control study, in which the vehicle was added once steady state was reached, the intracellular sodium content of the proximal tubules did not change significantly from the baseline level over the subsequent 20–30 min (Figure 3).

In a further set of 4 experiments, addition of ouabain 10^{-3} M, once steady state had been reached, caused a rapid and significant ($P<0.01$) increase in intracellular sodium content, by approximately 30% of the steady state, after 5 min and the effect was seen to plateau at about 70% after 30 min (Figure 3). The increase in $[Na]_i$ after addition of ouabain, over 30 min was significantly different from the steady state level ($P<0.01$).

Following the addition of ACTZ 10^{-3} M, in 5 experiments, the steady state intracellular sodium content of the proximal tubule suspension was seen to increase by approximately 35% within 5 min and thereafter increased in a time-dependent manner, peaking at about 45% after 30 min (Figure 4). The rise in intracellular sodium content due to ACTZ was significantly different from the steady state level ($P<0.001$) but the magnitude of increase was smaller than that seen with ouabain after 30 min ($P<0.05$).

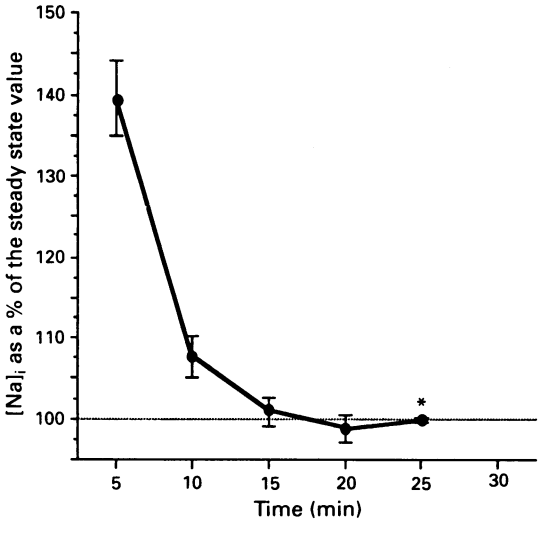

Figure 2 The effect of increasing temperature on intracellular sodium content in proximal tubules. The points are means of 17 experiments. At time 0 the tubule suspension was at 0–4°C and when placed in the n.m.r. probe it was warmed to the ambient temperature of the probe which was kept at 37°C. Steady state was reached after 15–20 min and was designated 100%. *$P<0.001$ for the decrease in intracellular sodium.

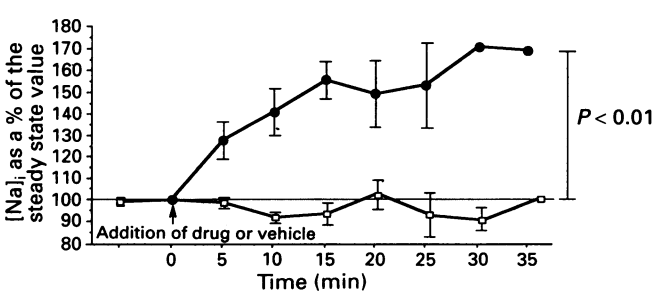

Figure 3 The effect of vehicle alone, in seven experiments (□) and ouabain 10^{-3} M, four experiments (●) on intracellular sodium content in proximal tubules. Steady state was reached after 15–20 min and was designated 100% and intracellular sodium was plotted as a percentage of this steady state. The profile of response seen over 30 min in the presence of vehicle alone was significantly different from that seen in the presence of ouabain ($P<0.01$).

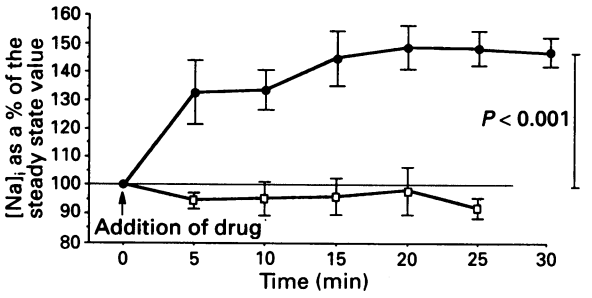

Figure 4 The effect of acetazolamide (ACTZ, 10^{-3} M) in five experiments (●) and amlodipine 10^{-4} M, in four experiments (□) on intracellular sodium content in proximal tubules. Intracellular sodium was plotted as percentage change in steady state, which was designated 100%. The profile of response seen in the presence of ACTZ was significantly different from that seen with the control study ($P<0.001$). The response seen with amlodipine was not significantly different from the baseline levels.

In a group of 4 experiments, addition of amlodipine to a final concentration of 10^{-4} M to the proximal tubule suspension appeared to have no effect on the steady state intracellular sodium level (Figure 4). The intracellular sodium content remained relatively constant after the addition of amlodipine over 30 min and did not vary by any significant amount from the level prior to drug treatment, nor was it significantly different from that observed when the vehicle was given alone.

Discussion

The purpose of this study was to follow changes in intracellular sodium content within the epithelial cells of suspensions of rat proximal tubules using ^{23}Na n.m.r. spectroscopy. The paramagnetic shift reagent, $Dy(PPP_i)_2^{7-}$, permitted the resolution of intra- and extracellular sodium in the n.m.r. spectrum (Figure 1), thus providing the possibility of assessing changes in intracellular sodium due to changes in the external environment and application of drugs. The concentration of $Dy(PPP_i)_2^{7-}$ chosen, 4 mM, had been previously reported to be non-toxic (Gullans *et al.*, 1985) and the initial trypan blue exclusion test supported this. Moreover, ATP levels in the tubules (Table 1) were similar to or greater than levels reported in the literature (Gesek *et al.*, 1987) and this provided further evidence to support the view that the tubules were functionally normal. Thus the tubules were respiring and able to generate and retain their intracellular ATP content at a level comparable to other studies (Balaban *et al.*, 1980). At 4 mM, $Dy(PPP_i)_2^{7-}$ also provided a shift between the two sodium peaks (about 8 p.p.m.) which was sufficient to permit accurate resolution of the intra- and extracellular sodium signals.

The study with ACTZ was aimed at examining whether it was able to change intracellular sodium and to this end a high dose was used which would completely block both luminal and cytosolic carbonic anhydrase. ACTZ increased intracellular sodium content in suspensions of proximal tubules by 45% compared to the steady state level after 30 min of incubation with ACTZ, which was taken to indicate a reduction in the rate of sodium flux. This action of ACTZ was probably achieved as the consequence of the blockade of the enzyme, carbonic anhydrase. Carbonic anhydrase (CA) has been positively identified by histological staining throughout the kidney and extensively in the proximal tubule in both the luminal membrane and cytosol (Lönnerholm & Ridderstale, 1980; Dobyan *et al.*, 1982). The enzyme facilitates the conversion of HCO_3^- and H^+ to H_2O and CO_2 at the luminal membrane and the regeneration of intracellular HCO_3^- and H^+. The consequence of the luminal

action of ACTZ would be to inhibit CA-catalysed HCO_3^- transport across the luminal membrane. In the cytosol, CA inhibition by ACTZ would reduce the intracellular levels of HCO_3^- and hence the total basolateral $NaHCO_3$ transport via the $Na^+/(HCO_3^-)_3$ symporter (Preisig *et al.*, 1987). Moreover, in other studies, ACTZ has been shown to decrease the activity of the $Na^+/(HCO_3^-)_3$ symporter on the basolateral membrane of rabbit isolated perfused S2 proximal tubules (Sasaki & Marumo, 1989). This could result in a reduction in the rate of total intracellular sodium efflux since it has been suggested that the $Na^+/(HCO_3^-)_3$ symporter is responsible for up to $\frac{1}{3}$ of the total sodium transported across the basolateral membrane (Moe *et al.*, 1990) while Sasaki & Marumo (1989) suggested that the symporter could account for 50% of the sodium removed from the proximal tubule cell at the basolateral membrane. Thus, in this present study the basolateral sodium exit could have been inhibited by ACTZ reducing the activity of the $Na^+/(HCO_3^-)_3$ symporter, the outcome of which was an increase in intracellular sodium content. $NaHCO_3$ transport into the cell would also have been inhibited but sodium entry would still occur via other transporters. The observed increase in intracellular sodium due to ACTZ was of a smaller magnitude than that seen by ouabain after 30 min ($P<0.05$) which suggests that the Na^+/K^+/ATPase provides the greater driving force for basolateral Na^+ transport.

Increasingly, calcium channel antagonists (CCA), especially the dihydropyridine variety, have been reported to have natriuretic and diuretic properties (Struyker-Boudier *et al.*, 1990). There is a possibility that the calcium channel antagonists act directly on tubular transport processes to cause natriuresis and Rodicio *et al.* (1990) reported that nifedipine increased sodium excretion in man without altering GFR and renal plasma flow, which suggested a tubular action. Figueiredo *et al.* (1982) also demonstrated that verapamil, a phenylalkylamine CCA, attenuated sodium reabsorption in rabbit isolated perfused proximal tubules when it was added to the bathing solution and felodipine has been shown to cause natriuresis and diuresis, without affecting renal haemodynamics, in anaesthetized normotensive dogs when administered via the renal artery (DiBona, 1990). Amlodipine is a recently developed dihydropyridine class CCA (Burges *et al.*, 1987) which has been demonstrated to have natriuretic properties *in vivo* (Johns, 1988). In this present study, amlodipine 10^{-4} M, a concentration which has been shown to block Ca^{2+}-induced contractions in rat isolated aorta (Burges *et al.*, 1987), was utilised to determine whether it had effects at the level of the proximal tubules. The addition of amlodipine to the proximal tubule suspension did not alter the Na^+ content from the steady state level which remained constant throughout the experiment, even 30 min after amlodipine was added. The present observations were in agreement with functional studies on rats, using lithium clearance as a measure of proximal Na^+ reabsorption (Johns, 1988) which found that amlodipine at concentrations of 200 $\mu g\ kg^{-1}$ and 400 $\mu g\ kg^{-1}$ did not have any significant action on Na^+ transport at the proximal tubule segment which suggested that the natriuretic action was due to an effect further along the tubule. This conclusion supports the findings that in this preparation amlodipine does not act directly at the proximal tubule to alter intracellular sodium content. Conversely studies have been conducted which indicate that the dihydropyridine class of calcium channel antagonists do have an influence on proximal tubule function. McCarty & O'Neil (1991) determined that rabbit proximal straight tubule had nifedipine-sensitive Ca^{2+} channels on the basolateral membrane which were activated during cell swelling. The reasons for these conflicting findings are not clear but it may be that these channels only become apparent under conditions of chemiosmotic stress and were not functional under the conditions of the present study.

We have used ^{23}Na n.m.r. spectroscopy to follow changes in intracellular sodium content in rat proximal tubular cells. The results presented in this study demonstrate that intracellular sodium levels are temperature-dependent, which probably reflects a dependency on the activity of Na^+/K^+/ATPase enzyme. This view was supported by the observation that, following blockade of the Na^+/K^+/ATPase with ouabain, sodium content gradually rose. Administration of the natriuretic agent ACTZ also increased intracellular sodium which was consistent with ACTZ's known action of blocking carbonic anhydrase activity. By contrast, the dihydropyridine calcium channel antagonist, amlodipine, appeared to have no effect on sodium transport at the proximal tubule suggesting that the compound does not act at this site.

The tubular cells became sodium-loaded during the preparation at 0–4°C and when allowed to warm to 37°C intracellular sodium decreased in an exponential way (Figure 4). The sodium efflux followed an exponential decay over 15–25 min. The rate constant, $k = 0.15 \pm 0.02\ min^{-1}$, was similar to that reported by Gullans *et al.* (1985) ($k = 0.14\ min^{-1}$) whose team used a similar approach, but with rabbit proximal tubules. In their case, the suspension warmed to 37°C over approximately 10 min whereas the $[Na]_i$ reached steady state after approximately 20 min which was similar to the results reported here. Gullans *et al.* (1985) undertook detailed metabolic studies to provide evidence that suggested that this time course and rate of efflux of intracellular sodium corresponded closely with the rate of ATP regeneration, which indicated that the re-energization of the cells involved an increase in ATP at the same time as a decline in intracellular sodium content.

The steady state intracellular sodium content of the proximal tubules prepared in the present study was about 80 nmol mg^{-1} protein, which corresponded to approximately 60 nmol mg^{-1} dry wt and by using cell volume estimation (Grantham *et al.*, 1977) gave a real intracellular sodium concentration of 19 mM. This value of intracellular sodium derived in the present study corresponded closely to those obtained by Kumar *et al.* (1986), 17 mM versus 19 mM, who also used suspensions of rat proximal tubules and Rayson & Gupta (1985) reported a n.m.r. visible $[Na]_i$ of 23 mM at 37°C in rat outer medullary tubules. In tests by Beck *et al.* (1980) using electron probe microanalysis, *in vitro*, reported values were 22.4 mM for the intracellular sodium content in the rat proximal tubule, which corresponds closely with the values obtained in the current study.

Ouabain was chosen as an accepted tool for blockade of the sodium pump in this tissue and was used at a high concentration, comparable to that utilised by Gullans *et al.* (1985) and by Kumar *et al.* (1986). Incubation with ouabain, a sodium pump inhibitor, rapidly increased $[Na]_i$ by 30% in the first 5 min and finally reached a plateau at 70% over the next 25 min. This pattern of response was comparable to results obtained by Gullans *et al.* (1985), who reported a rapid increase of 45% over the initial 2.5 min and then a more steady rise to 78% over the next 30 min and those observed by Boulanger *et al.* (1987), using the dog cortical tubules. The results of the present study clearly showed application of a known inhibitor of the sodium pump lead to appropriate and meaningful changes in sodium content in the proximal tubular epithelial cell.

P.S.K.W. was supported by an MRC collaborative research studentship. We are grateful to David Bowen, Michael Kinns and Alistair Swanson of Pfizer Central Research for their helpful advice and support.

References

BALABAN, R.S., SOLTOFF, S., STOREY, J.M. & MANDEL, L.J. (1980). Improved renal cortical tubule suspension: spectrophotometric study of O_2 delivery. *Am. J. Physiol.*, **238**, F50–F59.

BAUM, M. (1987). Evidence that parallel Na^+-H^+ and Cl^--HCO_3^-(OH^-) antiporters transport NaCl in the proximal tubule. *Am. J. Physiol.*, **252**, F338–F345.

BECK, F., BAUER, R., BAUER, U., MASON, J., DORGE, A., RICK, R. & THURAU, K. (1980). Electron microprobe analysis of intracellular elements in the rat kidney. *Kidney Int.*, **17**, 756–763.

BERRY, C.A. (1982). Heterogeneity of tubular transport processes in the nephron. *Annu. Rev. Physiol.*, **44**, 181–201.

BOULANGER, Y., VINAY, P. & BOULANGER, M. (1987). NMR monitoring of intracellular sodium in dog and rabbit tubules. *Am. J. Physiol.*, **253**, F904–F911.

BOULANGER, Y., VINAY, P. & DESROCHES, M. (1985). Measurement of a wide range of intracellular sodium concentrations in the erythrocytes by ^{23}Na nuclear magnetic resonance. *Biophys. J.*, **47**, 553–561.

BURGES, R.A., GARDINER, D.G., GWILT, M., HIGGINS, A.J., BLACKBURN, K.J., CAMPBELL, S.F., CROSS, P.E. & STUBBS, J.K. (1987). Calcium channel blocking properties of amlodipine in vascular smooth muscle *in vitro*: evidence for the voltage modulation of vascular dihydropyridine receptors. *J. Cardiovasc. Pharmacol.*, **9**, 110–119.

DIBONA, G.F. (1990). Renal effects of felodipine: a review of experimental evidence and clinical data. *J. Cardiovasc. Pharmacol.*, **15**, S29–S32.

DOBYAN, D.C., MAGILL, L.S., FRIEDMAN, P.A., HERBERT, S.C. & BULGER, R.E. (1982). Carbonic anhydrase histochemistry in rabbit and mouse kidneys. *Anat. Rec.*, **204**, 185–197.

DUBOSE, T.D.Jr. (1990). Reclamation of filtered bicarbonate. *Kidney Int.*, **38**, 584–589.

FIGUEIREDO, J.F., CONTI, D.F., SIGULEM, D. & RAMOS, O.L. (1982). Tetracaine, procaine and verapamil inhibition of fluid absorption in isolated perfused rabbit proximal convoluted tubules. *Brazilian J. Med. Biol. Res.*, **15**, 259–264.

GESEK, A.F., WOLFF, D.W. & STRANDHOY, J.W. (1987). Improved separation method for rat proximal and distal tubules. *Am. J. Physiol.*, **253**, F358–F365.

GESEK, F.A. & SCHOOLWERTH, A.C. (1990). Hormonal interactions with the proximal Na^+-H^+ exchanger. *Am. J. Physiol.*, **258**, F514–F521.

GRANTHAM, J.J., LOWE, C.M., DELLASEGA, M. & COLE, B.R. (1977). Effect of hypertonic medium on the K and Na content of proximal renal tubules. *Am. J. Physiol.*, **1**, F42–F49.

GULLANS, S.R., AVISON, M.J., OGINO, T., GIEBISCH, G. & SHULMAN, R.G. (1985). NMR Measurements of intracellular sodium in the rabbit proximal tubule. *Am. J. Physiol.*, **249**, F160–F168.

JOHNS, E.J. (1988). A study of the renal actions of amlodipine in the normotensive and spontaneously hypertensive rat. *Br. J. Pharmacol.*, **94**, 311–318.

KONDO, Y. & FRÖMTER, E. (1990). Evidence for chloride/bicarbonate exchange mediating bicarbonate efflux from S3 segments of rabbit renal proximal tubule. *Pflügers Arch.*, **415**, 726–733.

KRAPF, R. (1989). Physiology and molecular biology of the renal Na^+/H^+ antiporter. *Klin. Wochenschr.*, **67**, 847–851.

KUMAR, A.M., SPITZER, A. & GUPTA, R.K. (1986). ^{23}Na NMR spectroscopy of proximal tubule suspensions. *Kidney Int.*, **29**, 747–751.

LÖNNERHOLM, G. & RIDDERSTALE, Y. (1980). Intracellular distribution of carbonic anhydrase in the rat kidney. *Kidney Int.*, **17**, 162–174.

LOWRY, O.H., ROSEBROUGH, N.J., FARR, A.L. & RANDALL, R.J. (1951). Protein measurement with Folin phenol reagent. *J. Biol. Chem.*, **193**, 265–275.

MCCARTY, N.A. & O'NEIL, R.G. (1991). Calcium-dependent control of volume regulation in the renal proximal tubule cells: II. Roles of dihydropyridine-sensitive and -insensitive Ca^{2+} entry pathways. *J. Memb. Biol.*, **123**, 161–170.

MOE, O., PREISIG, P. & ALPERN, R. (1990). Cellular model of proximal tubule NaCl and $NaHCO_3$ absorption. *Kidney Int.*, **38**, 605–611.

PREISIG, P.A., TOTO, R.D. & ALPERN, R.J. (1987). Carbonic anhydrase inhibitors. *Renal Physiol.*, **10**, 136–159.

RAYSON, B.M. & GUPTA, R.K. (1985). ^{23}Na NMR studies of rat outer medullary kidney tubules. *J. Biol. Chem.*, **260**, 7276–7280.

RODICIO, J.L., MORALES, J.M. & RUILOPE, L.M. (1990). Calcium antagonists and the kidney. *Nephrol. Dial. Transplants*, **5**, 81–86.

SASAKI, S. & MARUMO, F. (1989). Effects of carbonic anhydrase inhibitors on the basolateral base transport of rabbit proximal straight tubule. *Am. J. Physiol.*, **26**, F947–F952.

SILBERNAGL, S., FOULKES, E.C. & DEETJEN, P. (1975). Renal transport of amino acids. *Rev. Physiol. Biochem. Pharmacol.*, **74**, 105–167.

STRUYKER-BOUDIER, H.A.J., SMITS, J.F.M. & DEMEY, J.G.R. (1990). The pharmacology of calcium antagonists: a review. *J. Cardiovasc. Pharm.*, **15**, S1–S10.

VINAY, P., GOUGOUX, A. & LEMIEUX, G. (1981). Isolation of a pure suspension of rat proximal tubules. *Am. J. Physiol.*, **241**, F403–F411.

(Received October 21, 1994
Revised March 7, 1994
Accepted April 7, 1994)

Br. J. Pharmacol. (1994), **112**, 887–894

Effects of selective ET_B-receptor stimulation on arterial, venous and capillary functions in cat skeletal muscle

[1]Ulf Ekelund, *Mikael Adner, *Lars Edvinsson & Stefan Mellander

Department of Physiology & Biophysics and *Department of Medicine, University and University Hospital of Lund, Sweden

1 This paper describes, in quantitative terms, the *in vivo* effects of two selective ET_B-receptor agonists (IRL 1620 and BQ 3020) on vascular resistance (tone) in the following consecutive sections of the vascular bed of sympathectomized cat skeletal muscle: large-bore arterial resistance vessels (>25 μm), small arterioles (<25 μm) and the veins. The effects on capillary pressure and transcapillary fluid exchange were also recorded.

2 Both IRL 1620 and BQ 3020, infused i.a. to the muscle preparation, evoked an initial transient dilator response followed by a moderate dose-dependent constrictor response, both being preferentially confined to the small arterioles. The dilator response was associated with a transient increase, and the constrictor response with a sustained decrease, in capillary pressure, the latter causing net transcapillary fluid absorption. The capillary filtration coefficient decreased during the constrictor response, indicating constriction of terminal arterioles/precapillary sphincters.

3 The vascular responses to the ET_B-receptor agonists were unaffected by blockade of endothelium-derived nitric oxide (N^G-nitro-L-arginine methyl ester) and by selective ET_A-receptor blockade (FR139317). However, blockade of prostacyclin production with indomethacin decreased the amplitude of the dilator response, and decreased the time required to reach a steady-state vasoconstrictor response to the ET_B-receptor agonists.

4 The effect of ET_B-receptor stimulation on vascular tone was also evaluated *in vitro* on the cat femoral artery and vein. IRL 1620 had no effect on the femoral artery but caused a weak dose-dependent relaxation in the femoral vein. This large vein relaxation response seemed to be mediated by endothelium-derived nitric oxide and not by prostacyclin.

5 It may be concluded that ET_B-receptor stimulation is responsible for the dilator response, and can contribute to the constrictor response, elicited by endothelins in cat skeletal muscle *in vivo*.

Keywords: Arteries; capillaries; capillary pressure; endothelins; ET_A-receptor; ET_B-receptor; microcirculation; prostacyclin; veins

Introduction

Endothelin-1, -2 and -3 exert their actions in the cardiovascular system via at least two different receptor subtypes, the ET_A- and ET_B-receptors (Rubanyi & Parker Botelho, 1991; Sakurai *et al.*, 1992). Binding to ET_A-receptors on vascular smooth muscle cells elicits contraction, whereas binding to ET_B-receptors, considered to be located on the endothelial cells, causes relaxation, as evidenced by *in vitro* experiments (for references see Sakurai *et al.*, 1992). The latter effect has been attributed to a secondary release of endothelium-derived nitric oxide (EDNO) and/or prostacyclin (see Rubanyi & Parker Botelho, 1991; Sakurai *et al.*, 1992). *In vivo*, activation of the vascular ET_A-receptor elicits a vasoconstrictor response (see Sakurai *et al.*, 1992; Masaki *et al.*, 1992), whereas the contribution of the ET_B-receptor to the vascular effect evoked by the endothelins in the peripheral circulation is more uncertain. Some recent *in vivo* studies of the effects of ET_B-receptor agonists suggest that the ET_B-receptor can mediate not only a vasodilator, but also a vasoconstrictor response (Bigaud & Pelton, 1992; Gardiner *et al.*, 1994). These results were based on observations of ET_B-induced effects on blood flow velocity in some major arteries in the systemic circulation in the presence of ET_A-receptor blockade.

To elucidate further the possible role of the ET_B-receptor in vascular regulation *in vivo*, there is a need for more detailed information about the effects of selective ET_B-receptor agonists on volume blood flow in homogeneous tissues, instead of composite organs. Further, their control of different vascular functions, and their site(s) of action in the consecutive segments of the vascular bed, need to be defined.

In the present study an attempt was made to provide such information by studying the circulatory effects of two different newly described selective ET_B-receptor agonists, IRL 1620 (Takai *et al.*, 1992) and BQ 3020 (Ihara *et al.*, 1992) in a pure lower leg muscle preparation in the cat. The technique used permitted quantitative analyses of the resistance responses to these agonists in the whole vascular bed, and its consecutive segments: large-bore arterial resistance vessels (>25 μm), small arterioles (<25 μm) and the veins. The associated effects on hydrostatic capillary pressure and transcapillary fluid exchange were also recorded. To elucidate the mechanisms underlying the vascular responses to IRL 1620 and BQ 3020, comparative observations were made in the absence and presence of selective ET_A-receptor blockade (FR139317; Sogabe *et al.*, 1992; 1993), blockade of the production of EDNO (N^G-nitro-L-arginine methyl ester; L-NAME) or prostacyclin (indomethacin). As a complement to the *in vivo* study, effects of the ET_B-receptor agonists on vascular tone were analysed *in vitro* in large conduit vessels supplying the cat hindlimb, i.e. the femoral artery and vein.

Methods

In vivo *experiments on the skeletal muscle circulation*

Skeletal muscle preparation and recordings The study was performed on young adult male cats (mean body wt 4.2 kg), anaesthetized intravenously with α-chloralose (50 mg kg^{-1} body wt, if necessary later supplemented by 20 mg kg^{-1} body wt) applied via a venous catheter inserted under local anaes-

[1] Author for correspondence.

thesia (lignocaine). After anaesthesia, a tracheal cannula was inserted to facilitate spontaneous respiration. Expiratory P_{CO_2} and body temperature were monitored continuously and stayed within normal limits during the experiments.

Observations were made on the acutely sympathectomized lower leg muscles of the right hindlimb, a preparation described in detail elsewhere (Mellander *et al.*, 1987). In brief, the muscle region was auto-perfused *in situ* via an arterial shunt placed between the femoral and popliteal artery. The muscle preparation, with intact arterial and venous supply, was enclosed in a Ringer fluid-filled plethysmograph, using special cannulation and instrumentation techniques described in detail elsewhere (Mellander *et al.*, 1987; Björnberg *et al.*, 1988). With this method, it is possible to obtain reliable continuous recordings of the following circulatory variables: arterial, arteriolar, capillary and venous pressures, regional blood flow, net transcapillary fluid flux, and resistances in the whole muscle vascular bed (R_T) and in the following consecutive vascular sections: large-bore arterial resistance vessels (> 25 μm; $R_{a,prox}$), small arterioles (< 25 μm; $R_{a,micro}$), and the veins (R_V). All parameters were recorded on a 10-channel Grass Polygraph.

After completion of surgery and instrumentation, the animals were left to equilibrate so as to permit the recovery of intrinsic myogenic vascular tone to a normal and stable level (Maspers *et al.*, 1990b) before the start of the experimental interventions.

Calculations and experimental protocols Total and segmental vascular resistances in the muscle preparation were derived as follows from the recorded regional blood flow (Q) and the relevant driving pressures obtained from the four pressure signals, arterial inflow pressure (P_A), pressure in arterioles of a size of about 25 μm ($P_{arteriole}$), capillary pressure towards the venous end of the capillaries ($P_{c,v}$) and the venous outflow pressure (P_V): $R_T = (P_A - P_V)/Q$; $R_{a,prox} = (P_A - P_{arteriole})/Q$; $R_{a,micro} = (P_{arteriole} - P_{c,v})/Q$; $R_v = (P_{c,v} - P_V)/Q$. Implicit in this methodological approach is that the sum of the three segmental resistances always equals the simultaneously recorded R_T value. These vascular resistances were continuously recorded with the aid of electronic divider circuits (for technical details see Björnberg *et al.*, 1988). All resistances are expressed as PRU values (peripheral resistance units; mmHg ml^{-1} min 100 g tissue).

The arterial versus venous resistance responses, i.e. changes in the pre- to postcapillary resistance ratio ($(R_{a,prox} + R_{a,micro})/R_v$) evoked by the ET_B-receptor agonists led to changes in hydrostatic capillary pressure and net transcapillary fluid exchange. Net transcapillary fluid movement during ET_B agonist infusion was assessed from the observed net change in tissue volume, after correction for the tissue volume change caused by the initial vascular capacitance response.

The capillary filtration coefficient (CFC) was used as an index of overall hydraulic conductivity across the exchange vessels in the muscle preparation, in turn reflecting the size of the functional capillary surface area available for fluid exchange (Folkow & Mellander, 1970). CFC (ml min^{-1} 100 g^{-1} mmHg^{-1}) was determined by raising venous outflow pressure by 5 mmHg and was calculated from the rate of the resulting net transcapillary fluid filtration divided by the directly observed increase in capillary pressure ($P_{c,v}$).

In vitro *experiments on femoral vessels*

Vessel preparation When the *in vivo* experiments were completed, the cat femoral artery and vein were rapidly removed, and placed in a 4°C aerated standard Na^+-Krebs buffer solution until use. The buffer solution contained (in mM): NaCl 119, $NaHCO_3$ 15, KCl 4.6, $MgCl_2$ 1.2, NaH_2PO_4 1.2, $CaCl_2$ 1.5 and glucose 11. The vessels were cut into small ring segments (1 mm long) under a dissecting microscope. For examination, each segment was carefully mounted on two L-shaped metal prongs (0.2 mm in diameter), one of which was connected to a Grass FT-03 transducer for continuous recordings of isometric tension. A basal tension of 5 mN was applied to the arterial segments, and of 1.5 mN to the venous segments, after which they were allowed to equilibrate for 2 h.

Experimental protocol The contractile capacity of the vessel segments was examined before the experimental interventions by a brief exposure to a high potassium (6×10^{-2} M) buffer solution (Högestätt *et al.*, 1983). In most cases precontraction of the vascular segments was produced with noradrenaline (3×10^{-5} M). To ascertain the specificity of the ET_B-induced vascular effects, paired experiments were always performed, one of the segments receiving the agonist, the other serving as a control. In some cases the response to ET-1 (10^{-11}–10^{-6} M) was tested at the end of the experiments.

The functional integrity of the endothelium was confirmed by the presence of a pronounced relaxation induced by acetylcholine (10^{-6} M), administered during stable precontraction with noradrenaline.

Endothelium denudation was performed by injection of 0.01% Triton X-100 through the vessel lumen for 10 s, followed by rinsing with buffer solution.

E_{max} was calculated as the maximum contractile effect compared to potassium-induced contraction and pD_2 as the negative logarithm of the molar concentration at half maximum of the response. The relaxant effect of the ET_B agonist was expressed as a percentage of the precontraction tension level. *n* refers to the number of segments tested.

Drugs

In the *in vivo* experiments, drugs were administered close-arterially to the muscle region via slow (0.01–0.2 ml min^{-1}) infusions (Harvard Apparatus, model 11) in the shunt between the femoral and the popliteal artery. The tip of the infusion needle was placed in the retrograde direction to facilitate the mixture of the drugs in the bloodstream. Control experiments in which isotonic saline was infused at the same rates demonstrated that infusion artifacts were negligible.

The following drugs were used: acetylcholine (Sigma, St Louis, MO, U.S.A.), BQ 3020 ([$Ala^{11,15}$]Ac-ET-1(6–21), Auspep, Parkville, Australia); endothelin-1 (Auspep); indomethacin (Dumex, Denmark); IRL 1620 (Suc-[Glu^9,$Ala^{11,15}$]-ET-1(8–21), Saxon Biochemicals, Hannover, Germany, and a generous gift from Ciba-Geigy, Japan); N^G-nitro-L-arginine methyl ester (L-NAME, Sigma); prazosin hydrochloride (Sigma); noradrenaline hydrochloride (Sigma); propranolol hydrochloride (ICI, Macclesfield, UK) and FR139317 ((R)2-[(R)-2-[(S)-2-[[1-(hexahydro-1H-azepinyl)] carbonyl]amino-4-methyl-pentanoyl]amino-3- [3- (1-methyl-1H-indolyl)] propionyl]amino-3-(2-pyridyl) propionic acid, Fujisawa Pharmaceutical Co., Osaka, Japan).

In previous studies (Ekelund *et al.*, 1993; Ekelund, 1994) on this muscle preparation *in vivo*, we have demonstrated that FR139317, administered i.a. at the dose of 1 mg kg^{-1} min^{-1}, entirely abolished the vasoconstrictor response to ET-1 (400 ng kg^{-1} min^{-1}, i.a.). This dose of FR139317 was therefore used in the present study. The dose of indomethacin used (10 mg kg^{-1}) can be considered to block effectively vascular cyclo-oxygenase and hence the production of prostacyclin in this muscle preparation (Ekelund, unpublished observations). Similarly, the dose of L-NAME (10 mg kg^{-1}, i.a.) used in this study is sufficient to inhibit EDNO formation (Ekelund *et al.*, 1992). Moreover, the doses of prazosin (1 mg kg^{-1}, i.a.) and propranolol (1.5 mg kg^{-1}, i.a.) used here are sufficient to block the α_1- and β-adrenoceptors (as evidenced by agonists in supramaximal doses) in this muscle preparation.

All drugs were dissolved in saline, and the solutions, when

necessary, were adjusted to isotonicity. Time data for the effects of the drugs given in Results are corrected for dead space delay in the tubings.

Statistics

Data are expressed as mean values ± s.e.mean. Group comparisons were performed by analysis of variance (ANOVA) followed by Bonferroni's test with a significance level of 5%, or by using paired (unless stated otherwise) Student's *t* test, differences being considered significant at P values <0.05.

Results

Vascular responses to ET_B-receptor agonists in skeletal muscle in vivo

General patterns of resistance response The two selective ET_B-receptor agonists, IRL 1620 and BQ 3020, were infused close-arterially in stepwise increasing doses (0.4, 0.8, 1.6, 3.2, 6.4 and 12.8 $\mu g\,kg^{-1}$ muscle tissue min^{-1}) to determine the dose-response characteristics and the smooth muscle effector sensitivity in the consecutive sections of the muscle vascular bed. The threshold dose for vascular response was 0.8 $\mu g\,kg^{-1}\,min^{-1}$ for both IRL 1620 and BQ 3020, and this response was found to be a constriction, not a dilatation. For both agonists, the constrictor response was clearly dose-dependent in the dose range up to 6.4 $\mu g\,kg^{-1}\,min^{-1}$, higher doses eliciting no further vasoconstriction. The maximal constrictor responses to IRL 1620 and BQ 3020 seemed to be equally great, implying that the two agonists had similar constrictor efficacy. In these experiments with stepwise infusion up to 12.8 $\mu g\,kg^{-1}\,min^{-1}$, a vasodilator response to these agonists was never observed. In addition, close-arterial (local) infusion of IRL 1620 or BQ 3020 did not result in any change in blood pressure (systemic effect).

The pattern of overall and segmental vascular resistance responses in the muscle preparation to IRL 1620, as well as their time characteristics, are exemplified by the original tracings depicted in Figure 1, in which the ET_B agonist was administered at a dose of 3.2 $\mu g\,kg^{-1}\,min^{-1}$ in a single infusion experiment. It can be seen that, under these circumstances, IRL 1620 elicited after some delay a biphasic response, consisting of an initial short-lasting vasodilator component, followed by a gradually developing moderate vasoconstriction. The latter reached an approximate steady state after about 6 min. Upon cessation of the infusion, the resistance responses, with some segmental variation, disappeared gradually, complete recovery being attained not until some 10 min after the end of the infusion. The vascular response to IRL 1620, both with regard to the vasoconstrictor and vasodilator component, was present in all three consecutive segments of the muscle vascular bed, yet with a preferential site of action in the small arterioles (<25 μm; $R_{a,micro}$).

The corresponding pattern of vascular response to BQ 3020 (3.2 $\mu g\,kg^{-1}\,min^{-1}$), both with regard to amplitude and time course, was very similar, with an initial short-lasting vasodilatation and a subsequent more sustained vasoconstriction, both being preferentially confined to the small arterioles.

Compiled data for the resistance responses to ET_B-receptor agonists Compiled data for resistance responses to IRL 1620 ($n = 6$) and BQ 3020 ($n = 7$), infused close-arterially to the muscle region at the dose of 3.2 $\mu g\,kg^{-1}$ muscle tissue min^{-1}, are illustrated in Figures 2 and 3. This dose corresponds to about 1.8 $nmol\,kg^{-1}\,min^{-1}$ for IRL 1620 and 1.6 $nmol\,kg^{-1}\,min^{-1}$ for BQ 3020. The infusions were made when basal vascular tone, after recovery from the preparatory surgery, had reached a normal steady-state level. In the experiments with IRL 1620, vascular tone in the control state (Figure 2) corresponded to an average overall vascular resistance (R_T, total height of the bar) of 19.8 ± 2.0 PRU, of which 9.5 ± 1.0 PRU resided in the large-bore arterial resistance vessels ($R_{a,prox}$), 8.3 ± 1.0 PRU in the small arterioles ($R_{a,micro}$) and 2.0 ± 0.2 PRU in the veins (R_v). In the BQ 3020

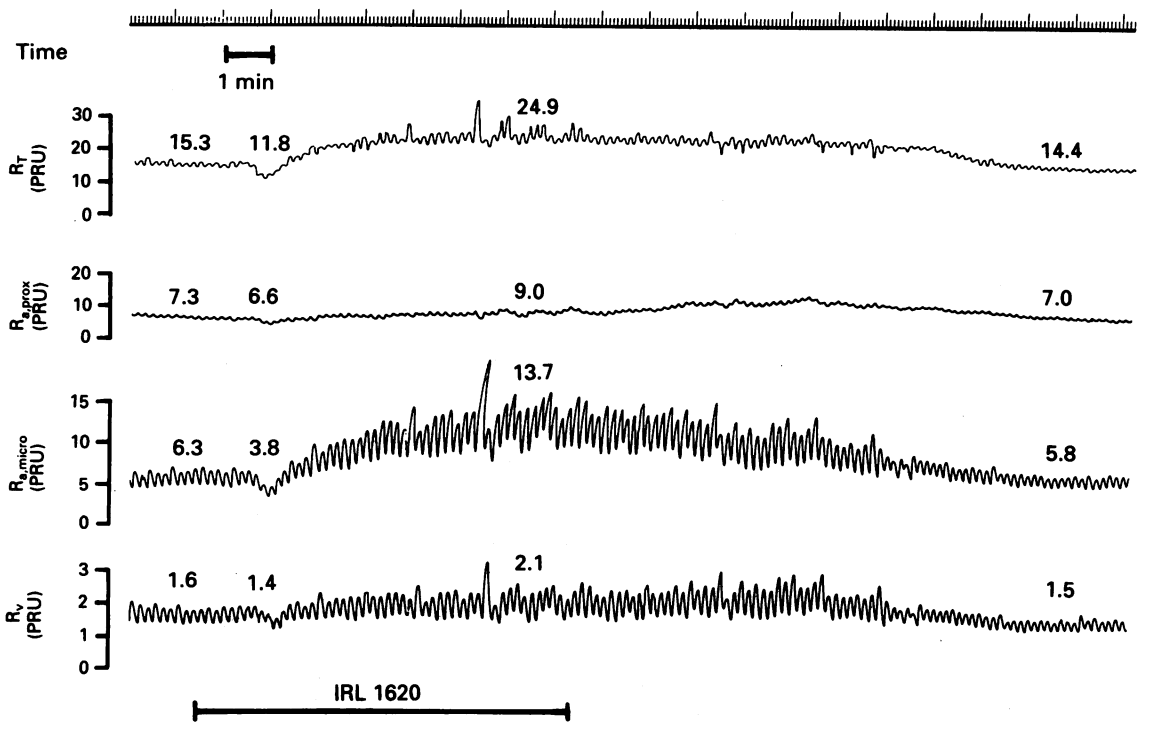

Figure 1 Pattern of vascular response in cat skeletal muscle to an i.a. infusion of IRL 1620 (3.2 $\mu g\,kg^{-1}\,min^{-1}$) on vascular resistance in the whole vascular bed (R_T) and its consecutive sections, large-bore arterial resistance vessels (>25 μm; $R_{a,prox}$), small arterioles (<25 μm; $R_{a,micro}$) and the veins (R_v). Note initial transient dilatation, followed by a slowly developing moderate vasoconstriction. Upon cessation of the infusion, the constrictor responses disappeared slowly.

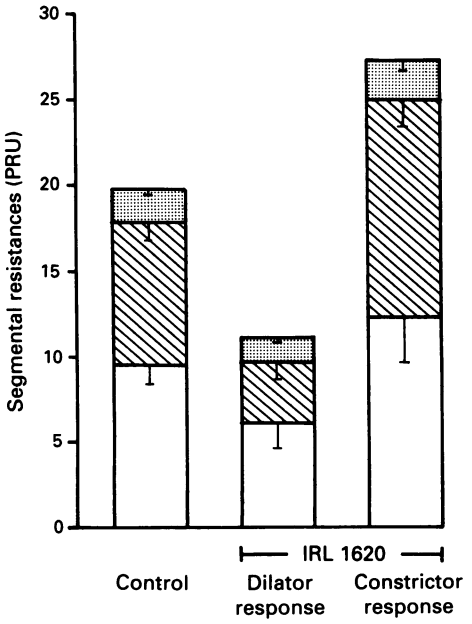

Figure 2 Compiled data ($n = 6$) for the initial transient peak dilator, and subsequent steady-state constrictor, response to IRL 1620 (3.2 $\mu g\ kg^{-1}\ min^{-1}$, i.a.) on total regional vascular resistance (total height of the columns), and its segmental distribution to the $R_{a,prox}$ (open area of column), $R_{a,micro}$ (hatched area of column) and R_v (stippled area of column) sections in cat skeletal muscle *in vivo*. Note that the vasodilator and subsequent vasoconstrictor responses were preferentially confined to the $R_{a,micro}$ section.

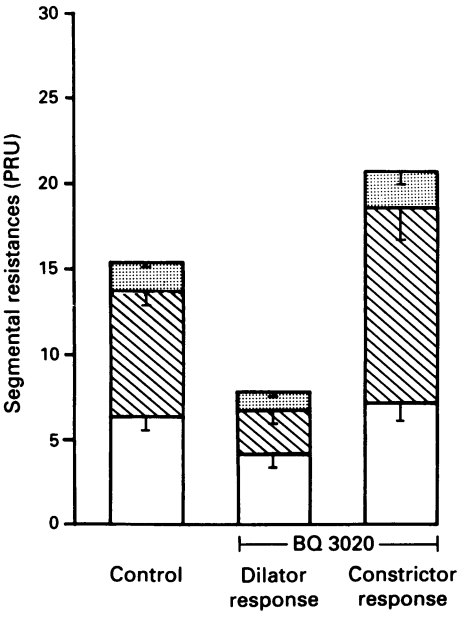

Figure 3 Compiled data ($n = 7$) for the initial transient peak dilator, and subsequent steady-state constrictor, response to BQ 3020 (3.2 $\mu g\ kg^{-1}\ min^{-1}$, i.a.) on total regional vascular resistance (total height of the columns), and its segmental distribution to the $R_{a,prox}$ (open area of column), $R_{a,micro}$ (hatched area of column) and R_v (stippled area of column) sections in cat skeletal muscle *in vivo*. Note that the vasodilator and subsequent vasoconstrictor responses were preferentially confined to the $R_{a,micro}$ section.

experiments, performed on another group of cats, R_T in the control state was 15.3 ± 0.7 PRU (Figure 3), of which 6.4 ± 0.7, 7.3 ± 0.7 and 1.7 ± 0.2 PRU resided in the $R_{a,prox}$, the $R_{a,micro}$ and the R_v sections, respectively.

Vasodilator component At the start of the infusions, both IRL 1620 and BQ 3020 elicited, after a delay of about 1 min, a clear-cut vasodilator response with its peak occurring about 90 s after the start of the infusion. For both agonists, the total duration of the dilator response was about 70 s. Compiled data for the total and segmental vascular resistance changes at the peak of these dilator responses to IRL 1620 and BQ 3020 are illustrated in Figures 2 and 3. The transient dilator response to IRL 1620 corresponded to an average decrease in R_T from the control value of 19.8 to 11.2 ± 2.0 PRU (-43%; $P<0.05$), in turn caused by a decrease in $R_{a,prox}$ of 36%, $R_{a,micro}$ of 57% and R_v of 25%. The initial dilator response to BQ 3020 was not significantly different, and corresponded to a decrease in R_T from 15.3 to 7.8 ± 0.8 PRU (-49%; $P<0.001$), in turn caused by a decrease in $R_{a,prox}$ by 36%, $R_{a,micro}$ by 64% and R_v by 35%. The vasodilator component to both ET_B agonists was thus present in all three consecutive sections, though preferentially confined to the small arterioles. From separate experiments in which single infusions of the ET_B agonists in doses other than $3.2\ \mu g\ kg^{-1}\ min^{-1}$ were made, the amplitude of this dilator response seemed to be dose-dependent.

In experiments ($n = 11$) in which a second infusion of either IRL 1620 or BQ 3020 was given after an interval with full recovery of vascular tone, the amplitude of the second dilator response was attenuated by about 55% compared to the first one, probably reflecting tachyphylaxis. The dilatation was further reduced during a third, and absent during a fourth, infusion. Moreover, cross-tachyphylaxis between the two ET_B-receptor agonists was observed. The data in Figures 2 and 3 refer to results from the first infusion in each animal.

Vasoconstrictor component After the initial dilator response to the ET_B agonists ($3.2\ \mu g\ kg^{-1}\ min^{-1}$), a gradually developing constrictor response always occurred, which, on average, reached a steady state after about 6.9 min for IRL 1620 and 5.6 min for BQ 3020. Compiled data from these experiments for the steady-state overall and segmental constrictor responses to IRL 1620 and BQ 3020 are shown in Figures 2 and 3. The constrictor response to IRL 1620 corresponded to a rise in R_T from the preinfusion control value of 19.8 to 27.3 ± 4.4 PRU ($+38\%$; $P<0.01$), explained by a resistance increase in the large-bore arterial resistance vessels to 12.3 PRU ($+29\%$), in the small arterioles to 12.7 ($+53\%$) and in the veins to 2.3 PRU ($+15\%$). The steady-state vasoconstriction elicited by BQ 3020 corresponded to an increase in R_T from 15.3 to 20.6 ± 2.3 PRU ($+35\%$; $P<0.05$), in turn caused by an increase in $R_{a,prox}$ to 7.2 ($+13\%$), $R_{a,micro}$ to 11.4 ($+56\%$) and R_v to 2.1 PRU ($+24\%$). These resistance changes were not significantly different from those evoked by IRL 1620. Thus, the vasoconstrictor response to both ET_B-receptor agonists was generalized, affecting all three consecutive vascular sections, yet with a preferential action, again, on the small arterioles.

Effects of ET_B-receptor agonists on capillary pressure and transcapillary fluid exchange Observations of ET_B-induced effects ($3.2\ \mu g\ kg^{-1}\ min^{-1}$) on hydrostatic capillary pressure ($P_{c,v}$) and transcapillary fluid movement were made on the same material as presented in Figures 2 and 3. $P_{c,v}$ in the control state averaged 19.5 ± 0.4 mmHg in the IRL 1620 experiments, and 19.5 ± 0.8 mmHg in the experiments with BQ 3020. An approximate transcapillary Starling fluid equilibrium (isovolumetric state) prevailed under these circumstances.

During the initial transient vasodilator response, IRL 1620 elicited an average peak increase in $P_{c,v}$ to 24.1 mmHg, due to its preferential dilator action on the precapillary vessels, in

turn decreasing the pre-/postcapillary resistance ratio (R_a/R_v) from 8.9 to 6.4. BQ 3020 infusion raised $P_{c,v}$ to 24.6 mmHg (decrease in R_a/R_v from 8.1 to 6.1).

During the steady-state constriction phase, IRL 1620 evoked a decrease in $P_{c,v}$ to 16.6 (− 2.9) mmHg ($P<0.01$), owing to an increase in R_a/R_v (from 8.9 to 10.9). BQ 3020 elicited a similar decrease in $P_{c,v}$ (to 16.7 mmHg; $P<0.01$). $P_{c,v}$ was maintained low as long as the vasoconstriction persisted, leading to a net transcapillary fluid absorption. The fluid absorption was, however, comparatively small, since there was a concomitant decrease in the capillary filtration coefficient (CFC). Thus, in separate experiments ($n = 11$), CFC was found to decrease from 0.010 ± 0.001 to 0.007 ± 0.001 ($P<0.05$, unpaired t test) during steady-state vasoconstriction evoked by IRL 1620.

Effects of blockade of cyclo-oxygenase, ET_A-receptors, EDNO production and adrenoceptors on vascular responses to ET_B-receptor agonists In separate experiments, the vascular resistance responses to IRL 1620 or BQ 3020 (3.2 μg kg^{-1} min^{-1}) were analysed in the absence and presence of blockade of prostacyclin with indomethacin, of EDNO with L-NAME, of ET_A-receptors with FR139317, of α_1-adrenoceptors with prazosin and of β-adrenoceptors with propranolol.

Illustrated in Figure 4a are the compiled data for the amplitude of the initial dilator response to IRL 1620 in the absence and presence of indomethacin ($n = 7$). Blockade of prostacyclin production attenuated ($P<0.05$; unpaired t test), but did not abolish ($P<0.05$), the initial dilator response to IRL 1620. However, the duration of the dilatation was unaffected by indomethacin.

Blockade of EDNO formation ($n = 7$) had no effect on the dilator response to IRL 1620. The dilatation in the presence of L-NAME (R_T − 44%) was not significantly different ($P<0.05$; unpaired t test) from that in the absence of L-NAME (R_T − 58%). Further, blockade of ET_A-receptors ($n = 3$) or β-adrenoceptors ($n = 6$) did not affect the initial dilator response to IRL 1620. The amplitude of the vasoconstrictor response (R_T) to IRL 1620 was not significantly different (unpaired t tests) in the absence and presence of indomethacin ($n = 13$), L-NAME ($n = 9$), FR139317 ($n = 10$) or prazosin ($n = 2$). However, the time required to reach steady-state constriction was significantly shorter in the presence (4.4 ± 0.3 min), than in the absence (7.2 ± 0.3 min), of indomethacin. L-NAME, FR139317 or prazosin had no effect in this respect. In the described experiments, L-NAME *per se* increased basal vascular tone (R_T) in the control state before IRL 1620 administration, due to inhibition of the basal endogenous release of EDNO, in agreement with previous results (Ekelund & Mellander, 1990). Therefore, an additional statistical analysis was made using matched controls with a corresponding level of basal vascular tone. The results from this analysis were not different from those described above.

Analogous experiments were performed with BQ 3020 in the absence and presence of indomethacin ($n = 7$), FR139317 ($n = 3$), L-NAME ($n = 6$) and prazosin ($n = 2$). The results were principally the same as those obtained with IRL 1620. As can be seen in Figure 4b, indomethacin attenuated ($P<0.05$; unpaired t test), but did not abolish ($P<0.05$), the vasodilator response to BQ 3020.

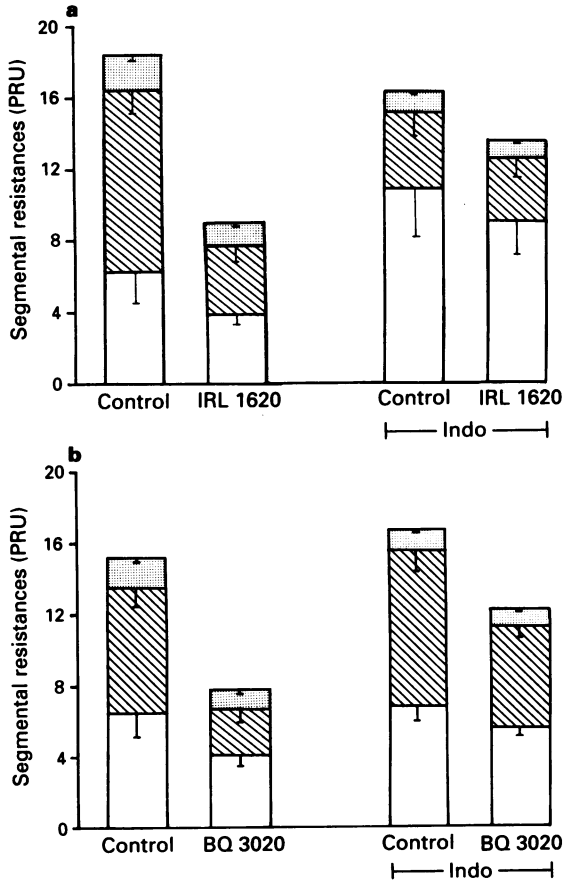

Figure 4 (a) Initial vasodilator response to IRL 1620 in the absence (left columns) and presence (Indo) of blockade of prostacyclin production with indomethacin ($n = 7$). (b) Initial vasodilator response to BQ 3020 in the absence (left columns) and presence (Indo) of blockade of prostacyclin production with indomethacin ($n = 7$). Prostacyclin blockade attenuated, but did not abolish, the dilator response to both ET_B-receptor agonists. Other details as in Figure 3.

In vitro *study of smooth muscle effects of ET_B-receptor agonists in femoral artery and vein*

In the absence of precontraction, IRL 1620 (10^{-10}–10^{-6} M) elicited no response in the femoral artery ($n = 12$) or vein ($n = 15$), nor did it induce a response in the noradrenaline-precontracted femoral artery ($n = 20$). These results were the same in the absence and presence of an intact endothelium.

Illustrated in Figure 5 is the effect of IRL 1620 (10^{-11}–10^{-6} M; $n = 16$) in the precontracted femoral vein. With

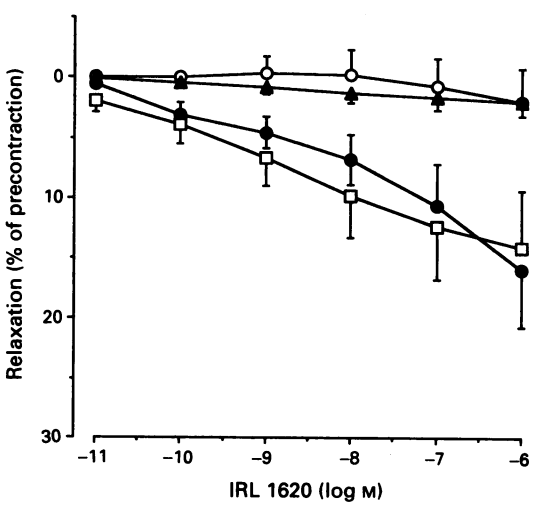

Figure 5 Concentration-response curve to IRL 1620 in cat isolated femoral vein precontracted with noradrenaline (3×10^{-5} M). Depicted are mean (± s.e.mean) responses in the control state (●, $n = 16$), in the presence of N^G-nitro-L-arginine methyl ester (L-NAME, 10^{-5} M; ▲, $n = 7$) or indomethacin (10^{-5} M; □, $n = 7$), and of the response to IRL 1620 in the absence of the endothelium (○, $n = 5$). The relaxation is expressed as a percentage of the precontraction tension level.

intact indothelium, the ET_B agonist elicited a dose-dependent relaxation, at a dose of 10^{-6} M reducing the precontraction tension by 17% ($P<0.01$). The relaxation to IRL 1620 was absent in endothelium-denuded vein segments. Segments with intact endothelium were also examined during blockade of EDNO and prostacyclin production (Figure 5). The relaxation response to IRL 1620 was abolished ($P<0.05$) by L-NAME at a dose of 10^{-5} M ($n=7$), but not at 10^{-6} M. The relaxation response was unaltered ($P>0.05$) in the presence of indomethacin (10^{-5} M; $n=7$).

In the femoral vein with intact endothelium, BQ 3020 ($10^{-11}-10^{-6}$; $n=3$) elicited a relaxation response which was similar to that evoked by IRL 1620, decreasing precontraction tension by an average of 22% at 10^{-6} M.

In both the femoral artery and vein, ET-1 ($10^{-11}-10^{-6}$ M) elicited strong dose-dependent contractions. FR139317 (10^{-6} M) caused parallel shifts to the right of the concentration-response curves (pD_2 significantly different for both artery and vein) but did not affect the E_{max} values.

Discussion

In some recent studies (Ekelund *et al.*, 1993; Ekelund, 1994), the vascular effects *in vivo* of ET-1, ET-2 and ET-3 were analysed in cat skeletal muscle with the same technical approach as was used in the present investigation. The results showed that all three endothelins elicited a transient dilatation followed by a slowly developing pronounced vasoconstrictor response. The constrictor response was preferentially confined to the small arterioles, and was mediated via the ET_A-receptor only, as indicated by abolition of the response by selective ET_A-receptor blockade (FR139317), and the observed rank order of constrictor activity, ET-1 > ET-2 > ET-3. The initial transient dilator response, however, was not mediated via the ET_A-receptor, but more likely via the ET_B-receptor. The present *in vivo* investigation aimed at defining, in quantitative terms, the site(s) of action of selective ET_B-receptor agonists on vascular resistances in the consecutive sections of the muscle vascular bed, and the effects on capillary pressure and transcapillary fluid exchange. The following results might warrant some comments.

The results demonstrated that both IRL 1620 and BQ 3020, infused i.a. to the muscle preparation, evoked an initial short-lasting dilator response and a subsequent dose-dependent vasoconstrictor response. The ET_B-receptor in the vascular bed of skeletal muscle thus mediates not only a vasodilator, but also a constrictor response. Although vascular smooth muscle adjustments in all three consecutive sections contributed to these responses, the effector reactivity in functional terms was greatest in the small arterioles ($<25\,\mu m$). Larger vessels were less responsive to ET_B-receptor stimulation, which was further supported by our *in vitro* observations on the femoral artery and vein. The pattern of segmental resistance response was thus similar to that evoked by the endothelins (Ekelund, 1994). These results, taken together, might suggest that both the ET_A- and the ET_B-receptors are especially abundant in the small arterioles.

There was no significant difference in the amplitude (peak resistance change) and time characteristics of the vascular responses between the two ET_B-receptor agonists. Moreover, the responses were unaffected by ET_A-receptor blockade. The effects of the two different ET_B agonists were thus strikingly similar, and the present comparative results indicate that, from a functional point of view, IRL 1620 and BQ 3020 can be considered equally effective and highly selective ET_B-receptor agonists in the vascular bed of skeletal muscle *in vivo*. Hence, these compounds might become useful as specific pharmacological tools for future functional investigations of the role of the ET_B-receptor in circulatory regulation in physiological and/or pathophysiological situations.

The initial transient vasodilator responses to IRL 1620 and BQ 3020 were not significantly different from those elicited by the endothelins (Ekelund *et al.*, 1993; Ekelund, 1994) with regard to amplitude, duration and time to peak dilatation. This finding seems to support our previous tentative conclusion (Ekelund, 1994) that the dilator responses to the endothelins are mediated via the ET_B-receptor.

The dilator response to ET_B-receptor stimulation by both agonists was attenuated, but not abolished, in the presence of indomethacin. On the assumption that the dose of indomethacin used completely blocked vascular cyclo-oxygenase, this observation indicates that the transient dilator response to ET_B-receptor stimulation in skeletal muscle is partly, but not entirely, mediated by secondary release of vasodilator cyclo-oxygenase products, most probably endothelium-derived prostacyclin. Thus, the findings in cat skeletal muscle seem to be compatible with the previous postulate (e.g. Sakurai *et al.*, 1992) that ET_B-receptor stimulation is responsible for endothelin-induced prostacyclin production. However, both the ET_A- and ET_B-receptor subtypes have been claimed to be capable of mediating endothelin-induced metabolism of arachidonic acid (Aramori & Nakanishi, 1992), and prostaglandin production. Hence the specific receptor subtype responsible for prostacyclin release may vary in different vessels and/or species. For instance, in the rat lung and rabbit kidney, the release of prostacyclin by ET-1 seems to be mediated by the ET_A-receptor (D'Orléans-Juste *et al.*, 1992; Télémaque *et al.*, 1992), whereas in the rat kidney both receptor subtypes (Warner *et al.*, 1993) may mediate the release of prostanoids.

The mechanism underlying the remaining ET_B-mediated dilator response *in vivo* during prostacyclin blockade is unclear, but could involve a direct effect of ET_B-receptors situated on the vascular smooth muscle, or an ET_B-mediated release of vasodilator substances other than those synthesized by vascular cyclo-oxygenase. EDNO did not seem to be involved in this mechanism, since the vasodilator response to ET_B-receptor stimulation was not significantly modified by EDNO blockade with L-NAME. This finding is in agreement with previous *in vivo* results obtained with ET-1 during EDNO blockade (e.g. Gardiner *et al.*, 1989; Ekelund *et al.*, 1993), and provides further evidence against the hypothesis derived from *in vitro* experiments (see Rubanyi & Parker Botelho, 1991; Sakurai *et al.*, 1992), that the vasodilatation and the consequent hyperaemic response to the endothelins is caused by ET_B-mediated release of EDNO.

The amplitude of the vasoconstrictor response was found not to be modified by indomethacin, which indicates that the ET_B-induced vasoconstrictor response was not due to the release of vasoconstrictor cyclo-oxygenase products. It is possible that the vasoconstrictor response to IRL 1620 and BQ 3020 is elicited by ET_B-receptors situated on the smooth muscle cells *proper* (cf. Moreland *et al.*, 1992).

Endothelin-1, at least *in vitro*, shows an about equal affinity for ET_A- and ET_B-receptors (Saeki *et al.*, 1991; Takai *et al.*, 1992). The present result, demonstrating that ET_B-receptor stimulation leads to a constrictor response, could *a priori* suggest that the vasoconstrictor response to ET-1 can be mediated by both receptor subtypes in skeletal muscle *in vivo*. However, we have previously demonstrated that the ET-1-mediated vasoconstriction in muscle *in vivo* can be abolished by selective ET_A-receptor blockade alone (FR 139317; Ekelund *et al.*, 1993). Further, in the present *in vitro* study, FR139317 competitively inhibited the ET-1-induced contraction of the femoral artery and vein. Future experiments with selective and true antagonists to the ET_B-receptor might permit more definite conclusions about the receptor mechanisms underlying the endothelin-induced vasoconstrictor response.

In the feline isolated femoral vein, IRL 1620 elicited a weak dose-dependent relaxation. This finding is one of the first demonstrations of a sustained relaxation to selective ET_B-receptor activation in a vein. The results indicated that this relaxation response was endothelium-dependent and abolished by L-NAME, which suggests that an endothelial

ET_B-receptor relaxed the vessel via EDNO release. Similar results with IRL 1620 have been reported for other large vessels, e.g. the rat aorta (Fujitani *et al.*, 1993). Thus, the ET_B-receptor-mediated vasodilator response in skeletal muscle *in vivo* (Figures 2 and 3), and the relaxation of the femoral vein *in vitro* (Figure 5), seem to be elicited via different postreceptor mechanisms, which in fact have been reported to differ considerably in different vessels (for references see Masaki, 1993; Simonson, 1993). The functional importance of the ET_B-mediated relaxation response in the femoral vein for blood flow regulation *in vivo* is probably very small, since the contribution of large conduit vessels to the overall vascular resistance regulation is almost insignificant. If the *in vivo* constrictor response to ET_B-receptor stimulation is caused by receptors situated on the vascular smooth muscle cells proper (see above), the absence of a constrictor response in the femoral vein could suggest a lack of such receptors in this vessel. The cat femoral artery might lack both types of ET_B-receptors, since it was non-reactive to ET_B-receptor stimulation.

It appears that the haemodynamic significance *in vivo* of the described vasodilator response to ET_B-receptor stimulation in skeletal muscle must be rather trivial in view of its transient nature. The subsequent sustained constrictor response may be more important in this respect. This response was also associated with a decrease in capillary pressure which seemed to be more pronounced per unit resistance increase than that to most other vasoconstrictors, e.g. neurally released noradrenaline (Maspers *et al.*, 1990a). As indicated by the observed decrease in CFC, this response further involved a maintained constriction of the terminal arterioles/precapillary sphincters, and a consequent reduction of the size of the functional capillary surface area. The decrease in CFC implies that the net transcapillary fluid absorption evoked by the capillary pressure drop becomes attenuated. A maintained constriction of precapillary sphincters is usually not evoked by other constrictor agents (e.g. neurally released noradrenaline), due to secondary metabolic/myogenic counteraction as a result of the associated decrease in blood flow and vascular transmural pressure. The sustained precapillary sphincter constrictor response to ET_B-receptor stimulation may thus present further evidence in support of the view of an abundance of ET_B-receptors in the microcirculation.

Our previous investigations, demonstrating quite unusual haemodynamic and capillary effects of the endothelins in muscle tissue (Ekelund *et al.*, 1993; Ekelund, 1994), suggested that they might be of importance in long-term, rather than short-term, regulation of vascular tone *in vivo*, perhaps especially during pathophysiological conditions. From the present results, it may be concluded that ET_B-receptor stimulation is responsible for the dilator response, and can contribute to the constrictor response, elicited by the endothelins in skeletal muscle *in vivo*.

This study was supported by grants from the Swedish Medical Research Council (2210 and 5958) and the Faculty of Medicine, University of Lund. The highly qualified technical assistance of Mrs Christine Wikstrand and Miss Helén Hansen is gratefully acknowledged.

References

ARAMORI, I. & NAKANISHI, S. (1992). Coupling of two endothelin receptor subtypes to differing signal transduction in transfected chinese hamster ovary cells. *J. Biol. Chem.*, **267**, 12468–12474.

BJÖRNBERG, J., GRÄNDE, P.-O., MASPERS, M. & MELLANDER, S. (1988). Site of autoregulatory reactions in the vascular bed of cat skeletal muscle as determined with a new technique for segmental vascular resistance recordings. *Acta Physiol. Scand.*, **133**, 199–210.

BIGAUD, M. & PELTON, J.T. (1992). Discrimination between ET_A- and ET_B-receptor-mediated effects of endothelin-1 and [$Ala^{1,3,11,15}$] endothelin-1 by BQ-123 in the anaesthetized rat. *Br. J. Pharmacol.*, **107**, 912–918.

D'ORLÉANS-JUSTE, P., TÉLÉMAQUE, S., CLAING, A., IHARA, M. & YANO, M. (1992). Human big-endothelin-1 and endothelin-1 release prostacyclin via the activation of ET_1 receptors in the rat perfused lung. *Br. J. Pharmacol.*, **105**, 773–775.

EKELUND, U. (1994). In-vivo effects of endothelin-2, endothelin-3 and ET_A receptor blockade on arterial, venous and capillary functions in cat skeletal muscle. *Acta Physiol. Scand.*, **140**, 47–56.

EKELUND, U., ALBERT, U., EDVINSSON, L. & MELLANDER, S. (1993). In-vivo effects of endothelin-1 and ET_A receptor blockade on arterial, venous and capillary functions in skeletal muscle. *Acta Physiol. Scand.*, **148**, 273–283.

EKELUND, U., BJÖRNBERG, J., GRÄNDE, P.-O., ALBERT, U. & MELLANDER, S. (1992). Myogenic vascular regulation in skeletal muscle in vivo is not dependent of endothelium-derived nitric oxide. *Acta Physiol. Scand.*, **144**, 199–207.

FOLKOW, B. & MELLANDER, S. (1970). Measurements of capillary filtration coefficient and its use in studies of the control of capillary exchange. In *Capillary Permeability. The Transfer of Molecules and Ions between Capillary Blood and Tissue.* ed. Crone, C. & Lassen, N.A. pp. 614–623. Copenhagen: Munksgaard.

FUJITANI, Y., UEDA, H., OKADA, T., URADE, Y. & KARAKI, H. (1993). A selective agonist of endothelin type B receptor, IRL 1620, stimulates cyclic GMP increase via nitric oxide formation in rat aorta. *J. Pharmacol. Exp. Ther.*, **267**, 683–689.

GARDINER, S.M., COMPTON, A.M., BENNETT, T., PALMER, R.M.J. & MONCADA, S. (1989). N^G-monomethyl-L-arginine does not inhibit the hindquarters vasodilator action of endothelin-1 in conscious rats. *Eur. J. Pharmacol.*, **171**, 237–240.

GARDINER, S.M., KEMP, P.A., MARCH, J.E., BENNETT, T., DAVENPORT, A.P. & EDVINSSON, L. (1994). Effects of an ET_A-receptor antagonist, FR139317, on regional haemodynamic responses to endothelin-1 and [$Ala^{11,15}$]Ac-endothelin-1(6–21) in conscious rats. *Br. J. Pharmacol.* (in press).

HÖGESTÄTT, E.D., ANDERSON, K.-E. & EDVINSSON, L. (1983). Mechanical properties of rat cerebral arteries as studied by a sensitive device for recording of mechanical activity in isolated small blood vessels. *Acta Physiol. Scand.*, **117**, 49–61.

IHARA, M., SAEKI, T., FUKURODA, T., KIMURA, S., OZAKI, S., PATEL, A.C. & YANO, M. (1992). A novel radioligand [^{125}I]BQ-3020 selective for endothelin (ET_B) receptors. *Life Sci.*, **51**, PL47–52.

MASAKI, T. (1993). Endothelins: homeostatic and compensatory actions in the circulatory and endocrine systems. *Endocrin. Rev.*, **14**, 256–268.

MASAKI, T., KIMURA, S., YANAGISAWA, M. & GOTO, K. (1992). Molecular and cellular mechanism of endothelin regulation: implications for vascular function. *Circulation*, **84**, 1457–1468.

MASPERS, M., BJÖRNBERG, J., GRÄNDE, P.-O. & MELLANDER, S. (1990a). Sympathetic α-adrenergic control of large-bore arterial vessels, arterioles and veins, and of capillary pressure and fluid exchange in whole-organ cat skeletal muscle. *Acta Physiol. Scand.*, **138**, 509–521.

MASPERS, M., BJÖRNBERG, J. & MELLANDER, S. (1990b). Relation between capillary pressure and vascular tone over the range from maximum dilatation to maximum constriction in cat skeletal muscle. *Acta Physiol. Scand.*, **140**, 73–83.

MELLANDER, S., BJÖRNBERG, J., MASPERS, M. & MYRHAGE, R. (1987). Method for continuous recording of hydrostatic exchange vessel pressure in cat skeletal muscle. *Acta Physiol. Scand.*, **129**, 325–335.

MORELAND, S., MCMULLEN, D.M., DELANEY, C.L., LEE, V.G. & HUNT, J.T. (1992). Venous smooth muscle contains vasoconstrictor ET_B-like receptors. *Biochem. Biophys. Res. Commun.*, **184**, 100–106.

RUBANYI, G.M. & PARKER BOTELHO, L.H. (1991). Endothelins. *FASEB J.*, **5**, 2713–2720.

SAEKI, T., IHARA, M., FUKURODA, T., YAMAGIWA, M. & YANO, M. (1991). [$Ala^{1,3,11,15}$]endothelin-1 analogs with ET_B agonistic activity. *Biochem. Biophys. Res. Commun.*, **179**, 286–292.

SAKURAI, T., YANAGISAWA, M. & MASAKI, T. (1992). Molecular characterization of endothelin receptors. *Trends Pharmacol. Sci.*, **13**, 103–108.

SIMONSON, M.S. (1993). Endothelins: multifunctional renal peptides. *Physiol. Rev.*, **73**, 375–411.

SOGABE, K., NIREI, H., SHOUBO, M., NOMOTO, A., AO, S., NOTSU, Y. & ONO, T. (1993). Pharmacological profile of FR139317, a novel, potent endothelin ET_A receptor antagonist. *J. Pharmacol. Exp. Ther.*, **264**, 1040–1046.

SOGABE, K., NIREI, H., SHOUBO, M., NOMOTO, A., HENMI, K., NOTSU, Y. & ONO, T. (1992). A novel endothelin receptor antagonist: studies with FR139317. *Jpn. J. Pharmacol.*, **58**, (suppl. 1), 105.

TAKAI, M., UMEMURA, I., YAMASAKI, K., WATAKABE, T., FUJITANI, Y., ODA, K., URADE, Y., INUI, T., YAMAMURA, T. & OKADA, T. (1992). A potent and specific agonist, Suc-[Glu^9, $Ala^{11,15}$]-endothelin-1(8–21), IRL 1620, for the ET_B receptor. *Biochem. Biophys. Res. Commun.*, **184**, 953–959.

TÉLÉMAQUE, S., LEMAIRE, D., CLAING, A. & D'ORLÉANS-JUSTE, P. (1992). Phosphoramidon-sensitive effects of big endothelins in the perfused rabbit kidney. *Hypertension*, **20**, 518–523.

WARNER, T.D., BATTISTINI, B., ALLCOCK, G.H. & VANE, J.R. (1993). Endothelin ET_A and ET_B receptors mediate vasoconstriction and prostanoid release in the isolated kidney of the rat. *Eur. J. Pharmacol.*, **250**, 447–453.

(Received November 15, 1993
Revised February 22, 1994
Accepted April 8, 1994)

Br. J. Pharmacol. (1994), **112**, 895–900

Poly-L-arginine-mediated release of acetylcholine from parasympathetic nerves in rat and guinea-pig airways

[1]D. Spina & R.G. Goldie

Department of Pharmacology, University of Western Australia, Nedlands 6009, Australia

1 The synthetic cationic polypeptide, poly-L-arginine (0.03–1 mg ml^{-1}) induced concentration-dependent contraction of guinea-pig and rat isolated trachea. In guinea-pig isolated trachea, this response was attenuated in the presence of the muscarinic cholinoceptor antagonist, atropine (0.1 μM) and augmented by the acetylcholinesterase inhibitor, ecothiophate (0.1 μM). The neuronal sodium channel blocker, tetrodotoxin (3 μM) failed to alter the contractile response to poly-L-arginine and acetylcholine.

2 The contractile response to poly-L-arginine in rat isolated trachea was inhibited in the presence of atropine (0.1 μM) and the 5-hydroxytryptamine (5-HT) receptor antagonist, methysergide (1 μM). Treatment of rat tracheal preparations with capsaicin (100 μM) or tetrodotoxin (3 μM) failed to alter the contractile response to poly-L-arginine. In contrast, ecothiophate (0.1 μM) augmented the contractile response to poly-L-arginine in rat isolated trachea.

3 Electrical field stimulation (5 Hz, 2 min) of epithelium-denuded guinea-pig tracheal preparations preloaded with [^{3}H]-choline resulted in a contractile response and the simultaneous efflux of radioactivity into the superfusate. Both these responses were abolished in the presence of tetrodotoxin (1.5 μM). Poly-L-arginine (1 mg ml^{-1}) also increased the efflux of total radioactivity from epithelium-denuded guinea-pig isolated tracheal preparations preloaded with [^{3}H]-choline, but this response was tetrodotoxin-insensitive. The negatively charged polyanion, heparin (1 mg ml^{-1}) failed to increase significantly the efflux of radioactivity from epithelium-denuded preparations.

4 In conclusion, the synthetic cationic polypeptide, poly-L-arginine, caused contraction of guinea-pig isolated tracheal preparations via the release of acetylcholine from parasympathetic nerves. Similarly, poly-L-arginine-induced contraction of rat isolated trachea is secondary to the release of acetylcholine from parasympathetic nerves and/or the release of mast cell-derived 5-HT.

Keywords: Poly-L-arginine; airway smooth muscle; isolated trachea of guinea-pig, rat; tetrodotoxin; [^{3}H]-choline release; capsaicin; parasympathetic nerves; acetylcholine

Introduction

We have recently demonstrated that synthetic polypeptides rich in arginine and lysine residues contract guinea-pig isolated tracheal smooth muscle. The exact mechanism of this effect is not known but might involve a direct effect on airway smooth muscle and/or the involvement of other cell types within this tissue (Spina & Goldie, 1994).

It has recently been demonstrated that the naturally occurring cationic polypeptide, eosinophil-derived major basic protein (MBP) mediated bronchoconstriction in primates (Gundel *et al.*, 1991) and contracted guinea-pig trachea *in situ* (White *et al.*, 1990). The contractile response to MBP was epithelium-dependent, although the chemical mediator involved was not identified. It has also been suggested that MBP and poly-L-lysine might mediate the release of sensory neuropeptides from neonatal rat dorsal root ganglion neurones in culture (Garland *et al.*, 1993). However, we found no evidence to suggest the involvement of sensory neuropeptides in the contractile response to poly-L-arginine in guinea-pig isolated trachea (Spina & Goldie, 1994).

The present study further investigated the mechanism of poly-L-arginine-induced contraction of isolated airway preparations.

[1] Author for correspondence at current address: The Sackler Institute of Pulmonary Pharmacology, Department of Thoracic Medicine, Kings College School of Medicine & Dentistry, Bessemer Road, London SE5 9PJ.

Methods

Tissue preparation

Male Albino guinea-pigs (300–500 g) and Wistar rats (250–350 g) were killed by cervical dislocation and the trachea removed and placed in cold (4°C) Krebs-Henseleit solution, aerated with 95% O_2 and 5% CO_2. Since it has previously been shown that the epithelium can influence guinea-pig tracheal smooth muscle sensitivity to spasmogens (Goldie *et al.*, 1986), the epithelium was removed from all preparations with a cotton wool probe.

Tracheal rings (2 mm) were suspended in dimethyldichlorosilane (40%)-treated 1 ml organ baths under an optimal tension of 1 g (guinea-pig trachea) and 0.5 g (rat trachea) in Krebs-Henseleit solution aerated with 95% O_2 and 5% CO_2 at 37°C. Tissues were allowed to equilibrate for 30 min with changes in Krebs-Henseleit solution made at 10 min intervals. Methacholine (0.2 and 10 μM) was added cumulatively to the bath and after the contractile response had reached plateau, the tissues were washed 5 times over a 15 min period and allowed to equilibrate for a further 30 min. This procedure was repeated a second time.

Guinea-pig trachea

Contraction studies Cumulative concentration-effect curves to poly-L-arginine (mol.wt. 8900; 0.03–1 mg ml^{-1}) were constructed in epithelium-denuded guinea-pig isolated tracheal preparations treated with the cyclo-oxygenase inhibitor, indomethacin (5 μM). In some experiments, guinea-pig

tracheal preparations were incubated with the acetylcholinesterase inhibitor, ecothiophate (0.1 μM) for 20 min followed by repeated washout over a 15 min period. Tissues were allowed to equilibrate for a further 30 min before concentration-effect curves to poly-L-arginine were obtained. In other experiments, contractile responses to poly-L-arginine were elicited in the absence or presence of the non-selective muscarinic cholinoceptor antagonist, atropine (0.1 μM; 30 min preincubation). Contractile responses to poly-L-arginine and acetylcholine were elicited in the absence or presence of the sodium channel blocker, tetrodotoxin (3 μM; 30 min preincubation).

In other experiments, guinea-pig isolated trachea was placed between 2 platinum electrodes and electrically stimulated at 10 Hz or 30 Hz (current = 600 mA, 0.5 ms pulse width, 10 s duration) in the absence or presence of tetrodotoxin (3 μM).

Release of radioactivity derived from [^{3}H]-choline incorporation The efflux of radioactivity from [^{3}H]-choline preloaded parasympathetic nerves was monitored by a modification of a previously described method (Wessler *et al.*, 1990). Male SRC tricolour guinea-pigs (300–650 g) were killed by cervical dislocation and the trachea removed and placed in cold (4°C) Krebs-Henseleit solution, aerated with 95% O_2 and 5% CO_2. The epithelium was removed and the trachea was cut longitudinally along its ventral surface. Zig-zag preparations consisting of 6–9 cartilagenous rings (200–400 mg) were suspended under 1 g tension (for the simultaneous measurement of isometric force) between two parallel platinum electrodes placed 2.5 mm apart. Tracheal preparations were superfused at 2 ml min^{-1} with Krebs-Henseleit solution previously aerated with 95% O_2 and 5% CO_2 at 37°C containing indomethacin (5 μM). Tissues were allowed to equilibrate for 30 min. During the last 10 min of this equilibration period, the preparations were stimulated electrically at 1 Hz (current = 600 mA, 1 ms pulse width) to elicit contraction.

Following this period, superfusion was stopped and the tissue and electrode assembly was immersed in Krebs-Henseleit solution aerated with 95% O_2 and 5% CO_2 at 37°C containing indomethacin (5 μM) and approximately 30 nM [^{3}H]-choline chloride (86.6 Ci mmol^{-1}) and continuously stimulated at 10 Hz for 60 min. Electrical stimulation was then terminated and the tracheal preparations were superfused at 2 ml min^{-1} with Krebs-Henseleit solution containing the choline uptake blocker, hemicholinium-3 (10 μM) and the muscarinic M_2-receptor antagonist, gallamine (100 μM) to inhibit M_2-autoreceptors.

Labelling was followed by a 90 min washout period. After the washout period, the efflux of radioactivity derived from [^{3}H]-choline was measured by collecting the superfusate at 3 min intervals and taking 1 ml aliquot for liquid scintillation counting. The release of radioactivity (d.p.m. g^{-1} 3 min^{-1}) from the tissue was also measured during periods of electrical field stimulation, S1 (5 Hz, 2 min, 12th–14th min after the washout period) and S2 (42nd–44th min after the washout period). In some experiments, tetrodotoxin (1.5 μM) was added between S1 and S2, 24 min before S2.

In other experiments the labelling protocol was followed by a washout period of 60 min. Thereafter superfusion was stopped and the tissue and electrode assembly placed in 2 ml organ baths containing Krebs-Henseleit solution together with indomethacin (5 μM), hemicholinium-3 (10 μM) and gallamine (100 μM). The bath solution was removed under vacuum and replaced 3 times with fresh Krebs-Henseleit solution. The bath solution was then changed at 5 min intervals for a further 60 min and 0.8 ml aliquots taken at each change for liquid scintillation counting. The release of radioactivity (d.p.m. g^{-1} ml^{-1}) from the tissue was then measured in the presence of 1 mg ml^{-1} poly-L-arginine or heparin (60th–65th min after washout period, S1). The release of radioactivity in response to poly-L-arginine was also measured a second time (S2, 100th–105th min after washout period). In some experiments, tissues were incubated for 30 min prior to S2 in the presence of tetrodotoxin (1.5 μM).

Rat trachea

Cumulative concentration-effect curves to poly-L-arginine (mol.wt. 8900; 0.03–1 mg ml^{-1}) were constructed in epithelium-denuded rat tracheal preparations in the absence or presence of the 5-HT receptor antagonist, methysergide (1 μM; 30 min preincubation), atropine (0.1 μM; 30 min preincubation) or tetrodotoxin (3 μM; 30 min preincubation). In other experiments, rat isolated tracheal preparations were incubated with ecothiophate (0.1 μM) for 20 min followed by a 15 min washout. Tissues were allowed to equilibrate for a further 30 min before concentration-effect curves to poly-L-arginine were obtained.

The response to poly-L-arginine was also evaluated in epithelium-denuded rat isolated tracheal preparations following acute desensitization to capsaicin. Tracheal rings were incubated with capsaicin (100 μM) for 15 min, then washed every 5 min over a 15 min period and allowed to equilibrate for a further 15 min. Rat tracheal preparations did not contract in response to capsaicin. The contractile response to poly-L-arginine was then investigated in capsaicin-treated tracheal preparations.

Rat isolated tracheal preparations were also placed between 2 platinum electrodes and electrically stimulated at 10 Hz and 30 Hz (current = 600 mA, 0.5 ms, 10 s duration) in the absence or presence of ecothiophate (0.1 μM) and/or tetrodotoxin (3 μM).

Analysis of results

The concentration of poly-L-arginine causing 25% (EC_{25}) and 15% (EC_{15}) of the maximum response to methacholine (100 μM) in the guinea-pig and rat respectively, was taken as a measure of potency and was expressed as the geometric mean together with 95% confidence limits. The concentration of acetylcholine causing 50% (EC_{50}) of the maximum response in the guinea-pig was taken as a measure of potency and was expressed as the geometric mean together with 95% confidence limits. In other cases, the arithmetic mean and s.e.mean was used. Contractile responses to poly-L-arginine were expressed in terms of the maximal contractile response (E_{max}) to methacholine (100 μM). Differences between means were assessed by Student's non-paired t test and considered significant if $P<0.05$.

Drugs

Indomethacin, atropine, acetylcholine chloride, methacholine chloride, poly-L-arginine (mol.wt. 8900), capsaicin, hemicholinium-3, gallamine triethiodide, tetrodotoxin (Sigma); ecothiophate (Wyeth, Aust.); methysergide (Sandoz, N.J., U.S.A.); standard unfractionated heparin (Delta West); [^{3}H]-choline chloride (86.6 Ci mmol^{-1}, New England Nuclear). All drugs were dissolved in Krebs-Henseleit solution. The composition of Krebs-Henseleit solution was as follows (mM): NaCl 117.6, KCl 5.4, $MgSO_4.7H_2O$ 0.57, $KH_2.PO_4$ 1.03, $NaHCO_3$ 25.0, glucose 11.1 and $CaCl_2.2H_2O$ 2.5. The stock concentration (0.01 M) of indomethacin was prepared in 0.5% Na_2CO_3. The stock concentration of capsaicin (0.01 M) was prepared in 100% ethanol. The appropriate dilution was then made in Krebs-Henseleit solution.

Results

Guinea-pig trachea

Contraction induced by poly-L-arginine, acetylcholine and electrical field stimulation Poly-L-arginine (0.03–1 mg ml^{-1})

caused concentration-dependent contraction in epithelium-denuded guinea-pig isolated trachea (Figure 1). The contractile response to 1 mg ml^{-1} poly-L-arginine (% methacholine E_{max} = 31 ± 5%, n = 7, Figure 1) was significantly attenuated in the presence of 0.1 μM atropine (8 ± 3%, n = 6, P<0.05 cf. control). In contrast, the acetylcholinesterase inhibitor, ecothiophate (0.1 μM) significantly increased the contractile potency of poly-L-arginine (EC_{25} 95% confidence limits; control: 758 μg ml^{-1} (263–2188) n = 7 vs ecothiophate: 174 μg ml^{-1} (100–302) n = 7, P<0.01; Figure 1). The neuronal sodium channel blocker, tetrodotoxin (3 μM) did not significantly alter the contractile response to 1 mg ml^{-1} poly-L-arginine (E_{max} control = 34 ± 8%, n = 4 vs E_{max} tetrodotoxin = 38 ± 7%, n = 4, P>0.05). In contrast, electrical field stimulation (EFS) of guinea-pig isolated tracheal preparations resulted in a contractile response (E_{max} 10 Hz = 35 ± 5%, n = 4; E_{max} 30 Hz = 48 ± 6%, n = 7) that was abolished in the presence of tetrodotoxin. The contractile potency of acetycholine (EC_{50}; 95% confidence limits) was not significantly altered by 3 μM tetrodotoxin (control, 1.3 μM (0.5–3.4), n = 3 vs tetrodotoxin 1.4 μM (0.6–3.3), n = 3, P>0.05, paired t test).

Release of radioactivity derived from [^{3}H]-choline incorporation The efflux of radioactivity decreased in a time-dependent manner, reaching a plateau by 60 min and remained stable over the next 60 min. Electrical field stimulation (5 Hz, 2 min) of guinea-pig superfused isolated trachea evoked a significant efflux of radioactivity during S1 (baseline = 4429 ± 657 d.p.m. g^{-1} 3 min^{-1}; EFS = 10 267 ± 1549 d.p.m. g^{-1} 3 min^{-1}, n = 4, Figure 2a). The ratio S2:S1 was 0.67 ± 0.04 (n = 4). Furthermore, the tracheal preparations contracted (% methacholine E_{max}) in response to EFS (5 Hz, 2 min) during S1 (21 ± 5%, n = 4) and S2 (23 ± 4%, n = 4). The neuronal origin of the radioactivity from epithelium-denuded trachea was confirmed by the significant reduction in efflux in the presence of the sodium channel blocker, tetrodotoxin (1.5 μM) (ratio S2:S1 = 0.15 ± 0.06, n = 3, P<0.05 cf. control, Figure 2b). The contractile response to EFS was also significantly reduced by tetrodotoxin (1.5 μM) (% methacholine E_{max}; S1 = 35 ± 5% vs S2 = 0.7 ± 0.7%, n = 3, P<0.05).

Poly-L-arginine (1 mg ml^{-1}, Figure 3a) also significantly increased the efflux of radioactivity above baseline during S1 (baseline = 3456 ± 413 d.p.m. g^{-1} ml^{-1}, poly-L-arginine stimulation = 5376 ± 464 d.p.m. g^{-1} ml^{-1}, n = 3). The ratio S2:S1 was 0.72 ± 0.09 (n = 4). Furthermore, tracheal preparations contracted (% methacholine E_{max}) in response to 1 mg ml^{-1} poly-L-arginine during S1 (21 ± 3%, n = 4) and S2 (14 ± 2%, n = 4). Tetrodotoxin (1.5 μM) failed to alter significantly the increase in the efflux of radioactivity (ratio S2:S1 = 0.74 ± 0.12, n = 3, P>0.05 cf. control, Figure 3b) or the contractile response (% methacholine E_{max}; S1 = 21 ± 8% vs S2 = 14 ± 6%, P>0.05) to poly-L-arginine (1 mg ml^{-1}). Poly-L-arginine (1 mg ml^{-1}) did not significantly alter the pH of the Krebs-Henseleit solution (control; 7.487 ± 0.056, n = 4 vs 1 mg ml^{-1} poly-L-arginine; 7.540 ± 0.041, n = 4, P>0.05).

The negatively charged polyanion, heparin (1 mg ml^{-1}), failed to alter significantly the efflux of radioactivity derived from [^{3}H]-choline in guinea-pig preparations (baseline = 2534 ± 134 d.p.m. g^{-1} min^{-1}, heparin = 2205 ± 150 d.p.m. g^{-1} ml^{-1}, n = 3, P>0.05).

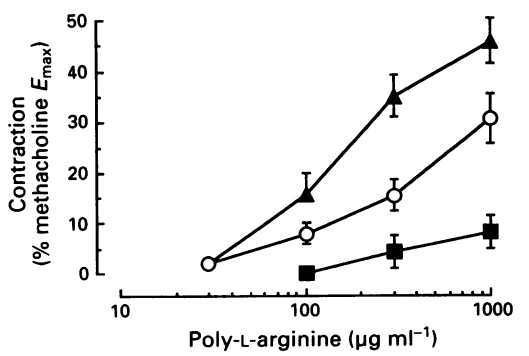

Figure 1 Concentration-dependent contraction of epithelium-denuded guinea-pig isolated trachea to poly-L-arginine in the absence (○) or in the presence of atropine (0.1 μM; ■), or in the presence of ecothiophate (0.1 μM; ●). Each point represents the mean ± s.e.mean of between 4–5 values. Indomethacin (5 μM) was present throughout all experiments.

Rat trachea

Contraction induced by poly-L-arginine and electrical field stimulation. Poly-L-arginine (0.03–1 mg ml^{-1}) caused concentration-dependent contraction in epithelium-denuded preparations (Figure 4). The contractile response to 1 mg ml^{-1} poly-L-arginine (% methacholine E_{max}: 35 ± 4%, n = 7) was significantly attenuated in the presence of atropine (7 ± 1%, n = 5, P<0.05 cf. control) and methysergide (7 ± 6%, n = 5, P<0.05 cf. control). In contrast, acute desensitization with capsaicin (100 μM) did not alter significantly either the contractile potency of poly-L-arginine (EC_{15}; 95% confidence limits: control 148 μg ml^{-1} (71–309), n = 7 vs capsaicin-treated 219 μg ml^{-1} (117–407), n = 7; P>0.05) or the maximum contractile response (E_{max} control = 35 ± 4%, n = 7 vs E_{max} capsaicin-treated = 40 ± 7%, n = 7, P>0.05).

Ecothiophate significantly augmented the contractile potency of poly-L-arginine (EC_{15}; 95% confidence limits: control 214 μg ml^{-1} (111–410), n = 6 vs ecothiophate: 76 μg ml^{-1} (43–135), n = 6; P<0.05 cf. control) and E_{max} to poly-

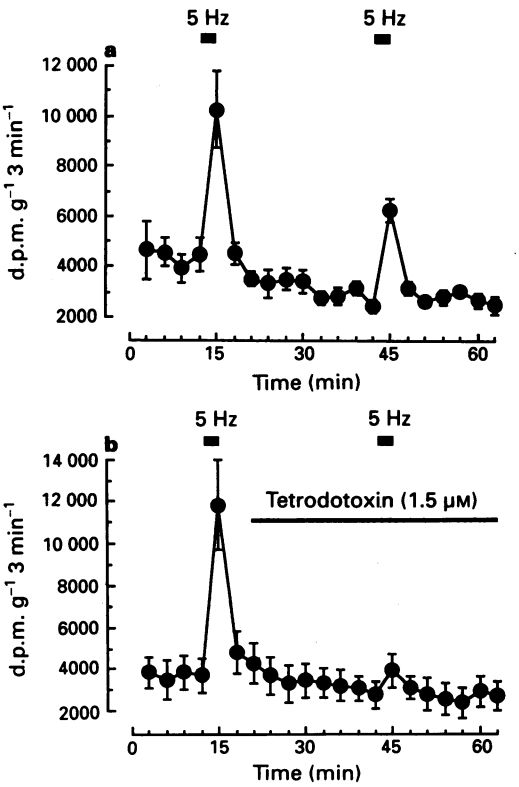

Figure 2 (a) The effect of electrical field stimulation (S1 and S2 = 5 Hz, 1 ms) on the efflux (d.p.m. g^{-1} 3 min^{-1}) of radioactivity derived from [^{3}H]-choline in superfused, epithelium-denuded guinea-pig isolated trachea. Each point represents the mean of 4 observations and vertical lines represent s.e.mean. (b) The effect of tetrodotoxin (1.5 μM) on electrically-induced efflux of radioactivity (n = 3). Tissues were superfused with Krebs-Henseleit solution containing indomethacin (5 μM), gallamine (100 μM) and hemicholinium-3 (10 μM).

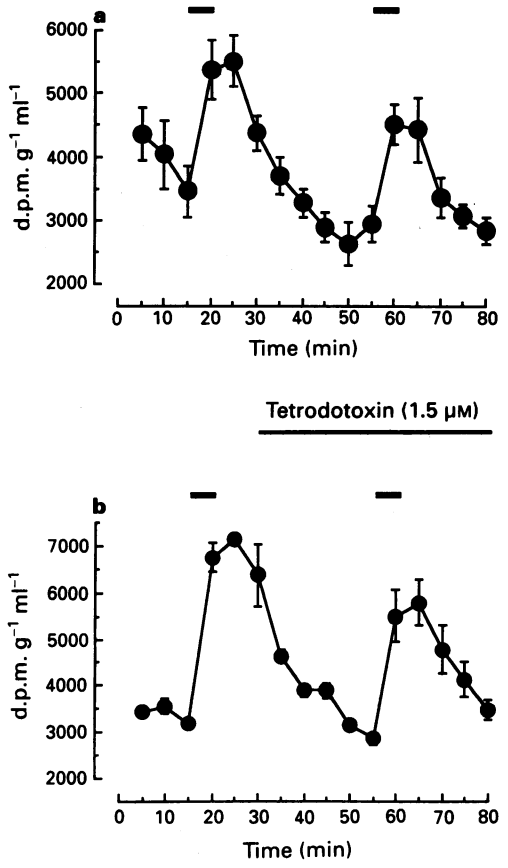

Figure 3 (a) The effect of poly-L-arginine (S1 and S2 = 1 mg ml^{-1}) on the efflux (d.p.m. g^{-1} ml^{-1}) of radioactivity derived from [^{3}H]-choline in epithelium-denuded guinea-pig isolated trachea. Each point represents the mean ± s.e.mean of 4 observations. (b) The effect of tetrodotoxin (1.5 μM) on poly-L-arginine (1 mg ml^{-1})-induced efflux of radioactivity ($n = 3$). Tissues incubated in Krebs-Henseleit solution containing indomethacin (5 μM), gallamine (100 μM) and hemicholinium-3 (10 μM).

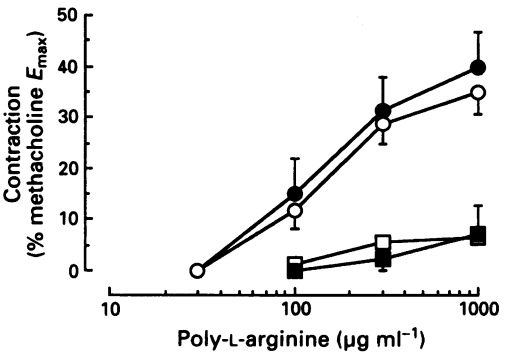

Figure 4 Concentration-dependent contraction of epithelium-denuded rat isolated trachea to poly-L-arginine in the absence (○) or presence of atropine (0.1 μM; □), or methysergide (1 μM; ■) or following acute desensitization to capsaicin (100 μM; ●). Each point represents the mean ± s.e.mean of 5–8 values.

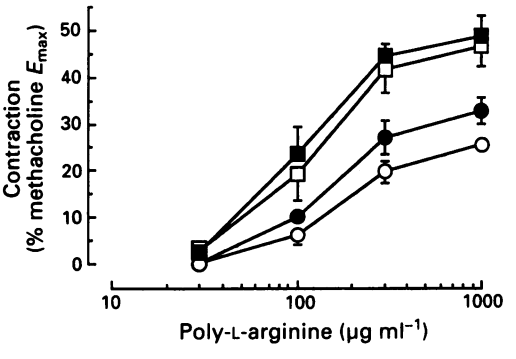

Figure 5 Concentration-dependent contraction of epithelium-denuded rat isolated trachea to poly-L-arginine in the absence (○) or presence of terodotoxin (3 μM; ●) or following treatment with ecothiophate (0.1 μM) in the absence (□) or presence (■) of tetrodotoxin (3 μM). Each point represents the mean ± s.e.mean of 3–6 values.

L-arginine (E_{max} control = 25 ± 1%, $n = 6$ vs E_{max} ecothiophate = 47 ± 4%, $n = 6$, $P < 0.05$ cf. control; Figure 5). In contrast, tetrodotoxin failed to alter significantly the contractile potency of poly-L-arginine in the absence (127 μg ml^{-1} (35–455), $n = 3$, $P > 0.05$ cf. control) or presence of ecothiophate (69 μg ml^{-1} (41–117), $n = 3$, $P > 0.05$ cf. ecothiophate).

Electrical field stimulation of rat isolated trachea resulted in a contractile response (E_{max} 10 Hz: 41 ± 4%, $n = 7$; E_{max} 30 Hz: 60 ± 5%, $n = 7$) that was abolished by tetrodotoxin. Furthermore, ecothiophate significantly increased the contractile responses to EFS at 10 Hz (78 ± 5% methacholine E_{max}; $n = 3$) and 30 Hz (88 ± 3% methacholine E_{max}, $n = 7$). Tetrodotoxin significantly attenuated the response to EFS at these frequencies (10 Hz: 1.4 ± 1.4%, $n = 3$, $P < 0.01$ cf. ecothiophate control; 30 Hz: 2.9 ± 2.9%, $n = 3$, $P < 0.01$ cf. ecothiophate control).

Discussion

We have previously shown that synthetic cationic polypeptides including poly-L-arginine caused charge-dependent, epithelium-independent contraction of guinea-pig isolated tracheal preparations. The contractile response was not mediated by products of cyclo-oxygenase pathway, mast cell-derived histamine or sensory neuropeptides (Spina & Goldie, 1994). The present study has demonstrated that the contractile response to poly-L-arginine was mediated via the release of acetylcholine from parasympathetic nerves. Furthermore, we have demonstrated that a similar mechanism underlies poly-L-arginine-induced contraction of rat isolated trachea, although mast cell derived mediators may also be involved.

In guinea-pig isolated trachea, atropine significantly attenuated the contractile response to poly-L-arginine whereas the acetylcholinesterase inhibitor, ecothiophate, augmented contraction, supporting the view that this response was dependent upon the release of acetylcholine from parasympathetic nerves. However, this effect did not involve the activation of neuronal sodium channels since tetrodotoxin failed to alter the contractile response to poly-L-arginine. In further support of this concept, the present study shows that poly-L-arginine stimulated the release of radioactivity derived from [^{3}H]-choline labelled parasympathetic nerves in guinea-pig isolated trachea. Electrical stimulation of epithelium-denuded guinea-pig isolated trachea resulted in a significant efflux of total radioactivity that was tetrodotoxin-sensitive, indicating the neuronal origin of the released radioactivity. Previous studies have demonstrated that the radioactivity derived from [^{3}H]-choline released by parasympathetic nerve stimulation was predominantly attributed to acetylcholine (D'Agostino *et al.*, 1990; Wessler *et al.*, 1990). Furthermore, we have shown that the poly-L-arginine-induced increase in the efflux of radioactivity was associated with smooth muscle contraction. This provides direct evidence for an interaction between poly-L-arginine and parasympathetic nerves leading to the release of acetylcholine and is consistent with the ability of atropine to inhibit and for ecothiophate to augment the contractile response to poly-L-arginine. The poly-L-arginine-induced increase in the efflux

of radioactivity from these preparations was tetrodotoxin-insensitive and was thus independent of the activation of neuronal sodium channels and neuronal depolarization.

Poly-L-arginine also caused contraction of rat isolated trachea. As in the guinea-pig, the contractile response to poly-L-arginine was augmented in tissues treated with the acetylcholinesterase inhibitor, ecothiophate, providing further evidence for the release of acetylcholine from parasympathetic nerves by poly-L-arginine. This response was abolished by atropine and by the 5-HT-antagonist, methysergide. These data suggest that poly-L-arginine caused contraction of rat trachea following the release of acetylcholine from parasympathetic nerves and/or release of mast cell derived 5-HT. This is consistent with the finding that poly-L-arginine mediated the release of 5-HT from rat peritoneal mast cells (Coleman *et al.*, 1981) and that 5-HT facilitated the electrically-induced contraction of rat isolated bronchi (Szarek *et al.*, 1993).

The possible role of sensory neuropeptides in the contractile response elicited by poly-L-arginine was also investigated. Recently, it has been shown that MBP and the synthetic cationic polypeptide, poly-L-lysine induced the release of substance P from neonatal rat dorsal ganglion neurones in culture (Garland *et al.*, 1993). Neuropeptides failed to contract rat isolated trachea, but mediated an epithelium-dependent, cyclo-oxygenase-sensitive relaxation of contracted rat trachea (Frossard & Muller, 1986; Devillier *et al.*, 1992). This is consistent with the localization of substance P binding sites to airway epithelium and blood vessels in the rat (Sertl *et al.*, 1988). In contrast, bronchoconstriction induced by intravenous administration of sensory neuropeptides, including, neurokinin A and substance P, in the rat was dependent on the release of acetylcholine from parasympathetic nerves and/or mast cell degranulation (Joos *et al.*, 1988). It was suggested that the receptors for the sensory neuropeptides were present on cells other than airway smooth muscle including, mast cells and parasympathetic nerves (Joos *et al.*, 1988). However, in epithelium-denuded rat isolated trachea, acute desensitization of sensory nerves with a high dose of capsaicin failed to alter the contractile potency to poly-L-arginine. It is of interest that the MBP-induced contraction of guinea-pig trachea *in situ* is not augmented following epithelium removal (White *et al.*, 1990). These findings suggest that the MBP-induced contraction of guinea-pig trachea is independent of the release of sensory neuropeptides. We have previously demonstrated that poly-L-arginine caused contraction of guinea-pig isolated trachea that was insensitive to acute desensitization with capsaicin and which was not augmented in the presence of the neutral endopeptidase inhibitor, phosphoramidon (Spina & Goldie, 1994). Thus, either poly-L-arginine did not induce the release of neuropeptides from airway sensory neurones, or neuropeptides released by poly-L-arginine failed to mediate contraction.

The mechanism of action of the poly-L-arginine-induced release of acetylcholine from parasympathetic nerves is not clear. Synthetic cationic polypeptides appear to increase cell membrane permeability as a consequence of binding to negatively charged residues on the cell membrane surface (Larsen, 1967), whereas ECP, but not MBP form transmembrane pores in plasma bilayers (Young *et al.*, 1986). At higher concentrations, MBP increases the permeability of the bilayers as a result of physical damage to the structural integrity of the membranes (Young *et al.*, 1986). It is thought that the charged nature of MBP facilitates binding to the cell surface, whereupon the hydrophobic regions of the molecule penetrate the lipid bilayer (Wasmoen *et al.*, 1989) and/or promote clustering of negatively charged components of the cell membrane (Abu-Ghazaleh *et al.*, 1992), thereby increasing cell membrane permeability. Whether poly-L-arginine increases neuronal cell membrane permeability or binds to a specific protein on the neuronal cell surface is not currently known.

A number of studies have demonstrated that synthetic cationic polypeptides including, poly-L-arginine (Hu *et al.*, 1992) and the related eosinophil-derived cationic polypeptide MBP (Jacoby *et al.*, 1993), behave as allosteric antagonists at cardiac muscarinic M_2-receptors. It has been suggested that during inflammation, the interaction of highly charged polypeptides, including MBP, with M_2-receptors located presynaptically on parasympathetic nerves in the lung, might account for the increase in airways sensitivity to spasmogens which activate vagal nerves in asthma (Jacoby *et al.*, 1992). We have previously shown that poly-L-arginine ($100\,\mu g\,ml^{-1}$) failed to augment the contractile response to electrical field stimulation in guinea-pig isolated trachea (Spina, 1992). This concentration of poly-L-arginine has previously been shown to produce near maximal deceleration of atropine-induced displacement of [^{3}H]-N-methylscopolamine ([^{3}H]-NMS) binding to rat cardiac M_2-receptors and to impair significantly [^{3}H]-NMS binding to rat cardiac M_2-receptors (Hu *et al.*, 1992). The findings in the present study support the view that the increased vagal activity observed during inflammation might also be a consequence of the ability of cationic polypeptides to facilitate the release of acetylcholine from parasympathetic nerves.

This research was supported by grants from the National Health and Medical Research Council of Australia, the Clive and Vera Ramaciotti Foundations of Australia and from the Government Employees Research Fund of New South Wales.

References

ABU-GHAZALEH, R.I., GLEICH, G.J. & PRENDERGAST, F.G. (1992). Interaction of eosinophil granule major basic protein with synthetic lipid bilayers: a mechanism for toxicity. *J. Memb. Biol.*, **128**, 153–164.

COLEMAN, J.W., HOLGATE, S.T., CHURCH, M.K. & GODFREY, R.C. (1981). Immunoglobulin E decapeptide-induced 5-hydroxytryptamine release from rat peritoneal mast cells. *Biochem. J.*, **198**, 615–619.

D'AGOSTINO, G., CHIARI, M.C., GRANA, E., SUBISSI, A. & KILBINGER, H. (1990). Muscarinic inhibition of acetylcholine release from a novel in vitro preparation of the guinea-pig trachea. *Naunyn-Schmied. Arch. Pharmacol.*, **342**, 141–145.

DEVILLIER, P., ACKER, G.M., ADVENIER, C., MARSAC, J., REGOLI, D. & FROSSARD, N. (1992). Activation of an epithelial neurokinin NK-1 receptor induces relaxation of rat trachea through release of prostaglandin E_2. *J. Pharmacol. Exp. Ther.*, **263**, 767–772.

FROSSARD, N. & MULLER, F. (1986). Epithelial modulation of tracheal smooth muscle responses to antigenic stimulation. *J. Appl. Physiol.*, **61**, 1449–1456.

GARLAND, A., JORDAN, J.E., NEELEY, S., WHITE, S.R., NECHELES, J., ALTER, L.E., SCULLY, M., HERNANDEZ, C., LEFF, A.R. & SOLWAY, J. (1993). Effects of eosinophil products upon sensory C-fiber neurons in cell culture. *Am. Rev. Respir. Dis.*, **147**, A816.

GOLDIE, R.G., PAPADIMITRIOU, J.M., PATERSON, J.W., RIGBY, P.J., SELF, H.M. & SPINA, D. (1986). Influence of the epithelium on responsiveness of guinea-pig isolated trachea to contractile and relaxant agonists. *Br. J. Pharmacol.*, **87**, 5–14.

GUNDEL, R.H., LETTS, G. & GLEICH, G.J. (1991). Human eosinophil major basic protein induces airway constriction and airway hyperresponsiveness in primates. *J. Clin. Invest.*, **87**, 1470–1473.

HU, J., WANG, S.-Z., FORRAY, C. & EL-FAKAHANY, E.E. (1992). Complex allosteric modulation of cardiac muscarinic receptors by protamine: potential model for putative endogenous ligands. *Mol. Pharmacol.*, **42**, 311–324.

JACOBY, D.B., GLEICH, G.J. & FRYER, A.D. (1993). Human eosinophil major basic protein is an endogenous allosteric antagonist at the inhibitory muscarinic M_2 receptor. *J. Clin. Invest.*, **91**, 1314–1318.

JOOS, G.F., PAUWELS, R.A. & VAN DER STRAETEN, M.E. (1988). The mechanism of tachykinin-induced bronchoconstriction in the rat. *Am. Rev. Respir. Dis.*, **137**, 1038–1044.

LARSEN, B. (1967). Increased permeability to albumin induced with protamine in modified gelatine membranes. *Nature*, **215**, 641–642.

SERTL, K., WIDERMANN, C.J., KOWALSKI, M.L., HURTADO, S., PLUTCHOK, J., LINNOILA, I., PERT, C.B. & KALINER, M.A. (1988). Substance P: the relationship between receptor distribution in rat lung and the capacity of substance P to stimulate vascular permeability. *Am. Rev. Respir. Dis.*, **138**, 151–159.

SPINA, D. (1992). Failure of poly-L-arginine to inhibit prejunctional M_2-receptors in guinea-pig trachea in vitro. *Am. Rev. Respir. Dis.*, **145**, A438.

SPINA, D. & GOLDIE, R.G. (1994). The effect of synthetic cationic polypeptides on guinea-pig isolated trachea. *Br. J. Pharmacol.*, **111**, 29–34.

SZAREK, J.L., ZHANG, J.Z. & GRUETTER, C.A. (1993). 5-HT_2 receptors augment cholinergic nerve-mediated contraction of rat bronchi. *Eur. J. Pharmacol.*, **231**, 339–346.

WASMOEN, T.L., BELL, M.P., LOEGERING, D.A., GLEICH, G.J., PRENDERGAST, F.G. & MCKEAN, D.J. (1989). Biochemical and amino acid sequence analysis of human eosinophil granule major basic protein. *J. Biol. Chem.*, **263**, 12559–12563.

WESSLER, I., HELLWIG, D. & RACKE, K. (1990). Epithelium-derived inhibition of [^{3}H]acetylcholine release from isolated guinea-pig trachea. *Naunyn-Schmied. Arch. Pharmacol.*, **342**, 387–393.

WHITE, S.R., OHNO, S., MUNOZ, N.M., GLEICH, G.J., ABRAHAMS, C., SOLWAY, J. & LEFF, A.R. (1990). Epithelium-dependent contraction of airway smooth muscle caused by eosinophil MBP. *Am. J. Physiol.*, **259**, L294–L303.

YOUNG, J.D.-E., PETERSON, C.G.B., VENGE, P. & COHN, Z.A. (1986). Mechanisms of membrane damage mediated by human eosinophil cationic protein. *Nature*, **321**, 613–616.

(Received December 16, 1993
Revised March 7, 1994
Accepted March 16, 1994)

Br. J. Pharmacol. (1994), **112**, 901–905

The effect of allosteric antagonists in modulating muscarinic M_2-receptor function in guinea-pig isolated trachea

[1]D. Spina, *E. Minshall, R.G. Goldie & *C.P. Page

[1]Department of Pharmacology, University of Western Australia, Nedlands 6009, Australia and *Department of Pharmacology, King's College London, London SW3 6LX

1 We have assessed the influence of a range of synthetic cationic polypeptides with putative inhibitory actions at prejunctional muscarinic M_2-receptors on electrical field stimulation-induced contraction of guinea-pig isolated tracheal preparations. Electrical field stimulation of epithelium-denuded guinea-pig trachea resulted in frequency-dependent contractile responses. As expected, tracheal smooth muscle sensitivity to electrical field stimulation was increased in tissues pretreated with the muscarinic M_2-receptor antagonist, gallamine. In contrast, gallamine did not significantly alter the contractile potency to acetylcholine.

2 Unlike gallamine, the synthetic cationic polypeptides, poly-L-arginine, poly-L-lysine, poly-D-lysine, the cationic dye ruthenium red and the anionic polysaccharide, heparin, failed to increase significantly tracheal smooth muscle sensitivity to electrical field stimulation.

3 Poly-L-arginine, ruthenium red and heparin had no effect on the contractile response to exogenously applied methacholine.

4 These data are consistent with the concept that in guinea-pig tracheal smooth muscle, gallamine is an allosteric antagonist of guinea-pig tracheal muscarinic M_2-receptors, whereas the various cationic polypeptides and the polyanion, heparin, are not.

Keywords: Muscarinic M_2-receptor, ruthenium red; poly-L-arginine; heparin; guinea-pig trachea

Introduction

It has recently been demonstrated that a number of cardioselective muscarinic receptor antagonists including gallamine (Lee & El-Fakahany, 1991; Ellis *et al.*, 1991), the cationic polypeptides protamine and poly-L-arginine (Hu *et al.*, 1992), eosinophil-derived major basic protein (MBP, Jacoby *et al.*, 1993) and the polyanion, heparin (Gerstin *et al.*, 1992) are allosteric antagonists at cardiac muscarinic M_2-receptors. This is of particular interest given that activation of prejunctional muscarinic M_2-receptors inhibits acetylcholine release from cholinergic nerves and that the function of these receptors in the lung is attenuated in virus-infected (Fryer & Jacoby, 1991) and ovalbumin-sensitized (Fryer & Wills-Karp, 1991; Fryer & Jacoby, 1992) guinea-pigs *in vivo*. Furthermore, muscarinic M_2-receptor function appears to be altered in asthma (Minette *et al.*, 1989).

It would appear that the function of muscarinic M_2-receptors might be modulated during an inflammatory response (Jacoby & Fryer, 1990). It has been suggested that the alteration of receptor function following an inflammatory stimulus might be a consequence of the removal of sialic acid residues present on the extracellular domain of the muscarinic M_2-receptor, presumably mediated by the action of viral and/or inflammatory cell-derived neuraminidase (Fryer *et al.*, 1990; Fryer & Jacoby, 1991; Fryer & Wills-Karp, 1991). Alternatively, cationic proteins released from inflammatory cells, notably eosinophil-derived MBP might act as allosteric antagonists at prejunctional muscarinic M_2-receptors (Fryer & Jacoby, 1992; Jacoby *et al.*, 1993).

We have therefore investigated the influence of drugs that are purported to act either as allosteric inhibitors at the muscarinic M_2-receptor on airway smooth muscle responses *in vitro* to electrical field stimulation. Some of the data presented in this paper have been communicated previously (Spina, 1992).

[1] Author for correspondence at current address: The Sackler Institute of Pulmonary Pharmacology, Department of Thoracic Medicine, King's College School of Medicine and Dentistry, Bessemer Road, London SE5 9PJ

Methods

Tissue preparation

Albino guinea-pigs (300–500 g) were killed by cervical dislocation and the trachea removed and placed in cold (4°C) Krebs-Henseleit solution, aerated with 95% O_2 and 5% CO_2. Since it has previously been shown that the epithelium can influence guinea-pig tracheal smooth muscle sensitivity to spasmogens (Goldie *et al.*, 1986), the epithelium was removed from all preparations with a wooden probe. To confirm the removal of the epithelium, paraffin embedded tracheal sections (8 μm) were stained with haematoxylin-eosin and examined at the light microscopic level.

Tracheal rings (2 mm) were suspended in dimethyldichlorosilane (40%)-treated 1 ml organ baths under an optimal tension of 1 g in Krebs-Henseleit solution aerated with 95% O_2 and 5% CO_2 at 37°C. Tissues were allowed to equilibrate for 30 min and changes in Krebs-Henseleit solution were made every 10 min. Methacholine (10 μM) was added to the bath to induce maximal contraction. After the contractile response had reached plateau, the tissues were washed 5 times over a 15 min period and allowed to equilibrate for a further 30 min.

Electrical field stimulation studies

In order to obtain a predominantly cholinergic response to electrical field stimulation, epithelium-denuded tracheal rings were incubated in Krebs-Henseleit solution containing, the cyclo-oxygenase inhibitor, indomethacin (5 μM), the non-selective β-adrenoceptor antagonist, propranolol (1 μM) and the nitric oxide synthetase inhibitor, N^G-nitro L-arginine methyl ester (L-NAME, 50 μM), 30 min prior to and during electrical field stimulation. Tracheal rings were placed between 2 platinum electrodes and electrically stimulated for 10 s (current = 600 mA, pulse width = 0.5 ms, 0.1–30 Hz) at 3.5 min intervals. Unless otherwise specified, tracheal rings were also incubated for 15 min with α-chymotrypsin (Type I-S; 2 units ml^{-1}) to degrade neuronally released vasointestinal peptide, before and during electrical field stimulation.

Under the conditions described above, frequency-response curves were obtained in the absence or following 30 min incubation in the presence of the muscarinic M_2-receptor antagonists, gallamine (30 and 100 μM) or methoctramine (1 μM), or 1 h incubation with the cationic dye, ruthenium red (1–10 μM), the cationic polypeptides, poly-L-arginine (mol. wt. 11600, 30 and 100 μg ml^{-1}), poly-L-lysine (mol. wt. 12000, 100 μg ml^{-1}), poly-D-lysine (mol. wt. 12000, 100 μg ml^{-1}) or the polysaccharide, heparin (1000 units ml^{-1}). These agents were also present during the construction of frequency-response curves. In the case of experiments with poly-L-arginine, poly-L, poly-D-lysine and heparin, tracheal rings were not incubated with α-chymotrypsin.

Spasmogen studies

In some experiments, acetylcholine cumulative concentration-response curves were constructed in tracheal tissue in the absence or presence of gallamine (30 and 100 μM). In other experiments, methacholine cumulative concentration-response curves were constructed in tracheal tissue in the absence or presence of poly-L-arginine (100 μg ml^{-1}), ruthenium red (3 and 10 μM), or heparin (1000 units ml^{-1}).

Analysis of results

Results have been expressed as the geometric mean together with 95% confidence limits or represented as the arithmetic mean and standard error of the mean. The linear portion of frequency-response curves (between 1 and 30 Hz) was analysed by one-way analysis of covariance (ANCOVA, Kenakin, 1987). Two way analysis of variance with repeated measures was also used to analyse the responses to electrical field stimulation. Where appropriate, data were analysed by an analysis of variance and a non-paired t test was performed to test significance between means. The Bonferroni correction was used in cases where multiple comparisons were made (Wallenstein *et al.*, 1980). Data were considered statistically significant if $P<0.05$.

Drugs

The following drugs were used: indomethacin, (±)-propranolol hydrochloride, α-chymotrypsin (Type I-S), N^G-nitro L-arginine methyl ester, acetylcholine, methacholine, ruthenium red, poly-L-arginine, poly-L-lysine, poly-D-lysine, gallamine triethiodide (Sigma); standard unfractionated heparin (Delta West); methoctramine (Research Biochemicals Inc). All drugs were dissolved in Krebs-Henseleit solution of the following composition, mM: NaCl 117.6, KCl 5.4, $MgSO_4.7H_2O$ 0.57, $KH_2.PO_4$ 1.03, $NaHCO_3$ 25.0, glucose 11.1 and $CaCl_2.2H_2O$ 2.5.

Results

Gallamine

Epithelium-denuded guinea-pig trachea contracted in a frequency-dependent manner in response to electrical field stimulation, this response was abolished in the presence of atropine (0.1 μM). At the maximum frequency tested (30 Hz), the contractile response was 73.7 ± 4.9% ($n=6$) of the maximal response (E_{max}) to methacholine (100 μM). The muscarinic M_2-receptor antagonist, gallamine, significantly increased airway smooth muscle sensitivity to electrical field stimulation in a concentration-dependent manner ($P<0.001$, Figure 1a). This was reflected in 3.4 fold (2.8–4.0, 95% confidence limits, $n=5$), and 6.6 fold (5.3–8.1) leftward shifts in the frequency-response curve in the presence of gallamine 30 μM and 100 μM, respectively. Furthermore, the potentiating effect of gallamine on the contractile response to electrical field stimulation was frequency-dependent ($P<0.01$). In contrast, no change in smooth muscle sensitivity (EC_{50}, 95% confidence limits; control, 2 μM (0.6–7), $n=3$; gallamine 30 μM, 2.1 μM (0.5–8.5), $n=3$, $P>0.05$ paired t test; gallamine 100 μM, 2.3 μM (0.4–12.6), $n=3$,

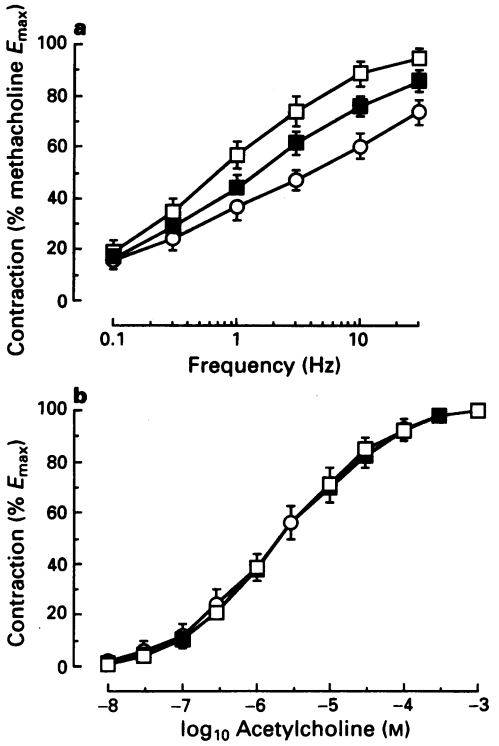

Figure 1 Effect of (a) electrical field stimulation and (b) exogenously applied acetylcholine on guinea-pig isolated tracheal smooth muscle tone in the absence (○) or presence of gallamine (■; 30 μM; □ 100 μM). Each point represents the mean ± s.e.mean of 4–6 observations.

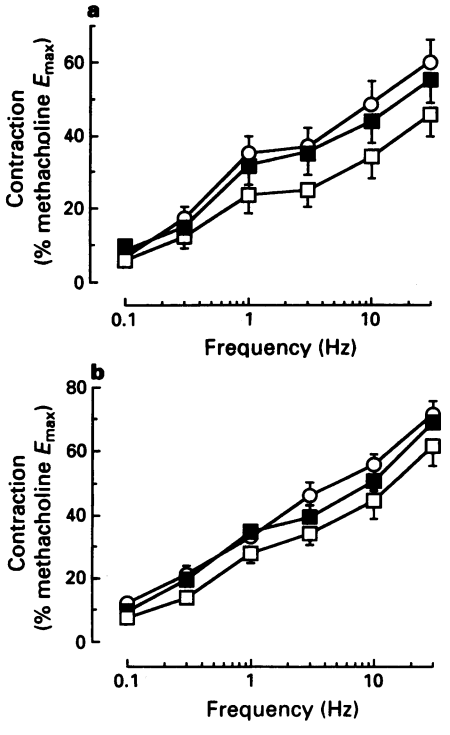

Figure 2 Frequency-dependent contractile response to electrical field stimulation in the absence (○) or presence of (a) poly-L-arginine (■, 30 μg ml^{-1}; □ 100 μg ml^{-1}; $n=4$) and (b) ruthenium red (■, 3 μM; □ 10 μM; $n=3$–6) in epithelium-denuded guinea-pig trachea rings. Each point represents the mean ± s.e.mean.

Table 1 The effect of ruthenium red, poly-L-arginine and heparin on the contractile potency (EC_{50}) and maximum response (E_{max}) of methacholine in epithelium-denuded guinea-pig trachea

	EC_{50} ($\times 10^{-7}$)	E_{max} (mg)	n
Control	3.4 (1.3–8.5)	1648 ± 446	3
Poly-L-arginine (30 μg ml^{-1})	3.6 (2.2–5.8)	1352 ± 184	3
Poly-L-arginine (100 μg ml^{-1})	2.5 (0.9–6.8)	1250 ± 203	3
Control	2.2 (1.1–4.6)	1566 ± 187	5
Ruthenium red (3 μM)	2.3 (1.0–5.4)	1649 ± 196	4
Ruthenium red (10 μM)	3.4 (2.2–5.2)	1375 ± 156	3
Control	2.4 (1.0–5.6)	1411 ± 398	4
Heparin (1000 units ml^{-1})	2.8 (0.9–8.8)	1142 ± 229	4

Results are expressed as geometric mean of n observations. Shown in parentheses are the 95% confidence limits. Poly-L-arginine, ruthenium red or heparin had no significant effect on the contractile potency or E_{max} to methacholine compared with control ($P>0.05$). Indomethacin (5 μM) was present throughout the experiment.

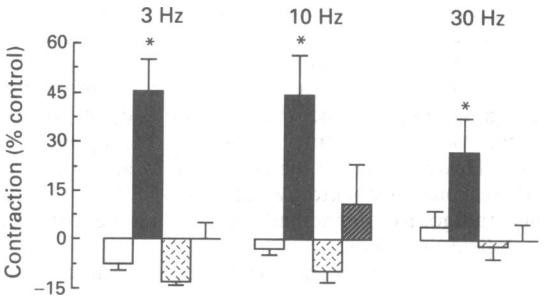

Figure 3 Graph representing the response to electrical field stimulation at 3, 10 and 30 Hz in the absence (open column) or presence of methoctramine (1 μM; solid column), poly-L-lysine (100 μg ml^{-1}; stippled column) and poly-D-lysine (100 μg ml^{-1}; hatched column). Each column represents the mean ± s.e.mean change in tone (% control); $n=5$. * $P<0.01$ versus control.

$P<0.05$ paired t test) or maximal contractile response (E_{max}; control 1305 ± 112 mg, $n=3$; gallamine 30 μM, 1149 ± 177 mg, $n=3$, $P<0.05$ paired t test; gallamine 100 μM, 912 ± 182 mg, $n=3$, $P<0.005$ paired t test) to acetylcholine was observed in gallamine-treated guinea-pig tracheal rings (Figure 1b).

Cationic polypeptides

Unlike gallamine, the synthetic cationic polypeptide, poly-L-arginine (Figure 2a) failed to increase smooth muscle sensitivity to electrical field stimulation. A reduction in airways sensitivity to electrical field stimulation was observed with poly-L-arginine (100 μg ml^{-1}) which was not statistically significant ($P>0.05$). Poly-L-arginine (100 μg ml^{-1}) induced a small increase in baseline tension of 13 ± 2% methacholine E_{max} ($n=4$) but had no significant effect on airway smooth muscle sensitivity to methacholine (Table 1).

Similarly, neither poly-L-lysine nor poly-D-lysine augmented contractile responses to electrical field stimulation (Figure 3). In contrast and as expected, the muscarinic M_2-receptor antagonist, methoctramine (1 μM) significantly increased contractile responses to electrical field stimulation of tissue preparations from the same animals ($P<0.01$).

In the absence of L-NAME, poly-L-arginine (100 μg ml^{-1}) failed to augment the contractile response to electrical field stimulation (10 Hz; −39 ± 8%, $n=3$). In contrast, in tissue preparations from the same animals, methoctramine enhanced the contractile response to EFS (10 Hz; 50 ± 8% of control, $n=3$, $P<0.05$ paired t test). The negatively charged polyanion, heparin (1000 units ml^{-1}) was also without effect on the contractile response to electrical field stimulation (10 Hz; −10.3 ± 11%, $n=3$).

Ruthenium red

Capsaicin (10 μM) caused a contraction of guinea-pig isolated trachea equivalent to 67 ± 2% methacholine E_{max}. Tachyphylaxis to capsaicin occurred such that a second challenge with this agonist resulted in a significantly reduced response (18 ± 4%, $n=6$, $P<0.05$). However, significant protection against capsaicin-induced desensitization was afforded in the presence of the cationic dye ruthenium red (3 μM) which is known to bind to sialic acid residues on the surface of cell membranes (first dose; 53 ± 6%; second dose 46 ± 2%, $n=5$, $P>0.05$). In contrast, ruthenium red failed to enhance airway smooth muscle sensitivity to electrical field stimulation (Figure 2b) or to exogenously administered methacholine (Table 1).

Discussion

Increases in contractile responses to electrical field stimulation induced in the presence of the muscarinic M_2-receptor antagonists, gallamine and methoctramine were observed, consistent with inhibition of muscarinic M_2-receptors located prejunctionally on postganglionic parasympathetic nerves and/or parasympathetic ganglia (Fryer & Maclagan, 1984; Faulkner *et al.*, 1986; Minette & Barnes, 1988; Yang & Biggs, 1991a). However, under conditions where we were able to demonstrate the presence of inhibitory muscarinic M_2-receptors, we were unable to demonstrate any effect on the function of these receptors by substances purported to behave as allosteric inhibitors of such receptors.

These results are not consistent with the suggestion that reduced muscarinic M_2-receptor function accompanying airway inflammation *in vivo*, might be a consequence of the removal of sialic acid residues present on the extracellular domain of the receptor (Fryer *et al.*, 1990; Fryer & Jacoby, 1991; Fryer & Wills-Karp, 1991) and/or an allosteric antagonist effect of MBP at prejunctional muscarinic M_2-receptors in the airways (Fryer & Jacoby, 1992; Jacoby *et al.*, 1993). Interestingly, no alteration in muscarinic M_2-receptor function was observed in guinea-pig trachea taken from ovalbumin challenged sensitized animals *in vitro* (Watson *et al.*, 1991; Yang & Biggs, 1991b) where an eosinophilia and elevated MBP levels might also be expected.

The cardiac muscarinic M_2-receptor contains 21 sialic acid residues (Peterson *et al.*, 1986). The cationic dye, ruthenium red is known to bind to neuraminidase-sensitive sites, i.e. sialic acid, in rat heart as assessed histologically (Woods *et al.*, 1982). It has been postulated that ruthenium red binds to sialic acid residues present on sensory nerves and protects them from damage by capsaicin (Amann & Maggi, 1991). Thus, it was expected that sialic acid residues present on the extracellular domain of the muscarinic M_2-receptor would have been a target for ruthenium red. However, ruthenium red failed to potentiate cholinergic responses in guinea-pig

isolated trachea despite protecting tracheal preparations from capsaicin-induced desensitization.

A number of studies have demonstrated that gallamine can act as an allosteric antagonist at muscarinic M_2-receptors, an action that is significantly enhanced in low ionic strength buffers (Lee & El-Fakahany, 1991; Ellis *et al.*, 1991). It has recently been demonstrated that the synthetic cationic polypeptide, poly-L-arginine (Hu *et al.*, 1992) and MBP (Jacoby *et al.*, 1993) also behave as allosteric antagonists at cardiac muscarinic M_2-receptors. However, we were unable to demonstrate this effect of poly-L-arginine as assessed by detectable changes in neuronal M_2-receptor mediated modulation of airway smooth muscle contraction. The reasons for the discrepancy between the binding data and our results might be attributable to the differences in the strengths of ionic buffers used. This seems unlikely given that both gallamine and methoctramine significantly inhibited airway muscarinic M_2-receptor function. It is also possible that the concentration of poly-L-arginine used in this study was not sufficiently high to antagonize M_2-receptor function. Both poly-L-arginine (Hu *et al.*, 1992) and gallamine (Ehlert, 1992) displaced 0.5 nM [^{3}H]-N-methylscopolamine ([^{3}H]-NMS) binding to M_2 receptors from rat cardiac membranes with similar affinity of 0.4 μM (approx. 5 μg ml^{-1}) and 1.1 μM, respectively. Furthermore, poly-L-arginine (Hu *et al.*, 1992) and gallamine (Ellis *et al.*, 1991; Ellis & Seidenberg, 1992) caused the deceleration of atropine-induced displacement of [^{3}H]-NMS (1 nM) binding from rat cardiac membranes with similar potency (IC_{50} value of 0.5 μM and 0.1–0.6 μM, respectively). Moreover, both poly-L-arginine (10 μM, approx. 100 μg ml^{-1}) and gallamine (10–100 μM) produced similar maximal effects (Ellis & Seidenberg, 1989; Hu *et al.*, 1992) with respect to deceleration of atropine-induced displacement of [^{3}H]-NMS binding to rat cardiac membranes. Poly-L-arginine and gallamine also have a similar negative co-operativity value (Stockton *et al.*, 1983; Hu *et al.*, 1992; Ehlert, 1992). Thus, the concentration of poly-L-arginine used in this study should have influenced M_2-receptor function if it were behaving as an allosteric antagonist. We could not use higher concentrations of poly-L-arginine due to the ability of this synthetic polypeptide to contract airway smooth muscle (Spina & Goldie, 1994a). Indeed, we have demonstrated that the poly-L-arginine-induced contraction of guinea-pig isolated trachea is mediated via the release of acetylcholine from parasympathetic nerves (Spina & Goldie, 1994b).

The anionic polysaccharide, heparin can also behave as an allosteric antagonist and thus, modulates the binding of the muscarinic antagonist [^{3}H]-NMS to cardiac muscarinic M_2-receptors in low but not high ionic strength buffer (Gerstin *et al.*, 1992). Furthermore, oxotremorine-induced inhibition of adenylate cyclase activity in myocardial homogenates was antagonized by heparin in a concentration-dependent manner (Gerstin *et al.*, 1992). In contrast, in the present study, heparin failed to augment the contractile response to electrical field stimulation *in vitro*. The difference between these studies is most likely due to the inability of heparin to penetrate nerve cells *in vitro*. This is consistent with the view that the ability of heparin to influence the binding of muscarinic (Gerstin *et al.*, 1992) and α-adrenoceptor radioligands (Huang *et al.*, 1989) to their respective receptors in membrane preparations, is a consequence of an interaction between the negatively charged heparin and positively charged residues either on the G protein or the receptor itself. This interaction would inhibit the coupling of receptor to G-protein (Huang *et al.*, 1989; Gerstin *et al.*, 1992). Thus, it is possible that poly-L-arginine failed to augment contractile responses to electrical field stimulation *in vitro*, due to the inability of the cationic polypeptide to interact with the cytoplasmic domain of the receptor and/or G protein. Poly-L-arginine and MBP have been shown to attenuate [^{3}H]-NMS binding to muscarinic M_2-receptors in cardiac membranes where access to the intracellular side of the cell membrane is possible (Hu *et al.*, 1992; Jacoby *et al.*, 1993). Alternatively, the inconsistency between these radioligand binding studies and the present study might be due to differences between airway and cardiac muscarinic M_2-receptors (Kilbinger *et al.*, 1991). It has been demonstrated that presynaptic muscarinic receptors might be classified as M_4-receptors (McKinney *et al.*, 1993). Thus, it is possible that the inability to detect changes in presynaptic receptor function in this study to poly-L-arginine might reflect the lower potency of polycations at M_4 than M_2-receptors (protamine 6 fold less potent; Hu *et al.*, 1992). However, gallamine is 2–20 fold less potent at M_4 than M_2-receptors (Stockton *et al.*, 1983; Ellis *et al.*, 1991), yet this antagonist augmented the contractile response to electrical field stimulation.

It has recently been demonstrated in functional and radioligand binding studies that the nitric oxide synthetase inhibitor L-NAME also acts as a muscarinic receptor antagonist (Buxton *et al.*, 1993). This might account for the lack of effect observed with a number of the agents used in this study. However, this seems unlikely, given that in the presence of L-NAME (50 μM), both gallamine and methoctramine were able to antagonize muscarinic M_2-receptor function. Furthermore, L-NAME potentiated electrical field stimulation-induced contractile responses in guinea-pig isolated trachea that was reversed by L-arginine (Belvisi *et al.*, 1991). L-Arginine failed to alter the purported ability of L-NAME to act as an M_2-antagonist (Buxton *et al.*, 1993). These findings would suggest that L-NAME does not act as an antagonist at prejunctional M_2-receptors in guinea-pig airways. Finally, the present data show that in the absence of L-NAME, poly-L-arginine still did not increase the contractile response to electrical field stimulation.

In conclusion, we were unable to demonstrate that synthetic cationic polypeptides behaved as allosteric inhibitors *in vitro*. Thus, inflammation-associated changes in airway M_2-receptor function might not be a consequence of an interaction between cationic polypeptides and the M_2-receptor.

This research was supported by grants from the National Health and Medical Research Council of Australia and the Government Employees Medical Research Fund of New South Wales. E.M. is supported by a Glaxo Group Research Scholarship.

References

AMANN, R. & MAGGI, C.A. (1991). Ruthenium red as a capsaicin antagonist. *Life Sci.*, **49**, 849–856.

BELVISI, M.G., STRETTON, D. & BARNES, P.J. (1991). Nitric oxide as an endogenous modulator of cholinergic neurotransmission in guinea-pig airways. *Eur. J. Pharmacol.*, **198**, 219–221.

BUXTON, I.L.O., CHEEK, D.J., ECKMAN, D., WESTFALL, D.P., SANDERS, K.M. & KEEF, K.D. (1993). N^G-nitro L-arginine methyl ester and other alkyl esters of arginine are muscarinic receptor antagonists. *Circ. Res.*, **72**, 387–395.

EHLERT, F.J. (1988). Gallamine allosterically antagonizes muscarinic receptor-mediated inhibition of adenylate cyclase activity in rat myocardium. *J. Pharmacol. Exp. Ther.*, **247**, 596–602.

ELLIS, J., HUYLER, J. & BRANN, H.R. (1991). Allosteric regulation of cloned m1-m5 muscarinic receptor subtypes. *Biochem. Pharmacol.*, **42**, 1927–1932.

ELLIS, J. & SEIDENBERG, M. (1992). Two allosteric modulators interact at a common site on cardiac muscarinic receptors. *Mol. Pharmacol.*, **42**, 638–641.

ELLIS, J. & SEIDENBERG, M. (1989). Gallamine exerts biphasic allosteric effects at muscarinic receptors. *Mol. Pharmacol.*, **35**, 173–176.

FAULKNER, D., FRYER, A.D. & MACLAGAN, J. (1986). Postganglionic muscarinic inhibitory receptors in pulmonary parasympathetic nerves in guinea-pig. *Br. J. Pharmacol.*, **88**, 181–187.

FRYER, A.D., EL-FAKAHANY, E.E. & JACOBY, D.B. (1990). Parainfluenza virus type 1 reduces the affinity of agonists for muscarinic receptors in guinea-pig lung and heart. *Eur. J. Pharmacol.*, **181**, 51–58.

FRYER, A.D. & JACOBY, D.B. (1991). Parainfluenza virus infection damages inhibitory M2 muscarinic receptors in pulmonary parasympathetic nerves in the guinea-pig. *Br. J. Pharmacol.*, **102**, 267–271.

FRYER, A.D. & JACOBY, D.B. (1992). Function of pulmonary M_2 muscarinic receptors in antigen-challenged guinea-pigs is restored by heparin and poly-L-glutamate. *J. Clin. Invest.*, **90**, 2292–2298.

FRYER, A.D. & MACLAGAN, J. (1984). Muscarinic inhibitory receptors in pulmonary parasympathetic nerves in the guinea-pig. *Br. J. Pharmacol.*, **83**, 973–978.

FRYER, A.D. & WILLS-KARP, M. (1991). Dysfunction of M_2 muscarinic receptors in pulmonary parasympathetic nerves after antigen challenged. *J. Appl. Physiol.*, **71**, 2255–2261.

GERSTIN Jr, E.H., LUONG, T. & EHLERT, F.J. (1992). Heparin, dextran and trypan blue allosterically modulate M_2 muscarinic receptor binding properties and interfere with receptor-mediated inhibition of adenylate cyclase. *J. Pharmacol. Exp. Ther.*, **263**, 910–917.

GOLDIE, R.G., PAPADIMITRIOU, J.M., PATERSON, J.W., RIGBY, P.J., SELF, H.M. & SPINA, D. (1986). Influence of the epithelium on responsiveness of guinea-pig isolated trachea to contractile and relaxant agonists. *Br. J. Pharmacol.*, **87**, 5–14.

HU, J., WANG, S.-Z., FORRAY, C. & EL-FAKAHANY, E.E. (1992). Complex allosteric modulation of cardiac muscarinic receptors by protamine: potential model for putative endogenous ligands. *Mol. Pharmacol.*, **42**, 311–324.

HUANG, R.-R., DEHAVEN, R.N., CHEUNG, A.H., DIEHL, R.E. DIXON, R.A.F. & STRADER, C.D. (1989). Identification of allosteric antagonists of receptor-guanine nucleotide-binding protein interactions. *Mol. Pharmacol.*, **37**, 304–310.

JACOBY, D.B. & FRYER, A.D. (1990). Abnormalities in neural control of smooth muscle in virus-infected airways. *Trends Pharmacol. Sci.*, **11**, 393–395.

JACOBY, D.B., GLEICH, G.J. & FRYER, A.D. (1993). Human eosinophil major basic protein is an endogenous allosteric antagonist at the inhibitory muscarinic M_2 receptor. *J. Clin. Invest.*, **91**, 1314–1318.

KENAKIN, T.P. (1987). *Pharmacologic Analysis of Drug-Receptor Interaction*. New York: Raven Press.

KILBINGER, H., SCHNEIDER, R., SIEFKEN, H., WOLF, D. & D'AGOSTINO, G. (1991). Characterization of prejunctional muscarinic autoreceptors in the guinea-pig trachea. *Br. J. Pharmacol.*, **103**, 1757–1763.

LEE, N.H. & EL-FAKAHANY, E.E. (1991). Allosteric interactions at the m1, m2 and m3 muscarinic receptor subtypes. *J. Pharmacol. Exp. Ther.*, **256**, 468–479.

MCKINNEY, M., MILLER, J.H. & AAGAARD, P.J. (1993). Pharmacological characterization of the rat hippocampal muscarinic receptor. *J. Pharmacol. Exp. Ther.*, **264**, 74–78.

MINETTE, P.A. & BARNES, P.J. (1988). Prejunctional inhibitory muscarinic receptors on cholinergic nerves in human and guinea pig airways. *J. Appl. Physiol.*, **64**, 2532–2537.

MINETTE, P., LAMMERS, J.W.J., DIXON, C.M.S., MCCUSKER, M.T. & BARNES, P.J. (1989). A muscarinic agonist inhibits reflex bronchoconstriction in normal but not in asthmatic subjects. *J. Appl. Physiol.*, **67**, 2461–2465.

PETERSON, G.L., ROSENBAUM, L.C., BRODERICK, D.J. & SCHIMERLIK, M.I. (1986). Physical properties of the purified cardiac muscarinic acetylcholine receptor. *Biochemistry*, **25**, 3189–3202.

SPINA, D. (1992). Failure of poly-L-arginine to inhibit prejunctional M_2-receptors in guinea-pig trachea in vitro. *Am. Rev. Respir. Dis.*, **145**, A438.

SPINA, D. & GOLDIE, R.G. (1994a). The contractile properties of poly-L-arginine in guinea-pig isolated trachea. *Br. J. Pharmacol.*, **111**, 29–34.

SPINA, D. & GOLDIE, R.G. (1994b). Poly-L-arginine-mediated release of acetylcholine from parasympathetic nerves in rat and guinea-pig airways. *Br. J. Pharmacol.*, **112**, 895–900.

STOCKTON, J.M., BIRDSALL, N.J.M., BURGEN, A.S.V. & HULME, E.C. (1983). Modification of the binding properties of muscarinic receptors by gallamine. *Mol. Pharmacol.*, **23**, 551–557.

WALLENSTEIN, S., ZUCKER, C.L. & FLEISS, J.L. (1980). Some statistical methods useful in circulation research. *Circ. Res.*, **47**, 1–9.

WATSON, N., OWEN, R., BARNES, P.J. & MACLAGAN, J. (1991). Pulmonary muscarinic receptors are functionally unaffected by ovalbumin sensitisation. *Am. Rev. Respir. Dis.*, **143**, A751.

WOODS, W.T., IMAMURA, K. & JAMES, T.N. (1982). Electrophysiological and electron microscopic correlations concerning the effects of neuraminidase on canine heart cells. *Circ. Res.*, **50**, 228–239.

YANG, Z.-J. & BIGGS, D.F. (1991a). Muscarinic receptors and parasympathetic neurotransmission in guinea-pig trachea. *Eur. J. Pharmacol.*, **193**, 301–308.

YANG, Z.-J. & BIGGS, D.F. (1991b). Muscarinic-receptor functioning in tracheas from normal and ovalbumin-sensitive guinea pigs. *Can. J. Pharmacol. Physiol.*, **69**, 871–876.

(Received December 16, 1993
Revised March 14, 1994
Accepted March 17, 1994)

Br. J. Pharmacol. (1994), **112**, 906–910

Stereoselective and non-stereoselective actions of isoflurane on the $GABA_A$ receptor

[1]A.C. Hall, W.R. Lieb & N.P. Franks

Biophysics Section, The Blackett Laboratory, Imperial College of Science, Technology and Medicine, South Kensington, London SW7 2BZ

1 Acutely dissociated cerebellar Purkinje neurones from 8–14 day old rats were studied under voltage clamp in the whole-cell patch-clamp configuration. Cl^- currents induced by bath application of γ-aminobutyric acid (GABA) were measured (using symmetrical Cl^- solutions) at both low (2 μM) non-desensitizing and high (300 μM) desensitizing concentrations of GABA.

2 At 2 μM GABA, the bicuculline-sensitive Cl^- currents were potentiated by racemic isoflurane and both of its optical isomers. Isoflurane had no effect on membrane current in the absence of GABA. The dose-response data for potentiation by racemic isoflurane could be fitted with a Hill equation with an $EC_{50} = 320 \pm 20$ μM isoflurane and a Hill coefficient of $h = 2.7 \pm 0.4$ (means ± s.e.mean).

3 The potentiations produced by the optical isomers of isoflurane at 2 μM GABA were stereoselective at moderate and high anaesthetic concentrations. The maximum stereoselectivity, about two fold, occurred at the EC_{50} concentration for general anaesthesia (310 μM isoflurane), with **S(+)**-isoflurane being more effective than **R(−)**-isoflurane. At sub-anaesthetic concentrations, the stereoselectivity was less marked and vanished at the lowest concentration used (77 μM isoflurane).

4 The sustained residual current remaining after exposure of neurones to a desensitizing concentration of GABA (300 μM) was inhibited non-stereoselectively, but only at high concentrations of isoflurane. The ratio of inhibitions by **S(+)**- and **R(−)**-isoflurane (mean ± s.e.mean) was 1.14 ± 0.21 at 770 μM isoflurane. At the EC_{50} concentration for general anaesthesia, however, the inhibition was barely significant.

5 The above results are discussed in relation to the possible role of the $GABA_A$ receptor channel in general anaesthesia.

Keywords: Inhalational general anaesthetics; isoflurane enantiomers; $GABA_A$ receptor; stereoselective actions; rat cerebellar Purkinje neurones

Introduction

Although it has long been recognized that barbiturates can interact directly with $GABA_A$ receptor channels, it has been less clear that volatile anaesthetics behave similarly (for reviews see Moody *et al.*, 1991; Tanelian *et al.*, 1993; and Franks & Lieb, 1994). For example, results from biochemical assays of $^{36}Cl^-$ uptake or release by CNS membrane vesicles have been contradictory, with some workers (Moody *et al.*, 1988) finding inhibition of agonist-induced Cl^- flux by volatile agents and others (Huidobro-Toro *et al.*, 1987; Longoni *et al.*, 1993) reporting enhancement. Electrophysiological data on inhibitory postsynaptic currents (i.p.s.cs) and potentials (i.p.s.ps) have also given equivocal results, with volatile anaesthetics being shown both to prolong i.p.s.cs (Gage & Robertson, 1985; Mody *et al.*, 1991) and inhibit i.p.s.ps (Yoshimura *et al.*, 1985; Fujiwara *et al.*, 1988; El-Beheiry & Puil, 1989) in mammalian central neurones. Recent voltage-clamp studies, however, have demonstrated clearly that volatile anaesthetics at relevant concentrations can markedly enhance GABA-induced Cl^- currents in neurones from rat hippocampus (Jones *et al.*, 1992), dorsal root ganglia (Nakahiro *et al.*, 1989) and nucleus tractus solitarius (Wakamori *et al.*, 1991). These recent voltage-clamp results add to the growing evidence (Tanelian *et al.*, 1993; Franks & Lieb, 1994) that the $GABA_A$ receptor channel is an important target for volatile general anaesthetics.

The recent report (Harris *et al.*, 1992) that isoflurane sleep times in mice are stereoselective (the **S(+)**-isomer induced longer sleep times than the **R(−)**-isomer) not only suggests a direct action of isoflurane on proteins rather than lipids (Franks & Lieb, 1991) but also provides a useful test for putative target proteins: they should interact stereoselectively, with **S(+)**-isoflurane being more effective than **R(−)**-isoflurane. Published studies on the $GABA_A$ receptor, however, have yielded conflicting results. Isoflurane has been reported to be non-stereoselective in enhancing GABA-induced $^{36}Cl^-$ flux in rat brain microvesicles (Quinlan *et al.*, 1992) and in inhibiting *t*-butylbicyclophosphorothionate (TBPS) binding to mouse cerebral cortical $GABA_A$ receptors (Moody *et al.*, 1993). On the other hand, isoflurane displays significant stereoselectivity in potentiating flunitrazepam binding (Moody *et al.*, 1993), and it is markedly stereoselective in its effects on evoked i.p.s.cs in cultured rat hippocampal neurones (Jones & Harrison, 1993). To clarify this problem, we have looked at the relative effects of isoflurane enantiomers under simple and well-controlled conditions, using bath application of known concentrations of both GABA and isoflurane to rat isolated cerebellar Purkinje neurones held under voltage clamp.

Methods

Preparation of rat cerebellar Purkinje neurones

The vermis of the cerebellum was dissected from the brain of a decapitated 8–14 day old Sprague-Dawley rat and cut into chunks of ~1 mm^3. Cells were dissociated with solutions and enzymes described by Mintz *et al.* (1992). Briefly, chunks of vermis were incubated under an O_2 atmosphere at 37°C for 7 to 8 min in a medium of the following composition (mM): Na_2SO_4 82, K_2SO_4 30, $MgCl_2$ 5, HEPES 2, glucose 10, 0.001% phenyl red indicator (titrated to pH 7.4 with NaOH) containing protease (type XXIII) 3 mg ml^{-1}. The protease

[1] Correspondence to any of the authors at the above address.

solution was decanted, and the tissue was resuspended in a medium composed of (mM): Na_2SO_4 82, K_2SO_4 30, $MgCl_2$ 5, HEPES 10, glucose 10, 0.001% phenyl red indicator (titrated to pH 7.4 with NaOH) containing trypsin inhibitor (type II-O, chicken egg white) 1 mg ml^{-1} and bovine serum albumin (fraction V) 1 mg ml^{-1} at 37°C, and then left to cool to room temperature (20–23°C) while continuously bubbling with O_2. An aliquot of the tissue was withdrawn and gently triturated by 10–15 passages through the tip of a lightly fire-polished Pasteur pipette. The resulting cell suspension was subsequently deposited uniformly in a glass-bottomed recording bath (bath volume $\approx$ 100 µl). Cells adhered to the glass within 5–10 min, after which time they were continuously superfused ($\sim$1 ml min^{-1}) with the control bathing medium (composition, mM): NaCl 124, KCl 5, $CaCl_2$ 2, $MgCl_2$ 1, HEPES 5 (titrated to pH 7.4 with NaOH). The Purkinje neurones were relatively easy to distinguish, due to their large size (15–25 µm diameter) and distinctive dendritic stumps. In preliminary investigation, identification was also confirmed by their selective staining with propidium iodide (Regan, 1991). After each recording, the layer of cells was wiped clean from the bath and a fresh aliquot was added. The tissue was used within 4 h of dissection. All chemicals (unless stated otherwise) were obtained from Sigma Chemical Co. Ltd. (Poole, Dorset).

Recording technique

Ionic currents evoked by bath application of GABA (2–300 µM) were recorded using the standard whole-cell voltage-clamp technique (Hamill *et al.*, 1981). Pipettes were fabricated from thin-walled filamented borosilicate glass (GC150TF, Clark Electromedical Instruments, Reading, Berkshire) using a two-stage pull (Narashige PB-7 micropipette puller, Tokyo, Japan). After light fire-polishing, they were filled with the internal recording solution (composition, mM): CsCl 130, $MgCl_2$ 1, HEPES 10, EGTA 11 (titrated to pH 7.4 with CsOH). The pipettes, with typical resistances of 3–5 MΩ, readily formed 'giga-ohm' seals with selected Purkinje neurones which, upon establishing the whole-cell configuration, were voltage-clamped at −60 mV. A few minutes were allowed for the cell interior to equilibrate with the internal solution prior to recording.

Isoflurane (diluted from saturated solutions) and GABA were dissolved in the bathing medium and applied at the same rate as the control solution. The chemical and optical purities of the S(+)- and R(−)-isoflurane isomers were determined to be >99% by chiral chromatography with an 80-metre Chiraldex G-TA column (Advanced Separation Technologies Inc., Whippany, New Jersey, U.S.A.). Currents were filtered at 10 Hz (−3 dB, 8-pole Bessel filter). Series resistance compensation was used (>75% of the series resistance was compensated). All experiments were performed at room temperature (20–23°C). Losses of volatile agents from the perfusion system were found to be negligible (as measured by gas chromatography). Racemic isoflurane was obtained from Abbott Laboratories Ltd. (Queenborough, Kent), and the two optical isomers of isoflurane were a gift from Anaquest Inc. (Murray Hill, New Jersey, U.S.A.).

Values are given as mean ± s.e.mean.

Results

GABA-induced currents in Purkinje neurones

Upon establishing the whole-cell recording configuration, Purkinje cells were routinely held at −60 mV. Inward currents, which reversed close to 0 mV with the symmetric Cl^- solutions used, were readily evoked by bath application of GABA. A concentration of GABA (2 µM), low compared to its EC_{50} (Kaneda *et al.*, 1989, reported a value of 50 µM for Purkinje neurones), produced non-desensitizing inward currents (140–1150 pA) that were generally maintained (up to 20 min) throughout the exposure (n = 94 cells; see Figures 1 and 3). In contrast, exposure of the cells to a high concentration of GABA (300 µM) produced large inward currents ($\sim$4–9 nA) that rapidly desensitized (within $\sim$20 s) and subsequently reached residual levels that were generally sustained for up to $\sim$10 min of continuous exposure (n = 16 cells; see Figure 5).

Effects of racemic isoflurane on currents evoked by GABA (2 µM)

Currents evoked by GABA, 2 µM, were markedly potentiated by racemic isoflurane (Figure 1) at a concentration (310 µM) equivalent to its EC_{50} concentration for general anaesthesia in mammals (Franks & Lieb, 1993). The effect was completely reversible, and repetitive exposures usually generated comparable currents unless there was substantial desensitization associated with the potentiation. Generally, anaesthetic-induced desensitization was only significant at higher concentrations ($\geq$ 610 µM) of isoflurane. Nonetheless, the duration of isoflurane exposure was kept as short as possible so as to minimize any desensitization.

In the absence of GABA, racemic isoflurane did not induce any measurable current in the Purkinje neurones (Figure 1, inset), even at concentrations up to 770 µM (n = 3 cells; data not shown). If after applying isoflurane (310 µM) alone, GABA (2 µM) was then added, comparable potentiations were observed to those found when GABA was applied first. In almost all the experiments described here, isoflurane was applied after initial exposure of the neurones to GABA (as illustrated in Figures 1 and 3).

Potentiations were calculated from the mean amplitude of the control currents in 2 µM GABA immediately before and after the anaesthetic exposure and the maximal current attained after addition of isoflurane. Percentage potentiations varied considerably between Purkinje neurones (for example, 310 µM racemic isoflurane gave values ranging from 66% to 240%) and appeared to vary roughly in inverse proportion to the size of the control current.

To establish the dose-response relationship for the potentiation produced by racemic isoflurane, recordings were made

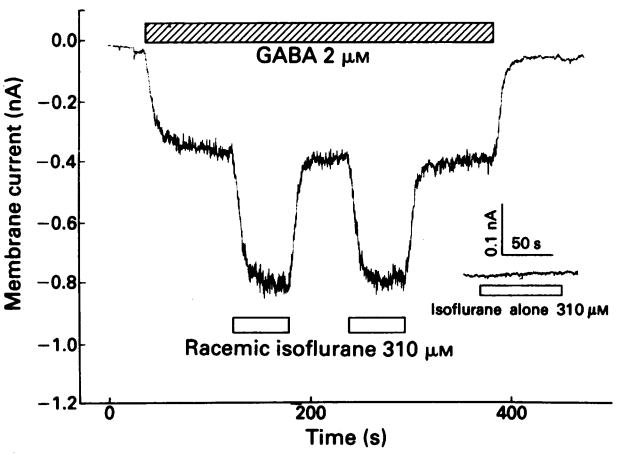

Figure 1 Isoflurane at clinically relevant concentrations (here 310 µM) markedly potentiates the current evoked by a low concentration of γ-aminobutyric acid (GABA, 2 µM) in cerebellar Purkinje neurones. The inward current evoked by bath application of GABA, 2 µM, was non-desensitizing. The effect of the anaesthetic was rapidly reversible, and repeated applications gave consistent potentiations of the Cl^- current. *Inset*: When applied in the absence of GABA, isoflurane 310 µM had no effect on the membrane current. In this and all other recordings, the neurone was voltage-clamped at −60 mV and whole-cell currents were recorded in symmetrical Cl^- solutions.

from individual neurones ($n = 5$) that were exposed to increasing concentrations of isoflurane (77–920 μM), with washout of anaesthetic after each exposure. Dose-response data from these neurones were then pooled. The percentage potentiation is plotted *versus* concentration in Figure 2. The data have been fitted to a Hill equation of the form $y = 100\ c^h/(c^h + EC_{50}^h)$, where y is the percentage potentiation, c is the isoflurane concentration, and h is the Hill coefficient. The best fit gave an EC_{50} of 320 ± 20 μM isoflurane (~EC_{50} for general anaesthesia) and a Hill coefficient of $h = 2.7 \pm 0.4$. The current induced by GABA (2 μM), whether in the absence or presence of isoflurane (310 μM), was completely abolished by 30 μM bicuculline (Figure 2, inset), and 3 μM bicuculline blocked the 2 μM GABA/310 μM isoflurane current by ~85% (data not shown).

Effects of isoflurane enantiomers on potentiation of $GABA_A$ currents

The pure enantiomers of isoflurane (77–920 μM) also produced marked potentiations of the 2 μM GABA-induced currents in cerebellar Purkinje neurones (Figure 3). At a very low concentration (77 μM) of S(+)- and R(−)-isoflurane, the degree of potentiation was identical for both isomers (Figure 3a); the ratio of potentiations [S(+)/R(−)-isoflurane] was 1.00 ± 0.09 ($n = 6$ cells: see Figure 4). However, at 310 μM, a concentration approximately equal to the EC_{50} for general anaesthesia (Franks & Lieb, 1993), S(+)-isoflurane produced a substantially larger potentiation of the GABA-activated current than did R(−)-isoflurane; this was true regardless of the order of exposure (Figure 3b). Stereoselectivity was equally apparent at both the 610 and 920 μM enantiomer concentrations (Figures 3c and 4), again independent of the order of isomer exposure.

Because the observed potentiation for a given anaesthetic concentration varied substantially between different neurones, maximum precision in estimating the degree of stereoselectivity for the isoflurane isomers was obtained by measuring the ratios of potentiations for individual neurones exposed to fixed concentrations of both isomers (as in Figure 3). The isoflurane dose-response data for these ratios are plotted in Figure 4.

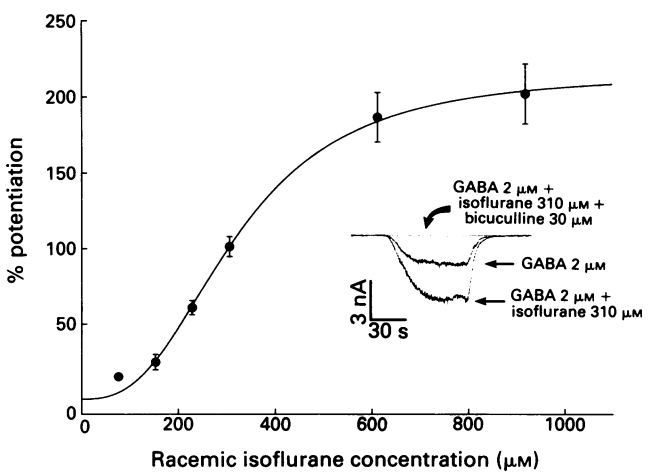

Figure 2 Dose-response curve for the potentiation of the GABA (2 μM)-induced inward current by racemic isoflurane. The mean percentage potentiations (see text) obtained from 5 recordings (on 5 different neurones) are plotted against racemic isoflurane concentration. Values are mean with s.e.mean and where standard errors are not shown they are smaller than the size of the symbol. The data were fitted to a Hill equation with an EC_{50} of 320 ± 20 μM isoflurane and a Hill coefficient $h = 2.7 \pm 0.4$. *Inset*: Bicuculline (30 μM) completely abolished the current evoked by GABA (2 μM) in both the presence (and absence: not shown) of isoflurane (310 μM).

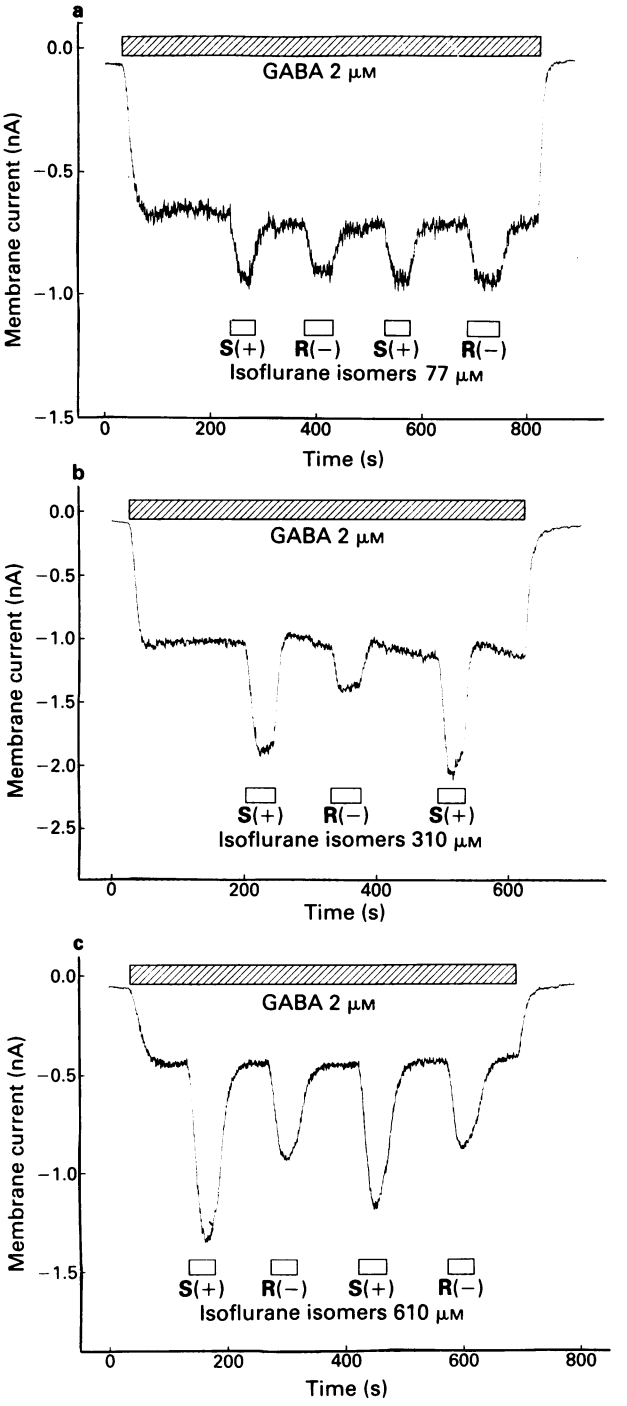

Figure 3 The optical isomers of isoflurane can act stereoselectively and non-stereoselectively in potentiating GABA-induced currents, depending on the isoflurane concentration. (a) Alternate additions of 77 μM S(+)- and R(−)-isoflurane to the superfusate resulted in small current potentiations, with the two isomers being equally effective. (b) At 310 μM isoflurane, the S(+)-isomer is roughly twice as effective as the R(−)-isomer. (c) A typical example of the responses to consecutive applications of 610 μM S(+)- and R(−)-isoflurane, showing marked stereoselectivity as well as the tendency for the currents in the presence of the higher concentrations of anaesthetic to show some desensitization. In all cases, reversal of the anaesthetic effect was rapid and complete.

Effects of isoflurane on residual 'desensitized' $GABA_A$ current

When cerebellar Purkinje neurones were exposed to a high GABA concentration (300 μM), a rapidly desensitizing current was observed that was followed by a residual component

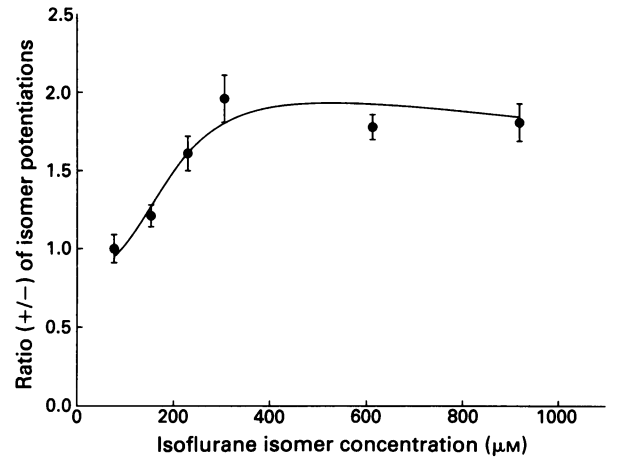

Figure 4 The degree of stereoselectivity of the isoflurane enantiomers depends on their concentration. Individual cells were exposed consecutively to a single concentration of each optical isomer of isoflurane after exposure to a low (2 μM) concentration of GABA. The ratio is the potentiation produced by the S(+)-isomer divided by that produced by the R(−)-isomer. The points represent means ($n \geq 5$ cells) with s.e.mean. The curve was fitted by eye.

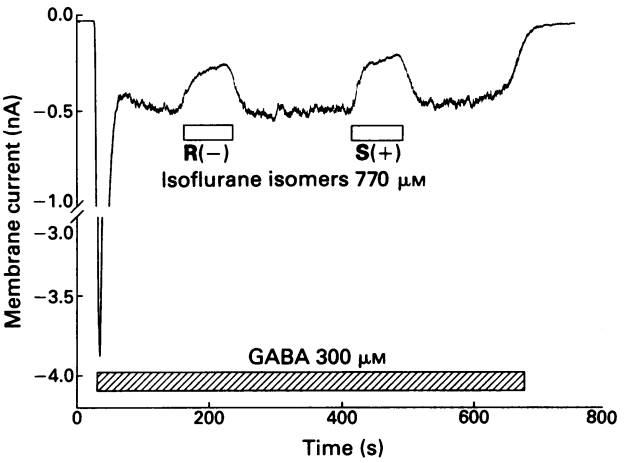

Figure 5 The sustained residual current following exposure to a high, desensitizing concentration (300 μM) of GABA is inhibited by both isomers of isoflurane in a non-stereoselective manner. Here, both the S(+)- and the R(−)-isomers at 770 μM caused a comparable (~50%) inhibition.

(see Figure 5). At an isoflurane concentration (310 μM) near to the EC_{50} for general anaesthesia, this residual current was only weakly inhibited (6.1 ± 3.5%, $n = 4$ cells) by addition of racemic isoflurane (not shown). However, at 770 μM isoflurane, the S(+)- and R(−)-isomers blocked 42.5 ± 5.6% and 37.2 ± 4.8% ($n = 6$ cells) of the residual component, respectively, giving a ratio [inhibition by S(+)/R(−)] of 1.14 ± 0.21. Thus isoflurane was not only relatively ineffective but also non-stereoselective at inhibiting this residual current.

Discussion and conclusions

Because of the traditional belief that most general anaesthetics (particularly the inhalational agents) produce their effects by acting non-specifically on lipids, little effort has, until recently, gone into synthesizing and testing optical isomers of inhalation agents. However, accumulating evidence (Franks & Lieb, 1991; 1994) that anaesthetics at clinically relevant levels act directly on proteins (rather than lipids) has motivated investigators to look for selective effects of anaesthetics. In particular, it has encouraged the synthesis (Huang *et al.*, 1992) of optically and chemically pure enantiomers of the widely used inhalation agent, isoflurane, and these have now been tested both on animals and neuronal ion channels. Although isoflurane was found to exhibit no stereoselectivity on lipid bilayers (Franks & Lieb, 1991), the surprising result has been that the isomers differentially affect a number of anaesthetic-sensitive ion channels (Franks & Lieb, 1991; Jones & Harrison, 1993; Moody *et al.*, 1993) as well as inducing different sleep times in mice (Harris *et al.*, 1992). In all cases where substantial stereoselective effects have been documented, the S(+)-optical isomer has been found to be more effective than the R(−)-isomer. To the extent that sleep time experiments are pertinent to general anaesthesia, this provides a new tool (in addition to anaesthetic sensitivity) for assessing pharmacological relevance: if S(+)-isoflurane is found to be more effective than R(−)-isoflurane at a given site and/or for a given behaviour, that site or behaviour is more likely to be involved in general anaesthesia.

We have used this test in the present experiments to distinguish between pharmacologically relevant and irrelevant effects of isoflurane on the $GABA_A$ receptor channel complex in rat cerebellar Purkinje neurones. It has been shown (and we have verified here) that volatile agents can both potentiate and inhibit GABA-induced Cl^- currents (Nakahiro *et al.*, 1989). Potentiating effects of racemic isoflurane (Figures 1 and 2) were observed with bath application of a low, non-desensitizing concentration of GABA and found to be dose-dependent and apparently highly cooperative (Hill coefficient = 2.7 ± 0.4). In addition, the EC_{50} concentration (320 ± 20 μM isoflurane) is very close to that for producing general anaesthesia (Franks & Lieb, 1993) in the rat (350 μM) and other mammals (320 μM on average). At this EC_{50} concentration, the GABA-induced current was potentiated by about 100%. Interestingly, isoflurane applied in the absence of GABA (see inset to Figure 1) had no effect.

When tested for stereoselectivity, the potentiation at an isoflurane concentration equivalent to the EC_{50} for general anaesthesia was found to be almost twice as great for the S(+)- as for the R(−)-enantiomer (Figures 3b and 4). This ratio is identical to the twofold effects found for activating the potassium current $I_{K(An)}$ in molluscan neurones (Franks & Lieb, 1991) and for prolonging evoked inhibitory postsynaptic currents (i.p.s.cs) in cultured rat hippocampal neurones (Jones & Harrison, 1993). It is also similar to the 50% differences in isoflurane association constants for binding to nicotinic acetylcholine receptors in molluscan neurones (Franks & Lieb, 1991) and for prolonging sleep times in mice at low doses of isoflurane (Harris *et al.*, 1992). On the other hand, we found no significant stereoselectivity for the inhibitory actions of isoflurane on the residual 'desensitized' current remaining after prolonged exposure to a high (300 μM) concentration of GABA (Figure 5). In addition, we found that the inhibition was very small at the isoflurane EC_{50} concentration for general anaesthesia. Thus our results show that the potentiating effects of isoflurane are not only very sensitive to isoflurane, but are stereoselective with the same order of selectivity as that observed in mammals. The inhibitory effects, on the other hand, are both relatively insensitive to isoflurane and non-stereoselective. Thus it seems likely that the potentiating, but not the inhibitory, effects of isoflurane on the $GABA_A$ receptor channel are pharmacologically relevant to mammalian general anaesthesia.

The nature of the dose-response relationship (Figure 4) for the ratio of potentiations by the S(+)- and R(−)-isomers has implications for the molecular mechanism by which isoflurane potentiates GABA responses. This ratio is close to unity for very low, sub-anaesthetic concentrations of isoflurane (see also Figure 3a), rapidly rises to a maximum

value at 310 μM isoflurane (~EC_{50} concentration for general anaesthesia), and remains high (although with a hint of a decrease) up to at least 920 μM isoflurane (≈three times the EC_{50} for general anaesthesia). This behaviour is consistent with isoflurane first binding to a low-affinity, achiral site on the $GABA_A$ receptor channel and allosterically modifying a second binding site for isoflurane, converting it into a chiral site of higher affinity. Although more work is needed to test the validity of this idea, such an allosteric effect is in line with the apparent positive cooperativity (Hill coefficient = 2.7 ± 0.4) that we have observed for potentiation by racemic isoflurane (see Figure 2).

Since our results suggest that the potentiating, but not the inhibitory, effects of inhalational anaesthetics on the $GABA_A$ receptor channel are relevant to general anaesthesia, the question arises as to how such potentiation might occur at inhibitory synapses. At these synapses, postsynaptic $GABA_A$ receptors are exposed to high aqueous concentrations of GABA for about a millisecond following invasion of the presynaptic nerve terminal by an action potential. This is a quite different situation from that in which we have studied potentiation (low GABA concentrations for many seconds). However, there is a connection between the two situations, in that it is well-known (see, for example, Parker *et al.*, 1986, and Wakamori *et al.*, 1991) that anaesthetics increase the apparent affinity of GABA for the $GABA_A$ receptor (i.e. they shift the GABA dose-response curve to lower GABA concentrations). It is this apparent increase in affinity that causes potentiation of GABA-induced currents during prolonged bath exposure to low concentrations of GABA. At a synapse, a similar increase in affinity would retard the dissociation of GABA from its receptor, so that substantial GABA would remain bound (and hence receptor channels remain open) for many milliseconds after free GABA has been removed from the synaptic cleft. This is consistent with the well-documented prolongation of $GABA_A$-mediated i.p.s.ps and i.p.s.cs by a wide variety of general anaesthetics and may account for much of the CNS depression caused by surgical levels of general anaesthetics.

We thank Jerry Vernice, Don Halpern, Grand Huang and Leo Rozov of Anaquest Inc. for kindly supplying the isoflurane isomers, Robert Dickinson for checking their purity and Ramin Nakisa for writing the acquisition software. We are grateful to the MRC, the NIH (grant GM 41609), Anaquest Inc., and the BOC Group Inc. for support.

References

EL-BEHEIRY, H. & PUIL, E. (1989). Anaesthetic depression of excitatory synaptic transmission in neocortex. *Exp. Brain Res.*, **77**, 87–93.

FRANKS, N.P. & LIEB, W.R. (1991). Stereospecific effects of inhalational general anesthetic optical isomers on nerve ion channels. *Science*, **254**, 427–430.

FRANKS, N.P. & LIEB, W.R. (1993). Selective actions of volatile general anaesthetics at molecular and cellular levels. *Br. J. Anaesthes.*, **71**, 65–76.

FRANKS, N.P. & LIEB, W.R. (1994). Molecular and cellular mechanisms of general anaesthesia. *Nature*, **367**, 607–614.

FUJIWARA, N., HIGASHI, H., NISHI, S., SHIMOJI, K., SUGITA, S. & YOSHIMURA, M. (1988). Changes in spontaneous firing patterns of rat hippocampal neurones induced by volatile anaesthetics. *J. Physiol.*, **402**, 155–175.

GAGE, P.W. & ROBERTSON, B. (1985). Prolongation of inhibitory postsynaptic currents by pentobarbitone, halothane and ketamine in CA1 pyramidal cells in rat hippocampus. *Br. J. Pharmacol.*, **85**, 675–681.

HAMILL, O.P., MARTY, A., NEHER, E., SAKMANN, B. & SIGWORTH, F.J. (1981). Improved patch-clamp techniques for high-resolution current recording from cells and cell-free membrane patches. *Pflüg. Arch.*, **391**, 85–100.

HARRIS, B., MOODY, E. & SKOLNICK, P. (1992). Isoflurane anesthesia is stereoselective. *Eur. J. Pharmacol.*, **217**, 215–216.

HUANG, C.G., ROZOV, L.A., HALPERN, D.F., VERNICE, G.G., BENVENGA, M.J. & JERUSSI, T.P. (1992). Preparation of the pure enantiomers of isoflurane. *Abstracts of Am. Chem. Soc.*, 203rd National Meeting, FLUO 18.

HUIDOBRO-TORO, J.P., BLECK, V., ALLAN, A.M. & HARRIS, R.A. (1987). Neurochemical actions of anesthetic drugs on the γ-aminobutyric acid receptor-chloride channel complex. *J. Pharmacol. Exp. Ther.*, **242**, 963–969.

JONES, M.V., BROOKS, P.A. & HARRISON, N.L. (1992). Enhancement of γ-aminobutyric acid-activated Cl^- currents in cultured rat hippocampal neurones by three volatile anaesthetics. *J. Physiol.*, **449**, 279–293.

JONES, M.V. & HARRISON, N.L. (1993). Effects of volatile anesthetics on the kinetics of inhibitory postsynaptic currents in cultured rat hippocampal neurons. *J. Neurophysiol.*, **70**, 1339–1349.

KANEDA, M., WAKAMORI, M. & AKAIKE, N. (1989). GABA-induced chloride current in rat isolated Purkinje cells. *Am. J. Physiol.*, **256**, C1153–C1159.

LONGONI, B., DEMONTIS, G.C. & OLSEN, R.W. (1993). Enhancement of γ-aminobutyric $acid_A$ receptor function and binding by the volatile anesthetic halothane. *J. Pharmacol. Exp. Ther.*, **266**, 153–159.

MINTZ, I.M., ADAMS, M.E. & BEAN, B.P. (1992). P-type calcium channels in rat central and peripheral neurons. *Neuron*, **9**, 85–95.

MODY, I., TANELIAN, D.L. & MACIVER, M.B. (1991). Halothane enhances tonic neuronal inhibition by elevating intracellular calcium. *Brain Res.*, **538**, 319–323.

MOODY, E.J., HARRIS, B.D. & SKOLNICK, P. (1993). Stereospecific actions of the inhalation anesthetic isoflurane at the $GABA_A$ receptor complex. *Brain Res.*, **615**, 101–106.

MOODY, E.J., SUZDAK, P.D., PAUL, S.M. & SKOLNICK, P. (1988). Modulation of the benzodiazepine/γ-aminobutyric acid receptor chloride channel complex by inhalation anesthetics. *J. Neurochem.*, **51**, 1386–1393.

MOODY, E.J., YEH, H.J.C. & SKOLNICK, P. (1991). The $GABA_A$ receptor complex: is it a locus of action for inhalation anesthetics? In *Neuropharmacology of Ethanol.* ed. Miller, R.E., Koob, G.F., Lewis, M.J. & Paul, S.M. pp. 77–92. Boston: Birkhauser.

NAKAHIRO, M., YEH, J.Z., BRUNNER, E. & NARAHASHI, T. (1989). General anesthetics modulate GABA receptor channel complex in rat dorsal root ganglion neurons. *FASEB J.*, **3**, 1850–1854.

PARKER, I., GUNDERSEN, C.B. & MILEDI, R. (1986). Actions of pentobarbital on rat brain receptors expressed in *Xenopus* oocytes. *J. Neurosci.*, **6**, 2290–2297.

QUINLAN, J.J., HUNTLEY, D. & FIRESTONE, L.L. (1992). Isoflurane's enhancement of GABA-gated chloride flux is not stereoselective. *Anesthesiology*, **77**, A701.

REGAN, L.J. (1991). Voltage-dependent calcium currents in Purkinje cells from rat cerebellar vermis. *J. Neurosci.*, **11**, 2259–2269.

TANELIAN, D.L., KOSEK, P., MODY, I. & MACIVER, M.B. (1993). The role of the $GABA_A$ receptor/chloride channel complex in anesthesia. *Anesthesiology*, **78**, 757–776.

WAKAMORI, M., IKEMOTO, Y. & AKAIKE, N. (1991). Effects of two volatile anesthetics and a volatile convulsant on the excitatory and inhibitory amino acid responses in dissociated CNS neurons of the rat. *J. Neurophysiol.*, **66**, 2014–2021.

YOSHIMURA, M., HIGASHI, H., FUJITA, S. & SHIMOJI, K. (1985). Selective depression of hippocampal inhibitory postsynaptic potentials and spontaneous firing by volatile anesthetics. *Brain Res.*, **340**, 363–368.

(Received January 11, 1994
Accepted March 2, 1994)

Br. J. Pharmacol. (1994), **112**, 911–919

Mediation of most atypical effects by species homologues of the β_3-adrenoceptor

Nathalie Blin, Clara Nahmias, Marie F. Drumare & [1]A. Donny Strosberg

Institut Cochin de Génétique Moléculaire, CNRS-UPR 0415 and Université Paris VII, 22 rue Méchain, 75014 Paris, France

1 A wide panel of compounds acting on β-adrenoceptors active either in mammalian heart or in rodent digestive tract and adipose tissues, were investigated for their effects on Chinese hamster ovary cells transfected with the human or murine β_3-adrenoceptor gene.

2 The β_3-agonists, bucindolol, CGP 12177A and pindolol exhibited the highest binding affinities; BRL 37344, LY 79771, ICI 201651 and SR 58611A presented high potencies in stimulating adenylyl cyclase; bupranolol appeared as the most efficient β_3-antagonist.

3 This pharmacological analysis further established that the β_3-adrenoceptor is the prototype of the adipose tissue atypical β-adrenoceptor, since these receptors share a number of pharmacological properties which differ strikingly from those of β_1- and β_2-adrenoceptors: low affinities for conventional β-adrenoceptor agonists and antagonists, high potencies for novel compounds active in adipose tissues, partial agonistic activites for several β_1/β_2-antagonists.

4 Although the pharmacological profiles of the human and murine β_3-receptor were very similar, some quantitative or even qualitative differences were observed for particular compounds such as propranolol, which exhibited weak and partial agonistic effects at the human β_3-receptors and antagonistic effects at the murine β_3-receptors. These differences may result from key amino-acid substitutions between the human and the murine β_3-receptor sequences, which may alter the binding site or signal processing.

5 Compounds active on atypical β-sites of other tissues such as heart and digestive tract were also potent on the β_3-adrenoceptor expressed in Chinese hamster ovary cells, suggesting that this receptor mediates most of the atypical properties described in various tissues, and that differences in ligand effects may result from tissue-related specificities.

Keywords: β_3-Adrenoceptors; atypical β-adrenoceptors; species-specificity; propranolol; adipose tissues; intestinal smooth muscle

Introduction

β-Adrenoceptors are integral membrane proteins mediating a wide variety of physiological actions of catecholamines, through coupling to guanine nucleotide-binding regulatory proteins (G proteins) and activation of adenylyl cyclase. It was initially thought that the β_1 and β_2 receptor subtypes modulate all the effects of adrenaline and noradrenaline. More recently however, an increasing number of reports proposed the existence in tissues of a new pharmacological entity with atypical β-adrenoceptor properties such as intrinsic sympathomimetic activities or low inhibition efficiencies for conventional β-antagonists (Zaagsma & Nahorski, 1990). These atypical properties were mostly derived from the pharmacological analyses of the metabolic responses in adipose tissues (i.e. oxygen consumption, mitochondrial GDP-binding and lipolysis); the strongest evidence for the existence of an atypical β-receptor came from studies with a series of novel agonists (e.g. BRL 35135, BRL 26830) that induced potent and selective thermogenic and anti-obesity activities in animal models (Wilson *et al.*, 1984; Arch *et al.*, 1984; 1989). In addition to the effects in rodent brown (BAT) and white (WAT) adipose tissues (Bojanic *et al.*, 1985; Hollenga & Zaagsma, 1989), atypical β-adrenoceptor pharmacological properties were described in gastro-intestinal tract of rodents (Bond & Clarke, 1988; Manara *et al.*, 1990; Bianchetti & Manara, 1990; MacLaughlin & MacDonald, 1990), and in cat heart (Kaumann, 1989). However, these functional approaches were hampered by the scarcity of pharmacological tools able to identify unambiguously the tissue atypical β-adrenoceptor, as well as by the simultaneous expression of different β-receptor subtypes in tissues. Therefore, confusing results were obtained for some compounds depending on the species or the tissue studied, and led to a controversy on the atypical nature of the β-receptor involved.

Emorine *et al.* (1989), provided the first molecular evidence for the existence of a third β-adrenoceptor subtype, by cloning a human gene which encoded a receptor resistant to blockade by conventional β-antagonists and highly sensitive to the novel thermogenic β-agonists. Expression of this gene was recently demonstrated in human brown adipose tissue by cDNA cloning (Lelias *et al.*, 1993), as well as in SK-N-MC human neuroblastoma cells by northern blot hybridization analysis (Esbenshade *et al.*, 1992). In human adipose tissue, colon and gallbladder, the presence of β_3-receptors has been proved by polymerase chain reaction assays (Krief *et al.*, 1993), while evidence for a functional β_3-receptor in human fat cells was shown by lipolysis stimulation studies (Lönnqvist *et al.*, 1993).

The murine gene (Nahmias *et al.*, 1991) and the rat cDNA (Granneman *et al.*, 1991; Muzzin *et al.*, 1991) coding for the β_3-receptor were also cloned and their functional characterization further established their similarity with the rodent atypical β-site (Fève *et al.*, 1991; Nahmias *et al.*, 1991; Emorine *et al.*, 1992). However, the pharmacological comparison of the cloned human rodent β_3-receptors expressed in the same cell line led to controversial interpretations (Granneman *et al.*, 1991; Muzzin *et al.*, 1991; Liggett, 1992), in analyses which were generally performed with only a few ligands and using different experimental conditions (reviewed by Emorine *et al.*, 1994). A thorough investigation of β_3-potent and -selective pharmacological tools thus remained essential to characterize further the β_3-adrenoceptor, as well as to examine accurately its relationships with the atypical β-receptors mostly described in rodent tissues.

In this study, a large panel of compounds known to interact with the atypical β-receptors described either in

[1] Author for correspondence.

adipose tissues or in intestinal smooth muscle and heart, were assessed for their binding capacities, as well as for their agonistic or antagonistic properties towards the adenylyl cyclase in Chinese hamster ovary (CHO) cells transfected with the human (CHO-Huβ3) or with the murine (CHO-Moβ3) β_3-adrenoceptor gene. The availability of cells expressing a single receptor subtype offered a unique opportunity for the characterization of a receptor, and this eukaryotic expression system was validated by testing conventional β-ligands (Tate *et al.*, 1991). The pharmacological patterns of the human and murine β_3-adrenoceptors are compared and discussed herein relative to those of the mammalian tissue atypical β-receptors in light of possible species- and tissue-specific effects.

Methods

Cell culture

Subclones of CHO cells, stably transfected with the human β_3-adrenoceptor (Emorine *et al.*, 1989; Tate *et al.*, 1991) or the murine β_3-adrenoceptors (Nahmias *et al.*, 1991), were grown as previously described. Chinese hamster CHW-1102 fibroblasts expressing the human β_3-receptor (Nantel *et al.*, 1993) were cultured in DMEM supplemented with 10% FCS, 2 mM L-glutamine and neomycin 150 μg ml^{-1} to maintain the selection of the transfectants.

Receptor binding assays

Preconfluent cells were harvested by treatment with EDTA and washed with Hank's balanced salt solution supplemented with 1 mM ascorbic acid and buffered with 20 mM HEPES to achieve a pH of 7.4. Aliquots of 10^5 cells were incubated with [^{125}I]-CYP in the absence or presence of a competitor, in a 500 μl buffered final volume with 0.1% (w/v) bovine serum albumin and 4 μM desipramine. The reaction was carried out for 45 min at 37°C under shaking in dark. After dilution with ice-cold PBS (pH 7.4), cells were immediately filtered and extensively washed over glass-fibre disks presoaked with 0.3% polyethyleneimine. Radioactivity was measured in a γ-radiation counter with an efficiency of 80%.

Saturation experiments were performed with [^{125}I]-CYP concentrations ranging from 50 to 5000 pM, and non-specific binding was determined in the presence of 100 μM (−)-isoprenaline. Competition experiments were performed with 1 nM [^{125}I]-CYP and varying concentrations of competitor (1 pM to 100 μM).

Adenylyl cyclase binding assays

Preconfluent cells in six-well dishes (≈1.2×10^6 cells/well) were washed twice with 2 ml ice-cold PBS, added to 1 ml of ice-cold Ham's F12 medium buffered with HEPES 20 mM (pH 7.4) and kept on ice for 30 min prior to the binding study. Cells were incubated at 4°C for 1 h with slow shaking, in 500 μl buffered [^{3}H]-forskolin, in the absence or presence of unlabelled forskolin or β-adrenoceptor ligands. Cells were then washed 3 times with 2 ml PBS, and dissolved in 1 ml 1 N NaOH for 30 min at 37°C, before counting the homogenate in a β-radiations scintillation spectrometer with an efficiency of 61%.

Forskolin stimulates the catalytic subunit of adenylyl cyclase directly, but displays a higher efficacy and potency when the catalytic domain interacts with the stimulatory G protein-α_S subunit (Alousi *et al.*, 1991). Saturation binding experiments were performed with 10 to 360 nM [^{3}H]-forskolin in the absence or presence of 10 μM forskolin or isoprenaline which stimulates the formation of a complex between the G protein-α_S subunit and the adenylyl cyclase-catalytic subunit, thus increasing forskolin affinity (K_d values changing from 230 ± 112 to 28 ± 5 nM). Experiments with doses of β-adrenoceptor ligands were performed in presence of 90 nM tritiated-forskolin.

Adenylyl cyclase stimulation assays

CHO-Huβ3 and CHO-Moβ3 were grown to preconfluence in six-well dishes (≈1.2×10^6 cells/well). After washing with 1 ml Ham's F12 medium buffered with 20 mM HEPES (pH 7.4) supplemented with 1 mM ascorbic acid and 1 mM IBMX, cell monolayers were incubated for 30 min at 37°C in 1 ml buffer, in the absence (basal level: 5–25 pmol/10^6 cells) or in the presence of 10 μM (−)-isoprenaline (maximal stimulation mediated by β-adrenoceptor: 170–400 pmol/10^6 cells), or 25 μM forskolin (direct adenylyl cyclase stimulation: 420–850 pmol/10^6 cells), or 1 pM to 100 μM of ligand. The reaction was stopped by washing once with 1 ml PBS and by immediate addition of 500 μl 1 N NaOH. After a period of 20 min at 37°C, dissolved cells were collected, buffered with 1 N acetic acid and centrifuged at 3000 *g* for 10 min at 4°C. The total adenosine 3′:5′-cyclic monophosphate (cyclic AMP) contained in an aliquot of supernatant was determined with commercial cyclic AMP determination assays.

For inhibition studies of adenylyl cyclase stimulation, cells were preincubated with the antagonist at 37°C for 10 min before addition of a reference agonist (i.e. (−)-isoprenaline) at its K_{act} concentration (5 nM), and incubated for a subsequent 20 min period. The resultant pD_2 (negative logarithm of the agonist equilibrium constant) value of 6.24 obtained for the (±)-propranolol-antagonism of (−)-isoprenaline-stimulation in CHO-Moβ3, was in complete agreement with the pA_2 (negative logarithm of the antagonism equilibrium constant) value of 6.31 deduced from the Schild plot representation, thus validating our procedure.

Statistical analyses

The data were expressed as the means ± standard error of the mean (s.e.mean) of at least three independent experiments performed in duplicate except for forskolin binding data which resulted from two experiments only. Saturation experiments were computer-analyzed with the EBDA programme (Biosoft-Elsevier, Cambridge, UK) using the Scatchard plot representation. IC_{50} and EC_{50} (or K_{act}) parameters (effective concentration inducing 50% of inhibition or effect (or activation), respectively) obtained from binding competition experiments or adenylyl cyclase inhibition or activation, were determined using a computerized iterative non-linear least squares curve-fitting programme (Graph-PAD Software, San Diego, CA, U.S.A.). IC_{50} values measured for binding competitions as well as cyclase antagonisms were corrected (K_i value) according to Cheng & Prusoff. The intrinsic activity (IA) of a compound was measured relative to the maximal cyclase stimulation obtained for (−)-isoprenaline. A ligand which possessed an IA inferior to 0.90 was defined as a partial agonist.

Drugs

Use in the text, in table or in figures of the name of β-adrenoceptor ligands without qualification implies that the (±)-isomer was used. (−)-Noradrenaline, (−)-adrenaline, (−)- and (+)-isoprenaline, (−)- and (±)-propranolol, IBMX (3-isobutyl-methyl-xanthine), bovine serum albumin, desipramine and polyethyleneimine were purchased from Sigma Chemical Co (St Louis, MO, U.S.A.). [^{125}I]-CYP ((−)-[3-^{125}I]-iodocyanopindolol) (specific activity 2000 Ci $mmol^{-1}$) and [12-^{3}H]forskolin (specific activity 20–35 Ci $mmol^{-1}$) came from Amersham (England) and New England Nuclear, respectively; cyclic AMP (adenosine 3′:5′-cyclic monophosphate) determinations were performed with the Amersham [^{3}H]-cyclic AMP assay or [^{125}I]-cyclic AMP scintillation proximity assay.

Other drug names are: BRL 37344 ((**RR,SS**)-(±)-4-(2′-[2-hydroxy-2-(3-chloro-phenyl)ethylamino] propyl)phenoxyacetate sodium salt sesquihydrate); BRL 28410 ((**RR,SS**)-(±)-4-(2′-[(2-hydroxy-2-phenylethyl)amino] propyl)-benzoate); bucin-

dolol (2-[2-hydroxy-3-([2-(3-indolyl)-1,1-dimethylethyl] amino) propoxy] benzonitrile hydrochloride); bupranolol (1-(2-chloro-5-methylphenoxy)-3-[(1, 1-dimethylethyl)amino]-2-propanol); CGP 12177A ((±)-4-(3-t-butylamino-2-hydroxypropoxy) benz-imidazol-2-one); CGP 20712A ((±)-[2-(3-carbomyl-4-hydroxyphenoxy)ethylamino]-3-[4-(1-methyl-4-trifluoromethyl-2-imidaz olyl)-phenoxy]-2-propanol methane sulphonate); cimaterol (2-amino-5-(1-hydroxy-2-[(1-methylethyl)amino]ethyl)]benzonitrile); ICI 118551 ((±)-D-1-(7-methylindan-4-yloxy) -3-isopropylaminobutan-2-ol); ICI 201651 ((**R**)-4-(2-hydroxy-3-phenoxypropylaminoethoxy)-*N*-(2-methoxyethyl)phenoxyaceticacid); LY 79771 ((**RS**)-(±)-4-(2'-[(2-hydroxy-3-phenylethyl)amino]butyl)-benzyl alcohol); SM 11044 (L-3-(3,4-dihydroxy phenyl)-*N*-[3-(4-fluorophenyl) propyl]serinepyrrolidineamide hydrobromide); SR 58611A ((**RS**)-*N*- [2**S**) -7-ethoxycarbonylmethoxy-1,2,3,4-tetrahydro napth-2-yl] -(2**R**) -2-(3-chlorophenyl)-2-hydroxyethanamine hydrochloride).

Results

To compare the effects of various compounds on the human and murine β_3-adrenoceptors, we analyzed in parallel the pharmacological intrinsic properties (number of receptors, coupling efficiency) in CHO-Huβ3 and CHO-Moβ3.

The presence of an additional carboxy-terminal six-residue sequence in the human and twelve-residue sequence in the murine β_3-receptor, resulting from splicing of an intron in the corresponding gene, was recently reported (Granneman *et al.*, 1992; Van Spronsen *et al.*, 1993). As expected, preliminary studies revealed very similar pharmacological patterns in CHO cells expressing recombinant human β_3-adrenoceptors with or without the additional carboxy-terminal six-residue (Granneman *et al.*, 1993).

[^{125}I]-CYP binding parameters, as determined by Scatchard analysis, were similar for the human ($K_d = 912 \pm 120$ pM, $B_{max} = 197{,}995 \pm 32{,}458$ sites/cell) and murine ($K_d = 880 \pm 88$ pM, $B_{max} = 202{,}644 \pm 49{,}040$ sites/cell) β_3-adrenoceptors expressed in CHO cells.

(−)-Isoprenaline/forskolin-adenylyl cyclase stimulation ratios were 0.25 and 0.85 in CHO-Huβ3 and CHO-Moβ3, respectively. This 3.4 fold difference was in line with the factor of 3.7 for (−)-isoprenaline intrinsic efficacy (K_{act}/K_i ratio) measured in CHO-Moβ3 ($K_{act}/K_i = 0.0017$) relative to CHO-Huβ3 ($K_{act}/K_i = 0.0063$). These ratios suggested either a better coupling efficiency of the murine β_3-adrenoceptor to adenylyl cyclase or a better intrinsic activity for isoprenaline at the murine β_3 site. We therefore evaluated the stoichiometry of receptor-G_S-adenylyl cyclase interactions in transfected CHO cells, according to Alousi *et al.* (1991). In CHO-Moβ3, (−)-isoprenaline-stimulated forskolin binding indicated the presence of 98,066 ± 5,056 sites per cell, whereas in CHO-Huβ3, only 37,029 ± 4,495 sites/cell were identified, thus suggesting that the level of coupling was 2.7 fold greater in cells expressing the murine relative to the human β_3-adrenoceptor.

In addition to natural hormones (noradrenaline, adrenaline) and reference β-adrenoceptor agonist (isoprenaline) or antagonists (propranolol, CGP 20712A, ICI 118551) used to characterize these receptors initially, thirteen drugs were chosen for their atypical properties described in adipose tissues (BRL 37344, BRL 28410, CGP 12177A, cimaterol, ICI 201651, LY 79771), intestinal smooth muscle (SM 11044, SR 58611A), and heart (alprenolol, bucindolol, bupranolol, oxprenolol, pindolol). Pharmacological parameters measured in [^{125}I]-CYP binding competition and adenylyl cyclase stimulation experiments on the previously described CHO-Huβ3 and CHO-Moβ3 subclones, allowed the classification of these compounds into four groups according to their full or partial agonistic effect or to their antagonistic effect on the human or murine β_3-adrenoceptors (Table 1).

Full agonists in CHO-β3

Bucindolol, BRL 37344, cimaterol, LY 79771, ICI 201651, SR 58611A, SM 11044, alprenolol and BRL 28410 behaved as full agonists (IA between 0.9 and 1.0 relative to isoprenaline) in CHO-Huβ3 as well as in CHO-Moβ3 (Table 1).

In CHO-Huβ3, bucindolol, BRL 37344, cimaterol, LY 79771 and SR 58611A exhibited high potencies in stimulating adenylyl cyclase, with K_{act} ranging from 7 to 25 nM. Bucindolol bound with the highest affinity ($K_i = 23$ nM) to the Huβ_3-adrenoceptors and appeared as a new useful tool to study atypical β-adrenoceptors in tissues. BRL 37344, LY 79771, ICI 201651 and alprenolol had affinities ranging from 100 to 500 nM, whereas cimaterol, SR 58611A and SM 11044 weakly competed with [^{125}I]-CYP at the human β_3 site ($K_i \approx 1-7$ μM). BRL 28410 was the weakest agonist ligand in CHO-Huβ3 ($K_i = 15$ μM; $K_{act} = 3$ μM).

In CHO-Moβ3, most of the compounds (bucindolol, BRL 37344, LY 79771, ICI 201651, SM 11044, alprenolol, BRL 28410) exhibited binding affinity properties equivalent to those obtained in CHO-Huβ3, whereas only half of them (LY 79771, ICI 201651, SR 58611A and SM 11044) displayed similar cyclase stimulation potencies in both cell lines. BRL 37344, the reference agonist for the atypical β-site (Arch *et al.*, 1984; Wilson *et al.*, 1984), possessed a cyclase stimulation constant 38 fold higher for the murine than for the human subclone, with a BRL 37344 potency relative to (−)-isoprenaline ($K_{act(Iso)}/K_{(BRL)}$) of 11.3 in CHO-Moβ3 and of 0.3 in CHO-Huβ3. BRL 28410, though very weak in β_3-adrenoceptor binding affinity or activation potency, also showed a 12 fold higher efficiency in CHO-Moβ3 than in CHO-Huβ3.

Partial agonists in CHO-β3

Compounds (oxprenolol, CGP 12177A, pindolol) which were first reported as possessing sympathomimetic activities in tissues, probably at the atypical β-adrenoceptor, behaved as partial agonists (IA ranging from 0.35 to 0.75 relative to (−)-isoprenaline) in CHO-Huβ3 and CHO-Moβ3 (Table 1). Among these, CGP 12177A was the most efficacious, exhibiting respective intrinsic activities of 0.68 and 0.75 in CHO-Huβ3 and CHO-Moβ3. With a cyclase stimulation constant of 41 nM, CGP 12177A was three fold more potent in CHO-Moβ3 than in CHO-Huβ3. The binding affinity measured to CGP 12177A in [^{125}I]-CYP binding competition in CHO-Huβ3 agreed with that obtained in direct tritiated-CGP 12177A binding (Fève *et al.*, 1991).

Oxprenolol and pindolol were less potent in stimulating adenylyl cyclase in CHO-Moβ3 than in CHO-Huβ3, with at least 10% decrease in IA and a 7 fold lower K_{act}. Interestingly, these compounds were less potent in cyclase stimulation (K_{act} between 100 and 1000 nM) than most of the full agonists described above, but their binding affinities were mostly higher (K_i ranging from 10 to 100 nM). Accordingly, K_{act}/K_i ratios yielded surprising values between 2 and 37, instead of 0.01 to 1 commonly observed for full agonists. These unexpected features could be explained by the difficulty for partial agonists (IA <0.90) to achieve receptor-effector coupling since, for these drugs, receptor occupancy is required to be at least 50% to induce a half-maximal stimulation of adenylyl cyclase. Curiously, alprenolol which we defined as a full agonist in CHO-Huβ3 and CHO-Moβ3 cells, exhibited the same inversion of K_i and K_{act} values. This compound was initially classified together with pindolol as a sympathomimetic agent in the heart (Kaumann, 1989).

Antagonists at the human and murine β3 sites

The β_1-selective CGP 20712A, the β_2-selective ICI 118551, and bupranolol behaved as antagonists at the human and murine β3 sites (Table 1). (−)-Bupranolol appeared to be the most potent β_3-receptor antagonist, with an [^{125}I]-CYP com-

Table 1 Comparison of the pharmacological properties of the human and murine β_3-adrenoceptors expressed in CHO cells

	Human β_3-adrenoceptors			*Mouse β_3-adrenoceptors*		
	Binding	*Adenylyl cyclase stimulation*		*Binding*	*Adenylyl cyclase stimulation*	
	K_i (nM)	K_{act} (nM)	*IA*	K_i (nM)	K_{act} (nM)	*IA*
Reference full agonists						
(−)-Isoprenaline	620 ± 220[a]	3.9 ± 0.4[a]	0.90 ± 0.02[a]	2,710 ± 820	4.5 ± 1.8[b]	1.00 ± 0.10[b]
(−)-Noradrenaline	475 ± 75[a]	6.3 ± 0.7[a]	1.00[a]	1,840 ± 600	13 ± 4[b]	1.06 ± 0.06[b]
(−)-Adrenaline	20,650 ± 2,810[a]	49 ± 5[a]	1.00 ± 0.04[a]	4,600 ± 1,850	23 ± 0.3[b]	0.91 ± 0.03[b]
(+)-Isoprenaline	18,950 ± 3,060[a]	111 ± 1[a]	0.97 ± 0.11[a]		99 ± 44[b]	1.40 ± 0.10[b]
Full agonists						
Bucindolol	23 ± 10	7.0 ± 1.2	1.01 ± 0.10	21 ± 5	40 ± 14	1.11 ± 0.06
BRL 37344	287 ± 92	15 ± 3	1.11 ± 0.12	290 ± 136	0.4 ± 0.1[b]	1.07 ± 0.08[b]
Cimaterol	4,700 ± 1,710	17 ± 3	1.15 ± 0.08	158 ± 71	76 ± 9	1.19 ± 0.13
LY 79771	555 ± 71	18 ± 3	1.06 ± 0.04	838 ± 16	9 ± 1	1.27 ± 0.05
ICI 201651	85 ± 12	20 ± 9	1.14 ± 0.14	239 ± 104	15 ± 1	1.02 ± 0.02
SR 58611A	6,640 ± 960	25 ± 5	1.23 ± 0.23	1,350 ± 270	19 ± 4	1.19 ± 0.05
SM 11044	1,300 ± 200	84 ± 10	0.98 ± 0.10	1,030 ± 60	64 ± 9	1.19 ± 0.07
Alprenolol	110 ± 30	219 ± 46	0.97 ± 0.07	91 ± 1	827 ± 89	0.95 ± 0.11
BRL 28410	14,800 ± 4,200[a]	2,710 ± 620	1.08 ± 0.02	14,600 ± 7,100	224 ± 22	1.19 ± 0.05
Partial agonists						
Oxprenolol	70 ± 10[a]	77 ± 13[a]	0.53 ± 0.07[a]	147 ± 31	535 ± 79[b]	0.44 ± 0.06[b]
CGP 12177A	88 ± 22	139 ± 44[b]	0.68 ± 0.02[b]	152 ± 19	41 ± 9[b]	0.75 ± 0.08[b]
Pindolol	11 ± 2[a]	153 ± 12[a]	0.55 ± 0.05[a]	315 ± 40	999 ± 187[b]	0.35 ± 0.03[b]
Antagonists						
(−)-Bupranolol	50 ± 14	antagonist 18 ± 5		42 ± 19	Antagonist 12 ± 1	
ICI 118551	257 ± 34[a]	antagonist 770 ± 80[a]		2,100 ± 920	Antagonist 4,969 ± 137[b]	
CGP 20712A	2,300 ± 450[a]	antagonist 6,700 ± 870[a]		13,000 ± 7,100	Antagonist 6,425 ± 584[b]	
Partial agonist/antagonist						
(−)-Propranolol		1,105 ± 15	0.31 ± 0.02	150 ± 22	Antagonist 406 ± 98	
(±)-Propranolol	145 ± 8	1,490 ± 550	0.51 ± 0.12		Antagonist 580 ± 148	

Binding competitions were carried out on intact cells for 45 min at 37°C in the presence of [^{125}I]-CYP as described in experimental procedures. Adenylyl cyclase stimulation assays were performed on intact cells incubated with agonists at 37°C for 30 min. For determining antagonists parameters, cells were preincubated with 5 nM (−)-isoprenaline at 37°C for 10 min. Concentration-response-curves were fitted using least squares regression analysis and deduced binding competition (K_i) and adenylyl cyclase stimulation (K_{act}) constants were expressed in nanomolar concentrations. Intrinsic activity (IA) was calculated for each drug relative to (−)-isoprenaline-induced maximal cyclic AMP accumulation. Values are means ± s.e.mean of at least three independent experiments performed in duplicate.

Ligands were classified as full or partial agonists and as antagonists, according to their ability to stimulate or inhibit the adenylyl cyclase in CHO-Huβ3 and CHO-Moβ3. All data were obtained under similar experimental conditions; [a]data from Emorine *et al.* (1989), with IA expressed relative to noradrenaline maximal cyclase stimulation; [b]results from Nahmias *et al.* (1991).

petition binding affinity of about 50 nM. In CHO-Huβ3, (−)-isoprenaline- or BRL 37344-stimulated adenylyl cyclase was antagonized by (−)-bupranolol with respective inhibition constants of 18 ± 5 nM and 37 ± 1 nM (data not shown), suggesting that bupranolol acts with similar efficiency to antagonize the β_3-potent agonists BRL 37344 and isoprenaline, despite the bulky N-substituent of BRL 37344 as compared to the short alkylamine chain of isoprenaline. In CHO-Huβ3, the potency order for the antagonists was (−)-bupranolol (1.0) > ICI 118551 (0.2) > CGP 20712A (0.02). In CHO-Moβ3, (−)-bupranolol exhibited a potency similar to that measured in CHO-Huβ3, whereas ICI 118551 and CGP 20712A were one to two orders less potent.

As expected for antagonists, a linear correlation existed between their inhibition constant measured in [^{125}I]-CYP binding competition (pKi) and in (−)-isoprenaline-stimulated cyclase antagonism (pD_2) in CHO-Huβ3 as well as in CHO-Moβ3 (Figure 1).

Propranolol as an agonist or as an antagonist at the β3 site

Surprisingly, propranolol established a clear distinction between the human and the murine β_3-adrenoceptors: this compound behaved as a weak (K_{act} = 1.49 μM) and partial (IA = 0.51) agonist in CHO-Huβ3, but as an antagonist in CHO-Moβ3 (Table 1). In CHO-Huβ3, (±)-propranolol antagonism of the concentration-response-curve to (−)-isoprenaline yielded a Schild plot with a slope of 1.11 and an expected pA_2 value of 5.88 ($K_{i\ cyclase}$ = 1.32 μM), indicating that propranolol competitively shifted the concentration-response-curve to isoprenaline to a value similar to its K_{act}. The β_3-specificity of the action of propranolol was further confirmed by the 100% and 80% inhibition of the (−)-propranolol-induced cyclase stimulation by 10 μM of (−)-bupranolol and ICI 118551, respectively (Figure 2). The adenylyl cyclase maximal stimulation induced by propranolol was also assayed by measuring the level of forskolin binding: (±)-propranolol stimulated forskolin binding relative to (−)-isoprenaline with a factor (F = 0.41) which was close to the IA value (IA = 0.51) of cyclase stimulation, whereas, as expected, the antagonist (−)-bupranolol produced no effect (Figure 3). These results were further supported by analyzing the effect of propranolol on another type of fibroblast

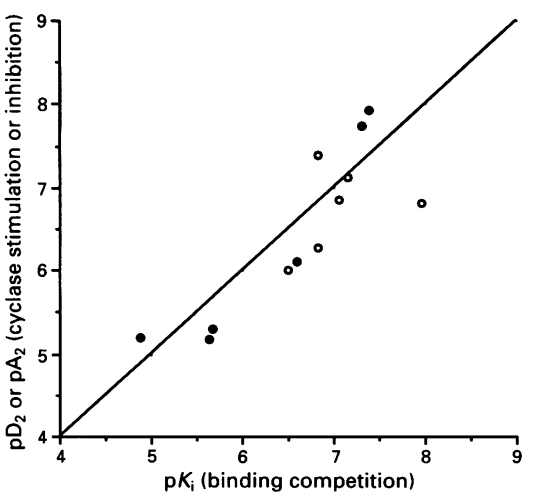

Figure 1 Relationship between adenylyl cyclase stimulation and binding competition parameters measured in CHO-Huβ3 and CHO-Moβ3. Correlation curve between $pK_i = -\log K_{ibinding}$ and pD_2 (or pA_2) = $-\log EC_{50}$ (or $IC_{50})_{cyclase}$ values measured for β-adrenoceptor partial agonists (○) and antagonists (●) in CHO-Huβ3 and CHO-Moβ3. Constants were obtained in [^{125}I]-CYP binding competition carried for 45 min at 37°C, or in (−)-isoprenaline-stimulated adenylyl cyclase experiments performed for 30 min at 37°C. Each value represents the mean of at least three independent experiments performed in duplicate.

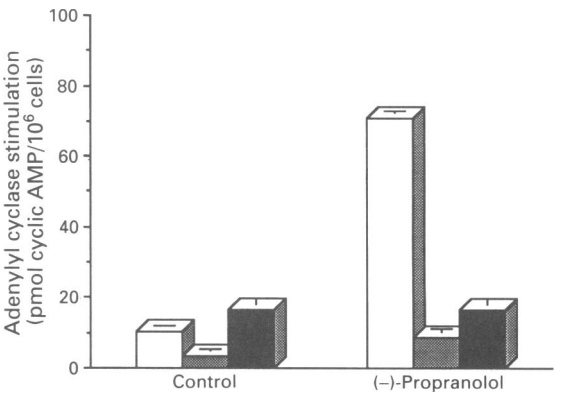

Figure 2 Antagonism of the propranolol-induced adenylyl cyclase stimulation in CHO-Huβ3. The amount of cyclic AMP accumulated per 10^6 CHO-Huβ3 was measured after a 100 μM (−)-propranolol stimulation for 30 min at 37°C, in absence (open columns) or in presence of 10 μM ICI 118551 (stippled columns) or 10 μM (−)-bupranolol (solid columns). The results are representative of one out of two separate experiments performed in duplicate.

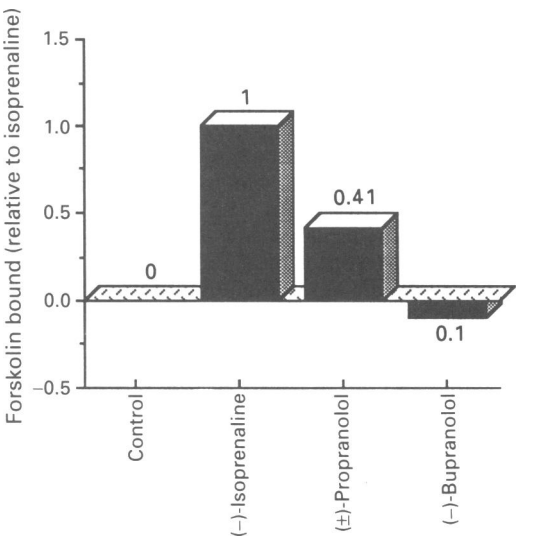

Figure 3 β-Adrenoceptor ligand-stimulated forskolin binding in CHO-Huβ3. Forskolin binding was measured during exposure of CHO-Huβ3 to 100 μM (−)-isoprenaline, (−)-propranolol or (−)-bupranolol, for 1 h at 4°C. Data were expressed relative to the (−)-isoprenaline-stimulated forskolin binding. The histogram results from one representative out of two independent experiments performed in duplicate.

(CHW) in which the human β_3-adrenoceptor was expressed at the level of 10,000 sites per cell (Nantel *et al.*, 1993): (±)-propranolol-induced cyclase stimulation properties measured in CHW-Huβ3 (K_{act} = 1.6 μM and F = 0.42) were similar to those obtained in CHO-Huβ3 (data not shown).

In CHO-Moβ3, (±)-propranolol inhibited the (−)-isoprenaline-induced cyclase stimulation with a constant of 580 ± 148 nM, in agreement with the value of 304 ± 78 nM reported by Nahmias *et al.* (1991). Moreover, (−)-propranolol, up to a concentration of 100 μM, was unable to stimulate forskolin binding, thus confirming its antagonistic effect at the murine β_3 site. Shift of the CRC to (−)-isoprenaline induced by varying concentrations of (±)-propranolol (0.1 to 100 μM) led to a Schild regression plot with a slope of 0.99, indicating simple competitive antagonism (data not shown). The deduced mean pA_2 value (6.3 ± 0.1) was in close agreement with that of 6.4 reported in murine BAT (Arch, 1989) and resulted in a functional K_i of 494 ± 80 nM, as compared with that measured in (−)-isoprenaline-stimulated cyclase antagonism ($K_{i\ cyclase}$ = 580 ± 148 nM).

Discussion

Tools to study the β_3-adrenoceptor

Reference β-adrenoceptor agonists as well as compounds reported to induce atypical β-adrenoceptor effects in brown and white adipose tissues or in cardiac and digestive tract tissues, were evaluated in CHO-Huβ3 and CHO-Moβ3 by determining their affinity in [^{125}I]-CYP binding competition experiments and their potency in stimulating adenylyl cyclase (Table 1).

Most of the full agonists (bucindolol, BRL 37344, LY 79771, ICI 201651, alprenolol) and all of the partial agonists (oxprenolol, CGP 12177A and pindolol) exhibited binding affinities higher or equivalent to those of noradrenaline and isoprenaline, whereas their adenylyl cyclase stimulation potencies were equivalent or lower. Because of their high affinity relative to isoprenaline, these compounds were defined as β_3-ligands. Among them, bucindolol, alprenolol, oxprenolol and pindolol, generally considered as 'cardiac compounds' possessed K_i values lower or similar to those of the 'adipose compounds', BRL 37344, LY 79771, ICI 201651, CGP 12177A, which in turn displayed higher affinities for the β_3-site than SM 11044 and SR 58611A, defined as 'gut compounds'.

Bucindolol displayed in CHO-Huβ3 and CHO-Moβ3 the most interesting binding and cyclase stimulation parameters. Alprenolol, oxprenolol, CGP-12177A and pindolol which exhibited weak efficacies in cyclase stimulation, seem to be ligands more dependable for binding characterization of the β_3 site, whereas BRL 37344, LY 79771, ICI 201651 and SR 58611SA which displayed low K_{act} values, appear to be better suited to investigate the β_3-adrenoceptor-mediated tissue physiological effects. Bupranolol, with a cyclase inhibition constant of about 15 nM in CHO-Huβ3 and CHO-Moβ3, is the most potent β_3-antagonist known to date. All these compounds could contribute to establish an accurate characterization of the β_3-adrenoceptor in cells and tissues.

The β_3-adrenoceptor as the adipose tissue atypical β site

The β_3-adrenoceptor displays six pharmacological properties, strikingly different from those of the β_1- and β_2-receptors, and which are shared with the atypical β-adrenoceptor of adipose tissue.

(1) Atypically low affinities for conventional β-radioligands: [^{125}I]-CYP binding saturation experiments in CHO-Huβ3 and CHO-Moβ3 led to a dissociation constant value close to 1 nM, that is more than one order lower than those measured for the conventional β_1- and β_2-adrenoceptors (Blin *et al.*, 1993) and similar to the K_d of 1.3 nM obtained at the rat β_3-site (Muzzin *et al.*, 1991), each expressed in CHO cells. The affinity of the β_3-receptors for the tritiated-CGP 12177A is also much lower than those of the β_1- and β_2-receptors, and is comparable in CHO-Huβ3 (K_d = 28 nM), in murine 3T3-F442A adipocytes (K_d = 38 nM), in CHO-Raβ3 (K_d = 44 nM), and in rat interscapular brown adipose tissue (K_d = 31 nM) (Fève *et al.*, 1991; Muzzin *et al.*, 1991; 1992).

(2) Atypically low stereoselectivity indices (SSI) for reference agonist and antagonist enantiomers as compared to those (SSI = 2–3) reported for conventional β_1- and β_2-receptors (Harms *et al.*, 1977): we measured for isoprenaline respective SSI or 1.45 and 1.34 in CHO-Huβ3 and CHO-Moβ3, in agreement with an SSI of 1.28 reported in rat white fat cells (Hollenga *et al.*, 1990).

(3) Atypically low potencies for the reference agonists: in CHO-Huβ3 and CHO-Moβ3, as well as in CHO-Raβ3 (Muzzin *et al.*, 1991), catecholamines-stimulated cyclase potencies were 10 to 100 fold lower than in CHO-Huβ1 and CHO-Huβ2 (Tate *et al.*, 1991). In murine 3T3-F442A adipocytes, such a difference in catecholamine potency between the atypical β-receptor and the β_1-receptor was also reported (Fève *et al.*, 1991).

(4) High potency for a novel class of compounds initially described as potent activators of lipolysis and thermogenesis in white (Wilson *et al.*, 1984) and brown (Arch *et al.*, 1984) adipose tissues: BRL 37344, the most representative compound of this class, exhibited a high potency in stimulating adenylyl cyclase in CHO-Huβ3 than in CHO-Moβ3.

In addition, we found that LY 79771, described as a potent and selective thermogenic anti-obesity agent (Arch *et al.*, 1991), and ICI 201651, the *in vivo* metabolized form of ICI D7114 reported to stimulate oxygen consumption and BAT activity (Holloway *et al.*, 1991), were also potent cyclase activators with K_{act} values around 20 nM in CHO-Huβ3 and 10 nM in CHO-Moβ3. Cimaterol, a rather potent stimulant of rat WAT lipolysis (Arch *et al.*, 1991), also potently stimulated the adenylyl cyclase in CHO-Huβ3 and CHO-Moβ3.

(5) Partial agonistic activities of several β_1/β_2-antagonists reflecting intrinsic sympathomimetic activities in tissues: oxprenolol, CGP 12177A and pindolol, initially described as displaying sympathomimetic activities in tissues (Kaumann, 1989), indeed behaved as agonists at the human and murine β_3 sites. They were less potent than most of the above described full agonist (1 to 3 log units higher K_{act} values) and exhibited only partial activities relative to isoprenaline (IA $\approx$0.35 to 0.75). The most efficacious, CGP 12177A, was reported as an atypical agonist able to stimulate the adenylyl cyclase in murine 3T3-F442A adipocytes (Fève *et al.*, 1991), and to exhibit potent thermogenic and lipolytic activities in rodent BAT (Mohell & Dicker, 1989) and WAT (Fève *et al.*, 1991; Langin *et al.*, 1991), respectively.

The β_3-receptor-mediated partial agonist action of these compounds may result in antagonism of full β-agonist effects, as described with the effect of CGP 12177A on the BRL 37344-stimulated lipolysis in rat WAT (Langin *et al.*, 1991). Moreover, they may account for underestimation of pA_2 values measured at the conventional β-sites coexisting in tissues (Zaagsma & Nahorski, 1990).

(6) Atypically low binding affinities and antagonistic potencies for conventional β-antagonists: the β_1-selective antagonist, CGP 20712A and the β_2-selective antagonist, ICI 118551 exhibited low potencies in inhibiting isoprenaline-stimulated adenylyl cyclase in CHO-Huβ3, in CHO-Moβ3, and in murine 3T3-F442A adipocytes (Fève *et al.*, 1991). In rodent WAT, Hollenga & Zaagsma (1989) also reported the low antagonism of isoprenaline-induced lipolysis by CGP 20712A and ICI 118551.

In addition, bupranolol behaved as the most potent antagonist (K_i $\approx$15 nM) towards isoprenaline-stimulated adenylyl cyclase in CHO-Huβ3 and in CHO-Moβ3, in agreement with Langin *et al.* (1991) who reported that bupranolol was the most effective blocker (K_i $\approx$50 nM) of the BRL 37344-induced lipolysis at the atypical β-receptor in rat and hamster fat cells.

The β_3-adrenoceptor in other tissues

Compounds herein defined as tools to study the β_3-adrenoceptor were also active at the atypical β-receptors described in cardiac or digestive-tract tissues. Moreover, their potencies measured in CHO-Huβ3 and CHO-Moβ3 were in agreement with those reported in literature: the atypical inotropic and chronotropic effects of pindolol in cat atria (K_{act} $\approx$100 nM), antagonized by high level of bupranolol and not by propranolol (Kaumann, 1989) resembled its pharmacological properties in CHO-Huβ3. The action of SR 58611A and SM 11044 revealed a close agreement between the pharmacology of the β_3-receptor expressed in CHO cells and that

of the atypical β-site described, respectively, in rat colon (Manara *et al.*, 1990) and in guinea-pig ileum (Sugasawa *et al.*, 1992). Moreover, atypical antagonistic effects were reported for pindolol and propranolol in guinea-pig ileum (Bond & Clarke, 1988) and in rat colon (Bianchetti & Manara, 1990; MacLaughlin & MacDonald, 1990).

In addition, a close relationship existed between the adipose tissue and the gut atypical β-adrenoceptors: ICI D7114 exhibited binding affinity for the atypical β-receptor described in guinea-pig ileum (Holloway *et al.*, 1991) and the potent lipolytic compound BRL 37344 was able to relax strongly pre-contracted guinea-pig ileum, through atypical β-receptors (Bond & Clarke, 1988). Similarly, a series of SR 58611A-related compounds exhibited considerable lipolytic effects on rat white adipocytes (Manara *et al.*, 1989), and behaved as full agonists with well-correlated orders of potency in activating adipocyte lipolysis (Langin *et al.*, 1991) and in inhibiting gut motility (Manara & Bianchetti, 1990). As a molecular proof for the expression of the human β_3-adrenoceptors in these tissues, Krief *et al.* (1993) detected β_3-transcripts in perirenal, omental and subcutaneous fat, as well as in human colon biopsies.

Taken together, these data suggest that a single β_3-adrenoceptor may mediate most of the atypical effects observed in various tissues. Experiments with BRL 37344 and SR 58611A showed, however, that SR 58611A is more specific for gut than is BRL 37344 (Manara *et al.*, 1990), and support the existence of tissue-specific properties. Variation of receptor density has been shown to modify the receptor-mediated response, and the presence of variable numbers of spare receptors may, for instance, complicate the comparison of binding tests with functional assays (George *et al.*, 1988; Lohse, 1992). The level of active G-protein and adenylyl cyclase effector available in a given cell type may also influence the level of second messenger; in particular, partial agonists should be more dependent on cellular or tissular intrinsic responsiveness, as attested by variations in K_{act} and IA measured for CGP 12177A in different tissues from different animals (Langin *et al.*, 1991).

Species-related variations of the β_3-adrenoceptor

Although the pharmacological profiles of the human and murine β_3-adrenoceptors were essentially similar, a detailed analysis revealed some differences, as attested by the BRL 37344 and propranolol compounds. Relative to isoprenaline, the cyclase stimulation potency of BRL 37344 was 30 to 40 fold lower in CHO-Huβ3 as compared to CHO-Moβ3, CHO-Raβ3 (Granneman *et al.*, 1991), murine 3T3-F442A adipocytes (Fève *et al.*, 1991) and rat BAT (Muzzin *et al.*, 1988). A recent study also reported the lower potency of BRL 37344 towards the human β_3-receptor as compared to the rat β_3-receptor (Ligget, 1992). Supporting these results, Hollenga *et al.* (1990) described the low potency of BRL 37344 as well as the weak intrinsic activities for catecholamines in human adipose tissues, and concluded that the atypical β-receptor adenylyl cyclase system of human adipocytes appeared to be less efficient than that of rat WAT cells. Another obvious pharmacological difference between the human and the murine β_3-receptors was apparent in the weak and partial agonism of propranolol in CHO-Huβ3, as compared to its antagonistic effect displayed in CHO-Moβ3 and in CHO-Raβ3 (Muzzin *et al.*, 1991). These differences, which were in a minority, suggested that pharmacological properties of ligands for a given receptor cannot be extrapolated across species, implying thus that caution should be exercised in using animal models such as rodents to select compounds active at the β_3 site for potential therapeutic applications in man.

On the basis of the overall amino-acid sequence identity (82%), chromosomal location and genomic organization, it has been demonstrated that the human and the murine β_3-adrenoceptor genes were derived from a common ancestor gene, therefore defining a single receptor subtype (Nahmias *et al.*, 1991; Van Spronsen *et al.*, 1993). Deletions or key amino-acid substitutions between the human rodent β_3-receptor sequences may thus suffice to explain species-related differences in pharmacology. Since the binding dissociation constant for BRL 37344 and propranolol were similar in CHO-Huβ3 and CHO-Moβ3, their ability to discriminate between receptors from different species should more likely be related to signal processing than to binding *per se*. The three-residue deletion (Val-Leu-Ala) in the first transmembrane region of the rodent as compared to the human β_3-sequence, is equivalent to the loss of one α-helix turn, thus inducing conformational modifications in a region located in the ligand binding site and that may be important for signal transduction (Blin *et al.*, 1993). The substitution of two Cys by two Arg in the second and third intra-cytoplasmic loops of the murine and rat as compared to the human β_3-adrenoceptor sequences, may also prevent the formation of a disulphide-bridge stabilizing the conformation in a region implicated in the coupling of the receptor with the G_S protein (Kjelsberg *et al.*, 1992).

Previous studies for other receptors have shown that minute sequence differences may actually result in important pharmacological differences: the substitution of Asp^{113} by Glu in the human β_2-adrenoceptor turned the antagonists oxprenolol and pindolol into partial agonists (Strader *et al.*, 1989). Pharmacological differences linked to the modification of a single key amino-acid between a human receptor and its murine counterpart were also reported for other G-protein coupled receptors like the α_{2A}-adrenoceptor (Link *et al.*, 1992), and the 5-$HT_{1D\beta}$ or 5-HT_{1B} receptor (Oksenberg *et al.*, 1992). These results support the idea that a single receptor subtype encoded by species-homologous genes may display different pharmacological patterns.

In conclusion, this detailed pharmacological analysis shows that the cloned human and murine β_3-adrenoceptors share extensive properties which closely resemble those of the atypical β-adrenoceptor sites described in heart, digestive tract, and adipose tissues. Variations reported in the literature are likely to arise from differences in the primary sequence of the β_3-adrenoceptor expressed in different species, or from differences in micro-environment for various tissues. A single receptor may thus account for most of the atypical pharmacological features described to date in different species and tissues.

We would like to acknowledge Dr B. Fève's helpful critical reading of the manuscript and Dr L.J. Emorine's constructive discussions.

This work was supported by grants from the Centre National de la Recherche Scientifique, the Institut National de la Santé et de la Recherche Médicale, the Ministère de la Recherche et de l'Espace, the Université Paris V, the Bristol-Myers-Squibb Company (Princeton, NJ, U.S.A.), the Fondation pour la Recherche Médicale, the Association pour le Développement de la Recherche sur le Cancer, and the Ligue Nationale Française contre la Cancer.

Bucindolol was provided by Bristol-Myers Squibb (Princeton, NJ, U.S.A.). CGP 12177A, CGP 20712A, alprenolol and oxprenolol were gifts from Ciba-Geigy Corporation (Basel, Schwitzerland). ICI 118551 and ICI 201651 were provided by Imperial Chemical Industries (Macclesfield, England). Cimaterol and LY 79771 were donated by American Cyanamid (Pearl River, NY, U.S.A.) and Lilly Research Labs (Indianapolis, IN, U.S.A.), respectively. Pindolol was provided by Sandoz (Basel, Switzerland). (−)-Bupranolol was a gift from Schwarz Pharma (Monheim, Germany). BRL 37344 and BRL 28410 were obtained from SmithKline Beecham Pharmaceuticals (Epsom, England). SM 11044 and SR 58611A were given by Sumitomo Pharmaceuticals (Osaka, Japan) and Sanofi-Midy (Milano, Italy), respectively.

References

ALOUSI, A.A., JASPER, J.R., INSEL, P.A. & MOTULSKY, H.J. (1991). Stoichiometry of receptor-G_S-adenylate cyclase interactions. *FASEB J.*, **5**, 2300–2303.

ARCH, J.R.S. (1989). The brown adipocyte β-adrenoceptor. *Proc. Nutr. Soc.*, **48**, 215–223.

ARCH, J.R.S., AINSWORTH, A.T., CAWTHORNE, M.A., PIERCY, V., SENNITT, M.V., THODY, V.E., WILSON, C. & WILSON, S. (1984). Atypical β-adrenoceptor on brown adipocytes as target for anti-obesity drugs. *Nature*, **309**, 163–165.

BIANCHETTI, A. & MANARA, L. (1990). In vitro inhibition of intestinal motility by phenylethanolaminotetralines: evidence of atypical β-adrenoceptors in rat colon. *Br. J. Pharmacol.*, **100**, 831–839.

BLIN, N., CAMOIN, L., MAIGRET, B. & STROSBERG, A.D. (1993). Structural and conformational features determining selective signal transduction in the β3-adrenergic receptor. *Mol. Pharmacol.*, **44**, 1094–1104.

BOJANIC, D., JANSEN, J.D., NAHORSKI, S.R. & ZAAGSMA, J. (1985). Atypical characteristics of the β-adrenoceptor mediating cyclic AMP generation and lipolysis in the rat adipocyte. *Br. J. Pharmacol.*, **84**, 131–137.

BOND, R.A. & CLARKE, D.E. (1988). Agonist and antagonist characterization of a putative adrenoceptor with distinct pharmacological properties from the α- and β-subtypes. *Br. J. Pharmacol.*, **95**, 723–734.

EMORINE, L.J., BLIN, N. & STROSBERG, A.D. (1994). The human β3-adrenoceptor: the search for a physiological function. *Trends Pharmacol. Sci.*, **15**, 3–7.

EMORINE, L.J., FÈVE, B., PAIRAULT, J., BRIEND-SUTREN, M.M., NAHMIAS, C., MARULLO, S., DELAVIER-KLUTCHKO, C. & STROSBERG, A.D. (1992). The human β3-adrenergic receptor: relationship with atypical receptors. *Am. J. Clin. Nutr.*, **55**, 215S–218S.

EMORINE, L.J., MARULLO, S., BRIEND-SUTREN, M.M., PATEY, G., TATE, K., DELAVIER-KLUTCHKO, C. & STROSBERG, A.D. (1989). Molecular characterization of the human β3-adrenergic receptor. *Science*, **245**, 1118–1121.

ESBENSHADE, T.A., HAN, C., THEROUX, T.L., GRANNEMAN, J.G. & P., M.K. (1992). Coexisting β1- and atypical β-adrenergic receptors cause redundant increases in cyclic AMP in human neuroblastoma cells. *Mol. Pharmacol.*, **42**, 753–759.

FÈVE, B., EMORINE, L.J., LASNIER, F., BLIN, N., BAUDE, B., STROSBERG, A.D. & PAIRAULT, J. (1991). Atypical β-adrenergic receptor in 3T3-F442A adipocytes. *J. Biol. Chem.*, **266**, 20329–20336.

GEORGE, S.T., BERRIOS, M., HADCOCK, J.R., WANG, H.Y. & MALBON, C.C. (1988). Receptor density and cAMP accumulation: analysis in CHO cells exhibiting stable expression of a cDNA that encodes the beta2-adrenergic receptor. *Biochem. Biophys. Res. Commun.*, **150**, 665–672.

GRANNEMAN, J.G., LAHNERS, K.N. & CHAUDHRY, A. (1991). Molecular cloning and expression of the rat β3-adrenergic receptor. *Mol. Pharmacol.*, **40**, 895–899.

GRANNEMAN, J.G., LAHNERS, K.N. & CHAUDHRY, A. (1993). Characterization of the human β3-adrenergic receptor gene. *Mol. Pharmacol.*, **44**, 264–270.

GRANNEMAN, J.G., LAHNERS, K.N. & RAO, D.D. (1992). Rodent and human β3-adrenergic receptor genes contain an intron within the protein-coding block. *Mol. Pharmacol.*, **42**, 964–970.

HARMS, H.H., ZAAGSMA, J. & DE VENTE, J. (1977). Differentiation of β-adrenoreceptors in rat atrium, diaphragm and adipose tissue of the rat, using stereoisomers of propranolol, alprenolol, nifenalol and practolol. *Life Sci.*, **21**, 123–128.

HOLLENGA, C., HAAS, M., DEINUM, J.T. & ZAAGSMA, J. (1990). Discrepancies in lipolytic activities induced by β-adrenoceptor agonists in human and rat adipocytes. *Horm. Metab. Res.*, **22**, 17–21.

HOLLENGA, C. & ZAAGSMA, J. (1989). Direct evidence for the atypical nature of functional β-adrenoceptors in rat adipocytes. *Br. J. Pharmacol.*, **98**, 1420–1424.

HOLLOWAY, B.R., HOWE, R., RAO, B.S., STRIBLING, D., MAYERS, R.M., BRISCOE, M.G. & JACKSON, J.M. (1991). ICI D7114 a novel selective β-adrenoceptor agonist selectively stimulates brown fat and increases whole-body oxygen. *Br. J. Pharmacol.*, **104**, 97–104.

KAUMANN, A.J. (1989). Is there a third heart β-adrenoceptor? *Trends Pharmacol. Sci.*, **10**, 316–320.

KJELSBERG, M.A., COTECCHIA, S., OSTROWSKI, J., CARON, M.G. & LEFKOWITZ, R.J. (1992). Constituitive activation of the α_{1B}-adrenergic receptor by all amino acid substitutions at a single site. *J. Biol. Chem.*, **267**, 1430–1433.

KRIEF, S., LÖNNQVIST, F., RAIMBAULT, S., BAUDE, B., VAN SPRONSEN, A., ARNER, P., STROSBERG, A.D., RICQUIER, D. & EMORINE, L.J. (1993). Tissue distribution of β3-adrenergic receptor mRNA in man. *J. Clin. Invest.*, **91**, 344–349.

LANGIN, D., PORTILLO, M.P., SAULNIER-BLACHE, J.S. & LAFONTAN, M. (1991). Coexistence of three β-adrenoceptor subtypes in white fat cells of various mammalian species. *Eur. J. Pharmacol.*, **199**, 291–301.

LELIAS, J.M., KAGHAD, M., RODRIGUEZ, M., CHALON, P., BONNIN, J., DUPRE, I., DELPECH, B., BENSAID, M., LEFUR, G., FERRARA, P. & CAPUT, D. (1993). Molecular cloning of a human β3-adrenergic receptor cDNA. *FEBS Lett.*, **324**, 127–130.

LIGGETT, S.B. (1992). Functional properties of the rat and human β3-adrenergic receptors: differential agonist activation of recombinant receptors in chinese hamster ovary cells. *Mol. Pharmacol.*, **42**, 634–637.

LINK, R., DAUNT, D., BARSH, G., CHRUSCINSKI, A. & KOBILKA, B. (1992). Cloning of two mouse genes encoding α2-adrenergic receptor subtypes and identification of a single amino acid in the mouse α2-C10 homolog responsible for an interspecies variation in antagonist binding. *Mol. Pharmacol.*, **42**, 16–27.

LOHSE, M.J. (1992). Stable overexpression of human β2-adrenergic receptors in mammalian cells. *Naunyn Schmied. Arch. Pharmacol.*, **345**, 444–451.

LÖNNQVIST, F., KRIEF, S., STROSBERG, A.D., NYBERG, B., EMORINE, L. & ARNER, P. (1993). Evidence for a functional β_3-adrenoceptor in man. *Br. J. Pharmacol.*, **110**, 929–936.

MACLAUGHLIN, D.P. & MACDONALD, A. (1990). Evidence for the existence of 'atypical' β-adrenoceptors (β_3-adrenoceptors) mediating relaxation in the rat distal colon *in vitro*. *Br. J. Pharmacol.*, **101**, 569–574.

MANARA, L. & BIANCHETTI, A. (1990). The phenylethanolaminotetralines: new selective agonists for atypical β-adrenoceptors. *Trends. Pharmacol. Sci.*, **11**, 229–230.

MANARA, L., GUZZI, U., AUREGGI, G., CROCI, T. & BIANCHETTI, A. (1990). On the selectivity of in vitro inhibition of rat colon motility by β-adrenergic substituted phenylethanolamines. *Eur. J. Pharmacol.*, **183**, 2197–2198.

MOHELL, N. & DICKER, A. (1989). The β-adrenergic radioligand [^{3}H]CGP-12177, generally classified as an antagonist, is a thermogenic agonist in brown adipose tissue. *Biochem. J.*, **261**, 401–405.

MUZZIN, P., REVELLI, J.P., FRASER, C.M .& GIACOBINO, J.P. (1992). Radioligand binding studies of the atypical β3-adrenergic receptor in rat brown adipose tissue using [^{3}H]CGP 12177. *FEBS Lett.*, **298**, 162–164.

MUZZIN, P., REVELLI, J.P., KUHNE, F., GOCAYNE, J.D., MACCOMBIE, W.R., VENTER, J.C., GIACOBINO, J.P. & FRASER, C.M. (1991). An adipose tissue-specific β-adrenergic receptor. *J. Biol. Chem.*, **266**, 24053–24058.

MUZZIN, P., SEYDOUX, J., GIACOBINO, J.P., VENTER, J.C. & FRASER, C. (1988). Discrepancies between the affinities of binding and action of the novel β-adrenergic agonist BRL 37344 in rat brown adipose tissues. *Biochem. Biophys. Res. Commun.*, **156**, 375–382.

NAHMIAS, C., BLIN, N, ELALOUF, J.M., MATTEI, M.G., STROSBERG, A.D. & EMORINE, L.J. (1991). Molecular characterization of the mouse β3-adrenergic receptor: relationship with the atypical receptor of adipocytes. *EMBO J.*, **10**, 3721–3727.

NANTEL, F., BONIN, H., EMORINE, L.J., ZILBERFARB, V., STROSBERG, A.D., BOUVIER, M. & MARULLO, S. (1993). The human β3-adrenergic receptor is resistant to short-term agonist-promoted desensitization. *Mol. Pharmacol.*, **43**, 548–555.

OKSENBERG, D., MARSTERS, S.A., O'DOWD, B.F., JIN, H., HAVLIK, S., PEROUTKA, S.J. & ASHKENAZI, A. (1992). A single amino-acid difference confers major pharmacological variation between human and rodent 5-HT_{1B} receptors. *Nature*, **360**, 161–163.

STRADER, C.D., CANDELORE, M.R., HILL, W.S. & DIXON, R.A.F. (1989). A single amino-acid substitution in the β-adrenergic receptor promotes partial agonist activity from antagonists. *J. Biol. Chem.*, **264**, 16470–16477.

SUGASAWA, T., MATSUZAKI, M., MOROOKA, S., FOIGNANT, N., BLIN, N. & STROSBERG, A.D. (1992). In vitro study of a novel atypical β-adrenoceptor agonist, SM-11044. *Eur. J. Pharmacol.*, **216**, 207–215.

TATE, K.M., BRIEND-SUTREN, M.M., EMORINE, L.J., DELAVIER-KLUTCHKO, C., MARULLO, S. & STROSBERG, A.D. (1991). Expression of three human β-adrenergic-receptor subtypes in transfected chinese hamster ovary cells. *Eur. J. Biochem.*, **612**, 1–5.

VAN SPRONSEN, A., NAHMIAS, C., KRIEF, S., BRIEND-SUTREN, M.M., STROSBERG, A.D. & EMORINE, L.J.E. (1993). The human and mouse beta3-adrenergic receptor genes: promoter and intron/exon structure. *Eur. J. Biochem.*, **213**, 1117–1124.

WILSON, C., WILSON, S., PIERCY, V., SENNITT, M.V. & ARCH, J.R.S. (1984). The rat lipolytic β-adrenoceptor: studies using novel β-adrenoceptor agonists. *Eur. J. Pharmacol.*, **100**, 309–319.

ZAAGSMA, J. & NAHORSKI, S.R. (1990). Is the adipocyte β-adrenoceptor a prototype for the recently cloned atypical 'β3-adrenoceptor'? *Trends Pharmacol. Sci.*, **11**, 3–7.

(Received September 9, 1993
Revised February 19, 1994
Accepted March 16, 1994)

Br. J. Pharmacol. (1994), **112**, 920–924

Blockade by oral or parenteral RPR 100893 (a non-peptide NK_1 receptor antagonist) of neurogenic plasma protein extravasation within guinea-pig dura mater and conjunctiva

Won S. Lee, *Saliha M. Moussaoui & [1]Michael A. Moskowitz

Stroke Research Laboratory, Neurosurgery and Neurology Services, Massachusetts General Hospital, Harvard Medical School, 32 Fruit Street, Boston, MA 02114, U.S.A. and *Rhone-Poulenc Rorer, Centre de Recherche de Vitry-Alfortville, 13, Quai Jules Guesda, 94403 Vitry-sur-Seine cedex, France

1 The ability of an NK_1 receptor antagonist, RPR 100893, and its enantiomer, RPR 103253 to block neurogenic plasma protein extravasation in guinea-pig dura mater and conjunctiva was assessed following ^{125}I-labelled bovine serum albumin ([^{125}I]-BSA, 50 μCi kg^{-1}, i.v.) and unilateral electrical stimulation of the trigeminal ganglion (0.6 mA, 5 ms, 5 Hz, 5 min) or capsaicin administration (150 μg kg^{-1}, i.v.).

2 When administered p.o. 60 min prior to electrical stimulation, RPR 100893 ($\geq$ 0.1 μg kg^{-1}) decreased plasma protein extravasation in dura mater in a dose-dependent manner, whereas the enantiomer (10 or 100 μg kg^{-1}, p.o.) was inactive.

3 When given i.v. 30 min prior to electrical stimulation, RPR 100893 ($\geq$ 0.5 ng kg^{-1}) significantly inhibited plasma protein extravasation in the dura mater evoked by electrical stimulation in a dose-dependent manner.

4 RPR 100893 (100 μg kg^{-1}, p.o.) also reduced the leakage when given 45 min before the guinea-pigs were killed and 10, 40 and 80 min after electrical trigeminal stimulation.

5 RPR 100893 given p.o. dose-dependently inhibited capsaicin-induced plasma protein extravasation with ID_{50}s of 7.4 μg kg^{-1} and 82 μg kg^{-1} for dura mater and conjunctiva, respectively.

6 These results are consistent with the contention that NK_1 receptors mediate neurogenic plasma protein leakage following trigeminal stimulation, and suggest that NK_1 receptor antagonists of the perhydroisoindolone series may be useful for treating migraine and cluster headaches.

Keywords: Migraine; neurogenic inflammation; tachykinins; trigeminal ganglion; NK_1 receptor antagonist

Introduction

Neurogenic inflammation (NI), a complex process characterized by vasodilatation, plasma extravasation, endothelium activation and mast cell degranulation develops in the dura mater following electrical or chemical stimulation of capsaicin-sensitive fibres projecting from neurones within trigeminal ganglia (Markowitz *et al.*, 1987; Dimitriadou *et al.*, 1992). There is considerable evidence that NI is mediated by the tachykinins, particularly substance P (SP), after release from perivascular trigeminovascular axons (Liu-Chen *et al.*, 1983; Moskowitz *et al.*, 1983; 1989; Dimitriadou *et al.*, 1991; Moussaoui *et al.*, 1993a,b; Shepheard *et al.*, 1993). SP binds preferentially to NK_1 receptors, whereas neurokinin A is a preferential ligand at NK_2 recognition sites (Quirion & Dam, 1985; Buck & Burcher, 1986; Regoli *et al.*, 1987). The selective antagonist, RP 67580 blocks neurogenic extravasation within dura mater after electrical or chemical trigeminal stimulation, thereby suggesting an NK_1 receptor-mediated response (Shepheard *et al.*, 1993; Moussaoui *et al.*, 1993a,b).

We have proposed that NI within dura mater may contribute to hyperalgesia and promote sensitization of dural trigeminovascular afferents to sustain headache pain (Moskowitz, 1984; 1991; 1992). Drugs useful for the treatment of acute migraine block NI within the dura mater. For example, sumatriptan or dihydroergotamine activate prejunctional 5-$HT_{1D/B}$ heteroreceptors and block the development of NI by inhibiting neuropeptide release from trigeminovascular fibres (Buzzi *et al.*, 1991).

RPR 100893, a novel, non-peptide, selective antagonist of human NK_1 receptors, is representative of the 7,7,4-triaryl-perhydroisoindol-4-ols, a new series of perhydroisoindolones of which RPR 67580 is a member (Tabart & Peyronel, 1994). We now demonstrate that low doses of orally or intravenously administered RPR 100893 potently block plasma protein extravasation in guinea-pig dura mater induced by electrical or chemical trigeminal stimulation, and that blockade can occur before as well as after nerve stimulation.

[1] Author for correspondence.

Methods

Male Hartley guinea-pigs (200–250 g, Charles River Laboratories, Wilmington, MA, U.S.A. and Charles River Laboratories, France) were housed under diurnal lighting conditions and allowed food and water *ad libitum*.

Electrical trigeminal ganglion stimulation

Anaesthetized animals (pentobarbitone sodium, 40 mg kg^{-1}, i.p.) were placed in a stereotaxic frame (DKI 900, David Kopf Instruments, Tujunga, CA, U.S.A.) with the incisor bar set at − 4.5 mm from the horizontal, and the calvarium was exposed by a midsagittal incision. The right femoral vein was exposed and ^{125}I-labelled bovine serum albumin ([^{125}I]-BSA, 50 μCi kg^{-1}) was injected as a bolus. Symmetrical burr holes of 2 mm diameter were drilled 4.0 mm posterior to the bregma and 4.0 mm laterally on each side of the sagittal suture for electrode placement. Bipolar electrodes (50 mm shaft, Rhodes Medical Instruments, Woodland Hills, CA, U.S.A.) were lowered into the trigeminal ganglia to a depth of 10.5 mm from the dura mater overlying the dorsal surface of the brain. The right trigeminal ganglion was stimulated for 5 min (0.6 mA, 5 ms, 5 Hz) (Pulsemaster A300, Stimulus Isolator A365, World Precision Instruments, San Carlos, CA, U.S.A.; Oscilloscope V-134, Hitachi Densi, Tokyo, Japan), as previously described (Markowitz *et al.*, 1987; Matsubara *et al.*, 1991).

Pre-stimulation treatment

RPR 100893 or its enantiomer, RPR 103253, was administered via nasogastric tube in a volume of 2.5 ml kg^{-1} 60 min before electrical stimulation of trigeminal ganglion. Sixty min was selected as the interval between administration and stimulation because previous studies had demonstrated that plasma levels of RPR 100893 peak at this time (Moussaoui *et al.*, 1994). By i.v. route, RPR 100893 was administered 30 min before electrical stimulation. Control animals received the same volume of vehicle. [^{125}I]-BSA was injected via the right femoral vein 5 min before electrical stimulation. Immediately after stimulation, animals were perfused via the left cardiac ventricle with 0.9% saline for 2 min at a constant pressure of 100 mmHg. The dura mater was then dissected bilaterally, as previously described (Markowitz *et al.*, 1987).

Post-stimulation treatment

RPR 100893 was administered p.o. 10, 40 and 80 min after electrical trigeminal stimulation. Forty min later, [^{125}I]-BSA was injected. Five min later, animals were perfused and then killed. During these experiments, supplementary pentobarbitone (15 mg kg^{-1}, i.p.) was administered every 60 min to maintain anaesthesia.

Capsaicin administration

Capsaicin (150 μg kg^{-1}) was administered via the left jugular vein of the anaesthetized guinea-pig 5 min after [^{125}I]-BSA injection. RPR 100893 or sumatriptan was administered p.o. 60 min prior to capsaicin. Ten min after capsaicin treatment, animals were perfused with 0.9% saline transcardially at a constant pressure of 100 mmHg for 3 min. Immediately after transcardiac perfusion, the dura mater and conjunctiva were dissected.

Drugs

^{125}I-labelled bovine serum albumin ([^{125}I]-BSA; New England Nuclear, Boston, MA, U.S.A. and Du Pont de Nemours, France) was diluted in saline. Capsaicin (Sigma, France) was dissolved in ethanol/polysorbate 80/distilled water (1:1:8). RPR 100893 and RPR 103253 were synthesized in the Department of Chemistry of Rhone-Poulenc Rorer, France. RPR 100893 and RPR 103253 were dissolved in polyethyleneglycol 400. Sumatriptan (Glaxo, U.K.) was dissolved in saline. RPR 100893, [^{125}I]-BSA and capsaicin were injected i.v. as a bolus in a volume of 1.0 ml kg^{-1}. The same volume of vehicle was administered to the animals in the control groups in each experiment.

Data analysis

[^{125}I]-BSA extravasation is expressed as the ratio of c.p.m. mg^{-1} of wet wt. (stimulated side)/c.p.m. mg^{-1} of wet wt. (unstimulated side) for experiments involving electrical stimulation. Data are given as mean ± s.e.mean. Results with capsaicin are expressed as a percentage of c.p.m. mg^{-1} tissue in the capsaicin- versus vehicle-treated animals.

Each data point was calculated from at least two separate experiments. ID_{50} (the dose at which [^{125}I]-BSA extravasation was inhibited by 50%) was determined by regression analysis. Student's unpaired *t* test was used for statistical comparisons between vehicle- and drug-treated groups. Probability values (*P*) of less than 0.05 were considered significant.

Results

Unilateral electrical trigeminal ganglion stimulation increased the leakage of [^{125}I]-BSA within the dura mater of guinea-pigs treated with vehicle (p.o.) from 29.2 ± 3.0 to 48.2 ± 4.3 c.p.m. mg^{-1} wet wt. ($P<0.005$, $n=10$). The ratio between the stimulated and unstimulated sides was 1.69 ± 0.07 and was similar to previously reported values after saline-vehicle administration (Buzzi & Moskowitz, 1990).

When administered p.o. 60 min before electrical stimulation (Figure 1), RPR 100893 significantly decreased the ratio to 1.42 ± 0.05 at a threshold dose of 0.1 μg kg^{-1} ($P<0.05$, $n=6$). The ID_{50} was 0.5 μg kg^{-1}. RPR 100893 dose-dependently decreased plasma extravasation. The ratio decreased to 1.24 ± 0.03 at 1 μg kg^{-1} ($P<0.001$, $n=7$), 1.15 ± 0.05 at 10 μg kg^{-1} ($P<0.001$, $n=6$), and 1.04 ± 0.06 at 100 μg kg^{-1} ($P<0.001$, $n=5$). Extravasation on the unstimulated side did not differ between the treated and untreated groups.

When administered p.o. at 10 or 100 μg kg^{-1}, 60 min before electrical stimulation, RPR 103253, the enantiomer of RPR 100893, did not affect plasma protein extravasation within dura mater: 1.51 ± 0.03 ($n=5$) and 1.47 ± 0.04 ($n=7$), respectively; 1.56 ± 0.06 in vehicle group ($n=4$).

Pretreatment with RPR 100893 (0.05–50 ng kg^{-1}, i.v.) 30 min before electrical stimulation dose-dependently reduced plasma protein extravasation with an ID_{50} of 2.5 ng kg^{-1} (Figure 2). The threshold dose was 0.5 ng kg^{-1} (1.40 ± 0.03, $P<0.05$, $n=5$) and the maximum response was achieved with 50 ng kg^{-1} (1.08 ± 0.07, $P<0.001$, $n=5$) as compared to the vehicle-treated group (1.69 ± 0.07, $n=5$).

Table 1 shows the effect of RPR 100893 on the delayed plasma protein extravasation response that develops during the poststimulation period. At 100 μg kg^{-1}, p.o. administered 10, 40 or 80 min after electrical stimulation, RPR 100893 markedly attenuated the delayed extravasation response in those animals killed within 85 min poststimulation. There was little extravasation to block at 125 min after stimulation.

Capsaicin increased the leakage of [^{125}I]-BSA within dura mater (133.2 ± 4.8%, $P<0.01$, $n=24$) and conjunctiva (177.9 ± 9.4%, $P<0.01$, $n=20$) as compared to vehicle-treated animals. RPR 100893 (1–1,000 μg kg^{-1}, p.o.) blocked the response in a dose-dependent manner when administered 60 min prior to capsaicin injection [in dura mater; 124.0 ± 11.3% at 1 μg kg^{-1} ($n=6$), 117.8 ± 12.5% at 10 μg kg^{-1} ($n=6$), 102.5 ± 7.9% at 100 μg kg^{-1} ($P<0.01$, $n=9$),

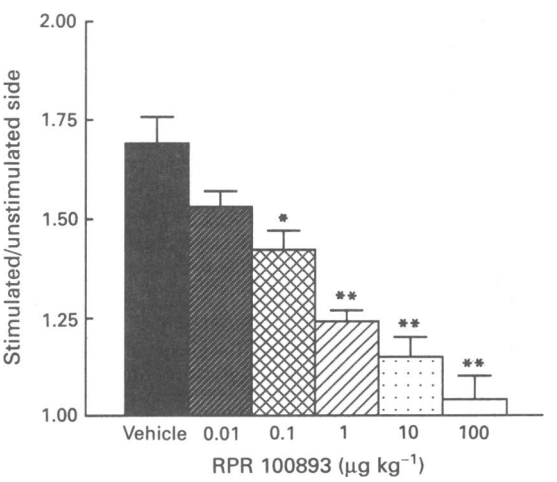

Figure 1 Oral RPR 100893 reduced plasma protein ([^{125}I]-BSA) extravasation within guinea-pig dura mater following electrical stimulation of trigeminal ganglion (0.6 mA, 5 ms, 5 Hz). Animals were treated with vehicle (solid column; $n=10$), 0.01 (heavily hatched column, $n=6$), 0.1 (cross-hatched column, $n=6$), 1 (hatched column, $n=7$), 10 (dotted column, $n=6$) or 100 (open column, $n=5$) μg kg^{-1} of RPR 100893 given 60 min before electrical stimulation and 55 min before [^{125}I]-BSA (50 μCi kg^{-1}) injection. Immediately after stimulation, animals were perfused with 0.9% saline and tissues harvested (see Methods). Results are expressed as the ratio of the c.p.m. mg^{-1} wet weight on the stimulated side to that on the unstimulated side (mean ± s.e.mean). *$P<0.05$, **$P<0.001$ as compared to vehicle-treated group.

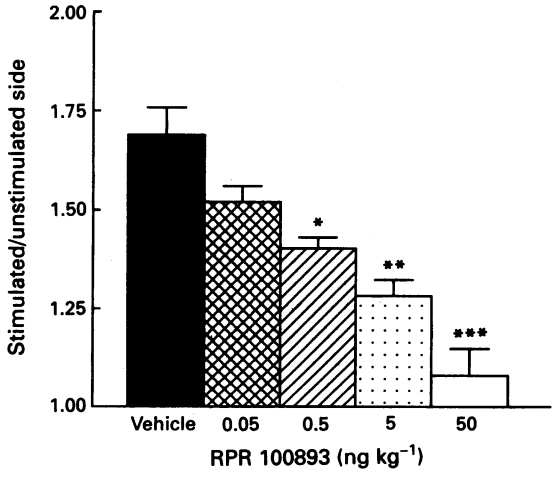

Figure 2 RPR 100893 administered i.v. decreased plasma protein extravasation within guinea-pig dura mater following electrical trigeminal ganglion stimulation. RPR 100893 was administered 0.05 (cross-hatched column), 0.5 (hatched column), 5 (dotted column) or 50 (open column) ng kg^{-1}, 30 min before electrical stimulation and 25 min before [^{125}I]-BSA injection. Immediately after stimulation, animals were perfused with 0.9% saline (see Methods). Data are expressed as described in legend to Figure 1. $*P<0.05$, $**P<0.01$; $***P<0.001$ as compared to vehicle-treated group ($n=5$ in each group).

101.3 ± 7.9% at 1,000 μg kg^{-1} ($P<0.01$, $n=8$): in conjunctiva; 161.3 ± 14.9% at 1 μg kg^{-1} ($n=6$), 138.5 ± 14.0% at 10 μg kg^{-1} ($P<0.05$, $n=6$), 130.6 ± 6.6% at 100 μg kg^{-1} ($P<0.01$, $n=8$), 117.7 ± 9.6% at 1,000 μg kg^{-1} ($P<0.01$, $n=6$)]. The ID_{50}s for dura mater and conjunctiva were 7.4 μg kg^{-1} and 82 μg kg^{-1}, respectively. Oral sumatriptan likewise administered 60 min prior to capsaicin injection was effective in dura mater only at a considerably higher dose [109.4 ± 10.4% at 10,000 μg kg^{-1} ($P<0.05$, $n=7$) vs. 155.6 ± 12.2% in vehicle group ($n=16$); ID_{50} of 1,000 μg kg^{-1}], but not in conjunctiva.

Discussion

The NK_1 receptor antagonist, RPR 100893 but not its stereoisomer RPR 103253, potently blocked NI within guinea-pig dura mater evoked by electrical trigeminal stimulation. RPR 100893 was effective at very low doses p.o. or i.v. when administered before, and also when given p.o. after electrical trigeminal stimulation. RPR 100893 was also effective against capsaicin-induced extravasation. When compared to RP 67580, pretreatment with RPR 100893 was about 240 times more potent. The ID_{50}s of RP 67580 (rat; Shepheard *et al.*, 1993) and RPR 100893 (guinea-pig) were 0.6 μg kg^{-1} and 2.5 ng kg^{-1}, i.v., respectively. Results of recent pilot experiments indicate that RPR 100893 does not alter basal plasma extravasation or vasodilatation in peripheral tissues (Moussaoui *et al.*, 1994).

RPR 100893

RPR 100893 binds with high affinity (nanomolar range) and selectively to the NK_1 recognition site on human IM9 cells and guinea-pig brain, but not to NK_2 or NK_3 binding sites (Fardin *et al.*, 1994). Its affinity for guinea-pig NK_1 receptors is 30 times greater than that of its enantiomer, RPR 103253 (Fardin *et al.*, 1994; Moussaoui *et al.*, 1994). RPR 100893 exhibits >1 μM affinity for a variety of other peptide receptors, receptors of classical neurotransmitters, calcium channels and the rat NK_1 receptor (Fardin *et al.*, unpublished data).

RPR 100893 inhibits nociceptive behaviours when administered to guinea-pigs, albeit at a lower potency than blockade of plasma extravasation within dura mater, and the response is not accompanied by a change in blood pressure. RPR 100893 but not its enantiomer blocked the licking response to formalin-injected guinea-pig paws (50 μl, 5%) with an ID_{50} of 3.1 mg kg^{-1}, s.c. (Moussaoui *et al.*, 1994). Although the mechanism may be complex and the specificity challenged (Rupniak *et al.*, 1993; Guard *et al.*, 1993), other NK_1 receptor antagonists, such as RP 67580 and CP-96,345 decreased pain-associated behaviours induced by chemical stimulation (formalin and phenylbenzoquinone tests in rat and mouse; Yamamoto & Yaksh, 1991; Nagahisa *et al.*, 1992; Carruette *et al.*, 1993). Moreover, RP 67580 blocked the nociception flexion reflex in an enantiomer-specific manner (Laird *et al.*, 1993). We recently found that relatively large doses of RPR 100893 (threshold, 1 μg kg^{-1}, i.v.) attenuated the expression of c-fos antigen within lamina I,II_o of guinea-pig trigeminal nucleus caudalis induced by intracisternal capsaicin (Cutrer *et al.*, unpublished data). The inhibition of c-fos antigen expression within this brain region was previously demonstrated after giving analgesics such as morphine, or after sumatriptan or dihydroergotamine following noxious meningeal stimulation (Presley *et al.*, 1990; Nozaki *et al.*, 1992; Moskowitz *et al.*, 1993).

Wang *et al.* (1994) noted certain structural similarities between non-peptide tachykinin receptor antagonists and local anaesthetics. They reported that RP 67580 and CP-96,345 blocked non-NK_1 related neurotransmission. RP 67580 and CP-96,345, like the anaesthetic bupivacaine, inhibited non-tachykinin-evoked neurotransmission in addition to tachykinin-evoked neurotransmission. Because RP

Table 1 Effect of RPR 100893 (100 μg kg^{-1}) administered p.o. 10, 40 or 80 min after electrical trigeminal stimulation on delayed plasma protein extravasation in guinea-pig dura mater

Poststimulation		*Stimulated side* (c.p.m. mg^{-1})	*Unstimulated side* (c.p.m. mg^{-1})	*Ratio*
55 min				
Vehicle	(8)	31.42 ± 0.47	21.90 ± 0.65	1.44 ± 0.03
RPR 100893	(8)	25.00 ± 1.05	23.11 ± 0.74	1.09 ± 0.07**
85 min				
Vehicle	(6)	32.54 ± 1.30	24.56 ± 1.09	1.33 ± 0.05
RPR 100893	(6)	26.98 ± 2.50	26.44 ± 2.73	1.03 ± 0.04*
125 min				
Vehicle	(6)	29.06 ± 1.97	26.40 ± 2.36	1.12 ± 0.06
RPR 100893	(6)	28.05 ± 3.27	27.93 ± 3.27	1.01 ± 0.05

RPR 100893 decreased plasma protein extravasation within the guinea-pig dura mater after 5 min of electrical trigeminal stimulation. RPR 100893 was administered p.o. 10, 40 or 80 min after electrical stimulation. Forty min later, [^{125}I]-BSA was injected and the animals perfused and killed after an additional 5 min. Numbers in parentheses represent the number of animals per group. $*P<0.01$, $**P<0.001$ as compared to corresponding vehicle-treated group.

67580 and RPR 100893 are structural analogues, the possibility that RPR 100893 possesses local anaesthetic-like actions in addition to actions at the NK_1 receptor cannot now be ruled out. However, the large concentrations of RP 67580 required to achieve non-specific blockade argues in favour of an NK_1 receptor-mediated mechanism in the studies reported herein. Additional work will be required to clarify this point.

NK_1 receptor and neurogenic inflammation in dura mater

The evidence supports NK_1 receptor involvement in the extravasation response. As noted above substance P (SP), the preferential NK_1 receptor endogenous ligand, is stored and released from trigeminal nerve terminals in the dura mater (Edvinsson *et al.*, 1983) where it produces vasodilatation and plasma protein extravasation (Moskowitz *et al.*, 1989). Exogenous SP and selective NK_1 receptor agonists, such as GR 73632 and SPOMe, but not NK_2 (GR 64349) or NK_3 (senktide) receptor agonists, enhance both plasma protein extravasation and vasodilatation in cranial tissues (Guard & Watson, 1991; Hagan *et al.*, 1991; Beattie *et al.*, 1993; O'Shaughnessy & Connor, 1993). Hence, the inhibition of NI by RPR 100893 is most consistent with selective blockade of NK_1 receptors.

RP 67580 (Moussaoui *et al.*, 1993c; Shepheard *et al.*, 1993) and RPR 100893 were more potent blockers of neurogenic extravasation within the dura mater than within extracranial tissues. When RP 67580 was administered prior to capsaicin treatment, its ID_{50} was as low as 35 $\mu g\,kg^{-1}$, i.v., whereas values of 109 and 309 $\mu g\,kg^{-1}$, i.v. were obtained in conjunctiva and bladder, respectively (Moussaoui *et al.*, 1993c). The explanation for this tissue-specific response is not yet known, but may suggest the existence of more than a single NK_1 receptor subtype.

The results after delayed RPR 100893 administration (Table 1) implicate sustained SP release as the mediator of plasma leakage developing beyond the period of electrical stimulation. Consistent with this formulation, endopeptidase 24.11 which degrades extracellular neuropeptides (Roques & Beaumont, 1990) blocks the delayed response as does 5-$HT_{1D/B}$ receptor agonists (Huang *et al.*, 1993). Together these findings are consistent with data showing that plasma extravasation in the skin can be blocked at the presynaptic level (by opioid agonists inhibiting SP release, by colchicine blocking axonal transport of neuromediators, or by neonatal capsaicin treatment destroying C-fibres; Moussaoui *et al.*, 1993a) as well as at the postsynaptic levels (by blocking NK_1 receptors or by dexamethasone which inhibits the mRNA expression of the NK_1 receptor; Ihara & Nakanishi, 1990). Our data showing that lignocaine (5 mg kg^{-1}, i.v.) blocked plasma protein extravasation in dura mater induced by SP (1 nmol kg^{-1}) or electrical trigeminal stimulation (Huang *et al.*, unpublished data) merit further study in view of one report showing that RP 67580 possesses local anaesthetic-like properties which are distinct from actions at the NK_1 receptor (Wang *et al.*, 1994).

In conclusion, the present work is the first to demonstrate the oral and parenteral effects of a potent human NK_1 receptor antagonist, RPR 100893, on neurogenic plasma extravasation, when administered either before or after chemical or electrical stimulation. If NI is important to the development of vascular headaches (Moskowitz *et al.*, 1989) and RPR 100893 exhibits antinociceptive activity (Moussaoui *et al.*, 1994), perhydroisoindoles such as RPR 100893 could be effective in the treatment of migraine and related headaches.

References

BEATTIE, D.T., STUBBS, C.M., CONNOR, H.E. & FENIUK, W. (1993). Neurokinin-induced changes in pial artery diameter in the anaesthetized guinea-pig. *Br. J. Pharmacol.*, **108**, 146–149.

BUCK, S.H. & BURCHER, E. (1986). The tachykinins: a family of peptides with a brood of 'receptors'. *Trends Pharmacol. Sci.*, **7**, 65–68.

BUZZI, M.G. & MOSKOWITZ, M.A. (1990). The antimigraine drug, sumatriptan (GR43175), selectively blocks neurogenic plasma extravasation from blood vessels in dura mater. *Br. J. Pharmacol.*, **99**, 202–206.

BUZZI, M.G., MOSKOWITZ, M.A., PEROUTKA, S.J. & BYUN, B. (1991). Further characterization of the putative 5-HT receptor which mediates blockade of neurogenic plasma protein extravasation in rat dura mater. *Br. J. Pharmacol.*, **103**, 1421–1428.

CARRUETTE, A., CHAMPION, A., GONIOT, P. & COTTEZ, D. (1993). Antinociceptive effect of RP 67580, a non-peptide substance P antagonist, in the formalin test in mice, rats and guinea-pigs. *7th World Congress on Pain* (Abstract 638), 230.

DIMITRIADOU, V., BUZZI, M.G., MOSKOWITZ, M.A. & THEOHARIDES, T.C. (1991). Trigeminal sensory fiber stimulation induces morphological changes reflecting secretion in rat dura mater mast cells. *Neuroscience*, **44**, 97–112.

DIMITRIADOU, V., BUZZI, M.G., THEOHARIDES, T.C. & MOSKOWITZ, M.A. (1992). Ultrastructural evidence for neurogenically mediated changes in blood vessels of the rat dura mater and tongue following antidromic trigeminal stimulation. *Neuroscience*, **48**, 187–203.

EDVINSSON, L., ROSENDAL-HELGESEN, S. & UDDMAN, R. (1983). Substance P: localization, concentration and release in cerebral arteries, choroid plexus and dura mater. *Cell Tissue Res.*, **234**, 1–7.

FARDIN, V., CARRUETTE, A., MENAGER, J., BOCK, M., FLAMAND, O., FOUCAULT, F., HEUILLET, E., MOUSSAOUI, S.M., TABART, M., PEYRONEL, J.F. & GARRET, C. (1994). In vitro pharmacological profile of RPR 100893, a novel non-peptide antagonist of the human NK_1 receptor. *Neuropeptides*, (in press).

GUARD, S., BOYLE, S.J., TANG, K.-W., WATLING, K.J., MCKNIGHT, A.T. & WOODRUFF, G.N. (1993). The interaction of the NK_1 receptor antagonist CP-96,345 with L-type calcium channels and its functional consequences. *Br. J. Pharmacol.*, **110**, 385–391.

GUARD, S. & WATSON, S.P. (1991). Tachykinin receptor types: classification and membrane signaling mechanisms. *Neurochem. Int.*, **18**, 149–165.

HAGAN, R.M., IRELAND, S.J., JORDAN, C.C., BERESFORD, I.J.M., DEAL, M.J. & WARD, P. (1991). Receptor-selective, peptidase-resistant agonists at neurokinin NK_1 and NK_2 receptors: new tools for investigating neurokinin function. *Neuropeptides*, **19**, 127–135.

HUANG, Z., BYUN, B., MATSUBARA, T. & MOSKOWITZ, M.A. (1993). Time-dependent blockade of neurogenic plasma protein extravasation in dura mater by 5-$HT_{1B/D}$ agonists and endopeptidase 24.11. *Br. J. Pharmacol.*, **108**, 331–335.

IHARA, H. & NAKANHISHI, S. (1990). Selective inhibition of expression of the substance P receptor mRNA in pancreatic acinar AR42J cells by glucocorticoids. *J. Biol. Chem.*, **265**, 22441–22445.

LAIRD, J.M., HARGREAVES, R.J. & HILL, R.G. (1993). Effect of RP 67580, a non-peptide neurokinin1 receptor antagonist, on facilitation of a nociceptive spinal flexion reflex in the rat. *Br. J. Pharmacol.*, **109**, 713–718.

LIU-CHEN, L.-Y., MAYBERG, M.R. & MOSKOWITZ, M.A. (1983). Immunohistochemical evidence for a substance P-containing trigeminovascular pathway to pial arteries in cat. *Brain Res.*, **268**, 162–166.

MARKOWITZ, S., SAITO, K. & MOSKOWITZ, M.A. (1987). Neurogenically mediated leakage of plasma protein occurs from blood vessels in dura mater but not brain. *J. Neurosci.*, **7**, 4129–4136.

MATSUBARA, T., MOSKOWITZ, M.A. & BYUN, B. (1991). CP-93,129, a potent and selective 5-HT_{1B} receptor agonist blocks neurogenic plasma extravasation within rat but not guinea pig dura mater. *Br. J. Pharmacol.*, **104**, 3–4.

MOSKOWITZ, M.A. (1984). The neurobiology of vascular head pain. *Ann. Neurol.*, **16,** 157–168.

MOSKOWITZ, M.A. (1991). The visceral organ brain: implications for the pathophysiology of vascular head pain. *Neurology*, **41,** 182–186.

MOSKOWITZ, M.A. (1992). Neurogenic versus vascular mechanisms of sumatriptan and ergot alkaloids in migraine. *Trends Pharmacol. Sci.*, **13,** 307–311.

MOSKOWITZ, M.A., BRODY, M. & LIU-CHEN, L.-Y. (1983). *In vitro* release of immunoreactive substance P from putative afferent nerve ending in bovine pia arachnoid. *Neuroscience*, **9,** 809–814.

MOSKOWITZ, M.A., BUZZI, M.G., SAKAS, D.E. & LINNIK, M.D. (1989). Pain mechanisms underlying vascular headaches. *Rev. Neurol.*, **145,** 181–193.

MOSKOWITZ, M.A., NOZAKI, K. & KRAIG, R.P. (1993). Neocortical spreading depression provokes the expression of c-fos protein-like immunoreactivity within trigeminal nucleus caudalis via trigeminovascular mechanisms. *J. Neurosci.*, **13,** 1167–1177.

MOUSSAOUI, S.M., CARRUETTE, A. & GARRET, C. (1993a). Further evidence that substance P is a mediator of both neurogenic inflammation and pain: two phenomena inhibited either by postsynaptic blockade of NK_1 receptors or by presynaptic action of opioid receptor agonist. *Regul. Pept.*, **46,** 424–425.

MOUSSAOUI, S.M., MONTIER, F., CARRUETTE, A., BLANCHARD, J.C., LADURON, P.M. & GARRET, C. (1993b). A non-peptide NK_1-receptor antagonist, RP 67580, inhibits neurogenic inflammation postsynaptically. *Br. J. Pharmacol.*, **109,** 259–264.

MOUSSAOUI, S.M., MONTIER, F., CARRUETTE, A., FARDIN, V., FLOCH, A. & GARRET, C. (1994). *In vivo* pharmacological properties of RPR 100893, a novel non-peptide antagonist of the human NK_1 receptor. *Neuropeptides*, (in press).

MOUSSAOUI, S.M., PHILIPPE, L., LE PRADO, N. & GARRET, C. (1993c). Inhibition of neurogenic inflammation in the meninges by a non-peptide NK_1 receptor antagonist, RP 67580. *Eur. J. Pharmacol.*, **238,** 421–424.

NAGAHISA, A., KANAI, Y., SUGA, O., TANIGUCHI, K., TSUCHIYA, M., LOWE, J.A. & HESS, H.-J. (1992). Antiinflammatory and analgesic activity of a non-peptide substance P receptor antagonist. *Eur. J. Pharmacol.*, **217,** 191–195.

NOZAKI, K., MOSKOWITZ, M.A. & BOCCALINI, P. (1992). CP-93,129, sumatriptan, dihydroergotamine block c-fos expression within rat trigeminal nucleus caudalis caused by chemical stimulation of the meninges. *Br. J. Pharmacol.*, **49,** 669–680.

O'SHAUGHNESSY, C.T. & CONNOR, H.E. (1993). Neurokinin NK_1 receptors mediate plasma protein extravasation in guinea-pig dura. *Eur. J. Pharmacol.*, **236,** 319–321.

PRESLEY, R.W., MENETREY, D., LEVINE, J.D. & BASBAUM, A.I. (1990). Systemic morphine suppresses noxious stimulus-evoked Fos protein-like immunoreactivity in the rat spinal cord. *J. Neurosci.*, **10,** 323–325.

QUIRION, R. & DAM, T.V. (1985). Multiple tachykinin receptors in guinea-pig brain. High densities of substance K (neuromedin K) binding sites in the substantia nigra. *Neuropeptides*, **6,** 191–194.

REGOLI, D., DRAPEAU, G., DION, S. & D'ORLEANS-JUSTE, P. (1987). Pharmacological receptors for substance P and neurokinins. *Life Sci.*, **40,** 109–117.

ROQUES, B. & BEAUMONT, A. (1990). Neutral endopeptidase-24.11 inhibitors: from analgesics to antihypertensives? *Trends Pharmacol. Sci.*, **11,** 245–249.

RUPNIAK, N.M.J., BOYCE, S., WILLIAMS, A.R., COOK, G., LONGMORE, J., SEABROOK, G.R., CAESER, M., IVERSEN, S.D. & HILL, R.G. (1993). Antinociceptive activity of NK_1 receptor antagonists: non-specific effects of racemic RP67580. *Br. J. Pharmacol.*, **110,** 1607–1613.

SHEPHEARD, S.L., WILLIAMSON, D.J., HILL, R.G. & HARGREAVES, R.J. (1993). The non-peptide neurokinin$_1$ receptor antagonist, RP 67580, blocks neurogenic plasma extravasation in the dura mater of rats. *Br. J. Pharmacol.*, **108,** 11–12.

TABART, M. & PEYRONEL, J.F. (1994). Synthesis of RPR 100893, prototype of a new series of potent and selective non-peptide NK_1 antagonists: the triarylperhydroisoindols. *Bioorg. Med. Chem. Lett.*, (in press).

WANG, Z.-Y., TUNG, S.R., STRICHARTZ, G.R. & HÅKANSON, R. (1994). Non-specific actions of the non-peptide tachykinin receptor antagonists, CP-96,345, RP 67580 and SR 48968, on neurotransmission. *Br. J. Pharmacol.*, **111,** 179–184.

YAMAMOTO, T. & YAKSH, T.L. (1991). Stereospecific effects of a nonpeptide NK_1 selective antagonist, CP96,345: antinociception in the absence of motor dysfunction. *Life Sci.*, **49,** 1955–1963.

(Received December 1, 1993
Revised March 7, 1994
Accepted March 14, 1994)

Br. J. Pharmacol. (1994), **112**, 925–933

Enhancement of arterial relaxation by long-term atenolol treatment in spontaneously hypertensive rats

[1]Mika Kähönen, Heikki Mäkynen, Pertti Arvola & Ilkka Pörsti

Department of Biomedical Sciences, University of Tampere, P.O. Box 607, FIN-33101 Tampere, Finland

1 The effects of long-term atenolol (25 mg kg^{-1} day^{-1}) therapy on arterial function were studied in spontaneously hypertensive rats (SHR) and Wistar-Kyoto (WKY) rats. The 14-week treatment attenuated the increase in blood pressure by approximately 30 mmHg in SHR, but did not affect blood pressure in WKY rats.

2 Responses of mesenteric arterial rings *in vitro* were examined at the end of the study. The relaxation to acetylcholine was similar in WKY rats and atenolol-treated SHR and more pronounced than in untreated SHR, whereas the relaxation to the nitric oxide donor 3-morpholinosydnonimine (SIN-1) was comparable in all study groups. Moreover, after maximal relaxations to acetylcholine, marked recontractions developed in untreated SHR but not in the other groups. Vasorelaxation to isoprenaline was also attenuated in SHR and was moderately improved by the atenolol therapy.

3 Arterial relaxation induced by return of potassium to the organ bath upon precontractions elicited by potassium-free solution were used to evaluate vascular smooth muscle Na^+,K^+-ATPase. The rate of potassium relaxation was fastest in WKY rats and was also faster in atenolol-treated than in untreated SHR.

4 The ability of vascular smooth muscle to sequester calcium was evaluated by eliciting responses to caffeine or noradrenaline after loading periods in different organ bath calcium concentrations. The subsequent contractions were lower in untreated SHR than in WKY rats, and augmented in SHR by the atenolol treatment.

5 Smooth muscle contractions to noradrenaline were comparable in SHR and WKY rats, while atenolol treatment slightly increased the maximal response to this agonist in SHR. Responses to potassium chloride were not affected by atenolol and contractions following cumulative re-addition of calcium to the organ bath after precontraction with potassium chloride and noradrenaline in calcium-free solution were comparable in all study groups.

6 In conclusion, the moderate antihypertensive effect of atenolol in SHR was accompanied by enhancement of β-adrenoceptor-mediated and normalization of endothelium-dependent arterial relaxation. Furthermore, ability to sequester calcium into cellular stores, and function of Na^+,K^+-ATPase were augmented in vascular smooth muscle. Therefore, the present results suggest that the long-term blood pressure-lowering action of atenolol in this type of genetic hypertension is accompanied by improved arterial relaxation and normalization of endothelial function.

Keywords: Arterial smooth muscle; atenolol; blood pressure; endothelium; spontaneously hypertensive rat

Introduction

The mechanisms beyond the antihypertensive action of β-adrenoceptor blockade have not been fully clarified, but reductions in adrenergic activity, cardiac output and renin release have been proposed to underlie the lowering of blood pressure (see Man in't Veld *et al.*, 1986; Meiracker *et al.*, 1989). Since different β-adrenoceptor blockers with quite dissimilar effects on the above variables have comparable effects on blood pressure, Man in't Veld *et al.* (1986) have suggested that the reductions observed in these factors are not essential for the antihypertensive action. The acute haemodynamic effect of β-adrenoceptor antagonism is a fall in cardiac output (Lysbo Svendsen *et al.*, 1979), and because of baroreflex-mediated compensatory mechanisms, total peripheral vascular resistance initially rises (Lund-Johansen, 1979). The long-term effect, however, is a reduction of arterial resistance associated with return of cardiac output towards baseline values. Therefore, it appears that β-blockers lower blood pressure by influencing the regulation of vascular tone, which leads to vasodilatation in the resistance vasculature (Man in't Veld, 1991).

The mechanism of the vasodilatation during β-adrenoceptor antagonism is not fully understood. Interference with vasoconstrictor nerve activity through blockade of prejunctional β-adrenoceptors with subsequent inhibition of noradrenaline (NA) release could lead to diminished arterial contractility, and thus explain the antihypertensive effect (Meiracker *et al.*, 1989). In addition, endothelial influences may play a role, since arterial preparations of normotensive animals have been shown to relax in the presence of β-blockers if the endothelium is left intact (Mostaghim *et al.*, 1986; Janczewski *et al.*, 1987). Moreover, treatment with atenolol has been reported to stimulate vasodepressor prostaglandin generation in the kidney and aorta of hypertensive rats (Hirawa *et al.*, 1991).

Since the long-term effects of β-blockade on arterial function are largely unknown, the aim of the present study was to elucidate the influences of treatment with atenolol, a hydrophilic β_1-selective compound, on vascular responses in spontaneously hypertensive rats (SHR) and normotensive Wistar-Kyoto (WKY) rats. We examined arterial contractions induced by membrane depolarization and α-adrenoceptors, and relaxations to endothelium-dependent and -independent agents after the atenolol therapy. In addition, vascular smooth muscle ability to sequester calcium into cellular stores and to induce relaxation via Na^+,K^+-ATPase were evaluated by indirect methods (Kojima *et al.*, 1991; Arvola *et al.*, 1992).

[1] Author for correspondence.

Methods

Animals and experimental design

Male SHR (Okamoto-Aoki strain) and age-matched WKY rats were obtained from Møllegaard's Breeding Centre, Ejby, Denmark. The animals were housed four to a cage in a standard experimental animal laboratory (illuminated 06 h 00 min–18 h 00 min, temperature + 22°C), and had free access to drinking fluid (tap water) and food pellets (Ewos, Södertälje, Sweden). The systolic blood pressures of conscious animals were measured at + 28°C by the tail-cuff method (Model 129 Blood Pressure Meter; IITC Inc., Woodland Hills, Ca., U.S.A.). At 8 weeks of age both SHR and WKY rats were divided into two groups of equal mean systolic blood pressures. Thereafter, SHR ($n = 10$) and WKY rats ($n = 10$) were given atenolol in drinking water in light-proof bottles, (average dose 25 mg kg^{-1} day^{-1}, fresh drug solutions daily prepared), while untreated SHR ($n = 15$) and normotensive WKY rats ($n = 15$) were kept on normal drinking fluid. This daily dose of the drug was chosen, since in the range 15–45 mg kg^{-1} atenolol has been reported to induce a comparable and nearly maximal affect on blood pressure in SHR (Takeda *et al.*, 1982). The concentration of atenolol in the drinking water was adjusted weekly to the drinking habits of the animals. Atelolol therapy and indirect blood pressure measurements continued for 14 more weeks until the animals were 22 weeks old. Thereafter atenolol administration was withdrawn 1 day before the rats were decapitated and exsanguinated. The blood samples were drawn into polystyrene tubes containing heparin (100 units ml^{-1}) as anticoagulant for lymphocyte intracellular free calcium concentration ($[Ca^{2+}]_i$) measurements, which were performed as previously described (Pörsti *et al.*, 1992; Wuorela *et al.*, 1992). The hearts were removed and weighed, and the superior mesenteric arteries carefully excised and cleaned of adherent connective tissue. The experimental design of the study was approved by the Animal Experimentation Committee of the University of Tampere, Finland.

Mesenteric arterial responses in vitro

Four successive standard sections (3 mm in length) of the mesenteric artery from each animal were cut, beginning 1 cm distally from the mesenteric artery-aorta junction. The most distal ring was left with the endothelium intact and from the other three vascular endothelium was removed by gently rubbing with a jagged injection needle (Arvola *et al.*, 1992). The average medial thickness in this preparation is about 110 and 80 μm in SHR and WKY rats, respectively (Arvola *et al.*, 1993; Wuorela *et al.*, 1994). The rings were placed between stainless steel hooks (diameter 30 μm) and suspended in an organ bath chamber (volume 20 ml) in physiological salt solution (PSS) (pH 7.4) of the following composition (mM): NaCl 119.0, $NaHCO_3$ 25.0, glucose 11.1, $CaCl_2$ 1.6, KCl 4.7, KH_2PO_4 1.2, $MgSO_4$ 1.2, and aerated with 95% O_2 and 5% CO_2. The rings were initially equilibrated for 1 h at 37°C with a resting tension of 1.5 g. The force of contraction was measured with an isometric force-displacement transducer and registered on a polygraph (FT03 transducer and model 7E Polygraph; Grass Instrument Co., Quincy, Ma., U.S.A.). The presence of intact endothelium in vascular preparations was confirmed by an almost complete relaxation response (>75%) to 1 μM acetylcholine (ACh) in 1 μM NA-precontracted rings, and the absence of endothelium by the lack of this relaxation response. If any relaxation was seen in endothelium-denuded rings, the endothelium was further rubbed.

Vascular preparation 1 After a 30 min stabilization, the endothelium-denuded mesenteric arterial ring was contracted with 10 μM NA to provide a reference contraction. When the maximal reponse had fully developed, the rings were rinsed with Ca^{2+}-free PSS, and once the resting tension was restored the contraction to NA was repeated in Ca^{2+}-free medium to deplete the cellular calcium stores. After a further 10 min equilibration in resting tension at 0 mM calcium with 1 mM ethylene glycol *bis*(β-aminoethyl ether)-*N,N,N',N'*-tetraacetic acid (EGTA), the rings were rinsed several times with Ca^{2+}-free buffer without EGTA and again contracted with NA (10 μM, in Ca^{2+}-free PSS). When the response had reached a plateau, calcium was cumulatively readded to the organ bath in concentrations of 0.05, 0.1, 0.2, 0.4, 0.8, 1.2 and 2.5 mM. and the increase in contractile force registered. After the maximal response, rings were rinsed with normal PSS and allowed a 20 min recovery period. Then the cycle was repeated with 125 mM KCl used as the agonist instead of NA. In solutions containing high concentrations of potassium, NaCl was substituted with KCl on an equimolar basis.

Vascular preparation 2 After a 30 min stabilization period, the endothelium-denuded vascular ring was contracted with 10 μM NA (reference contraction). When the maximal contraction was reached, the ring was rinsed with Ca^{2+}-free PSS. After a 10-min period in Ca^{2+}-free PSS, 1 mM EGTA was introduced and maximal response with 10 μM NA was elicited 1 min later. This induced rapidly fading contraction, the peak of the response reflecting the amount of calcium liberated from cellular stores (Dohi *et al.*, 1990). The following cycle was then used to evaluate calcium sequestration into cellular stores: (1) The preparations were incubated for 6 min in Ca^{2+}-free PSS containing 1 mM EGTA (depletion of cellular stores). (2) The rings were allowed a 10-min recovery period in PSS with calcium (calcium loading period; no EGTA in organ bath). (3) The Ca^{2+}-free PSS containing 0.1 mM EGTA was returned to the organ bath and 1 min later contractions to 10 μM NA were again elicited and maximal responses registered. This cycle was repeated 5 times, the following organ bath calcium concentrations during the calcium loading period being tested: 0, 0.033, 0.1, 0.4 and 1.2 mM. After a 20-min recovery period similar cycles were repeated with 30 mM caffeine as the contractile agent.

Vascular preparation 3 After 30 min the endothelium-denuded preparation was contracted with 125 mM KCl (reference response). After another 30 min the rings were exposed to K^+-free buffer solution (pH 7.4), which was prepared by substituting KH_2PO_4 and KCl of normal PSS with NaH_2PO_4 and NaCl, respectively, on an equimolar basis. The omission of potassium induced gradual contractions in all vascular rings. Once the contraction had reached a plateau, 1 mM potassium was re-added and the subsequent relaxation registered.

Vascular preparation 4 In the most distal ring with intact vascular endothelium, concentration-response curves for NA, and 30 min later for KCl, were determined cumulatively. After another 30 min recovery period, vascular responses to ACh, 3-morpholinosydnonimine (SIN-1), and isoprenaline were examined. The rings were precontracted with 1 μM NA, and after the contraction had developed fully increasing concentrations of the relaxing agent were cumulatively added to the organ bath. The next concentration of the relaxant was added only after the previous level of relaxation was stable. The rings were allowed a 20-min recovery in resting tension between the study of each relaxant.

The KCl-, NA- and K^+-free medium-induced contractile responses were expressed in g. The EC_{50} for KCl and NA in each ring was calculated as percentage of maximal response. Calcium cumulative responses in Ca^{2+}-free buffer solution with KCl and NA as the agonists, and the maximal contractile forces induced by 30 mM caffeine and 10 μM NA after each calcium loading period were normalized by relating them to the previously determined reference contractions. After potassium repletion upon K^+-free contractions, the greatest reduction in smooth muscle contractile force during

a 1 min period was considered the maximal relaxation rate, the mean relaxation rate being calculated from the time which was required to reach the maximal level of potassium relaxation. The relaxations in response to potassium repletion, ACh, SIN-1 and isoprenaline were presented as percentage of pre-existing contractile force. The EC_{50} for the latter 3 relaxants was calculated as a percentage of the 1 μM NA-induced precontraction. All EC_{50} values were calculated with a computer programme and presented as the negative logarithm (pD_{50}), which values were also used in the statistical analysis.

Drugs

The following drugs were used: acetylcholine chloride, calcium salt of ionomycin, EGTA, isoprenaline hydrochloride, ammonium salt of heparin (Sigma Chemical Co., St. Louis, Mo., U.S.A.), atenolol (Leiras Pharmaceutical Co., Turku, Finland), acetoxymethyl ester of quin-2, Triton X100 (Aldrich Chemical Co., Milwaukee, Wis., U.S.A.), 3-morpholinosydnonimine (GEA Ltd., Copenhagen, Denmark) and (−)-noradrenaline L-hydrogentartrate (Fluka Chemie AG, Buchs SG, Switzerland). Atenolol was dissolved directly in tap water. The stock solutions of the compounds used in the *in vitro* studies were dissolved in distilled water, with the exception of ionomycin (in absolute ethanol) and quin-2 (in dimethylsulphoxide). All solutions were freshly prepared before use and protected from light.

Analysis of results

Statistical analysis was carried out by one-way analysis of variance (ANOVA) supported by Bonferroni confidence intervals in the case of pairwise between-group comparisons. When the data consisted of repeated observations at successive time points ANOVA for repeated measurements was applied to investigate between-group differences. Differences were considered significant when $P < 0.05$. All results are expressed as mean ± s.e.mean.

Results

Blood pressure, heart rate, heart and body weights, and intracellular free calcium

The systolic blood pressure of SHR was higher at the beginning of the study than in WKY rats, and during the 14-week-long follow up it increased steadily in both SHR groups, whereas no significant change was observed in either of the WKY groups. Furthermore, the rise in blood pressure was significantly attenuated in atenolol-treated SHR (Figure 1 and Table 1). Heart rate was also reduced by atenolol administration in SHR, and it remained lower throughout the study than in control SHR (Table 1).

The atenolol therapy did not affect heart or body weights in either strain (Table 1). Lymphocyte $[Ca^{2+}]_i$, measured by the fluorescent indicator quin-2, was comparable in control and atenolol-treated SHR, and markedly higher than in the WKY groups (Table 1).

Mesenteric arterial responses in vitro

The relaxations of endothelium-intact mesenteric arterial rings to ACh were greatly impaired in untreated SHR when compared with the WKY groups. Interestingly, the response to ACh was markedly improved in SHR by the atenolol treatment, the relaxation not differing from that in the WKY groups. Moreover, following maximal dilatations to ACh the force of contraction rapidly increased in untreated SHR, but these recontractions were practically absent in WKY rats and

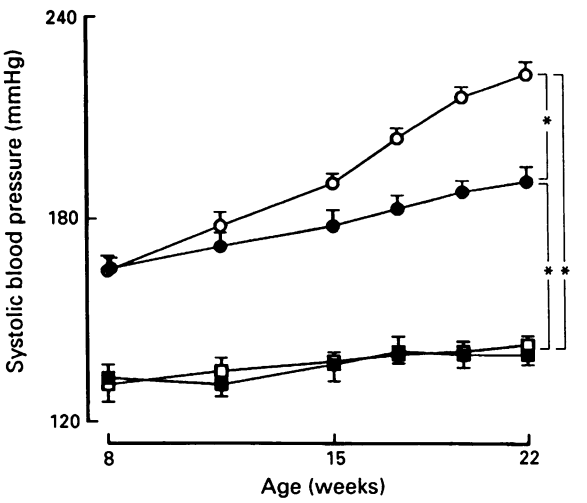

Figure 1 Systolic blood pressure in untreated spontaneously hypertensive rats (SHR, ○), atenolol-treated SHR (●, 25 mg kg^{-1} day^{-1}), untreated Wistar-Kyoto (WKY, □) rats, and atenolol-treated WKY rats (■). Symbols indicate means with s.e.means, $n = 10-12$ in each group; $^*P < 0.05$, ANOVA for repeated measurements.

Table 1 Blood pressure, body weight and heart rate during the study, and heart weight and lymphocyte intracellular free calcium concentration at the close of the 13-week study

Variable	*SHR*	*Aten-SHR*	*WKY*	*Aten-WKY*
Systolic blood pressure (mmHg)				
week 0	165 ± 4*	166 ± 3*	131 ± 5	133 ± 3
week 14	223 ± 3*	191 ± 4*†	143 ± 3	140 ± 4
Body weight (g)				
week 0	197 ± 6	199 ± 4	200 ± 9	205 ± 8
week 14	374 ± 4	368 ± 6	379 ± 7	370 ± 8
Heart weight (g kg^{-1} body weight)	3.6 ± 0.1*	3.6 ± 0.1*	3.2 ± 0.1	3.1 ± 0.1
Heart rate (beats min^{-1})				
week 0	374 ± 4*	375 ± 3*	328 ± 5	330 ± 4
week 14	335 ± 8*	302 ± 3*†	289 ± 5	285 ± 6
Intracellular free calcium concentration in lymphocytes (nM)	98 ± 3*	99 ± 6*	72 ± 3	74 ± 4

Values are mean ± s.e.mean; $n = 10-12$ in each group. SHR, spontaneously hypertensive rats; WKY, Wistar-Kyoto rats; Aten, atenolol-treated rats. The 14-week long atenolol treatment commenced at study week 0 when the animals were 8 weeks old. $^*P < 0.05$ compared with WKY rats, $^\dagger P < 0.05$ Aten-SHR versus SHR (Bonferroni test).

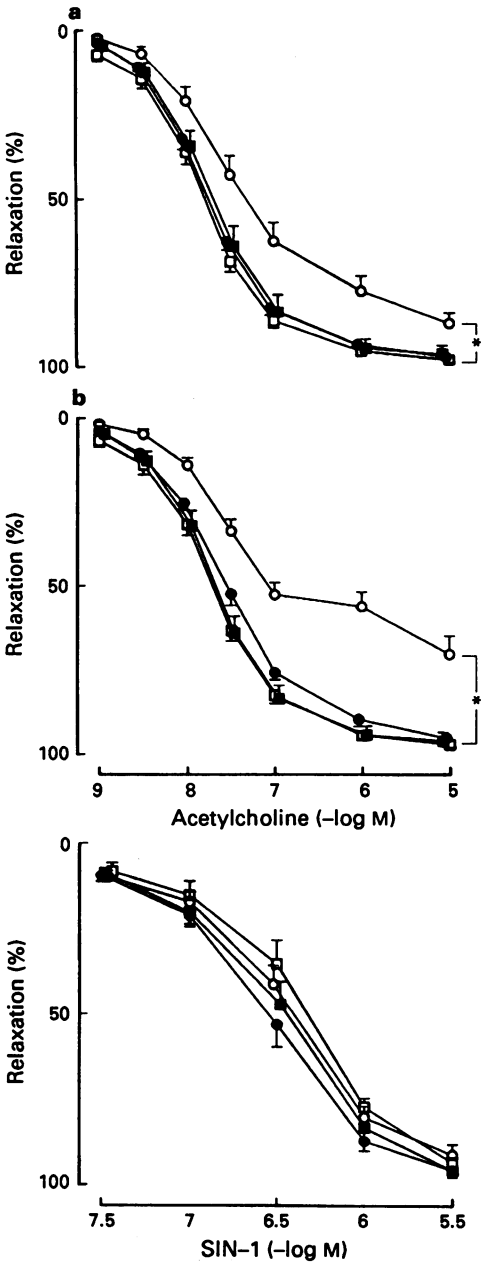

atenolol-treated SHR (Table 2 and Figure 2). No differences were found in the nitric oxide donor SIN-1-induced responses between the study groups (Figure 2). However, the relaxation to isoprenaline was attenuated in untreated SHR when compared with WKY rats. The atenolol therapy also improved this response in SHR, but the relaxation nevertheless remained less marked than in WKY rats (Table 2 and Figure 3).

The maximal contractions elicited by K^+-free solution did not differ between the four study groups (Table 3). After the return of potassium to the organ bath upon K^+-free contractions the rate of the subsequent relaxation was faster in the two WKY groups than in SHR. Furthermore, the atenolol therapy clearly enhanced the rate of potassium relaxation in SHR (Figure 3). However, the time to reach baseline tension after washout of 125 mM KCl, i.e. the washout time, which was clearly prolonged in SHR when compared with WKY rats, was not shortened by the atenolol treatment in SHR (Table 3).

In endothelium-denuded mesenteric arterial rings maximal contractile force generation to high concentrations of KCl was more pronounded in SHR than in WKY rats, and these responses were not affected by the atenolol treatment in either strain. The contractions to NA, however, were comparable in untreated SHR and WKY rats, while atenolol slightly increased the maximal response in SHR but not in WKY rats (Figure 4). pD_{50} values of KCl- and NA-induced contractions were corresponding in all study groups (Table 2).

The effect of organ bath calcium concentration on 125 mM KCl- and 10 μM NA-induced contractions, i.e. the calcium sensitivity of the vascular rings during depolarization and α-adrenoceptor stimulation, respectively, were comparable in all four study groups (Figure 5).

The contractile responses induced by 30 mM caffeine and

Figure 2 Relaxations of endothelium-intact mesenteric arterial rings after precontraction with 1 μM noradrenaline from untreated spontaneously hypertensive rats (SHR, ○), atenolol-treated SHR (●), untreated Wistar-Kyoto (WKY, □) rats, and atenolol-treated WKY rats (■). The relaxation to acetylcholine consisted of the maximal response (a) and the subsequent recontraction (b). Relaxations were also induced by 3-morpholinosydnonimine (SIN-1) (c). Symbols indicate means with s.e.mean, $n = 8$ in each group; $*P < 0.05$, ANOVA for repeated measurements.

Table 2 Parameters of contractile and relaxation responses of isolated endothelium-intact arterial rings

Variable	*SHR*	*Aten-SHR*	*WKY*	*Aten-WKY*
Relaxation responses				
pD_{50}				
Acetylcholine	7.20 ± 0.20*	7.70 ± 0.05†	7.79 ± 0.05	7.64 ± 0.07
SIN-1	6.34 ± 0.11	6.53 ± 0.10	6.38 ± 0.03	6.54 ± 0.11
Isoprenaline	4.89 ± 0.23*	5.22 ± 0.10*	5.83 ± 0.22	5.70 ± 0.25
Maximal relaxation (% of 1 μM noradrenaline -induced precontraction)				
Acetylcholine (10 μM)	87 ± 3*	97 ± 1†	98 ± 1	96 ± 1
SIN-1 (3.3 μM)	91 ± 3	96 ± 2	95 ± 2	98 ± 2
Isoprenaline (0.1 mM)	63 ± 5*	76 ± 1*†	84 ± 2	85 ± 3
Contractile responses				
pD_{50}				
Noradrenaline	6.33 ± 0.04	6.33 ± 0.02	6.37 ± 0.08	6.45 ± 0.08
Potassium chloride	1.32 ± 0.01	1.30 ± 0.02	1.36 ± 0.03	1.37 ± 0.03
Maximal force (g)				
Noradrenaline (10 μM)	3.0 ± 0.2	3.5 ± 0.2*†	2.9 ± 0.2	3.1 ± 0.2
Potassium chloride (125 mM)	3.3 ± 0.1*	3.5 ± 0.1*	2.6 ± 0.2	2.5 ± 0.2

Values are mean ± s.e.mean; $n = 10-12$ in each group. SHR, spontaneously hypertensive rats; WKY, Wistar-Kyoto rats; Aten, atenolol-treated rats. EC_{50} values are presented at the negative logarithm (pD_{50}) of concentration of the agonist. $*P < 0.05$ compared with WKY rats, $†P < 0.05$ Aten-SHR versus SHR (Bonferroni test).

10 μM NA after loading periods in increasing organ bath calcium concentrations were clearly less marked in SHR than in WKY rats. These contractions, reflecting the ability of arterial smooth muscle to sequester calcium into cellular stores, were improved in SHR by the atenolol treatment (Figure 6).

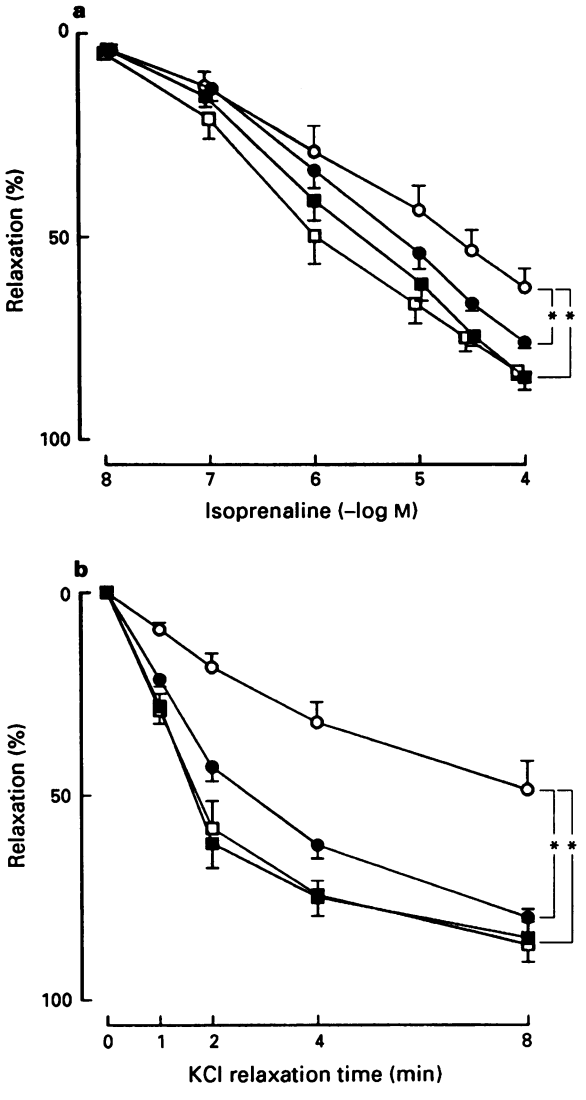

Figure 3 Relaxations to isoprenaline after precontraction with 1 μM noradrenaline in endothelium-intact mesenteric arterial rings (a), and relaxations to re-addition of 1.0 mM K^+ after precontraction induced by K^+-free buffer solution in endothelium-denuded rings (b). The groups were untreated spontaneously hypertensive rats (SHR, ○), atenolol-treated SHR (●), untreated Wistar-Kyoto (WKY, □) rats, and atenolol-treated WKY rats (■). Symbols indicate means with s.e.mean, $n = 8-10$ in each group; $^*P < 0.05$, ANOVA for repeated measurements.

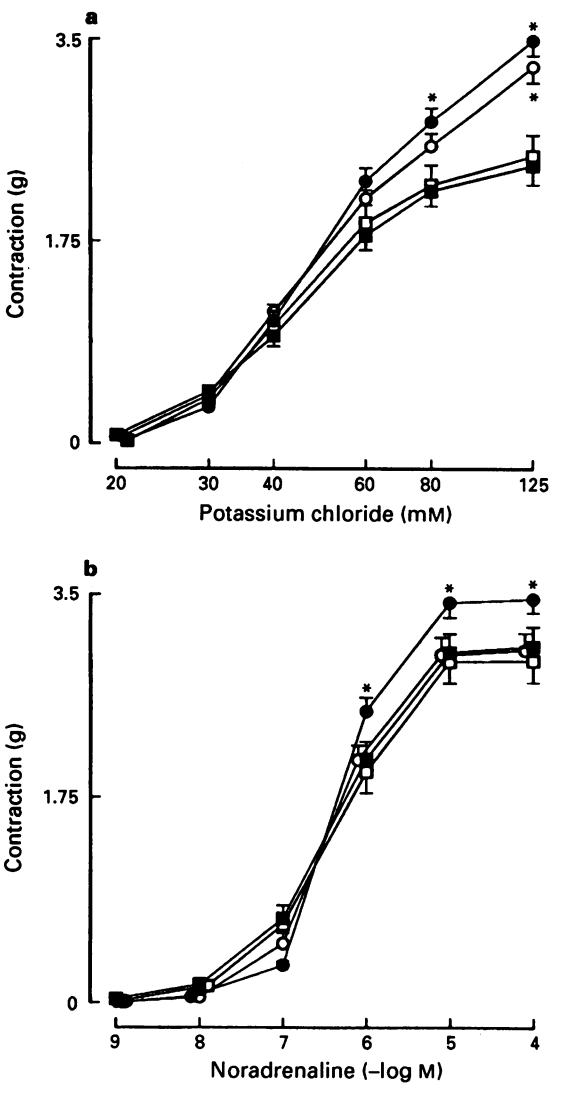

Figure 4 Concentration-response curves of endothelium-denuded mesenteric arterial rings to potassium chloride (a) and noradrenaline (b) in untreated spontaneously hypertensive rats (SHR, ○), atenolol-treated SHR (●), untreated Wistar-Kyoto (WKY, □) rats, and atenolol-treated WKY rats (■). Contractile force generation to potassium chloride was more pronounced in SHR than WKY rats, and atenolol treatment slightly increased maximal responses to noradrenaline in SHR. Symbols indicate means with s.e.mean, $n = 8$ in each group; $^*P < 0.05$, one-way ANOVA.

Table 3 Parameters of potassium-free buffer solution-induced contractions and subsequent relaxations induced by 1.0 mM potassium chloride in isolated endothelium-denuded mesenteric arterial rings

Variable	*SHR*	*Aten-SHR*	*WKY*	*Aten-WKY*
Reference response to 125 mM potassium chloride				
Maximal force (g)	2.3 ± 0.1	2.5 ± 0.2	2.4 ± 0.2	2.4 ± 0.2
Washout time (min)	16.0 ± 1.0*	13.3 ± 0.8*	7.7 ± 0.6	7.5 ± 0.4
Potassium-free contraction				
Time to onset (min)	3.0 ± 0.5	3.3 ± 0.6	5.1 ± 1.3	4.8 ± 0.4
Maximal force (g)	1.0 ± 0.1	1.1 ± 0.1	1.0 ± 0.1	1.1 ± 0.1
Potassium-relaxation				
Maximal rate (mg min^{-1})	75 ± 13*	245 ± 31†	317 ± 64	330 ± 80
Mean rate (mg min^{-1})	51 ± 8*	113 ± 10†	111 ± 17	121 ± 14

Values are mean ± s.e.mean; $n = 10-12$ in each group. SHR, spontaneously hypertensive rats; WKY, Wistar-Kyoto rats; Aten, atenolol-treated rats. $^*P < 0.05$ compared with WKY rats, $\dagger P < 0.05$ Aten-SHR versus SHR (Bonferroni test).

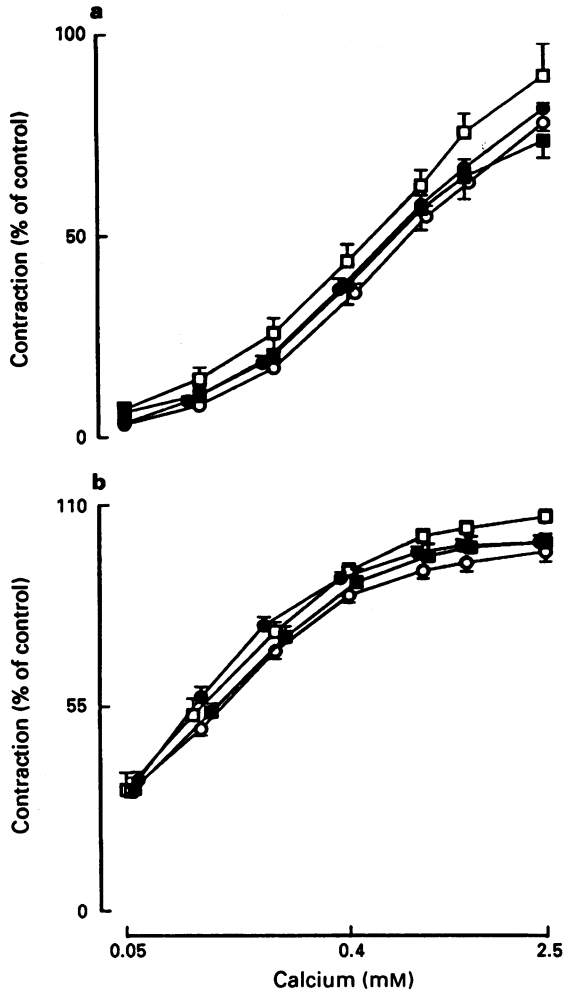

Figure 5 Contractile responses of endothelium-denuded mesenteric arterial rings from untreated spontaneously hypertensive rats (SHR, ○), atenolol-treated SHR (●), untreated Wistar-Kyoto rats (WKY, □) and, atenolol-treated WKY rats (■). Line graphs show the effect of organ bath calcium concentration on 125 mM KCl- (a), and 10 μM noradrenaline-induced contractions (b). Symbols indicate means with s.e.mean, $n = 8-10$ in each group.

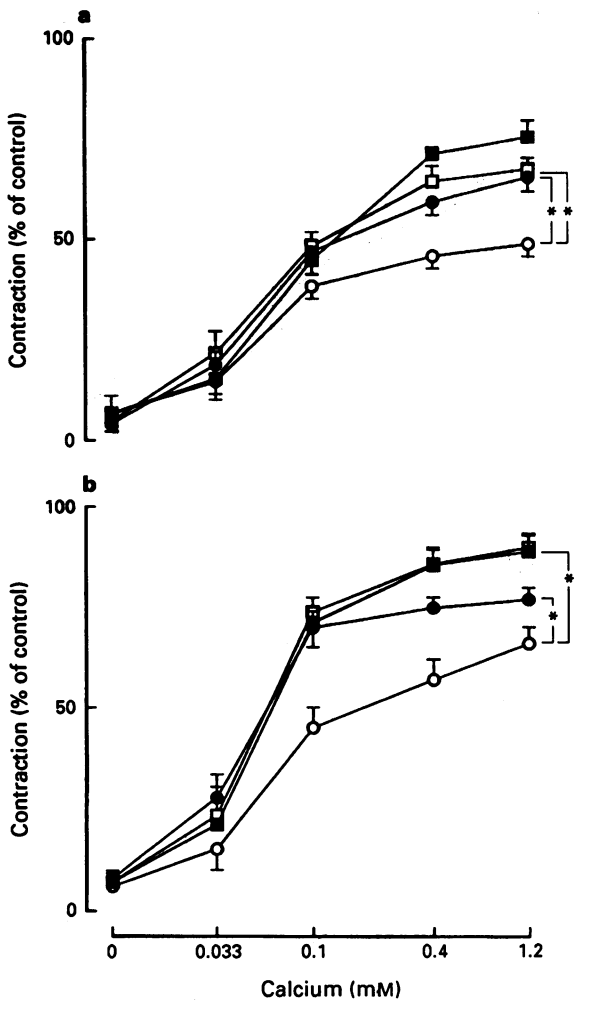

Figure 6 Contractile responses reflecting the ability to sequester calcium into cellular stores in endothelium-denuded mesenteric arterial rings from untreated spontaneously hypertensive rats (SHR, ○), atenolol-treated SHR (●), untreated Wistar-Kyoto (WKY, □) rats, and atenolol-treated WKY rats (■). Initially, cellular calcium stores were depleted, whereafter calcium was returned to the organ bath for 10 min, the concentrations 0, 0.033, 0.1, 0.4 and 1.2 mM being tested. The contractions induced by 30 mM caffeine (a) and 10 μM noradrenaline (b) after each calcium loading period were normalized by comparing them to the previously determined reference responses. Symbols indicate means with s.e.means, $n = 8-10$ in each group; $^*P < 0.05$, ANOVA for repeated measurements.

Discussion

In the present study, the atenolol therapy had a moderate antihypertensive action in SHR, whereas blood pressure in WKY rats was not affected. However, heart weights were not decreased by the treatment in SHR. Apparently the reduction in afterload accompanying the moderately lowered blood pressure was not sufficient to attenuate cardiac hypertrophy. Moreover, the degree of cardiovascular hypertrophy in SHR is not only governed by the level of blood pressure, but also by enhanced cellular responses to various growth factors such as angiotensin II (Dzau *et al.*, 1991). Previous reports have shown either no change (Chatelain *et al.*, 1981) or an attenuated increase (Lauva & Tomanek, 1985) in heart weights after chronic β_1-adrenoceptor blockade in SHR.

ACh relaxes arteries endothelium-dependently via the release of the endothelium-derived relaxing factor (EDRF), which stimulates smooth muscle soluble guanylate cyclase and elevates intracellular guanosine 3':5'-cyclic monophosphate (cyclic GMP) (Moncada *et al.*, 1991). EDRF is probably identical with nitric oxide (NO) (Moncada *et al.*, 1991), the production of which is also the mechanism of action of the endothelium-independent vasodilator, SIN-1 (Feelisch *et al.*, 1989). Previously several studies have reported impaired endothelium-dependent relaxation in human and experimental forms of hypertension (Watt & Thurston, 1989; Treasure *et al.*, 1991; Arvola *et al.*, 1993), a finding which was confirmed in the present study. Interestingly, the moderate antihypertensive effect of the atenolol treatment was accompanied by normalization of the response to ACh in SHR. However, no significant differences in the relaxations elicited by SIN-1 were found between the study groups. Thus, the sensitivity of arterial smooth muscle to NO was comparable in both hypertensive and normotensive rats, and was not altered by β-adrenoceptor antagonism. Furthermore, arterial relaxation elicited by isoprenaline has in general been considered to be mediated endothelium-independently via β-adrenoceptor stimulation and the subsequent increase in intracellular adenosine 3':5'-cyclic monophosphate (cyclic AMP) in smooth muscle (Bülbring & Tomita, 1987). However, the endothelium, too, contains β-adrenoceptors (Steinberg *et al.*, 1984), the activation of which increases cyclic AMP within the endothelial cells, which, in turn, augments the release of NO and promotes vascular relaxation (Gray & Marshall, 1992; Graves & Poston, 1993). Since β-adrenoceptor agonists

thus are partially endothelium-dependent vasodilators, this mechanism may have contributed to the augmented relaxation to isoprenaline observed in atenolol-treated SHR. Upregulation of β-adrenoceptors in smooth muscle remains another possibility to explain the improved isoprenaline response (Meiracker *et al.*, 1989). Taken together, the normalized response to ACh together with enhanced relaxation to isoprenaline in SHR following the atenolol therapy suggest improved endothelial function in these animals.

Previously, treatment with angiotensin converting enzyme inhibitors has been shown to normalize the relaxation to ACh in SHR (Clozel *et al.*, 1990; Arvola *et al.*, 1993), whereas diuretic therapy with trichlormethiazide only moderately augmented the response (Kähönen *et al.*, unpublished observations), and hydralazine treatment was without effect on the endothelium-dependent relaxation (Clozel *et al.*, 1990). Thus, although all of these antihypertensive therapies reduced blood pressure, their effects on endothelium-dependent relaxation appeared diverse. Therefore, the enhanced ACh-induced relaxation after the long-term atenolol treatment may not be related exclusively to the reduction of blood pressure but to other mechanisms affecting endothelial function as well.

After maximal relaxations to ACh, marked recontractions developed in untreated SHR but not in WKY rats and atenolol-treated SHR. ACh is known to evoke contractions in blood vessels of SHR but not of WKY rats via the release of endothelium-derived contractile factors (EDCF) (Lüscher & Vanhoutte, 1986). Furthermore, the production of EDCF appears to parallel closely the increase in blood pressure (Iwama *et al.*, 1992), and the impaired dilator response to ACh in SHR probably does not result from deficient NO production, but from enhanced simultaneous release of contractile factors from the endothelium (Lüscher & Vanhoutte, 1986; Ito & Carretero, 1992; Auch-Schwelk *et al.*, 1992). Thus, in the present study the absence of the recontractions after maximal relaxations to ACh in the treated SHR suggests that the release of contractile factors from the endothelium was diminished by the atenolol therapy, the mechanism of which may also underlie the improved relaxations to ACh. This conclusion is further supported by the fact that no significant differences in the relaxations to SIN-1 were detected in the study groups. Hence, the balance between endothelium-dependent relaxation and contraction may be beneficially modified by atenolol. Previous investigations have shown that several β-blockers can relax arterial preparations from normotensive animals, and that this effect is more pronounced in the presence of an intact endothelium (Mostaghim *et al.*, 1986). Moreover, carteolol has been reported to augment the basal release of relaxing factors from the endothelium of canine femoral artery (Janczewski *et al.*, 1987), and nebivolol to induce endothelium-dependent relaxation of canine coronary artery (Gao *et al.*, 1991), while celiprolol has neither direct nor indirect relaxing effects in rat arteries and veins (O'Rouke & Vanhoutte, 1990). Therefore, further investigations are clearly needed to clarify the acute and chronic effects of β-adrenoceptor blockade on endothelial function in hypertension.

Vascular contractions induced by Na^+,K^+-ATPase inhibition with a K^+-free medium in arterial rings result from sodium leak to the smooth muscle cells, which causes depolarization and increases calcium influx through voltage-dependent channels (Mulvany, 1985). In addition, the depolarization of vascular adrenergic nerve-endings releases NA, which contributes to the contraction (Vanhoutte & Lorenz, 1984). In the present study, vascular Na^+,K^+-ATPase function was evaluated indirectly by readdition of potassium upon full K^+-free medium-induced precontractions (Arvola *et al.*, 1992). The return of potassium activates Na^+,K^+-ATP which repolarizes the cell membrane and initiates the relaxation of smooth muscle (Bonaccorsi *et al.*, 1977). The potassium relaxation rate was markedly slower in SHR than WKY rats, in agreement with earlier observations (Arvola *et al.*, 1992; Pörsti *et al.*, 1992), and was clearly enhanced in SHR after the atenolol therapy. However, the washout time after maximal contractions to KCl was not significantly shortened by atenolol. The markedly prolonged interval required to reach baseline tension after washout of 125 mM KCl in SHR presumably reflects abnormal excitation-contraction uncoupling mechanisms with impaired sequestration and extrusion of intracellular calcium, and dephosphorylation of contractile proteins. Therefore, the enhanced potassium relaxation indicates promoted recovery rate of ionic gradients across the cell membrane in SHR following long-term β-adrenoceptor blockade, probably via improved function of vascular Na^+,K^+-ATPase.

In the study described here, the ability of arterial smooth muscle to sequester calcium was examined by means of caffeine- and NA-induced contractions after loading periods in different organ bath calcium concentrations. Of these two agonists, caffeine directly (see Karaki & Weiss, 1988) and NA via the stimulation of 1,4,5-inositol triphosphate accumulation (Guild *et al.*, 1992; Itoh *et al.*, 1992) opens the calcium channels in the sarcoplasmic reticulum. The refilling of the calcium stores without cell activation and $[Ca^{2+}]_i$ elevation presumably occurs via a direct link between the extracellular space and intracellular calcium stores (Rink, 1990). After the calcium loading periods the contractions to both NA and caffeine were lower in SHR than WKY rats, in agreement with previous reports (Dohi *et al.*, 1990; Wuorela *et al.*, 1994), and atenolol treatment improved these responses in SHR. Thus, the present results suggest that the ability of the sarcoplasmic reticulum to take up and store NA- and caffeine-releasable calcium is improved in SHR by atenolol treatment.

The concentration of intracellular free calcium is a primary determinant of arterial tone (Rembold, 1992). Previously, abnormalities in calcium metabolism have been reported to be prior events rather than subsequent to the development of hypertension in SHR, since elevated $[Ca^{2+}]_i$ has been found in vascular smooth muscle of prehypertensive animals (Sugiyama *et al.*, 1990), and in circulating as well as in non-circulating cells (Oshima *et al.*, 1991; Pörsti *et al.*, 1992). Moreover, normalization of blood pressure and arterial relaxation in SHR by ACE-inhibitor therapy has been reported to normalize the elevated $[Ca^{2+}]_i$ in platelets and lymphocytes of these animals (Arvola *et al.*, 1993). In the present study, basal $[Ca^{2+}]_i$ was clearly higher in lymphocytes of SHR when compared with WKY rats, and was not reduced by atenolol therapy in SHR. Thus, assuming that the observed changes in lymphocytes $[Ca^{2+}]_i$ also reflected cellular calcium metabolism in other tissues, the reduction in blood pressure following long-term β-adrenoceptor blockade was not associated with reduced basal cytosolic calcium in SHR. However, the above results on the ability of sarcoplasmic reticulum to take up and store calcium in smooth muscle suggest that the atenolol therapy had a beneficial effect on cellular calcium handling even though the basal calcium concentration was not reduced.

Arterial contractions to the classical contractile agents KCl and NA, and vascular calcium sensitivity during stimulation with these agonists were also examined. KCl-induced contractions were not affected by atenolol therapy in the two strains, and also the sensitivity to NA remained unchanged. The maximal contractile force generation to NA, however, was slightly increased by atenolol in SHR but not in WKY rats. The explanation for this remains unclear, since any residual β-adrenoceptor blockade would be expected to produce increased maximal contractions and sensitivity to NA in both rat strains. Furthermore, when inducing contractions to NA in a Ca^{2+}-free medium, the response primarily reflects calcium release from the sarcoplasmic reticulum, a minor source of the activator calcium being the inner surface of the plasmalemma, whereas the response to KCl depends mainly upon extracellular calcium (Johns *et al.*, 1987). Thus, the increase in contractile force during cumulative calcium addition to the organ bath results from calcium entry through the

plasmalemma (Karaki & Weiss, 1988). In the present study, the response to calcium addition with KCl (125 mM) or NA (10 μM) as the agonists did not significantly differ in SHR and WKY rats and was not affected by the atenolol therapy in either strain. Therefore, long-term β-adrenoceptor blockade did not appear to change arterial calcium sensitivity. In addition, the present findings on contractile responses further support the conclusion that alterations in endothelial function and not in contractile sensitivity or total calcium entry to the smooth muscle explain the augmented arterial relaxation in atenolol-treated SHR. Finally, the beneficial changes in calcium sequestration ability in arterial smooth muscle of atenolol-treated SHR appear to correlate with alterations in relaxation but not in contractile responses. This finding is in agreement with the fact that inhibitors of sarcoplasmic reticulum Ca^{2+}-ATPase also inhibit the relaxation of arterial smooth muscle (Luo *et al.*, 1993).

In conclusion, the moderate antihypertensive effect of atenolol in SHR was accompanied by enhancement of β-adrenergic and normalization of endothelium-dependent arterial relaxation. Furthermore, the responses reflecting the ability to sequester calcium into cellular stores and to induce vascular relaxation via function of the Na^+,K^+-ATPase were augmented. In contrast, the contractions to KCl and NA, as well as vascular calcium sensitivity, remained practically unaffected after the chronic β-adrenoceptor blockade. Therefore, the present results suggest that enhanced arterial relaxation and improved smooth muscle calcium handling participate in the long-term blood pressure-lowering action of atenolol in this type of genetic hypertension.

This study was supported by the Finnish Cultural Foundation, Häme Fund (M.K.) and the Paavo Nurmi Foundation, Finland (I.P.). Atenolol was kindly donated by Leiras Pharmaceutical Company, Turku, Finland. The valuable discussions with Dr Kazuhide Ayajiki are sincerely acknowledged.

References

ARVOLA, P., PÖRSTI, I., VUORINEN, P., PEKKI, A. & VAPAATALO, H. (1992). Contractions induced by potassium-free solution and potassium relaxation in vascular smooth muscle of hypertensive and normotensive rats. *Br. J. Pharmacol.*, **106**, 157–165.

ARVOLA, P., RUSKOAHO, H., WUORELA, H., PEKKI, A., VAPAATALO, H. & PÖRSTI, I. (1993). Quinapril treatment and arterial smooth muscle responses in spontaneously hypertensive rats. *Br. J. Pharmacol.*, **108**, 980–990.

AUCH-SCHWELK, W., KATUSIC, Z.S. & VANHOUTTE, P.M. (1992). Nitric oxide inactivates endothelium-derived contracting factor in the rat aorta. *Hypertension*, **19**, 442–445.

BÜLBRING, E. & TOMITA, T. (1987). Catecholamine action on smooth muscle. *Pharmacol. Rev.*, **39**, 49–96.

BONACCORSI, A., HERMSMEYER, K., APRIGLIANO, O., SMITH, C.B. & BOHR, D.F. (1977). Mechanisms of potassium relaxation of arterial muscle. *Blood Vessels*, **14**, 261–276.

CHATELAIN, P., WAELBROECK, M., CAMUS, J.-C., DE NEEF, P., ROBBERECHT, P., ROBA, J. & CHRISTOPHE, J. (1981). Comparative effects of α-methyldopa, propranolol and hydralazine therapy on cardiac adenylate cyclase activity in normal and spontaneously hypertensive rats. *Eur. J. Pharmacol.*, **72**, 17–25.

CLOZEL, M., KUHN, H. & HEFTI, F. (1990). Effects of angiotensin converting enzyme inhibitors and of hydralazine on endothelial function in hypertensive rats. *Hypertension*, **16**, 532–540.

DOHI, Y., AOKI, K., FUJIMOTO, S., KOJIMA, M. & MATSUDA, T. (1990). Alteration in sarcoplasmic reticulum-dependent contraction of tail arteries in response to caffeine and noradrenaline in spontaneously hypertensive rats. *J. Hypertens.*, **8**, 261–267.

DZAU, V.J., GIBBONS, G.H. & PRATT, R.E. (1991). Molecular mechanisms of vascular renin-angiotensin system in myointimal hyperplasia. *Hypertension*, **18**, (suppl. II), II-100–II-105.

FEELISCH, M., OSTROWSKI, J. & NOACK, E. (1989). On the mechanism of NO release from sydnonimines. *J. Cardiovasc. Pharmacol.*, **14**, (suppl. 11), S13–S22.

GAO, Y., NAGAO, T., BOND, R.A., JANSSENS, W.J. & VANHOUTTE, P.M. (1991). Nebivolol induces endothelium-dependent relaxations of canine coronary arteries. *J. Cardiovasc. Pharmacol.*, **17**, 964–969.

GRAVES, J. & POSTON, L. (1993). β-Adrenoceptor agonist mediated relaxation of rat isolated resistance arteries: a role for the endothelium and nitric oxide. *Br. J. Pharmacol.*, **108**, 631–637.

GRAY, D.W. & MARSHALL, I. (1992). Novel signal transduction pathway mediating endothelium-dependent β-adrenoceptor vasorelaxation in rat thoracic aorta. *Br. J. Pharmacol.*, **107**, 684–690.

GUILD, S.B., JENKINSON, S. & MUIR, T.C. (1992). Noradrenaline-stimulated inositol phosphate accumulation in arteries from spontaneously hypertensive rats. *Br. J. Pharmacol.*, **106**, 859–864.

HIRAWA, N., UEHURA, Y., NUMABE, A., TAKADA, S., MATSUOKA, H., IKEDA, T., SUGIMOTO, T., YAGI, S. &, ISHII, M. (1991). Stimulating effects of atenolol on vasodepressor prostaglandin generation in spontaneously hypertensive rats. *Clin. Sci.*, **81**, 499–507.

ITO, S. & CARRETERO, O.A. (1992). Impaired response to acetylcholine despite intact endothelium-derived relaxing factor/nitric oxide in isolated microperfused afferent arterioles of the spontaneously hypertensive rats. *J. Cardiovasc. Pharmacol.*, **20**, (suppl. 12), S187–S189.

ITOH, T., KAJIKURI, J. & KURIYAMA, H. (1992). Characteristic features of noradrenaline-induced Ca^{2+} mobilization and tension in arterial smooth muscle of the rabbit. *J. Physiol.*, **457**, 297–314.

IWAKA, Y., KATO, T., MURAMATSU, M., ASANO, H., SHIMIZU, K., TOKI, Y., MIYAZAKI, Y., OKUMURA, K., HASHIMOTO, H., ITO, T. & SATAKE, T. (1992). Correlation with blood pressure of the acetylcholine-induced endothelium-derived contracting factor in the rat aorta. *Hypertension*, **19**, 326–332.

JANCZEWSKI, P., BOULANGER, C., IQBAL, A. & VANHOUTTE, P.M. (1987). Endothelium-dependent effects of carteolol. *J. Pharmacol. Exp. Ther.*, **247**, 590–595.

JOHNS, A., LEIJTEN, P., YAMAMOTO, H., HWANG, K. & VAN BREEMEN, C. (1987). Calcium regulation in vascular smooth muscle contractility. *Am. J. Cardiol.*, **59**, 18A–23A.

KARAKI, H. & WEISS, G.B. (1988). Calcium release in smooth muscle. *Life Sci.*, **42**, 111–122.

KOJIMA, M., AOKI, K., ASANO, M., FUJIMOTO, S. & MATSUDA, T. (1991). Malfunction of arterial sarcoplasmic reticulum leading to faster and greater contraction induced by high-potassium depolarization in young spontaneously hypertensive rats. *J. Hypertens.*, **9**, 783–788.

LAUVA, I.K. & TOMANEK, R.J. (1985). Left ventricular performance in spontaneously hypertensive rats after chronic β_1-adrenoceptor blockade with atenolol. *J. Cardiovasc. Pharmacol.*, **7**, 232–237.

LUND-JOHANSEN, P. (1979). Hemodynamic consequences of long-term beta-blocker therapy: A 5-year follow-up study of atenolol. *J. Cardiovasc. Pharmacol.*, **1**, 487–495.

LUO, D.-L., NAKAZAWA, M., ISHIBASHI, T., KATO, K. & IMAI, S. (1993). Putative, selective inhibitors of sarcoplasmic reticulum Ca^{++}-pump ATPase inhibit relaxation by nitroglycerin and atrial natriuretic factor of the rabbit aorta contracted by phenylephrine. *J. Pharmacol. Exp. Ther.*, **265**, 1187–1192.

LÜSCHER, T.F. & VANHOUTTE, P.M. (1986). Endothelium-dependent contractions to acetylcholine in the aorta of the spontaneously hypertensive rat. *Hypertension*, **8**, 344–348.

LYSBO SVENDSEN, T., HARTLING, O. & TRAP-JENSEN, J. (1979). Immediate haemodynamic effects of propranolol, practolol, pindolol, atenolol and ICI 89,406 in healthy volunteers. *Eur. J. Clin. Pharmacol.*, **15**, 223–228.

MAN IN'T VELD, A.J., MEIRACKER, A. & SCHALEKAMP, M.A.D.H. (1986). The effect of β blockers on total peripheral resistance. *J. Cardiovasc. Pharmacol.*, **8**, (suppl. 4), S49–S60.

MAN IN'T VELD, A.J. (1991). Vasodilatation, not cardiodepression, underlies the antihypertensive effect of beta-adrenoceptor antagonists. *Am. J. Cardiol.*, **67**, 13B–17B.

MEIRACKER, A.H., MAN IN'T VELD, A.J., BOOMSMA, F., FISCHBERG, D.J., MOLINOFF, P.B. & SCHALEKAMP, M.A.D.H. (1989). Hemodynamic and β-adrenergic receptor adaptations during long-term β-adrenoceptor blockade: studies with acebutolol, atenolol, pindolol, and propranolol in hypertensive patients. *Circulation*, **80**, 903–914.

MONCADA, S., PALMER, R.M.J. & HIGGS, E.A. (1991). Nitric oxide: physiology, pathophysiology, and pharmacology. *Pharmacol. Rev.*, **43**, 109–142.

MOSTAGHIM, R., MADDOX, Y.T. & RAMWELL, P.W. (1986). Endothelial potentiation of relaxation response to beta adrenoceptor blocking agents. *J. Pharmacol. Exp. Ther.*, **239**, 797–801.

MULVANY, M.J. (1985). Changes in sodium pump activity and vascular contraction. *J. Hypertens.*, **3**, 429–436.

O'ROURKE, S.T. & VANHOUTTE, P.M. (1990). Celiprolol has no direct or indirect effects in isolated arteries and veins. *J. Cardiovasc. Pharmacol.*, **15**, 831–835.

OSHIMA, T., YOUNG, E.W. & MCCARRON, D.A. (1991). Abnormal platelet and lymphocyte calcium handling in prehypertensive rats. *Hypertension.*, **18**, 111–115.

PÖRSTI, I., ARVOLA, P., WUORELA, H. & VAPAATALO, H. (1992). High calcium diet augments vascular potassium relaxation in spontaneously hypertensive rats. *Hypertension*, **19**, 85–92.

REMBOLD, C.M. (1992). Regulation of contraction and relaxation in arterial smooth muscle. *Hypertension*, **20**, 129–137.

RINK, T.J. (1990). Receptor-mediated calcium entry. *FEBS Lett.*, **268**, 381–385.

STEINBERG, S.F., JAFFE, E.A. & BILEZIKIAN, J.P. (1984). Endothelial cells contain beta adrenoceptors. *Naunyn-Schmied. Arch. Pharmacol.*, **325**, 310–313.

SUGIYAMA, T., YOSHIZUMI, M., TAKAKU, F. & YAZAKI, Y. (1990). Abnormal calcium handling in vascular smooth muscle cells of spontaneously hypertensive rats. *J. Hypertens.*, **8**, 369–375.

TAKEDA, K., NAKAGAWA, Y., CHIN, W.P. & IMAI, S. (1982). A comparison of antihypertensive effects of atenolol and propranolol in the spontaneously hypertensive, DOCA/saline hypertensive and renal hypertensive rats. *Jpn. J. Pharmacol.*, **32**, 283–289.

TREASURE, C.B., MANOUKIAN, S.V., KLEIN, J.L., VITA, J.A., NABEL, E.G., RENWICK, G.H., SELWYN, A.P., ALEXANDER, R.W. & GANZ, P. (1992). Epicardial coronary artery responses to acetylcholine are impaired in hypertensive patients. *Circ. Res.*, **71**, 776–781.

VANHOUTTE, P.M. & LORENZ, R.R. (1984). Na^+,K^+-ATPase inhibitors and the adrenergic neuroeffector interaction in the blood vessel wall. *J. Cardiovasc. Pharmacol.*, **6**, (suppl. 1), S88–S94.

WATT, P.A.C. & THURSTON, H. (1989). Endothelium-dependent relaxation in resistance vessels from the spontaneously hypertensive rats. *J. Hypertens.*, **7**, 661–666.

WUORELA, H., ARVOLA, P., KÄHÖNEN, M., VAPAATALO, H. & PÖRSTI, I. (1994). Arterial smooth muscle responses in adult and moderately aged spontaneously hypertensive rats. *Pharmacol. Toxicol.*, **74**, 167–173.

WUORELA, H., PÖRSTI, I., ARVOLA, P., MÄKYNEN, H. & VAPAATALO, H. (1992). Three levels of dietary calcium-effects on blood pressure and electrolyte balance in spontaneously hypertensive rats. *Naunyn-Schmied. Arch. Pharmacol.*, **346**, 524–549.

(Received October 21, 1993
Revised March 14, 1994
Accepted March 28, 1994)

Br. J. Pharmacol. (1994), **112**, 934–938

Des-Arg^9-bradykinin-induced increases in intracellular calcium ion concentration in single bovine tracheal smooth muscle cells

[1]Katrina A. Marsh & Stephen J. Hill

Department of Physiology and Pharmacology, University of Nottingham Medical School, Queen's Medical Centre, Nottingham, NG7 2UH

1 Dynamic video imaging was used to measure the des-Arg^9-bradykinin-induced changes in the intracellular free calcium ion concentration ($[Ca^{2+}]_i$) of single bovine tracheal smooth muscle (BTSM) cells.

2 In the presence of extracellular calcium ions, des-Arg^9-bradykinin (1 nM–10 μM) produced a concentration-dependent increase in the $[Ca^{2+}]_i$ over basal levels yielding an EC_{50} value of 316 nM. The percentage of cells responding to each concentration of des-Arg^9-bradykinin also increased in a concentration-dependent manner (from 9% to 100%).

3 The bradykinin B_2 receptor antagonist, D-Arg[Hyp^3,Thi^{5,8},D-Phe^7]-bradykinin (10 μM), was without effect on the calcium response of the cells when added 2 min prior to des-Arg^9-bradykinin (100 nM). However, the B_1 receptor antagonist, des-Arg^{9}Leu^8-bradykinin (10 μM), completely abolished the des-Arg^9-bradykinin-induced response.

4 Under calcium-free conditions, des-Arg^9-bradykinin induced an increase in $[Ca^{2+}]_i$ at concentrations of 1 μM and 10 μM. The response to 10 μM des-Arg^9-bradykinin was reduced by preincubation of either D-Arg[Hyp^3,Thi^{5,8},D-Phe^7]-bradykinin (10 μM) or des-Arg^{9}Leu^8-bradykinin (10 μM).

5 We conclude that bradykinin B_1 receptors are expressed by cultured BTSM cells and mediate the des-Arg^9-bradykinin-induced influx of calcium ions at low agonist concentrations (< 1 μM). At higher concentrations, des-Arg^9-bradykinin (1 μM and 10 μM) can stimulate both B_1 and B_2 receptors to effect intracellular calcium release under calcium-free conditions.

Keywords: Des-Arg^9-bradykinin; smooth muscle; intracellular calcium; trachea; bradykinin

Introduction

The involvement of kinins in inflammatory airway disease is not entirely understood although the nonapeptide, bradykinin, has been implicated in the pathogenesis of allergic asthma (Christiansen *et al.*, 1987). The receptors mediating responses to bradykinin have typically been divided into two subtypes, B_1 and B_2 receptors (Regoli & Barabé, 1980). Although present in a variety of tissues, B_2 receptors and not B_1 receptors, are found to be in great abundance in the rabbit jugular vein whereas the less commonly expressed B_1 receptors are found in the rabbit aorta (Regoli *et al.*, 1981). Bradykinin has been shown to elicit an increase in intracellular calcium ion concentration ($[Ca^{2+}]_i$) of human (Murray & Kotlikoff, 1991) and guinea-pig (Farmer *et al.*, 1991a,b) airway smooth muscle cells although the characteristics of these responses remain unclear. An increase in $[Ca^{2+}]_i$ is a mechanism necessary for the contraction of smooth muscle and can be mediated either via an influx of calcium ions from the extracellular space (Benham & Tsien, 1987; Murray & Kotlikoff, 1991) or via a release of calcium from the intracellular stores which may result from an increase in production of inositol 1,4,5-trisphosphate (Somlyo *et al.*, 1988; Berridge & Irvine, 1989).

In previous studies we have shown that bradykinin B_2 receptor subtype-stimulation can cause an increase in phosphoinositide hydrolysis in cultures of bovine tracheal smooth muscle (BTSM) cells (Marsh & Hill, 1992). In the same study we noted that the bradykinin B_1 receptor agonist, des-Arg^9-bradykinin, caused a small increase in the phosphoinositide hydrolysis (16% of that produced by bradykinin) of cultured BTSM cells (Marsh & Hill, 1992) indicating the presence of B_1 receptors in this system. In addition to these studies, we have demonstrated that bradykinin, via activation of the B_2 receptor, can also induce an increase in $[Ca^{2+}]_i$ both in the presence and absence of extracellular calcium ions (Marsh & Hill, 1993).

The presence of the B_1 receptor coupled to calcium ion mobilisation in airway smooth muscle cells from other species, such as guinea-pig, is doubted (Farmer *et al.*, 1989). We have therefore extended our studies to evaluate the ability of this receptor, which upon stimulation mediates an increase in phosphoinositide turnover, to mediate increases in $[Ca^{2+}]_i$ of cultured BTSM cells. This has been performed by use of dynamic video imaging of single BTSM cells in both calcium-containing and calcium-free conditions in order to evaluate the characteristics of the response. The present study demonstrates the presence of functional B_1 receptors coupled to intracellular calcium ion mobilisation in single BTSM cells.

Methods

Cell culture

BTSM cell cultures were established from fresh tissue as described previously (Marsh & Hill, 1992). Briefly, tracheal smooth muscle, dissected free of surrounding connective tissue and mucosa, was chopped into 1 mm^3 pieces. The explant tissue was then transferred to tissue culture-treated plastic flasks and covered with a D-Val-substituted minimum essential medium supplemented with 10% foetal calf serum (FCS) and antibiotics (100 u ml^{-1} penicillin G; 100 μg ml^{-1} streptomycin; 250 ng ml^{-1} amphotericin B). Smooth muscle cells were then maintained at 37°C in a humidified 10% CO_2 atmosphere until confluency and were routinely subcultured using trypsin (0.05% w/v in versene, Glasgow formula). Mycoplasmal contamination was shown to be negative by the Hoechst 33258 staining method of Chen (1977). Identity of smooth muscle cells was confirmed by indirect immunocyto-

[1] Author for correspondence.

chemical analysis using the monoclonal antibody to alpha smooth muscle actin as described previously in detail (Marsh & Hill, 1992). For the image analysis procedure, smooth muscle cells from passages 4 to 10 were seeded onto 22 mm circular glass coverslips at a 1:10 split ratio. These were maintained under the above conditions in Dulbecco's modified Eagle's medium with 10% FCS for 72 h until use.

Image analysis

Cells attached to the glass coverslips were washed three times in a physiological saline solution (PSS) containing (in mM): NaCl 145, KCl 5, $MgSO_4$ 1, N-2-hydroxyethylpiperazine-*N'*-2-ethanesulphonic acid (HEPES) 10, glucose 10 and $CaCl_2$ 2, pH 7.4. Cells were then incubated at 37°C for 30 min with PSS containing 10% FCS and 5 μM fura-2 acetoxymethylester. After washing a further three times, coverslips were transferred to a metal holder which was then mounted in a heated chamber in order to maintain the temperature at 37°C. A volume of 900 μl of PSS was then added to the chamber and agents were added directly to the cells in a volume of 100 μl PSS. For experiments requiring calcium-free conditions, any PSS added to the chamber was deficient in $CaCl_2$ and supplemented with 0.1 mM EGTA. All coverslips were used within 90 min of the end of loading time.

Image analysis was performed by use of MagiCal hardware and TARDIS software supplied by Applied Imaging International Ltd. (Hylton Park, Sunderland, Tyne & Wear) as described previously in detail (Neylon *et al.*, 1990). Briefly, fluorescent images were detected by a Nikon Diaphot epifluorescence microscope with a 10 × quartz objective lens then relayed through an image intensifying charged couple device camera (Photonic Science) to the TARDIS software where the images underwent analogue to digital conversion.

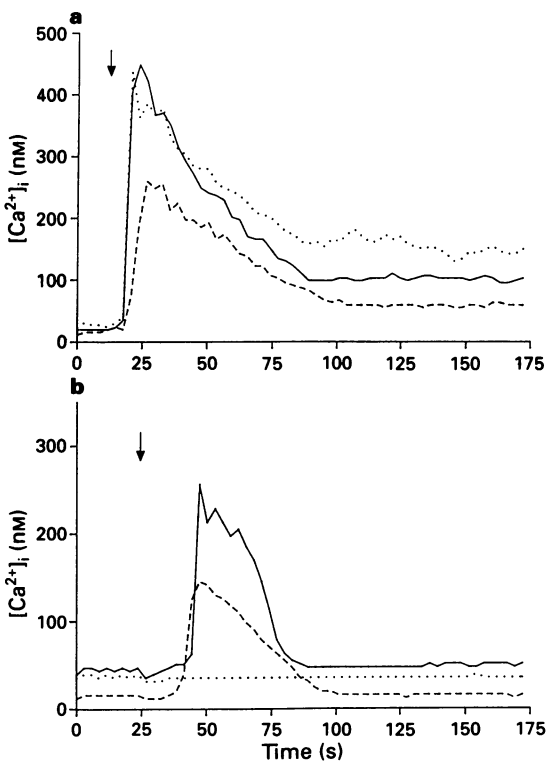

Figure 1 Des-Arg^9-bradykinin-induced changes in intracellular calcium ion concentration in single bovine tracheal smooth muscle cells. Individual traces represent the changes in intracellular calcium ion concentration of individual cells within the same field of view and are representative of responses from other cells measured. The arrow indicates the addition of des-Arg^9-bradykinin (1 μM) (a) in the presence of extracellular calcium ions (2 mM $CaCl_2$) or (b) in the absence of extracellular calcium ions (with 0.1 mM EGTA).

Images captured were 256 × 256 pixels in size and each frame was averaged 8 times with analogue hardware averaging to reduce camera noise. Incident light of alternating 340 and 380 nm wavelength was supplied to the sample by means of a rotating filter wheel so that the time between image pairs was 1.5 s. Once a sequence of images had been captured they were subjected to a background subtraction. For this purpose, an averaged image of each of the 340 and 380 nm types was captured from an area of the coverslip devoid of any cells using the same parameters as for cell measurements. The 340 nm background was then subtracted from each of the 340 nm images on a pixel-by-pixel basis and similar processing was performed with the 380 nm background and images.

After digital conversion background-corrected image pairs were ratioed (340/380) on a pixel-by-pixel basis and calcium ion concentration was calculated using a 2-D look up table utilising the Grynkiewicz *et al.* (1985) equation below

$$[Ca] = K_D \beta [(R - R_{min})/(R_{max} - R)]$$

where R is the measured ratio and β is the fluorescence ratio at 380 nm of R_{min} to R_{max}. R_{max} and R_{min} values were calculated for calibration purposes by exposing the cells firstly to 20 μM ionomycin in the presence of 10 mM calcium allowing for flooding of the cell with calcium and a maximum fluorescence ratio (R_{max}) to be obtained. R_{min} (minimum fluorescence ratio) was calculated by chelation of the free calcium ions with 6 mM EGTA. A dissociation constant (K_D) of 224 nM for fura-2 and calcium at 37°C was incorporated into the 2-D look up table.

Image analysis software performed quantification of mean calcium ion concentration as a function of time (e.g. Figure 1) and whole cell intracellular calcium ion quantification was obtained by outlining each individual cell using a light pen. Graphical representation was automatically produced from the pixel data contained within the defined region.

Data analysis

Concentration-response curves were fitted to a Hill equation using the non-linear curve-fitting programme ALLFIT (DeLean *et al.*, 1978). The equation fitted was

$$\text{Response} = E_{max} \times D^n/(D^n + (EC_{50})^n)$$

where D is the agonist concentration, n is the Hill coefficient, EC_{50} is the concentration of agonist giving half maximal response and E_{max} is the maximal effect. The data point at each concentration of bradykinin was calculated from accumulated data from a single field of view (containing 4–10 cells) from each of at least five different coverslips each arising from different animals.

Chemicals

D-Val minimum essential medium and the antibiotic/antimycotic solution used in culture were obtained from Gibco. Dulbecco's modified Eagle's medium and foetal calf serum were purchased from Northumbrian Biologicals Ltd. Powdered trypsin (3 × crystalized and dialysed) was bought from Worthington Biochemicals. Fura-2 acetoxymethylester was obtained from Calbiochem. D-Arg[Hyp^3,Thi^{5,8},D-Phe^7]-bradykinin, des-Arg^{9}Leu^8-bradykinin, des-Arg^{9}bradykinin and Hoechst 33258 were obtained from Sigma. Anti-alpha smooth muscle actin monoclonal antibody was purchased from Dako Ltd.

Results

In the presence of extracellular calcium ions, addition of the bradykinin B_1 receptor agonist, des-Arg^9-bradykinin, to BTSM cells produced a sharp increase in $[Ca^{2+}]_i$ which fell to a level above basal that was maintained for the duration of the experiment (Figure 1a). The increase in $[Ca^{2+}]_i$ observed

appeared to be uniform across the cell throughout the duration of the response. On analysis of data from 27 to 43 cells at each concentration, des-Arg^9-bradykinin was found to produce a concentration-dependent increase in $[Ca^{2+}]_i$ over basal levels (mean basal level = 51 ± 3 nM; n = 107; maximum increase = 373 ± 28 nM at 10 μM des-Arg^9-bradykinin; n = 29; Figure 2a). As we have noted previously, when using bradykinin as an agonist in this system (Marsh & Hill, 1993), not all the cells in any one field of view were responsive to des-Arg^9-bradykinin. Responding cells were identified by an increase in $[Ca^{2+}]_i$ above their basal levels and conversely, non-responders showed no variation in the baseline response on addition of the agonist (e.g. one cell in Figure 1b). We have therefore calculated the number of cells which responded to a particular concentration of des-Arg^9-bradykinin as a percentage of the total number of cells observed at that concentration (frequency). By evaluating data in this manner it was found that des-Arg^9-bradykinin also caused a concentration-dependent increase in the frequency of response of the BTSM cells from 9% at 1 nM to 100% at 10 μM des-Arg^9-bradykinin (Figure 2b). A randomised pattern of response to des-Arg^9-bradykinin was observed in the cells of any one field of view. Cellular contact did not appear to be a contributing factor to the nature of the responses of the cells.

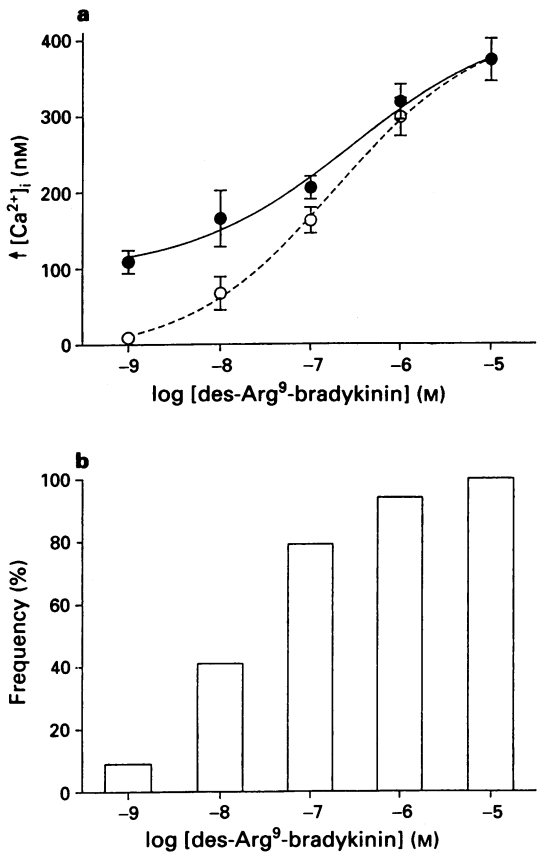

Figure 2 Concentration-response relationships to des-Arg^9-bradykinin (1 nM–10 μM) in the presence of extracellular calcium. (a) Values represent the mean increase in intracellular calcium ion concentration over basal levels of all bovine tracheal smooth muscle (BTSM) cells observed (○) or responding cells only (●). Means ± s.e.means at each concentration were calculated from at least five separate coverslips each arising from different animals. (b) Columns represent the frequency of response of BTSM cells. Frequency is defined as the percentage of the total number of cells observed which respond to des-Arg^9-bradykinin.

In order to establish the nature of the mean cellular response (rather than the mean population response) to des-Arg^9-bradykinin, the remaining results have been calculated from data obtained from des-Arg^9-bradykinin-sensitive cells only. As a result of these calculations, the EC_{50} value for des-Arg^9-bradykinin was found to be 316 nM in the presence of extracellular calcium ions (Figure 2a).

Addition of the bradykinin B_1 receptor antagonist, des-Arg^{9}Leu^8-bradykinin (10 μM), 2 min prior to the addition of agonist completely abolished the increase in $[Ca^{2+}]_i$ induced by 100 nM des-Arg^9-bradykinin (Table 1). However, there was no significant difference between the response to des-Arg^9-bradykinin alone and that obtained in the presence of the bradykinin B_2 receptor antagonist, D-Arg[Hyp^3,Thi^{5,8},D-Phe^7]-bradykinin (10 μM; Table 1). We have previously shown that this concentration of D-Arg[Hyp^3,Thi^{5,8},D-Phe^7]-bradykinin attenuates the bradykinin-induced calcium response in these cells (Marsh & Hill, 1993). The frequency of response of the cells to 100 nM des-Arg^9-bradykinin was reduced to 0% by the B_1 receptor antagonist but was of a similar magnitude in the presence of the B_2 receptor antagonist (Table 1).

In the absence of extracellular calcium ions, des-Arg^9-bradykinin was found to elicit a calcium response characterized by a rise in $[Ca^{2+}]_i$ followed by a fall to basal level (mean basal level = 32 ± 2 nM; n = 37) within 60–80 s (Figure 1b). However, only concentrations of des-Arg^9-bradykinin equal to or greater than 1 μM were found to induce a calcium response in BTSM cells under these conditions. Des-Arg^9-bradykinin, 1 μM, produced a mean increase of 184 ± 24 nM (n = 8) at a frequency of 18% and 10 μM des-Arg^9-bradykinin elicited an increase of 210 ± 21 nM (n = 29) at a frequency of 62%. These two responses were found not to be significantly different from each other (unpaired t test). Table 1 also demonstrates that, in a separate series of experiments, des-Arg^{9}Leu^8-bradykinin (10 μM) and D-Arg[Hyp^3,Thi^{5,8},D-Phe^7]-bradykinin (10 μM) were each able to attenuate the calcium response of the cells

Table 1 Responses of single bovine tracheal smooth muscle cells to des-Arg^9-bradykinin in calcium-containing and calcium-free conditions

	$\Delta[Ca^{2+}]_i$ (nM)	Frequency of response (%)
+ Calcium		
des-Arg^9-bradykinin 100 nM	190 ± 21	62 (18/29)
+ B_1 antagonist 10 μM	0	0 (0/25)
+ B_2 antagonist 10 μM	149 ± 16	59 (13/22)
– Calcium		
des-Arg^9-bradykinin 10 μM	239 ± 30	79 (19/24)
+ B_1 antagonist 10 μM	145 ± 13*	46 (12/26)
+ B_2 antagonist 10 μM	138 ± 10*	52 (12/23)

Experiments were performed as described in the text in the absence or presence of des-Arg^{9}Leu^8-bradykinin (B_1 antagonist) and D-Arg[Hyp^3,Thi^{5,8},D-Phe^7]-bradykinin (B_2 antagonist). The results are calculated from a sample of cells taken from at least four different coverslips each originating from different animals. Matching coverslips were used for the three different conditions (agonist ± antagonist) on each experimental day. Numbers in parentheses indicate the number of cells responding to des-Arg^9-bradykinin/the total number of cells observed. *P<0.05 (unpaired t test).

to des-Arg^9-bradykinin (10 μM) to a similar extent under calcium-free conditions.

Discussion

The present study demonstrates the presence of functional bradykinin B_1 receptors on cultured BTSM cells which can elicit an increase in $[Ca^{2+}]_i$. The bradykinin B_1 receptor agonist, des-Arg^9-bradykinin, can induce a concentration-dependent increase in $[Ca^{2+}]_i$ of BTSM cells in the presence of extracellular calcium ions suggesting activation of the bradykinin B_1 receptor. The pattern of increase of $[Ca^{2+}]_i$ induced by the agonist demonstrates an initial peak followed by the much lower plateau component of the response which is likely to be due to a continued influx of calcium ions from the extracellular environment. The EC_{50} value of 316 nM obtained under these conditions is consistent with that previously calculated in this laboratory from phosphoinositide studies on cultured BTSM cells (EC_{50} = 199 nM; Marsh & Hill, 1992). These values are similar to that obtained from calcium studies of the B_1 receptor in rat mesangial cells (560 nM; Bascands *et al.*, 1993) and are in the same concentration-range as those observed in the 'classic' B_1 receptor system, contractile responses of the rabbit aorta, where the EC_{50} was found to be 50 nM (Regoli *et al.*, 1981).

We have also demonstrated in this study that the calcium response to des-Arg^9-bradykinin (100 nM) in calcium-containing medium was insensitive to the B_2 receptor antagonist (D-Arg[Hyp^3,Thi^{5,8},D-Phe^7]-bradykinin) but was completely abolished by the B_1 receptor antagonist used (des-Arg^{9}Leu^8-bradykinin). These data further suggest that des-Arg^9-bradykinin is acting via stimulation of B_1 receptors as des-Arg^{9}Leu^8-bradykinin has previously been shown to be selective for B_1 receptors since it is active in the rabbit aorta (B_1 system) yet without effect in the rabbit jugular vein (B_2 system; Regoli *et al.*, 1990). It is possible, however, that the responses observed in the presence of extracellular calcium ions to concentrations of des-Arg^9-bradykinin above 100 nM are in part due to activation of B_2 receptors. This suggestion has arisen from the observation in this study that the responses to des-Arg^9-bradykinin at these concentrations obtained under calcium-free conditions are sensitive to the B_2 receptor antagonist. Furthermore a recent study demonstrated that the cDNA from the murine B_2 receptor encodes for two populations of receptors which exhibit the pharmacological properties of a B_1-like receptor and the B_2 receptor; however, it is noteworthy that receptors cloned from human and rat sources in the same study demonstrated pharmacological properties of B_2 receptors only (McIntyre *et al.*, 1993).

The results obtained in this study are consistent with the observation made in our previous studies where des-Arg^9-bradykinin elicited an increase in phosphoinositide hydrolysis in these cells (Marsh & Hill, 1992) demonstrating the presence of functional bradykinin B_1 receptors on cultured BTSM cells. The mean data represented by Figure 4b of that paper demonstrate that des-Arg^9-bradykinin was able to increase significantly the phosphoinositide hydrolysis over basal levels in BTSM cells at concentrations of 1 μM and 10 μM. It is only at these concentrations that, in the absence of extracellular calcium ions, an increase in $[Ca^{2+}]_i$ of BTSM cells was observed in this study. This increase observed in the absence of extracellular calcium must be due to a release of calcium from intracellular stores which, from the evidence available (Marsh & Hill, 1992 and present study), is likely to occur via an increase in phosphoinositide turnover and production of IP_3.

In a previous study we demonstrated that bradykinin, through activation of B_2 receptors, can induce an 'all-or-nothing' release of calcium from intracellular stores (Marsh & Hill, 1993). From the results obtained in the present studies it is possible that des-Arg^9-bradykinin also induces an 'all-or-nothing' release of intracellular calcium in experiments conducted in the absence of extracellular calcium ions. Consistent with this view is the fact that no response in any cell was observed below a concentration of 1 μM des-Arg^9-bradykinin yet the responses elicited by 1 μM and 10 μM agonist were of a similar magnitude in each cell and the mean responses were not significantly different from each other, i.e. no intermediate response was obtained between zero and approximately 200 nM even though the frequency of responding cells increased from 18% to 62% as the concentration rose from 1 μM to 10 μM antagonist. This value is similar to that obtained in our previous study where, in the presence of extracellular calcium ions, bradykinin stimulated B_2 receptors to produce an 'all-or-nothing' increase in $[Ca^{2+}]_i$ of approximately 180 nM (Marsh & Hill, 1993). It is of interest to note that the concentration of des-Arg^9-bradykinin required to elicit a response under calcium-free conditions (1 μM) is much higher than that of bradykinin shown to produce a similar increase (10 pM; Marsh & Hill, 1993).

In the present study both the B_1 and B_2 receptor antagonists used (des-Arg^{9}Leu^8-bradykinin and D-Arg[Hyp^3,-Thi^{5,8},D-Phe^7]-bradykinin) were found to be equiactive in attenuating the calcium response of BTSM cells to 10 μM des-Arg^9-bradykinin under calcium-free conditions. This suggests that B_2 receptors are also stimulated by this high concentration of B_1 agonist in the absence of extracellular calcium ions. However, the fact that both receptors are activated by the high concentrations of des-Arg^9-bradykinin needed to release intracellular calcium, makes the pharmacology of the B_1 receptor, stimulated under these conditions, very difficult to evaluate. Furthermore, this partial antagonism of the response to des-Arg^9-bradykinin, in the absence of intracellular calcium ions, by both B_1 and B_2 antagonists is not readily consistent with the 'all-or-nothing' release of intracellular calcium observed with bradykinin (Marsh & Hill, 1993). Nevertheless, the data obtained at the lower concentrations of des-Arg^9-bradykinin suggest that the calcium response observed is mediated via stimulation of B_1 receptors to produce an influx of calcium ions from the extracellular environment.

The present study also demonstrates that the latency of response of the cells to des-Arg^9-bradykinin in the presence of extracellular calcium ions (Figure 1a) is much shorter than that under calcium-free conditions (Figure 1b). The latency present in intracellular calcium release may, as we have suggested previously (Marsh & Hill, 1993), be a result of the interaction between IP_3-sensitive and IP_3-insensitive calcium stores. This would lead to the filling of IP_3-insensitive calcium stores and subsequent transient calcium-induced calcium release from these stores leading to the observed delay in response. The most likely explanation for the short latency of response observed at low agonist concentrations in the presence of extracellular calcium ions is that des-Arg^9-bradykinin can stimulate calcium entry directly and/or be able to act via IP_3-insensitive stores that are not accessible to calcium released from IP_3-sensitive stores.

An interesting study using populations of rat mesangial cells demonstrated that the profiles of the calcium response to B_1 stimulation (des-Arg^9-bradykinin) and to B_2 stimulation (bradykinin) were different in that the plateau, or influx, phase of the response was much greater upon B_1 stimulation (Bescands *et al.*, 1993). This led the authors to suggest that B_1 stimulation resulted in a larger part of the response being due to calcium influx whereas B_2 activation preferentially stimulated the release of calcium from intracellular stores. In our studies to date we have observed no apparent differences in the plateau phase of the calcium response upon B_2 stimulation (Marsh & Hill, 1993) or B_1 stimulation (present study). However, our data also suggest that des-Arg^9-bradykinin predominantly causes an influx of calcium ions from the extracellular space, particularly at the lower concentrations of the agonist where no response was observed in the absence of extracellular calcium ions. Our results also dem-

onstrate that only the high and non-specific concentrations of des-Arg^9-bradykinin are able to induce a release of calcium from intracellular stores which is mediated via activation of both B_1 and B_2 receptors. The results presented in this study provide us with a unique system with which to study the effects of B_1 receptor activation on airway smooth muscle tissue.

We would like to thank the AFRC for their financial support of this work.

References

BASCANDS, J.L., PECHER, C., RAUOUD, S., EMOND, C., TACK, J.L., BASTIE, M.J., BURCH, R., REGOLI, D. & GIROLAMI, J.-P. (1993). Evidence for the existence of two distinct bradykinin receptors on rat mesangial cells. *Am. J. Physiol.*, **264**, F548–F556.

BENHAM, C.D. & TSIEN, R.W. (1987). A novel receptor-operated Ca^{2+}-permeable channel activated by ATP in smooth muscle. *Nature*, **328**, 275–278.

BERRIDGE, M.J. & IRVINE, R.F. (1989). Inositol phosphates and cell signalling. *Nature*, **341**, 197–205.

CHEN, T.R. (1977). *In situ* detection of mycoplasma contamination in cell cultures by fluorescent Hoechst stain 33258. *Exp. Cell Res.*, **104**, 255–259.

CHRISTIANSEN, S.C., PROUD, D. & COCHRANE, C.G. (1987). Detection of tissue kallikrein in the bronchoalveolar lavage fluid of asthmatic patients. *J. Clin. Invest.*, **79**, 188–197.

DELEAN, A., MUNSON, P.J. & RODBARD, D. (1978). Simultaneous analysis of families of sigmoidal curves: application to bioassay, radioligand assay and physiological dose-response curves. *Am. J. Physiol.*, **235**, E97–E102.

FARMER, S.G., BURCH, R.M., KYLE, D.J., MARTIN, J.A., MEEKER, S.N. & TOGO, J. (1991a). D-Arg[Hyp^3-Thi^5-D-Tic^8]-bradykinin, a potent antagonist of smooth muscle BK_2 receptors and BK_3 receptors. *Br. J. Pharmacol.*, **102**, 785–787.

FARMER, S.G., BURCH, R.M., MEEKER, S.A. & WILKINS, D.E. (1989). Evidence for a pulmonary B_3 bradykinin receptor. *Mol. Pharmacol.*, **36**, 1–8.

FARMER, S.G., ENSOR, J.E. & BURCH, R.M. (1991b). Evidence that cultured airway smooth muscle cells contain bradykinin B_2 and B_3 receptors. *Am. J. Respir. Cell Mol. Biol.*, **4**, 273–277.

GRYNKIEWICZ, G., POENIE, M. & TSIEN, R.Y. (1985). A new generation of Ca^{2+} indicators with greatly improved fluorescence indicators. *J. Biol. Chem.*, **260**, 3440–3450.

MARSH, K.A. & HILL, S.J. (1992). Bradykinin B_2 receptor-mediated phosphoinositide hydrolysis in bovine cultured tracheal smooth muscle cells. *Br. J. Pharmacol.*, **107**, 443–447.

MARSH, K.A. & HILL, S.J. (1993). Characteristics of the bradykinin-induced changes in intracellular calcium ion concentration of single bovine tracheal smooth muscle cells. *Br. J. Pharmacol.*, **110**, 29–35.

MCINTYRE, P., PHILLIPS, E., SKIDMORE, E., BROWN, M. & WEBB, M. (1993). Cloned murine bradykinin receptors exhibit a mixed B_1 and B_2 pharmacological selectivity. *Mol. Pharmacol.*, **44**, 346–355.

MURRAY, R.K. & KOTLIKOFF, M.I. (1991). Receptor-activated calcium influx in human airway smooth muscle cells. *J. Physiol.*, **435**, 123–144.

NEYLON, C.B., HOYLAND, J., MASON, W. & IRVINE, R.F. (1990). Spatial dynamics of intracellular calcium in agonist-stimulated vascular smooth muscle cells. *Am. J. Physiol.*, **259**, C657–C686.

REGOLI, D. & BARABÉ, J. (1980). Pharmacology of bradykinin and related kinins. *Pharmacol. Rev.*, **32**, 1–46.

REGOLI, D.C., MARCEAU, F. & LAVIGNE, J. (1981). Induction of B_1 receptors for kinins in the rabbit by a bacterial lipopolysaccharide. *Eur. J. Pharmacol.*, **71**, 105–115.

REGOLI, D., RHALEB, N.-E., DRAPEAU, G. & DION, S. (1990). Kinin receptor subtypes. *J. Card. Pharmacol.*, **15**, S30–S38.

SOMLYO, A.P., WALKER, J.W., GOLDMAN, Y.E., TRENTHAM, D.R., KOBAYASHI, S., KITAZAWA, T. & SOMLYO, A.V. (1988). Inositol triphosphate, calcium and muscle contraction. *Phil. Trans. R. Soc. B.*, **320**, 399–404.

(Received November 15, 1993
Revised March 7, 1994
Accepted March 14, 1994)

Br. J. Pharmacol. (1994), **112**, 939–945

Mediation by 5-HT_{1D} receptors of 5-hydroxytryptamine-induced contractions of rabbit middle and posterior cerebral arteries

[1]Valérie Deckert, Didier Pruneau & *Jean-Luc Elghozi

Laboratoires Fournier, 50 rue de Dijon, 21121 Daix, France and *Laboratoire de Pharmacologie, CNRS URA 1482, Faculté de Médecine Necker-Enfants Malades, 156, rue de Vaugirard 75015 Paris, France

1 5-Hydroxytryptamine (5-HT) receptor-mediated contraction of endothelium denuded rabbit middle (MCA) and posterior (PCA) cerebral arteries was characterized by use of selective agonists and antagonists for different 5-HT receptor subtypes.

2 5-HT and various 5-HT receptor agonists contracted the arteries with the following rank order of potency in MCA: 5-carboxamidotryptamine (5-CT) > 5-HT > 5-methoxytryptamine (5-MeOT) > sumatriptan > α-methyl-5-HT (α-Me-5-HT) >> 8-hydroxy-2-(di-n-propylamino) tetralin (8-OH-DPAT) and in PCA: 5-CT > 5-HT > sumatriptan > 5-MeOT > α-Me-5-HT >> 8-OH-DPAT. With few exceptions, the maximal contractile responses of these agonists were similar to that induced by 5-HT.

3 The selective antagonists of 5-$HT_{2A/2C}$ (ketanserin), 5-HT_4 (SDZ 205-557) and 5-$HT_{1A/1B}$ (S-(−)-propranolol) sites were devoid of inhibitory effect on 5-HT-mediated contraction in both MCA and PCA, thus excluding activation of the corresponding receptors.

4 In both arteries, the contraction-response curve to 5-HT was unaffected by the 5-HT_3 receptor antagonist, ICS 205-930 (0.01 and 0.1 μM) whilst a small (3 and 6 fold displacement) was seen with MDL 72222 (0.1 and 1 μM).

5 The mixed 5-HT_1-like/5-HT_{2A} receptor antagonist, methiothepin (0.001–0.1 μM), was a potent antagonist of 5-HT-induced contractions in both arteries, giving pA_2 values of 9.4 ± 0.7 and 9.6 ± 0.8 in MCA and PCA, respectively.

6 Rauwolscine (0.1–10 μM) and yohimbine (0.3, 3 μM) inhibited contractions to 5-HT in a competitive manner, pA_2 values of 7.1 ± 0.6 and 6.7 ± 0.6 were determined for rauwolscine in MCA and PCA, respectively. An apparent pA_2 value of 6.9 ± 0.2 was calculated for yohimbine (3 μM) in both MCA and PCA.

7 In conclusion, these results suggest that the contractile response to 5-HT in rabbit isolated MCA and PCA is predominantly mediated by the 5-HT_{1D} receptor subtype, although a small contribution by 5-HT_3 receptors cannot be excluded.

Keywords: Rabbit cerebral arteries; 5-hydroxytryptamine (5-HT); 5-HT receptors; 5-HT_{1D} receptor subtype; sumatriptan

Introduction

5-Hydroxytryptamine (5-HT) is a potent constrictor of cerebral arteries in mammals. 5-HT has been localized in platelets (Tranzer *et al.*, 1972), and mast cells (Aubineau & Dimitriadou, 1989). In addition, nerves containing 5-HT have been identified in animal and human brain vessels (Griffith *et al.*, 1982; Edvinsson *et al.*, 1983; Griffith & Burnstock, 1983; Scatton *et al.*, 1985; Saito & Lee, 1987). 5-HT may therefore contribute to the control of cerebral blood flow and has been implicated in the aetiology of several cerebrovascular disorders, such as migraine.

Four main types of 5-HT receptors have been defined, the 5-HT_1, 5-HT_2, 5-HT_3 and 5-HT_4 receptors and a new nomenclature has been proposed to introduce additional subtypes (see Humphrey *et al.*, 1993). Attempts have been made to characterize the type of receptor mediating the contraction to 5-HT in a number of cerebral arteries including basilar, pial, meningeal and middle cerebral arteries and it appears that the distribution of 5-HT receptor subtypes varies according to the species. Thus, in the rat (Deckert & Angus, 1992) and the sheep (Gaw *et al.*, 1990) 5-HT_{2A} (Humphrey *et al.*, 1993) receptors predominantly mediate the contraction of cerebral arteries whilst in other species, including man (Parsons *et al.*, 1989; Hamel & Bouchard, 1991), rabbit (Parsons & Whalley, 1989), guinea-pig (Chang & Owman, 1989), dog and primate (Connor *et al.*, 1989), 5-HT_1-like receptors are primarily involved. 5-HT_1-like receptors which underly the contraction of the rabbit basilar artery appear to share some similarities with 5-HT_1-like receptors that mediate contractions to 5-HT in cerebral blood vessels from man, primate and dog (Parsons *et al.*, 1989). While the 5-HT_{1D} receptor subtype mediates contraction to 5-HT in human cerebral arteries (Hamel & Bouchard, 1991; Jansen *et al.*, 1993), the subtype of 5-HT_1 receptors implicated in the contraction of rabbit cerebral arteries remains to be fully characterized.

Therefore, this study was undertaken to determine the type of 5-HT receptors involved in the contraction of rabbit isolated middle (MCA) and posterior (PCA) cerebral arteries. By using selective agonists and antagonists for 5-HT_1, 5-HT_2, 5-HT_3 and 5-HT_4 receptor subtypes, we have shown that 5-HT-induced contractions of MCA and PCA are dependent on the 5-HT_{1D} receptor subtype.

Methods

Preparation of vessels

Vessels were prepared according to a method previously described (Deckert *et al.*, 1994). Briefly, New Zealand white rabbits, weighing 3–3.5 kg, were killed by an overdose of pentobarbitone sodium via the marginal ear vein. The brain

[1] Author for correspondence at: Faculté de Médecine, Laboratoire de Biochimie des Lipoprotéines, 7, Bd Jeanne d'Arc, 21033 Dijon Cedex, France.

was rapidly removed and placed in a Krebs solution bubbled with 95% O_2:5% CO_2. The Krebs solution had the following composition (in mM): NaCl 119, KCl 4.7, KH_2PO_4 1.18, $MgSO_4$ 1.17, $CaCl_2$ 2.5, ethylenediaminetetracetic acid (EDTA) 0.027, glucose 5.5 and $NaHCO_3$ 15, pH 7.3. The arteries were carefully dissected out under a binocular microscope (Nachet Z45P, Dijon, France). Two millimeter long segments of the arteries were threaded onto 40 μm stainless steel wires and mounted as ring preparations in a dual channel isometric myograph (J-P Trading, Aarhus, Denmark). The endothelium was mechanically removed by gentle rubbing of the luminal surface of the artery with a thin cotton thread previously hardened by coating with cyanoacrylate glue. Artery segments were left unstretched on the wires for 30 min at 37°C in Krebs solution containing 10 μM indomethacin. The vessels were then submitted to a resting tension of 100 mg and left to equilibrate for 30 min before concentration-effect curves to 5-HT or to agonists were constructed. 5-HT or agonists were added to the organ bath cumulatively in 0.5 log unit increments. In all experiments, a 1 h delay was allowed between two consecutives concentration-effect curves while three washings with fresh (drug-free apart from indomethacin) solution was performed after obtaining the maximal effect for each curve. Previous experiments showed that at least three consecutive concentration-effect curves to 5-HT were reproducible in both arterial preparations (Deckert *et al.*, 1994).

Determination of agonist potency

After completion of the control concentration-effect curve to 5-HT, cumulative concentration-effect curves to either 5-carboxamidotryptamine (5-CT), 5-methoxytryptamine (5-MeOT), α-methyl-5-HT (α-Me-5-HT), sumatriptan and 8-hydroxy-2-(di-n-propylamino)tetralin (8-OH-DPAT) were constructed. Only one agonist other than 5-HT was tested per artery.

Determination of antagonist potency

Concentration-effect curves to 5-HT were established first in the absence and then repeated in the presence of methiothepin (0.001–0.1 μM), ketanserin (0.003–0.3 μM), MDL 72222 (0.01–1 μM), S-(−)-propranolol (0.1, 1 μM), yohimbine (0.3, 3 μM), rauwolscine (0.1–10 μM), ICS 205-930 (0.01, 0.1 μM) or SDZ 205-557 (0.1, 1 μM). In each case, the antagonist was present for 45 min before 5-HT was added. No more than two concentrations of antagonist were tested on the same artery.

Test for functional endothelium

The integrity of the endothelium was assessed functionally, at the end of the experiment, by application of acetylcholine (ACh, 10 μM) on a sustained tension to 30 mM KCl. Vessels relaxing to ACh were discarded.

Analysis of data

The concentration-effect curves to agonists or to 5-HT (in the absence or in the presence of an antagonist) were expressed as percentage of the maximum contraction induced by 5-HT (% 5-HT max. contraction) in a control concentration-response curve constructed within the same artery. The mean maximal contraction (E_{max}) ± s.e.mean was determined from experimental data whereas the mean pD_2 ± s.e.mean (the negative logarithm of the concentration required to produce a half maximum contractile effect (EC_{50})) was calculated after fitting each curve according to a sigmoidal equation of the form:

$$Y = P_1 + P_2/[1 + e^{P_3(\log X - P_4)}]$$

in which, X = agonist concentration, P_1 = lower plateau response, P_2 = range between the lower and the maximal plateau of the concentration-effect curve, P_3 = a negative curvature index indicating the slope independently of the range and P_4 = log EC_{50} (Elghozi & Head, 1990). The relative potency of the agonist was determined by calculating the concentration ratio: EC_{50} for agonist divided by EC_{50} for 5-HT obtained from the corresponding control curve.

Antagonist potency was assessed by calculating the pA_2 value giving a concentration-ratio of two, according to the relation pA_2 = log (CR − 1) − log (B), where (B) is the antagonist concentration, (CR) the concentration ratio of 5-HT EC_{50} values in the absence and in the presence of the antagonist (Van Den Brink, 1977). When concentration-effect curves to 5-HT were shifted in parallel in the presence of three concentrations of antagonist, the pA_2 was determined from a Schild plot analysis and linear regression (Arunlakshana & Schild, 1959). When concentration-effect curves to 5-HT were shifted in parallel in the presence of one or two concentrations of antagonist, we calculated an apparent pA_2 from the formula given above, by assuming that the slope of the Schild plot did not differ from unity.

A one-way analysis of variance followed by a Student's *t* test was used to establish significant differences between mean values of pD_2 or E_{max}. A *P* value less than 0.05 was considered to be statistically significant.

Drugs

The following drugs were used, 5-hydroxytryptamine creatinine sulphate, indomethacin, acetylcholine chloride, yohimbine hydrochloride; 5-methoxytryptamine hydrochloride, S-(−)-propranolol hydrochloride (Sigma Chemical Co., St. Louis, U.S.A.), 5-carboxamidotryptamine maleate, α-methyl-5-hydroxytryptamine maleate, 8-hydroxy-2-(di-n-propylamino) tetralin hydrobromide, ketanserin tartrate, rauwolscine hydrochloride (Research Biochemicals Inc., Natick, U.S.A.), methiothepin maleate (gift from Drs E. Kyburz and P. Weber, Hoffman La Roche, Basel, Switzerland), sumatriptan (3-[2-dimethylamino]-ethyl-N-methyl-1H-indole-5-methane sulphonamid, Glaxo, Greenford, U.K.), MDL 72222 (1αH,3α,5αH-tropan-3-yl 3,5-dichlorobenzoate methanesulphonate, gift from Drs R.C. Miller and C.D. Houldsworth, Marion Merrel Dow Research Institute, Strasbourg, France). ICS 205-930 ([3α-tropanyl]-1-H-indole-3-carboxylic acid ester hydrochloride) and SDZ 205-557 (2-methoxy-4-amino-5-chloro-benzoic acid 2-(diethylamino)-ethyl ester hydrochloride) (gifts from Drs J.R. Fozard, D. Römer and E. Rissi, Sandoz Pharma Ltd. Basel, Switzerland).

All drugs were freshly dissolved and diluted in distilled water and kept on ice for the duration of the experiment. Indomethacin was freshly dissolved in dimethylsulphoxide (DMSO) and kept at room temperature.

Results

Agonist studies

No significant differences occurred between the resting force of the vessels prior to concentration-effect curves to 5-HT and to the 5-HT agonists. 5-HT was a potent agonist causing contraction of rabbit MCA and PCA with pD_2 values of 7.32 ± 0.12 and 7.16 ± 0.13, respectively (Table 1). 5-CT, sumatriptan, 5-MeOT, α-Me-5-HT and 8-OH-DPAT also produced concentration-dependent contractions of rabbit MCA and PCA. The corresponding concentration-effect curves are presented in Figure 1 and the pD_2 and E_{max} values are given in Table 1. A comparison of the relative potency of each agonist in respect to 5-HT gave the following rank order of potency in MCA: 5-CT > 5-HT > 5-MeOT > sumatriptan > α-Me-5-HT >> 8-OH-DPAT; and in PCA: 5-CT > 5-HT > sumatriptan > 5-MeOT > α-Me-5-HT >> 8-OH-DPAT. In MCA and PCA, all the agonists, except 8-OH-DPAT, produced maximal contractions of similar magnitude

Table 1 Potencies of various 5-hydroxytryptamine (5-HT) receptor agonists for inducing contraction of rabbit middle and posterior cerebral arteries

	Middle cerebral artery				*Posterior cerebral artery*			
Agonist	*n*	pD_2 ($-\log EC_{50}$)	Relative potency	E_{max} (%5-HT E_{max})	*n*	pD_2 ($-\log EC_{50}$)	Relative potency	E_{max} (%5-HT E_{max})
5-HT	32	7.32 ± 0.12	1	100	31	7.16 ± 0.13	1	100
5-CT	7	8.06 ± 0.13*	0.07	107 ± 28	6	7.41 ± 0.22	0.31	76 ± 16
		(6.90 ± 0.16)	(0.02–0.22)			(6.90 ± 0.22)	(0.06–1.64)	
Sumatriptan	7	7.01 ± 0.32*	5.6	116 ± 10	6	6.98 ± 0.12	2.3	135 ± 14
		(7.76 ± 0.17)	(1.3–24.3)			(7.35 ± 0.08)	(0.1–5.7)	
5-MeOT	5	5.93 ± 0.36	3.6	108 ± 6	6	5.84 ± 0.22*	4.1	90 ± 11
		(6.49 ± 0.14)	(0.5–24.7)			(6.45 ± 0.15)	(1.9–8.8)	
α-Me-5-HT	6	5.79 ± 0.32*	74.1	130 ± 17	6	6.16 ± 0.12*	33.9	132 ± 17
		(7.67 ± 0.22)	(15.9 ± 345.5)			(7.69 ± 0.05)	(16.6–68.9)	
8-OH-DPAT	7	–	–	32 ± 10*	7	–	–	24 ± 10*
		(7.59 ± 0.29)				(7.52 ± 0.33)		

Values are mean ± s.e.mean for pD_2, E_{max} (maximal contraction expressed as % of E_{max} obtained for 5-HT) and geometric mean (95% confidence limits) for relative potency (EC_{50} agonist/EC_{50} 5-HT). pD_2 values obtained from respective control response curve to 5-HT constructed before each agonist response curve are given in brackets. The EC_{50} for 8-OH-DPAT could not be determined (see Results section for details). *$P<0.05$ compared with respective 5-HT data. For abbreviations, see text.

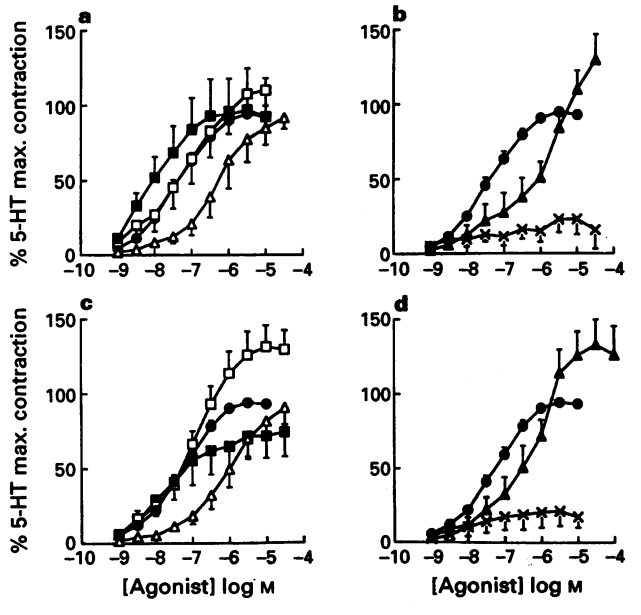

Figure 1 Average concentration-effect curves to 5-hydroxytryptamine (5-HT) and to 5-HT receptor agonists in rabbit middle (a,b) and posterior (c,d) cerebral arteries. 5-HT control curve (●); 5-carboxamidetryptamine (■); sumatriptan (□); 5-methoxytryptamine (△); α-methyl-5-HT (▲); 8-hydroxy-2-(di-n-ptopylamino) tetralin (×). The average control curve to 5-HT, which is the same curve in left and right panels, represents the pooled data obtained with all tissues. Mean ± s.e.mean is shown of $n = 5$ to 32 experiments.

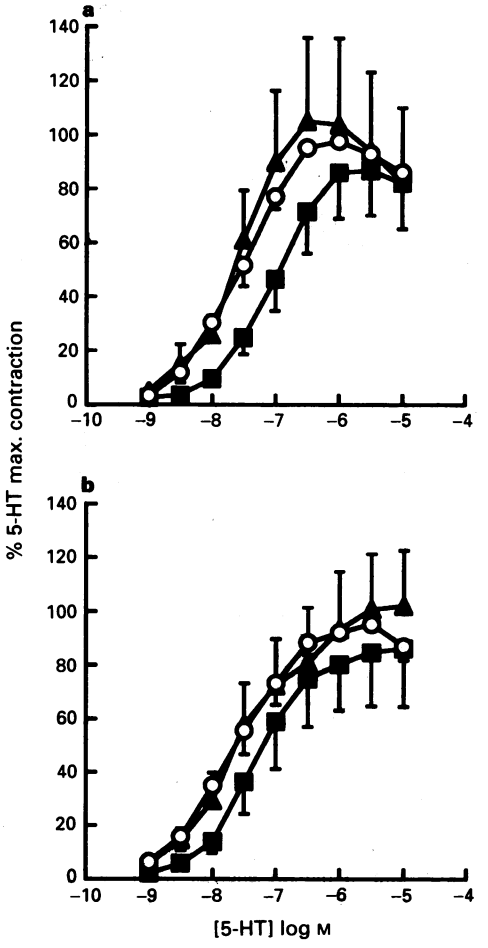

Figure 2 Average concentration-effect curves to 5-hydroxytryptamine (5-HT) in rabbit middle (a) and posterior (b) cerebral arteries in the absence (○) and in the presence of ketanserin 3 nM (▲) and 300 nM (■). Mean ± s.e.mean of $n = 6$ to 9 experiments.

to that of 5-HT (Table 1). Although the maximum response to α-Me-5-HT in MCA appeared larger than that to 5-HT, this was not statistically significant (Table 1). 8-OH-DPAT was the weakest contractile agent in both rabbit MCA and PCA ($P<0.05$). Because of the non-sigmoid form of its concentration-effect curve and the poor contraction it elicited, EC_{50} values for this agonist could not be determined.

Antagonist studies

The effects of various antagonists with known selectivity towards 5-HT receptor subtypes were assessed against 5-HT-induced contraction of rabbit isolated MCA and PCA. The contractile response to 5-HT in both arteries was resistant to ketanserin, a selective $5\text{-HT}_{2A/2C}$ receptor antagonist (Figure 2), to SDZ 205-557 an antagonist of 5-HT_4 receptor and to S-(−)-propranolol, a β-adrenoceptor blocker with a relatively high affinity for 5-HT_{1A} and 5-HT_{1B} receptors (Table 2).

MDL 72222, an antagonist of 5-HT_3 receptors, produced a significant 3 and 6 fold rightward shift of the 5-HT concentration-effect curve at 0.1 and 1 μM, respectively (Figure 3). The maximum contractile response was un-

Table 2 Effects of antagonists on 5-hydroxytryptamine (5-HT)-induced contraction of rabbit middle and posterior cerebral arteries

			Middle cerebral artery				*Posterior cerebral artery*		
Antagonist	μM	*n*	5-HT conc.ratio	Apparent pA_2	E_{max}	*n*	5-HT conc.-ratio	Apparent pA_2	E_{max}
Propranolol	0.1	4	1.2 (0.1–20.4)	–	88 ± 6	4	1.5 (0.4–5.6)	–	99 ± 9
	1	4	1.1 (0.5–2.5)	–	84 ± 17	4	2.0 (0.91–4.6)	–	85 ± 15
Yohimbine	0.3	6	1.9 (0.8–4.7)	6.77 ± 0.22	80 ± 9	6	3.6 (2.4–5.5)	6.93 ± 0.09	74 ± 15
	3	5	23.4 (7.9–69.5)	6.86 ± 0.18	68 ± 14	6	28.5 (7.0–116.0)	6.95 ± 0.24	91 ± 21
SDZ 205-557	0.1	4	1.6 (0.15–16.5)	–	74 ± 10	4	0.7 (0.1–5.3)	–	98 ± 8
	1	4	2.2 (0.5–9.4)	–	72 ± 12	4	2.7 (0.3–20.7)	–	87 ± 16
ICS 205-930	0.01	6	0.8 (0.2–2.7)	–	78 ± 9	4	0.7 (0.33–1.25)	–	85 ± 10
	0.1	6	1.9 (0.2–20.2)	–	88 ± 24	4	1.5 (0.4–5.4)	–	76 ± 13

5-HT concentration-ratio in the presence of indicated antagonist concentration are given as geometric mean (95% confidence limits), apparent pA_2 and 5-HT E_{max} are given as mean value ± s.e.mean of *n* experiments. $^*P<0.05$ compared with respective 5-HT data.

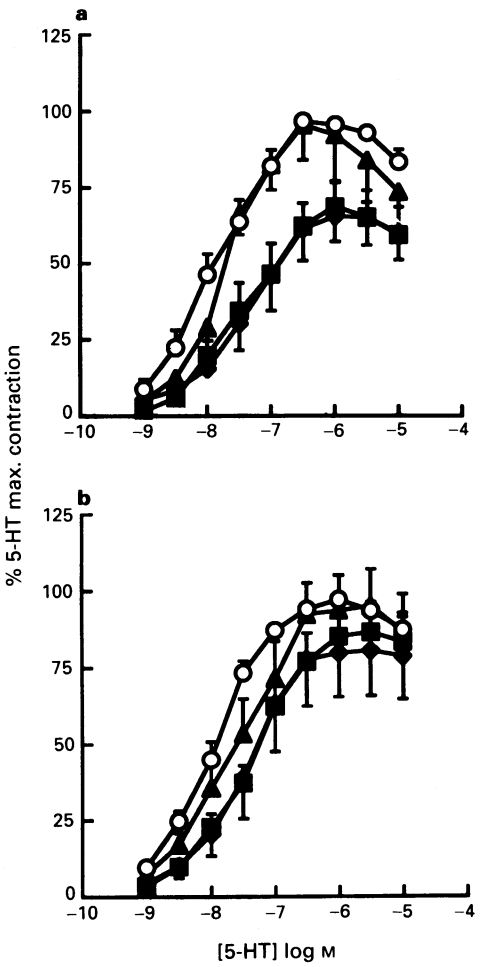

Figure 3 Average concentration-effect curves to 5-hydroxytryptamine (5-HT) in rabbit middle (a) and posterior (b) cerebral artery in the absence (○) and in the presence of MDL 72222 0.01 μM (▲), 0.1 μM (■) and 1 μM (◆). Mean ± s.e.mean of $n = 4$ to 9 experiments.

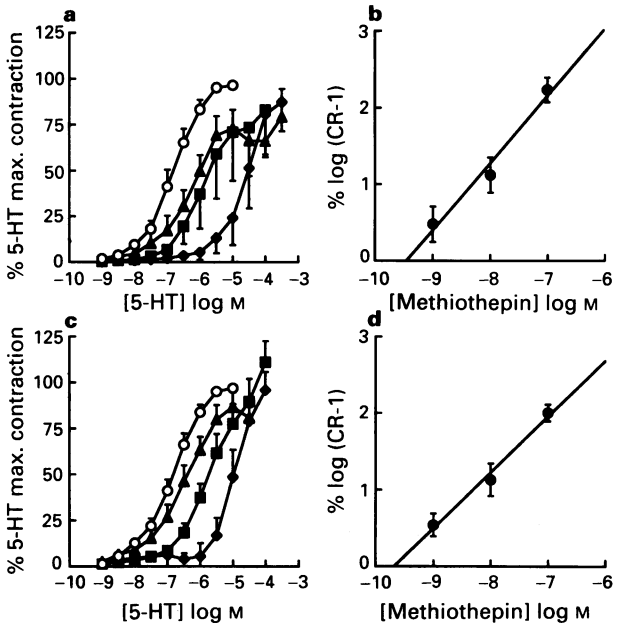

Figure 4 Average concentration-effect curves to 5-hydroxytryptamine (5-HT) in rabbit middle (a,b) and posterior (c,d) cerebral arteries in the absence (○) and in the presence of methiothepin 0.001 μM (▲), 0.01 μM (■) and 0.1 μM (◆). The respective Schild regression plots are given on the right part of the figure. Mean ± s.e.mean of $n = 5$ to 10 experiments.

changed in PCA but was significantly reduced in MCA by MDL 72222 ($P<0.05$). ICS 205-930 at low concentrations (0.1–10 nM) has a known antagonist action on 5-HT_3 receptors whilst at higher concentrations (1 μM) it antagonizes 5-HT_4 receptors (Clarke *et al.*, 1989). ICS 205-930, at 0.01 and 0.1 μM, did not affect in terms of maximal contraction and sensitivity the 5-HT-induced contraction in either MCA or PCA (Table 2).

Methiothepin (0.001–0.1 μM), a mixed 5-HT_1-like/5-HT_{2A} receptor antagonist, behaved as a potent antagonist causing a concentration-dependent parallel rightward shift of the concentration-response curve to 5-HT with no significant depression of the maximum response (Figure 4). The Schild plot analysis of methiothepin against 5-HT gave a pA_2 value of 9.4 ± 0.7 for MCA and a pA_2 value of 9.6 ± 0.8 for PCA. The regression line had a slope of 0.9 ± 0.15 for MCA and of 0.75 ± 0.15 for PCA. The slopes were not significantly different from one indicating competitive antagonism.

Concentration-dependent shifts of the 5-HT concentration effect curve were observed with both yohimbine and its enantiomer, rauwolscine (Table 2 and Figure 5). 5-HT concentration-ratios and corresponding apparent pA_2 values of yohimbine are given in Table 2. Schild plot analysis of rauwolscine effects against 5-HT (Figure 5), gave a pA_2 value of 7.1 ± 0.6 and a slope of 1.05 ± 0.2 for MCA. For PCA, a pA_2 value of 6.7 ± 0.6 and a slope of 1.13 ± 0.26 were determined. In each case, the slopes were not significantly different from 1, indicating competitive antagonism.

Discussion

These results demonstrate that contractions of rabbit isolated MCA and PCA to 5-HT are mediated by 5-HT_{1D} receptors with no contribution by 5-HT_{1A}, 5-HT_{2A}, 5-HT_{2C} and 5-HT_4

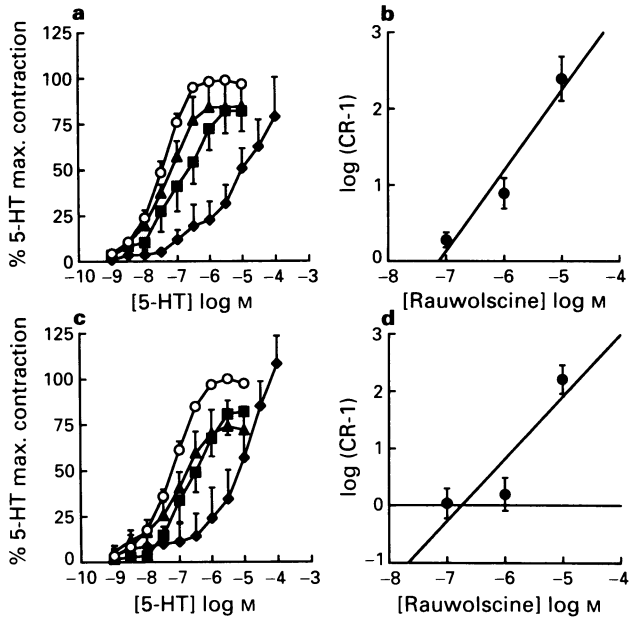

Figure 5 Average concentration-effect curves to 5-hydroxytryptamine (5-HT) in rabbit middle (a,b) and posterior (c,d) cerebral arteries in the absence (○) and in the presence of rauwolscine 0.1 μM (▲), 1 μM (■) and 10 μM (◆). The respective Schild regression plots are given on the right side of the figure. Mean ± s.e.mean of $n = 4$ to 8 experiments.

receptors. Nevertheless, a participation of 5-HT_3 receptors could not be ruled out.

In some cerebrovascular preparations such as the rabbit (Trezise *et al.*, 1992) and the dog basilar artery (Connor & Feniuk, 1989), the reactivity of smooth muscle has been shown to be influenced by the presence of the endothelium (see Cocks & Angus, 1983). In particular, endothelial removal potentiated the response to 5-HT and increased the maximum of the contraction. Therefore, in order to assay the full constrictor effect of 5-HT and 5-HT agonists, we conducted all the experiments on arteries without endothelium. Under these condtions, the involvement of 5-HT_{2A} receptors was first ruled out in the 5-HT-mediated contraction of rabbit MCA and PCA. This was based on the observation that the potent 5-HT_{2A} antagonist, ketanserin was devoid of antagonist activity. 5-HT_{2A} receptors, however, have been shown to mediate 5-HT contractions of rabbit vertebral artery (Griffith & Burnstock, 1982) and rabbit aorta (Feniuk *et al.*, 1985). In the latter preparation, ketanserin was a potent antagonist with a pA_2 value of 8.7 (Feniuk *et al.*, 1985). In addition, Parsons & Whalley (1989) showed that in the rabbit basilar artery, 5-HT activated a small population of 5-HT_{2A} receptors. Thus, marked differences in the contribution of 5-HT_{2A} receptors to 5-HT-induced contractions exist between cerebral arteries from the same species. It is also unlikely that activation of vascular 5-HT_4 receptors (Cocks & Arnold, 1993) mediated contractions to 5-HT in rabbit MCA and PCA since the 5-HT_4 receptor antagonist, SDZ 205-557, a compound previously shown to be a potent selective antagonist of 5-HT_4 receptors in the guinea-pig isolated ileum had no effect (Buchheit *et al.*, 1992). MDL 72222, an antagonist of 5-HT_3 receptors (Fozard, 1984) produced a 6 fold shift at 1 μM of the concentration-effect curve to 5-HT in both arteries which was associated with a decrease in the maximum contraction in MCA only. ICS 205-930, an antagonist of 5-HT_3 receptors at low concentrations (0.1–10 nM; Clarke *et al.*, 1989) had no effect at 0.01 and 0.1 μM against the contraction to 5-HT in either artery; ICS 205-930 has been shown to have a greater affinity for 5-HT_3 receptors than MDL 72222 (Hoyer, 1990) and thus it is possible that MDL 72222 produced some non specific effect in our experiments. Although we cannot reach a definite conclusion on the role of 5-HT_3 receptors in the 5-HT-mediated contraction, their participation is likely to be minor. In support of this, previous reports showed that the contractions to 5-HT of the rabbit, dog and primate basilar artery (Parsons & Whalley, 1989; Connor *et al.*, 1989), the cat middle cerebral artery (Hamel *et al.*, 1989), the human basilar artery (Parsons *et al.*, 1989) and the human pial arterioles (Hamel & Bouchard, 1991) were not mediated by 5-HT_3 receptors. So far, 5-HT_3 receptors have been found only on neurones where they are responsible for eliciting the depolarizing action of 5-HT (Bradley *et al.*, 1986) and further studies would be needed to investigate such a mechanism in our vessel preparations.

The mixed 5-HT_1-like/5-HT_{2A} receptor antagonist, methiothepin, was a potent competitive antagonist of 5-HT-induced contractions in rabbit MCA and PCA. Respective pA_2 values of 9.4 (MCA) and 9.6 (PCA) were determined suggesting that 5-HT was acting at the same receptor type in the two vessels to produce contraction. These observations are consistent with the presence of 5-HT_1-like receptors in both preparations, with similar pA_2 values to those found in vessels where 5-HT_1-like receptors mediate vasoconstriction; 8.8 in human basilar artery (Parsons *et al.*, 1989), 8.6 in rabbit renal artery (Tadipatri *et al.*, 1992) and 8.5 in human pial arterioles (Hamel & Bouchard, 1991). Interestingly, our pA_2 values are also close to the pA_2 value of 10.3 reported by Parsons & Whalley (1989) in the rabbit basilar artery.

When comparing the contractile potency of various agonists, 5-CT, a selective agonist at 5-HT_1-like receptors, was found to be the most potent in both types of arteries. The EC_{50} values for 5-CT were 7.1 fold and 1.3 fold higher than that for 5-HT in MCA and PCA, respectively. In addition, sumatriptan, another selective 5-HT_1-like agonist effective in the acute treatment of migraine (Doenicke *et al.*, 1988), was found to be a potent vasoconstrictor of rabbit MCA and PCA.

Taken together, the ineffectiveness of ketanserin, ICS 205-930 and SDZ 205-557 in preventing the contractile effect of 5-HT and the potent antagonism by methiothepin as well as the higher potency of 5-CT as compared with 5-HT and the agonist effect of sumatriptan, strongly suggest, according to the criteria of classification proposed by Bradley *et al.* (1986), that 5-HT_1-like receptors are predominantly involved in the contraction of rabbit MCA and PCA.

Both α-Me-5-HT and 5-MeOT contracted the rabbit MCA and PCA. These compounds are usually considered as selective for 5-HT_{2A} and 5-HT_4 receptors, respectively (Bradley *et al.*, 1986; Saxena & Villalon, 1990). Nevertheless, their ability to contract rabbit MCA and PCA could result from a stimulation of 5-HT_1-like receptors rather than 5-HT_{2A} or 5-HT_4 receptors since it has been demonstrated by Tadipatri *et al.* (1992) that these agonists contracted the rabbit isolated renal artery via 5-HT_1-like receptors. Thus, the selectivity of these tryptamine derivatives is questionable, particularly since α-Me-5-HT and 5-MeOT have identical binding affinity at 5-HT_1, 5-HT_{2A} and 5-HT_4 sites (Hoyer & Fozard, 1991).

The β-adrenoceptor blocker, S-(−)-propranolol, did not alter the 5-HT concentration-effect curve, ruling out an involvement of 5-HT_{1A} and 5-HT_{1B} receptor subtypes. Furthermore, the weak effect of 8-OH-DPAT a highly selective agonist at 5-HT_{1A} receptors argues against the presence of 5-HT_{1A} receptors. Involvement of 5-HT_{2C} receptors was also unlikely since ketanserin which in addition to its high affinity for 5-HT_{2A} sites, exhibits an affinity for 5-HT_{2C} sites (pK_D values of 8.9 and 7, respectively, Hoyer & Fozard, 1991) was without effect. However, we found that yohimbine (0.3, 3 μM) and rauwolscine (0.1–10 μM), two drugs with affinity for 5-HT_{1D} sites (Hoyer & Fozard, 1991) antagonized the contractile effect of 5-HT. The apparent pA_2 value for yohimbine and the pA_2 value for rauwolscine were close to their respective affinity constants reported at 5-HT_{1D} binding

sites in mammalian brain membranes (7.1 and 7.7, respectively, Hoyer & Fozard, 1991), an observation which would favour the activation of 5-HT_{1D} receptors in rabbit MCA and PCA. In addition, agonists displaying high affinity towards 5-HT_{1D} binding site such as, 5-CT (pK_D, 9), 5-MeOT (pK_D, 8.4) and sumatriptan (pK_D, 7.5) matched the effect of 5-HT (pK_D, 8.4) better than α-Me-5-HT ($pK_D = 6.2$, Hoyer & Fozard, 1991). Furthermore, the apparent pA_2 value for methiothepin and yohimbine as well as the pD_2 values for 5-HT and 5-CT found in this study are in accordance with the corresponding values observed for these compounds at the presynaptic 5-HT autoreceptor in the rabbit brain cortex (Limberger *et al.*, 1991). Taken together our results support the view that the receptor underlying 5-HT-mediated contraction of rabbit middle and posterior cerebral arteries is of the 5-HT_{1D} subtype. Interestingly, such a subtype of 5-HT receptor was not found in the rabbit basilar artery, where yohimbine failed to antagonize the contractile effect of 5-HT and of sumatriptan (Parsons & Whalley, 1989). Such a difference seems to reflect a differential distribution of 5-HT receptors along the cerebral vasculature of the rabbit.

This study provides the first demonstration of 5-HT_{1D} receptor-mediated contractile response in rabbit cerebral arteries. Since this type of 5-HT receptor has been shown to be involved in 5-HT-induced contraction of human cerebral arterioles (Hamel & Bouchard, 1991) and human cerebral arteries (Jansen *et al.*, 1993), the rabbit isolated MCA and PCA might constitute useful pharmacological preparations for the development of new compounds acting at the 5-HT_{1D} receptor. Recently, two genes encoding the human 5-HT_{1D} receptor subtypes have been cloned and named 5-$HT_{1D\alpha}$ and 5-$HT_{1D\beta}$ (Weinshank *et al.*, 1992). A weak homology of sequence (63%) between 5-$HT_{1D\beta}$ and 5-$HT_{1D\alpha}$ receptors has been reported but their pharmacological profiles appeared almost indistinguishable (Hartig *et al.*, 1992). While it appears that the human 5-$HT_{1D\beta}$ is the species homolgous of the rat 5-HT_{1B} receptor (Hartig *et al.*, 1992), further studies will be needed to determine the subtype of 5-HT_{1D} receptor present in rabbit MCA and PCA.

The authors thank Drs T.M. Cocks and N.M.B. Martin for their helpful comments regarding the manuscript.

References

ARUNLAKSHANA, O. & SCHILD, H.O. (1959). Some quantitative uses of drug antagonists. *Br. J. Pharmacol. Chemother.*, **14**, 48–58.

AUBINEAU, P. & DIMITRIADOU, V. (1989). Mast cells in the cerebral circulation. Characterization and possible function. In *Neurotransmitter and Cerebrovascular Function*. ed. Seylaz, J. & Sercombe, R. Volume II, p. 293. Amsterdam: Elsevier.

BRADLEY, P.B., ENGEL, G., FENIUK, W., FOZARD, J.R., HUMPHREY, P.P.A., MIDDLEMISS, D.N., MYLECHARANE, E.J., RICHARDSON, B.P. & SAXENA, P.R. (1986). Proposals for the classification and nomenclature of functional receptors for 5-hydroxytryptamine. *Neuropharmacol.*, **25**, 563–576.

BUCHHEIT, K.-H., GAMSE, R. & PFANNKUCHE, H.-J. (1992). SDZ 205-557, a selective, surmountable antagonist for 5-HT_4 receptors in the isolated guinea pig ileum. *Naunyn-Schmied. Arch. Pharmacol.*, **345**, 387–393.

CHANG, J.Y. & OWMAN, C.H. (1989). Cerebrovascular serotonergic receptors mediating vasoconstriction: further evidence for the existence of 5-HT_2 receptors in rat and 5-HT_1-like receptors in guinea-pig basilar arteries. *Acta Physiol. Scand.*, **136**, 59–67.

CLARKE, D.E., GRAIG, D.A. & FOZARD, J.R. (1989). The 5-HT_4 receptor: naughty, but nice. *Trends Pharmacol. Sci.*, **10**, 385–386.

COCKS, T.M. & ANGUS, J.A. (1983). Endothelium-dependent relaxation of coronary arteries by noradrenaline and serotonin. *Nature*, **305**, 627–630.

COCKS, T.M. & ARNOLD, P. (1993). 5-hydroxytryptamine (5-HT) mediates relaxation in the sheep isolated pulmonary vein via activation of 5-HT_4 receptors. *Br. J. Pharmacol.*, **107**, 591–596.

CONNOR, H.E. & FENIUK, W. (1989). Influence of the endothelium on contractile effects of 5-hydroxytryptamine and selective 5-HT agonists in canine basilar artery. *Br. J. Pharmacol.*, **96**, 170–178.

CONNOR, H.E., FENIUK, W. & HUMPHREY, P.P.A. (1989). Characterisation of 5-HT receptors mediating contraction of canine and primate basilar artery by use of GR43175, a selective 5-HT_1-like receptor agonist. *Br. J. Pharmacol.*, **96**, 379–387.

DECKERT, V. & ANGUS, J.A. (1992). Evidence that 5-HT_2 receptors predominantly mediate the contraction of the rat basilar artery to 5-hydroxytryptamine. *Eur. J. Pharmacol.*, **221**, 17–25.

DECKERT, V., PRUNEAU, D. & ELGHOZI, J.-L. (1994). Evidence for pH as an important parameter to control when studying the contractility of isolated rabbit cerebral arteries. *Fundam. Clin. Pharmacol.*, **8**, 34–42.

DOENICKE, A., BRAND, J. & PERRIN, V.L. (1988). Possible benefits of GR 43175, a novel 5-HT_1-like receptor agonist, for acute treatment of severe migraine. *Lancet*, **i**, 1309–1311.

EDVINSSON, L., DEGUERCE, A., DUVERGER, D., MACKENZIE, E.T. & SCATTON, B. (1983). Central serotoninergic nerves project to the pial vessels of the brain. *Nature*, **306**, 55–57.

ELGHOZI, J.-L. & HEAD, G. (1990). Spinal noradrenergic pathways pressor responses to central angiotensin II. *Am. J. Physiol.*, **258**, H240–H246.

FENIUK, W., HUMPHREY, P.P.A., PERREN, M.J. & WATTS, A.D. (1985). A comparison of 5-hydroxytryptamine receptors mediating contraction in rabbit aorta and dog saphenous vein: evidence for different receptor types obtained by use of selective agonists and antagonists. *Br. J. Pharmacol.*, **86**, 697–704.

FOZARD, J.R. (1984). MDL 72222, a potent and highly selective antagonist at neuronal 5-hydroxytryptamine receptors. *Naunyn Schmied. Arch. Pharmacol.*, **326**, 36–44.

GAW, A.J., WADSWORTH, R.M. & HUMPHREY, P.P.A. (1990). Pharmacological characterisation of postjunctional 5-HT receptors in cerebral arteries from the sheep. *Eur. J. Pharmacol.*, **179**, 35–44.

GRIFFITH, S.G. & BURNSTOCK, G. (1983). Immunohistochemical demonstration of serotonin in nerves supplying human cerebral and mesenteric blood vessels. *Lancet*, **i**, 561–562.

GRIFFITH, S.G., LINCOLN, J. & BURNSTOCK, G. (1982). Serotonin as a neurotransmitter in cerebral arteries. *Brain Res.*, **247**, 388–392.

HAMEL, E. & BOUCHARD, D. (1991). Contractile 5-HT_1 receptors in human isolated pial arterioles: correlation with 5-HT_{1D} binding sites. *Br. J. Pharmacol.*, **102**, 227–233.

HAMEL, E., ROBERT, J.-P., YOUNG, A.R. & MACKENZIE, E.T. (1989). Pharmacological properties of the receptor(s) involved in the 5-hydroxytryptamine-induced contraction of the feline middle cerebral artery. *J. Pharmacol. Exp. Ther.*, **249**, 879–889.

HARTIG, P.R., BRANCHEK, T.A. & WEINSHANK, R.L. (1992). A subfamily of 5-HT_{1D} receptor genes. *Trends Pharmacol. Sci.*, **13**, 152–159.

HOYER, D. (1990). Serotonin 5-HT_3, 5-HT_4 and 5-HT-M receptors. *Neuropsychopharmacol.*, **3**, 371–383.

HOYER, D. & FOZARD, J.R. (1991). 5-Hydroxytryptamine receptors. In *Receptor Data For Biological Experiments*. ed. Doods, H.N. & Van Meel, J.C.A. pp. 35–41. New York: Ellis Horwood.

HUMPHREY, P.P.A., HARTIG, P. & HOYER, D. (1993). A proposed new nomenclature for 5-HT receptors. *Trends Pharmacol. Sci.*, **14**, 233–236.

JANSEN, I., OLESEN, J. & EDVINSSON, L. (1993). 5-Hydroxytryptamine receptor characterization of human cerebral, middle meningeal and temporal arteries: regional differences. *Acta Physiol. Scand.*, **147**, 141–150.

LIMBERGER, N., DEICHER, R. & STARKE, K. (1991). Species differences in presynaptic serotonin autoreceptors: mainly 5-HT_{1B} but possibly in addition 5-HT_{1D} in the rat, 5-HT_{1D} in the rabbit and guinea-pig brain cortex. *Naunyn Schmied. Arch. Pharmacol.*, **343**, 353–364.

PARSONS, A.A. & WHALLEY, E.T. (1989). Evidence for the presence of 5-HT_1-like receptors in rabbit isolated basilar arteries. *Eur. J. Pharmacol.*, **174**, 189–196.

PARSONS, A.A., WHALLEY, E.T., FENIUK, W., CONNOR, H.E. & HUMPHREY, P.P.A. (1989). 5-HT_1-like receptors mediate 5-hydroxytryptamine-induced contraction of human isolated basilar artery. *Br. J. Pharmacol.*, **96**, 434–449.

SAITO, A. & LEE, J.-F. (1987). Serotonin as an alternative transmitter in sympathetic nerves of large cerebral arteries of the rabbit. *Circ. Res.*, **60**, 220–228.

SAXENA, P.R. & VILLALON, C.M. (1990). Cardiovascular effects of serotonin agonists and antagonists. *J. Cardiovasc. Pharmacol.*, **15** (Suppl. 7), S17–S34.

SCATTON, B., DUVERGER, D., L'HEUREUX, R., SERRANO, A., FAGE, D., NOWICKI, J.-P. & MACKENZIE, E.T. (1985). Neurochemical studies on the existence, origin and characteristics of the serotoninergic innervation of small pial vessels. *Brain Res.*, **345**, 219–229.

TADIPATRI, S.D., FENIUK, W. & SAXENA, P.R. (1992). Rabbit isolated renal artery contractions by some tryptamine derivatives, including 2-methyl-5-HT, are mediated by a 5-HT_1-like receptor. *Br. J. Pharmacol.*, **107**, 322–328.

TRANZER, J.P., PRADA, D.A. & PLETSHER, A. (1972). Storage of 5-hydroxytryptamine in Mega Karyocytes. *J. Cell. Biol.*, **52**, 191–197.

TREZISE, D.J., DREW, G.M. & WESTON, A.H. (1992). Analysis of the depressant effect of the endothelium on contractions of rabbit isolated basilar artery to 5-hydroxytryptamine. *Br. J. Pharmacol.*, **106**, 587–592.

VAN DEN BRINK, F.G. (1977). General theory of drug-receptor interactions. Drug-receptor interaction models. Calculation of drug parameters. In *Kinetics of Drug Action*. ed. Van Rossum, J.M. pp. 169–254. Berlin: Springer-Verlag.

WEINSHANK, R.L., ZGOMBICK, J.M., MACCHI, M.J., BRANCHEK, T.A. & HARTIG, P.R. (1992). Human serotonin 1D receptor is encoded by a subfamily of two distinct genes: 5-$HT_{1D\alpha}$ and 5-$HT_{1D\beta}$. *Proc. Natl Acad. Sci. U.S.A.*, **89**, 3630–3634.

(Received September 27, 1993
Revised February 24, 1994
Accepted March 14, 1994)

Br. J. Pharmacol. (1994), **112**, 946–950

The P_{2Z}-purinoceptor of human lymphocytes: actions of nucleotide agonists and irreversible inhibition by oxidized ATP

[1]James S. Wiley, Joan R. Chen, Marie B. Snook & Gary P. Jamieson

Haematology Department, Austin Hospital, Heidelberg, Victoria 3084, Australia

1 Extracellular adenosine triphosphate (ATP) is known to open a receptor-operated ion channel (P_{2Z} class) in human lymphocytes which conducts a range of cationic permeants. The activity of a range of different agonists and inhibitors towards the P_{2Z}-purinoceptor was investigated by measuring the agonist-induced influx of Ba^{2+} into fura-2 loaded lymphocytes.

2 The most potent agonist was 2′ & 3′-0-(4-benzoylbenzoyl)-ATP (benzoylbenzoic ATP) which gave 2 fold greater maximum Ba^{2+} influx and had a 10 fold lower EC_{50} than for ATP. The rank order of agonist potency in K^+-media was benzoylbenzoic ATP>>ATP = 2-methylthio ATP = 2-chloro ATP > ATP-γ-S. ADP, UTP and α,β-methylene ATP were unable to stimulate Ba^{2+} influx.

3 Extracellular Na^+ inhibited the increment of Ba^{2+} influx induced by all concentrations of ATP, 2-methylthio ATP, 2-chloroATP and ATP-γ-S. This inhibitory effect of extracellular Na^+ is also reflected in the different EC_{50}s for benzoylbenzoic ATP (8 μM in K^+-media, 18 μM in Na^+-media) but the maximal response to this agonist was the same in the presence or absence of Na^+.

4 Treatment of lymphocytes with 2,3 dialdehyde ATP (oxidized ATP) at 300 μM for 60 min gave total and irreversible inhibition of ATP-induced Ba^{2+} influx. 5′-*p*-Fluorosulphonyl benzoyladenosine (FSBA) also was an irreversible inhibitor but the maximal inhibition achieved was 90%.

5 It is concluded that the P_{2Z}-purinoceptor of human lymphocytes has a rank order of agonist potency which clearly distinguishes it from other P_2-receptors and that oxidized ATP is a convenient irreversible inhibitor for the P_{2Z}-purinoceptor.

Keywords: P_{2Z}-purinoceptor; ion channel, lymphocyte; lymphocytes, human leukaemic; barium influx, lymphocytes; ATP-receptor, extracellular; 2-chloro ATP; 2-methylthio ATP; oxidized ATP; benzoylbenzoic ATP; fluorosulphonylbenzoyladenosine

Introduction

Extracellular adenosine 5′-triphosphate (ATP) mediates a wide range of effects by acting on P_2-purinoceptors on many tissues throughout the body. Some 5 classes of P_2-receptors have been recognized (P_{2X}, P_{2Y}, P_{2U}, P_{2Z} and P_{2T}) from their characteristic agonist selectivity and sensitivity to inhibitors (reviewed by Gordon, 1986; Burnstock, 1990; Dubyak & El-Moatassim, 1993). In smooth muscle, extracellular ATP can act in signal transduction at P_{2X}-purinoceptors (Benham & Tsien, 1987) by an action which opens an ion channel and which usually brings about contraction. In endothelial cells extracellular ATP causes formation of nitric oxide and vascular relaxation. This action of ATP is mediated via a P_{2Y}-receptor which is coupled to activation of the phosphoinositide signalling cascade, formation of inositol (1,4,5)-trisphosphate (IP3) and release of Ca^{2+} from intracellular organelles. Many features of this P_{2Y}-receptor are functionally similar to the endothelial P_{2U}-receptor except that UTP is the preferred agonist for the latter. ATP also induces the formation of ion-conducting channels (pores) in mouse and human lymphocytes (Wiley & Dubyak, 1989; Wiley *et al.*, 1990; 1992; El-Moatassim *et al.*, 1990; Pizzo *et al.*, 1991), rat peritoneal mast cells (Tatham & Lindau, 1990), rat parotid acinar cells (Soltoff *et al.*, 1992) and mouse macrophages (Greenberg *et al.*, 1988). A subclass of purinoceptors termed P_{2Z} was first proposed for the receptor associated with this channel based on a specificity for the fully ionized ATP^{4-} and need for relatively high (ca. 100 μM) ATP concentrations to open the channel (Gordon, 1986).

Several general features characterize the ionic fluxes associated with opening of the P_{2Z}-associated ion channel of lymphocytes (El-Moatassim *et al.*, 1990; Wiley *et al.*, 1990; 1992; 1993; Pizzo *et al.*, 1991). First, ATP-induced increments in permeant fluxes show a sigmoid dependence on agonist concentration. Second, amiloride analogues such as hexamethylene amiloride potently inhibit ATP-induced ion fluxes. Third, ATP-induced fluxes are inhibited to a variable extent by high concentrations of extracellular Na^+. Finally the P_{2Z} channel accepts certain large inorganic and organic cations so that influx of Ba^{2+} into fura-2 loaded lymphocytes can be used to study the kinetics of opening of this P_2-channel. Thus Ba^{2+} influx was used in the present study to characterize the potency of various agonists of the P_2-purinoceptor of lymphocytes and the effect of irreversible antagonists. Lymphocytes showed no ATP-induced release of internal Ca^{2+} (a P_{2Y} effect) and no response to UTP, ADP or α,β-methylene ATP, agonists which are specific for the P_{2U}, P_{2T} and P_{2X} purinoceptors respectively. These results confirm that lymphocytes possess only P_{2Z}-purinoceptors and are an ideal cell type to study the characteristics of this receptor. 2′ & 3′-0-(4-benzoylbenzoyl) ATP (benzoylbenzoic ACP) which potently stimulates Ca^{2+} responses in macrophages (El-Moatassim & Dubyak, 1992) showed the greatest potency for opening this P_{2Z} channel of lymphocytes. The present study reports a rank order of agonist potency for the lymphocyte P_{2Z}-receptor which clearly distinguishes it from other classes of P_2-purinoceptors.

Methods

Source of lymphocytes

Peripheral blood lymphocytes were obtained from eight separate patients with B-cell chronic lymphocytic leukaemia whose cells showed permeability responses in our previous study (Wiley *et al.*, 1992). Our previous work has shown that these leukaemic lymphocytes show similar ATP-induced

[1] Author for correspondence.

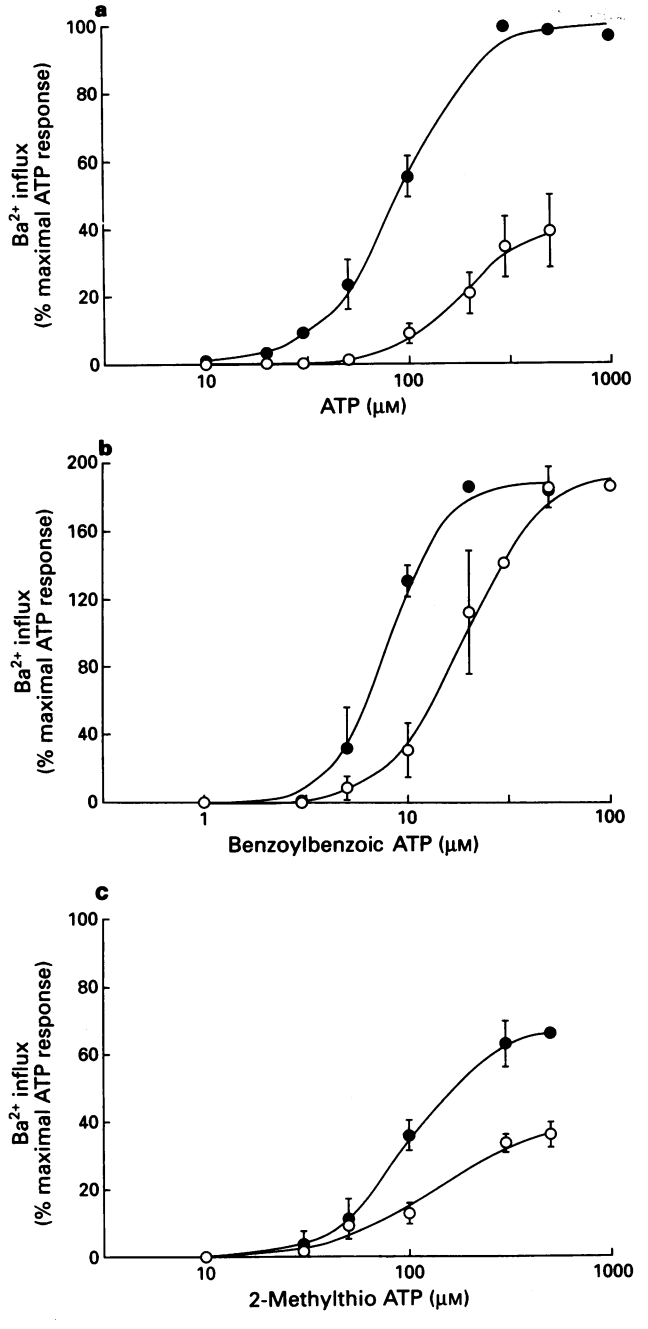

permeability responses to lymphocytes of normal subjects (Wiley & Dubyak, 1989).

Lymphocyte preparation

Venous blood (20 ml) from patients was added to heparin anti-coagulant and diluted with 2 vol HEPES buffered saline (composition mM: NaCl 145, KCl 5, HEPES 10, pH 7.4, $CaCl_2$ 1, D-glucose 5 and bovine serum albumin (BSA) 1 g l^{-1}). Mononuclear cells were separated by density gradient centrifugation over Ficoll-Paque. Cytocentrifuge preparations showed that >99% of the mononuclear cells were small mature lymphocytes.

Cytosolic Ba^{2+} measurements by fluorometry

Washed cells (1×10^7 ml^{-1}) suspended in HEPES buffered saline were loaded with fura-2 by incubation in the dark with 2 μM fura-2-acetoxymethyl ester for 20 min at 37°C. The cells were then washed twice and resuspended in HEPES buffered saline. Cells (1.0×10^8 ml^{-1}) were kept at 20°C in the dark and diluted to 2×10^6 ml^{-1} in 3 ml of either 150 mM NaCl medium or 150 mM KCl medium containing HEPES 10 mM, pH 7.4, BSA 1 g l^{-1} and D-glucose 5 mM for fluorometric analysis in a stirred cuvette at 37°C. $BaCl_2$ (3 μl of 1.0 M stock) and nucleotides were added as indicated. Fluorescence measurements were made in a Johnson Foundation fluorometer (Dubyak & De Young, 1985) with excitation at 340 nm and emission at 500 nm. Calibration was performed after each run by adding 10 μl digitonin (7.5 mg ml^{-1}) followed by 5 mM EGTA (Grynkiewicz & Tsien, 1985) with additional NaOH added to elevate pH above 8.5 to obtain minimum fluorescence.

Materials

Ficoll-Plaque (density 1.077) was obtained from Pharmacia (Uppsala, Sweden). ATP, ADP, UTP, 2',3'-dialdehyde ATP (oxidized ATP), 5'-*p*-fluorosulphonybenzoyladenosine (FSBA)

Figure 1 Dose-response curves of Ba^{2+} influx for various nucleotides and analogues. (a) ATP, (b) benzoylbenzoic ATP and (c) 2-methylthio ATP measured in either isotonic KCl media (●) or NaCl media (○). The increment of Ba^{2+} influx produced by each nucleotide was expressed as a percentage of the maximal response to 1.0 mM ATP in KCl media which was defined as 100% response. The curves shown were calculated by non linear regression analyses. Mean values ± s.e. mean from experiments on three donors are shown.

Table 1 Effect of various ATP analogues in inducing Ba^{2+} uptake

	NaCl medium			*KCl medium*		
Agonist	pEC_{50}	(EC_{50} μM)	*Maximal rate**	pEC_{50}	(EC_{50} μM)	*Maximal rate**
ATP	3.73 ± 0.14	(187)	44 ± 11	4.05 ± 0.03	(89)	100 ± 4
Benzoylbenzoic ATP	4.74 ± 0.06	(18)	193 ± 16	5.11 ± 0.05	(8)	189 ± 11
2-Methylthio ATP	3.84 ± 0.19	(146)	42 ± 10	4.03 ± 0.04	(94)	67 ± 3
2-Chloro ATP	3.86 ± 0.15	(137)	26 ± 4	3.81 ± 0.08	(154)	86 ± 15
ATP-γ-S (1 mM)	–		5 ± 3	–		25 ± 8
α,β-Methylene ATP (2 mM)	–		0	–		0
ADP (2 mM)	–		0	–		0
UTP (2 mM)	–		0	–		0
FSBA (100 μM)	–		0	–		0
Oxidized ATP (100 μM)	–		0	–		0

*Maximal rates are expressed as a percentage relative to maximal rate for ATP in KCl media.
Extracellular Ba^{2+} concentration was 1.0 mM. Maximal rates, pEC_{50}s ($-\log_{10}EC_{50}$) and respective standard errors were calculated by non-linear regression analysis of plots of response versus log agonist concentration using the programme Flexifit (Guardabasso *et al.*, 1988). Each value was obtained using data obtained from at least three experiments. Agonists without EC_{50}s were added at the concentration indicated in parentheses.

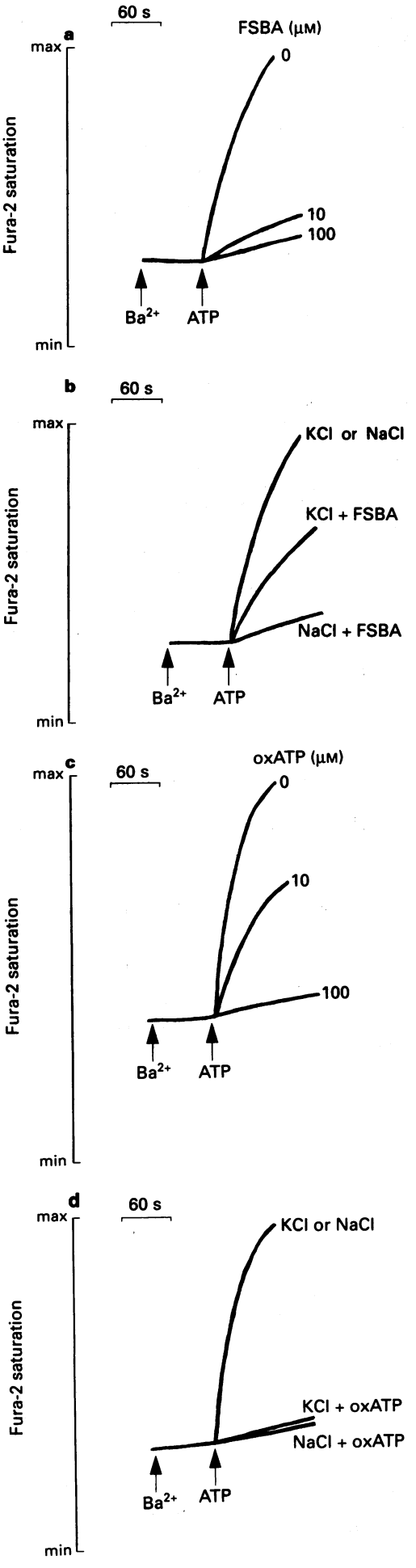

and benzoylbenzoic ATP were from Sigma Chemical Co. (St. Louis, MO, U.S.A.). Fura-2-acetoxymethyl ester was from Molecular Probes (Eugene, OR, U.S.A.). α,β-Methylene ATP, 2-chloroadenosine triphosphate (2-chloro ATP) and 2-methylthio ATP were obtained from Research Biochemicals Inc. (Natick, MA, U.S.A.). Adenosine 5'-0-(3-thiotriphosphate) (ATP-γ-S) was from Boehringer-Mannheim (Sydney, Australia).

Results

Nucleotide specificity of the lymphocyte P_2-receptor

The use of Ba^{2+} as a permeant for the P_{2Z} channel offers a unique advantage over Ca^{2+} since the increase in the fluorescent signal reflects uptake and the Ba^{2+} taken up is neither sequestered nor pumped by transport ATP-ases (Wiley *et al.*, 1983; Yamaguchi *et al.*, 1989; Schilling *et al.*, 1989). Addition of either 1 mM Ba^{2+} or 1 mM ATP to fura-2 loaded lymphocytes incubated in Ca^{2+}-free media resulted in little change in fura-2 fluorescence. This confirms our previous report that extracellular ATP does not cause release of intracellular Ca^{2+} stores in lymphocytes. However, addition of ATP (0.05–1.0 mM) with Ba^{2+} gave a prompt increase in fura-2 fluorescence due to influx of Ba^{2+} ions. The initial slope of the increase in fluorescence was taken as a measure of Ba^{2+} influx. Figure 1a shows the increment in Ba^{2+} influx following addition of ATP showed a sigmoid dependence on the concentration of agonist. EC_{50} values for this effect of ATP are shown in Table 1 and are similar to values (ca. 100 μM) previously reported (Wiley *et al.*, 1993). Figure 1a shows that the maximal Ba^{2+} influx was 2.5 fold greater in KCl media than in NaCl media. Figure 1b shows that benzoylbenzoic ATP was 10 fold more potent than ATP in inducing Ba^{2+} influx in either medium and as little as 8 μM agonist gave half maximal Ba^{2+} influx in KCl media. It is of note that the maximal Ba^{2+} influx induced by benzoylbenzoic ATP was the same in KCl as in NaCl media (Figure 1b). 2-Methylthio ATP was also effective in inducing Ba^{2+} influx into lymphocytes although the maximal Ba^{2+} influx was only 2 fold greater in KCl than in NaCl (Figure 1c). Hill analyses of the data in Figure 1a,b,c gave slope parameters between 1.6 and 3.6, consistent with a positive co-operative effect of all the nucleotide agonists. Table 1 shows maximal Ba^{2+} influx values for different nucleotide agonists together with their EC_{50} values in NaCl and KCl media. The greatest Ba^{2+} influx was achieved with benzoylbenzoic ATP either in NaCl or KCl media. The EC_{50} values showed a rank order of agonist potency in KCl media of: benzoylbenzoic ATP$\geq$ ATP = 2-methylthio ATP = 2-chloro ATP > ATP-γ-S. Neither ADP, UTP nor α,β-methylene ATP at 2 mM concentration could substitute for ATP in stimulating Ba^{2+} influx (Table 1).

Inhibition of P_{2Z}-purinoceptors by 5'-p-fluorosulphonyl benzoyladenosine (FSBA)

FSBA is a known irreversible inhibitor of many ATP-requiring enzymes such as ecto-ATPase (Filippini *et al.*,

Figure 2 Inhibition of ATP-induced Ba^{2+} uptake by 5'-*p*-fluorosulphonylbenzoyladenosine (FSBA) and oxidized ATP. Fura-2 loaded cells were suspended at 2×10^8 ml^{-1} in KCl medium and additions of 1.0 mM Ba^{2+} and 0.1 mM ATP were made as indicated. (a) Cells were preincubated with 0, 10 and 100 μM FSBA in NaCl medium at 37°C for 30 min and then washed twice with KCl medium. (b) Cells were preincubated with 100 μM FSBA in either NaCl or KCl medium at 37°C for 30 min and then washed twice with KCl medium. (c) Cells were preincubated with 0, 10 and 100 μM oxidized ATP in NaCl medium at 37°C for 60 min and then washed twice with KCl medium. (d) Cells were preincubated with 100 μM oxidized ATP in either NaCl or KCl medium at 37°C for 60 min and then washed twice with KCl medium.

1990) as well as the P_2-purinoceptor which mediates ADP-induced platelet activation (Figures *et al.*, 1981). FSBA (100 μM) was not able to induce Ba^{2+} influx into lymphocytes. Preincubation of lymphocytes with 10–100 μM FSBA for 30 min at 37°C inhibited subsequent ATP-induced Ba^{2+} influx whether the inhibitor was still present or was removed by washing (Figure 2a). The maximal inhibition achieved with 100 μM FSBA was ca. 90% and complete inhibition could not be achieved even when inhibitor was present in both pre-incubation and subsequent assay. Neither increasing FSBA concentration to 200 μM nor extending the pre-incubation time achieved 100% inhibition of ATP-induced Ba^{2+} influx. The inhibitory effect of FSBA was greater when the pre-incubation with inhibitor was in Na media than in K-media. Figure 2b shows that FSBA pre-incubation in Na-medium gave 90% inhibition of Ba^{2+} influx compared with 60% inhibition following pre-incubation in K-media.

Irreversible inhibition of P_{2Z}-purinoceptor by oxidized ATP

The 2, 3 dialdehyde derivative of ATP (oxidized ATP) is a potent irreversible inhibitor of P_{2Z}-purinoceptors of mouse macrophages (Murgia *et al.*, 1993). Added alone, oxidized ATP was unable to induce Ba^{2+} influx into lymphocytes (Table 1). Preincubation of lymphocytes with 100 μM oxidized ATP for 60 min followed by washing gave >95% inhibition of ATP-induced Ba^{2+} influx (Figure 2c). Increasing the concentration of oxidized ATP to 300 μM during 60 min preincubation gave 100% inhibition of both ATP-induced and benzoylbenzoic ATP-induced Ba^{2+} influx. Figure 2d shows that this complete inhibition of P_{2Z}-mediated Ba^{2+} influx was independent of whether the preincubation of cells with oxidized ATP (100 μM) was in Na^+ or K^+-media. The irreversible inhibition by oxidized ATP was still evident in cells exposed to inhibitor for 60 min, washed and then incubated for 4 h prior to assay of P_{2Z} channel fluxes.

Discussion

Various subtypes of P_2-purinoceptors have been recognized by characteristic profiles of agonist activities. There are few studies comparing agonist potencies for the P_{2Z}-purinoceptor since few cell types express the P_{2Z} subtype in isolation. Previous studies in mast cells and in human and mouse lymphocytes have shown that 2-chloro ATP, 2-methylthio ATP and ATP-γ-S are all agonists for the P_{2Z}-associated channel in these cell types (Tatham *et al.*, 1988; Wiley *et al.*, 1990; El-Moatassim *et al.*, 1990). Table 1 and Figure 1c show that these three nucleotide agonists are active in stimulating Ba^{2+} influx into human lymphocytes. In a murine macrophage cell line (expressing P_{2Y}, P_{2U} and P_{2Z}), benzoylbenzoic ATP powerfully stimulated influx of Ca^{2+} from the medium without triggering release of internal Ca^{2+} and this effect was attributed to a specific occupancy of P_{2Z}-purinoceptors (El Moatassim & Dubyak, 1992). Our study confirms that benzoylbenzoic ATP is a far more potent agonist than ATP for the P_{2Z}-purinoceptor in human lymphocytes, and produced 2 fold greater maximal Ba^{2+} influx compared to ATP. Indeed benzoylbenzoic ATP stimulated Ba^{2+} influx with EC_{50}s of 8 and 18 μM compared with 89 and 187 μM for ATP in K^+ and Na^+ media respectively. Benzoylbenzoic ATP has also been reported to be >10 fold more potent than ATP in stimulating $^{45}Ca^{2+}$ influx via the P_{2Z}-purinoceptor of rat parotid acinar cells (Soltoff *et al.*, 1992). Table 1 also shows that recognized agonists for P_{2X} (α,β-methylene ATP), for P_{2T} (ADP) and for P_{2U} (UTP) had no activity in human lymphocytes. Furthermore, 2-methylthio ATP and 2-chloro ATP which are potent agonists for P_{2Y}-receptors had only moderate agonist activity in lymphocytes. Finally these data establish a rank order of agonist-induced Ba^{2+} flux for the lymphocyte P_{2Z}-purinoceptor as: benzoylbenzoic ATP>> ATP = 2-methylthio ATP = 2-chloro ATP > ATP-γ-S. A major feature of the P_{2Z}-associated ion channel in lymphocytes is the inhibition of ion fluxes which is observed at high extracellular Na^+ concentrations (Figure 1a).

A similar inhibitory action of extracellular Na^+ on ATP-induced Ca^{2+} transients has been reported for mouse thymocytes (Pizzo *et al.*, 1991) and human lymphocytes but is not observed with Ca^{2+} transients produced by agonists such as anti human immunoglobulin antibody (Wiley *et al.*, 1992), an observation which excludes some generalized effect of extracellular Na^+ on Ca^{2+} homeostasis, e.g. by Ca^{2+}-Na^+ countertransport. Could this inhibitory effect of extracellular Na^+ be due to direct competition between Na^+ and Ba^{2+} (or Ca^{2+}) for passage through the channel? Our previous studies have shown that both Na^+ and Ba^{2+} are permeants for the P_{2Z}-associated ionic channel of lymphocytes (Wiley *et al.*, 1989; 1993). Competitive interactions between Na^+ and Ba^{2+} must occur and provides a partial explanation for the lower Ba^{2+} influxes in the presence of Na^+ (Figure 1a,b,c). However, the data in Figure 1b show maximal Ba^{2+} influx achieved with benzoylbenzoic ATP was independent of the presence or absence of Na^+-ions. This effect is difficult to explain but may result from benzoylbenzoic ATP altering the conformation of the channel in such a way that Na^+ no longer competes effectively with other permeants. Direct effects of external Na^+ ions on ion-channel conformation have been described for the amiloride-sensitive Na^+ channel in frog skin, where Na^+ ions react with modifying sites located on or near the Na^+-conductive protein to self-inhibit the Na^+ current (Sariban-Sohraby & Benos, 1986). Likewise Na^+ ions have been reported to reduce the Ca^{2+} current through L-type calcium channels by modulating the conformation of the channel (Balke & Wier, 1992).

Finally, the irreversible inhibition of ATP-induced Ba^{2+} influx in human lymphocytes by oxidized ATP confirms the proposal of Murgia *et al.* (1993) who suggest that this 2, 3 dialdehyde derivative of ATP is a potent inhibitor of P_{2Z}-channels in the J774 mouse macrophage cell line. Our data also show that FSBA irreversibly inhibits 60–90% of the P_{2Z} channel fluxes of lymphocytes and the inhibition was more complete when the inhibitor was added to the cells in Na^+ media than in K^+ media (Figure 2b). This observation provides further evidence that extracellular Na^+ ions may modify the conformation of the ATP-binding site on the P_{2Z} channel. Although the role of the ATP^{4-} receptor-operated ion channel in lymphocyte function is yet to be elucidated, the application of these irreversible inhibitors may enable a role for this channel to be tested in processes as diverse as apoptosis and intercellular signalling.

We thank Dr Arthur Conigrave and Dr David Satchell for helpful comments. This work was supported by a grant from the National Health and Medical Research Council of Australia.

References

BALKE, C.W. & WIER, W.G. (1992). Modulation of L-type calcium channels by sodium ions. *Proc. Natl. Acad. Sci. U.S.A*, **89**, 4417–4421.

BENHAM, C.D. & TSIEN, R.W. (1987). A novel receptor-operated Ca^{2+}-permeable channel activated by ATP in smooth muscle. *Nature*, **328**, 275–278.

BURNSTOCK, G. (1990). Purinergic mechanisms. *Ann. N.Y. Acad. Sci.*, **603**, 1–17.

DUBYAK, G.R. & DE YOUNG, M.B. (1985). Intracellular Ca^{2+} mobilisation activated by extracellular ATP in Ehrlich ascites tumor cells. *J. Biol. Chem.*, **260**, 10653–10661.

DUBYAK, G.R. & EL-MOATASSIM, C. (1993). Signal transduction via P_2-purinergic receptors for extracellular ATP and other nucleotides. *Am. J. Physiol.*, **265**, C577–C606.

EL-MOATASSIM, C. & DUBYAK, G.R. (1992). A novel pathway for the activation of phospholipase D by P_2Z purinergic receptors in BAC1.2F5 macrophages. *J. Biol. Chem.*, **267**, 23664–23673.

EL-MOATASSIM, C., MANI, J.C. & DORNAND, J. (1990). Extracellular ATP4- permeabilizes thymocytes not only to cations but also to low-molecular-weight solutes. *Eur. J. Pharmacol.*, **181**, 111–118.

FIGURES, W.R., NIEWIAROWSKI, S., MORINELLI, T.A., COLMAN, R.F. & COLMAN, R.W. (1981). Affinity labelling of a human platelet membrane protein with 5'-p-fluorosulfonylbenzoyl adenosine. *J. Biol. Chem.*, **256**, 7789–7795.

FILIPPINI, A., TAFFS, R.E., AGIU, T. & SITKOVSKY, M. (1990). Ecto-ATPase activity in Cytolytic T-lymphocytes. Protection from the cytolytic effects of extracellular ATP. *J. Biol. Chem.*, **265**, 334–340.

GORDON, J.L. (1986). Extracellular ATP: effects, sources and fate. *Biochem. J.*, **233**, 309–319.

GREENBERG, S., DIVIRGILIO, F., STEINBERG, T.H. & SILVERSTEIN, S.C. (1988). Extracellular nucleotides mediate Ca^{2+} fluxes in J774 macrophages by two distinct mechanisms. *J. Biol. Chem.*, **263**, 10337–10343.

GRYNKIEWICZ, G.P.M. & TSIEN, R.Y. (1985). A new generation of Ca^{2+} indicators with greatly improved fluorescence properties. *J. Biol. Chem.*, **260**, 3440–3450.

GUARDABASSO, V., MUNSON, P.J. & RODBARD, D. (1988). A versatile method for simultaneous analysis of families of curves. *FASEB J.*, **2**, 209–215.

MURGIA, M., HANAU, S., PIZZO, P., RIPPA, M. & DIVIRGILLIO, F. (1993). Oxidised ATP. An irreversible inhibitor of the macrophage purinergic P_2Z receptor. *J. Biol. Chem.*, **268**, 8199–8203.

PIZZO, P., ZANOVELLO, P., BRONTE, V. & DIVIRGILIO, F. (1991). Extracellular ATP causes lysis of mouse thymocytes and activates a plasma membrane ion channel. *Biochem. J.*, **274**, 139–144.

SARIBAN-SOHRABY, S. & BENOS, D.J. (1986). The amiloride-sensitive sodium channel. *Am. J. Physiol.*, **250**, C175–C190.

SCHILLING, W.P., RAJAN, L. & STROBL-JAGER, E. (1989). Characterization of the bradykinin-stimulated calcium influx pathway of cultured vascular endothelial cells. *J. Biol. Chem.*, **264**, 12838–12848.

SOLTOFF, S.P., MCMILLAN, M.K. & TALAMO, B.R. (1992). ATP activates a cation-permeable pathway in rat parotid acinar cells. *Am. J. Physiol.*, **262**, C934–C940.

TATHAM, P.E.R., CUSACK, N.J. & GOMPERTS, B.D. (1988). Characterization of the ATP^{4-} receptor that mediates permeabilisation of rat mast cells. *Eur. J. Pharmacol.*, **147**, 13–21.

TATHAM, P.E.R. & LINDAU, M. (1990). ATP induces pore formation in the plasma membrane of rat peritoneal mast cells. *J. Gen. Physiol.*, **95**, 459–476.

WILEY, J.S., CHEN, R. & JAMIESON, G.P. (1993). The ATP^{4-} receptor-operated channel (P_2Z class) of human lymphocytes allows Ba^{2+} and ethidium$^+$ uptake: inhibition of fluxes by suramin. *Arch. Biochem. Biophys.*, **305**, 54–60.

WILEY, J.S., CHEN, R., WILEY, M.J. & JAMIESON, G.P. (1992). The ATP^{4-} receptor-operated ion channel of human lymphocytes. Inhibition of ion fluxes by amiloride analogues and by extracellular sodium ions. *Arch. Biochem. Biophys.*, **292**, 411–418.

WILEY, J.S. & DUBYAK, G.R. (1989). Extracellular adenosine triphosphate increases cation permeability of chronic lymphocytic leukemic lymphocytes. *Blood*, **73**, 1316–1323.

WILEY, J.S., JAMIESON, G.P., MAYGER, W., CRAGOE, E.J.Jr. & JOPSON, M. (1990). Extracellular ATP stimulates an amiloride-sensitive sodium influx in human lymphocytes. *Arch. Biochem. Biophys.*, **280**, 263–268.

YAMAGUCHI, D.T., GREEN, J., KLEEMAN, C.R. & MUALLEM, S. (1989). Properties of the depolarization-activated calcium and barium entry in osteoblast-like cells. *J. Biol. Chem.*, **264**, 197–204.

(Received January 4, 1994
Revised February 25, 1994
Accepted March 31, 1994)

Br. J. Pharmacol. (1994), **112**, 951–957

Lack of effect of microinjection of noradrenaline or medetomidine on stimulus-evoked release of substance P in the spinal cord of the cat: a study with antibody microprobes

[1]C.W. Lang, [2]P.J. Hope, [3]B.D. Grubb & [4]A.W. Duggan

Department of Preclinical Veterinary Sciences, Royal (Dick) School of Veterinary Studies, University of Edinburgh, Summerhall, Edinburgh EH9 1QH

1 Experiments were performed on barbiturate anaesthetized, spinalized cats to investigate the effect of microinjected noradrenaline or medetomidine on the release of immunoreactive substance P in the dorsal spinal cord following peripheral nerve stimulation. The presence of immunoreactive substance P was assessed with microprobes bearing C-terminus-directed antibodies to substance P.

2 Noradrenaline or medetomidine were microinjected into the grey matter of the spinal cord, near microprobe insertion sites, at depths of 2.5, 2.0, 1.5 and 1.0 mm below the spinal cord surface with volumes of approximately 0.125 μl and a concentration of 10^{-3}M.

3 In the untreated spinal cord, electrical stimulation of the ipsilateral tibial nerve (suprathreshold for C-fibres) elicited release of immunoreactive substance P which was centred in and around lamina II. Neither noradrenaline nor medetomidine administration in the manner described produced significant alterations in this pattern of nerve stimulus-evoked release.

4 In agreement with recent ultrastructural studies these results do not support a control of substance P release by catecholamines released from sites near to the central terminals of small diameter primary afferent fibres.

Keywords: Antibody microprobes; substance P release; spinal cord; peripheral nerve stimulation; microinjection; noradrenaline; medetomidine

Introduction

Although there is considerable information on the brainstem sites of origin of descending pathways controlling spinal transmission of nociceptive information, comparatively little is known about the mechanisms operating at the spinal termination of these pathways. A wealth of evidence suggests that release of the monoamines, noradrenaline (NA) and 5-hydroxytryptamine (5-HT), mediates, in part, brainstem control of spinal nociceptive transmission. This evidence includes the effects of agonists applied either topically to the spinal cord (mouse: (Hylden & Wilcox, 1983) rat: (Camarata & Yaksh, 1985; Sullivan *et al.*, 1987; Solomon & Gebhart, 1988; Gordh *et al.*, 1989; Tseng & Tang, 1989; Danzebrink & Gebhart, 1990; Tjolsen *et al.*, 1990; Uhlen *et al.*, 1990; Fisher *et al.*, 1991; Hylden *et al.*, 1991; Takano & Yaksh, 1991) cat: (Collins *et al.*, 1984; Nakagawa *et al.*, 1990) sheep (Waterman *et al.*, 1988)) or near to single neurones in the dorsal spinal cord (Headley *et al.*, 1978; Jeftinija *et al.*, 1981; Nagy & Hunt, 1982; Curtis *et al.*, 1983; Davies & Quinlan, 1985; Fleetwood-Walker *et al.*, 1985; Zhao & Duggan, 1987) and the behavioural effects of electrical stimulation of brain stem areas exhibiting monamine containing cell bodies (rat: (Reynolds, 1969), and man (Meyerson *et al.*, 1979)). In addition there is a dense plexus of catecholamine containing nerve terminals (rat: (Schroder & Skagerberg, 1985; Rajaofetra *et al.*, 1992), cat: (Lackner, 1980; Doyle & Maxwell, 1991a), primate (Westlund *et al.*, 1984)), and a marked density of catecholamine bindings sites (rat: (Young & Kuhar, 1980), Jones *et al.*, 1982; Unnerstall *et al.*, 1984; Giron *et al.*, 1985), sheep: (Bouchenafa & Livingston, 1987) and man: (Unnerstall *et al.*, 1984)), in the superficial dorsal spinal cord, the main area of termination of small diameter primary afferent fibres.

One hypothesis for a mechanism of selective analgesia at the spinal level is a presynaptic reduction in transmitter release from primary afferent terminals of nociceptive origin. This has been investigated by a number of methods for several compounds including NA. These methods include both *in vivo* and *in vitro* transmitter release studies (Kuraishi *et al.*, 1985; Pang & Vasko, 1986; Ono *et al.*, 1991) and electrophysiological assessments of changes in the excitability of the spinal terminations of primary afferent fibres in response to compounds administered microionophoretically (Jeftinija *et al.*, 1981; Nagy & Hunt, 1982; Curtis *et al.*, 1983). Such studies however, have produced controversial results and the spinal mechanisms underlying supraspinal controls involving monoamines remain unresolved.

The most direct method of investigating a possible presynaptic control by monoamines of transmission of information conveyed by nociceptors is to measure transmitter release in the dorsal spinal cord, in response to defined peripheral noxious stimuli, before and after monoamine application close to the releasing terminals. The tachykinin neuropeptide substance P (SP) has been shown, by a variety of techniques, to be released in the spinal dorsal horn following peripheral noxious stimuli. With the antibody microprobe technique, such release in spinal cats has been shown to be centered on laminae I and II, the major sites of termination of cutaneous small diameter primary afferents (Duggan *et al.*, 1988b; 1991; 1992; Schaible *et al.*, 1992). Controls of transmitter release from the central terminals of peripheral nociceptors might, therefore, be reasonably expected to influence the stimulus-evoked release of SP in laminae I and II of spinal cats. In the present series of experiments antibody microprobes have been used to measure the release of immunoreactive SP (irSP) in the superficial dorsal horn in

Present addresses: [1] Department of Physiology, Medical School, University of Bristol, Bristol, BS8 1TD; [2] Syntex Research Centre, Research Park South, Riccarton, Edinburgh, EH14 4AP; [3] Department of Cell Physiology and Pharmacology, University of Leicester, PO Box 138, Leicester, LE1 9HN.
[4] Author for correspondence.

response to electrical stimulation of unmyelinated primary afferent fibres. The effects of NA microinjection from a micropipette with its tip positioned in the region of the substantia gelatinosa have been evaluated in terms of any change in the subsequent pattern of stimulus evoked irSP detection. Because of existing evidence that the relevant receptors mediating the antinociceptive action of spinal NA are of the α_2-adrenoceptor type (Fleetwood-Walker *et al.*, 1985), the effects of the highly selective α_2-adrenoceptor agonist, medetomidine hydrochloride, were also studied.

Methods

Animal preparation

Experiments were carried out on 7 barbiturate-anaesthetized cats. These were skeletally mature animals, males and females, bred specifically for research purposes and with body weights in the range of 2.5–3 kg. Induction of anaesthesia was by intraperitoneal injection of pentobarbitone sodium (35 mg kg^{-1}) and maintenance was by a continuous intravenous infusion of the same compound (3 mg kg^{-1} h^{-1}). All animals were artificially ventilated following neuromuscular paralysis with gallamine (4 mg kg^{-1} h^{-1}). Gallamine was subsequently administered intermittently to allow adequate checks on the level of anaesthesia. Blood pressure was monitored via a cannulated carotid artery and end-tidal CO_2 levels were continually monitored and maintained at 4%.

The lumbar spinal cord was exposed by removal of the overlying bony laminae and the spinal cord was then transected at the thoraco-lumbar junction following intraspinal injection of 0.1 ml of a 2% lignocaine solution. The lumbar dura mater was cut longitudinally and retracted laterally. A thin layer of Ringer/agar was then placed over the dorsal surface of the exposed spinal cord. At sites of proposed microprobe insertion an area of agar and a small part of the underlying pia-arachnoid were removed with sterile fine forceps. The area of the spinal cord exposed in this way was then irrigated with a sterile Ringer solution held at 37°C by a heat exchanger jacket around the delivery tube. Following the induction of anaesthesia, cats received two intramuscular injection of ampicillin, 25 mg kg^{-1}, 10 h apart. When measuring neuropeptide release by any method it is important to have near sterile conditions (Duggan, 1992).

Although irSP release in the superficial dorsal horn is evoked by a variety of noxious peripheral stimuli (Duggan *et al.*, 1988b), it is difficult to deliver such stimuli repeatedly without damaging peripheral tissues and thus altering the firing of peripheral nociceptors to successive stimuli. For this reason, electrical stimulation of unmyelinated primary afferent fibres in the tibial nerve was used to elicit spinal release of irSP in the present series of experiments. The right and left tibial nerves were exposed in the lower limb, immersed in liquid paraffin and mounted on platinum stimulating electrodes. Stimulation was with square wave pulses, 0.3 ms duration, with an amplitude of at least 80 times the threshold stimulus needed to produce a short latency field potential as measured with a recording electrode placed in the upper dorsal horn. Stimulus frequency was 20 Hz and stimulation duration was 10 min in every case.

Microprobe preparation

Antibody microprobes were prepared as previously described (Duggan *et al.*, 1988a; Duggan, 1992). Briefly, fine glass micropipettes, heat sealed at both ends, were incubated in a 10% solution of aminopropyltriethoxysilane in toluene. This produced a siloxane polymer layer on the outer surfaces of the microprobes and glutaraldehyde was then used to immobilize protein A (Sigma) to this polymer. Protein A then bound immunoglobulins present in a polyclonal antiserum containing antibodies directed at the C-terminus of SP (Peninsula Laboratories). These antibodies bind SP and fragments of SP containing at least the last five amino acid residues; data from the manufacturer indicates negligible cross-reactivity with either neurokinin A or neurokinin B.

Microprobes were inserted into the spinal cord, in pairs, with stepping motor micromanipulators. Prior to insertion, microprobes had both ends removed to allow filling with a solution of pontamine sky blue to aid visualization of the tips. With the first probe introduced into a particular area of the spinal cord, it was usual to obtain extracellular recordings during introduction into the spinal cord in order to confirm that fibres in the ipsilateral tibial nerve did project to that area. All microprobes were inserted to a depth of 4 mm which, in the lumbar spinal cord of the adult cat, places the tip in the ventral horn. Microprobes were left *in situ* for 10 min following insertion into the cord, during which time either (a) no peripheral stimulus was applied to allow detection of basal irSP levels or (b) the ipsilateral tibial nerve was stimulated as previously described, with or without prior drug application (see results). Insertions of consecutive pairs of antibody microprobes, in the same area of the spinal cord, were at intervals of at least 25 min.

The antibody microprobe technique detects bound endogenous ligand by the subsequent failure of binding of exogenous radiolabelled ligand. Thus, following removal from the spinal cord, microprobes were washed for 15 min in a cold solution of phosphate-buffered saline (PBS) containing Tween (0.1%) and then incubated for 24 h at 6°C in a PBS-azide solution of (Bolton-Hunter) ^{125}I-radiolabelled SP (Amersham) containing 0.5% bovine serum albumin. This solution was diluted to give approximately 2000 counts min^{-1} μl^{-1}. After this incubation, microprobes were again washed for 15 min in cold PBS-Tween, while continually drawing the solution through the tips to remove any radiolabelled SP from the inside. The tips were then carefully broken off about 1 cm back and glued to a sheet of paper which was placed in an X-ray film cassette with a sheet of monoemulsion film (Kodak NMB).

The resulting X-ray film images of microprobes were analysed with an image analysis system employing an Imaging Technology PC Vision Plus frame grabber board operating in a Data Control Systems 286e (AT based) computer. A CCD camera scanned each image and, as described previously (Hendry *et al.*, 1988), after background subtraction in a transverse integration of the optical density of the image of each microprobe was executed at defined intervals. With the magnification used and the resolution of the image analysis system (512 by 512 locations per frame) this corresponds to a 10 μm interval for transverse integrations. The resultant integrals were stored on a hard disk record which included 40 coded values for each individual image relevant to the experimental conditions surrounding it. An analysis programme subsequently obtained groups of microprobes which met stated criteria and obtained the mean image analysis of each group. This mean image analysis was plotted with respect to distance from spinal cord surface (see Figures 1a, 2 and 3a). In addition, differences between the mean image analyses of control and experimental groups were obtained, t statistics were then calculated and a probability of significance assigned to the difference in the mean grey scale values at each analysis point (see Figures 1b and 3b). It is important to emphasize the spatial resolution of this technique. For microprobes inserted into the spinal cord events are examined optically at 100 sites per mm. Since such a resolution exceeds the biological resolution of the microprobe technique, the mean of 3 successive sites was calculated and stored giving an approximate resolution of 33 sites per mm.

During *in vitro* tests of antibody microprobes, [^{125}I]-SP was bound to a representative group of probes. At least 50% suppression of this binding of radioactive SP was achieved by prior incubation of the microprobes in a solution of 10^{-7} M unlabelled SP for 30 min at 37°C.

Microinjection of drug solutions

NA and medetomidine (a gift from Farmos) solutions (10^{-3} M in sterile Ringer) were microinjected into the dorsal horn from micropipettes (tip diameter 20–40 μm) positioned with a micromanipulator to the appropriate regions and at depths of 1.0, 1.5, 2.0, and 2.5 mm below the dorsal spinal cord surface. Although in the cat, the peak release of irSP evoked by tibial nerve stimulation is in the superficial dorsal horn, 1.1 mm below the cord surface, (Duggan *et al.*, 1988b; 1991; 1992; Schaible *et al.*, 1992), there is significant release from approximately 0.5 to 1.0 mm deep in this area. Hence the microinjections were performed at sites deep in the region of the substantia gelatinosa. The total drug volume was 0.5 μl, i.e. 0.125 μl at each site. Previous experiments (Duggan *et al.*, 1991; 1992; Schaible *et al.*, 1992) have shown that microinjections of Ringer solution (or of PBS), in comparable or larger volumes to those used in the present study, have no effect on the stimulus-evoked release of irSP in this region of the spinal cord.

The timing of microinjections in relation to the application of stimuli evoking release of irSP is important in experiments of this type for several reasons. Firstly, if a compound is inactivated quickly, the microinjection may need to be performed whilst a microprobe is already *in situ* and a stimulus being delivered. Previous experiments with neuropeptide (NPY) microinjection (Duggan *et al.*, 1991), inhibitors of endopeptidase 24.11 (Duggan *et al.*, 1992) and calcitonin gene-related peptide (CGRP) (Schaible *et al.*, 1992) showed that this was not necessary with these compounds. Secondly, the injected compound may need to diffuse within the spinal cord for an effect of irSP release to be detected; this implies a need to inject some time prior to testing for inhibition of release. In the present experiments injections of NA or medetomidine were performed after control microprobes (either no stimulus or nerve stimulus controls) had been removed from the cord and these microinjections were then given gradually over a 5 min period. Subsequent pairs of microprobes were then inserted as rapidly as possible into the cord and were typically *in situ* 1–2 min after cessation of drug microinjection. Drug microinjections and subsequent microprobe insertions during nerve stimulation were always at least 25 min after the preceding period of ipsilateral tibial nerve stimulation.

Both NA and medetomidine were microinjected using 10^{-3} M solutions and in volumes of approximately 0.125 μl at each site. These volumes correspond to spheres with a radius of approximately 340 μm and in the absence of a removal mechanism, such as neuronal uptake, a 10 fold reduction in concentration (to 10^{-4} M) will occur with an expansion of this sphere, by diffusion, to a radius of 736 μm. Drug absorption into local blood vessels will reduce the concentration still further, but as the starting concentrations for both NA and medetomidine were relatively high and the drugs were also administered close to the major zone of primary afferent fibre termination, the concentrations of drug used should have been sufficient to reveal any action at such sites. This methodology has successfully altered the pattern of release of SP following microinjection of NPY or CGRP (Duggan *et al.*, 1991; Schaible *et al.*, 1992).

Results

Stimulus-evoked release of immunoreactive substance P

The mean image analyses of 13 microprobes inserted 4 mm into the spinal cord and left for 10 min in the absence of peripheral nerve stimulation, and 24 microprobes inserted for the same time and to the same depth but during electrical stimulation of myelinated and unmyelinated primary afferents of the ipsilateral tibial nerve are illustrated in Figure 1a. These microprobes are derived from the same experiments.

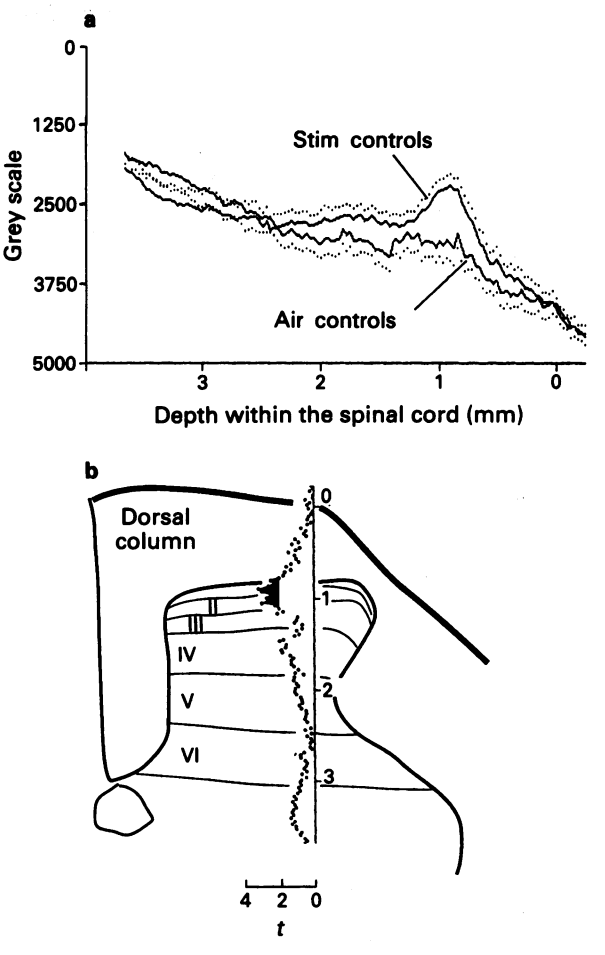

Figure 1 Nerve stimulus-evoked release of immunoreactive-substance P in the superficial dorsal horn. (a) The mean image analysis of two groups of microprobes are plotted: those which remained in the spinal cord for 10 min and no peripheral stimulus was applied (air controls, $n = 13$) and those present in the spinal cord during electrical stimulation of myelinated and unmyelinated afferents of the ipsilateral tibial nerve (skin controls, $n = 24$). The mean grey scale of microprobes was calculated in 30 μm intervals and a line joins these points. At each point the s.e.mean (+ for Stim controls, – for air controls) is plotted. (b) A plot of the t statistics derived from the differences of the means from the two groups of microprobes shown in (a). This plot is superimposed on a diagram of a cross section of the lumbar spinal cord of the cat and the hatched area indicates where these differences are significant with a probability of <0.05.

Significant differences between these mean image analyses occur from 0.7 to 1.2 mm from the dorsal surface of the spinal cord, and there is also a smaller zone of significance approximately 1.5 mm below the cord surface. The distribution of significant differences between the two groups is illustrated in Figure 1b. The maximal difference occurs at a depth of 1.0 mm below the spinal cord surface. This site of maximal release approximates to the substantia gelatinosa and lamina I of the dorsal grey matter and agrees with the findings of previous studies (Duggan *et al.*, 1988b; 1991; 1992; Schaible *et al.*, 1992). When dye is ejected from the tip of a single microprobe and its position in the spinal cord subsequently determined in a spinal cord section, then sites of neuropeptide release can be inferred with great accuracy. With mean image analyses, as presented here, the location of sites of release is less precise. With microprobes inserted a fixed distance into the spinal cord (4 mm in this series of experiments) the relationship of spinal laminae to distance from the tip will vary between individual animals, and also with distance from the midline. When encoding the information describing the position of a microprobe, a correction

factor is included when appropriate, but the relative broadness of the sites of release of irSP results in part from these anatomical differences.

Microprobes present in the spinal cord following microinjection of noradrenaline

The mean image analyses of 38 microprobes inserted 4 mm into the spinal cord for 10 min with concurrent electrical stimulation of myelinated and unmyelinated afferents of the ipsilateral tibial nerve (stim. controls) and 35 microprobes inserted under the same conditions but following the injection of 10^{-3} M NA at depths of 1.0, 1.5, 2.0 and 2.5 mm below cord surface in the area of subsequent microprobe insertions (post NA) are illustrated in Figure 2. The two groups of microprobes are derived from the same experiments. The two mean image analyses are virtually identical and at no points do the differences between them approach statistical significance (at $P<0.05$).

Microprobes present in the spinal cord following microinjection of medetomidine

The mean image analyses of 31 microprobes inserted 4 mm into the spinal cord for 10 min with concurrent electrical stimulation of the myelinated and unmyelinated afferents of the ipsilateral tibial nerve (stim. controls) and 20 microprobes inserted under the same conditions but following the microinjection of 10^{-3} M medetomidine at depths of 1.0, 1.5, 2.0 and 2.5 mm below the spinal cord surface in the area of subsequent microprobe insertion (post Med) are illustrated in Figure 3a. These two groups are again derived from the same experiments, i.e. the 'Stim control' groups illustrated in Figures 2 and 3a do not represent the same microprobes. Although the post medetomidine group is displaced above the control group at sites deep to the superficial dorsal horn, (suggestive of increased release) there are no statistically significant differences between the two groups within the spinal cord at shown in Figure 3b. A small area of increased irSP detection following medetomidine microinjection is evident at the cord surface. This has been an observation in previous studies with microprobes and has been related to the late development of inflammation at the sites of removal of pia mater at the cord surface (Duggan *et al.*, 1988b) in some experiments. Hence it is more likely to be seen in the post injection than pre injection microprobes.

Thus, neither 10^{-3} M NA nor 10^{-3} M medetomidine, microinjected directly into the dorsal spinal cord, had any significant effect on the subsequent nerve stimulus-evoked release of irSP.

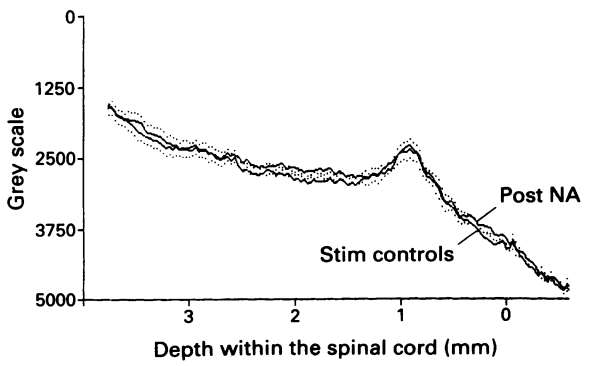

Figure 2 Lack of effect of microinjection of noradrenaline (NA) into the dorsal horn on the nerve-stimulus-evoked release of immunoreactive-substance P. The mean image analysis of two groups of microprobes are plotted: those present in the spinal cord for 10 min during electrical stimulation of myelinated and unmyelinated afferents of the ipsilateral tibial nerve (Stim controls, $n=38$) and those with comparable stimulation but inserted after microinjection of noradrenaline (10^{-3} M) into the dorsal horn (post NA, $n=35$). The format of plotting is similar to that of Figure 1a.

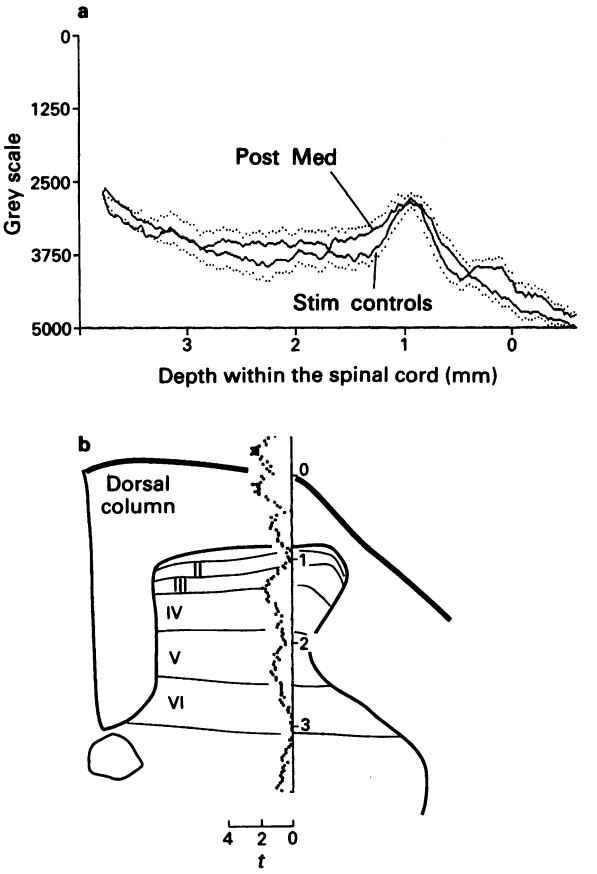

Figure 3 Lack of effect of microinjection of medetomidine into the dorsal horn on the nerve stimulus-evoked release of immunoreactive-substance P. (a) The mean image analysis of microprobes present in the spinal cord for 10 min during electrical stimulation of myelinated and unmyelinated primary afferents of the ipsilateral tibial nerve (Stim controls, $n=31$) and those with comparable stimulation but inserted after microinjection of medetomidine (10^{-3} M) into the dorsal horn (post Med, $n=20$). (b) A plot of the t-statistics derived from the differences of means of the two groups shown in (a) is superimposed on a diagram of the lumbar spinal cord of the cat. The hatched area indicates significant differences with a probability of <0.05.

Discussion

The present results are part of an extended study of possible presynaptic controls of tachykinin release from the central terminals of nociceptors. Presynaptic inhibition of transmitter release from such terminals has been proposed as important in several mechanisms of analgesia, including that resulting from impulses arriving in large diameter afferents (Melzack & Wall, 1965) and that produced by electrical stimulation of certain brainstem regions (Reynolds, 1969; Meyerson *et al.*, 1979).

There is evidence that, in acutely spinalized cats, the irSP detected by microprobes and localized to the region of the substantia gelatinosa following peripheral nerve stimulation, is largely released from the central terminals of primary afferent fibres. The substantia gelatinosa is the major site of termination of cutaneous unmyelinated primary afferent fibres (Sugiura *et al.*, 1986), and a proportion of these are known to contain substance P (Nagy & Hunt, 1982; Price, 1985). A contribution from intrinsic substance P-containing spinal neurones is possible, but in the spinalized animal

release from fibres of supraspinal origin cannot have occurred. Thus physiological controls acting on the terminals of unmyelinated primary afferents should be revealed by this methodology, provided the compounds are administered in a relevant manner.

Although microinjection of NA directly into the substantia gelatinosa had no effect on the stimulus-evoked release of irSP, administration of drugs in this manner has previously been shown to be an effective way of modulating stimulus-evoked irSP release. Microinjection of NPY was shown to reduce irSP detection following peripheral nerve stimulation (Duggan *et al.*, 1991). Conversely, microinjection of CGRP or of a mixture of the peptidase inhibitor drugs, kelatorphan and enalaprilat, enhanced post-stimulus detection of irSP by antibody microprobes (Duggan *et al.*, 1992; Schaible *et al.*, 1992). Microinjections of comparable volumes of Ringer or PBS solutions in these studies were without effect. NA may, following microinjection, have been subject to rapid re-uptake and degradation in the spinal cord. Medetomidine, a synthetic compound, does not appear to be subject to any re-uptake mechanism (R. Virtanen, Farmos, personal communication). Following systemic administration, medetomidine is metabolized by hydroxylation in the liver (Salonen & Eloranta, 1990) but little is known of its elimination from the central nervous system.

The current observation that NA was ineffective in reducing noxious stimulus-evoked irSP release disagrees with earlier studies of catecholamines and SP release from the spinal cord. Ono *et al.* (1991) demonstrated that clonidine (10^{-5} M) and tizanidine (10^{-9} M), both α_2-adrenoceptor agonist drugs, reduced the veratridine-induced release of SP from slices of rat spinal cord *in vitro*. This effect was blocked by yohimbine (10^{-5} M) and also by prazosin (10^{-5} M), suggesting the involvement of α_{2B}-adrenoceptors. Pang & Vasko (1986), reported that NA (10^{-5} M) inhibited the high potassium-evoked release of SP from a rat spinal cord slice. Veratridine application or simple elevation of extracellular potassium levels do not selectively activate primary afferent fibres and perfusion of cord slices allows no spatial resolution of the source of neurotransmitter release. Thus SP will probably be released from a host of structures in these experiments, including fibres of supraspinal/propriospinal origin and intrinsic neurones of the slice as well as primary afferent terminals. Thus the action of α_2-agonists cannot necessarily be related to an action on primary afferent terminals.

More directly comparable to the present study are the experiments of Kuraishi *et al.* (1985) who reported that NA (10^{-5} M) added to the perfusate of a push-pull cannula inserted into the upper dorsal horn of rabbit spinal cord *in vivo* reduced the release of irSP in response to a peripheral noxious mechanical stimulus. The cannulae used were of 600 μm outer diameter and the flow rate was 50 μl min^{-1} (0.83 μl s^{-1}). Although it is uncertain how much of the perfusate passing through a push-pull cannula escapes into the surrounding tissue, 0.83 μl s^{-1} is a relatively large flow rate in relationship to the dimensions of the dorsal horn of the rabbit. The distance from the dorsal surface of the spinal cord to lamina I of the grey matter is approximately 1 mm and as 1 μl represents 1 mm^3, it is probable that administration of NA in this way results in activation of adrenoceptors over a very wide area of the spinal grey and white matter.

Indeed, an important distinction between the present study and those in which effects on SP release have been observed is the method of drug administration. In our experiments, NA and medetomidine microinjections were restricted to the dorsal horn and the volumes were relatively small.

Experiments in which large volumes of drug containing solutions are administered will access the intraspinal preterminal regions of primary afferents running rostally and caudally in the white matter and this could be a cause of reduced stimulus-evoked release of SP which is not related to a physiological mechanism. There is good evidence for 5-HT receptors on the peripheral branches of unmyelinated primary afferents (Neto, 1978) and for γ-aminobutyric acid (GABA) receptors on undefined peripheral nerve fibres (Sakatani *et al.*, 1991). A recent study (Sakatani *et al.*, 1993) found that GABA, 10^{-4} M, applied to the hemisected spinal cord of the neonatal rat, reduced the amplitude of the compound action potential resulting from propagation of impulses along dorsal column fibres. This was a receptor-mediated and not a local anaesthetic type of effect since it was reversed by bicuculline. Such a block of conduction in some fibres would reduce transmitter release at the relevant terminals. Thus caution is needed in interpreting the results of experiments in which adrenoceptor agonists are administered either diffusely to a slice preparation or intraspinally in large volumes as necessarily revealing a physiological control of SP released from the central terminals of nociceptors. Although we do not know the precise areas at which pharmacologically active doses of these compounds were present in our experiments, it is probable that restricting administration to areas near the central terminals of nociceptors is more likely to study controls acting at those terminals.

Ultrastructural studies have also failed to find evidence for a synaptic control by catecholamines of transmitter release from the central terminals of nociceptors. In both the rat (Sugiura *et al.*, 1986) and cat (Doyle & Maxwell, 1991a,b; 1993a) axo-axonic contacts containing dopamine-β-hydroxylase or tyrosine hydroxylase in the presynaptic element were not identified in the region of the substantia gelatinosa, the major site of termination of small diameter primary afferent fibres. Axo-dendritic and axo-somatic contacts were readily identified in the same area. These contacts have also been observed with identified lamina I spinothalamic tract cells of the monkey (Price, 1985). It is interesting to note that previous results from our laboratory which provided evidence for a control by NPY of the spinal release of SP following activation of peripheral nociceptors (Duggan *et al.*, 1991) have been supported by recent ultrastructural studies (Doyle & Maxwell, 1993b).

Electrophysiological studies of the effects of NA and 5-HT on the electrical excitability of the central terminals of small diameter primary afferents have given results allowing for more than one interpretation, and have not helped resolve the issue of whether presynaptic α_2-adrenoceptors are involved in physiological controls at such sites. With large diameter primary afferents, presynaptic inhibition by GABA is mediated by a terminal depolarization detected as an increased excitability to stimulation by an adjacent microelectrode (Curtis *et al.*, 1977). Both Carstens *et al.* (1982) and Jeftinija *et al.* (1981) found that microiontophoretically administered monoamines increased the electrical threshold of the central terminals of small diameter afferents. Curtis *et al.* (1983) suggested that this was an artifact due to an altered current distribution during electrical stimulation as a result of glial uptake of administered NA or 5-HT, rather than a novel mechanism of presynaptic inhibition.

The present results do not support the proposal that there is a physiological control of SP release from the central terminals of nociceptors mediated by α_2-adrenoceptors. This is in accord with ultrastructural and electrophysiological observations. It is more probable that the potent effects of α_2-adrenoceptor agonists in suppressing spinal transmission of nociceptive information result from postsynaptic actions on neurones of the spinal cord. We believe that experiments purporting to support presynaptic control mechanisms are difficult to interpret both in terms of the source of the released SP by the stimuli used, and/or the sites accessed by the method of drug administration.

Assistance with this work was provided by M. Arnott, E. Rogers, C. Warwick and E.J. Chalmers. Animals were cared for in the Wellcome Animal Unit of the Faculty of Veterinary Medicine. Support was provided by the Wellcome Trust and the Agricultural Food Research Council.

References

BOUCHENAFA, O. & LIVINGSTON, A. (1987). Autoradiographic localisation of alpha 2 adrenoceptor binding sites in the spinal cord of the sheep. *Res. Vet. Sci.*, **42**, 382–386.

CAMARATA, P.J. & YAKSH, T.L. (1985). Characterization of the spinal adrenergic receptors mediating the spinal effects produced by microinjection of morphine into the periaqueductal gray. *Brain Res.*, **336**, 133–142.

CARSTENS, E., KLUMPP, D., RANDIC, M. & ZIMMERMAN, M. (1981). Effect of iontophoretically applied 5-hydroxytryptamine on the excitability of single primary afferent C- and A-fibres in cat spinal cord. *Brain Res.*, **220**, 151–158.

COLLINS, J.G., KITIHATA, L.M., MATSUMOTO, M., HOMMA, E. & SUZUKAWA, M. (1984). Spinally administered epinephrine suppresses noxiously evoked activity of WDR neurons in the dorsal horn of the spinal cord. *Anesthesiology*, **60**, 269–275.

CURTIS, D.R., LEAH, J.D. & PEET, M.J. (1983). Effects of noradrenaline and 5-hydroxytryptamine on spinal Ia afferent terminations. *Brain Res.*, **258**, 328–332.

CURTIS, D.R., LODGE, D. & BRAND, S.J. (1977). GABA and spinal afferent terminal excitability in the cat. *Brain Res.*, **130**, 360–363.

DANZEBRINK, R.M. & GEBHART, G.F. (1990). Antinociceptive effects of intrathecal adrenoceptor agonists in a rat model of visceral nociception. *J. Pharmacol. Exp. Ther.*, **253**, 698–705.

DAVIES, J. (1989). Effects of tizanidine, eperisone and afloqualone on feline dorsal horn neuronal responses to peripheral cutaneous noxious and innocuous stimuli. *Neuropharmacology*, **28**, 1357–1362.

DAVIES, J. & QUINLAN, J.E. (1985). Selective inhibition of responses of feline dorsal horn neurones to noxious cutaneous stimuli by tizanidine (DS103-282) and noradrenaline: involvement of alpha 2-adrenoceptors. *Neuroscience*, **16**, 673–682.

DOYLE, C.A. & MAXWELL, D.J. (1991a). Catecholaminergic innervation of the spinal dorsal horn: a correlated light and electron microscopic analysis of tyrosine hydroxylase-immunoreactive fibres in the cat. *Neuroscience*, **45**, 161–176.

DOYLE, C.A. & MAXWELL, D.J. (1991b). Ultrastructural analysis of noradrenergic nerve terminals in the cat lumbosacral spinal dorsal horn: a dopamine-beta-hydroxylase immunocytochemical study. *Brain Res.*, **563**, 329–333.

DOYLE, C.A. & MAXWELL, D.J. (1993a). Direct catecholaminergic innervation of spinal dorsal horn neurones with axons ascending the dorsal columns in cat. *J. Comp. Neurol.*, **331**, 434–444.

DOYLE, C.A. & MAXWELL, D.J. (1993b). Neuropeptide Y-immunoreactive terminals form axo-axonic synaptic arrangements in the substantia gelatinosa (lamina II) of the cat spinal dorsal horn. *Brain Res.*, **603**, 157–161.

DUGGAN, A.W. (1992). Antibody Microprobes. In *Monitoring Neuronal Activity: A Practical Approach*. ed. Stamford, J. pp. 181–202. Oxford: Oxford University Press.

DUGGAN, A.W., HENDRY, J.A., GREEN, J.L., MORTON, C.R. & HUTCHISON, W.D. (1988a). The preparation and use of antibody microprobes. *J. Neurosci. Methods*, **23**, 241–247.

DUGGAN, A.W., HENDRY, I.A., MORTON, C.R., HUTCHISON, W.D. & ZHAO, Z.Q. (1988b). Cutaneous stimuli releasing immunoreactive substance P in the dorsal horn of the cat. *Brain Res.*, **451**, 261–273.

DUGGAN, A.W., HOPE, P.J. & LANG, C.W. (1991). Microinjection of neuropeptide Y into the superficial dorsal horn reduces stimulus evoked release of immunoreactive substance P in the anaesthetized cat. *Neuroscience*, **44**, 733–740.

DUGGAN, A.W., SCHAIBLE, H.-G., HOPE, P.J. & LANG, C.W. (1992). Effect of peptidase inhibition on the pattern of intraspinally released immunoreactive substance P detected with antibody microprobes. *Brain Res.*, **579**, 261–269.

FISHER, B., ZORNOW, M.H., YAKSH, T.L. & PETERSON, B.M. (1991). Antinociceptive properties of intrathecal dexmedetomidine in rats. *Eur. J. Pharmacol.*, **192**, 221–225.

FLEETWOOD-WALKER, S.M., MITCHELL, R., HOPE, P.J., MOLONY, V. & IGGO, A. (1985). An alpha-2 receptor mediates the selective inhibition by noradrenaline of nociceptive responses of identified dorsal horn neurones. *Brain Res.*, **334**, 243–254.

GIRON, L.T.Jr., MCCANN, S.A. & CRIST ORLANDO, S.G. (1985). Pharmacological characterization and regional distribution of alpha-noradrenergic binding sites of rat spinal cord. *Eur. J. Pharmacol.*, **115**, 285–290.

GORDH, T.Jr., JANSSON, I., HARTVIG, P., GILLBERG, P.G. & POST, C. (1989). Interactions between noradrenergic and cholinergic mechanisms involved in spinal nociceptive processing. *Acta Anaesthesiol. Scand.*, **33**, 39–47.

HEADLEY, P.M., DUGGAN, A.W. & GRIERSMITH, B.T. (1978). Selective reduction by noradrenaline and 5-hydroxytryptamine of nociceptive responses of cat dorsal horn neurones. *Brain Res.*, **145**, 185–189.

HENDRY, I.A., MORTON, C.R. & DUGGAN, A.W. (1988). Analysis of antibody microprobe autoradiographs by computerized image processing. *J. Neurosci. Methods*, **23**, 249–256.

HYLDEN, J.L., THOMAS, D.A., IADAROLA, M.J., NAHIN, R.L. & DUBNER, R. (1991). Spinal opioid analgesic effects are enhanced in a model of unilateral inflammation/hyperalgesia: possible involvement of noradrenergic mechanisms. *Eur. J. Pharmacol.*, **194**, 135–143.

HYLDEN, J.L. & WILCOX, G.L. (1983). Pharmacological characterization of substance P-induced nociception in mice: modulation by opioid and noradrenergic agonists at the spinal level. *J. Pharmacol. Exp. Ther.*, **226**, 398–404.

JEFTINIJA, S., SEMBA, K. & RANDIC, M. (1981). Norepinephrine reduces excitability of single cutaneous afferent C-fibers in the cat spinal cord. *Brain Res.*, **219**, 456–463.

JONES, D.J., KENDALL, D.E. & ENNA, S.J. (1982). Adrenergic receptors in rat spinal cord. *Neuropharmacology*, **21**, 191–195.

KURAISHI, Y., HIROTA, N., SATO, Y., KANEKO, S., SATOH, M. & TAKAGI, H. (1985). Noradrenergic inhibition of the release of substance P from primary afferents in the rabbit spinal dorsal horn. *Brain Res.*, **359**, 177–182.

LACKNER, K.J. (1980). Mapping of monoamine neurons and fibres in the cat lower brainstem and spinal cord. *Anat. Embryol.*, **161**, 169–195.

MELZACK, R. & WALL, P.D. (1965). Pain mechanisms: a new theory. *Science*, **150**, 973–979.

MEYERSON, B.A., BOETHIUS, J. & CARLSSON, A.M. (1979). Alleviation of malignant pain by electrical stimulation of the periventricular-periaqueductal region: pain relief as related to stimulation sites. In *Advances in Pain Research and Therapy*. ed. Bonica, J., Liebeskind, J.C. & Albe-Fessard, D.G. pp. 525–583. New York: Raven Press.

NAGY, J.I. & HUNT, S.P. (1982). Fluoride resistant acid phosphatase – containing neurones in dorsal root ganglia are separate from those containing substance P or somatostatin. *Neuroscience*, **7**, 89–98.

NAKAGAWA, I., OMOTE, K., KITAHATA, L.M., COLLINS, J.G. & MURATA, K. (1990). Serotonergic mediation of spinal analgesia and its interaction with noradrenergic systems. *Anesthesiology*, **73**, 474–478.

NETO, F.R. (1978). The depolarizing action of 5-HT on mammalian non-myelinated nerve fibres. *Eur. J. Pharmacol.*, **49**, 351–352.

ONO, H., MISHIMA, A., ONO, S., FUKUDA, H. & VASKO, M.R. (1991). Inhibitory effects of clonidine and tizanidine on release of substance P from slices of rat spinal cord and antagonism by alpha-adrenergic receptor antagonists. *Neuropharmacology*, **30**, 585–589.

PANG, I.-H. & VASKO, M.R. (1986). Morphine and norepinephrine but not 5-hydroxytryptamine and gamma-aminobutyric acid inhibit the potassium-stimulated release of substance P from rat spinal cord slices. *Brain Res.*, **376**, 268–279.

PRICE, J. (1985). An immunocytochemical and quantitative examination of dorsal root ganglion neuronal subpopulations. *J. Neurosci.*, **5**, 2051–2059.

RAJAOFETRA, N., RIDET, J.-L., POULAT, P., MARLIER, L., SANDILLON, F., GEFFARD, M. & PRIVAT, A. (1992). Immunocytochemical mapping of noradrenergic projections to the rat spinal cord with an antiserum against noradrenaline. *J. Neurocytol.*, **21**, 481–494.

REYNOLDS, D.V. (1969). Surgery in the rat during electrical analgesia induced by focal brain stimulation. *Science*, **164**, 44–45.

SAKATANI, K., CHESLER, M. & HASSAN, A.Z. (1991). GABA receptors modulate axonal conduction in dorsal columns of neonatal rat spinal cord. *Brain Res.*, **542**, 273–279.

SAKATANI, K., CHESLER, M., HASSAN, A.Z., LEE, M. & YOUNG, W. (1993). Non-synaptic modulation of dorsal column conduction by endogenous GABA in neonatal rat spinal cord. *Brain Res.*, **622**, 43–50.

SALONEN, J.S. & ELORANTA, M. (1990). Biotransformation of medetomidine in the rat. *Xenobiotica*, **20**, 471–480.

SCHAIBLE, H.-G., HOPE, P.J., LANG, C.W. & DUGGAN, A.W. (1992). Calcitonin gene-related peptide causes intraspinal spreading of Substance P released by peripheral stimulation. *Eur. J. Neurosci.*, **4**, 750–757.

SCHRODER, H.D. & SKAGERBERG, G. (1985). Catecholamine innervation of the caudal spinal cord in the rat. *J. Comp. Neurol.*, **242,** 358–368.

SOLOMON, R.E. & GEBHART, G.F. (1988). Intrathecal morphine and clonidine: antinociceptive tolerance and cross-tolerance and effects on blood pressure. *J. Pharmacol. Exp. Ther.*, **245,** 444–454.

SUGIURA, Y., LEE, C.L. & PERL, E.R. (1986). Central projections of identified unmyelinated (C) afferent fibers innervating mammalian skin. *Science*, **234,** 358–361.

SULLIVAN, A.F., DASHWOOD, M.R. & DICKENSON, A.H. (1987). Alpha 2-adrenoceptor modulation of nociception in rat spinal cord: location, effects and interactions with morphine. *Eur. J. Pharmacol.*, **19,** 138, 169–177.

SULLIVAN, A.F., KALSO, E.A., McQUAY, H.J. & DICKENSON, A.H. (1992). The antinociceptive actions of dexmedetomidine on dorsal horn neuronal responses in the anaesthetized rat. *Eur. J. Pharmacol.*, **215,** 127–133.

TAKANO, Y. & YAKSH, T.L. (1991). Relative efficacy of spinal alpha-2 agonists, dexmedetomidine, clonidine and ST-91, determined in vivo by using N-ethoxycarbonyl-2-ethoxy-1,2-dihydroquinoline, an irreversible antagonist. *J. Pharmacol. Exp. Ther.*, **258,** 438–446.

TJOLSEN, A., LUND, A. & HOLE, K. (1990). The role of descending noradrenergic systems in regulation of nociception: the effects of intrathecally administered alpha-adrenoceptor antagonists and clonidine. *Pain*, **43,** 113–120.

TSENG, L.L. & TANG, R. (1989). Differential actions of the blockade of spinal opioid, adrenergic and serotonergic receptors on the tail-flick inhibition induced by morphine microinjected into the dorsal raphe and central gray in rats. *Neuroscience*, **33,** 93–100.

UHLEN, S., PERSSON, M.L., ALARI, L., POST, C., AXELSSON, K.L. & WIKBERG, J.E. (1990). Antinociceptive actions of alpha 2-adrenoceptor agonists in the rat spinal cord: evidence for antinociceptive alpha 2-adrenoceptor subtypes and dissociation of antinociceptive alpha 2-adrenoceptors from cyclic AMP. *J. Neurochem.*, **55,** 1905–1914.

UNNERSTALL, J.R., KOPAJTIC, T.A. & KUHAR, M.J. (1984). Distribution of alpha-2 agonist binding sites in the rat and human central nervous system: analysis of some functional, anatomical correlates of the pharmacological effects of clonidine and related adrenergic agents. *Brain Res.*, **319,** 69–101.

WATERMAN, A., LIVINGSTON, A. & BOUCHENAFA, O. (1988). Analgesic effects of intrathecally-applied alpha 2-adrenoceptor agonists in conscious, unrestrained sheep. *Neuropharmacology*, **27,** 213–216.

WESTLUND, K.M., BOWKER, R.M., ZIEGLER, M.G. & COULTER, J.D. (1984). Origins and terminations of descending noradrenergic projections to the spinal cord of monkey. *Brain Res.*, **292,** 1–16.

YOUNG, W.S.I. & KUHAR, M.J. (1980). Noradrenergic alpha 1 and alpha 2 receptors: light microscopic autoradiographic localization. *Proc. Natl. Acad. Sci. U.S.A.*, **77,** 1696–1700.

ZHAO, Z.Q. & DUGGAN, A.W. (1987). Clonidine and the hyperresponsiveness of dorsal horn neurones following morphine withdrawal in the spinal cat. *Neuropharmacology*, **26,** 1499–1502.

(Received January 17, 1994
Revised March 7, 1994
Accepted March 15, 1994)

Br. J. Pharmacol. (1994), **112**, 958–962

Involvement of apamin-sensitive K^+ channels in antigen-induced spasm of guinea-pig isolated trachea

Hideyuki Yamauchi, Motohiko Miura, Masakazu Ichinose, Jun Ishikawa, Natsuko Nakajima, Masafumi Tomaki, Hiroshi Inoue, *Kazutaka Maeyama, *Takehiko Watanabe & [1]Kunio Shirato

First Department of Internal Medicine and *Pharmacology I, Tohoku University School of Medicine, Sendai 980, Japan

1 In order to examine whether K^+ channels play a role in antigen-induced airway responses, the effect of K^+ channel blockers on antigen-induced airway smooth muscle contraction and mediator release was examined *in vitro* in guinea-pigs actively sensitized with ovalbumin (OA).

2 Tracheal strips from sensitized animals were suspended in organ baths under a resting tension of 1 g and isometric tension was continuously measured. Cumulative concentration-response curves to OA (0.1–1000 ng ml^{-1}) or histamine (10 nM–1 mM) were obtained in the presence and absence of K^+ channel blockers.

3 OA (10, 100 or 1000 ng ml^{-1}) was incubated with minced lung tissues from the same animals for 15 min in the presence and absence of K^+ channel blockers, and released histamine and leukotriene C_4 (LTC_4) in the incubating medium were measured.

4 Apamin, a small conductance Ca^{2+}-activated K^+ channel ($P_{K,Ca}$) blocker, (0.1, 0.3 and 1 μM) significantly inhibited OA-induced smooth muscle contraction, while charybdotoxin (ChTX, 10 nM), an intermediate and large conductance $P_{K,Ca}$ blocker, and iberiotoxin (IbTX, 3 nM), a large conductance $P_{K,Ca}$ blocker, were without effect. Apamin (0.3 μM) had no effect on exogenously administered histamine-induced airway smooth muscle contraction, suggesting that the inhibition of OA-induced contraction by apamin did not occur at the smooth muscle level.

5 The inhibition of OA-induced contraction by apamin (0.3 μM) was not significantly affected by pretreatment with a leukotriene antagonist, ONO-1078 (10 μM), but was abolished by pretreatment with a histamine H_1-receptor blocker, pyrilamine (1 μM).

6 Apamin by itself (up to 0.1 μM) had no effect on spontaneous histamine release from minced lung tissues. Histamine release induced by low and intermediate concentrations of OA (10 and 100 ng ml^{-1}) was significantly suppressed by apamin pretreatment ($P<0.05$ and $P<0.001$), whereas LTC_4 release was not affected. ChTX (0.1 μM) and IbTX (10 nM) had no significant effect on either spontaneous or OA (100 ng ml^{-1})-induced histamine release.

7 These results suggest that apamin partially but substantially inhibits antigen-induced smooth muscle contraction, presumably by inhibiting antigen-induced histamine release from airway mast cells through small conductance $P_{K,Ca}$ closure.

Keywords: Apamin; K^+ channel; antigen; mast cell degranulation; histamine; leukotriene C_4; charybdotoxin; iberiotoxin

Introduction

The role of K^+ channels has been demonstrated in many types of airway cells (Black & Barnes, 1990). In airway smooth muscle cells, K^+ channels play a role not only in regulating membrane potential (Kotlikoff, 1990) but also in the relaxation responses induced by β-adrenoceptor agonists (Jones *et al.*, 1990; Miura *et al.*, 1992). The activation of certain types of K^+ channels is also involved in neural function including repolarization of nerve fibres (Conti & Neher, 1980) and presynaptic modulation of neurotransmission (Ichinose & Barnes, 1990; Stretton *et al.*, 1992). Moreover, airway non-excitable cells such as airway epithelial cells (McCann & Welsh, 1990) and T-lymphocytes (Leonard *et al.*, 1992) possess K^+ channels on the cell membrane which play a role in the exocytotic process.

The present study was designed to examine whether K^+ channels are involved in antigen-induced airway responses, consisting of mast cell degranulation and subsequent smooth muscle contraction. Whether IgE-mediated mast cell degranulation requires the opening of ion channels has not yet been established. Lindau & Fernandez (1986) reported that mast cells do not use ion channels in stimulation-secretion coupling, whereas Ca^{2+} influx through membrane ion channels is thought to be necessary to complete or maintain the degranulation of mast cells (Penner & Neher, 1988). Recently, changes in membrane permeability to other ions, including Cl^-, Na^+ and K^+, have also been recognized as an important element of the signal transduction process in mast cells (Janizsewski *et al.*, 1992).

Several studies on rat basophilic leukaemia (RBL) cells (Mohr & Fewtrell, 1987; Labrecque *et al.*, 1991), which may be regarded as mast cell analogues, suggested the involvement of K^+ channels in mast cell degranulation. However, little is known about the involvement of K^+ channels in mast cell degranulation, especially in airway mast cells. For this reason, we have examined the effects of K^+ channel blockers on antigen-induced mediator release from lung parenchyma and smooth muscle contraction using guinea-pigs actively sensitized with ovalbumin (OA). We used three types of Ca^{2+}-activated K^+ channel ($P_{K,Ca}$) blockers: apamin, a blocker of small conductance $P_{K,Ca}$ (Banks *et al.*, 1979), charybdotoxin (ChTX), an intermediate and large conductance $P_{K,Ca}$ blocker (Miller *et al.*, 1985; Beech *et al.*, 1987) and iberiotoxin (IbTX), a selective blocker of large conductance $P_{K,Ca}$ (Suarez-Kurtz *et al.*, 1991). We chose these blockers since $P_{K,Ca}$ activity is thought to be important in the degranulation of guinea-pig and human basophils (Labrecque *et al.*, 1991; Beauvais *et al.*, 1992).

[1] Author for correspondence.

Methods

Animal sensitization and preparation

Male Dunkin-Hartley guinea-pigs, weighing 250–300 g, were sensitized by subcutaneous injection of 0.5 ml of saline containing 10 μg of ovalbumin (OA) and 100 mg of aluminum hydroxide on 2 consecutive days. Three weeks after the sensitization procedure, the animals were anaesthetized by intraperitoneal injection of urethane (2 g kg^{-1}) and killed by exsanguination. The trachea and lungs were quickly removed and placed in Krebs-Henseleit (K-H) solution cooled to 4°C. The composition of the K-H solution was as follows (mM): NaCl 118, KCl 5.9, $MgSO_4$ 1.2, $CaCl_2$ 2.5, NaH_2PO_4 1.2, $NaHCO_3$ 25.5 and glucose 5.6. After being cleaned of connective tissue, the trachea was opened longitudinally by cutting through the cartilage and cut into segments so that each segment contained 3–4 cartilage rings. Each segment of tracheal tissue was mounted in a 10 ml organ bath containing K-H solution maintained at 37°C and gassed with 95% O_2 and 5% CO_2, giving a pH of 7.4. Strips were connected via silk threads to force displacement transducers (UL-10GR, Minebea Co., Ltd., Tokyo, Japan) for the measurement of isometric changes in tension, and the responses were recorded on a polygraph (Rectigraph-8K, San-ei, Tokyo, Japan). The tissues were allowed to equilibrate for 1 h with frequent washing under a resting tension of 1 g which was found to be optimal for measuring the changes in tension. The remaining lungs were dissected free of large vessels and bronchi and cut into small pieces (1–2 mm thick) for the minced lung preparation.

Contraction studies

Indomethacin (10 μM) was present throughout the experiment in order to avoid a possible modulation of contractile responses by prostaglandins derived from epithelium (Holtzman, 1992). After the equilibration period, cumulative concentration-response curves to OA (0.1–1000 ng ml^{-1}) or exogenously applied histamine (0.1 μM–1 nM) were obtained in the tracheal strips in the presence and absence of apamin (0.1, 0.3 or 1 μM). Apamin or its vehicle (saline with 0.25% bovine serum albumin (BSA)) was preincubated with tissues for 20 min before the contraction studies. In another set of experiments, the effects of other K^+ channel blockers, ChTX (10 nM) and IbTX (3 nM), on OA-induced concentration-response curves were also similarly examined. The concentrations of ChTX and IbTX chosen in these experiments were the maximal concentrations which, by themselves, had no effect on baseline tone.

We have previously shown that OA-induced contraction is abolished under similar experimental conditions by pretreatment with a combination of the histamine H_1-receptor blocker, pyrilamine (1 μM), and a leukotriene antagonist, ONO-1078 (10 μM; Obata *et al.*, 1992). Thus, in a separate series of experiments, the effect of apamin (0.3 μM) on the OA-induced contractile response was also examined in the presence and absence of pyrilamine (1 μM) or ONO-1078 (10 μM), respectively.

Mediator release assay

Minched lung fragments (80 mg) were suspended in Eppendorf tubes with 1 ml of Tyrode solution containing $CaCl_2$ (2 mM) and $MgCl_2$ (1 mM) prewarmed to 37°C for 15 min. Suspended tissues were preincubated with apamin (0.01, 0.1 and 1 μM), ChTX (0.1 μM), IbTX (0.01 μM) or its vehicle (saline with 0.25% BSA) for 15 min and then challenged with saline and OA (10, 100 or 1000 ng ml^{-1}). After a 30 min incubation at 37°C, tubes were cooled to stop further reactions and centrifuged (10,000 *g*, 3 min, 4°C).

Histamine was determined fluorimetrically by high performance liquid chromatography (h.p.l.c.; Yamatodani *et al.*, 1985). In brief, 0.2 ml of supernatant was collected from each tube. Then, 20 μl of 60% perchloric acid was added to both the supernatant and tissue fractions. The tissue fraction was homogenized with a Polytron homogenizer (Kinematica, Luzern, Switzerland) at maximal speed for 15 s. The supernatant and homogenate were centrifuged at 10,000 *g* for 3 min. An aliquot of 50 μl of each supernatant was injected into an h.p.l.c. system, and fluorescence was determined by a fluoromonitor (F-1100, Hitachi, Tokyo, Japan). Net histamine release is expressed as a percentage of the total histamine content of the supernatant and tissue fractions and corrected for the spontaneous release of histamine. Immunoreactive LTC_4 was measured by an enzyme immunoassay system, with a claimed cross-reactivity of $<0.15\%$ with other eicosanoids (Amersham International PLC, Amersham). Supernatants of 0.5 ml were collected from each tube, and concentrations of LTC_4 in the supernatants were measured, normalized by tissue weight (mg tissue) and corrected for the spontaneous release of LTC_4. In the mediator release assays, all values were based on means of duplicate or triplicate determinations.

Drugs

The following drugs were used; apamin (Research Biochemicals Inc., Baltimore, U.S.A.), charybdotoxin and iberiotoxin (Peptide Institute Inc., Osaka, Japan), histamine hydrochloride (Wako Chemicals, Sendai, Japan), indomethacin (Sumitomo Pharmaceutical Company, Osaka, Japan), ovalbumin and pyrilamine (Sigma Chemical Co., St Louis, U.S.A.) and ONO-1078 (4-oxo-8-[4-(4-phenylbutoxy)benzoylamino]-2-(tertrazol-5-yl)-4H-1-benzopyran hemihydrate; ONO Pharmaceutial Company, Osaka, Japan).

Statistical analysis

The effect of apamin on OA-induced tracheal contraction was assessed by calculating the EC_{40}, namely the concentration of OA producing 40% of the maximal contraction of the tissue induced by 1 mM of histamine. The geometric mean of EC_{40} with 95% confidence interval (CI) was calculated in each group. All other data are expressed as the arithmetic means ± s.e.mean. The effect of K^+ channel blockers on OA or histamine-induced concentration-response studies of airway smooth muscle contraction was statistically analyzed by two-way analysis of variance (two-way ANOVA). Comparisons between paired or unpaired mean data were performed by Wilcoxon's signed rank test or Mann-Whitney *U* test, respectively. In each case, $P<0.05$ was considered statistically significant.

Results

Effect of K^+ channel blockers on OA-induced smooth muscle contraction

OA (0.1–1000 ng ml^{-1}) evoked concentration-dependent smooth muscle contraction in trachea removed from all the experimental animals. Apamin (0.1, 0.3 and 1 μM) pretreatment by itself had no effect on baseline tone. Compared with the concentration-response curves in control tissues ($n = 10$), apamin at 0.3 ($n = 7$) and 1 μM ($n = 4$) significantly suppressed OA-induced contraction concentration-response curves ($P<0.01$ and $P<0.05$, respectively, two-way ANOVA, Figure 1), while apamin at 0.1 μM ($n = 8$) failed to affect the curves significantly ($P>0.05$, two-way ANOVA). The geometric mean of EC_{40} for ovalbumin in control tissues was 8.2 ng ml^{-1} (95% CI, 7.1–9.3 ng ml^{-1}), which was significantly increased by pretreatment with each concentration of apamin (0.1, 0.3 and 1 μM) in a concentration-dependent manner; the EC_{40} values with 95% CI for ovalbumin in the presence of apamin 0.1, 0.3 and 1 μM were 14.2

(12.9 to 15.5) ng ml^{-1} 29.0 (27.8 to 30.3) ng ml^{-1} and 31.2 (29.6 to 32.9) ng ml^{-1} ($P<0.05$, $P<0.01$ and $P<0.05$, respectively, Mann-Whitney U test).

Neither ChTX (10 nM, $n = 5$) nor IbTX (3 nM, $n = 5$) had effects on either the spontaneous basal tone or OA-induced contraction concentration-response curves, compared with their control tissues (both $n = 5$).

Effect of apamin on histamine-induced smooth muscle contraction

Pretreatment with apamin (0.3 μM) did not affect exogenously applied histamine (0.1 μM–1 mM)-induced contraction concentration-response curves ($n = 6$, $P>0.05$, two-way ANOVA, Figure 2).

Effect of H_1 blocker and leukotriene antagonist on inhibitory effect of apamin

Neither the H_1 blocker, pyrilamine (1 μM), nor the leukotriene antagonist, ONO-1078 (10 μM), had an effect on baseline smooth muscle tone. However, both drugs significantly suppressed OA-induced smooth muscle contraction in our preliminary experiments. After pyrilamine pretreatment, apamin (0.3 μM) failed to show a significant inhibition of OA-induced smooth muscle contraction ($n = 6$, $P>0.05$, two-way ANOVA, Figure 3a), while apamin (0.3 μM) still significantly inhibited OA-induced contraction

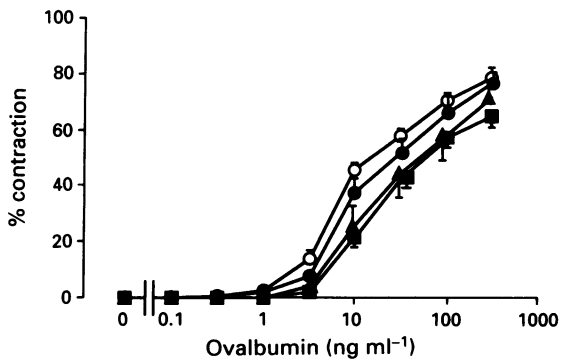

Figure 1 Effect of apamin on ovalbumin (OA)-induced smooth muscle contraction in actively sensitized guinea-pig trachea. Apamin at 0.3 μM (■, $n = 7$) and 1 μM (▲, $n = 4$) but not at 0.1 μM (●, $n = 8$) significantly suppressed OA (0.1–300 ng ml^{-1})-induced cumulative concentration-response curves, compared with vehicle-treated tissues (○, $n = 10$). Contractile response is expressed as a percentage of maximal contraction induced by 1 mM of histamine (% contraction) in each tissue. All points represents mean ± s.e.mean.

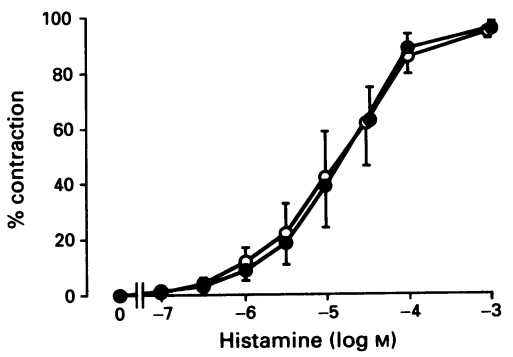

Figure 2 Effect of apamin on exogenously administered histamine-induced smooth muscle contraction in actively sensitized guinea-pig trachea. Apamin (0.3 μM, ●, $n = 6$) had no significant effect on histamine (0.1 μM–1 mM)-induced cumulative concentration-response curves, compared with vehicle-treated tissues (○, $n = 6$). Contractile response is expressed as a percentage of the maximal contraction induced by 1 mM histamine, which was obtained before the concentration-response study (% contraction) in each tissue. Each value represents mean ± s.e.mean.

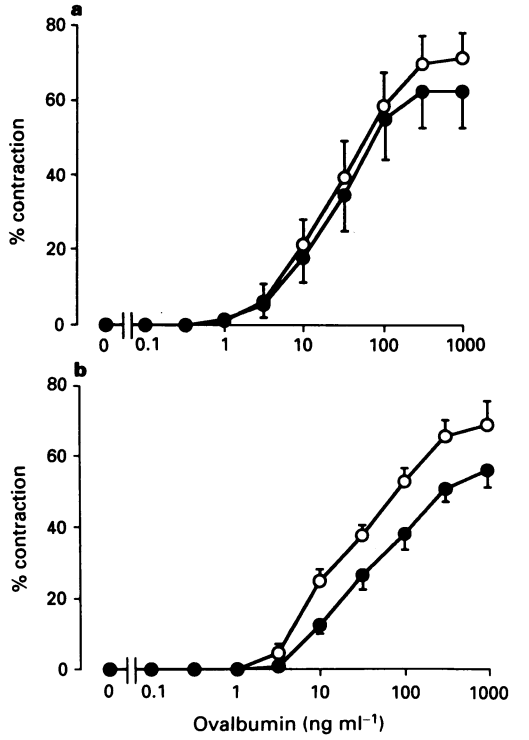

Figure 3 Effects of a histamine H_1-receptor blocker and a leukotriene antagonist on the inhibition of ovalbumin (OA)-induced smooth muscle contraction by apamin in actively-sensitized guinea-pig trachea. In the presence of pyrilamine (1 μM; a) apamin (0.3 μM, ●, $n = 6$) failed to affect OA (0.1–1000 ng ml^{-1})-induced cumulative concentration-response curves, compared with vehicle-treated tissues (○, $n = 6$), while ONO-1078 (10 μM; b) did not influence the inhibition of OA-induced contraction by apamin (0.3 μM, $n = 7$) in vehicle-treated tissues (○, $n = 7$). Contractile response is expressed as a percentage of the maximal contraction induced by 1 mM histamine (% contraction) in each tissue. Each value represents mean ± s.e.mean.

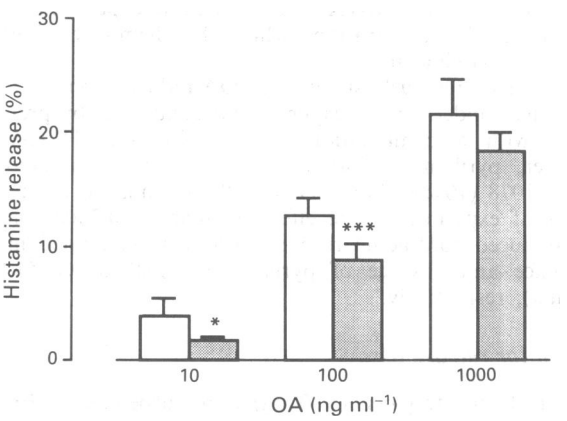

Figure 4 Effect of apamin on ovalbumin (OA)-induced histamine release from minced lung tissues of actively sensitized guinea-pigs. Apamin (0.1 μM, stippled columns, $n = 8$) significantly inhibited low concentrations of OA (10 and 100 ng ml^{-1})-induced histamine release, compared with vehicle-treated tissues (open columns, $n = 8$), although 1000 ng ml^{-1} of OA-induced histamine release was not significantly affected. Histamine release is expressed as a percentage of the total histamine content, corrected for spontaneous release. Each value represents mean ± s.e.mean. Significant difference from vehicle-treated tissues of $^*P<0.05$ and $^{***}P<0.001$, respectively.

in the presence of ONO-1078 pretreatment ($n = 7$, $P < 0.05$, two-way ANOVA, Figure 3b).

Effect of K^+ channel blockers on OA-induced mediator release

Apamin (0.01 and 0.1 μM, $n = 5$ and $n = 8$, respectively) had no effect on spontaneous histamine release from minced lung tissues. In the presence of apamin (0.1 μM), histamine release induced by 10 and 100 ng ml^{-1} of OA, but not that induced by 1000 ng ml^{-1}, was significantly suppressed (Figure 4). OA-induced LTC_4 release from minced lung tissues ($n = 4$) was not affected by apamin (0.1 μM) pretreatment at any concentration of OA; OA (10, 100 and 1000 ng ml^{-1})-induced LTC_4 release was 6.7 ± 3.5, 23.4 ± 5.3 and 23.0 ± 5.1 pg mg^{-1} tissue without and 6.3 ± 4.2, 22.7 ± 6.4 and 22.7 ± 6.6 pg mg^{-1} tissue with apamin 0.1 μM. Higher concentrations of ChTX (0.1 μM) and IbTX (0.01 μM) than those used in the contraction studies had no significant effect on OA (100 ng ml^{-1})-induced histamine release. Mean histamine release by OA (100 ng ml^{-1}) from control tissues was $12.7 \pm 0.7\%$ ($n = 6$), which was not significantly different from that in the presence of ChTX ($13.6 \pm 1.5\%$) and IbTX ($13.8 \pm 2.9\%$, both $P > 0.05$, Wilcoxon's signed rank test), respectively.

Discussion

The present study shows that apamin, a small conductance $P_{K,Ca}$ blocker, significantly inhibited antigen-induced airway smooth muscle contraction in trachea isolated from actively-sensitized guinea-pigs *in vitro*. This suggests that small conductance $P_{K,Ca}$ play a role in antigen-induced airway contractile responses.

The sensitization procedure used has been demonstrated predominantly to produce IgE antibody (Andersson, 1980), suggesting that OA-induced airway responses were mainly mediated by IgE receptors. Since both pyrilamine and ONO-1078 significantly suppressed OA-induced smooth muscle contraction, histamine and leukotrienes appear to participate in mediating antigen-induced airway smooth muscle contraction. Histamine released by OA challenge is thought to be mainly derived from airway mast cells, because mast cells are a major source of histamine in airways (Riley & West, 1966) and possess high affinity Fc receptors to IgE (FcεRI; Ishizaka *et al.*, 1970). On the other hand, leukotrienes released by OA could be derived from eosinophils as well as mast cells, as eosinophils have low affinity Fc receptors for IgE (FcεRII; Capron *et al.*, 1986). Therefore, as far as histamine is concerned, antigen-induced responses are likely to reflect mast cell function through FcεRI.

The mechanisms by which apamin inhibited antigen-induced airway smooth muscle contraction in the present study are still unclear. However, a direct action of apamin on airway smooth muscle is unlikely to explain the inhibitory effect obtained in the present study as the existence of apamin-sensitive K^+ channels on airway smooth muscle cells has not been reported. It could be suggested rather that apamin inhibits OA-induced smooth muscle contraction by suppressing histamine release from mast cells in guinea-pig airways. This is supported by the following findings in the present study. First, the inhibition of OA-induced contraction by apamin was abolished by pretreatment with a H_1 receptor blocker, pyrilamine, suggesting that the inhibitory effect of apamin is expressed against a histamine component of the OA-induced contraction. Second, the contraction induced by exogenously administered histamine was not affected by apamin in sensitized tracheal smooth muscle, implying that the inhibition by apamin was not due to the change in responsiveness of airway smooth muscle to histamine. Finally, in lung parenchyma, the histamine release induced by lower concentrations of OA (10 and 100 ng ml^{-1}) was significantly suppressed by apamin.

In studies using rat basophilic leukaemia (RBL)-2H3 cells, depolarization induced by extracellular high K^+ inhibited not only Ca^{2+} uptake but also exocytosis (Labrecque *et al.*, 1989). In another study from the same group, evidence was obtained to suggest that Ca^{2+}-activated K^+ efflux pathways serve to sustain Ca^{2+} influx which is necessary for IgE receptor-mediated triggering of degranulation (Labrecque *et al.*, 1991). In human basophils, decreasing K^+ channel conductance using K^+ channel blockers such as 4-aminopyridine and quinine is also known to inhibit histamine release (Beauvais *et al.*, 1992). These findings from mast cell analogue cells raise the possibility that K^+ channel activation is involved in the maintenance of Ca^{2+} influx to promote mediator release in mast cells. In this case, apamin-sensitive K^+ channels appear to play this role in the mast cell degranulation of guinea-pig airways.

OA-induced LTC_4 release was not affected by apamin, whereas lower concentrations of OA-induced histamine release were significantly suppressed. This observation may reflect the possibility that leukotrienes are released by antigen challenge not only from mast cells but also from eosinophils. Alternatively, the difference may be explained by the different releasing mechanisms between preformed mediators such as histamine and non-performed mediators such as leukotrienes, as shown in skin mast cells (Benyon *et al.*, 1989).

In the present study, ChTX and IbTX were without effect on both OA-induced smooth muscle contraction and mediator release. Since airway smooth muscle contains large conductance $P_{K,Ca}$ (McCann & Welsh, 1986), higher concentrations of the blockers for these channels, ChTX (100 nM) and IbTX (10 nM), by themselves increased baseline tone in guinea-pig trachea (Jones *et al.*, 1990; Suarez-Kurtz *et al.*, 1991). Therefore, these concentrations of the blockers could not be used in the contraction studies. However, in the mediator release study, even higher concentrations of the toxins did not show a significant effect on mediator release, suggesting that small conductance $P_{K,Ca}$ but not intermediate or large conductance $P_{K,Ca}$ are involved in airway mast cell degranulation mechanisms.

In summary, apamin, a blocker of small conductance $P_{K,Ca}$, significantly inhibited antigen-induced airway smooth muscle contraction, presumably by suppressing histamine release from airway mast cells in actively-sensitized guinea-pigs. This result provides evidence that the activation of apamin-sensitive K^+ channels is involved in antigen-induced airway responses.

The authors thank Mr Brent Bell for reading the manuscript and Dr E. Sakurai for technical assistance.

References

ANDERSSON, P. (1980). Antigen-induced bronchial anaphylaxis in actively sensitized guinea-pigs. *Allergy*, **35**, 65–71.

BANKS, B.E.C., BROWN, C., BURGESS, G.M., BURNSTOCK, G., CLARET, M., COCKS, T.M. & JENKINSON, D.H. (1979). Apamin blocks certain transmitter-induced increase in potassium permeability. *Nature*, **282**, 415–417.

BEAUVAIS, F., SHIMAHARA, T., INOUE, I., HIEBLOT, C., BURTIN, C. & BENVENISTE, J. (1992). Regulation of human basophil activation: II. Histamine release is potentiated by K^+ efflux and inhibited by Na^+ influx. *J. Immunol.*, **148**, 149–154.

BEECH, D.J., BOLTON, T.B., CASTLE, N.A. & STRONG, P.N. (1987). Characterization of a toxin from scorpion (*Leiurus quinquestriatus*) venom that blocks *in vitro* both large (BK) K^+-channels in rabbit vascular smooth muscle and intermediate (IK) conductance Ca^{2+}-activated K^+ channels in human red cells. *J. Physiol.*, **387**, 32P.

BENYON, R.C., ROBINSON, C. & CHURCH, M.K. (1989). Differential release of histamine and eicosanoids from human skin mast cells activated by IgE-dependent and non-immunological stimuli. *Br. J. Pharmacol.*, **97**, 898–904.

BLACK, J.L. & BARNES, P.J. (1990). Potassium channels and airway function: new therapeutic prospects. *Thorax*, **45**, 213–218.

CAPRON, A., DESSAINT, J.P., CAPRON, M., JOSEPH, M., AMEISEN, J.C. & TONNEL, A.B. (1986). From parasites to allergy: a second receptor for IgE. *Immunol. Today*, **7**, 15–18.

CONTI, F. & NEHER, E. (1980). Single channel recordings of K^+ currents in squid axon. *Nature*, **303**, 250–253.

HOLTZMAN, M.J. (1992). Arachidonic acid metabolism in airway epithelial cells. *Annu. Rev. Physiol.*, **54**, 303–329.

ICHINOSE, M. & BARNES, P.J. (1990). A potassium channel activator modulates both excitatory noncholinergic and cholinergic neurotransmission in guinea pig airways. *J. Pharmacol. Exp. Ther.*, **252**, 1207–1212.

ISHIZAKA, K., TOMIOKA, H. & ISHIZAKA, T. (1970). Mechanisms of passive sensitization. I. Presence of IgE and IgG molecules on human leukocytes. *J. Immunol.*, **105**, 1459–1467.

JANISZEWSKI, J., HUIZINGA, J.D. & BLENNERHASSETT, M.G. (1992). Mast cell ionic channels: significance for stimulus-secretion coupling. *Can. J. Physiol. Pharmacol.*, **70**, 1–7.

JONES, T.R., CHARETTE, L., GARCIA, M.L. & KACZOROWSKI, G.J. (1990). Selective inhibition of relaxation of guinea-pig trachea by charybdotoxin, a potent Ca^{2+}-activated K^+ channel inhibitor. *J. Pharmacol. Exp. Ther.*, **255**, 697–706.

KOTLIKOFF, M.I. (1990). Potassium currents in canine airway smooth muscle cells. *Am. J. Physiol. (Lung Cell. Mol. Physiol.)*, **259**, L384–L395.

LABRECQUE, G.F., HOLOWKA, D. & BAIRD, B. (1989). Antigen-triggered membrane potential changes in IgE-sensitized rat basophilic leukemia cells: evidence for a repolarizing response that is important in the stimulation of cellular degranulation. *J. Immunol.*, **142**, 236–243.

LABRECQUE, G.F., HOLOWKA, D. & BAIRD, B. (1991). Characterization of increased K^+ permeability associated with the stimulation of receptors for immunoglobulin E on rat basophilic leukemia cells. *J. Biol. Chem.*, **266**, 14912–14917.

LEONARD, R.J., GARCIA, M.L., SLAUGHTER, R.S. & REUBEN, J.P. (1992). Selective blockers of voltage-gated K^+ channels depolarize human T lymphocytes: mechanism of the antiproliferative effect of charybdotoxin. *Proc. Natl. Acad. Sci. USA*, **89**, 10094–10098.

LINDAU, M. & FERNANDEZ, J.M. (1986). IgE-mediated degranulation of mast cells does not require opening of ion channels. *Nature*, **319**, 150–153.

MCCANN, J.D. & WELSH, M.J. (1986). Calcium-activated potassium channels in canine airway smooth muscle. *J. Physiol.*, **372**, 113–127.

MCCANN, J.D. & WELSH, M.J. (1990). Basolateral K^+ channels in airway epithelia. II. Role in Cl^- secretion and evidence for two types of K^+ channel. *Am. J. Physiol. (Lung Cell. Mol. Physiol.)*, **258**, L343–L348.

MILLER, C., MOCZYDLOWSKI, E., LATORRE, R. & PHILLIPS, M. (1985). Charybdotoxin, a protein inhibitor of single Ca^{++}-activated K^+ channels from mammalian skeletal muscle. *Nature*, **313**, 316–318.

MIURA, M., BELVISI, M.G., YACOUB, M.H. & BARNES, P.J. (1992). Role of potassium channels in bronchodilator responses in human airways. *Am. Rev. Respir. Dis.*, **146**, 132–136.

MOHR, F.C. & FEWTRELL, C. (1987). Depolarization of rat basophilic leukemia cells inhibits calcium uptake and exocytosis. *J. Cell. Biol.*, **104**, 783–792.

OBATA, T., KOBAYASHI, T., OKADA, Y., NAKAGAWA, N., TERAWAKI, T. & AISHITA, H. (1992). Effect of a peptide leukotriene antagonist, ONO-1078 on antigen-induced airway microvascular leakage in actively sensitized guinea pigs. *Life Sci.*, **51**, 1577–1583.

PENNER, R. & NEHER, E. (1988). Secretory responses of rat peritoneal mast cells to high intracellular calcium. *FEBS Lett.*, **226**, 307–313.

RILEY, J.F. & WEST, G.B. (1966). The occurrence of histamine in mast cells. In *Handbook of Experimental Pharmacology*, ed. Eichler, O. & Farah, A. Berlin: Springer.

STRETTON, C.D., MIURA, M., BELVISI, M.G. & BARNES, P.J. (1992). Calcium-activated potassium channels mediate prejunctional inhibition of peripheral sensory nerves. *Proc. Natl. Acad. Sci. U.S.A.*, **89**, 1325–1329.

SUAREZ-KURTZ, G., GARCIA, M.L. & KACZOROWSKI, G.J. (1991). Effects of charybdotoxin and iberiotoxin on the spontaneous motility and tonus of different guinea pig smooth muscle tissues. *J. Pharmacol. Exp. Ther.*, **259**, 439–443.

YAMATODANI, A., FUKUDA, H., WADA, H., IWAEDA, T. & WATANABE, T. (1985). High-performance liquid chromatographic determination of plasma and brain histamine without previous purification of biological samples: cation-exchange chromatography coupled with post-column derivatization fluorometry. *J. Chromatogr.*, **344**, 115–123.

(Received February 25, 1994
Revised March 29, 1994
Accepted March 31, 1994)

Br. J. Pharmacol. (1994), **112**, 963–971

Endothelin-1-induced myocardial ischaemia and oedema in the rat: involvement of the ET_A receptor, platelet-activating factor and thromboxane A_2

[1]János G. Filep, *Alain Fournier & Éva Földes-Filep

Research Center, Maisonneuve-Rosemont Hospital, University of Montréal, Montréal, P.Q., Canada H1T 2M4 and *Institut National de la Recherche Scientifique-Santé, Pointe-Claire, P.Q., Canada H9R 1G6

1 The objectives of the present experiments were to assess the role of ET_A receptors in mediating endothelin-1 (ET-1)-induced myocardial ischaemia and oedema and to study the involvement of platelet-activating factor (PAF) and thromboxane A_2 (TxA_2) in these actions of ET-1 in rats.

2 Intravenous bolus injection of ET-1 (0.1–2 nmol kg^{-1}) into anaesthetized rats induced ST segment elevation of the electrocardiogram in a dose-dependent manner without causing arrhythmias. ST segment elevation developed within 20–90 s and persisted for at least 10–20 min following administration of ET-1.

3 Pretreatment of the animals with the selective endothelin ET_A receptor antagonist, FR 139317 (2.5 mg kg^{-1}, i.v.) inhibited by 86% the ST segment elevation elicited by ET-1 (1 nmol kg^{-1}). Pretreatment with intravenous administration of BM 13505 (1 mg kg^{-1}), a TxA_2 receptor antagonist, OKY-046 (10 mg kg^{-1}), a thromboxane synthase inhibitor or the specific PAF receptor antagonist, WEB 2086 (1 mg kg^{-1}) or BN 52021 (10 mg kg^{-1}) markedly suppressed ST segment elevation in response to ET-1. Infusion of indomethacin (3 mg kg^{-1} bolus plus 2 mg kg^{-1} h^{-1}) did not significantly affect ET-1-induced ST segment elevation.

4 Bolus injection of ET-1 (1 nmol kg^{-1}, i.v.) to conscious rats resulted in a prolonged pressor effect preceded by a transient depressor response. Corresponding to changes in blood pressure, a small transient tachycardia was followed by a sustained bradycardia. ET-1 enhanced albumin leakage by 87 and 120% in the left ventricle and right atrium, respectively, as measured by the extravasation of Evans blue dye.

5 The selective ET_A receptor antagonist, FR 139317 (2.5 mg kg^{-1}) significantly blunted the pressor action of ET-1 and the accompanying bradycardia without affecting the depressor response. Furthermore, FR 139317 almost completely abolished the permeability effect of ET-1 in both vascular beds studied.

6 Pretreatment of the animals with BM 13505 (1 mg kg^{-1}), OKY-046 (10 mg kg^{-1}), WEB 2086 (1 mg kg^{-1}) or BN 52021 (10 mg kg^{-1}) significantly reduced ET-1 (1 nmol kg^{-1})-induced albumin extravasation both in the left ventricle and right atrium. The PAF receptor antagonists, WEB 2086 and BN 52021 were equally potent inhibitors in the left ventricle, whereas BN 52021 appeared to be a more potent inhibitor than WEB 2086 in the right atrium. Pretreatment with indomethacin (3 mg kg^{-1} plus 2 mg kg^{-1} h^{-1}) did not modify the permeability response to ET-1. None of these compounds affected significantly ET-1-induced changes in mean arterial blood pressure and heart rate.

7 These results indicate that intravenous administration of ET-1 provokes ST segment elevation and myocardial oedema and suggest that these events are mediated, in part, through release of secondary mediators, such as PAF and TxA_2 via the activation of ET_A receptors.

Keywords: Endothelin; ET_A receptor; FR139317; ST segment elevation; protein extravasation; myocardial ischaemia; PAF; thromboxane; rat heart

Introduction

An increasing body of evidence suggests that endothelin-1 (ET-1) plays an important role in coronary ischaemic diseases. Elevated plasma concentrations of ET-1 can be detected in the coronary circulation both in patients with ischaemic heart diseases (Yasuda *et al.*, 1990; Matsuyama *et al.*, 1991; Toyo-oka *et al.*, 1991; Ray *et al.*, 1992) and in laboratory animals during experimental myocardial ischaemia and reperfusion (Tsuji *et al.*, 1991; Watanabe *et al.*, 1991). Coronary arteries from man and other species are very sensitive to the vasoconstrictor action of ET-1 *in vitro* (Yanagisawa *et al.*, 1988; Chester *et al.*, 1989; Cocks *et al.*, 1989; Franco-Cereceda, 1989). Administration of ET-1 directly into the coronary artery of dogs, pigs and rats dramatically increased coronary resistance and ST segment elevations of the electrocardiogram, similar to the clinical phenomenon of Prinzmetal angina, were observed (Ezra *et al.*, 1989; Kurihara *et al.*, 1989; Nichols *et al.*, 1990; Hom *et al.*, 1992; Harada *et al.*, 1993). Furthermore, intravenous injection of ET-1 has been reported to enhance albumin extravasation in the rat coronary circulation (Filep *et al.*, 1992) and therefore contributing to oedema formation, a characteristic feature of the inflammatory reaction associated with acute myocardial ischaemia (Entman *et al.*, 1991).

The cardiac actions of ET-1 may be mediated through activation of one or more endothelin receptor subtypes. Both ET_A (which is highly selective for ET-1) and ET_B (non isopeptide-selective) receptor subtypes are expressed in cardiac tissues (Arai *et al.*, 1990; Sakurai *et al.*, 1990; Lin *et al.*, 1991; Molenaar *et al.*, 1993). In addition, pharmacological studies have suggested the existence of a third, non ET_A/ET_B receptor subtype in the pig coronary artery, which, like ET_A receptors, may mediate the vasoconstrictor action of ET-1 (Harrison *et al.*, 1992). It remains to be determined whether

[1] Author for correspondence.

this ET receptor subtype is similar to those described on bovine cultured endothelial cells (Emori *et al.*, 1990) or rat pituitary gland (Samson *et al.*, 1990). The mechanism of action of ET-1 on the coronary vasculature *in vivo* is far from being fully understood. Results from studies on isolated coronary arteries have implicated the involvement of voltage-gated calcium channels (Yanagisawa *et al.*, 1988) and stimulation of phosphoinositide hydrolysis with subsequent release of intracellular calcium (Kasuya *et al.*, 1989; Pang *et al.*, 1989) in mediating the contractile action of ET-1. The findings that the *in vivo* coronary vasoconstrictor action of ET-1 can be only partially antagonized by calcium channel blockers (Hom *et al.*, 1992; Harada *et al.*, 1993) indicate that mechanisms other than calcium influx through voltage-operated channels are also involved. Indeed, recent evidence suggests that secondary mediators, such as platelet-activating factor (PAF) and thromboxane A_2 (TxA_2) may mediate certain actions of ET-1. Both PAF and TxA_2 have been implicated in ET-1-induced mobilization of intracellular Ca^{2+} in cultured vascular smooth muscle cells (Takayashu *et al.*, 1989). PAF receptor antagonists have been reported to attenuate albumin extravasation elicited by ET-1 in the rat pulmonary and gastrointestinal circulation (Filep *et al.*, 1991b) and to protect against ET-1-induced sudden-death in mice and rats (Terashita *et al.*, 1989). In the present study, we examined the effects of a selective ET_A receptor antagonist, FR 139317 (Aramori *et al.*, 1993; Sogabe *et al.*, 1993) on the coronary vascular responses to ET-1 and studied the involvement of PAF and TxA_2 in mediating the coronary vascular actions of ET-1 in the rat.

Methods

Vascular permeability measurements

The experiments were performed on conscious, chronically catheterized male Wistar rats weighing 205–290 g. The animals were housed in individual metabolic cages and catheters were implanted into the abdominal aorta and vena cava as described previously (Filep *et al.*, 1987). During the experiments the animals could move freely and had free access to food and water. Mean arterial blood pressure (MABP) and heart rate were monitored continuously by a blood pressure analyzer (Micro-Med, Louisville, KY, U.S.A.) using a COBE CDX III pressure transducer.

On the day of the experiment, following an equilibrium period of 1 h, basal cardiovascular parameters were measured for 20 min before drug administration. To measure protein extravasation, Evans blue dye (20 mg kg^{-1}), which binds to plasma albumin (Rawson, 1943), was injected i.v. together with ET-1 (1 nmol kg^{-1}). Previous experiments showed that at this dose, ET-1 markedly enhances albumin extravasation in the rat coronary circulation (Filep *et al.*, 1992). The animals were divided into six groups and were pretreated with one of the following drugs: FR 139317 (2.5 mg kg^{-1}, i.v., 5 min prior to ET-1), a selective ET_A receptor antagonist (Aramori *et al.*, 1993; Sogabe *et al.*, 1993); indomethacin (3 mg kg^{-1} bolus followed by an infusion of 2 mg kg^{-1} h^{-1} started 60 min before injection of ET-1); OKY-046, a thromboxane synthase inhibitor (10 mg kg^{-1}, i.v., 60 min prior to ET-1) (Garcia-Szabo *et al.*, 1984); the TxA_2 receptor antagonist, BM 13505 (1 mg kg^{-1}, i.v., 5 min before injection of ET-1) (Patscheke *et al.*, 1987); the platelet-activating factor receptor antagonists, WEB 2086 (1 mg kg^{-1}, i.v.) (Casals-Stenzel *et al.*, 1987) or BN 52021 (10 mg kg^{-1}, i.v.) (Braquet *et al.*, 1985; Földes-Filep *et al.*, 1987) 10 min before administration of ET-1. Previous studies have demonstrated that indomethacin and OKY-046 at the dose employed inhibited prostaglandin (Filep *et al.*, 1987) and thromboxane A_2 formation (Garcia-Szabo *et al.*, 1984), BM 13505 inhibited the effects of the thromboxane A_2-mimetic, U 44069 (Patscheke *et al.*, 1984) and both WEB 2086 and BN 52021 blocked the hypotensive effect of exogenous platelet-activating factor in rats (Filep *et al.*, 1991b). Ten minutes after injection of ET-1, the animals were anaesthetized with sodium pentobarbitone (50 mg kg^{-1}), and the heart was perfused with 40 ml 0.9% NaCl solution through a catheter inserted into the abdominal aorta. Portions of the anterior wall of the left ventricle and right atrium were excised and weighed. Tissue Evans blue content was measured by spectrophotometry following extraction with formamide (4 ml per g wet tissue weight). The Evans blue content of each sample was expressed as μg dye per g dry weight of tissue to avoid underestimation of changes due to plasma fluid extravasation.

Electrocardiogram measurements

Male Wistar rats weighing 210–295 g were anaesthetized with sodium pentobarbitone (50 mg kg^{-1}). Catheters were inserted into the right femoral artery and vein and electrodes were placed on the left and right forlegs and left hindleg. The change in ST-segment of the Lead II electrocardiogram (ECG) was used to monitor coronary ischaemia. Following control cardiovascular and ECG measurements, ET-1 (0.1, 1 or 2 nmol kg^{-1}) was injected i.v. in a volume of 25 μl kg^{-1} body weight followed by 30 μl 0.9% NaCl. In another series of experiments, the animals were pretreated with FR 139317, indomethacin, OKY-046, BM 13505, WEB 2086 or BN 52021 as described above before injection of ET-1 (1 nmol kg^{-1}, i.v.). The animals were monitored for 20 min following the injection of ET-1. Each animal received only one dose of ET-1 and one type of pretreatment. Lead II ECG was recorded using a Siemens Sirecust 341 electrocardiograph (Germany).

Drugs and chemicals

ET-1 was synthesized in our laboratories by solid-phase methodology. The purity of the preparation was greater than 97% as measured by high performance liquid chromatography. ET-1 was dissolved in distilled water and stored at −20°C. On the day of the experiments, an aliquot was removed and diluted further with 0.9% NaCl. Other drugs were freshly prepared each day and includeed FR 139317 ((**R**)2-[(**R**)-2-[(**S**)-2-[[1-(hexahydro-1*H*-azepinyl)]-carbonyl] amino-4-methylpentanoyl] amino-3-[3-(1-methyl-1*H*-indoyl)] propionyl]amino-3-(2-pyridyl) propionic acid, Fujisawa Pharmaceutical Co., Osaka, Japan); OKY-046 ((E)-3-[4-(1-imidazolylmethyl)phenyl]-2-propenoic acid hydrochloride, ONO Pharmaceuticals, Japan); BM 13505 (4-[2-(4-chlorobenzene sulphonylamino) ethyl) benzene] acetic acid, Boehringer-Mannheim GmbH, Mannheim, Germany); WEB 2086 (3-[4-(2-chlorphenyl)-9-methyl-6H-thienol [3,2-f] [1,2,4] triazolo-[4,3-a] [1,4]-diazepine-2-yl]-1-(morpholinyl)-1-propanon, Boehringer-Ingelheim KG, Ingelheim, Germany) and BN 52021 (ginkgolide B, 9H-1,7a-(epoxymethanol)-1H,6aH,cyclopenta [c] [2-3-b] furo-[3,2':3,4] cyclopenta-[1,2-d]furan 5,9,12-[4H] trione, 3 *tert*-butyl-hexahydro 4,7b,11, hydroxy-8-methyl, Institut Henri Beaufour, Le Plessis Robinson, France). Drugs were dissolved in 0.9% saline with the exception of indomethacin and BM 13505 which were dissolved in ethanol, and BN 52021 which was dissolved in dimethylsulphoxide and were diluted further with 0.9% NaCl as appropriate. Indomethacin and Evans blue dye were purchased from Sigma Chemical Co., St. Louis, MO, U.S.A.

Statistical analysis

Results are expressed as means ± s.e.mean. Statistical analysis of the data was performed by two-way analysis of variance using ranks (Friedman's test) followed by a Wilcoxon-Wilcox test (Wilcoxon & Wilcox, 1964) to identify differences between control and repeated measurements on the same animals; by one-way analysis of variance using

ranks (Kruskal-Wallis test) followed by Dunn's multiple contrast hypothesis test (Dunn, 1964), when various treatments were compared to the same control group; or by Wilcoxon signed rank test and Mann-Whitney U test, for paired and unpaired observations, respectively. A level of $P<0.05$ was considered significant for all tests.

Results

Effects of FR 139317, indomethacin, thromboxane and PAF receptor blockade on ET-1-induced changes in blood pressure and heart rate in conscious and anaesthetized rats

In agreement with previous studies, intravenous bolus injection of ET-1 (1 nmol kg^{-1}) to conscious rats evoked biphasic effects on MABP with a transient decrease followed by a prolonged pressor action. Corresponding to the changes in MABP, a small transient tachycardia was followed by a sustained bradycardia (Figure 1). Administration of FR 139317 (2.5 mg kg^{-1}) by itself did not produce significant changes in MABP and heart rate, whereas it inhibited by 76% the pressor action of 1 nmol kg^{-1} ET-1 and the concomitant bradycardia, without affecting the depressor response to ET-1 (Figure 1). Increasing the dose of FR 139317 did not cause further inhibition of the pressor effect of ET-1.

Pretreatment of the animals with indomethacin (3 mg kg^{-1} plus 2 mg kg^{-1} h^{-1}), WEB 2086 (1 mg kg^{-1}) or BN 52021 (10 mg kg^{-1}) caused neither significant changes in MABP and heart rate nor modified the depressor and pressor actions of ET-1 (1 nmol kg^{-1}) (Table 1). Administration of BM 13505 (1 mg kg^{-1}) 5 min before injection of ET-1, increased MABP from 112 ± 4 to 125 ± 4 mmHg ($n = 6$, $P<0.05$). BM 13505 treatment prolonged the duration of the depressor action of 1 nmol kg^{-1} ET-1 up to 75 s without affecting its magnitude. The pressor response to ET-1 was similar in control and BM 13505-treated animals (Table 1). MABP rose from 111 ± 3 to 123 ± 4 mmHg ($n = 6$, $P<0.05$) following OKY-046 (10 mg kg^{-1}) treatment. However, OKY-046 failed to affect the depressor and pressor responses to ET-1 (Table 1). None of these inhibitors and antagonists affected significantly ET-1-induced changes in heart rate (Table 1).

The basal values for MABP and heart rate were significantly higher in anaesthetized than in conscious animals

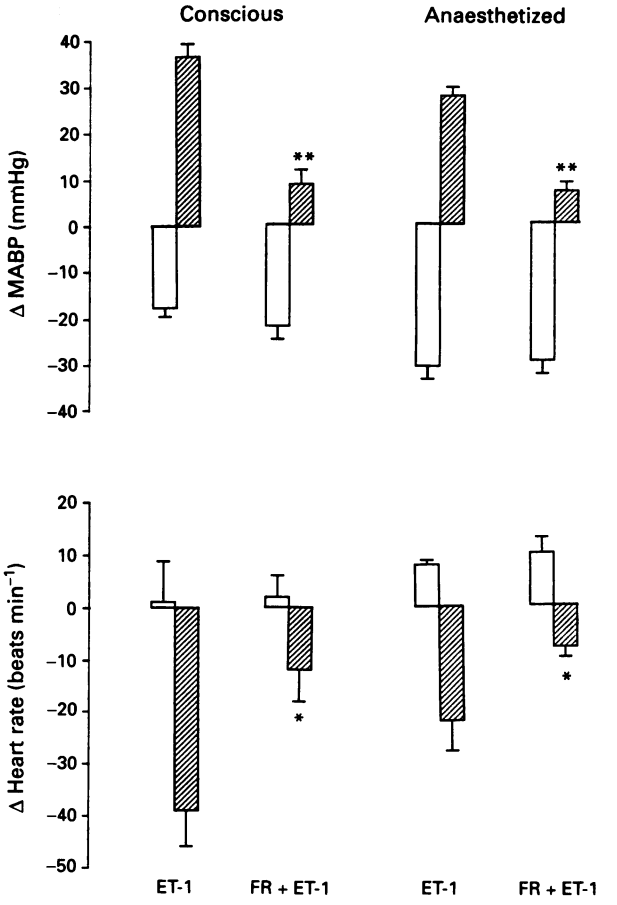

Figure 1 Effect of FR 139317 (FR, 2.5 mg kg^{-1}, i.v.) on the peak depressor (open columns) and pressor (hatched columns) responses elicited by endothelin-1 (ET-1, 1 nmol kg^{-1}, i.v.) and accompanying changes in heart rate in conscious and anaesthetized rats. The basal values for mean arterial blood pressure (MABP) and heart rate in conscious rats were 107 ± 2 mmHg and 335 ± 8 beats min^{-1} ($n = 10$), respectively, and in anaesthetized rats were 124 ± 2 mmHg and 426 ± 10 beats min^{-1} ($n = 10$), respectively. Values are means with s.e.mean for five experiments. $^*P<0.05$, $^{**}P<0.01$ (compared to ET-1 by the Mann-Whitney U test).

Table 1 Endothelin-1 (ET-1)-induced maximum decrease and increase in mean arterial blood pressure (MABP) and accompanying changes in heart rate in conscious and anaesthetized rats

		Basal		*Maximum depressor response*		*Maximum pressor response*	
		MABP (mmHg)	*Heart rate* (beats min^{-1})	*ΔMABP* (mmHg)	*ΔHeart rate* (beats min^{-1})	*ΔMABP* (mmHg)	*ΔHeart rate* (beats min^{-1})
Conscious rats							
ET-1	8	112 ± 3	343 ± 9	-18 ± 2	2 ± 6	39 ± 3	-42 ± 9
Indomethacin + ET-1	5	115 ± 3	342 ± 12	-18 ± 3	-2 ± 6	47 ± 4	-45 ± 8
OKY-034 + ET-1	6	111 ± 3	326 ± 11	-22 ± 2	0 ± 7	36 ± 6	-32 ± 9
BM 13505 + ET-1	6	112 ± 4	338 ± 12	-29 ± 4	3 ± 8	34 ± 3	-31 ± 5
WEB 2086 + ET-1	6	111 ± 2	312 ± 9	-22 ± 4	5 ± 7	41 ± 2	-41 ± 10
BN 52021 + ET-1	6	118 ± 2	334 ± 12	-25 ± 3	3 ± 7	30 ± 3	-29 ± 5
Anaesthetized rats							
ET-1	5	$125 \pm 2^{**}$	$440 \pm 15^{**}$	$-31 \pm 3^{**}$	8 ± 1	$28 \pm 2^{*}$	$-22 \pm 6^{*}$
Indomethacin + ET-1	4	124 ± 5	455 ± 10	-31 ± 2	12 ± 8	37 ± 7	-29 ± 11
OKY-034 + ET-1	5	122 ± 5	445 ± 15	-34 ± 5	10 ± 6	28 ± 2	-35 ± 4
BM 13505 + ET-1	6	126 ± 2	428 ± 22	-27 ± 3	5 ± 3	22 ± 3	-16 ± 5
WEB 2086 + ET-1	5	126 ± 4	439 ± 16	-29 ± 5	6 ± 5	23 ± 6	-24 ± 12
BN 52021 + ET-1	4	126 ± 3	416 ± 26	-32 ± 3	12 ± 3	28 ± 6	-27 ± 8

Following control measurements, the animals were pretreated with indomethacin (3 mg kg^{-1} plus 2 mg kg^{-1} h^{-1} for 60 min), OKY-046 (10 mg kg^{-1} for 60 min), BM 13505 (1 mg kg^{-1} for 5 min), WEB 2086 (1 mg kg^{-1} for 10 min) or BN 52021 (10 mg kg^{-1} for 10 min) before injection of ET-1 (1 nmol kg^{-1}, i.v.). The values are means ± s.e.mean for n experiments. Kruskal-Wallis test indicated that variation among median values for all parameters in various treatment groups was not significantly greater (P values were between 0.08 and 0.83) than expected by chance both in conscious and anaesthetized rats. $^*P<0.05$; $^{**}P<0.01$ (compared to ET-1 injection in conscious rats by the Mann-Whitney U test).

(MABP were 113 ± 1 mmHg, $n = 37$ and 124 ± 1 mmHg, $n = 34$ in conscious and anaesthetized animals, respectively, $P < 0.05$; heart rate were 333 ± 5 and 433 ± 6 beats min^{-1}, respectively, $P < 0.01$). Both MABP and heart rate remained stable for 80 min following control measurements. The magnitude of the transient fall in MABP following injection of ET-1 (1 nmol kg^{-1}) was significantly greater in anaesthetized than in conscious rats, whereas the pressor effect of ET-1 was more pronounced in conscious than in anaesthetized animals (Table 1). As observed in conscious rats, FR 139317 significantly attenuated, but did not completely prevent the pressor response to ET-1 and the accompanying bradycardia without affecting the depressor response (Figure 1). Intravenous administration of BM 13505 or OKY-046 resulted in significant increases in MABP in anaesthetized rats. For instance, MABP rose from 126 ± 2 mmHg to 135 ± 5 mmHg ($n = 6$, $P < 0.05$) and from 122 ± 5 mmHg to 127 ± 7 mmHg ($n = 5$, $P < 0.05$) following BM 13505 and OKY-046 treatment, respectively. However, neither BM 13505 nor OKY-046 affected the depressor and pressor responses to ET-1 (1 nmol kg^{-1}) (Table 1). In addition, indomethacin, WEB 2086 or BN 52021 also failed to modify the effects of ET-1 on MABP (Table 1). None of the TxA_2 and PAF receptor antagonists and TxA_2 synthase inhibitors affected the ET-1-induced changes in heart rate (Table 1).

Effects of ET_A, thromboxane and PAF receptor blockade on ET-1-induced albumin extravasation

In agreement with our previous observations, ET-1 at 1 nmol kg^{-1} increased the Evans blue content in the left ventricle and right atrium by 87 and 120%, respectively (Figure 2). These increases were almost completely abolished by FR 139317 (Figure 2). BM 13505 and OKY-046 reduced ET-1-induced albumin extravasation in the left ventricle by 85 and 71%, respectively and in the right atrium by 82 and 47%, respectively (Figure 3). Pretreatment of animals with indomethacin did not modify the increase in permeability elicited by ET-1 (Figure 3). The PAF receptor antagonists, WEB 2086 and BN 52021, appeared to be equally potent inhibitors of the permeability effect of ET-1 in the left ventricle (73 and 86% inhibition, respectively), whereas BN 52021 was a more potent inhibitor of ET-1-induced albumin extravasation than WEB 2086 in the right atrium (99% versus 69% inhibition) (Figure 3). None of the drugs alone affected tissue Evans blue content (data not shown).

Effects of intravenous administration of ET-1 on ECG

Bolus i.v. injections of ET-1 (0.1, 1 or 2 nmol kg^{-1}) produced ST segment elevation in a dose-dependent manner (Figure 4). Statistically significant, albeit small, elevations were observed following ET-1 at a dose as low as 0.1 nmol kg^{-1}. ST segment elevations were observed within 60–90, 30–50 and 20–40 s corresponding to the three doses of ET-1 used. ST segment elevation persisted for 10–14 min following 0.1 nmol kg^{-1} ET-1, whereas no complete recovery to control levels was observed within 20 min following the injection of the two highest doses of ET-1 (Figure 4). Administration of ET-1 up to a dose of 2 nmol kg^{-1} did not produce arrhythmias.

Effects of ET_A, thromboxane and PAF receptor blockade on ET-1-induced ST segment elevation

The ET_A receptor antagonist, FR 139317 (2.5 mg kg^{-1}) attenuated the ST segment elevation induced by ET-1 (1 nmol kg^{-1}, i.v.) by 86% (Figure 5). Pretreatment of the animals with indomethacin (3 mg kg^{-1} plus 2 mg kg^{-1} h^{-1}) did not affect the ST segment elevation elicited by ET-1 (Figure 5). On the other hand, both the thromboxane synthase inhibitor OKY-046 (10 mg kg^{-1}) and the TxA_2 receptor antagonist BM 13505 (1 mg kg^{-1}) suppressed ST segment elevation elicited by ET-1 (Figure 5). Similarly, pretreatment of the animals with the PAF receptor antagonist, WEB 2086 (1 mg kg^{-1}) or BN 52021 (10 mg kg^{-1}) markedly attenuated the ET-1-induced ST segment elevation (Figure 5). None of the inhibitors or antagonists alone caused significant changes in ST segment (data not shown).

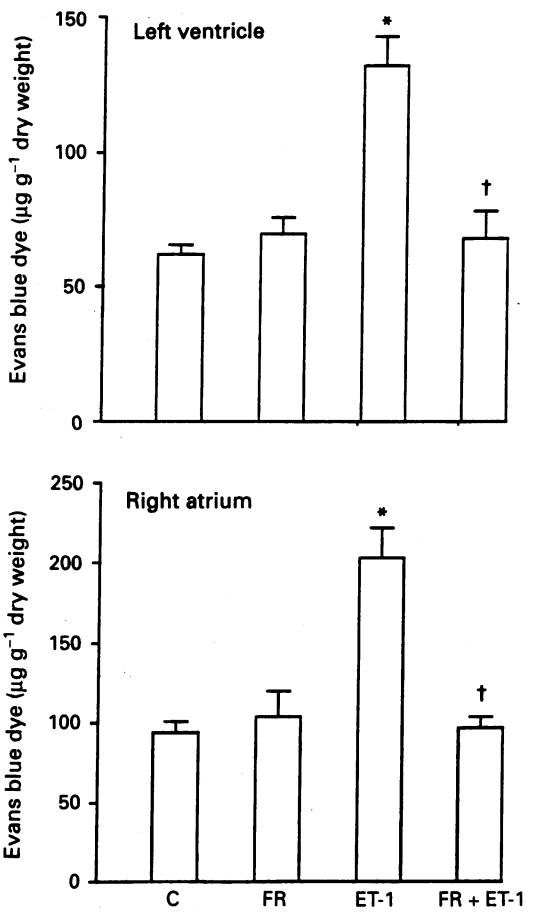

Figure 2 Effects of FR 139317 on endothelin-1 (ET-1)-induced albumin extravasation in the coronary circulation of conscious rats. The animals were pretreated with 0.9% NaCl (C, control) or FR 139317 (FR, 2.5 mg kg^{-1}, i.v. for 5 min), then ET-1 (1 nmol kg^{-1}) or its vehicle (C) were injected together with Evans blue dye (20 mg kg^{-1}). Ten minutes later, the animals were anaesthetized and the heart was perfused with 0.9% NaCl. The permeability measurements were made 15 min after injection of ET-1. Values are means with s.e.mean. $n = 4$ for FR 139317 and FR 139317 plus ET-1, $n = 5$ for control and ET-1. $^*P < 0.05$ (compared to control), $^\dagger P < 0.05$ (compared to ET-1 by Dunn's multiple contrast hypothesis test).

Discussion

The present results showed that i.v. injection of ET-1 produced ST segment elevation and myocardial oedema in the rat. These effects of ET-1 were significantly attenuated by a selective ET_A receptor antagonist, a thromboxane synthase inhibitor, and specific TxA_2 or PAF receptor antagonists.

Since we are not equipped to perform ECG measurements on freely moving rats, and anaesthesia is known to alter cardiovascular control mechanisms (Cox & Bagshaw, 1980), we compared the effects of the above mentioned inhibitors on the haemodynamic effects of ET-1 in conscious and anaesthetized rats. In confirmation of earlier observations, the present study also shows a biphasic change of MABP in response to i.v. bolus injection of ET-1 in both conscious (Gardiner *et al.*, 1989; Le Monnier de Gouville *et al.*, 1990) and anaesthetized rats (Yanagisawa *et al.*, 1988; De Nucci *et*

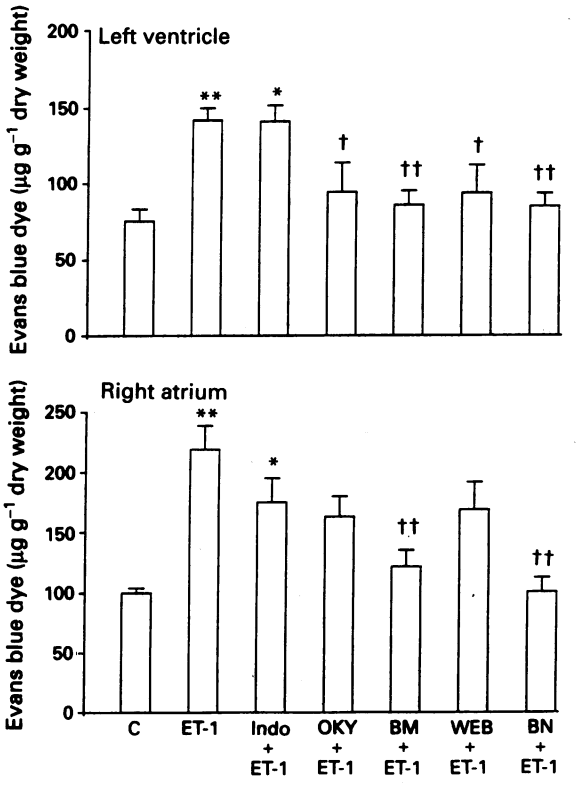

Figure 3 Pharmacological modulation of endothelin-1 (ET-1)-induced albumin extravasation in the coronary circulation of conscious rats. The animals were pretreated with 0.9% NaCl (C, control), indomethacin (Indo, 3 mg kg^{-1} plus 2 mg kg^{-1} h^{-1} for 60 min), OKY-046 (OKY, 10 mg kg^{-1} for 60 min), BM 13505 (BM, 1 mg kg^{-1} for 5 min), WEB 2086 (WEB, 1 mg kg^{-1} for 10 min) or BN 52021 (BN, 10 mg kg^{-1} for 10 min) before i.v. bolus injection of ET-1 (1 nmol kg^{-1}) or its vehicle (C) plus Evans blue dye (20 mg kg^{-1}). Ten minutes later, the rats were anaesthetized and the heart was perfused with 0.9% NaCl. The permeability measurements were made 15 min after the injection of ET-1. Values are mean with s.e.mean, $n = 8$ for control and ET-1, $n = 5$ for indomethacin plus ET-1 and $n = 6$ for all other treatments. $^*P<0.05$; $^{**}P<0.01$ (compared to control), $\dagger P<0.05$; $\dagger\dagger P<0.01$ (compared to ET-1 by Dunn's multiple contrast hypothesis test).

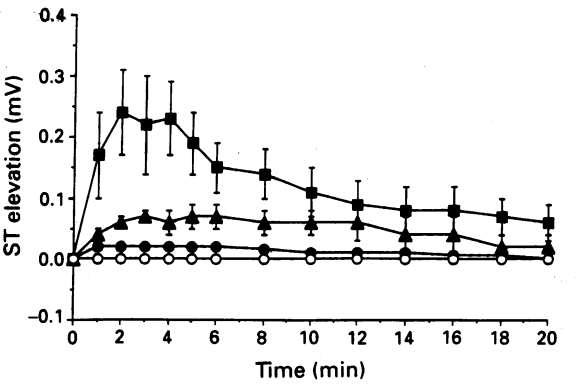

Figure 4 ST segment elevation elicited by intravenous bolus injection of endothelin-1 (ET-1) in anaesthetized rats. The animals received 0.9% NaCl (vehicle of ET-1, $n = 5$) (○), ET-1, 0.1 nmol kg^{-1} (●, $n = 4$), 1 nmol kg^{-1} (▲, $n = 6$) or 2 nmol kg^{-1} (■, $n = 5$) at 0 min. Each point represents mean ± s.e.mean.

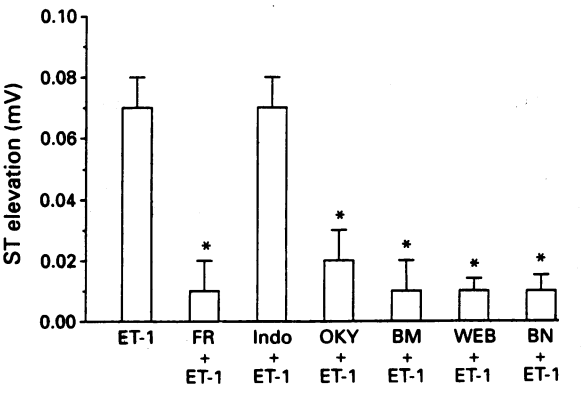

Figure 5 Effects of FR 139317, indomethacin, OKY-046, BM 13505, WEB 2086 and BN 52021 on ST segment elevation induced by intravenous administration of endothelin-1 (ET-1) in anaesthetized rats. The animals were pretreated with 0.9% NaCl, FR 139317 (FR, 2.5 mg kg^{-1} for 5 min, $n = 5$), indomethacin (Indo, 3 mg kg^{-1} plus 2 mg kg^{-1} h^{-1} for 60 min, $n = 4$), OKY-046 (OKY, 10 mg kg^{-1} for 60 min, $n = 5$), BM 13505 (BM, 1 mg kg^{-1} for 5 min, $n = 6$), WEB 2086 (WEB, 1 mg kg^{-1} for 10 min, $n = 5$) or BN 52021 (BN, 10 mg kg^{-1} for 10 min, $n = 5$) before injection of ET-1 (1 nmol kg^{-1}). Values are means ± s.e.mean. $^*P<0.05$ (compared to ET-1 by Dunn's multiple contrast hypothesis test).

al., 1988; Le Monnier de Gouville *et al.*, 1990). The depressor and pressor responses were accompanied by a transient reflex tachycardia and a prolonged reflex bradycardia, respectively. However, the magnitude of the changes in MABP and heart rate were different in anaesthetized and conscious rats. ET-1 produced significantly greater decreases in MABP in anaesthetized than in conscious rats, whereas it evoked greater increases in MABP in conscious than in anaesthetized rats. These observations can be explained by differences in the resting MABP of conscious and anaesthetized rats. Elevations in basal MABP (anaesthetized rats relative to conscious rats) would result in augmentation of the apparent vasodepressor activity and attenuation of the apparent vasopressor activity of various substances.

FR 139317 significantly attenuated the pressor response to ET-1 without affecting its depressor action in both conscious and anaesthetized rats (Sogabe *et al.*, 1993 and the present study). FR 139317 has been reported to be 7000 times more potent in inhibiting the binding of ET-1 to ET_A than ET_B receptors *in vitro* (Aramori *et al.*, 1993). Since ET_B receptors located on the vascular endothelium have been implicated in the mediation of the transient depressor action of ET-1 (Saeki *et al.*, 1991; Douglas & Hiley, 1991), it might be concluded that at the dose used, FR 139317 does not block ET_B receptors *in vivo*. It should be noted, however, that the degree of inhibition of the pressor action of ET-1 by FR 139317 did not exceed 80% either in anaesthetized or conscious rats confirming previous results (Sogabe *et al.*, 1993). Increasing of the dose of FR 139317 did not reduce further the maximum increase in MABP evoked by ET-1 (Sogabe *et al.*, 1993 and the present study). These observations lend further support to the notion that more than one subtype of endothelin receptor is involved in the generation of the pressor effect of ET-1 in the rat (Ihara *et al.*, 1992; Filep *et al.*, 1992, 1993b; Cristol *et al.*, 1993; McMurdo *et al.*, 1993a). The observations that ET-1-induced bradycardia was also markedly attenuated by FR 139317 suggest that ET-1-induced changes in heart rate were secondary to changes in MABP (i.e. a pressor response resulted in reflex bradycardia).

Pretreatment of the animals with indomethacin, OKY-046, BM 13505, WEB 2086 or BN 52021 failed to affect the ET-1-induced changes in MABP and heart rate in both conscious and anaesthetized rats. These findings indicate that neither cyclo-oxygenase products nor PAF are involved in mediating these actions of ET-1. In contrast to these observations, indomethacin was found to potentiate the pressor effect of ET-1 in pithed rats with resting blood pressure of about 50 mmHg (De Nucci *et al.*, 1988). This apparent discrepancy might be, in part, attributed to differences in cardiovascular

control mechanisms operant in conscious and pithed rats. Thus, one may speculate that mechanisms other than release of vasodilator prostanoids are involved in limiting the pressor activity of ET-1 in conscious rats. One of these mechanisms may be endothelium-derived nitric oxide, as inhibition of nitric oxide synthesis markedly potentiated the pressor effect of ET-1 in conscious rats (Filep *et al.*, 1993a). Another possibility might be that ET-1 is less active in releasing vasodilator prostaglandins in conscious than pithed rats, and consequently prostaglandins might be more important in limiting the pressor effects of ET-1 in pithed than conscious rats. The observations that cyclo-oxygenase inhibitors can attenuate the depressor response to ET-1 in anaesthetized dogs (Hermán *et al.*, 1989), and either inhibit or potentiate the pressor action of ET-1 in anaesthetized guinea-pigs (Whittle *et al.*, 1989) or rabbits (Thiemermann *et al.*, 1990; Rogerson *et al.*, 1993), respectively, indicate important species differences in the mechanisms mediating the vascular actions of ET-1. It is uncertain at present which receptor subtypes mediate the ET-1-induced release of vasodilator prostanoids in the rat. The finding that FR 139317 did not modify the depressor response elicited by ET-1, which is thought to be partly mediated by prostacyclin (De Nucci *et al.*, 1988), would argue against the involvement of ET_A receptors. This suggestion is further supported by the observations that ET-1 induces prostacyclin release from bovine cultured aortic endothelial cells (Filep *et al.*, 1991a) which do not possess ET_A receptors (Saeki *et al.*, 1991) and that the prostacyclin releasing properties of ET-1 were not affected by ET_A receptor antagonists in the anaesthetized dog (Hermán *et al.*, 1993) and rabbit (McMurdo *et al.*, 1993b). On the other hand, the supposedly selective ET_A receptor antagonist, BQ-123 (Ihara *et al.*, 1992) was found to inhibit the vasoconstrictor effects of ET-1 and its ability to release prostacyclin from the isolated perfused rat lung (D'Orleans-Juste *et al.*, 1992). However, these latter experiments did not exclude the possibility that prostacyclin release was a consequence of a non-specific defence mechanism of the vasculature in response to drastic elevations in perfusion pressure following administration of ET-1. Furthermore, the selectivity of BQ-123 has recently been questioned (see below). It is also possible that both ET_A and ET_B receptors could mediate prostacyclin release, but their involvement may differ from vascular region to vascular region.

Previous studies demonstrated that intracoronary administration of ET-1 dramatically increases coronary resistance and causes ST segment elevations and arrhythmias in pigs (Ezra *et al.*, 1989), dogs (Kurihara *et al.*, 1989; Nichols *et al.*, 1990; Hom *et al.*, 1992) and rats (Harada *et al.*, 1993). The present results extend these observations by demonstrating that i.v. administration of ET-1 can also produce ST segment elevation without associated arrhythmias. Following i.v. injection of 2 nmol kg^{-1} ET-1, the peak plasma concentration of the peptide in the coronary circulation might be about 100 fold lower than those levels that might have been achieved by intracoronary injections of 6–7 nmol kg^{-1} ET-1 in rats (Harada *et al.*, 1993). The doses of ET-1 used in the present study result in peak plasma ET-1 levels that are two-to-three orders of magnitude higher than those detected under pathological conditions (Yasuda *et al.*, 1990; Matsuyama *et al.*, 1991; Toyo-oka *et al.*, 1991; Tsuji *et al.*, 1991; Watanabe *et al.*, 1991; Ray *et al.*, 1992). It should, however, be noted that plasma ET-1 levels may not necessarily reflect local production and/or concentration of the peptide. The ST segment elevation by endothelin-1 is thought to be due to myocardial ischaemia related to coronary vasoconstriction, whereas a direct action on the myocardium has been implicated in inducing arrhythmias (Harada *et al.*, 1993). Therefore, one may assume that under the present experimental conditions (i.e. at lower coronary plasma concentrations) ET-1 acted primarily on the coronary vascular smooth muscle. The selective ET_A receptor antagonist, FR 139317 protected the heart from ST segment elevation. The observations that FR 139317 did not inhibit completely this action of ET-1 are consistent with the hypothesis that in addition to ET_A receptors, non ET_A/ET_B receptors are also involved in the generation of the vasoconstriction in the coronary circulation (Harrison *et al.*, 1992).

ET-1-induced ST segment elevation was significantly attenuated by the TxA_2 synthesis inhibitor, OKY-046, the TxA_2 receptor blocker, BM 13505 or by the PAF receptor antagonists, WEB 2086 or BN 52021. Numerous studies have shown that ET-1 could activate phospholipase A_2 via various intracellular signalling pathways, leading to release of arachidonic acid and PAF (for recent reviews see Simonson & Dunn, 1992; Sokolovsky, 1992). Arterial tissue and the heart actively convert arachidonic acid to cyclo-oxygenase products including TxA_2 (Hirsh *et al.*, 1981). Both TxA_2 and PAF are potent coronary vasoconstrictors (Hirsh *et al.*, 1981; Feuerstein *et al.*, 1984). Although we did not measure TxA_2 and PAF levels in the coronary circulation in the present experiments, previous studies have documented the capability of ET-1 to release TxA_2 from various tissues (cf. Simonson & Dunn, 1992; Sokolovsky, 1992) and ET-1 has also been reported to enhance PAF release from glomerular mesangial cells (López-Farré *et al.*, 1991). Interestingly, the cyclo-oxygenase inhibitor, indomethacin, failed to inhibit ST segment elevation produced by ET-1. The reason for this observation is not known at present. One possible explanation might be that cyclo-oxygenase blockade diverted arachidonic acid to the lipoxygenase pathway, leading to formation of, for example, sulphidopeptide leukotrienes, which are also known to provoke coronary vasoconstriction (cf. Piper, 1984). Taken together, the protective effects of TxA_2 and PAF receptor blockade on ST segment elevation appear to be due to the inhibitory action on the coronary vasoconstrictor action of ET-1.

In addition to inducing vasoconstriction, ET-1 also enhanced albumin extravasation in the coronary vascular bed of conscious rats. Pretreatment of the animals with FR 139317 almost completely abolished the ET-1-induced increase in albumin extravasation in both the left ventricle and right atrium. These results are consistent with our previous findings with another supposedly selective ET_A receptor antagonist, BQ-123 (Filep *et al.*, 1992). However, recent studies have questioned the selectivity of BQ-123 as it had a preferential antagonistic effect on the ET-3 response in the rat vas deferens (Eglezos *et al.*, 1993). These observations raised the possibility that BQ-123 may also antagonize a non ET_A/ET_B receptor. Whether the atypical endothelin receptor described in the rat vas deferens might be similar to that found in the coronary arteries (Harrison *et al.*, 1992), is not known at present. The findings that FR 139317 markedly attenuated, but did not inhibit completely the ET-1-induced ST segment elevation suggest that FR 139317 may not be an antagonist of this receptor subtype.

The presents results also showed that the permeability effect of ET-1 is mediated through release of secondary mediators, such as TxA_2 and PAF. As with coronary vasoconstriction, indomethacin failed to inhibit albumin extravasation evoked by ET-1, whereas tissue Evans blue accumulation was significantly attenuated by the TxA_2 synthase inhibitor, OKY-046 and the TxA_2 receptor antagonist, BM 13505. However, in addition to inhibition of TxA_2 production, cyclo-oxygenase blockade might have led to enhanced formation of other arachidonic acid metabolites, e.g. leukotrienes (see above), which are known to promote protein extravasation (Dahlén *et al.*, 1981). The PAF receptor antagonists, WEB 2086 and BN 52021 at the doses employed were equally potent in attenuating ET-1-induced accumulation of Evans blue dye in the left ventricle, whereas BN 52021 appeared to be a more potent inhibitor than WEB 2086 in the right atrium. We have found similar differences in the inhibitory action of these PAF antagonists in the lower bronchi and spleen of rats (Filep *et al.*, 1991b). These differences occurred despite the fact that WEB 2086 and BN 52021 at the doses used, caused similar inhibition of the

hypotensive action of exogenous PAF in the conscious rat (Filep *et al.*, 1991b). The different responses to WEB 2086 and BN 52021 suggest that one of the antagonists might act on a different PAF receptor population (Hwang, 1988). An increase in MABP, *per se*, could not be the basis for the observed albumin extravasation as TxA_2 and PAF receptor antagonists were highly effective in inhibiting albumin leakage elicited by ET-1 without affecting the pressor action of this peptide. Indeed, mediator-stimulated increase in protein extravasation is primarily attributable to interendothelial cells gap formation in the venules (Grega *et al.*, 1986). Vasoconstrictors, like noradrenaline that can elevate capillary hydrostatic pressure, but do not elicit gap formation could not promote protein efflux (Grega *et al.*, 1986). ET-1 may induce gap formation directly or more likely through release of secondary mediators, including TxA_2 and PAF. An increase in systemic blood pressure and/or elevation in capillary hydrostatic pressure would, however, facilitate protein extravasation and oedema formation provided that gaps are formed. Thus, attenuation of ET-1-induced coronary vasoconstriction by FR 139317 would lead to a reduction in hydrostatic pressure in the coronary circulation, which, in turn, could contribute to the decrease in albumin extravasation.

In conclusion, the present results demonstrates that i.v. injection of ET-1 provokes ST segment elevation and enhances myocardial albumin extravasation in the rat and suggest that these actions of ET-1 are mediated, in part, through release of secondary mediators, such as TxA_2 and PAF via the activation of ET_A receptors. These data also suggest a therapeutic potential for ET_A receptor antagonists in the treatment of acute ischaemic heart diseases where ET-1 production is enhanced.

FR 139317 was a generous gift of Fujisawa Pharmaceutical Co., Ltd., Osaka, Japan. We thank Drs P. Braquet (Institut Henri Beaufour, Le Plessis Robinson, France), H. Heuer (Boehringer-Ingelheim GmbH, Ingelheim, Germany) and K. Stegmeier (Boehringer-Mannheim KG, Mannheim, Germany) for generously supplying us with BN 52021, WEB 2086 and BM 13505, respectively. This study was supported by the Foundation of the Maisonneuve-Rosemont Hospital. A.F. and J.G.F. are scholars of the Fonds de la Recherche en Santé du Québec (FRSQ).

References

ARAI, H., HORI, S., ARAMORI, I., OHKUBO, H. & NAKANISHI, S. (1990). Cloning and expression of a cDNA encoding an endothelin receptor. *Nature*, **348**, 731–732.

ARAMORI, I., NIREI, H, SHOUBO, M., SOGABE, K., NAKAMURA, K., KOJO, H., NOTSU, Y., ONO, T. & NAKANISHI, S. (1993). Subtype selectivity of a novel endothelin antagonist, FR 139317, for the two endothelin receptors in transfected chinese hamster ovary cells. *Mol. Pharmacol.*, **43**, 127–131.

BRAQUET, P., SPINNEWYN, B., BRAQUET, M., BOURGAIN, R.M., TAYLOR, J.E., NUNEZ, D. & DRIEU, K. (1985). BN 52021 and related compounds: A new series of highly specific PAF-acether receptor antagonists isolated from Ginkgo biloba. *Blood Vessels*, **16**, 559–572.

CASALS-STENZEL, J., MUACEVIC, G. & WEBER, K.H. (1987). Pharmacological actions of WEB 2086, a new specific antagonist of platelet-activating factor. *J. Pharmacol. Exp. Ther.*, **241**, 974–981.

CHESTER, A.H., DASHWOOD, M.R., CLARKE, J.G., LARKIN, S.W., DAVIES, G.J., TADJKARIMI, S., MASERI, A. & YACOUB, M.H. (1989). Influence of endothelin on human coronary arteries and localisation of its binding sites. *Am. J. Cardiol.*, **63**, 1395–1398.

COCKS, T.M., FAULKNER, N.L., SUDHIR, K. & ANGUS, J. (1989). Reactivity of endothelin-1 on human and canine large veins compared with large arteries *in vitro*. *Eur. J. Pharmacol.*, **171**, 17–24.

COX, R.H. & BAGSHAW, R.J. (1980). Effect of anesthesia on carotid sinus reflex control of arterial hemodynamics in the dog. *Am. J. Physiol.*, **239**, H681–H691.

CRISTOL, J.-P., WARNER, T.D., THIEMERMANN, C. & VANE, J.R. (1993). Mediation via different receptors of the vasoconstrictor effects of endothelins and sarafotoxins in the systemic circulation and renal circulation of the anaesthetized rat. *Br. J. Pharmacol.*, **108**, 776–779.

DAHLÉN, S.E., BJORK, J., HEDQVIST, P., ARFORS, K.E., HAMMARSTRÖM, S., LINDGREN, J.A. & SAMUELSSON, B. (1981). Leukotrienes promote plasma leakage and leukocyte adhesion in postcapillary venules: in vivo effects with relevance to the acute inflammatory response. *Proc. Natl. Acad. Sci. U.S.A.*, **78**, 3887–3891.

DE NUCCI, G., THOMAS, R., D'ORLEANS-JUSTE, P., ANTUNES, E., WALDER, C., WARNER, T.D. & VANE, J.R. (1988). Pressor effects of circulating endothelin are limited by its removal in the pulmonary circulation and by the release of prostacyclin and endothelium-derived relaxing factor. *Proc. Natl. Acad. Sci. U.S.A.*, **85**, 9797–9800.

D'ORLEANS-JUSTE, P., TELEMAQUE, S., CLAING, A., IHARA, M. & YANO, M. (1992). Human big endothelin-1 and endothelin-1 release prostacyclin via the activation of ET_1 receptors. *Br. J. Pharmacol.*, **105**, 773–775.

DOUGLAS, S.A. & HILEY, C.R. (1991). Endothelium-dependent mesenteric vasorelaxant effects and systemic action of endothelin (16–21) and other endothelin-related peptides in the rat. *Br. J. Pharmacol.*, **104**, 311–320.

DUNN, O.J. (1964). Multiple comparisons using rank sums. *Technometrics*, **6**, 241–252.

EGLEZOS, A., CUCCHI, P., PATACCHINI, R., QUARTARA, L., MAGGI, C.A. & MIZRAHI, J. (1993). Differential effects of BQ-123 against endothelin-1 and endothelin-3 on the rat vas deferens: evidence for an atypical endothelin receptor. *Br. J. Pharmacol.*, **109**, 736–738.

EMORI, T., HIRATA, Y. & MARUMO, F. (1990). Specific receptor for endothelin-1 in cultured endothelial cells and its cellular mechanism of action. *FEBS Lett.*, **263**, 261–264.

ENTMAN, M.L., MICHAEL, L., ROSSEN, R.D., DREYER, W.J., ANDERSON, D.C., TAYLOR, A.A. & SMITH, C.W. (1991). Inflammation in the course of early myocardial ischemia. *FASEB J.*, **5**, 2529–2537.

EZRA, D., GOLDSTEIN, R.E., CZAJA, J.F. & FEUERSTEIN, G.Z. (1989). Lethal ischemia due to intracoronary endothelin in pigs. *Am. J. Physiol.*, **257**, H339–H343.

FEUERSTEIN, G., BOYD, L.M., EZRA, D. & GOLDSTEIN, R.E. (1984). Effect of platelet-activating factor on coronary circulation of the domestic pig. *Am. J. Physiol.*, **246**, H466–H471.

FILEP, J.G., BATTISTINI, B., COTE, Y.P., BEAUDOIN, A.R. & SIROIS, P. (1991a). Endothelin-1 induces prostacyclin release from bovine aortic endothelial cells. *Biochem. Biophys. Res. Commun.*, **177**, 171–176.

FILEP, J., FÖLDES-FILEP, E. & FRÖLICH, J.C. (1987). Vascular responses to leukotrienes B_4, C_4 and D_4 following FPL 55712, indomethacin, saralasin, phentolamine and verapamil in the conscious rat. *Br. J. Pharmacol.*, **90**, 431–439.

FILEP, J.G., FÖLDES-FILEP, E., ROUSSEAU, A., FOURNIER, A., SIROIS, P. & YANO, M. (1992). Endothelin-1 enhances vascular permeability in rat heart through the ET_A receptor. *Eur. J. Pharmacol.*, **219**, 343–344.

FILEP, J.G., FÖLDES-FILEP, E., ROUSSEAU, A., SIROIS, P. & FOURNIER, A. (1993a). Vascular responses to endothelin-1 following inhibition of nitric oxide synthesis in the conscious rat. *Br. J. Pharmacol.*, **110**, 1213–1221.

FILEP, J.G., SIROIS, M.G., FÖLDES-FILEP, E., ROUSSEAU, A., PLANTE, G.E., FOURNIER, A., YANO, M. & SIROIS, P. (1993b). Enhancement by endothelin-1 of microvascular permeability via the activation of ET_A receptors. *Br. J. Pharmacol.*, **109**, 880–886.

FILEP, J.G., SIROIS, M.G., ROSSEAU, A., FOURNIER, A. & SIROIS, P. (1991b). Effects of endothelin-1 on vascular permeability in the conscious rat: interactions with platelet-activating factor. *Br. J. Pharmacol.*, **104**, 797–804.

FÖLDES-FILEP, E., BRAQUET, P. & FILEP, J. (1987). Inhibition by BN 52021 (Ginkgolide B) of the specific binding of [^{3}H]-platelet-activating factor to human neutrophil granulocytes. *Biochem. Biophys. Res. Commun.*, **148**, 1412–1417.

FRANCO-CERECEDA, A. (1989). Endothelin- and neuropeptide Y-induced vasoconstriction of human epicardial coronary arteries *in vitro*. *Br. J. Pharmacol.*, **97**, 968–972.

GARCIA-SZABO, R., KERN, D.F. & MALIK, A.B. (1984). Pulmonary vascular response to thrombin: effects of thromboxane synthase inhibition with OKY-046 and OKY-1581. *Prostaglandins*, **28**, 851–866.

GARDINER, S.M., COMPTON, A.M. & BENNETT, T. (1989). Regional haemodynamic effects of endothelin-1 in conscious, unrestrained, Wistar rats. *J. Cardiovasc. Pharmacol.*, **13** (Suppl. 5), S202–S204.

GREGA, G.J., ADAMSKI, S.W. & DOBBINS, D.E. (1986). Physiological and pharmacological evidence for the regulation of permeability. *Fed. Proc.*, **45**, 96–100.

HARADA, K., MIWA, A., KANETA, S., IZAWA, T., FUKUSHIMA, H. & OGAWA, N. (1993). Effects of KRN 2391, nicorandil and diltiazem on the changes in the electrocardiogram caused by endothelin-1 in anaesthetized rats. *Br. J. Pharmacol.*, **109**, 679–684.

HARRISON, V.J., RANDRIANTSOA, A. & SCHOEFFTER, P. (1992). Heterogeneity of endothelin-sarafotoxin receptors mediating contraction of pig coronary artery. *Br. J. Pharmacol.*, **105**, 511–513.

HERMÁN, F., MAGYAR, K., CHABRIER, P.E., BRAQUET, P. & FILEP, J. (1989). Prostacyclin mediates antiaggregatory and hypotensive actions of endothelin in anaesthetized beagle dogs. *Br. J. Pharmacol.*, **98**, 38–40.

HERMÁN, F., YANO, M. & FILEP, J.G. (1993). The in vivo antiaggregatory action of endothelin-1 is not mediated through the endothelin ET_A receptor. *Eur. J. Pharmacol.*, **236**, 143–146.

HIRSH, P.D., HILLIS, L.D., CAMPBELL, W.B., FIRTH, B.G. & WILLERSON, J.T. (1981). Release of prostaglandins and thromboxane into the coronary circulation in patients with ischemic heart disease. *N. Engl. J. Med.*, **304**, 685–691.

HOM, G.J., TOUHEY, B. & RUBANYI, G.M. (1992). Effects of intracoronary administration of endothelin in anesthetized dogs: comparison with Bay K 8644 and U 46619. *J. Cardiovasc. Pharmacol.*, **19**, 194–200.

HWANG, S.B. (1988). Identification of a second putative receptor of platelet-activating factor from human polymorphonuclear leukocytes. *J. Biol. Chem.*, **263**, 3225–3233.

IHARA, M., NOGUCHI, K., SAEKI, T., FUKURODA, T., TSUCHIDA, S., KIMURA, S., FUKAMI, T., ISHIKAWA, K., NISHIKIBE, M. & YANO, M. (1992). Biological profiles of a highly potent novel endothelin antagonist selective for the ET_A receptor. *Life Sci.*, **50**, 247–255.

KASUYA, Y., TAKUWA, Y., YANAGISAWA, M., KIMURA, S., GOTO, K. & MASAKI, T. (1989). Endothelin-1 induces vasoconstriction through two functionally distinct pathways in porcine coronary artery: contribution of phosphoinositide turnover. *Biochem. Biophys. Res. Commun.*, **161**, 1049–1055.

KURIHARA, H., YAMAOKI, K., NAGAI, R., YOSHIZUMI, M., TAHAKU, F., SATOH, M., INUI, J. & YAZAKI, Y. (1989). Endothelin: a potent vasoconstrictor associated with coronary vasospasm. *Life Sci.*, **44**, 1937–1943.

LE MONNIER DE GOUVILLE, A.C., MONDOT, S., LIPPTON, H., HYMAN, A. & CAVERO, I. (1990). Hemodynamic and pharmacological evaluation of the vasodilator and vasoconstrictor effects of endothelin in rats. *J. Pharmacol. Exp. Ther.*, **252**, 300–311.

LIN, H.Y., KAJI, E.H., WINKEL, G.K., IVES, H.E. & LADISH, H.F. (1991). Cloning and functional expression of a vascular smooth muscle endothelin-1 receptor. *Proc. Natl. Acad. Sci. U.S.A.*, **88**, 3185–3189.

LÓPEZ-FARRÉ, A., GÓMEZ-GARRE, D., BERNABEU, F., MONTANÉS, I., MILLÁS, I. & LÓPEZ-NOVOA, J. (1991). Renal effects and mesangial cell contraction induced by endothelin are mediated by PAF. *Kidney Int.*, **39**, 624–630.

MATSUYAMA, K., YASUE, H., OKUMURA, K., SAITO, Y., NAKAO, K., SHIRAKAMI, G. & IMURA, H. (1991). Increased plasma level of endothelin-1-like immunoreactivity during coronary spasm in patients with coronary spastic angina. *Am. J. Cardiol.*, **68**, 991–995.

MCMURDO, L., CORDER, R., THIEMERMANN, C. & VANE, J.R. (1993a). Incomplete inhibition of the pressor effects of endothelin-1 and related peptides in the anaesthetized rat with BQ-123 provides evidence for more than one vasoconstrictor receptor. *Br. J. Pharmacol.*, **108**, 557–561.

MCMURDO, L., LIDBURY, C., THIEMERMANN, C. & VANE, J.R. (1993b). Mediation of endothelin-1-induced inhibition of platelet aggregation via the ET_B receptor. *Br. J. Pharmacol.*, **109**, 530–534.

MOLENAAR, P., O'REILLY, G., SHARKEY, A., KUC, R.E., HARDING, D.P., PLUMTON, C., GRESHAM, G.A. & DAVENPORT, A.P. (1993). Characterization and localization of endothelin receptor subtypes in the human atrio-ventricular conducting system and myocardium. *Circ. Res.*, **72**, 526–538.

NICHOLS, A.J., KOSTER, P.F. & OHLSTEIN, E.H. (1990). The effect of diltiazem on the coronary haemodynamic and cardiac functional effects produced by intracoronary administration of endothelin-1 to anaesthetized dogs. *Br. J. Pharmacol.*, **99**, 597–601.

PANG, D.C., JOHNS, A., PATTERSON, K., BOTELHO, L. & RUBANYI, G.M. (1989). Endothelin-1 stimulates phosphatidylinositol hydrolysis and calcium uptake in isolated canine coronary arteries. *J. Cardiovasc. Pharmacol.*, **13** (Suppl. 5), S75–S79.

PATSCHEKE, H., STEGMEIER, K., HORNBERGER, W., STAIGER, C.H. & NEUGEBAUER, G. (1987). Inhibition of platelet activation by the novel thromboxane receptor antagonist BM 13505. *Thromb. Haemostasis*, **58**, 182.

PIPER, P.J. (1984). Formation and actions of leukotrienes. *Physiol. Rev.*, **64**, 744–761.

RAWSON, R.A. (1943). The binding of T-1824 and structurally related diazo dyes by the plasma protein. *Am. J. Physiol.*, **138**, 708–717.

RAY, S.G., MCMURRAY, J.J., MORTON, J.J. & DARGIE, H.J. (1992). Circulating endothelin in acute ischaemic syndromes. *Br. Heart J.*, **67**, 383–386.

ROGERSON, M.E., CAIRNS, H.S., FAIRBANKS, L.D., WESTWICK, J. & NEILD, G.H. (1993). Endothelin-1 in the rabbit – Interaction with cyclooxygenase and NO-synthase products. *Br. J. Pharmacol.*, **108**, 838–843.

SAEKI, T., IHARA, M., FUKURODA, T., YAMAGIWA, M. & YANO, M. (1991). [$Ala^{1,3,11,15}$]endothelin-1 analogues with ET_B agonistic activity. *Biochem. Biophys. Res. Commun.*, **179**, 286–292.

SAKURAI, T., YANAGISAWA, M., TUKURA, Y., MIYAZAKI, H., KIMURA, S., GOTO, K. & MASAKI, T. (1990). Cloning of a cDNA encoding a non-isopeptide-selective subtype of the endothelin receptor. *Nature*, **348**, 732–735.

SAMSON, W.K., SKALA, K.P., ALEXANDER, B.D. & HUANG, F.L.S. (1990). Pituitary site of action of endothelin: selective inhibition of prolactin release in vitro. *Biochem. Biophys. Res. Commun.*, **169**, 737–743.

SIMONSON, M.S. & DUNN, M.J. (1992). The molecular mechanisms of cardiovascular and renal regulation of endothelin peptides. *J. Lab. Clin. Med.*, **119**, 622–639.

SOGABE, K., NIREI, H., SHOUBO, M., NOMOTO, A., AO, S., NOTSU, Y. & ONO, T. (1993). Pharmacological profile of FR 139317, a novel, potent endothelin ET_A receptor antagonist. *J. Pharmacol. Exp. Ther.*, **264**, 1040–1046.

SOKOLOVSKY, M. (1992). Endothelins and sarafotoxins: physiological regulation, receptor subtypes and transmembrane signaling. *Pharmacol. Ther.*, **54**, 129–149.

TAKAYASHU, M., KONDO, K. & TERAO, S. (1989). Endothelin-induced mobilization of Ca^{2+} and possible involvement of platelet-activating factor and thromboxane A_2. *Biochem. Biophys. Res. Commun.*, **160**, 751–757.

TERASHITA, Z., SHIBOUTA, Y., IMURA, Y., IWASAKI, K. & NISHIKAWA, K. (1989). Endothelin-induced sudden-death and the possible involvement of platelet-activating factor. *Life Sci.*, **45**, 1911–1918.

THIEMERMANN, C., MAY, G.R., PAGE, C.P. & VANE, J.R. (1990). Endothelin-1 inhibits platelet aggregation *in vivo*: a study with ^{111}indium-labelled platelets. *Br. J. Pharmacol.*, **99**, 303–308.

TOYO-OKA, T., AIZAWA, T., SUZUKI, N., HIRATA, Y., MIYAUCHI, T., SHIN, W.S., YANAGISAWA, M., MASAKI, T. & SUGIMOTO, T. (1991). Increased plasma level of endothelin-1 and coronary spasm induction in patients with vasospastic angina pectoris. *Circulation*, **83**, 476–483.

TSUJI, S., SAWAMURA, A., WATANABE, H., TAKIHARA, K., PARK, S.E. & AZUMA, J. (1991). Plasma endothelin levels during myocardial ischemia and reperfusion. *Life Sci.*, **48**, 1745–1749.

WATANABE, T., SUZUKI, N., SHIMAMOTO, N., FUJINO, M. & IMADA, A. (1991). Contribution of endogenous endothelin to the extension of myocardial infarct size in rats. *Circ. Res.*, **69**, 370–377.

WHITTLE, B.J.R., PAYNE, A.N. & ESPLUGUES, J.V. (1989). Cardiopulmonary and gastric ulcerogenic actions of endothelin-1 in the guinea pig and rat. *J. Cardiovasc. Pharmacol.*, **13** (Suppl 5.), S103–S107.

WILCOXON, F. & WILCOX, R.A. (1964). *Some Rapid Approximate Statistical Procedures*. pp. 36–38. Pearl River NY: Lederle Laboratories.

YANAGISAWA, M, KURIHARA, H., KIMURA, S., TOMOBE, Y., KOBAYASHI, M., MITSUI, Y., YAZAKI, Y., GOTO, K. & MASAKI, T. (1988). A novel potent vasoconstrictor peptide produced by vascular endothelial cells. *Nature*, **332**, 411–415.

YASUDA, M., KOHNO, M., TAHARA, A., ITAGANE, H., TODA, I., AKIOKA, K., TERAGAKI, M., OKU, H., TAKEUCHI, K. & TAKEDA, T. (1990). Circulating immunoreactive endothelin in ischemic heart disease. *Am. Heart J.*, **119**, 801–806.

(Received December 7, 1993
Revised March 17, 1994
Accepted March 22, 1994)

Br. J. Pharmacol. (1994), **112**, 972–976

All-or-nothing responses to carbachol in single intestinal smooth muscle cells of rat

[1]Toshio Ohta, Shigeo Ito & Yoshikazu Nakazato

Department of Pharmacology, Faculty of Veterinary Medicine, Hokkaido University, Sapporo 060, Japan

1 Concentration-response relationships for carbachol (CCh)-induced increases in the cytosolic calcium concentration ($[Ca^{2+}]_i$) and membrane currents were studied by use of fura-2 microfluorimetry and nystatin-perforated whole-cell recording in single smooth muscle cells isolated from rat intestine.

2 CCh produced an initial peak rise in $[Ca^{2+}]_i$ followed by a small sustained rise. In individual cells, the peak rise in $[Ca^{2+}]_i$ did not increase in amplitude even with increasing concentrations of CCh, though the threshold concentration varied in different cells. The initial peak rise in $[Ca^{2+}]_i$, but not the sustained rise, was due to the release of stored Ca^{2+}, because it was unchanged after removal of external Ca^{2+} and the addition of nifedipine (1 μM) or La^{3+} (1 mM).

3 CCh elicited an outward and inward current in a cell dialyzed with a pipette solution containing KCl at a holding potential of − 30 mV and with one containing NaCl at − 60 mV, respectively. In individual cells, the amplitude of each current was similar in cells stimulated at over the threshold concentration of CCh, but the threshold was different among cells.

4 The percentage of cells showing Ca^{2+}-transient responses to CCh at given concentrations was similar to those showing current responses and contractile responses.

5 In thin muscle bundles, a concentration-dependent contraction was evoked by CCh in the absence of external Ca^{2+}. Its threshold was similar to those of Ca^{2+}-transient and current responses in single cells.

6 These results suggest that CCh-induced release of stored Ca^{2+} takes place in an all-or-nothing fashion in individual cells of the rat intestinal smooth muscle.

Keywords: Calcium release; carbachol; intestinal smooth muscle cell; intracellular Ca^{2+} stores; ion channel; whole-cell voltage-clamp

Introduction

In various smooth muscle cells, the activation of muscarinic receptors produces an increase of cytosolic calcium concentration ($[Ca^{2+}]_i$) due to the influx of external Ca^{2+} and the release of Ca^{2+} from intracellular stores (Bolton, 1979). It is now widely accepted that inositol 1,4,5-trisphosphate (IP_3) is the intracellular messenger which stimulates the release of Ca^{2+} from intracellular stores following receptor activation (Berridge & Irvine, 1984).

Recently, it has been shown that IP_3-induced Ca^{2+} release is potentiated in the presence of submicromolar concentrations of Ca^{2+} and receives positive feedback regulation by Ca^{2+} (Iino, 1990; Bezprozvanny *et al.*, 1991; Finch *et al.*, 1991; Iino & Endo, 1992). The feedback mechanism could account for the oscillations in $[Ca^{2+}]_i$ sometimes seen (DeLisle & Welsh, 1992; Miyazaki *et al.*, 1992). Therefore, it is suggested that IP_3-induced Ca^{2+} release is regenerative, that is it occurs in an all-or-nothing fashion, once Ca^{2+} release has been initiated by IP_3 (Iino *et al.*, 1994). From this suggestion, it is expected that CCh-induced release of stored Ca^{2+} occurs dose-independently, if cells are stimulated by CCh concentrations that exceed the threshold for IP_3 formation, resulting in Ca^{2+} release from intracellular stores.

We have recently demonstrated that the muscarinic agonist carbachol (CCh), activates two different ionic channel in rat intestinal smooth muscle cells, probably due to Ca^{2+} release from intracellular Ca^{2+} stores through production of IP_3 (Ito *et al.*, 1993). One is an outward K^+ current as reported in vascular (Byrne & Large, 1988; Amédée *et al.*, 1990a) and visceral smooth muscle cells (Bolton & Lim, 1989; Komori & Bolton, 1991; Ohta *et al.*, 1992), and the other is an inward current mainly due to an increase in membrane Cl^- conductance, the properties of which are similar to those in vascular (Byrne & Large, 1988; Pacaud *et al.*, 1989; Amédée *et al.*, 1990a,b) and tracheal smooth muscle cells (Janssen & Sims, 1992). If CCh causes the release of stored Ca^{2+} in an all-or-nothing fashion, the Ca^{2+}-activated CCh-induced current responses are also expected to occur in a similar manner.

The purpose of the present study was to determine whether CCh causes Ca^{2+} release from intracellular stores and evokes current responses in an all-or-nothing fashion. We investigated, therefore, the effects of various concentrations of CCh on increases in $[Ca^{2+}]_i$ and outward and inward currents in single dispersed intestinal smooth muscle cells of the rat.

Methods

Cell preparation

Male Wistar rats (200–250 g) were killed by stunning and bleeding. Smooth muscle cells were enzymatically isolated from the longitudinal muscle of rat intestine with collagenase and papain as described previously (Ohta *et al.*, 1993). Small aliquots of the dispersed cells were stored in normal external solution on cover-slips in a moist chamber at 4°C for use the same day.

Fluorescence and membrane current measurements

The cytosolic Ca^{2+} concentration, $[Ca^{2+}]_i$, was estimated in single cells by fura-2 fluorescence with the ratio method using dual-wavelength excitation and single emission (Grynkiewicz *et al.*, 1985). The cells adhering to cover-slips were incubated with fura-2 in the normal external solution containing 5 μM fura-2 AM for 30 min at room temperature (approximately 25°C). Then the cover-slips were transferred to an experimental chamber (volume about 0.2 ml) on the stage of an inverted microscope attached to a fluorometer (CAM-200, Japan Spectroscopic) as described previously (Ohta *et al.*,

[1] Author for correspondence.

1993). The fluorescence signal was detected with a Nikon CF u.v. lens (× 40) and the emission light, which was passed through a pinhole diaphragm slightly larger than a cell, was collected by a photomultiplier through a 500 nm filter. The ratio of the fluorescence due to excitation at 340 nm to that at 380 nm was calculated and was considered to be an index of $[Ca^{2+}]_i$.

Membrane currents were recorded with the nystatin-perforated patch-clamp technique to prevent the run-down of receptor-mediated responses (Horn & Marty, 1988; Ito *et al.*, 1993) using a patch-clamp amplifier (CEZ-2300, Nihon-Koden, Japan). Nystatin (50–200 $\mu g\ ml^{-1}$) was introduced into the pipette solution. The patch-pipette resistance ranged from 2.5 to 4 MΩ. The experiments were carried out 5–10 min after formation of a gigaseal at which the access resistance decreased to 10–30 MΩ. Data recording and illustration were carried out as described previously (Ohta *et al.*, 1992).

Cells were constantly superfused with the external solution at a flow rate of 2–3 $ml\ min^{-1}$ and CCh was applied to the cell through a puffer pipette placed close to it (Ito *et al.*, 1993). Using this puffer system, the solution around the cell was completely exchanged within 0.5 s. Therefore, when the time required to attain peak response was estimated, this lag time was neglected. All these experiments were performed at room temperature.

Measurement of mechanical activity

Thin longitudinal muscle bundles (0.1 mm in width, 0.7–1 mm in length) were prepared from tension recording. Mechanical activity was measured isometrically using the experimental setup described previously (Ohta *et al.*, 1992). To examine the contractile responses to CCh utilizing Ca^{2+} released from intracellular stores, the following procedure was carried out. After the disappearance of 0.1 mM CCh-induced contraction in Ca^{2+}-free solution containing 2 mM EGTA, the muscle bundles were exposed to the normal external solution containing 2.5 mM Ca^{2+} for 2 min for the purpose of Ca^{2+} loading of intracellular stores. The muscle bundles were washed with a fresh Ca^{2+}-free solution containing 2 mM EGTA for 1 min and then stimulated by various concentrations of CCh under Ca^{2+}-free conditions. These procedures were repeated and the interval between CCh-stimulations was more than 10 min to avoid possible receptor-desensitization.

Solutions

The ionic composition of the normal external solution was as follows (mM): NaCl 126, KCl 6, $MgCl_2$ 1.2, $CaCl_2$ 2.5, HEPES 10, glucose 14 (pH 7.2 with NaOH). For the Ca^{2+}-free solution, $CaCl_2$ was omitted and 2 mM EGTA was added. The K^+-containing pipette solution contained (mM): KCl 132, $MgCl_2$ 1.2, $ATPNa_2$ 2, HEPES 10, EGTA 0.1 (pH 7.2 with KOH). The Na^+-containing pipette solution was prepared by substitution of equimolar NaCl for KCl (pH 7.2 with NaOH).

Drugs

Chemicals used were $ATPNa_2$ (Boehringer, Germany), carbamylcholine chloride (carbachol), collagenase, nystatin, papain (Sigma, U.S.A.), EGTA, fura-2AM, HEPES (Dojindo, Japan) and nifedipine (Wako Pure Chem, Japan).

Statistics

The results were expressed as the mean value ± s.e.mean (n = number of observations), and statistical significance was assessed with Student's t test. P values of less than 0.05 were considered to be significant.

Results

Change in cytosolic Ca^{2+} concentration induced by CCh

Single smooth muscle cells loaded with fura-2 were stimulated for 10 s by increasing concentrations of CCh at about 4 min intervals. Figure 1a shows typical $[Ca^{2+}]_i$ changes induced by CCh in two cells. In the cell shown in the upper traces, no changes in $[Ca^{2+}]_i$ occurred in response to 0.2 μM CCh. However, 0.5 μM CCh was effective in increasing $[Ca^{2+}]_i$, which occurred in three phases, a slow upstroke, an initial peak and a small sustained phase. When the concentration of CCh was increased to 1 to 10 μM, the rate of increase in $[Ca^{2+}]_i$ became more rapid, being 6.1 ± 0.6 s at 1 μM and 2.8 ± 0.2 s at 10 μM (n = 10), without change in the peak amplitude of $[Ca^{2+}]_i$. As shown in Figure 1b, the amplitudes of the peak rise in $[Ca^{2+}]_i$ were not significantly different among doses of CCh over 0.2 μM. The sustained phase of the Ca^{2+}-transient tended to elevate with increasing concentrations of CCh. Qualitatively, the same results were obtained in another cell, shown in the lower traces, in which a higher concentration of CCh (1 μM) was needed to initiate the rise in $[Ca^{2+}]_i$ than in the cell shown in the upper traces.

The peak rise in $[Ca^{2+}]_i$ elicited by 1 μM CCh was little affected by 2 min exposure of cells to Ca^{2+}-free solution containing 2 mM EGTA (91.9 ± 7.1% of control response, n = 6), a voltage-dependent Ca^{2+} channel blocker, 1 μM nifedipine (96.0 ± 2.2%, n = 4), or a non-specific Ca^{2+} entry blocker, 1 mM La^{3+} (81.9 ± 6.0%, n = 6). These results indicated that the CCh-induced initial peak rise in $[Ca^{2+}]_i$

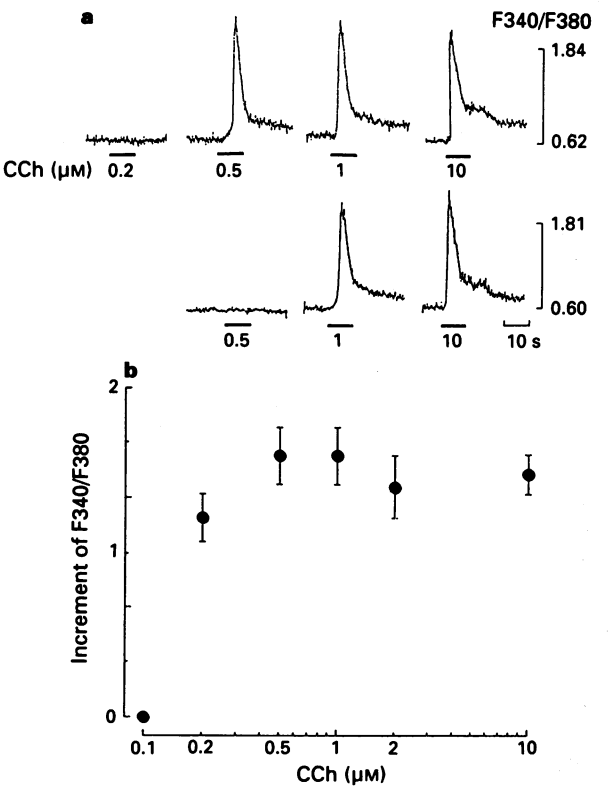

Figure 1 Ca^{2+}-transient responses of single rat intestinal smooth muscle cells to various concentrations of carbachol (CCh). In this and the following two figures, cells were stimulated by CCh for 10 s (—) with increasing concentrations from 0.1 to 10 μM at intervals of more than 4 min. (a) Representative data obtained from two cells; (b) the increment of peak rise in $[Ca^{2+}]_i$ (F340/F380) in the single cells plotted against the concentration of CCh (mean ± s.e.mean, n = 16). Each cell was stimulated with three or four concentrations of CCh, the last concentration being 10 μM. The increment of F340/F380 was estimated by subtracting the resting ratio before stimulation from the peak ratio.

was attributable to Ca^{2+} released from internal stores. In contrast, the sustained rise in $[Ca^{2+}]_i$ evoked by 1 μM CCh was decreased by the external Ca^{2+} removal (17.2 ± 5.2%), nifedipine (42.9 ± 7.8%) and La^{3+} (32.8 ± 3.8%).

Membrane current responses to CCh

To study the membrane currents induced by CCh, the nystatin-perforated whole-cell patch clamp technique was adopted to eliminate run-down of receptor-mediated current responses. First, we examined the effects of various concentrations of CCh on the outward K^+ current, which has been reported to be activated by Ca^{2+} released from intracellular stores, using K^+-containing pipette solution (KCl, 132 mM). Cells were voltage-clamped at − 30 mV to avoid full activation of K^+ channels. The representative data obtained from two different cells are shown in Figure 2. In the cell shown in the upper traces, CCh failed to evoke any current responses at 0.2 μM but elicited a large outward current at 0.5 μM. There was practically no increase in the amplitude of the current with increases in concentration to 1 and 10 μM. The lower traces show that the outward current started to appear at 1 μM CCh and again that no further increase in the amplitude of the current response was observed at 10 μM. As shown in Figure 2b, there was no significant difference between the amplitudes of the outward current induced by CCh with concentrations over 0.2 μM.

The effects of various concentrations of CCh on the inward current were examined in cells dialyzed with KCl-free, NaCl (140 mM)-containing pipette solution to prevent the development of an outward K^+ current at a holding potential of − 60 mV. Similar to the outward current response, an almost full magnitude of the inward current response was elicited by threshold doses of CCh, which differed slightly among cells, and thus there was no further increase in the amplitude with increasing concentrations of CCh (Figure 3).

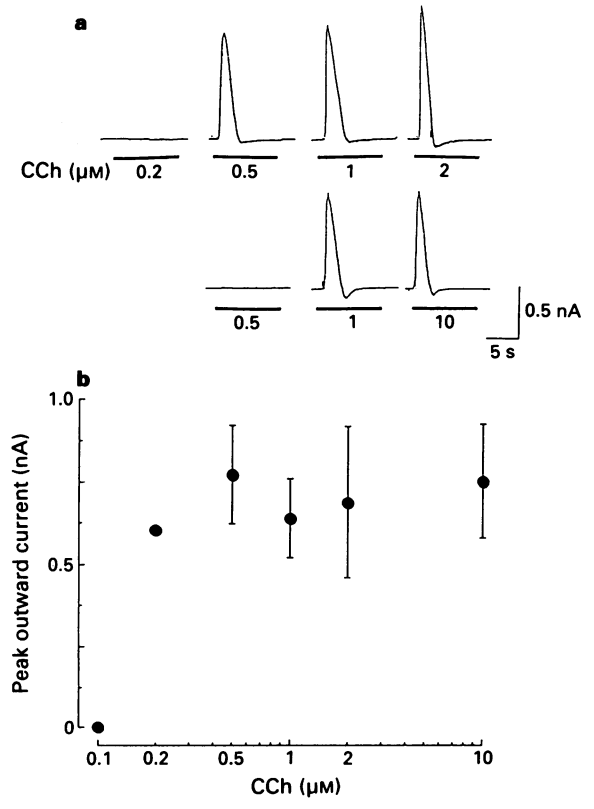

Figure 2 Outward current responses to various concentrations of carbachol (CCh). Membrane currents were recorded with nystatin-perforated whole-cell recording at a holding potential of − 30 mV using a KCl (134 mM)-containing pipette. (a) Representative data obtained from two different cells; (b) the peak amplitude of outward current plotted against CCh concentrations (mean ± s.e.mean, $n = 8$).

Concentration-dependent increase in the number of cells responding to CCh

There was no concentration-dependent increase in the amplitudes of Ca^{2+}-transient and membrane currents evoked by

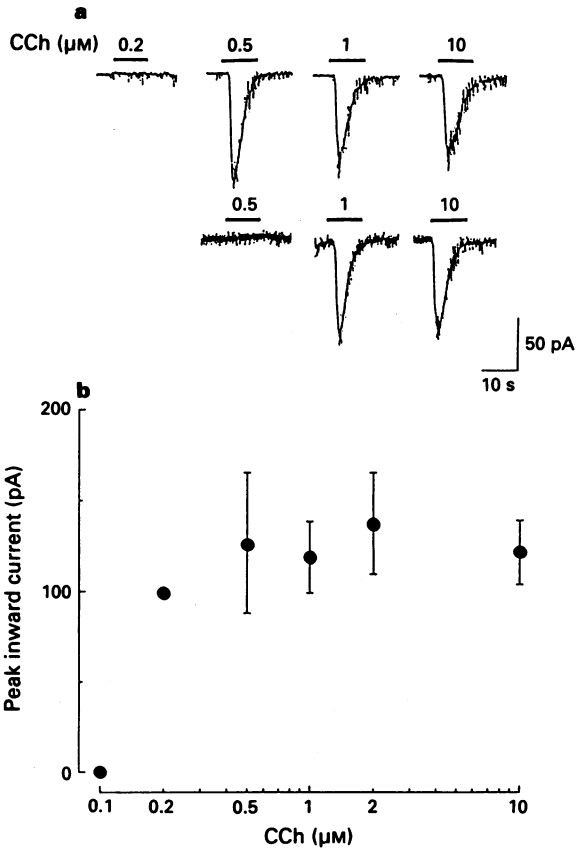

Figure 3 Inward current responses to various concentrations of carbachol (CCh). Holding potential of − 60 mV using an NaCl (134 mM)-containing pipette. (a) Typical inward current responses in two cells; (b) the peak amplitude of inward current plotted against CCh concentrations (mean ± s.e.mean, $n = 11$).

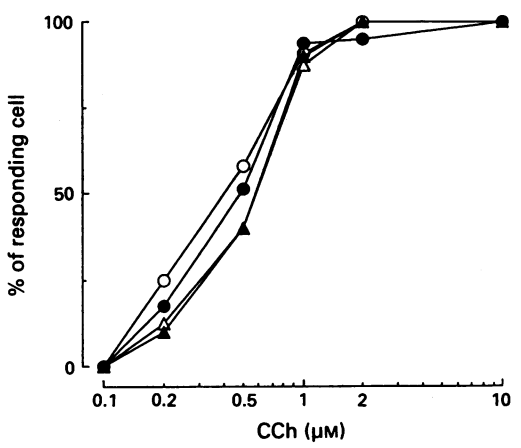

Figure 4 Concentration-dependent increase in the number of single cells responding to given concentrations of carbachol (CCh). The number of cells responding to each concentration of CCh is expressed as a percentage of those responding to 10 μM CCh. The number of contracted cells was counted by direct microscopical observation. (○) CCh-induced Ca^{2+}-transient ($n = 12$); (△) outward current ($n = 10$), (▲) inward current ($n = 8$) and (●) contractile response ($n = 64$).

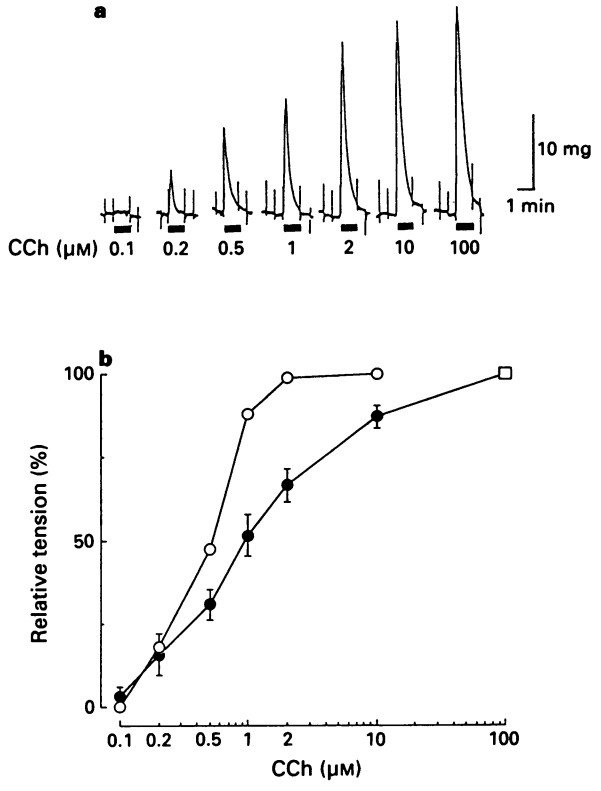

Figure 5 Carbachol (CCh)-induced contractile responses utilizing Ca^{2+} released from intracellular stores in thin muscle bundles. After 2 min exposure of the muscle fibres to the normal external solution containing 2.5 mM Ca^{2+}, they were stimulated by various concentrations of CCh for 1 min (■) in Ca^{2+}-free solution containing 2 mM EGTA. (a) CCh-induced contractile responses in the absence of external Ca^{2+}. (b) (●) the percent amplitude of each contractile response (mean ± s.e.mean, $n = 6$) as compared to that induced by 100 μM CCh (□); (○) the concentration-response curve of the mean value of the number of cells showing Ca^{2+}-transient, outward and inward currents, and contraction in single cells taken from Figure 4.

CCh in the same cells, but the threshold for CCh varied from cell to cell. Therefore, the numbers of cells responding to various concentrations of CCh in evoking Ca^{2+}-transient and current responses were estimated as a percentage of the total number of cells examined. In addition, the numbers of cells contracted by CCh were counted by microscopical observation. The percentage of the responding cells was plotted against the log concentrations of CCh (Figure 4). The concentration-response curves for all CCh-induced responses were sigmoidal and overlapped each other.

CCh-induced contraction utilizing Ca^{2+} released from intracellular stores in muscle bundles

To determine the concentration-response relationships in CCh-induced muscle contractions utilizing Ca^{2+} released from internal stores, thin muscle bundles were loaded with Ca^{2+} and then stimulated by various concentrations of CCh in a Ca^{2+}-free solution containing 2 mM EGTA. Under these conditions, CCh over 0.2 μM evoked a transient contraction, the amplitude of which increased in a concentration-dependent manner (Figure 5a). The threshold concentration of CCh (0.2 μM) inducing transient contraction was similar to those for Ca^{2+}-transient, membrane currents and contractile responses obtained in single cells. As shown in Figure 5b, the concentration-response curve for CCh-induced contraction in muscle bundles extended to higher concentrations of CCh than those obtained from single cells.

Discussion

The present results indicated that CCh evoked a peak rise in $[Ca^{2+}]_i$, and outward and inward currents in an all-or-nothing fashion, that is, there was no dose-dependent increase in the amplitude of each response with concentrations of CCh over threshold in individual cells, though the threshold concentration varied from cell to cell.

CCh has been shown to evoke outward and inward currents by activating Ca^{2+}-dependent K^+ channels and mainly Ca^{2+}-dependent Cl^- channels, respectively, and both current responses were mediated by Ca^{2+} released from intracellular stores in rat intestinal smooth muscle cells (Ito *et al.*, 1993). In the present experiments, both current responses were closely similar to Ca^{2+}-transient responses, with regard to the lack of concentration-dependency and the value of the threshold concentration of CCh. It seems likely therefore that CCh-induced current responses reflect the properties of Ca^{2+}-transient responses. These results may provide further evidence that CCh-induced outward and inward currents are dependent on an increase in $[Ca^{2+}]_i$.

The peak rise in $[Ca^{2+}]_i$ in response to CCh was due to Ca^{2+} released from intracellular stores, because the Ca^{2+}-transient was not influenced by the removal of external Ca^{2+} or by Ca^{2+} channel blockers. In general, IP_3 has been proposed as a second messenger substance provoking Ca^{2+} release from intracellular stores (Berridge & Irvine, 1984) in response to the activation of muscarinic receptor in smooth muscle cells (Gardner *et al.*, 1988; Parekh & Brading, 1991). Recently, it has been reported that IP_3-induced Ca^{2+} release receives positive feedback regulation by $[Ca^{2+}]_i$ and in consequence, Ca^{2+} released by IP_3 further accelerates IP_3-induced Ca^{2+} release (Iino, 1990; Bezprozvanny *et al.*, 1991; Finch *et al.*, 1991; Iino & Endo, 1992). If this is the case in the present experiments, then our results may be explained by the regenerative all-or-nothing Ca^{2+} release induced by IP_3. Similarly, CCh-induced release of stored Ca^{2+} took place in an all-or-nothing fashion in the freshly dispersed smooth muscle cells of guinea-pig taenia coli (Iino *et al.*, 1994), but not in cultured tracheal smooth muscle cells of the rat (Yang *et al.*, 1993). This difference may be due to the difference in the tissue or cells cultured.

It was noted that the percentage of the cells showing Ca^{2+}-transient responses to various concentrations of CCh agreed well with those responding with contractions in single cells. These results suggest that Ca^{2+} release from intracellular stores plays a role in initiating contractions in single intestinal smooth muscle cells of the rat, as reported in the tracheal (Janssen & Sims, 1992) and gastric smooth muscle cells (Sims, 1992). The threshold concentration of CCh required to evoke a contraction of thin muscle bundles in the absence of external Ca^{2+} was almost equal to that evoking Ca^{2+}-transient, current and contractile responses in single cells. This indicates that the threshold concentration of CCh to induce Ca^{2+} release from intracellular stores was similar regardless of differences in the preparations, muscle bundles or single cells. However, the diffusion rate for CCh should be slower in muscle bundles than in single cells and this may account for why the concentration-response curve for CCh extended to higher concentrations in muscle bundles than in single cells.

This work was supported by a Grant-in-Aid for Scientific Research from the Ministry of Education, Science and Culture of Japan, and by The Naito Foundation (Japan).

References

AMÉDÉE, T., BENHAM, C.D., BOLTON, T.B., BYRNE, N.G. & LARGE, W.A. (1990a). Potassium, chloride and non-selective cation conductances opened by noradrenaline in rabbit ear artery cells. *J. Physiol.*, **423**, 551–568.

AMÉDÉE, T., LARGE, W.A. & WANG, Q. (1990b). Characteristics of chloride currents activated by noradrenaline in rabbit ear artery cells. *J. Physiol.*, **428**, 501–516.

BERRIDGE, M.J. & IRVINE, R.F. (1984). Inositol trisphosphate, a novel second messenger in cellular signal transduction. *Nature*, **312**, 315–321.

BEZPROZVANNY, I., WATRAS, J. & EHRLICH, B.E. (1991). Bell-shaped calcium-response curves of ins(1,4,5)P_3- and calcium-gated channels from endoplasmic reticulum of cerebellum. *Nature*, **351**, 751–754.

BOLTON, T.B. (1979). Mechanisms of action of transmitters and other substances on smooth muscle. *Physiol. Rev.*, **59**, 606–718.

BOLTON, T.B. & LIM, S.P. (1989). Properties of calcium stores and transient outward currents in single smooth muscle cells of rabbit intestine. *J. Physiol.*, **409**, 385–401.

BYRNE, N.G. & LARGE, W.A. (1988). Membrane ionic mechanisms activated by noradrenaline in cells isolated from the rabbit portal vein. *J. Physiol.*, **404**, 557–573.

DELISLE, S. & WELSH, M.J. (1992). Inositol trisphosphate is required for the propagation of calcium waves in *Xenopus* oocytes. *J. Biol. Chem.*, **267**, 7963–7966.

FINCH, E.A., TURNER, T.J. & GOLDIN, S.M. (1991). Calcium as a coagonist of inositol 1,4,5-trisphosphate-induced calcium release. *Science*, **252**, 443–446.

GARDNER, A.L., CHOO, L.K. & MITCHELSON, F. (1988). Comparison of the effects of some muscarinic agonists on smooth muscle function and phosphatidylinositol turnover in the guinea-pig taenia caeci. *Br. J. Pharmacol.*, **94**, 199–211.

GRYNKIEWICZ, G., POENIE, M. & TSIEN, R.Y. (1985). A new generation of Ca^{2+} indicators with greatly improved fluorescence properties. *J. Biol. Chem.*, **260**, 3440–3450.

HORN, R. & MARTY, A. (1988). Muscarinic activation of ionic currents measured by a new whole-cell recording method. *J. Gen. Physiol.*, **92**, 145–159.

IINO, M. (1990). Biphasic Ca^{2+} dependence of inositol 1,4,5-trisphosphate-induced Ca release in smooth muscle cells of the guinea-pig taenia caeci. *J. Gen. Physiol.*, **95**, 1103–1122.

IINO, M. & ENDO, M. (1992). Calcium-dependent immediate feedback control of inositol 1,4,5-trisphosphate-induced Ca^{2+} release. *Nature*, **360**, 76–78.

IINO, M., YAMAZAWA, T., MIYASHITA, Y., ENDO, M. & KASAI, H. (1994). Critical intracellular Ca^{2+} concentration for all-or-nothing Ca^{2+} spiking in single smooth muscle cells. *EMBO J.*, **12**, 5287–5291.

ITO, S., OHTA, T. & NAKAZATO, Y. (1993). Inward current activated by carbachol in rat intestinal smooth muscle cells. *J. Physiol.*, **470**, 395–409.

JANSSEN, L.J. & SIMS, S.M. (1992). Acetylcholine activates non-selective cation and chloride conductances in canine and guinea-pig tracheal myocytes. *J. Physiol.*, **453**, 197–218.

KOMORI, S. & BOLTON, T.B. (1990). Role of G-proteins in muscarinic receptor inward and outward currents in rabbit jejunal smooth muscle. *J. Physiol.*, **427**, 395–419.

MIYAZAKI, S., YUZAKI, M., NAKADA, K., SHIRAKAWA, H., NAKANISHI, S., NAKADE, S. & MIKOSHIBA, K. (1992). Block of Ca^{2+} wave and Ca^{2+} oscillation by antibody to the inositol 1,4,5-trisphosphate receptor in fertilized hamster eggs. *Science*, **257**, 251–255.

OHTA, T., ITO, S. & NAKAZATO, Y. (1993). Chloride currents activated by caffeine in rat intestinal smooth muscle cells. *J. Physiol.*, **465**, 149–162.

OHTA, T., ITO, S., NOTO, T., TACHIBANA, R., NAKAZATO, Y. & OHGA, A. (1992). The inhibitory action of cyclic AMP on responses to carbachol dependent calcium stores in rat gastric smooth muscle. *J. Physiol.*, **453**, 367–384.

PACAUD, P., LOIRAND, G., MIRRONNEAU, C. & MIRONNEAU, J. (1989). Noradrenaline activates a calcium-activated chloride conductance and increases the voltage-dependent calcium current in cultured single cells of rat portal vein. *Br. J. Pharmacol.*, **97**, 139–146.

PAREKH, A.B. & BRADING, A.F. (1991). The sources of calcium for carbachol-induced contraction in the circular smooth muscle of guinea-pig stomach. *Br. J. Pharmacol.*, **104**, 412–418.

SIMS, S.M. (1992). Cholinergic activation of a non-selective cation current in canine gastric smooth muscle is associated with contraction. *J. Physiol.*, **449**, 377–398.

YANG, C.M., YO, Y.-L. & WANG, Y.-Y. (1993). Intracellular calcium in canine cultured tracheal smooth muscle cells is regulated by M_3 muscarinic receptors. *Br. J. Pharmacol.*, **110**, 983–988.

(Received February 21, 1994
Revised March 18, 1994
Accepted March 22, 1994)

Br. J. Pharmacol. (1994), **112**, 977–984

Action of niflumic acid on evoked and spontaneous calcium-activated chloride and potassium currents in smooth muscle cells from rabbit portal vein

R.C. Hogg, Q. Wang & [1]W.A. Large

Department of Pharmacology and Clinical Pharmacology, St. George's Hospital Medical School, Cranmer Terrace, London SW17 0RE

1 The action of niflumic acid was studied on spontaneous and evoked calcium-activated chloride ($I_{Cl(Ca)}$) and potassium ($I_{K(Ca)}$) currents in rabbit isolated portal vein cells.

2 With the nystatin perforated patch technique in potassium-containing solutions at a holding potential of −77 mV (the potassium equilibrium potential), niflumic acid produced a concentration-dependent inhibition of spontaneous transient inward current (STIC, calcium-activated chloride current) amplitude. The concentration to reduce the STIC amplitude by 50% (IC_{50}) was 3.6×10^{-6} M.

3 At −77 mV holding potential, niflumic acid converted the STIC decay from a single exponential to 2 exponential components. In niflumic acid the fast component of decay was faster, and the slow component was slower than the control decay time constant. Increasing the concentration of niflumic acid enhanced the decay rate of the fast component and reduced the decay rate of the slow component.

4 The effect of niflumic acid on STIC amplitude was voltage-dependent and at −50 and +50 mV the IC_{50} values were 2.3×10^{-6} M and 1.1×10^{-6} M respectively (cf. 3.6×10^{-6} M at −77 mV).

5 In K-free solutions at potentials of −50 mV and +50 mV, niflumic acid did not induce a dual exponential STIC decay but just increased the decay time constant at both potentials in a concentration-dependent manner.

6 Niflumic acid, in concentrations up to 5×10^{-5} M, had no effect on spontaneous calcium-activated potassium currents.

7 Niflumic acid inhibited noradrenaline- and caffeine-evoked $I_{Cl(Ca)}$ with an IC_{50} of 6.6×10^{-6} M, i.e. was less potent against evoked currents compared to spontaneous currents. In contrast niflumic acid (2×10^{-6} M–5×10^{-5} M) increased noradrenaline- and caffeine-induced $I_{K(Ca)}$.

8 The results are discussed with respect to the mechanism of block of $I_{Cl(Ca)}$ by niflumic acid and its suitability as a pharmacological tool for assessing the role of $I_{Cl(Ca)}$ in physiological mechanisms.

Keywords: Niflumic acid; vascular smooth muscle; calcium-activated chloride current; calcium-activated potassium current

Introduction

Experiments with patch pipette techniques have revealed that noradrenaline acts on α_1-adrenoceptors to stimulate simultaneously a calcium-activated chloride current ($I_{Cl(Ca)}$), calcium-activated potassium current ($I_{K(Ca)}$) and a calcium-permeable cation current (I_{cat}) in the rabbit portal vein (Byrne & Large, 1988; Wang & Large, 1991) and in the rabbit ear artery (Amédée *et al.*, 1990). Since it has been shown that an anion and a cation conductance increase is responsible for the noradrenaline-induced depolarization recorded with microelectrodes in isolated cells of the rabbit portal vein (Amédée & Large, 1989), it is possible that $I_{Cl(Ca)}$ and I_{cat} may have important roles in producing depolarization and contraction in vascular smooth muscle. Also it is relevant that $I_{Cl(Ca)}$ has now been observed in several types of smooth muscle and can be activated by various pharmacological agents (see Introduction of Hogg *et al.*, 1994). Therefore it would be interesting to assess the contribution of $I_{Cl(Ca)}$ and I_{cat} to agonist-induced depolarization in smooth muscle. In order to do this it would be necessary to have selective blocking drugs to dissect out the roles of these conductance mechanisms.

Recently we have embarked on a series of experiments to investigate the characteristics of established chloride channel antagonists in blocking $I_{Cl(Ca)}$ in vascular smooth muscle cells. It has been demonstrated that 4-acetamido-4′-isothiocyanatostilbene-2,2′-disulphonic acid (SITS), 4,4′-diisothiocyanatostilbene-2,2′-disulphonic acid (DIDS) and anthracene-9-carboxylic acid (A-9-C) inhibit evoked $I_{Cl(Ca)}$ in rat portal vein (Baron *et al.*, 1991). Also it was shown in rabbit portal vein that these compounds were more potent against spontaneous transient inward currents (STICs, chloride currents activated by spontaneous release of calcium from caffeine-sensitive intracellular stores) than against $I_{Cl(Ca)}$ elicited by noradrenaline and caffeine (Hogg *et al.*, 1994). It was found that all 3 compounds had low potency as the concentration to inhibit $I_{Cl(Ca)}$ by 50% was greater than 10^{-4} M i.e. the potency against $I_{Cl(Ca)}$ is less than the action of DIDS and SITS against their well-established effects on $Cl^- - HCO_3^-$ exchange in smooth muscle (e.g. see Aickin & Brading, 1983). Consequently it seems unlikely that these channel blockers would be of use as pharmacological tools for assessing the physiological role of $I_{Cl(Ca)}$. A more promising candidate might be niflumic acid, a non-steroidal anti-inflammatory agent, which at a concentration of 10 μM produced marked attenuation of $I_{Cl(Ca)}$ in rat portal vein (Pacaud *et al.*, 1989). The relatively high potency of niflumic acid has been confirmed in canine and guinea-pig tracheal cells (Janssen & Sims, 1992) and in rabbit oesophageal smooth muscle (Akbarali & Giles, 1993).

In the present work we have undertaken a quantitative study of the action of niflumic acid against spontaneous and evoked $I_{Cl(Ca)}$ in the rabbit portal vein. Evidence will be presented to substantiate the relatively high potency of niflumic acid and experiments will be described which indicate that niflumic acid inhibits $I_{Cl(Ca)}$, at least partly, by an open channel blocking mechanism.

[1] Author for correspondence.

Methods

Experiments were carried out on freshly dispersed smooth muscle cells from the rabbit portal vein. Rabbits (2–2.5 kg) of either sex were killed by an overdose of i.v. sodium pentobarbitone and single cells were obtained by enzymatic dissociation with collagenase and papain as described previously (Hogg *et al.*, 1993). The cells were stored in a physiological salt solution with 0.75 mM Ca^{2+} at 4°C and were used on the same day. Whole-cell currents were measured with the perforated patch method with a patch clamp amplifier (List EPC7; List-Electronic; Darmstadt, Germany) at room temperature. In order to obtain a perforated patch nystatin (75–200 $\mu g\,ml^{-1}$) was contained in the patch pipette solution. The external salt solution contained (mM): NaCl 126, KCl 6, $MgCl_2$ 1.2, $CaCl_2$ 1.5, HEPES 10 and glucose 11 and the pH was adjusted to 7.2 with NaOH. In potassium-free conditions, 6 mM KCl was omitted and in some experiments 5 mM tetraethylammonium chloride (TEA-Cl) was added to the bathing solution. The pipette solution contained (mM): KCl 126, $MgCl_2$ 1.2, HEPES 10, glucose 11 and EGTA 0.2. In potassium-free conditions 126 mM KCl was replaced by an equimolar amount of NaCl. In some experiments the effect of niflumic acid on voltage-gated divalent cation currents was studied. For these studies 10 mM $BaCl_2$ was added to the bathing solution instead of calcium so that Ba^{2+} was the charge carrier. Also in these latter studies the pipette solution contained 126 mM CsCl and 10 mM EGTA.

In experiments where noradrenaline was used, 10^{-6} M propranolol was included in the bathing solution to remove any β-adrenoceptor-mediated response. The recordings were made in a static bathing solution and the external solution was changed with a push-pull arrangement with syringes.

Some records were illustrated by playback from videotape onto a Gould brush recorder. Analysis of the time course of spontaneous transient currents was carried out on a personal computer. Signals were filtered at 400 Hz prior to digitisation and currents were sampled at 800 Hz using a CED 1401 laboratory interface and captured on the hard disk of the computer. Capture and averaging of signals were performed with SIGAVG signal-averaging programme and curve fitting was done with a voltage clamp analysis programme (both Cambridge Electronic Design, Science Park, Cambridge). Exponential fits were obtained using a least squares fitting routine and the fitting procedure was weighted towards large current values. From each cell 10–20 spontaneous chloride or potassium currents were averaged to obtain amplitude and time course values. The Langmuir adsorbtion isotherm curve in Figure 1b was drawn using an IC_{50} value (concentration of niflumic acid to inhibit STIC amplitude to 50% of the control value) obtained by linear regression of the experimental data points. In the text, *n* values refer to the number of cells used to obtain the mean determinations. The values given in the text are means ± s.e.mean and statistical significance was estimated with either Student's *t* test or paired *t* test. Chemicals used were bovine serum albumin (fatty acid free), caffeine, dithiothreitol, noradrenaline bitartrate, nystatin, papain (type IV), TEA-Cl (all Sigma, Poole, Dorset); niflumic acid (Aldrich, Gillingham, Dorset); collagenase (CLS2 247 u mg^{-1}, Worthington, Reading, Berkshire).

Results

Effect of niflumic acid on STICs

In the first series of experiments we investigated the action of niflumic acid on STICs in potassium-containing solutions. Figure 1a shows records from a cell which was held under voltage clamp at a command potential of − 77 mV (the potassium equilibrium potential, E_K) and niflumic acid was added to the bathing solution in a cumulative manner. It can be seen quite clearly that there was progressive diminution of STIC amplitude and in the presence of 10^{-4} M niflumic acid the STICs were blocked. The onset of inhibition was rapid and was apparent within about 10 s of adding niflumic acid to the external solution. Also the antagonism was readily reversible and usually complete washout occurred within 1–3 min after removing niflumic acid from the cells (Figure 1a). The concentration-effect of niflumic acid on STIC amplitude is illustrated graphically in Figure 1b. The continuous curve is drawn according to the Langmuir isotherm and the estimated concentration to inhibit STIC amplitude to 50% of the control value (IC_{50}) at − 77 mV with potassium containing solutions was 3.6×10^{-6} M. The potency of niflumic acid against STIC amplitude at any given membrane potential did not differ in potassium-free conditions which were used in some experiments to investigate the voltage-dependence of the action of niflumic acid.

It was apparent in the majority of cells at − 77 mV that the reduction in STIC amplitude by niflumic acid was accompanied by a marked alteration of the STIC time course. Figure 2a illustrates averaged STICs in the absence and presence of various concentrations of niflumic acid taken from the same cell as shown in Figure 1. In control conditions the STIC decay time course can be described by a single exponential with a time constant (τ_{con}) of 77 ms (control curve in Figure 2b). In the presence of niflumic acid the STIC decay time course became more complex and appeared to consist of two distinct phases (Figure 2a). The semilogarithmic plots show that the initial decay was faster than the control while the slow component was slower than the control decay (Figure 2b). In Figure 2b the straight lines with niflumic acid represent the slow exponential component from which the slow time constant (τ_s) was calculated. The fast time constant (τ_f) was obtained by subtracting the slow component from the total current. In the presence of 5×10^{-6} M niflumic acid, τ_f was 28 ms and τ_s was 196 ms and in 5×10^{-5} M niflumic acid τ_f was 18 ms and τ_s was 711 ms. Thus an increase in the concentration of niflumic acid accelerated the fast component of the STIC decay but reduced the rate of decay of the slow component but both components remained exponential in niflumic acid. It should be emphasized that the fast phase is not a spontaneous transient outward current (calcium-activated potassium current, STOC) which theoretically might be observed if inadequate cell dialysis with the pipette solution had occurred. First, because of their voltage-dependence STOCs are very rarely observed at potentials negative to − 50 mV. Secondly and most convincingly, the rapid component of the STIC decay was very sensitive to niflumic acid (Figure 2a) whereas STOCs are insensitive to niflumic acid (see Figure 6).

Evidence has been put forward to suggest that the STIC decay represents closure of the calcium-activated chloride channels (Hogg *et al.*, 1993) and the alteration of the STIC decay by niflumic acid could therefore be explained by blockade of open ion channels. The usual scheme (see Colquoun & Sheridan, 1981) to describe open channel block is:

$$(1)\quad \text{closed channel} \underset{\alpha}{\overset{\beta'}{\rightleftharpoons}} \text{open channel} \underset{k_{-B}}{\overset{k_{+B}}{\rightleftharpoons}} \text{blocked channel}$$

Assuming the normal opening rate (β') is faster than the closure rate (α) of calcium-activated chloride channels then STIC decay in control conditions is determined by $\alpha (= 1/\tau_{con}$ see Hogg *et al.*, 1993). In the presence of an open channel blocking agent (with association and dissociation rate constants of respectively k_{+B} and k_{-B}) it is expected that the STIC decay should consist of two components as was seen experimentally. Moreover it is predicted with certain assumptions (see Colquhoun & Sheridan, 1981) that

$$(2)\quad 1/\tau_f + 1/\tau_s - 1/\tau_{con} = k_{+B}C_B + k_{-B}$$

where C_B is the antagonist concentration. If open channel block was responsible for the reduction in STIC amplitude

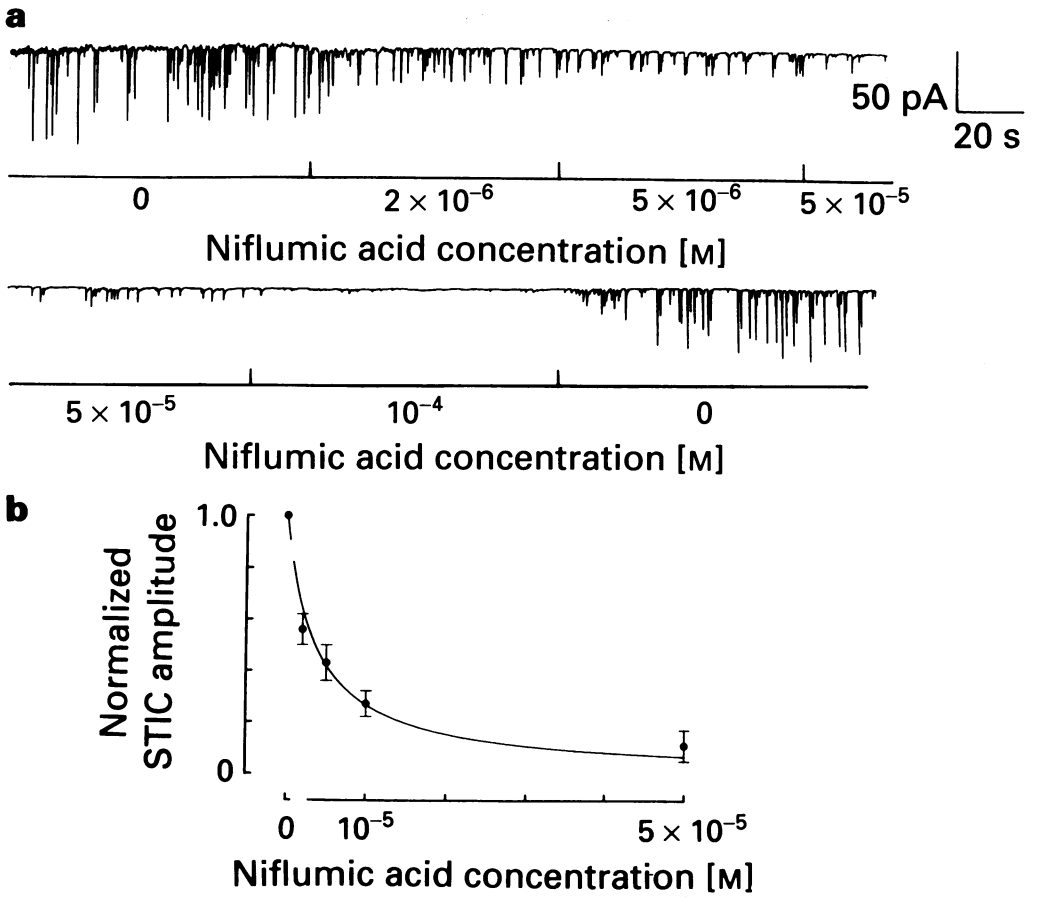

Figure 1 The effect of niflumic acid on spontaneous transient inward current (STIC) amplitude. (a) Shows experimental records in a single cell where niflumic acid was added cumulatively. Inward currents are represented as downward deflections and the records in (a) are continuous. Note the rapid reversal on washout. Potassium-containing solutions and the holding potential was − 77 mV. (b) Illustrates the concentration-effect relationship of niflumic acid on STIC amplitude. The amplitude is normalised to the individual control values as 1 and the mean control amplitudes were between 43 and 125 pA. Each point is the mean from 6 cells.

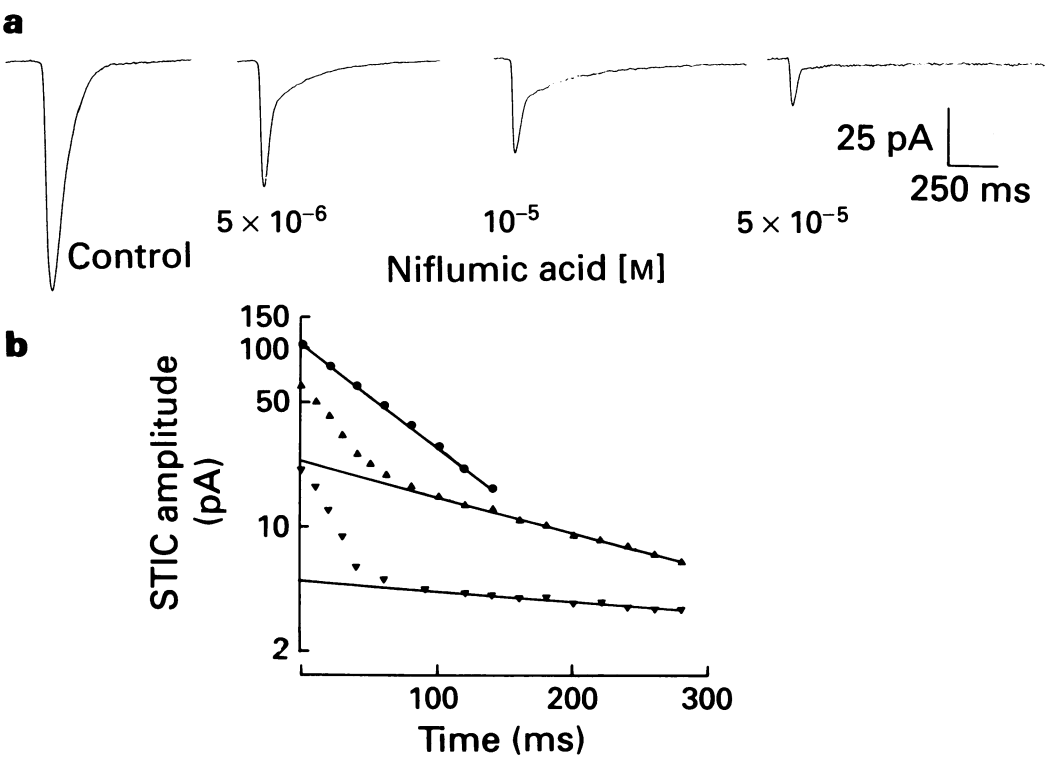

Figure 2 The effect of niflumic acid on spontaneous transient inward current (STIC) time course at − 77 mV. (a) Shows averaged STICs in increasing concentrations of niflumic acid. Note the long tail in the presence of 5×10^{-5} M niflumic acid; (b) illustrates the decay of STICs plotted on a semi-logarithmic scale. The amplitude of the currents are plotted on a logarithmic scale and the straight lines were drawn by eye. In niflumic acid the lines represent the slow exponential components which were used to calculate the fast components by subtraction from the total current. (●), Control; (▲) 5×10^{-6} M; (▼) 5×10^{-5} M niflumic acid.

then it is expected that a plot of $(1/\tau_f + 1/\tau_s - 1/\tau_{con})$ against niflumic acid concentration would be linear. The results from the cell in Figure 2 are plotted according to equation (2) in Figure 3. It can be seen that a linear relationship fits the data points well and the intercept (k_{-B}) is 25 s^{-1} and the slope (k_{+B}) was 3.8×10^5 M^{-1} s^{-1}. In 5 out of 6 cells in potassium-containing solutions at − 77 mV, niflumic acid produced similar results to those illustrated in Figures 2 and 3 and the mean k_{+B} was $5.8 \pm 1.1 \times 10^5$ M^{-1} s^{-1} and k_{-B} was 26 ± 5.1 s^{-1}. In the sixth cell the fast component was not present and niflumic acid appeared only to increase the τ value (i.e. corresponding to τ_s). It seems unlikely that the fast component was not seen in this cell because of the voltage-dependent action of niflumic acid and the fast component was not observed at more depolarized potentials (e.g. see Figure 5 and see discussion). Nevertheless, overall the data are consistent with open channel block by niflumic acid.

Voltage-dependent effect of niflumic acid

Previously we had demonstrated that A-9-C reduced STICs in a voltage-dependent manner whereas the inhibitory action of DIDS and SITS was not influenced by membrane potential (Hogg *et al.*, 1994). We have carried out similar experiments with niflumic acid in potassium-free bathing and pipette solutions to eliminate STOCs which become prominent at potentials positive to − 50 mV. Figure 4a shows the effect of 10^{-6} M niflumic acid at − 50 mV and + 50 mV in the same cell. At − 50 mV this concentration of the blocker reduced the STIC amplitude by about 10% whereas at + 50 mV the attenuation was more marked (about 30%). The concentration-effect curves for several cells are shown in Figure 4b at − 50 and + 50 mV and the curve at − 77 mV from Figure 1b is also added for comparison. The calculated IC_{50} values at − 50 and + 50 mV were respectively 2.3×10^{-6} M and 1.1×10^{-6} M (3.6×10^{-6} M at − 77 mV). Therefore it is concluded that the potency of niflumic acid was increased by depolarization by about two fold between − 50 and + 50 mV.

We also investigated the effect of niflumic acid on the STIC τ at various membrane potentials and these experiments were also carried out in potassium-free conditions to remove any interference from STOCs. Figure 5a shows averaged STICs in the absence (control) and in the presence of 5×10^{-6} M niflumic acid at holding potentials of − 50 mV and + 50 mV. It was apparent that the fast component of decay was no longer observed in the presence of niflumic acid at these potentials (to be discussed later) and that only the slow component was present (cf. Figure 2a). At − 50 and + 50 mV, niflumic acid greatly prolonged the STIC decay in addition to reducing the STIC amplitude (i.e. qualitatively similar to the effect of niflumic acid on the slow component of decay at − 77 mV, Figure 2). The decays of the averaged currents in Figure 5a are plotted on a semi-logarithmic scale in Figure 5b. In both the absence and presence of niflumic

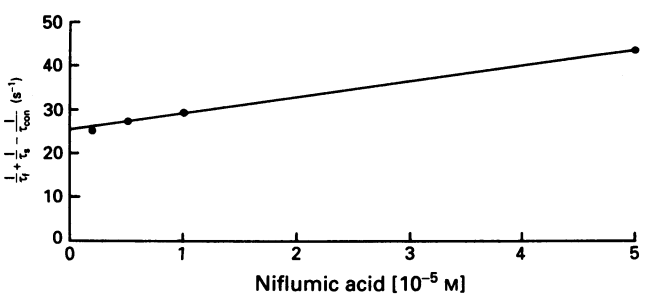

Figure 3 Sum of fast and slow rate constants in niflumic acid minus the control rate constant plotted against the concentration of niflumic acid. Data taken from the cell shown in Figure 2. Straight line was drawn by eye.

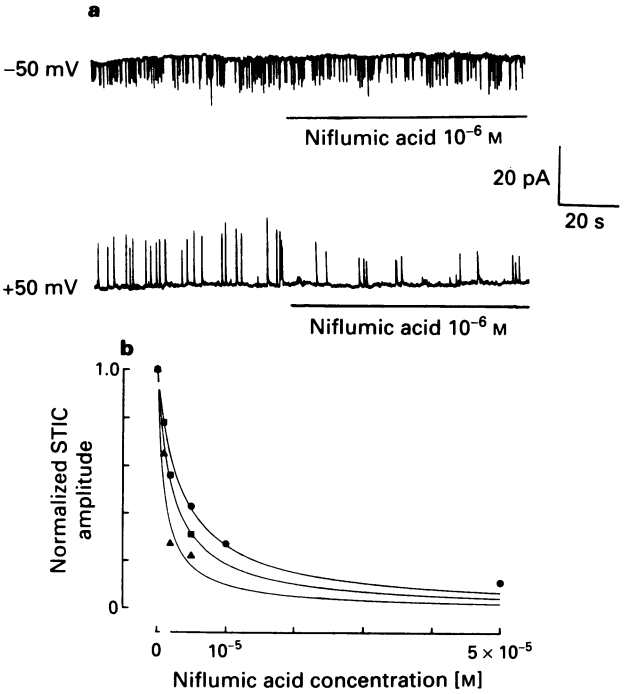

Figure 4 Voltage-dependent inhibition of spontaneous transient inward current (STIC) amplitude by niflumic acid; (a) shows experimental traces of the effect of 10^{-6} M niflumic acid on STICs at − 50 mV and + 50 mV in the same cell recorded in K-free conditions. Niflumic acid was washed out from the cell at − 50 mV holding potential before clamping the cell at + 50 mV when niflumic acid was reapplied. (b) Is the concentration-effect relationship of niflumic acid at 3 membrane potentials: (▲) + 50 mV, (■) − 50 mV, and (●) − 77 mV taken from Figure 1b. Each point is the mean from 6–7 cells and the s.e.mean have been omitted for clarity but were similar to the error bars shown in Figure 1b.

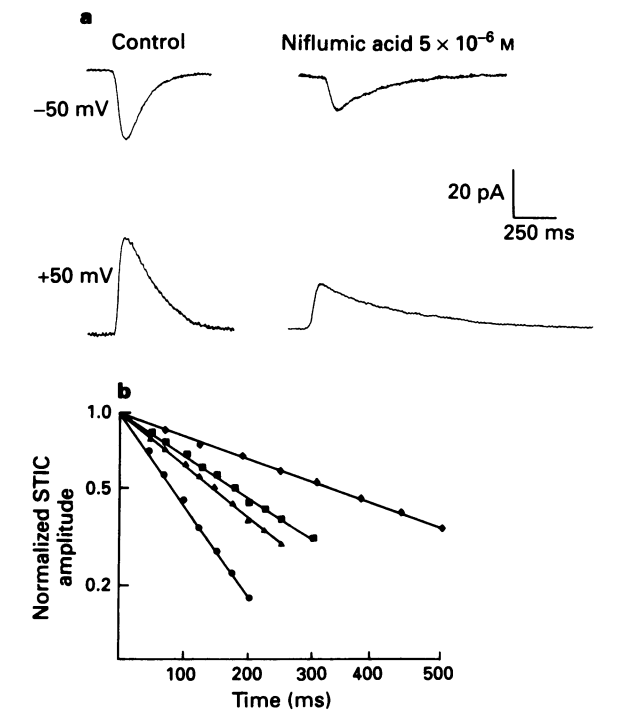

Figure 5 Voltage-dependent effect of niflumic acid on spontaneous transient inward current (STIC) time course: (a) averaged STICs at − 50 mV and + 50 mV in the absence and presence of niflumic acid. Experiment carried out in K-free conditions. (b) Shows the decay of the current plotted on a semi-logarithmic scale. (●) − 50 mV, (▲) + 50 mV controls; (■) − 50 mV, (◆) + 50 mV in 5×10^{-6} M niflumic acid.

acid the STICs decayed exponentially and the control time constants at − 50 and + 50 mV were respectively 96 ms and 213 ms. In the presence of 5×10^{-6} M niflumic acid the τ values were 263 ms (− 50 mV) and 485 ms (+ 50 mV). The effect of two concentrations of niflumic acid at − 50 mV and + 50 mV are shown in Table 1 and there are several conclusions. First, the increase in the STIC τ value was concentration-dependent as 5×10^{-6} M niflumic acid produced a greater effect on τ than 10^{-6} M niflumic acid. Secondly, although the absolute τ values are larger at + 50 mV than − 50 mV (see Hogg *et al.*, 1993), the ratios of the τ values (drug:control) are no greater at + 50 mV than at − 50. Therefore the increase in τ does not appear to be voltage-dependent.

Effect of niflumic acid on STOCs

In order to ensure that the effect of niflumic acid was not mediated by an action on the intracellular calcium store which is the primary source of calcium for triggering STICs we investigated the action of niflumic acid on spontaneous transient outward currents (STOCs). These are spontaneous calcium-activated potassium currents which are triggered by the same calcium store responsible for STICs (Wang *et al.*, 1992). Figure 6a shows a continuous record of STOCs in a cell held at 0 mV (i.e. close to E_{Cl}) before and after the addition of 5×10^{-5} M niflumic acid to the bathing solution. From this trace and averaged STOCs illustrated in Figure 6b it is apparent that niflumic acid did not affect STOCs. With 5×10^{-6} M, 10^{-5} M and 5×10^{-5} M, ($n = 3$ at each concentration) niflumic acid did not alter the amplitude, time to peak, half-decay time and frequency of STOCs. It can be concluded that niflumic acid does not modify the intracellular calcium store or the calcium-activated potassium channels responsible for STOCs.

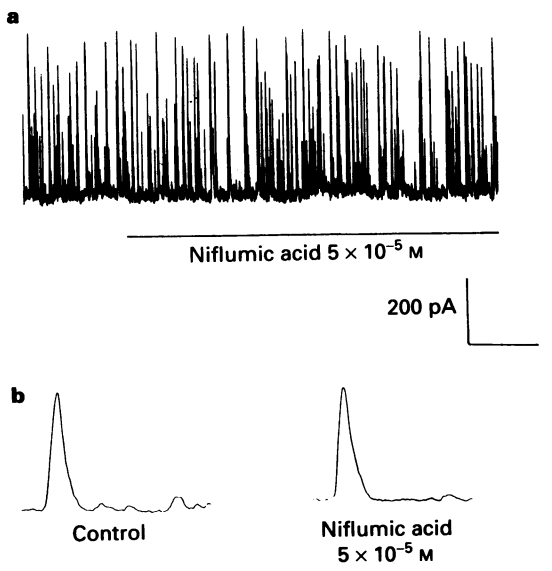

Figure 6 Effect of niflumic acid on spontaneous transient outward currents (STOCs): (a) is an experimental trace of a cell held at 0 mV with K-containing solutions; 5×10^{-5} M niflumic acid was added to the bathing solution as indicated by the horizontal bar. (b) Averaged STOCs on an expanded time base in the absence and presence of 5×10^{-5} M niflumic acid. Horizontal calibration for, 20 s for (a) and 200 ms for (b).

Effect of niflumic acid on evoked calcium-activated chloride and potassium currents

It has been demonstrated previously that DIDS, SITS and A-9-C were less potent in inhibiting evoked chloride currents compared to STICs (Hogg *et al.*, 1994). Consequently we investigated the effect of niflumic acid on noradrenaline- and caffeine-evoked $I_{Cl(Ca)}$ in potassium-free conditions at a holding potential of − 50 mV. Figure 7 shows the effect of two concentrations of niflumic acid on noradrenaline-induced $I_{Cl(Ca)}$ (Figure 7a) and caffeine-evoked $I_{Cl(Ca)}$ (Figure 7b) and it can be seen that niflumic acid produces a concentration-

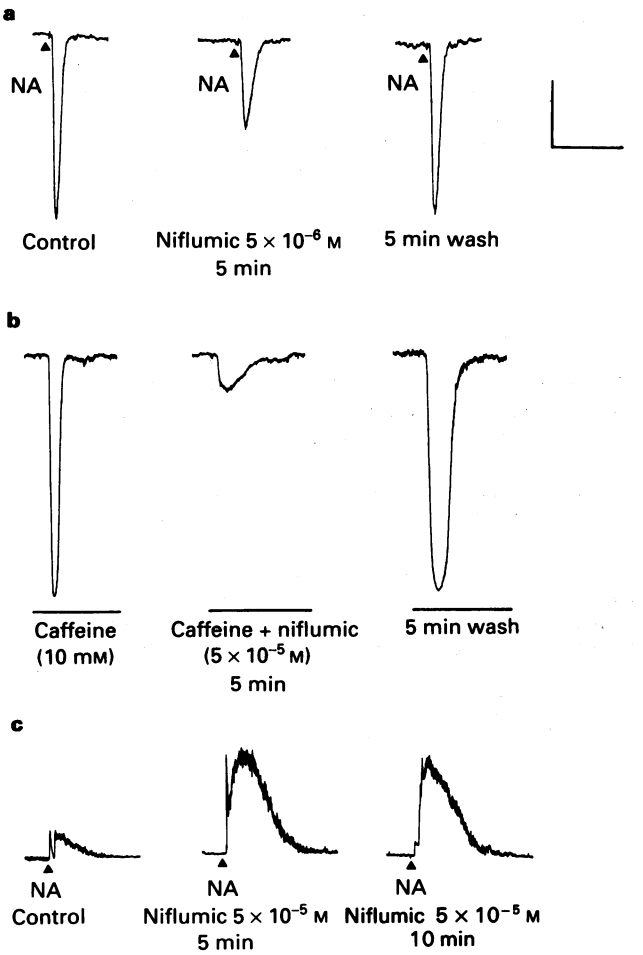

Figure 7 Effect of niflumic acid on evoked calcium-activated chloride and potassium currents. (a) Effect of niflumic acid on noradrenaline (NA)-evoked $I_{Cl(Ca)}$. Ionophoretic pulse, 50 nA for 150 ms. (b) Niflumic acid on caffeine-evoked $I_{Cl(Ca)}$. Caffeine (10 mM) was applied in the bathing solution. In (a) and (b) the holding potential was − 50 mV in K-free conditions. In (c), the effect of niflumic acid on noradrenaline-evoked $I_{K(Ca)}$ is shown. Holding potential of 0 mV in K-containing solutions. Ionophoretic pulse: 50 nA for 600 ms. Vertical calibration bar: 20 pA in (a), 30 pA in (b) and 200 pA in (c). Horizontal bar: 20 s in (a), 40 s in (b) and 4 s in (c).

Table 1 Effect of niflumic acid on the spontaneous transient inward current (STIC) decay time constant

Niflumic acid concentration	*Control* τ (ms)		*In niflumic acid* τ (ms)			
	− 50 mV (a)	+ 50 mV (b)	− 50 mV (c)	+ 50 mV (d)	*c/a*	*d/b*
10^{-6} M ($n = 8$)	99 ± 12	195 ± 19	133 ± 39	295 ± 39	1.34	1.51
5×10^{-6} M ($n = 5$)	115 ± 12	257 ± 21	303 ± 38	595 ± 50	2.63	2.32

dependent inhibition of $I_{Cl(Ca)}$ which is rapidly reversible. It is interesting that in Figure 7b niflumic acid appears to prolong the duration of the induced current which persisted after washout of the drug. There is no obvious explanation for this observation. Niflumic acid produced similar effects on both noradrenaline- and caffeine-evoked currents and consequently the data were pooled. Figure 8 illustrates the concentration-effect relationship of niflumic acid on evoked $I_{Cl(Ca)}$ at -50 mV obtained from several cells and the estimated IC_{50} was 6.6×10^{-6} M. Also included on this graph are the data on STICs at -50 mV (appropriate curve from Figure 4b) and it can be seen quite clearly that the potency of niflumic acid against STICs ($IC_{50} = 2.3 \times 10^{-6}$ M) is greater than against evoked chloride currents.

We also studied the effect of niflumic acid on $I_{K(Ca)}$ stimulated by noradrenaline in potassium-containing solutions at 0 mV (which is close to the chloride equilibrium potential, -2 mV). A typical experiment is shown in Figure 7c where it can be seen that 5×10^{-5} M niflumic acid potentiates the noradrenaline-evoked $I_{K(Ca)}$ and this enhancement is sustained in the continued presence of niflumic acid. The potentiating effect of niflumic acid was concentration-dependent as in the presence of 2×10^{-6} M and 5×10^{-5} M niflumic acid the noradrenaline-evoked $I_{K(Ca)}$ was increased respectively 1.7 ± 0.4 fold ($n = 6$) and 2.5 ± 0.3 ($n = 8$) fold. Therefore niflumic acid increases the amplitude of evoked $I_{K(Ca)}$ without affecting spontaneous calcium-activated potassium currents.

Effect of niflumic acid on voltage-activated divalent cation currents

The relative high potency (see Discussion) of niflumic acid against $I_{Cl(Ca)}$ suggests that this agent might be used to appraise the role of calcium-activated chloride currents in producing membrane depolarization and contraction evoked by noradrenaline (or other excitants) in smooth muscle. Consequently it seemed worthwhile to see if niflumic acid inhibited voltage-gated calcium currents which might be expected to be the essential link between depolarization which is generated by $I_{Cl(Ca)}$ and muscle contraction. In these experiments we used pipettes filled with 126 mM CsCl and 10 mM EGTA (see Methods) and the external solution contained 10 mM $BaCl_2$ (no added calcium) so that Ba^{2+} was the charge carrier. Full current-voltage experiments were not carried out but in experiments where the holding potential was -70 mV the amplitude of inward currents evoked by command steps duration of (1500 ms) to 0 mV was not altered by 2×10^{-6} M -5×10^{-5} M niflumic acid. For example, in one series of experiments the amplitude of the control barium current was 58 ± 12 pA and in the presence of 2×10^{-6} M niflumic acid the current 59 ± 9 pA ($n = 4$). In another series of experiments in 5×10^{-5} M niflumic acid the inward current was 79 ± 13 pA compared to a control value of 73 ± 12 pA ($n = 3$). Therefore it can be concluded that niflumic acid in concentrations up to 5×10^{-5} M does not inhibit the influx of divalent cations through voltage-gated calcium channels.

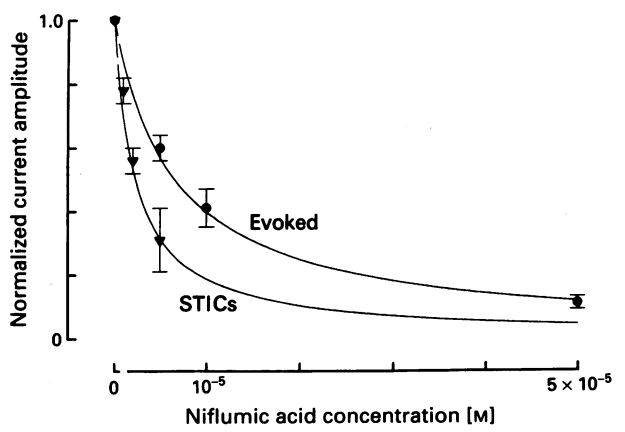

Figure 8 Comparison of concentration-effect curves of niflumic acid against evoked $I_{Cl(Ca)}$ and spontaneous transient inward currents (STICs). Both curves derived from data in cells held at -50 mV in K-free conditions. For evoked currents (●) each point is the mean from 4–8 cells. The amplitudes have been normalized but the individual mean values of the control evoked currents were between 18 and 260 pA. The curve for STICs (▼) was taken from Figure 4b and included for comparison.

Discussion

This paper demonstrates that niflumic acid is a relatively potent blocker of calcium-activated chloride currents in rabbit portal vein and inhibits $I_{Cl(Ca)}$ in the micromolar range. It will be suggested later that niflumic acid inhibits $I_{Cl(Ca)}$ by blocking open chloride channels and therefore comparison of quantitative data in different preparations might give an indication whether the calcium-activated chloride conductance differs from tissue to tissue. Dose-response curves with niflumic acid have not been constructed in other smooth muscle tissues but it has been reported that in the presence of 10^{-4} M niflumic acid a tail current, presumed to be chloride current activated by the influx of calcium, was greatly reduced but a small component still persisted in the presence of 10^{-4} M niflumic acid in rabbit oesophageal smooth muscle (Akbarali & Giles, 1993) whereas this concentration of niflumic acid blocked STICs in the present work. This suggests that there might be a difference in $I_{Cl(Ca)}$ in portal vein and oesophagus or that another conductance might contribute to the tail current in rabbit oesophageal smooth muscle cells. The IC_{50} of niflumic acid against $I_{Cl(Ca)}$ in *Xenopus* oocytes was estimated to be 17 μM (White & Aylwin, 1990) which is almost an order less potent than against STICs at -50 mV (IC_{50} of 2.2×10^{-6} M) in the present study. This difference is sufficiently large to suggest that there might be a difference between $I_{Cl(Ca)}$ in rabbit portal vein and oocytes. It should be noted that niflumic acid is not specific for $I_{Cl(Ca)}$ because this agent inhibits cyclic AMP-activated chloride currents in amphibian retinal pigment epithelial cells with an IC_{50} of about 2.5×10^{-5} M (Hughes & Segawa, 1993). Also niflumic acid is a potent inhibitor (IC_{50} of 6.3×10^{-7} M) of anion exchange in human red cells where it has been suggested that niflumic acid interacts with the band 3 protein (Cousin & Motais, 1979). It is interesting that many compounds that block chloride channels also inhibit anion transport in red blood cells (also see Cousin & Motais, 1982a,b).

A striking result was that niflumic acid inhibited STICs more potently than evoked currents. Since niflumic acid increased the noradrenaline-evoked $I_{K(Ca)}$ without altering STOCs (spontaneous calcium-activated potassium currents) it is possible that this compound increases the evoked release of calcium from the intracellular store without altering the spontaneous release of calcium. It was observed previously that DIDS, SITS and A-9-C increased the evoked $I_{K(Ca)}$ (Hogg *et al.*, 1994) and it may be a general property of chloride channel blocking agents to enhance the amount of calcium released from the intracellular store.

There is some evidence to suggest that niflumic acid inhibits $I_{Cl(Ca)}$ by blocking open chloride channels. First, the action of niflumic acid is voltage-dependent which suggests the blocking site is within the membrane electrical field. The rapid onset and reversibility indicates the site with which niflumic acid binds is readily accessible from the external solution and therefore taking these two points together it is tempting to speculate that the ion channel is the site of action. Secondly, at -77 mV in the presence of niflumic acid the STIC decay consisted of two exponentials rather than one and the time constants of both exponentials were depen-

dent on concentration of niflumic acid in a manner consistent with open channel block according to scheme (1). Moreover the data represented in Figure 3 give quantitative support for an open channel blocking mechanism over a large concentration range. However, it is necessary to explain why in the presence of niflumic acid the STIC decay was described by two exponentials at − 77 mV but only a single component was observed at more positive potentials. It should be emphasized that the fast component at − 77 mV was not a STOC (see Results for arguments) but was a chloride current. The STIC decay at − 50 mV and + 50 mV (e.g. see Figure 5a) resemble in some respects the slow component recorded at − 77 mV (e.g. Figure 2a). At − 50 and + 50 mV in the presence of niflumic acid the STIC decay was exponential and had a similar absolute value, for any given concentration of niflumic acid, to τ_s at − 77 mV. Therefore it can be concluded that the fast component is not observed at potentials more positive than − 77 mV. A common observation is that STOCs and STICs often occur as biphasic events which suggests that the same calcium pulse activates both potassium and chloride currents (see Hogg *et al.*, 1993). Therefore since the STOC time course is not altered by niflumic acid it is unlikely that the slow decay of STICs in the presence of the blocking agents can be attributed to a prolonged time course of the calcium signal that triggers the STIC. From scheme (1) two components of STIC decay would be recorded only if chloride channel opening was rapid compared to the blocking rate by niflumic acid. We have no information on the rate of opening of calcium-activated chloride channels in smooth muscle but the STIC rise time is 40–60 ms which is likely to be slow relative to chloride channel opening. There are no data on the factors that determine the STIC rise time although the rate of rise of calcium at the internal surface of the cell membrane which contains calcium-activated chloride channels remains a distinct possibility. Nevertheless since the STIC rise time is relatively slow it is probable that significant block of the chloride channels will occur during the STIC rise time. If the rate of association (k_{+B}) of niflumic acid with the chloride channel was rapid compared to the STIC rise time it might not be expected to record all (or any) of the rapid phase of block and only the component associated with unblocking of the channel might be observed. In the context of the present work it might be necessary to postulate that the fast component of block is resolved at − 77 mV but not at − 50 mV or + 50 mV because the rate of association of niflumic acid with the channel is slow compared to the STIC rise time at − 77 mV but not at more positive potentials. For this to occur it would be necessary for k_{+B} to be voltage-dependent and at more depolarized potentials block of channels might occur during the STIC rise time and only the unblocking slow component is observed. The experimental data confirm that membrane depolarization increases the potency of niflumic acid which indicates that as the inside of membrane is made more positive the rate of association of the negatively changed molecules of niflumic acid with binding sites inside the open chloride channel is increased. Previously it has been demonstrated at the frog motor endplate in the presence of lignocaine derivatives, which block channels opened by acetylcholine, the decay of the endplate current (e.p.c.) is prolonged but remains mono-exponential at − 30 mV whereas at more negative potentials the e.p.c. decay is obviously bi-exponential (Beam, 1976). These data are qualitatively similar to the results of the present experiments. In conclusion, it seems likely that at least part of the blocking action of niflumic acid on $I_{Cl(Ca)}$ can be attributed to block of open chloride channels.

The equilibrium constant of niflumic acid for the open chloride channel (K_B) can be estimated from k_{-B}/k_{+B} which is calculated to be 4.5×10^{-5} M at − 77 mV. This is about an order greater than the IC_{50} (3.6×10^{-6} M) calculated from inhibition of STIC amplitude at − 77 mV which suggests that niflumic acid might have an additional action (other than blocking open channels) to inhibit $I_{Cl(Ca)}$. Alternatively the value of K_B might be an overestimate resulting from the imperfections of using STICs as a model as outlined in the previous paragraph.

Finally, it is worth commenting on the potential usefulness of niflumic acid as a pharmacological tool. It is evident that niflumic acid does not inhibit either the α_1-adrenoceptor recognition site (as the noradrenaline-induced $I_{K(Ca)}$ was not blocked) or the voltage-dependent calcium channel. Also in two cells, noradrenaline-evoked I_{cat} (unpublished observation) was not reduced and thus it seems that niflumic acid might be useful in defining the role of $I_{Cl(Ca)}$ in producing noradrenaline-evoked depolarization and contraction. However it seems that niflumic acid appears to increase the amount of calcium released from the intracellular store in response to stimulation with noradrenaline. If this increased release of calcium can activate contractile proteins niflumic acid will tend to increase contractility of smooth muscle to excitants such as noradrenaline in addition to blocking calcium-activated chloride channels which are also stimulated by noradrenaline. Therefore the effect of niflumic acid to inhibit $I_{Cl(Ca)}$ in smooth muscle and subsequent contraction might be overcome, at least partly, by the ability to increase the release of calcium from the sarcoplasmic reticulum and hence the contractility of vascular smooth muscle. In these circumstances it might be difficult to assess the role of $I_{Cl(Ca)}$ in smooth muscle contraction with niflumic acid.

This work was supported by The Wellcome Trust.

References

AICKIN, C.C. & BRADING, A.F. (1983). Towards an estimate of chloride permeability in the smooth muscle of guinea-pig vas deferens. *J. Physiol.*, **336**, 179–197.

AKBARALI, H.I. & GILES, W.R. (1993). Ca^{2+} and Ca^{2+}-activated Cl^- currents in rabbit oesophageal smooth muscle. *J. Physiol.*, **460**, 117–133.

AMÉDÉE, T., BENHAM, C.D., BOLTON, T.B., BYRNE, N.G. & LARGE, W.A. (1990). Potassium, chloride and non-selective cation conductances opened by noradrenaline in rabbit ear artery cells. *J. Physiol.*, **423**, 551–568.

AMÉDÉE, T. & LARGE, W.A. (1989). Microelectrode study on the ionic mechanisms which contribute to the noradrenaline-induced depolarization in isolated cells of the rabbit portal vein. *Br. J. Pharmacol.*, **97**, 1331–1337.

BARON, A., PACAUD, P., LOIRAND, G., MIRONNEAU, C. & MIRONNEAU, J. (1991). Pharmacological block of Ca^{2+}-activated Cl^- current in rat vascular smooth muscle cells in short term primary culture. *Pflügers Archiv.*, **419**, 553–558.

BEAM, K.G. (1976). A voltage-clamp study of the effect of two lidocaine derivatives on the time course of end-plate currents. *J. Physiol.*, **258**, 279–300.

BYRNE, N.G. & LARGE, W.A. (1988). Membrane ionic mechanisms activated by noradrenaline in cells isolated from the rabbit portal vein. *J. Physiol.*, **404**, 557–573.

COLQUHOUN, D. & SHERIDAN, R.E. (1981). The modes of action of gallamine. *Proc. R. Soc. B.*, **211**, 181–203.

COUSIN, J.L. & MOTAIS, R. (1979). Inhibition of anion permeability by amphiphilic compounds in human red cell: evidence for an interaction of niflumic acid with the band 3 protein. *J. Memb. Biol.*, **46**, 125–153.

COUSIN, J.L. & MOTAIS, R. (1982a). Inhibition of anion transport in the red blood cell by anionic amphiphilic compounds. II. Chemical properties of the flufenamate-binding site on the band 3 protein. *Biochim. Biophys. Acta*, **687**, 147–155.

COUSIN, J.L. & MOTAIS, R. (1982b). Inhibition of anion transport in the red blood cell by anionic amphiphilic compounds II. Chemical properties of the flufenamate-binding site on the band 3 protein. *Biochim. Biophys. Acta.*, **687**, 156–164.

HOGG, R.C., WANG, Q. & LARGE, W.A. (1993). Time course of spontaneous calcium-activated chloride currents in smooth muscle cells from the rabbit portal vein. *J. Physiol.*, **464**, 15–31.

HOGG, R.C., WANG, Q. & LARGE, W.A. (1994). Effects of Cl channel blockers on Ca-activated chloride and potassium currents in smooth muscle cells from rabbit portal vein. *Br. J. Pharmacol.*, **111**, 1333–1341.

HUGHES, B.A. & SEGAWA, Y. (1993). cAMP-activated chloride currents in amphibian retinal pigment epithelial cells. *J. Physiol.*, **466**, 749–766.

JANSSEN, L.J. & SIMS, S.M. (1992). Acetylcholine activates non-selective cation and chloride conductances in canine and guinea-pig tracheal myocytes. *J. Physiol.*, **453**, 197–218.

PACAUD, P., LOIRAND, G., LAVIE, J.L., MIRONNEAU, C. & MIRONNEAU, J. (1989). Calcium-activated chloride current in rat vascular smooth muscle cells in short-term primary culture. *Pflügers Archiv.*, **413**, 629–636.

WANG, Q., HOGG, R.C. & LARGE, W.A. (1992). Properties of spontaneous inward currents in smooth muscle cells isolated from the rabbit portal vein. *J. Physiol.*, **451**, 525–537.

WANG, Q. & LARGE, W.A. (1991). Noradrenaline-evoked cation conductance recorded with the nystatin whole-cell method in rabbit portal vein cells. *J. Physiol.*, **435**, 21–39.

WHITE, M.M. & AYLWIN, M. (1990). Niflumic acid and flufenamic acids, are potent, reversible blockers of Ca^{2+}-activated Cl^- channels in *Xenopus* oocytes. *Mol. Pharmacol.*, **37**, 720–724.

(Received February 2, 1994
Revised March 17, 1994
Accepted March 21, 1994)

Br. J. Pharmacol. (1994), **112**, 985–991

Typical and atypical NK_1 tachykinin receptor characteristics in the rabbit isolated iris sphincter

[1]Judith M. Hall, Debra Mitchell & Ian K.M. Morton

Pharmacology Group, Biomedical Sciences Division, King's College London, Manresa Road, Chelsea, London SW3 6LX

1 A contraction of the rabbit isolated iris sphincter smooth muscle follows activation of either tachykinin NK_1 or NK_3 receptors. We have here characterized the pharmacological activity profiles of various tachykinin receptor agonists considered to have NK_1-receptor-preferring activity in this preparation.

2 Two groups of NK_1-receptor-preferring agonists could be distinguished in terms of a common pharmacological profile. The first group (Group 1) included [Glp^6,L-Pro^9]-SP(6-11) (septide), [Glp^6]-SP (6-11), substance P methyl ester, δ-aminovaleryl-[L-Pro^9, *N*-MeLeu^{10}]-SP(7-11) (GR73632), and [Apa$^{9\text{-}10}$]-SP. The second group (Group 2) included [Pro^9]-SP, substance P, physalaemin and ranamargarin.

3 Under control conditions, the responses to Group 1 agonists were relatively fast in offset (time for reversal of maximal responses, 11.2–18.2 min), and were antagonized by NK_1-receptor-selective antagonists (range of pK_B estimates *vs* various agonists; GR82334, 7.1–8.2; (±)-CP-96,345, 8.9–9.5; RP67580, 7.0–7.4). Following incubation of the tissue with phenoxybenzamine (20 μM, 10 min), the affinity of GR82334, tested against the Group 1 agonists, substance P methyl ester and septide, was not significantly different ($P < 0.05$; $n = 7$–18) to that determined in untreated tissues (substance P methyl ester pK_B 7.5 ± 0.1 and 7.2 ± 0.2, respectively; septide 7.7 ± 0.2 and 7.9 ± 0.2, respectively). Further, response offset times (5.0–8.5 min) were little reduced as compared to those observed in untreated tissues.

4 Under control conditions, the response to Group 2 agonists was markedly slow in offset (times for reversal of maximal responses, 51.4–70.4 min), and was not attenuated significantly by the NK_1-receptor-selective antagonists GR82334 (1 μM), (±)-CP-96,345 (0.1 μM) or RP67580 (1 μM). In contrast, after phenoxybenzamine pretreatment, responses to Group 2 agonists reversed rapidly (times for reversal of maximal responses, 13.1–24.2 min), and were now antagonized by GR82334 (pK_B estimates, 6.4–7.1).

5 The responses to the NK_3-receptor-selective agonist Succ-[Asp^6,Me-Phe^8]-SP(6-11) (senktide) were relatively fast in offset (time for reversal of maximal response was 18.6 ± 1.7 min) and were not inhibited by GR82334 (10 μM; $n = 5$). The contractile response resulting from co-application of the Group 1 agonist, septide together with senktide, did not exhibit prolonged response offset kinetics.

6 Assuming simple competition at equilibrium, these data from the rabbit iris smooth muscle could be explained either by interaction of the various ligands with two separately-existing NK_1 receptor-subtypes or -isoforms; or alternatively by a preferential interaction of the two agonist groups with different binding domains on a common NK_1 receptor.

Keywords: Tachykinin receptors; iris sphincter; substance P; NK_1 antagonist; GR82334; phenoxybenzamine; neurokinin; (±)-CP-96,345; RP67580; receptor subtypes

Introduction

Stimulation both of NK_1 and NK_3 receptors, causes contraction in the rabbit isolated iris sphincter preparation (Hall *et al.*, 1991; 1993b; Håkanson *et al.*, 1991; see Hall, 1994). However, in our preliminary studies we identified profound differences in the pharmacological characteristics of certain tachykinins and analogues considered to act preferentially at NK_1 receptors in this preparation (Hall *et al.*, 1991; 1993c). Thus, the contractile responses to several NK_1-receptor-preferring tachykinins including substance P methyl ester, [Glp^6,L-Pro^9]-SP(6-11) (septide), and δ-aminovaleryl-[L-Pro^9, *N*-MeLeu^{10}]-SP(7-11) (GR73632) reverse rapidly (< 20 min; see Hall *et al.*, 1991; 1994) and are readily inhibited by NK_1 receptor antagonists with affinities typical of NK_1 receptors in rabbit preparations (Hall *et al.*, 1994). In contrast, other agonist ligands including substance P and physalaemin, show 'atypical' responses since these are maintained for very long periods (> 1 h) and, further, are relatively resistant to blockade by NK_1 receptor antagonists (Muramatsu *et al.*, 1987; Too *et al.*, 1988; Hall *et al.*, 1994). These contrasting washout-kinetics of tachykinins and analogues seem not to result from differences in the metabolic stability of the peptides (Hall *et al.*, 1991), nor from the differential release of other mediators (Too *et al.*, 1988). We have previously referred to the former group of agonists with 'typical' responses as Group 1, and those with 'atypical' responses as Group 2 (Hall *et al.*, 1994): this convention will be adopted here for simplicity of description, and the division will be re-examined in the Discussion.

There are reports of responses to substance P being mediated through activation of atypical tachykinin receptors in other preparations (Petitet *et al.*, 1992). Indeed there are proposals both for the existence of distinct subtypes of NK_1 receptors, and for inter-species variants or homologues (see Hall *et al.*, 1993a; Maggi *et al.*, 1993). In view of these issues, it would be of the greatest pharmacological significance if subtypes of NK_1 receptor could be demonstrated within a single tissue from a given animal species. The aim of our study, therefore, was to investigate whether NK_1-receptor-preferring agonists interact with two different NK_1 receptor subtypes in rabbit iris sphincter, or if other reasons can be advanced to explain the profoundly different pharmacological profiles of these groups of NK_1-receptor-preferring agonists. To this end, we have compared the con-

[1] Author for correspondence.

tractile responses of a number of NK_1-receptor-preferring agonists with respect to their washout-kinetics, sensitivity to inhibition by the NK_1-receptor selective antagonists GR82334 (Hagan *et al.*, 1991); (±)-CP-96,345 (Snider *et al.*, 1991); RP67580 (Garret *et al.*, 1991; see Maggi *et al.*, 1993); and modification of these characteristics by pretreatment with phenoxybenzamine. There are previous reports of phenoxybenzamine pretreatment showing agonist-dependent effects with certain tachykinins in various preparations, including the rabbit iris (Too *et al.*, 1988; Hall *et al.*, 1993c; 1994).

Preliminary accounts of this work have been communicated to the British Pharmacological Society (Hall *et al.*, 1994) and to the International Symposium on Substance P and Related Peptides, Shizuoka, Japan (Hall *et al.*, 1993c).

Methods

Tissue preparation and recording arrangements

Male New Zealand albino rabbits (2.5–3.0 kg) were killed by an overdose of i.v. pentobarbitone sodium (Sagatal). The eyes were enucleated immediately after death and opened by an incision 2–3 mm dorsal to the limbus, followed by excision of the iris from the ciliary margin. The sphincter pupillae muscles were dissected free of dilator muscle and mounted intact on stainless steel tissue-holders in 2.5 ml silanised glass organ baths in Krebs solution at 37°C. The preparations were attached to isometric Grass FT03B force-displacement transducers under an initial resting tension of 150 mg. The mechanical activity was recorded on Grass model 7E polygraphs. The composition of the Krebs solution was (mM): Na^+ 140, K^+ 5.9, Cl^- 104.8, $H_2PO_4^-$ 1.2, HCO_3^- 24.9, Ca^{2+} 2.6, Mg^{2+} 1.15, SO_4^{2-} 1.15, glucose 10. The Krebs solution was maintained at pH 7.4 by constant bubbling with 95% O_2:5% CO_2, and contained hexamethonium (100 μM), mepyramine, cimetidine, guanethidine and ibuprofen (all 1 μM), and atropine (1 μM) (except in experiments with phenoxybenzamine since effective phenoxybenzamine treatment was estimated in terms of muscarinic blockade, where atropine treatment would preclude this).

Tachykinin receptor antagonist studies

An equilibration period of 60 min was allowed. In all experiments, paired irises from the same animal were used. Full cumulative concentration-response curves were obtained for agonists (see Results), either in the absence (concurrent time control preparations), or the presence (test preparations), of GR82334 (1, 3.2 or 10 μM), RP67580 (1, 3.2 or 10 μM) or (±)-CP-96,345 (32, 100 or 320 nM), with up to four agonists applied to each preparation in a random order. In experiments with substance P, physalaemin, ranamargarin and [Pro^9]-SP, the prolonged washout of responses did not allow determination of more than one concentration-response curve in a single preparation at the end of the experiment (see Results). With GR82334, additional experiments were carried out as above, but in preparations pretreated with phenyoxybenzamine (20 μM, 10 min application followed by washing every 5 min for 20 min; see Too *et al.*, 1988). In these experiments, carbachol was included as an independent test for effective (muscarinic) receptor alkylation, which was feasible since in these experiments atropine was omitted from the medium. Antagonist incubation time was 5 min, except in some additional experiments with GR82334 against responses to substance P; where in testing for possible non-equilibrium conditions, the antagonist incubation time was increased to 30 min.

Co-administration of septide and senktide

The time course was investigated of the composite response following co-administration *ca.* EC_{50} concentrations of both the NK_1-receptor-selective agonist septide (1–3 nM) and the NK_3-receptor-selective agonist senktide (1–3 nM).

Washout of responses to agonists

In preparations where tachykinin receptor antagonists had not been used, the rates of offset of responses to tachykinins were estimated. After cumulative application of doses to reach a maximum response, the organ bath was thoroughly washed out and this was repeated at 5 min intervals until tension had resumed the pre-dose level. Because of their very slow offset rates, estimates for Group 2 agonists were made only at the end of experiments: other agonists were applied in a random order.

Source of agents used

Agents were obtained as follows: Sagatal (RMB Animal Health Ltd., U.K.), carbamylcholine chloride (carbachol), hexamethonium bromide, ibuprofen, (Sigma, U.K.), mepyramine maleate (May & Baker, U.K.), guanethidine sulphate (CIBA, U.K.), substance P, substance P methyl ester (Bachem, U.K.), [Glp^6]-SP(6-11), physalaemin, Succ-[Asp^6, Me-Phe^8]-SP(6-11) (senktide), ranamargarin (Peninsula Laboratories, Europe), δ-aminovaleryl-[L-Pro^9, *N*-MeLeu^{10}]-SP(7-11) (GR73632), and [D-Pro^9[Spiro-γ-lactam]Leu^{10},Trp^{11}]-physalaemin(1-11) (GR82334) (Peninsula Laboratories Europe; or Glaxo Group Research, U.K.), phenoxybenzamine (Smith, Kline & French, U.K.), [Glp^6, L-Pro^9]-SP(6-11) (septide, gift Dr B. Williams, Merck, Sharp and Dohme, U.K.), [Pro^9]-SP(1-11) (Neosystems, France), [Apa$^{9-10}$]-SP(1-11) (Apa = aminopentanoic acid) (gift Dr S. Lavielle, Université Pierre et Marie Curie, Paris, France), (3αR, 7αR)-7,7-diphenyl-2-[1-imino-2-(2-methoxyphenyl)ethyl]-perhydroisoindol-4-one (RP67580); gift Dr C. Garret (Rhône-Poulenc Rorer, France), [(2s,3s)-*cis*-2-(diphenylmethyl)-*N*-(2-iodophenyl)-methyl]-1-azabicyclo-[2,2,2]octan-3-amine ((±)-CP-96,345); gift Dr C.A. Maggi (A. Menarini Pharmaceuticals, Italy). All salts were of analytical grade and were obtained from B.D.H., U.K.

Senktide and (±)-CP-96,345 were dissolved in dimethylsulphoxide, RP67580 was dissolved in 0.05 M HCl, [Glp^6]-SP(6-11) was dissolved in formic acid, and ibuprofen was dissolved in 5% Na_2CO_3. All other agents, and all dilutions, were made up in distilled water. Peptides and non-peptide tachykinin receptor antagonists were stored at −20°C. Phenoxybenzamine was dissolved and diluted in 0.05 M hydrochloric acid (see Too *et al.*, 1988). Dimethylsulphoxide and hydrochloric acid (0.05 M) (administered in volumes used in experiments), did not effect basal tension *per se* or the concentration-response curve to neurokinin A ($n = 4$ each, data not shown).

Expression of results and statistical analysis

For estimation of time of reversal of agonist responses, the times to reach 75%, 50%, 25% and 0% of maximal agonist-induced tension were measured from individual traces, and from these values the arithmetic mean and s.e.mean were calculated.

In all other experiments, responses were calculated as % maximal response to carbachol (obtained with 1–10 mM carbachol, in view of the presence of atropine in the Krebs medium) in individual preparations, determined at the start of experiments. Data from individual experiments were combined and analysed in two ways. To allow conventional graphical display, responses were calculated for each concentration of test agonist in individual experiments, and plotted as mean responses ± s.e.mean. For the purposes of obtaining objective slope and EC_{50} estimates, individual agonist concentration-response relationships were analysed by determining the least-squares fit of data to the logistic function $y = y_{max} A^p/(A^p + A_{50}^p)$; where y is the response (expressed in

terms of maximum responses to carbachol), y_{max} is the estimated maximum response to that tachykinin, A is the tachykinin concentration, A_{50} is the concentration producing 50% of that agonist's maximum response (the EC_{50}), and p is the slope factor (equivalent to the Hill slope). These curve-fitting procedures were carried out using ORIGIN version 2.8 computer software (MicroCal Software Inc., MA, U.S.A.). Tests for significant differences were made using Student's *t* test for single- or two-samples, as appropriate. The pK_B estimates were determined from individual dose-ratios using the Gaddum-Schild equation: $pK_B = -\log K_B = \log (x-1) - \log [A]$, where x is the dose-ratio and [A] the applied antagonist concentration. Affinities are described as pK_B values when Schild plot analysis showed no significant departure from unity slope, or as apparent pK_B values when such analysis could not be carried out because a limited antagonist concentration range was used (see Results). In experiments measuring the effect of antagonists against responses to substance P, [Pro^9]-SP, physalaemin or ranamargarin under normal control conditions, in view of the prolonged washout of responses, dose-ratios were estimated between control log concentration-response curves obtained in concurrent time-control preparations (no antagonist) and log concentration-response curves obtained in test preparations (with antagonist), studied in parallel in paired preparations taken from the same animal. Estimates of pK_B obtained with this protocol, and calculated in this manner, with Group 1 agonists did not differ significantly ($P > 0.05$) from those obtained using within-preparation controls. In all cases *n* refers to the number of estimates (pK_B) or preparations (all other estimates), and represents data obtained from 4–8 animals (except as indicated in Table 1).

Results

Kinetics

The NK_1-receptor-preferring agonists differed in their relative potencies, but not in any consistent way in their slopes or maxima (Table 1; see also Hall *et al.*, 1991; 1993b). The rates of offset of contractile responses to tachykinins and analogues after washout, differed markedly. The responses to Group 1 agonists (GR73632, substance P methyl ester, septide, [Apa$^{9-10}$]-SP, [Glp^6]-SP(6-11)) had relatively fast offset kinetics (12.0 ± 1.8, 15.6 ± 3.6, 13.0 ± 2.0, 11.2 ± 1.7, 18.2 ± 3.8 min respectively; $n = 5-8$), and were similar to the muscarinic receptor agonist, carbachol (10.5 ± 2.3 min; $n = 6$). Responses to Group 2 agonists (substance P, physalaemin, ranamargarin and [Pro^9]-SP) were very slow indeed in offset (70.4 ± 8.4, 54.0 ± 6.7, 51.4 ± 3.8, 58.0 ± 3.9 min respectively; $n = 3-4$). Response washout kinetics of substance P methyl ester and substance P are represented in Figure 1. Co-application of EC_{50} concentrations of the Group 1 agonist, septide together with the NK_3-receptor-selective agonist, senktide, did not result in prolonged response offset kinetics (e.g. $t_{1/2}$ of the mixture, 3.4 ± 0.9 min, $n = 4$; *cf.* substance P, $t_{1/2}$ 35.3 ± 5.4 min; Hall *et al.*, 1991). Tissue pretreatment with phenoxybenzamine greatly accelerated the previously very slow washout-time of Group 2 agonists (e.g. substance P and [Pro^9]-SP; 24.2 ± 2.4 and 18.3 ± 2.4 min respectively ($P < 0.01$, $n = 7$; $P < 0.01$, $n = 11$; respectively)). There was less acceleration of the time of offset of Group 1 agonists (e.g. substance P methyl ester, septide; 8.5 ± 2.6 and 6.7 ± 0.8 min ($P > 0.05$, $n = 5$; $P < 0.05$, $n = 7$; respectively)), or of carbachol (5.3 ± 1.1 min ($P > 0.05$, $n = 6$)) (see Figure 1).

Antagonist studies

GR82334, (±)-CP-96,345 and RP67580 antagonized responses to Group 1 agonists (GR73632, substance P methyl ester, septide, [Apa$^{9-10}$]-SP, [Glp^6]-SP(6-11)) (Table 2). Schild analysis indicated that the antagonism by GR82334 of responses to substance P methyl ester was competitive (Figure 2). However, even at high concentrations the NK_1 antagonists did not inhibit, or only weakly attenuated, the responses to Group 2 agonists (substance P, physalaemin, ranamargarin and [Pro^9]-SP) (Table 2). Indeed, in some preparations, there was slight potentiation of agonist responses. The effect of GR82334 (10 μM) on the averaged log concentration-response curve to substance P is shown in Figure 2. Despite increasing the incubation time for GR82334 (10 μM) to 30 min, the antagonist was still without effect on the log concentration-response curve to substance P ($n = 4$; data not shown).

Phenoxybenzamine studies

Concentration-response parameters for two representative agonists from Group 1 and from Group 2 analogues, in control and phenoxybenzamine pretreated (test) preparations, are compared in Table 1. Though there were some significant changes ($P < 0.05$) in the slope or maxima, there seemed little

Table 1 Activities of tachykinin-receptor agonists in contracting the rabbit iris sphincter preparation: effect of phenoxybenzamine pretreatment

	Slope			*Maximum*			pD_2		
	Control	*Test*	*Δ (%)*	*Control*	*Test*	*Δ (%)*	*Control*	*Test*	*Δ (log)*
Agonist groups	*s.e.mean*	*s.e.mean*	*P*	*s.e.mean*	*s.e.mean*	*P*	*s.e.mean*	*s.e.mean*	*P*
Group 1									
Substance P methyl ester	0.62	1.07	172.6	100.4	116.0	115.5	9.16	7.86	1.30
	0.04; 17	0.19; 5	<0.01	4.8; 17	9.7; 5	>0.05	0.10; 17	0.23; 5	<0.01
Septide	0.77	0.75	97.5	95.3	95.8	100.5	9.47	8.84	0.63
	0.05; 13	0.11; 5	>0.05	2.8; 13	5.7; 5	>0.05	0.12; 13	0.31; 5	<0.05
Group 2									
Substance P	0.73	0.91	124.6	92.1	107.9	117.1	8.45	9.58	−1.13
	0.10; 13	0.14; 9	>0.05	4.3; 13	4.6; 9	<0.05	0.26; 13	0.24; 9	<0.01
[Pro^9]-SP	0.74	0.64	85.5	80.8	109.8	136.0	9.15	8.86	0.29
	0.12; 10	0.08; 5	>0.05	3.1; 10	11.4; 5	<0.05	0.16; 10	0.14; 5	>0.05

Contractile activities of two groups of tachykinin agonists (Group 1 and Group 2) with differing receptor selectivities (see text), described in terms of logistic parameters (see Methods). Maxima are expressed in terms of % carbachol maximum (where appropriate, prior to phenoxybenzamine treatment), and slope in terms of a slope factor (equivalent to the Hill slope). Differences between the control and the (test) phenoxybenzamine-pretreated (20 μM, 10 min) preparations, are expressed as % of control (Δ%, together with significance of difference, *P*) on an arithmetic scale for slope and maximum (i.e. 100% indicates no change). Differences in pD_2 values following phenoxybenzamine treatment are shown as logarithms (i.e. 1.0 would indicate a ten fold rightward shift, and − 1.0 a ten fold leftward shift.

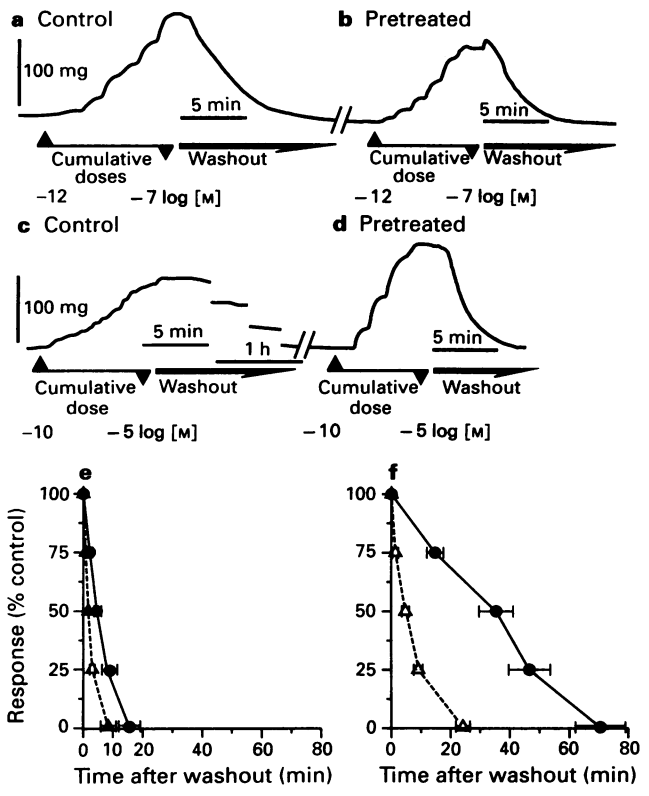

Figure 1 Kinetics of offset of contractions in the rabbit iris sphincter after washout of subtance P methyl ester or substance P; and effect of phenoxybenzamine pretreatment (20 μM, 10 min). The upper and middle panels show representative trace of cumulative concentration-responses curves over the concentration-ranges indicated, for substance P (a) and substance P methyl ester (c), respectively; untreated control preparations (a and c), or phenoxybenzamine pretreated preparations (b and d). Note the changed time scale in the latter part of (c). The lower panel shows averaged response *versus* time washout-curves for substance P methyl ester (e) or substance P (f); untreated control preparations (●), or phenoxybenzamine pretreated preparations (Δ). Points shown are means and s.e.means of times to reach set response levels expressed as % of pre-washout control level (in 4–11 preparations).

consistent difference between the groups. There was a marked rightward-shift of the concentration-response curves for the Group 1 agonists substance P methyl ester (twenty fold), though this was not so marked with septide (four fold) (Table 1). In contrast, there was a marked leftward-shift of the curve to the Group 2 agonist substance P (thirteen fold), though with no significant change for [Pro^9]-SP (Table 1). In contrast to the findings with controls, in phenoxybenzamine-pretreated preparations, GR82334 now antagonized the responses to substance P, physalaemin, ranamargarin and [Pro^9]-SP (Table 2). The overall results for substance P are shown in Figure 2, where antagonism was found to be compatible with simple equilibrium competitive interaction at a single site (see Table 2). Following phenoxybenzamine pretreatment, the pK_B estimates obtained for GR82334 against the Group 1 agonists substance P methyl ester and septide showed no difference ($P<0.05$) as compared to controls (Table 2): further, Schild analysis (Figure 2) showed that the antagonism by GR82334 of responses to substance P methyl ester was apparently competitive under both conditions. It may be noted that GR82334 always produced an initial fast contractile response in phenoxybenzamine-treated preparations, and occasionally in untreated preparations (data not shown).

Discussion

Within the tachykinin receptor analogues that are considered to be NK_1-receptor-preferring, two groups could be distinguished in terms of their common profile of pharmacological properties in the rabbit iris sphincter preparation. Group 1 consisted of septide, [Glp^6]-SP(6-11), substance P methyl ester, GR73632 and [Apa$^{9-10}$]-SP; whereas Group 2 included substance P, physalaemin, ranamargarin and [Pro^9]-SP. The responses to Group 1 agonists reversed rapidly on washout and were inhibited with high affinity by various NK_1-receptor-selective antagonists. In contrast, responses to Group 2 agonists reversed only very slowly on washout, and were not inhibited by NK_1 receptor antagonists under normal conditions: only after phenoxybenzamine pretreatment were such antagonists effective. These contrasting characteristics of the two groups seem not to result from differences in

Table 2 Affinity estimates in the rabbit iris preparation for three tachykinin receptor antagonists tested against two groups of tachykinin receptor agonists

Agonist groups	*(±)CP-96,345*	*RP67580*	*GR82334*	
	– PBZ	*+ PBZ*	*– PBZ*	*+ PBZ*
Group 1				
Substance P methyl ester	8.9 (0.3; 6)	7.0 (0.1; 6)	7.5 (0.1; 18)	7.2 (0.2; 15)
Septide	9.3 (0.3; 6)	7.4 (0.2; 6)	7.7 (0.2; 9)	7.9 (0.2; 7)
[Apa$^{9-10}$]-SP	9.5 (0.5; 6)	n.d.	7.1 (0.1; 7)	7.1 (2)
[Glp^6]-SP(6-11)	n.d.	n.d.	8.2 (0.3; 7)	7.7 (2)
GR73632	n.d.	n.d.	7.5 (0.2; 15)	n.d.
Group 2				
Substance P	<7.0 (3)	<6.0 (3)	<5.5 (6)	6.4 (0.1, 15)
[Pro^9]-SP	<7.0 (3)	<6.0 (3)	<6.0 (5)	6.8 (0.3, 7)
Physalaemin	n.d.	n.d.	<6.0 (4)	7.1 (2)
Ranamargarin	n.d.	n.d.	<6.0 (8)	6.8 (2)

Antagonist affinity estimates are given as apparent pK_B values (± s.e.mean; *n*), when tested against two groups of agonists (Group 1 and Group 2) with differing receptor selectivities. The antagonist GR82334 was tested both with and without pretreatment of preparations with phenoxybenzamine (20 μM, 10 min; see Methods); n.d. denotes not determined.

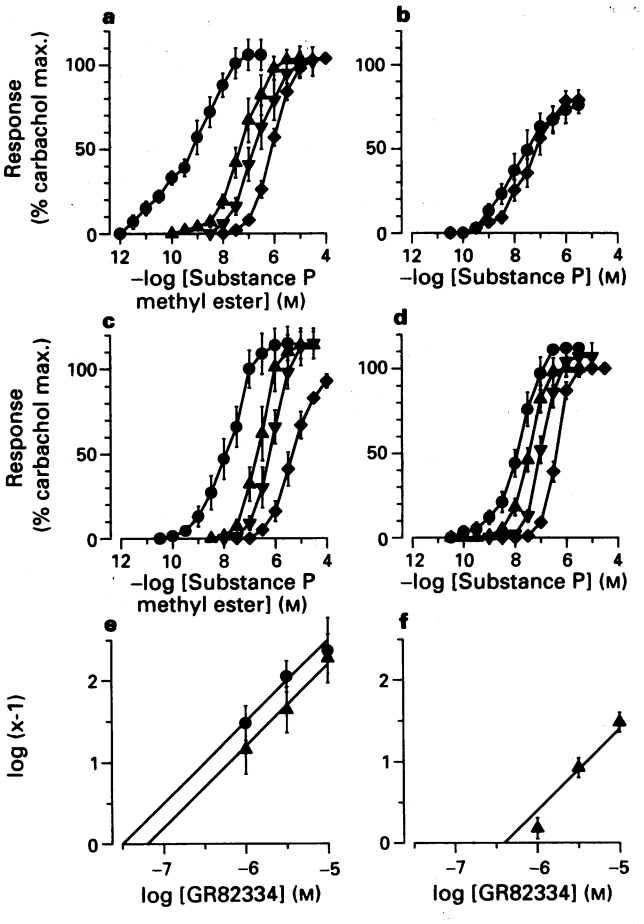

Figure 2 The effect of NK_1-receptor selective antagonists on responses to substance P, or substance P methyl ester, in control and phenoxybenzamine pretreated (20 μM, 10 min) preparations of rabbit iris sphincter. The top panels show averaged log concentration-response curves to substance P methyl ester (a) or substance P (b) determined in control tissue or, middle panels, in phenoxybenzamine pretreated tissues (c and d). Each panel shows control curves in the absence (●), or test, after a 5 min incubation with the NK_1-receptor-selective antagonist GR82334 at 1 μM (▲), 3.2 μM (▼), or 10 μM (◆). The lower panels show Schild regressions for antagonism by GR82334 of responses to substance P methyl ester in control preparations (●), and in preparations pretreated with phenoxybenzamine (▲) (e); and of responses to substance P in phenoxybenzamine-treated preparations only (f). The calculated slopes are (b ± s.e.mean; *n*) 0.87 ± 0.36; 18; 1.12 ± 0.42; 15; and 1.30 ± 0.18; 15, respectively: in no case do these Schild regressions differ significantly from unity ($P<0.05$), so unity slopes are imposed. For pK_B estimates, see Table 2. Experiments were carried out in the presence of hexamethonium (100 μM)., mepyramine, cimetidine, guanethidine and ibuprofen (all 1 μM). Atropine (1 μM) was included only in experiments without phenoxybenzamine.

metabolic stability of the peptides, since we have shown elsewhere (Hall *et al.*, 1991), that in the rabbit iris, even in combination, inhibitors of several different peptidases have little effect on activities of a number of such tachykinin receptor agonists; though we have found in certain other preparations that these inhibitors can modestly prolong tachykinin action (Hall *et al.*, 1990).

Interactions of Group 1 agonists with 'typical' NK_1 receptors

The Group 1 agonists (GR73632, substance P methyl ester, septide, [Apa^{9-10}]-SP, [Glp^6]-SP(6-11)) certainly can contract the rabbit iris sphincter via an interaction with 'typical' NK_1 receptors, since conventional NK_1 receptor antagonists (GR82334, RP67580, (±)-CP-96,345) competitively inhibited their responses with affinities consistent with published data for NK_1 receptors in other rabbit preparations (Hall *et al.*, 1993a; see Maggi *et al.*, 1993). For example, (±)-CP-96,345 had a similar affinity in the iris (pK_B 8.9–9.5) to that reported in the rabbit jugular vein (pK_B 8.33; Patacchini *et al.*, 1992), jugular vein and vena cava (pK_B 8.9 and 9.5, respectively; Rouissi *et al.*, 1991), and rabbit aorta (pK_B 8.81; Beresford *et al.*, 1991). It should be noted that for the present experiments in the rabbit iris sphincter, antagonism of responses to substance P methyl ester by GR82334 (both under control and phenoxybenzamine-pretreated conditions) was compatible with fully competitive equilibrium interaction at a single site, since the Schild regression appeared linear with a slope close to unity. However, there was some variation in the apparent affinity of a given antagonist depending on the agonist under study, and it may well be that some of the particular agonists which we designed as Group 1 for the purposes of discussion, do not have a total selectivity for this site. In preparations treated with the protein alkylator phenoxybenzamine, the log concentration-response curves to Group 1 agonists were shifted markedly to the right (twenty fold for substance P methyl ester or four fold for septide) (Table 1). However, most interestingly, there was no significant change ($P>0.05$) in the affinity of GR82334 tested against Group 1 agonists (Table 2; e.g. pK_B against substance P methyl ester, 7.5 and 7.2; and against septide 7.7 and 7.9, respectively). These various observations, taken together, suggest that phenoxybenzamine pretreatment reduces the receptor number at the sites where Group 1 agonists act (as might be expected by analogy with other receptor types) but does not change the receptor recognition properties.

'Atypical' characteristics of Group 2 agonists

The responses to the Group 2 agonists (substance P, physalaemin, ranamargarin, [Pro^9]-SP) had very prolonged response offset kinetics and were little inhibited, or in some instances potentiated, by the NK_1 receptor antagonists. Thus, Group 2 agonists must mediate contraction of iris smooth muscle via another route as compared to that of Group 1 agonists. An interaction with NK_2 receptors can be ruled out, since we have previously demonstrated insignificant activity of various NK_2-receptor-selective ligands in the iris preparation (Hall *et al.*, 1991; 1993b). Further, it seems unlikely that simultaneous synergistic activation of NK_1 and NK_3 receptors account for the unusual pharmacology of Group 2 ligands, since the co-administration of Group 1 NK_1-, and NK_3-receptor-selective, ligands (septide and senktide, respectively) does not result in a contractile response similar in profile to that of the Group 2 agonists. Also, it may be noted that the Group 2 agonist, [Pro^9]-SP, is well established in other systems as a very selective NK_1 receptor agonist, being virtually inactive at NK_3 receptors (Lavielle *et al.*, 1986; Beaujouan *et al.*, 1991; Petitet *et al.*, 1992). Moreover, tachykinins such as neurokinin A which are known to activate both NK_1 and NK_3 receptors, do not exhibit prolonged offset kinetics (Too *et al.*, 1988; Hall *et al.*, 1993b); and, as might be expected, the responses to such non-selective agonists are indeed partially inhibited by NK_1-receptor antagonists (Hall *et al.*, 1993b). Another mechanism that needs to be considered in attempting to explain the unusual characteristics of Group 2 agonists, is whether they act indirectly via the release of further mediators which, in principle, could influence both offset kinetics and sensitivity of responses to antagonism by NK_1 antagonists. Of the possible mediators that we have tested (endothelin, [Arg^8]-vasopressin, bombesin, angiotensin II, bradykinin), only endothelin had prolonged response offset kinetics in the rabbit iris sphincter, but was found to be insensitive to phenoxybenzamine pretreatment (unpublished observations).

It must be considered whether Group 2 agonists do, in fact, interact with 'typical' NK_1 receptors, but perhaps their

prolonged action and insensitivity to NK_1 receptor antagonists results from, for example, some prolonged non-equilibrium state in the biophase. There have been a number of reports of peptide antagonists that appear to become inserted in the membrane by some lipophilic binding (e.g. Hoe 140; Hall, 1992), and a similar phenomenon might well occur for agonists (as established for the nonpeptide β_2-adrenoceptor agonist salmeterol (Ball *et al.*, 1991)). It is difficult to test for such phenomena, but it may be noted that the prolonged action of Group 2 agonists is not prevented even by 30 min prior incubation with NK_1 antagonists. That phenoxybenzamine-pretreatment prevents the agonists' prolonged effect, could be interpreted in a number of ways, given this reagent's wide-ranging alkylating actions. Possible explanations include: (1) reduction of the receptor density reducing the diffusional drag limiting washout of agonist molecules from high-affinity binding in the biophase (see Bailey, 1985); and here it is noteworthy that several NK_1 agonists have unusually high potency in this preparation (Hall *et al.*, 1991) suggesting a large receptor concentration and/or good coupling-efficiency (this supposition of a large receptor reserve being supported by the failure of phenoxybenzamine alkylation to reduce agonists' maximum responses or slope, even when there was a substantial shift of the concentration-response curve to the right); (2) reduction of high-affinity binding at sites not actually involved in the response ('silent receptors') but which exert a diffusional drag; or (3) modification of the receptor-effector coupling-mechanisms downstream of the receptor site (for instance, by blocking Ca^{2+}-channels). However, no single explanation seems to account for all the atypical characteristics of Group 2 agonists. It would be helpful if the differences in pharmacology of Group 1 and Group 2 agonists could be attributed to some specific chemical feature; but though all the Group 2 agonists are full-length peptides, whereas several Group 1 agonists are made up of the truncated SP(6-11) sequence, there are the notable exceptions within Group 1 of the full-sequence agonists substance P methyl ester and [Apa^{9-10}]-SP(1-11).

Discounting the potential complications discussed above, the simplest remaining explanation for our findings is that the rabbit iris sphincter contains two differing 'NK_1-like' receptor populations. Here, there is the possibility that these represent two genetically-distinct receptor subtypes: alternatively they may reflect receptor isoforms, resulting, for example, from alternative pre-mRNA splicing (as has been shown with the cloned human NK_1 receptor; Fong *et al.*, 1992). One receptor subtype in the iris, which Group 1 agonists preferentially activate, appears to have characteristics similar to those previously described for 'typical' rabbit NK_1 receptors. Thus, (±)-CP-96,345, GR82334 and RP67580 have their characteristic affinities (see Maggi *et al.*, 1993), and responses following receptor activation reverse fairly rapidly on agonist washout. In contrast, Group 2 agonists seem preferentially to activate a very different (in terms of recognition properties) 'atypical' receptor-subtype or receptor-isoform, which is insensitive to blockade by (±)-CP-96,345, GR82334 or RP67580, and where receptor activation results in prolonged washout offset-kinetics. It might be supposed that phenoxybenzamine preferentially alkylates this form of receptor, unmasking the 'typical' NK_1 receptor at which Group 2 agonists have some agonist activity, so that their actions are now rapid in offset and are inhibited by NK_1 receptor antagonists. However, since Group 1 agonist activities are attenuated by phenoxybenzamine, it would seem that 'typical' NK_1 sites are also susceptible to alkylation.

In practice, it is difficult to distinguish between the above proposal of the presence of two distinct receptor proteins, from a plausible and similar model where Group 1 and Group 2 agonists bind to different domains of the *same* (NK_1) receptor protein. For instance, Group 2 agonists may bind to additional domains not accessible to NK_1 agonists, and this could induce conformational or allosteric changes resulting in prolonged responses, and prevention of antagonist binding or the ability of the antagonists actually to interfere with agonist binding. Binding of agonist and antagonist ligands each to different domains of NK_1 receptors, has been described as the cloned NK_1 receptors of rat and man (see Hall *et al.*, 1993a). It could be envisaged that the additional binding domain occupied by Group 2 agonists is susceptible to alkylation by phenoxybenzamine; and thus following alkylation of this site, Group 2 agonists interact with the same receptor domains as those recognizing Group 1 agonists.

It is of interest that Petitet *et al.* (1992) have recently reported pharmacological and radioligand binding data which they interpret as indicating the existence of two NK_1-like tachykinin receptor subtypes in the guinea-pig ileum. In their studies, two groups of agonists could also be distinguished. Substance P, [Pro^9]-SP and [Sar^9, $Met(O_2)^{11}$]-SP were proposed to belong to one group which had high affinity for [^{3}H]-[Pro^9]-SP binding sites; and further, contractile responses to a representative agonist from this group ([Pro^9]-SP) were only weakly inhibited by the NK_1 receptor antagonist GR71251 (pK_B 6.5). In contrast, [Glp^6, L-Pro^9]-SP(6-11) (septide), substance P methyl ester, [Apa^{9-10}]-SP and [$Pro^{9,10}$]-SP were all considered to belong to a second group having low affinity for [^{3}H]-[Pro^9]-SP binding sites, and responses to agonists in this group (septide and [Apa^{9-10}]-SP) were inhibited by the NK_1 antagonist, GR71251 with relatively high affinity (pK_B 7.9 and 8.1, respectively). Further evidence for the existence of subtypes of the NK_1 receptor in the guinea-pig ileum was provided by the fact that [D-Pro^9,$MeLeu^{10}$,Trp^{11}]-SP was equipotent as an antagonist against either [Pro^9]-SP or septide evoked contractions (pA_2 6.6) (Chassaing *et al.*, 1992). Unfortunately, in the rabbit iris sphincter, we found this analogue to be a partial agonist (unpublished observations).

The grouping of agonists by Petitet *et al.* (1992) in the guinea-pig ileum is largely in accord with our own grouping of agonists in the rabbit iris sphincter. An obvious interpretation of this correspondence, is that there are two within-preparations subtypes of the NK_1 receptor; which in turn have some common between-preparations properties. Indeed, others have claimed some inter-species similarities in NK_1 receptors of the guinea-pig and rabbit (see Hall *et al.*, 1993a). However, it would be premature to propose intra-species variants of the NK_1 receptor on the present evidence, especially given some of our reservations over interpretation of the experimental evidence. Final conclusions would be aided by the development of selective antagonists for the NK_1 receptor antagonist-insensitive 'atypical' site; but more important would be the demonstration, by the techniques of molecular biology, of the existence of genetically-distinct NK_1 receptor-subtypes, or of receptor-isoforms, within the single species; or alternatively, the identification of different binding domains, for each of the two agonist groups, on a single NK_1-receptor-protein. However, irrespective of such conclusions, the contrasting operational pharmacological characteristics of the two groups of ligands is striking, and the physiological importance of this, at the level of receptor function, may well be considerable.

We wish to thank the following for discussion or gifts of compounds: Dr S.P. Watson, University Department of Pharmacology, University of Oxford; Dr C.A. Maggi, A. Menarini Pharmaceuticals, Florence, Italy ((±)-CP-96,345); Dr C. Garret, Rhône-Poulenc Rorer, Vitry sur Seine, France (RP67580); Dr S. Lavielle, Université Pierre et Marie Curie, Paris, France ([Apa^{9-10}]-SP) and Drs R.M. Hagan and S.J. Ireland, Glaxo Group Research, UK, (GR82334 and GR73632). This study was supported by the Wellcome Trust.

References

BAILEY, S.J. (1985). Theoretical models for the actions of tachykinin antagonists in the guinea-pig ileum. In *Tachykinin Antagonists*. ed. Håkanson, R. & Sundler, F. pp. 323–331. Amsterdam: Elsevier.

BALL, D.I., BRITTAIN, R.T., COLEMAN, R.A., DENYER, L.H. JACK, D., JOHNSON, M., LUNTS, L.H.C., NIALS, A.T., SHELDRICK, K.E. & SKIDMORE, I.F. (1991). Salmeterol, a novel, long-acting β_2-adrenoceptor agonist: characterization of pharmacological activity. *Br. J. Pharmacol.*, **104**, 665–671.

BEAUJOUAN, J.-C., SAFFROY, M., TORRENS, Y., CHASSAING, G., LAVIELLE, S., BESSEYRE, J., GARRET, C., CARUETTE, A. & GLOWINSKI, J. (1991). Further demonstration that (Pro^9)-substance P is a potent and selective ligand of NK-1 tachykinin receptor. *J. Neurochem.*, **56**, 879–889.

BERESFORD, I.J.M., BIRCH, P.J., HAGAN, R.M. & IRELAND, S.J. (1991). Investigation into species variants in tachykinin NK_1 receptors by use of the non-peptide antagonist, CP-96,345. *Br. J. Pharmacol.*, **104**, 292–293.

CHASSAING, G., LAVIELLE, S., BRUNISSEN, A., CARRUETTE, A., GARRET, C., PETITET, F., SAFFROY, M., BEAUJOUAN, J.-C., TORRENS, Y. & GLOWINSKI, J. (1992). [PRO^9]SP and [pGLU^6,PRO^9]SP(6-11) interact with two different receptors in the guinea-pig ileum as demonstrated with new substance P antagonists. *Neuropeptides*, **23**, 73–79.

FONG, T.M., ANDERSON, S.A., YU, H., HUANG, R.-R.C. & STRADER, C.D. (1992). Differential activation of intracellular effector by two isoforms of human neurokinin-1 receptor. *Mol. Pharmacol.*, **41**, 24–30.

GARRET, C., CARRUETTE, A., FARDIN, V., MOUSSAOUI, S., PEYRONEL, J.-F., BLANCHARD, J.-C. & LADURON, P.M. (1991). Pharmacological properties of a potent and selective nonpeptide substance P antagonist. *Proc. Natl. Acad. Sci. U.S.A.*, **88**, 10208–10212.

HAGAN, R.M., IRELAND, S.J., BAILEY, F., McBRIDE, C., JORDAN, C.C. & WARD, P. (1991). GR82334, a spirolactam conformationally-constrained analogue of physalaemin which is a peptidase-resistant, selective neurokinin NK-1 receptor antagonist. *Br. J. Pharmacol.*, **102**, 360P.

HÅKANSON, R., WANG, Z. & FOLKERS, K. (1991). Comparison of spantide II and CP-96,345 for blockade of tachykinin-evoked contractions in smooth muscle. *Biochem. Biophys. Res. Commun.*, **178**, 297–301.

HALL, J.M. (1992). Bradykinin receptors: pharmacological properties and biological roles. *Pharmacol. Ther.*, **56**, 131–190.

HALL, J.M. (1994). Receptor function in the periphery. In *The Tachykinins Receptors*. ed. Buck, S.H., Chapter 17, NJ, USA: Humana Press.

HALL, J.M., FOX, A.J. & MORTON, I.K.M. (1990). Peptidase activity a determinant of agonists potencies in some smooth muscle preparations. *Eur. J. Pharmacol.*, **176**, 127–134.

HALL, J.M., CAULFIELD, M.P., WATSON, S.P. & GUARD, S. (1993a). Receptor subtypes or species homologues: relevance to drug discovery. *Trends Pharmacol. Sci.*, **14**, 376–383.

HALL, J.M., MITCHELL, D. & MORTON, I.K.M. (1991). Neurokinin receptors in the rabbit iris sphincter characterised by novel agonist ligands. *Eur. J. Pharmacol.*, **199**, 9–14.

HALL, J.M., MITCHELL, D. & MORTON, I.K.M. (1993b). Tachykinin receptors mediating responses to sensory nerve stimulation and exogenous tachykinins and analogues in the rabbit isolated iris sphincter. *Br. J. Pharmacol.*, **109**, 1008–1013.

HALL, J.M., MITCHELL, D. & MORTON, I.K.M. (1993c). Does substance P release mediate NANC nerve-mediated responses to field stimulation and ligands, in rabbit isolated sphincter pupillae? *Regul. Pept.*, **46**, 278–281.

HALL, J.M., MITCHELL, D. & MORTON, I.K.M. (1994). Tachykinin NK_1 receptor ligands show two distinct pharmacological profiles in rabbit iris sphincter. *Br. J. Pharmacol.*, **111**, 48P.

LAVIELLE, S., CHASSAING, G., JULIEN, S., MARQUET, A., BERGSTRÖM, L., BEAUJOUAN, J.-C., TORRENS, Y. & GLOWINSKI, J. (1986). Specific recognition of SP and NKB receptors by analogues of SP substituted at positions 8 and 9. *Eur. J. Pharmacol.*, **125**, 461–462.

MAGGI, C.A., PATACCHINI, R., ROVERO, P. & GIACHETTI, A. (1993). Tachykinin receptors and tachykinin receptor antagonists. *J. Autonom. Pharmacol.*, **13**, 23–93.

MURAMATSU, I., NAKANISHI, S. & FUJIWARA, M. (1987). Comparison of the responses to the sensory neuropeptides, substance P, neurokinin A, neurokinin B and calcitonin gene-related peptide and to trigeminal nerve stimulation in the iris sphincter muscle of the rabbit. *Jpn. J. Pharmacol.*, **44**, 85–92.

PATACCHINI, R., SANTICIOLI, P., ASTOLFI, M., ROVERO, P., VITI, G. & MAGGI, C.A. (1992). Activity of peptide and non-peptide antagonists at peripheral NK_1 receptors. *Eur. J. Pharmacol.*, **215**, 93–98.

PETITET, F., SAFFROY, M., TORRENS, Y., LAVIELLE, S., CHASSAING, G., LOEUILLET, D., GLOWINSKI, J. & BEAUJOUAN, J.-C. (1992). Possible existence of a new tachykinin receptor subtype in the guinea-pig ileum. *Peptides*, **13**, 383–388.

ROUISSI, N., GITTER, B.D., WATERS, D.C., HOWBERT, J.J., NIXON, J.A. & REGOLI, D. (1991). Selectivity and specificity of new, non-peptide, quinuclidine antagonists of substance P. *Biochem. Biophys. Res. Commun.*, **176**, 894–901.

SNIDER, R.M., CONSTANTINE, J.W., LOWE, J.A., III, LONGO, K.P., LEBEL, W.S., WOODY, H.A., DROZDA, S.E., DESAI, M.C., VINIC, F.J., SPENCER, R.W. & HESS, H.-J. (1991). A potent nonpeptide antagonist of the substance P (NK_1) receptor. *Science*, **251**, 435–437.

TOO, H.P., UNGER, W.G. & HANLEY, M.R. (1988). Evidence for multiple tachykinin receptor subtypes on the rabbit iris sphincter muscle. *Mol. Pharmacol.*, **33**, 64–71.

(Received January 13, 1994
Revised March 7, 1994
Accepted March 22, 1994)

Br. J. Pharmacol. (1994), **112**, 992–997

Potentiation by adenosine of ATP-evoked dopamine release via a pertussis toxin-sensitive mechanism in rat phaeochromocytoma PC12 cells

Schuichi Koizumi, Tomokazu Watano, Ken Nakazawa & [1]Kazuhide Inoue

Division of Pharmacology, National Institute of Health Sciences, 1-18-1 Kamiyoga, Setagaya-ku, Tokyo 158, Japan

1 The effects of adenosine on adenosine 5'-triphosphate (ATP)-evoked dopamine release from rat phaeochromocytoma PC12 cells was investigated to determine whether adenosine exerts a regulatory effect on the ATP-evoked response. Adenosine potentiated ATP (30 μM)-evoked dopamine release in a concentration-dependent manner over a concentration-range of 1 to 100 μM. Adenosine (100 μM) shifted the concentration-dependence of the ATP-evoked response to the left without affecting the maximal response.

2 Aminophylline, a non-selective adenosine receptor antagonist, and CP66713, a selective antagonist at the A_2 subclass of adenosine receptors, abolished the adenosine-induced potentiation. Furthermore, 8-cyclopentyltheophylline, a selective antagonist at the adenosine A_1 receptor partially inhibited the adenosine-evoked potentiation. CGS22492, a selective A_2 receptor agonist, potentiated ATP-evoked dopamine release whereas N^6-cyclohexyladenosine (CHA), a selective A_1 receptor agonist, had no effect.

3 Pertussis toxin (PTX), a bacterial exotoxin which catalyzes the ADP-ribosylation of guanosine 5'-triphosphate (GTP)-binding proteins (G-proteins), inhibited the adenosine-induced potentiation of dopamine release. Dibutyryl cyclic AMP (db cyclic AMP), an analogue of cyclic AMP, had no effect on the release on the ATP-evoked response.

4 Adenosine potentiated the ATP-evoked rise in intracellular Ca^{2+} concentration ($[Ca]_i$) in PC12 cells. This potentiation was also observed with CGS 22492 but not with CHA. PTX completely inhibited the adenosine-induced potentiation of the rise in $[Ca]_i$.

5 On the basis of these findings, we suggest that the adenosine-induced potentiation of ATP-evoked dopamine release was due to an increase in $[Ca]_i$ in the cells. Although the potentiation is most likely mediated by a subclass of A_2 receptors, the subclass may be different from those previously reported since the potentiation was sensitive to PTX and was not reproduced by db cyclic AMP.

Keywords: ATP; adenosine; PC12 cells; dopamine release; intracellular Ca^{2+} concentration; pertussis toxin

Introduction

Adenosine 5'-triphosphate (ATP) has a functional role as a neurotransmitter or modulator in smooth muscle (Burnstock & Kennedy, 1985) and in neural tissues (Bean, 1990; Evans, 1992), including the central nervous system (Inoue & Nakazawa, 1992; Edwards *et al.*, 1992; Edwards & Gibb, 1993). ATP activates non-selective cation channels (Bean, 1992), leading to muscle contraction (Bean, 1992) and catecholamine secretion (Inoue *et al.*, 1989; Nakazawa & Inoue, 1992). We previously characterized the ATP-activated channels in PC12 cells, a cell line derived from a rat phaeochromocytoma (Green & Tischler, 1975), and demonstrated that these cells are suitable for the study of the channels and secretion triggered by channel activation (Inoue *et al.*, 1989; Inoue & Nakazawa, 1992; Nakazawa & Inoue, 1992).

Few previous reports have dealt with the modulatory effects of endogenous substances on the ATP-evoked effects. Agents acting on dopamine receptors were shown to potentiate ATP-evoked currents in PC12 cells (Inoue & Nakazawa, 1992; Nakazawa *et al.*, 1993). ATP-activated phosphatidyl inositide breakdown and arachidonate release are reported to be affected by adenosine, a product of ATP metabolism, in rat thyroid FRTL-5 cells (Okajima *et al.*, 1989; Nazarea *et al.*, 1991). ATP and adenosine act synergistically to mobilize intracellular Ca^{2+} via the formation of inositol 1,4,5-trisphosphate in a smooth muscle cell line (Gerwins & Fredholm, 1992). Adenosine has also been proposed as a neuromodulator or neurotransmitter in various neuronal cells or tissues, with mainly inhibitory action (Phillis *et al.*, 1975; Okada & Kuroda, 1980). PC12 cells have been reported to have functional adenosine receptors (Hide *et al.*, 1991), raising the possibility that adenosine can modulate ATP-evoked responses in PC12 cells. We have therefore examined the effects of adenosine on ATP-evoked dopamine release and the increase in intracellular Ca^{2+} concentration ($[Ca]_i$) in the cells.

In the present study, we demonstrate that adenosine increases ATP-evoked dopamine release by potentiating the $[Ca]_i$ rise in the cells. This potentiation is achieved via a pertussis toxin-sensitive and adenosine 3':5'-cyclic monophosphate (cyclic AMP)-independent mechanism.

Methods

Cell culture

PC12 cells were the kind gift of Dr Terry Rogers (Johns Hopkins University School of Medicine, Baltimore, MD, U.S.A.). Culture conditions were as described previously (Inoue & Kenimer, 1988). In brief, the cells were received in our laboratory at passage 46 and were expanded, and a seed lot was frozen at passage 47 and stored in liquid nitrogen. All experiments described in this manuscript were performed with cells at passage number between 53 and 68. Cells were cultured in 75 cm^2 flask in Dulbecco's Modified Eagle's Medium containing 7% foetal bovine serum (GIBCO, NY, U.S.A.), 7% heat-inactivated (56°C, 40 min) horse serum (Cell culture Laboratories, Ohio, U.S.A.), 2 mM L-glutamine (M.A. Bioproducts, MD, U.S.A.), and 50 μg ml^{-1} gentamicin

[1] Author for correspondence.

sulphate (Boehringer Mannheim GmbH, Germany) in a humidified atmosphere of 90% air and 10% CO_2 at 37°C. Cells were removed from flasks for subculture and for plating into assay dishes using a Ca^{2+}/Mg^{2+} -free solution containing (mM): NaCl 172, KCl 5.4, NaH_2PO_4 1 and glucose 5.6, pH 7.4. Afer about 5 min in this solution, the cells were detached by gently tapping the side of the flask. The cells were removed, plated onto collagen-coated 35 mm polystyrene dishes (1×10^6 cells/dish) and used 2 days later. For measurement of $[Ca]_i$ in single cells, cells were plated onto poly-L-lysine (Sigma, MO, U.S.A.)-coated glass coverslips ($24 \times 60 \times 0.15$ mm, Flexiperm, W.C. Haraeus GmbH, Hanau, Germany) at a density of 2.5×10^5 cells per well (8×11 mm), and cultured for an additional 2 days.

Dopamine release

Released dopamine was measured as described by Ohara-Imaizumi *et al.* (1991). All the procedures including incubation, washing, and drug application, were made using 1 ml/dish of a balanced salt solution (BSS) with the following composition (mM): NaCl 150, KCl 5.0, $CaCl_2$ 1.2, $MgCl_2$ 1.2, NaH_2PO_4 1.2, D-glucose 10, ethylenediaminetetraacetic acid (EDTA) 0.1 and N-2-hydroxyethylpiperazine-*N'*-2-ethanesulphonic acid (HEPES) 25, pH adjusted to 7.4 with NaOH. Dishes were washed twice and incubated with BSS for 1 h at room temperature. After washing once with BSS, ATP was added to the dishes and incubated for 1 min. Agonists and antagonists to adenosine receptors were added to the medium 1 min before and during ATP application. At the end of the incubation period, the solutions were transferred immediately to sample cups containing 0.25 ml of 1 N $HClO_4$ for measurement of dopamine released into the solution. The cellular dopamine was extracted with 0.2 N $HClO_4$ by sonication in the dish. After centrifugation (at 4°C for 2 min, 1000 *g*), supernatants of both the incubation solutions and the sonicated cellular solutions were collected for measurement of dopamine content. Dopamine content was determined with a high performance liquid chromatography-electrochemical detection system (Bioanalytical systems, West Lafayette, IN, U.S.A.). The percentage of release was calculated using the values obtained for the dopamine content in the incubation solution (A) and the dopamine content remaining in the cells (B) using the following equation: % of total dopamine = $100 \times A/(A + B)$.

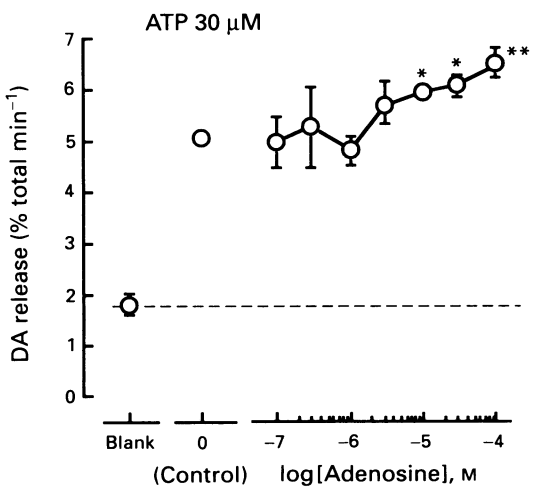

Figure 1 Effect of adenosine on ATP (30 μM)-evoked dopamine (DA) release from PC12 cells. Adenosine was present 1 min before and during ATP application. Values represent the released dopamine (% of total content per min) of 2 separate experiments ($n = 6$). Broken line indicates spontaneous release (1.8 ± 0.11% of total content per min). Data are mean ± s.e.mean. Asterisks indicate significant differences from the response by ATP alone (control): $*P < 0.05$; $**P < 0.01$.

$[Ca]_i$ concentration

The increase in $[Ca]_i$ in single cells was measured by the fura-2 method as described by Grynkiewicz *et al.* (1985) with minor modifications. All the procedures including incubation, washing, and drug application, were made using balanced salt solution (BSS). The cells were washed with BSS and incubated with 10 μM fura-2 acetoxymethylester at 37°C in BSS. After 30 min incubation, the cells were washed with 0.2 mM of BSS. The coverslips were mounted on an Olympus IMT-2 inverted epifluorescence microscope equipped with a 75 W xenon-lamp and band-pass filters of 340 nm wavelength, for measurement of the Ca^{2+}-dependent signal, and 360 nm wavelength, for measurement of the Ca^{2+}-independent signal. Image data, recorded by a high-sensitivity silicon intensifier target camera (C-2741-08, Hamamatsu Photonics, Co., Hamamatsu, Japan) were processed by a personal computer. Fluorescence ratio images were obtained and calibrated as described elsewhere (Miyakawa *et al.*, 1989). The cells were treated twice with ATP, and the second treatment was made with drugs. The ratio of the second response over the first response (S2/S1) was calculated and adopted as an index to compare the data among different cells.

Pretreatment with PTX

Pretreatment of PC12 cells with PTX was performed as described previously (Inoue & Kenimer, 1988). PTX was added to the conditioned medium at a final concentration of 2 ng ml^{-1}, and the cells were incubated for 20 h at 37°C. With this procedure, a 41-kDa PTX-sensitive G-protein, was almost completely ADP-ribosylated in PC12 cells (Inoue & Kenimer, 1988).

Drugs

Drugs and chemicals were obtained from the following sources: ATP (Yamasa Co., Choshi, Japan), adenosine and N^6-cyclohexyladenosine (CHA; A_1 agonist) were from Sigma (MO, U.S.A.). 8-cyclopentyl-1,3-dimethylxanthine (8-CPT; A_1 antagonist) (Research Biochemicals Inc., MA, U.S.A.), CP66713 (A_2 antagonist) (Pfizer, CT, U.S.A.), EGTA, HEPES and fura-2AM (Dojin, Kumamoto, Japan). Other drugs were purchased from Hayashi Pure Chemical (Tokyo, Japan).

Statistics

Statistical differences in values for dopamine release and $[Ca]_i$ increase were determined by analysis of variance and Scheffe's test for multiple comparisons.

Results

Figure 1 shows the concentration-dependence of the adenosine-induced potentiation of ATP-evoked dopamine release from PC12 cells. Adenosine potentiated ATP (30 μM)-evoked dopamine release significantly in a concentration-dependent manner over a concentration-range from 10 to 100 μM. At the highest concentration, adenosine potentiated the ATP-evoked response by approximately 50%. Figure 2a shows the effect of adenosine (100 μM) on the concentration-dependent curves of ATP-evoked dopamine release from the cells. Adenosine (100 μM) shifted the ATP-response curve to the left but did not change the maximal response to ATP. Adenosine potentiated the response evoked by 30 μM ATP yet had no effect on the response evoked by 300 μM ATP (Figure 2b).

To examine the involvement of PTX-sensitive G-proteins on the adenosine-induced responses, the cells were preincubated with 2 ng ml^{-1} of PTX for 20 h at 37°C as described previously (Inoue & Kenimer, 1988). Figure 3 shows the

effects of PTX on the adenosine-induced potentiation of the ATP-evoked response. PTX abolished the effect of adenosine almost completely, suggesting that the adenosine-induced potentiation is mediated via a PTX-sensitive G-protein.

The effects of adenosine antagonists on the potentiation of the ATP-induced response was investigated. Figure 4 shows the effects of aminophylline, a non selective adenosine receptor antagonist, 8-cyclopentyltheophylline (8-CPT), a selective adenosine A_1 subtype antagonist, and CP66713, a selective adenosine A_2 subtype antagonist, on the adenosine-evoked potentiation. Aminophylline ($<100\,\mu M$) had no effect on dopamine release stimulated by $30\,\mu M$ ATP alone; however, it inhibited the potentiation seen with adenosine almost completely. The release was reduced to the control level

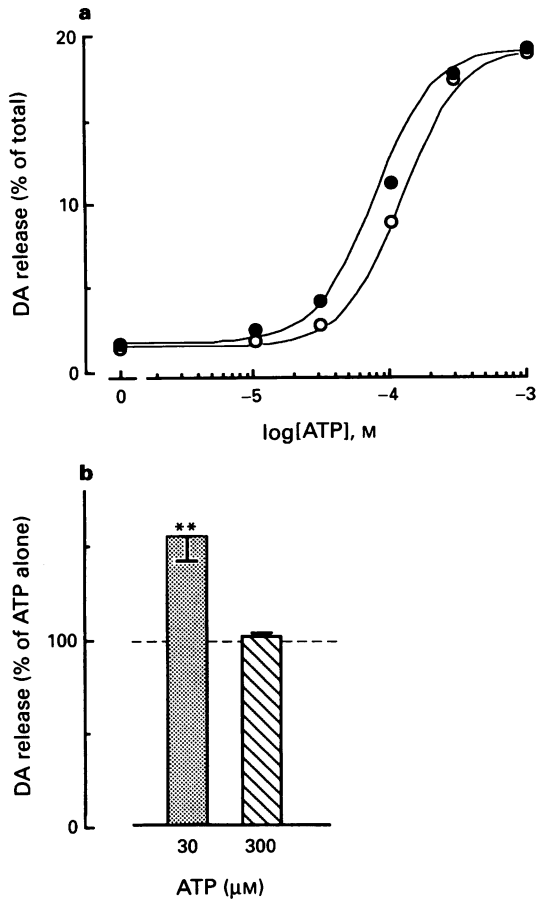

Figure 2 Effect of adenosine ($100\,\mu M$, ●) on the concentration-dependent curves of ATP-evoked dopamine release from the cells (a). Adenosine shifted the curves to the left without affecting the maximal response. Values represent the released dopamine (% of total content per min) of 3 separate experiments ($n=9$). (○) Control curve (b) Shows effect of adenosine ($100\,\mu M$) on $30\,\mu M$ ATP (stippled column) and $300\,\mu M$ ATP (hatched column). Values represent % of the response evoked by ATP alone. Each column indicates mean ± s.e.mean of 3–9 of dishes. Asterisks show significant difference from ATP alone: $^{**}P<0.01$.

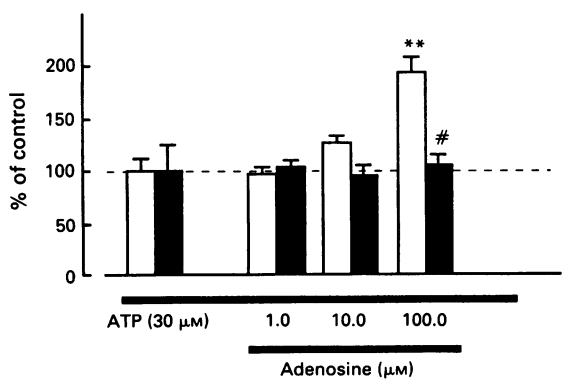

Figure 3 The involvement of pertussis toxin (PTX) on adenosine (1–100 μM)-induced potentiation in ATP (30 μM)-evoked dopamine release. The cells were treated with PTX as described in Methods. Values represent % of the response evoked by ATP alone in control (open columns) and the PTX (2 ng ml^{-1}, 20 h)-treated (solid columns) cells, respectively. Data are mean ± s.e.mean of 3 separate experiments ($n=9$). Symbols represent significant differences from the response to ATP alone ($^{**}P<0.01$) or corresponding response in intact cells ($\#P<0.05$), respectively.

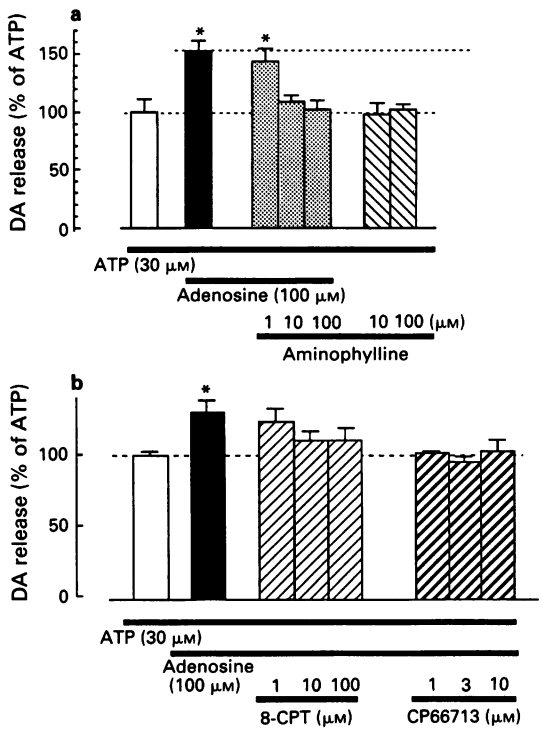

Figure 4 Inhibitory effect of adenosine antagonists on adenosine-induced potentiation of ATP-evoked dopamine (DA) release. Aminophylline (1–100 μM) (a), 8-cyclopentyltheophylline (8-CPT, 1–100 μM) and CP66713 (1–10 μM) (b) inhibited adenosine (100 μM)-induced potentiation of the ATP (30 μM)-evoked release. Values represent % of the response by ATP alone. Data are mean ± s.e. mean obtained from at least 3 separate experiments ($n=9-12$). Asterisks indicate significant difference from ATP alone: $^{*}P<0.05$.

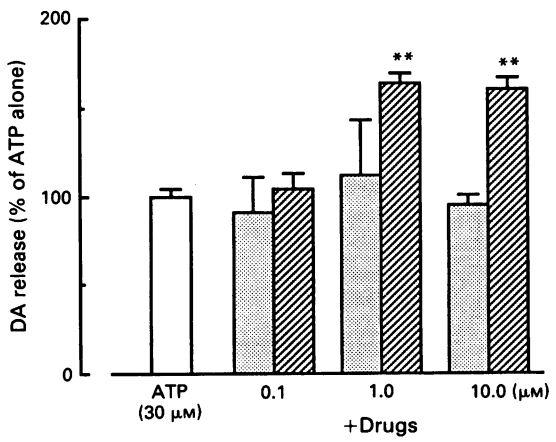

Figure 5 Effects of N^6-cyclohexyladenosine (CHA) (an adenosine A_1 agonist) or CGS22492 (an adenosine A_2 agonist) on ATP (30 μM)-evoked dopamine (DA) release from the cells. Stippled columns: CHA; hatched columns CGS 22492. Values represent % of the response by ATP alone. Data are mean ± s.e.mean obtained from 2 separate experiments ($n=6$). Asterisks indicate significant differences from ATP alone: $^{**}P<0.01$.

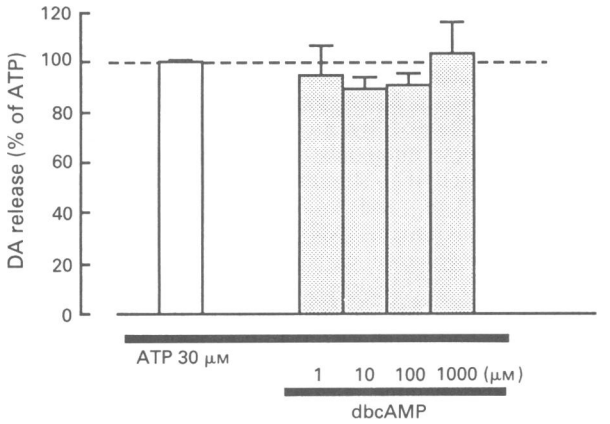

Figure 6 Effect of dibutyryl cyclic AMP (dbcAMP, 1–1000 μM) on ATP (30 μM)-evoked dopamine (DA) release from PC12 cells. Each column represents % of the response to ATP alone. Data are mean ± s.e.mean obtained from 2 separate experiments ($n = 6$).

(102.1 ± 7.3% of ATP alone, Figure 4a). Similarly, neither 8-cyclopentyltheophylline (8-CPT, 100 μM) nor CP66713 (10 μM) affected dopamine release stimulated by 30 μM ATP alone (data not shown), but they inhibited the adenosine-induced potentiation (Figure 4b). Next we examined the effects of CHA, a selective adenosine A_1 receptor agonist, and CGS22492, a selective adenosine A_2 receptor agonist, on ATP-evoked release (Figure 5). These agonists had no effects on spontaneous dopamine release. CHA failed to enhance the response, while CGS22492 potentiated over a concentration-range of 1 to 10 μM. These results suggest that adenosine-induced potentiation of ATP-stimulated dopamine release involves a subclass of adenosine A_2 receptors.

We investigated the effects of dibutyryl cyclic AMP, a cyclic AMP analogue, on ATP-evoked response because coupling between A_2 receptors and activation of adenylate cyclase has been suggested (Gilman, 1984). As shown in Figure 6, dibutyryl cyclic AMP did not affect ATP-evoked dopamine release from PC12 cells, even at concentrations up to 1 mM.

Finally, we observed the effects of adenosine on ATP-

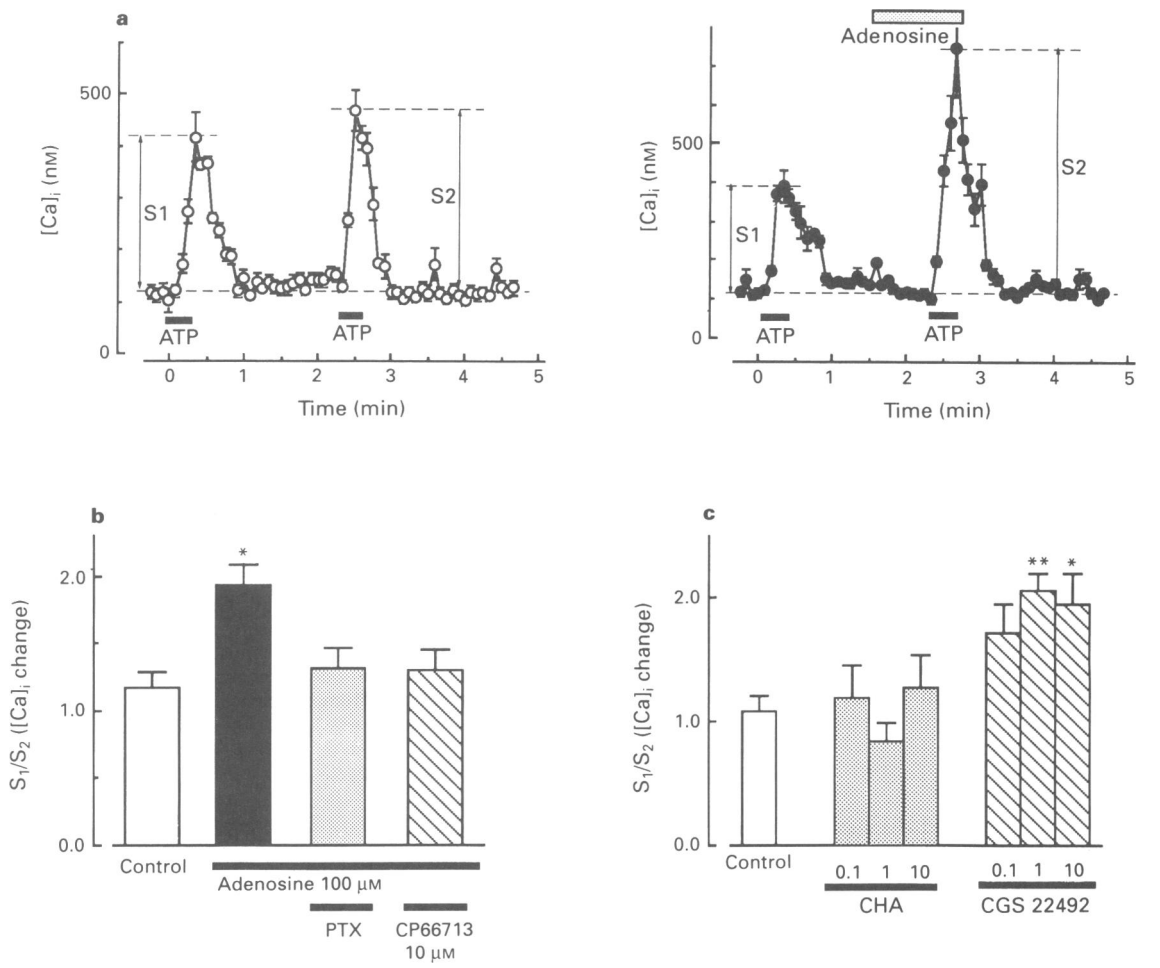

Figure 7 Potentiation by adenosine and its analogue of the ATP-evoked increase in $[Ca]_i$ in PC12 cells. (a) Ca^{2+} response to repeated applications of 30 μM ATP (15 s) to the same cells. In the left panel, both of the ATP applications were made in the absence of adenosine. In the right panel, adenosine was applied for 1 min before and during the second ATP application. Each symbol represents the mean ± s.e.mean from 14 (control) and 8 (100 μM adenosine) cells tested. (b) Comparison of the increase in $[Ca]_i$ upon the second application of 30 μM ATP. The Ca^{2+} response upon the first (S_1) and that upon the second (S_2) were measured as shown in (a), and the ratio of S_2/S_1 was determined in individual cells. Adenosine (100 μM) and CP66713 (10 μM) was applied 1 min before and during the second ATP stimulation. Each column represent mean ± s.e.mean from 5 (adenosine), 7 pertussis toxin (PTX) and 8 (CP66713) cells tested. (c) Effects of adenosine agonists on ATP-evoked $[Ca]_i$ rise. Values indicate the ratio (S_2/S_1) of the first and the second Ca^{2+} response to ATP (30 μM) as described in (b). The agents were applied 1 min before and during the second ATP stimulation. Data are mean ± s.e.mean from 13–19 (N^6-cyclohexyladenosine, CHA) and 11–14 (CGS22492) cells tested. Asterisks indicate significant differences from control: $*P < 0.05$; $**P < 0.01$.

evoked increase in $[Ca]_i$. Figure 7a shows the time-course of ATP-evoked $[Ca]_i$ rise in the cells. ATP was applied twice for 15 s with a 2 min interval between applications. ATP (30 μM, 15 s) stimulated transient increase in $[Ca]_i$ in the cells and the S_2/S_1 ratio was 1.2 ± 0.11 ($n = 5$). In PTX-treated PC12 cells, the ratio of repeated ATP application was unaffected (1.2 ± 0.11, $n = 7$). The first response to ATP was measured in the absence of adenosine (Figure 7a, left panel) and the second response to ATP was measured in the presence of adenosine (Figure 7a, right panel), and the ratio of S_2/S_1 was determined in individual cells. Adenosine (10 and 100 μM) potentiated the magnitude of $[Ca]_i$ rise (S_2/S_1 ratio: 10 μM; 1.6 ± 0.18, $n = 6$; 100 μM 1.9 ± 0.16, $n = 8$). These values were significantly larger compared with ATP alone ($P < 0.05$). Figure 7b indicates the effects of PTX and CP66713 (10 μM) on adenosine (100 μM)-induced potentiation of the ATP-evoked $[Ca]_i$ rise. PTX and CP66713 significantly attenuated the potential $[Ca]_i$ rise by adenosine. Furthermore, CGS22492 (1 and 10 μM) potentiated the ATP-evoked response significantly whereas CHA did not (Figure 7c).

Discussion

We have demonstrated here that adenosine (100 μM) potentiated ATP (30 μM)-evoked dopamine release in PC12 cells. Adenosine (100 μM) shifted the concentration-dependent curve of ATP-evoked dopamine release to the left without affecting the maximal ATP response, suggesting that adenosine does not increase the number of functional P_2-purinoceptors, but facilitates the efficiency of the response. Adenosine acts on at least two types of receptors (Stiles, 1992), namely, A_1 receptors that inhibit adenylate cyclase and A_2 receptors that stimulate adenylate cyclase. Nazarea et al. (1991) has shown that adenosine A_1 receptors attenuate ATP-evoked phosphoinositide turnover and arachidonate release in rat thyroid FRTL-5 cells, and that this inhibition involves a PTX-sensitive G-protein. In PC12 cells, pretreatment of the cells with PTX inhibited the adenosine-induced potentiation almost completely (Figure 3). This observation suggests that the modification by adenosine of ATP-evoked release is mediated by a PTX-sensitive pathway. Thus, our present data are in agreement with those of Nazarea et al. (1991) as to sensitivity to PTX. However, although 8-CPT, an A_1 antagonist, inhibited the potentiation, CP66713, an A_2 antagonist, abolished the potentiation and CGS22492, an A_2 agonist, potentiated ATP-evoked responses in the present study (Figures 4, 5, 7). These results suggest that the adenosine A_2 subclass receptors are involved in the potentiation. The observation that 5'-(N-cyclopropyl)-carboxamidoadenosine, another selective A_2 receptor agonist, also potentiated ATP-evoked dopamine release supports this idea (S. Koizumi & K. Inoue, unpublished data). The fact that 8-CPT also depressed adenosine-evoked potentiation may be explained by its poor selectivity: 8-CPT may also affect another subclass of A_2 receptors. Alternatively, this potentiation may be caused by an unknown adenosine receptor, sensitive to these antagonists and CGS22492.

It is suggested that stimulation of A_2 receptors activates adenylate cyclase, and causes cytoplasmic cyclic AMP accumulation (Gilman, 1984). An elevated cyclic AMP by forskolin can enhance carbachol-evoked dopamine release from PC12 cells (Meldolesi et al., 1988). We found that dibutyryl cyclic AMP, a membrane permeable analogue of cyclic AMP, had no effect on ATP-evoked dopamine release (Figure 6). The observation suggests that the potentiation of ATP-evoked dopamine release may not be mediated by the accumulation of cytoplasmic cyclic AMP. The lack of contribution of cyclic AMP seems to be reasonable since the subclass of adenosine A_2 receptors that mediates cyclic AMP accumulation are PTX-insensitive (Gilman, 1984) whereas the potentiation by adenosine in the present study was abolished by PTX-treatment (Figures 3 and 7b).

Adenosine (100 μM) potentiated the ATP-evoked increase in $[Ca]_i$ in PC12 cells (Figure 7a,b). As with the potentiation of the evoked release, PTX abolished the potentiation of $[Ca]_i$ increase and CGS22492 potentiated the Ca^{2+} response to ATP (Figure 7b,c). It is likely that the facilitation of ATP-evoked dopamine release by adenosine is due to an enhancement of the $[Ca]_i$ increase. The enhancement of $[Ca]_i$ increase, may at least partly, be mediated by an increase in Ca^{2+}-influx from extracellular media. This view is supported by our recent results using whole-cell voltage-clamp (Inoue et al., 1993) where adenosine (100 μM) potentiated the ATP (30 μM)-evoked inward current by a PTX-sensitive G-protein-mediated mechanism. As the ATP-activated channels are Ca^{2+}-permeable (Inoue & Nakazawa, 1992), this current enhancement may result in augmentation of Ca^{2+}-influx.

In conclusion, adenosine potentiates ATP-evoked dopamine release by facilitating the $[Ca]_i$ rise in PC12 cells. Evidence is most consistent with a role for a subclass of adenosine A_2 receptors in the observed potentiation. However, we cannot exclude the possibility that the potentiation may be mediated via a new type of adenosine receptor which is sensitive to PTX, and cannot readily be classified into the A_1 or A_2 subclasses. Detailed cellular mechanisms and the receptor subtypes are currently under investigation.

We would like to thank Ms T. Obama and Ms A. Kawahara for skilful assistance in experiments and cell culture, Dr James G. Kenimer for improving the manuscript, and Drs A. Takanaka and K. Fujimori for continuous encouragement. S.K. is a recipient of a Fellowship of the Human Science Foundation in Japan.

References

BEAN, B.P. (1990). ATP-activated channels in rat and bullfrog sensory neurons: concentration-dependence and kinetics. *J. Neurosci.*, **10**, 1–10.

BEAN, B.P. (1992). Pharmacology and electrophysiology of ATP-activated ion channels. *Trends Pharmacol. Sci.*, **13**, 87–90.

BURNSTOCK, G. & KENNEDY, C. (1985). A dual function for adenosine 5'-triphosphate in the regulation of vascular tone; excitatory cotransmitter with noradrenaline from perivascular nerves and locally released inhibitory intravascular agent. *Circ. Res.*, **58**, 319–391.

EDWARDS, F.A. & GIBB, A.J. (1993). ATP- a fast neurotransmitter. *FEBS Lett.*, **325**, 86–89.

EDWARDS, F.A., GIBB, A.J. & COLQUHOUN, D. (1992). ATP receptor-mediated synaptic currents in the central nervous system. *Nature*, **359**, 145–147.

EVANS, R.J., DERKACH, V. & SURPRENANT, A. (1992). ATP-mediates fast synaptic transmission in mammalian neurons. *Nature*, **357**, 503–505.

GERWINS, P. & FREDHOLM, B.B. (1992). ATP and its metabolite adenosine act synergically to mobilize intracellular calcium via the formation of inositol 1,4,5-triphosphate in a smooth muscle cell line. *J. Biol. Chem.*, **267**, 16081–16087.

GILMAN, A.G. (1984). G-proteins and dual control of adenylate cyclase. *Cell*, **36**, 577–579.

GREEN, L.A. & TISCHLER, A.S. (1976). Establishment of noradrenergic clonal line of rat adrenal pheochromocytoma cells which respond to nerve growth factor. *Proc. Natl. Acad. Sci. U.S.A.*, **73**, 2424–2428.

GRYNKIEWICZ, G., POENIE, M. & TSIEN, R.Y. (1985). A new generation of Ca^{2+} indicators with greatly improved fluorescence properties. *J. Biol. Chem.*, **260**, 3440–3450.

HIDE, I., PADGETT, W.L., JACOBSON, K.A. & DALY, J.D. (1991). A_{2A} adenosine receptors from rat PC12 cells: characterization with radioligand binding and by activation of adenylate cyclase. *Mol. Pharmacol.*, **41**, 352–359.

INOUE, K. & KENIMER, J.G. (1988). Muscarinic stimulation of calcium influx and norepinephrine release in PC12 cells. *J. Biol. Chem.*, **263**, 8157–8161.

INOUE, K. & NAKAZAWA, K. (1992). ATP receptor-operated Ca^{2+} influx and catecholamine release from neuronal cells. *News Physiol. Sci.*, **7**, 56–59.

INOUE, K., NAKAZAWA, K., FUJIMORI, K. & TAKANAKA, A. (1989). Extracellular adenosine 5'-triphosphate-evoked norepinephrine release coupled with receptor-operated Ca permeable channels in PC12 cells. *Neurosci. Lett.*, **106**, 294–299.

INOUE, K., WATANO, T., KOIZUMI, S. & BURNSTOCK, G. (1993). G-protein dependent dual modulation by adenosine of ATP-evoked inward currents and intracellular Ca increase in PC12 cells. *Jpn. J. Pharmacol.*, Suppl., **61**, 131p.

MELDOLESI, J., GATTI, G., AMBROSINI, A., POZZAN, T. & WEST-HEAD, E.W. (1988). Second-messenger control of catecholamine release from PC12 cells. *Biochem. J.*, **255**, 761–768.

MIYAKAWA, A., MAKINO, T., TAMAGAWA, A. & OZAKI, K. (1989). Determination of intracellular free calcium ion distribution with fluorescent calcium reagent Fura-2 using video image processing. *Bunseki Kagaku*, **28**, 643–649.

NAKAZAWA, K. & INOUE, K. (1992). Roles of Ca^{2+} influx through ATP-activated channels in catecholamine release from pheochromocytoma PC12 cells. *J. Neurophysiol.*, **68**, 2026–2032.

NAKAZAWA, K., WATANO, T. & INOUE, K. (1993). Mechanisms underlying facilitation of dopamine of ATP-activated currents in rat pheochromocytoma cells. *Pflügers Arch.*, **422**, 458–464.

NAZAREA, M., OKAJIMA, F. & KONDO, Y. (1991). P_2-purinergic activation of phosphoinositide turnover is potentiated by A1-receptor stimulation in thyroid cells. *Eur. J. Pharmacol. (Mol. Pharmacol. Section)*, **206**, 47–52.

OHARA-IMAIZUMI, M., NAKAZAWA, K., OBAMA, T., FUJIMORI, K., TAKANAKA, A. & INOUE, K. (1991). Inhibitory action of peripheral-type benzodiazepines on dopamine release from PC12 pheochromocytoma cells. *J. Pharmacol. Exp. Ther.*, **259**, 484–489.

OKADA, Y. & KURODA, Y. (1980). Inhibitory action of adenosine and adenosine analogs on neurotransmission in the olfactory cortex slice of guinea pig-structure-activity relationships. *Eur. J. Pharmacol.*, **61**, 137–146.

OKAJIMA, F., SATO, K., NAZAREA, M., SHO, K. & KONDO, Y. (1989). A permissive role of pertussis toxin substrate G-protein in P_2-purinergic stimulation of phosphoinositide turnover and arachidonate release in FRTL-5 thyroid cells. *J. Biol. Chem.*, **264**, 13029–13037.

PHILLIS, J.W., KOSTOPOULOS, G.K. & LIMACHER, J.J. (1975). A potent depressant action of adenosine derivatives on cerebral cortical neurons. *Eur. J. Pharmacol.*, **30**, 125–129.

STILES, G.L. (1992). Adenosine receptors. *J. Biol. Chem.*, **267**, 6451–6454.

(Received January 4, 1994
Revised February 21, 1994
Accepted March 8, 1994)

British Journal of Pharmacology

VOLUME 112 (3) JULY 1994

BRITISH JOURNAL OF PHARMACOLOGY

The *British Journal of Pharmacology* welcomes contributions in all fields of experimental pharmacology including neuroscience, biochemical, cellular and molecular pharmacology. The Board of Editors represents a wide range of expertise and ensures that well-presented work is published as promptly as possible, consistent with maintaining the overall quality of the journal.

Edited for the British Pharmacological Society by

Submission of manuscripts: Manuscripts (two copies) should be sent to The Editorial Office, British Journal of Pharmacology, St. George's Hospital Medical School, Cranmer Terrace, London SW17 0RE.

Authors should consult the Instructions to Authors and the Nomenclature Guidelines for Authors in Vol. **111,** 378–387. These Instructions and Guidelines also appear with the journal Index for Volumes **108–110,** 1993. A checklist of the essential requirements is summarised in each issue of the journal, or as the last page of the issue.

The *British Journal of Pharmacology* is published by Macmillan Press Ltd.

Scope The *British Journal of Pharmacology* is published monthly. It welcomes contribution in all field of experimental pharmacology including neuroscience, biochemical, cellular and molecular pharmacology. The Board of Editors represents a wide range of expertise and ensures that well-presented work is published as promptly as possible, consistent with maintaining the overall qulaity of the journal

This journal is covered by Current Contents, Excerpta Medica, BIOSIS and Index Medicus.

Editorial Manuscripts (plus two copies) and all editorial correspondence should be sent to: The Editorial Office, British Journal of Pharmacology, St George's Hospital Medical School, Cranmere Terrace, London SW17 0RE, UK. Tel: +44 81 767 6765; Fax: +44 81 767 5645.

Advertisements Enquires concerning advertisements should be addressed to: Michael Rowley, Hasler House, High Street, Great Dunmow, Essex CM6 1AP. Tel: +44 371 874613; Fax: +44 371 872273.

Publisher All business correspondence, supplement enquiries and reprint requests should be addressed to British Journal of Pharmacology, Scientific and Medical Division, Macmillan Press Ltd, Houndmills, Basingstoke, Hampshire RG21 2XS, UK. Tel: +44 256 29242; Fax: +44 256 810526. Publisher: Marija Vukovojac. Editorial Assistant: Alice Ellingham. Production Controller: Kath Parr.

Subscription Subscription price per annum (one volume, twelve issues) £540, rest of world £714 (Airmail), £595 (Surface mail) or equivalent in any other currency. Orders must be accompanied by remittance. Cheques should be made payable to Macmillan Magazines and sent to: The Subscription Department, Macmillan Press Ltd, Houndmills, Basingstoke, Hampshire RG21 2XS, UK. Where appropriate, subscribers may make payments into UK Post Office Giro Account No. 519 2455. Full details must accompany the payment. Subscribers from EC territories should add sales tax at the local rate.

British Journal of Pharmacology (ISSN 0007–1188) is published monthly by Macmillan Press Ltd, c/o Mercury Airfreight International Ltd, 2323 Randolph Avenue, Avenel, NJ 07001, USA. Subscription price for institutions is $950 per annum. 2nd class postage is paid at Rahway NJ. Postmaster: send address corrections to Macmillan Press Ltd, c/o Mercury Airfreight International Ltd, 2323 Randolph Avenue, Avenel NJ 07001.

Reprints of any article in this journal are available from Scientific and Medical Division, Macmillan Press Ltd, Houndmills, Basingstoke, Hampshire RG21 2XS, UK. Tel: +44 256 29242; Fax: +44 256 810526.

ISSN 0007–1188

Official publication of the British Pharmacological Society.

PREPARATION OF MANUSCRIPTS

Authors are strongly recommended to read the full *Instructions to Authors* and *Nomenclature Guidelines for Authors* (*Br. J. Pharmacol.* 1994, **111,** 378–387) before submitting a manuscript for publication in the *British Journal of Pharmacology*. The manuscript and cover letter should be checked against the following list before mailing.

The original and one copy of the manuscript must be supplied. Manuscripts must be typed in double-line spacing on one side of A4 paper, in type not smaller than 12 characters per inch or 10 point. Both copies to include Tables and a set of labelled Figures. One set of Figures without numbers or letters is also to be included. The text to be arranged in the following subsections:

1. **Title**—To have no more than 150 characters on a separate page, which should also include a Short Title (50 characters maximum) and the name and address of the author for correspondence.
2. **Summary**—To be arranged in numbered paragraphs (Full Papers) or a single paragraph (Special Reports).
   —to include aims, principal results and conclusions.
   —to include Key words (10 maximum) at end of summary.
3. **Introduction**—To contain concise statements of the problem and the aims of the investigation.
4. **Methods**—To have brief but adequate account of the procedures; *full names of drugs (including those referred to by manufacturer's code)*, sources of drugs and statistical tests to be stated.
5. **Results**—To have no repetition of data in Figures, Tables and text.
6. **Discussion**—Findings and conclusions to be placed in context of other relevant work.
   NB Simple repetition of results and unwarranted speculation are not acceptable.
7. **Acknowledgements**—Sources of support. Sources of drugs not widely available commercially.
8. **References**—All references in the text to be included in the Reference List and *vice versa*. References in alphabetical order with complete citations; Journals publishing 'in press' papers identified.
   References to manuscripts submitted to other journals but not yet accepted are not allowed.
9. **Tables**—Each on a separate page and prepared in accordance with current requirements of the Journal.
10. **Figures**—Both labelled and non-labelled Figures to be prepared in accordance with current requirements of the Journal (see *Instructions to Authors*, 1993, **108,** 275–281) and provided with Figure Number and Authors' names on back (*in pencil*).
    —each legend to be typed on a separate page and carrying keys to symbols.
    —keys to symbols and histograms must not appear on the figures themselves, but in the respective legends.
    —'box style' figures are not in keeping with the Journal style; line drawings etc must have only left-hand and bottom axes.
11. **Manuscripts**—To be accompanied by a declaration signed by each author that
    (a) results are original
    (b) approval of all persons concerned has been given to submit manuscripts for consideration (see also 12b)
    (c) the same material is neither 'in press' (i.e. is in proof or has definitely been accepted for publication) nor under consideration elsewhere. Furthermore it will not be submitted or published elsewhere before a decision has been reached by the Editorial Board of the *British Journal of Pharmacology* and will not be submitted elsewhere if accepted by the *British Journal of Pharmacology*.
    (d) Copyright assignment is included.
12. **Cover letter**—To state clearly
    (a) Corresponding author's full postal address, telephone, telex or Fax number
    (b) where appropriate, that *either* ethical approval has been given for investigation *or* Company or Institutional permission to publish work has been received.
13. **Reminder**—Packaging to be sufficiently robust to protect Figures and to withstand mailing.

Failure to comply with *Instructions to Authors* may lead to substantial delays in processing, review and publication and may even jeopardize acceptance of the manuscript.

NOMENCLATURE

Authors are reminded that accepted receptor and associated terminology is laid out in *Nomenclature Guidelines for Authors*, as published in the *British Journal of Pharmacology, Br. J. Pharmacol.*, 1994, **111,** 385–387.

SPECIAL REPORTS

The purpose of *Special Reports* is to provide rapid publication for **new** and **important** results which the Editorial Board considers are likely to be of special pharmacological significance. *Special Reports* will have publication priority over all other material and so authors are asked to consider carefully the status of their work before submission.

In order to speed publication there is normally no revision allowed beyond very minor typographical or grammatical corrections. If significant revision is required, the Board may either invite rapid re-submission or, more probably, propose that it be re-written as a Full Paper and be re-submitted for consideration. In order to reduce delays, proofs of *Special Reports* will be sent to authors but **essential corrections must reach the Production Office within 48 hours of receipt.** Authors should ensure that their submitted material conforms exactly to the following requirements.

Special Reports should normally occupy no more than two printed pages of the Journal; two illustrations (Figures or Tables, with legends) are permitted. As a guideline, with type face of 12 pitch and double-line spacing, a page of A4 paper could contain about 400 words. The absolute maximum length of the *Special Report* is 1700 words. For each Figure or Table, please deduct 200 words. The manuscript should comprise a Title page with key words (maximum of 10), a Summary consisting of a single short paragraph, followed by Introduction, Methods, Results, Discussion and References (maximum of 10). In all other respects, the requirements are the same as for Full Papers (see current 'Instructions to Authors').

BRITISH JOURNAL OF PHARMACOLOGY VOLUME 112 (3) 1994

Contents continue inside back cover

Typeset by Elite Typesetting Techniques, Southampton, Hampshire
and printed in Great Britain by Unwin Brothers Ltd., The Gresham Press, Old Woking, Surrey